

# **Introduction to NUCLEAR REACTOR THEORY**

**John R. Lamarsh**  
**NEW YORK UNIVERSITY**

**ADDISON-WESLEY PUBLISHING COMPANY**

# Contents

## Chapter 1 Review of Nuclear Physics

1-1	The Constituents of Nuclei . . . . .	1
1-2	Particle Wavelengths . . . . .	1
1-3	Nuclear Radii . . . . .	2
1-4	Nuclear Mass . . . . .	3
1-5	Binding Energy . . . . .	3
1-6	Excited States in Nuclei. . . . .	5
1-7	Radioactivity . . . . .	7
1-8	The Decay of Excited States . . . . .	9
1-9	Nuclear Reactions . . . . .	11

## Chapter 2 Interaction of Neutrons with Matter

2-1	Cross Sections . . . . .	17
2-2	Neutron Interactions and Macroscopic Cross Sections . . . . .	20
2-3	Cross Sections of Mixtures and Molecules . . . . .	22
2-4	Angular Distributions and Differential Cross Sections . . . . .	22
2-5	Center-of-Mass Coordinates . . . . .	24
2-6	Mechanisms of Neutron Interactions . . . . .	31
2-7	The Total Cross Section . . . . .	34
2-8	Elastic Scattering . . . . .	42
2-9	Transport Cross Section . . . . .	54
2-10	Nonelastic Cross Section . . . . .	57
2-11	Inelastic Scattering . . . . .	57
2-12	Absorption Reactions . . . . .	61
2-13	Neutron Producing Reactions . . . . .	66
2-14	The Doppler Effect . . . . .	68
2-15	On Cross-Section Compilations . . . . .	74

## Chapter 3 Nuclear Fission

3-1	The Mechanics of Fission . . . . .	82
3-2	Practical Fission Fuels . . . . .	86
3-3	Cross Sections of Fissionable Nuclei . . . . .	89
3-4	The Products of Fission . . . . .	92
3-5	Energy Release from Fission . . . . .	103
3-6	Reactor Power, Fuel Burnup, and Fuel Consumption . . . . .	105

**Chapter 4 Neutron Chain-Reacting Systems**

4-1	Multiplication Factor . . . . .	109
4-2	Neutron Balance and Conditions for Criticality . . . . .	109
4-3	Conversion and Breeding . . . . .	110
4-4	Types of Nuclear Reactors . . . . .	113
4-5	General Considerations of Reactor Design . . . . .	116

**Chapter 5 The Diffusion of Neutrons**

5-1	Interaction Rates and Neutron Flux . . . . .	118
5-2	Neutron Current Density . . . . .	122
5-3	The Equation of Continuity . . . . .	123
5-4	Fick's Law . . . . .	125
5-5	Physical Interpretation of Fick's Law . . . . .	128
5-6	Validity of Fick's Law . . . . .	129
5-7	The Diffusion Equation . . . . .	132
5-8	Boundary Conditions for the Steady-State Diffusion Equation . . . . .	133
5-9	Elementary Solutions of the Steady-State Diffusion Equation . . . . .	137
5-10	General Diffusion Problems . . . . .	144
5-11	The Diffusion Length . . . . .	153
5-12	The Reciprocity Theorem . . . . .	155

**Chapter 6 Neutron Moderation without Absorption**

6-1	Energy Loss in Elastic Collisions . . . . .	167
6-2	Collision and Slowing-Down Densities . . . . .	171
6-3	Moderation of Neutrons in Hydrogen . . . . .	171
6-4	Lethargy and $\xi$ . . . . .	174
6-5	Moderation of Neutrons for $A > 1$ . . . . .	176
6-6	Nonmonoenergetic Sources . . . . .	182
6-7	Slowing Down in Mixtures of Nuclides . . . . .	183
6-8	Multiscattered Neutrons . . . . .	185
6-9	Space-Dependent Slowing Down—Fermi Age Theory . . . . .	187
6-10	Boundary Conditions for the Age Equation . . . . .	190
6-11	Solutions to the Age Equation . . . . .	192
6-12	Physical Significance of Fermi Age . . . . .	196
6-13	Validity of Age Theory—Slowing Down in Hydrogen . . . . .	199
6-14	Measurement of Neutron Age . . . . .	201
6-15	Inelastic Scattering in the Slowing Down of Neutrons . . . . .	204
6-16	Methods of Calculating Age . . . . .	207

6-17	Elastic Moderation Time . . . . .	207
6-18	Slowing-Down Kernels . . . . .	208

## **Chapter 7 Neutron Moderation with Absorption and Fission**

7-1	Hydrogen and an Infinite Mass Absorber . . . . .	216
7-2	Moderators with $A > 1$ ; The NR and NRIM Approximations . .	222
7-3	Temperature Dependence of Resonance Escape . . . . .	229
7-4	Widely Spaced and Narrow Resonances . . . . .	230
7-5	Slowing Down with Weak Absorption . . . . .	232
7-6	Numerical Computations of Resonance Escape . . . . .	233
7-7	Measurements of Resonance Escape . . . . .	235
7-8	Space-Dependent Moderation with Absorption . . . . .	236
7-9	Fast Fission . . . . .	238

## **Chapter 8 Low-Energy Neutrons**

8-1	Thermal Neutron Spectra . . . . .	243
8-2	Interaction Rates for Thermal Neutrons . . . . .	251
8-3	Reactor Power . . . . .	257
8-4	Average $\eta$ in a Thermal Flux . . . . .	258
8-5	Diffusion of Thermal Neutrons . . . . .	260
8-6	Thermalization Time . . . . .	264
8-7	Age from Indium Resonance to Thermal . . . . .	266
8-8	Slowing Down and Diffusion . . . . .	268
8-9	Measurements of the Thermal Diffusion Parameters . . . . .	270

## **Chapter 9 Fermi Theory of the Bare Thermal Reactor**

9-1	Criticality of an Infinite Homogeneous Reactor . . . . .	282
9-2	The One-Region Finite Thermal Reactor . . . . .	285
9-3	Criticality for Other Reactor Geometries . . . . .	292
9-4	The Critical Equation . . . . .	299
9-5	Large Reactors . . . . .	301
9-6	Practical Applications of the Critical Equation . . . . .	302
9-7	Dependence of Critical Mass on Size and Composition . . . . .	307
9-8	Optimum Reactor Shapes . . . . .	309
9-9	Quasi-Homogeneous Reactors . . . . .	310

**Chapter 10 Multiregion Reactors—The Group Diffusion Method**

10-1	One Group of Neutrons . . . . .	319
10-2	Two-Group Method . . . . .	323
10-3	Two-Group Calculations of Nonuniform Reactors . . . . .	342
10-4	The Multigroup Method . . . . .	346
10-5	Reflector Savings . . . . .	354
10-6	Totally Reflected Reactors . . . . .	355
10-7	Experimental Determination of Critical Reactor Parameters .	359

**Chapter 11 Heterogeneous Reactors**

11-1	Eta . . . . .	371
11-2	Thermal Utilization . . . . .	371
11-3	Resonance Escape Probability . . . . .	390
11-4	The Fast Effect . . . . .	401
11-5	The Value of $k_\infty$ . . . . .	407
11-6	Other Reactor Parameters . . . . .	408

**Chapter 12 Reactor Kinetics**

12-1	Infinite Reactor with No Delayed Neutrons . . . . .	418
12-2	Mean Generation Time with Delayed Neutrons . . . . .	420
12-3	Infinite Reactor with Delayed Neutrons . . . . .	421
12-4	Response of a Bare Reactor to a Step-Change Reactivity .	428
12-5	The Value of $\beta$ . . . . .	436
12-6	The Stable Period . . . . .	437
12-7	The Prompt Jump . . . . .	439
12-8	The Prompt Critical Condition . . . . .	441
12-9	Small Reactivities . . . . .	441
12-10	Large Negative Reactivities; Scram and Shutdown . . . .	442
12-11	Linear Change in Reactivity . . . . .	443

**Chapter 13 Changes in Reactivity**

13-1	Changes in Temperature—Temperature Coefficients . . . .	448
13-2	Fission-Product Poisoning . . . . .	467
13-3	Burnup and Conversion . . . . .	479
13-4	Reactor Properties Over Life—Estimating Core Life . . . .	480

**Chapter 14 Control Rods**

14-1	Control-Rod Worth . . . . .	499
14-2	One Central Rod—Modified One-Group Theory . . . . .	503
14-3	Two-Group Theory of Control Rod . . . . .	506
14-4	The Eccentric Control Rod . . . . .	509
14-5	Ring of Rods . . . . .	512
14-6	Noncylindrical Rods . . . . .	517
14-7	Many Rods . . . . .	517

**Chapter 15 Perturbation Theory**

15-1	Reactivity and Perturbations . . . . .	524
15-2	Some Mathematical Preliminaries . . . . .	525
15-3	One-Group Perturbation Theory . . . . .	530
15-4	Two-Group Perturbation Theory . . . . .	534
15-5	Physical Interpretation of the Adjoint Flux . . . . .	541
15-6	Some Applications of Perturbation Theory . . . . .	543
15-7	Orthogonality and Adjointness . . . . .	547

**Appendix I Miscellaneous Constants and Data . . . . .** 555**Appendix II Special Functions . . . . .** 562

II-1	The Delta Function—Singular Source Distributions . . . . .	562
II-2	The Exponential Integral Function . . . . .	564
II-3	The Functions $E_n(x)$ . . . . .	564
II-4	The Error Function . . . . .	565
II-5	Bessel Functions . . . . .	566

**Index . . . . .** 573

*To Barbara, Michele, and Louie*

# Preface

This book is based on a one-year course in nuclear reactor theory which I have given over a number of years at Cornell and New York Universities. The major objective of this course is to provide the student with an understanding of the fundamental physical principles underlying the operation of a nuclear reactor. At the same time, it is expected that by the end of the course the student will be able to perform some of the more elementary calculations necessary in reactor design.

The prerequisites for this course, and hence for this book, are an undergraduate course in atomic and nuclear physics and a study of mathematics through advanced calculus. A knowledge of quantum mechanics is not assumed.

The selection and processing of nuclear data, especially cross-section data, is the starting point for many reactor calculations, and it is important for the nuclear engineer to be able to interpret and use such data correctly. These data and the physical processes from which they stem are discussed in the first portion of this book. It would not be necessary to include these chapters were it not for the fact that this material is not ordinarily covered in sufficient detail in prerequisite courses in nuclear physics. Physicists understandably are no longer so concerned with these matters as they once were. Where adequate prerequisite courses exist, the first three chapters can be omitted.

Most of the phenomena involving the transport of neutrons in a reactor can be understood within the framework of diffusion theory, and this model of neutron transport is used throughout much of this book. The cumbersome mathematical machinery of space-dependent transport theory is not included, because these techniques do not contribute substantially to an understanding of the basic physical principles. At the same time, a discussion of such techniques in a textbook of finite size requires the exclusion of other matters of greater importance. In certain important situations, however, where diffusion theory gives especially poor results, namely, in calculations of heterogeneous reactors, more accurate methods based on escape probabilities are introduced.

The notation used in this book is that recommended by the Commission on Symbols, Units, and Nomenclature (SUN Commission) of the International Union of Pure and Applied Physics; the physical constants are those recommended by the Committee on Fundamental Constants of the National Academy of Sciences—National Research Council (1963); and the cross-section data have been updated to include the second supplement to the second edition of BNL-325 [1964, 1965 and 1966 (to appear)].

The problems are arranged, in so far as possible, in the order of presentation of the material and not according to their difficulty. Some of the problems are pa-

tently trivial but are included because they demonstrate important physical principles. On the other hand, some problems are long and tedious and lend themselves well to machine computations. However, no problem specifically requires the use of a computer.

I have been aided by many persons in the preparation of this book. I especially wish to thank J. Chernick, N. R. Corngold, S. Glasstone, H. Goldstein, C. C. Graves, H. Hurwitz, Jr., I. Kaplan, M. S. Nelkin, L. W. Nordheim, D. S. St. John, and E. P. Wigner for comments on specific questions and/or reviews of portions of the manuscript. I am also indebted to B. A. Magurno and J. R. Stehn for sending me cross-section data prior to publication in the current supplement of BNL-325. My colleagues at New York University, R. Aronson, J. J. Herbst, R. W. Kupp, and E. Starr, have been most helpful in their comments on the evolving manuscript.

I also wish to acknowledge the assistance of many present and former students, especially S. J. Fierberg, J. S. Ingley, C. R. MacVean, J. R. Roth and R. A. Shaw, whose comments and suggestions over the years have helped to shape the final product. Mr. Joel Adir performed most of the calculations and provided many of the curves used in the figures, and I am pleased to acknowledge his vital assistance. The manuscript was prepared for publication by my wife, and it is doubtful that this work would have reached completion were it not for her untiring efforts in this project.

J. R. L.

Larchmont, New York

# 1

## Review of Nuclear Physics

Those portions of nuclear physics that are particularly important in reactor theory will be reviewed briefly in this chapter and in Chapter 2. It is presumed that the reader has already become acquainted with much of the subject matter of these chapters through prerequisite courses in atomic and nuclear physics.

### 1-1 The Constituents of Nuclei

The atomic nucleus consists of  $Z$  protons and  $N$  neutrons, where  $Z$  and  $N$  are the *atomic number* and *neutron number*, respectively. The total number of *nucleons* in the nucleus, that is, neutrons and protons, is equal to  $Z + N = A$ , where  $A$  is the *atomic mass number*.

Nuclei having the same atomic numbers but different neutron numbers are known as *isotopes*. Oxygen, for instance, has three stable isotopes,  $O^{16}$ ,  $O^{17}$ , and  $O^{18}$ , and three unstable isotopes,  $O^{14}$ ,  $O^{15}$ , and  $O^{19}$ . A table of some of the more important isotopes encountered in nuclear engineering appears in Appendix I. More complete tabulations are given in the references at the end of this chapter.

The mass of the proton is  $1.67252 \times 10^{-24}$  gram (gm). It carries a positive charge of  $1.60210 \times 10^{-19}$  coulombs (coul), equal in magnitude to the charge of the electron, and is a stable particle.

The mass of the neutron, for reasons which until recently were not entirely understood,\* is slightly larger than the mass of the proton, namely,  $1.67482 \times 10^{-24}$  gm, and it is electrically neutral. The neutron is not stable, however, unless it is bound in a nucleus. A free neutron decays to a proton with the emission of a  $\beta$ -ray and an antineutrino, a process which occurs on the average in about 12 min. It will be shown later in this book that the average lifetime of neutrons in a nuclear reactor before they are absorbed or leak from the system is only about  $10^{-3}$  sec. The instability of the neutron is therefore of no importance in reactor theory.

### 1-2 Particle Wavelengths

All particles in nature have a split personality, behaving sometimes like individual particles and sometimes like waves. The wavelength  $\lambda$  associated with a particle having momentum  $p$  is given by

$$\lambda = \frac{h}{p},$$

\* This question evidently has been settled at last; the neutron-proton mass difference can now be calculated from first principles. Cf. R. F. Dashen, *Phys. Rev.* **135B**, 1196 (1964).

where  $\hbar$  is Planck's constant.\* It is now customary to speak of a particle's *reduced wavelength*, denoted by  $\lambda$ , which is simply its wavelength divided by  $2\pi$ . Thus  $\lambda$  can be written as

$$\lambda = \frac{\hbar}{p}, \quad (1-1)$$

where  $\hbar$  is Planck's constant divided by  $2\pi$ . For neutrons, Eq. (1-1) gives

$$\lambda = \frac{4.55 \times 10^{-10}}{\sqrt{E}} \text{ cm}, \quad (1-2)$$

where  $E$  is the neutron energy in electron volts.†

### 1-3 Nuclear Radii

To a first approximation, the atomic nucleus can be considered to be a sphere of radius  $R$  given by the expression

$$R = 1.25 \times 10^{-13} A^{1/3} \text{ cm}, \quad (1-3)$$

where  $A$  is the atomic mass number. The constant 1.25 is derived from neutron scattering experiments, and since other types of measurements give somewhat different values, radii computed from Eq. (1-3) should not be taken too seriously. It should also be noted that this equation is not valid for the very light nuclei.

It is often convenient to express the nuclear radius in terms of the classical radius of the electron,  $r_e$ , which is defined by the formula

$$r_e = \frac{e^2}{m_e c^2}, \quad (1-4)$$

where  $e$  and  $m_e$  are the electronic charge and mass, respectively, and  $c$  is the velocity of light. The numerical value of  $r_e$  is  $2.82 \times 10^{-13}$  cm, so that  $R$  can be written roughly as

$$R = \frac{r_e}{2} A^{1/3}. \quad (1-5)$$

Although Eq. (1-5) is not numerically exact, it is sufficiently accurate for many computational purposes.

The volume  $V$  of a nucleus is proportional to  $R^3$ , and, in view of Eq. (1-3),  $V$  is proportional to  $A$ . Thus the average number of nucleons per unit volume in a nucleus, that is,  $A/V$ , is constant for all nuclei. Such a uniform density of nuclear matter suggests that nuclei are similar to little liquid drops, which, it will be recalled, have the same density whether they are large or small. This *liquid-drop model* of the nucleus has been widely used in nuclear physics and accounts for many properties of nuclei. It will be discussed further in Chapter 2.

\* A table of physical constants is given in Appendix I.

† 1 electron volt = 1 eV is the unit of energy equal to  $1.60 \times 10^{-19}$  joule.

## 1-4 Nuclear Mass

The masses of atoms are expressed in terms of the *atomic mass unit*, or *amu*. Until comparatively recently the amu was defined as one-sixteenth of the mass of the neutral O<sup>16</sup> atom. For a number of reasons, chiefly to bring the atomic mass unit closer to the chemical scale of atomic weights, nuclear masses are now measured relative to the mass of C<sup>12</sup> rather than O<sup>16</sup>. The amu is therefore currently defined as one-twelfth the mass of the neutral C<sup>12</sup> atom, and is equal to  $1.660438 \times 10^{-24}$  gm. In energy units the amu (using the C<sup>12</sup> standard) is equivalent to 931.478 MeV. In terms of this unit the proton and neutron have the following masses:

$$\begin{aligned} M_p &= 1.007277 \text{ amu}, \\ M_n &= 1.008665 \text{ amu}. \end{aligned}$$

Compilations of nuclear masses are noted in the references at the end of this chapter. Before using any compilation of data, however, the reader is cautioned to determine whether the values of mass are based on O<sup>16</sup> or C<sup>12</sup>.

## 1-5 Binding Energy

The masses of all nuclei are slightly less than the sum of the masses of the individual neutrons and protons contained in them. This difference in mass is called the *mass defect*, and is given by

$$\Delta = ZM_p + NM_n - M_A, \quad (1-6)$$

where  $M_A$  is the mass of the nucleus. Equation (1-6) can also be written as

$$\Delta = Z(M_p + m_e) + NM_n - (M_A + Zm_e), \quad (1-7)$$

where  $m_e$  is the mass of an electron. The quantity  $M_p + m_e$  is approximately equal to the mass  $M_H$  of neutral hydrogen, while  $M_A + Zm_e$  is approximately equal to the mass  $M$  of the neutral atom in question. The mass defect of the nucleus is therefore

$$\Delta \approx ZM_H + NM_n - M. \quad (1-8)$$

Equations (1-6) and (1-8) are not precisely equivalent owing to differences in electronic binding energies, but this is not important for most purposes.

When  $\Delta$  is expressed in energy units, it is equal to the energy which is necessary to break the nucleus into its constituent nucleons. This energy is known as the *binding energy* of the system, since it represents the energy with which the nucleus is held together. On the other hand, when a nucleus is produced from  $A$  nucleons,  $\Delta$  is equal to the energy released in the process. For example, when a neutron and proton combine to form a deuteron, the nucleus of H<sup>2</sup>, a 2.23-MeV  $\gamma$ -ray is emitted. Since this energy escapes as the deuteron is formed, the mass of the deuteron in energy units is 2.23 MeV less than the sum of the masses of neutron and proton. The neutron and proton can later be separated again, provided the binding energy

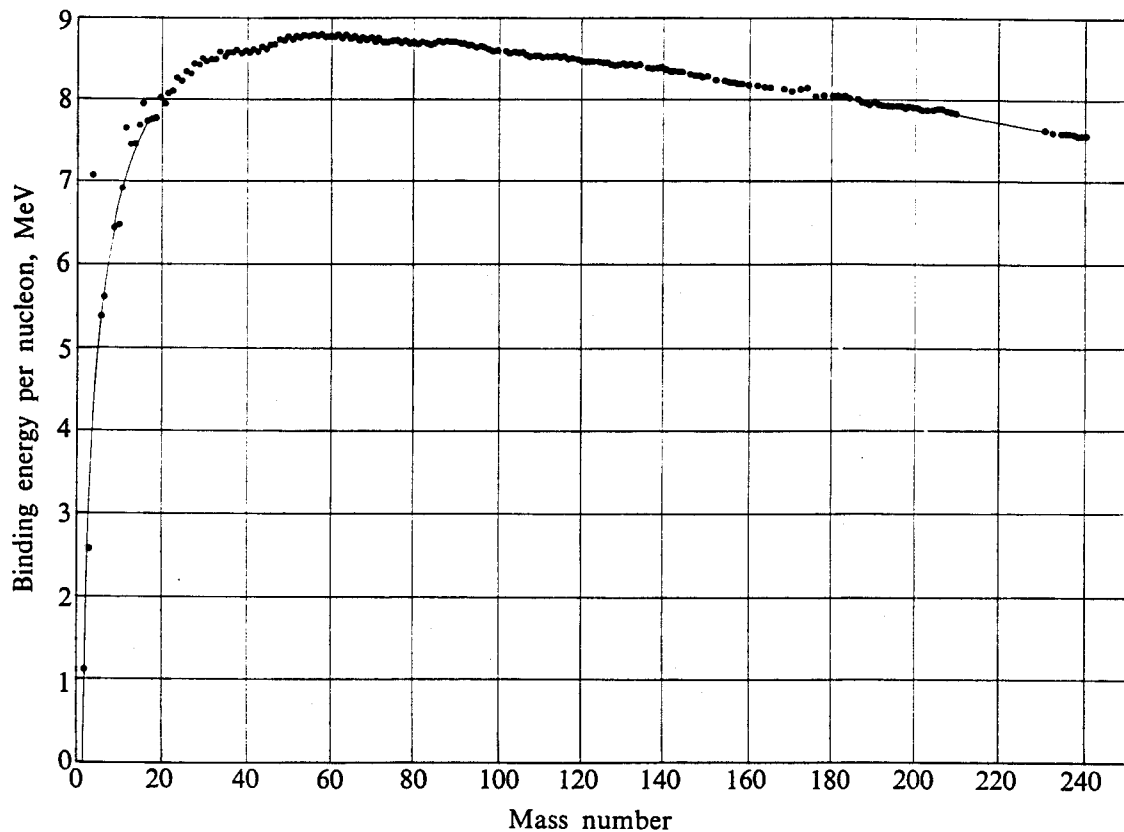


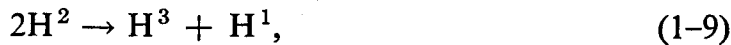
Fig. 1-1. Binding energy per nucleon as a function of mass number.

is resupplied to the system. This can be done in a number of ways, for instance by bombarding deuterium with  $\gamma$ -rays having an energy greater than 2.23 MeV.

The total binding energy of nuclei is an increasing function of the atomic mass number  $A$ . It does not increase, however, at a constant rate. This can be seen most conveniently when the average binding energy per nucleon is plotted versus  $A$ , as shown in Fig. 1-1. It will be noted that there are a number of deviations from the curve at low  $A$ , while above about  $A = 50$  the curve is a smooth but *decreasing* function of  $A$ . The behavior of the binding energy is particularly important in determining possible sources of nuclear energy.

Those nuclei in which the binding energy per nucleon is high are particularly stable or "tightly bound," and a relatively large amount of energy must be supplied to these systems to break them apart. On the other hand, nuclei with low binding energy per nucleon are less stable and can be disrupted more easily.

Whenever it is possible to form a more stable configuration by combining two less stable nuclei, energy is released in the process. Such reactions are possible with a great many pairs of isotopes. For instance, when two deuterons, each with a binding energy of 2.23 MeV, react to form  $H^3$ , having a total binding energy of 8.48 MeV, according to the equation



there is a net gain in the binding energy of the system of  $8.48 - 2 \times 2.23 = 4.02$  MeV. In this case, this energy appears as kinetic energy of the product nuclei H<sup>3</sup> and H<sup>1</sup>.

Reactions such as Eq. (1-9), in which at least one heavier, more stable nucleus is produced from two lighter, less stable nuclei, are known as *fusion reactions*. Reactions of this type are responsible for the enormous release of energy in hydrogen bombs and may some day provide unlimited sources of thermonuclear power.

Moving now to regions of large  $A$  in Fig. 1-1, it will be seen that a more stable configuration is formed when a heavy nucleus splits into two parts. The binding energy per nucleon in U<sup>238</sup>, for instance, is about 7.5 MeV, while it is about 8.4 MeV in the neighborhood of  $A = 238/2 = 119$ . Thus if a uranium nucleus divides into two lighter nuclei, each with about half the uranium mass, there is a gain in the binding energy of the system of approximately 0.9 MeV per nucleon, which amounts to a total energy release of about  $238 \times 0.9 = 214$  MeV. This process, of course, is called nuclear *fission*, and is the source of energy in nuclear reactors.

Before leaving the discussion of nuclear binding energy, it should be noted that nuclei containing 2, 6, 8, 14, 20, 28, 50, 82, or 126 neutrons or protons are especially stable. These nuclei are said to be *magic*, and their associated numbers of nucleons are known as *magic numbers*. These correspond to the numbers of neutrons or protons that are required to fill shells (or subshells) of nucleons in the nucleus in much the same way that electron shells are filled in atomic structures.

The existence of magic nuclei has a number of practical consequences in nuclear engineering. For instance, nuclei with a magic neutron number absorb neutrons to only a very small extent, and materials of this type can be used where neutron absorption must be avoided. Zirconium, for example, whose most abundant isotope contains 50 neutrons, has been widely used as a structural material in reactors, and bismuth (in liquid form), whose only naturally occurring isotope has 126 neutrons, has been proposed as a reactor coolant.

## 1-6 Excited States in Nuclei

The preceding sections pertain to nuclei in their *ground state*, that is, in the state of lowest energy. Nuclei also have *excited states* or *energy levels*. Figure 1-2 shows the known energy levels of C<sup>12</sup>, Al<sup>28</sup>, and U<sup>235</sup>, which are typical light, intermediate, and heavy nuclei, respectively. It will be observed that in every case the density of levels increases with increasing excitation energy. Furthermore, it should be noted that the density of levels at a given excitation energy also increases with increasing mass of the nucleus. While it is generally true that energy levels become increasingly dense with increasing mass number, the magic nuclei are important exceptions to this rule, and their excited states tend to resemble those of the lighter nuclei. This is shown in Fig. 1-3 for the nucleus Bi<sup>209</sup>. Such a level scheme has little in common with those of other heavy nuclei.

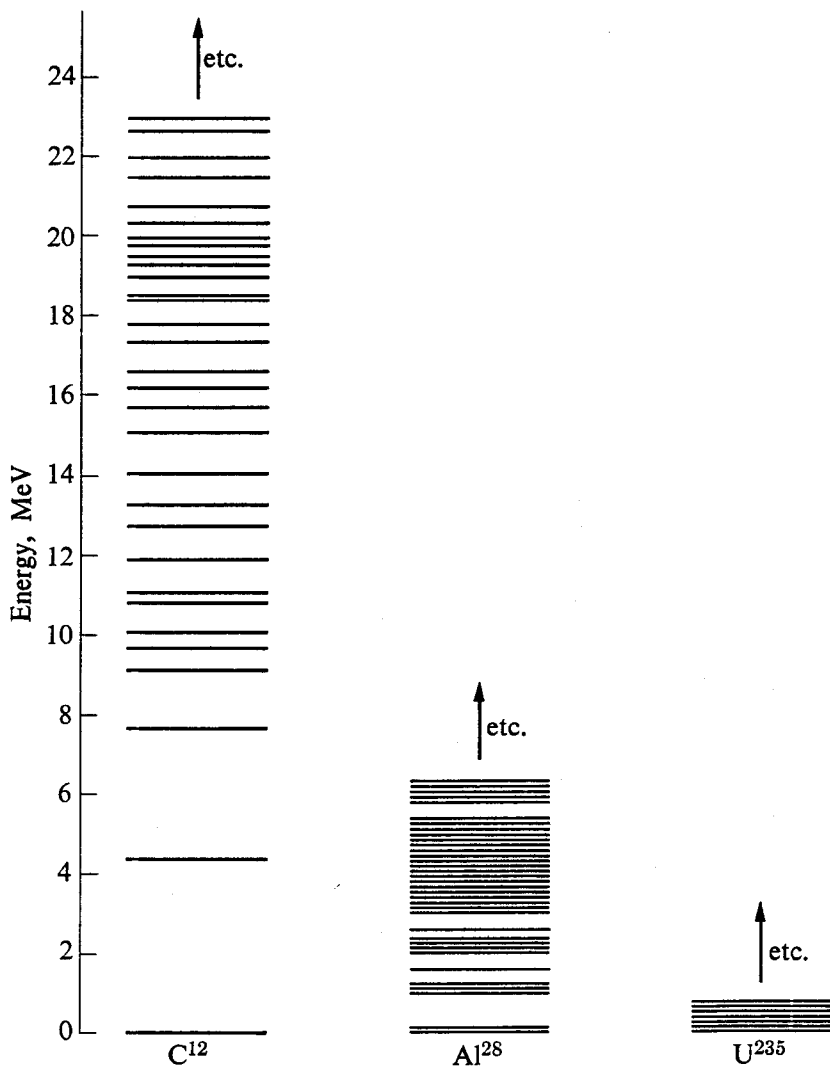


Fig. 1-2. The energy levels of  $\text{C}^{12}$ ,  $\text{Al}^{28}$ , and  $\text{U}^{235}$ .

It is interesting to compare the origins of excited states in nuclei and atoms. It will be recalled that in atoms the excited states are formed as the result of the continued excitation of only *one* electron at a time. That is, the states are formed by raising one electron through a succession of levels until it finally escapes from the system and the atom is ionized. More highly excited states of the atom are then formed by the excitation of a second electron until the atom is doubly ionized, and so on. Atomic energy states arise in this way because *it always takes less energy to raise an electron, already in an excited state, to a higher level than to place two or more electrons in excited states.*

The situation is quite different with nuclear energy levels. Once a nucleon has been raised to an excited level, it very frequently requires less energy for a second nucleon to make the same or another transition than it does to raise the first nucleon to a higher level. Thus the excited states of nuclei differ from those of atoms in that the higher excited states of nuclei usually result from the *simultaneous excita-*

*tion of a number of nucleons*; they are not due to the continued excitation of a single nucleon. For this reason, excited states in nuclei can exist above the “ionization” or binding energy of a single nucleon, a situation which is only rarely found in atomic structure. Thus an energy level can occur at 10 MeV in a nucleus in which only 8 MeV is necessary to remove a nucleon, simply because the 10 MeV of excitation energy is shared among several nucleons.

The binding energy of the least bound nucleon in a nucleus is called the *virtual energy*. This is the minimum energy which must be added to the nucleus in order to remove a nucleon, and is entirely analogous to the first ionization energy of an atom. Nuclear excited states above the virtual energy are called *virtual states* or *virtual levels*, while states below the virtual energy are called *bound states* or *bound levels*. It is clearly possible for nuclei in virtual states to decay by nucleon emission, whereas this is not possible for nuclei in bound states. It may be noted, however, that in order for a nucleon to be emitted from a virtual state, other excited nucleons must give up some of their own energy so that escape from the system is possible. Such a concentration of energy upon only one nucleon can occur as the result of collisions between the nucleons in the nucleus. However, when the energy of the excited nucleus is shared among a great many nucleons, such an unlikely distribution of energy among the nucleons rarely occurs. On the other hand, if only a few nucleons are involved in the formation of a virtual level, the chance that one nucleon can receive enough energy to escape from the nucleus is much greater.

## 1-7 Radioactivity

The spontaneous disintegration of nuclei, a process known under the (now) somewhat erroneous name “radioactivity,” is governed by only one fundamental law, namely, that the probability per unit time that a nucleus decays is a constant independent of time. This constant is called the *decay constant* and is denoted by  $\lambda$ .

Consider the decay of a sample of radioactive material. If at time  $t$  there are  $n(t)$  atoms which have not as yet decayed, then in view of the definition of  $\lambda$ ,  $\lambda n(t) dt$  of these will decay *on the average* in the time  $dt$  between  $t$  and  $t + dt$ . The rate of decay of the sample at time  $t$  is therefore simply  $\lambda n(t)$ . This decay rate is also called the *activity* of the sample, and is measured in *curies*. One curie is defined as  $3.700 \times 10^{10}$  disintegrations per second.

The decrease in the number of undecayed nuclei in time  $dt$  is given by

$$-dn(t) = \lambda n(t) dt. \quad (1-10)$$

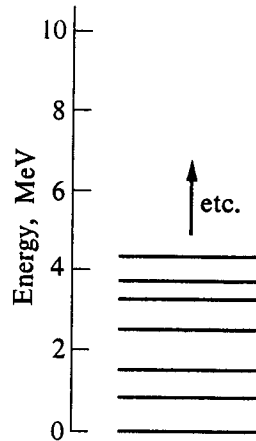


Fig. 1-3. The energy levels of  $\text{Bi}^{209}$ . (There may be a few additional levels in the vicinity of 3 MeV.)

This equation can be integrated to obtain

$$n(t) = n_0 e^{-\lambda t}, \quad (1-11)$$

where  $n_0$  is the number of atoms at  $t = 0$ .

The time during which the activity of a radioactive sample falls by a factor of two is known as the *half-life*, and is denoted by the symbol  $T_{1/2}$ . Writing

$$n(T_{1/2}) = n_0/2$$

in Eq. (1-11), it is easy to see that

$$T_{1/2} = \frac{\ln 2}{\lambda} = \frac{0.693}{\lambda}. \quad (1-12)$$

Consider next a sample of radioactive material containing  $n_0$  nuclei at time  $t = 0$ . In view of Eq. (1-11), there will be  $n_0 e^{-\lambda t}$  nuclei remaining after  $t$  sec. The *fraction* of the original nuclei which has not decayed is therefore  $e^{-\lambda t}$ . This fraction can also be viewed as the *probability* that any nucleus will not decay in the interval from  $t = 0$  to  $t = t$ . Now let  $p(t) dt$  be the probability that a nucleus decays in the time  $dt$  between  $t$  and  $t + dt$ . In other words,  $p(t) dt$  is the probability that a nucleus survives up to the time  $t$  and then decays in the interval from  $t$  to  $t + dt$ . This is evidently equal to the probability that the nucleus has not decayed up to the time  $t$  *times* the probability that it does in fact decay in the additional time  $dt$ . It follows therefore that

$$\begin{aligned} p(t) dt &= e^{-\lambda t} \times \lambda dt \\ &= \lambda e^{-\lambda t} dt. \end{aligned} \quad (1-13)$$

If Eq. (1-13) is integrated over all  $t$ , there is obtained

$$\int_0^\infty p(t) dt = \lambda \int_0^\infty e^{-\lambda t} dt = 1. \quad (1-14)$$

This shows that the probability that a radioactive nucleus eventually decays is equal to unity, as would be expected.

The *mean-life* of a nucleus can now be determined by finding the average value of  $t$  over the probability distribution  $p(t)$ . Denoting the mean-life by  $\bar{t}$ ,

$$\bar{t} = \int_0^\infty t p(t) dt = 1/\lambda. \quad (1-15)$$

In view of Eq. (1-12), the mean-life can also be written as

$$\bar{t} = \frac{T_{1/2}}{0.693} = 1.44 T_{1/2}. \quad (1-16)$$

It is frequently necessary to consider situations in which radioactive isotopes are produced and decay within a reactor. If they are produced at a rate of  $R(t)$  atoms/sec at the time  $t$ , the change in the number of atoms of the isotope in the subsequent interval  $dt$  is

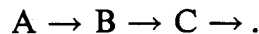
$$dn(t) = -\lambda n(t) dt + R(t) dt. \quad (1-17)$$

This equation can be solved directly by multiplying each term by the integrating factor  $e^{\lambda t}$ . Thus

$$n(t) = n_0 e^{-\lambda t} + e^{-\lambda t} \int_0^t R(t') e^{\lambda t'} dt', \quad (1-18)$$

where  $n_0$  is the number of atoms present at  $t = 0$ . The function  $n(t)$  can easily be found once the explicit form of  $R(t)$  is known.

Equation (1-18) can also be used to find the amount of an isotope at any point in a radioactive decay chain of the type



Consider, for example, the accumulation of the isotope B. Since the disintegration of one atom of A gives one atom of B, the rate of production of B is equal to the activity of A, that is

$$R(t) = \lambda_A n_A(t) = \lambda_A n_{A0} e^{-\lambda_A t}. \quad (1-19)$$

Inserting this into Eq. (1-18) and performing the integration gives the result

$$n_B(t) = n_{B0} e^{-\lambda_B t} + \frac{n_{A0} \lambda_A}{\lambda_B - \lambda_A} (e^{-\lambda_A t} - e^{-\lambda_B t}), \quad (1-20)$$

where  $n_{A0}$  and  $n_{B0}$  are the numbers of atoms of A and B at  $t = 0$ .

## 1-8 The Decay of Excited States

It has been found that the fundamental law of natural radioactivity, i.e., the probability per unit time that a system decays is a constant, also applies to the spontaneous decay of nuclei in excited states. It is customary, however, in discussing the decay of an excited state to express the decay constant  $\lambda$  in terms of a new quantity,  $\Gamma$ , called the *level width*, which is defined by the relation

$$\Gamma = \hbar \lambda. \quad (1-21)$$

Since  $\hbar$  has the units of energy *times* time, and  $\lambda$  has units of inverse time, it is evident that  $\Gamma$  has units of energy. In other words,  $\Gamma$  is the decay constant of an excited state expressed in energy units.

The level width can be used instead of the usual decay constant to describe the decay of nuclei from excited states. If, for example, there are  $n_0$  nuclei in a certain

excited state at  $t = 0$ ,  $t$  sec later there will be

$$n = n_0 e^{-\Gamma t/\hbar} \quad (1-22)$$

nuclei left in this state. Formulas such as Eq. (1-22) are not often useful, however, since the decay of excited states usually occurs so quickly that the time dependence of the process is not easily observed.

From Eqs. (1-15) and (1-21) it follows that the mean-life of a state of width  $\Gamma$  is given by

$$\bar{t} = 1/\lambda = \hbar/\Gamma. \quad (1-23)$$

Thus a state of large width tends to be short-lived; a state of small width is long-lived.

The widths of a great many excited states have been measured. For instance, the first virtual state of  $U^{239}$  is at 6.67 eV above the virtual energy and has a width of 27 millivolts (i.e., 0.027 eV). The mean-life of this state is therefore about

$$6.58 \times 10^{-16}/0.027 = 2.4 \times 10^{-14} \text{ sec.}$$

Lifetimes as short as this cannot be measured by ordinary methods, and this state appears to decay (in this case primarily by  $\gamma$ -ray emission) as soon as it is formed.

The decay of a nucleus from an excited state can frequently occur in a number of ways. If the nucleus is in a bound state, however, nucleon emission cannot occur, and, with few exceptions,\* the nucleus decays by the emission of  $\gamma$ -rays. On the other hand, if the nucleus is in a virtual state, then one or more nucleons, in addition to  $\gamma$ -rays, may be emitted, depending on the energy of the state.

The probability per unit time of each mode of decay of an excited state is described in terms of a *partial width* characteristic of each process. For instance, the partial width for  $\gamma$ -ray emission,  $\Gamma_\gamma$ , which is also known as the *radiation width*, is the probability per unit time (expressed in energy units) that the excited nucleus decays by  $\gamma$ -ray emission. Similarly,  $\Gamma_n$ , the *neutron width*, gives the probability per unit time that the state decays by neutron emission, etc. Since the total decay probability is the sum of the probabilities for all possible processes, the total width is the sum of the partial widths:

$$\Gamma = \Gamma_\gamma + \Gamma_n + \dots \quad (1-24)$$

The *relative* probability that an excited state decays by a given mode is evidently the ratio of the partial width of the particular mode to the total width. For example, the relative probability that a state decays by  $\gamma$ -ray emission is  $\Gamma_\gamma/\Gamma$ , that it decays by neutron emission is  $\Gamma_n/\Gamma$ , and so on.

---

\* The first excited state of  $O^{16}$  at 6.06 MeV, for example, decays by emitting an electron-positron pair; decay by  $\beta$ -ray emission is also possible from certain long-lived (isomeric) states.

### 1-9 Nuclear Reactions

When two nuclear particles, that is, two nuclei or a nucleus and a nucleon, interact to produce two or more nuclear particles or gamma radiation, a *nuclear reaction* is said to have taken place. If the initial nuclei are denoted by  $a$  and  $b$ , and the product nuclei (for simplicity it will be assumed that there are only two) are denoted by  $c$  and  $d$ , the reaction can be represented by the equation



In equations of this type, the interacting particles are always written in terms of neutral atoms, although some of the particles may be ionized.

In the usual experimental arrangement, one of the particles, say  $a$ , is at rest in some sort of target, and the particle  $b$  is projected against the target. In this case, Eq. (1-25) is often written in the abbreviated form

$$a(b, c)d,$$

or

$$a(b, d)c, \quad (1-26)$$

whichever is the more appropriate. For example, when oxygen is bombarded by energetic neutrons, one of the reactions that can occur is



In abbreviated form this is

$$\text{O}^{16}(\text{n}, \text{p})\text{N}^{16}, \quad (1-28)$$

where the symbols  $n$  and  $p$  refer to the incident neutron and emergent proton, respectively.

The detailed theoretical treatment of nuclear reactions is beyond the scope of this book. For present purposes, however, it is sufficient to note four of the fundamental laws governing these reactions:

(1) *Conservation of nucleons.* The number of nucleons before and after a reaction must be equal.

(2) *Conservation of charge.* The sum of the charges on all the particles before and after a reaction must be equal.

(3) *Conservation of linear and angular momentum.* The total momentum of the interacting particles before and after a reaction are the same since no external forces act upon the particles. The importance of the conservation of momentum will be discussed further in Chapter 2.

(4) *Conservation of energy.* Energy is conserved in all nuclear reactions.

The principle of the conservation of energy can be used to predict whether a certain reaction is energetically possible. Consider, for example, a reaction of the type given in Eq. (1-25). The total energy *before* the reaction is the sum of the

kinetic energies of the particles  $a$  and  $b$  plus the rest-mass energy of each particle. Similarly, the energy *after* the reaction is the sum of the kinetic energies of particles  $c$  and  $d$  plus their rest-mass energies. By conservation of energy it follows that

$$E_a + E_b + M_a c^2 + M_b c^2 = E_c + E_d + M_c c^2 + M_d c^2, \quad (1-29)$$

where  $E_a$ ,  $E_b$ , etc. are the kinetic energies of particles  $a$ ,  $b$ , etc. Equation (1-29) can be rearranged in the form

$$(E_c + E_d) - (E_a + E_b) = [(M_a + M_b) - (M_c + M_d)]c^2. \quad (1-30)$$

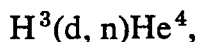
Thus it is seen that the *change* in the kinetic energies of the particles before and after the reaction is equal to the difference in the rest-mass energies of the particles before and after the reaction.

The right-hand side of Eq. (1-30) is known as the *Q-value* of the reaction; that is,

$$Q = [(M_a + M_b) - (M_c + M_d)]c^2. \quad (1-31)$$

From Eq. (1-30) it is clear that when  $Q$  is positive, there is a net *increase* in the kinetic energies of the particles. Such reactions are called *exothermic*. When  $Q$  is *negative*, on the other hand, there is a net *decrease* in the energies of the particles, and the reaction is said to be *endothermic*. With exothermic reactions, nuclear mass is converted into kinetic energy, while in endothermic reactions, kinetic energy is converted into mass.

The  $Q$ -value can be calculated without difficulty for any reaction involving atoms whose masses are known, provided the product nuclei are formed in their ground states. Consider, for instance, the reaction



which is of considerable importance both as a laboratory source of neutrons and as a possible source of thermonuclear power. The  $Q$ -value of the reaction is found from the following (atomic) masses:

$$\begin{array}{rcl} M(\text{H}^3) & = & 3.016049 \\ M(\text{H}^2) & = & 2.014102 \\ \hline M(\text{H}^3) + M(\text{H}^2) & = & 5.030151 \end{array} \quad \begin{array}{rcl} M(\text{He}^4) & = & 4.002604 \\ M(\text{n}) & = & 1.008665 \\ \hline M(\text{He}^4) + M(\text{n}) & = & 5.011269 \end{array}$$

Thus  $Q = 5.030151 - 5.011269 = 0.018882$  amu, which is equivalent to 17.6 MeV. This means that if, for instance, a stationary tritium ( $\text{H}^3$ ) target is bombarded with 1-MeV deuterons, the sum of the energies of the emergent neutron and alpha particle will be 18.6 MeV. On the other hand, if both the deuteron and  $\text{H}^3$  have essentially zero kinetic energy, the emergent neutron and alpha particle share only 17.6 MeV. In this latter case, it is easy to show that in order to conserve linear momentum, the neutron actually has an energy of 14.1 MeV while the alpha particle has 3.5 MeV.

When a reaction leads to nuclei in excited states, the  $Q$ -value cannot be calculated directly from the masses of the neutral atoms. In this case, either the masses of the nuclei in their excited states must be inferred from the neutral masses and the energies of the excited states, or else the  $Q$ -value can be calculated for the reaction proceeding to the ground states of the product nuclei, and then adjusted to take into account their state of excitation.

## References

### General

- BURCHAM, W. E., *Nuclear Physics*. New York: McGraw-Hill, 1963, Parts A and C.  
 EISBERG, R. M., *Fundamentals of Modern Physics*. New York: Wiley, 1961, Chapters 1-14, 16.  
 ENDT, P. M., and M. DEMEUR, *Nuclear Reactions*, Vol. I. Amsterdam: North Holland, 1959, Chapter 2.  
 EVANS, R. D., *The Atomic Nucleus*. New York: McGraw-Hill, 1955, Chapters 1-9, 11, 12, 15.  
 GREEN, A. E. S., *Nuclear Physics*. New York: McGraw-Hill, 1955, Chapters 1-6, 8, 12.  
 KAPLAN, I., *Nuclear Physics*, 2nd ed. Reading, Mass.: Addison-Wesley, 1963, Chapters 1-15, 17.  
 LITTLER, D. J., and J. F. RAFFLE, *An Introduction to Reactor Physics*, 2nd ed. New York: McGraw-Hill, 1957, Chapters 1-3.  
 MAYER, M. G., and J. H. D. JENSEN, *Elementary Theory of Nuclear Shell Structure*. New York: Wiley, 1955.  
 SEGRE, E., Editor, *Experimental Nuclear Physics*, Vol. III. New York: Wiley, 1959.

### Data

GIBBS, R. C., and K. WAY, *A Directory to Nuclear Data Tabulations*. Nuclear Data Project, National Academy of Sciences-National Research Council, U. S. Government Printing Office, Washington, D.C., 1958.

WAY, K., Editor, *Nuclear Data Tables* (in several parts). National Academy of Sciences-National Research Council, U. S. Government Printing Office, Washington, D.C., 1959, 1960.

WAY, K., Editor, *World-Wide News of Compilations in Nuclear Physics*. Nuclear Data Project, Oak Ridge National Laboratory, Oak Ridge, Tennessee. This newsletter contains the latest information on newly available and forthcoming data compilations.

STROMINGER, HOLLANDER, and SEABORG, "Tables of Isotopes," *Rev. Mod. Phys.* **30**, 585 (1958).

### Tables of masses based on C<sup>12</sup> can be found in:

- Handbook of Chemistry and Physics*, 45th ed. Cleveland: Chemical Rubber Co., 1964.  
 EVERLING, KONIG, MATTAUCH, and WAPSTRA, "Atomic Masses of Nuclides,  $A \leq 70$ ," *Nucl. Phys.* **15**, 342 (1960); **18**, 529 (1960).  
 BHANOT, JOHNSON, and NIER, "Atomic Masses in the Heavy Mass Region," *Phys. Rev.* **120**, 235 (1960).

Tables of nuclear energy levels are given in:

AJZENBERG-SELOVE, F., and T. LAURITSEN, "Energy Levels in Light Nuclei," *Nucl. Phys.* **11**, 1-340 (1959).

HELLWEGE, A. M., and K. H. HELLWEGE, Editors, "Energy Levels of Nuclei:  $A = 5$  to  $A = 257$ ," Landolt-Bornstein, New Series, Group I, Volume I, Berlin: Springer Verlag, 1961.

### Problems

1-1. The isotopic abundances of  $H^1$  and  $H^2$ , in atom percent, are 99.9851 and 0.0149, respectively. Compute the atom densities ( $\text{atoms}/\text{cm}^3$ ) of  $H^1$  and  $H^2$  in ordinary water.

1-2. The isotopic abundance of  $U^{235}$  is 0.714 atom percent. Compute the atom densities of  $U^{235}$  and  $U^{238}$  in (a) natural uranium, (b) uranium enriched to 1 atom percent in  $U^{235}$ . [Note: In both (a) and (b) take the density of the uranium to be  $18.7 \text{ gm}/\text{cm}^3$ .]

1-3. The useful substance *rubber* has a density of approximately unity and can be represented by the chemical formula  $(C_5H_8)_x$ , where  $x$  depends on the degree of polymerization. Find the atom densities of carbon and hydrogen in this material.

1-4. The density of thorium at  $0^\circ\text{C}$  is approximately  $11.3 \text{ gm}/\text{cm}^3$ . Its coefficient of linear expansion between  $0^\circ\text{C}$  and  $100^\circ\text{C}$  is constant and equal to  $12.3 \times 10^{-6}/^\circ\text{C}$ . Find the fractional change in its atom density as thorium is raised from  $0^\circ\text{C}$  to  $100^\circ\text{C}$ .

1-5. A certain reactor is fueled with a mixture of  $UO_2SO_4$  (uranyl sulfate) dissolved in water. The ratio of the atom density of the uranium to the molecular density of the water is only 0.00141, so that it may be assumed that the  $UO_2SO_4$  takes up no space whatever in the solution. Find the concentration of the  $UO_2SO_4$  in grams/liter.

1-6. Show that the speed of a neutron is given by

$$v = c\sqrt{E/470},$$

where  $c$  is the speed of light and  $E$  is the kinetic energy of the neutron in MeV.

1-7. Beryllium has a density of  $1.85 \text{ gm}/\text{cm}^3$ . At what energy is the wavelength of a neutron comparable to the average interatomic distance in this material?

1-8. Using the data in the table below, compute the fractions of the molecules of  $\text{LiH}$  that have molecular weights of approximately 7, 8, and 9.

Isotope	Abundance, atom percent
$H^1$	99.9851
$H^2$	0.0149
$Li^6$	7.42
$Li^7$	92.58

1-9. Using atomic mass tables, compute the binding energy of the "last neutron," that is, the energy required to remove a neutron from the following nuclei.

- (a)  $H^2$
- (d)  $Be^9$
- (g)  $U^{235}$

- (b)  $H^3$
- (e)  $C^{13}$
- (h)  $U^{236}$

- (c)  $He^4$
- (f)  $Pb^{208}$
- (i)  $U^{239}$

1-10. Using atomic mass tables, compute the average binding energy per nucleon of the following nuclei.

- (a) H<sup>2</sup>      (b) He<sup>4</sup>      (c) O<sup>16</sup>      (d) Fe<sup>56</sup>      (e) Bi<sup>209</sup>      (f) U<sup>235</sup>

1-11. Complete the following reactions and determine their  $Q$ -values.

- |                                     |                                      |                                      |
|-------------------------------------|--------------------------------------|--------------------------------------|
| (a) Be <sup>9</sup> ( $\alpha$ , n) | (b) Li <sup>6</sup> (p, $\alpha$ )   | (c) C <sup>12</sup> (n, 2n)          |
| (d) N <sup>14</sup> (n, p)          | (e) Al <sup>27</sup> (d, p)          | (f) Th <sup>232</sup> (n, $\gamma$ ) |
| (g) U <sup>235</sup> (n, 2n)        | (h) U <sup>236</sup> ( $\gamma$ , n) | (i) U <sup>238</sup> (n, 3n)         |

1-12. The radiation and neutron widths of the first virtual state in Xe<sup>136</sup> are 86 mV (millivolts) and 24 mV, respectively. (a) What is the mean-life of the state? (b) What is the relative probability that the state decays by neutron emission?

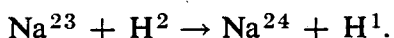
1-13. An indium foil is irradiated to saturation in a reactor and then removed. One-half hour later its activity (which is due to the decay of In<sup>116</sup> with a half-life of 54.1 min) is measured in a device that registers 1000 counts in 1 min. Had the activity been measured 5 min after its removal from the reactor, how many counts would the detector have registered in 1 min?

1-14. In nuclear reactors a newly-formed radioactive isotope *A* may be transformed into another isotope *B* by neutron absorption before it has had an opportunity to decay. Neutron absorption occurs at a rate proportional to the amount of isotope *A* present in the system. If the proportionality constant is denoted by *c*, and the rate of production (atoms of *A*/sec) is denoted by *R*(*t*), show that the number of atoms of isotope *A* present in the reactor at time *t* is given by

$$n(t) = n_0 e^{-(\lambda+c)t} + e^{-(\lambda+c)t} \int_0^t e^{(\lambda+c)t'} R(t') dt',$$

where *n*<sub>0</sub> is the number of atoms of *A* present at *t* = 0.

1-15. The isotope Na<sup>24</sup> ( $T_{1/2} = 15.0$  hr) can be produced by bombarding a Na<sup>23</sup> target with deuterons. The reaction is



If the *yield* of Na<sup>24</sup>, i.e., the number of Na<sup>24</sup> atoms produced per second multiplied by the decay constant, is 100  $\mu$ curies/hr, (a) what is the activity of the Na<sup>24</sup> after a 5 hr bombardment? (b) If the bombardment is ceased after 5 hr, what is the activity 10 hr later? (c) What is the maximum possible activity (the *saturation* activity) of Na<sup>24</sup> in the target?

1-16. Many coolant materials become radioactive as they pass through a reactor. Consider a circulating liquid coolant which spends an average of *t*<sub>1</sub> sec in a reactor and *t*<sub>2</sub> sec in the external circuit as indicated in Fig. 1-4. While in the reactor it becomes activated at the rate of *R* atoms/cm<sup>3</sup>-sec. (a) Show that the activity *a* added per cm<sup>3</sup> of the coolant per transit of the reactor is given by

$$\alpha = R(1 - e^{-\lambda_A t_1}).$$

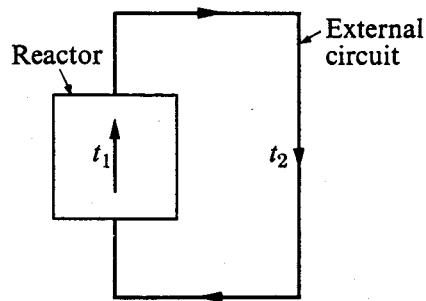


Figure 1-4

(b) Show that after  $m$  cycles the activity per  $\text{cm}^3$  of the coolant leaving the reactor is

$$\alpha_m = R \frac{(1 - e^{-\lambda_A t_1})(1 - e^{-m\lambda_A(t_1+t_2)})}{1 - e^{-\lambda_A(t_1+t_2)}}.$$

(c) What is the maximum coolant activity at the exit?

1-17. Isotope  $A$  is produced in a reactor at the constant rate of  $R$  atoms/sec and decays by way of the chain  $A \rightarrow B \rightarrow C$ , where the half-life of  $B$  is much longer than that of  $A$ .

(a) If the reactor is operated for the time  $t_0$  and then shut down, derive expressions for the activity of  $A$  and  $B$  at shutdown. (b) If  $t_0$  is large compared to  $T_{1/2}(A)$  but small compared to  $T_{1/2}(B)$ , at what time after shutdown is the activity of  $B$  the greatest? (c) Repeat part (b) for the case of  $t_0$  much larger than  $T_{1/2}(B)$ . What is the maximum activity of  $B$  in this case?

# 2

## Interaction of Neutrons with Matter

The operation of a nuclear reactor depends fundamentally on the way in which neutrons interact with atomic nuclei. It is necessary, therefore, to consider the nature of these interactions in some detail.

Neutrons interact with nuclei in a variety of ways. For instance, if the nucleus is unchanged in either isotopic composition or internal energy after interacting with a neutron, the process is called *elastic scattering*. On the other hand, if the nucleus, still unchanged in composition, is left in an excited state, the process is called *inelastic scattering*. The symbols  $(n, n)$  and  $(n, n')$  are often used to denote these processes. In referring to these interactions it is common to say that the incident neutron has been "scattered," elastically or inelastically, as the case may be, because a neutron reappears after the interaction. However, this term is somewhat misleading, since the emerging neutron may not be the same neutron that originally struck the nucleus.

Neutrons disappear in a reactor as the result of *absorption reactions*, the most important of which is the  $(n, \gamma)$  reaction. This process is also known as *radiative capture*, since one of the products of the reaction is  $\gamma$ -radiation. Neutrons also disappear in charged-particle reactions such as the  $(n, p)$  or  $(n, \alpha)$  reactions. Occasionally, two or more neutrons are emitted when a nucleus is struck by a high-energy neutron. The processes involved here are of the  $(n, 2n)$  or  $(n, 3n)$  type. A closely related process is the  $(n, pn)$  reaction, which also occurs with highly energetic incident neutrons. Finally, when a neutron collides with certain heavy nuclei, the nucleus splits into two large fragments with the release of considerable energy. This, of course, is the *fission* process, which will be discussed in Chapter 3.

In one way or another, most of these interactions must be taken into account in the design of a nuclear reactor. Before considering the specific interactions, however, it is necessary to set up a framework with which these interactions can be discussed quantitatively.

### 2-1 Cross Sections

The interactions of neutrons with matter are described in terms of quantities known as *cross sections* which are defined in the following way. Consider a thin target of area  $\mathcal{A}$  and thickness  $X$  containing  $N$  atoms per unit volume, placed in a uniform,

monodirectional beam of neutrons of intensity\*  $I$ , which strikes the entire target normal to its surface as shown in Fig. 2-1. In such an experiment, it is found that the rate at which interactions occur within the target is proportional to the beam intensity and to the atom density, area, and thickness of the target. If, for instance, the area of the target is doubled, the interaction rate is also doubled, provided, of course, the beam still has the same intensity over the entire target. On the other hand, if the intensity is doubled, the number of interactions which take place in a given time is also doubled, and so on.

These observations can be summarized by the equation:

$$\text{Interaction rate (in the entire target)} = \sigma IN\alpha X, \quad (2-1)$$

where the proportionality constant,  $\sigma$ , is known as the *cross section*. Solving Eq. (2-1) for  $\sigma$  gives

$$\sigma = \text{Interaction rate}/IN\alpha X. \quad (2-2)$$

However,  $N\alpha X$  is equal to the total number of atoms in the target, and it follows therefore that  $\sigma$  is the *interaction rate per atom in the target per unit intensity of the incident beam*.

It may be noted that in view of the definition of beam intensity,  $I\alpha$  neutrons strike the target per second, and according to Eq. (2-1),  $\sigma IN\alpha X$  interact. The relative probability that any one neutron in the beam interacts is therefore

$$\frac{\sigma IN\alpha X}{I\alpha} = \left( \frac{\sigma}{\alpha} \right) (N\alpha X). \quad (2-3)$$

Since the quantity  $N\alpha X$  is the number of nuclei in the target, it follows that  $\sigma/\alpha$  is the probability per target nucleus that a neutron in that portion of the beam striking the target will interact. Therefore, since the area of the target is fixed by the experiment, the *probability of an interaction is determined by  $\sigma$  alone*. It is in this sense, that of a *probability of interaction*, that the concept of cross section has its widest application.

It was assumed in the preceding discussion that the incident neutron beam strikes the entire target, which is the case when the target is smaller in area than

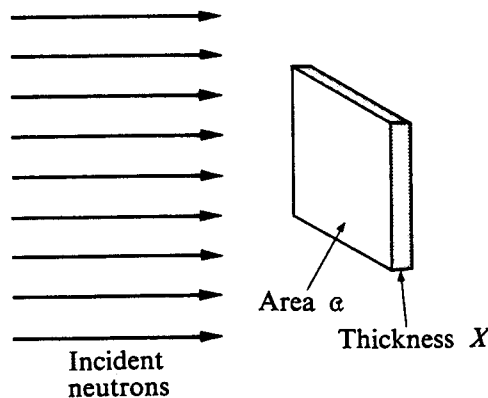


Fig. 2-1. Neutrons incident on a target.

\* The intensity of a monodirectional beam is defined as the number of neutrons which strike the target per  $\text{cm}^2/\text{sec}$ . If there are  $n$  neutrons/ $\text{cm}^3$  in the beam and if these neutrons move with the speed  $v$ , then  $I = nv$ , since all neutrons within the distance  $v \text{ cm}$  in front of the target strike it in 1 sec.

the beam. In many experiments the reverse is true, and the beam is smaller than the target. When this is the case, it is merely necessary to replace the target area appearing in the above formulas by the *interaction area*, that is, the area of the target exposed to the beam. The definition of cross section, of course, is the same in both cases.

It can be seen from Eq. (2-2) that  $\sigma$  has the dimensions of area. Cross sections are usually measured in units of barns, where 1 barn, abbreviated as b, is equal to  $10^{-24} \text{ cm}^2$ .

As mentioned in the introduction to this chapter, neutrons interact with nuclei in a number of ways, and it is convenient to describe each type of interaction in terms of a characteristic cross section. Thus elastic scattering is described by the *elastic scattering cross section*,  $\sigma_s$ ; inelastic scattering by the *inelastic scattering cross section*,  $\sigma_i$ ; the  $(n, \gamma)$  reaction (radiative capture) by the *capture cross section*,  $\sigma_\gamma$ ; fission by the *fission cross section*,  $\sigma_f$ ; etc. The sum of the cross sections for all possible interactions is known as the *total cross section* and is denoted by the symbol  $\sigma_t$ ; that is,

$$\sigma_t = \sigma_s + \sigma_i + \sigma_\gamma + \sigma_f + \dots \quad (2-4)$$

The total cross section measures the probability that an interaction of *any* type will occur when neutrons strike a target.

The sum of the cross sections of all absorption reactions is known as the *absorption cross section* and is denoted by  $\sigma_a$ . Thus,

$$\sigma_a = \sigma_\gamma + \sigma_f + \sigma_p + \sigma_\alpha + \dots, \quad (2-5)$$

where  $\sigma_p$  and  $\sigma_\alpha$  are the cross sections for the  $(n, p)$  and  $(n, \alpha)$  reactions. As indicated in Eq. (2-5), fission, by convention, is treated as an absorption process.

Finally, the difference between the total and elastic cross sections is known as the *nonelastic cross section*, and is usually denoted by  $\sigma_{ne}$ . In symbols, this is

$$\sigma_{ne} = \sigma_t - \sigma_s. \quad (2-6)$$

The nonelastic cross section is occasionally called the "inelastic cross section." This terminology is not correct, however, unless inelastic scattering is the only nonelastic process that can occur.\*

---

\* A somewhat different cross-section notation has recently been proposed by the Nuclear Cross Section Advisory Group of the U. S. Atomic Energy Commission [See H. Goldstein in *Fast Neutron Physics*, J. B. Marion and J. L. Fowler, Editors, p. 2227, New York: Interscience, 1963]. This group prefers to use  $\sigma_n$  and  $\sigma_{n'}$  for elastic and inelastic scattering cross sections, respectively,  $\sigma_T$  for the total cross section,  $\sigma_A$  for the absorption cross section, and  $\sigma_X$  for the nonelastic cross section. Despite certain advantages of this proposed notation, particularly in connection with calculations of fast reactors, the older notation given above will be used throughout this book. However, the reader should be alert for a possible general adoption of this alternative notation.

## 2-2 Neutron Interactions and Macroscopic Cross Sections

Suppose that a target of thickness  $X$  is placed in a monodirectional beam of intensity  $I_0$ , and that a neutron detector is placed at some distance behind the target as shown in Fig. 2-2. It will be assumed that both the target and the detector are small so that the detector subtends a small solid angle at the target. In this case every neutron that interacts in the target will be lost from the beam, and only those neutrons that do not interact will enter the detector.

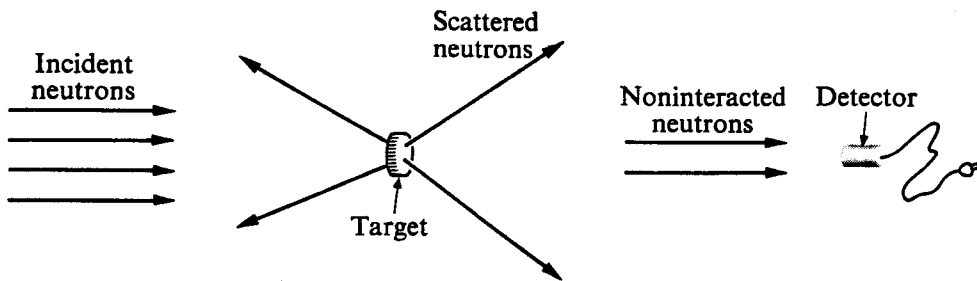


Fig. 2-2. Measurement of neutrons that have not interacted in the target.

Let  $I(x)$  be the intensity of the *noninteracted* neutrons after penetrating the distance  $x$  into the target. In traversing an additional distance  $dx$ , the intensity of the beam will be decreased by the number of neutrons that have interacted in the thin sheet of thickness  $dx$ . In view of Eq. (2-1), this decrease in intensity is given by

$$-dI(x) = N\sigma_t I(x) dx, \quad (2-7)$$

where  $N$  is the atom density of the target. The total cross section must be used in Eq. (2-7) since by definition any interaction removes a neutron from the non-interacted beam. Equation (2-7) can be integrated with the result

$$I(x) = I_0 e^{-N\sigma_t x}. \quad (2-8)$$

The intensity of the noninteracted beam thus decreases exponentially with distance inside the target. The intensity of the noninteracted beam *emerging* from the target is then

$$I(X) = I_0 e^{-N\sigma_t X}, \quad (2-9)$$

and this is the intensity measured by the detector.

The product of the atom density and a cross section, which appears in the exponential in Eq. (2-9), occurs quite frequently in the equations of reactor theory; it is given the special symbol  $\Sigma$ , and is called the *macroscopic cross section*. In particular, the product  $N\sigma_t = \Sigma_t$  is called the *macroscopic total cross section*,  $N\sigma_s = \Sigma_s$  is called the *macroscopic scattering cross section*, etc. Macroscopic cross sections evidently have the dimensions of  $\text{cm}^{-1}$ .

In terms of  $\Sigma_t$ , Eq. (2-7) can be written as

$$-dI(x) = \Sigma_t I(x) dx. \quad (2-10)$$

Dividing this expression by  $I(x)$  gives

$$-\frac{dI(x)}{I(x)} = \Sigma_t dx. \quad (2-11)$$

The quantity  $dI(x)/I(x)$  in this equation is equal to the fraction of the neutrons that have penetrated the distance  $x$  into the target without interacting, which subsequently interact in the distance  $dx$ . This, in turn, is equivalent to the probability that a neutron which survives up to  $x$  interacts in the next  $dx$ . Thus from Eq. (2-11),  $\Sigma_t dx$  is the probability that a neutron interacts in  $dx$ , and it follows that  $\Sigma_t$  is the *probability per unit path length* that a neutron will undergo some sort of interaction. In a similar manner, it is easy to show that  $\Sigma_s$ , the macroscopic scattering cross section, is equal to the probability per unit path length that a neutron will undergo elastic scattering. Analogous interpretations hold for all other macroscopic cross sections.

Returning to Eq. (2-8), it should be noted that in view of the fact that  $I(x)$  refers to those neutrons that have *not* interacted in penetrating the distance  $x$ , the ratio  $I(x)/I_0 = e^{-N\sigma_t x} = e^{-\Sigma_t x}$  is equal to the probability that a neutron can move through this distance without interacting. Now let the quantity  $p(x) dx$  be the probability that a neutron will have its *first interaction* in  $dx$  in the neighborhood of  $x$ . This is evidently equal to the probability that the neutron survives up to  $x$  without interaction *times* the probability that it does in fact interact in the additional distance  $dx$ . Since  $\Sigma_t$  is the probability of interaction per path length,  $p(x) dx$  is given by

$$\begin{aligned} p(x) dx &= e^{-\Sigma_t x} \times \Sigma_t dx \\ &= \Sigma_t e^{-\Sigma_t x} dx. \end{aligned} \quad (2-12)$$

The similarity between  $p(x)$  and the function  $p(t)$  for radioactive decay should be particularly noted [cf. argument preceding Eq. (1-13)].

The first interaction probability distribution function  $p(x)$  can be used in a number of ways. For instance, the probability  $P(a, b)$  that a neutron will have its first interaction between  $x = a$  and  $x = b$  is simply the integral of  $p(x) dx$  between these limits. That is,

$$\begin{aligned} P(a, b) &= \Sigma_t \int_a^b e^{-\Sigma_t x} dx \\ &= e^{-\Sigma_t a} - e^{-\Sigma_t b}. \end{aligned} \quad (2-13)$$

In particular, the probability that a neutron will interact at least once in an infinite medium is obtained by placing  $a = 0$  and  $b = \infty$ ; thus

$$P(0, \infty) = \int_0^\infty p(x) dx = 1,$$

as would be expected.

The distance that a neutron moves between interactions is called a *free path*, and the average distance between interactions is known as the *mean free path*. This

quantity, which is usually designated by the symbol  $\lambda$  (not to be confused with the radioactive decay constant or neutron wavelength), is equal to the average value of  $x$ , the distance traversed by a neutron without interaction, over the interaction probability distribution  $p(x)$ , that is,

$$\begin{aligned}\lambda &= \int_0^\infty xp(x) dx \\ &= \Sigma_t \int_0^\infty xe^{-\Sigma_t x} dx \\ &= 1/\Sigma_t.\end{aligned}\tag{2-14}$$

### 2-3 Cross Sections of Mixtures and Molecules

Consider a homogeneous mixture of two nuclear species  $X$  and  $Y$ , containing  $N_X$  and  $N_Y$  atoms/cm<sup>3</sup> of each type, and let  $\sigma_X$  and  $\sigma_Y$  be the cross sections of the two nuclei for some particular interaction. According to the discussion in the previous section, the probability per unit path that a neutron interacts with a nucleus of the first type is  $\Sigma_X = N_X\sigma_X$ , and with the second is  $\Sigma_Y = N_Y\sigma_Y$ . The total probability per unit path that a neutron interacts with either nucleus is, therefore,

$$\Sigma = \Sigma_X + \Sigma_Y = N_X\sigma_X + N_Y\sigma_Y.\tag{2-15}$$

If the nuclei are in atoms that are bound together in a molecule, Eq. (2-15) can be used to define an equivalent cross section for the molecule. This is done simply by dividing the macroscopic cross section of the mixture by the number of molecules per unit volume. If, for instance, the molecular formula is  $X_m Y_n$ , the resulting cross section for the molecule is

$$\sigma = m\sigma_X + n\sigma_Y.\tag{2-16}$$

Equations (2-15) and (2-16) are based on the assumption that the nuclei  $X$  and  $Y$  act independently of one another when they interact with neutrons. In some cases, particularly for low-energy elastic scattering by molecules and solids, this assumption is not valid and Eqs. (2-15) and (2-16) do not apply. This question will be considered again in Section 2-8.

### 2-4 Angular Distributions and Differential Cross Sections

Returning now to the experiment discussed in Section 2-1 in which a small detector was placed at some distance behind the target, it will be recalled that with the detector in this position, only those neutrons that do not interact in the target are counted. However, if the detector is moved off the axis of the incident beam, as shown in Fig. 2-3, neutrons that have been elastically or inelastically scattered or produced by reactions in the target will be observed in the detector, provided they are scattered in the proper direction.

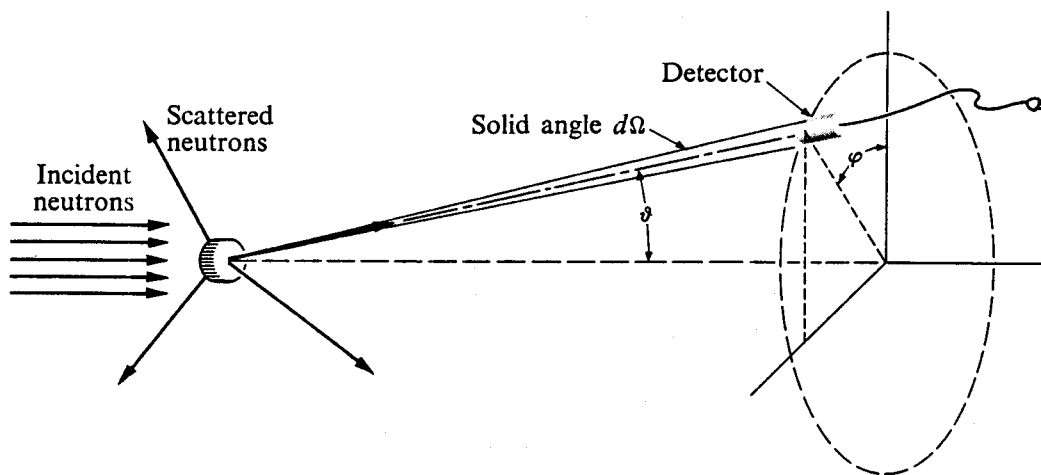


Fig. 2-3. Experimental arrangement for measuring angular distributions.

When such experiments are performed it is found that the number of neutrons scattered into the detector per unit time is often a function of the angle  $\vartheta$  but rarely depends on  $\varphi$ , the angle of rotation of the detector about the direction of the incident beam. In addition, it is found that this number is proportional to the beam intensity; to the atom density, area, and thickness of the target; and, in addition, to the solid angle subtended by the detector at the target. This last result is reasonable, since if the aperture of the detector is doubled, for instance, roughly twice as many neutrons are able to enter it per unit time. Consider for the moment only those neutrons that arrive in the detector as a result of elastic scattering; these results can then be summarized by the equation

$$dn(\vartheta) = \sigma_s(\vartheta) IN\alpha X d\Omega(\vartheta), \quad (2-17)$$

where  $dn(\vartheta)$  is the number of neutrons of the scattered beam entering the detector per unit time,  $I$  is the intensity of the incident beam;  $N$ ,  $\alpha$ , and  $X$  are, respectively, the atom density, area, and thickness of the target; and  $d\Omega(\vartheta)$  is the solid angle subtended by the detector at the target (cf. Fig. 2-3). Equation (2-17) defines the proportionality factor,  $\sigma_s(\vartheta)$ , which is called the *differential elastic scattering cross section*. Differential cross sections for other types of interactions such as inelastic scattering, the  $(n, 2n)$  and  $(n, 3n)$  reactions, etc., are defined in a similar manner.

Since  $dn(\vartheta)$  is the number of neutrons scattered per unit time from the beam into solid angle  $d\Omega(\vartheta)$ , it is easy to see that the differential cross section  $\sigma_s(\vartheta)$  is proportional to the probability that a neutron interacting in the target will be elastically scattered into the solid angle  $d\Omega(\vartheta)$ . The *total* probability that a neutron will be scattered through *any* angle is therefore equal to the integral of  $\sigma_s(\vartheta)$  over all solid angle. This, in turn, must be equal to the scattering cross section  $\sigma_s$ , which was defined in Section 2-1. Thus,

$$\sigma_s = \int_{4\pi} \sigma_s(\vartheta) d\Omega(\vartheta), \quad (2-18)$$

where the  $4\pi$  on the integral indicates that the integration is to be carried out over all solid angle. Since  $\sigma_s(\vartheta)$  in this integral does not depend upon the angle  $\varphi$ , the differential solid angle can be written as

$$d\Omega(\vartheta) = 2\pi \sin \vartheta d\vartheta, \quad (2-19)$$

and Eq. (2-18) becomes

$$\sigma_s = 2\pi \int_0^\pi \sigma_s(\vartheta) \sin \vartheta d\vartheta. \quad (2-20)$$

It is often necessary to evaluate integrals of the form given in Eq. (2-20) and this is usually facilitated by making the transformation  $\mu = \cos \vartheta$ . Then  $d\mu = -\sin \vartheta d\vartheta$ , and Eq. (2-20) becomes

$$\sigma_s = 2\pi \int_{-1}^{+1} \sigma_s(\mu) d\mu. \quad (2-21)$$

## 2-5 Center-of-Mass Coordinates

As will be shown presently, calculations of the kinematics of neutron interactions are considerably simplified when the interactions are described by a coordinate system in which the center of mass of the interacting particles is at rest. Such a coordinate system is known as the *center-of-mass system*. To be specific, let  $\mathbf{r}_l$  and  $\mathbf{R}_l$  be vectors describing the positions of the neutron and nucleus with respect to an arbitrary zero of coordinates at rest in the laboratory, as shown in Fig. 2-4. The center of mass of the system is the point defined by the vector  $\rho$  given by

$$\rho = \frac{m\mathbf{r}_l + M\mathbf{R}_l}{m + M}, \quad (2-22)$$

where  $m$  and  $M$  are the masses of the neutron and nucleus, respectively. The center-of-mass coordinates are simply those coordinates which describe the positions of the particles with respect to the center of mass. Thus, for the neutron and nucleus, the center-of-mass coordinates  $\mathbf{r}_c$  and  $\mathbf{R}_c$  are defined by the equations

$$\mathbf{r}_c = \mathbf{r}_l - \rho, \quad (2-23)$$

$$\mathbf{R}_c = \mathbf{R}_l - \rho. \quad (2-24)$$

If the particles are in motion, the vectors in Eqs. (2-23) and (2-24) are functions of time. Differentiating each with respect to time, there is obtained

$$\mathbf{v}_c = \mathbf{v}_l - \mathbf{v}_0, \quad (2-25)$$

$$\mathbf{V}_c = \mathbf{V}_l - \mathbf{v}_0. \quad (2-26)$$

Here,  $\mathbf{v}_c = d\mathbf{r}_c/dt$  and  $\mathbf{V}_c = d\mathbf{R}_c/dt$  are the velocities of the neutron and nucleus with respect to the center of mass,  $\mathbf{v}_l$  and  $\mathbf{V}_l$  are their velocities in the laboratory, and  $\mathbf{v}_0 = d\rho/dt$  is the velocity of the center of mass as observed in the laboratory.

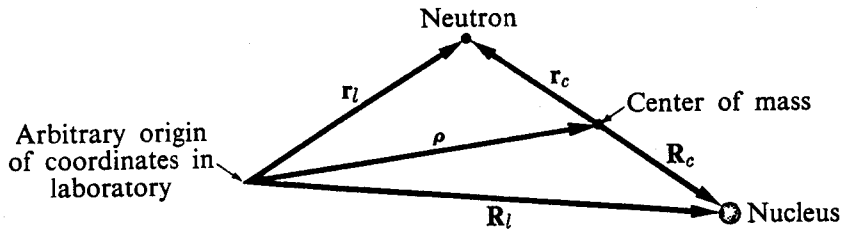


Fig. 2-4. Laboratory and center-of-mass coordinates.

The velocity  $v_0$  can be found by differentiating Eq. (2-22); thus,

$$v_0 = \frac{mv_l + M\mathbf{V}_l}{m + M}. \quad (2-27)$$

In many encounters between neutrons and nuclei, the velocity of the neutron is much larger than the velocity of the nucleus, and the latter can be assumed to be at rest in the laboratory. In this case, the second term in the numerator of Eq. (2-27) is zero, and

$$v_0 = \frac{m}{m + M} v_l. \quad (2-28)$$

Since  $m$  and  $M$  are about one amu and  $A$  amu, respectively, where  $A$  is the atomic mass number, this equation can also be written approximately as

$$v_0 \approx \frac{1}{A + 1} v_l. \quad (2-29)$$

It is clear from Eqs. (2-28) or (2-29) that for large  $A$ ,  $v_0$  is essentially zero, and in this case, the laboratory and center-of-mass coordinates are identical.

The velocity of the neutron in the center-of-mass system can be found by substituting Eq. (2-28) into Eq. (2-25); thus

$$\begin{aligned} v_c &= v_l - \frac{m}{m + M} v_l \\ &= \frac{M}{m + M} v_l \approx \frac{A}{A + 1} v_l. \end{aligned} \quad (2-30)$$

Finally, with the nucleus assumed to be at rest in the laboratory,  $\mathbf{V}_l = 0$ , and Eq. (2-26) gives

$$\mathbf{V}_c = -\mathbf{v}_0 = -\frac{m}{m + M} v_l \approx -\frac{1}{A + 1} v_l. \quad (2-31)$$

In other words, the velocity of the nucleus in the center-of-mass system is simply the negative of the velocity of the center of mass as observed in the laboratory.

The total momentum of the neutron and nucleus in the center-of-mass system is given by

$$\mathbf{p}_c = m\mathbf{v}_c + M\mathbf{V}_c.$$

Introduction of Eqs. (2-30) and (2-31) gives

$$\mathbf{p}_c = \frac{mM}{m+M} \mathbf{v}_l - \frac{mM}{m+M} \mathbf{v}_l = 0.$$

Hence the total momentum in the center-of-mass system is precisely zero. As will be seen below, this result simplifies calculations of two-particle collisions.

Consider now the energies of the neutron and nucleus as observed in the laboratory and center-of-mass systems. If the nucleus is at rest in the laboratory, the total energy  $E_l$  of the two particles in this system is just the kinetic energy of the neutron; that is,

$$E_l = \frac{1}{2}mv_l^2. \quad (2-32)$$

With respect to the center-of-mass system, however, both the neutron and the nucleus are in motion, and the total kinetic energy  $E_c$  in this system is

$$E_c = \frac{1}{2}mv_c^2 + \frac{1}{2}MV_c^2. \quad (2-33)$$

In view of Eqs. (2-30) and (2-31), this can be written as

$$E_c = \frac{1}{2} \frac{mM}{m+M} v_l^2 = \frac{1}{2}\mu v_l^2. \quad (2-34)$$

The quantity  $\mu$  [not to be confused with the cosine of the scattering angle; cf. Eq. (2-21)], which is defined as

$$\mu = \frac{mM}{m+M}, \quad (2-35)$$

is known as the *reduced mass* of the two-particle system.

It may be noted at this point that in the derivation of Eq. (2-34) it was assumed that the nucleus is at rest in the laboratory system. If this is not the case and the nucleus is also in motion, it is easily shown (cf. Prob. 2-8) that the total kinetic energy in the center-of-mass system is obtained by replacing  $v_l$  in Eq. (2-34) by the relative speed of the particles  $v_r$ . Thus in general for two particles,

$$E_c = \frac{1}{2}\mu v_r^2. \quad (2-36)$$

Equations (2-34) and (2-36) express the familiar result from classical mechanics, that the kinetic energy of two particles with respect to their center of mass is equal to the kinetic energy of a fictitious particle of mass equal to the reduced mass of the particles moving with a speed equal to the relative speed of the two particles.

By combining Eqs. (2-32) and (2-34), it is easy to see that with the nucleus at rest in the laboratory the total energy in the laboratory and center-of-mass systems are related by

$$E_c = \frac{M}{m+M} E_l, \quad (2-37)$$

which can also be written approximately as

$$E_c \approx \frac{A}{A + 1} E_l. \quad (2-38)$$

From Eq. (2-38) it follows that the total energy of two particles in the center-of-mass system is always somewhat *less* than it is in the laboratory system.

It will be recalled that in many interactions, such as elastic and inelastic scattering, neutrons emerge from their encounter with the nucleus at some angle with respect to the direction of the incident beam. It is in connection with such problems that center-of-mass coordinates are most helpful, because the kinematics of these interactions are particularly simple when viewed in this system. This, in turn, is due to the fact that the total momentum of the particles in the center-of-mass system is precisely zero before the collision, and, since momentum must be conserved, it is also zero after the collision. As a consequence, if only two particles emerge from a collision, they must necessarily part company back to back when observed in the center-of-mass system.

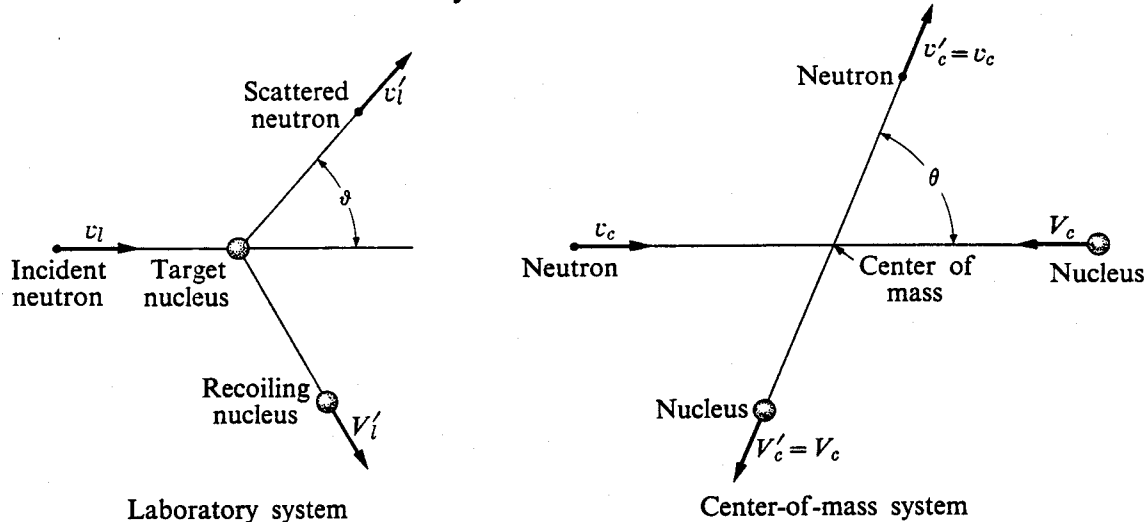


**Fig. 2-5.** Elastic scattering of neutron by nucleus, as observed in laboratory and center-of-mass coordinates.

As an illustration, consider the elastic scattering of a neutron as seen in the laboratory and center-of-mass systems (cf. Fig. 2-5). Viewed in the laboratory, the incident neutron moves with the speed  $v_l$  and strikes the nucleus which is initially at rest. As a result of the collision, the neutron emerges with the speed  $v'_l$  at the angle  $\vartheta$  with respect to its original direction, and the nucleus recoils in another direction with speed  $V'_l$ . Viewed from the center-of-mass system, the neutron and the nucleus are observed to approach each other with speeds of  $v_c$  and  $V_c$ . After the collision, the scattered neutron and residual nucleus leave back to back, as shown in the figure, with speeds  $v'_c$  and  $V'_c$ , respectively.

With elastic scattering, the situation is further simplified by the fact that *in the center-of-mass system* the speeds of the neutron and nucleus do not change in the

collision. This can be seen by the following argument. The relative speed of approach of the particles before the collision is

$$v_l = v_c + V_c, \quad (2-39)$$

and from Eq. (2-34) the total energy in the center-of-mass system can be written as

$$E_c = \frac{1}{2}\mu(v_c + V_c)^2. \quad (2-40)$$

After the collision the relative speed of neutron and nucleus is  $v'_c + V'_c$ , but the total energy is unchanged since the collision is elastic. Therefore after the collision,  $E_c$  is given by

$$E_c = \frac{1}{2}\mu(v'_c + V'_c)^2. \quad (2-41)$$

Thus, in view of Eqs. (2-40) and (2-41) it follows that

$$v_c + V_c = v'_c + V'_c. \quad (2-42)$$

The total linear momentum in the center-of-mass system is zero both before and after the collision, however, so that

$$mv_c = MV_c, \quad (2-43)$$

and

$$mv'_c = MV'_c. \quad (2-44)$$

Using Eq. (2-43) to eliminate  $V_c$  from the left-hand side of Eq. (2-42) and Eq. (2-44) to eliminate  $V'_c$  from the right-hand side of Eq. (2-42) gives

$$\left(1 + \frac{m}{M}\right)v_c = \left(1 + \frac{m}{M}\right)v'_c, \quad (2-45)$$

so that  $v_c = v'_c$ . From Eq. (2-42) it is also seen that  $V_c = V'_c$ . In other words, the speeds of the neutron and nucleus with respect to the center of mass are unchanged in an elastic collision. This result, incidentally, is also true if both the neutron and nucleus are initially in motion in the laboratory system.

With interactions other than elastic scattering,  $v'_c$  is not equal to  $v_c$ , but is larger or smaller depending upon whether the  $Q$ -value for the interaction is positive or negative. In any event, the particles emerging from the interaction must leave back

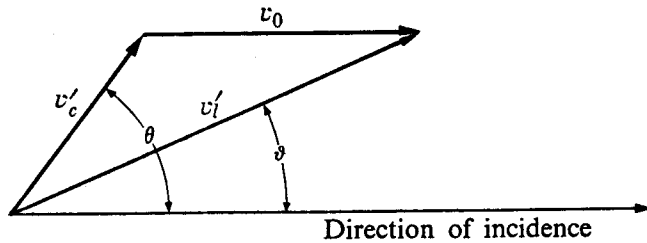


Fig. 2-6. Vector diagram relating laboratory and center-of-mass scattering angles.

to back in the center-of-mass system since the total momentum in this system must always remain zero.

It will be noted in Fig. 2-5 that the angle  $\vartheta$  at which an elastically scattered neutron appears in the laboratory system is not, in general, the same as the angle  $\theta$  at which it is observed in the center-of-mass system. The relationship between  $\vartheta$  and  $\theta$  can be found by noting that Eq. (2-25) relating the neutron velocities in the center-of-mass and laboratory systems is a general result, valid both before and after the interaction. The velocities of the scattered neutron in the two systems are therefore related by

$$\mathbf{v}'_c = \mathbf{v}'_l - \mathbf{v}_0. \quad (2-46)$$

This equation is depicted as a vector diagram in Fig. 2-6. From the figure it is clear that

$$v'_l \sin \vartheta = v'_c \sin \theta, \quad (2-47)$$

and

$$v'_l \cos \vartheta = v_0 + v'_c \cos \theta. \quad (2-48)$$

Dividing these equations gives

$$\tan \vartheta = \frac{v'_c \sin \theta}{v_0 + v'_c \cos \theta}. \quad (2-49)$$

Using Eqs. (2-29) and (2-30) and noting that for elastic scattering  $v'_c = v_c$ , Eq. (2-49) can be written as

$$\tan \vartheta = \frac{\sin \theta}{\frac{1}{A} + \cos \theta}. \quad (2-50)$$

Equation (2-50) is valid only for elastic scattering. For other types of neutron interactions, the relation between the angles  $\vartheta$  and  $\theta$  is of the same form, namely,

$$\tan \vartheta = \frac{\sin \theta}{\gamma + \cos \theta}, \quad (2-51)$$

where

$$\gamma = \frac{v_0}{v'_c}. \quad (2-52)$$

The parameter  $\gamma$  depends upon such things as bombarding energy,  $Q$ -value, etc., in addition to the mass of the struck nucleus (cf. Prob. 2-11).

Another useful formula relating  $\vartheta$  and  $\theta$  can be obtained by writing Eq. (2-48) as

$$\cos \vartheta = \frac{v_0 + v'_c \cos \theta}{v'_l}. \quad (2-53)$$

Then, from the law of cosines,

$$v'_l = \sqrt{(v'_c)^2 + v_0^2 + 2v'_c v_0 \cos \theta}, \quad (2-54)$$

and again noting that  $v'_c = v_c$  for elastic scattering, Eq. (2-53) gives

$$\cos \vartheta = \frac{1 + A \cos \theta}{\sqrt{A^2 + 2A \cos \theta + 1}}. \quad (2-55)$$

For interactions other than elastic scattering, Eq. (2-55) becomes

$$\cos \vartheta = \frac{\gamma + \cos \theta}{\sqrt{\gamma^2 + 2\gamma \cos \theta + 1}}, \quad (2-56)$$

where  $\gamma$  is given by Eq. (2-52).

Because the laboratory and center-of-mass scattering angles are not equal, the angular distributions of the emergent particles expressed in the two systems are also different. The relation between the two angular distributions may be obtained by noting that the number of neutrons appearing in a given element of solid angle must be the same in both systems. It follows therefore that

$$\sigma(\vartheta) d\Omega(\vartheta) = \sigma(\theta) d\Omega(\theta), \quad (2-57)$$

where  $\sigma(\theta)$  is the differential cross section measured in the center-of-mass system.\* Since  $d\Omega = 2\pi \sin \vartheta d\vartheta$ , Eq. (2-57) is equivalent to

$$\sigma(\vartheta) \sin \vartheta d\vartheta = \sigma(\theta) \sin \theta d\theta. \quad (2-58)$$

Equation (2-58), together with Eqs. (2-51) or (2-56), can be used to convert angular distributions from one system to the other. For instance, suppose the differential cross section in the laboratory must be found from values given in the center-of-mass system. From Eq. (2-58),  $\sigma(\vartheta)$  is

$$\sigma(\vartheta) = \sigma(\theta) \frac{\sin \theta}{\sin \vartheta} \frac{d\theta}{d\vartheta} = \sigma(\theta) \frac{d(\cos \theta)}{d(\cos \vartheta)}, \quad (2-59)$$

and from Eq. (2-56)

$$\frac{d(\cos \theta)}{d(\cos \vartheta)} = \frac{(\gamma^2 + 2\gamma \cos \theta + 1)^{3/2}}{1 + \gamma \cos \theta}. \quad (2-60)$$

Thus

$$\sigma(\vartheta) = \sigma(\theta) \frac{(\gamma^2 + 2\gamma \cos \theta + 1)^{3/2}}{1 + \gamma \cos \theta}, \quad (2-61)$$

which is the desired relation.

---

\* Equation (2-57) is an example of the standard prescription for relating distribution functions of different but related statistical variables. Thus, if  $x$  and  $y$  are two such variables, their associated distribution functions  $f(x)$  and  $F(y)$  are connected by the equation  $f(x) dx = F(y) dy$ . Since  $f(x)$  and  $F(y)$  are different functions, they are usually (*always* by mathematicians) represented by different symbols. The cross sections  $\sigma(\vartheta)$  and  $\sigma(\theta)$  are also different functions but it is the usual practice to denote them both by the symbol  $\sigma$ , since this is standard symbol for cross section. This hopefully not too-confusing procedure will be met throughout this book.

If both sides of Eq. (2-57) are integrated over all solid angle, the result is:

$$\int_{4\pi} \sigma(\vartheta) d\Omega(\vartheta) = \int_{4\pi} \sigma(\theta) d\Omega(\theta). \quad (2-62)$$

The left-hand side of Eq. (2-62) is the cross section for the process as observed in the laboratory, while the right-hand side is the cross section as observed in the center-of-mass system. Equation (2-62) shows that although the *differential* cross sections may not be equal, the *integrated* cross sections are identical. This is no surprise, however, since the integrated cross sections are directly related to the probability that the process will occur at all, and this clearly must be independent of the coordinate system in which the process is expressed.\*

## 2-6 Mechanisms of Neutron Interactions

Each of the various neutron interactions discussed at the beginning of this chapter may occur by way of one or more of three fundamentally different mechanisms. These are called, respectively, *compound nucleus formation*, *potential or shape scattering*, and *direct interaction*.

**Compound nucleus formation.** In this process the incident neutron is absorbed by the nucleus, and a system known as the *compound nucleus* is formed. If the target nucleus is  $Z^A$ , the compound nucleus will be  $Z^{A+1}$ .

It is interesting to consider how the formation of the compound nucleus appears when observed in the center-of-mass system. In this system, it will be remembered, the target nucleus and incident neutron approach each other and collide *at the center of mass* which is at rest. If the neutron is absorbed and a compound nucleus is produced, this nucleus must necessarily remain motionless at this point since the center of mass now resides with the compound system. It follows that when the compound nucleus is formed, the kinetic energies of both neutron and target nucleus with respect to the center-of-mass system are transferred into internal energy of the compound nucleus. This energy,  $E_c$ , was computed in Section 2-5 and is given by Eq. (2-34).

The excitation of the compound nucleus is considerably higher than  $E_c$ , however. In Chapter 1 it was pointed out that energy is required to remove a neutron from a nucleus, and, conversely, this energy reappears when the neutron is replaced in the nucleus. Thus, when the incident neutron coalesces with the target nucleus  $Z^A$  to form the compound system  $Z^{A+1}$  it brings with it, so to speak, its binding energy  $B$  to the nucleus  $Z^{A+1}$ . The compound nucleus is formed therefore at the energy  $E_c + B$  above the ground state. This situation is illustrated schematically in Fig. 2-7. The compound nucleus in this excited state could immediately decay

---

\* This assumes that the target nuclei are at rest in the laboratory before the interaction. If they are in motion the cross sections in the laboratory and center-of-mass systems may be different (cf. Section 2-8).

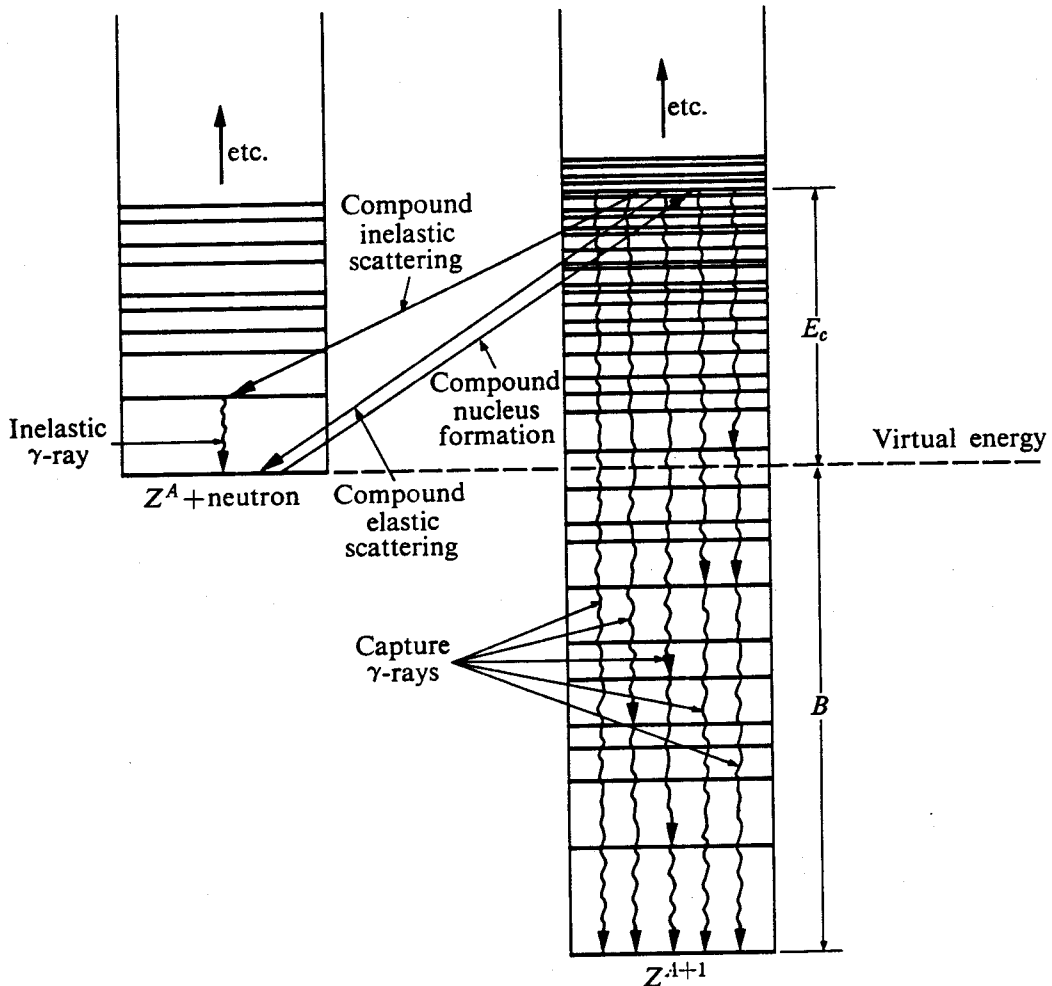


Fig. 2-7. Diagram showing role of compound nucleus in neutron interactions.

with the reemission of the neutron, were it not for the fact that the energy of excitation of the compound system is usually shared among many nucleons. The nucleus therefore may remain in this state for a long time, and, as discussed in Section 1-6, can decay by the emission of a nucleon (or a group of nucleons, such as an  $\alpha$ -particle) only if, as a result of random collisions within the nucleus, the nucleon receives enough energy to enable it to escape from the system.

If the emitted nucleon is a neutron and the residual nucleus  $Z^A$  is returned to its ground state the process is known as *compound elastic scattering* or sometimes *resonance elastic scattering*. On the other hand, if the emitted neutron leaves the residual nucleus in an excited state, the process is called *compound inelastic scattering* or *resonance inelastic scattering*. These processes are shown in Fig. 2-7.

The compound nucleus may also decay by the emission of one or more *capture  $\gamma$ -rays*, as indicated in Fig. 2-7, and in this way the highly excited compound nucleus eventually reaches the ground state. While the nucleus  $Z^{A+1}$  may not be stable with respect to  $\beta$ -decay, it can no longer decay by nucleon emission once it has decayed by  $\gamma$ -rays to a bound state.

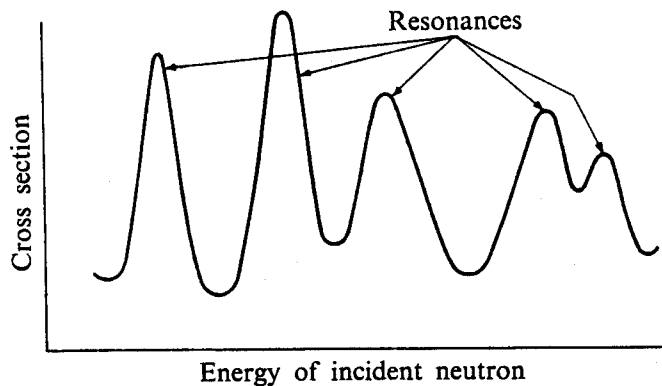


Fig. 2-8. Resonances in cross section.

The characteristic feature of an interaction that proceeds by way of the compound nucleus is that it is first necessary to form the compound system as an intermediate state. Furthermore, it can be shown using quantum mechanics that the probability of formation of the compound nucleus is high if there is an excited state in the nucleus  $Z^{A+1}$  in the vicinity of the energy  $E_c + B$ . When such a state exists, the probability of the formation of the compound nucleus is very large and the cross sections for whatever interactions are energetically possible are correspondingly quite high. On the other hand, if there is no excited state in  $Z^{A+1}$  near the energy  $E_c + B$ , the probability that a compound nucleus will be formed is much smaller, and so are the corresponding cross sections. The dependence of the cross sections on the energy of the incident neutron for interactions that proceed via compound-nucleus formation can therefore be quite pronounced. This type of behavior is shown schematically in Fig. 2-8. Distinct peaks in a cross section, like those shown in the figure, are called *resonances*.

The cross sections for neutron interactions that involve the compound nucleus as an intermediate state can be written as the product of two terms; namely, the cross section for the formation of the compound nucleus *times* the relative probability that this system decays in a specified way. In this connection, it will be recalled from Section 1-8 that the probability that the nucleus decays by the emission of an elastic neutron is  $\Gamma_n/\Gamma$ ; the probability that it decays by inelastic neutron emission is  $\Gamma_{n'}/\Gamma$ ; and so on. If, therefore, the cross section for the formation of a compound nucleus is denoted by  $\sigma_{CN}(E_c)$ , the cross section for compound elastic scattering is

$$\sigma_s(E_c) = \sigma_{CN}(E_c) \frac{\Gamma_n}{\Gamma}. \quad (2-63)$$

Analogous expressions hold for all the other compound nucleus processes.

The energy dependence of  $\sigma_{CN}(E_c)$  is fairly complicated in general, but near an isolated resonance at the energy  $E_1$  it can be shown to behave roughly as

$$\sigma_{CN}(E_c) = \frac{\text{constant}}{(E_c - E_1)^2 + \Gamma^2/4}. \quad (2-64)$$

In view of Eq. (2-63), the elastic scattering cross section and the cross sections for other compound-nucleus processes also follow Eq. (2-64). According to this equation,  $\sigma_{CN}(E_c)$  is peaked as shown in Fig. 2-8 in the vicinity of  $E_c = E_1$ . It is also easy to see from Eq. (2-64) that when  $E_c = E_1 \pm \Gamma/2$ ,  $\sigma_{CN}$  is equal to one-half its maximum value. Thus,  $\Gamma$  is a measure of the *width* of the resonance, and it is for this reason that  $\Gamma$  is called a "width."

**Potential scattering.** While the cross section for compound elastic scattering is only significant in the neighborhood of a resonance, *potential scattering* is a type of elastic scattering which occurs with neutrons of any energy. This mode of scattering does not involve the formation of a compound nucleus; it arises simply because of the *presence* of the nucleus. It is similar in this respect to the scattering of one billiard ball by another, which ordinarily does not occur through the formation of a compound billiard ball. Potential scattering is only a function of the forces which act upon a neutron as it moves in or near the nucleus, and since these depend upon the size and shape of the nucleus this process is sometimes called *shape elastic scattering*.

**Direct interaction.** Neutrons with comparatively high energy by reactor physics standards can also interact with nuclei by *direct interaction*. In this process the incident neutron collides directly with one of the nucleons in the nucleus. If, as a result of the collision, a proton is ejected from the nucleus and the incident neutron is retained, the process is called a *direct interaction ( $n, p$ ) reaction*. On the other hand, if the incident neutron merely knocks the struck nucleon into an excited state, emerging itself with a reduced energy, the process is called *direct-interaction inelastic scattering*. Very few neutrons in a reactor have the energy necessary to cause direct interactions, however, and this mode of interaction is of little importance in reactor theory.

## 2-7 The Total Cross Section

Having concluded with the preliminary discussion of neutron interactions, it is now possible to consider actual experimental cross-section data and their interpretation. It will be seen that these data depend on both the energy of the incident neutron and the nature of the target nucleus. It is possible, however, to classify the data into a few rather broad categories, depending upon whether the target nucleus is light ( $A \lesssim 25$ ) or magic, intermediate ( $25 \lesssim A \lesssim 150$ ), or heavy ( $A \gtrsim 150$ ). It is logical to begin by considering the total cross section, since this represents a composite of all possible interaction processes.

**Total cross section—data.** The total cross section is usually measured in transmission experiments of the type discussed in Section 2-2. In such measurements, it will be recalled, only those neutrons which pass directly through the target are detected, and any neutron that interacts in the target is removed from

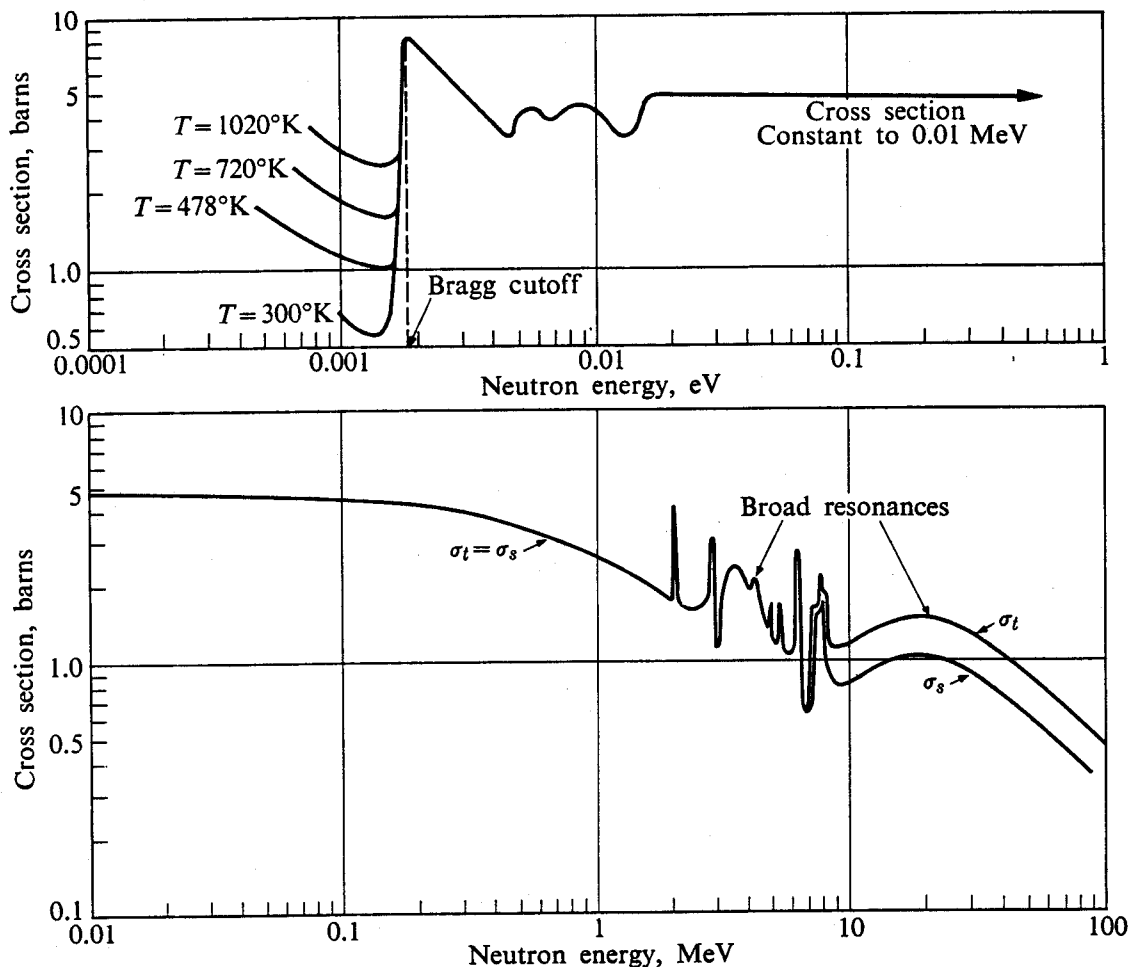


Fig. 2-9. The total and elastic scattering cross sections of  $\text{C}^{12}$ . [Based on BNL-325, Second Edition (1958).]

the beam. Because of the inherent simplicity of these experiments, more data have been accumulated on total cross sections than on any other cross section. Most of the data discussed below can be found in the report, *Neutron Cross Sections*, BNL-325, Second Edition, plus supplements to this report which are issued from time to time.

The results of these measurements can be summarized as follows:

(1) *Light and some magic nuclei.* At low energy\*  $\sigma_t$  usually behaves as

$$\sigma_t = C_1 + \frac{C_2}{\sqrt{E}}, \quad (2-65)$$

where  $C_1$  and  $C_2$  are constants. Since the neutron velocity is proportional to  $\sqrt{E}$ ,  $\sigma_t$  can also be written as

$$\sigma_t = C_1 + \frac{C'_2}{v}, \quad (2-66)$$

\* The term "low energy" in this section means energies from approximately 0.01 eV to 1.0 eV.

where  $C'_2$  is another constant. As will be shown later in this chapter, the value of  $C_1$  is determined by the elastic-scattering cross section, while the value of  $C_2$  (or  $C'_2$ ) depends upon the cross section for radiative capture or any other exothermic reaction which may be possible at these energies. The energy dependence of  $\sigma_t$  thus depends upon the relative magnitudes of the cross sections of elastic scattering and those other interactions. When the second term in the above equations predominates over the first, the cross section is said to exhibit a  $1/v$  behavior.

The total cross section of  $C^{12}$  is shown in Fig. 2-9. It will be observed that  $\sigma_t$  is approximately constant in the entire region from 0.01 eV to 0.1 MeV. Thus for this nucleus the constant  $C_2$  is much less than  $C_1$ . It will also be noted that at *very* low energy ( $E \lesssim 0.01$  eV), much lower, in fact, than the average energy of thermal agitation ( $\sim 0.025$  eV), the cross section exhibits a complicated and temperature-dependent behavior. This rapid variation in cross section is due to various crystalline effects which will be discussed in Section 2-8.

Figure 2-10 shows  $\sigma_t$  for  $B^{10}$ . It will be noted that, in contrast to the low-energy cross section of  $C^{12}$ , this nucleus shows a pronounced  $1/v$  behavior.

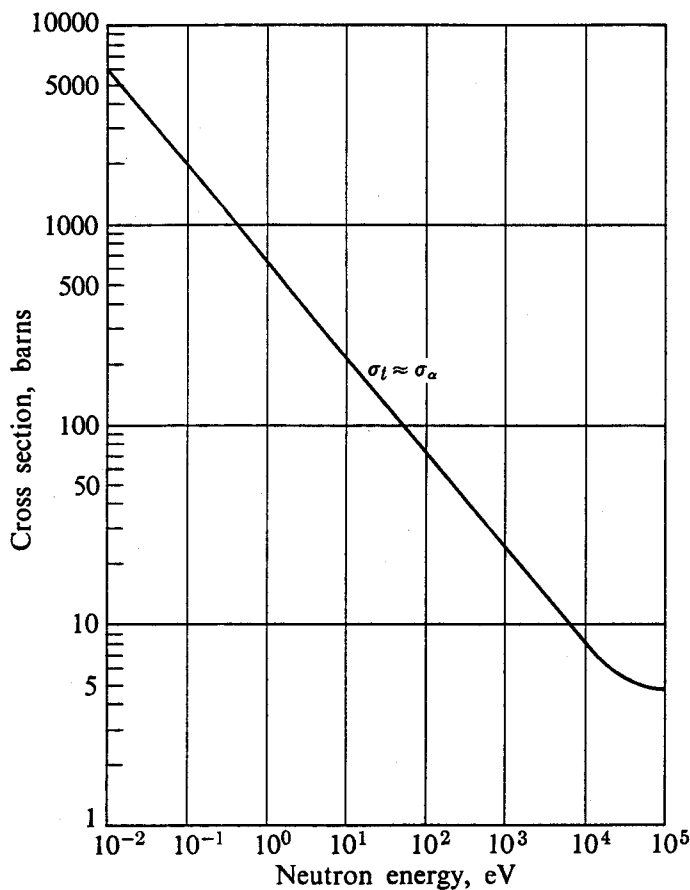


Fig. 2-10. The total cross section of  $B^{10}$  from 0.01 eV to  $10^5$  eV.  
[From BNL-325, Second Edition (1958).]

Moving now to higher energy,  $\sigma_t$  of the light nuclei eventually ceases to be either flat or  $1/v$  and a number of resonances are observed in the MeV-region. These resonances may persist up to about 6 or 8 MeV where the cross section becomes rather smooth and rolling. It should be noticed that these resonances are fairly wide. In C<sup>12</sup> (cf. Fig. 2-9), the total width of the 2-MeV resonance is 7 keV; the width of the 3.65-MeV resonance is 1.2 MeV; etc.

All light nuclei do not, of course, show the same behavior as boron or carbon; but the total cross sections of most of them are quite similar in general character,

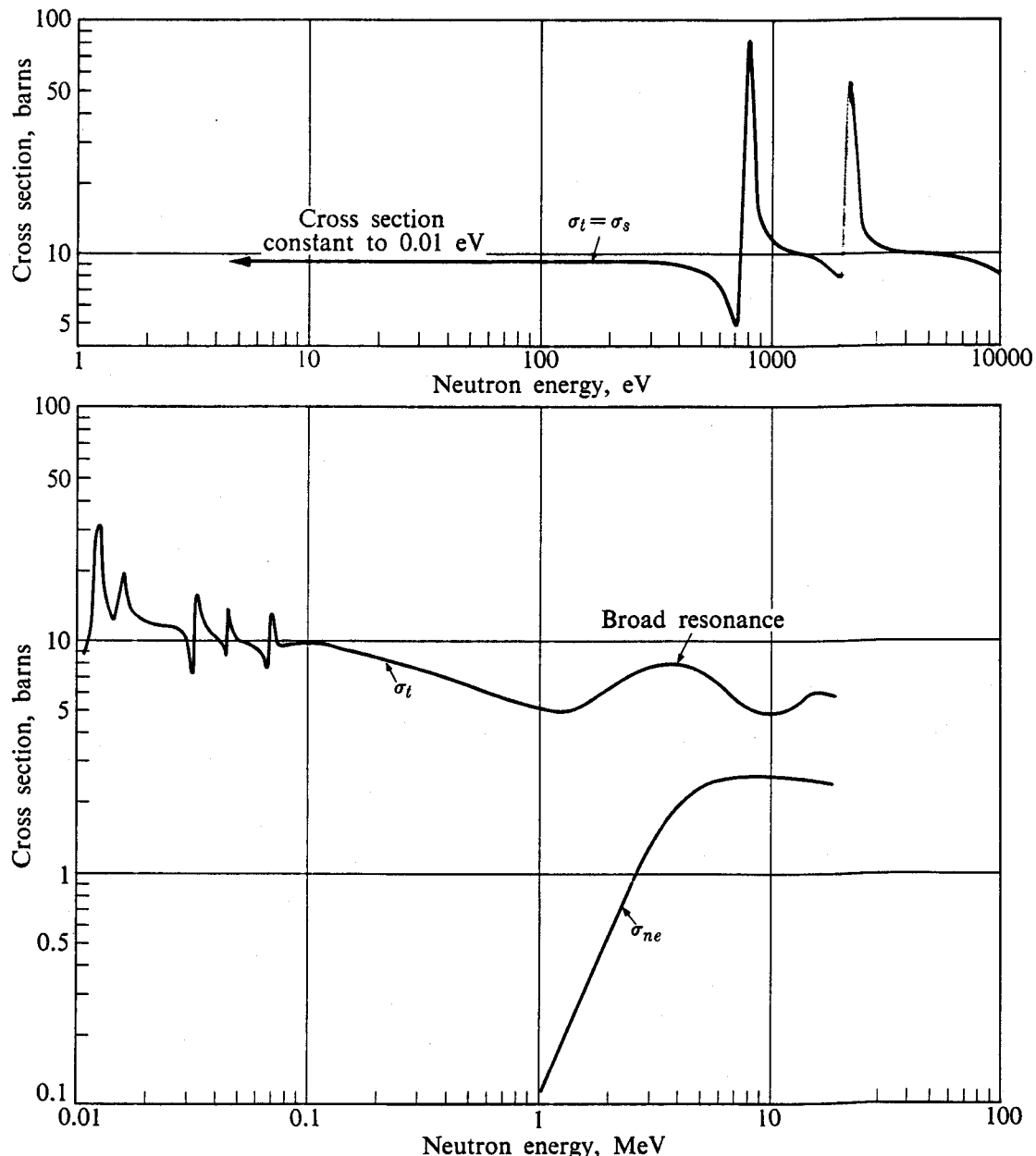


Fig. 2-11. The total and nonelastic cross sections of Bi<sup>209</sup>. [From BNL-325, Second Edition (1958).]

with the exception of the two lightest isotopes,  $H^1$  and  $H^2$ , which do not show any resonances whatever.

The above remarks concerning  $\sigma_t$  for light nuclei apply equally well to some magic nuclei. This is illustrated in Fig. 2-11 for  $Bi^{209}$ , which contains the magic number of 126 neutrons. The cross section of this nucleus strongly resembles that of a lighter nucleus such as  $C^{12}$ , and bears no resemblance to the cross sections of heavy nuclei discussed below.

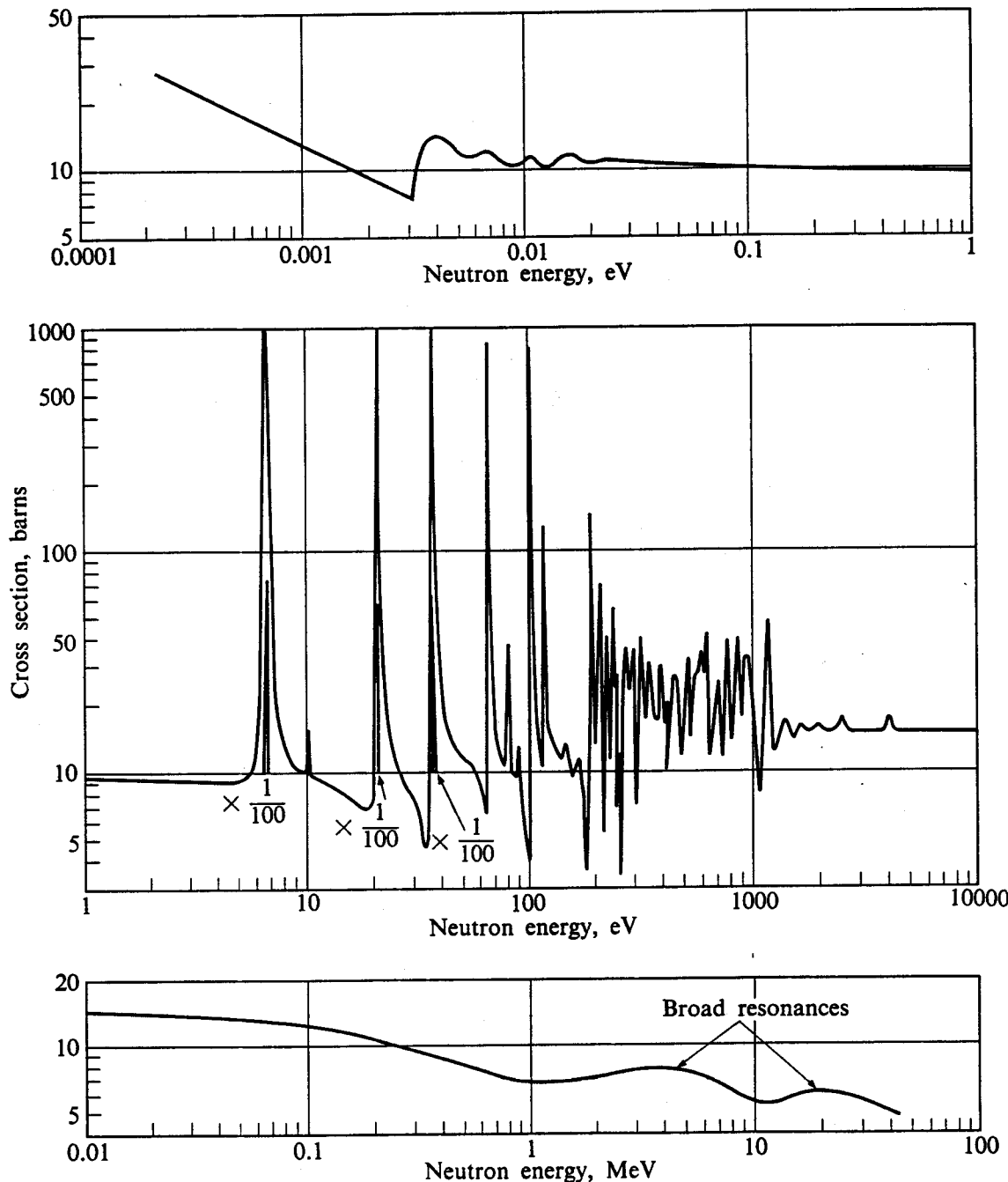


Fig. 2-12. The total cross section of  $U^{238}$ . [From BNL-325, Second Edition (1958).]

(2) *Heavy nuclei.* With heavy (but nonmagic) nuclei, such as  $U^{238}$ , whose total cross section is given in Fig. 2-12,  $\sigma_t$  again may be constant or exhibit a  $1/v$  behavior at low energy. This is followed in the electron-volt region by a spectacular series of resonances. Here, in marked contrast to the resonances in light nuclei, the resonances are very sharp, with widths usually much less than 1 eV, and the cross section rises to great heights. Moving to higher energies, at some point, usually between 3 keV and 5 keV, the resonances can no longer be resolved experimentally and  $\sigma_t$  becomes a smooth function of energy. By contrast, it will be recalled that for light nuclei, the end of the resonance region occurs at several MeV.

(3) *Intermediate nuclei.* The total cross sections of intermediate nuclei, as would be expected, are somewhat intermediate in character between those of light and heavy nuclei. Thus the total cross section may or may not be  $1/v$  at low energy, the resonance region tends to lie somewhere in the range from 100 eV to 1 keV, and the resonances are neither as narrow nor as high as in the heavy nuclei, nor as wide and short as they are in light nuclei.

**Total cross section—theory.** It is not possible to calculate from first principles, the total cross sections of nuclei in the region of the discrete resonances in the cross section. Above the resonance region, however, where the resonances overlap and the cross section is smooth,  $\sigma_t$  can be computed using a phenomenological theory known as the *optical model* of the nucleus. A detailed description of this theory is beyond the scope of this book, and only the underlying principles will be considered here.

The central feature of this model is that the nucleus is treated as a diffuse absorbing medium. Thus, a neutron which strikes the nucleus, that is, passes within range of the nuclear forces, is not immediately absorbed by the nucleus, but moves within the nuclear matter with a finite-absorption mean free path. If the neutron is, in fact, absorbed, a compound nucleus is formed which decays in the manner described in Section 2-6. There is, however, a good chance that the neutron can pass entirely through the nucleus without being absorbed. In this case the neutron merely reappears, having been elastically scattered by the potential field of the nucleus. It is in this context that this potential scattering is usually called *shape elastic scattering*.

To carry out a calculation using the optical model, the incident neutrons are represented by a plane wave, whose amplitude  $\psi$  varies with position according to the usual formula

$$\psi = \text{const } e^{ikz},$$

where the wave has been assumed to be moving in the  $z$ -direction. The constant  $k$  is called the *wave number* of the neutrons and is the reciprocal of the neutron reduced wavelength  $\lambda$  (cf. Section 1-2), that is,

$$k = \frac{1}{\lambda}. \quad (2-67)$$

It is now convenient to describe the motion of the incident neutrons in terms of a spherical coordinate system centered on the nucleus,\* as shown in Fig. 2-13. Then  $z = r \cos \vartheta$ , and  $\exp(ikz) = \exp(ikr \cos \vartheta)$ . It is possible to show that this function can be expanded in the series

$$e^{ikr \cos \vartheta} = \sum_{l=0}^{\infty} (2l+1) i^l f_l(r) P_l(\cos \vartheta), \quad (2-68)$$

where the functions  $f_l(r)$  are related to Bessel functions, although their precise definition is not important in the present discussion, and  $P_l(\cos \vartheta)$  are the familiar Legendre polynomials. According to Eq. (2-68), a plane wave of neutrons can be viewed as a superposition of an infinite number of *partial waves*, each characterized by the functions  $f_l(r)$  and  $P_l(\cos \vartheta)$ . The importance of this *partial-wave expansion* will be clear in a moment.

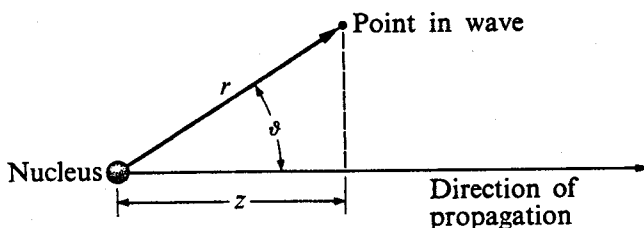


Fig. 2-13. Coordinates of a plane wave.

It is also convenient to divide the incident wave into *cylindrical zones* of radii  $\lambda$ ,  $2\lambda$ ,  $3\lambda$ , etc., as indicated in Fig. 2-14. The virtue of this construction lies in the fact that it can be shown that the neutrons in the  $l$ th partial wave in the above expansion are almost always to be found in the zone bounded by radii  $l\lambda$  and  $(l+1)\lambda$ . For example, the neutrons in the partial wave having  $l = 0$ , which are called *s-wave* neutrons,† are almost always found in the first zone of radius  $\lambda$ ; the  $l = 1$  neutrons, which are also called *p-wave* neutrons, lie in the next zone; and so on.

If the reduced wavelength  $\lambda$  of the incident neutrons is *larger* than the nuclear radius  $R$ , it will be evident that only the *s-wave* neutrons can interact with the nucleus. If, however,  $\lambda \approx R$ , both *s-* and *p-wave* neutrons can interact. In general, all partial waves in the incident beam up to those having  $l = R/\lambda = kR$  can interact with the nucleus. Since  $\lambda \sim 1/\sqrt{E}$  [cf. Eq. (1-2)],  $k \sim \sqrt{E}$ , and it follows

\* More precisely, the zero of the coordinate system should be taken at the center of mass of the neutron and nucleus.

† This notation is borrowed from optical spectroscopy. The correspondence between  $l$  and the wave notation is as follows:

$l$	0	1	2	3	4	etc.
Wave	<i>s</i>	<i>p</i>	<i>d</i>	<i>f</i>	<i>g</i>	etc.

that the number of partial waves which can interact with the nucleus increases with the energy of the incident neutrons.

One of the most important virtues of the optical model is that it accounts for the existence of *giant* or *broad resonances* in the total cross section. These resonances were not mentioned earlier because they are not so easy to recognize in the cross-section data as compound nucleus resonances, owing to the fact that their widths are so very large. Several broad resonances are indicated in Figs. 2-9, 2-11, and 2-12, where it will be observed that the resonances are several MeV wide. Such resonances are found in all nuclei at both high and low energy, though they are most easily distinguished at high energy, where the compound-nucleus resonances overlap and the total cross section is a smooth function of energy.

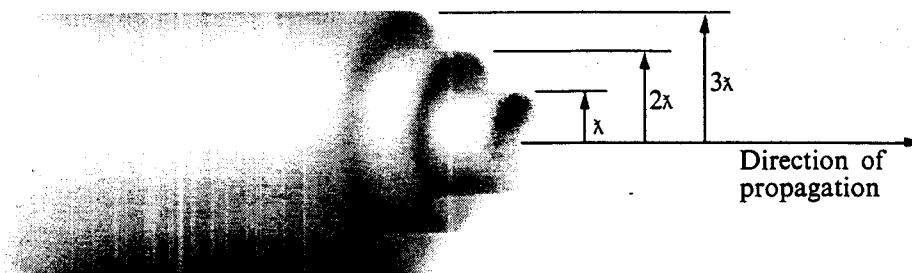
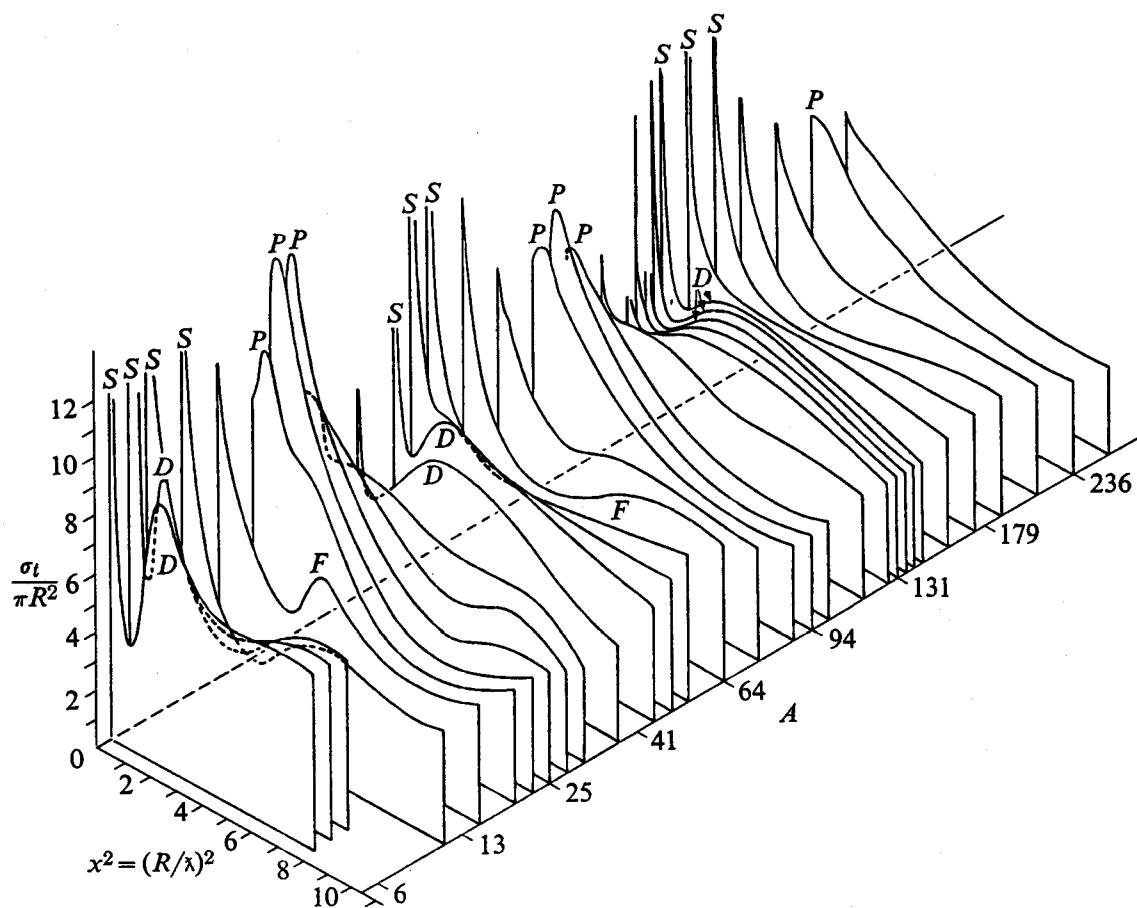


Fig. 2-14. Partial wave zones of a plane wave.

The broad resonances are explained with the optical model in the following way. It will be recalled that according to this theory the incident neutrons move freely within the nucleus, which is treated as a diffuse absorbing medium. It can be shown, however, that at various neutron energies, certain partial waves "fit better" within the nuclear volume than at other energies. When this is the case, the amplitude of a particular partial wave in the nucleus is greatly increased, with the result that the scattering of neutrons in this partial wave is enhanced, and the total cross section is therefore somewhat larger. This phenomenon has many counterparts in other branches of physics. Thus it resembles the resonances observed in the forced vibration of a string, the scattering of sound by a hollow pipe, etc. In view of this explanation, it is possible to identify the particular partial wave that gives rise to each broad resonance. For instance, the general rise of the cross section from about 2 to 4 MeV, in  $C^{12}$  (cf. Fig. 2-9) is due to  $l = 2$  neutrons and is therefore called a *d*-wave resonance, while the resonance at about 20 MeV is due to  $l = 3$  neutrons and is an *f*-wave resonance.

The optical model can be used to compute the total cross section with good accuracy, at least at energies where this cross section is reasonably smooth. These calculations are quite complicated, however, and they are usually performed with an electronic computer. The results of a number of calculations are shown in Fig. 2-15 where the total cross section is plotted as a function of both  $A$  and  $E$  (note that the parameter  $x^2$  is proportional to  $E$ ). It will be observed that  $\sigma_t$



**Fig. 2-15.** Optical model calculations of the total cross section as a function of energy and mass number. (After H. Feshbach in *Nuclear Spectroscopy*, Part B, F. Ajzenberg-Selove, Ed., New York: Academic Press, 1960.)

changes rather smoothly from nucleus to nucleus. This fact can be used to estimate the value of an unknown cross section by interpolating between known values for nearby nuclei. In the region of the narrower compound-nucleus resonances, the optical model is also useful in obtaining the average behavior of the total cross section, which is often adequate for many types of reactor calculations. Predictions of other cross sections, in particular the cross section for the formation of the compound nucleus, can also be made using the optical model. This will be discussed later in the chapter.

## 2-8 Elastic Scattering

Elastic scattering is one of the more difficult neutron interactions to measure and the most complicated to analyze theoretically. Yet it is one of the most important nuclear processes which occur in reactors. With elastic scattering, it is necessary to consider the differential elastic cross section, which describes the angular distribution of the scattered neutrons, as well as the total elastic cross section.

**Elastic scattering—data.** Because of experimental difficulties, the elastic scattering cross section is not usually measured directly; it is obtained by subtracting the cross sections for all other processes from the total cross section. Of course, at those energies where nonelastic processes do not occur, the total and elastic cross sections are identical.

The data on elastic scattering can be summarized as follows:

(1) *Light and some magic nuclei.* With these nuclei,  $\sigma_s$  is constant from low energy up to about the MeV region, where a number of fairly wide ( $\Gamma \approx \text{keV}$ ) scattering resonances are observed. Above the resonance region,  $\sigma_s$  becomes smooth and rolling, and broad resonances in  $\sigma_s$  are found at the same energies as for  $\sigma_t$ . The elastic cross section of  $C^{12}$  is shown in Fig. 2-9. The behavior of the cross section at very low energy will be explained later in this section.

(2) *Heavy nuclei.* Here,  $\sigma_s$  is again constant at low energy, although the data in this region are frequently rather inaccurate. In the resonance region,  $\sigma_s$  varies rapidly with energy in the vicinity of each resonance, while in between resonances,  $\sigma_s$  is constant. (The exact variation of  $\sigma_s$  with energy at a resonance will be discussed below.) At energies above this region,  $\sigma_s$  becomes smooth and rolling.

(3) *Intermediate nuclei.* The elastic cross sections of these nuclei, as expected, exhibit a behavior intermediate between those of the light and heavy nuclei.

**Elastic scattering—theory.** It is possible to write a general theory of elastic scattering in the resonance region in terms of phenomenological parameters such as the nuclear radius, neutron widths, etc., but unfortunately, the resulting expressions for the elastic cross section are so complicated they have little practical application in reactor calculations.

At low energy, however, where only *s*-wave scattering can occur ( $kR \ll 1$ ), and provided the resonances in the cross section are well separated, these formulas simplify considerably. Under these conditions near a resonance at the center-of-mass energy  $E_1$ , it can be shown that  $\sigma_s$  is given by

$$\sigma_s(E_c) = \frac{\pi\lambda_1^2 g \Gamma_n^2}{(E_c - E_1)^2 + \Gamma^2/4} + \frac{4\pi\lambda_1 g R(E_c - E_1)\Gamma_n}{(E_c - E_1)^2 + \Gamma^2/4} + 4\pi R^2. \quad (2-69)$$

In this equation,  $E_c$  is the total kinetic energy of the incident neutron and the target nucleus with respect to the center-of-mass system. In view of Eq. (2-38), if the nucleus is at rest in the laboratory,  $E_c$  is essentially equal to the laboratory energy of the neutron except for the very lightest nuclei. Also in Eq. (2-69),  $\lambda$  is the reduced wavelength of a particle of reduced mass  $\mu$  and energy  $E_1$ , that is,  $\lambda_1 = \hbar/\sqrt{2\mu E_1}$ ,  $\Gamma$  and  $\Gamma_n$  are the total and neutron widths, respectively,  $R$  is the nuclear radius, and  $g$  is a statistical factor which is given by the formula

$$g = \begin{cases} 1, & I = 0, \\ \frac{1}{2} \left( \frac{2J+1}{2I+1} \right), & I \neq 0, \end{cases} \quad (2-70)$$

where  $I$  is the spin of the target nucleus, and  $J$  is the spin of the compound nucleus. Equation (2-69) is known as the *Breit-Wigner one-level formula for s-wave resonance scattering*. Tables of  $E_1$ ,  $\Gamma$ , and  $\Gamma_n$  are given in BNL-325 for a large number of resonances. It should be noted, however, that these tables present these data in the laboratory system.\*

By defining the quantities

$$\sigma_1 = \frac{4\pi\lambda_1^2 g\Gamma_n}{\Gamma} \quad (2-71)$$

and

$$x = \frac{2}{\Gamma} (E_c - E_1), \quad (2-72)$$

Eq. (2-69) can be written in the more convenient form

$$\sigma_s(x) = \frac{\sigma_1\Gamma_n}{\Gamma} \frac{1}{1+x^2} + \frac{2\sigma_1 R}{\lambda_1} \frac{x}{1+x^2} + 4\pi R^2. \quad (2-73)$$

It will be recalled from Section 2-6 that elastic scattering can occur by way of two interaction mechanisms, namely, potential scattering and compound elastic scattering. This can also be seen from Eqs. (2-69) or (2-73). Thus the first term in these equations represents the compound-elastic scattering, while the last term is the potential scattering. The middle term is somewhat more complicated, and arises as the result of the interference between the neutron waves emitted in compound-elastic scattering and potential scattering. When  $E_c < E_1$ , this term is negative, whereas it is positive when  $E_c > E_1$ . As a consequence,  $\sigma_s$  exhibits a pronounced asymmetry in the neighborhood of the resonance, as illustrated in Fig. 2-16. As indicated in the figure,  $\sigma_s$  approaches the constant value  $4\pi R^2$  at energies far from the resonance. It is for this reason that the usual practice is to assume that  $\sigma_s$  is a constant at low energy even when the cross sections for competing reactions, such as radiative capture or fission, are so large that direct measurements of  $\sigma_s$  are impossible. At energies above the resonance,  $\sigma_s$  takes on the value  $4\pi R^2$  up to the point where another resonance appears, provided  $kR$  remains much less than unity.

The asymmetric behavior of  $\sigma_s$  at a resonance is ordinarily found only in *s*-wave resonance scattering, and this fact can be used to identify this type of scattering. Thus, minima will be found in the total cross section just below a resonance if the principal contribution to  $\sigma_t$  is scattering, and the scattering is *s*-wave. Examples

---

\* Equation (2-69) is also valid if all energies are given in the laboratory system (as they are in BNL-325), and  $\mu$  is interpreted as the mass of the neutron. In this connection, it must be noted that level widths transform as kinetic energy between center-of-mass and laboratory coordinates. Except for the lightest nuclei, of course, the distinction between the two systems need not be made.

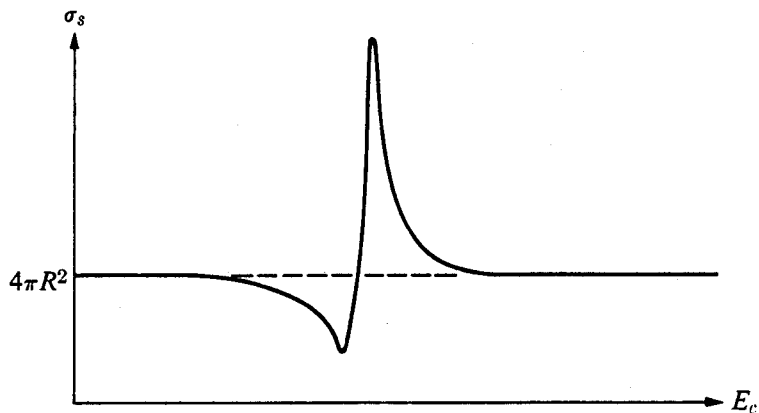


**Fig. 2-16.** The elastic scattering cross section for  $l = 0$  neutrons in the vicinity of a resonance. The energy is the total kinetic energy of neutron and nucleus in the center-of-mass system.

of this phenomenon may be seen in Fig. 2-11 for  $\text{Bi}^{209}$  and Fig. 2-12 for  $\text{U}^{238}$ . It is interesting to note that in the case of  $\text{U}^{238}$ , minima are found before all of the prominent resonances except the one at 6.67 eV. Since  $kR \ll 1$  at this energy, only  $s$ -wave scattering is possible, and it must be concluded that elastic scattering is not the principal mode of interaction at this resonance—a conclusion which is verified by the fact that  $\Gamma_n$  is only 1.5 mV for this resonance whereas  $\Gamma_\gamma$  is about 26 mV.

The difference between the actual scattering in the neighborhood of a resonance and the (constant) potential scattering is known as *anomalous scattering*. The cross section for this anomalous scattering is given by the first two terms of Eqs. (2-69) or (2-73), and the sum of these terms is called the *anomalous scattering cross section*.

At energies where the resonances are closely spaced, the formulas for elastic scattering are too complicated to be useful in ordinary applications. It should be particularly noted that due to interference effects from the scattering of neutrons from different resonances, the cross section in this case is *not* equal to the sum of the cross sections for each resonance computed from the one-level formula. Above the resonance region where the cross section becomes smooth,  $\sigma_s$  can be estimated theoretically from optical model calculations discussed in the preceding section. It will be recalled that with this model it is possible to calculate the total cross section and the cross section for the formation of the compound nucleus. The difference between these two cross sections is equal to the potential, or shape-elastic, scattering cross section. However, the shape-elastic cross section is not the entire elastic cross section, since the compound nucleus formed by the absorption of the incident neutron can also decay by the emission of an elastic neutron. Fortunately, at high energy it can be shown that compound elastic scattering is much less probable than shape elastic scattering, and the computed shape-elastic cross section can therefore be used as a good estimate of the elastic cross section.

**Low-energy scattering by molecules and solids.** If the energy,  $E$ , of an incident neutron is large compared with the chemical binding energy,  $B_m$ , of the atoms in a molecule, the molecule is generally disrupted when the neutron is scattered by one of the atoms. In this case, the fact that the atoms (nuclei) are bound together in the form of a molecule can be ignored. The scattering cross section for the molecule is then the sum of the cross sections of its constituent nuclei, weighted by the numbers of each atomic species in the molecule, as given by Eq. (2-16). On the other hand, when  $E$  is of the order of or less than  $B_m$ , the nuclei cannot be considered to be free, and there is no simple prescription for computing the cross section of the molecule in terms of the free cross section of its individual nuclei. The same is true for the scattering of low energy neutrons by solids. At energies comparable to or less than the binding energy of an atom to a solid, the macroscopic scattering cross section of the solid is not equal to the sum of the cross sections of the free nuclei.

In the scattering of neutrons by molecules, there are several factors which may contribute to the failure of Eq. (2-16). One of the most important of these is that the scattering of slow neutrons by nuclei is *greater* when the nuclei are bound in molecules than when they are free. Suppose for the moment that the atoms in the molecule are at rest in the laboratory system; this is the case if the target material is at a temperature of absolute zero. It can then be shown using elementary quantum mechanics that the cross section for the scattering of a neutron by a single nucleus is proportional to the square of the reduced mass of the two particles. At neutron energies above  $B_m$ , where the nucleus can be considered to be free, the cross section can thus be written as

$$\sigma_{\text{free}} \sim \mu^2 = \left( \frac{mM}{m+M} \right)^2 \approx \left( \frac{A}{A+1} \right)^2.$$

On the other hand, at energies comparable to or less than  $B_m$ , the nucleus is no longer free, and as a result its mass effectively increases. As the ratio  $E/B_m$  decreases, this effective nuclear mass increases; and in the limit as  $E/B_m \rightarrow 0$ , it becomes equal to the mass of the entire molecule. Except for light molecules, therefore, the reduced mass of neutron and nucleus approaches the mass of the neutron alone. Thus at a temperature of 0°K, the cross section of the completely bound nucleus,  $\sigma_{\text{bound}}$ , is

$$\sigma_{\text{bound}} \sim \mu^2 = (1)^2.$$

It follows that in the limit as  $E/B_m \rightarrow 0$ , the bound and free cross sections are related by

$$\sigma_{\text{bound}} = \left( \frac{A+1}{A} \right)^2 \sigma_{\text{free}}. \quad (2-74)$$

This phenomenon is illustrated schematically in Fig. 2-17, where the cross section of a nucleus in a molecule is shown as a function of  $E/B_m$ . It will be observed that for  $E/B_m \gg 1$ , this cross section is approximately equal to  $\sigma_{\text{free}}$ .

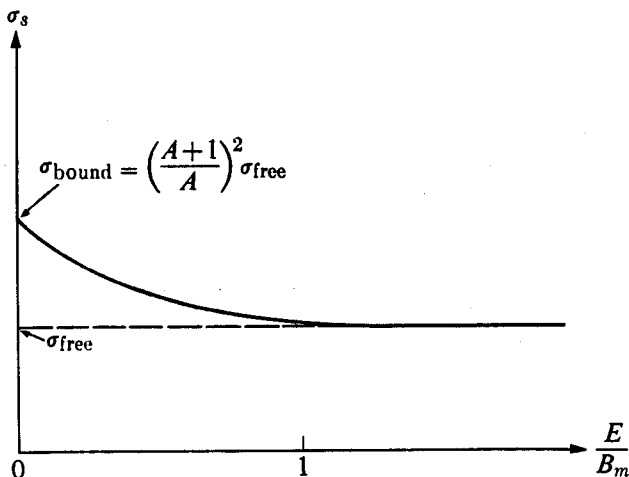


Fig. 2-17. The low energy scattering cross section at 0°K of an atom (nucleus) bound in a molecule as a function of  $E/B_m$ , where  $E$  is the incident neutron energy and  $B_m$  is the binding energy of the atom to the molecule.

However, for  $E/B_m \lesssim 1$ , it is larger than  $\sigma_{\text{free}}$  and approaches  $\sigma_{\text{bound}}$  as  $E/B_m \rightarrow 0$ . Since the factor  $[(A + 1)/A]^2$  in Eq. (2-74) increases with decreasing  $A$ , this bound-nucleus effect is evidently of greatest importance for the light nuclei. In particular, in the limit as the neutron energy approaches zero, the cross section of bound hydrogen at absolute zero is four times its free cross section.

For temperatures above absolute zero there is another effect on low-energy scattering which arises from the thermal motion of the atoms. To understand this effect consider the rate at which scattering collisions occur in a target as observed in the center-of-mass system. By analogy with Eq. (2-1), the interaction rate can be written as the product of a scattering cross section and a beam intensity, both measured in the center-of-mass system. In this case, the beam intensity is proportional to the relative speed of the neutrons and nuclei. At sufficiently low neutron energy, however, the neutron speed is small compared to the speed of the nuclei, and, as a result, the beam intensity observed in the center-of-mass system is relatively independent of the neutron speed. Furthermore, the scattering cross section in the center-of-mass system can be shown to be a constant at low energy. It follows that the interaction rate is independent of the neutron energy, although it is a function of the temperature of the medium. With respect to the laboratory system this constant interaction rate is written as the product of the scattering cross section and the beam intensity, both measured in this system. However, the beam intensity is now proportional to the *laboratory* speed,  $v$ , of the neutrons, and as a consequence

$$\sigma_s v = \text{constant},$$

where  $\sigma_s$  is the cross section as observed in the laboratory. Hence at sufficiently low energy,  $\sigma_s$  varies as  $1/v$ , and increases without limit as  $E \rightarrow 0$ . Only at  $T = 0^\circ\text{K}$  does  $\sigma_s$  approach the constant value given in Eq. (2-74). These conclusions

hold for solids as well as molecules. An example of this temperature-dependent,  $1/v$  scattering can be seen in Fig. 2-9 for graphite (note the portion of the figure below 0.002 eV) and in Fig. 2-12 for metallic  $U^{238}$  ( $E < 0.003$  eV).

The low-energy scattering cross section of a molecule may also be complicated by the occurrence of *coherent scattering*. This effect arises as the result of the interference of neutron waves scattered from different nuclei in the molecule, and it can lead to anomalous values of the cross section. Fortunately, in the important case of molecules containing hydrogen, it can be shown that the coherent scattering from different hydrogen nuclei (protons) can be ignored, and these atoms can be treated independently. This considerably simplifies calculations of scattering from such molecules.

A molecule, of course, is a complex dynamical system, which, to a good approximation, can be pictured as a group of atoms held together as if by springs. A neutron that collides with such a system may excite one or more of its vibrational modes, it may cause the molecule to rotate or twist, or it may set the molecule into translational motion. All of these factors must be taken into account in a detailed calculation of the low-energy cross section, and they contribute in one way or another to the observed cross section. To complicate matters further, the molecule may not be able to vibrate, rotate, or translate freely due to various intermolecular forces acting between the molecules in the medium. That is, the normal reaction of the molecule to the interaction with a neutron may be impeded by the presence of other molecules. The scattering cross section thus depends upon the coupling of the molecule to the surrounding medium as well as upon the structure of the molecule itself.

The above considerations are particularly important in nuclear engineering in connection with the scattering of neutrons by  $H_2O$  or  $D_2O$ . Figure 2-18 shows the total cross section (which is essentially all scattering) of water, along with the quantity  $2\sigma_t(H) + \sigma_t(O)$  where  $\sigma_t(H)$  and  $\sigma_t(O)$  are the free cross sections of

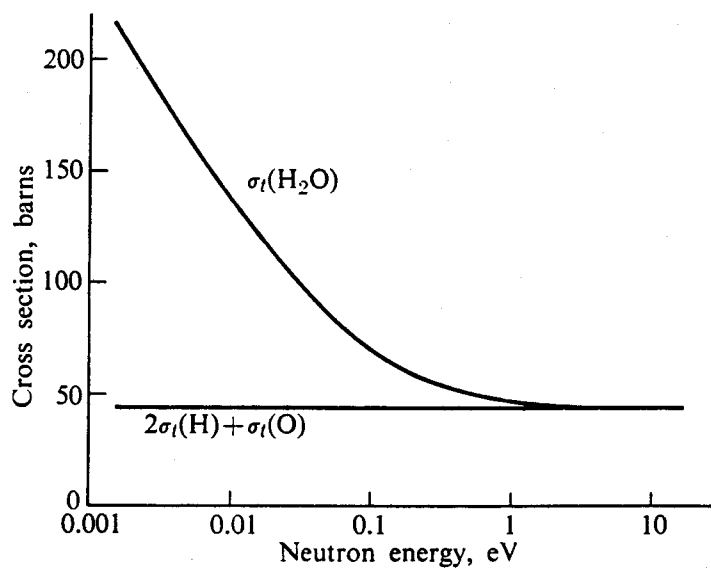


Fig. 2-18. Measured total cross section of  $H_2O$  and the quantity  $2\sigma_t(H) + \sigma_t(O)$ .

hydrogen and oxygen, respectively. As indicated in the figure, the water cross section rises to large values at low energies while the free cross sections remain constant. It is of interest to mention that in recent years it has been possible to derive the observed cross section from reasonable assumptions regarding the vibrational frequencies of the molecule and by assuming that the molecule undergoes impeded rotation and translation. These calculations are very complicated, however, and are well beyond the scope of this book.

With regard to the scattering of neutrons by solids,\* it has already been mentioned that for incident neutron energies comparable to or less than the chemical binding energy of atoms in a solid, the individual atoms cannot be treated as if they were free, and the observed cross section reflects the fact that the neutron has interacted with a complex dynamical system. Indeed, for this reason, it is not logical to describe the observed interaction rate in terms of a microscopic cross section. Only the macroscopic cross section has a precise meaning. While it is always possible to write the macroscopic cross section as  $\Sigma_s = N\sigma_s$ , the microscopic cross section so-defined is only an *effective* one-nucleus cross section and must not be construed to mean that the nuclei scatter independently.

One of the principal effects which is responsible for the observed scattering cross section of solids at low energy is *Bragg scattering*, which may be familiar to the reader in connection with the scattering of x-rays. Suppose that a beam of mono-energetic neutrons is incident upon a crystal at the angle  $\vartheta$  with respect to one of the planes of the crystal lattice (these planes are called *Bragg planes*) as shown in Fig. 2-19. It is not difficult to show that neutrons will be reflected from these

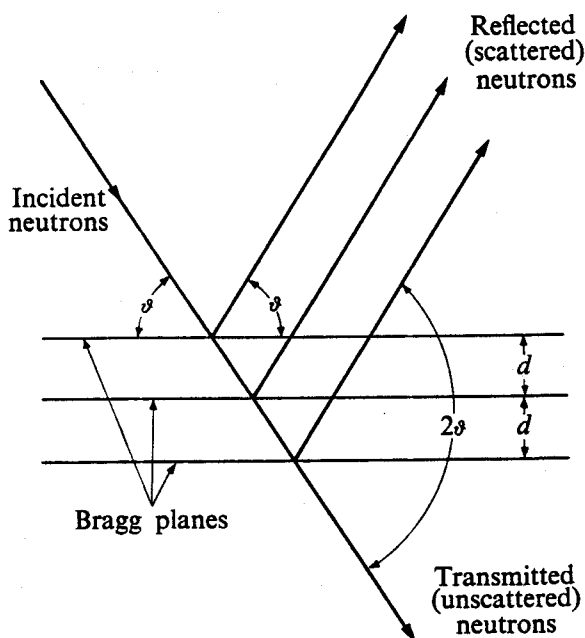


Fig. 2-19. Diagram showing Bragg reflection from three Bragg planes.

\* The solids of interest in reactor analysis, i.e., graphite, beryllium, beryllium oxide, various metals, and so on, are polycrystalline in nature. That is, they are composed of large numbers of tiny microcrystals, each of which consists of an ordered array of atoms.

planes, i.e., scattered through the angle  $2\vartheta$ , provided the neutron wavelength  $\lambda$  satisfies the relation

$$n\lambda = 2d \sin \vartheta, \quad (2-75)$$

where  $n = 1, 2, 3, \dots$  and  $d$  is the distance between adjacent Bragg planes. At neutron energies corresponding to the wavelengths satisfying Eq. (2-75), the scattering cross section is much enhanced. Also, according to Eq. (2-75) there is a maximum wavelength above which Bragg scattering cannot occur. By placing  $\vartheta = \pi/2$  and  $n = 1$ , this wavelength,  $\lambda_{\max}$ , is found to be

$$\lambda_{\max} = 2d. \quad (2-76)$$

Since  $\lambda$  increases with decreasing neutron energy, it follows that there is a minimum energy, called the *Bragg cutoff*, below which Bragg scattering cannot occur. This cutoff and several Bragg peaks are evident at low energy in the cross section of carbon shown in Fig. 2-9 (in this figure the target is graphite).

At energies, both above and below the Bragg cutoff but still below the binding energy of the atoms in the crystal, it is possible for neutrons to excite vibrational modes of the crystal. Such vibrational modes are known as *phonons*. This type of interaction is actually a form of inelastic scattering, since the internal energy of the crystal is increased at the expense of the energy of the incident neutron. By contrast, neutrons do not lose energy in Bragg scattering, that is, Bragg scattering is an entirely elastic process. In view of the nature of phonon excitation and Bragg scattering, it will be evident that low-energy scattering of neutrons by a solid depends in detail upon its crystalline structure and upon the forces which act between the atoms in the crystal. It should also be pointed out that this scattering is a function of the size of the microcrystals in the solid. The cross sections of different samples of the same material may be somewhat different if the samples have different microcrystalline structure.

It must be emphasized that the above discussion pertains only to *scattering*. With other interactions, such as radiative capture or fission, the individual atoms in a molecule or solid interact independently with the incident neutrons at all energies. The molecular cross section is then given by Eq. (2-16) and the macroscopic cross section for a solid is simply the sum of the contributions from all nuclei per cubic centimeter.

**Elastic angular distributions.** It has been found experimentally and it can also be shown theoretically that the scattering of *s*-wave neutrons is always *isotropic in the center-of-mass system*. It will be recalled that *s*-wave scattering is the only mode of potential scattering possible when  $kR \ll 1$ . Since  $k \sim \sqrt{E}$ , this condition is always satisfied if the energy of the incident neutron is sufficiently low. Also, in view of the fact that  $R$  increases with  $A$ , it follows that isotropic *s*-wave scattering is observed in light nuclei up to a much higher energy than in heavy nuclei. When, however, either the neutron energy or the nuclear radius become

sufficiently large so that  $kR \approx 1$ , the  $p$ -waves begin to interact with the nucleus, and the scattering ceases to be isotropic in the center-of-mass system. The angular distribution in this case tends to become forward peaked; that is, the neutrons are most frequently scattered through small angle. As the value of  $kR$  is increased still further, more partial waves interact and the scattering becomes increasingly forward peaked.

As an illustration of this situation the differential cross section in the center-of-mass system is shown in Fig. 2-20 for  $C^{12}$  for 0.5 MeV and 14 MeV neutrons. In the first case  $kR = 0.4$ , and it will be observed that the angular distribution is indeed isotropic. At the higher energy, however, where  $kR \approx 3$ ,  $\sigma_s(\theta)$  is forward peaked. By way of contrast,  $\sigma_s(\theta)$  is shown in Fig. 2-21 for  $U^{238}$ , again at 0.5 MeV and 14 MeV. It will be noted that now even at 0.5 MeV where  $kR = 1.3$ , the

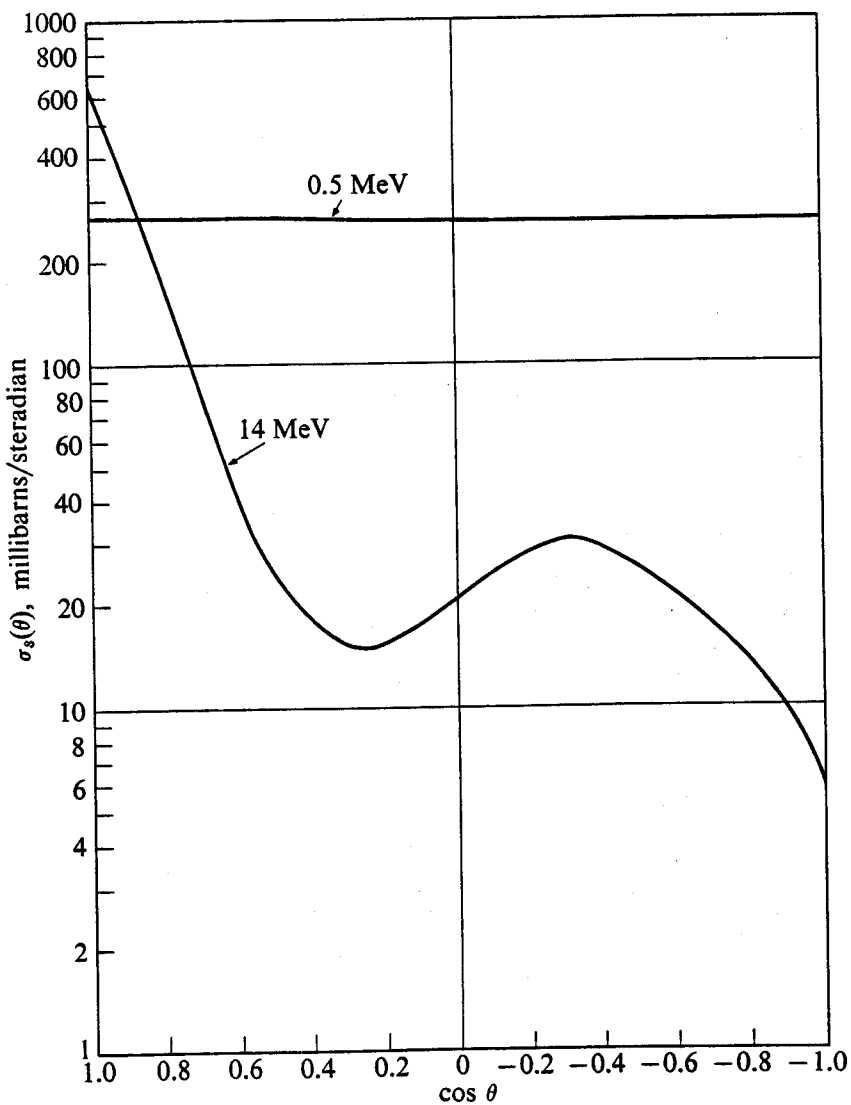


Fig. 2-20. Differential elastic scattering cross sections of  $C^{12}$  at 0.5 MeV and 14 MeV as a function of the cosine of the scattering angle in the center-of-mass system. [From BNL-400, Second Edition (1962).]

angular distribution is markedly forward peaked, and at 14 MeV with  $kR = 7.4$ , it is very peaked in the forward direction. Incidentally, the series of maxima and minima shown in Fig. 2-21 are due to the interference between the scattered waves, a phenomenon similar to the diffraction of light by a small obstacle.

In the region of scattering resonances, for example, at about 6 MeV in  $C^{12}$ , the situation is more complicated, and it is difficult to make general statements regarding  $\sigma_s(\theta)$ . If, however, a scattering resonance is reasonably isolated,  $\sigma_s(\theta)$  is usually forward peaked at energies above the resonance; backward peaked below the resonance; and near the center of the resonance,  $\sigma_s(\theta)$  is fairly symmetric about  $90^\circ$ ; all, of course, in the center-of-mass system.

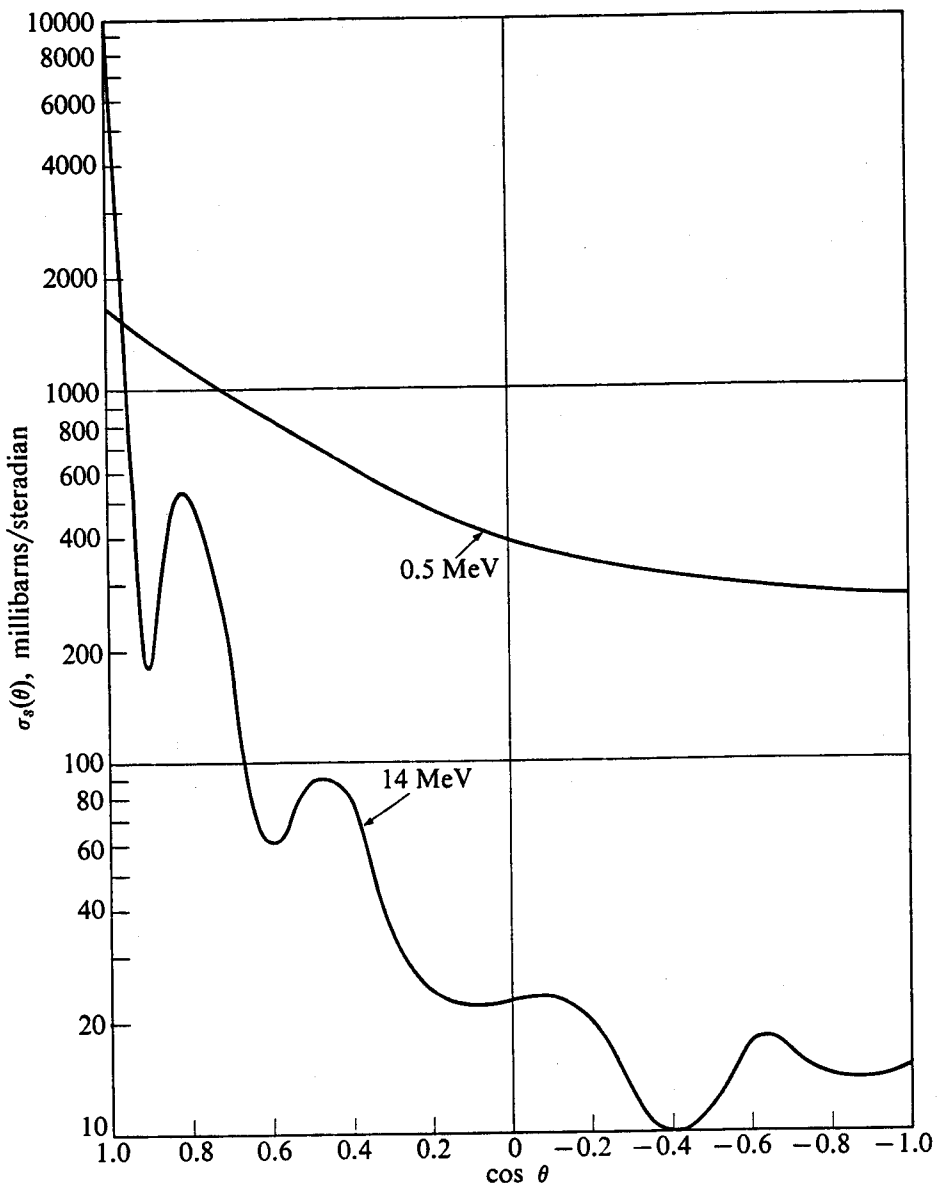


Fig. 2-21. Differential elastic scattering cross sections of  $U^{238}$  at 0.5 MeV and 14 MeV as a function of the cosine of the scattering angle in the center-of-mass system. [From BNL-400, Second Edition (1962).]

It is possible to derive formulas for the differential cross section in the resonance region, but they are quite lengthy and will not be reproduced here. Above the resonance region,  $\sigma_s(\theta)$  can be computed using the optical model. However, this model gives only the angular distribution of the shape-elastic (i.e. potential) scattering; it does not include compound elastic scattering. Fortunately, at energies where the model is most useful, that is, beyond the resonance region, compound elastic scattering is not usually an important process and it can often be ignored. A more accurate procedure is to add a constant to computed values of the shape-elastic differential cross section, since compound elastic scattering at these energies is isotropic. This constant can then be adjusted so that the integrated cross section is equal to the correct value of the total elastic cross section  $\sigma_s$ .

The above discussion refers entirely to scattering in the center-of-mass system, and, using Eq. (2-61), it is a simple matter to transform the differential cross section to the laboratory system. Since the two systems tend to become identical with increasing mass of the target nucleus, it is not usually necessary to make a distinction between the two systems for nuclei heavier than nitrogen or oxygen, and the difference is often ignored even for carbon. (For one thing, the present experimental data on  $\sigma_s(\theta)$  are generally too inaccurate to warrant making the transformation.) With the very light nuclei, however, the transformation must always be made.

In this connection, the scattering of neutrons by hydrogen is particularly interesting. At all energies of importance in reactor theory *the scattering of neutrons by hydrogen ( $H^1$ ) is isotropic in the center-of-mass system*. The angular distribution is quite different when viewed in the laboratory. In this case, since  $A = 1$ , Eq. (2-50) gives

$$\tan \vartheta = \frac{\sin \theta}{1 + \cos \theta}.$$

Using the identities

$$\sin \theta = 2 \sin \frac{\theta}{2} \cos \frac{\theta}{2}$$

and

$$1 + \cos \theta = 2 \cos^2 \frac{\theta}{2},$$

this reduces to

$$\tan \vartheta = \tan \frac{\theta}{2},$$

and therefore

$$\vartheta = \frac{\theta}{2}.$$

Thus, as  $\theta$  varies from 0 to  $\pi$ ,  $\vartheta$  ranges only from 0 to  $\pi/2$ . In other words, as viewed in the laboratory, *there is no back scattering (i.e.,  $\vartheta > \pi/2$ ) of neutrons from hydrogen.*

The differential cross section of hydrogen in the laboratory system can be found from either Eq. (2-59) or Eq. (2-61). Using the former, and writing  $\sigma_s(\theta) = \sigma_s/4\pi$  since the scattering is isotropic in the center-of-mass system, gives

$$\sigma_s(\vartheta) = \frac{\sigma_s}{4\pi} \frac{\sin \theta d\theta}{\sin \vartheta d\vartheta}.$$

Since  $\theta = 2\vartheta$ , this becomes

$$\begin{aligned}\sigma_s(\vartheta) &= \frac{\sigma_s}{4\pi} \frac{2 \sin \vartheta \cos \vartheta 2d\vartheta}{\sin \vartheta d\vartheta} \\ &= \frac{\sigma_s}{\pi} \cos \vartheta.\end{aligned}$$

It may be noted that this is the equation of a sphere tangent to the plane  $\vartheta = \pi/2$ , perpendicular to the direction of incidence.

## 2-9 Transport Cross Section

The effect of the scattering angular distribution on the motion of a neutron in a scattering medium may be taken into account very roughly by the use of the *transport cross section*. To define this new cross section, consider the motion of a neutron which is injected into an infinite medium that scatters but does not absorb neutrons. It will be assumed that the energy of the neutron does not change as the result of collisions.

From the point where it is injected into the system, the neutron moves, on the average, the distance  $\bar{x}_0 = \lambda_s$  before having its first collision, where  $\lambda_s$  is the scattering mean free path. As a result of this collision, the neutron is scattered through the angle  $\vartheta_1$ , as shown in Fig. 2-22, and then travels another mean free path in this direction before it has a second collision. As indicated in the figure, this is equivalent to moving the distance  $x_1 = \lambda_s \cos \vartheta_1$ , in the original direction. The average value of  $x_1$  is then  $\bar{x}_1 = \overline{\lambda_s \cos \vartheta_1} = \lambda_s \bar{\mu}$ , where  $\bar{\mu}$  is the average value of the cosine of the scattering angle.

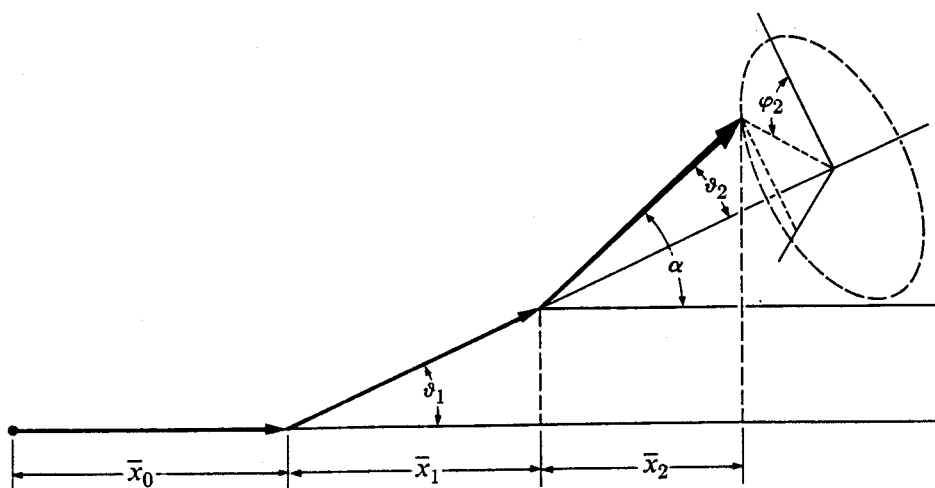


Fig. 2-22. Diagram for calculating the transport cross section.

At the second collision the situation is somewhat more complicated. The angle of scattering,  $\vartheta_2$ , is measured from the direction of the second mean free path, and the average distance which the neutron travels in its original direction before a third encounter is now  $x_2 = \lambda_s \cos \alpha$ , where  $\alpha$  is the angle between the direction of motion after the second collision and the original direction. With a little trigonometry it is easy to show that

$$\cos \alpha = \cos \vartheta_1 \cos \vartheta_2 + \sin \vartheta_1 \sin \vartheta_2 \cos \varphi_2, \quad (2-77)$$

where  $\varphi_2$  is the angle of rotation of the third mean free path with respect to the plane of the first two paths (see Fig. 2-22). Since all values of  $\varphi_2$  are equally probable, the average value of the second term in Eq. (2-77) is zero, so that

$$\bar{x}_2 = \overline{\lambda_s \cos \alpha} = \overline{\lambda_s \cos \vartheta_1 \cos \vartheta_2} = \lambda_s \bar{\mu}^2.$$

In a similar way it can be demonstrated that after the  $n$ th collision the neutron moves the distance  $\bar{x}_n = \lambda_s \bar{\mu}^n$  in the original direction before its next collision. Since  $\bar{\mu}$  is necessarily less than unity, it follows that  $\bar{x}_n$  approaches zero as  $n \rightarrow \infty$ . Physically, a zero value of the average of the mean free path projection in the direction of motion implies that on its next collision the neutron will be scattered with equal probability in both directions, i.e., forward and backward from the original direction of motion. In other words, after a succession of collisions in which the neutron has been carried the distance

$$\begin{aligned} \bar{x}_0 + \bar{x}_1 + \bar{x}_2 + \cdots &= \lambda_s + \lambda_s \bar{\mu} + \lambda_s \bar{\mu}^2 + \cdots \\ &= \frac{\lambda_s}{1 - \bar{\mu}}, \end{aligned}$$

the neutron has effectively "forgotten" its original direction of motion. The quantity  $\lambda_s/(1 - \bar{\mu})$  is known as the *transport mean free path* and is denoted by  $\lambda_{\text{tr}}$ , i.e.,

$$\lambda_{\text{tr}} = \frac{\lambda_s}{1 - \bar{\mu}}. \quad (2-78)$$

It will be noted that if the elastic angular distribution is forward peaked,  $\bar{\mu}$  is positive and  $\lambda_{\text{tr}}$  is somewhat greater than  $\lambda_s$ . This is to be expected on physical grounds since, with forward scattering, neutrons tend to propagate in their original direction of motion. On the other hand, if  $\sigma_s(\vartheta)$  is peaked in the backward direction,  $\bar{\mu}$  is negative and  $\lambda_{\text{tr}} < \lambda_s$ .

By analogy with other cross sections, the transport cross section,  $\sigma_{\text{tr}}$ , is defined by the relation

$$\lambda_{\text{tr}} = \frac{1}{N\sigma_{\text{tr}}}. \quad (2-79)$$

Thus in view of Eq. (2-78),

$$\sigma_{\text{tr}} = \sigma_s(1 - \bar{\mu}). \quad (2-80)$$

In general, the average value of the cosine of the scattering angle can be found by evaluating the integral

$$\bar{\mu} = \frac{1}{\sigma_s} \int_{4\pi} \sigma_s(\vartheta) \cos \vartheta d\Omega.$$

Writing  $d\Omega = 2\pi \sin \vartheta d\vartheta$  gives

$$\bar{\mu} = \frac{2\pi}{\sigma_s} \int_0^\pi \sigma_s(\vartheta) \cos \vartheta \sin \vartheta d\vartheta. \quad (2-81)$$

With the substitution  $\mu = \cos \vartheta$ , Eq. (2-81) becomes

$$\bar{\mu} = \frac{2\pi}{\sigma_s} \int_{-1}^{+1} \sigma_s(\mu) \mu d\mu. \quad (2-82)$$

From Eqs. (2-81) or (2-82) and Eq. (2-80),  $\sigma_{tr}$  can be computed from either experimental or theoretical values of  $\sigma_s(\vartheta)$ .

It may be mentioned for future reference that it is possible to obtain a simple formula for  $\bar{\mu}$  in the important case of isotropic scattering in the center-of-mass system. Since  $\sigma_s(\vartheta) d\Omega(\vartheta) = \sigma_s(\theta) d\Omega(\theta)$ , where  $\theta$  is the center-of-mass angle, Eq. (2-81) becomes

$$\bar{\mu} = \frac{2\pi}{\sigma_s} \int_0^\pi \sigma_s(\theta) \cos \vartheta \sin \theta d\theta. \quad (2-83)$$

With isotropic scattering in the center-of-mass system,  $\sigma_s(\theta) = \sigma_s/4\pi$ , and Eq. (2-83) reduces to

$$\bar{\mu} = \frac{1}{2} \int_0^\pi \cos \vartheta \sin \theta d\theta. \quad (2-84)$$

From Eq. (2-55), however,

$$\cos \vartheta = \frac{1 + A \cos \theta}{\sqrt{A^2 + 2A \cos \theta + 1}}.$$

Inserting this expression into Eq. (2-84) and performing the integration, the result is

$$\bar{\mu} = \frac{2}{3A}. \quad (2-85)$$

It has been assumed so far, that elastic scattering is the only possible mode of interaction. If absorption is present, it is necessary to generalize the definition of  $\sigma_{tr}$  as follows:

$$\begin{aligned} \sigma_{tr} &= \sigma_a + \sigma_s(1 - \bar{\mu}), \\ &= \sigma_t - \sigma_s \bar{\mu}. \end{aligned} \quad (2-86)$$

The transport mean free path is then given by

$$\frac{1}{\lambda_{tr}} = \frac{1}{\lambda_t} - \frac{\bar{\mu}}{\lambda_s}. \quad (2-87)$$

## 2-10 Nonelastic Cross Section

The nonelastic cross section  $\sigma_{ne}$  was defined in Section 2-1 as the difference between the total and elastic cross sections. In view of this definition,  $\sigma_{ne}$  is also equal to the sum of the cross sections for all nonelastic processes. The importance of this cross section lies in the fact that it can be used to infer the elastic and inelastic cross sections above about 3 MeV, where these cross sections cannot accurately be measured at the present time.

Many measurements of  $\sigma_{ne}$  have been performed in recent years and the resulting data are given in BNL-325. Values of  $\sigma_{ne}$  for  $Bi^{209}$  are shown in Fig. 2-11. With this nucleus virtually all of  $\sigma_{ne}$  up to about 8 MeV is due to inelastic scattering. Above 8 MeV the  $(n, 2n)$  reaction also contributes to the value of  $\sigma_{ne}$  (cf. Section 2-13). The behavior of  $\sigma_{ne}$  for other nuclei is very similar to that of  $Bi^{209}$ , except that the threshold for nonelastic processes usually occurs at much lower energies for nuclei as heavy as bismuth. Being magic,  $Bi^{209}$  tends to be a somewhat exceptional heavy nucleus.

The nonelastic cross section can also be computed using the optical model. It will be recalled from Section 2-7 that this theory gives  $\sigma_{CN}$ , the cross section for formation of the compound nucleus. Since all nonelastic processes (with the exception of direct interaction which is usually negligible) proceed by way of compound nucleus formation, it follows that  $\sigma_{CN} = \sigma_{ne}$ , provided the cross section for compound elastic scattering is small. As pointed out in Section 2-8, this is the case at energies above the resonance region in all nuclei, where elastic scattering is primarily shape elastic, i.e., potential scattering. Computations based on the optical model must be used in the absence of experimental data on  $\sigma_{ne}$ .

## 2-11 Inelastic Scattering

Inelastic scattering plays an important role in nuclear reactor theory. It will be shown in Chapter 6, that because of inelastic scattering, heavy nuclei are more effective than light nuclei in slowing down neutrons at high energies.

**Threshold energy.** Consider the collision of a neutron with a nucleus as viewed in the center-of-mass system. In this system the two particles are seen to approach each other and collide at the center-of-mass, and the sum of the kinetic energies of the two particles in the center-of-mass system is available to induce a reaction. If their total kinetic energy is greater than  $\epsilon_1$ , the energy of the first excited state, this state can be excited in the collision; that is, inelastic scattering can occur. Following such an interaction, the excited nucleus and inelastic neutron part company back to back in order to conserve momentum, and the total kinetic energy of the two is reduced by an amount equal to the excitation of the nucleus.

According to Eq. (2-38), the kinetic energy of the neutron in the laboratory  $E_l$  and the total energy of the neutron and nucleus in the center-of-mass system  $E_c$  are related by

$$E_l = \frac{A + 1}{A} E_c.$$

Since  $E_c$  must be greater than  $\epsilon_1$  for inelastic scattering to occur, it follows that  $E_t$  must be greater than  $E_l$ , where

$$E_t = \frac{A+1}{A} \epsilon_1. \quad (2-88)$$

The energy  $E_t$  is known as the *inelastic threshold*, and in view of Eq. (2-88) it is evident that  $E_t$  is always greater than the energy of the first excited state. For example, the first state of  $C^{12}$  is at 4.43 MeV, but inelastic scattering does not occur unless the neutrons have a laboratory energy greater than  $\frac{13}{12} \times 4.43 = 4.80$  MeV. Of course, the difference between  $E_t$  and  $\epsilon_1$  is of the order of  $1/A$ , so that the distinction is unimportant except for light nuclei.

Although there are a great many exceptions, in particular, the magic nuclei, the energy of the first excited state, i.e.,  $\epsilon_1$ , generally decreases with increasing mass number, as indicated in Fig. 1-2. As a practical matter, therefore, inelastic scattering tends to be more important for heavy nuclei than for light nuclei. Thus in calculations of a reactor consisting of an assembly of uranium and water, for example, inelastic scattering by oxygen (inelastic threshold = 6.42 MeV) can ordinarily be ignored, whereas inelastic scattering by uranium must be included.

**Inelastic scattering cross-section data.** Modern time-of-flight techniques have made it possible to obtain considerable data on inelastic scattering where, until recently, comparatively little data were available. Figure 2-23 shows the cross sections for the excitation of the first three levels in  $U^{238}$ , along with the total inelastic cross section  $\sigma_i$ .

When a great many levels can be excited,  $\sigma_i$  is not usually measured directly. It can be found, however, by subtracting the cross sections of other nonelastic processes from the nonelastic cross section. These calculations are particularly simple for intermediate and heavy nuclei in the MeV region, for as mentioned in the next section, the cross sections for all nonelastic interactions except inelastic scattering are usually small. Thus in this case,  $\sigma_{ne}$  and  $\sigma_i$  can be taken to be equal.

**Calculations of inelastic cross sections.** For energies near the inelastic threshold, and except for the very lightest nuclei,  $\sigma_i$  can be computed by a method due to Hauser and Feshbach. The details of this method are too complicated to be given here, and the reader is referred to the references at the end of the chapter. In any event, this method can be used to predict  $\sigma_i$  when one or at most a few levels are excited. At energies where several levels can be excited the method becomes too involved for practical calculations. At these energies, however,  $\sigma_i$  and  $\sigma_{ne}$  are usually very nearly identical at least for intermediate and heavy nuclei, and values of  $\sigma_{ne}$  computed from the optical model (cf. Section 2-7) can be used when nonelastic cross-section data is not available.

**Energy distribution of inelastically scattered neutrons.** When the energy of the incident neutron is only high enough to excite a few levels in the target nucleus, the inelastic neutrons appear in the center-of-mass system in distinct energy groups, each group corresponding to the excitation of a single level.

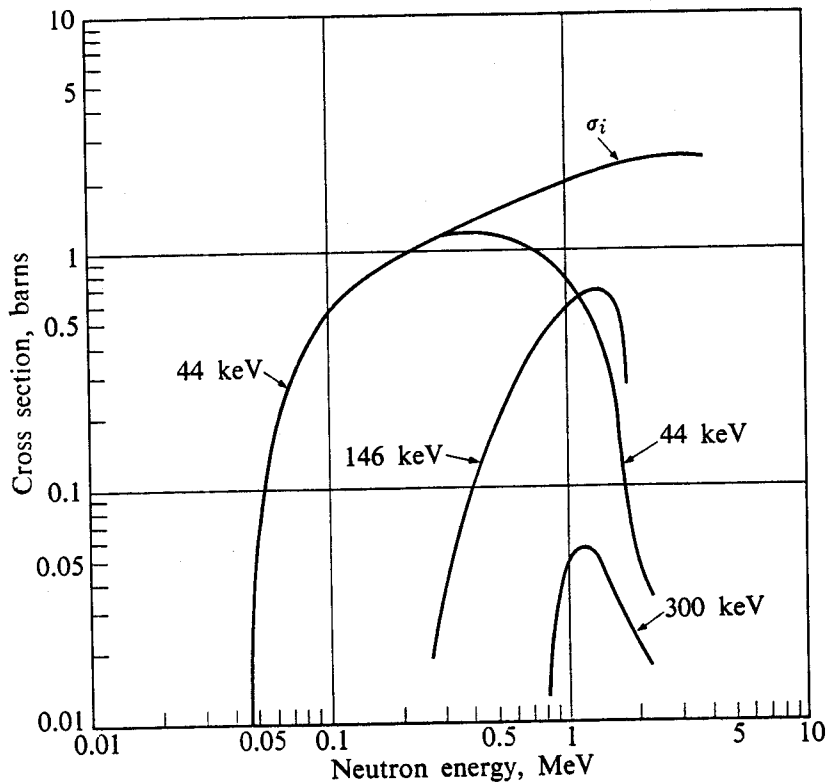


**Fig. 2-23.** The cross sections for the excitation of the 44 keV, 146 keV, and 300 keV levels and the total inelastic cross section of  $\text{U}^{238}$ . The cross sections for the excitation of several levels above 300 keV are not shown. (From S. Yiftah, D. Okrent, P. A. Moldauer, *Fast Reactor Cross Sections*, New York: Pergamon Press, 1960.)

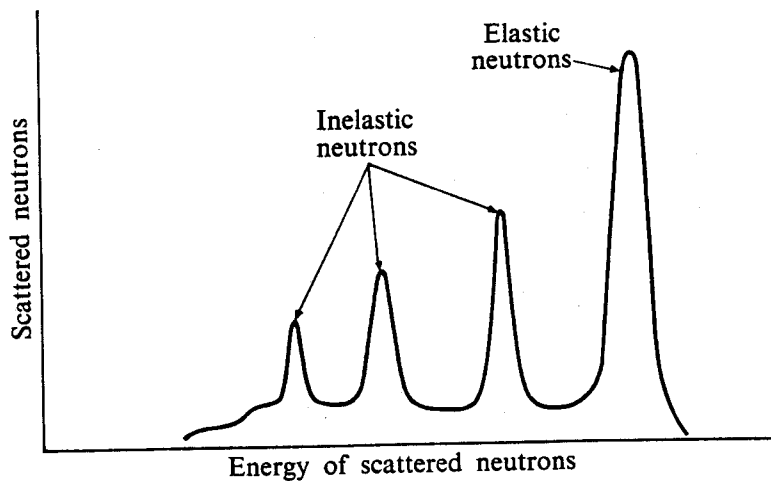


**Fig. 2-24.** Discrete energy spectrum of inelastic neutrons.

When observed in the laboratory system, however, this line spectrum of energies is modified to some extent by the motion of the center of mass. Nevertheless, provided the energy of the incident neutron is not too high, a fairly discrete spectrum of inelastic neutrons is observed as shown in Fig. 2-24.

If the energy of the incident neutron is raised to a point where many levels can be excited, the neutron groups corresponding to the more closely spaced levels

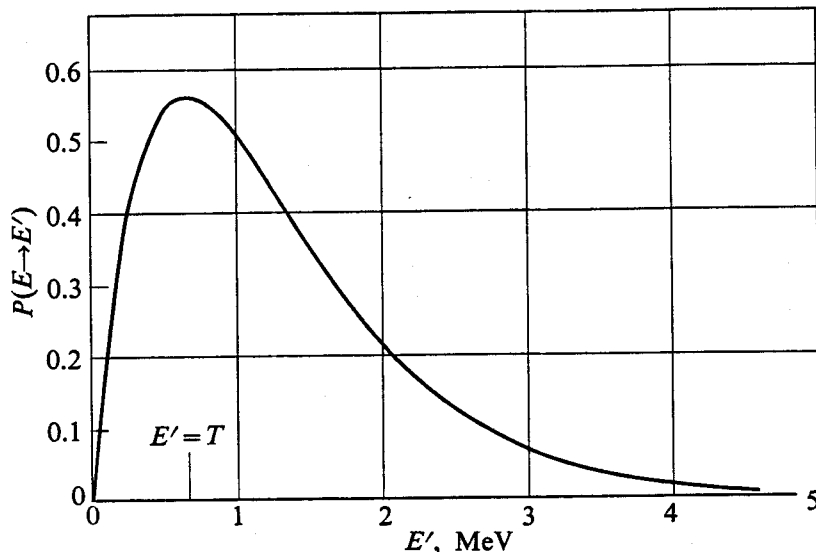


Fig. 2-25. Continuous energy spectrum of inelastic neutrons from inelastic scattering of 10 MeV neutrons by  $\text{U}^{238}$ , as computed from Eqs. (2-89) and (2-90).

cannot be resolved and a continuous spectrum is observed in addition to the discrete spectrum. The shape of the continuous spectrum can be derived on the basis of the liquid-drop model mentioned in Chapter 1. In this theory it is assumed that the inelastic neutrons simply "boil off" from the compound nucleus and then appear with the energy distribution:

$$P(E \rightarrow E') = \frac{E'}{T^2} e^{-E'/T}. \quad (2-89)$$

The function  $P(E \rightarrow E')$  is defined so that  $P(E \rightarrow E') dE'$  is the probability that an inelastic neutron will be emitted with an energy between  $E'$  and  $E' + dE'$  when the nucleus is struck by a neutron of energy  $E$ . The parameter  $T$  is called the *nuclear temperature* and is given approximately by the formula

$$T = 3.2\sqrt{E/A}, \quad (2-90)$$

where  $T$  and  $E$  are in MeV and  $A$  is the mass of the target nucleus. It must be emphasized that Eq. (2-90) is *very* approximate and is particularly erroneous when used for magic or near-magic nuclei.

The function  $P(E \rightarrow E')$  is plotted in Fig. 2-25 for 10-MeV neutrons incident on  $\text{U}^{238}$ . It should be noted that the peak of the curve, which corresponds to the *most probable energy* of the emitted neutrons, occurs at  $E' = T = 0.66$  MeV. Thus, when  $\text{U}^{238}$  is bombarded with 10-MeV neutrons, the inelastic neutrons are most likely to appear with an energy of only about 0.66 MeV.

**Angular distribution of inelastic neutrons.** The angular distributions of inelastically scattered neutrons are quite simple over most of the energy range of interest in reactor theory. Up to around 10 MeV these neutrons are

emitted isotropically, or nearly so, in the center-of-mass system. Above approximately 10 MeV, the angular distribution tends to become forward peaked and exhibits a diffraction pattern similar to that found in elastic scattering at these energies. This forward-peaked distribution is due to the neutrons which have undergone the direct-interaction type of inelastic scattering discussed in Section 2-6. Since there are comparatively few neutrons with such a large energy in nuclear reactors, it is usually adequate in reactor theory to assume that inelastic scattering is always isotropic in the center-of-mass system.

## 2-12 Absorption Reactions

The disappearance of neutrons as the result of absorption reactions has an important bearing on the design of a reactor. By far the most important reaction of this kind is radiative capture.

**Radiative capture—data and theory.** This process can occur at all neutron energies, but it is most probable at low energies and in particular at those energies that lead to *long-lived* states of the compound nucleus. The requirement that the compound state must be long-lived is due to the fact that the emission of  $\gamma$ -radiation by a nucleus can be shown to be a very lengthy process when measured on a nuclear time scale. For instance, it takes a nucleon on the order of  $10^{-21}$  sec to move once around an orbit in the nucleus, whereas the emission of a  $\gamma$ -ray requires about  $10^{-14}$  sec, a difference of a factor of  $10^7$ .

In Section 2-6 it was pointed out that when a neutron is first absorbed by the nucleus  $Z^A$ , the compound nucleus  $Z^{A+1}$  is formed in a highly excited (virtual) state because the neutron brings into the system both its original kinetic energy and its binding energy. Since the compound state lies above the virtual energy, the system can decay either by the reemission of a neutron, as in elastic scattering, or by emitting a  $\gamma$ -ray. However, as discussed in Chapter 1, the excitation energy of the compound nucleus is divided among several nucleons, and the emission of a nucleon is delayed until one nucleon obtains an energy in collisions with other nucleons greater than its binding energy in the nucleus. It is reasonable to expect, therefore, that when the excitation energy is shared among a large number of nucleons, the average time that elapses before a nucleon can be emitted is much longer than when only a few nucleons are involved. If nucleon emission is delayed by much more than about  $10^{-14}$  sec, the average time required for  $\gamma$ -ray emission, the compound nucleus may decay by emitting a  $\gamma$ -ray. Since it is logical to assume that a given excitation energy is shared among many more nucleons in a heavy nucleus than in a light nucleus, it follows that radiative capture is comparatively unimportant in light nuclei but becomes increasingly important in the heavier nuclei.

The fact that radiative capture requires a long-lived compound state can be used to determine whether the more important process at a particular resonance is scattering or capture. As shown in Section 1-8, the lifetime of a compound state is

inversely proportional to its total width. Narrow resonances therefore correspond to capture while the wider resonances are due to scattering. For example, the first resonance in  $U^{238}$  at 6.67 eV, which corresponds to the first virtual level in  $U^{239}$ , has a total width of only 0.027 eV, and the mean life of this state is  $2.4 \times 10^{-14}$  sec. By contrast, the resonance observed at 443 keV in  $O^{16}$ , which corresponds to the first virtual state in  $O^{17}$ , has a total width of 41 keV, giving a mean lifetime of  $1.5 \times 10^{-21}$  sec. Thus it is highly likely that the compound state in  $U^{239}$  decays at least to some extent by  $\gamma$ -ray emission, while the compound state in  $O^{17}$  must decay primarily by nucleon emission. The 443-keV resonance in  $O^{16}$  is clearly a *scattering resonance*, whereas the 6.67-eV resonance in  $U^{238}$  is in part (and almost entirely, as it turns out) a *capture resonance*.

In view of the fact that the cross section for radiative capture is only large at low energy, it follows that it is primarily *s*-wave neutrons which are involved in this

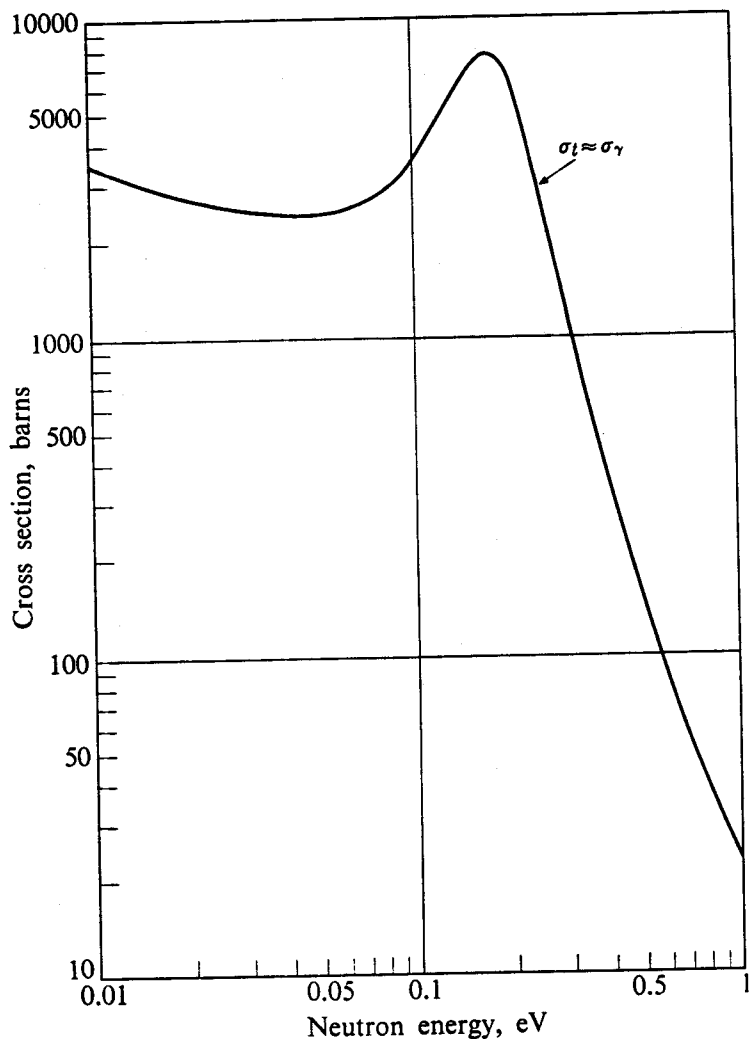


Fig. 2-26. The total  $\approx$  radiative capture cross section of cadmium at low energy. [From BNL-325, Second Edition (1958).]

process. In this case, near an isolated resonance at the energy  $E_1$ ,  $\sigma_\gamma$  is given by the *Breit-Wigner one-level formula*:

$$\sigma_\gamma(E_c) = \pi \lambda_1^2 g \left( \frac{E_1}{E_c} \right)^{1/2} \frac{\Gamma_n \Gamma_\gamma}{(E_c - E_1)^2 + \Gamma^2/4}. \quad (2-91)$$

Here,  $\Gamma_n$  and  $\Gamma_\gamma$  are the neutron and radiation widths, respectively, and the other symbols have the same meaning as in Eq. (2-69). Since capture resonances are found only in intermediate and heavy nuclei, the center-of-mass energy  $E_c$  is essentially equal to the laboratory energy  $E$  of the incident neutron. This is true, of course, provided the target nucleus is at rest in the laboratory system. (This point will be reconsidered in Section 2-14.)

It should be observed from Eq. (2-91) that when  $E(\approx E_c)$  is very much less than  $E_1$ ,  $\sigma_\gamma$  behaves as  $1/\sqrt{E}$ , that is, as  $1/v$ , where  $v$  is the speed of the neutron. The magnitude of  $\sigma_\gamma$  at low energy depends, however, upon whether or not there is a resonance in this energy region. If there is a low energy resonance,  $\sigma_\gamma$  is quite large and the  $1/v$ -portion of  $\sigma_\gamma$  is short. This situation is illustrated in Fig. 2-26 for cadmium, where the first resonance (which is due to  $Cd^{113}$ ) occurs at only 0.178 eV. It is of some interest to note that it is actually rather unlikely to find a resonance at such a low energy. This is because the corresponding level in the compound nucleus, which lies just slightly above the virtual energy, is, in fact, at an energy of about 7 MeV above the ground state of the compound nucleus. The spacing of levels at this energy and for nuclei with  $A$  about 113 has been found to be about 40 eV; that is, this is the average energy between levels. The probability that a level will be found in the small energy interval between zero and 0.2 eV is therefore only  $0.2/40 = 0.5\%$ . The more usual situation is shown in Fig. 2-27, where  $\sigma_\gamma \approx \sigma_t$  is shown for  $Au^{197}$ . Here the long  $1/v$ -tail is quite evident.

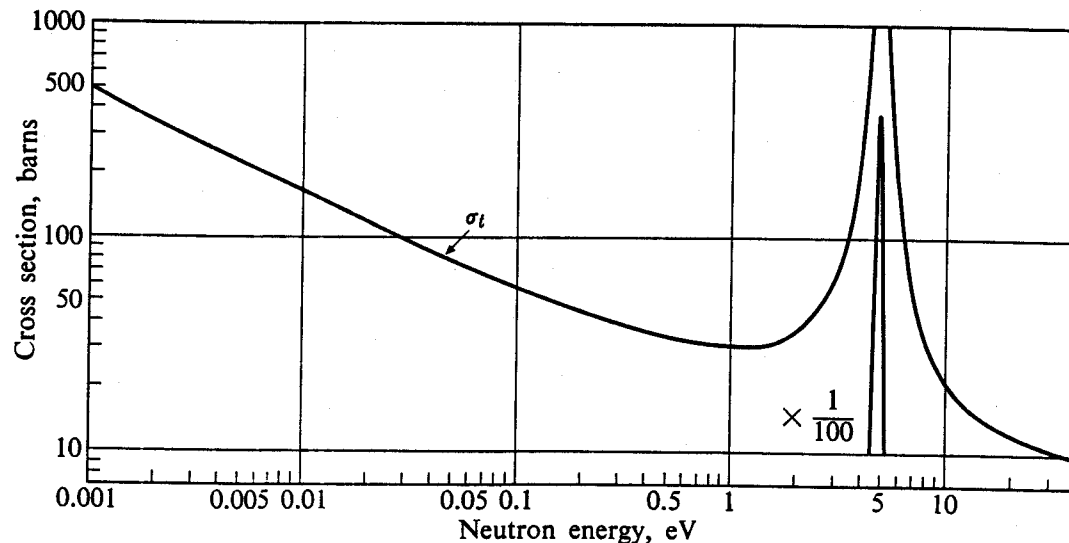


Fig. 2-27. The total  $\approx$  radiative capture cross section of  $Au^{197}$  at low energy. [From BNL-325, Second Edition (1958).]

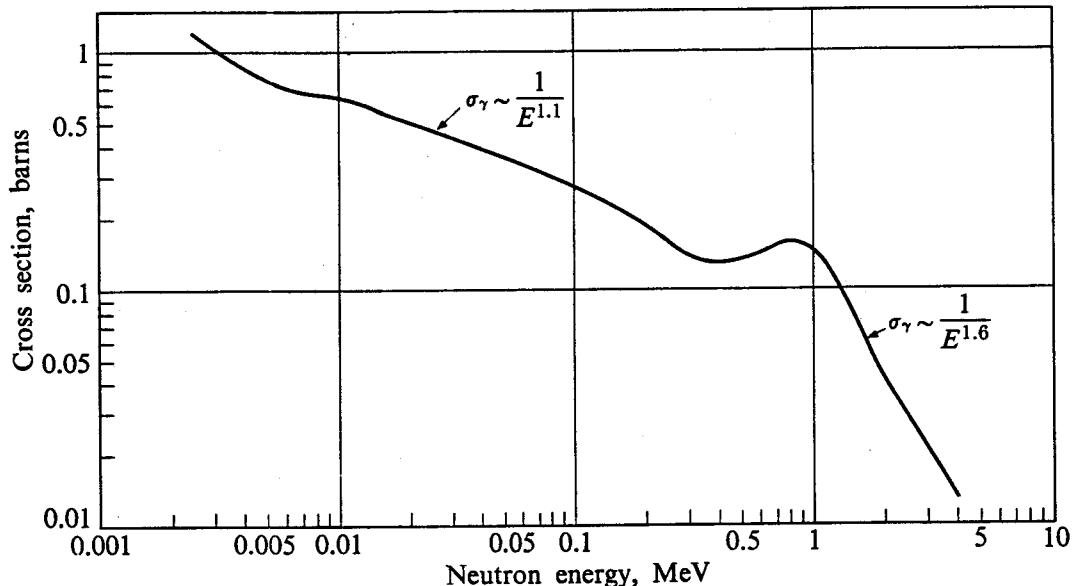


Fig. 2-28. The radiative capture cross section of  $\text{U}^{238}$  at high energy. [From BNL-325, Second Edition (1958).]

By introducing the quantities  $\sigma_1$  and  $x$  defined in Eqs. (2-71) and (2-72), the Breit-Wigner one-level formula can be written in the more convenient form

$$\sigma_\gamma(x) = \frac{\sigma_1 \Gamma_\gamma}{\Gamma} \left( \frac{E_1}{E_c} \right)^{1/2} \frac{1}{1 + x^2}. \quad (2-92)$$

In the immediate vicinity of a narrow absorption resonance the term  $(E_1/E_c)^{1/2}$  in Eq. (2-92) is approximately constant and equal to unity, and  $\sigma_\gamma$  reduces to

$$\sigma_\gamma(x) = \frac{\sigma_1 \Gamma_\gamma}{\Gamma} \frac{1}{1 + x^2}. \quad (2-93)$$

In a region of several *s*-wave resonances the capture cross section can be found by merely adding together the contributions from each resonance as computed from Eq. (2-91). This is in marked contrast to the situation with elastic scattering. It will be recalled from Section 2-8 that the elastic cross section in a region of closely spaced resonances is given by a complicated formula and is *not* the sum of contributions from each resonance.

At energies above the resonance region  $\sigma_\gamma$  drops rapidly as  $1/E$ , or faster, to very small values. An example of this behavior is shown for  $\text{U}^{238}$  in Fig. 2-28. The reason for the rapid decrease in  $\sigma_\gamma$  is that with increasing energy of the incident neutron, the compound nucleus is formed in more highly-excited states which can more readily decay by neutron emission (or fission, if this is energetically possible) than by  $\gamma$ -ray emission. At the higher energies, inelastic scattering and the  $(n, 2n)$  reaction thus become the dominant compound nucleus process, at the expense of both elastic scattering and radiative capture.

Measurements of  $\sigma_\gamma$  have been carried out at low energy and in the resonance regions of most nuclei. These data, including both the cross sections and resonance widths, are given in BNL-325. Above the resonance region, the experiments are more difficult to perform since, among other things, the cross section is so small, and considerably less data are available.

**Charged-particle reactions.** Neutrons also disappear as a result of charged-particle reactions, such as the (n, p) or (n,  $\alpha$ ) reactions. These reactions are usually endothermic and do not occur below a threshold energy. For a few light nuclei, however, they are exothermic.

The most important exothermic reaction of this type is the  $B^{10}(n, \alpha)Li^7$  reaction. The low-energy cross section for this reaction is very high, and for this reason boron is widely used to absorb slow neutrons. The total cross section of  $B^{10}$  at low energies, which is almost entirely due to the (n,  $\alpha$ ) reaction, is shown in Fig. 2-10. It will be noted that  $\sigma_t \approx \sigma_\alpha$  is  $1/v$  over a wide range of energy. The reason for this is as follows. It can be shown that except in the vicinity of resonances the cross section of *any* reaction of the type  $X(a, b)Y$  is given by the formula\*

$$\sigma_{a,b} = \left( \frac{E_b}{E_a} \right)^{1/2} H(E_a), \quad (2-94)$$

where  $E_a$  and  $E_b$  are the kinetic energies of the incident and emergent particles, respectively, and  $H(E_a)$  is a slowly varying function of  $E_a$ . If the reaction is exothermic,  $E_b$  will usually exceed  $E_a$  by several MeV. Hence, at low energies of the incident neutron, i.e.,  $E_a \approx$  eV, changes in  $E_a$  have almost no effect on  $E_b$ . The cross section therefore behaves essentially like  $1/\sqrt{E_a}$ , that is, like  $1/v_a$ .

A similar exothermic reaction which also shows a strong  $1/v$  behavior is  $Li^6(n, \alpha)H^3$ . This reaction is used for the production of tritium,  $H^3$ .

Another important charged-particle reaction which occurs with low-energy neutrons is the  $N^{14}(n, p)C^{14}$  reaction. Although the cross section is not particularly high (1.8 barns at 0.025 eV), many neutrons emitted from nuclear explosions are absorbed in the atmosphere via this reaction and produce the long-lived and potentially dangerous  $\beta$ -emitter  $C^{14}$ .

Some endothermic charged-particle reactions are important in reactors even though their thresholds are high. In water reactors, for example, the  $O^{16}(n, p)N^{16}$  reaction is the principal source of the radioactivity of the water (the  $N^{16}$  undergoes  $\beta$ -decay with a half-life of approximately 7 sec, which is accompanied by the emission of 6- to 7-MeV  $\gamma$ -rays), despite the fact that ordinarily only one neutron in several thousand has an energy greater than the 9-MeV threshold for this reaction.

---

\* It may be noted that the Breit-Wigner formula for radiative capture at energies far from a resonance is a special case of this more general relation.

With intermediate and heavy nuclei, the cross sections for charged-particle reactions are so small they cannot usually be measured. This is because the emitted charged particle must pass through a coulomb barrier in order to escape from the nucleus in much the same way that  $\alpha$ -particles do when emitted from radioactive nuclei. Except for light nuclei, this barrier is so high and the associated delay in charged-particle emission is so long that the compound system almost always decays by the emission of an elastic or inelastic neutron before a charged particle can be emitted.

### 2-13 Neutron Producing Reactions

The principal source of neutrons in reactors is nuclear fission, and this reaction is discussed in detail in Chapter 3. Neutrons are also produced in certain other reactions, however, though to a much smaller extent.

**The ( $n$ ,  $2n$ ) and ( $n$ ,  $3n$ ) reactions.** The ( $n$ ,  $2n$ ) reaction usually proceeds in two steps. First, the incident neutron is inelastically scattered by the target nucleus. Then, if the residual nucleus is left with an excitation energy above the binding energy of its least bound neutron, this neutron is free to escape from the system. According to the discussion of Section 2-11 and as shown in Fig. 2-25, inelastically scattered neutrons usually leave most of their initial energy in the residual nucleus. This means that if the incident neutron has an energy above the threshold for the ( $n$ ,  $2n$ ) reaction it is likely that a second neutron will appear. As a result, the ( $n$ ,  $2n$ ) cross section rises rapidly above its threshold at the expense of the inelastic cross section, since the bulk of the inelastic neutrons are now included as part of the ( $n$ ,  $2n$ ) reaction. This situation is illustrated in Fig. 2-29, where the inelastic and ( $n$ ,  $2n$ ) cross sections are shown for  $U^{238}$ .

The  $Q$ -value of the ( $n$ ,  $2n$ ) reaction is equal, of course, to the binding energy of the "loosest" neutron in the target nucleus. As in other reactions, the threshold energy in the laboratory system is then given by

$$E_t = - \left( \frac{A+1}{A} \right) Q. \quad (2-95)$$

Nuclei which contain a loosely bound neutron, thus have a low ( $n$ ,  $2n$ ) threshold. One of the most important examples of this kind is  $Be^9$ , whose ( $n$ ,  $2n$ ) threshold is only 1.8 MeV. Beryllium is often used in substantial quantities in reactors, and when this is the case special attention must be given to this reaction. With most nuclei, however, the ( $n$ ,  $2n$ ) threshold is in the range from about 7 to 10 MeV.

The relationship of the ( $n$ ,  $3n$ ) reaction to the ( $n$ ,  $2n$ ) reaction is similar to that of the ( $n$ ,  $2n$ ) reaction to inelastic scattering. Thus a third neutron will be emitted provided the nucleus retains sufficient excitation energy after the emission of the second neutron in the ( $n$ ,  $2n$ ) reaction. The ( $n$ ,  $3n$ ) cross section therefore rises from the ( $n$ ,  $3n$ ) threshold at the expense of the ( $n$ ,  $2n$ ) cross section, as indicated in Fig. 2-29. Ordinarily, however, the ( $n$ ,  $3n$ ) threshold is so high (it ranges from

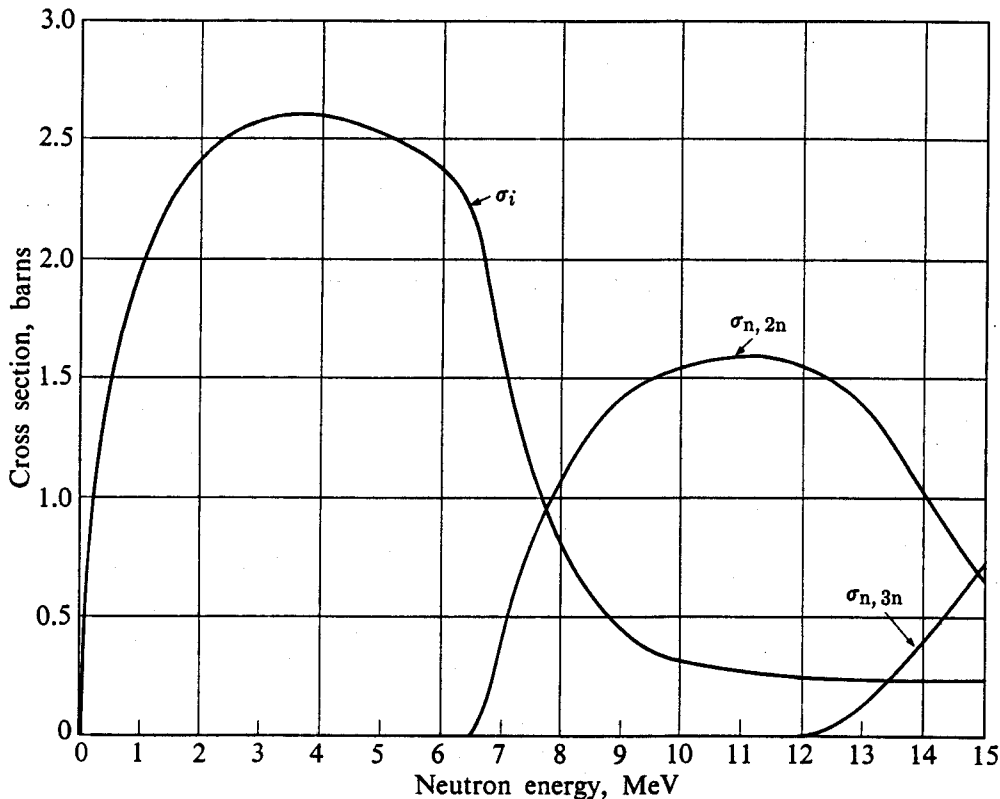


Fig. 2-29. The inelastic,  $(n, 2n)$  and  $(n, 3n)$  cross sections of  $U^{238}$ . (Based on R. J. Howerton, "Semi-empirical Neutron Cross Sections 0.5-15 MeV," UCRL-5351, November 1958.)

about 11 MeV to 30 MeV) that this reaction is not important in most reactor calculations. In this connection, it may be mentioned that if a nucleus has a low  $(n, 2n)$  threshold, it does not necessarily follow that its  $(n, 3n)$  threshold will also be low. For instance, while the  $(n, 2n)$  threshold of  $Be^9$  is only 1.8 MeV, its  $(n, 3n)$  threshold is 21 MeV. The origin of this disparity lies in the fact that although it may require only a small amount of energy to remove one neutron from a nucleus it may take considerably more energy to remove a second neutron.

**The  $(\gamma, n)$  reaction.** When a nuclear reactor is in operation, a great many energetic  $\gamma$ -rays are produced in its interior as the result of fission, from the decay of radioactive fission products, and from various neutron interactions, in particular, radiative capture and inelastic scattering. The more energetic of these  $\gamma$ -rays can produce neutrons by the  $(\gamma, n)$  reaction. This reaction is similar to the  $(n, 2n)$  reaction in that a neutron originally bound in the nucleus is ejected in the process. It is easy to see, in fact, that except for center-of-mass effects, the thresholds for the  $(\gamma, n)$  and  $(n, 2n)$  reactions are identical, and these reactions are therefore important for the same nuclei. However, unlike the  $(n, 2n)$  reaction, the  $(\gamma, n)$  reaction continues to produce neutrons even after a reactor is shut down, owing to the continuing decay of the fission products.

## 2-14 The Doppler Effect

Up to this point, it has been assumed that prior to a neutron-nucleus interaction the nucleus is at rest in the laboratory system. This is never strictly true, however, since the atoms containing the nuclei are in continual motion due to their thermal energy. It will be recalled from Section 2-5 that the energy available for an interaction is the sum of the kinetic energies of the neutron and nucleus with respect to their center of mass. This energy,  $E_c$ , is given by

$$E_c = \frac{1}{2}\mu v_r^2, \quad (2-96)$$

where  $\mu$  is the reduced mass of the particles and  $v_r$  is their relative speed of approach. If the nucleus is at rest,  $v_r$  is equal to the laboratory speed of the neutron. On the other hand, if the nucleus is in motion,  $v_r$  has a range of values. It is larger, for instance, if the two particles are approaching each other, as in Fig. 2-30(a), than if the neutron must "catch up with" the nucleus, as in Fig. 2-30(b). It follows, therefore, that because of the thermal motion of the target nuclei, a beam of neutrons that is monoenergetic in the laboratory appears to have a smear of energies insofar as their interactions with the nuclei are concerned. By analogy to similar phenomena encountered in acoustics and optics this effect is known as the *nuclear Doppler effect*.

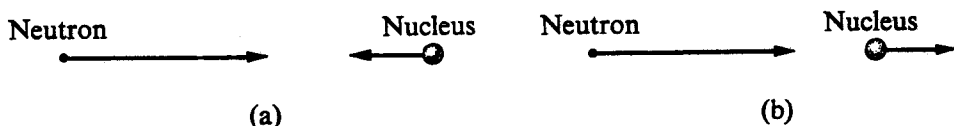


Fig. 2-30. Motions of neutron and nucleus.

Because of this effect, the observed interaction rate of a beam of monoenergetic neutrons depends upon the temperature  $T$  of the target as well as on the laboratory energy  $E$  of the neutrons. By analogy with Eq. (2-1), the interaction rate/cm<sup>3</sup> is written

$$\text{interaction rate}/\text{cm}^3 = IN\bar{\sigma}(E, T), \quad (2-97)$$

where  $I$  is the intensity of the beam,  $N$  is the atom density of the target, and  $\bar{\sigma}(E, T)$  for reasons that will be clear momentarily, is called the average *Doppler-broadened cross section*.

To compute  $\bar{\sigma}(E, T)$ , let  $N(V) dV$  be the number of atoms (nuclei)/cm<sup>3</sup> in the target moving with velocities between  $V$  and  $V + dV$ . With respect to these nuclei, the incident neutrons approach with the speed  $v_r$  and with an intensity  $nv_r$ , where  $n$  is the density of neutrons in the beam, and interact at the rate of  $nv_r\sigma(E_c)N(V) dV$  interactions per cm<sup>3</sup>/sec. The total interaction rate for all nuclei is therefore

$$IN\bar{\sigma}(E, T) = \int nv_r\sigma(E_c)N(V) dV, \quad (2-98)$$

$$g(E, T) = \frac{N_0}{I} \int u_n g(E_n) N(V_z) dV_z. \quad (2-103)$$

where  $N(V_z) dV_z$  is the number of atoms/cm<sup>3</sup> with  $V_z$  between  $V_z$  and  $V_z + dV_z$ , Eq. (2-99) becomes

$$\int N(V) dV = \iiint N(V_x, V_y, V_z) dV_x dV_y dV_z = \int N(V_z) dV_z$$

In view of the fact that  $E_n$ , and therefore also  $u_n$ , depends upon only the z-component of  $V$ , the integral over  $dV_x$  and  $dV_y$  in Eq. (2-99) can be carried out directly.

Computations show that the Doppler effect is of greatest significance in the immediate vicinity of narrow resonances such as those in the  $\bar{e}V$ -region of heavy nuclei. In this case,  $m/(m + M) \approx 0$  while  $M/(m + M) \approx 1$ , and Eq. (2-101) reduces to

$$E_n \approx E - \frac{\mu}{(2E)^{1/2}} V_z. \quad (2-102)$$

Thus, since

$$E_n \approx E - \frac{\mu}{(2E)^{1/2}} V_z. \quad (2-102)$$

reduces to

$$E_n \approx E - \frac{\mu}{(2E)^{1/2}} V_z. \quad (2-102)$$

where  $m$  and  $M$  are the masses of neutron and nucleus, respectively,  $E$  and  $E_n$  are

their laboratory energies, and  $V_z$  is the component of the velocity of the nucleus

along the direction of motion of the neutron, as shown in Fig. 2-31.

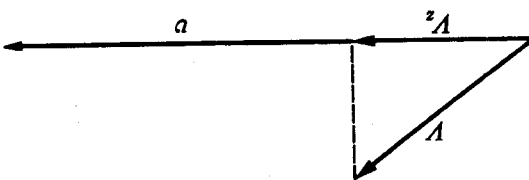


Fig. 2-31. Diagram defining  $V_z$ .

where  $m$  and  $M$  are the masses of neutron and nucleus, respectively,  $E$  and  $E_n$  are their laboratory energies, and  $V_z$  is the component of the velocity of the nucleus along the direction of motion of the neutron, as shown in Fig. 2-31.

$$E_n = \frac{m}{M} E + \frac{m}{m + M} E_n - \frac{\mu}{(2E)^{1/2}} V_z. \quad (2-101)$$

This equation can be put in the more convenient form

$$E_n = \frac{1}{2} \mu v^2 + \frac{1}{2} \mu V_z^2 - \mu V \cdot V$$

$$E_n = \frac{1}{2} \mu |V| - V|^2$$

In order to evaluate the integral in Eq. (2-99), it is necessary to express  $E_n$  and  $|V - V_z|$ , Eq. (2-96) can be written as

$$g(E, T) = \frac{N_0}{I} \int u_n g(E_n) N(V) dV. \quad (2-99)$$

Since  $I = \mu v$ , where  $v$  is the laboratory speed of the neutrons,  $g(E, T)$  becomes

where the integration is carried out over the three components  $V_x$ ,  $V_y$ , and  $V_z$  of  $V$ .

If the target is a gas (a rather unusual situation)  $N(V_z)$  is given by the Maxwellian distribution function for a velocity component, namely,

$$N(V_z) = N \left( \frac{M}{2\pi kT} \right)^{1/2} e^{-MV_z^2/2kT}, \quad (2-104)$$

where  $k$  is Boltzmann's constant ( $k = 8.617 \times 10^{-5}$  eV/ $^{\circ}$ K) and  $T$  is the absolute temperature of the gas. For a solid target it can be shown that  $N(V_z)$  is given approximately by the same function, except that the parameter  $T$  is somewhat different from the temperature of the target. The difference is small, however, for temperatures above approximately 300 $^{\circ}$ K, and it can frequently be assumed that  $T$  refers to the actual temperature of the target.

Consider first the radiative capture cross section near an isolated resonance at energy  $E_1$ ;  $\sigma(E_c)$  is then given by the Breit-Wigner formula (Eq. 2-91). Inserting this expression and Eq. (2-104) into Eq. (2-103), and noting that since  $\mu \approx m$ ,  $v_r/v \approx \sqrt{E_c/E}$ , the result is

$$\bar{\sigma}_\gamma(E, T) = \left( \frac{\sigma_1 \Gamma_\gamma}{\Gamma} \right) \left( \frac{E_1}{E} \right)^{1/2} \left( \frac{M}{2\pi kT} \right)^{1/2} \int_{-\infty}^{\infty} \frac{\exp(-MV_z^2/2kT)}{[2(E_c - E_1)/\Gamma]^2 + 1} dV_z. \quad (2-105)$$

This integral can be simplified by making the following substitutions:\*

$$x = \frac{2}{\Gamma} (E - E_1), \quad (2-106)$$

$$y = \frac{2}{\Gamma} (E_c - E_1), \quad (2-107)$$

$$\xi = \frac{\Gamma}{\Gamma_D}, \quad (2-108)$$

and

$$\Gamma_D = \left( \frac{4E_1 k T}{A} \right)^{1/2}, \quad (2-109)$$

where the quantity  $\Gamma_D$  is known as the *Doppler width*. Equation (2-105) can then be written as

$$\bar{\sigma}_\gamma(E, T) = \frac{\sigma_1 \Gamma_\gamma}{\Gamma} \left( \frac{E_1}{E} \right)^{1/2} \psi(\xi, x), \quad (2-110)$$

where  $\psi(\xi, x)$  is a function defined by the integral

$$\psi(\xi, x) = \frac{\xi}{2\sqrt{\pi}} \int_{-\infty}^{\infty} \frac{\exp[-\frac{1}{4}\xi^2(x-y)^2]}{1+y^2} dy. \quad (2-111)$$

---

\* Note that the parameter  $x$  in Eq. (2-106) is different from the  $x$  defined by Eq. (2-72). In the literature the parameter  $\xi$  is also denoted by  $\theta$ ,  $\xi$ , and  $t^{-1/2}$ .

Table 2-1. Tables of  $\psi(\xi, x)$  and  $\chi(\xi, x)^*$   
THE  $\psi$ -FUNCTION

$x$	0	0.5	1	2	4	6	8	10	20	40
$\xi$										
0.05	0.04309	0.04308	0.04306	0.04298	0.04267	0.04216	0.04145	0.04055	0.03380	0.01639
0.10	0.08384	0.08379	0.08364	0.08305	0.08073	0.07700	0.07208	0.06623	0.03291	0.00262
0.15	0.12239	0.12223	0.12176	0.11989	0.11268	0.10165	0.08805	0.07328	0.01695	0.00080
0.20	0.15889	0.15854	0.15748	0.15331	0.13777	0.11540	0.09027	0.06614	0.00713	0.00070
0.25	0.19347	0.19281	0.19086	0.18324	0.15584	0.11934	0.08277	0.05253	0.00394	0.00067
0.30	0.22624	0.22516	0.22197	0.20968	0.16729	0.11571	0.07042	0.03880	0.00314	0.00065
0.35	0.25731	0.25569	0.25091	0.23271	0.17288	0.10713	0.05724	0.02815	0.00289	0.00064
0.40	0.28679	0.28450	0.27776	0.25245	0.17359	0.09604	0.04566	0.02109	0.00277	0.00064
0.45	0.31477	0.31168	0.30261	0.26909	0.17052	0.08439	0.03670	0.01687	0.00270	0.00064
0.50	0.34135	0.33733	0.32557	0.28286	0.16469	0.07346	0.03025	0.01446	0.00266	0.00063

THE  $\chi$ -FUNCTION

$x$	0	0.5	1	2	4	6	8	10	20	40
$\xi$										
0.05	0	0.00120	0.00239	0.00478	0.00951	0.01415	0.01865	0.02297	0.04076	0.05221
0.10	0	0.00458	0.00915	0.01821	0.03573	0.05192	0.06626	0.07833	0.10132	0.05957
0.15	0	0.00986	0.01968	0.03894	0.07470	0.10460	0.12690	0.14096	0.12219	0.05341
0.20	0	0.01680	0.03344	0.06567	0.12219	0.16295	0.18538	0.19091	0.11754	0.05170
0.25	0	0.02515	0.04994	0.09714	0.17413	0.21909	0.23168	0.22043	0.11052	0.05103
0.30	0	0.03470	0.06873	0.13219	0.22694	0.26757	0.26227	0.23199	0.10650	0.05069
0.35	0	0.04529	0.08940	0.16976	0.27773	0.30564	0.27850	0.23236	0.10437	0.05049
0.40	0	0.05674	0.11160	0.20890	0.32442	0.33286	0.28419	0.22782	0.10316	0.05037
0.45	0	0.06890	0.13498	0.24880	0.36563	0.35033	0.28351	0.22223	0.10238	0.05028
0.50	0	0.08165	0.15927	0.28875	0.40075	0.35998	0.27979	0.21729	0.10185	0.05022

\* From T. D. Beynon and I. S. Grant, "Evolution of the Doppler-Broadened Single Level and Interference Functions," *Nucl. Sci. Eng.* 17, 547 (1963).

This function cannot be expressed in terms of elementary functions. It has been tabulated, however, and a short table is given in Table 2-1. More extensive tabulations may be found in the references at the end of the chapter.

Unless the resonance is located at a very low energy, the expression for  $\bar{\sigma}_\gamma(E, T)$  near the resonance can be simplified by taking the factor  $\sqrt{E_1/E}$  in Eq. (2-110) to be unity; then

$$\bar{\sigma}_\gamma(E, T) = \frac{\sigma_1 \Gamma_\gamma}{\Gamma} \psi(\xi, x). \quad (2-112)$$

The similarity in form of Eqs. (2-110) and (2-112) to Eqs. (2-92) and (2-93) should be particularly noted.

According to these results the temperature dependence of  $\bar{\sigma}_\gamma(E, T)$  is contained in the function  $\psi(\xi, x)$ . To clarify the nature of this function, it should first be noted that the quantity  $\exp[-\frac{1}{4}\xi^2(x - y)^2]$  in the integrand of Eq. (2-111) is a Gaussian centered about the point  $y = x$ , whose width (standard deviation) is proportional to  $1/\xi$ . In view of Eqs. (2-108) and (2-109), however,  $1/\xi$  varies as  $\sqrt{T}$ , so that at low temperature the Gaussian in the integrand is rather narrow. As a consequence, the bulk of the integral in Eq. (2-111) comes from the region in the immediate vicinity of  $y = x$ , and the denominator in the integrand can be extracted from the integral as  $1 + x^2$ . The remaining Gaussian can then be integrated, and it is easily seen that  $\bar{\sigma}_\gamma(E, T)$  reduces to the original Breit-Wigner formula. This is to be expected since at low temperature there is little thermal motion of the nuclei and therefore no Doppler effect.

At high temperature, on the other hand,  $1/\xi$  is large, the Gaussian is broad, and the integral in Eq. (2-111) is now dominated by the term  $1/(1 + y^2)$ . Since this term is peaked at  $y = 0$ , the Gaussian can be extracted as  $\exp(-\xi^2 x^2/4)$  and the remaining integral can then be evaluated. The resulting expression for  $\bar{\sigma}_\gamma(E, T)$  is

$$\bar{\sigma}_\gamma(E, T) = \frac{\sigma_1 \Gamma_\gamma \sqrt{\pi}}{2\Gamma_D} \exp\left[-\frac{(E - E_1)^2}{\Gamma_D^2}\right]. \quad (2-113)$$

Equation (2-113) shows that at high temperature the resonance exhibits a Gaussian dependence on the energy of the incident neutron. Furthermore, the width of the resonance is only a function of  $\Gamma_D$  which, in view of Eq. (2-109), does not depend upon any of the nuclear properties of the resonance such as  $\Gamma$ ,  $\Gamma_\gamma$ , etc. In this case, the resonance is said to exhibit a *pure Doppler shape*.

The above extremes are not usually met in practice, and the actual shape of an absorption resonance must be computed from Eq. (2-110) and the tables. Resonances are then always found to be broader than their natural width and they are said to be *temperature broadened* or *Doppler broadened*. This is illustrated in Fig. 2-32, where the first resonance in  $U^{238}$  is shown for three different temperatures. The curve for  $T = 0^\circ K$ , of course, is just the ordinary Breit-Wigner formula.

It is easy to show (cf. Prob. 2-31) that although the shape of a resonance is changed by the Doppler effect, the total area under the resonance is a constant,

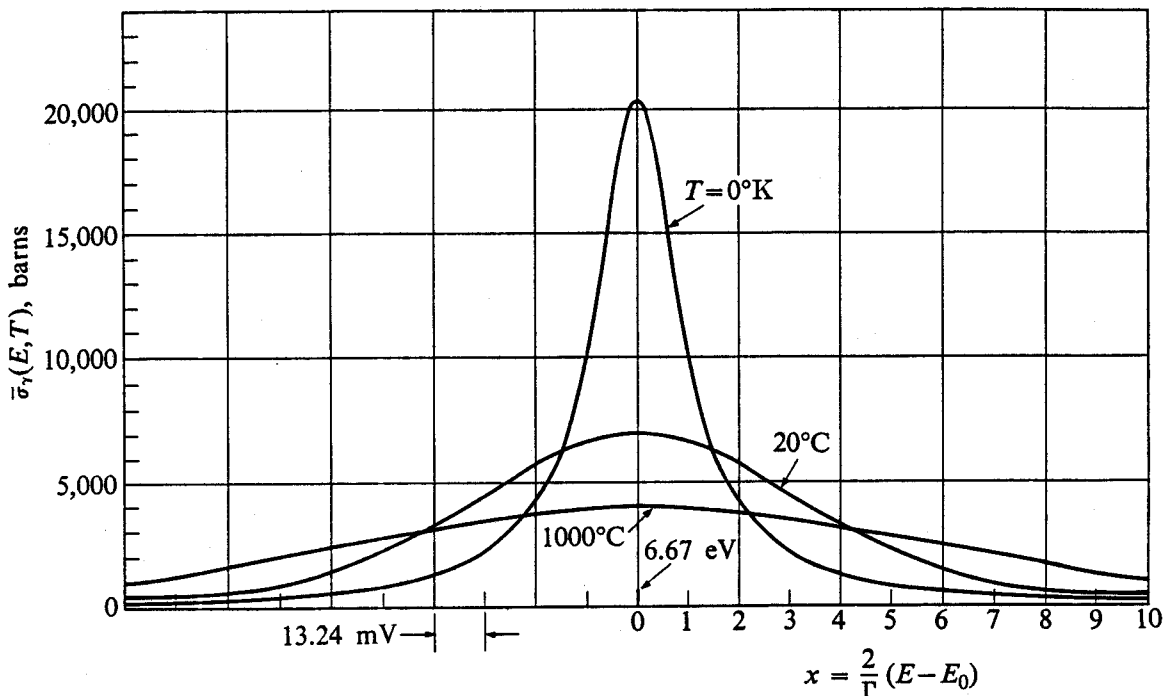


**Fig. 2-32.** Doppler broadening of the capture cross section of  $\text{U}^{238}$  at the 6.67 eV resonance.

independent of temperature. It might appear, therefore, that Doppler broadening would have no effect on the absorption of neutrons in a reactor. This is not the case, however, for as will be shown in Chapter 7, the number of neutrons in the vicinity of a resonance increases with temperature. Neutron capture in the resonance therefore tends to increase with temperature, an effect which has an important bearing on reactor control. This is discussed further in Chapter 13.

At low energy, i.e., where  $E \ll E_1$ , the function  $\psi(\xi, x)$  approaches a constant value. From Eq. (2-110),  $\bar{\sigma}_\gamma(E, T)$  then varies as  $1/v$ , as does the ordinary Breit-Wigner formula at these energies. This result is more general than indicated by the form of Eq. (2-110). Thus if  $\sigma_\gamma(E_c) = \text{constant}/v_r$  is inserted into Eq. (2-103), the  $v_r$ 's cancel giving

$$\bar{\sigma}_\gamma(E, T) = \frac{\text{constant}}{Nv} \int N(V_z) dV_z. \quad (2-114)$$

The remaining integral is just the atom density,  $N$ , so that

$$\bar{\sigma}_\gamma(E, T) = \frac{\text{constant}}{v}. \quad (2-115)$$

This result does not depend on the form assumed for the function  $N(V_z)$  and obviously holds for any  $1/v$  cross section, i.e., all absorption reactions, not just radiative capture. Equation (2-115) shows that when a monoenergetic beam of neutrons strikes a target consisting of  $1/v$  absorbers, the observed cross section is also  $1/v$ , regardless of the velocity distribution of the nuclei in the target.

In the case of scattering, the Doppler effect can usually be ignored for the scattering resonances found at high energies in light and intermediate nuclei, since the natural widths of these resonances are so large compared to the Doppler width. It must be included, however, in calculations of the scattering cross section at the narrow resonances in heavier nuclei. The average scattering cross section  $\bar{\sigma}_s(E, T)$  can be found by introducing  $\sigma_s(E_c)$  from Eq. (2-69) into Eq. (2-103) and proceeding as in the derivation of  $\bar{\sigma}_\gamma(E, T)$ .\* The result is

$$\bar{\sigma}_s(E, T) = \frac{\sigma_1 \Gamma_n}{\Gamma} \psi(\xi, x) + \frac{\sigma_1 R}{\lambda_1} x(\xi, x) + 4\pi R^2, \quad (2-116)$$

where  $x(\xi, x)$  is the function

$$x(\xi, x) = \frac{\xi}{\sqrt{\pi}} \int_{-\infty}^{\infty} \frac{y \exp[-\frac{1}{4}\xi^2(x-y)^2]}{1+y^2} dy. \quad (2-117)$$

A short table of  $x(\xi, x)$  is also given in Table 2-1. More comprehensive tabulations are noted in the references.

## 2-15 On Cross-Section Compilations

It should be reiterated that compilations of cross sections such as BNL-325 present *experimental data* which are not corrected for either Doppler broadening or the resolution of the instruments used in the measurements. For this reason the cross sections, particularly in the resonance regions of intermediate and heavy nuclei, appear considerably different from values computed with the formulas discussed in this chapter. For example, as noted in the introduction to BNL-325, the maximum value of the total cross section at the 6.67-eV resonance in  $U^{238}$ , as shown in the tables and in Fig. 2-12, is about 7000 b. With perfect resolution, however, the maximum cross section would be measured as 8000 b at room temperature. Correcting for Doppler broadening gives a true peak cross section of 20,000 b, which is the value obtained from the Breit-Wigner formula.

## References

### General

AMALDI, E., "The Production and Slowing Down of Neutrons," *Handbuch der Physik*, Berlin: Springer-Verlag, Vol. 38, Part 2, 1959, Sections A and B.

BECKURTS, K. H., and K. WIRTZ, *Neutron Physics*. Berlin: Springer-Verlag, 1958 (translated edition, 1964), Part I.

BURCHAM, W. E., *Nuclear Physics*. New York: McGraw-Hill, 1963, Part D.

CURTISS, L. F., *Introduction to Neutron Physics*. Princeton, N. J.: Van Nostrand, 1959.

---

\* It is also necessary to assume in the case of scattering that  $v_r \approx v \approx$  constant in the vicinity of the resonance. This is so if the resonance is narrow and located at an energy well above thermal energies.

- EISBERG, R. M., *Fundamentals of Modern Physics*. New York: Wiley, 1961, Chapters 15 and 16.
- EVANS, R. D., *The Atomic Nucleus*. New York: McGraw-Hill, 1955, Chapter 14.
- GLASSTONE, S., and A. SESONSKE, *Nuclear Reactor Engineering*. Princeton, N.J.: Van Nostrand, 1963, Chapter 2.
- GREEN, A. E. S., *Nuclear Physics*. New York: McGraw-Hill, 1955, Chapters 7 and 13.
- HUGHES, D. J., *Neutron Cross Sections*. New York: Pergamon Press, 1957.
- ISBIN, H. S., *Introductory Nuclear Reactor Theory*. New York: Reinhold, 1963, Chapter 2.
- KAPLAN, I., *Nuclear Physics*, 2nd ed. Reading, Mass.: Addison-Wesley, 1963, Chapters 16 and 18.
- LITTLER, D. J., and J. F. RAFFLE, *An Introduction to Reactor Physics*, 2nd ed. New York: McGraw-Hill, 1957, Chapter 5.

#### At a somewhat more advanced level see:

- AJZENBERG-SELOVE, F., Editor, *Nuclear Spectroscopy*. New York: Academic Press, 1960, Part A, Chapter III and IV A; Part B, Chapter V A and VI D.
- ENDT, P. M., and M. DEMEUR, *Nuclear Reactions*, Vol. I. Amsterdam: North Holland, 1959, Chapters 5, 6, 7, 8.
- Inelastic Scattering of Neutrons in Solids and Liquids*. Vienna, Austria: International Atomic Energy Agency, 1961, 1963. These books contain a collection of papers on the various interactions of low-energy neutrons with matter. Some of the latest information on this difficult subject is to be found in these papers.
- MARION, J. B., and J. L. FOWLER, Editors, *Fast Neutron Physics*. New York: Interscience, 1963, Part II.
- PHILLIPS, G. C., J. B. MARION, and J. R. RISSER, Editors, *Progress in Fast Neutron Physics*. Chicago: University of Chicago Press, 1963.
- SEGRE, E., Editor, *Experimental Nuclear Physics*. New York: Wiley, 1959, Volume II.
- WEINBERG, A. M., and E. P. WIGNER, *The Physical Theory of Neutron Chain Reactors*. Chicago: University of Chicago Press, 1958, Chapters 2, 3, 4, 6.

#### Laboratory—Center-of-mass tables

MARION, J. B., T. I. ARNETTE, and H. C. OWENS, "Tables for the Transformation Between the Laboratory and Center-of-Mass Coordinate Systems and for the Calculations of the Energies of Reaction Products," ORNL-2574, 1959. These tables facilitate calculations involving the transformation between center-of-mass and laboratory coordinates.

#### Cross-section data

HUGHES, D. J., *et al.*, *Neutron Cross Sections*. BNL-325, Second Edition (1958) plus supplements (1960, 1964 and 1965). Tables of low-energy (thermal) cross sections and resonance parameters, and curves of neutron cross sections as a function of energy will be found in these reports. The cross-section curves show raw experimental data.

HOWERTON, R. J., "Semi-Empirical Neutron Cross Sections 0.5 to 15 MeV," UCRL-5351, November 1958, plus supplements. In addition to data from BNL-325, this report contains computed and extrapolated values of cross sections where data are not presently available.

HOWERTON, R. J., "Tabulated Neutron Cross Sections, 0.001–14.5 MeV," UCRL-5226, May 1958, plus supplements. Cross sections are given in tabular form in this report; this saves time in reading the curves in BNL-325 or UCRL-5351.

HOWERTON, R. J., D. BRAFF, W. J. CAHILL, and N. CHAZAN, "Thresholds of Nuclear Reactions," UCRL-14000, May 1964.

GOLDBERG, M. D., V. M. MAY, and J. R. STEHN, "Angular Distributions in Neutron Induced Reactions," BNL-400, Second Edition, October 1962.

The Neutron Cross-Section Compilation Group at Brookhaven National Laboratory compiles data on neutron cross sections. This group is responsible for the preparation of new supplements to the neutron cross-section reports BNL-325 and BNL-400. The Reactor Cross-Section Compilation Group, also at Brookhaven, evaluates and analyzes neutron cross sections and from time to time publishes analyses of selected cross sections. The Compilation Group and Evaluation Group together comprise the "Sigma Center" at Brookhaven.

The Computerized Bibliographic Index of Neutron Cross Section Data ("CINDA-65"), EANDC-46, May 1, 1965. This report contains a tabulation of references to measurements of neutron cross sections. The report represents an international effort to provide a systematic bibliography of measurements of neutron cross-section data.

Charged-particle cross sections are compiled by the Charged-Particle Cross-Section Data Center at Oak Ridge National Laboratory. Reports of this group are designated ORNL-CPX-1, ORNL-CPX-2, etc. Cross sections of charged-particle interactions will also be found in *Charged-Particle Cross Sections*, N. JARMIE, J. D. SEAGRAVE, and D. B. SMITH, Editors, Los Alamos Scientific Laboratory Reports LA-2014 (1956) and LA-2424 (1960).

### Tables of Doppler functions

BEYNON, T. D., and I. S. GRANT, "Evaluation of the Doppler-Broadened Single-Level and Interference Functions," *Nucl. Sci. Eng.* 17, 547–550 (1963).

ROSE, M. E., W. MIRANKER, and P. LEAK, "A Table of the Integral  $\psi(x, t)$ ," WAPD-SR-506, October 1954. (Note that the parameter  $t$  in this reference is related to the parameter  $\xi$  used in Section 2-14 by  $t = \xi^{-2}$ .)

SAILOR, V. L., "A Table of the Integral  $\psi(x, t)$ ," BNL-257, (1953). (See note in reference to Rose, *et al.*)

SETH, K. K., and R. H. TABONY, "A Tabulation of the Doppler Integrals  $\psi(x, t)$  and  $\emptyset(x, t)$ ," United States Atomic Energy Commission Report TID-21304, February 1964. This is the most extensive tabulation of Doppler functions available. In this report the function  $X$  is denoted by  $\emptyset$ ; note also that  $t = \xi^{-2}$ .

### Problems

[*Note:* Helpful data will be found in Appendix I.]

- 2-1. A beam of 0.025 eV neutrons which has a cross-sectional area of  $0.01 \text{ cm}^2$  strikes a thin  $\text{Li}^6$  target, inducing the exothermic reaction  $\text{Li}^6(n, \alpha)\text{H}^3$ . The beam intensity is  $5 \times 10^{10}$  neutrons/ $\text{cm}^2\text{-sec}$ . The target has an area of  $0.5 \text{ cm}^2$  and it is  $0.005 \text{ cm}$  in thickness. The cross section for this reaction at 0.025 eV is 945 barns. (a) What is the density of neutrons in the beam? (b) What is the atom density of the target? (c) What is the rate of production of tritium in the target? (d) What is the maximum tritium activity

in curies which can be induced in the target by this beam? [Note: The density of Li<sup>6</sup> is 0.5 gm/cm<sup>3</sup> and the half-life of H<sup>3</sup> is approximately 12 yr.] The atomic weight of Li<sup>6</sup> is 6.01513.

2-2. A monoenergetic beam of neutrons of intensity  $10^{10}$  neutrons/cm<sup>2</sup>-sec is incident upon a thin sheet of material. Confining attention to a particular atom, how long must one wait, on the average, before a neutron interacts with it, if the total cross section is 10 barns?

2-3. Compute the minimum intensity of a beam of 0.025 eV neutrons required to produce 10  $\mu$ curies of Al<sup>28</sup> ( $T_{1/2} = 2.3$  min) in an aluminum target (100% Al<sup>27</sup>) having an area of 1 cm<sup>2</sup> and a thickness of 0.1 cm.

2-4. Stainless steel No. 347 (density 7.86 gm/cm<sup>3</sup>) has been used in the fuel elements of many reactors. (a) Using the information given in the table below, compute the macroscopic absorption cross section of SS-347 at 0.025 eV. (b) If a fuel element consists of a homogeneous mixture of SS-347 and U<sup>235</sup> with atom ratio  $N(\text{Fe})/N(\text{U}^{235}) = 150$ , compute the macroscopic absorption cross section of the fuel element at 0.025 eV.

**Composition, weight %**

C	Si	P	S	Cr	Mn	Ni	Nb	Fe
0.08	1.00	0.04	0.05	18.00	2.00	10.00	0.80	remainder

2-5. What is the probability that a neutron can move 2 mean free paths without interacting in a medium? What is this probability for 1/2 mean free path?

2-6. Using the data in BNL-325, compute the mean free paths of neutrons with the following energies in the specified media.

	Energy	Medium
(a)	14 MeV	air
(b)	2 MeV	air
(c)	0.025 eV	air
(d)	14 MeV	water
(e)	2 MeV	water
(f)	0.025 eV	water
(g)	14 MeV	uranium
(h)	0.025 eV	uranium

2-7. Derive a formula for the relative probability that a neutron will undergo radioactive decay before being absorbed in an infinite medium. What is this probability for a 0.025 eV neutron if the medium is D<sub>2</sub>O?

2-8. Using Eqs. (2-25), (2-26), and (2-27) show that the total kinetic energy of two particles in the center-of-mass system is given by

$$E_c = \frac{1}{2}\mu v_r^2,$$

where  $\mu$  is the reduced mass of the particles and  $v_r$  is their relative speed.

2-9. Show that when a neutron is scattered from hydrogen, the angle between the laboratory velocities of the scattered neutron and the recoiling proton is always 90°.

2-10. It was shown in Section 1-9 that in the laboratory system the difference between the kinetic energies of the final and initial particles in a nuclear reaction is equal to the

*Q*-value. In the center-of-mass system, what is the difference between the initial and final kinetic energies of the particles equal to? Explain.

2-11. (a) Show that the angles in the laboratory and center-of-mass systems at which the particle *c* emerges from the reaction  $a(b, c)d$  are related by

$$\tan \vartheta = \frac{\sin \theta}{\gamma + \cos \theta},$$

where

$$\gamma \approx \sqrt{\frac{M_b M_c}{M_a M_d} \frac{E_b}{E_b + Q(1 + M_b/M_a)}},$$

and  $M_a$ ,  $M_b$ , etc. are the masses of the particles,  $E_b$  is the laboratory energy of particle *b*, and  $Q$  is the *Q*-value of the reaction. (b) Show that the kinetic energy of the particle *c* in the laboratory is given by

$$(E_c)_{\text{lab}} = \frac{M_b M_c S^2 E_b}{(M_a + M_b)^2},$$

where

$$S = \cos \vartheta + \gamma^{-1} \cos(\theta - \vartheta).$$

2-12. A 1-MeV neutron is elastically scattered from Be<sup>9</sup>. (a) Find the energy of the incident neutron in the center-of-mass system. (b) Find the maximum energy loss of the neutron after scattering. (c) If the angle of scattering of the neutron in the center-of-mass system is 90°, find the recoil energy of the target nucleus in the laboratory.

2-13. One-MeV deuterons bombard a stationary target containing tritium and produce neutrons by the H<sup>3</sup>(d, n)He<sup>4</sup> reaction. Find the maximum and the minimum energy of the emergent neutrons in the laboratory system.

2-14. Show that the laboratory and center-of-mass angles are related by the formula

$$\sin(\theta - \vartheta) = \gamma \sin \vartheta,$$

where  $\gamma$  is given by Eq. (2-52) (see also Problem 2-11). This formula is more convenient than Eq. (2-51) for transformations from laboratory to center-of-mass coordinates.

2-15. Resonances are observed in the neutron total cross section of B<sup>10</sup> at the following (laboratory) energies: 0.530 MeV, 1.90 MeV, 2.80 MeV, 3.40 MeV, 4.20 MeV, etc. If the *Q*-value of the reaction B<sup>10</sup>(d, p)B<sup>11</sup> is 9.217 MeV, at what energies, measured from the ground state, are the excited states which give rise to the above resonances?

2-16. The first resonance in the total cross section of Li<sup>6</sup> occurs at a laboratory energy of 0.255 MeV. (a) Using the fact that the threshold for the Li<sup>7</sup>(n, 2n) reaction is 8.442 MeV, find the binding energy of the last neutron in Li<sup>7</sup>. (b) At what energy above the ground state of Li<sup>7</sup> does the energy level occur that gives rise to the first resonance in  $\sigma_t$  for Li<sup>6</sup>?

2-17. It so happens that the square of the atomic fine structure constant ( $\hbar c/e^2 = 137$ ) is about 10 times the ratio of the mass of the neutron to the mass of the electron ( $M_n/m_e \approx 1835$ ). Using this fact, show that the quantity  $kR$  in Section 2-7 is given approximately by

$$kR \approx A^{1/3} \sqrt{E/10},$$

where  $A$  is the mass number of the target nucleus and  $E$  is the neutron energy in MeV. (This is a handy formula for determining the number of partial waves involved in a neutron interaction.)

2-18. A small detector with an aperture of  $0.4\text{cm}^2$  is placed in a beam of 14 MeV neutrons and registers 1000 counts/sec. (a) If a graphite target 0.2 cm thick is placed in the beam 1 m from the detector, what is the new count rate? (b) If the detector is placed  $20^\circ$  from the direction of incidence what is the new count rate? [Hint: Use Fig. 2-20.]

2-19. Using the cross-section data in BNL-325, estimate the nuclear radii of the following nuclei.

(a)  $\text{C}^{12}$

(b)  $\text{Ba}^{135}$

(c)  $\text{Bi}^{209}$

(d)  $\text{U}^{238}$

Compare these values with radii computed from Eq. (1-3).

2-20. A hydrogen target 0.1 cm in area contains  $6.6 \times 10^{22}$  hydrogen atoms/cm<sup>3</sup>. A 100% efficient neutron detector having an aperture of  $1\text{cm}^2$  is placed 100 cm from the target and at  $45^\circ$  to the direction of incidence. If the target is bombarded by a beam of 1 MeV neutrons having an intensity of  $10^8$  neutrons/cm<sup>2</sup>-sec, what is the counting rate in the detector?

2-21. (a) Using the data in BNL-400, determine the differential elastic cross section of  $\text{Be}^9$  in the laboratory system for 7.0 MeV neutrons. (b) Compute the transport cross section of  $\text{Be}^9$  at 7.0 MeV.

2-22. The differential elastic cross section of  $\text{He}^4$  in the center-of-mass system at a certain energy is given by

$$\sigma_s(\theta) = \frac{\sigma_s}{4\pi} (1 + \cos \theta).$$

(a) Find the elastic cross section at this energy. (b) What fraction of the elastic neutrons appears at angles greater than  $90^\circ$  in the center-of-mass system? (c) Plot the differential cross section in the center-of-mass and laboratory systems. (d) Compute the transport cross section at this energy.

2-23. The energies of the excited states of two *hypothetical* nuclei of mass numbers 10 and 11 are given in the table below. All energies are in MeV and measured from the ground state. The binding energy of the last neutron in these nuclei is 6.10 MeV and 4.80 MeV, respectively, and the absorption cross section is negligible.

$A = 10$	$A = 11$
1.60	2.00
3.00	4.50
4.00	4.60
4.25	5.20
4.60	5.70
5.10	6.00
6.15	6.35
6.20	6.70
6.25	7.20
6.95	8.00
7.80	etc.
	etc.

Make a rough plot of the total and inelastic cross sections of nuclide  $A = 10$  as a function of the laboratory energy of incident neutrons. Show clearly at what energies resonances may be expected to occur, and indicate the inelastic threshold.

2-24. Plot the total, elastic, and inelastic cross sections of bismuth from 0.1 MeV to 14 MeV.

2-25. (a) When 10-MeV neutrons strike  $\text{Th}^{232}$ , what is the temperature of the compound nucleus that is formed? (b) What is the most probable energy of the inelastic neutrons? (c) What is the average energy of the inelastic neutrons?

2-26. The first excited state of the nucleus  $Z^A$  is at the energy  $\epsilon_1$ . (a) Show that the angles of emission of the inelastic neutron in the laboratory and in the center-of-mass system are related by

$$\tan \vartheta = \frac{\sin \theta}{\gamma + \cos \theta},$$

where

$$\gamma = \frac{1}{A} \sqrt{\frac{AE}{AE - (A + 1)\epsilon_1}},$$

and  $E$  is the laboratory energy of the incident neutron. (b) Show that the angular distribution of the inelastic neutrons becomes increasingly forward peaked with *decreasing* energy of the incident neutron. Explain this result on physical grounds.

2-27. The total and nonelastic cross sections of a certain heavy, nonmagic, and nonfissionable nucleus at 7 MeV are 3 barns and 1.5 barns, respectively. Give reasonable values of the following cross sections at this energy.

(a)  $\sigma_s$

(b)  $\sigma_i$

(c)  $\sigma_\gamma$

(d)  $\sigma_a$

2-28. Determine in the most appropriate manner  $\sigma_\gamma$  for the following nuclei (or molecules) at the specified energies.

	Nucleus	Energy		Nucleus	Energy
(a)	$\text{H}^1$	0.025 eV	(f)	$\text{Sm}$	0.1 eV
(b)	$\text{H}^1$	1.0 eV	(g)	$\text{Cd}^{113}$	1.0 eV
(c)	$\text{H}_2\text{O}$	1.0 eV	(h)	$\text{U}^{236}$	1.0 eV
(d)	$\text{C}^{12}$	10 eV	(i)	$\text{U}^{238}$	1.0 eV
(e)	$\text{N}^{14}$	0.025 eV	(j)	$\text{U}^{235}\text{O}_2$	10 keV

2-29. Using atomic mass tables, compute the threshold energies for the following reactions.

(a)  $\text{O}^{16}(\text{n}, \text{p})\text{N}^{16}$

(d)  $\text{C}^{12}(\text{n}, \text{n}')3\alpha$

(b)  $\text{H}^2(\text{n}, 2\text{n})\text{H}^1$

(e)  $\text{H}^2(\text{d}, \text{n})\text{He}^3$

(c)  $\text{Be}^9(\text{n}, 2\text{n})2\alpha$

(f)  $\text{H}^2(\gamma, \text{n})\text{H}^1$

2-30. The partial widths of the first resonance in  $\text{U}^{236}$  at 5.49 eV are  $\Gamma_\gamma = 29 \text{ mV}$  and  $\Gamma_n = 1.8 \text{ mV}$ . Plot the Doppler-broadened capture cross section at the following temperatures.

(a) 0°K

(b) 200°C

(c) 1000°C

2-31. Show that the total area under a Doppler-broadened resonance is essentially independent of temperature.

2-32. Plot the maximum value of the capture cross section at the first resonance in  $U^{238}$  at 6.67 eV as a function of temperature from  $T = 0^{\circ}\text{K}$  to  $1000^{\circ}\text{C}$ . [Note:  $\Gamma_\gamma = 26 \text{ mV}$  and  $\Gamma_n = 1.52 \text{ mV}$ .]

2-33. Show that at low temperature the Doppler-broadened capture cross section reduces to the ordinary Breit-Wigner formula.

2-34. The first resonance in  $In^{115}$  is at 1.457 eV and has the following parameters:  $\Gamma_\gamma = 72 \text{ mV}$ ,  $\Gamma_n = 3.03 \text{ mV}$ , and  $g = 11/20$ . Plot  $\sigma_\gamma$  for this resonance at  $0^{\circ}\text{K}$  and  $20^{\circ}\text{C}$  and compare with the data in BNL-325.

2-35. Show that at high temperature the Doppler-broadened capture cross section is given by Eq. (2-113).

2-36. Derive the following properties of the function  $\psi(\xi, x)$ .

$$(a) \psi(\infty, x) = (1 + x^2)^{-1} \quad (b) \int_{-\infty}^{\infty} \psi(\xi, x) dx = \pi$$

2-37. Derive the following properties of the function  $\chi(\xi, x)$ .

$$(a) \chi(\infty, x) = 2x(1 + x^2)^{-1} \quad (b) \int_{-\infty}^{\infty} \chi(\xi, x) dx = 0$$

$$(c) \chi(\xi, 0) = 0$$

2-38. Show that the functions  $\chi(\xi, x)$  and  $\psi(\xi, x)$  are related by the following:

$$\chi(\xi, x) = 2x\psi(\xi, x) + \frac{4}{\xi^2} \frac{d\psi(\xi, x)}{dx}.$$

2-39. A thin disc of radius  $R$ , rotating at an angular speed of  $\omega$  rad/sec is exposed near its outer edge to a monoenergetic neutron beam of area  $a$  as shown in Fig. 2-33. (a) If the disc is maintained at a temperature of  $T = 0^{\circ}\text{K}$ , compute the interaction rate in the target as a function of  $\omega$  and the laboratory energy of the incident neutrons. (b) Discuss the effect which changing  $\omega$  has on the interaction rate in the case of  $1/v$  absorption and at an absorption resonance.

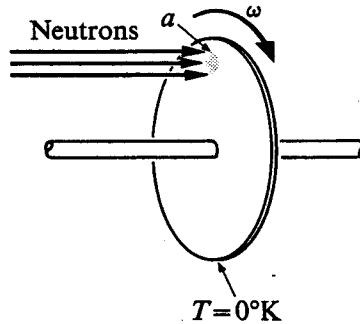


Figure 2-33

# 3

## Nuclear Fission

Nuclear *fission* is the process in which a heavy nucleus splits into two fragments, with the release of considerable energy and the emission of neutrons and  $\gamma$ -rays. In the present chapter, those aspects of the fission process that are of the greatest practical importance in reactor theory will be discussed.

### 3-1 The Mechanics of Fission

It will be recalled from Chapter 1 that the binding energy per nucleon decreases with increasing mass number for  $A$  greater than about 50. A more stable configuration is obtained, therefore, when a heavy nucleus splits into two lighter nuclei, and this is the origin of the fission process. On this basis, however, it might be expected that all heavy nuclei would spontaneously undergo fission, and, indeed, heavy nuclei should not exist at all. While such *spontaneous fission* is possible, in fact, for all nuclei with  $A$  greater than about 50, it happens only rarely. For fissions to take place with a reasonable probability, energy must be supplied to the nucleus in one way or another. This is because of the manner in which the fission process occurs.

For simplicity, the initial state of a fissioning nucleus  $Z^A$  can be assumed to be a sphere of radius  $R$  as shown in Fig. 3-1(a). At the end of the process, two nuclei  $Z_1^{A_1}$  and  $Z_2^{A_2}$  are formed having radii  $R_1$  and  $R_2$ , respectively, as shown in Fig. 3-1(c). The details of how the nucleus is transformed from the initial state (a) to the final state (c) are not completely understood, but it is reasonable to assume that this involves a sequence of dumbbell-shaped intermediate states of the type shown in Fig. 3-1(b).

It is interesting to consider the potential energy of the fissioning nucleus as a function of the distance  $r$  between the two separating lobes. This is equal to the

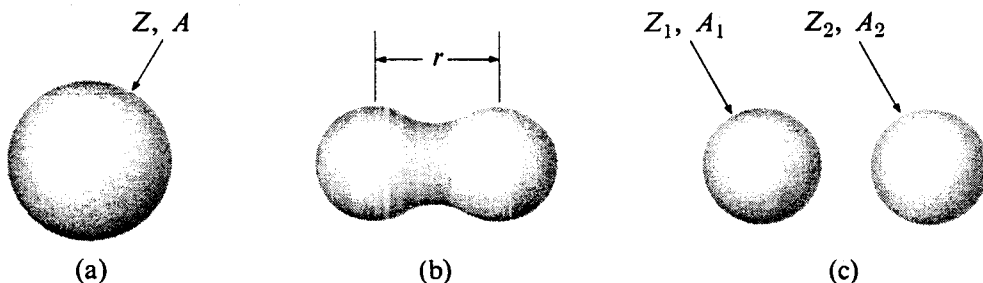


Fig. 3-1. Stages in fission.

total energy of the system at any point minus the kinetic energy. When  $r = 0$ , the total energy is  $M_A c^2$ , where  $M_A$  is the mass of the initial nucleus, and the kinetic energy is zero. In order to deform the nucleus into a dumbbell configuration, energy must be added to the system. This is due to the fact that since nucleons attract one another, energy is required to increase the average distance between them. The nucleus in an intermediate state thus has a larger potential energy than it had originally. The potential energy continues to increase in this way with increasing  $r$  as shown in Fig. 3-2 until a point is reached where the two lobes of the dumbbell begin to separate. From this point on, the nuclear energy of the two fragments remains constant while the potential energy decreases, owing to the decreasing Coulomb repulsive energy of the two fragments.

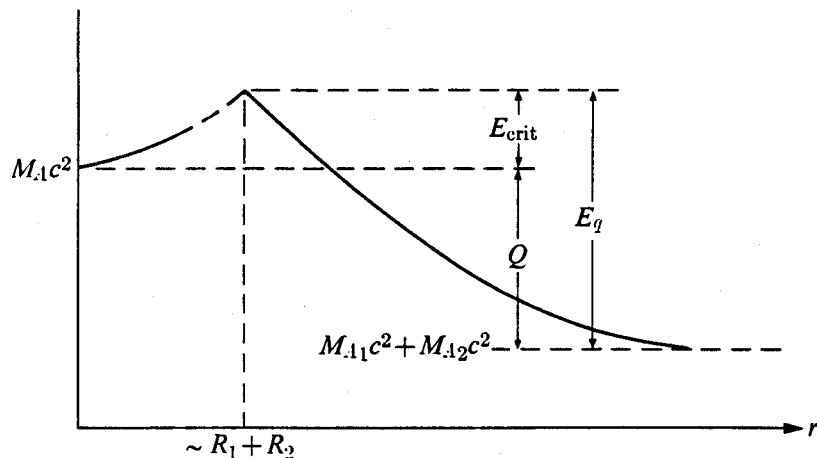


Fig. 3-2. Potential energy of fissioning nucleus as a function of the distance between the separating lobes.

The energy which must be supplied to a nucleus in order for it to undergo fission immediately is known as the *critical energy* or *threshold energy*,  $E_{\text{crit}}$ , and can be estimated with the help of Fig. 3-2. First it will be remembered that the difference between the initial and final energies of the system is just the  $Q$ -value of the fission reaction. Then, as indicated in the figure,  $E_{\text{crit}}$  is simply equal to the Coulomb energy  $E_q$  computed at the point where the fragments separate, minus the  $Q$ -value of the reaction; that is,

$$E_{\text{crit}} = E_q - Q. \quad (3-1)$$

As will be discussed in Section 3-4, all fissioning nuclei do not split in the same way. Thus, although the mass of the initial nucleus is well defined, the masses of the fission fragments are not. The  $Q$ -value for fission leading to one set of fission fragments is therefore somewhat different from the  $Q$ -value for fission leading to another, and for this reason there is no single  $Q$ -value for fission. What is ordinarily referred to as the fission  $Q$ -value is actually an average of the  $Q$ -values over all modes of fission. This fission  $Q$ -value is determined experimentally by measuring the total energy released from a mass of nuclei undergoing fission.

A rough estimate of the Coulomb energy can be made by assuming that each fragment is a uniform sphere unaffected by the presence of the other. In this case,  $E_q$  is given by

$$E_q = \frac{Z_1 Z_2 e^2}{R_1 + R_2}. \quad (3-2)$$

Recalling from Chapter 1 (cf. Section 1-3) that nuclear radii are given approximately by the formula

$$R = \frac{r_e}{2} A^{1/3},$$

where  $r_e = e^2/m_e c^2$  is the classical radius of the electron, Eq. (3-2) becomes

$$\begin{aligned} E_q &= \frac{Z_1 Z_2 e^2}{(r_e/2)(A_1^{1/3} + A_2^{1/3})} \\ &= \frac{Z_1 Z_2}{A_1^{1/3} + A_2^{1/3}} 2m_e c^2. \end{aligned}$$

Since  $2m_e c^2 \approx 1$  MeV,  $E_q$  is

$$E_q = \frac{Z_1 Z_2}{A_1^{1/3} + A_2^{1/3}} \text{ MeV.} \quad (3-3)$$

If, for simplicity, it is also assumed that fission leads to fragments of equal mass and equal charge, i.e.,  $A_1 = A_2 = A/2$  and  $Z_1 = Z_2 = Z/2$ , Eq. (3-3) reduces to

$$E_q = 0.16 Z^2 / A^{1/3}. \quad (3-4)$$

For uranium,  $E_q$  is approximately 218 MeV, the average  $Q$ -value is 212 MeV, and the critical energy is therefore about 6 MeV. For nuclei lighter than uranium the critical energies are considerably higher; for example,  $E_{\text{crit}} \approx 20$  MeV for  $\text{Pb}^{208}$ . It is for this reason that fission is of practical importance only for the heaviest nuclei. Critical energies of several heavy nuclei are given in Table 3-1; it should be noted that in the table it is the indicated nucleus which fissions.

Fission can also occur without the addition of the critical energy by the quantum-mechanical process of "leaking through" the Coulomb barrier, much like  $\alpha$ -particles do in  $\alpha$ -decay. Such *spontaneous fission* proceeds, however, with very small probability. In  $\text{U}^{238}$ , for example, only one spontaneous fission occurs per gm/100 sec, which is equivalent to a half-life of  $5.5 \times 10^{15}$  years. The spontaneous fission rates of  $\text{U}^{233}$ ,  $\text{U}^{235}$ , and  $\text{Pu}^{239}$  might reasonably be expected to be larger than that of  $\text{U}^{238}$  since according to Table 3-1 the critical energies of these nuclei are somewhat smaller. In actual fact, however, the spontaneous fission rate of  $\text{U}^{238}$  is several orders of magnitude larger than those of  $\text{U}^{233}$ ,  $\text{U}^{235}$ , and  $\text{Pu}^{239}$ . This unexpected situation is not understood at the present time. Despite the slow rate at which spontaneous fission occurs, it is not unimportant in reactor analysis,

**Table 3-1**  
**Critical Energies for Fission**

Fissioning nucleus $Z^A$	Critical energy	Binding energy of last neutron in $Z^A$
$\text{Th}^{232}$	5.9	*
$\text{Th}^{233}$	6.5	5.1
$\text{U}^{233}$	5.5	*
$\text{U}^{234}$	4.6	6.6
$\text{U}^{235}$	5.75	*
$\text{U}^{236}$	5.3	6.4
$\text{U}^{238}$	5.85	*
$\text{U}^{239}$	5.5	4.9
$\text{Pu}^{239}$	5.5	*
$\text{Pu}^{240}$	4.0	6.4

\* Neutron binding energies are not relevant for these nuclei since they cannot be formed by the absorption of neutrons by the nuclei  $Z^{A-1}$ .

since it represents an uncontrolled source of extraneous neutrons in all reactors, particularly those containing large amounts of  $\text{U}^{238}$ .

For practical purposes, however, the energy  $E_{\text{crit}}$  represents a real threshold for fission, and any method which supplies this energy is said to "induce" the fission. By far the most important method is neutron absorption. In this connection it will be recalled from Chapter 2 that when a neutron is absorbed, the compound nucleus is formed with an excitation energy equal to the kinetic energy of the incident neutron plus its binding energy to the compound system. If this binding energy is greater than the critical energy of the compound nucleus, fission can be induced with neutrons of essentially zero kinetic energy. For example, according to Table 3-1, the binding energy of the last neutron in  $\text{U}^{236}$  is 6.4 MeV, while the critical energy is only 5.3 MeV. Thus, when a neutron with zero kinetic energy is absorbed by  $\text{U}^{235}$ , the compound nucleus  $\text{U}^{236}$  is produced at about 1.1 MeV above the critical energy, and fission may immediately occur. Nuclei such as  $\text{U}^{235}$  that lead to fission following the absorption of a zero energy neutron are called *fissile*. Note, however, that although in this example it is the  $\text{U}^{235}$  which is said to be fissile, the nucleus that actually fissions is  $\text{U}^{236}$ . From Table 3-1 it will be evident that  $\text{U}^{233}$  and  $\text{Pu}^{239}$  are also fissile. In addition,  $\text{Pu}^{241}$  and several other nuclei not indicated in the table, are also fissile.

With most heavy nuclei other than  $\text{U}^{233}$ ,  $\text{U}^{235}$ ,  $\text{Pu}^{239}$ , and  $\text{Pu}^{241}$ , the binding energy of the incident neutron is not sufficient in itself to supply the compound nucleus with the critical energy, and a neutron must have some kinetic energy in order to induce fission. In particular, this is always the case when the struck nucleus contains an *even* number of nucleons, since the binding energy of the incident

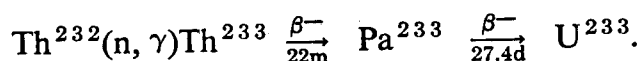
neutron to an even-*A* nucleus is always less than to an odd-*A* nucleus. (This odd-even variation in binding energy is evident in Table 3-1.) For instance, the binding energy of the last neutron in  $U^{239}$  is only 4.9 MeV, and this is the excitation of the compound nucleus when a neutron of zero kinetic energy is absorbed by  $U^{238}$ . The critical energy of  $U^{239}$ , however, is 5.5 MeV, and fission cannot occur, therefore, unless the incident neutron has an energy greater than about 0.6 MeV. Nuclei such as  $U^{238}$  are said to be *fissionable*, provided the critical energy is not so high that neutron energies in excess of about 10 MeV are required to induce fission.\* Thus although  $Pb^{208}$  may fission when struck by a neutron of energy greater than about 20 MeV, this nucleus is not ordinarily said to be fissionable.

Fission can also be induced by  $\gamma$ -rays, a process that is known as *photofission*, provided the  $\gamma$ -rays have an energy greater than the critical energy. In most reactors there are comparatively few  $\gamma$ -rays with such high energy, and photofission can usually be ignored in the design of nuclear reactors. This process is useful, however, for determining critical energies, and many of the values of  $E_{crit}$  in Table 3-1 were obtained in this way.

### 3-2 Practical Fission Fuels

For a number of reasons, isotopes such as  $U^{238}$ , which only fission with energetic neutrons, cannot alone be used to fuel nuclear reactors. It is the fissile isotopes  $U^{233}$ ,  $U^{235}$ , and  $Pu^{239}$  that are the practical fuels of nuclear power. The fissile isotope  $Pu^{241}$  as discussed below is not a practical nuclear fuel in the ordinary sense. Of these nuclei, only  $U^{235}$  is naturally occurring. It is present in the amount of 0.71 atom percent of natural uranium and can be extracted by various separation processes such as gaseous diffusion, ultracentrifuging, etc. Several large  $U^{235}$  separation plants are in existence, and in the United States it is possible to obtain uranium with any desired enrichment, that is, any specified atom percent of  $U^{235}$ .

The isotope  $U^{233}$  can be produced by the absorption of neutrons by  $Th^{232}$ . The reactions involved are:



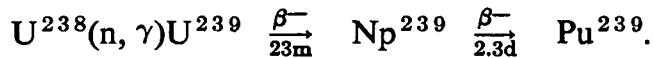
Although, in principle,  $U^{233}$  can be obtained in sizable quantities by the above reactions, only small amounts of this isotope have been produced to date. No large-scale facilities specifically designed for the production of  $U^{233}$  exist, at least in the United States, and  $U^{233}$  has not been used to fuel nuclear reactors up to the present time. However, for reasons that will be discussed in Chapter 4,  $U^{233}$  holds considerable promise for fueling certain advanced types of reactors, and this isotope will undoubtedly receive increasing attention in the future. It should be mentioned

---

\* Note that the term "fissile" represents a special case of the more general term "fissionable." All nuclei that fission when struck by neutrons of energy  $\lesssim 10$  MeV are said to be fissionable. But while both  $U^{235}$  and  $U^{238}$  are "fissionable" only  $U^{235}$  is "fissile" [cf. E. P. Blizzard, editorial in *Nucl. Sci. Eng.* 9, No. 3 (1961)].

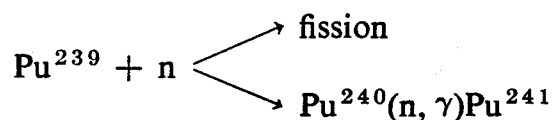
that isotopes such as  $\text{Th}^{232}$  which are not themselves fissile (though they may be fissionable), but which can be used as the raw material for the production of fissile isotopes are called *fertile*.

$\text{Pu}^{239}$  is produced by the absorption of neutrons by  $\text{U}^{238}$  via the following reactions:



Plutonium was first produced during World War II for use in weapons, and this production has been continued since the war on an even greater scale. It has been used comparatively little as a reactor fuel, however, for several reasons: (1)  $\text{Pu}^{239}$  is more expensive to produce than  $\text{U}^{235}$ ; (2) it is less satisfactory than  $\text{U}^{235}$  for fueling most of the reactors built since World War II (because of its high value of  $\alpha$ ; cf. Section 3-3); (3) the physical and chemical properties of plutonium make it a difficult material to work with; (4) little  $\text{Pu}^{239}$  has been available because of the competing demand of the weapons program. Nevertheless, as in the case of  $\text{U}^{233}$ ,  $\text{Pu}^{239}$  appears to be a far better fuel than  $\text{U}^{235}$  for certain advanced types of reactors, and the future will undoubtedly see increased use of this isotope.

A certain amount of  $\text{Pu}^{239}$  accumulates in any reactor containing  $\text{U}^{238}$ , as the result of neutron absorption. In a similar fashion the fissile isotope  $\text{Pu}^{241}$  accumulates in reactors containing  $\text{Pu}^{239}$  by the absorption of two additional neutrons. (It may be noted at this point that the absorption of a neutron by  $\text{Pu}^{239}$  does not always lead to fission; cf. Section 3-3.) The reactions involved are:



The operation of a reactor is necessarily affected by the presence of  $\text{Pu}^{241}$  and this must be taken into account in the design of  $\text{Pu}^{239}$ -fueled reactors or reactors containing large amounts of  $\text{U}^{238}$ . However,  $\text{Pu}^{241}$  has never been used to fuel a reactor directly and there are no facilities for the specific production of this isotope. Indeed, it appears that the cost of  $\text{Pu}^{241}$  is much too high for it to be used as a principal reactor fuel.

During World War II the heavy isotopes of nuclear technology were identified by code numbers, and this nomenclature persists to some extent today. According to this code each isotope is identified by a two-digit number. The first digit is the atomic number minus 90, and the second digit is the last digit of the mass number.\* Thus  $\text{U}^{235}$  is known simply as "25";  $\text{Pu}^{239}$  is known as "49"; etc. Note that  $\text{Pu}^{241}$  is "41" not "51."

---

\* More precisely the code number is  $10Z(\text{mod } 10) + A(\text{mod } 10)$ , where  $Z$  and  $A$  are the atomic and mass numbers, respectively. A number  $x(\text{mod } 10)$  is the smallest positive number obtained by repeatedly subtracting 10 from  $x$ ; e.g.,  $92(\text{mod } 10) = 2$ ,  $238(\text{mod } 10) = 8$ , etc.

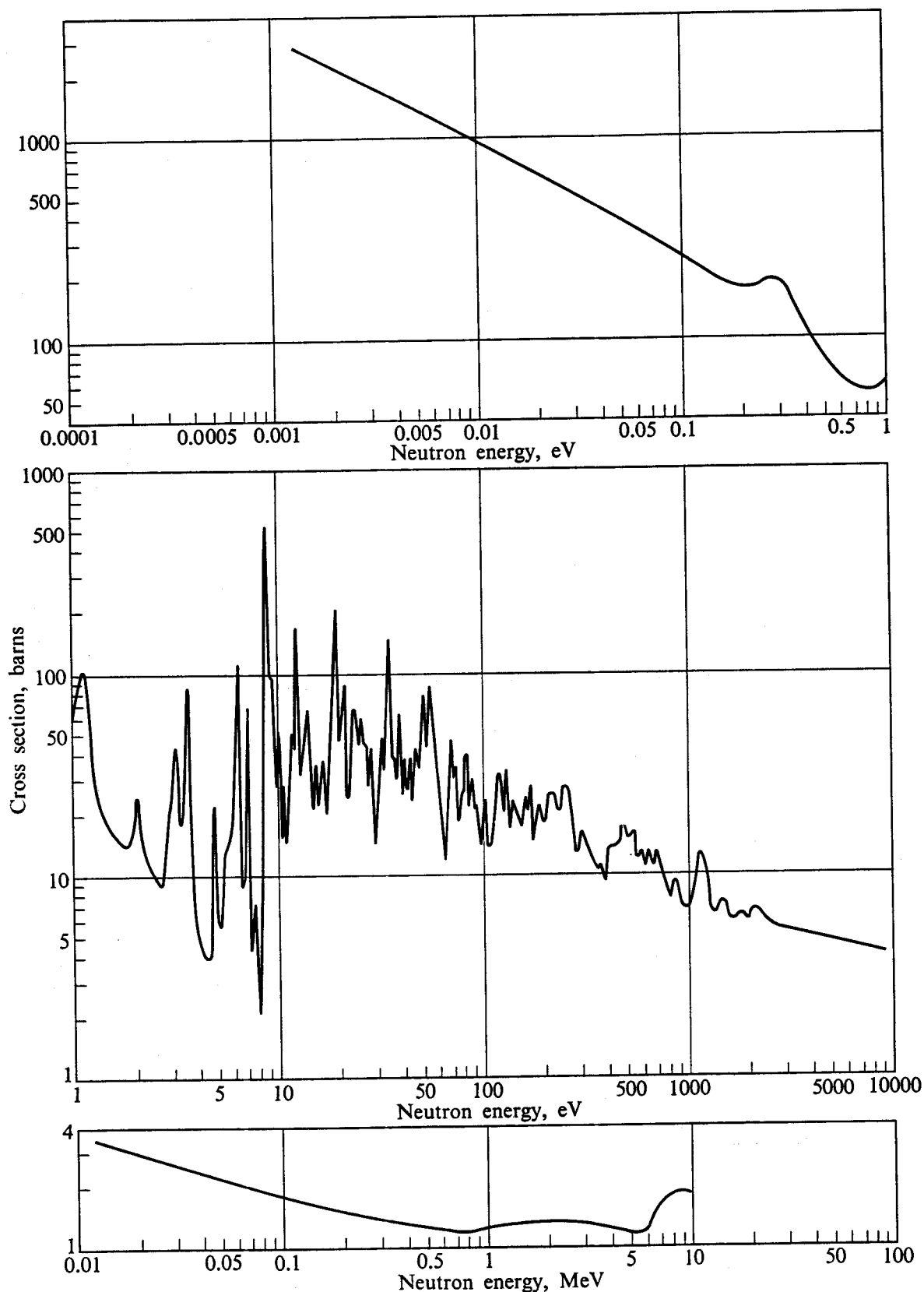


Fig. 3-3. The fission cross section of  $\text{U}^{235}$ . [From BNL-325, Second Edition (1958).]

### 3-3 Cross Sections of Fissionable Nuclei

The probability of neutron-induced fission is described by the *fission cross section*,  $\sigma_f$ , and as is true for any other cross section,  $\sigma_f$  is a function both of the target nucleus and the energy of the incident neutron. For the fissile nuclei,  $\sigma_f$  is quite large (as cross sections go) at low energy, and drops roughly as  $1/v$  with increasing energy up to the electron-volt region where several resonances appear. Above approximately 1 keV, the resonances can no longer be resolved by present measuring techniques\*, and the cross section becomes rather smooth. This type of behavior is illustrated in Fig. 3-3, where  $\sigma_f$  is shown for  $U^{235}$ .

The fission cross section is somewhat different for nuclei such as  $U^{238}$  that require an energetic neutron to induce fission. Now  $\sigma_f$  is zero up to the threshold energy for fission, where it rises rapidly with increasing energy. This is shown in Fig. 3-4 for  $U^{238}$  and several other even- $A$  nuclei. Since the fission threshold usually occurs at energies above the region of resolvable resonances, the fission cross sections of these nuclei tend to be smooth everywhere.

For reasons which will be explained in Chapter 8, it is the usual practice to tabulate low-energy cross sections at an energy of 0.0253 eV. This value is called the *thermal energy* since neutrons in thermal equilibrium with their surroundings at room temperature have approximately this energy. The corresponding cross sections are called *thermal cross sections*. These are given in the first two columns of Table 3-2 for  $U^{233}$ ,  $U^{235}$ , natural uranium,  $Pu^{239}$ , and  $Pu^{241}$ . Additional data on these and other heavy nuclei will be found in Appendix I and in the references at the end of the chapter.

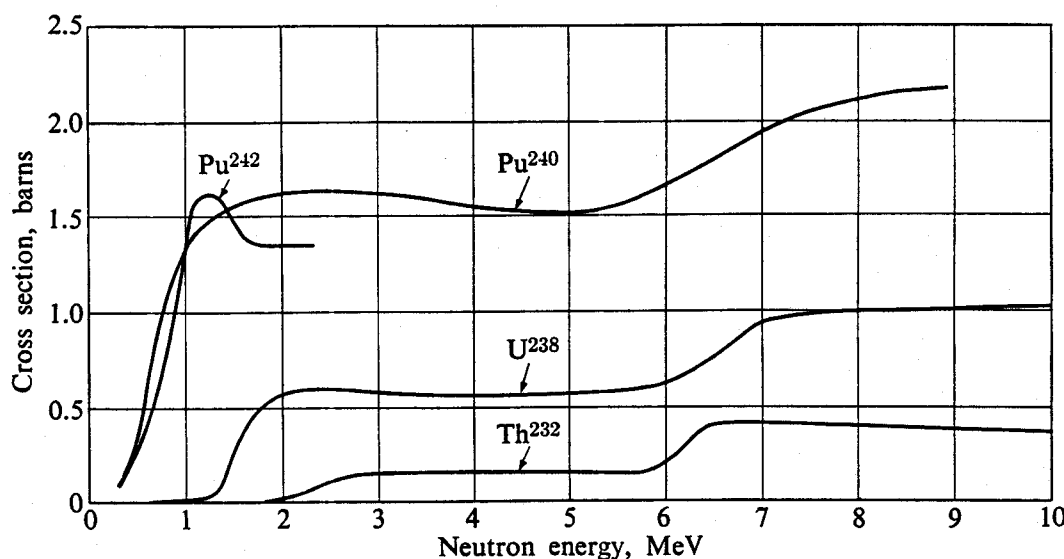


Fig. 3-4. The fission cross sections of  $Th^{232}$ ,  $U^{238}$ ,  $Pu^{240}$ , and  $Pu^{242}$ . [From BNL-325, Second Edition (1958).]

\* The actual overlapping of the levels, that is, where the Doppler width and the level spacing are approximately equal, probably occurs at about 5 keV.

Table 3-2\*

**Thermal (0.025 eV) Data for  $U^{233}$ ,  $U^{235}$ , Natural Uranium,  
 $Pu^{239}$ , and  $Pu^{241}$**

	$\sigma_a \dagger$	$\sigma_f$	$\alpha$	$\eta$	$\nu$
$U^{233}$	573	525	0.093	2.29	2.50
$U^{235}$	678	577	0.175	2.08	2.44
Natural uranium	7.59	4.16	0.910	1.31	2.50
$Pu^{239}$	1015	741	0.370	2.12	2.90
$Pu^{241}$	1375	950	0.357	2.21	3.00

\* From BNL-325, Second ed. (1958), Supplement No. 2, Volume III, February, 1965. For an evaluation of the measurements of these important parameters and their errors see R. Sher and J. Felberbaum, BNL-918 (March, 1965). See also Table I-3 in Appendix I for further data on these and other heavy nuclei.

†  $\sigma_a = \sigma_\gamma + \sigma_f$ .

Aside from the fact that they undergo fission, fissionable nuclei are not essentially different from other heavy nuclei, and they interact with neutrons in the many ways discussed in the preceding chapter. In the case of fissile nuclei, however, the low-energy cross sections are dominated by fission and radiative capture. Elastic scattering cannot be measured at low energies, but  $\sigma_s$  is presumably constant. On the other hand, with fissionable nuclei such as  $U^{238}$ , the fission cross section is zero at low energies, and the capture cross sections tend to be small. The elastic cross section can be determined more easily in this case, and  $\sigma_s$  is indeed found to be constant. In the resonance region, the elastic cross sections of fissionable nuclei are roughly constant, except, of course, as discussed in the preceding chapter, in the immediate vicinity of resonances. At considerably higher energies, that is, above the resonance region,  $\sigma_s$  can be estimated as the difference between the total cross section and the nonelastic cross section, and in this region is smooth.

Inelastic scattering cannot occur below the kilovolt region in any of the fissionable nuclei.\* The inelastic thresholds for several of these nuclei are given in Table 3-3. The inelastic cross section can be measured up to about 2 MeV by time-of-flight techniques. The cross sections for the excitation of the first three levels in  $U^{238}$  are shown in Fig. 2-23. At higher energies,  $\sigma_i$  can be inferred by subtracting the cross sections for other nonelastic interactions from  $\sigma_{ne}$ .

The radiative capture cross sections of fissionable nuclei are not essentially different from those of other heavy nuclei. At low energy,  $\sigma_\gamma$  is usually  $1/v$  (or nearly so). This is followed by a region of resonances, and beyond the resonance region  $\sigma_\gamma$  becomes smooth and decreases approximately as  $1/E$  or faster.

\* It should be mentioned that there is a curious excited state in  $U^{235}$  at only 23 eV above ground. However, this level apparently is not excited by *s*-wave neutrons.

**Table 3-3**  
Inelastic Scattering Thresholds in Heavy Nuclei

Nucleus	Threshold (keV)
$U^{233}$	40
$U^{235}$	14
$U^{238}$	44
$Pu^{239}$	8

When a fissile nucleus absorbs a neutron, the compound nucleus that is formed can usually decay in several ways. At low energies, however, inelastic scattering cannot occur, the elastic cross section is comparatively small, and fission and radiative capture are the principal modes of decay of the compound system. It has been found that the relative probability of these two processes is not a constant, but depends upon the energy of the incident neutron. This situation is described by the energy-dependent parameter  $\alpha$ , known as the *capture-to-fission ratio*, which is defined as

$$\alpha = \frac{\sigma_\gamma}{\sigma_f}. \quad (3-5)$$

In terms of  $\alpha$ , the relative probability that the compound nucleus decays by fission is  $1/(1 + \alpha)$ , and the relative probability that it decays by the emission of capture  $\gamma$ -rays is  $\alpha/(1 + \alpha)$ . Thus a high value of  $\alpha$  means a low probability of fission following neutron absorption, and conversely, a low value of  $\alpha$  means a high probability of fission. Figure 3-5 shows the behavior of  $\alpha$  as a function of energy

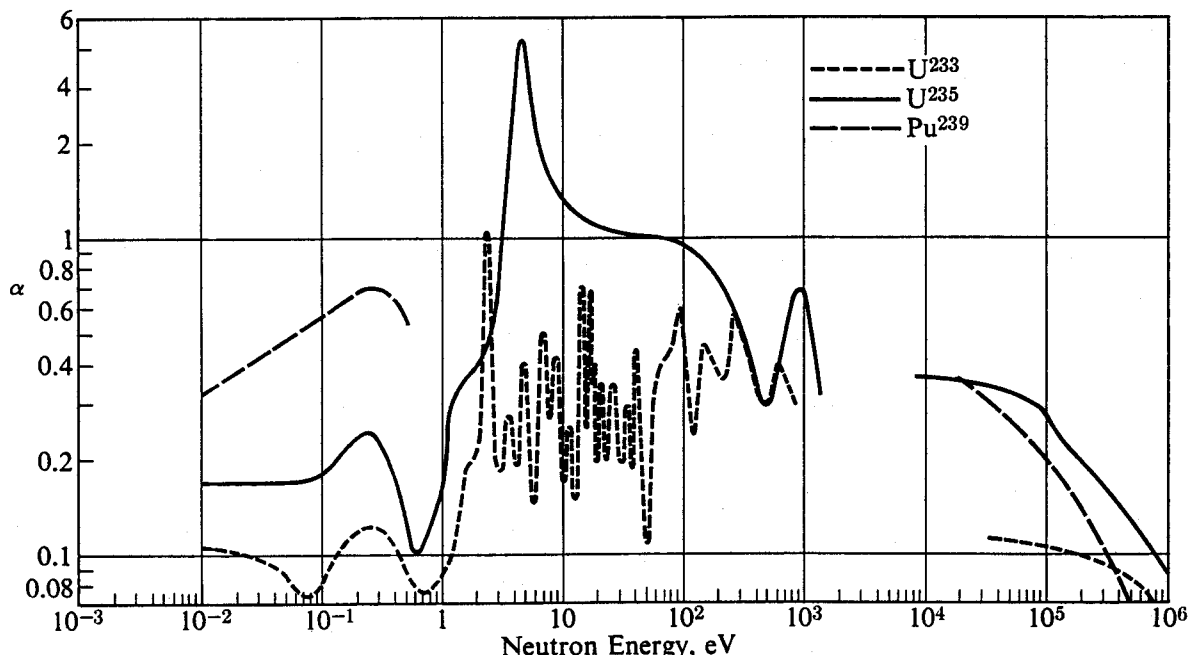


**Fig. 3-5.** Variation of  $\alpha$  with energy for  $U^{233}$ ,  $U^{235}$ , and  $Pu^{239}$ . The  $U^{235}$  curve has been smoothed in the eV region. [From BNL-325, Second Ed. (1958 plus supplements).]

**Table 3-4**  
**Thresholds (in MeV) for the (n, 2n) and (n, 3n) Reactions in Heavy Nuclei**

Nucleus	(n, 2n)	(n, 3n)
$U^{233}$	5.9	13.2
$U^{235}$	5.2	12.0
$U^{238}$	6.1	11.5
$Pu^{239}$	5.5	12.5

for  $U^{233}$ ,  $U^{235}$ , and  $Pu^{239}$ . In Chapter 4 it will be shown that the parameter  $\alpha$  plays a central role in the design of certain reactors.

The cross sections of all charged-particle reactions with fissionable nuclei are essentially zero at energies of interest in reactor theory because, as explained in Section 2-12, an emitted charged particle has to pass through a large Coulomb barrier. The only other important interactions for these nuclei are the (n, 2n) and (n, 3n) reactions. As discussed in Section 2-13, these reactions are of the threshold type, and their cross sections rise sharply from the threshold energy. The (n, 2n) and (n, 3n) thresholds are given in Table 3-4 for a number of the more important heavy nuclei; the (n, 2n) and (n, 3n) cross sections of  $U^{238}$  are shown in Fig. 2-29.

### 3-4 The Products of Fission

When a nucleus undergoes fission, a number of products are formed. There are, of course, the fission fragments, but in addition, neutrons,  $\gamma$ -rays,  $\beta$ -rays, and neutrinos are emitted, either at the instant of the fission or sometime later as the fission fragments undergo radioactive decay.

**Fission fragments and asymmetric fission.** It will be recalled from Chapter 1 that the binding energy per nucleon is a decreasing function of  $A$ , when  $A$  is greater than about 50. This means that although the total binding energy of nuclei increases with  $A$ , it does so at a decreasing rate. This situation is depicted in Fig. 3-6, where the total binding energy is indicated schematically as a function of  $A$ , for  $A$  above 50. Suppose now that a heavy nucleus undergoes fission. It is easy to see from the figure that the most stable configuration of the final nuclei, that is, the two fragments with the largest total binding energy, is obtained

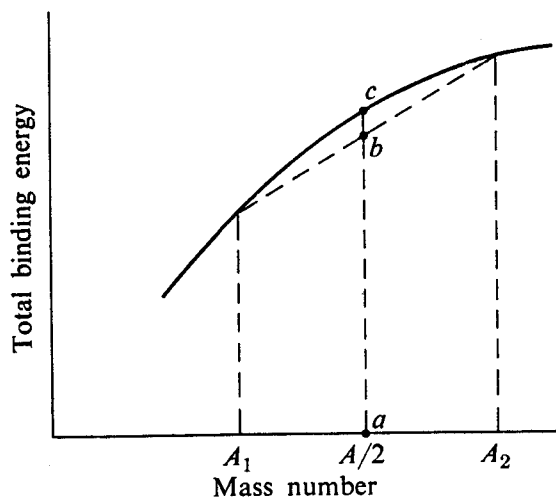
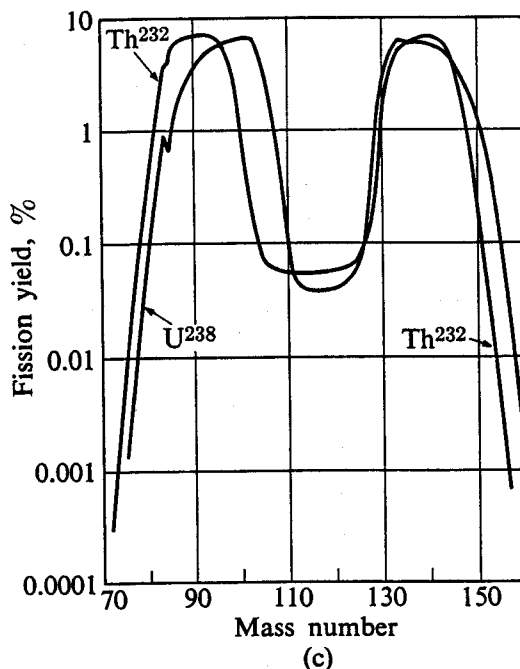
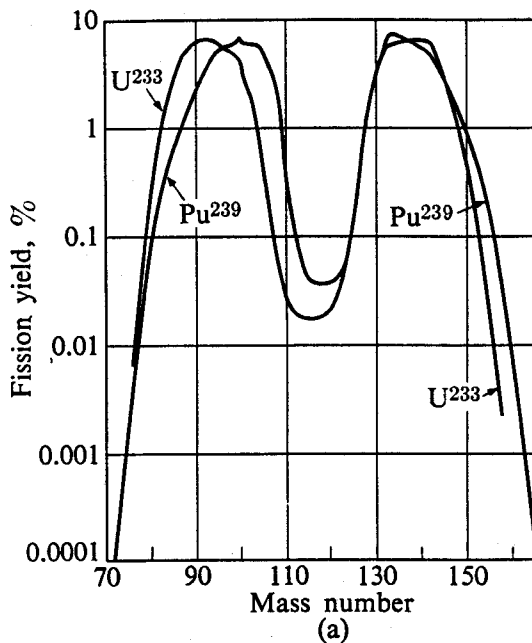
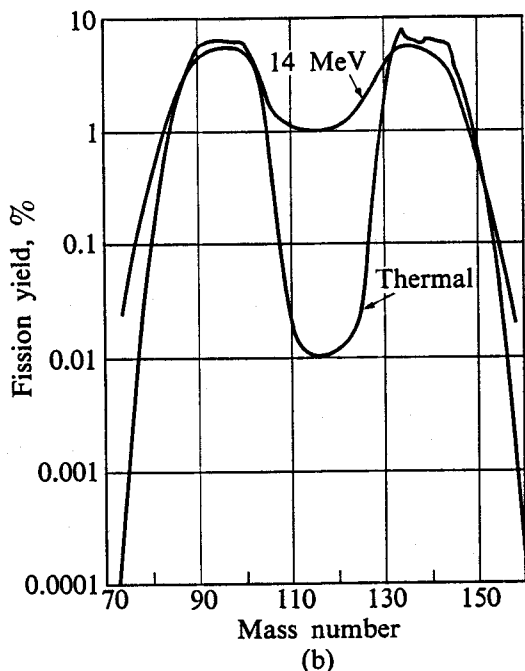


**Fig. 3-6.** Total nuclear binding energy versus  $A$  for  $A \gtrsim 50$ .

**Fig. 3-7.** Fission product yields: (a) thermal fission of  $U^{233}$  and  $Pu^{239}$ ; (b) thermal and 14-MeV fission of  $U^{235}$ ; (c) fission by prompt spectrum of  $Th^{232}$  and  $U^{238}$ . [Reprinted by permission from S. Katcoff, "Fission-Product Yields from Neutron Induced Fission," *Nucleonics* 18, 11, 201 (November 1960).]

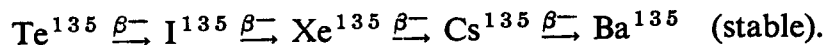


when the parent nucleus splits *exactly in half*. If this were not the case, and unequal fragments  $A_1$  and  $A_2$  were produced, the final binding energy would be twice the distance  $ab$  shown in the figure, which is clearly less than the binding energy  $2ac$  obtained in symmetric fission.

It is rather surprising, therefore, to find that fission almost always occurs in an asymmetric fashion, and that symmetric fission is, in fact, a comparatively rare event. This is shown in Fig. 3-7 where the observed yields of fission products are shown as a function of mass number. In these curves the ordinate is the probability

expressed in percent that a fission fragment of a given mass number is produced in fission. Figure 3-7(a) gives the fission yield for fission induced by slow neutrons (thermal neutrons) in  $U^{233}$  and  $Pu^{239}$ ; Fig. 3-7(b) shows the yield for fission induced by both slow neutrons and 14-MeV neutrons in  $U^{235}$ ; and Fig. 3-7(c) gives the yield for fission induced by prompt fission neutrons (cf. below) in  $Th^{232}$  and  $U^{238}$ . It should be noted that the ordinates in these curves are plotted on a logarithmic scale; fission-product distributions are therefore much more asymmetric than might be thought from a casual glance at the curves. For example, fission fragments corresponding to symmetric fission from low energy neutrons in  $U^{235}$  ( $A = 236 \div 2 = 118$ ) have a yield of only 0.01 percent which means that symmetric fission occurs only once in 20,000 events.\* As indicated in Fig. 3-7(b), however, fission becomes more symmetric when the energy of the incident neutron is increased.

**The decay of fission fragments.** When the fission fragments are formed, they are excessively "neutron rich." That is, they contain too many neutrons for stability and therefore decay with the emission of one or more negative  $\beta$ -rays. For instance, the isotope  $Te^{135}$ , which is produced directly in fission, decays by the following chain:



The decay of fission products in reactors is important for a number of reasons. First, the energy emitted in the form of  $\beta$ - and  $\gamma$ -rays during reactor operation represents an important contribution to the recoverable energy of fission, since the bulk of this radiation cannot escape from a reactor. Also, since the decay of fission fragments continues after a reactor is shut down, the decay energy provides a continuing source of heat that in many reactors must be removed following shutdown. Finally, the radiation associated with fission product decay, particularly the  $\gamma$ -rays, presents an important biological hazard and usually makes many parts of reactors inaccessible after shutdown.

Several expressions have been given for the rate at which energy is released from decaying fission fragments. If  $\beta(t)$  and  $\gamma(t)$  represent the *average energy* emitted per second in the form of  $\beta$ - and  $\gamma$ -rays, respectively,  $t$  sec after *one* fission, these quantities are given approximately by:

$$\beta(t) = 1.26t^{-1.2} \text{ MeV/sec,} \quad (3-6)$$

$$\gamma(t) = 1.40t^{-1.2} \text{ MeV/sec.} \quad (3-7)$$

These formulas are valid in the range from about  $t = 1$  sec to  $t = 10^6$  sec. While it is possible to write exact expressions for fission product decay based on detailed experimental data, Eqs. (3-6) and (3-7) are usually accurate enough for most

---

\* Note that there are *two* fragments per fission; hence the number 20,000, not 10,000.

purposes. It should be noted that these formulas only give the *rate* of energy release but do not specify the energy distribution. Although the  $\beta$ -rays are emitted in a continuous spectrum, it is usually assumed that they are monoenergetic and have an average energy of about 0.4 MeV. Up to about 250 sec after a fission, the fission product  $\gamma$ -rays can be represented by the spectrum

$$N(E) \approx e^{-1.10E}, \quad (3-8)$$

where  $N(E) dE$  is the number of  $\gamma$ -rays emitted with energy between  $E$  and  $E + dE$ , and  $E$  is in MeV.

In many engineering design calculations, it is necessary to know the energy released by fission products following the shutdown of a reactor that has been operating at a specified power level for a given length of time. In this case, Eqs. (3-6) and (3-7) can be integrated over the period of operation of the reactor and the following useful expression is obtained:<sup>\*</sup>

$$P(t, T) = 4.10 \times 10^{11} [t^{-0.2} - (t + T)^{-0.2}] \text{ MeV/sec} \quad (3-9)$$

Here  $P(t, T)$  is the total power (MeV/sec) emitted in the form of  $\beta$ -rays and  $\gamma$ -rays by the decaying fission products in a reactor that has been operated for  $T$  sec at a power of one watt,  $t$  sec after it has been shut down. The function  $P(t, T)$  is often called the *Borst-Wheeler function*.

**Prompt neutrons.** One of the most important products of fission is the neutrons which are emitted in the process. The majority of these appear essentially instantaneously, that is, within about  $10^{-17}$  sec of the fission event, and are called *prompt neutrons*. A very small number of neutrons appear long after fission occurs, and these are referred to as *delayed neutrons*. These delayed neutrons are discussed later in this section.

The number of prompt neutrons emitted in fission varies from fission to fission. Thus in some fissions no neutrons appear at all, while occasionally as many as five neutrons are emitted. However, only the *average* number of neutrons released per fission is needed in reactor calculations and this quantity is given the symbol  $\nu$ .<sup>†</sup> As usually defined,  $\nu$  refers to both the prompt and delayed neutrons, and its value depends both on the fissioning isotope and on the energy of the incident neutron. In particular, it has been found experimentally that  $\nu$  increases approximately linearly with energy, over large ranges in energy; i.e.,

$$\nu(E) = \nu_0 + aE, \quad (3-10)$$

---

\* Equation (3-9) is based on a recoverable energy of 200 MeV per fission (cf. Section 3-5). The constant in the equation is somewhat different for other recoverable energies.

† To indicate that  $\nu$  is an average quantity, it is often denoted by the symbol  $\bar{\nu}$ . This somewhat more cumbersome notation will not be used in this book.

where  $\nu_0$  and  $a$  are constants given in Table 3-5, and  $E$  is the incident neutron energy in MeV. The quantity  $\nu_0$  for Th<sup>232</sup> and U<sup>238</sup> was assigned to reproduce the data above the fission thresholds of these nuclei; Eq. (3-10) is not applicable, of course, below threshold for these nuclei. It should be noted from the table that above 1 MeV  $a^{-1}$  is about 6 or 7 MeV, so that one additional neutron is emitted per fission for every 6- or 7-MeV increase in energy of the incident neutron.

Table 3-5  
The Constants,  $\nu_0$  and  $a$ , for Eq. (3-10)\*

Isotope	$\nu_0$	$a$ , MeV <sup>-1</sup>	Energy range, MeV
Th <sup>232</sup>	1.87	0.164	all $E$
U <sup>233</sup>	2.48	0.075	$0 \leq E \leq 1$
	2.41	0.136	$E > 1$
U <sup>235</sup>	2.43	0.065	$0 \leq E \leq 1$
	2.35	0.150	$E > 1$
U <sup>238</sup>	2.30	0.160	all $E$
Pu <sup>239</sup>	2.87	0.148	$0 \leq E \leq 1$
	2.91	0.133	$E > 1$

\* From G. R. Keepin, *Physics of Nuclear Kinetics*, Reading, Mass.: Addison-Wesley, 1965.

It was pointed out in the preceding section that the absorption of a low-energy neutron by a fissile nucleus does not always lead to fission. A  $\gamma$ -ray may be emitted before the nucleus fissions, and in this case the neutron is merely captured. With U<sup>235</sup>, for instance, radiative capture occurs in about  $\alpha/(1 + \alpha) = 15$  percent of slow neutron absorptions. To describe this situation it is convenient to introduce a parameter which is equal to the average number of neutrons emitted in fission *per neutron absorbed* in the fissile isotope. This quantity, which is denoted by  $\eta$ , is equal to  $\nu$  times the relative probability that neutron absorption leads to fission; thus

$$\eta = \nu \frac{\sigma_f}{\sigma_a} . \quad (3-11)$$

At low energy  $\sigma_a = \sigma_f + \sigma_\gamma$ , so that

$$\eta = \frac{\nu}{1 + \alpha} , \quad (3-12)$$

where  $\alpha$  is defined in Section 3-3. It should be noted that since  $\nu$  and  $\alpha$  are functions of neutron energy,  $\eta$  is also energy dependent.

The quantity  $\eta$  is also defined for a mixture of fissile and nonfissile isotopes; such a mixture is frequently called "fuel." In this case,  $\eta$  is the average number of neutrons produced per neutron absorbed in the mixture. For example, if the fuel

where  $E$  is in MeV. This function is shown in Fig. 3-8. It is generally believed that this spectrum is independent of the energy of the neutron inducing the fission. Also, although Eq. (3-14) is based largely on measurements of  $U_{235}$ , the prompt spectra of all other fissile nuclei are presumably very similar.

$$\chi(E) = 0.453e^{-1.036E} \sinh \sqrt{2.29}E, \quad (3-14)$$

Several expressions have been given over the years for the prompt neutron spectrum; a comparatively recent formula is

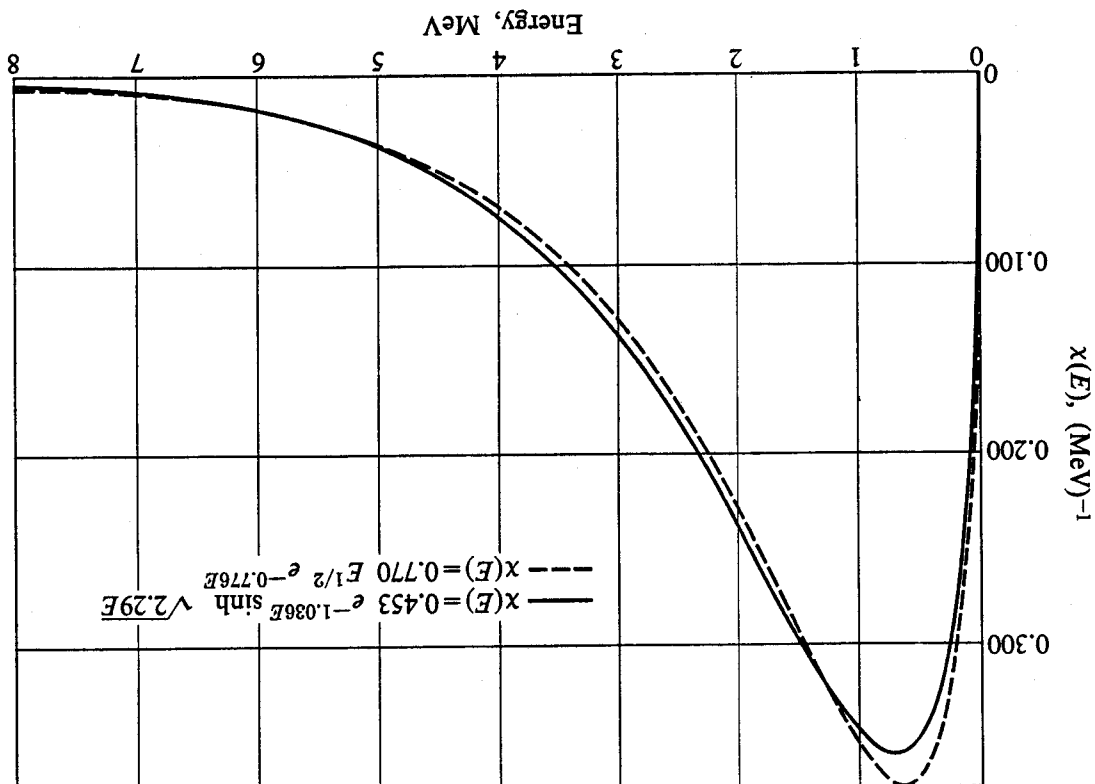
$$\cdot 1 = Ep(E)x \int_0^\infty$$

where the numbers 25 and 28 refer to  $U_{235}$  and  $U_{238}$ , respectively (cf. Section 3-2). The prompt fission neutrons are emitted with a continuous distribution of energies. This distribution is described by the function  $x(E)$ , which is called the prompt-neutron spectrum. This is defined so that  $x(E) dE$  is the number of neutrons emitted with laboratory energy between  $E$  and  $E + dE$  per fission neutron, that is,  $x(E)$  is normalized so that

$$\eta = \frac{\mathbb{E}^a(25) + \mathbb{E}^a(28)}{\mathbb{E}(25)\mathbb{E}(25)}, \quad (3-13)$$

consists of a mixture of  $U^{235}$  and  $U^{238}$  (such as natural uranium),  $\eta$  is given by

Fig. 3-8. The prompt neutron spectrum computed from Eqs. (3-14) and (3-15).



A somewhat simpler expression for  $\chi(E)$ , but one which less accurately reproduces the data, is

$$\chi(E) = 0.770E^{1/2}e^{-0.776E}, \quad (3-15)$$

where  $E$  is again in MeV. Equation (3-15) is also plotted in Fig. 3-8.

The *average* energy of the prompt neutrons can be found in the usual way by integrating over the prompt-neutron spectrum, viz.,

$$\bar{E} = \int_0^{\infty} Ex(E) dE = 1.98 \text{ MeV.}$$

On the other hand, the *most probable* neutron energy, that is, the energy corresponding to the peak of the  $\chi(E)$  curve, is only about 0.73 MeV, as shown in Fig. 3-8.

**Delayed neutrons.** Although less than one percent of the fission neutrons are delayed, these neutrons, as will be shown in Chapter 12, play a central role in the operation of a reactor. Delayed neutrons originate in the decay by neutron emission of nuclei produced following the  $\beta$ -decay of certain fission fragments. For example, the  $\beta$ -decay of the fission product  $\text{Br}^{87}$  leads either to the ground state of  $\text{Kr}^{87}$  or to the excited states at about 5.4 MeV, as shown in Fig. 3-9. However,  $\text{Kr}^{87}$  contains 51 neutrons, just one more than the magic number of 50, and the binding energy of the 51st neutron is quite low, namely 5.1 MeV. The levels at 5.4 MeV can therefore decay by the emission of a neutron with a kinetic energy of about 0.3 MeV. Since the neutron is emitted in a time which is short

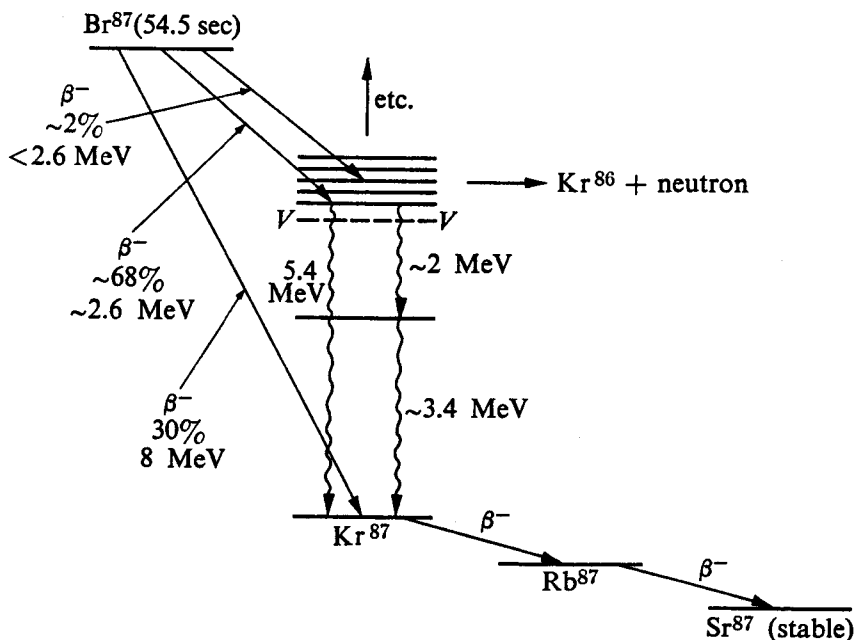


Fig. 3-9. The origin of delayed neutrons from the precursor  $\text{Br}^{87}$ . The virtual energy of  $\text{Kr}^{87}$  is indicated by  $V - V'$ . There may be other energy levels at low energy in addition to those shown.

\* Until comparatively recently it was thought that each delayed group originated with one and only one precursor. If this were the case, the half-lives of corresponding groups would be the same for all fissile nuclei.

It will be recalled from Fig. 3-7 that the distribution of fission products depends on both the fissioning nucleus and the energy of the neutron inducing the fission. As a result, the distribution of delayed neutron precursors, and so also the yields of the delayed neutrons and their average group half-lives, are functions of the fissioning nucleus and neutron energy.\* The yields and the average half-lives of delayed neutrons are given in Table 3-7 for fission induced by low energy (thermal) neutrons in  $U_{233}$ ,  $U_{235}$ , and  $Pu_{239}$ . Similar data are given in Table 3-8 for fission induced by a continuous neutron spectrum resembling that of the prompt fission neutrons.

Nuclei such as  $\text{Br}^{87}$  whose production in fission may eventually lead to the emission of a delayed neutron are known as *delayed-neutron precursors*. At the present time, it is believed that there may be as many as twenty precursors responsible for delayed-neutron emission, although only about a half dozen have been positively identified. These precursors and their respective half-lives are given in Table 3-6. As indicated in the table, the precursors can conveniently be divided into six groups according to their half-lives.

compared with the half-life of the  $\text{Br}^{87}$ , it appears to be emitted with the  $54.5\text{-sec}$  half-life of  $\text{Br}^{87}$ .

\*From G. R. Keepin, *Physics of Nuclear Kinetics*, Readings, Mass.: Addison-Wesley, 1965.

Precursor	Precursor half-life (sec)	and group assignment
$\text{Br}^{87}$	54.5	Group 1
$\text{I}^{137}$	24.4	Group 2
$\text{Br}^{88}$	16.3	{ Group 3 RB(89) Br(89) RB(93, 94) Br(93, 94)
$\text{I}^{138}$	6.3	{ Group 4 (Cs, Sb or Te) Br(90, 92) Kr(93)
$\text{I}^{139}$	4.4	{ Group 4 (Cs, Sb or Te) Br(90, 92) Kr(93)
	~6	{ Group 4 (Cs, Sb or Te) Br(90, 92) Kr(93)
	2.0	{ Group 4 (Cs, Sb or Te) Br(90, 92) Kr(93)
	1.6	{ Group 4 (Cs, Sb or Te) Br(90, 92) Kr(93)
	~1.5	{ Group 4 (Cs, Sb or Te) Br(90, 92) Kr(93)
	0.5	{ Group 5 $\text{I}^{140} + \text{Kr}?$
	0.2	{ Group 6 $\text{Br}, \text{Rb}, \text{As} + ?$

Delayed-Neutron Precursors. Uncertain Quantities  
are Indicated by Parentheses.\*

Table 3-6

**Table 3-7**  
**Delayed Neutron Data for Thermal Fission in  $\text{U}^{233}$ ,  $\text{U}^{235}$ , and  $\text{Pu}^{239}$ \***

$\text{U}^{233}$				
Group	Half-life (sec)	Decay constant $\lambda_i (\text{sec}^{-1})$	Yield (neutrons per fission)	Fraction $\beta_i$
1	55.00	0.0126	0.00057	0.000224
2	20.57	0.0337	0.00197	0.000777
3	5.00	0.139	0.00166	0.000655
4	2.13	0.325	0.00184	0.000723
5	0.615	1.13	0.00034	0.000133
6	0.277	2.50	0.00022	0.000088
Total yield: 0.0066				
Total delayed fraction ( $\beta$ ): 0.0026				
$\text{U}^{235}$				
Group	Half-life (sec)	Decay constant $\lambda_i (\text{sec}^{-1})$	Yield (neutrons per fission)	Fraction $\beta_i$
1	55.72	0.0124	0.00052	0.000215
2	22.72	0.0305	0.00346	0.001424
3	6.22	0.111	0.00310	0.001274
4	2.30	0.301	0.00624	0.002568
5	0.610	1.14	0.00182	0.000748
6	0.230	3.01	0.00066	0.000273
Total yield: 0.0158				
Total delayed fraction ( $\beta$ ): 0.0065				
$\text{Pu}^{239}$				
Group	Half-life (sec)	Decay constant $\lambda_i (\text{sec}^{-1})$	Yield (neutrons per fission)	Fraction $\beta_i$
1	54.28	0.0128	0.00021	0.000073
2	23.04	0.0301	0.00182	0.000626
3	5.60	0.124	0.00129	0.000443
4	2.13	0.325	0.00199	0.000685
5	0.618	1.12	0.00052	0.000181
6	0.257	2.69	0.00027	0.000092
Total yield: 0.0061				
Total delayed fraction ( $\beta$ ): 0.0021				

\* Based on G. R. Keepin, *Physics of Nuclear Kinetics*, Reading, Mass.: Addison-Wesley, 1965.

In reactor calculations it is more convenient to use the *delayed-neutron fractions*  $\beta_i$  than the absolute yields of the delayed neutrons. The number  $\beta_i$  is defined as the fraction of the fission neutrons which appear as delayed neutrons in the  $i$ th group. Since  $\nu$  is the total number of neutrons emitted in fission, it follows that  $\beta_i\nu$  is equal to the absolute yield of neutrons in the  $i$ th group. The *total delayed fraction* is denoted by  $\beta$  and is simply the sum of the  $\beta_i$  over all groups;  $\beta\nu$  is then the total yield of delayed neutrons in all groups. Values of  $\beta_i$  and  $\beta$  are also given in Tables 3-7 and 3-8.

In contrast to the prompt neutrons, which are emitted with a continuous energy spectrum, the neutrons in each delayed group appear with a more or less well-

**Table 3-8**  
**Delayed Neutron Data for Fission Induced by a Prompt-Neutron Spectrum\***

$\text{Th}^{232}$				
Group	Half-life (sec)	Decay constant $\lambda_i$ (sec $^{-1}$ )	Yield (neutrons per fission)	Fraction $\beta_i$
1	56.03	0.0124	0.00169	0.000690
2	20.75	0.0334	0.00744	0.003045
3	5.74	0.121	0.00769	0.003147
4	2.16	0.321	0.02212	0.009054
5	0.571	1.21	0.00853	0.003492
6	0.211	3.29	0.00213	0.000873
Total yield: 0.0496				
Total delayed fraction ( $\beta$ ): 0.0203				
$\text{U}^{233}$				
Group	Half-life (sec)	Decay constant $\lambda_i$ (sec $^{-1}$ )	Yield (neutrons per fission)	Fraction $\beta_i$
1	55.11	0.0126	0.00060	0.000224
2	20.74	0.0334	0.00192	0.000712
3	5.30	0.131	0.00159	0.000590
4	2.29	0.302	0.00222	0.000824
5	0.546	1.27	0.00051	0.000190
6	0.221	3.13	0.00016	0.000060
Total yield: 0.0070				
Total delayed fraction ( $\beta$ ): 0.0026				

*(Continued)*

\* Based on G. R. Keepin, *Physics of Nuclear Kinetics*, Reading, Mass.: Addison-Wesley, 1965.

Table 3-8 (Continued)

$U^{235}$				
Group	Half-life (sec)	Decay constant $\lambda_i$ (sec $^{-1}$ )	Yield (neutrons per fission)	Fraction $\beta_i$
1	54.51	0.0127	0.00063	0.000243
2	21.84	0.0317	0.00351	0.001363
3	6.00	0.115	0.00310	0.001203
4	2.23	0.311	0.00672	0.002605
5	0.496	1.40	0.00211	0.000819
6	0.179	3.87	0.00043	0.000166
Total yield: 0.0165				
Total delayed fraction ( $\beta$ ): 0.0064				
$U^{238}$				
Group	Half-life (sec)	Decay constant $\lambda_i$ (sec $^{-1}$ )	Yield (neutrons per fission)	Fraction $\beta_i$
1	52.38	0.0132	0.00054	0.000192
2	21.58	0.0321	0.00564	0.002028
3	5.00	0.139	0.00667	0.002398
4	1.93	0.358	0.01599	0.005742
5	0.490	1.41	0.00927	0.003330
6	0.172	4.02	0.00309	0.001110
Total yield: 0.0412				
Total delayed fraction ( $\beta$ ): 0.0148				
$Pu^{239}$				
Group	Half-life (sec)	Decay constant $\lambda_i$ (sec $^{-1}$ )	Yield (neutrons per fission)	Fraction $\beta_i$
1	53.75	0.0129	0.00024	0.000076
2	22.29	0.0311	0.00176	0.000560
3	5.19	0.134	0.00136	0.000432
4	2.09	0.331	0.00207	0.000656
5	0.549	1.26	0.00065	0.000206
6	0.216	3.21	0.00022	0.000070
Total yield: 0.0063				
Total delayed fraction ( $\beta$ ): 0.0020				

The energy of the  $\gamma$ -rays is also recoverable since almost all reactors are designed only a short distance within a reactor, and their energy is therefore recoverable. and 12 MeV in the form of neutrinos. The  $\beta$ -rays, being charged particles, travel and these fragments decay, they emit about 8 MeV in  $\beta$ -rays, 7 MeV in  $\gamma$ -rays, a reactor and the kinetic energy of the fission fragments is entirely recoverable.

About  $10^{-3}$  cm from the site of the fission. Thus none of this energy escapes from particles moving through matter, and their energy is deposited no farther than as highly-charged particles. They soon come to rest, however, as do any charged electrons of the fissioning nucleus, and pass into the surrounding matter the electronic shells of the fission fragments. With their large energy, the fragments rip through energy of the fission fragments. By far the bulk of the fission energy, namely, about 168 MeV, appears as kinetic energy in  $U_{235}$ .

In discussing the energy of fission, it is important to distinguish between the total energy released in the process and the energy which can be recovered in a reactor and is therefore available for the production of heat. This recoverable energy and the total energy, in general, are different. To illustrate, consider fission occurring

### 3-5 Energy Release from Fission

**Prompt gamma rays.** A number of  $\gamma$ -rays are emitted at the instant of fission, and these are referred to as *prompt*  $\gamma$ -rays, to distinguish them from the delayed neutrons accompanying fission-product decay. The spectrum of the prompt  $\gamma$ -radiation accompanying fission-product decay between 1 and 7 MeV by the same distribution function as for the fission product  $\gamma$ -rays, i.e., Eq. (3-8). The prompt-gamma spectra of all fissionable nuclei are believed to be identical or nearly so.

Delayed neutrons are much less energetic than the majority of the prompt neutrons. (thermal) fissions in  $U_{235}$  are given in Table 3-9. It should be noted that the delayed energy. The energies of the delayed neutrons emitted following low-energy fission, and these are referred to as *prompt*  $\gamma$ -rays, to distinguish them from the delayed neutrons are much less energetic than the majority of the prompt neutrons.

\* From R. Bachelor and H. R. Mck. Hyder,  
J. Nuc. Energy, 3, 7 (1956).

Group	Energy (keV)
1	—
2	560
3	405
4	450
5	—
6	—

Table 3-9  
Mean Energies of Delayed Neutrons from Thermal Fission in  $U_{235}$ \*

Table 3-9

so that comparatively little  $\gamma$ -radiation can escape. The neutrinos, by contrast, pass through even the largest reactor without interacting, and their energy is irrevocably lost. About 6% of the fission energy of all reactors is lost in this way.

The total energy of the prompt  $\gamma$ -rays is about 7 MeV. This energy is recoverable, since again comparatively little  $\gamma$ -radiation ever leaves a reactor.

**Table 3-10**  
**Emitted and Recoverable Energies for Fission of  $U^{235}$**

Form	Emitted energy, MeV	Recoverable energy, MeV
Fission fragments	168	168
Fission product decay		
$\beta$ -rays	8	8
$\gamma$ -rays	7	7
neutrinos	12	—
Prompt $\gamma$ -rays	7	7
Fission neutrons (kinetic energy)	5	5
Capture $\gamma$ -rays	—	3-12
Total	207	198-207

The total kinetic energy of the prompt fission neutrons is about 5 MeV, and this is recoverable since few neutrons escape from most reactors. Because these neutrons remain within the reactor, they eventually are captured by the nuclei in the system. It will be shown in the next chapter, however, that one of the  $\nu$ -neutrons emitted per fission must be absorbed by a fissionable nucleus and produce another fission in order for a reactor to remain in operation. It follows, therefore, that the remaining ( $\nu - 1$ ) neutrons per fission must be absorbed parasitically in the reactor, that is, absorbed in a nonfission reaction. Each absorption usually leads to the production of one or more capture  $\gamma$ -rays, whose energy depends on the binding energy of the neutron to the compound nucleus. Since  $\nu$  is approximately 2.44 for  $U^{235}$  (its precise value depends on the energy of the neutrons causing the fission), this means that from about 3 to 12 MeV of capture  $\gamma$ -radiation is produced per fission, depending upon the material in the reactor. All this  $\gamma$ -ray energy is, of course, recoverable.

Total and recoverable energies are summarized in Table 3-10 for fission in  $U^{235}$ . It will be observed that the energy of the capture  $\gamma$ -rays compensates to some extent for the energy lost by neutrino emission. The recoverable energy per fission is approximately 2% smaller for  $U^{233}$  and 4% larger for  $Pu^{239}$ .

### 3-6 Reactor Power, Fuel Burnup, and Fuel Consumption

Consider a reactor which is operating at a power of  $P$  megawatts (MW). If the recoverable energy per fission is  $E_R$  MeV, the total number of fissions occurring per second in the entire reactor is

$$\begin{aligned}
 \text{Fission rate} &= P \text{ MW} \times \frac{10^6 \text{ joules}}{\text{MW-sec}} \times \frac{\text{fission}}{E_R \text{ MeV}} \\
 &\quad \times \frac{\text{MeV}}{1.60 \times 10^{-13} \text{ joule}} \\
 &\quad \times \frac{86400 \text{ sec}}{\text{day}} \\
 &= 5.40 \times 10^{23} \frac{P}{E_R} \text{ fissions/day.} \tag{3-16}
 \end{aligned}$$

If the atomic weight ( $\approx$  mass number) of the fissile nucleus is  $A$ , this requires the fissioning or *burnup*, as it is usually called, of

$$\begin{aligned}
 \text{Burnup rate} &= 5.40 \times 10^{23} \frac{P}{E_R} \times \frac{A}{0.602 \times 10^{24}} \\
 &= 0.895 \frac{PA}{E_R} \text{ gm/day.} \tag{3-17}
 \end{aligned}$$

With  $\text{U}^{235}$  fuel and a recoverable energy of 200 MeV, Eq. (3-17) gives a burnup rate of  $1.05P$  gm/day. Thus if the reactor is operating at a power of 1 MW, the  $\text{U}^{235}$  undergoes fission at the rate of approximately 1 gm/day. To put this another way, the release of 1 megawatt-day of energy requires the fission of 1 gram of  $\text{U}^{235}$ .

It must be remembered, however, that fissile nuclei are *consumed* both in fission and in radiative capture. Since the total absorption rate is  $\sigma_a/\sigma_f = (1 + \alpha)$  times the fission rate, it follows from Eq. (3-17) that fissile material is consumed at the rate of

$$\text{Consumption rate} = 0.895 (1 + \alpha) \frac{PA}{E_R} \text{ gm/day.} \tag{3-18}$$

For  $\text{U}^{235}$ , the thermal value of  $\alpha$  is 0.175 and Eq. (3-18) shows that this isotope is consumed at the rate of about 1.24 gm/day per megawatt of power if the fissions are induced primarily by thermal neutrons.

It is desirable to have a special unit to describe the energy release from nuclear fuels. Unfortunately, there is no universally accepted unit of this kind.\* Frequently the unit megawatt-days per metric ton of fuel, abbreviated MWD/T, is used where a metric ton (written tonne) is  $1000 \text{ kgm} = 10^6 \text{ gm}$ . As an example of

---

\* The High Temperature Fuels Committee of the U.S. Atomic Energy Commission has recommended the adoption of the unit "fissions/cm<sup>3</sup>", but this unit is not widely used.

the use of this unit, suppose that the fuel consists of pure U<sup>235</sup>. If it were possible to fission all of the U<sup>235</sup> nuclei, the total energy release would be 1 MWD/gm, which is equivalent to 10<sup>6</sup> MWD/T. Because of parasitic absorption, however, the maximum energy release from U<sup>235</sup> is actually about 800,000 MWD/T.

In most reactors the fissile atoms are contained in solid *fuel elements*, the bulk of whose atoms are not fissile. For example, rods of natural uranium are used as fuel in some reactors, and in this case only 0.72 % of the atoms are fissile. In other reactors the fuel elements are mixtures or alloys of uranium, enriched in U<sup>235</sup>, and various structural materials, such as aluminum, stainless steel, or zirconium, having low neutron absorption cross sections. The ratio of fissile atoms to non-fissile atoms is again usually of the order of 1/100.

When a fission occurs in a solid fuel element the microscopic structure of the material is disrupted in the vicinity of the fission site, an effect which is called *radiation damage*. The cumulative effect of many fissions eventually leads to a loss of structural integrity of the element. As a general rule, such materials failure is found to occur when more than about 1 % of the atoms have undergone fission. This condition is referred to as *one percent burnup*,\* and corresponds to an energy release of somewhere in the neighborhood of 10,000 to 20,000 MWD/T, depending on the fuel element. While this appears to represent a very small utilization of the fuel, this is not the case in view of the small concentration of fissile isotopes in most fuel elements. Thus one percent burnup in a fuel element containing the order of one atom percent of fissile material is actually equivalent to 100 percent burnup of the fissile isotope.

## References

### General

- BURCHAM, W. E., *Nuclear Physics*. New York: McGraw-Hill, 1963, Appendix 6.  
ENDT, P. M., and P. B. SMITH, Editors, *Nuclear Reactions*, Vol. II. Amsterdam: North Holland, 1962, Chapter 2.  
EVANS, R. D., *The Atomic Nucleus*. New York: McGraw-Hill, 1955, Chapter 14.  
GREEN, A. E. S., *Nuclear Physics*. New York: McGraw-Hill, 1955, Chapter 9.  
HALPERN, I., "Nuclear Fission," *Ann. Rev. Nucl. Sci.*, 9, 245 (1959).  
KAPLAN, I., *Nuclear Physics*, 2nd ed. Reading, Mass.: Addison-Wesley, 1963, Chapter 19.  
KEEPIN, G. R., *Physics of Nuclear Kinetics*. Reading, Mass.: Addison-Wesley, 1965.  
LITTLER, D. J., and J. F. RAFFLE, *An Introduction to Reactor Physics*, 2nd ed. New York: McGraw-Hill, 1957, Chapter 4.  
WEINBERG, A. M., and E. P. WIGNER, *The Physical Theory of Neutron Chain Reactors*. Chicago: University of Chicago Press, 1958, Chapter 5.  
WHEELER, J. A., "Fission," *Handbook of Physics*, Part 9, E. U. CONDON and H. ODISHAW (Editors). New York: McGraw-Hill, 1958, Chapter 11.

\* It must be emphasized that the term "burnup" refers to atoms fissioned, not atoms consumed.

**Data**

Cross sections may be found in the tables of data noted in the references to Chapter 2.  
See also:

ETHERINGTON, H., Editor, *Nuclear Engineering Handbook*. New York: McGraw-Hill, 1958, Section 2.

SOODAK, H., Editor, *Reactor Handbook*, 2nd ed., Vol. III, Part A. New York: Wiley, 1962, Chapter 1.

TEMPLIN, L. J., Editor, "Reactor Physics Constants," ANL-5800, 2nd ed. (1963), Sections 1 and 2.

**Problems**

[*Note*: Where necessary in the following problems, evaluate cross sections at 0.025 eV and take the recoverable energy of fission to be 200 MeV.]

3-1. How does the Coulomb energy between fission fragments depend upon the degree of asymmetry of the fission? In particular, does  $E_q$  increase or decrease with increasingly asymmetric fission?

3-2. If the  $Q$ -value for fission of  $\text{Bi}^{209}$  is approximately 160 MeV, estimate the critical energy for fission of this nucleus.

3-3. Derive the Borst-Wheeler function (Eq. 3-9).

3-4. In a bad accident all the fission products are released from a reactor which had been operating at a power of 100 megawatts for one year. Rescue crews reaching the area one day after the accident find a fission product activity equivalent to the explosion of roughly how large a nuclear warhead? Which activity would die off more rapidly; that of the reactor or the bomb? [*Note*: The yield of a nuclear weapon is measured in kilotons, where 1 kiloton =  $2.6 \times 10^{25}$  MeV.]

3-5. A small training reactor is operated an average of two hours every day for two years at a power of 1000 watts and is then shut down. If the average energies of the fission product  $\beta$ -rays and  $\gamma$ -rays are taken to be 0.4 MeV and 0.7 MeV, respectively, what is the total activity of the fuel one year after shutdown?

3-6. Radioactive fallout (mainly dust particles and water droplets to which fission products have adhered) settles in an area at the time  $t_0$  after the detonation of a nuclear warhead. The initial radiation dose rate (which is proportional to the fission product activity) is  $R_0$ . Show that the total dose which will be received in the area is equal to  $5t_0R_0$ .

3-7. Using Eq. (3-8) find the average energy of a fission product  $\gamma$ -ray.

3-8. The prompt fission neutron spectrum is often represented by the function

$$\chi(E) = Ce^{-aE} \sinh \sqrt{bE},$$

where  $C$ ,  $a$ , and  $b$  are constants. (a) If the function  $\chi(E)$  is normalized to one neutron, that is, if

$$\int_0^{\infty} \chi(E) dE = 1,$$

show that the constant  $C$  is given by

$$C = 2\sqrt{a^3/\pi b} \exp(-b/4a).$$

(b) Find a (transcendental) expression for the most probable energy. (c) Show that the average energy  $\bar{E}$  is given by

$$\bar{E} = \frac{3}{2a} + \frac{b}{4a^2}.$$

3-9. Compute and plot the parameter  $\eta$  for uranium enriched in  $U^{235}$ , as a function of its enrichment (atom percent of  $U^{235}$ ) at an energy of 0.025 eV.

3-10. Although fission is observed with neutrons of much lower energy, the threshold for fission of  $U^{238}$  is often taken to be 1.4 MeV, since the fission cross section is small below this energy. Using this threshold, what fraction of the prompt fission neutrons are capable of inducing fission in  $U^{238}$ ?

3-11. The propulsion plant of a nuclear submarine delivers 25,000 shaft horsepower at a cruising speed of 20 knots (1 knot = 1.15 statute miles/h). Assuming an overall plant efficiency of about 25%, how much fuel ( $U^{235}$ ) is consumed on a 40,000-mile cruise around the world at this speed?

3-12. Show that for fuel elements of natural or slightly enriched uranium the total energy release  $W$  is given approximately by

$$W = 7.9 \times 10^5 \beta \text{ MWD/T},$$

where  $\beta$  is the fraction of the atoms consumed.

# 4

## Neutron Chain-Reacting Systems

It was pointed out in the preceding chapter that more than one neutron is emitted, on the average, when a nucleus fissions. In the proper environment of fissionable material, these fission neutrons are capable of inducing further fissions with the release of more neutrons, and so on. This sequence of events is known as a *chain reaction*, and is the process by which nuclear energy is utilized in practical applications. A *nuclear reactor* is a device in which things are so arranged that a self-sustained fission chain reaction can occur in a controlled manner. In this chapter the essential features of the fission chain reaction will be considered along with the types of reactors that have been developed to utilize this process.

### 4-1 Multiplication Factor

The required condition for a stable, self-sustained chain reaction in a nuclear reactor is that exactly one neutron must be produced per fission which eventually succeeds in inducing another fission. In other words, one fission must lead to another, and if this is the case, the number of fissions occurring per unit time within the system will be constant. If, on the other hand, each fission eventually leads to more than one fission, the fission rate will increase in time, and conversely, it will decrease with time if less than one additional fission occurs per fission.

These ideas can be expressed conveniently in terms of the *multiplication factor*. This is defined as the *ratio of the number of fissions in any one generation to the number of fissions in the immediately preceding generation*. When this factor is exactly equal to unity the number of fissions in each succeeding generation is a constant, and a chain reaction initiated in the system will continue at a constant rate. Such a system is said to be *critical*. If the multiplication factor is greater than unity, the number of fissions increases with each succeeding generation. In this case, the chain reaction diverges and the reactor is said to be *supercritical*. Finally, if the multiplication factor is less than unity, the chain reaction eventually dies out, and the system is called *subcritical*.

### 4-2 Neutron Balance and Conditions for Criticality

In order to maintain a self-sustained chain reaction in a reactor, a careful balance must be established between the rate at which neutrons are produced in the system and the rate at which they disappear. Neutrons disappear in two ways; they either leak from the surface of the reactor or are absorbed within its interior.

The rates at which neutron leakage and absorption occur are governed by the size and composition of the system. Consider, for example, a reactor consisting of a bare sphere of pure  $U^{235}$ . This type of reactor is known (for obvious reasons) as a *Godiva* reactor. If the sphere is very small, most of the fission neutrons immediately escape from the system, and too few fissions are produced to sustain the chain reaction. The fraction of neutrons which leak from the system can be reduced, however, by simply increasing the radius of the sphere. As the radius becomes large compared to the neutron mean free path, the leakage of neutrons occurs from regions near the surface of the sphere, whereas the fission-producing reactions occur throughout the interior. Thus as the radius is increased the leakage increases as  $r^2$  while the total fission rate increases as  $r^3$ . The ratio of neutron leakage to neutron production therefore goes down as  $1/r$ , and at a particular radius  $r_c$ , the number of neutrons which are produced in the reactor is just sufficient to compensate for losses owing to leakage and absorption. If a chain reaction is initiated in a sphere of this size, it will continue at a constant rate; in other words, the system is critical. The radius  $r_c$  is known as the *critical radius*, and the required amount of fuel is called the *critical mass*. For pure  $U^{235}$ ,  $r_c$  is about 8.7 cm and the critical mass is 52 kg.

In the preceding example, a critical system was obtained by adjusting the size of a system of given composition, in this case, the mass of fissionable material. Criticality can also be attained in a system of specified size and shape by adjusting its composition. Consider, for instance, a large tank of water of fixed dimensions. If initially there is no fissionable material in the tank, there clearly can be no chain reaction. When fuel is added, say in the form of a soluble  $U^{235}$  salt, fissions will begin to occur. In this system the fast fission neutrons are produced in an environment of essentially pure water and they rapidly slow down to thermal energies in collisions with the water. These thermalized neutrons remain in the system until they are either absorbed by the fuel or by the water; comparatively few neutrons leak from the tank since it has been assumed to be large. If only a small amount of fuel is present in the tank, most of the neutrons are absorbed by the water and relatively few by the fuel. The necessary neutron balance for a self-sustained chain reaction is not obtained and the system remains subcritical. However, as more fuel is added, the *fraction* of neutrons absorbed by the fuel increases, and eventually, at some particular fuel concentration, the system will become critical.

### 4-3 Conversion and Breeding

In view of the inevitable losses of neutrons by leakage and absorption, it is clear that  $\eta$ , the number of neutrons emitted per neutron absorbed by a fissile or fissionable nucleus, must be greater than unity in order to achieve criticality. In actual fact,  $\eta$  is considerably larger than unity for  $U^{233}$ ,  $U^{235}$ , and  $Pu^{239}$ , and also for natural uranium. The question immediately arises as to whether the neutrons in excess of the number required to maintain a chain reaction can be utilized to advantage.

Aside from such uses as the production of radioactive isotopes or for research, the excess neutrons can also be used to produce fissile isotopes from fertile material, a process known as *conversion*. For instance, as discussed in Section 3-2, the fissile isotope  $\text{Pu}^{239}$ , which does not occur naturally, can be made in a reactor by the absorption of some of the excess fission neutrons by  $\text{U}^{238}$ . In this way the  $\text{U}^{238}$ , which only fissions at high energies and hence is of comparatively little value in most reactors, is converted to the important fissile isotope  $\text{Pu}^{239}$ . Reactors which are built specifically for converting fertile materials are called *converters*. The large natural uranium-graphite reactors, for example, that were constructed at Hanford, Washington, during and since World War II, operate as converters for the production of  $\text{Pu}^{239}$ .

The conversion process is described quantitatively by the *conversion ratio* or sometimes, loosely, the *breeding ratio*. This quantity, which is denoted by  $C$ , is defined as the average number of fissile atoms produced in a reactor per fuel atom consumed either by fission or absorption. If the newly-produced isotope is not the same as the one that fuels the reactor, the consumption of  $N$  atoms of primary fuel leads to the conversion of  $NC$  atoms of the fertile isotope. On the other hand, if the new isotope is the same one that fuels the reactor, the situation is somewhat more complicated since it is not possible to distinguish between the new and the old fuel. In this case, it can be shown (cf. Prob. 4-4) that when  $N$  atoms of primary fuel are consumed, a total of  $NC/(1 - C)$  atoms of fertile material are converted, provided  $C$  is less than unity. When  $C$  is unity, one new fissile atom is produced for every atom of fuel consumed, and in this situation, fertile material can be converted in the reactor indefinitely without adding new fuel to the system.

The most important case, however, occurs when  $C$  is greater than unity. Now, *more* fuel is produced than is consumed in the system and the reactor is said to *breed*.\* The extent to which breeding occurs in a reactor is measured by the *breeding gain*  $G$ . This is equal to the number of fissile nuclei *gained* in the system per fuel atom consumed. Since  $C$  is the total number of fissile atoms produced per fuel atom consumed, the *increase* in the number of fuel atoms, that is,  $G$ , is simply  $C - 1$ .

Since it is only necessary that  $\eta$  be greater than unity in order for conversion to occur, it is a fairly simple matter to build reactors which operate, at least to some extent, as converters. Unfortunately, it is much more difficult to build reactors that breed, since now  $\eta$  must be somewhat greater than 2. This is due to the fact

---

\* It should be noted that in recent usage the term "breeding" is used simply to describe the situation in which more fuel is produced than consumed, whether or not the new fuel is the same isotope as the old. Thus a  $\text{U}^{235}$ -fueled reactor which converts  $\text{U}^{238}$  to  $\text{Pu}^{239}$  is said to "breed," provided more  $\text{Pu}^{239}$  is produced than  $\text{U}^{235}$  consumed. However, breeding is relatively unimportant for nuclei such as  $\text{U}^{235}$  which cannot be produced from fertile material, since the  $\text{U}^{235}$  can only be used once. The pressing question, therefore, is always whether the breedable isotopes such as  $\text{U}^{233}$  and  $\text{Pu}^{239}$  can themselves be used to fuel reactors that breed.

that one neutron on the average must be absorbed in fuel and produce another fission in order to sustain the chain reaction, and at the same time *more than one neutron* must be absorbed by fertile material if a reactor is to breed.

Table 3-2 gives the thermal values of  $\eta$ , that is, at a neutron energy of 0.025 eV. Reactors in which most of the fissions are induced by neutrons of about this energy, from approximately 0.01 eV to 0.3 eV, are known as *thermal reactors*.

Breeding is probably not feasible in a thermal reactor using  $U^{235}$  or  $Pu^{239}$  as fuel, for although  $\eta$  of both these isotopes is somewhat greater than 2, neither is evidently large enough to compensate for the leakage and parasitic capture of neutrons that inevitably occur to some extent in every reactor.

The situation with regard to  $U^{233}$  is considerably better, however, since  $\eta$  of this isotope is almost 2.3. Although no reactor fueled with  $U^{233}$  has as yet been built, it is generally believed that a thermal reactor of this type could successfully be made to breed.

While thermal reactors fueled with  $U^{235}$  or  $Pu^{239}$  probably cannot breed, it is possible to breed, at least with  $Pu^{239}$ , provided the energy of the neutrons which induce the fissions is raised sufficiently. It will be recalled from Chapter 3 that although  $v$ , the average number of neutrons emitted in fission, changes very slowly with the energy of the incident neutron, the capture-to-fission ratio,  $\alpha$ , is a sensitive function of energy. As a consequence,  $\eta$  is also strongly energy dependent as shown in Fig. 4-1. It will be noted that at low energies  $\eta$  is approximately constant for  $U^{233}$  and  $U^{235}$  but decreases with increasing energy for  $Pu^{239}$ . In the resonance region, from about 1 eV to 1 keV,  $\eta$  is much smaller, on the average, than

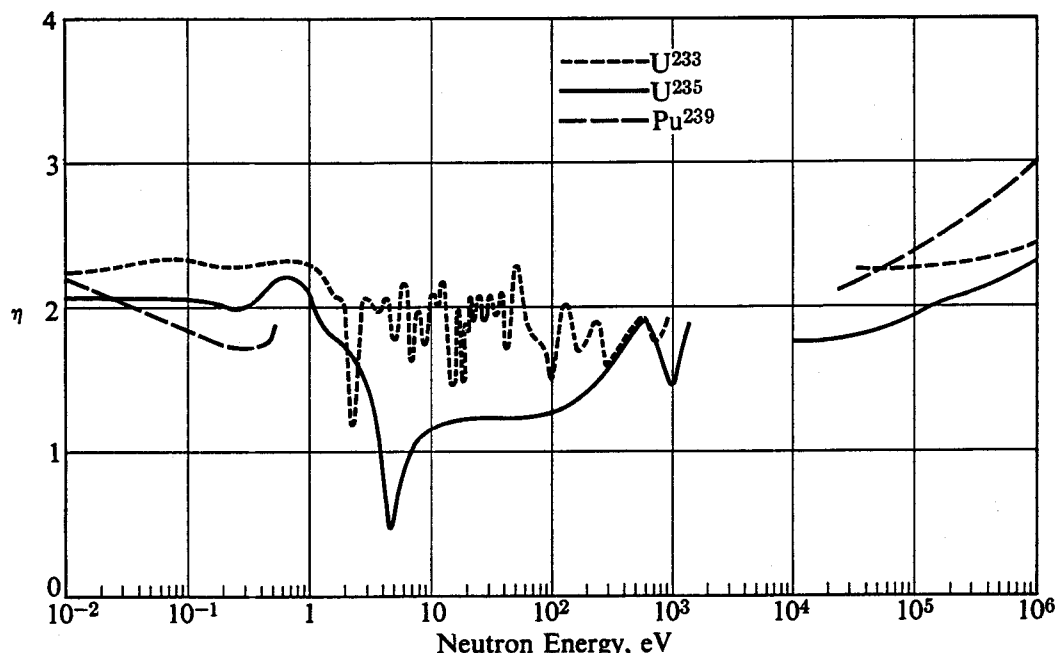


Fig. 4-1. Variation of  $\eta$  with energy for  $U^{233}$ ,  $U^{235}$ , and  $Pu^{239}$ . The  $U^{235}$  curve has been smoothed in the eV region. [From BNL-325, Second Edition (1958 plus supplements).]

at low energies. (This is true also for  $\text{Pu}^{239}$ , although there is too little data to draw a curve for this nucleus in this region.) Because of experimental difficulties there is almost no data on  $\eta$  between about 1 keV and 10 keV. However, beyond 10 keV it will be observed that  $\eta$  increases and, particularly in the case of  $\text{Pu}^{239}$ , rises to comparatively large values. It follows from Fig. 4-1 that a reactor fueled with  $\text{Pu}^{239}$  will breed provided the fissions in the reactor are induced by neutrons with an energy in the vicinity of 100 keV or larger. This conclusion also holds for  $\text{U}^{233}$ ; for  $\text{U}^{235}$  to breed the energy of the neutrons must be substantially higher. Reactors in which the chain reaction is sustained by such fast neutrons are called *fast reactors*. These reactors are discussed more fully in the next section.

#### 4-4 Types of Nuclear Reactors

For classification purposes nuclear reactors are divided into three types depending upon the average energy of the neutrons which cause the bulk of the fissions in the system. These are, respectively, *thermal reactors*, in which most fissions are induced by neutrons that are more or less in thermal equilibrium with the atoms in the system and have an energy below approximately 0.3 eV; *intermediate reactors*,\* in which neutrons having an energy from somewhat above thermal to approximately 10 keV are largely responsible for producing fissions; and *fast reactors*, in which fissions are induced primarily by neutrons with an energy of the order of 100 keV and above.

**Thermal reactors.** Almost all of the reactors which have been built to date are of the thermal type. The principal reason for the popularity of this kind of reactor is that it is the easiest to make critical, that is, the amount of fissionable material required is much smaller than for a comparable intermediate or fast reactor. This, in turn, is due to the fact that the fission cross sections of the fissile nuclei (i.e.,  $\text{U}^{233}$ ,  $\text{U}^{235}$ , and  $\text{Pu}^{239}$ ) increase with decreasing neutron energy. At 2 MeV, for instance,  $\sigma_f$  of  $\text{U}^{235}$  is only 1.3 barns, whereas it is 577 barns at 0.025 eV. In a system of given composition, the probability per unit path that a neutron will induce fission is therefore much larger for a slow neutron than for a fast neutron, and as a result considerably less fuel is needed for a thermal reactor than for, say, a comparable fast reactor.

In a thermal reactor the fission neutrons are slowed down by the use of a *moderator*. This is a mass of lightweight material, such as carbon, beryllium, or water, which is distributed throughout the fueled region or *core* of the reactor. Light material is used because, as will be explained in Chapter 6, neutrons slow down in a light material in a much shorter distance than in a heavy material. This tends to reduce the leakage of neutrons from the reactor and thereby reduces the reactor size. In order to reduce the leakage of neutrons still further, it is usual to surround the core of a thermal reactor with an additional region of moderating

\* Intermediate reactors are sometimes also called *resonance reactors* because most of the neutrons responsible for fission lie in the resonance region of the heavy elements.

material called the *reflector*. In this way, many neutrons that would ordinarily leak from a bare system have collisions in the reflector and are returned to the core. In liquid-moderated reactors, the moderator frequently serves also as the coolant. With water-moderated reactors, for example, the water is continually circulated through and around the core and acts simultaneously as coolant, moderator, and reflector.

Hundreds of thermal reactors have been built in recent years for a variety of purposes: for power, research, isotope production, and so on. These reactors are safe, reliable, and probably about as well understood as ordinary gasoline engines.

**Intermediate reactors.** At one time when there were little data on fission and radiative capture sections, it was thought that  $\alpha$ , the capture-to-fission ratio, would ordinarily be much less than unity since fission was believed to be a far more rapid process than capture. Although it was known that the values of  $\alpha$  for  $U^{235}$  and  $Pu^{239}$  were high at thermal energies, this fact was interpreted as resulting from an unusual property of the 0.3-eV resonance which is common to both nuclei. It was felt, therefore, that a reactor in which the neutron spectrum was sufficiently elevated to avoid the 0.3-eV resonance would have a low effective value of  $\alpha$ . Had this been the case, it would have been possible to build a reactor capable of breeding, with a critical mass considerably smaller than that required for a fast reactor. At the same time, there was some hope that higher power densities and longer fuel lifetimes would be possible compared to those attainable in a fast reactor.

It is a relatively simple matter to build a reactor having the desired neutron spectrum. This is done by using a somewhat smaller quantity of moderator than in a thermal reactor and at the same time increasing the concentration of the fuel. The fission neutrons are then absorbed by the fuel before they have an opportunity to slow down to thermal energies. However, an intermediate breeder reactor was never actually constructed. Preliminary experiments showed that a high value of  $\alpha$  was the rule rather than the exception at low energies, and that it is necessary, in fact, to go to energies of the order of 100 keV before  $\alpha$  becomes small enough to permit breeding.

Nevertheless, it was also pointed out that in several ways an intermediate reactor might be more attractive for propulsion purposes than a comparable thermal reactor. The most important of these is the possibility of using liquid metal coolants, such as sodium, which have excellent heat transfer properties, without having to increase the core volume as is the case when these coolants are used in a thermal reactor. Thus as will be shown in Chapter 6, materials such as sodium are not very effective in slowing down neutrons at energies below several keV, and when these are used as coolants in a thermal reactor it is necessary to enlarge the core with compensating moderator to ensure that the reactor will indeed be thermal. With the intermediate system, however, the inclusion of liquid metals does not materially disturb the spectrum, and so the core of an intermediate reactor and therefore the reactor itself, can be considerably smaller than an equivalent

thermal reactor. This is a most important consideration in a mobile installation such as a submarine.

In addition to its small size, an intermediate reactor has the additional advantage over a thermal system in that it is immune from effects of certain fission products which have very large thermal cross sections. Thus, as discussed in Chapter 13, under certain circumstances these *fission-product poisons*, as they are called, can seriously impede the operation of a thermal reactor and interfere with the mobility of the installation. Since there are few thermal neutrons in an intermediate reactor, these poisons have little or no effect on the operation of the system.

With these advantages in mind, the Submarine Intermediate Reactor (SIR) was constructed at West Milton, New York, and a similar reactor was installed on the second American nuclear submarine Sea Wolf. The performance of the reactor reportedly exceeded expectations, but it was later replaced by a pressurized water reactor when the Navy adopted this system as its fleet standard.

It is now generally felt that the additional complications inherent in an intermediate reactor, in particular, the presence of large quantities of hot, radioactive coolant, militate against the use of these reactors for mobile installations. For stationary power plants, on the other hand, where size is less important, it is considered more reasonable to build thermal reactors when breeding is not an important consideration, or fast reactors when it is. Intermediate reactors, therefore, are not being developed at the present time. Nevertheless, it should be recognized that compact thermal reactors have a substantial fraction of fissions produced by neutrons in the intermediate energy region, i.e., from a few eV to approximately 10 keV. Fast reactors also have a large fraction of fissions occurring in the intermediate region because of inelastic scattering of fast neutrons and some elastic moderation by the coolant. For these reasons, the study of the effects of intermediate energy neutrons continues to be an important part of reactor theory.

**Fast reactors.** One of the most promising types of reactors is the fast reactor. This system contains no moderator whatever and is simply an assembly of fissionable material and coolant. The coolant, of course, must not be a lightweight material such as  $H_2O$  or  $D_2O$ , since these materials would tend to moderate the neutrons. The fast fission neutrons thus slow down much less than they do in other reactors, and the bulk of fissions occurs at energies of the order of 100 keV. Figure 4-1 shows that it is in this energy region that  $\eta$  becomes large, and as mentioned earlier, these reactors are therefore capable of breeding.

The first large-scale reactor of this type built in the United States was the Fermi Reactor. The core of this reactor consists of assemblies of uranium enriched to 25.6%  $U^{235}$ . Surrounding the core is the principal breeding region or *blanket* consisting of assemblies of uranium depleted in  $U^{235}$  to 0.35%. This depleted uranium is the residue or "tailings" from the gaseous diffusion plants at Oak Ridge. The core and blanket are both immersed in the liquid-sodium coolant which is continually circulated through the system.

Since the fission cross section is so small at the operating neutron energies of fast reactors, these reactors require a large mass of fuel to become critical. The critical mass of the Fermi Reactor, for example, is 444 kg of U<sup>235</sup>. By contrast, a thermal water reactor of the same size would have a critical mass of only about 20 kg. Because they require such large critical masses, and for a number of other reasons, the construction of large fast reactors has only been attempted in recent years.

#### 4-5 General Considerations of Reactor Design

Nuclear reactors are potentially dangerous devices, and for this reason they must be designed with care. The accidental release of the accumulated fission products from even a small power reactor can lead to a disaster of major proportions. Even if the fission products are prevented from escaping to the surrounding community by a suitable containment vessel, repairs to the reactor can be a lengthy and expensive undertaking.

The fundamental process which underlies the operation of a reactor is, of course, the fission chain reaction, and the central problem of the reactor designer is to provide a system in which a self-sustained chain reaction can occur with complete safety. At the same time, the reactor must be capable of fulfilling the function for which it is designed, i.e., the production of power, isotopes, etc. To design such a system the reactor engineer must be able to calculate every aspect of the chain reaction in some detail. In the following chapters it will be shown how many of the necessary calculations can be made.

### References

#### General

EL-WAKIL, M. M., *Nuclear Power Engineering*. New York: McGraw-Hill, 1962, Part 3.

ETHERINGTON, H., Editor, *Nuclear Engineering Handbook*. New York: McGraw-Hill, 1958, Sections 12 and 13.

GLASSTONE, S., and A. SESONSKE, *Nuclear Reactor Engineering*. Princeton, N.J.: Van Nostrand, 1963, Chapter 13.

ISBIN, H. S., *Introductory Nuclear Reactor Theory*. New York: Reinhold, 1963, Chapter 1.

MURRAY, R. L., *Introduction to Nuclear Engineering*, 2nd ed. Englewood Cliffs, N.J.: Prentice-Hall, 1961, Chapters 3, 4 ,and 5.

STEPHENSON, R., *Introduction to Nuclear Engineering*, 2nd ed. New York: McGraw-Hill, 1958, Chapter 3.

WEINBERG, A. M., and E. P. WIGNER, *The Physical Theory of Neutron Chain Reactors*. Chicago: University of Chicago Press, 1958, Chapters 1 and 7.

#### Specific Reactors

DIETRICH, J. R., and W. H. ZINN, Editors, *Solid Fuel Reactors*. Reading, Mass.: Addison-Wesley, 1958.

HURWITZ, H., JR., and R. EHRLICH, "Highly Enriched Intermediate and Thermal Assemblies," *Progress in Nuclear Energy*, Series I, Volume I. New York: McGraw-Hill, 1956.

KRAMER, A. W., *Boiling Water Reactors*. Reading, Mass.: Addison-Wesley, 1958.

LANE, J. A., H. G. MACPHERSON, and F. MASLAN, Editors, *Fluid Fuel Reactors*. Reading, Mass.: Addison-Wesley, 1958.

PALMER, R. G., and A. PLATT, *Fast Reactors*. London: Temple Press, 1961.

*Proceedings of 2nd U.N. International Conference on Peaceful Uses of Atomic Energy*, Geneva, 1958. New York: United Nations, 1958, Volumes 7 through 10.

*The Shippingport Pressurized Water Reactor*. Reading, Mass.: Addison-Wesley, 1958.

STARR, C., and R. W. DICKINSON, *Sodium-Graphite Reactors*. Reading, Mass.: Addison-Wesley, 1958.

## Problems

4-1. In a certain thermal reactor fueled with  $U^{235}$ , it is observed that 25% of the neutrons emitted in fission escape from the system while 30% are captured in the moderator, structure, and other nonfissile materials. Was the reactor critical at the time these observations were made? Explain.

4-2. Given any conceivable assembly of fissile material, what is the maximum value of the multiplication factor?

4-3. Consider a bare lump of fissile material. Let  $P$  be the average probability that a fission neutron born anywhere within the lump will have a collision in the lump. (a) If  $\sigma_s \approx 0$ , show that the condition for the lump to be critical is  $\eta P = 1$ , where  $\eta$  is the average number of neutrons emitted per neutron absorbed. (b) If  $\sigma_s$  is not zero, but it is assumed that the fission neutrons do not lose energy in scattering collisions, show that the condition for criticality becomes

$$\frac{\eta P \sigma_a}{\sigma_t - P \sigma_s} = 1.$$

(c) Using 1 MeV cross sections, estimate  $P$  for a bare sphere of  $U^{235}$ . [Hint: In part (b), note that at each collision  $\sigma_a/\sigma_t$  neutrons are absorbed, on the average, and  $\sigma_s/\sigma_t$  are scattered. Then compute the total number of fission neutrons produced per initial fission neutron.]

4-4. If the primary and newly-produced fuel in a converter reactor are the same, show that a total of  $NC/(1 - C)$  atoms of fertile material are converted when  $N$  atoms of fuel are consumed, provided the conversion ratio,  $C$ , is less than unity.

4-5. The rate at which breeding occurs in a reactor is occasionally measured in terms of the *doubling time*,  $t_D$ . This is defined as the time required for the amount of fissile material in a reactor to double. Show that

$$t_D = \frac{ME_R}{0.895(1 + \alpha)PAG},$$

where  $M$  is the original fuel inventory of the reactor in grams,  $E_R$  is the recoverable energy in MeV,  $P$  is the operating power in MW,  $A$  is the atomic weight of the fuel, and  $G$  is the breeding gain.

# 5

## The Diffusion of Neutrons

Neutrons move about in a reactor in complicated, zigzag paths due to repeated collisions with nuclei. As a consequence of this motion, neutrons that were originally in one part of a reactor and moving in a particular direction with a particular energy appear at a later time in another part of the system, moving in another direction with some other energy. The neutrons in this case are said to have been *transported* from the first region and energy to the second, and the study of this phenomenon is known as *transport theory*.

Transport theory is relatively simple in principle, and an exact equation governing transport phenomena can easily be derived. This is called the *Boltzmann equation*, or the *transport equation*, and the study of transport theory is essentially the study of this equation. Unfortunately, it is much easier to derive the Boltzmann equation than it is to solve it. Under certain conditions, however, the equation simplifies considerably and can be treated in a rather straightforward way. This simplified version of transport theory is called *diffusion theory* and is the subject of the present chapter. While the requirements for the validity of diffusion theory are seldom fully realized in practical reactor problems, the use of this method usually provides a good approximation to the exact transport solution, and, due to its simplicity, it is commonly used in many reactor design problems.

For the most part it will be assumed in this chapter that all neutrons have the same energy, and the theory to be developed is called *one-velocity diffusion theory*.<sup>\*</sup> The diffusion of polyenergetic neutrons is discussed in Chapter 6 and later chapters. Preliminary to considering neutron diffusion, however, it is necessary to set up a framework for describing the rate at which neutrons interact at any point in a reactor.

### 5-1 Interaction Rates and Neutron Flux

It will be recalled from Chapter 2 that the rate at which interactions occur within a thin target, placed in a beam of monoenergetic neutrons of intensity  $I$ , is equal to  $I\Sigma_t$  interactions per  $\text{cm}^3/\text{sec}$ , where  $\Sigma_t$  is the macroscopic total cross section. Consider now the situation shown in Fig. 5-1, in which a small target is exposed simultaneously to several beams of intensities  $I_A, I_B, I_C$ , etc., all neutrons having

---

\* More precisely, one-velocity diffusion theory should be called *one-speed*, or *monoenergetic*, diffusion theory. Clearly, neutrons with a single *velocity* cannot diffuse, since velocity is a vector quantity.

the same energy. In view of the fact that the interaction of neutrons is independent of the angle at which they strike the target, the total interaction rate is evidently just  $(I_A + I_B + I_C + \dots) \Sigma_t$  interactions per  $\text{cm}^3/\text{sec}$ .

The situation at any point in a nuclear reactor is similar to the experiment shown in Fig. 5-1, except that the neutrons move in *all* directions. The interaction rate (or *collision density*, as the interaction rate is often called in reactor calculations) can therefore be found by a straightforward generalization of the above results. For this purpose it is convenient to introduce the function  $n(\mathbf{r}, \omega)$  which is known as the *neutron density distribution function*. This function is defined so that  $n(\mathbf{r}, \omega) d\Omega$  is the number of neutrons per  $\text{cm}^3$  at the point  $\mathbf{r}$  whose velocity vectors lie within the differential solid angle  $d\Omega$  about the direction  $\omega$ , as indicated in Fig. 5-2. In terms of this function, the total number of neutrons per  $\text{cm}^3$  at  $\mathbf{r}$ , denoted by  $n(\mathbf{r})$ , is given by

$$n(\mathbf{r}) = \int_{4\pi} n(\mathbf{r}, \omega) d\Omega, \quad (5-1)$$

where the  $4\pi$  on the integral means that the integration is to be carried out over all solid angle, that is, over all possible directions of motion of the neutrons.

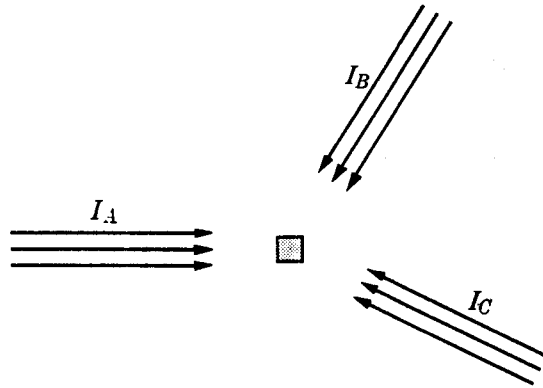


Fig. 5-1. A small target exposed to several neutron beams.

As discussed in Chapter 2, the intensity of a beam of monoenergetic neutrons is equal to the density of neutrons in the beam multiplied by their speed. It is possible, therefore, to think of the neutrons which are moving into the solid angle  $d\Omega$  about  $\omega$  as comprising a differential beam of intensity  $dI(\mathbf{r}, \omega)$  which is given by

$$dI(\mathbf{r}, \omega) = n(\mathbf{r}, \omega)v d\Omega, \quad (5-2)$$

where  $v$  is the speed of the neutrons. The interaction rate  $dF(\mathbf{r}, \omega)^*$  due to this beam is evidently

$$dF(\mathbf{r}, \omega) = \Sigma_t dI(\mathbf{r}, \omega), \quad (5-3)$$

and the total interaction rate at  $\mathbf{r}$  is

$$F(\mathbf{r}) = \int dF(\mathbf{r}, \omega) = \Sigma_t \int_{4\pi} n(\mathbf{r}, \omega)v d\Omega. \quad (5-4)$$

---

\* In this chapter and in the remainder of this book, interaction rates will be denoted by the symbol  $F$ .

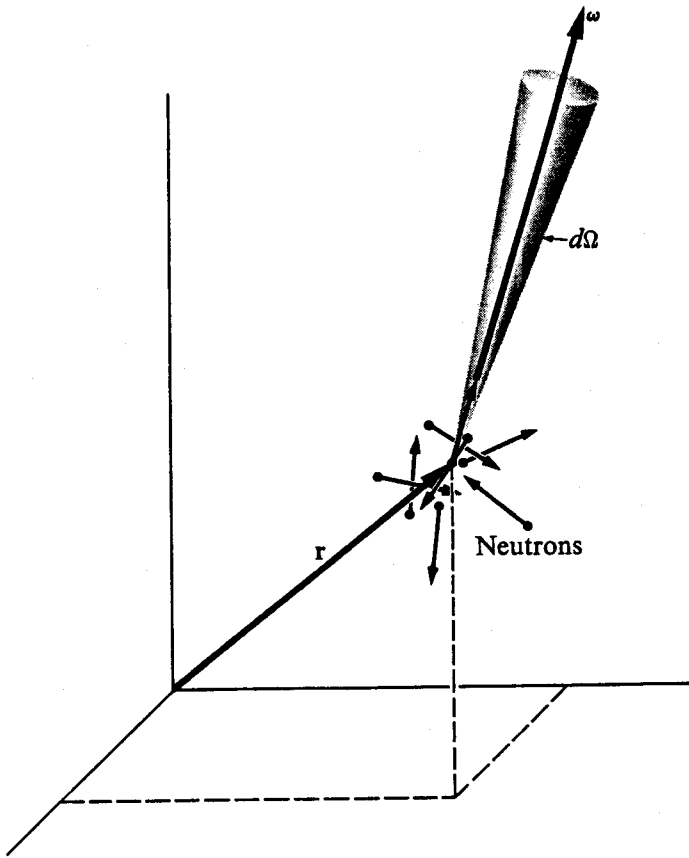


Fig. 5-2. Neutron motions near the point  $\mathbf{r}$ .

Since  $v$  has been assumed to be constant, it can be extracted from the integral in Eq. (5-4). Then in view of Eq. (5-1),  $F(\mathbf{r})$  can also be written as

$$F(\mathbf{r}) = \Sigma_t n(\mathbf{r})v. \quad (5-5)$$

The quantity  $n(\mathbf{r})v$  appearing in Eq. (5-5) occurs very frequently in nuclear engineering. It is called the *one-velocity neutron flux* and is denoted by  $\phi(\mathbf{r})$ , that is,

$$\phi(\mathbf{r}) = n(\mathbf{r})v. \quad (5-6)$$

From Eq. (5-5) the interaction rate is then

$$F(\mathbf{r}) = \Sigma_t \phi(\mathbf{r}). \quad (5-7)$$

Although the present chapter is limited to monoenergetic neutrons, it is convenient for future reference to generalize the above results at this point to include situations where the neutrons are not monoenergetic. This can easily be done by incorporating the energy distribution of the neutrons in the neutron density distribution function. Thus the new function  $n(\mathbf{r}, E, \omega)$  is defined so that  $n(\mathbf{r}, E, \omega) dE d\Omega$  is equal to the number of neutrons per  $\text{cm}^3$  having an energy between  $E$  and  $E + dE$  and which are moving into a solid angle  $d\Omega$  about the

direction  $\omega$ . The total number of neutrons per  $\text{cm}^3$  with energies between  $E$  and  $E + dE$  is then

$$n(\mathbf{r}, E) dE = \int_{4\pi} n(\mathbf{r}, E, \omega) d\Omega dE, \quad (5-8)$$

and the total neutron density is

$$n(\mathbf{r}) = \int_0^\infty \int_{4\pi} n(\mathbf{r}, E, \omega) d\Omega dE. \quad (5-9)$$

The limits on the first integral are 0 and  $\infty$  to indicate that the integration is to be carried out over all neutron energies.

Let  $F(\mathbf{r}, E) dE$  be the number of interactions occurring per  $\text{cm}^3/\text{sec}$  at  $\mathbf{r}$  in the energy interval  $dE$ . The function  $F(\mathbf{r}, E)$  is clearly the *interaction rate per unit energy*. From Eq. (5-5),

$$F(\mathbf{r}, E) dE = \Sigma_t(E) n(\mathbf{r}, E) v(E) dE, \quad (5-10)$$

where the energy dependence has been written explicitly in every term. The quantity  $n(\mathbf{r}, E)v(E)$  in Eq. (5-10) is called the *energy-dependent flux* or the *flux per unit energy* and is denoted by  $\phi(\mathbf{r}, E)$ , that is,

$$\phi(\mathbf{r}, E) = n(\mathbf{r}, E)v(E). \quad (5-11)$$

The interaction rate per unit energy at  $\mathbf{r}$  can then be written as

$$F(\mathbf{r}, E) = \Sigma_t(E)\phi(\mathbf{r}, E), \quad (5-12)$$

and the total interaction rate at  $\mathbf{r}$  is

$$F(\mathbf{r}) = \int_0^\infty \Sigma_t(E)\phi(\mathbf{r}, E) dE. \quad (5-13)$$

When  $\phi(\mathbf{r}, E)$  is known throughout a reactor (and much of the remainder of this book will be devoted to finding this function) then the total interaction rate at any point can be computed from Eq. (5-13). The rates of any particular nuclear interaction can also be computed in a rather obvious way. Thus the *scattering interaction rate* at the point  $\mathbf{r}$  is

$$F_s(\mathbf{r}) = \int_0^\infty \Sigma_s(E)\phi(\mathbf{r}, E) dE; \quad (5-14)$$

the *absorption rate* is

$$F_a(\mathbf{r}) = \int_0^\infty \Sigma_a(E)\phi(\mathbf{r}, E) dE; \quad (5-15)$$

and so on.

There is frequently confusion regarding the concept of neutron flux, due in part to the unfortunate use of the term "flux" in nuclear engineering. In view of the foregoing discussion, it should be noted that the neutron flux is a measure of the combined effect of the motions of neutrons, as evidenced by the interaction rate to which they give rise, but it has nothing whatsoever (at least not directly)

to do with the *flow* of neutrons. Thus neutron flux is a scalar, not a vector; and it is *not* analogous to such things as heat flux, light flux, or magnetic flux that are encountered in other branches of engineering and physics. Indeed, since neutron flux is proportional to the density of neutrons at a point, it is therefore a concept more akin to chemical concentration or atom density (or temperature).

It may also be noted that the units of neutron flux are the same as the units of beam intensity, namely, neutrons per  $\text{cm}^2/\text{sec}$ . This is to be expected, of course, since the flux is merely the sum of the intensities of an infinite number of differential neutron beams.

## 5-2 Neutron Current Density

The net flow of neutrons (from here on assumed to be monoenergetic) in a reactor is described by the vector  $\mathbf{J}$ , which is called the *neutron current density vector*. This vector is defined in the following way. It was shown in the preceding section that neutron motions at any point in a reactor involve the superposition of an infinite number of differential neutron beams, each having an intensity  $dI(\mathbf{r}, \omega)$ , given by Eq. (5-2). The neutron current density vector is obtained by first constructing a vector whose magnitude is equal to  $dI(\mathbf{r}, \omega)$  and which points in the direction of  $\omega$ , that is, in the direction of motion of the neutrons in this differential beam. This can be done simply by replacing the speed  $v$  in the Eq. (5-2) by the velocity  $\mathbf{v}$ , that is,

$$d\mathbf{I}(\mathbf{r}, \omega) = n(\mathbf{r}, \omega)\mathbf{v} d\Omega. \quad (5-16)$$

The vector  $\mathbf{J}$  is then defined as the integral of  $d\mathbf{I}(\mathbf{r}, \omega)$  over all solid angles:

$$\mathbf{J} = \int_{4\pi} n(\mathbf{r}, \omega)\mathbf{v} d\Omega. \quad (5-17)$$

The physical significance of  $\mathbf{J}$  may be understood most readily by evaluating one of its components. Consider, for instance, the  $x$ -component of  $\mathbf{J}$ , that is,  $J_x$ . From Eq. (5-17) this is

$$J_x = \int_{4\pi} n(\mathbf{r}, \omega)v \cos \vartheta_x d\Omega, \quad (5-18)$$

where  $\vartheta_x$  is the angle between  $\mathbf{v}$  and the  $x$ -axis. The quantity  $v \cos \vartheta_x$  is equal to the volume of a slant cylinder of length  $v$  with ends of unit area lying in the  $yz$ -plane, as indicated in Fig. 5-3. Clearly, all the neutrons in this volume having velocities within the solid angle  $d\Omega$  of  $\mathbf{v}$ , namely  $n(\mathbf{r}, \omega)v \cos \vartheta_x d\Omega$ , will pass through the end of the cylinder in

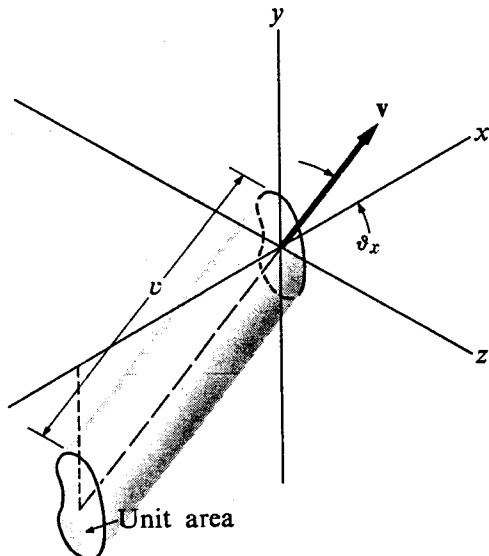


Fig. 5-3. The flow of neutrons through a surface.

one second. It follows therefore that the integration in Eq. (5-18) gives the net number of neutrons which cross the unit area per second perpendicular to the  $x$ -axis.

It should be noted that  $J_x$  measures the *net* rate of flow in the *positive*  $x$ -direction. The integration in Eq. (5-18) automatically subtracts the number of neutrons which pass from right to left through the area in Fig. 5-3 from those which pass from left to right, the  $\cos \vartheta_x$  being negative in the first instance and positive in the second. Thus if  $J_x$  is positive, there is a net flow of neutrons from left to right; whereas if  $J_x$  is negative, there is a net flow in the opposite direction.

In this discussion, the direction of the  $x$ -axis has not been specified, and the interpretation of  $J_x$  is therefore equally valid for *any* component of  $\mathbf{J}$ . Hence, the component of  $\mathbf{J}$  in the direction of the unit vector  $\mathbf{n}$ , which is given by

$$J_n = \mathbf{J} \cdot \mathbf{n},$$

is equal to the net rate at which neutrons pass through a unit area normal to  $\mathbf{n}$ .

### 5-3 The Equation of Continuity

Consider an arbitrary volume  $V$  of material containing monoenergetic neutrons. As time goes on, some of these neutrons will interact with nuclei and be scattered or absorbed; some may leave the volume and others may enter. Also, if neutron sources are present within the volume, additional neutrons may appear as they are emitted from the sources. In any event, the neutrons within this volume satisfy the *condition of continuity*, namely, the time rate of change of the total number of neutrons in  $V$  must be equal to the rate at which neutrons are produced within  $V$  minus the rate at which they are absorbed or escape from  $V$ . If  $n(\mathbf{r}, t)$  is the neutron density at the point  $\mathbf{r}$  and at the time  $t$ , the total number of neutrons in  $V$  is simply  $\int_V n(\mathbf{r}, t) dV$ . The condition of continuity can then be written as

$$\frac{d}{dt} \int_V n(\mathbf{r}, t) dV = \text{production rate} - \text{absorption rate} - \text{leakage rate}. \quad (5-19)$$

The production of neutrons can be represented by a *source distribution function*  $s(\mathbf{r}, t)$ , which is equal to the number of neutrons emitted per  $\text{cm}^3/\text{sec}$  by sources at the point  $\mathbf{r}$  and at time  $t$ . The total rate of production of neutrons in  $V$  is therefore

$$\text{production rate} = \int_V s(\mathbf{r}, t) dV. \quad (5-20)$$

As discussed in Section 5-1, the rate of absorption of neutrons in  $V$  can be written in terms of the neutron flux, i.e.,

$$\text{absorption rate} = \int_V \Sigma_a(\mathbf{r})\phi(\mathbf{r}, t) dV, \quad (5-21)$$

where, for generality, spatial variation of the absorption cross section has been included.

The leakage of neutrons from  $V$  can be expressed in terms of the neutron current density vector which was defined in the preceding section. Thus it will be recalled that  $\mathbf{J}(\mathbf{r}, t) \cdot \mathbf{n}$  is equal to the net rate of flow of neutrons through a unit area normal to  $\mathbf{n}$  at  $\mathbf{r}$ . If, therefore,  $\mathbf{n}$  is taken to be a unit normal pointing *outward* from the surface  $A$  bounding  $V$ , then  $\mathbf{J}(\mathbf{r}, t) \cdot \mathbf{n} dA$  is the net rate of flow of neutrons outward through  $dA$ . The total rate at which neutrons leak from the entire surface is then

$$\text{leakage rate} = \int_A \mathbf{J}(\mathbf{r}, t) \cdot \mathbf{n} dA. \quad (5-22)$$

Inserting the last three equations into Eq. (5-19), there follows:

$$\begin{aligned} \frac{d}{dt} \int_V n(\mathbf{r}, t) dV &= \int_V s(\mathbf{r}, t) dV - \int_V \Sigma_a(\mathbf{r})\phi(\mathbf{r}, t) dV \\ &\quad - \int_A \mathbf{J}(\mathbf{r}, t) \cdot \mathbf{n} dA. \end{aligned} \quad (5-23)$$

Equation (5-23) can be put in a more convenient form by using the divergence theorem to transform the last term from a surface integral to a volume integral. Thus

$$\int_A \mathbf{J}(\mathbf{r}, t) \cdot \mathbf{n} dA = \int_V \operatorname{div} \mathbf{J}(\mathbf{r}, t) dV,$$

and Eq. (5-23) becomes

$$\begin{aligned} \frac{d}{dt} \int_V n(\mathbf{r}, t) dV &= \int_V s(\mathbf{r}, t) dV - \int_V \Sigma_a(\mathbf{r})\phi(\mathbf{r}, t) dV \\ &\quad - \int_V \operatorname{div} \mathbf{J}(\mathbf{r}, t) dV. \end{aligned} \quad (5-24)$$

Since all integrals now involve the same volume of integration, the integrands on both sides of Eq. (5-24) must necessarily be equal; that is

$$\frac{\partial n(\mathbf{r}, t)}{\partial t} = s(\mathbf{r}, t) - \Sigma_a(\mathbf{r})\phi(\mathbf{r}, t) - \operatorname{div} \mathbf{J}(\mathbf{r}, t). \quad (5-25)$$

Equation (5-25) is called the *equation of continuity* and is of central importance in reactor theory.

When the flux, current, and sources are all independent of time, a system is said to be in a *steady state*. In this case, Eq. (5-25) reduces to

$$\operatorname{div} \mathbf{J}(\mathbf{r}) + \Sigma_a(\mathbf{r})\phi(\mathbf{r}) - s(\mathbf{r}) = 0, \quad (5-26)$$

which is known as the *steady-state equation of continuity*. On the other hand, if the neutron density and flux are independent of position,  $\operatorname{div} \mathbf{J} = 0$  and Eq. (5-25) becomes

$$\frac{dn(t)}{dt} = s(t) - \Sigma_a\phi(t). \quad (5-27)$$

For future reference, it may be noted that the quantity  $\text{div } \mathbf{J}(\mathbf{r})$ , which appears repeatedly in the equations of reactor theory, is equal to the net rate of neutron leakage per unit volume at the point  $\mathbf{r}$ . Thus the net rate at which neutrons leak from the volume  $dV$  at  $\mathbf{r}$  is  $\text{div } \mathbf{J}(\mathbf{r}) dV$ . This result follows directly from either Eq. (5-25) or (5-26), or may be seen by applying the divergence theorem to the integral of  $\mathbf{J}$  over the surface  $dA$  surrounding  $dV$ .

#### 5-4 Fick's Law

As pointed out in the introduction to this chapter, the general problem of neutron transport is a very complicated one. However, it will now be shown that the neutron flux and current are related in a simple way if certain conditions are met. When this is the case it is possible to obtain elementary solutions to transport problems. This relationship between  $\phi$  and  $\mathbf{J}$  is identical in form with *Fick's law*, which has been used for many years to describe diffusion phenomena in liquids and gases. For this reason, the use of Fick's law in reactor theory leads to what is known as the *diffusion approximation*.

Fick's law can be derived by calculating, under a number of simplifying assumptions, the neutron current density at any point in a medium containing neutrons. For the moment, at least, the following assumptions will be made:

- (a) the medium is infinite;
- (b) the medium is uniform, so that all cross sections are constants, independent of position;
- (c) there are no neutron sources in the medium;
- (d) scattering is isotropic in the *laboratory* coordinate system;
- (e) the neutron flux is a slowly varying function of position;
- (f) the neutron flux is not a function of time.

It will be possible to relax certain of these restrictions later in the discussion.

The point at which the current density is computed will be taken to be the center of a coordinate system, as shown in Fig. 5-4. To specify the current density vector  $\mathbf{J}$ , its three components  $J_x$ ,  $J_y$ , and  $J_z$  must be evaluated. Beginning with  $J_z$ , consider the rate at which neutrons flow through the area  $dA_z$  lying in the  $xy$ -plane at the origin. It is an obvious but important fact that since there are no neutron sources present in the medium, every neutron which passes through  $dA_z$  has just arrived from a scattering collision. Neutrons therefore flow downward through  $dA_z$  as the result of collisions above the  $xy$ -plane, and they flow upward through  $dA_z$  from collisions below the  $xy$ -plane.

The number of scattering collisions that occur per second in the volume element  $dV$  located at the point  $\mathbf{r}$  is  $\Sigma_s \phi(\mathbf{r}) dV$ , where  $\Sigma_s$  is the macroscopic scattering cross section and  $\phi(\mathbf{r})$  is the neutron flux at  $\mathbf{r}$ . Since scattering has been assumed to be isotropic in the laboratory system, the fraction of these neutrons that are scattered in the direction of  $dA_z$  is just the fraction of the total solid angle subtended by  $dA_z$ ,

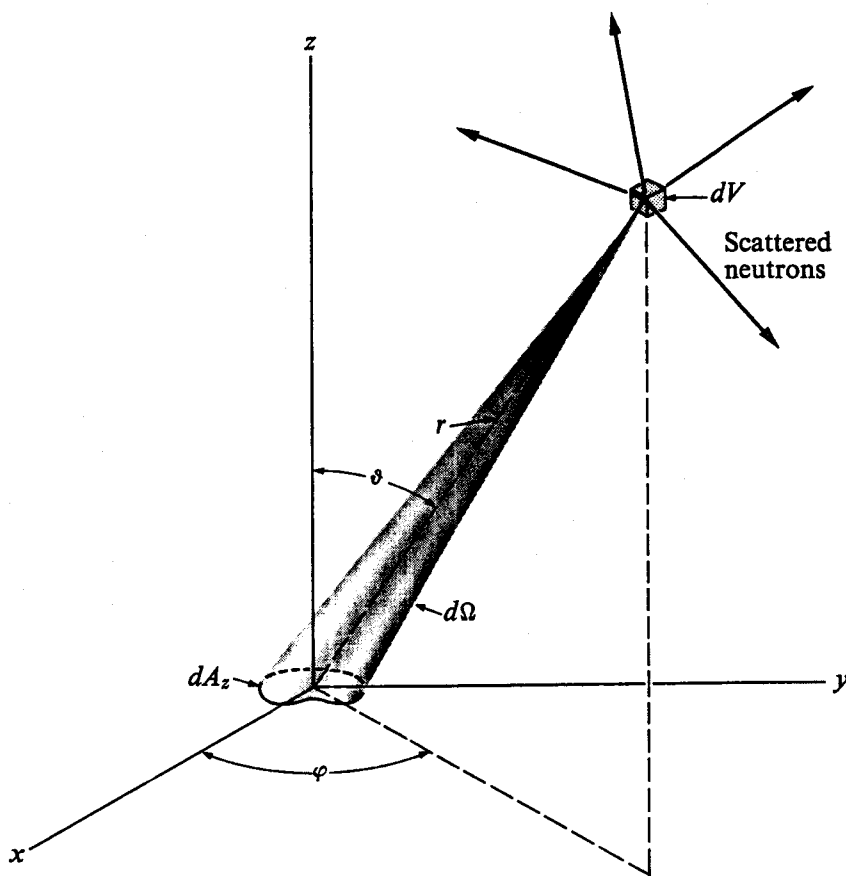


Fig. 5-4. Diagram for deriving Fick's law.

at  $dV$ . From the definition of solid angle, this fraction is

$$\frac{dA_z \cos \vartheta}{4\pi r^2},$$

so that the number of neutrons scattered per second in  $dV$  which head toward  $dA_z$  is

$$\frac{\Sigma_s \phi(\mathbf{r}) \cos \vartheta \, dA_z \, dV}{4\pi r^2}.$$

All of these neutrons do not, however, succeed in reaching  $dA_z$ ; some are scattered or absorbed enroute. In view of the discussion in Section 2-2, the number which does reach  $dA_z$  per second is

$$\frac{e^{-\Sigma_t r} \Sigma_s \phi(\mathbf{r}) \cos \vartheta \, dA_z \, dV}{4\pi r^2},$$

where  $\Sigma_t$  is the macroscopic total cross section of the medium.

It is convenient to consider separately the contributions to  $J_z$  of neutrons which pass downward through  $dA_z$  and those which pass upward. With  $dV$  written in spherical coordinates, that is,  $dV = r^2 \sin \vartheta \, dr \, d\vartheta \, d\varphi$ , the total number of neutrons

which flow *downward* through  $dA_z$  per second is

$$\frac{\Sigma_s dA_z}{4\pi} \int_{\varphi=0}^{2\pi} \int_{\vartheta=0}^{\pi/2} \int_{r=0}^{\infty} e^{-\Sigma_t r} \phi(\mathbf{r}) \cos \vartheta \sin \vartheta dr d\vartheta d\varphi.$$

Now if  $J_z^-$  denotes the number of neutrons passing per second in the negative  $z$ -direction through a unit area, this is just the above number divided by  $dA_z$ , namely,

$$J_z^- = \frac{\Sigma_s}{4\pi} \int_{\varphi=0}^{2\pi} \int_{\vartheta=0}^{\pi/2} \int_{r=0}^{\infty} e^{-\Sigma_t r} \phi(\mathbf{r}) \cos \vartheta \sin \vartheta dr d\vartheta d\varphi. \quad (5-28)$$

The integral in Eq. (5-28) cannot be evaluated as it stands, since the flux  $\phi(\mathbf{r})$  is an unknown function. If as assumed, however,  $\phi(\mathbf{r})$  varies slowly with position, it can be expanded in the Taylor's series:

$$\phi(\mathbf{r}) = \phi_0 + x \left( \frac{\partial \phi}{\partial x} \right)_0 + y \left( \frac{\partial \phi}{\partial y} \right)_0 + z \left( \frac{\partial \phi}{\partial z} \right)_0 + \dots, \quad (5-29)$$

where the subscripts indicate that  $\phi$  and its derivatives are to be evaluated at the origin. Writing  $x$ ,  $y$ , and  $z$  in spherical coordinates:

$$x = r \sin \vartheta \cos \varphi, \quad y = r \sin \vartheta \sin \varphi, \quad z = r \cos \vartheta,$$

and inserting Eq. (5-29) into Eq. (5-28), it is found that the terms containing  $\cos \varphi$  and  $\sin \varphi$  immediately integrate to zero. Thus  $J_z^-$  reduces to

$$J_z^- = \frac{\Sigma_s}{4\pi} \int_{\varphi=0}^{2\pi} \int_{\vartheta=0}^{\pi/2} \int_{r=0}^{\infty} e^{-\Sigma_t r} \left[ \phi_0 + \left( \frac{\partial \phi}{\partial z} \right)_0 r \cos \vartheta \right] \cos \vartheta \sin \vartheta dr d\vartheta d\varphi,$$

which, when evaluated, gives

$$J_z^- = \frac{\Sigma_s \phi_0}{4\Sigma_t} + \frac{\Sigma_s}{6\Sigma_t^2} \left( \frac{\partial \phi}{\partial z} \right)_0. \quad (5-30)$$

The calculation of  $J_z^+$ , the number of neutrons moving per second in the positive  $z$ -direction through a unit area in the  $xy$ -plane, is essentially the same as the preceding calculation of  $J_z^-$ ; it is necessary only to rewrite the limits of integration on  $\vartheta$ . The resulting expression for  $J_z^+$  is easily found to be

$$J_z^+ = \frac{\Sigma_s \phi_0}{4\Sigma_t} - \frac{\Sigma_s}{6\Sigma_t^2} \left( \frac{\partial \phi}{\partial z} \right)_0. \quad (5-31)$$

The  $z$ -component of current density, as explained in Section 5-2, refers to the *net* flow of neutrons per unit area so that

$$J_z = J_z^+ - J_z^- = - \frac{\Sigma_s}{3\Sigma_t^2} \left( \frac{\partial \phi}{\partial z} \right)_0. \quad (5-32)$$

In this computation, attention was centered on the  $z$ -component of  $\mathbf{J}$ . There is, however, nothing special about this component, since the orientation of the coordinate system is purely arbitrary. Thus the other components of  $\mathbf{J}$  at the origin must also be given by expressions of the same form as Eq. (5-32), but with  $z$  everywhere replaced by  $x$  or  $y$ ; that is,

$$J_x = - \frac{\Sigma_s}{3\Sigma_t^2} \left( \frac{\partial \phi}{\partial x} \right)_0, \quad (5-33)$$

and

$$J_y = - \frac{\Sigma_s}{3\Sigma_t^2} \left( \frac{\partial \phi}{\partial y} \right)_0. \quad (5-34)$$

The vector  $\mathbf{J}$  is now

$$\mathbf{J} = iJ_x + jJ_y + kJ_z = - \frac{\Sigma_s}{3\Sigma_t^2} \operatorname{grad} \phi. \quad (5-35)$$

The subscript denoting evaluation at the origin has been dropped in Eq. (5-35), since the location of the origin of coordinates in this derivation is also arbitrary. This equation is therefore valid at any point in the medium where the initial assumptions are satisfied.

Equation (5-35) is called Fick's law, which states that *the current density vector is proportional to the negative gradient of the flux*. The proportionality constant is called the *diffusion coefficient* and is denoted by the symbol  $D$ . With this notation, Fick's law becomes

$$\mathbf{J} = -D \operatorname{grad} \phi, \quad (5-36)$$

where, according to the preceding derivation,

$$D = \frac{\Sigma_s}{3\Sigma_t^2}. \quad (5-37)$$

## 5-5 Physical Interpretation of Fick's Law

Before Fick's law is applied to specific problems, it is important to understand on physical grounds why such a relationship between flux and current would be expected to occur. This can be seen from the simple example shown in Fig. 5-5, in which the flux is a function of only one spatial variable. Thus consider the flow of neutrons through the plane at  $x = 0$ . It will be evident that neutrons pass through this plane from left to right as the result of collisions to the left of the plane; and, conversely, they flow from right to

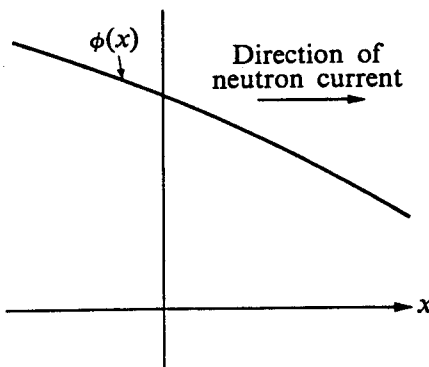


Fig. 5-5. Neutron current from nonuniform flux.

left as the result of collisions to the right of the plane. Since the flux is larger for negative values of  $x$ , the number of collisions per  $\text{cm}^3/\text{sec}$ , that is, the collision density, is greater on the left than it is on the right. As a consequence, more neutrons are scattered from left to right through the plane than from right to left, with the result that a net positive flow of neutrons occurs through the plane. This, of course, is just what Fick's law predicts; the gradient of the flux is negative, and from Eq. (5-36), the current is positive.

## 5-6 Validity of Fick's Law

In the light of the derivation of Fick's law given in Section 5-4, it is possible to reexamine the assumptions that were made in that derivation to determine under what conditions this law can be expected to hold. Each of these assumptions will now be considered in turn.

(a) *Infinite versus finite media.* It was necessary in Section 5-4 to assume that the diffusing medium was infinite in order to be able to integrate over all space. However, because the exponential function which appears in the integrand of Eq. (5-28) dies off rapidly with distance, neutrons coming from distances of more than a few mean free paths from the point where  $J$  is computed make very little contribution to the integral. It follows, therefore, that Fick's law is valid in finite media at points which are more than a few mean free paths from the edges of the medium. Thus Fick's law may be expected to be valid in the interior of a reactor, but not near its outer surface. Methods for treating regions near the surface of a diffusing medium are discussed in Section 5-8.

(b) *Uniform versus nonuniform media.* If the medium is nonuniform, it might reasonably be expected that Fick's law would have to be modified. In particular, according to the discussion in Section 5-5, a neutron current is simply the result of a larger collision density at one point than at another. Therefore, since the collision density is given by the product  $\Sigma_s \phi$ , it is logical to expect that spatial variations in  $\Sigma_s$ , as well as in  $\phi$  would give rise to a neutron current.

To illustrate this point consider the situation shown in Fig. 5-6, where  $\phi$  is a constant but  $\Sigma_s$  is a function of position. In this case, as in Fig. 5-5, the collision rate is greater to the left of the  $x = 0$  plane than to the right, and a positive neutron current might well be anticipated, in contradiction to Fick's law, which gives  $J = -D(d\phi/dx) = 0$ . Such a current does not occur, however, for the following reason. While it is perfectly true that the collision rate is larger on the left, the attenuation of the neutrons in this region is also larger, due to the larger value of  $\Sigma_s$ . The probability that a neutron that is

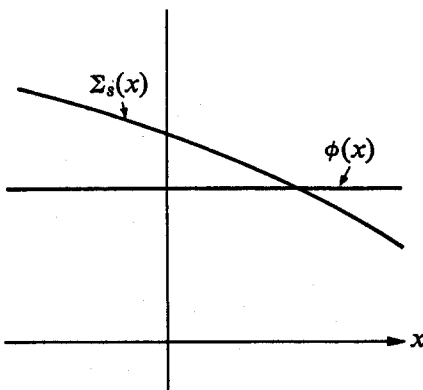


Fig. 5-6. Hypothetical nonuniform medium with a uniform flux.

scattered on the left actually reaches the  $x = 0$  plane is therefore smaller than for a comparable neutron scattered at the same distance to the right of the plane. It can be shown that the effects of increased collision density and increased attenuation exactly cancel, so that there is no net current.

The assumption of a uniform medium which was used in the derivation of Fick's law in Section 5-4 is therefore not a strict requirement for its validity.\* Thus even at the boundary between two media of entirely different scattering properties, Fick's law will still be valid provided none of the other assumptions in Section 5-4 are violated. In this connection it should be noted that sharp changes in the properties of a medium often lead to a rapidly varying flux distribution which may violate assumption (e).

(c) *Sources.* In the computation of  $\mathbf{J}$  in Section 5-4, it was assumed that all neutrons contributing to  $\mathbf{J}$  originated in scattering collisions in the medium. This is not necessarily the case, of course, if sources are present in the system. However, in view of the exponential attenuation factor in the integral for  $\mathbf{J}$ , very few of the source neutrons will survive as such to contribute to the value of  $\mathbf{J}$  if the sources are located more than a few mean free paths from the point where  $\mathbf{J}$  is evaluated. It follows that Fick's law is valid in media containing sources but at distances from the sources that are larger than a few mean free paths.

(d) *Anisotropic laboratory scattering—transport corrections.* In deriving Fick's law, it was also necessary to assume that the neutrons were scattered isotropically in the *laboratory* system. This is true only at low energies, and even then not for the very light nuclei (cf. Section 2-8); it is certainly not true in general. Nevertheless, it is possible to show by the methods of transport theory that Fick's law is still approximately valid even with moderately anisotropic laboratory scattering, provided that the diffusion coefficient is taken to be of a more complicated form than that given in Eq. (5-37). This expression for  $D$  cannot be written in closed form and must be determined by solving the following transcendental equation:

$$\frac{\Sigma_s}{2} \sqrt{\frac{D}{\Sigma_a}} \ln \left[ \frac{\Sigma_t + \sqrt{\Sigma_a/D}}{\Sigma_t - \sqrt{\Sigma_a/D}} \right] = \frac{1 + 3D\Sigma_s\bar{\mu}}{1 + 3D\Sigma_t\bar{\mu}}. \quad (5-38)$$

Here  $\Sigma_t$ ,  $\Sigma_s$ , and  $\Sigma_a$  are the macroscopic total, scattering, and absorption cross sections, respectively, and  $\bar{\mu}$  is the average value of the cosine of the scattering angle in the laboratory coordinate system. In the important case of isotropic scattering in the center-of-mass system, it will be recalled from Section 2-9 that  $\bar{\mu}$  is given by

$$\bar{\mu} = \frac{2}{3A}. \quad (5-39)$$

---

\* It should be mentioned that this conclusion is valid only when there is negligible absorption in the medium, or when the scattering and absorption cross sections vary with position in the same way, so that the ratio  $\Sigma_s/\Sigma_t$  is a constant.

When Eq. (5-38) is expanded in a series of powers of  $\Sigma_a/\Sigma_t$  and solved for  $D$ , the following expression is obtained:

$$D = \frac{1}{3\Sigma_t(1 - \bar{\mu})(1 - 4\Sigma_a/5\Sigma_t + \dots)}. \quad (5-40)$$

If  $\Sigma_a/\Sigma_t \ll 1$ , Eq. (5-40) reduces to

$$D = \frac{1}{3\Sigma_s(1 - \bar{\mu})},$$

which can also be written as

$$D = \frac{\lambda_{tr}}{3}, \quad (5-41)$$

where  $\lambda_{tr}$  is the transport mean free path discussed in Section 2-9.

(e) *Slowly-varying flux.* In the derivation of Fick's law, the flux was expanded in a Taylor series only to first-order terms. It is easily shown, however, that even if the second-order terms are retained, they give no contribution to  $J_z$ . They either integrate to zero directly or make identical contributions to both  $J_z^+$  and  $J_z^-$ , which cancel when

$$J_z = J_z^+ - J_z^-$$

is computed.

In order for Fick's law to be valid, it is therefore necessary only that the terms in the Taylor series containing *third derivatives* of the flux make a small contribution to the integral for  $J$ . This, in turn, will be the case provided that the second derivative of the flux does not change significantly over a few mean free paths, since the bulk of the integral is accumulated over this distance.

In this connection, it should be mentioned that in practice the flux tends to vary rapidly with position in strongly absorbing media. It is necessary, therefore, to restrict Fick's law to systems in which  $\Sigma_a \ll \Sigma_s$ . Incidentally, when absorption is present,  $D$  should always be computed from Eq. (5-38) rather than Eqs. (5-37) or (5-41).

(f) *Time-dependent flux.* It was assumed in Section 5-4 that the flux is independent of time. If this is not the case, the flux which enters the integral in Eq. (5-28) must be evaluated at an *earlier* time, due to the finite time required for a neutron to travel from the collision site to the point where the current density is evaluated. As already noted, however, regions beyond a few scattering mean free paths do not contribute significantly to  $J$ . Thus it is possible to relax the requirement of a time-independent flux, provided the fractional change in  $\phi$  is small during a time required for a neutron to travel about three mean free paths. Since the slowest neutrons in any reactor have a speed of about 1000 m/sec, Fick's law will therefore be valid if the inequality

$$\left| \frac{1}{\phi} \frac{d\phi}{dt} \right| \ll \frac{10^5}{3\lambda_s} \text{ sec}^{-1} \quad (5-42)$$

is satisfied, where the scattering mean free path  $\lambda_s$  is in centimeters.

### 5-7 The Diffusion Equation

Fick's law provides a relationship between the flux and current. Using the equation of continuity it is now possible to derive an equation involving the neutron flux alone. Thus, substitution of Eq. (5-36) into Eq. (5-25) yields the following equation:

$$\operatorname{div} D \operatorname{grad} \phi - \Sigma_a \phi + s = \frac{\partial n}{\partial t}, \quad (5-43)$$

where for simplicity all of the independent variables have been omitted.

Throughout most of this book, only systems consisting of uniform materials will be considered. In this case,  $D$  is a constant, and the first term in Eq. (5-43) can be written as

$$D \operatorname{div} \operatorname{grad} \phi = D \nabla^2 \phi,$$

where  $\nabla^2$  is the Laplacian operator. Also, since all neutrons have been assumed to have the same energy, the flux is given by  $\phi = nv$  (cf. Eq. 5-6), and Eq. (5-43) becomes

$$D \nabla^2 \phi - \Sigma_a \phi + s = \frac{1}{v} \frac{\partial \phi}{\partial t}. \quad (5-44)$$

This equation is known as the *neutron diffusion equation* and it is of great importance in nuclear reactor theory.

The form of the Laplacian to be used in Eq. (5-44) depends upon the coordinate system appropriate to a given problem. In reactor calculations, it is usually necessary to consider only three coordinate systems: namely, rectangular, cylindrical, and spherical coordinates. In these coordinate systems,  $\nabla^2$  is given by

$$\text{rectangular: } \nabla^2 = \frac{\partial^2}{\partial x^2} + \frac{\partial^2}{\partial y^2} + \frac{\partial^2}{\partial z^2}, \quad (5-45)$$

$$\text{cylindrical: } \nabla^2 = \frac{1}{r} \frac{\partial}{\partial r} r \frac{\partial}{\partial r} + \frac{1}{r^2} \frac{\partial^2}{\partial \vartheta^2} + \frac{\partial^2}{\partial z^2}, \quad (5-46)$$

$$\begin{aligned} \text{spherical: } \nabla^2 &= \frac{1}{r^2} \frac{\partial}{\partial r} r^2 \frac{\partial}{\partial r} + \frac{1}{r^2 \sin \vartheta} \frac{\partial}{\partial \vartheta} \sin \vartheta \frac{\partial}{\partial \vartheta} \\ &\quad + \frac{1}{r^2 \sin^2 \vartheta} \frac{\partial^2}{\partial \varphi^2}. \end{aligned} \quad (5-47)$$

If the flux is not a function of time, the right-hand side of Eq. (5-44) vanishes, and the equation reduces to

$$D \nabla^2 \phi - \Sigma_a \phi + s = 0. \quad (5-48)$$

This equation is known as the *steady-state diffusion equation*. Mathematicians also refer to Eq. (5-48) as the *scalar Helmholtz equation*.

\* See, for instance, Morse, P. M., and H. Feshbach, *Methods of Theoretical Physics*. New York: McGraw-Hill, 1953, Chapter 6.

<sup>†</sup> Equation (5-49) can also be written as  $d/dn(\ln\phi) = -1/d$ . This equation is sometimes referred to as a logarithmic boundary condition and  $d$  is also known as the *re-*

*ciprocal logarithmic derivative*.

where  $d\phi/dn$  is the normal derivative of the flux and  $d$  is a parameter known (for reasons discussed below) as the *extrapolation distance or extrapolation length*.<sup>†</sup> The

$$\frac{1}{\phi} \frac{d\phi}{dn} = -\frac{d}{1}, \quad (5-49)$$

**Boundary conditions at surfaces.** Some of the most important types of boundary condition at the surface of the medium of the form to handle such problems in a special way. What is done is first to assume a boundary condition that diffusion theory is not valid near such a surface, and it is necessary recalled that diffusion theory is usually possible to treat it as a vacuum in reactor calculations. It will be and it is usually possible to treat it as air is much larger than in nonabsorbing materials, mean free path of neutrons in air is much larger than in vacuum, the ion of this kind. Although the surrounding atmosphere is not truly a vacuum, the and essentially vacuous media. The exterior surface of a reactor represents a situation of this kind. Some of the most important types of boundary conditions that occur in reactor problems are those between comparatively dense boundaries that occur in reactor problems based on physical arguments, the requirements of this mathematical theorem must not (and will not) be violated.

In imposing boundary conditions based on physical arguments, the requirements both  $\phi$  and its normal derivative cannot be specified independently; or the normal derivative of  $\phi$ , or a linear combination of the two must be specified; On the boundaries of a region in which  $\phi$  satisfies the differential equation, either  $\phi$ ,

Boundary conditions cannot be imposed arbitrarily; however, it can be shown that corresponding to every differential equation there is an appropriate set of these conditions that leads to a reasonable solution. For equations of the scalar that corresponds to the differential equation there is an appropriate set of these boundary conditions that uniquely determine the solution to every problem.

Boundary conditions corresponding to every real physical problem, there is only one function that corresponds to the differential equation. In order to distinguish the proper function, certain restrictions must be placed on the solution in addition to the requirement that it correctly represents the flux. In order to satisfy the differential equation the physical problem and are known as boundary conditions. These restrictions are imposed by the physical restrictions must be placed on the solution in addition to the requirement that it corresponds to every real physical problem, there is only one function that corresponds to the differential equation, it has an infinite number of functions which satisfy the equation. However, there are an infinite number of functions which satisfy the equation. In other words, differential equation, it has an infinite number of solutions. In partial differential steady-state diffusion equation, since the steady-state diffusion equation is a partial differential equation, it has an infinite number of solutions. In other words, considered in later chapters. Since the steady-state diffusion problem is a partial differential steady-state diffusion equation; time-dependent diffusion problems will be considered in later chapters. Since the steady-state diffusion equation is a partial differential equation, it has an infinite number of solutions. In other words,

The remainder of this chapter will be devoted largely to finding solutions of the steady-state diffusion equation; time-dependent diffusion problems will be con-

### Equation

## 5-8 Boundary Conditions for the Steady-State Diffusion

value of  $d$  is then chosen so that the solution to the diffusion equation satisfying Eq. (5-49) matches as nearly as possible the rigorous solution given by transport theory in the interior of the medium. It should be noted that when Eq. (5-49) is written as

$$\frac{d\phi}{dn} + \frac{\phi}{d} = 0, \quad (5-50)$$

this boundary condition is of the form required by the above theorem.

In considering an appropriate value of  $d$  to use in condition (i), it is necessary to distinguish between two types of surface. These are known, respectively, as *reentrant* and *nonreentrant* surfaces, and are defined in the following way. A surface is called reentrant if it is possible to draw, through any point on the surface, one straight line outward which eventually reenters the medium. On the other hand, if no straight line that reenters the medium can be drawn through the surface, the surface is said to be nonreentrant. Examples of these surfaces are shown in Fig. 5-7. The essential difference between these two surfaces is that a neutron leaving a reentrant surface may reappear elsewhere in the system, whereas a neutron that passes through a nonreentrant surface is permanently lost from the system.

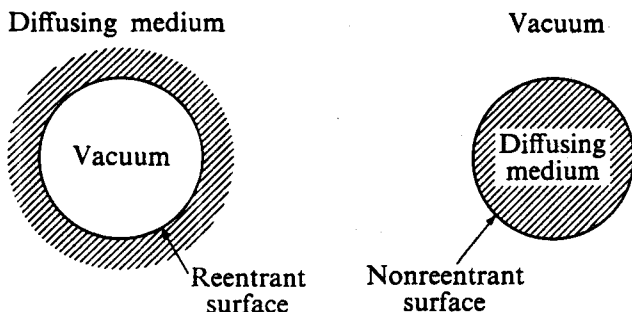
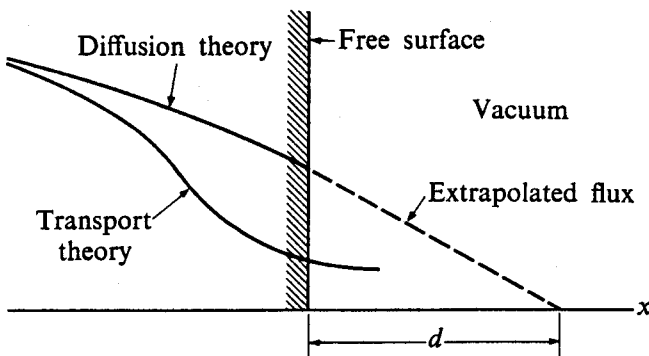


Fig. 5-7. Simple reentrant and nonreentrant surfaces.

The value of  $d$  at a reentrant surface depends in a complicated way upon the size and shape of the void space adjacent to the surface. The situation is considerably simpler at a nonreentrant surface, which, incidentally, is also called a *free surface* in reactor theory. In particular, for a planar free surface it can be shown by transport theory that if  $d$  is taken to have the value

$$d = 0.71\lambda_{tr}, \quad (5-51)$$

where  $\lambda_{tr}$  is the transport mean free path of the medium, the flux obtained by solving the diffusion equation, subject to boundary condition (i), provides a good approximation to the actual flux everywhere within the medium except near the surface. This situation is illustrated in Fig. 5-8, where the flux is shown near a free surface as calculated by exact transport theory and by diffusion theory using the above boundary condition. It will be observed that while the two solutions are very nearly the same in the interior of the medium, they differ substantially in the immediate vicinity of the surface.



**Fig. 5-8.** Neutron flux as a function of position near a free surface according to diffusion theory and transport theory.

With curved free surfaces (for example, the outer edge of a cylindrical or spherical reactor) the extrapolation distance is given by a somewhat more complicated formula than Eq. (5-51) and depends upon the radius of curvature  $R$  of the surface. However,  $d$  approaches the planar value in the limit of large radius of curvature, i.e., as  $d/R \rightarrow 0$ . It is possible therefore to use Eq. (5-51) at the surfaces of cylindrical and spherical reactors provided (as is usually the case) that  $d \ll R$ .

In view of Eq. (5-49), the solution to the diffusion equation vanishes at the distance  $d$  from the surface if the solution is extended *linearly* beyond the surface (cf. Fig. 5-8). Such an extrapolation of the flux introduces negligible error into solutions of the diffusion equation, since, as shown below,  $d$  is ordinarily very small compared with the dimensions of practical systems. It is possible therefore to replace boundary condition (i) by the simpler condition:

(i') *The solution to the diffusion equation vanishes at the extrapolation distance beyond the edge of a free surface.*

It should be emphasized that this boundary condition is only a mathematical device for simplifying the problem of obtaining solutions to the diffusion equation. The neutron flux does *not*, in fact, vanish at the extrapolation distance, and solutions obtained by this device do not give the correct flux near the boundary.

It will be recalled from Eq. (5-41) that the diffusion coefficient is given approximately by  $D = \lambda_{tr}/3$ , so that from Eq. (5-51) the extrapolation distance is about equal to  $2D$ . For most diffusing media,  $D$  is of the order of 1 cm or less, and, as a consequence,  $d$  is never more than 2 cm, and it is frequently much less. Most reactors, on the other hand, are of the order of meters in size, so that in many calculations the extrapolation distance can be neglected altogether. In such cases, the flux is assumed to vanish at the actual surface of the reactor.

**Boundary conditions at an interface.** In problems involving the diffusion of neutrons in systems containing several different materials, it is necessary to know how the neutron currents and fluxes are related across the interfaces between the different media. This leads to what are known as the *interface boundary conditions*. To derive these relations, consider the flow of neutrons across the interface between two regions  $A$  and  $B$ . The normal component of the current density

computed in region  $A$  at the interface is equal to the net number of neutrons (which may be either positive or negative) leaving  $A$  per second per unit area. Since there can be no accumulation of neutrons at the interface, this is equal to the number of neutrons that enter  $B$  per second per unit area, which, in turn, is equal to the normal component of the current density computed in  $B$ . In symbols this boundary condition is

$$(ii) \quad (J_A)_n = (J_B)_n,$$

where the subscript  $n$  refers to the component of  $\mathbf{J}$  normal to the surface. It may be noted that boundary condition (ii) is exact, and is not based on diffusion theory.

Since neutrons cross an interface between two media without hindrance, the neutron density distribution function must be continuous across the boundary. As a consequence, the flux, which is simply an integral of this function over solid angle (cf. Section 5-1), must also be continuous:

(iii) *The flux is continuous across the boundary between two different media.*

In many reactors, rather thin sheets of structural material are often used to separate different portions of the system. For example, the reactor core is often separated from the reflector or blanket by a comparatively thin-walled container. With such systems, it is sometimes possible to expedite the solution of diffusion problems by replacing the structural region by a suitable boundary condition. This can be done provided that the mean free path of neutrons in the structure is much greater than the structure thickness. In this case it is easy to show that the flux across the region is approximately constant, but that the current density is decreased by an amount equal to the number of neutrons absorbed in the material. The *thin-interface boundary conditions* are therefore

$$(iv) \quad \phi_A = \phi_B,$$

$$(iv') \quad (J_A)_n = (J_B)_n + x\Sigma_a\phi_A,$$

where  $\Sigma_a$  is the macroscopic absorption cross section of the structure and  $x$  is its thickness. It should be noted in using this boundary condition that the normal components are taken to be positive when pointing from region  $A$  to region  $B$ . If the normal components are assumed to point in the opposite direction, the sign in the second equation is negative.

**Other conditions.** The above boundary conditions together with the diffusion equation provide a unique solution to every physical diffusion problem involving one or more diffusing media and/or free surfaces. While no additional conditions are required to obtain the correct solution (within the limitations of diffusion theory) it is often expedient to utilize certain other rather obvious physical requirements on the solution.

For example, a negative or imaginary flux has no meaning, and the proper solution of the diffusion equation must therefore be real and nonnegative. This condition applies, of course, only in those regions where the diffusion equation is valid. Thus in finding the flux in a block of moderator surrounded by a vacuum, for instance, the fact that a solution is negative in the vacuum is of no significance, since the diffusion equation is not valid there. In summary:

- (v) *The solution to the diffusion equation must be real, nonnegative, and single-valued in those regions where the equation applies.*

The neutron flux also can never be infinite. Although this statement is technically correct, it will be seen in this chapter that solutions to certain artificial diffusion problems occasionally include points at which the flux is infinite. This occurs in problems where the neutron source distribution is represented by a function that is itself infinite at certain points. This procedure, however, is just another mathematical device, since no real source density is ever infinite, and the singularities that such functions introduce into the flux have no physical significance. Thus, although the actual neutron flux must always be finite, there is the slightly less restrictive condition on the solutions to the diffusion equation:

- (vi) *The solution to the diffusion equation must be finite in those regions where the equation is valid except (but not necessarily) at singular points of the source distribution.*

It must be emphasized that conditions (v) and (vi) are automatically satisfied by the function (there is only one) which satisfies the diffusion equation and the previous boundary conditions. Conditions (v) and (vi) add nothing new to the solution. Nevertheless, as will be seen repeatedly in this chapter, these new conditions often provide a means for quickly eliminating extraneous functions from the solution.

### **5-9 Elementary Solutions of the Steady-State Diffusion Equation**

It is not always a simple matter to find solutions of Eq. (5-48) that satisfy the boundary conditions discussed in the preceding section. In certain cases, however, the mathematics is quite straightforward, and a few problems of this type are considered in the present section for illustrative purposes. It must be realized that these problems are necessarily rather artificial, since among other things it is assumed that all neutrons are emitted and diffuse at one energy. More realistic problems will be treated in later chapters.

Before proceeding, it is convenient to rewrite Eq. (5-48) in the form

$$\nabla^2 \phi - \frac{1}{L^2} \phi = -\frac{s}{D}, \quad (5-52)$$

where the constant  $L^2$  is defined as

$$L^2 = \frac{D}{\Sigma_a}. \quad (5-53)$$

The quantity  $L$  appears very frequently in the equations of reactor theory and is known as the *diffusion length*. Since  $D$  and  $\Sigma_a$  have dimensions of cm and  $\text{cm}^{-1}$ , respectively, it is easy to see from Eq. (5-53) that  $L$  has dimensions of cm. The physical significance of the diffusion length will be discussed in Section 5-11; for the present,  $L$  should be viewed simply as a parameter appearing in the diffusion equation.

**Infinite planar source.** As a first example, consider an infinite planar source which emits (at a constant rate)  $S$  neutrons per second per unit area into an infinite homogeneous medium. Since the source plane and the medium are both infinite, the flux at any point in the medium can be a function only of the distance from the plane. Calling this distance  $x$ , Eq. (5-52) becomes

$$\frac{d^2\phi}{dx^2} - \frac{1}{L^2} \phi = - \frac{s(x)}{D}. \quad (5-54)$$

The source density function  $s(x)$  in Eq. (5-54) is an unusual function of  $x$ . Since there are no sources present in the medium itself,  $s(x)$  is zero everywhere in the medium. At  $x = 0$ , however,  $s(x)$  is infinite. This is because the source density function was defined in Section 5-3 to be the number of neutrons emitted per second *per unit volume*. When the neutrons are emitted from an infinitely thin plane, the source density is necessarily infinite at the plane, since a finite number of neutrons are produced in zero volume.

Functions such as  $s(x)$ , which are zero everywhere except at  $x = 0$ , can be represented in terms of the *Dirac delta function*  $\delta(x)$ , which is defined by the equations

$$\begin{aligned} \delta(x) &= 0, \quad x \neq 0, \\ \int_a^b \delta(x) dx &= \begin{cases} 1, & a < 0 < b, \\ 0, & \text{otherwise.} \end{cases} \end{aligned} \quad (5-55)$$

This somewhat pathological function is described in more detail in Appendix II. In any case,  $s(x)$  can be written as

$$s(x) = S \delta(x). \quad (5-56)$$

In view of Eq. (5-55), the total number of neutrons emitted per second per unit area of the source plane is just

$$\int_{-\epsilon}^{\epsilon} s(x) dx = S \int_{-\epsilon}^{\epsilon} \delta(x) dx = S,$$

as required, where  $\epsilon$  has any value.

Inserting Eq. (5-56) into Eq. (5-54), the diffusion equation is now

$$\frac{d^2\phi}{dx^2} - \frac{1}{L^2} \phi = - \frac{S \delta(x)}{D}. \quad (5-57)$$

This is an ordinary, inhomogeneous, linear differential equation and it can be solved by methods that are normally employed with inhomogeneous equations. (Some of these methods are discussed in Section 5-10.) The unusual nature of the function appearing in the inhomogeneous term in no way complicates the solution.

There is, however, a more physical approach to problems of this type. First, it will be noted that except at  $x = 0$ , Eq. (5-57) is the simple homogeneous equation

$$\frac{d^2\phi}{dx^2} - \frac{1}{L^2} \phi = 0, \quad x \neq 0. \quad (5-58)$$

The source at  $x = 0$  can now be taken into account by means of a *source condition*, rather than by using the source density function directly.

To derive the source condition, a small "pillbox" of unit surface area and thickness  $2x$  is constructed at the source plane, as shown in Fig. 5-9. In view of the symmetry of the problem, the net flow of neutrons through both ends of the pillbox is equal to  $2J(x)$ , where  $J(x)$  is the magnitude of the neutron current density at either end. There is no net flow of neutrons through the sides of the pillbox since the source plane is infinite. In the limit as  $x$  approaches zero the net flow of neutrons out of the pillbox must be equal to  $S$ , and it follows that

$$\lim_{x \rightarrow 0} J(x) = \frac{S}{2}. \quad (5-59)$$

This result is the required source condition.\*

Equation (5-58) has the following general solution:

$$\phi = Ae^{-x/L} + Ce^{x/L},$$

where  $A$  and  $C$  are constants to be determined.† Considering for the moment only positive values of  $x$ , it is evident that  $C$  must be taken equal to zero; otherwise the flux would become infinite with increasing  $x$ . The constant  $A$  can be found

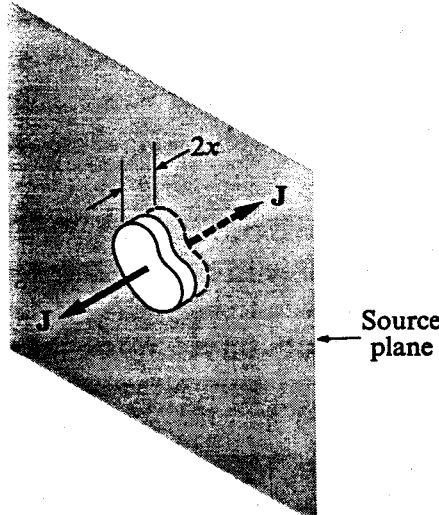


Fig. 5-9. Construction to derive the planar source condition.

\* It may be noted that this source condition is also valid if the sources are emitted non-uniformly from the plane, or if the plane is finite rather than infinite. In these situations there is a net flow of neutrons through the sides of the pillbox. This vanishes, however, in the limit as the size of the pillbox goes to zero and Eq. (5-59) is again obtained.

† The constant  $B$  has a special meaning in reactor theory, and it is usually reserved for that purpose.

from the source condition. From Fick's law,

$$J = -D \frac{d\phi}{dx} = \frac{DA}{L} e^{-x/L}.$$

Inserting this into Eq. (5-59), it is found that

$$A = \frac{SL}{2D},$$

and therefore

$$\phi = \frac{SL}{2D} e^{-x/L}.$$

This result is valid only for positive values of  $x$ . However, because of the symmetry of the problem, a solution valid for all  $x$  can be obtained by merely replacing  $x$  by its absolute value  $|x|$ ; hence

$$\phi = \frac{SL}{2D} e^{-|x|/L}. \quad (5-60)$$

It will be observed from Eq. (5-60) that the flux is everywhere proportional to the source strength  $S$ . This is a consequence of the fact that the diffusion equation is linear. Thus, if the intensity of the source is doubled, for example, the flux is also doubled, and so on. Furthermore, it may be noted that the diffusion length appears as a *relaxation length* for the flux. That is, the flux decreases by the factor  $e$  every  $L$  cm from the source plane. It must be remembered, however, that Fick's law does not apply within a few mean free paths of neutron sources. Equation (5-60) is not valid, therefore, near  $x = 0$ .

**Point source in an infinite medium.** Consider next a point source emitting  $S$  neutrons per second isotropically in an infinite medium. If the source point is taken to be at the center of a spherical coordinate system, the flux obviously depends only on  $r$ . When the form of the Laplacian given in Eq. (5-47) is used, only the first term remains, and the diffusion equation is

$$\frac{1}{r^2} \frac{d}{dr} r^2 \frac{d\phi}{dr} - \frac{1}{L^2} \phi = 0, \quad (5-61)$$

except at the origin, that is,  $r = 0$ . The appropriate source condition for this problem is obtained by drawing a small sphere around the source and computing the net number of neutrons that pass through its surface per second. If the sphere has the radius  $r$ , this number is just  $4\pi r^2 J(r)$ , so that in the limit, as  $r$  goes to zero, the following condition is obtained:

$$\lim_{r \rightarrow 0} r^2 J(r) = \frac{S}{4\pi}. \quad (5-62)$$

In order to solve Eq. (5-61), it is convenient to introduce a new variable  $w$ , defined by

$$w = r\phi. \quad (5-63)$$

When Eq. (5-63) is substituted into Eq. (5-61), the following equation is found for  $w$ :

$$\frac{d^2w}{dr^2} - \frac{1}{L^2} w = 0.$$

The general solution to this equation is

$$w = Ae^{-r/L} + Ce^{r/L},$$

and  $\phi$  is therefore

$$\phi = A \frac{e^{-r/L}}{r} + C \frac{e^{r/L}}{r},$$

where  $A$  and  $C$  are unknown constants. Again, as in the preceding example,  $\phi$  must remain finite as  $r$  becomes infinite, and  $C$  must be zero. The constant  $A$  is found from the source condition, Eq. (5-62); thus

$$J = -D \frac{d\phi}{dr} = DA \left( \frac{1}{rL} + \frac{1}{r^2} \right) e^{-r/L}$$

and

$$A = \frac{S}{4\pi D}.$$

Finally, the flux is given by

$$\phi = \frac{Se^{-r/L}}{4\pi Dr}. \quad (5-64)$$

It will be noted that in this example,  $\phi$  is again proportional to the source strength  $S$ . However, unlike the preceding problem of the planar source,  $\phi$  is infinite at the source. As pointed out in Section 5-8, this is unimportant, since, on the one hand, point sources do not actually exist, and, on the other, the solution given in Eq. (5-64) is not valid near the source.

**Systems with a free surface.** Imagine an infinite slab of thickness  $a$  (including the extrapolation distance), which has an infinite planar source at its center emitting  $S$  neutrons per second per unit area. Since the dimension  $a$  includes the extrapolation distance, the physical thickness of the slab is  $a - 2d$ , where  $d = 0.71\lambda_{tr}$ . Taking the zero of the coordinate system at the center of the slab, the diffusion equation is again Eq. (5-58), the source condition is given by Eq. (5-59), and the boundary conditions are

$$\phi\left(\pm\frac{a}{2}\right) = 0.$$

For positive values of  $x$ , the general solution is

$$\phi = Ae^{-x/L} + Ce^{x/L}, \quad (5-65)$$

and in view of the boundary condition at  $a/2$ ,

$$\phi\left(\frac{a}{2}\right) = Ae^{-a/2L} + Ce^{a/2L} = 0,$$

so that

$$C = -Ae^{-a/L}.$$

Substituting this result into Eq. (5-65) gives

$$\phi = A[e^{-x/L} - e^{-(a-x)/L}].$$

The constant  $A$  is found from the source condition (Eq. 5-59) in the usual way, and is

$$A = \frac{SL}{2D} (1 + e^{-a/L})^{-1}.$$

For positive  $x$ , therefore,  $\phi$  is given by

$$\phi = \frac{SL}{2D} \frac{e^{-x/L} - e^{-(a-x)/L}}{1 + e^{-a/L}}.$$

In view of the symmetry of the problem, a solution valid for all  $x$  is obtained by substituting  $|x|$  for  $x$ ; thus

$$\phi = \frac{SL}{2D} \frac{e^{-|x|/L} - e^{-(a-|x|)/L}}{1 + e^{-a/L}}. \quad (5-66)$$

If the numerator and denominator of Eq. (5-66) are multiplied by  $e^{a/2L}$ , the solution can be written in the more convenient form:

$$\phi = \frac{SL}{2D} \frac{\sinh [(a - 2|x|)/2L]}{\cosh (a/2L)}, \quad (5-67)$$

where the hyperbolic functions are defined as

$$\sinh x = \frac{e^x - e^{-x}}{2}, \quad \cosh x = \frac{e^x + e^{-x}}{2}.$$

These functions could have been used from the beginning of this problem, since the general solution of Eq. (5-58) can also be written as

$$\phi = A \cosh \frac{x}{L} + C \sinh \frac{x}{L}.$$

Both methods, of course, lead to the same final answer, and the choice of procedure is a matter of taste. As a general rule, however, it is better to use the hyper-

bolic functions in problems involving *finite* media, such as the present problem, and exponential functions for *infinite* media. This is because  $\sinh x$  has a zero, which is a useful property when dealing with finite media, whereas the exponentials do not. Similarly, one of the exponential solutions goes to zero at infinity, a useful property for problems involving infinite media, while both hyperbolic functions are singular at infinity. Furthermore,  $\cosh x$  is an even function, and can be used quite naturally in problems where it is clear that the flux is an even function.

**Multiregion problems.** With problems involving two or more different media, the interface boundary conditions must be satisfied at each interface separating regions. Consider, for instance, an infinite slab of thickness  $a$ , containing at its center a planar source emitting  $S$  neutrons per second per unit area as in the preceding problem, but which is now surrounded by an infinitely thick medium.

With the subscripts  $_1$  and  $_2$  denoting the inner and outer regions, respectively, the flux is determined by the following diffusion equations:

$$\frac{d^2\phi_1}{dx^2} - \frac{1}{L_1^2} \phi_1 = 0, \quad (5-68)$$

for  $|x| < a/2$  and  $x \neq 0$ , and

$$\frac{d^2\phi_2}{dx^2} - \frac{1}{L_2^2} \phi_2 = 0, \quad (5-69)$$

for  $|x| > a/2$ . The following boundary conditions must be satisfied:

- (i)  $\phi_2$  must remain finite as  $|x| \rightarrow \infty$ ,
- (ii)  $\lim_{x \rightarrow 0} J(x) = \frac{S}{2}$  (the source condition),
- (iii)  $\phi_1\left(\pm \frac{a}{2}\right) = \phi_2\left(\pm \frac{a}{2}\right)$ ,
- (iv)  $D_1 \frac{d\phi_1}{dx}\Big|_{x=\pm a/2} = D_2 \frac{d\phi_2}{dx}\Big|_{x=\pm a/2}$ .

The appropriate general solutions to Eqs. (5-68) and (5-69) are

$$\phi_1 = A_1 \cosh \frac{x}{L_1} + C_1 \sinh \frac{x}{L_1} \quad (5-70)$$

and

$$\phi_2 = A_2 e^{-x/L_2} + C_2 e^{x/L_2}, \quad (5-71)$$

where the four constants  $A_1$ ,  $A_2$ ,  $C_1$ , and  $C_2$  must be determined. With attention for the moment centered on positive values of  $x$ , it is easy to see from condition (i) that  $C_2 = 0$ . Next, using condition (ii) in the usual way yields  $C_1 = -SL_1/2D_1$ . Thus, only  $A_1$  and  $A_2$  remain to be determined. These can

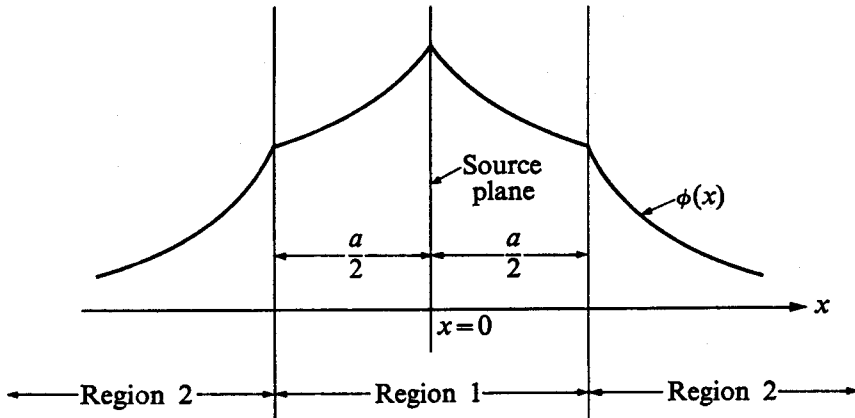


Fig. 5-10. Neutron flux in a simple two-region diffusion problem.

be found using conditions (iii) and (iv). From condition (iii) and Eqs. (5-70) and (5-71),

$$A_1 \cosh \frac{a}{2L_1} - \frac{SL_1}{2D_1} \sinh \frac{a}{2L_1} = A_2 e^{-a/2L_2}, \quad (5-72)$$

and similarly from condition (iv),

$$-\frac{D_1 A_1}{L_1} \sinh \frac{a}{2L_1} + \frac{S}{2} \cosh \frac{a}{2L_1} = \frac{D_2 A_2}{L_2} e^{-a/2L_2}. \quad (5-73)$$

When these equations are solved for  $A_1$  and  $A_2$ , the following results are obtained:

$$A_1 = \frac{SL_1}{2D_1} \frac{D_1 L_2 \cosh(a/2L_1) + D_2 L_1 \sinh(a/2L_1)}{D_2 L_1 \cosh(a/2L_1) + D_1 L_2 \sinh(a/2L_1)} \quad (5-74)$$

and

$$A_2 = \frac{SL_1 L_2}{2} \frac{e^{a/2L_2}}{D_2 L_1 \cosh(a/2L_1) + D_1 L_2 \sinh(a/2L_1)}. \quad (5-75)$$

With all the constants determined, the solution is complete. Again, it should be noted from the expressions for  $A_1$ ,  $A_2$ , and  $C_1$ , that despite the more complicated nature of this problem,  $\phi$  is still everywhere proportional to the source strength  $S$ . The resulting flux is indicated in Fig. 5-10. It is evident from the figure that while  $\phi$  is continuous at  $x = \pm a/2$ , its derivative  $d\phi/dx$  is discontinuous. This is due to the fact that it is  $D(d\phi/dx)$  which is continuous, and not  $d\phi/dx$ , and the diffusion coefficients  $D_1$  and  $D_2$  are, in general, different.

## 5-10 General Diffusion Problems

The problems discussed in the preceding section were comparatively simple due to the special types of source distributions that were assumed, namely, planar sources, point sources, etc. It is frequently necessary, however, to consider more complicated problems involving arbitrary source distributions. The mathematical methods which are useful in such problems depend on whether the diffusing medium is finite or infinite.

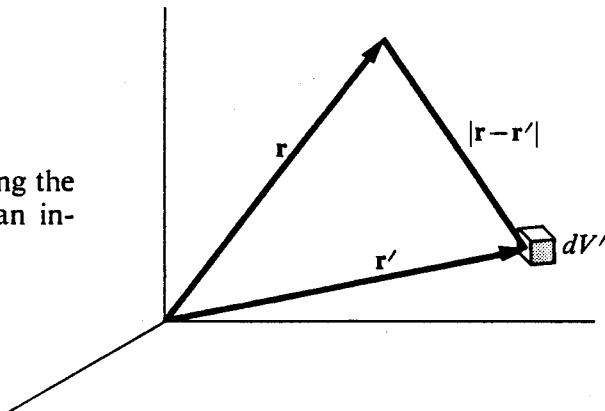


**Fig. 5-11.** Geometry for computing the flux from distributed sources in an infinite medium.

**Distributed sources in an infinite medium.** Consider an infinite medium containing an arbitrary distribution of isotropic neutron sources. If the source distribution is described by the function  $s(r')$ , then by definition  $s(r') dV'$  neutrons are emitted per second from the volume element  $dV'$  located at  $r'$  (cf. Fig. 5-11). Since  $dV'$  is small, these neutrons are emitted as from a point source, and in view of Eq. (5-64), they contribute to the flux at  $r$  the amount

$$d\phi(r) = \frac{s(r') dV' e^{-|r-r'|/L}}{4\pi D|r - r'|}. \quad (5-76)$$

Here,  $|r - r'|$  is the distance between the points located by the vectors  $r$  and  $r'$ . Equation (5-76) is a more general form of Eq. (5-64), which was derived for a point source located at the origin, i.e., for  $r' = 0$ . The total flux at  $r$  is simply the sum of the contributions  $d\phi$  arising from all sources throughout space. It follows that

$$\phi(r) = \int_{\text{all space}} s(r') \frac{e^{-|r-r'|/L}}{4\pi D|r - r'|} dV'. \quad (5-77)$$

In view of this result, the problem of finding the flux at any point in an infinite medium due to an arbitrary source distribution reduces to the evaluation of the above integral.

The quantity defined by

$$G_{\text{pt}}(r, r') = \frac{e^{-|r-r'|/L}}{4\pi D|r - r'|}, \quad (5-78)$$

which appears in the integral of Eq. (5-77), is known as the *point diffusion kernel for an infinite medium*.\* It will be noted that  $G_{\text{pt}}(r, r')$  is equal to the flux at the point  $r$  arising from a *unit point source* of neutrons placed at  $r'$ . In terms of the diffusion kernel, Eq. (5-77) can be written as

$$\phi(r) = \int_{\text{all space}} s(r') G_{\text{pt}}(r, r') dV'. \quad (5-79)$$

---

\* Diffusion kernels are examples of a large class of functions called *Green's functions* by mathematicians and physicists.

The point diffusion kernel given in Eq. (5-78) is appropriate for problems involving arbitrary sources spread throughout space. When the sources are distributed in some symmetric fashion, however, other forms of diffusion kernel may be more convenient. If, for instance, the source distribution is only a function of one rectangular variable, say  $x$ , then both the sources and the resulting flux have planar symmetry; and the *planar kernel in an infinite medium*  $G_{\text{pl}}(x, x')$  is the one appropriate for the problem.

To find  $G_{\text{pl}}(x, x')$ , it will be recalled from the preceding section that the flux from a planar source at  $x = 0$  is given by Eq. (5-60):

$$\phi = \frac{SL}{2D} e^{-|x|/L},$$

where  $S$  is the source strength. Had the source plane been located at  $x'$ ,  $\phi$  would obviously be

$$\phi = \frac{SL}{2D} e^{-|x-x'|/L}. \quad (5-80)$$

If the actual source distribution  $s(x')$  is now divided into thin slabs of thickness  $dx'$ , each slab is equivalent to a planar source of strength  $s(x') dx'$ . By an argument similar to the one given above, it follows that the flux at any point is

$$\phi(x) = \frac{L}{2D} \int_{-\infty}^{\infty} s(x') e^{-|x-x'|/L} dx'. \quad (5-81)$$

Thus if  $G_{\text{pl}}(x, x')$  is defined as

$$G_{\text{pl}}(x, x') = \frac{L}{2D} e^{-|x-x'|/L}, \quad (5-82)$$

then the flux can be written in the form

$$\phi(x) = \int_{-\infty}^{\infty} s(x') G_{\text{pl}}(x, x') dx'. \quad (5-83)$$

Several other diffusion kernels are discussed in the problems at the end of the chapter.

If the source distribution is a function of only one spatial variable, it is sometimes easier to find the flux by solving the diffusion equation directly, since it reduces to an ordinary differential equation in this case. For sources of planar symmetry, this is

$$\frac{d^2\phi(x)}{dx^2} - \frac{1}{L^2} \phi(x) = - \frac{s(x)}{D}; \quad (5-84)$$

with spherically symmetric sources it is

$$\frac{1}{r^2} \frac{d}{dr} r^2 \frac{d\phi(r)}{dr} - \frac{1}{L^2} \phi(r) = - \frac{s(r)}{D}, \quad (5-85)$$

and so on. In general, the diffusion equation is of the form

$$M\phi(x) = f(x), \quad (5-86)$$

where  $M$  is a linear, second-order differential operator.

The complete solution to an inhomogeneous equation of this type is the sum of the two independent solutions to the homogeneous equation

$$M\phi(x) = 0, \quad (5-87)$$

plus a particular solution. With the solutions to Eq. (5-87) denoted by  $\phi_{h1}(x)$  and  $\phi_{h2}(x)$  and the particular solution by  $\phi_p(x)$ , the flux can then be written as

$$\phi(x) = A\phi_{h1}(x) + C\phi_{h2}(x) + \phi_p(x), \quad (5-88)$$

where  $A$  and  $C$  are constants.

In many problems, the function  $\phi_p(x)$  can be found by inspection or by guessing the solution (the method of undetermined coefficients). If these attempts prove unsuccessful,  $\phi_p(x)$  can be calculated in terms of the functions  $\phi_{h1}(x)$  and  $\phi_{h2}(x)$  using the formula\*

$$\phi_p(x) = \phi_{h2}(x) \int_a^x \frac{f(x')\phi_{h1}(x') dx'}{W[\phi_{h1}(x'), \phi_{h2}(x')]} - \phi_{h1}(x) \int_b^x \frac{f(x')\phi_{h2}(x') dx'}{W[\phi_{h1}(x'), \phi_{h2}(x')]} \quad (5-89)$$

In this expression,  $W[\phi_{h1}(x'), \phi_{h2}(x')]$  is the Wronskian of the functions and is defined as

$$W[\phi_{h1}(x), \phi_{h2}(x)] = \begin{vmatrix} \phi_{h1}(x) & \phi_{h2}(x) \\ \phi'_{h1}(x) & \phi'_{h2}(x) \end{vmatrix}. \quad (5-90)$$

The limits  $a$  and  $b$  on the integrals in Eq. (5-89) and the constants  $A$  and  $C$  in Eq. (5-88) must be chosen in such a manner that the boundary conditions for the problem are satisfied.†

As an example of this procedure, consider the solution of the diffusion equation for an infinite planar source in an infinite medium (cf. Eq. 5-57) which was handled earlier using a source condition. The appropriate solutions to the homogeneous equation are

$$\phi_{h1}(x) = e^{-x/L}, \quad (5-91)$$

and

$$\phi_{h2}(x) = e^{x/L}. \quad (5-92)$$

\* See, for instance, *Advanced Calculus for Engineers* by Hildebrand, F. B., Englewood Cliffs, New Jersey: Prentice Hall, 1949, p. 29.

† Although there appear to be four unknown constants, there are only two;  $a$  and  $b$  cannot be chosen independently of  $A$  and  $C$ , and vice versa.

The Wronskian of these functions is easily seen to be

$$W[\phi_{h1}(x), \phi_{h2}(x)] = \frac{2}{L}. \quad (5-93)$$

The inhomogeneous function is  $f(x) = -S \delta(x)/D$ ; so Eqs. (5-88) and (5-89) give

$$\begin{aligned} \phi(x) = & Ae^{-x/L} + Ce^{x/L} + \frac{SL}{2D} e^{x/L} \int_x^{\infty} \delta(x') e^{-x'/L} dx' \\ & + \frac{SL}{2D} e^{-x/L} \int_{-\infty}^x \delta(x') e^{x'/L} dx'. \end{aligned} \quad (5-94)$$

The limits on the integrals in this expression have been chosen so that neither the third nor fourth term is infinite at  $\pm\infty$ . (Note that the limits have been exchanged on the first integral; hence the positive sign before that term.) The first term in Eq. (5-94) is infinite at  $x = -\infty$ , and the second is infinite at  $x = +\infty$ . Both  $A$  and  $C$  therefore must be taken to be zero. Finally, in view of the definition of the delta function, the first integral is zero when  $x > 0$ , while the second is zero when  $x < 0$ . It follows that Eq. (5-94) reduces to

$$\phi(x) = \frac{SL}{2D} e^{-|x|/L},$$

which was obtained earlier (cf. Eq. 5-60).

**Distributed sources in a finite medium.** When sources are distributed within a finite medium in such a manner that the diffusion equation reduces to an ordinary differential equation, the flux can be found either by inspection or by using Eqs. (5-88) and (5-89). The flux can also be determined by another technique known as the *method of eigenfunctions*. As an illustration of this method, consider an infinite slab of extrapolated thickness  $a$  containing the source distribution  $s(x)$ . To simplify the discussion, it will be assumed that these sources are distributed symmetrically about the midplane of the slab. In other words, the function  $s(x)$  is an *even* function of  $x$ , that is,  $s(-x) = s(x)$ , where  $x$  is measured from the center of the slab. The flux in the slab must necessarily be an even function also, because a symmetric source distribution cannot possibly give rise to an asymmetric flux. Since the flux is a function only of  $x$ , the diffusion equation is

$$\frac{d^2\phi}{dx^2} - \frac{1}{L^2} \phi = -\frac{s}{D}, \quad (5-95)$$

and the boundary conditions are

$$\phi(a/2) = \phi(-a/2) = 0.$$

The central idea of the eigenfunction method is that it is possible to obtain a solution to the diffusion equation in terms of solutions to another differential

equation. Thus consider the equation

$$\frac{d^2\varphi}{dx^2} + B^2\varphi = 0, \quad (5-96)$$

where  $B$  is a constant and the function  $\varphi$  is required to satisfy the *same boundary conditions as the flux*. Because  $\phi$  has been assumed to be an even function, it will be necessary to consider only the even solutions of Eq. (5-96). Thus, although the general solution to Eq. (5-96) is

$$\varphi = A \cos Bx + C \sin Bx, \quad (5-97)$$

the constant  $C$  may be taken to be zero, since  $\sin Bx$  is an odd function.

The boundary condition at  $x = a/2$  (or at  $x = -a/2$ ; it makes no difference which is used, since the cosine is an even function) gives

$$\varphi\left(\frac{a}{2}\right) = A \cos \frac{Ba}{2} = 0. \quad (5-98)$$

This equation can be satisfied either by taking  $A = 0$ , which leads to the trivial solution  $\varphi = 0$ , or by requiring that  $\cos(Ba/2) = 0$ . This, in turn, will be satisfied provided  $B$  takes on certain values,  $B_n$ , namely,

$$B_n = \frac{n\pi}{a}, \quad (5-99)$$

where  $n$  is an odd integer.

The numbers  $B_n$  are known as *eigenvalues*, and the solutions to Eq. (5-96) corresponding to these eigenvalues are called *eigenfunctions*. Thus the solution

$$\varphi_n(x) = \cos \frac{n\pi x}{a} \quad (5-100)$$

is the  $n$ th eigenfunction corresponding to the  $n$ th eigenvalue  $B_n$ . It will be noted that  $\varphi_n$  satisfies both the differential equation (Eq. 5-96) and the boundary conditions. By analogy to problems in acoustics, the eigenfunction corresponding to the lowest value of  $n$ , that is,  $n = 1$ , is called the *fundamental eigenfunction* or *first harmonic*. All other eigenfunctions are referred to as *higher harmonics*.

One of the most important properties of eigenfunctions is the fact that the integral of the product of any two *different* eigenfunctions over a region specified by the boundary conditions is zero.\* Thus by direct integration it is easy to show that

$$\int_{-a/2}^{a/2} \varphi_m(x)\varphi_n(x) dx = \int_{-a/2}^{a/2} \cos \frac{m\pi x}{a} \cos \frac{n\pi x}{a} dx$$

---

\* In general, for the integral to vanish, it is also necessary to multiply the two eigenfunctions by another function called the *weighting function*. See, for example, Appendix II for a discussion of the integration of Bessel functions.

vanishes when  $m$  is not equal to  $n$ . When  $m = n$ , the integral is no longer zero, and has the value  $a/2$ . This property of eigenfunctions is known as *orthogonality*, and functions of this type are said to be *orthogonal* to one another.

Because of the orthogonality property of eigenfunctions, it is possible to expand any function that is reasonably well behaved (and many that are not) in a series of eigenfunctions. However, since the functions  $\varphi_n$  discussed above are even, they can be used to expand only even functions (cf. Prob. 5-35 for the more general case). To be specific, consider the even, but otherwise arbitrary, function  $f(x)$ . The expansion in eigenfunctions can be carried out by writing

$$f(x) = \sum_{n \text{ odd}} c_n \varphi_n(x). \quad (5-101)$$

The constants  $c_n$  can be determined by multiplying both sides of this equation by  $\varphi_m(x)$  and integrating from  $x = -a/2$  to  $a/2$ ; that is,

$$\int_{-a/2}^{a/2} f(x) \varphi_m(x) dx = \sum_{n \text{ odd}} c_n \int_{-a/2}^{a/2} \varphi_n(x) \varphi_m(x) dx.$$

The integral on the right-hand side of this equation vanishes unless  $m = n$ , and as a result, the entire sum reduces to only one term, namely, the  $m$ th term. Thus

$$c_m = \frac{2}{a} \int_{-a/2}^{a/2} f(x) \varphi_m(x) dx. \quad (5-102)$$

With this formula all of the constants in Eq. (5-101) can be computed. This procedure of expanding an arbitrary function in terms of eigenfunctions is widely used in reactor theory and will be employed throughout this book.

Returning now to the original problem of solving the diffusion equation (Eq. 5-95), this can be accomplished by first expanding both  $\phi(x)$  and  $s(x)$  in series of eigenfunctions, namely,

$$\phi(x) = \sum_{n \text{ odd}} A_n \varphi_n(x), \quad (5-103)$$

and

$$s(x) = \sum_{n \text{ odd}} S_n \varphi_n(x). \quad (5-104)$$

Since the source distribution  $s(x)$  is known, the constants  $S_n$  can be computed using Eq. (5-102), and the problem reduces to the finding of the constants  $A_n$ .

Inserting Eqs. (5-103) and (5-104) into Eq. (5-95) yields

$$\sum_{n \text{ odd}} A_n \left[ \frac{d^2 \varphi_n}{dx^2} - \frac{1}{L^2} \varphi_n \right] = -\frac{1}{D} \sum_{n \text{ odd}} S_n \varphi_n. \quad (5-105)$$

Since  $\varphi_n$  satisfies the equation

$$\frac{d^2 \varphi_n}{dx^2} + B_n^2 \varphi_n = 0,$$

where  $B_n$  is defined by Eq. (5-99), Eq. (5-105) can also be written as

$$\sum_{n \text{ odd}} A_n \left( B_n^2 + \frac{1}{L^2} \right) \varphi_n = \frac{1}{D} \sum_{n \text{ odd}} S_n \varphi_n. \quad (5-106)$$

Now, in view of the orthogonality of the  $\varphi_n$  functions, the  $n$ th terms on each side of Eq. (5-106) must be equal\* so that

$$A_n = \frac{S_n/D}{B_n^2 + 1/L^2} = \frac{S_n/\Sigma_a}{1 + B_n^2 L^2}, \quad (5-107)$$

where use has been made of the definition of  $L^2$  (cf. Eq. 5-53). With this result inserted into Eq. (5-103), the flux is

$$\phi(x) = \frac{1}{\Sigma_a} \sum_{n \text{ odd}} \frac{S_n \varphi_n(x)}{1 + B_n^2 L^2}. \quad (5-108)$$

Equation (5-108) is the complete solution to the problem;  $\phi(x)$  satisfies both the diffusion equation and the boundary conditions.

It is interesting to carry the solution one step further. In view of Eq. (5-102), the constants  $S_n$  are given by the integral

$$S_n = \frac{2}{a} \int_{-a/2}^{a/2} s(x) \varphi_n(x) dx. \quad (5-109)$$

Inserting this expression into Eq. (5-108) and writing  $x'$  instead of  $x$  in the integrand to avoid confusion, the result is

$$\phi(x) = \frac{2}{a \Sigma_a} \sum_{n \text{ odd}} \frac{\varphi_n(x)}{1 + B_n^2 L^2} \int_{-a/2}^{a/2} s(x') \varphi_n(x') dx'. \quad (5-110)$$

With a little rearrangement this equation can also be written as

$$\phi(x) = \int_{-a/2}^{a/2} s(x') \left[ \frac{2}{a \Sigma_a} \sum_{n \text{ odd}} \frac{\varphi_n(x) \varphi_n(x')}{1 + B_n^2 L^2} \right] dx'. \quad (5-111)$$

The expression in the brackets can be identified at once as the diffusion kernel for the problem. Thus with

$$G(x, x') = \frac{2}{a \Sigma_a} \sum_{n \text{ odd}} \frac{\varphi_n(x) \varphi_n(x')}{1 + B_n^2 L^2}, \quad (5-112)$$

---

\* To see this in detail, multiply both sides of Eq. (5-106) by  $\varphi_m$  and integrate from  $-a/2$  to  $+a/2$ . Only the  $m$ th terms on each side of the equation will remain, and Eq. (5-107) follows.

the flux becomes

$$\phi(x) = \int_{-a/2}^{a/2} s(x') G(x, x') dx'. \quad (5-113)$$

This result is simply a generalization of Eq. (5-83) to a finite system.

One of the great advantages of the eigenfunction method is that it can be extended without difficulty to problems involving more than one dimension. Thus it is easy to show that the kernel for *any* finite region enclosed by a free surface is always of the form

$$G(\mathbf{r}, \mathbf{r}') = \text{constant} \times \sum \frac{\varphi_n(\mathbf{r})\varphi_n(\mathbf{r}')}{1 + B_n^2 L^2}, \quad (5-114)$$

where the functions  $\varphi_n(\mathbf{r})$  satisfy the equation

$$\nabla^2 \varphi_n(\mathbf{r}) + B_n^2 \varphi_n(\mathbf{r}) = 0, \quad (5-115)$$

and vanish at the extrapolated surface of the medium. The flux arising from the general source distribution  $s(\mathbf{r})$  is then

$$\phi(\mathbf{r}) = \int_V s(\mathbf{r}') G(\mathbf{r}, \mathbf{r}') dV', \quad (5-116)$$

where  $V$  is the volume of the region.

**Numerical methods.** Many of the diffusion problems met in practice cannot be solved by the analytical techniques discussed above. These problems must be handled by numerical methods. Numerical computation is also frequently used even where an analytical solution is known, simply because it may be less time consuming to solve the diffusion equation directly by numerical methods than to evaluate a complicated, albeit elegant, analytical expression. This is particularly true when the calculations must be repeated many times in connection with parametric studies of reactors.

With the advent of modern high-speed computing machinery, it has become possible to make computations using the transport equation as well as the diffusion equation, and a large number of programs, or "codes" as they are usually called, have been developed to handle a variety of problems with these equations. Since the transport equation is more complicated than the diffusion equation, computations using transport codes generally take longer to perform on a computer and therefore tend to be more expensive to use than comparable diffusion codes. Nevertheless, because transport calculations give more nearly exact results than calculations based on diffusion theory and in view of the increased capabilities of modern computing equipment, transport codes are rapidly replacing diffusion codes in the design of nuclear reactors.

While a discussion of numerical methods lies outside the scope of this book, it may be mentioned that these methods generally fall into two broad categories, namely, *numerical integration* and *Monte Carlo*.\* The first category consists

---

\* "Monte Carlo" was the code name given to this method at the Los Alamos Laboratory during World War II.

essentially of a large number of techniques for numerically integrating a differential or integral equation. These methods are similar in principle to Simpson's rule for evaluating integrals, familiar from elementary calculus. Monte Carlo represents a considerably different approach to numerical computation. In this method, the life histories of individual neutrons are duplicated in detail on a computer. It may be recalled that at each stage in the life of a neutron, its future behavior is determined by various probability distribution functions. For instance, the location of an interaction is determined by the function  $p(x) = \Sigma_t \exp(-\Sigma_t x)$  (cf. Eq. 2-12); the type of interaction which it undergoes is determined by ratios of cross sections (for example,  $\sigma_s/\sigma_t$  is the probability that an interaction is elastic scattering); the angle of scattering of the neutron (if it is scattered) is determined by the differential cross section  $\sigma_s(\vartheta)$ ; and so on. In a Monte Carlo calculation, these various probability distributions are sampled by the computer in such a way that the computed histories of the neutrons are reproduced exactly as they would occur in the actual physical problem. With this method it is possible, therefore, to obtain the exact neutron distribution for all problems involving neutron transport. Unfortunately, this method also has a number of serious drawbacks (in particular, computation times often are very long), and it is not as widely used in reactor computations as the numerical techniques mentioned above. (A simple problem illustrating the Monte Carlo technique is given in Prob. 5-40.)

For a complete discussion of numerical methods, including Monte Carlo, the reader should consult the references at the end of the chapter. Information on computer codes is also noted in the references.

### 5-11 The Diffusion Length

In Section 5-9, it was shown that  $L$  is the relaxation length for the flux produced by a planar source in an infinite medium. In other words, the flux from this source falls off by a factor of  $e$  in the distance  $L$ . This is a rather special situation, however, and it is desirable to have a more general interpretation of the diffusion length.

For this purpose, consider a point source emitting  $S$  neutrons per second in an infinite medium. These neutrons diffuse about in the medium, moving in complicated paths like the one shown in Fig. 5-12, until they are eventually absorbed; none can escape since the medium is infinite. According to Eq. (5-64), the flux

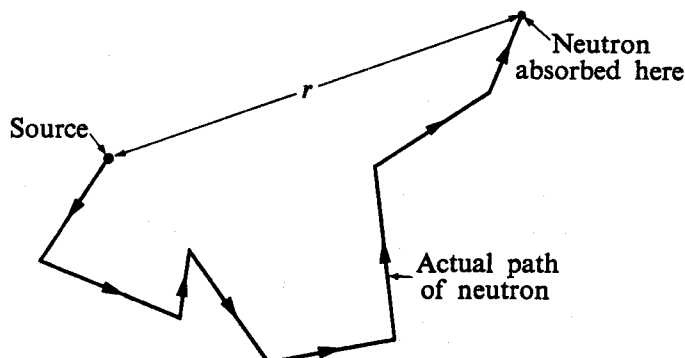


Fig. 5-12. Trajectory of a diffusing neutron from emission to absorption.

at the distance  $r$  from this source is given by

$$\phi(r) = \frac{Se^{-r/L}}{4\pi Dr}.$$

The number of neutrons,  $dN$ , which are absorbed per second in a spherical shell of volume  $dV = 4\pi r^2 dr$  located between  $r$  and  $r + dr$  is therefore

$$dN = \Sigma_a \phi(r) dV = \frac{S\Sigma_a}{D} r e^{-r/L} dr.$$

Since by definition  $L^2 = D/\Sigma_a$ , this can also be written as

$$dN = \frac{S}{L^2} r e^{-r/L} dr.$$

If a total of  $S$  neutrons are emitted per second by the source, and  $dN$  neutrons are absorbed per second between  $r$  and  $r + dr$ , the probability  $p(r) dr$  that a neutron emitted by the source is absorbed in  $dr$  is clearly just  $dN/S$ , that is,

$$p(r) dr = \frac{dN}{S} = \frac{r}{L^2} e^{-r/L} dr,$$

and the probability distribution function  $p(r)$  is

$$p(r) = \frac{r}{L^2} e^{-r/L}. \quad (5-117)$$

In view of the formula

$$\int_0^\infty x^n e^{-ax} dx = \frac{n!}{a^{n+1}}, \quad (5-118)$$

in which  $n$  is an integer, it is easy to see that

$$\int_0^\infty p(r) dr = 1.$$

Thus the probability that a source neutron is eventually absorbed *somewhere* in the infinite medium is unity, as it must be.

The  $n$ th *moment* of a probability distribution such as  $p(r)$  is defined as the average value of  $r^n$  over the distribution. Denoting this quantity by  $\bar{r}^n$ , it follows that

$$\bar{r}^n = \int_0^\infty r^n p(r) dr. \quad (5-119)$$

Using Eqs. (5-117) and (5-118), the moments of  $p(r)$  can easily be obtained.

For reasons that will be discussed in Chapter 9, it is the *second moment* of  $p(r)$  that is of the greatest importance in reactor theory. This is

$$\bar{r}^2 = \frac{1}{L^2} \int_0^\infty r^3 e^{-r/L} dr = 6L^2.$$

Thus the following result is obtained:

$$L^2 = \frac{1}{6} \bar{r^2}. \quad (5-120)$$

In other words, the square of the diffusion length is equal to one-sixth the average of the square of the crow-flight distance\* that a neutron travels from the point where it is emitted to the point where it is absorbed. Incidentally, the parameter  $L^2$ , for obvious reasons, is called the *diffusion area*.

This discussion of diffusion length has been based entirely upon diffusion theory. There are, however, many situations in which diffusion theory is not valid because of anisotropic scattering in the laboratory system, a rapidly varying flux, or for some other reason. Nevertheless, it is still convenient to define a diffusion length, and in these cases Eq. (5-120) is taken to be the definition of  $L^2$ . Thus whether diffusion theory is valid or not,  $L^2$  is defined to be  $\bar{r^2}/6$ . Only if diffusion theory is valid is  $L^2$  also given by the formula  $L^2 = D/\Sigma_a$ . Methods for measuring  $L$  in the important case of thermal neutrons will be discussed in Chapter 8.

## 5-12 The Reciprocity Theorem

At this point it is convenient to derive an important theorem regarding neutron diffusion. This theorem, which is known as the *reciprocity theorem*, will be used in a number of practical problems later in this book, particularly in connection with calculations of heterogeneous reactors in Chapter 11.

Let  $G(\mathbf{r}, \mathbf{r}')$  be the steady-state, one-velocity flux at  $\mathbf{r}$  due to a unit source at  $\mathbf{r}'$  in any uniform or nonuniform, finite or infinite medium in which Fick's law is valid. The function  $G(\mathbf{r}, \mathbf{r}')$  is the one-velocity point diffusion kernel for the medium in question. For the special case of a uniform, infinite medium,  $G(\mathbf{r}, \mathbf{r}')$  is the function  $G_{pt}(\mathbf{r}, \mathbf{r}')$  which was derived in Section 5-10. If the medium is finite,  $G(\mathbf{r}, \mathbf{r}')$  vanishes at the extrapolated surface; if the medium is infinite,  $G(\mathbf{r}, \mathbf{r}')$  vanishes at infinity.

According to Eq. (5-43),  $G(\mathbf{r}, \mathbf{r}')$  is determined by the equation

$$\operatorname{div} D \operatorname{grad} G(\mathbf{r}, \mathbf{r}') - \Sigma_a G(\mathbf{r}, \mathbf{r}') = -\delta(\mathbf{r} - \mathbf{r}'), \quad (5-121)$$

where  $D$  and  $\Sigma_a$  may be functions of  $\mathbf{r}$ , and  $\operatorname{div}$  and  $\operatorname{grad}$  operate on the variable  $\mathbf{r}$ , since  $\mathbf{r}'$  is merely the source point. With a source located at the point  $\mathbf{r}''$ , the diffusion equation becomes

$$\operatorname{div} D \operatorname{grad} G(\mathbf{r}, \mathbf{r}'') - \Sigma_a G(\mathbf{r}, \mathbf{r}'') = -\delta(\mathbf{r} - \mathbf{r}''). \quad (5-122)$$

If Eq. (5-121) is now multiplied by  $G(\mathbf{r}, \mathbf{r}'')$  and Eq. (5-122) is multiplied by  $G(\mathbf{r}, \mathbf{r}')$ , and the resulting equations are then subtracted and integrated over the

---

\* Crows, it seems, travel in straight lines before they alight. The "crow-flight distance" is thus the shortest distance from the point where the neutron is emitted to where it is ultimately absorbed (cf. Fig. 5-12).

volume of the medium, it is found that

$$\begin{aligned} \int_V [G(\mathbf{r}, \mathbf{r}'') \operatorname{div} D \operatorname{grad} G(\mathbf{r}, \mathbf{r}') - G(\mathbf{r}, \mathbf{r}') \operatorname{div} D \operatorname{grad} G(\mathbf{r}, \mathbf{r}'')] dV \\ = - \int_V G(\mathbf{r}, \mathbf{r}'') \delta(\mathbf{r} - \mathbf{r}') dV + \int_V G(\mathbf{r}, \mathbf{r}') \delta(\mathbf{r} - \mathbf{r}'') dV \\ = - G(\mathbf{r}', \mathbf{r}'') + G(\mathbf{r}'', \mathbf{r}'). \end{aligned} \quad (5-123)$$

The left-hand side of this equation can be transformed by use of the identity

$$f \operatorname{div} D \operatorname{grad} g = \operatorname{div}(fD \operatorname{grad} g) - D \operatorname{grad} f \cdot \operatorname{grad} g. \quad (5-124)$$

Thus

$$\begin{aligned} \int_V [G(\mathbf{r}, \mathbf{r}'') \operatorname{div} D \operatorname{grad} G(\mathbf{r}, \mathbf{r}') - G(\mathbf{r}, \mathbf{r}') \operatorname{div} D \operatorname{grad} G(\mathbf{r}, \mathbf{r}'')] dV \\ = \int_V \operatorname{div} D[G(\mathbf{r}, \mathbf{r}'') \operatorname{grad} G(\mathbf{r}, \mathbf{r}') - G(\mathbf{r}, \mathbf{r}') \operatorname{grad} G(\mathbf{r}, \mathbf{r}'')] dV \\ = \int_A D[G(\mathbf{r}, \mathbf{r}'') \operatorname{grad} G(\mathbf{r}, \mathbf{r}') - G(\mathbf{r}, \mathbf{r}') \operatorname{grad} G(\mathbf{r}, \mathbf{r}'')] \cdot \mathbf{n} dA, \end{aligned} \quad (5-125)$$

where use has been made of the divergence theorem.\* However, since both  $G(\mathbf{r}, \mathbf{r}')$  and  $G(\mathbf{r}, \mathbf{r}'')$  vanish on the surface, this integral is zero and it follows from Eq. (5-123) that

$$G(\mathbf{r}', \mathbf{r}'') = G(\mathbf{r}'', \mathbf{r}'). \quad (5-126)$$

By definition, the first variable in the  $G$  function is the point where the flux is observed; the second variable is the location of the source. Equation (5-126) shows, therefore, that the source and observation points can be exchanged. That is, *the one-velocity flux at  $\mathbf{r}'$  due to a unit source at  $\mathbf{r}''$  is the same as the one-velocity flux observed at  $\mathbf{r}''$  when the source is moved to  $\mathbf{r}'$ .* This is the reciprocity theorem.

This result is more general than it might appear from the above derivation which is based on diffusion theory. Thus it can be shown that Eq. (5-126) holds rigorously whether diffusion theory is valid or not. It must be emphasized, however, that the reciprocity theorem only applies in the one-velocity case. (The precise requirement for the validity of the reciprocity theorem is that the integrodifferential operator determining the flux must be self-adjoint. This condition is satisfied in all one-velocity problems. Self-adjoint operators will be discussed in Chapter 15.)

## References

### General

CASE, K. M., F. DEHOFFMANN, and G. PLACZEK, *Introduction to the Theory of Neutron Diffusion*. Washington, D.C.: U. S. Government Printing Office, 1953.

---

\* Equation (5-125) is a form of *Green's theorem* (see any book on advanced calculus).

DAVISON, B., *Neutron Transport Theory*. Oxford: Clarendon Press, 1957. This is the classic work on neutron transport theory. Diffusion theory is discussed in Chapter 7.

GALANIN, A. D., *Thermal Reactor Theory*, 2nd ed., New York: Pergamon Press, 1960, Sections 1 and 2.

GLASSTONE, S., and M. C. EDLUND, *The Elements of Nuclear Reactor Theory*. Princeton, N.J.: Van Nostrand, 1952, Chapter 5.

ISBIN, H. S., *Introductory Nuclear Reactor Theory*. New York: Reinhold, 1963, Chapter 4.

LITTLER, D. J., and J. F. RAFFLE, *An Introduction to Reactor Physics*, 2nd ed. New York: McGraw-Hill, 1957, Chapter 7.

MEGHREBLIAN, R. V., and D. K. HOLMES. *Reactor Analysis*. New York: McGraw-Hill, 1960, Chapter 5.

MURRAY, R. L., *Nuclear Reactor Physics*. Englewood Cliffs, N.J.: Prentice-Hall, 1957, Chapters 2 and 3.

WALLACE, P. R., and J. LECAINE, *Elementary Approximations in the Theory of Neutron Diffusion*. National Research Council of Canada (NRC No. 1480-MT-12; AECL-336), August 1946. This useful report contains the solutions to a large number of diffusion problems.

WEINBERG, A. M., and E. P. WIGNER, *The Physical Theory of Neutron Chain Reactors*. Chicago: University of Chicago Press, 1958, Chapters 8 and 9.

#### Analytical mathematics

HILDEBRAND, F. B., *Advanced Calculus for Engineers*. Englewood Cliffs, N.J.: Prentice-Hall, 1949.

KAPLAN, W., *Advanced Calculus*. Reading, Mass.: Addison-Wesley, 1952.

MORSE, P. M., and H. FESHBACH, *Methods of Theoretical Physics*. New York: McGraw-Hill, 1953. These volumes contain many examples of the use of Green's functions and eigenfunctions; see particularly Chapters 6 and 7.

SOKOLNIKOFF, I. S., and R. M. REDHEFFER, *Mathematics of Physics and Modern Engineering*. New York: McGraw-Hill, 1958.

WYLIE, C. R., JR., *Advanced Engineering Mathematics*, 2nd ed. New York: McGraw-Hill, 1960.

#### Numerical methods

CASHWELL, E. D., and C. J. EVERETT, *A Practical Manual on the Monte Carlo Method for Random Walk Problems*. New York: Pergamon Press, 1960.

HAMMING, R. W., *Numerical Methods for Scientists and Engineers*. New York: McGraw-Hill, 1962.

HILDEBRAND, F. B., *Introduction to Numerical Analysis*. New York: McGraw-Hill, 1956.

ROOS, B. W., and W. C. SANGREN, "Some Aspects of the Use of Digital Computers in Nuclear Reactor Design," *Advances in Nuclear Science and Technology*, Volume 2. New York: Academic Press, 1964.

SANGREN, W., *Digital Computers and Nuclear Reactor Calculations*. New York: Wiley, 1960.

STIEFEL, E. L., *An Introduction to Numerical Methods*. New York: Academic Press, 1963.

### Reactor codes

*Reactor Physics Constants*, USAEC Report ANL-5800, 2nd ed., 1963. Section 10 of this report contains information on a large number of reactor codes.

Abstracts of reactor codes are issued from time to time by the Argonne Code Center at the Argonne National Laboratory and distributed by the American Nuclear Society.

### Problems

[Note: Except where otherwise specified, the neutrons are to be treated as monoenergetic. Cross sections where needed should be computed at 0.025 eV.]

5-1. At one point in a block of graphite the remarkable situation is found that the neutrons are traveling in only the positive and negative  $x$ -directions (see Fig. 5-13), and all have the energy 0.025 eV. There are  $10^{10}$  neutrons/sec crossing unit area normal to the  $x$ -axis in the positive direction and  $0.5 \times 10^{10}$  neutrons/sec crossing unit area in the negative direction. (a) Compute the neutron flux and current at this point. (b) Compute the collision density.

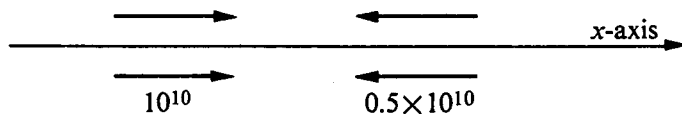


Figure 5-13

5-2. Two monoenergetic neutron beams, each of intensity  $5 \times 10^8$  neutrons/cm<sup>2</sup>-sec, cross at an angle of  $45^\circ$ . Compute the neutron flux and current in the region where the beams intersect.

5-3. The neutron density distribution function at the point  $r$  is

$$n(r, \omega) = n e^{-z/\lambda} (1 + \cos \vartheta),$$

where  $n$  and  $\lambda$  are constants, and  $\vartheta$  is the angle between  $\omega$  and the  $z$ -axis. Compute at  $r$ : (a) the neutron density, (b) the flux, (c) the current.

5-4. At a certain point in a reactor, the neutron density distribution function is given by

$$n(r, E, \omega) = n E^{1/2} e^{-aE} \cos \frac{\vartheta}{2},$$

where  $n$  and  $a$  are constants, and  $\vartheta$  is the angle between  $\omega$  and the  $z$ -axis. Determine (a) the total neutron density, (b) the energy-dependent flux, (c) the neutron current.

5-5. Show that the neutron density distribution function at any point in a monodirectional beam of monoenergetic neutrons moving along the  $x$ -axis is given by

$$n(x, \omega) = \frac{n}{\pi} \delta(\mu - 1),$$

where  $n$  is the neutron density,  $\delta(\mu - 1)$  is the Dirac delta function, and  $\mu$  is the cosine of the angle between  $\omega$  and the  $x$ -axis.

5-6. Consider a point where the flux is isotropic, that is, where there are equal numbers of neutrons moving into solid angles  $d\Omega$  about every direction  $\omega$ . (a) Show that the neutron density distribution function is given by

$$n(\omega) = \frac{\phi}{4\pi v},$$

where  $\phi$  is the flux. (b) Show that the magnitude of the current density of neutrons moving into any direction is given by

$$J^+ = \frac{\phi}{4}.$$

(c) What is the total current at this point?

5-7. Consider a unit area on the surface of a semi-infinite medium, i.e., the region defined by  $0 \leq x < \infty$ . (a) If the flux is a constant in the medium and zero outside, and the scattering is isotropic in the laboratory system, show that the number of neutrons passing through this area into a solid angle  $d\Omega$  about  $\omega$  is proportional to the cosine of the angle between  $\omega$  and the normal to the surface. This result is called *Lambert's cosine law*. (b) If the flux, in fact, increases with distance into the medium from a value of near zero at the surface, as it does in most practical problems, discuss qualitatively how this affects the angular distribution of the neutrons emitted through unit area of the surface.

5-8. Neutrons are produced uniformly and isotropically throughout a spherical chamber containing a mixture of  $H^3$  and  $H^2$  gases at high temperature ( $\sim 10^8 K$ ) and low density. (The neutrons originate in the  $H^3(d, n)He^4$  and  $H^2(d, n)He^3$  fusion reactions.) Show that the neutron flux and current at any point on the surface of the chamber are given by  $\phi = SR/2$  and  $J = SRa_r/3$ , respectively, where  $S$  is the source density (neutrons/cm<sup>3</sup>-sec),  $R$  is the radius of the chamber, and  $a_r$  is a unit radial vector. The neutron mean free path in the medium is essentially infinite. [Note: It considerably simplifies the calculations if the origin of coordinates is chosen to be on the surface of the chamber.]

5-9. Isotropic neutron sources are uniformly distributed over the planar surface of a semi-infinite diffusing medium. If  $S$  neutrons are emitted per cm<sup>2</sup>/sec of the surface, show that the flux of uncollided neutrons in the medium is given by

$$\phi_u(x) = \frac{S}{2} E_1(\Sigma_t x),$$

where (cf. Appendix II)

$$E_1(z) = \int_z^\infty \frac{e^{-z}}{z} dz.$$

5-10. A spherical target is placed in a monodirectional beam of neutrons of intensity  $I$ . The area of the beam is larger than the cross sectional area of the sphere. Show that the total reaction rate within the sphere in such a beam is equal to the reaction rate when the sphere is completely immersed in an isotropic flux of magnitude equal to  $I$ .

5-11. Show by direct calculation that the second-order terms in the derivation of Fick's law vanish identically.

5-12. Using Eq. (5-38), compute the diffusion coefficients of the following materials at 0.025 eV: (a) iron, (b) natural uranium, (c) uranium enriched to 2.5%  $U^{235}$ .

5-13. Show that Eq. (5-38) reduces to Eq. (5-37) when  $\bar{\mu} = 0$  and  $\Sigma_a/\Sigma_t \ll 1$ .

5-14. Two isotropic point sources each emitting  $S$  neutrons/sec are placed in an infinite diffusing medium as shown in Fig. 5-14. (a) Find the flux at the point  $P$ . (b) Find the current at the point  $P$ .

5-15. Three isotropic point sources each emitting  $S$  neutrons/sec are placed in an infinite moderator at the vertices of an equilateral triangle of side  $a$ . Find the flux and current at the midpoint of any side of the triangle.

5-16. A bare sphere of moderator of radius  $a$  contains uniformly distributed sources of neutrons emitting  $S$  neutrons/cm<sup>3</sup>-sec. (a) Find the flux and current within the sphere. (b) What is the neutron current exterior to the sphere? (c) What is the probability that a source neutron does not leak from the sphere?

5-17. Neutron sources are distributed over the plane at  $x = 0$  according to the function  $S(y, z)$ . Show that the source condition is

$$\lim_{x \rightarrow 0} J_x(x, y, z) = \frac{S(y, z)}{2}.$$

5-18. A 0.025-eV neutron is incident normally on a slab of graphite 100 cm thick. (a) What is the probability that the neutron passes through the slab without a collision? (b) What is the probability that it ultimately passes through the slab? (c) What is the probability that it is reflected from the slab?

5-19. An infinite line source emits  $S$  neutrons/sec per unit length of the source into an infinite homogeneous medium. Show that the appropriate source condition is

$$\lim_{r \rightarrow 0} rJ(r) = \frac{S}{2\pi},$$

and that the flux is given by

$$\phi = \frac{S}{2\pi D} K_0(r/L),$$

where  $K_0$  is the modified Bessel function of the second kind (cf. Appendix II).

5-20. Along the axis of an infinitely long bare cylinder of radius  $a$  there is a line source of neutrons emitting  $S$  neutrons/sec per unit length of the source. (a) Find the flux and current within the cylinder. (b) What is the neutron current exterior to the cylinder? (c) What is the probability that a neutron from the source does not escape from the cylinder?

5-21. Monoenergetic sources of neutrons emitting  $S$  neutrons/cm<sup>3</sup>-sec are distributed uniformly throughout an infinite moderator. (a) Show that the flux is given by

$$\phi_0 = \frac{S}{\Sigma_a}.$$

(b) If an infinite sheet of thin absorber is inserted in the medium at  $x = 0$ , show that the flux becomes

$$\phi(x) = \phi_0 \left[ 1 - \frac{\gamma e^{-|x|/L}}{\gamma + (2D/L)} \right],$$

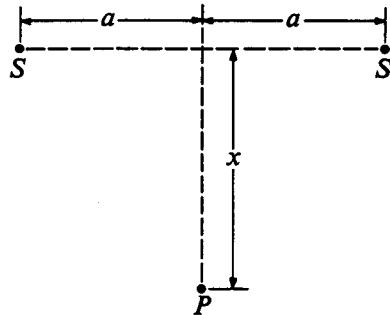


Figure 5-14

in which  $\gamma = \Sigma'_a t$ , where  $\Sigma'_a$  and  $t$  are respectively the absorption cross section and thickness of the sheet; the other parameters refer to the moderator. *Hint:* Treat the absorbing sheet by a "source" condition

$$\lim_{x \rightarrow 0} J(x) = -\Sigma'_a t \phi(0)/2.$$

5-22. A monodirectional beam of neutrons of intensity  $I$  impinges on a semi-infinite diffusing medium. The flux in the medium can be found in two ways: (1) by solving the diffusion equation subject to the boundary condition  $J^+(0) = I$ , or (2) by treating the first collision density as a distributed source within the medium. Compute and sketch the flux using these two methods and discuss the validity of each solution.

5-23. The neutron flux at the surface of a submerged nuclear submarine is found to be given by the expression

$$\phi = a + b \cos \vartheta,$$

where  $a$  and  $b$  are constants and  $\vartheta$  is the cylindrical angle measured from the vertical (cf. Fig. 5-15). Find the flux in the surrounding sea water. [Hint: Solve the diffusion equation in cylindrical coordinates using the method of separation of variables. (See any book on advanced calculus or see Section 9-3.)]

5-24. Consider two adjacent diffusing regions  $A$  and  $B$ .  $A$  contains neutron sources;  $B$  does not. The *albedo* or *reflection coefficient*  $\beta$  of region  $B$  with respect to  $A$  is defined as the ratio

$$\beta = \frac{J_{\text{out}}}{J_{\text{in}}},$$

where  $J_{\text{in}}$  and  $J_{\text{out}}$  are, respectively, the neutron currents entering and emerging from  $B$ ; both are computed at the interface between the two media. (a) If region  $B$  is an infinite slab of thickness  $a$ , show that its albedo is given by

$$\beta = \frac{1 - (2D/L) \coth(a/L)}{1 + (2D/L) \coth(a/L)},$$

where all parameters refer to region  $B$ . (b) Plot  $\beta$  as a function of  $a$  if region  $B$  is  $H_2O$ . (c) Compute  $\beta$  when region  $B$  is infinitely thick for the four common moderators  $H_2O$ ,  $D_2O$ ,  $Be$ ,  $C$ .

5-25. A sphere of moderator  $A$  of radius  $a$  is immersed in an infinite region of moderator  $B$ . An isotropic source emitting  $S$  neutrons/sec is located at the center of moderator  $A$ . Find the flux throughout the system.

5-26. Consider an infinite, uniform, source-free medium containing neutrons. (a) If the scattering is isotropic in the laboratory system show that the flux satisfies the integral equation:

$$\phi(\mathbf{r}) = \frac{\Sigma_s}{4\pi} \int \phi(\mathbf{r}') \frac{e^{-\Sigma_t |\mathbf{r}-\mathbf{r}'|} dV'}{|\mathbf{r}-\mathbf{r}'|^2},$$

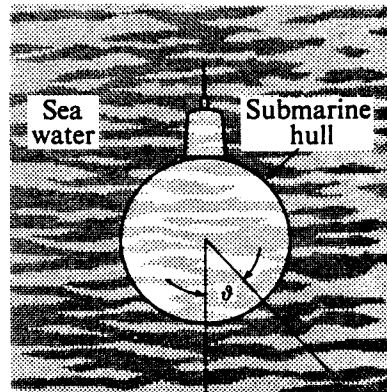


Figure 5-15

where the integral is carried out over all space. This equation is the integral form of the transport equation. (b) Taking  $\mathbf{r} = 0$ , for simplicity, expand  $\phi(\mathbf{r}')$  in the Taylor series:

$$\phi(\mathbf{r}') = \phi(0) + x\phi_x(0) + y\phi_y(0) + z\phi_z(0) + \frac{1}{2}x^2\phi_{xx}(0) + \frac{1}{2}xy\phi_{xy}(0) + \dots,$$

where differentiation is indicated by subscripts. By direct substitution into the integral equation show that if the series is truncated after second-order terms, the flux satisfies the diffusion equation and  $D$  is given by Eq. (5-37). [This result can be generalized as follows. When the complete series is inserted into the integral equation it is found that only terms in  $\nabla^2\phi, \nabla^4\phi, \dots, \nabla^{2n}\phi$  remain after the integration is performed. The flux will then satisfy the diffusion equation only if  $D$  is computed from the equation

$$\frac{\Sigma_s}{2} \sqrt{\frac{D}{\Sigma_a}} \ln \left[ \frac{\Sigma_t + \sqrt{\Sigma_a/D}}{\Sigma_t - \sqrt{\Sigma_a/D}} \right] = 1.$$

This is one derivation of Eq. (5-38), in the case of isotropic scattering ( $\mu = 0$ ).]

5-27. (a) By solving the diffusion equation for a planar source located at  $x'$ , show that the diffusion kernel for an infinite slab of thickness  $a$  is given by

$$G(x, x') = \frac{L}{D \sinh(a/L)} \begin{cases} \sinh \frac{1}{L} \left( \frac{a}{2} - x \right) \sinh \frac{1}{L} \left( \frac{a}{2} + x' \right), & x > x', \\ \sinh \frac{1}{L} \left( \frac{a}{2} + x \right) \sinh \frac{1}{L} \left( \frac{a}{2} - x' \right), & x < x'. \end{cases}$$

(b) Using this kernel calculate the flux in a slab containing uniformly distributed sources emitting  $S$  neutrons/cm<sup>3</sup>-sec.

5-28. (a) By computing the flux due to a thin spherical shell of neutron sources of radius  $r'$ , show that the diffusion kernel for a spherically symmetric source distribution in an infinite medium is given by

$$G(r, r') = \frac{L}{8\pi rr'D} \begin{cases} [e^{-(r-r')/L} - e^{-(r'+r)/L}], & r > r', \\ [e^{-(r'-r)/L} - e^{-(r'+r)/L}], & r < r'. \end{cases}$$

[Hint: Use the source condition  $4\pi(r')^2 \lim_{\epsilon \rightarrow 0} [J_r(r' + \epsilon) - J_r(r' - \epsilon)] = 1$ .] (b) Using this kernel compute the flux at any point in an infinite medium containing uniformly distributed sources emitting  $S$  neutrons/cm<sup>3</sup>-sec.

5-29. Using the diffusion kernel derived in Problem 5-28 calculate the flux throughout a sphere of radius  $R$  containing uniformly distributed sources emitting  $S$  neutrons/cm<sup>3</sup>-sec.

5-30. The diffusion kernel,  $G(x, x')$ , for a semi-infinite medium, i.e. the region  $0 \leq x < \infty$ , can be calculated by supposing that for every planar source at  $x'$  there is a negative planar source at  $-x'$  (cf. Fig. 5-16), and that for the purposes of the calculation, the medium is extended to  $-\infty$ . The flux due to the two planar sources then satisfies the diffusion equation and vanishes at the surface of the medium. This technique is known as the *method of images*. (a) In this way, show that the diffusion kernel for a semi-infinite

medium is

$$G(x, x') = \frac{L}{2D} [e^{-|x-x'|/L} - e^{-|x'+x|/L}].$$

(b) Using this kernel, compute the flux in a semi-infinite medium containing uniformly distributed neutron sources.

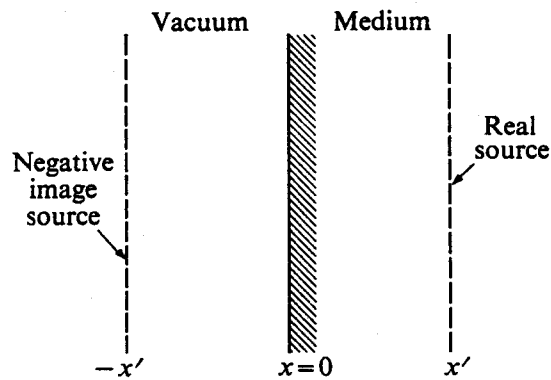


Figure 5-16

5-31. Neutron sources are distributed in a bare infinite slab of extrapolated thickness  $a$  according to the relation

$$s(x) = S(x + a/2),$$

where  $S$  is a constant and  $x$  is measured from the center of the slab. Show that the flux within the slab is given by

$$\phi = \frac{Sa}{\Sigma_a} \left[ \frac{x}{a} + \frac{1}{2} - \frac{\sinh[(x + a/2)/L]}{\sinh(a/L)} \right].$$

5-32. Verify that

$$\int_{-a/2}^{a/2} \cos \frac{m\pi x}{a} \cos \frac{n\pi x}{a} dx$$

vanishes unless  $m = n$ .

5-33. Expand the function

$$f(x) = A(a^2 - 4x^2), \quad -\frac{a}{2} \leq x \leq \frac{a}{2},$$

in a series of slab eigenfunctions.

5-34. A bare slab of moderator of extrapolated thickness  $a$  contains a uniformly distributed source of thermal neutrons emitting  $S$  neutrons/cm<sup>3</sup>-sec. Find the thermal neutron flux and current in the slab (a) by directly solving the diffusion equation and (b) by using the eigenfunction method. Show that the two solutions are equivalent.

5-35. The eigenfunctions derived in Section 5-10 are even functions of  $x$  and hence are appropriate for problems involving source distributions which are also even in  $x$ . (a) Show that the eigenfunctions appropriate for arbitrary source distributions in a slab are

$$\varphi_n = \begin{cases} \cos \frac{n\pi x}{a}, & n = \text{odd}, \\ \sin \frac{n\pi x}{a}, & n = \text{even}. \end{cases}$$

(b) Show that these functions form an orthogonal set.

5-36. A planar source emitting  $S$  neutrons/cm<sup>2</sup>-sec is placed in the center of an infinite bare slab of moderator or extrapolated thickness  $a$ . (a) Find the rate at which neutrons are absorbed in the slab. (b) Find the rate at which neutrons leak from the slab. (c) What is the probability that a neutron emitted by the source will not escape from the slab?

5-37. Consider the infinite slab containing an arbitrary distribution of neutron sources which was discussed in Section 5-10 by the eigenfunction method. In the steady state the total number of neutrons emitted by the sources within the slab must be equal to the number absorbed in the slab plus the number escaping from the surface. Verify this condition using the expression for  $\phi(x)$  given in Eq. (5-110).

5-38. A bare cube of moderator of side  $a$  contains at its center an isotropic point source emitting  $S$  neutrons/sec. (a) Show that the flux is given by

$$\phi = \frac{8S}{a^3 \Sigma_a} \sum_{\substack{l,m,n \\ \text{odd}}} \frac{1}{1 + B_{lmn}^2 L^2} \cos \frac{l\pi x}{a} \cos \frac{m\pi y}{a} \cos \frac{n\pi z}{a},$$

where

$$B_{lmn}^2 = (l^2 + m^2 + n^2) \left( \frac{\pi}{a} \right)^2.$$

(b) Derive an expression for the probability that a source neutron will escape from the cube. [Hint: In part (a) expand  $\phi$  in the triple eigenfunction series

$$\phi = \sum A_{lmn} \cos \frac{l\pi x}{a} \cos \frac{m\pi y}{a} \cos \frac{n\pi z}{a},$$

and find  $A_{lmn}$  by substituting this series into the diffusion equation.]

5-39. An isotropic point source emitting  $S$  neutrons/sec is placed at the center of a right circular cylinder of moderator of radius  $R$  and height  $H$ . (a) With the origin of cylindrical coordinates at the center of the cylinder, show that the source function is given by

$$s(r, z) = \frac{S\delta(r)\delta(z)}{\pi r}.$$

(b) Show that the flux is given by

$$\phi(r, z) = \frac{2S}{\Sigma_a V} \sum_{\substack{m \text{ odd} \\ n=1, 2, 3, \dots}} \frac{\cos(m\pi z/H) J_0(x_n r/R)}{(1 + B_{mn}^2 L^2) J_1^2(x_n)},$$

where  $V$  is the volume of the cylinder;  $x_n$  is the  $n$ th zero of  $J_0(x)$ , that is,  $J_0(x_n) = 0$ ; and

$$B_{mn}^2 = \left( \frac{m\pi}{H} \right)^2 + \left( \frac{x_n}{R} \right)^2.$$

[Hint: In part (a) consult Appendix II. In part (b) use the orthogonality of the Bessel functions discussed in Appendix II, and expand both  $s(r, z)$  and  $\phi(r, z)$  in a double eigenfunction series, viz.,

$$\phi(r, z) = \sum A_{mn} \cos \left( \frac{m\pi z}{H} \right) J_0 \left( \frac{x_n r}{R} \right).$$

Determine  $A_{mn}$  by substituting into the diffusion equation.]

5-40. The underlying principle of a Monte Carlo computation may be seen from the following example. A college professor from upstate New York on a visit to New York City goes out for a random walk in midtown Manhattan (the cartesian part of town).

At each intersection he tosses a coin twice. If it falls heads-heads he turns north; heads-tails, east; tails-tails, south; and tails-heads, west. By tossing coins, duplicate this random walk and estimate the average distance, as the crow flies, that he has traveled from his room at the YMCA when he has walked a total distance of 10 blocks. Assume that the blocks are square.

5-41. A point source of neutrons is located in an infinite medium which absorbs but does not scatter neutrons, that is,  $\Sigma_a \gg \Sigma_s$ . (a) Find the probability distribution function describing the absorption of the neutrons. (b) Compute the second moment of this function and compare with the comparable second moment for a diffusing medium.

5-42. A monoenergetic isotropic point source emitting  $S$  neutrons/sec is located at the distance  $R/2$  from the center of a sphere of moderator of radius  $R$ . Derive an expression for the flux at the center of the sphere.

# 6

## Neutron Moderation Without Absorption

It will be recalled from Chapter 3 that fission neutrons are fairly energetic, having an average energy of about 2 MeV. Before these neutrons induce additional fissions to sustain a chain reaction, their energy is reduced, often by several orders of magnitude, as the result of successive elastic and inelastic collisions with the nuclei in the system. In thermal reactors, for instance, almost all of the fission neutrons slow down to thermal energies before they induce further fissions. By contrast, they only slow down to the order of 100 keV or so in fast reactors before they interact with the fuel and produce fissions.

In considering the slowing down of neutrons in a thermal reactor it is convenient to divide the energy scale of the neutrons into two more or less distinct regions defined by a cutoff energy  $E_m$ . The value of  $E_m$  is chosen in such a way that for interactions at energies above  $E_m$  the nuclei in the system can be assumed to be free, that is, unencumbered by chemical binding effects, and at rest with respect to an incident neutron. In this case, the laws governing the energy loss of neutrons in scattering collisions are comparatively simple, and it is possible to develop an analytical theory of neutron slowing down using elementary methods. By contrast, at energies below  $E_m$  the various chemical binding effects discussed in Section 2-8 must be taken into account, along with the fact that due to its thermal motion the energy of a nucleus may be comparable to or even larger than that of an incident neutron. In practice, it is found that  $E_m$  is of the order of 1 eV.

The energy region above  $E_m$  is called the *moderating* region, and the slowing down of neutrons in this region is known as *moderation*. Neutron moderation in the absence of absorption forms the subject of the present chapter; moderation with absorption is covered in Chapter 7. The behavior of neutrons at energies below  $E_m$  will be considered in Chapter 8.

In systems composed of light nuclei the moderation of neutrons is due almost entirely to elastic scattering, due to the fact that the inelastic thresholds of light nuclei are so high. If large amounts of intermediate or heavy nuclei are present, however, inelastic scattering by these nuclei may make an important contribution to the moderation of the neutrons and must be taken into account. In the first sections of this chapter it is assumed that the neutrons interact only by elastic scattering; moderation by inelastic scattering is discussed in Section 6-15.

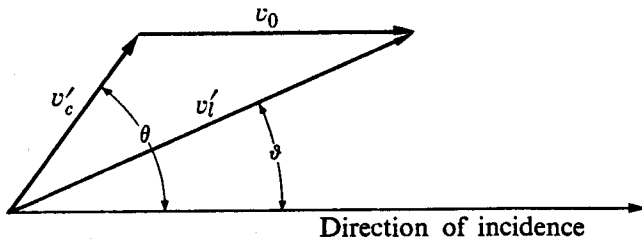


**Fig. 6-1.** Vector diagram for relating the center-of-mass and laboratory speeds of an elastically-scattered neutron.

### 6-1 Energy Loss in Elastic Collisions

When a neutron is elastically scattered by a nucleus which is initially at rest in the laboratory, the nucleus recoils, since momentum must be conserved in the collision. As a result, the laboratory energy of the incident neutron is diminished by an amount equal to the energy acquired by the recoiling nucleus. When the collision is viewed in the center-of-mass system, as explained in Section 2-5, the energies of neutron and nucleus remain the same and only the direction of motion of the two is changed. Figure 6-1 shows the vector diagram relating the neutron velocities in the laboratory and center-of-mass systems for a neutron scattered through an angle  $\vartheta$  in the laboratory, which corresponds to the angle  $\theta$  in the center-of-mass system. In the figure,  $v'_l$  and  $v'_c$  are the neutron speeds after the collision in the laboratory and center-of-mass systems, respectively, and  $v_0$  is the speed of the center of mass. If the scattering is elastic,  $v'_c = v_c$ , where  $v_c$  is the initial speed in the center-of-mass system, and from the law of cosines it is evident that

$$(v'_l)^2 = v_c^2 + v_0^2 + 2v_0v_c \cos \theta. \quad (6-1)$$

In view of Eqs. (2-29) and (2-30),  $v_c = Av_l/(A + 1)$  and  $v_0 = v_l/(A + 1)$ , where  $v_l$  is the initial speed of the neutron in the laboratory. It follows that

$$\begin{aligned} (v'_l)^2 &= \left(\frac{Av_l}{A + 1}\right)^2 + \left(\frac{v_l}{A + 1}\right)^2 + \frac{2Av_l^2}{(A + 1)^2} \cos \theta \\ &= \frac{v_l^2(A^2 + 2A \cos \theta + 1)}{(A + 1)^2}. \end{aligned} \quad (6-2)$$

The laboratory kinetic energies of the neutron before and after the collision,  $E_l$  and  $E'_l$ , are given by  $E_l = \frac{1}{2}mv_l^2$  and  $E'_l = \frac{1}{2}m(v'_l)^2$ , and Eq. (6-2) can be written as

$$E'_l = E_l \left[ \frac{A^2 + 2A \cos \theta + 1}{(A + 1)^2} \right]. \quad (6-3)$$

This equation relating  $E_l$ ,  $E'_l$ , and the angle  $\theta$  can be put in a more convenient form upon introducing the parameter  $\alpha$  (not to be confused with the capture-to-fission ratio) defined by

$$\alpha = \left(\frac{A - 1}{A + 1}\right)^2. \quad (6-4)$$

With a little algebra Eq. (6-3) then becomes

$$E'_l = \frac{1}{2}E_l[(1 + \alpha) + (1 - \alpha)\cos\theta]. \quad (6-5)$$

From Eq. (6-5) it is easy to see that the energy of the scattered neutron is greatest for  $\theta = 0$ , namely,

$$(E'_l)_{\max} = E_l, \quad (6-6)$$

as would be expected. On the other hand, the minimum value of  $E'_l$  occurs when  $\theta = \pi$ , that is,

$$(E'_l)_{\min} = \alpha E_l. \quad (6-7)$$

Thus the minimum energy of a neutron after an elastic collision is determined by the parameter  $\alpha$ , which, from Eq. (6-4), depends only upon the mass of the struck nucleus.

**Table 6-1**  
**Elastic Slowing-Down Parameters**

Nucleus	Mass no.	$\alpha$	$\xi$ or $\bar{\xi}$
Hydrogen	1	0	1.000
H <sub>2</sub> O		*	0.920
Deuterium	2	0.111	0.725
D <sub>2</sub> O		*	0.509
Beryllium	9	0.640	0.209
Carbon	12	0.716	0.158
Oxygen	16	0.779	0.120
Sodium	23	0.840	0.0825
Iron	56	0.931	0.0357
Uranium	238	0.983	0.00838

\* Not defined.

According to Eq. (6-4)  $\alpha$  is equal to zero when  $A = 1$ , i.e., for hydrogen, and increases to unity with increasing  $A$  (cf. Table 6-1). In view of Eq. (6-7), it is evident that a neutron can lose all its energy in a single collision with hydrogen, while for collisions with all other nuclei it can lose at most only a fraction of its original energy. For example,  $\alpha$  is 0.716 for carbon, so that  $(E'_l)_{\min} = 0.716E_l$ . Neutrons can lose therefore at most only 28.4% of their energy in an elastic collision with a carbon nucleus. On the other hand, for U<sup>238</sup>,  $\alpha$  is 0.983, and in this case no more than 1.7% of a neutron's energy can be lost in an elastic collision. To summarize, *the maximum fractional energy loss in a single elastic collision decreases with increasing mass of the struck nucleus*.

In any case, the energy of an elastically scattered neutron always lies between  $\alpha E$  and  $E$ , where  $E$  is its original energy. (The subscript denoting the laboratory system will be dropped from here on, since only laboratory energies will be con-

sidered.) It is important now to consider where in the interval from  $\alpha E$  to  $E$  the energy of the scattered neutron is likely to fall. For this purpose, it is convenient to introduce the probability distribution function  $P(E \rightarrow E')$ , which is defined so that  $P(E \rightarrow E') dE'$  is the probability that a neutron with the laboratory energy  $E$  will emerge from a collision with an energy between  $E'$  and  $E' + dE'$ .

From the above discussion it is clear that  $P(E \rightarrow E') = 0$  for  $E < E' < \alpha E$ . Within the region  $\alpha E < E' < E$ ,  $P(E \rightarrow E')$  can be determined by the following argument. First, it will be noted that in view of Eq. (6-5), the energy of the scattered neutron depends upon the angle through which the neutron is scattered. (Either laboratory or center-of-mass scattering angles can be used here, but it is more convenient to use the latter.) The neutrons which emerge with energies between  $E'$  and  $E' + dE'$  are therefore the same neutrons that are scattered between angles  $\theta$  and  $\theta + d\theta$ . Now, as shown in Section 2-4, the probability that a neutron is scattered between  $\theta$  and  $\theta + d\theta$  is given by  $\sigma_s(\theta) d\Omega(\theta)/\sigma_s = 2\pi\sigma_s(\theta) \sin \theta d\theta/\sigma_s$ , where  $\sigma_s(\theta)$  and  $\sigma_s$  are the differential and total elastic cross sections, respectively. It follows that

$$P(E \rightarrow E') dE' = - \frac{2\pi\sigma_s(\theta) \sin \theta d\theta}{\sigma_s}. \quad (6-8)$$

The minus sign appears in this equation because  $E'$  decreases with increasing  $\theta$ , and a positive value of  $d\theta$  necessarily implies a negative value of  $dE'$ ; with the minus sign included in Eq. (6-8), it is assured that  $P(E \rightarrow E')$  is a positive quantity.

Returning to Eq. (6-5) and taking differentials, the result is

$$dE' = -\frac{1}{2}E(1 - \alpha) \sin \theta d\theta. \quad (6-9)$$

Dividing Eq. (6-8) by Eq. (6-9) gives

$$P(E \rightarrow E') = \frac{4\pi\sigma_s(\theta)}{E(1 - \alpha)\sigma_s}$$

for  $E'$  in the interval  $\alpha E < E' < E$ . In summary, therefore,  $P(E \rightarrow E')$  is given by

$$P(E \rightarrow E') = \begin{cases} \frac{4\pi\sigma_s(\theta)}{E(1 - \alpha)\sigma_s}, & \alpha E < E' < E, \\ 0, & E < E' < \alpha E. \end{cases} \quad (6-10)$$

Equation (6-10) shows that the energy distribution of elastically scattered neutrons is directly proportional to the differential scattering cross section. An important special case is that of isotropic scattering in the *center-of-mass system*. It will be recalled from Chapter 2 that this occurs when  $kR \ll 1$ , where  $k$  is the wave number of the incident neutron and  $R$  is the radius of the struck nucleus. In this case,  $\sigma_s(\theta)$  is a constant, namely,

$$\sigma_s(\theta) = \frac{\sigma_s}{4\pi}, \quad (6-11)$$

and Eq. (6-10) becomes

$$P(E \rightarrow E') = \begin{cases} \frac{1}{E(1 - \alpha)}, & \alpha E < E' < E, \\ 0, & E < E' < \alpha E. \end{cases} \quad (6-12)$$

Hence, when the scattering is isotropic in the center-of-mass system, the energy distribution of the scattered neutrons is a constant, independent of  $E'$ . In other words, the energy of a scattered neutron will be found with equal probability in any interval  $dE'$  between  $E' = \alpha E$  and  $E' = E$ .

Incidentally, it is easy to show by direct calculation (cf. Prob. 6-2) that the integral of  $P(E \rightarrow E')$  between  $\alpha E$  and  $E$  is equal to unity. This is to be expected, since a scattered neutron necessarily must appear with an energy *somewhere* in this interval. In particular, for isotropic center-of-mass scattering,  $P(E \rightarrow E')$  is given by Eq. (6-12) and

$$\int_{\alpha E}^E P(E \rightarrow E') dE' = \frac{1}{E(1 - \alpha)} \int_{\alpha E}^E dE' = 1.$$

When the scattering is *not* isotropic in the center-of-mass system,  $P(E \rightarrow E')$  is not independent of  $E'$ , since  $\theta$  and  $E'$  are related by Eq. (6-5) and  $\sigma_s(\theta)$  is no longer a constant. If the scattering is forward peaked, that is, neutrons are preferentially scattered through small angles,  $P(E \rightarrow E')$  is larger near  $E' = E$  than near  $E' = \alpha E$ , since neutrons lose comparatively little energy in small angle scattering. On the other hand, if  $\sigma_s(\theta)$  is peaked in the backward direction,  $P(E \rightarrow E')$  is larger near  $E' = \alpha E$ . The function  $P(E \rightarrow E')$  is shown in Fig. 6-2 for these cases and also for isotropic scattering. The area under each of these curves is equal to unity.

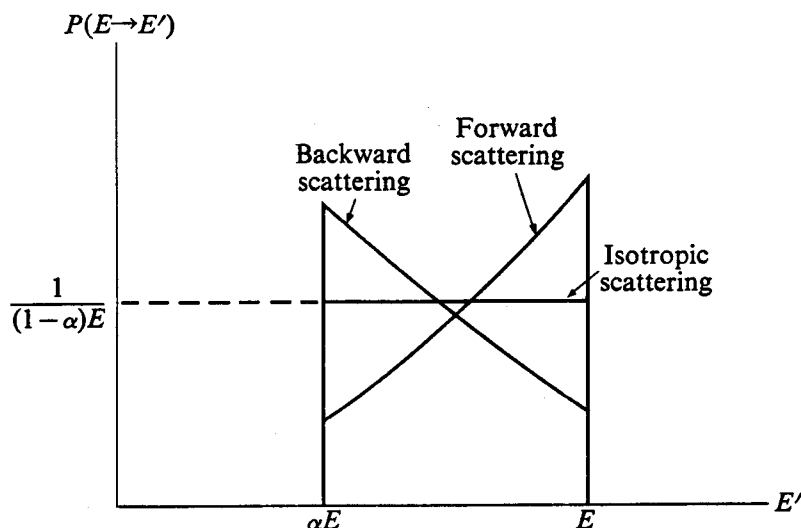


**Fig. 6-2.** Elastic scattering distribution functions  $P(E \rightarrow E')$  for forward scattering, backward scattering, and isotropic scattering, all in the center-of-mass system.

The average energy  $\bar{E}'$  of elastically scattered neutrons can be found by computing the integral

$$\bar{E}' = \int_{\alpha E}^E E' P(E \rightarrow E') dE'. \quad (6-13)$$

For isotropic scattering in the center-of-mass system,  $P(E \rightarrow E')$  is given by Eq. (6-12), and  $\bar{E}'$  is easily found to be  $E(1 + \alpha)/2$ . The average energy of the scattered neutron thus lies midway between  $E$  and  $\alpha E$ . The average energy loss per collision is then  $E - E(1 + \alpha)/2 = E(1 - \alpha)/2$  and depends upon the energy of the neutron before the collision, as one would expect. The average fractional energy loss, however, is independent of the initial energy of the neutron and is simply  $E(1 - \alpha)/2 \div E = (1 - \alpha)/2$ . With hydrogen, for example, since  $\alpha = 0$ , neutrons, on the average, lose half of their energy in each collision regardless of their initial energy.

## 6-2 Collision and Slowing-Down Densities

The energy-dependent flux  $\phi(\mathbf{r}, E)$ , which was defined in Section 5-1, is proportional to the number of neutrons/cm<sup>3</sup> at the point  $\mathbf{r}$  which have an energy between  $E$  and  $E + dE$ . The function  $\phi(\mathbf{r}, E)$  can therefore be used to describe quantitatively the slowing down of neutrons. A knowledge of  $\phi(\mathbf{r}, E)$  at every point in a reactor necessarily specifies to what extent the fission neutrons have been moderated within the system.

For calculational purposes, however, it is somewhat more convenient to describe the slowing down of neutrons in terms of the interaction rate or collision density  $F(\mathbf{r}, E)$ , which was also introduced in Section 5-1. This function, it will be recalled, is defined so that  $F(\mathbf{r}, E) dE$  is equal to the number of neutron-nucleus interactions occurring per cm<sup>3</sup>/sec at the point  $\mathbf{r}$  in the energy interval  $dE$  between  $E$  and  $E + dE$ . In view of this definition, it should be remembered that  $F(\mathbf{r}, E)$  is the number of interactions per cm<sup>3</sup>/sec *per unit energy*.

Another important quantity which is also used to describe the slowing down of neutrons is the *slowing-down density* denoted by  $q(\mathbf{r}, E)$ . This is defined as the number of neutrons/cm<sup>3</sup> at the point  $\mathbf{r}$  whose energy falls below  $E$  per sec. Since neutrons obviously lose energy only at collisions with nuclei (and not in between collisions),  $q(\mathbf{r}, E)$  is equal to the total number of collisions per cm<sup>3</sup>/sec at  $\mathbf{r}$  in which the energies of the colliding neutrons fall below  $E$ . If, for instance, at a certain point there are a total of  $10^{10}$  collisions per cm<sup>3</sup>/sec at energies above 1 MeV, and the energies of the neutrons fall below this energy in one-half of the collisions, the slowing down density at 1 MeV would be  $0.5 \times 10^{10}$  per cm<sup>3</sup>/sec.

## 6-3 Moderation of Neutrons in Hydrogen

In developing a quantitative theory of the slowing down of neutrons, it is easiest to begin with hydrogen. This is because, as shown in Section 6-1, neutrons can lose all their energy in a single collision with hydrogen, whereas they can lose at

most only a fraction of their original energy in collisions with all other nuclei. It will soon be evident that this fact considerably simplifies the analytical problem.

To simplify the problem further, all spatial variation in the slowing down of the neutrons will be ignored temporarily and only the distribution in energy of the neutrons will be considered. For this purpose consider an infinite, homogeneous, hydrogenous medium containing uniformly distributed sources emitting neutrons with the energy  $E_0$  at the constant rate of  $S$  neutrons per  $\text{cm}^3/\text{sec}$ . Following their emission, these neutrons travel about through the medium, and as the result of elastic collisions lose energy in the manner discussed in the preceding sections. However, since the medium is infinite and the neutrons are emitted uniformly throughout, the number of neutrons in any energy interval below  $E_0$  must be independent of position. Consequently, the energy-dependent flux, the collision density, and the slowing-down density will not be functions of position, although they may depend upon energy. As already noted, it will also be assumed that the medium does not absorb neutrons. (In fact, hydrogen does not absorb neutrons to any appreciable extent, except at very low energy.)

The collision density  $F(E)^*$  for hydrogen can be determined by considering the scattering of neutrons into and out of an energy interval  $dE$  at  $E$ , as indicated in Fig. 6-3. Neutrons arrive in  $dE$  as the result of scattering collisions that occur at higher energies. Since a collision with hydrogen can drop the energy of a neutron to any lower value, some of the source neutrons may acquire an energy in  $dE$  as the result of only one collision. By the same token, neutrons that have had one or more collisions but whose energy  $E'$  is still above  $E$  may also fall into  $dE$  with their next collision (cf. Fig. 6-3).

Consider first the source neutrons. In the steady state, if  $S$  of these neutrons are produced per  $\text{cm}^3/\text{sec}$ , exactly this number of neutrons must be scattered per  $\text{cm}^3/\text{sec}$  at this energy. If this were not so, there would be an accumulation of neutrons at  $E_0$ . From Eq. (6-12), since  $\alpha = 0$ , the probability that one of these neutrons will be scattered into  $dE$  is

$$P(E_0 \rightarrow E) dE = dE/E_0.$$

It follows that a total of  $S dE/E_0$  source neutrons are scattered directly into  $dE$  per  $\text{cm}^3/\text{sec}$ .

Turning next to the neutrons having energies between  $E$  and  $E_0$ , there are, by definition,  $F(E') dE'$  scattering collisions per  $\text{cm}^3/\text{sec}$  in the energy interval  $dE'$  at  $E'$ . The probability that one of these neutrons is scattered into  $dE$  is  $dE/E'$ ,

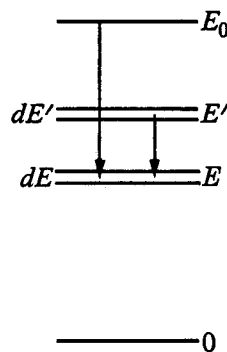


Fig. 6-3. Diagram for analysis of slowing down in hydrogen.

\* The subscript on  $F(E)$  denoting elastic scattering will be omitted in this chapter.

so that  $F(E') dE' dE/E'$  neutrons are scattered per second from  $dE'$  to  $dE$ . The number of neutrons arriving in  $dE$  from all  $dE'$  above  $E$  is therefore

$$\int_E^{E_0} \frac{F(E') dE' dE}{E'}.$$

Since in the steady state the number of neutrons scattered into  $dE$  must be equal to the number scattered out, it follows that

$$F(E) dE = \frac{S dE}{E_0} + \int_E^{E_0} \frac{F(E') dE' dE}{E'}.$$

After cancellation of  $dE$  from both sides, the following integral equation for  $F(E)$  is obtained:

$$F(E) = \frac{S}{E_0} + \int_E^{E_0} \frac{F(E') dE'}{E'}. \quad (6-14)$$

This equation is a special case of the transport equation which was mentioned in the introduction to Chapter 5. In particular, Eq. (6-14) is the space-independent transport equation describing the transport of neutrons in energy in an infinite hydrogen medium.

Equation (6-14) can be solved by differentiating both sides of the equation with respect to  $E$ . This gives

$$\frac{dF(E)}{dE} = -\frac{F(E)}{E}, \quad (6-15)$$

where the minus sign appears because the variable  $E$  occurs in the lower limit of the integral. The general solution of Eq. (6-15) is

$$F(E) = \frac{C}{E}, \quad (6-16)$$

where  $C$  is a constant that must be determined. The value of  $C$  can be found by placing  $E = E_0$  in Eq. (6-14); this gives

$$F(E_0) = \frac{S}{E_0}.$$

Comparing this result with Eq. (6-16), it is evident that  $C = S$ , so that

$$F(E) = \frac{S}{E}. \quad (6-17)$$

The energy-dependent flux  $\phi(E)$  can now be computed using Eq. (6-17). Since in the present case

$$F(E) = \Sigma_s(E)\phi(E), \quad (6-18)$$

it follows that

$$\phi(E) = \frac{S}{E\Sigma_s(E)}. \quad (6-19)$$

While Eq. (6-19) is strictly correct only for an infinite hydrogen medium, it is often used to give rough estimates of the energy-dependent flux in finite hydrogenous systems such as water-moderated reactors. Incidentally, it is interesting to note that  $F(E)$  and  $\phi(E)$  are independent of the energy of the source neutrons.

The slowing-down density in hydrogen can also be found from  $F(E)$  by computing the number of collisions which occur at energies above  $E$ , and multiplying this number by the relative probability that these collisions carry neutrons to energies below  $E$ . Consider first the source neutrons. When these are scattered, their energies lie uniformly between zero and  $E_0$ , so that the probability that a source neutron is scattered to below  $E$  is just  $E/E_0$ . This can be viewed in Fig. 6-3 as the distance from zero to  $E$ , divided by the distance from zero to  $E_0$ . The total number of source neutrons slowing down below  $E$  per  $\text{cm}^3/\text{sec}$  is therefore  $SE/E_0$ . In the same manner, the number of neutrons scattered in  $dE'$  at  $E'$  which slow down below  $E$  is  $F(E') dE' \times E/E'$ , and the total number of these is

$$E \int_E^{E_0} \frac{F(E') dE'}{E'}.$$

With these contributions, the total slowing down density at  $E$  is

$$q(E) = \frac{SE}{E_0} + E \int_E^{E_0} \frac{F(E') dE'}{E'}. \quad (6-20)$$

Comparing this equation with Eq. (6-14) shows that

$$q(E) = EF(E), \quad (6-21)$$

and by using Eq. (6-17) it follows that

$$q(E) = S. \quad (6-22)$$

This result, that the slowing-down density is constant and equal to the source density, is not surprising and could have been anticipated from the beginning. Thus if  $S$  neutrons are produced per  $\text{cm}^3/\text{sec}$  throughout an infinite medium and none are absorbed, exactly  $S$  neutrons necessarily must be slowing down at every energy in a steady-state situation. If this were not the case, there would clearly be an accumulation of neutrons somewhere between  $E = 0$  and  $E = E_0$ .

#### 6-4 Lethargy and $\xi$

According to Eq. (6-17), the collision density in hydrogen increases with decreasing energy. Thus as fast neutrons slow down in hydrogen they undergo, on the average,  $10^6$  times as many collisions per unit energy at 1 eV, for example, as they do at

1 MeV. For this reason, it is desirable to write the collision density in terms of an independent variable other than the energy. This variable, which is denoted by the symbol  $u$ , is called the *lethargy*, and is defined as

$$u = \ln \frac{E_0}{E}, \quad (6-23)$$

where  $E_0$  is an arbitrary energy. It is the usual practice to choose  $E_0$  to be the energy of the most energetic neutrons in whatever system is under consideration so that  $u$  will always be a positive quantity. The lethargy is then zero for neutrons with energy  $E_0$  and increases with decreasing energy. In other words, as their energy decreases, neutrons become more lethargic; hence, the term "lethargy."

The collision density can be expressed in terms of lethargy by noting that the collisions which occur in the lethargy interval  $du$ , namely  $F(u) du$ , are the same collisions that occur in the energy interval  $dE$ , specifically  $F(E) dE$ . That is\*

$$F(u) du = -F(E) dE, \quad (6-24)$$

where the minus sign is necessary since  $u$  increases as  $E$  decreases. From Eq. (6-23) however,

$$du = -\frac{dE}{E}, \quad (6-25)$$

so that

$$F(u) = EF(E). \quad (6-26)$$

By inserting Eq. (6-17), it follows that

$$F(u) = S. \quad (6-27)$$

Thus the collision density per unit lethargy is a constant for hydrogen.

With every collision the energy of a neutron decreases, and its lethargy therefore increases. The change in lethargy  $\Delta u$  as a result of a single collision is given by  $\Delta u = \ln(E_0/E') - \ln(E_0/E) = \ln(E/E')$ , where  $E$  and  $E'$  are the energies before and after the collision, respectively. The *average increase in lethargy per collision* is an important quantity which often appears in calculations of the slowing down of neutrons. This is denoted by the symbol  $\xi$ † and can be calculated from the integral

$$\overline{\Delta u} = \xi = \int_{\alpha E}^E \ln \left( \frac{E}{E'} \right) P(E \rightarrow E') dE', \quad (6-28)$$

where  $P(E \rightarrow E')$  is the energy distribution function of the scattered neutrons

\* See footnote on page 30 regarding this notation.

† In the original literature on neutron moderation, the variable  $\xi$  was used to denote the change in  $u$  at any collision. The average value of  $\xi$  was then denoted by  $\bar{\xi}$ . This older notation has largely been discarded.

(cf. Section 6-1). The range of integration is over all possible final energies, i.e., from  $E' = \alpha E$  to  $E' = E$ .

The integral in Eq. (6-28), in general, cannot be carried out analytically. For isotropic scattering in the center-of-mass system, however, Eq. (6-12) can be used for  $P(E \rightarrow E')$ , and then

$$\xi = \frac{1}{E(1 - \alpha)} \int_{\alpha E}^E \ln\left(\frac{E}{E'}\right) dE'.$$

The integral can be evaluated by making the substitution  $x = E'/E$ ; thus

$$\begin{aligned} \xi &= \frac{1}{1 - \alpha} \int_1^\alpha \ln x \, dx \\ &= 1 + \frac{\alpha}{1 - \alpha} \ln \alpha. \end{aligned} \quad (6-29)$$

In terms of the mass number  $A$ , this can also be written (using Eq. 6-4)

$$\xi = 1 - \frac{(A - 1)^2}{2A} \ln\left(\frac{A + 1}{A - 1}\right). \quad (6-30)$$

Except for small values of  $A$ , the logarithm in Eq. (6-30) can be expanded in a series which is closely approximated by the simple formula

$$\xi = \frac{2}{A + \frac{2}{3}}. \quad (6-31)$$

Values of  $\xi$  for several nuclei are given in Table 6-1.

## 6-5 Moderation of Neutrons for $A > 1$

In Section 6-3 the collision density, energy-dependent flux, and slowing-down density were calculated for an infinite hydrogen medium containing uniformly distributed sources which emit monoenergetic neutrons. When a similar problem is considered for a medium having  $A$  greater than unity, the fact that a neutron cannot lose all its energy in a single encounter, leads to a number of complications which did not appear in the earlier problem. In particular, the collision density  $F(E)$  cannot be written in terms of a single expression that is valid for all energies, as was the case for hydrogen. Several series representations of  $F(E)$  can be obtained, however, one of which will now be considered in detail. A second, and in some ways more practical, method of obtaining a series for  $F(E)$  is illustrated in Prob. 6-12. Throughout the following discussion it will be assumed that the neutrons are scattered isotropically in the center-of-mass system.

To generate the series for  $F(E)$ , neutrons in the energy interval  $dE$  at  $E$  are classified according to the number of times they have collided in reaching  $dE$ . All these neutrons, of course, eventually have their *next* collision in the interval  $dE$ . Neutrons which reach  $dE$  as the result of one collision have their second collision

in  $dE$ ; neutrons reaching  $dE$  following two collisions have their third collision in  $dE$ ; etc. Now let  $F_1(E)$  be the collision density at  $E$  for neutrons which have previously had one collision; similarly, let  $F_2(E)$  be the collision density for neutrons which have previously had two collisions; and so on. Clearly the total collision density at  $E$  is given by

$$F(E) = F_1(E) + F_2(E) + F_3(E) + \dots \quad (6-32)$$

The function  $F(E)$  will now be found by computing separately each of the individual collision densities.

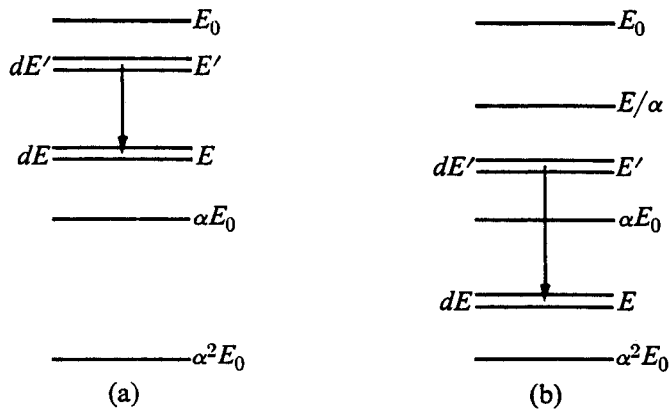


**Fig. 6-4.** Diagrams for calculating  $F_2(E)$  when (a)  $\alpha E_0 < E < E_0$  and (b)  $\alpha^2 E_0 < E < \alpha E_0$ .

Since all neutrons have their first collision as source neutrons, only these neutrons must be taken into consideration in computing  $F_1(E)$ . From Eq. (6-12) the probability that a source neutron is scattered into  $dE$  is  $dE/(1 - \alpha)E_0$ , provided that  $E$  is greater than  $\alpha E_0$ , and is zero for  $E$  less than  $\alpha E_0$ . The number of neutrons reaching  $dE$  as the result of only one collision is therefore  $S dE/(1 - \alpha)E_0$ , if  $E$  lies in the interval  $\alpha E_0 < E < E_0$ . It follows that  $F_1(E)$  is given by

$$F_1(E) = \begin{cases} \frac{S}{(1 - \alpha)E_0}, & \alpha E_0 < E < E_0, \\ 0, & E < \alpha E_0. \end{cases} \quad (6-33)$$

By definition,  $F_1(E') dE'$  neutrons have their second collision in  $dE'$ , and since the probability that such a collision carries a neutron into  $dE$  is  $dE/(1 - \alpha)E'$ , provided that  $\alpha E' < E < E'$ , a total of  $F_1(E') dE' \times dE/(1 - \alpha)E'$  neutrons arrive in  $dE$  per second from second collisions in  $dE'$ . If  $E$  lies between  $\alpha E_0$  and  $E_0$ , as shown in Fig. 6-4(a), a collision at any energy between  $E$  and  $E_0$  may scatter a neutron into  $dE$ . Hence  $F_2(E)$  is given by the integral

$$F_2(E) = \int_E^{E_0} \frac{F_1(E') dE'}{(1 - \alpha)E'}, \quad \alpha E_0 < E < E_0. \quad (6-34)$$

Inserting  $F_1(E)$  from Eq. (6-33) yields

$$F_2(E) = \frac{S}{(1 - \alpha)^2 E_0} \ln\left(\frac{E_0}{E}\right), \quad \alpha E_0 < E < E_0.$$

On the other hand, if  $E$  lies between  $\alpha^2 E_0$  and  $\alpha E_0$ , as shown in Fig. 6-4(b), neutrons can reach  $dE$  only as the result of second collisions at energies between  $E$  and  $E/\alpha$ . Then, since  $F_1(E)$  is zero for  $E < \alpha E_0$ ,  $F_2(E)$  is given by

$$F_2(E) = \int_{\alpha E_0}^{E/\alpha} \frac{F_1(E') dE'}{(1 - \alpha) E'}.$$

This integral has the value

$$F_2(E) = \frac{S}{(1 - \alpha)^2 E_0} \ln\left(\frac{E}{\alpha^2 E_0}\right), \quad \alpha^2 E_0 < E < \alpha E_0.$$

Finally, if  $E$  is less than  $\alpha^2 E_0$ , then  $F_2(E) = 0$ , since neutrons simply cannot fall into this region as the result of only two collisions. In summary,

$$F_2(E) = \begin{cases} \frac{S}{(1 - \alpha)^2 E_0} \ln\left(\frac{E_0}{E}\right), & \alpha E_0 < E < E_0, \\ \frac{S}{(1 - \alpha)^2 E_0} \ln\left(\frac{E}{\alpha^2 E_0}\right), & \alpha^2 E_0 < E < \alpha E_0, \\ 0, & E < \alpha^2 E_0. \end{cases} \quad (6-35)$$

In a similar fashion, the other terms in the series given in Eq. (6-32) for  $F(E)$  can easily be obtained. The functions  $F_1(E)$ ,  $F_2(E)$ , and  $F_3(E)$  are plotted in Fig. 6-5 for a unit source density of 1-MeV neutrons in a beryllium medium. It

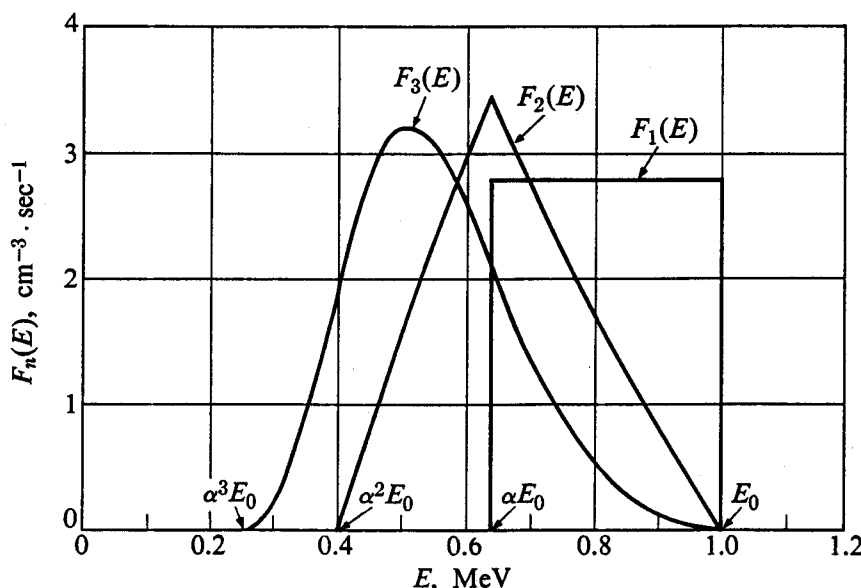


Fig. 6-5. The first, second, and third collision densities for unit source of 1-MeV neutrons in beryllium.

will be observed that  $F_1(E)$  is discontinuous at both  $E_0$  ( $= 1 \text{ MeV}$ ) and  $\alpha E_0$ . On the other hand,  $F_2(E)$  is continuous everywhere although its first derivative  $F'_2(E)$  is discontinuous at  $E_0$ ,  $\alpha E_0$ , and  $\alpha^2 E_0$ , as can readily be seen from the figure or from Eq. (6-35). Lastly,  $F_3(E)$  is continuous everywhere;  $F'_3(E)$  is also continuous everywhere except at  $\alpha^3 E_0$ , but  $F''_3(E)$  is discontinuous at  $E_0$ ,  $\alpha E_0$ ,  $\alpha^2 E_0$ , and  $\alpha^3 E_0$ . Therefore it may be concluded that, in general, the  $n$ th collision density  $F_n(E)$  becomes an increasingly smooth function of  $E$  with increasing values of  $n$ . It can be shown, in fact, that in the limit of large  $n$ ,  $F_n(E)$  becomes Gaussian (cf. Section 6-8).

The discontinuities in  $F_1$  and in the derivatives of  $F_2$ ,  $F_3$ , etc., lead, of course, to similar discontinuities in the total collision density and its derivatives. However, these appear only near the source energy, and as will be shown later in this section, they do not persist much below approximately  $\alpha^3 E_0$ . At energies below  $\alpha^3 E_0$ ,  $F(E)$  becomes a smooth function of energy, due to the fact the neutrons at these energies have had several collisions and the functions  $F_n(E)$  are all well-behaved.

At energies well below the source energy, i.e.,  $E \lesssim \alpha^3 E_0$ , which is also known as the *asymptotic energy region*, it is possible to obtain a simple expression for the collision density from the integral equation for  $F(E)$ . Since source neutrons do not scatter directly into this energy region, it is easy to see by using Fig. 6-6 that  $F(E)$  is determined by the equation

$$F(E) = \int_E^{E/\alpha} \frac{F(E') dE'}{(1 - \alpha)E'}. \quad (6-36)$$

The upper limit on this integral is  $E/\alpha$  because this is the highest energy from which a neutron can be scattered into  $dE$  at  $E$ .

When the function

$$F(E) = \frac{C}{E} \quad (6-37)$$

is substituted into Eq. (6-36), it is found to satisfy the equation.\* The constant  $C$  cannot be determined from Eq. (6-36), however, since it appears in every term and cancels out of the equation.

To find  $C$  it is necessary to set up an expression for the slowing-down density in the asymptotic region. Neutrons scattered in the interval  $dE'$  at  $E'$  (see Fig. 6-7) can appear with energies anywhere from  $E'$  to  $\alpha E'$ . Since the probability function  $P(E \rightarrow E')$  is a constant for isotropic scattering in the center-of-mass system, the relative probability that a collision carries a neutron from  $E'$  to below  $E$  is simply the ratio of the size of the interval  $E - \alpha E'$  to the interval  $E' - \alpha E'$ . Thus, since there are  $F(E') dE'$  collisions per second in the interval  $dE'$ ,  $F(E') dE' \times (E - \alpha E')/(E' - \alpha E')$  neutrons slow down past  $E$  per  $\text{cm}^3/\text{sec}$  from  $dE'$ . The

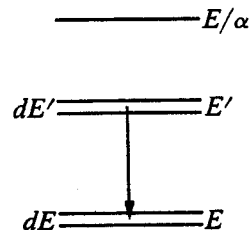


Fig. 6-6. Diagram for calculating the collision density in the asymptotic energy region.

\* It may be mentioned that it is not particularly easy to show that Eq. (6-37) is the *only* solution valid at asymptotic energies.

total number slowing down below  $E$ , that is, the slowing-down density at  $E$ , is therefore

$$q = \int_E^{E/\alpha} F(E') dE' \frac{E - \alpha E'}{(1 - \alpha) E'}. \quad (6-38)$$

Substituting Eq. (6-37) for  $F(E)$  and performing the integration yields

$$q = C \left( 1 + \frac{\alpha}{1 - \alpha} \ln \alpha \right).$$

The term in the parentheses is just  $\xi$  (cf. Eq. 6-29); therefore

$$q = C\xi. \quad (6-39)$$

In the absence of absorption, and since no neutrons leak from an infinite system, the slowing-down density must be equal to the source density, i.e.,  $q = S$ . Thus the constant  $C$  is given by

$$C = \frac{S}{\xi}.$$

From Eq. (6-37) the collision density is therefore

$$F(E) = \frac{S}{\xi E}, \quad (6-40)$$

and the energy-dependent flux is

$$\phi(E) = \frac{S}{\xi E \Sigma_s(E)}. \quad (6-41)$$

This important result shows that in the asymptotic region, that is,  $E \lesssim \alpha^3 E_0$ , aside from a multiplicative constant,  $F(E)$  and  $\phi(E)$  are the same for moderators with  $A > 1$  as for hydrogen (cf. Eqs. 6-17 and 6-19). Furthermore, as in hydrogen,  $F(E)$  and  $\phi(E)$  are independent of the energy of the source neutrons. Rewriting  $F(E)$  in terms of the lethargy variable gives

$$F(u) = \frac{S}{\xi}, \quad (6-42)$$

so that the collision density expressed in lethargy units approaches a constant value for large  $u$ .

The complete collision density per unit lethargy, multiplied by a scale factor  $(1 - \alpha)$ , is shown in Fig. 6-8 for a number of moderators and a unit source density of energy  $E_0$ . [It is more convenient to plot  $F(u)$  than  $F(E)$ , since  $F(u)$  approaches a constant with increasing  $u$  whereas  $F(E)$  varies as  $1/E$ .] The independent variable,  $u/\ln(1/\alpha)$ , on the upper scale of the abscissa is chosen so that unit distances along the abscissa correspond to different collision intervals as indicated on the lower scale. For  $A = 1$  (hydrogen),  $F(u)$  is equal to unity for all values of  $u$  and coincides

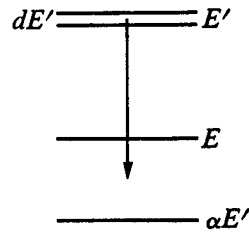
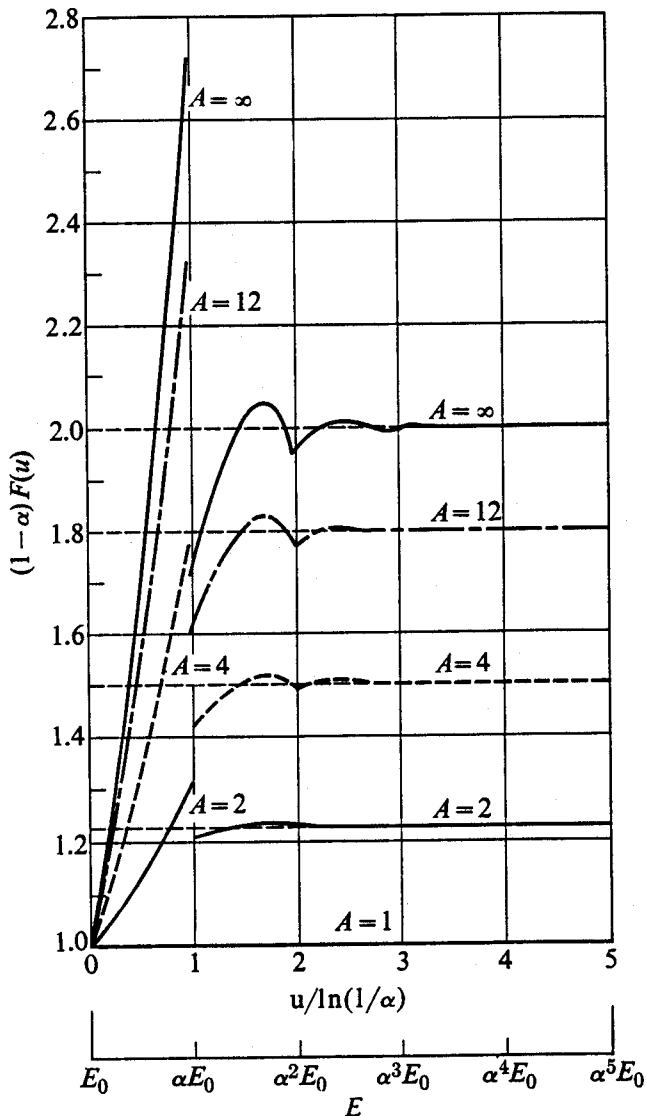


Fig. 6-7. Diagram for computing the slowing-down density in the asymptotic energy region.



**Fig. 6-8.** The collision density per unit lethargy for various moderators. (After A. M. Weinberg and E. P. Wigner, *The Physical Theory of Neutron Chain Reactors*. Chicago: University of Chicago Press, 1958.)

with the abscissa as indicated in the figure. With all other moderators, it will be observed that  $F(u)$  is discontinuous at  $E = \alpha E_0$ . This discontinuity arises as the result of the discontinuity in  $F_1(E)$  at this energy (cf. Fig. 6-5). Similarly, the first derivative of  $F(u)$  is discontinuous at  $E = \alpha^2 E_0$  due to the discontinuity in  $F'_2(E)$ . The other discontinuities cannot be seen as easily in the figure.

It should also be noted in Fig. 6-8 that, as mentioned previously, the *transient region* in  $F(u)$ , that is, the wavelike behavior of  $F(u)$ , dies out below approximately  $E = \alpha^3 E_0$ . Since  $\alpha$  increases with  $A$  but is always less than unity, the size of this region therefore increases with decreasing  $A$ . For example, if the source energy is 1 MeV, the end of the transient region occurs at about 0.37 MeV for carbon, whereas it persists down to about 1.4 keV for deuterium. At the same time, how-

ever, it will be observed that the transients are much more pronounced for the heavier nuclei. The magnitude of the discontinuities in  $F$  and its derivatives is considered in the problems at the end of this chapter.

## 6-6 Nonmonoenergetic Sources

Up to this point it has been assumed that the neutron sources are monoenergetic. Since this situation is not usually found in practical problems, it is necessary to consider the flux distributions arising from sources emitting neutrons with a distribution of energies. Imagine an infinite medium throughout which neutrons are emitted with the energy spectrum  $S(E')$ , that is,  $S(E') dE'$  neutrons are emitted per  $\text{cm}^3/\text{sec}$  having energies between  $E'$  and  $E' + dE'$ .

With hydrogen the problem is quite simple since, as shown in Section 6-3, the energy-dependent flux is independent of the energy of the source. The flux  $d\phi(E)$  from neutrons emitted between  $E'$  and  $E' + dE'$  is therefore

$$d\phi(E) = \frac{S(E') dE'}{E\Sigma_{sH}(E)}, \quad (6-43)$$

provided that  $E < E'$ . For  $E > E'$ ,  $d\phi(E) = 0$ . The total flux arising from sources with energies above  $E$  is thus

$$\phi(E) = \frac{1}{E\Sigma_{sH}(E)} \int_E^\infty S(E') dE'. \quad (6-44)$$

The energy distributions of many sources fall effectively to zero at some lower energy, that is,  $S(E') = 0$  for  $E' < E_s$ . For example, less than 1% of all fission neutrons are emitted at energies below 50 keV. In this case for energies below  $E_s$ ,  $\phi(E)$  for hydrogen is given by

$$\phi(E) = \frac{1}{E\Sigma_{sH}(E)} \int_{E_s}^\infty S(E') dE' \quad (6-45)$$

$$= \frac{S}{E\Sigma_{sH}(E)}, \quad (6-46)$$

where  $S$  is the total source density.

For moderators other than hydrogen, the evaluation of  $\phi(E)$  is complicated by the fact that the flux from source neutrons of energy  $E'$  depends upon both  $E$  and  $E'$ . Thus if  $d\phi(E, E')$  is the flux at  $E$  due to sources at  $E'$ ,  $\phi(E)$  must be found by numerically evaluating the integral:

$$\phi(E) = \int_E^\infty d\phi(E, E'). \quad (6-47)$$

However, at energies much below the low-energy cutoff of the source distribution, that is,  $E \lesssim \alpha^3 E_s$ , the flux  $d\phi(E, E')$  takes on its asymptotic value and, as with

hydrogen, depends on the magnitude but not the energy of the source. From Eq. (6-41) the flux from neutrons emitted between  $E'$  and  $E' + dE'$  is then

$$d\phi(E) = \frac{S(E') dE'}{\xi E \Sigma_s(E)}, \quad E \lesssim \alpha^3 E', \quad (6-48)$$

and  $\phi(E)$  becomes

$$\phi(E) = \frac{1}{\xi E \Sigma_s(E)} \int_{E_s}^{\infty} S(E') dE' \quad (6-49)$$

$$= \frac{S}{\xi E \Sigma_s(E)}, \quad E \lesssim \alpha^3 E_s, \quad (6-50)$$

where again  $S$  is the total source density.

Equations (6-46) and (6-50) show that at energies sufficiently below the low-energy cutoff of the source distribution, the flux is determined by the total number of source neutrons and is independent of their energy distribution. This important result considerably simplifies many reactor calculations, particularly in connection with the design of thermal reactors. For these reactors, as will be shown later in this book, it is frequently necessary to know  $\phi(E)$  only at energies below the low-energy end of the fission spectrum. In this case, it is possible to lump together all fission neutrons and assume that they are emitted with a single energy.

## 6-7 Slowing Down in Mixtures of Nuclides

It is often necessary to make computations of the slowing down of neutrons in systems containing a mixture of two or more nuclides, and the preceding discussion must be generalized to cover situations of this kind. For this purpose, let  $F^{(i)}(E)$  be the collision density of neutrons elastically scattered by nuclei of the  $i$ th variety. Then if  $\Sigma_s^{(i)}(E)$  is the macroscopic scattering cross section of these nuclei, evidently

$$\begin{aligned} F^{(i)}(E) &= \Sigma_s^{(i)}(E)\phi(E) \\ &= \frac{\Sigma_s^{(i)}(E)}{\Sigma_s(E)} F(E), \end{aligned} \quad (6-51)$$

where  $\Sigma_s(E)$  is the total macroscopic scattering cross section and  $F(E)$  is the total collision density.

Consider now the calculation of  $F(E)$  in the asymptotic region. In the energy interval  $dE'$  at  $E'$  there are  $F^{(i)}(E') dE'$  collisions with nuclei of the  $i$ th type, and as a result,  $F^{(i)}(E') dE' \times dE / (1 - \alpha_i) E'$  neutrons are scattered into  $dE$  per second, where  $\alpha_i$  is the slowing-down constant of the  $i$ th nuclide. The total collision density at  $E$  is therefore

$$F(E) = \sum_i \int_E^{E/\alpha_i} \frac{F^{(i)}(E') dE'}{(1 - \alpha_i) E'}, \quad (6-52)$$

where the summation extends over all nuclear species in the system.

It is easy to see by direct substitution that the functions

$$F^{(i)}(E) = \frac{C_i}{E}, \quad (6-53)$$

where  $C_i$  are constants, satisfy Eq. (6-52). To determine  $C_i$  it is necessary to set up an expression for the slowing-down density in the asymptotic region, as was done in Section 6-5. If the reasoning that led to Eq. (6-36) is used,  $q$  is found to be given by

$$q = \sum_i \int_E^{E/\alpha_i} F^{(i)}(E') \left( \frac{E - \alpha_i E'}{E' - \alpha_i E'} \right) dE'. \quad (6-54)$$

Next, by inserting Eq. (6-53) and noting that in the absence of absorption  $q$  must be equal to the source density, it is found that

$$q = S = \sum_i C_i \left( 1 + \frac{\alpha_i}{1 - \alpha_i} \ln \alpha_i \right). \quad (6-55)$$

The quantity in parentheses is just  $\xi_i$  (cf. Eq. 6-29), the average lethargy change per collision for the  $i$ th nuclide, so that

$$S = \sum_i C_i \xi_i. \quad (6-56)$$

From Eq. (6-53), however,  $C_i = EF^{(i)}(E)$ , so Eq. (6-56) can be written as

$$S = E \sum_i \xi_i F^{(i)}(E) = EF(E) \sum_i \frac{\xi_i \Sigma_s^{(i)}(E)}{\Sigma_s(E)}.$$

Finally, defining the quantity  $\bar{\xi}(E)$  as

$$\bar{\xi}(E) = \frac{1}{\Sigma_s(E)} \sum_i \xi_i \Sigma_s^{(i)}(E), \quad (6-57)$$

the collision density becomes

$$F(E) = \frac{S}{\bar{\xi}(E)E} \quad (6-58)$$

and the energy-dependent flux is

$$\phi(E) = \frac{S}{\bar{\xi}(E)E\Sigma_s(E)}. \quad (6-59)$$

Equations (6-58) and (6-59) are generalizations of Eqs. (6-40) and (6-41) for mixtures of nuclides.

It will be recalled that the scattering cross sections of most light nuclei are constant except at high energy. If a medium consists of light nuclei,  $\bar{\xi}(E)$  is then also constant and  $F(E)$  has the familiar  $1/E$  dependence on energy. The situation is more complicated when heavy nuclei are present, as they always are in reactors.

Their scattering cross sections are usually complex functions of energy, even at low energy, and  $\bar{\xi}(E)$  may be expected to be energy dependent. As a practical matter, however, the values of  $\xi$  for heavy nuclei are very small (cf. Table 6-1). Thus  $\bar{\xi}(E)$  is not appreciably affected by the presence of these nuclei, and  $\bar{\xi}(E)$  is again more or less constant except at high energies.

### 6-8 Multiscattered Neutrons

Consider a neutron slowing down in an infinite scattering medium consisting of a single nuclear species such as graphite. If the initial lethargy of the neutron is taken to be zero, its lethargy  $u_n$  after  $n$  collisions will be

$$u_n = \sum_{i=1}^n \Delta u_i, \quad (6-60)$$

where  $\Delta u_i$  is the increase in lethargy of the neutron at its  $i$ th collision. The average value of  $u_n$  after  $n$  collisions is therefore

$$\bar{u}_n = \sum_{i=1}^n \overline{\Delta u_i}, \quad (6-61)$$

where  $\overline{\Delta u_i}$  is the average increase in lethargy at the  $i$ th collision. If the scattering is isotropic in the center-of-mass system,  $\overline{\Delta u_i} = \xi$  for all collisions,\* and it follows that

$$\bar{u}_n = n\xi. \quad (6-62)$$

Equation (6-62) can be used in an obvious way to compute the number of collisions required to increase the average lethargy to the value  $\bar{u}_n$ , that is,

$$n = \frac{\bar{u}_n}{\xi}. \quad (6-63)$$

If the initial energy of the neutron is  $E_0$  and the energy corresponding to  $\bar{u}_n$  is  $E$ , then  $n$  is given by

$$n = \frac{1}{\xi} \ln \frac{E_0}{E}. \quad (6-64)$$

This formula must be interpreted with some care. Thus  $n$  is *not* the average number of collisions necessary to reduce the energy from  $E_0$  to  $E$ , nor is it the number of collisions necessary to reduce the average energy to  $E$ . It is the number of collisions required to increase the average lethargy to the value  $\bar{u}_n$  whose corresponding energy is  $E$ . All these numbers represent somewhat different concepts and they are slightly different numerically. Values of  $n$  computed from Eq. (6-64) with  $E_0 = 2$  MeV and  $E = 1$  eV are given in Table 6-2.

---

\* Or  $\bar{\xi}$  if the system contains a mixture of nuclides.

In addition to the average value of the lethargy after  $n$  collisions, it is also important to determine the lethargy distribution. This distribution can be described by the function  $P_n(u)$  which is defined in such a way that  $P_n(u) du$  is the probability that the lethargy of a neutron lies in the interval  $du$  at  $u$  after the neutron has undergone exactly  $n$  collisions. The function  $P_n(u)$  may be recognized as the  $n$ th collision density  $F_n(u)$  defined in Section 6-5, per unit source neutron. However, whereas it was the purpose of Section 6-5 to find the total collision density  $F(u)$ , the aim of the present section is to consider the lethargy distribution after neutrons have undergone several collisions. For this purpose it is more convenient to use the probability function  $P_n(u)$  rather than the collision density.

Table 6-2

**Number of Collisions,  $n$ , Necessary to Increase the Average Lethargy of 2-MeV Neutrons to a Value whose Corresponding Energy is 1 eV, Assuming Isotropic Scattering in the Center-of-Mass System**

Medium	H	H <sub>2</sub> O	D	D <sub>2</sub> O	Be	C	O	Fe	U
$n$	14.5	15.8	20.0	28.5	69.4	91.3	121	407	1730

The problem of finding  $P_n(u)$  for large  $n$  turns out to be a standard problem in statistics. It is completely analogous, for instance, to the problem of determining the distribution of the total distance traveled by a golf ball down a fairway after a given number of whacks at the ball. Accordingly, it can be shown by the *central limit theorem\** that  $P_n(u)$  rapidly approaches a Gaussian function

$$P_n(u) \approx \exp \left[ -\frac{(u - \bar{u}_n)^2}{2\sigma^2} \right], \quad (6-65)$$

where  $\bar{u}_n$  is given by Eq. (6-62) and  $\sigma$  is the standard deviation. For isotropic scattering in the center-of-mass system, it is easy to show (cf. Prob. 6-15) that  $\sigma^2$  is given by the formula

$$\sigma^2 = n \left[ 1 - \frac{(1 - \xi)^2}{\alpha} \right], \quad (6-66)$$

where  $\alpha$  is the collision parameter defined by Eq. (6-4).

To see the significance of these results it should first be recalled that the standard deviation is a measure of the width or spread of the distribution, that is, the extent to which the value of  $u$  after  $n$  collisions may be expected to deviate from the value  $\bar{u}_n = n\xi$ . In particular, there is about a 70% chance that  $u$  will lie within the range  $n\xi \pm \sigma$ . The *fractional deviation* in the expected value of  $u$  is simply  $\sigma/n\xi$ , which

\* See any book on statistics.

in view of Eq. (6-66) is

$$\text{fractional deviation in } u = \frac{\sigma}{n\xi} = \frac{1}{\xi\sqrt{n}} \left[ 1 - \frac{(1 - \xi)^2}{\alpha} \right]^{1/2}. \quad (6-67)$$

This result shows that the fractional deviation from the mean decreases with increasing  $n$  as  $1/\sqrt{n}$ . Furthermore, it is easily shown that the quantity  $[1 - (1 - \xi)^2/\alpha]^{1/2}/\xi$  in Eq. (6-67) decreases with increasing  $A$ . Thus for a given change in lethargy, the fractional deviation in the lethargy is smaller for larger values of  $A$  for two reasons. First, the number of collisions required for the lethargy change increases with  $A$ , and second, the aforementioned factor multiplying  $1/\sqrt{n}$  in Eq. (6-67) also decreases with increasing  $A$ .

As an application of these results consider the slowing down of a 1-MeV neutron in an infinite graphite moderator. In this case,  $\xi = 0.158$ ,  $\alpha = 0.716$ , and  $\sigma^2 = 0.00925n$ . After 10 collisions,  $\bar{u}_n = 1.58$  and  $\sigma = 0.304$ . The fractional deviation in  $\bar{u}_n$  is therefore  $0.304/1.58 = 19\%$ . In energy units,  $\bar{u}_n$  corresponds to 206 keV and the lethargy interval defined by  $\bar{u}_n \pm \sigma$  is equivalent to an energy spread of approximately 150 keV. After 100 collisions,  $\bar{u}_n = 15.8$ , which corresponds to an energy of 0.14 eV,  $\sigma = 0.962$ , and the fractional deviation in  $u$  is  $0.962/15.8 = 6.1\%$ . However, the spread in energy corresponding to the lethargy interval  $\bar{u}_n \pm \sigma$  is now only 0.31 eV. Thus it is seen that *as the number of collisions increases, the lethargies (and energies) of the neutrons cluster closer to their average value.* Although this conclusion is based on a moderator composed of a single nuclear species, it can easily be shown to be valid also for systems containing a mixture of nuclides.

### 6-9 Space-Dependent Slowing Down—Fermi Age Theory

In the preceding sections the neutron sources were assumed to be uniformly distributed throughout all space. This assumption considerably simplified the calculations of neutron moderation, since spatial variables were not involved. Reactors, however, are finite in size, and fission neutrons are rarely produced uniformly in them. The earlier discussion must therefore be enlarged to include spatially dependent sources and finite media, and in this case it is necessary to consider how the neutrons move about while they are slowing down. Unfortunately, problems of this more general nature cannot be handled analytically except in special cases, and then only by methods which are beyond the scope of this book. Frequently, however, satisfactory results can be obtained on the basis of the following simple model which is due to Fermi. In the present discussion it will be assumed for simplicity that the moderator consists of a single nuclide and that the scattering is isotropic in the center-of-mass system. In this case,  $\xi$  is independent of energy. The results can easily be modified later to include situations in which  $\xi$  may be a function of energy. It will also be assumed for the moment that the neutron sources are monoenergetic.

It was shown in the preceding section that the average lethargy of neutrons after  $n$  collisions is equal to  $n\xi$ ; therefore a neutron may be said to gain  $\xi$  units of

lethargy *on the average* at each collision. In the Fermi model it is assumed that all neutrons gain *exactly*  $\xi$  in lethargy at every collision, that is, all neutrons are treated, so to speak, as average neutrons. However, if the lethargy did, in fact, change only in units of  $\xi$ , the neutrons in the system would have only the lethargies  $u = 0, \xi, 2\xi, \text{etc.}$ , as shown in Fig. 6-9, and the neutron flux would be defined only at these lethargies. Since it is desirable to deal with continuous rather than discrete variables, it is postulated that the lethargy is a continuous variable which takes on the required value  $n\xi$  after  $n$  collisions, as indicated in Fig. 6-9. Thus the collision number  $n$  can also be viewed as a continuous variable, and for this reason the Fermi model is often referred to as the "continuous slowing down model." In view of the results of the preceding section, this model may be expected to be most appropriate for the heavier moderators, since for a given change in lethargy, the fluctuations from the average behavior decrease with increasing mass number. In the Fermi model it is also assumed that diffusion theory is valid at all energies (or lethargies). There is one additional assumption in this model which will be mentioned below.

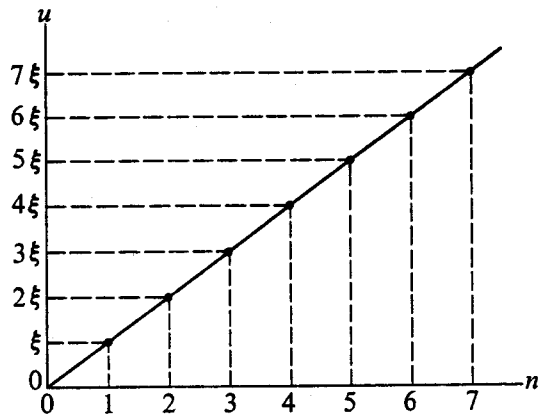


Fig. 6-9. Lethargy as a continuous function of the collision density.

Consider now the arrival and departure of neutrons with lethargies between  $u$  and  $u + du$  in the volume element  $dV$  at  $\mathbf{r}$ . Neutrons in this lethargy interval flow into and out of  $dV$  as the result of collisions in and around  $dV$ . If  $\mathbf{J}(\mathbf{r}, u)$  is the current density per unit lethargy at  $\mathbf{r}$ , then (cf. Section 5-3)  $\text{div } \mathbf{J}(\mathbf{r}, u) du dV$  is equal to the net rate at which neutrons in  $du$  flow out of  $dV$ .

Neutrons are also produced in or lost from the lethargy interval  $du$  in  $dV$  as the result of collisions in  $dV$  in which their lethargy either falls into or is knocked out of  $du$ . The net rate at which neutrons are lost can be found by noting that since, by definition,  $q(\mathbf{r}, u) dV$  neutrons slow down per second to lethargies above  $u$  in  $dV$  and  $q(\mathbf{r}, u + du) dV$  slow down per second above  $u + du$ , it follows that

$$[q(\mathbf{r}, u + du) - q(\mathbf{r}, u)] dV = \frac{\partial q(\mathbf{r}, u)}{\partial u} du dV$$

neutrons are knocked out of (slowed down from)  $du$  in  $dV$  per second.

In the steady state and in the absence of sources at the lethargy  $u$  or absorption, the number of neutrons in  $du$  and in  $dV$  must be constant, so that from the equation of continuity (Eq. 5-26)

$$\operatorname{div} \mathbf{J}(\mathbf{r}, u) + \frac{\partial q(\mathbf{r}, u)}{\partial u} = 0. \quad (6-68)$$

This equation is exact, but it is not very useful as it stands. To obtain a more useful equation,  $\mathbf{J}$  must be expressed in terms of  $q$ . From Fick's law,  $\mathbf{J}(\mathbf{r}, u)$  can be written as

$$\mathbf{J}(\mathbf{r}, u) = -D(u) \operatorname{grad} \phi(\mathbf{r}, u), \quad (6-69)$$

where  $\phi(\mathbf{r}, u)$  is the lethargy-dependent flux, and explicit note has been taken of the fact that the diffusion coefficient may be a function of lethargy.

A relationship between  $q$  and  $\phi$  can be found by using the assumption that neutrons gain  $\xi$  in lethargy at every collision. In this case, all collisions in the lethargy interval from  $u - \xi$  to  $u$  contribute to the slowing-down density at  $u$ , and

$$q(\mathbf{r}, u) = \int_{u-\xi}^u F(\mathbf{r}, u') du'. \quad (6-70)$$

Now, provided that the collision density  $F(\mathbf{r}, u)$  is reasonably constant over a lethargy interval equal to  $\xi$  (this question is considered in Problem 6-19), Eq. (6-70) gives

$$q(\mathbf{r}, u) = \xi F(\mathbf{r}, u) = \xi \Sigma_s(u) \phi(\mathbf{r}, u). \quad (6-71)$$

When Eq. (6-71) is solved for  $\phi(\mathbf{r}, u)$  and inserted into Eq. (6-69), and the resulting expression for  $\mathbf{J}(\mathbf{r}, u)$  is substituted into Eq. (6-68), the result is

$$\frac{D(u)}{\xi \Sigma_s(u)} \nabla^2 q(\mathbf{r}, u) = \frac{\partial q(\mathbf{r}, u)}{\partial u}. \quad (6-72)$$

This equation can be written in a more convenient form by introducing a new variable  $\tau(u)$  defined by the integral

$$\tau(u) = \int_0^u \frac{D(u')}{\xi \Sigma_s(u')} du. \quad (6-73)$$

The parameter  $\xi$  is written inside the integral to call attention to the fact that if the moderator consists of a mixture of nuclides,  $\xi$  is to be replaced by  $\bar{\xi}$  (cf. Section 6-7), which may be a function of lethargy. This is the only adjustment that must be made in order to apply age theory to mixtures. From Eq. (6-73),

$$\frac{\partial}{\partial u} = \frac{d\tau}{du} \frac{\partial}{\partial \tau} = \frac{D(u)}{\xi \Sigma_s(u)} \frac{\partial}{\partial \tau},$$

and Eq. (6-72) becomes

$$\nabla^2 q(\mathbf{r}, \tau) = \frac{\partial q(\mathbf{r}, \tau)}{\partial \tau}. \quad (6-74)$$

Equation (6-74) is known as the *Fermi age equation*, and the quantity  $\tau$  defined by Eq. (6-73) is called the *Fermi age*.

Despite its name, it must be emphasized that age does not have units of time; as can readily be seen from Eq. (6-73)  $\tau$  actually has units of square centimeters. Nevertheless,  $\tau$  is a monotonically increasing function of the time during which a neutron has been slowing down. This can be shown by noting that when a neutron moves the distance  $dx$  it undergoes, on the average,  $\Sigma_s dx$  collisions and its lethargy increases the amount

$$du = \xi \Sigma_s dx. \quad (6-75)$$

Substituting  $du$  into Eq. (6-73) gives

$$\begin{aligned} \tau(u) &= \int_0^u D(u) dx \\ &= \bar{D}l(u), \end{aligned}$$

where  $\bar{D}$  is an average value of  $D$  between 0 and  $u$  and where  $l(u) = \int_0^u dx$  is the total distance a neutron moves from the time it is emitted with zero lethargy until it attains the lethargy  $u$ . Since  $l$  obviously increases monotonically with time, it follows that the age does also.

According to the definition of  $\tau$  given by Eq. (6-73), it should be noted that neutron ages are additive. For instance, if  $\tau_1$  is the age of neutrons from  $u = 0$  to  $u = u_1$ , and  $\tau_{12}$  is the age from  $u_1$  to  $u_2$ , then the age from  $u = 0$  to  $u = u_2$  is simply  $\tau_2 = \tau_1 + \tau_{12}$ .

The preceding derivation was carried out in terms of the lethargy variable, and  $\tau$  was therefore expressed as a function of  $u$ . It is possible, however, to write  $\tau$  as a function of energy by a simple change of variables. Thus the age of neutrons from the source energy  $E_0$ , which corresponds to zero lethargy, to the energy  $E$ , which is written either as  $\tau(E)$  or  $\tau(E_0 \rightarrow E)$ , can be found by substituting  $du = -dE/E$  from Eq. (6-25) into Eq. (6-73). The result is

$$\tau(E) = \tau(E_0 \rightarrow E) = \int_E^{E_0} \frac{D(E) dE}{\xi \Sigma_s(E) E}. \quad (6-76)$$

## 6-10 Boundary Conditions for the Age Equation

The age equation is identical in form with the time-dependent diffusion equation with no absorption (cf. Eq. 5-44) and to the familiar time-dependent heat flow equation. The boundary conditions for all these equations are also essentially the same.

In the derivation of the age equation, the source neutrons were assumed to be emitted monoenergetically at zero lethargy, that is, at  $\tau = 0$ . According to the continuous slowing-down model, however, the neutrons begin to slow down just as soon as they are emitted from the sources. Therefore, if  $s(\mathbf{r})$  is the source density at the point  $\mathbf{r}$ , the slowing-down density at that point at zero age must be equal

to  $s(\mathbf{r})$ . Thus the first boundary condition (or source condition) is obtained:

$$(i) \quad q(\mathbf{r}, 0) = s(\mathbf{r}). \quad (6-77)$$

This relation is analogous to an initial condition for the time-dependent diffusion or heat flow equations. The procedure to be followed when neutrons are emitted with more than one energy, as they are in fission, will be discussed later in this chapter.

The boundary conditions for  $q(\mathbf{r}, \tau)$  at the surfaces of media and at interfaces between different media can be obtained by expressing  $q(\mathbf{r}, \tau)$  in terms of the flux using Eq. (6-71), that is,  $q(\mathbf{r}, u) = \xi \Sigma_s(u) \phi(\mathbf{r}, u)$ , and then noting the boundary conditions on  $\phi(\mathbf{r}, u)$  discussed in Section 5-8. Thus, since the flux must vanish at the extrapolated edge of a free surface, it follows that:

(ii) *The slowing-down density is zero at the extrapolated edge of a free surface.*

It will be recalled from Chapter 5 that the extrapolated distance  $d$  is a function of the transport mean free path of the medium. Since, however,  $\lambda_{tr}$  depends upon neutron cross sections,  $d$ , in general, is a function of energy. This means that the point where  $q(\mathbf{r}, \tau)$  must be placed equal to zero is also a function of energy and therefore a function of  $\tau$  through Eq. (6-73). Such a  $\tau$ -dependent boundary condition is very difficult to handle mathematically. Fortunately,  $d$  is not usually a rapidly varying function of energy and a single, average value of  $d$  can be used without introducing substantial errors. Furthermore, as pointed out in Chapter 5,  $d$  is frequently small compared with the dimensions of reactors and can often be neglected entirely. The flux is then assumed to vanish at the free surface itself, and in this case, boundary condition (ii) can be replaced by the following condition:

(ii') *The slowing-down density vanishes at a free surface.*

The boundary conditions on  $q(\mathbf{r}, \tau)$  at an interface between two different media result from the requirements of continuity of flux and current discussed in Chapter 5. It is easy to obtain in this manner the following interface conditions:

(iii)  $\frac{q(\mathbf{r}, \tau)}{\xi \Sigma_s}$  is continuous,

(iv)  $\frac{D}{\xi \Sigma_s} \text{ grad } q(\mathbf{r}, \tau)$  is continuous.

Unfortunately, boundary conditions (iii) and (iv) are ordinarily of little more than academic interest, since it is difficult to obtain solutions of the age equation for systems consisting of more than one medium. This situation is similar to the problem of solving the time-dependent heat flow equation in multiregion systems. For example, it may be remembered that although the steady-state flow of heat through several layers of insulation is a comparatively simple problem familiar to all engineers, the *transient* flow of heat in such a system is a considerably more difficult problem which cannot be handled by elementary analytical techniques.

Similarly, in nuclear engineering, age theory is almost never used for systems involving more than one moderating region. Other methods must be used for multiregion problems; these will be discussed in Chapter 10.

### 6-11 Solutions to the Age Equation

Several solutions to the age equation will now be obtained. For reasons mentioned above, these will pertain to single-region problems only.

**Planar source in an infinite slab.** Consider an infinite slab of moderator of extrapolated thickness  $a$  (energy-independent) containing at its center an infinite planar source emitting  $S$  fast neutrons per  $\text{cm}^2/\text{sec}$  at the energy  $E_0$ . In this problem, the slowing-down density can be a function of only one spatial variable, and the age equation is

$$\frac{\partial^2 q(x, \tau)}{\partial x^2} = \frac{\partial q(x, \tau)}{\partial \tau}, \quad (6-78)$$

where  $x$  is measured from the center of the slab.

The source density  $s(x)$  is zero everywhere in the slab except at  $x = 0$ , where  $s(x)$  is infinite because a finite number of neutrons are emitted from an infinitely thin source plane. As explained in Section 5-9, the source density can then be represented as

$$s(x) = S \delta(x), \quad (6-79)$$

where  $\delta(x)$  is the Dirac delta function (cf. Appendix II). The source condition (i) is therefore

$$q(x, 0) = S \delta(x). \quad (6-80)$$

The boundary conditions at the (extrapolated) surfaces of the slab are  $q(\pm a/2, \tau) = 0$ . Finally, because of the symmetry of the problem,  $q(x, \tau)$  must be an even function of  $x$ , that is,  $q(-x, \tau) = q(x, \tau)$ .

Equation (6-78) can be solved in terms of the slab eigenfunctions,

$$\varphi_n(x) = \cos B_n x,$$

discussed in Section 5-10, where  $B_n = n\pi/a$  and  $n$  is an odd integer. Thus, it will be assumed that  $q(x, \tau)$  can be expanded in the series

$$q(x, \tau) = \sum_{n \text{ odd}} f_n(\tau) \cos B_n x, \quad (6-81)$$

where  $f_n(\tau)$  are functions of  $\tau$  that must be determined. Substituting this expression into Eq. (6-78) gives

$$-\sum_{n \text{ odd}} B_n^2 f_n \cos B_n x = \sum_{n \text{ odd}} \frac{df_n}{d\tau} \cos B_n x. \quad (6-82)$$

In view of the orthogonality of the eigenfunctions, the  $n$ th terms on each side of this equation are equal, and the following differential equation for  $f_n(\tau)$  is obtained:

$$\frac{df_n}{d\tau} = -B_n^2 f_n. \quad (6-83)$$

The solution to Eq. (6-83) is

$$f_n = A_n e^{-B_n^2 \tau}, \quad (6-84)$$

where  $A_n$  is an arbitrary constant. Returning to Eq. (6-81),  $q(x, \tau)$  is now given by

$$q(x, \tau) = \sum_{n \text{ odd}} A_n e^{-B_n^2 \tau} \cos B_n x. \quad (6-85)$$

The constants  $A_n$  can be determined from the source condition. Letting  $\tau = 0$  in Eq. (6-85), it follows that

$$q(x, 0) = S\delta(x) = \sum_{n \text{ odd}} A_n \cos B_n x. \quad (6-86)$$

Next, multiplying both sides of this equation by  $\cos B_m x$  and integrating from  $-a/2$  to  $+a/2$  as in Section 5-10, it is easily found that  $A_n = 2S/a$ . Finally,  $q(x, \tau)$  becomes

$$q(x, \tau) = \frac{2S}{a} \sum_{n \text{ odd}} e^{-B_n^2 \tau} \cos B_n x. \quad (6-87)$$

Equation (6-87) is the complete solution to the problem;  $q(x, \tau)$  satisfies the age equation, the source condition, and the boundary condition at the free surface. The interpretation of this result is a little complicated, however, and a physical insight into age theory is better obtained from the following, somewhat more difficult, analytical problem.

**Planar source in an infinite medium.** Consider next the infinite planar source of the preceding example placed in an infinite medium. The age equation is again given by Eq. (6-78), and the source condition is Eq. (6-79), but now  $q(x, \tau)$  must vanish at infinity. The discrete set of eigenfunctions used in the preceding example cannot be applied to the present problem, since those eigenfunctions only had relevance to the finite slab. Now, all values of the eigenvalue  $B$  are possible and it is reasonable to expect that the solution will be given by an integral rather than by a series. (This is the familiar transition from a Fourier series, valid over a finite region, to the Fourier integral, valid over the infinite interval.)

Thus a solution of the following form is suggested:

$$q(x, \tau) = \int_{-\infty}^{\infty} F(B, \tau) \cos Bx dB, \quad (6-88)$$

where  $F(B, \tau)$  is a function to be determined. When Eq. (6-88) is substituted into

the differential equation (6-78), there is obtained

$$-\int_{-\infty}^{\infty} B^2 F(B, \tau) \cos Bx dB = \int_{-\infty}^{\infty} \frac{\partial F(B, \tau)}{\partial \tau} \cos Bx dB. \quad (6-89)$$

It follows that  $F(B, \tau)$  must be given by the equation

$$\frac{\partial F(B, \tau)}{\partial \tau} = -B^2 F(B, \tau), \quad (6-90)$$

whose general solution is

$$F(B, \tau) = G(B)e^{-B^2 \tau}, \quad (6-91)$$

where  $G(B)$  is a function of  $B$ . [Note that Eq. (6-90) is a partial differential equation whose integral involves an arbitrary *function* instead of an arbitrary constant, as with an ordinary differential equation.] Next, inserting Eq. (6-91) into Eq. (6-88) gives

$$q(x, \tau) = \int_{-\infty}^{\infty} G(B)e^{-B^2 \tau} \cos Bx dB. \quad (6-92)$$

The function  $G(B)$  can be found from the source condition by placing  $\tau = 0$  in Eq. (6-92); thus,

$$S\delta(x) = \int_{-\infty}^{\infty} G(B) \cos Bx dB. \quad (6-93)$$

It can be shown without difficulty that the delta function can be written in the form

$$\delta(x) = \frac{1}{2\pi} \int_{-\infty}^{\infty} \cos Bx dB. \quad (6-94)$$

By comparing the last two equations it is evident that  $G(B) = S/\sqrt{2\pi}$ , so that

$$q(x, \tau) = \frac{S}{2\pi} \int_{-\infty}^{\infty} e^{-B^2 \tau} \cos Bx dB. \quad (6-95)$$

The evaluation of the integral in Eq. (6-95) is somewhat tedious and will not be reproduced here. The final result for  $q(x, \tau)$  is

$$q(x, \tau) = \frac{S}{\sqrt{4\pi\tau}} e^{-x^2/4\tau}. \quad (6-96)$$

**Point source in an infinite medium.** Instead of solving the age equation again for this case, it is much easier to construct the solution from the results obtained above for the planar source. Let  $q_{pl}(x, \tau)$  be the slowing-down density at the distance  $x$  from a planar source emitting *one* neutron per  $\text{cm}^2/\text{sec}$ . Then, from Eq. (6-96),

$$q_{pl}(x, \tau) = \frac{1}{\sqrt{4\pi\tau}} e^{-x^2/4\tau}. \quad (6-97)$$

Similarly, let  $q_{pt}(r, \tau)$  be the slowing-down density at the distance  $r$  from a unit point source in the same medium. The function  $q_{pt}(r, \tau)$  can be found by the following device.

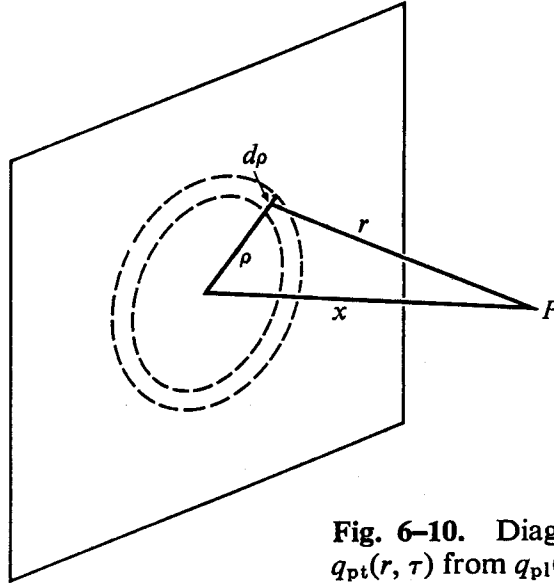


Fig. 6-10. Diagram for determining  $q_{pt}(r, \tau)$  from  $q_{pl}(x, \tau)$ .

The slowing-down density at  $P$  in Fig. 6-10 which arises from neutrons emitted from the differential ring of radius  $\rho$  and width  $d\rho$  is given by

$$dq_{pl}(x, \tau) = 2\pi q_{pt}(r, \tau)\rho d\rho.$$

The total slowing-down density at  $P$  is therefore

$$q_{pl}(x, \tau) = 2\pi \int_0^\infty q_{pt}(r, \tau)\rho d\rho. \quad (6-98)$$

By changing the integration variable from  $\rho$  to  $r$ , and noting that  $x^2 + \rho^2 = r^2$ , so that  $\rho d\rho = r dr$ , Eq. (6-98) becomes

$$q_{pl}(x, \tau) = 2\pi \int_x^\infty q_{pt}(r, \tau)r dr. \quad (6-99)$$

Next, differentiating Eq. (6-99) with respect to  $x$  yields

$$\frac{\partial q_{pl}(x, \tau)}{\partial x} = -2\pi x q_{pt}(x, \tau), \quad (6-100)$$

and so

$$q_{pt}(x, \tau) = -\frac{1}{2\pi x} \frac{\partial q_{pl}(x, \tau)}{\partial x}. \quad (6-101)$$

By substituting Eq. (6-97), and returning to the use of the variable  $r$ , which is more appropriate for describing problems involving point sources, Eq. (6-101) gives

$$q_{pt}(r, \tau) = \frac{e^{-r^2/4\tau}}{(4\pi\tau)^{3/2}}. \quad (6-102)$$

This result applies to a point source emitting one neutron per second. It is easy to see, however, that for a point source emitting  $S$  neutrons per second the slowing-down density is

$$q(r, \tau) = \frac{Se^{-r^2/4\tau}}{(4\pi\tau)^{3/2}}. \quad (6-103)$$

### 6-12 Physical Significance of Fermi Age

The slowing-down density from a unit point source in an infinite medium as computed from Eq. (6-102) is shown in Fig. 6-11 as a function of  $r$  for three values of  $\tau$ . Since the source neutrons have zero age, it follows from the source condition (Eq. 6-77) that  $q(r, 0)$  must be zero everywhere except at  $r = 0$ , where it is infinite. In the figure,  $q(r, 0)$  is therefore represented by the positive vertical axis.

For nonzero values of  $\tau$ ,  $q(r, \tau)$  is the familiar Gaussian curve which becomes increasingly broad with increasing  $\tau$ . The physical reason for this is simply that the larger values of  $\tau$  correspond to neutrons which have been slowing down longer, and these neutrons have had an opportunity to diffuse further from the source.

Incidentally, it should be noted that the areas under the curves in Fig. 6-11 are all equal to the source strength  $S = 1$ . This is because in an infinite system and in the absence of absorption, the total number of neutrons in the system slowing down past any value of lethargy must be independent of lethargy, and hence of  $\tau$ . If this were not the case, there would be an accumulation of neutrons at some lethargy or age somewhere in the system. The areas are equal to unity, since this is the total number slowing down at zero age.

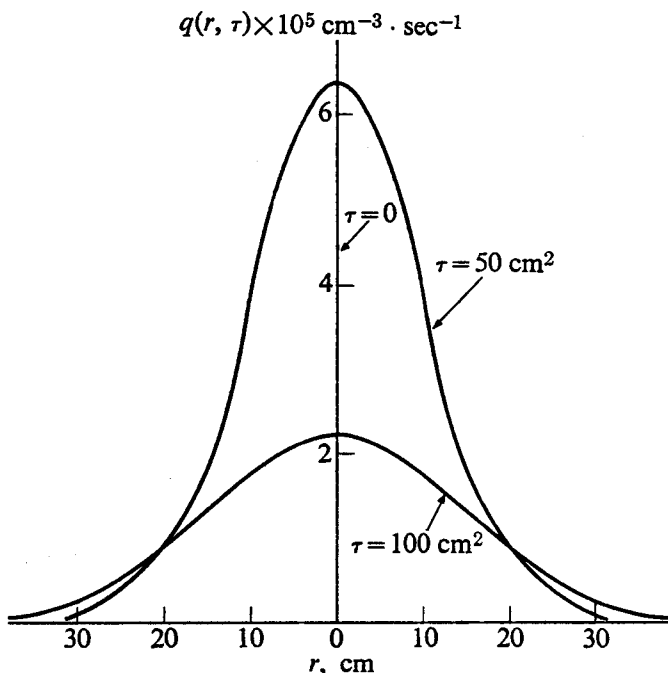
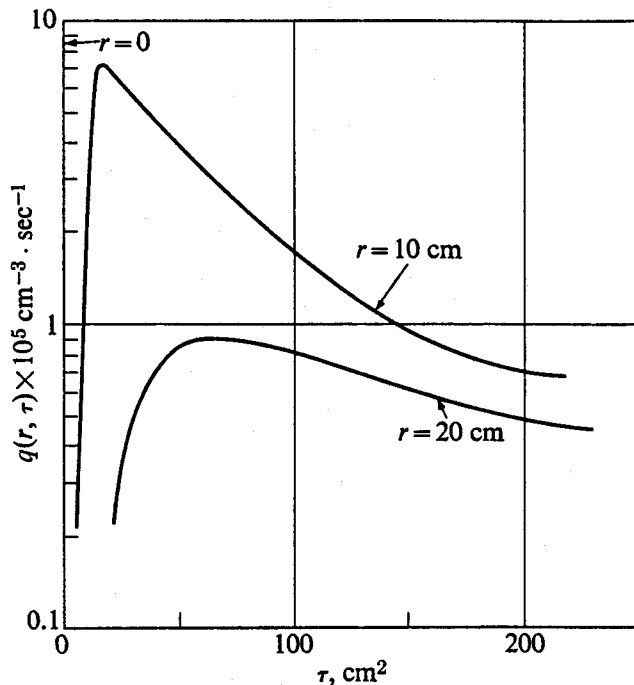


Fig. 6-11. The slowing-down density as a function of the distance from a unit point source of fast neutrons in an infinite medium for various values of age.



**Fig. 6-12.** The slowing-down density as a function of age for a unit point source of fast neutrons in an infinite medium.

Figure 6-12 shows  $q(r, \tau)$  as a function of  $\tau$  for fixed values of  $r$ . It will be observed that the maximum slowing-down density occurs at values of  $\tau$  which increase with  $r$ . In other words, the bulk of the neutrons slowing down near the source have a small age, whereas at larger distances most neutrons have a larger age. This again would be expected on physical grounds since the farther neutrons migrate from the source the more likely it is that they have acquired a larger age.

It is frequently desirable to have a more succinct interpretation of  $\tau$  than that given above, but one which has a more physical basis than the integral in Eq. (6-73). This can be obtained by an argument similar to that used in connection with the interpretation of  $L^2$  in Section 5-11. Consider, therefore, a point isotropic source emitting  $S$  neutrons per second in an infinite medium. The number of neutrons slowing down at age  $\tau$  within a spherical shell located between  $r$  and  $r + dr$  is  $q(r, \tau) dV = 4\pi r^2 q(r, \tau) dr$ . Let  $p(r) dr$  be the probability that a single neutron emitted from the source will acquire the age  $\tau$  between  $r$  and  $r + dr$ . Then  $p(r) dr$  is given by  $q(r, \tau) dV/S$ , so that from Eq. (6-103),

$$p(r) = \frac{4\pi r^2 e^{-r^2/4\tau}}{(4\pi\tau)^{3/2}}. \quad (6-104)$$

The second moment of the distribution function  $p(r)$ , denoted by  $\bar{r^2}$ , is defined by the integral

$$\bar{r^2} = \int_0^\infty r^2 p(r) dr. \quad (6-105)$$

In view of Eq. (6-104), this is equal to

$$\bar{r}^2 = \frac{4\pi}{(4\pi\tau)^{3/2}} \int_0^\infty r^4 e^{-r^2/4\tau} dr. \quad (6-106)$$

Using the formula

$$\int_0^\infty x^{2n} e^{-ax^2} dx = \frac{1 \cdot 3 \cdot 5 \cdots (2n-1)}{2^{n+1} a^n} \sqrt{\frac{\pi}{a}}, \quad (6-107)$$

Eq. (6-106) gives  $\bar{r}^2 = 6\tau$ , and therefore,

$$\tau = \frac{1}{6} \bar{r}^2. \quad (6-108)$$

Thus, *the Fermi age is equal to one-sixth the average of the square of the crow-flight distance from the point where a neutron enters a system with zero age to the point where it acquires the age  $\tau$ .*

The age to thermal energies, for instance, which is denoted by  $\tau_T$ , is one-sixth the average value of the square of the crow-flight distance from the point where a neutron is emitted to the point where it can be said to have acquired thermal energies. In this case, the quantity  $\sqrt{\tau_T}$  is called the *slowing-down length*.

The above discussion is based, of course, on age theory. As shown in the next section, however, age theory is not always valid, and for this reason it is convenient to generalize the concept of neutron age to include other situations. Henceforth, therefore,  $\tau$  will be *defined* by Eq. (6-108) regardless of how the neutrons actually slow down in a medium, that is, whether age theory is valid or not. In general, the probability  $p(r) dr$  that a neutron emitted from a point isotropic source will slow down past lethargy  $u$  between  $r$  and  $r + dr$  is given by

$$p(r) dr = \frac{4\pi q(r, u) r^2 dr}{S}. \quad (6-109)$$

From Eqs. (6-105) and (6-108), the age corresponding to the lethargy  $u$  is then

$$\tau(u) = \frac{4\pi}{6S} \int_0^\infty r^4 q(r, u) dr. \quad (6-110)$$

Also, since in an infinite system with no absorption

$$S = 4\pi \int_0^\infty r^2 q(r, u) dr, \quad (6-111)$$

it follows that the age is given by

$$\tau(u) = \frac{1}{6} \frac{\int_0^\infty r^4 q(r, u) dr}{\int_0^\infty r^2 q(r, u) dr}. \quad (6-112)$$

This generalized definition of age is similar to the redefinition of  $L^2$  discussed in Section 5-11.

The fundamental reason for the failure of theory in hydrogenous media is the fact that Fick's law is not valid in hydrogen, at least not at high energies. This in turn is due to the unusual nature of the hydrogen scattering cross section and the fact that neutrons lose so much of their energy in a collision with hydrogen. As shown in Fig. 6-13,  $\sigma_H$  is constant from 1 eV to about 10 keV and thereafter decreases rapidly with energy. Consider now the slowing down of a single fast neutron emitted in an infinite hydrogen medium with the energy  $E_0$ , where  $E_0$  is in the MeV region. The neutron undergoes its first collision after moving, on the average, one mean free path, i.e., the distance  $1/\Sigma_s(E_0)$ . At this point, since  $\Sigma_s = 1$ , its energy increases by one unit, on the average, which is equivalent to a reduction in energy by a factor of  $e$ . The cross section for a second collision is now much larger, and the second mean free path is considerably shorter than the first. As a consequence, the second collision occurs comparatively near the site of the first collision. This process is repeated at all succeeding collisions, the mean free path decreasing with each encounter, until the result that the neutron migrates only a short distance from the point where it was first scattered. After the energy

As shown earlier, the fluctuations in the letthargies of neutrons from their average letthargy decrease with increasing  $A$ . The Fermi age model is therefore clearly more appropriate for describing the slowing down of neutrons in heavy rather than light moderators. However, this does not entirely rule out the use of this model, even for the lightest moderators. With hydrogen, for example, although only about 14.5 collisions are required to increase the average letthargy of a 2-MeV neutron to a value whose corresponding energy is 1 eV, the fluctuation in letthargy (from Eq. 6-67) is only 26%. This corresponds to a spread in energy from 0.014 eV to 70 eV. While this represents a very substantial fluctuation in energy, age theory might still provide useful information regarding the moderation of neutrons in hydrogen, and, indeed, age theory can be used for hydrogen in certain cases as described below.

According to Section 6-9, age theory is based essentially on three assumptions:  
 (1) All neutrons can be described in terms of their average behavior. (2) The collision density  $F(r, u)$  is essentially constant over any lethargy interval of size  $\delta$ . (3) Diffusion theory is valid at all energies. These assumptions will now be examined to determine under what circumstances age theory might be expected to be valid. In particular, age theory cannot ordinarily be used to describe the slowing down of neutrons in hydrogenous media, and in view of the importance of moderators containing hydrogen (especially water) it is appropriate to understand

### 6-13 Validity of Age Theory—Slow ing Down in Hydrogen

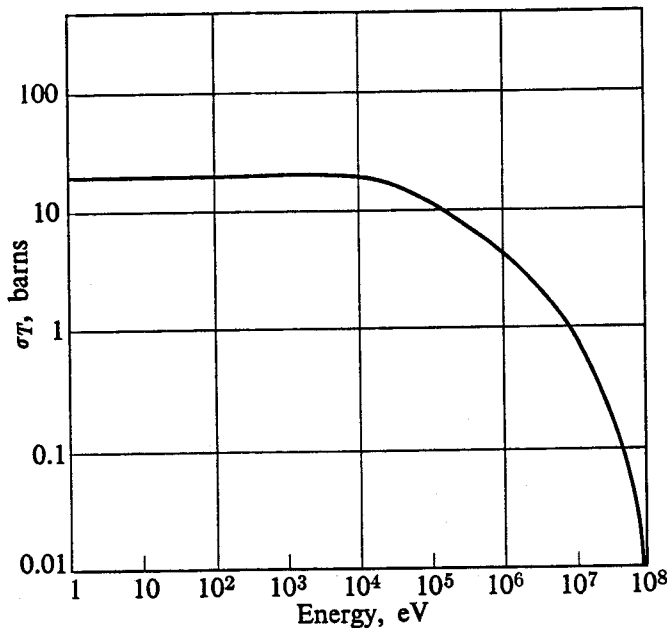


Fig. 6-13. The total cross section of hydrogen.

of the neutron falls below 10 keV, the mean free path remains approximately constant, but now the cross section is large and the neutron does not move much farther at the lower energies.

To a rough approximation, therefore, the neutrons slow down in hydrogen at the point where they have their first collision. It will be recalled, however, that Fick's law cannot be used at distances within a few mean free paths of sources. In view of the foregoing discussion, it is clear that by the time a neutron reaches the point where Fick's law and hence diffusion theory is valid, it has moved just about as far from the point where it was emitted as it is ever going to go. In other words, it is the first mean free path and not the subsequent diffusion of the neutrons which largely determines their slowing-down distribution in hydrogen. Of course, if the source neutrons are emitted with energies below 10 keV, that is, in the region where  $\sigma_H$  is constant, the situation is quite different. At these energies it is permissible to use the age equation for hydrogen, although the fluctuations from the predicted behavior of the neutrons may be expected to be very large.

Since neutrons slow down in hydrogen in the vicinity of their first collision, it follows that the slowing-down density is about equal to the first-collision density. This, in turn, is given by the product of the uncollided flux and the macroscopic scattering cross section at the source energy. For a point source emitting  $S$  neutrons per second at the energy  $E_0$  in an infinite medium,  $q(r)$  is therefore

$$q(r) = \frac{S \Sigma_s(E_0) e^{-\Sigma_s(E_0)r}}{4\pi r^2}. \quad (6-113)$$

It should be noted that the spatial dependence of  $q$  in Eq. (6-113) is considerably different from the Gaussian behavior predicted by age theory (cf. Eq. 6-103). Furthermore,  $q(r)$  is not a function of  $\tau$ , since every neutron is presumed to slow

down fully at its first collision. Equation (6-113) is a fair (but *only* fair) representation of the slowing down of neutrons in water.

The age of neutrons in hydrogenous media is still defined, of course, even though age theory is not valid (see preceding section). In this connection, it is interesting to note that although it is the hydrogen which is primarily responsible for the moderation of the neutrons in these media, other nuclei which are present can play an important role in determining the age. For example, the age of fission neutrons to 1.45 eV in a hydrogen medium having an atom density equal to that of the hydrogen in water is  $41 \text{ cm}^2$ , while the age of the same neutrons in water is only about  $26 \text{ cm}^2$ . The oxygen thus reduces the age by over 35%. This appears puzzling at first, since neutrons lose very little energy in elastic collisions in oxygen compared with hydrogen, and the threshold for inelastic scattering (6.5 MeV) is so high that this process cannot play a significant role in neutron moderation. Furthermore, there is twice as much hydrogen as oxygen in water. Nevertheless, while the oxygen itself does not slow the neutrons down appreciably, collisions with oxygen tend to prevent the neutrons from traveling very far from the source. In other words, the oxygen acts rather like a uniformly distributed reflector, holding the neutrons near the source where they can be slowed down in collisions with hydrogen.

### 6-14 Measurement of Neutron Age

The concept of neutron age is most useful in connection with thermal reactors and is rarely used in calculations of intermediate or fast reactors. It is the age to thermal energies,  $\tau_T$ , that is therefore of greatest importance in nuclear engineering.

In view of the general definition of age given in Eq. (6-112), the experimental determination of  $\tau_T$  requires the measurement of the slowing-down density at thermal energies as a function of position from a point source. However, this quantity cannot be measured directly, since it is not possible to distinguish between neutrons that have "just become" thermal and those that have been diffusing as thermal neutrons for some time. As a consequence, the slowing-down density must be measured at an energy above thermal, and corrections can then be made to take into account the additional slowing down required for the neutrons to reach the thermal region.

These measurements are usually carried out using thin foils of an isotope having a strong, isolated absorption resonance just above thermal. Foils of indium, whose principal isotope  $\text{In}^{115}$  has a resonance at 1.45 eV, are often used for this purpose. These are covered with thin sheets of cadmium, whose absorption cross section is large below the indium resonance but small at higher energies. The cadmium thus prevents thermal neutrons from reaching the indium foil, but permits the 1.45-eV neutrons to pass through to the indium, where they are absorbed. The foils are put in suitable holders and placed in the moderating medium at various distances from the source. The saturation activity of each foil (from the 54.1-minute beta decay of  $\text{In}^{116}$ ) is then a measure of the slowing-down density at about 1.45 eV in the vicinity of the foil, as can be seen by the following argument.

The saturation activity of an indium foil is equal to the rate of production of  $\text{In}^{116}$  nuclei, namely,

$$\text{saturation activity} = V \int \phi(r, E) \Sigma_{a\text{In}}(E) dE, \quad (6-114)$$

where  $V$  is the volume of the foil,  $\phi(r, E)$  is the energy-dependent flux at the foil,  $\Sigma_{a\text{In}}(E)$  is the macroscopic absorption cross section of  $\text{In}^{115}$ , and the integral is evaluated over the 1.45-eV resonance. According to Eq. (6-71), the slowing-down density and lethargy-dependent flux are related by

$$\phi(r, u) = \frac{q(r, u)}{\xi \Sigma_s(u)}, \quad (6-115)$$

provided the sources are monoenergetic. Since  $\phi(r, u) du = -\phi(r, E) dE$ , it follows from Eq. (6-25) that  $\phi(r, u) = E\phi(r, E)$ , and Eq. (6-115) becomes

$$\phi(r, E) = \frac{q(r, E)}{\xi E \Sigma_s(E)}, \quad (6-116)$$

where, of course,  $\Sigma_s(E)$  refers to the moderator. Assuming that  $q(r, E)$ ,  $\xi$ , and  $\Sigma_s(E)$  are reasonably constant over the limits of the integral in Eq. (6-114), this can be written as

$$\text{saturation activity} = \frac{V q(r, E_{\text{In}})}{\xi \Sigma_s} \int \frac{\Sigma_{a\text{In}}(E) dE}{E}, \quad (6-117)$$

where  $E_{\text{In}} = 1.45$  eV. Thus measurements of the saturation activities of the various foils give  $q(r, E_{\text{In}})$ , and the age to 1.45 eV can then be obtained by numerically evaluating the integrals in Eq. (6-112). As shown in Eq. (6-112) and in Eq. (6-119) below, it is not necessary, however, to know the absolute magnitude of  $q(r, E_{\text{In}})$  in order to determine  $\tau$ ; it is sufficient to know the relative values of  $q$  as a function of position.

As a practical matter, it is usually necessary to deal with sources that emit neutrons with a continuous energy spectrum. In this case, the measured value of the age depends upon the nature of the spectrum, and different source spectra lead to different values of the age.

To find the average age of neutrons from a source spectrum  $S(E)$ , let  $q(r; E \rightarrow E_{\text{In}})$  be the slowing-down density at the indium resonance arising from unit neutron sources at the energy  $E$ . The total slowing-down density at  $r$  is then

$$q(r, E_{\text{In}}) = \int_0^\infty S(E) q(r; E \rightarrow E_{\text{In}}) dE. \quad (6-118)$$

The average age to indium resonance, denoted by  $\tau_{\text{In}}$ , can now be found by inserting this expression into Eq. (6-112); thus

$$\tau_{\text{In}} = \frac{1}{6} \frac{\int_0^\infty \int_0^\infty S(E) r^4 q(r; E \rightarrow E_{\text{In}}) dE dr}{\int_0^\infty \int_0^\infty S(E) r^2 q(r; E \rightarrow E_{\text{In}}) dE dr}. \quad (6-119)$$

In an infinite system, however, with no absorption,

$$\frac{4\pi}{6} \int_0^\infty r^2 q(r; E \rightarrow E_{In}) dr = 1,$$

and Eq. (6-119) reduces to

$$\tau_{In} = \frac{4\pi}{6S} \int_0^\infty \int_0^\infty S(E) r^4 q(r; E \rightarrow E_{In}) dE dr, \quad (6-120)$$

where  $S$  is the strength of the source. From Eq. (6-110), however, the quantity

$$\frac{4\pi}{6} \int_0^\infty r^4 q(r; E \rightarrow E_{In}) dr$$

is equal to the age of neutrons from the energy  $E$  to indium resonance, that is,  $\tau(E \rightarrow E_{In})$ . It follows therefore from Eq. (6-120) that the measured value of the age to indium resonance of a continuous source of neutrons in the absence of absorption is related to the age of monoenergetic neutrons by

$$\tau_{In} = \frac{1}{S} \int_0^\infty S(E) \tau(E \rightarrow E_{In}) dE. \quad (6-121)$$

Measured values of  $\tau_{In}$  for fission neutrons are given in Table 6-3 for several moderators.

**Table 6-3**  
**Ages (in cm<sup>2</sup>) of Fission Neutrons to Indium Resonance (1.45 eV)  
in Various Moderators**

Moderator	H <sub>2</sub> O	D <sub>2</sub> O	Be	BeO	Graphite
$\tau_{In}$	$\sim 26$	111	85	80	311

In order to determine the age to thermal energies, it is necessary to know the age from indium resonance to thermal,  $\tau(E_{In} \rightarrow E_{th})$ . Then since ages are additive\*

$$\tau_T = \tau_{In} + \tau(E_{In} \rightarrow E_{th}). \quad (6-122)$$

As mentioned earlier,  $\tau(E_{In} \rightarrow E_{th})$  cannot be measured and must be inferred

---

\* As mentioned in Section 6-9, ages defined by age theory, that is, by Eq. (6-73), are additive. This is *not* necessarily the case, however, when age is given the more general definition of Eq. (6-112). Nevertheless, it is usual practice to assume that ages are always additive.

from theoretical calculations. Furthermore, age theory, at least in the form described in the present chapter, cannot be used to compute  $\tau(E_{In} \rightarrow E_{th})$  because of chemical binding and other effects at these energies. A more appropriate method for determining  $\tau(E_{In} \rightarrow E_{th})$  will be discussed in Chapter 8 (cf. Section 8-7).

### 6-15 Inelastic Scattering in the Slowing Down of Neutrons

The slowing down of neutrons as the result of inelastic scattering has not been considered up to this point. This is not because it is an unimportant mechanism of neutron moderation, but merely because it cannot be treated by simple analytical methods. As will be shown in this section, inelastic scattering is very effective in slowing down neutrons and must be included in one way or another in most reactor calculations.

In discussing the loss in energy which accompanies inelastic scattering, it will be recalled from Chapter 2 that two situations must be considered. First, if the incident neutron has sufficient kinetic energy to excite only a few levels in the struck nucleus, the inelastic neutrons appear in a few discrete energy groups. In this case, the average energy of the emitted neutrons depends upon the energies of the various levels of the target nucleus as well as upon the relative cross sections for their excitation, and no general statement can be made regarding the effective energy loss of the incident neutron.

On the other hand, if the energy of the incident neutron is high enough to excite many levels, the energies of the emitted neutrons can be represented reasonably well by a smooth function. Thus the probability that an inelastic neutron will be emitted with an energy between  $E'$  and  $E' + dE'$  when the nucleus is struck by neutrons of energy  $E$  is given approximately by (cf. Section 2-11)

$$P(E \rightarrow E') dE' = \frac{E'}{T^2} e^{-E'/T} dE'. \quad (6-123)$$

In this formula,  $T$  is the nuclear temperature, which can be represented by the formula

$$T = 3.2 \sqrt{E/A}, \quad (6-124)$$

where both  $T$  and  $E$  are in MeV and  $A$  is the mass number of the nucleus. Using Eq. (6-123), the average energy of an inelastic neutron is

$$\begin{aligned} \bar{E}' &= \int_0^\infty E' P(E \rightarrow E') dE' \\ &= 2T. \end{aligned} \quad (6-125)$$

According to Eq. (6-125) the energy loss associated with inelastic scattering can be considerable. For example, if  $U^{238}$  is bombarded by 10-MeV neutrons,  $T$  is about 0.66 MeV, and  $\bar{E}'$  is 1.32 MeV. In other words, the incident neutron on the average loses 8.68 MeV as a result of a single inelastic collision with  $U^{238}$ . (Of

course, since neutrons are indistinguishable, it is not necessarily the incident neutron which is emitted. This distinction is unimportant, however, so long as *some* neutron appears.) By contrast, it should be noted that the average energy loss by elastic scattering in  $U^{238}$  is  $\frac{1}{2}(1 - \alpha) \times 10 \text{ MeV} = 0.085 \text{ MeV}$ , if the scattering were isotropic in the center-of-mass system. In fact, the scattering is strongly forward peaked at 10 MeV (cf. Fig. 2-21) and the actual energy loss by elastic scattering is therefore *considerably* less than 0.085 MeV. It should be evident from this example that at least in certain cases, inelastic scattering can be a far more important mechanism for the slowing down of neutrons than elastic scattering.

It must be remembered, however, that while elastic scattering occurs at all energies, inelastic scattering does not take place below the inelastic threshold. This threshold is rather high for many light nuclei; it is 4.8 MeV for carbon, 6.4 MeV for oxygen, and with hydrogen and deuterium, inelastic scattering does not occur at all. Inelastic scattering can therefore be ignored in most light nuclei except at high energy. With intermediate and heavy nuclei, on the other hand, the inelastic thresholds are much lower, and inelastic scattering must be taken into account whenever materials of this type are present in large amounts in a reactor.

Many reactors do, in fact, contain substantial quantities of intermediate and heavy nuclei. The structural parts are often iron or aluminum, the coolant may be sodium or a mixture of sodium and potassium (called NaK), all of which are intermediate nuclei, and the fuel itself always consists of heavy nuclei. In fast and intermediate reactors, as mentioned in Chapter 4, there are essentially no light nuclei present, and in these systems virtually all the slowing down arises from inelastic scattering. Methods for incorporating inelastic scattering in the calculations for these types of reactors will be considered in Chapter 10.

A simple way of handling inelastic scattering in thermal reactors is to use values of the age in which this process is explicitly included. These can be obtained either from measurements of the age in assemblies which duplicate the composition of the intended reactor, or from computations using one of the numerical methods discussed in the next section in which inelastic scattering can be included. Results of calculations of this type are shown in Fig. 6-14, where the age of fission neutrons to 1.45 eV is shown for various metal-water mixtures as a function of the ratio of the volume of the metal to the volume of the water. (Experiments, of course, give similar curves; however, these have been carried out only at comparatively few points.) In these calculations it was assumed that the metal is in the form of thin elements, so thin, in fact, that the mixture can be assumed to be homogeneous insofar as the moderation of the neutrons is concerned. (Such systems are often called *quasihomogeneous*; cf. Section 9-9.)

It will be observed in Fig. 6-14 that with the exception of the uranium curve, the age increases with increasing metal-to-water-volume ratio. This is to be expected, since one of the effects of increasing the volume of metal in the system is to decrease the amount of water, and, of course, water is very effective in slowing down neutrons. However, the curves cannot be explained by assuming that the only effect of the metal is to change the average water density, that is, that the

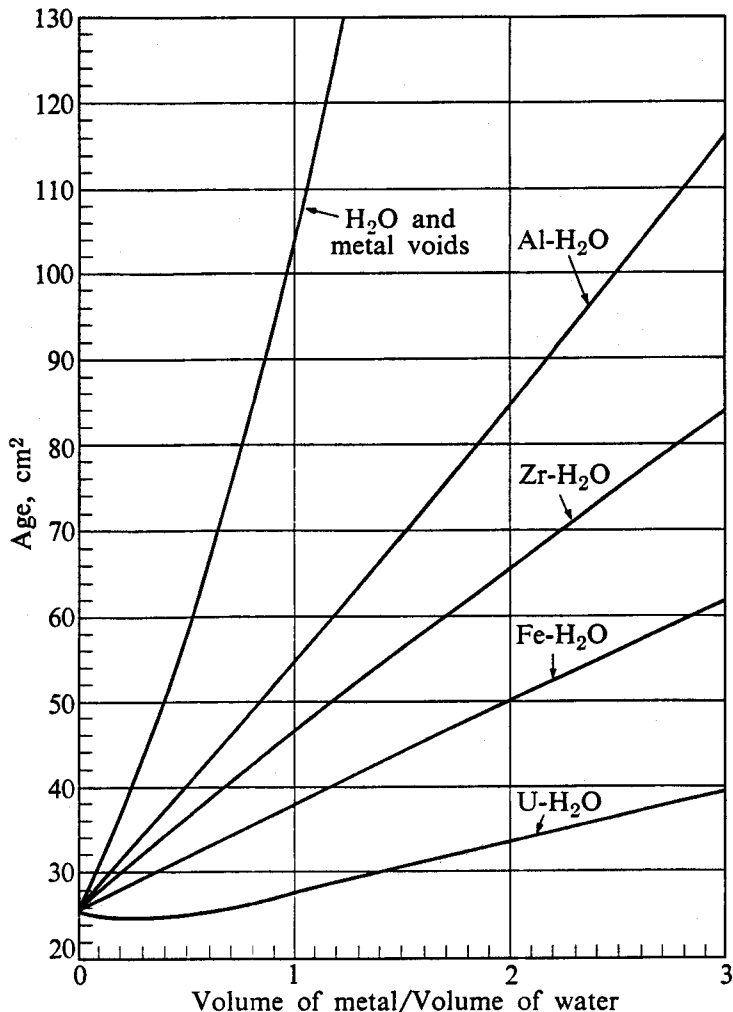


Fig. 6-14. The age of fission neutrons to 1.45 eV in metal-water mixtures. Age is also shown assuming that the metal acts only as a void. (Metal-water curves courtesy of G. D. Joanou, General Atomic.)

metal acts only as a void. According to Eq. (6-73) it is easy to see that  $\tau$  varies inversely as the square of the moderator density. Thus if the moderation of neutrons were due only to the water,  $\tau$  would increase as

$$\tau = \tau_w \left( \frac{V_w + V_m}{V_w} \right)^2 = \tau_w \left( 1 + \frac{V_m}{V_w} \right)^2, \quad (6-126)$$

where  $\tau_w$  is the age of neutrons in pure water and  $V_m/V_w$  is the metal-water ratio. As shown in Fig. 6-14, the actual ages of metal-water mixtures are much less than the values computed from Eq. (6-126), and it must be concluded that the presence of the metal considerably reduces the age over what would be expected if the metal acted simply as a void. In particular, returning to the curve for uranium, it will be seen that  $\tau$  actually decreases slightly as uranium is added to the system and then increases comparatively little over the entire range of metal-water ratios. Since

none of these metals moderate neutrons appreciably by elastic scattering, it follows that it is inelastic scattering by the metal which accounts for the low values of age. Indeed, in view of Fig. 6-14, it must even be concluded that because of inelastic scattering, uranium is about as effective as water in moderating neutrons.\*

### 6-16 Methods of Calculating Age

Measurements of the ages of fission neutrons in various systems are expensive to carry out, and so it is desirable to be able to calculate ages from first principles. The simple formula for  $\tau$  given in Eq. (6-73) rarely gives sufficiently accurate values for design purposes, however, since all the assumptions of age theory are seldom valid simultaneously for a real system and, in addition, moderation by inelastic scattering was ignored in its derivation.

Fortunately, age can be calculated exactly by a number of numerical-analytical methods. These methods, like those discussed in Section 5-10 for handling neutron diffusion, fall roughly into two categories. The first consists of a number of techniques for finding the age by solving the energy-dependent transport equation; the second is the Monte Carlo method (cf. Section 5-10). Needless to say, a complete discussion of these techniques lies well beyond the scope of this text, and the reader should consult the references for the details. What is important to note at this point is the fact that it is possible using these methods to treat all neutron interactions exactly and so obtain (presumably) exact values of age. Indeed, the confidence in such calculations is so high (particularly on the part of theoreticians) that, at least until recently, the calculated age of neutrons in water was considered to be more reliable than the experimental value. Results of calculations of this type for various homogeneous mixtures of metals and water were shown in Fig. 6-14; their interpretation was discussed in Section 6-15.

### 6-17 Elastic Moderation Time

The average time required for a neutron to slow down from one energy to another by elastic scattering in the moderating region, i.e., at energies above about 1 eV, can be estimated by using age theory. In the time  $dt$ , the neutron moves the distance  $dx = v dt$ , where  $v$  is the neutron speed, and according to Eq. (6-75), it increases in lethargy by the amount

$$du = \xi \Sigma_s v dt. \quad (6-127)$$

---

\* This may not be the whole story, however. It was pointed out in Section 6-13 that the oxygen in water has a surprisingly important effect on the age of neutrons. Thus, even though the oxygen plays little or no role in moderating the neutrons, it acts as a distributed reflector and tends to keep the neutrons near the source, where they are slowed down in collisions with hydrogen. The metals in the mixtures shown in Fig. 6-14 presumably act in much the same way, though clearly to a much lesser extent.

Since  $du = -dE/E$ , Eq. (6-127) is equivalent to

$$-\frac{dE}{E} = \xi \Sigma_s v dt; \quad (6-128)$$

and since  $E = \frac{1}{2}mv^2$ , where  $m$  is the mass of the neutron, Eq. (6-128) can also be written as

$$-\frac{dv}{v^2} = \frac{1}{2}\xi \Sigma_s dt. \quad (6-129)$$

The time which a neutron spends in slowing down from an initial speed  $v_i$  to the speed  $v$  is therefore

$$t = \int_0^t dt = -2 \int_{v_i}^v \frac{dv}{\xi \Sigma_s v^2}. \quad (6-130)$$

In general,  $\Sigma_s$  (and possibly also  $\xi$ ) is a function of energy and hence of  $v$ . However, an estimate of  $t$  can be obtained by replacing  $\Sigma_s$  in the integral by an appropriate average value. Then,

$$t = \frac{2}{\xi \Sigma_s} \left( \frac{1}{v} - \frac{1}{v_i} \right). \quad (6-131)$$

An especially important case of Eq. (6-131) is the time required for fission neutrons to slow down to the cutoff of the moderation region at about 1 eV. This time is called the *moderation time* and is denoted by  $t_m$ . Since the speed  $v_m$  corresponding to  $E_m$  is so much smaller than the speeds of fission neutrons, the second term in Eq. (6-131) can be neglected and  $t_m$  becomes

$$t_m = \frac{2}{\xi \Sigma_s v_m}. \quad (6-132)$$

Values of  $t_m$  for several moderators, which were computed using Eq. (6-132), are given in Table 6-4.

Table 6-4  
Moderation Times (in  $\mu$ sec)

Moderator	$t_m$
H <sub>2</sub> O	1.0
D <sub>2</sub> O	8.1
Be	9.3
BeO	12
C	23

### 6-18 Slowing-Down Kernels

According to age theory, the slowing-down density at the distance  $r$  from a point source emitting  $S$  fast neutrons isotropically in an infinite medium is given by Eq. (6-103),

$$q(r, \tau) = \frac{Se^{-r^2/4\tau}}{(4\pi\tau)^{3/2}}.$$

In deriving this expression in Section 6-11, the source was assumed to be located at the center of coordinates. If the source is located at the point  $\mathbf{r}'$ , then  $q(\mathbf{r}, \tau)$  becomes

$$q(\mathbf{r}, \tau) = \frac{Se^{-|\mathbf{r}-\mathbf{r}'|^2/4\tau}}{(4\pi\tau)^{3/2}}, \quad (6-133)$$

since the slowing-down density depends only on the distance between the source and the observation point.

Consider now the slowing-down density arising from isotropic neutron sources distributed continuously in an infinite medium. If  $s(\mathbf{r}')$  is the source density at  $\mathbf{r}'$ , then  $s(\mathbf{r}') dV'$  fast neutrons are emitted from the volume element  $dV'$ , and they make a contribution to the slowing-down density at  $\mathbf{r}$  which is equal to

$$dq(\mathbf{r}, \tau) = \frac{s(\mathbf{r}')e^{-|\mathbf{r}-\mathbf{r}'|^2/4\tau}}{(4\pi\tau)^{3/2}} dV'. \quad (6-134)$$

The total slowing-down density at  $\mathbf{r}$  is therefore

$$q(\mathbf{r}, \tau) = \frac{1}{(4\pi\tau)^{3/2}} \int_{\text{all space}} s(\mathbf{r}') e^{-|\mathbf{r}-\mathbf{r}'|^2/4\tau} dV'. \quad (6-135)$$

This result can be written as

$$q(\mathbf{r}, \tau) = \int_{\text{all space}} s(\mathbf{r}') G(\mathbf{r}, \mathbf{r}') dV', \quad (6-136)$$

where

$$G(\mathbf{r}, \mathbf{r}') = \frac{1}{(4\pi\tau)^{3/2}} e^{-|\mathbf{r}-\mathbf{r}'|^2/4\tau} \quad (6-137)$$

is known as the *Fermi point slowing-down kernel*, or sometimes the *Gaussian point slowing-down kernel*, for the infinite medium. It should be noted that  $G(\mathbf{r}, \mathbf{r}')$  is equal to the slowing-down density at  $\mathbf{r}$  due to a unit source of fast neutrons placed at  $\mathbf{r}'$ . These results are completely analogous to those obtained for neutron diffusion in Section 5-10.

The expression for  $G(\mathbf{r}, \mathbf{r}')$  given by Eq. (6-137) is based, of course, on age theory, and it can be used only when that theory is valid. If this is not the case,  $q(\mathbf{r}, \tau)$  can still be computed from Eq. (6-136), but  $G(\mathbf{r}, \mathbf{r}')$  must be replaced by another, more appropriate, slowing-down kernel. This can either be obtained from one of the numerical methods discussed in Section 6-16, or it can be measured experimentally. Thus, since  $G(\mathbf{r}, \mathbf{r}')$  is equal to the slowing-down density due to a point source in an infinite medium, the measurements discussed in Section 6-14 for determining  $\tau$  also give the slowing-down kernel, at least to indium resonance.

## References

- AMALDI, E., "The Production and Slowing Down of Neutrons," *Handbuch der Physik*. Berlin: Springer Verlag, Vol. 38, Part 2, 1959, pp. 1-659.
- BECKURTS, K. H., and K. WIRTZ, *Neutron Physics*. Berlin: Springer Verlag, 1958 (translated edition, 1964), Chapters 7, 8, and 9.
- GALANIN, A. D., *Thermal Reactor Theory*, 2nd ed. New York: Pergamon Press, 1960, Sections 3 and 4.
- GLASSTONE, S., and M. C. EDLUND, *The Elements of Nuclear Reactor Theory*. Princeton, N.J.: Van Nostrand, 1952, Chapter 6.
- ISBIN, H. S., *Introductory Nuclear Reactor Theory*. New York: Reinhold, 1963, Chapter 3.
- MEGHREBLIAN, R. V., and D. K. HOLMES, *Reactor Analysis*. New York: McGraw-Hill, 1960, Chapters 4 and 6.
- MURRAY, R. L., *Nuclear Reactor Physics*. Englewood Cliffs, N.J.: Prentice-Hall, 1957, Chapters 2 and 3.
- WEINBERG, A. M., and E. P. WIGNER, *The Physical Theory of Neutron Chain Reactors*. Chicago: University of Chicago Press, 1958, Chapters 10 and 11.

## Problems

6-1. The differential elastic cross section of oxygen at 0.95 MeV in the center-of-mass system can be written as

$$\sigma_s(\mu) = 0.212 (1 + 2.45 \mu^2) \text{ barns/steradian}$$

where  $\mu$  is the cosine of the scattering angle. (a) Find the total elastic cross section at this energy. (b) Compute and plot the scattering distribution function  $P(E \rightarrow E')$  for oxygen at this energy. (c) Find the average energy of the scattered neutrons.

6-2. Show by direct integration that for elastic scattering

$$\int_{\alpha E}^E P(E \rightarrow E') dE' = 1,$$

independent of the scattering angular distribution.

6-3. Let  $P(v \rightarrow v')dv'$  be the probability that a neutron with laboratory speed  $v$  is elastically scattered into the interval  $dv'$  between  $v'$  and  $v' + dv'$ . (a) With isotropic scattering in the center-of-mass system, show that

$$P(v \rightarrow v') = \begin{cases} \frac{2v'}{(1 - \alpha)v^2}, & v\sqrt{\alpha} < v' < v, \\ 0, & \text{otherwise.} \end{cases}$$

(b) Show that the average speed after a collision is

$$\bar{v}' = \frac{2v}{3} \frac{1 - \alpha^{3/2}}{1 - \alpha}.$$

(c) Compute  $\bar{v}'$  for 1 MeV neutrons scattered from hydrogen.

6-4. Show that for isotropic scattering in the center-of-mass system the probability function  $P(u \rightarrow u')$  for elastic scattering between lethargies  $u$  and  $u'$  is given by the formula

$$P(u \rightarrow u') = \begin{cases} \frac{1}{1 - \alpha} e^{(u-u')}, & u < u' < u + \ln(1/\alpha), \\ 0, & \text{otherwise.} \end{cases}$$

6-5. Show that a good approximation for  $\xi$  is

$$\xi \approx \frac{2}{A + \frac{2}{3}}.$$

6-6. The differential elastic scattering cross section in the center-of-mass system at some energy can be represented by the formula

$$\sigma_s(\theta) = a + b \cos \theta.$$

(a) Derive a formula for  $\xi$  at this energy. (b) What is the limit of this formula as  $b \rightarrow 0$ ?

6-7. Show that

$$\xi = \frac{1}{2}X - \frac{1}{12}X^2 + \dots,$$

where  $X = \ln(1/\alpha)$ .

6-8. Show that for isotropic scattering in the center-of-mass system and for large  $A$ , the average increase in lethargy in an elastic collision is one-half the maximum lethargy increase.

6-9. (a) By introducing the variable  $x = E/E_0$ , show that the function  $P_A(x) = E_0 F(E)$  depends only upon  $A$  and  $x$ . (b) Derive an exact integral equation for  $P_A(x)$ . [Note: The function  $P_A(x)$  is called the *Placzek function*.]

6-10. Show that the function

$$F(E) = CE^{-\beta}$$

is a solution to the asymptotic equation for  $F(E)$  (Eq. 6-36) provided

$$\beta(\alpha - 1) = \alpha^\beta - 1.$$

Discuss the values of  $\beta$  which satisfy this equation.

6-11. Compute and plot the collision density function  $F_3(E)$  for neutrons that have had three collisions. Discuss the continuity of  $F_3(E)$  and its derivatives at  $E = E_0, \alpha E_0, \alpha^2 E_0$ , and  $\alpha^3 E_0$ .

6-12. The collision density for a moderator with  $A > 1$ , which was found in Section 6-5 by the method of successive collisions, can also be found using the method of *successive collision intervals*. The energy region  $\alpha E_0 < E < E_0$  is known as the first collision interval, where  $E_0$  is the energy of the source neutrons; the region  $\alpha^2 E_0 < E < \alpha E_0$  is the second collision interval; and so on. In this method the collision density for the  $n$ th collision interval,  $F^{(n)}(E)$ , is determined by using the previously-computed collision density  $F^{(n-1)}(E)$ . (a) In the first collision interval show that

$$F^{(1)}(E) = \frac{S}{(1 - \alpha)E_0} + \int_E^{E_0} \frac{F^{(1)}(E') dE'}{(1 - \alpha)E},$$

(b) By transforming this integral equation to a differential equation show that

$$F^{(1)}(E) = \frac{S}{(1 - \alpha)E_0} \left( \frac{E_0}{E} \right)^{1/(1-\alpha)}.$$

(c) For the second collision interval show that

$$F^{(2)}(E) = \int_{\alpha E_0}^{E/\alpha} \frac{F^{(1)}(E') dE'}{(1 - \alpha)E'} + \int_E^{\alpha E_0} \frac{F^{(2)}(E') dE'}{(1 - \alpha)E'}.$$

(d) Show that

$$F^{(2)}(E) = \frac{S}{(1 - \alpha)E_0} \left( \frac{E_0}{E} \right)^{1/(1-\alpha)} \left[ 1 - \alpha^{1/(1-\alpha)} + \frac{\alpha^{1/(1-\alpha)}}{1 - \alpha} \ln \left( \frac{E}{\alpha E_0} \right) \right].$$

(e) Show that, in general,

$$F^{(n)}(E) = \int_{\alpha^{n-1} E_0}^{E/\alpha} \frac{F^{(n-1)}(E') dE'}{(1 - \alpha)E'} + \int_E^{\alpha^{n-1} E_0} \frac{F^{(n)}(E') dE'}{(1 - \alpha)E'}.$$

6-13. (a) Using the results of Problem 6-12, determine the discontinuity in  $F(E)$  at  $\alpha E_0$

(b) How does the magnitude of the discontinuity vary with  $A$ ?

6-14. Neutrons are emitted with an energy of 2 MeV in an infinite medium. Estimate the fractional deviation in the lethargy of the neutrons when their average lethargy corresponds to an energy of 1 eV if the medium is

- (a) H, (b) D, (c) C, (d) U.

6-15. The variance (square of the standard deviation) of the distribution in lethargy of neutrons that have undergone  $n$  collisions is defined in statistics as

$$\sigma^2 = \overline{\sum_{i=1}^n (\Delta u_i)^2} - \left( \overline{\sum_{i=1}^n \Delta u_i} \right)^2,$$

where  $\Delta u_i$  is the change in lethargy at the  $i$ th collision. With isotropic scattering in the center-of-mass system all collisions are identical and  $\sigma^2$  is  $\sigma^2 = n[\overline{(\Delta u)^2} - \overline{(\Delta u)^2}]$ . The quantity  $\overline{\Delta u}$  has already been shown to be equal to  $\xi$ . (a) Using the same procedure, show that

$$\overline{(\Delta u)^2} = 2\xi - (1 - \xi) \ln \frac{1}{\alpha}.$$

(b) Show also that

$$\frac{\sigma}{\overline{u}_n} = \frac{1}{\xi \sqrt{n}} \left[ 1 - \frac{(1 - \xi)^2}{\alpha} \right]^{1/2}.$$

(c) Show that in the limit of large  $A$  the fractional deviation from the mean in the lethargy of neutrons which have undergone  $n$  collisions approaches

$$\frac{\sigma}{\overline{u}_n} \rightarrow \frac{1}{\sqrt{3n}}.$$

(d) Plot the quantity

$$\frac{1}{\xi} \left[ 1 - \frac{(1 - \xi)^2}{\alpha} \right]^{1/2}$$

as a function of  $A$ .

- 6-16. (a) Derive an exact expression for the average number of collisions which neutrons undergo as their energy decreases from  $E_0$  to  $E_1$  in a hydrogen medium. (Note that this is not equivalent to finding the average energy after a given number of collisions.)  
 (b) Find a similar but approximate expression for neutrons slowing down in a medium with  $A > 1$ . [Hint: Use the collision densities computed in Sections 6-3 and 6-5.]

- 6-17. (a) Show that the energy of a neutron after  $n$  elastic collisions can be expressed as

$$E_n = E \prod_{j=1}^n 2^{-j} [(1 + \alpha) + (1 - \alpha) \cos \theta_j],$$

- where  $E$  is its initial energy, and  $\theta_j$  is the angle of scattering after the  $j$ th collision. (b) By treating  $E_n$  as a function of the  $n$  independent variables  $\theta_j$ , show that with isotropic scattering in the center-of-mass system the average value of  $E_n$  is given by

$$\bar{E}_n = \left( \frac{1 + \alpha}{2} \right)^n E.$$

- 6-18. Estimate the age of 2 MeV neutrons to 1 eV for graphite using the Fermi formula (Eq. 6-73). Compare this answer with the experimental value of  $311 \text{ cm}^2$  for fission neutrons.

- 6-19. Show that a criterion for the validity of Eq. (6-71) is

$$\frac{d}{du} \ln F(r, u) \ll \frac{1}{\xi}.$$

- 6-20. Show that according to age theory the slowing down density at the distance  $r$  from an infinitely long line source emitting  $S$  neutrons/sec per unit length is given by

$$q(r, \tau) = \frac{Se^{-r^2/4\tau}}{4\pi\tau}.$$

[Hint: Treat the line source as a set of point sources.]

- 6-21. Sources of monoenergetic fast neutrons are distributed in an infinite slab of moderator according to the function

$$s(x) = S \cos \left( \frac{\pi x}{a} \right),$$

- where  $S$  is a constant and  $a$  is the thickness of the slab. (a) Using age theory, calculate the slowing down density of neutrons of age  $\tau$ . (b) What is the average probability that a source neutron leaks from the slab while slowing down to the age  $\tau$ ?

- 6-22. An isotropic point source emitting  $S$  fast neutrons/sec is located at the center of a sphere of moderator of radius  $R$ . (a) Using age theory, show that the slowing down density of neutrons of age  $\tau$  is

$$q(r, \tau) = \frac{S}{2\pi r R} \sum_{n=1}^{\infty} B_n e^{-B_n^2 \tau} \sin B_n r,$$

where  $B_n = n\pi/R$ . (b) Derive an expression giving the probability that a source neutron will leak from the sphere while slowing down to the age  $\tau$ . Hint: It may be helpful to use the expansion (cf. Appendix II)

$$\delta(r) = \frac{r}{R} \sum_{n=1}^{\infty} B_n \sin B_n r.$$

6-23. An isotropic point source emitting  $S$  fast neutrons/sec is placed at the center of a bare cylindrical tank of moderator of radius  $R$  and height  $H$ . (a) Using age theory, show that the slowing down density of neutrons of age  $\tau$  is given by

$$q(r, z, \tau) = \frac{2S}{V} \sum_{\substack{m=1, 2, 3, \dots, n \\ \text{odd}}} \frac{e^{-B_{mn}^2 \tau}}{J_1^2(x_m)} J_0\left(\frac{x_m r}{R}\right) \cos\left(\frac{n\pi z}{H}\right),$$

where  $V$  is the volume of the cylinder,  $x_m$  is the  $m$ th zero of  $J_0(x)$ , and

$$B_{mn}^2 = \left(\frac{x_m}{R}\right)^2 + \left(\frac{n\pi}{H}\right)^2.$$

(b) Show that for  $H \gg \sqrt{\tau}$  the slowing down density along the axis of the tank, not near the top or bottom, is given by

$$\ln q = C - \frac{z^2}{4\tau},$$

where  $C$  is a known constant. [Hint: For part (a) see Problem 5-39.]

6-24. Based on age theory, what fraction of the neutrons emitted at the energy  $E_0$  slow down below  $E$  at distances greater than  $\sqrt{\tau(E_0 \rightarrow E)}$  from their point of birth?

6-25. (a) Show that if neutrons actually slowed down at the site of their first collision in hydrogen the age of neutrons from  $E_0$  to  $E$  would be

$$\tau(E_0 \rightarrow E) = \frac{1}{3\Sigma_s^2(E_0)},$$

where  $\Sigma_s(E)$  is the macroscopic scattering cross section of hydrogen. (b) Compare the age in water of 2-MeV neutrons to indium resonance computed from this formula with the measured age of fission neutrons.

6-26. Neutrons striking target nuclei of mass number  $A$  excite a level at the energy  $\epsilon$ . (a) If the angular distribution of the inelastic neutrons is isotropic in the center-of-mass system, show that

$$E' = \frac{E}{(A+1)^2} \left[ 1 + \frac{1}{\gamma^2} + \frac{2}{\gamma} \cos \theta \right],$$

where  $E$  and  $E'$  are the laboratory energies of the incident and inelastic neutrons, respectively,  $\theta$  is the angle of scattering in the center-of-mass system and  $\gamma$  is given by (cf. Problem 2-26)

$$\gamma = \frac{1}{A} \sqrt{\frac{AE}{AE - (A+1)\epsilon}}.$$

(b) What are the maximum and minimum energies of the inelastic neutrons in the laboratory? (c) Show that the inelastic probability distribution function  $P(E \rightarrow E')$  is given by

$$P(E \rightarrow E') = \frac{\gamma(A + 1)^2}{4E}.$$

(d) Compute the average energy of the inelastic neutrons in the laboratory system.

6-27. Show that in an inelastic collision the average increase in the lethargy  $\xi_i$  is given by the formula

$$\xi_i = \frac{\gamma - 1 + \ln x + e^{-x} + E_1(x)}{1 - (1 + x)e^{-x}},$$

in which  $\gamma = 0.5772$  is Euler's constant;  $x = E/T(E)$ , where  $E$  is the laboratory energy of the incident neutron and  $T(E)$  is the nuclear temperature; and  $E_1(x)$  is the exponential integral (see Appendix II).

6-28. Within the slab region  $-\frac{a}{2} \leq x \leq \frac{a}{2}$  of an infinite homogeneous moderator, fast neutrons are emitted uniformly at the rate of  $S$  neutrons/cm<sup>3</sup>-sec. Compute the slowing down density everywhere in the medium using Fermi age theory.

# 7

## Neutron Moderation with Absorption and Fission

In the preceding chapter it was assumed that neutrons interact only by elastic or inelastic scattering while slowing down. In fact, they may also be captured by the fuel or some other absorbing material, or they may induce fissions as the result of interactions with the fuel. Both of these processes have an obvious bearing on the criticality of a reactor and are considered in this chapter. The discussion is restricted to thermal reactors; methods for computing absorption and fission in other reactors are discussed in Chapter 10.

Considering absorption first, it will be recalled that this process occurs whenever a neutron undergoes a reaction such as  $(n, \gamma)$ ,  $(n, p)$ ,  $(n, \alpha)$ , etc. Among these possibilities, the  $(n, \gamma)$  reaction (radiative capture) is ordinarily the most important in thermal reactors. As discussed in Chapter 2, the radiative capture cross section,  $\sigma_\gamma$ , usually follows the  $1/v$  law at low energies; it is quite large in the resonance regions of intermediate and heavy nuclei, i.e., from about 1 eV to 1000 eV; and above the resonances it drops rapidly as  $1/E$  or faster to very low values. Most of the absorption of neutrons while they are slowing down occurs therefore at resonance energies.

### 7-1 Hydrogen and an Infinite Mass Absorber

The slowing down of neutrons in an absorbing medium cannot be handled analytically except in special cases. One of the simplest of these is an infinite medium, consisting of a uniform mixture of hydrogen and an infinitely heavy absorber, throughout which there are uniformly distributed sources emitting  $S$  fast neutrons per  $\text{cm}^3/\text{sec}$  at the energy  $E_0$ . In this problem, since the absorbing nucleus is infinitely heavy, it plays no part in the elastic slowing down of the neutrons; inelastic scattering by this nucleus is also ignored.

Consider now the continual arrival and departure of neutrons in the energy interval  $dE$  at  $E$ . These neutrons arrive in  $dE$  both as the result of single collisions at the source energy and from multiple collisions at energies between  $E$  and  $E_0$  (cf. Fig. 6-3). If  $E_0$  is well above the resonance region, which is true in all practical

cases, the source neutrons will not be absorbed on their first collision, and, from the argument given in Section 6-3,  $S dE/E_0$  of these neutrons will arrive per sec in  $dE$ . At the same time, there are  $F(E') dE'$  interactions/sec in the interval  $dE'$  above  $dE$  of which the fraction  $\Sigma_s(E')/[\Sigma_s(E') + \Sigma_a(E')]$  are elastic collisions with hydrogen. Thus  $F(E') dE' \Sigma_s(E')/[\Sigma_s(E') + \Sigma_a(E')]$  neutrons survive their interaction in  $dE'$  and the fraction  $dE'/E'$  are scattered into  $dE$ . In the steady state the number of neutrons falling into  $dE$  per sec is equal to the number which interact per sec in  $dE$ ; hence

$$F(E) dE = \frac{S dE}{E_0} + \int_E^{E_0} F(E') \frac{\Sigma_s(E')}{\Sigma_s(E') + \Sigma_a(E')} \frac{dE' dE}{E'}. \quad (7-1)$$

Upon canceling  $dE$  from both sides of the equation, the following integral equation is obtained for  $F(E)$ :

$$F(E) = \frac{S}{E_0} + \int_E^{E_0} F(E') \frac{\Sigma_s(E')}{\Sigma_s(E') + \Sigma_a(E')} \frac{dE'}{E'}. \quad (7-2)$$

This equation can be solved by differentiating with respect to  $E$ ; that is,

$$\frac{dF(E)}{dE} = - \frac{F(E)}{E} \frac{\Sigma_s(E)}{\Sigma_s(E) + \Sigma_a(E)}. \quad (7-3)$$

Preliminary to integrating Eq. (7-3), it is convenient to rearrange the equation in the following way:

$$\frac{dF(E)}{F(E)} = - \frac{dE}{E} + \frac{\Sigma_a(E)}{\Sigma_s(E) + \Sigma_a(E)} \frac{dE}{E}.$$

Integration of each term from  $E$  to  $E_0$  then gives

$$\ln \frac{F(E_0)}{F(E)} = - \ln \frac{E_0}{E} + \int_E^{E_0} \frac{\Sigma_a(E')}{\Sigma_s(E') + \Sigma_a(E')} \frac{dE'}{E'},$$

which is equivalent to

$$F(E) = \frac{F(E_0)E_0}{E} \exp \left[ - \int_E^{E_0} \frac{\Sigma_a(E')}{\Sigma_s(E') + \Sigma_a(E')} \frac{dE'}{E'} \right]. \quad (7-4)$$

The quantity  $F(E_0)$  can be found by placing  $E = E_0$  in Eq. (7-2) which gives  $F(E_0) = S/E_0$ . Equation (7-4) thus becomes

$$F(E) = \frac{S}{E} \exp \left[ - \int_E^{E_0} \frac{\Sigma_a}{\Sigma_s + \Sigma_a} \frac{dE'}{E'} \right], \quad (7-5)$$

where the energy dependence of  $\Sigma_s$  and  $\Sigma_a$  has been omitted for simplicity.

With absorption present in the system, the slowing-down density is obviously not a constant as it was in Sections 6-3 and 6-5, but it can be computed in exactly

the same way as it was earlier. Thus it is easy to show that

$$q(E) = \frac{SE}{E_0} + \int_E^{E_0} F(E') \frac{\Sigma_s(E')}{\Sigma_s(E') + \Sigma_a(E')} \frac{E}{E'} dE'. \quad (7-6)$$

Comparing Eq. (7-6) with Eq. (7-2) shows that

$$q(E) = EF(E), \quad (7-7)$$

so that in view of Eq. (7-5),

$$q(E) = S \exp \left[ - \int_E^{E_0} \frac{\Sigma_a}{\Sigma_s + \Sigma_a} \frac{dE'}{E'} \right]. \quad (7-8)$$

Now, if  $S$  source neutrons are emitted per  $\text{cm}^3/\text{sec}$  with energy  $E_0$ , and  $q(E)$  actually slow down below  $E$ , the quantity  $q(E)/S$  must be equal to the probability that a source neutron is *not* absorbed while slowing down from  $E_0$  to  $E$ . Since this absorption occurs primarily in resonances,  $q(E)/S$  is called the *resonance escape probability* and is denoted by  $p(E)$ . Therefore, for a mixture of hydrogen and an infinitely heavy nucleus,

$$p(E) = \frac{q(E)}{S} = \exp \left[ - \int_E^{E_0} \frac{\Sigma_a}{\Sigma_s + \Sigma_a} \frac{dE'}{E'} \right]. \quad (7-9)$$

As an example of the application of Eq. (7-9), consider the capture of neutrons in a single resonance at the energy  $E_1$ . Since the absorption cross section of hydrogen is small at resonance energies, only capture by the heavy absorber need be included. When Eq. (7-9) is written out in detail, the escape probability for this resonance,  $p_1$ , becomes

$$p_1 = \exp \left[ - \int_{E_1}^{E_0} \frac{N_A \sigma_{\gamma A}(E')}{N_H \sigma_{sH}(E') + N_A \sigma_{\gamma A}(E')} \frac{dE'}{E'} \right]. \quad (7-10)$$

Here  $N_A$  and  $N_H$  are the atom densities of absorber and hydrogen, respectively,  $\sigma_{\gamma A}$  is the radiative capture cross section of the absorber, and  $\sigma_{sH}$  is the scattering cross section of hydrogen. The subscript on the integral indicates that the integration is to be carried out over energies where  $\sigma_{\gamma A}$  is significantly different from zero.

To evaluate Eq. (7-10), it is necessary to substitute expressions for  $\sigma_{sH}$  and  $\sigma_{\gamma A}$ . However, since the major part of the integral comes from the region in the immediate vicinity of the resonance,  $\sigma_{sH}$  can be taken to be constant. The Breit-Wigner formula, with Doppler broadening, must be used for  $\sigma_{\gamma A}$ .

Although Doppler broadening must be included in the calculation of  $p_1$  for systems at room temperature or above, it is instructive to consider for a moment the evaluation of  $p_1$  when this effect is ignored. Near the resonance,  $\sigma_{\gamma A}$  is then

given by (cf. Eq. 2-93)

$$\sigma_{\gamma A} = \frac{\sigma_1 \Gamma_\gamma}{\Gamma} \frac{1}{1 + x^2}, \quad (7-11)$$

where

$$x = \frac{2}{\Gamma} (E - E_1) \quad (7-12)$$

and

$$\sigma_1 = \frac{4\pi \lambda_1^2 g \Gamma_n}{\Gamma}. \quad (7-13)$$

In these formulas,  $E$  is the energy in the center-of-mass system (which is equal to the laboratory energy of the neutron in an interaction with an intermediate or heavy nucleus),  $\Gamma_\gamma$  and  $\Gamma$  are the radiative and total widths of the resonance, respectively,  $\lambda_1$  is the neutron reduced wavelength corresponding to the energy  $E_1$ , and  $g$  is a statistical factor.

If the concentration of absorber in the medium is so low that

$$N_A \sigma_{\gamma A}(E) \ll N_H \sigma_{sH}, \quad (7-14)$$

the second term in the denominator of Eq. (7-10) can be ignored. This is known as the *infinite dilution* case and  $p_1$  is denoted by  $p_1^\infty$ . Since, according to Eq. (7-11), the maximum value of  $\sigma_{\gamma A}$  at an unbroadened resonance is  $\sigma_1 \Gamma_\gamma / \Gamma$ , Eq. (7-14) is equivalent to

$$\frac{N_A \sigma_1 \Gamma_\gamma}{\Gamma} \ll N_H \sigma_{sH}. \quad (7-15)$$

Equation (7-10) then reduces to

$$p_1^\infty = \exp \left[ - \frac{N_A}{N_H \sigma_{sH}} \int_{E_1} \sigma_{\gamma A}(E') \frac{dE'}{E'} \right]. \quad (7-16)$$

Except for a few resonances which occur at very low energy (for example, the 0.178-eV resonance in Cd<sup>113</sup> whose width is 0.113 eV), the width of an absorption resonance is much less than  $E_1$ . Little error is made therefore if the term  $1/E'$  in the integral is extracted as  $1/E_1$ ; thus

$$p_1^\infty = \exp \left[ - \frac{N_A}{N_H \sigma_{sH} E_1} \int_{E_1} \sigma_{\gamma A}(E') dE' \right]. \quad (7-17)$$

Inserting Eq. (7-11) results in

$$p_1^\infty = \exp \left[ - \frac{N_A \sigma_1 \Gamma_\gamma}{2 N_H \sigma_{sH} E_1} \int_{-\infty}^{\infty} \frac{dx}{1 + x^2} \right], \quad (7-18)$$

where the limits of integration have been arbitrarily extended from  $-\infty$  to  $\infty$  because the bulk of the integral comes from a small region in the vicinity of the

resonance. Performing the integration gives

$$p_1^\infty = \exp \left[ - \frac{\pi N_A \sigma_1 \Gamma_\gamma}{2 N_H \sigma_{sH} E_1} \right]. \quad (7-19)$$

With *finite dilution* and no Doppler broadening, Eq. (7-10) becomes

$$p_1 = \exp \left[ - \frac{N_A \sigma_1 \Gamma_\gamma}{2 N_H \sigma_{sH} E_1} \int_{-\infty}^{\infty} \frac{dx}{a^2 + x^2} \right], \quad (7-20)$$

where

$$a^2 = 1 + \frac{N_A \sigma_1 \Gamma_\gamma}{N_H \sigma_{sH} \Gamma}. \quad (7-21)$$

Carrying out the integration,  $p_1$  is now given by

$$p_1 = \exp \left[ - \frac{\pi N_A \sigma_1 \Gamma_\gamma}{2 N_H \sigma_{sH} E_1 a} \right]. \quad (7-22)$$

It will be observed that Eq. (7-22) properly reduces to Eq. (7-19) for infinite dilution, since  $a \rightarrow 1$  as  $N_H \sigma_{sH}/N_A \sigma_1 \rightarrow \infty$ .

When Doppler broadening is included, the Breit-Wigner formula is modified and becomes (cf. Eq. 2-112)

$$\sigma_{\gamma A} = \frac{\sigma_1 \Gamma_\gamma}{\Gamma} \psi(\xi, x), \quad (7-23)$$

where  $\psi(\xi, x)$  is a tabulated function and  $\xi$  is

$$\xi = \Gamma \left( \frac{A}{4 E_1 k T} \right)^{1/2}. \quad (7-24)$$

Consider first the infinite dilution\* case; then

$$p_1^\infty = \exp \left[ - \frac{N_A \sigma_1 \Gamma_\gamma}{2 N_H \sigma_{sH} E_1} \int_{-\infty}^{\infty} \psi(\xi, x) dx \right], \quad (7-25)$$

where Eq. (7-23) has been inserted into Eq. (7-17). It is not difficult to show that

$$\int_{-\infty}^{\infty} \psi(\xi, x) dx = \pi, \quad (7-26)$$

and so

$$p_1^\infty = \exp \left[ - \frac{\pi N_A \sigma_1 \Gamma_\gamma}{2 N_H \sigma_{sH} E_1} \right]. \quad (7-27)$$

This expression for  $p_1^\infty$  does not contain any temperature-dependent quantities,

---

\* The maximum value of  $\sigma_{\gamma A}$  at a Doppler-broadened resonance is  $\sigma_1 \Gamma_\gamma \psi(\xi, 0)/\Gamma$ , so that the condition for infinite dilution, Eq. (7-15), becomes  $N_A \sigma_1 \Gamma_\gamma \psi(\xi, 0)/\Gamma \ll N_H \sigma_{sH}$ .

and is, in fact, identical with Eq. (7-19), which was derived without taking Doppler broadening into account. It follows, therefore, that the escape probability, at least for a single resonance, is not a function of temperature in a sufficiently dilute mixture of hydrogen and an infinitely heavy absorber. This result could have been anticipated from the start, for in the infinitely dilute case,  $p_1$  depends only on the area under the resonance (cf. Eq. 7-17), and this area, as mentioned in Section 2-14, is independent of temperature. Incidentally, this conclusion regarding the

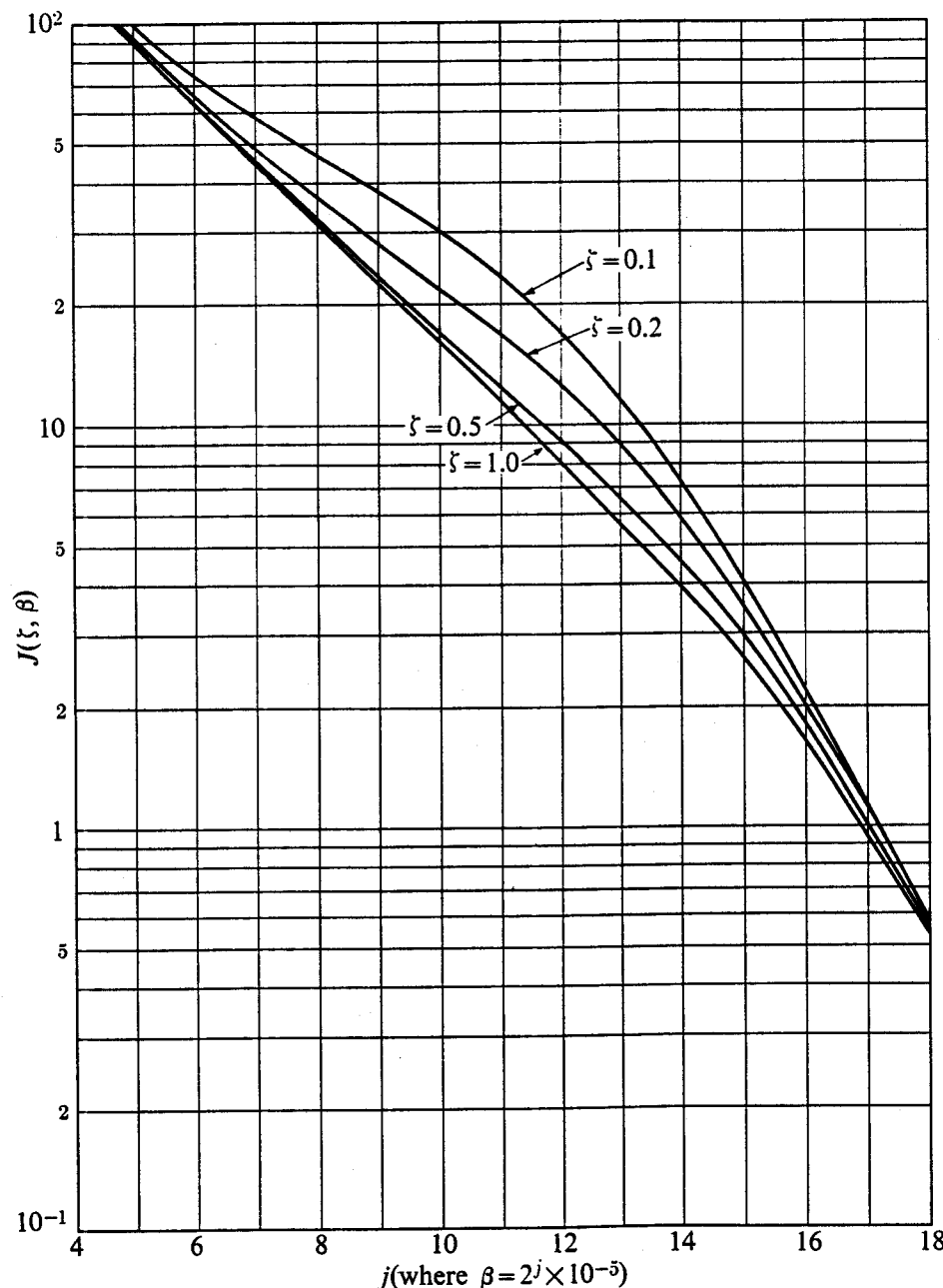


**Fig. 7-1.** The function  $J(\xi, \beta)$ . (From L. Dresner, *Resonance Absorption in Nuclear Reactors*. New York: Pergamon Press, 1960.)

temperature dependence of  $p_1$  is a very general one. Thus, it can be shown that the resonance escape probability is *always* independent of temperature, provided the mixture is sufficiently dilute.

With finite dilution, the integral in Eq. (7-10) can no longer be carried out analytically when Doppler broadening is included. The value of  $p_1$  is then usually expressed in the form

$$p_1 = \exp \left[ -\frac{\Gamma}{E_1} J(\xi, \beta) \right], \quad (7-28)$$

where  $J(\xi, \beta)$  is defined by the integral

$$J(\xi, \beta) = \int_0^\infty \frac{\psi(\xi, x) dx}{\beta + \psi(\xi, x)}, \quad (7-29)$$

and

$$\beta = \frac{N_H \sigma_{sH} \Gamma}{N_A \sigma_1 \Gamma_\gamma}. \quad (7-30)$$

The function  $J(\xi, \beta)$  is shown in Fig. 7-1.

It is important to note that in all the above formulas for  $p_1$ , the energy of the resonance  $E_1$  appears in the denominator of the exponential. Thus, all other things being equal, more neutrons are absorbed in a low-energy resonance than in a high-energy resonance. The reason for this is simply that the energy-dependent flux increases rapidly with decreasing energy and more neutrons are therefore available to interact with a lower-energy resonance. This result is true also for moderators other than hydrogen, as will be seen presently.

## 7-2 Moderators with $A > 1$ ; The NR and NRIM Approximations

For moderators with  $A > 1$ , an analytical solution to the slowing-down problem with absorption is not possible even if the mass of the absorber is assumed to be infinite. Good estimates of the escape probability for individual resonances can be determined, however, by one or the other of the two approximate methods discussed in this section. These methods can also be used if the moderator is hydrogen, and *must* be used in this case if it is not possible to assume, as in the preceding section, that the absorber is infinitely heavy.

**Resonance escape.** Consider again an infinite medium consisting of a homogeneous mixture of moderator and absorber, which contains uniformly distributed sources emitting  $S$  neutrons per  $\text{cm}^3/\text{sec}$  at the energy  $E_0$ . The total number of neutrons absorbed per  $\text{cm}^3/\text{sec}$  between  $E$  and  $E_0$  is given by

$$\text{Neutrons absorbed from } E \text{ to } E_0 = \int_E^{E_0} \Sigma_a(E') \phi(E') dE'.$$

Now, if  $S$  neutrons are emitted by the sources per  $\text{cm}^3/\text{sec}$ , the probability  $p(E)$

that a neutron survives to the energy  $E$  is evidently

$$\begin{aligned} p(E) &= \frac{S - \text{Neutrons absorbed from } E \text{ to } E_0}{S} \\ &= 1 - \frac{1}{S} \int_E^{E_0} \Sigma_a(E') \phi(E') dE'. \end{aligned} \quad (7-31)$$

Equation (7-31) is exact, and once the flux is known,  $p$  can be computed directly.\* Unfortunately, it is not possible to calculate  $\phi(E)$  analytically at energies within a resonance, and it is for this reason that it is necessary to resort to approximate methods. This is due to the fact that absorption acts much like a negative source and introduces transients, like those shown in Fig. 6-8, into the collision density and hence the flux. As is evident from the discussion in Section 6-5, these transients are very difficult to handle analytically. It will be recalled that the transients arise as the result of multiple scattering of the neutrons at energies near the source (in this case, a negative source). Thus it is the multiple scattering of the neutrons at energies within the resonance that is the underlying reason why analytical calculations of  $p$  cannot be made in general. In the methods discussed below, this multiple scattering is treated approximately. Before these methods are considered, however, the concept of the *practical width* must be introduced.

**The practical width.** Consider a homogeneous mixture of moderator and a heavy absorber, which has an isolated resonance at the energy  $E_1$ . The *practical width* of this resonance, which is denoted by  $\Gamma_P$ , is defined as the energy interval over which the resonance cross section, i.e., the sum of the cross sections for resonance absorption and resonance scattering, is greater than the macroscopic potential scattering cross section.† It will be recalled that at energies far from the resonance the total cross section is due only to potential scattering. It follows that  $\Gamma_P$  is a measure of the extent of the influence of the resonance, that is, the energy range over which the resonance is felt above the background potential scattering.

It is possible to obtain a simple formula for  $\Gamma_P$  in the case of a system which is at a temperature of 0°K. The cross sections are then given by the ordinary Breit-Wigner formulas without Doppler broadening. The absorption cross section is given by Eq. (2-93) and the resonance scattering cross section is given by

\* It may be noted that Eq. (7-31) can be used to compute  $p$  for a mixture of hydrogen and an infinitely heavy absorber, which was handled quite differently in Section 7-1 (cf. Prob. 7-8).

† The practical width has also been defined in the literature as (1) the energy interval over which the macroscopic *total* cross section is equal to twice the potential scattering cross section and (2) the energy interval over which the ratio  $\Sigma_a/(\Sigma_p + \Sigma_s)$  is greater than  $\frac{1}{2}$ . Both of these alternate definitions of  $\Gamma_P$  are equivalent to the definition given above for resonances which are primarily due to absorption, i.e., resonances at which  $\Gamma_\gamma \gg \Gamma_n$ . However, for resonances with  $\Gamma_\gamma < \Gamma_n$ , definition (1) gives larger values of  $\Gamma_P$ , while definition (2) gives  $\Gamma_P = 0$ .

the first term in Eq. (2-73). In the notation of these equations, the practical width is equal to the difference between the energies at which the equation

$$\frac{N_A \sigma_1}{1 + 4(E - E_1)^2/\Gamma^2} = \Sigma_p$$

is satisfied. Here

$$\Sigma_p = N_A \sigma_{pA} + N_M \sigma_{sM}$$

is the macroscopic potential scattering cross section of the mixture,  $N_A$  and  $N_M$  are the atom densities of the absorber and moderator, respectively,  $\sigma_{pA}$  is the potential scattering cross section of the absorber ( $\sigma_{pA} \approx 4\pi R^2$ ), and  $\sigma_{sM}$  is the scattering (which is all potential scattering) cross section of the moderator. Substituting  $E = E_1 \pm \frac{1}{2}\Gamma_P$  into this relation and anticipating that  $\Gamma_P/\Gamma \gg 1$ , gives the useful formula

$$\Gamma_P = \Gamma \sqrt{\frac{N_A \sigma_1}{\Sigma_p}}.$$

As a specific example of the use of this formula, consider the first resonance in  $U^{238}$  at  $E_1 = 6.67$  eV for a mixture of  $U^{238}$  and hydrogen with  $N_U = N_H$ . For this resonance  $\Gamma = 0.027$  eV,  $\sigma_1 = 21,000$  b,  $\sigma_p(U^{238}) \approx 10$  b,  $\sigma_H \approx 20$  b, and the above formula gives  $\Gamma_P = 0.72$  eV. Thus  $\Gamma_P$  is considerably larger than  $\Gamma$ . This is the usual situation. The practical width is generally from about ten to thirty times the natural width, although its exact value depends on the concentration of the absorber and the temperature of the system. Ordinarily, however, as shown in the problems at the end of the Chapter,  $\Gamma_P$  is not a sensitive function of the temperature.

**The narrow resonance (NR) approximation.** If the average energy loss in an elastic collision with either the moderator or the absorber is much larger than the practical width of a resonance, it is very unlikely that a neutron will have a second collision within the resonance and be absorbed. At energies relevant to calculations of resonance escape, scattering is isotropic in the center-of-mass system, and the average energy loss is  $(1 - \alpha)E/2$  (cf. Section 6-1). The requirement that a neutron will have no more than one collision in a resonance at  $E_1$  is therefore

$$\Gamma_P \ll \frac{(1 - \alpha)E_1}{2}, \quad (7-32)$$

where  $\alpha$  refers both to the absorber and to the moderator. This is the principal assumption in the *narrow resonance (NR) approximation*; its validity will be considered later in this section.

Consider now an energy interval  $dE$  within the resonance. In view of the narrow resonance assumption, neutrons can only arrive in  $dE$  as the result of collisions

at energies *above* the resonance; neutrons which interact within the resonance are either absorbed or are scattered out of the resonance. However, neutrons with energies above the resonance obviously have no way of knowing whether there is a nucleus in the system with a resonance at a lower energy, and the number of neutrons scattered into  $dE$  is therefore the same whether the resonance is present or not. This number is equal to  $F(E) dE$ , where  $F(E)$  is the collision density in the *absence* of the resonance. Furthermore, if the resonance is located in the asymptotic region of the collision density,  $F(E) dE = S dE / \bar{\xi}(E) E$ , in which  $\bar{\xi}(E)$  includes scattering by both moderator and absorber and is computed at the energy  $E$  in the absence of the resonance. In particular,  $\bar{\xi}(E)$  is given by

$$\bar{\xi}(E) = \frac{\xi_M \Sigma_{sM} + \xi_A \Sigma_{pA}}{\Sigma_{sM} + \Sigma_{pA}}, \quad (7-33)$$

where the subscripts M and A again refer to the moderator and absorber, respectively, and  $\Sigma_{pA}$  is the macroscopic potential scattering cross section of the absorber.

In the steady state the number of neutrons which arrive in  $dE$  must be equal to the number that interact in  $dE$ , namely,  $\Sigma_t(E)\phi(E) dE$ , where  $\Sigma_t(E)$  is the macroscopic total cross section. It follows that

$$\frac{S}{\bar{\xi}(E) E} = \Sigma_t(E)\phi(E),$$

and so

$$\phi(E) = \frac{S}{\bar{\xi}(E) E \Sigma_t(E)}. \quad (7-34)$$

Inserting  $\phi(E)$  from Eq. (7-34) into Eq. (7-31), the result is

$$p_1 = 1 - \int_{E_1} \frac{\Sigma_a(E')}{\Sigma_t(E')} \frac{dE'}{\bar{\xi}(E') E'}.$$

It is reasonable to assume that  $\Sigma_{sM}$  is constant over the resonance;  $\Sigma_{pA}$  is also constant, and therefore so is  $\bar{\xi}$ . Then, after extracting  $1/E'$  as  $1/E_1$ , as in Section 7-1, Eq. (7-34) reduces to

$$p_1 = 1 - \frac{1}{\bar{\xi} E_1} \int_{E_1} \frac{\Sigma_a(E')}{\Sigma_t(E')} dE'. \quad (7-35)$$

When this equation is written out in terms of microscopic cross sections, it becomes

$$p_1 = 1 - \frac{1}{\bar{\xi} E_1} \int_{E_1} \frac{N_A \sigma_{\gamma A}(E') dE'}{N_M \sigma_{sM}(E') + N_A \sigma_{sA}(E') + N_A \sigma_{\gamma A}(E')}. \quad (7-36)$$

To evaluate Eq. (7-36), the Doppler-broadened cross sections must be substituted for  $\sigma_{\gamma A}$  and  $\sigma_{sA}$ ;  $\sigma_{sM}$  can be taken to be constant. Again, however, as in

the earlier discussion of hydrogen, it is instructive to consider the nonbroadened case first. Then  $\sigma_{\gamma A}$  is given by Eq. (7-11), and according to Eq. (2-73),  $\sigma_{sA}$  is

$$\sigma_{sA} = \frac{\sigma_1 \Gamma_n}{\Gamma} \frac{1}{1+x^2} + \frac{2\sigma_1 R}{\lambda_1} \frac{x}{1+x^2} + 4\pi R^2. \quad (7-37)$$

It may be recalled from Section 2-8 that the first and last terms in Eq. (7-37) are due to resonance scattering and potential scattering, respectively, while the middle term arises as the result of interference between these two interaction modes. Inserting Eqs. (7-11) and (7-37) into Eq. (7-36) yields

$$p_1 = 1 - \frac{N_A \sigma_1 \Gamma_\gamma}{2 N_M \sigma_{sM} \bar{\xi} E_1} \int_{-\infty}^{\infty} \frac{dx}{ax^2 + bx + c}, \quad (7-38)$$

where

$$a = 1 + \frac{4\pi R^2 N_A}{N_M \sigma_{sM}}, \quad (7-39)$$

$$b = \frac{2N_A \sigma_1 R}{N_M \sigma_{sM} \lambda_1}, \quad (7-40)$$

$$c = a + \frac{N_A \sigma_1}{N_M \sigma_{sM}}. \quad (7-41)$$

The integral in Eq. (7-38) can easily be carried out, and  $p_1$  is

$$p_1 = 1 - \frac{\pi N_A \sigma_1 \Gamma_\gamma}{2 N_M \sigma_{sM} \bar{\xi} E_1} \frac{1}{\sqrt{ac - b^2/4}}. \quad (7-42)$$

When Doppler broadening is included,  $\sigma_{\gamma A}$  is given by Eq. (7-23) and  $\sigma_{sA}$  is (cf. Eq. 2-116)

$$\sigma_{sA} = \frac{\sigma_1 \Gamma_n}{\Gamma} \psi(\xi, x) + \frac{\sigma_1 R}{\lambda_1} x(\xi, x) + 4\pi R^2, \quad (7-43)$$

where  $\psi(\xi, x)$  and  $x(\xi, x)$  are tabulated functions. In this case, the integral in Eq. (7-36) cannot be evaluated analytically. In many practical cases, however, the interference term in Eq. (7-43) can be neglected and  $p_1$  can then be expressed in the form

$$p_1 = 1 - \frac{\Gamma_\gamma}{\bar{\xi} E_1} J(\xi, \beta), \quad (7-44)$$

where  $J(\xi, \beta)$  is defined by Eq. (7-29) and  $\beta$  is now

$$\beta = \frac{N_M \sigma_{sM}}{N_A \sigma_1} + \frac{4\pi R^2}{\sigma_1}. \quad (7-45)$$

**The narrow resonance-infinite mass (NRIM) approximation.\*** There are a number of important situations, particularly at low-energy resonances, where the average energy loss in a scattering collision with the absorber is *not* large compared with the practical width. In this case, the neutron may be scattered more than once within the resonance. However, if this energy loss is *small* compared with  $\Gamma_P$ , it is reasonable to ignore scattering by the absorber altogether. This is equivalent to assuming that the mass of the absorber is infinite. Thus, in the NRIM approximation it is required that

$$\Gamma_P \gg \frac{(1 - \alpha_A)E_1}{2}, \quad (7-46)$$

where  $\alpha_A$  refers to the absorber. It is still necessary that  $\Gamma_P$  be small compared with the energy loss in collisions with the moderator; i.e., Eq. (7-32) must still hold for the moderator.

As a practical matter, the only difference between the NRIM and NR methods is that the scattering cross section of the absorber is omitted from the formulas for  $p_1$ . Thus, omitting  $\sigma_{sA}$  from Eq. (7-36) results in

$$p_1 = 1 - \frac{1}{\bar{\xi}E_1} \int_{E_1}^{\infty} \frac{N_A \sigma_{\gamma A}(E') dE'}{N_M \sigma_{sM}(E') + N_A \sigma_{\gamma A}(E')} . \quad (7-47)$$

In Eq. (7-47),  $\bar{\xi}$  includes scattering only by the moderator.

Treating the non-Doppler case first,  $p_1$  is now given by the integral

$$p_1 = 1 - \frac{N_A \sigma_1 \Gamma_\gamma}{2N_M \sigma_{sM} \bar{\xi} E_1} \int_{-\infty}^{\infty} \frac{dx}{a^2 + x^2} , \quad (7-48)$$

where

$$a^2 = 1 + \frac{N_A \sigma_1 \Gamma_\gamma}{N_M \sigma_{sM} \Gamma} . \quad (7-49)$$

Performing the integration gives

$$p_1 = 1 - \frac{\pi N_A \sigma_1 \Gamma_\gamma}{2N_M \sigma_{sM} \bar{\xi} E_1 a} . \quad (7-50)$$

When Doppler broadening is included,  $p_1$  can again be expressed in terms of the  $J(\zeta, \beta)$  function; i.e.,

$$p_1 = 1 - \frac{\Gamma}{\bar{\xi} E_1} J(\zeta, \beta), \quad (7-51)$$

where now

$$\beta = \frac{N_M \sigma_{sM} \Gamma}{N_A \sigma_1 \Gamma_\gamma} . \quad (7-52)$$

---

\* The NRIM method was originally called the NRIA method. Because of the possibility of interpreting "IA" as "infinite absorption" rather than "infinite mass absorber," the original notation has been largely discarded.

It is interesting to compare Eqs. (7-50) and (7-51) of the NRIM method with the exact results of Section 7-1 for hydrogen and an infinitely heavy absorber [cf. Eqs. (7-22) and (7-28)]. With  $N_M\sigma_{sM} = N_H\sigma_{sH}$ , it will be observed that Eqs. (7-50) and (7-51) are merely the first two terms in the expansion of the exponential in the hydrogen problem. It may be concluded therefore that the NRIM approximation (and this is true also for the NR approximation) is valid only when the probability of absorption is small, that is, when  $p_1$  is close to unity.

**Comparison of NR and NRIM approximations.** The NR and NRIM approximations differ only in the way in which scattering within the resonances of the absorbing nuclei is taken into account. Since a neutron loses, on the average, the energy  $\frac{1}{2}(1 - \alpha)E$ , where  $E$  is its initial energy, it follows that it loses more energy in a collision at a high-energy resonance than at a low-energy resonance. Other things being equal, therefore, it is more likely that as the result of such a collision a neutron will be knocked out of a resonance at high energy than at low energy. In short, it is more likely that Eq. (7-32) will be valid at the higher-energy resonances than Eq. (7-46), and, conversely, Eq. (7-46) is more likely to be valid for the lower-energy resonances than Eq. (7-32). Thus it may be expected that the NR approximation would be more appropriate for the higher-energy resonances, while the NRIM approximation would be more appropriate for the lower-energy resonances.

That this conclusion is borne out in practice may be seen from Table 7-1, where the results of NR, NRIM, and exact calculations are shown for the 6.67-eV and 273.7-eV resonances of  $U^{238}$ , for a mixture of  $U^{238}$  and hydrogen with  $N_U = N_H$  at room temperature. The quantities  $1 - p$  are given rather than  $p$  in order to magnify the differences between the numerical values. The exact values were obtained using a numerical method to be discussed in Section 7-6. Also shown in the table are the natural and practical widths of the resonances and the average energy losses of neutrons having collisions with hydrogen and  $U^{238}$  at the energies

Table 7-1

Comparison of NR and NRIM Methods with Exact Values of the Escape Probabilities at Individual Resonances

Resonance energy, eV	$\Gamma$ , eV	$\Gamma_p$ , eV	Average energy loss, eV		Values of $1 - p$		
			H	U	NR	NRIM	Exact*
6.67	0.027	0.72	3.34	0.0551	0.2376	0.1998	0.1963
273.7	0.048	0.62	136.8	2.27	0.004185	0.005208	0.004408

\* Courtesy of B. R. Sehgal, Brookhaven National Laboratory.

of the resonances. In both cases, it will be observed that the average energy loss in a collision with the hydrogen is larger than  $\Gamma_P$ . On the other hand, the energy loss in a collision with the uranium is smaller than  $\Gamma_P$  for the 6.67-eV resonance but larger than  $\Gamma_P$  for the 273.7-eV resonance. It is no surprise, therefore, to observe that the NRIM calculation is more accurate than the NR calculation for the 6.67-eV resonance, while the converse is true for the 273.7-eV resonance.

### 7-3 Temperature Dependence of Resonance Escape

According to the formulas for the resonance escape probability derived in the preceding sections,  $p$  is a function of temperature except in dilute systems. This variation with temperature is illustrated in Fig. 7-2, where  $p_1$  is shown for the 6.67-eV resonance of  $U^{238}$  as computed by the NRIM method for three different  $U^{238}$ -hydrogen mixtures. It will be observed that in every case  $p_1$  decreases with increasing temperature, that is, *the absorption of neutrons in the resonance increases with temperature*.

To understand physically the temperature dependence of resonance absorption, it is instructive to consider a hypothetical resonance which is rectangular in shape as shown in Fig. 7-3. This resonance has the Doppler-broadened width  $w$  and height  $\sigma_{\gamma 0}$ . It is assumed that as the temperature increases  $w$  increases and  $\sigma_{\gamma 0}$

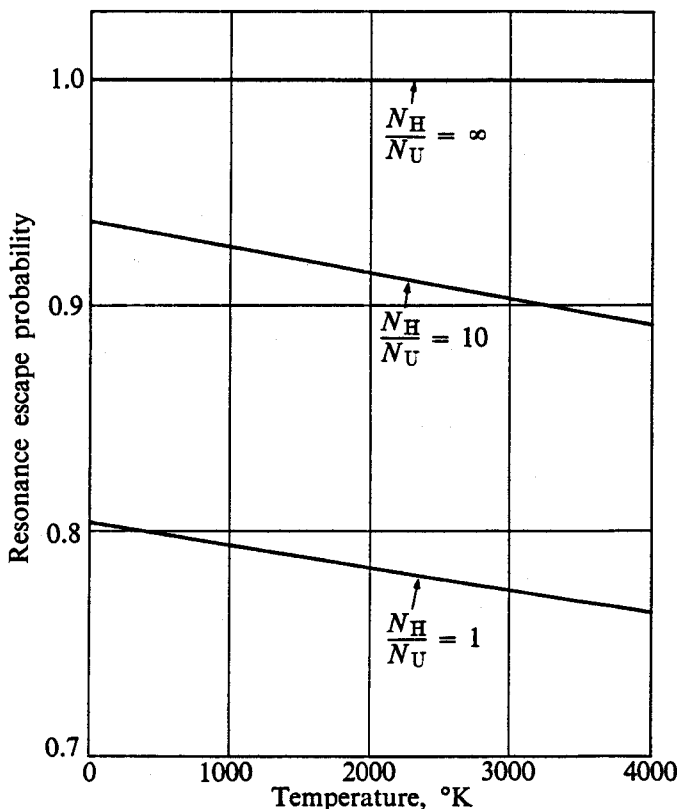


Fig. 7-2. The escape probability for the 6.67-eV resonance of  $U^{238}$  as a function of temperature for various concentrations of uranium in an infinite hydrogen moderator.

decreases in such a way that the total area under the resonance  $\sigma_{\gamma 0}w$  remains constant. Thus this simple resonance is assumed to behave with temperature in the same way as does an actual resonance.

Consider now the value of  $p_1$  as computed by the NRIM method, i.e., using Eq. (7-47). In the dilute case, that is, when  $N_A\sigma_{\gamma 0} \ll N_M\sigma_{sM}$ , the integral in Eq. (7-47) is proportional to  $\sigma_{\gamma 0}w$ , and  $p_1$  is independent of temperature. With finite dilution, on the other hand, Eq. (7-47) gives

$$p_1 = 1 - \frac{1}{\bar{\xi}E_1} \frac{N_A\sigma_{\gamma 0}w}{N_M\sigma_{sM} + N_A\sigma_{\gamma 0}}. \quad (7-53)$$

The numerator in the second term of this expression is again independent of temperature. However, the denominator *decreases* with increasing temperature, and as a result  $p_1$  also decreases. This, of course, is just the behavior of  $p_1$  which is shown in Fig. 7-2.

The origin of the increased absorption is evidently in the factor

$$\frac{1}{N_M\sigma_{sM} + N_A\sigma_{\gamma 0}} = \frac{1}{\Sigma_t}$$

in Eq. (7-53). According to Eq. (7-34), this factor is proportional to the flux within the resonance, and it follows that *as the temperature increases, the flux in a resonance increases*. This is quite reasonable on physical grounds. Thus as the temperature rises, the resonance broadens, the absorption cross section goes down and so naturally the flux in the resonance increases. It is this increased flux at the resonance rather than the broadening of the resonance itself (although they are related, of course) which ultimately is the origin of the increase in resonance absorption with temperature.

Although this discussion has been limited to a single resonance and computations based on the NRIM method, the above conclusions are valid for any sequence of resonances, and they do not depend on a particular model for computing  $p$ . The increase in resonance absorption with temperature will be considered again in Chapter 13, where it will be shown that this phenomenon has an important bearing on the safety of reactor operation.

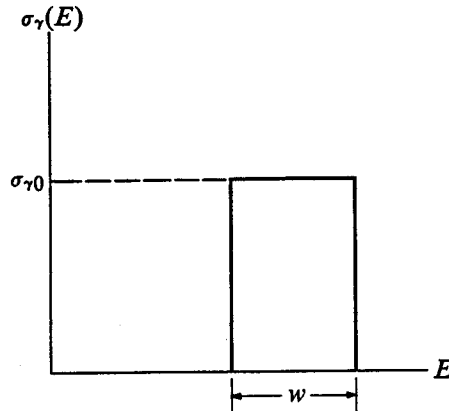


Fig. 7-3. A hypothetical rectangular resonance.

#### 7-4 Widely Spaced and Narrow Resonances

In practice, it is always necessary to deal with absorbers having many resonances. Such a sequence of resonances can be handled in a straightforward way provided that they are all narrow or wide in the sense of the NR and NRIM approximations, and provided that they are also well separated in energy. The second requirement is necessary because if the resonances were too close together, the moderation transients introduced into the collision density due to absorption at one resonance

would persist into the region of another resonance. In particular, if a second resonance at the energy  $E_2$  lies in the transient "wake" of the resonance at  $E_1$ , that is, if  $\alpha^3 E_1 \lesssim E_2 < E_1$ , the escape probability for the second resonance cannot be calculated analytically. However, if the resonances are sufficiently separated so that every resonance lies in an asymptotic region of the collision density, each resonance can be calculated independently using the formulas derived in Sections 7-1 and 7-2. The escape probability  $p_i$  for the  $i$ th resonance at the energy  $E_i$  is then given by

$$p_i = 1 - \int_{E_i} \frac{\Sigma_a}{\Sigma_s + \Sigma_a} \frac{dE}{\xi E}, \quad (7-54)$$

where scattering by the absorbing nucleus is included in  $\Sigma_s$  in the NR approximation and is omitted in the NRIM approximation.

The probability that a neutron will not be captured in any of a sequence of  $N$  independent resonances is clearly the product of the escape probabilities for all resonances; that is,

$$\begin{aligned} p &= p_1 p_2 p_3 \cdots p_N \\ &= \prod_{i=1}^N \left[ 1 - \int_{E_i} \frac{\Sigma_a}{\Sigma_s + \Sigma_a} \frac{dE}{\xi E} \right]. \end{aligned} \quad (7-55)$$

This expression can be written more succinctly by taking logarithms of both sides of the equation:

$$\ln p = \sum_{i=1}^N \ln \left[ 1 - \int_{E_i} \frac{\Sigma_a}{\Sigma_s + \Sigma_a} \frac{dE}{\xi E} \right]. \quad (7-56)$$

The integrals in the bracket are usually much less than unity, and using the first term in the expansion of the logarithm, that is,  $\ln(1 + x) \approx x$ , Eq. (7-56) becomes

$$\ln p = - \sum_{i=1}^N \int_{E_i} \frac{\Sigma_a}{\Sigma_s + \Sigma_a} \frac{dE}{\xi E}. \quad (7-57)$$

The summation sign and the subscripts on the integrals can now be dropped with the understanding that the integration extends over the entire region of discrete resonances. Equation (7-57) then reduces to

$$p = \exp \left[ - \int \frac{\Sigma_a}{\Sigma_s + \Sigma_a} \frac{dE}{\xi E} \right]. \quad (7-58)$$

In using Eq. (7-58) it is customary to separate the scattering cross section of the absorber into the anomalous-scattering cross section  $\sigma'_{sA}$ , namely, the first two terms of Eq. (7-37) or (7-43), and the potential-scattering cross section  $\sigma_{pA}$ , the last term in these equations. Then  $p$  can be written as

$$p = \exp \left[ - \int \frac{N_A \sigma_{\gamma A}}{N_M \sigma_{sM} + N_A (\sigma'_{sA} + \sigma_{pA} + \sigma_{\gamma A})} \frac{dE}{\xi E} \right]. \quad (7-59)$$

If, as usual,  $\sigma_{sM}$  is assumed to be constant in the resonance region, then  $\bar{\xi}$  is also constant (cf. Eq. 7-33), and Eq. (7-59) can be written as

$$p = \exp \left[ - \frac{N_A}{\bar{\xi} \Sigma_p} \int \frac{\sigma_{\gamma A}}{1 + (N_A/\Sigma_p)(\sigma'_{sA} + \sigma_{\gamma A})} \frac{dE}{E} \right], \quad (7-60)$$

where  $\Sigma_p$  is the (constant) cross section

$$\Sigma_p = N_A \sigma_{pA} + \Sigma_{sM}. \quad (7-61)$$

It is understood, of course, that  $\sigma'_{sA}$  and  $\sigma_{pA}$  are to be omitted from Eqs. (7-60) and (7-61) (the NRIM approximation) for low-energy resonances.

It will be noted that the integral in Eq. (7-60) depends upon the nature of the absorber (through the quantities  $\sigma'_{sA}$  and  $\sigma_{\gamma A}$ ) and upon the *dilution factor*,  $N_A/\Sigma_p$ , but does not depend explicitly upon the moderator. Hence homogeneous mixtures containing a specified resonance absorber will have the same integral, provided they all have the same value of  $N_A/\Sigma_p$ . This integral is known as the *effective resonance integral* (in this case, for a sequence of widely spaced resonances) and is denoted by the symbol  $I$ , that is,

$$I = \int \frac{\sigma_{\gamma A}}{1 + (N_A/\Sigma_p)(\sigma'_{sA} + \sigma_{\gamma A})} \frac{dE}{E}. \quad (7-62)$$

Equation (7-60) then becomes

$$p = \exp \left[ - \frac{N_A I}{\bar{\xi} \Sigma_p} \right] = \exp \left[ - \frac{N_A I}{\xi_A \Sigma_{pA} + \xi_M \Sigma_{sM}} \right]. \quad (7-63)$$

Unfortunately, all resonances are not isolated and, indeed, at high energies the resonances overlap. Analytical expressions for the escape probability for this end of the resonance region have been given in the literature but will not be discussed here. In any event, it must be emphasized that Eqs. (7-62) and (7-63) by themselves do not give the entire resonance escape probability for actual absorbers. Nevertheless, these equations are of great importance for they suggest an analytical form which is useful in correlating experimental data and exact numerical computations of resonance escape (cf. Sections 7-6 and 7-7).

## 7-5 Slowing Down with Weak Absorption

If the absorption cross section is very small, the slowing down of neutrons can be estimated in the following way. Because of the absorption, the slowing-down density is clearly smaller at  $E - dE$  than at  $E$ . This decrease is equal to the number of neutrons absorbed in the interval  $dE$ , namely,  $\phi(E)\Sigma_a(E)dE$ , so that

$$dq(E) = \phi(E)\Sigma_a(E)dE. \quad (7-64)$$

The flux  $\phi(E)$  in the presence of absorption is not known, of course, but if the

absorption is very weak, it is possible to write from Eq. (6-41) that

$$\phi(E) \approx q(E)/\bar{\xi}E\Sigma_s(E).$$

Inserting this into Eq. (7-64) and carrying out the integration gives

$$q(E) = S \exp \left[ - \int_E^{E_0} \frac{\Sigma_a}{\Sigma_s} \frac{dE'}{\bar{\xi}E'} \right], \quad (7-65)$$

where  $q(E_0) = S$  is the source density. The probability  $p(E)$  that a neutron will escape capture in slowing down to the energy  $E$  is given by

$$p(E) = \frac{q(E)}{S} = \exp \left[ - \int_E^{E_0} \frac{\Sigma_a}{\Sigma_s} \frac{dE'}{\bar{\xi}E'} \right]. \quad (7-66)$$

In view of its derivation, Eq. (7-66) would not be expected to be valid in the neighborhood of strongly absorbing resonances. Nevertheless, it is interesting (and also somewhat disconcerting) to note the similarity between Eqs. (7-58) and (7-66). Thus when  $\Sigma_a \ll \Sigma_s$ , Eq. (7-58) reduces to Eq. (7-66) despite the fact that Eq. (7-58) was derived specifically for sharp resonances.

## 7-6 Numerical Computations of Resonance Escape

According to Eq. (7-31),  $p$  can be rigorously computed once the energy-dependent flux is known. This is true regardless of the nature of the resonances, that is, whether or not they are narrow, closely spaced, and so on. For the reasons mentioned earlier, however,  $\phi(E)$  cannot be calculated exactly by analytical methods. Fortunately, it can be computed numerically, and as a consequence it is possible to determine  $p$  as accurately as the nuclear data permits.

As a first step, it is necessary to set up an exact equation for determining  $\phi(E)$ . For simplicity, it will be assumed that the system, which again is taken to be uniform and infinite, consists of a mixture of a single-nuclide moderator such as graphite and one species of absorber. The results can easily be generalized to more complicated mixtures of nuclides.

Consider now an energy interval  $dE$  at  $E$ . By the argument which has been used repeatedly in earlier sections, the number of neutrons scattered into  $dE$  per  $\text{cm}^3/\text{sec}$  from elastic collisions with the moderator is

$$\int_E^{E/\alpha_M} \frac{\Sigma_{sM}(E')\phi(E') dE' dE}{(1 - \alpha_M)E'},$$

where  $\alpha_M$  is the collision parameter for the moderator. A similar expression, with the subscript M replaced by A, holds for elastic collisions with the absorber. Since in the steady state the total number of neutrons falling into  $dE$  is equal to the

number interacting in  $dE$ , it follows that  $\phi$  must satisfy the following integral equation:

$$\begin{aligned}\Sigma_t(E)\phi(E) = & \frac{1}{1 - \alpha_M} \int_E^{E/\alpha_M} \Sigma_{sM}(E')\phi(E') \frac{dE'}{E'} \\ & + \frac{1}{1 - \alpha_A} \int_E^{E/\alpha_A} \Sigma_{sA}(E')\phi(E') \frac{dE'}{E'},\end{aligned}\quad (7-67)$$

where  $\Sigma_t$  is the total cross section.

In deriving Eq. (7-67), it was assumed that the interval  $dE$  is at energies sufficiently below the source energy so that neutrons cannot reach  $dE$  in one collision. If this is not the case, an appropriate source term must be added to the equation. In particular, if the moderator is hydrogen, this term is  $S/E_0$ , where  $S$  and  $E_0$  are the source density and energy, respectively.

Equations of the form of Eq. (7-67) can be handled directly by machine computation. (As a practical matter, the form of the equation can be improved considerably prior to programming for a computer.) The details of this procedure are discussed in the references at the end of the chapter. (See, in particular, the articles by Nordheim.)

If the absorption occurs in discrete resonances, it is convenient to compute  $\phi(E)$  from Eq. (7-67) for each resonance separately. The escape probability for the  $i$ th resonance is then

$$p_i = 1 - \frac{1}{S} \int_{E_i} \Sigma_a(E)\phi(E) dE,$$

where the integration is carried out over the resonance. If, in addition, the absorption is small at each resonance, the total resonance escape probability  $p$  is given by

$$p = \prod p_i \approx \exp \left[ - \frac{N_A I}{\xi \Sigma_p} \right], \quad (7-68)$$

where  $\Sigma_p$  is defined by Eq. (7-61) and  $I$  is the resonance integral

$$I = \frac{\xi \Sigma_p}{S} \int \sigma_a(E)\phi(E) dE. \quad (7-69)$$

Equation (7-69) can be used to obtain an interesting physical interpretation of the resonance integral. Thus let it be supposed that the flux in the resonance region is equal to its value in the *absence* of the resonances, namely,  $\phi(E) = S/\xi E \Sigma_p$ , but that the actual absorption cross section is modified from  $\sigma_a(E)$  to an effective value  $[\sigma_a(E)]_{\text{eff}}$ , so that the integral in Eq. (7-69) remains unchanged. When these functions are substituted into Eq. (7-69) this reduces to

$$I = \int [\sigma_a(E)]_{\text{eff}} \frac{dE}{E},$$

### \* Room temperature.

$a$	$b$	$c$
8.33	2.73	0.486
U <sub>238</sub>	Th <sub>232</sub>	0.253

The Parameters  $a$  and  $c$  in the Formula for  $I$  of  $U^{238}$  and  $Th^{232}*$

Table 7-2

It was shown earlier (cf. Eq. 7-62) that the resonance escape probability for a sequence of widely spaced resonances can be written in terms of an effective resonance integral  $I$  which depends only on the absorber and the dilution factor  $N_A/Z^2$ , but not on the nature of the moderator. This conclusion has been found to be approximately valid for the experimental values of  $p$ , which, of course,

The resonance escape probability is usually measured by observing the activity induced in an absorber as the result of resonance capture. To find the resonance escape probability for a mixture of  $U_{238}$  and moderator, for example, thin rods of this isotope are placed in a moderating medium containing known sources of fast neutrons and the activity of the  $U_{239}$  ( $T_{1/2} = 23 \text{ min}$ ) formed by neutron capture in  $U_{238}$  is measured. In the taking of these measurements the uranium rods must be wrapped in sheets of a strong thermal neutron absorber such as cadmium to eliminate the activity induced by thermal neutron absorption. The measured activity is then caused primarily by resonance absorption. A comparison of the induced activity with the known source strength gives the resonance escape probability directly.

## 7-7 Measurements of Resonance Escape

It may be mentioned that it is possible to derive the NR and NRM formulas for  $p$ , which were discussed in Section 7-2, by replacing  $\phi(E)$  in the integrals in Eq. (7-67) by appropriate asymptotic functions. This procedure is discussed in the problems and will be reconsidered in Chapter 11 in connection with the calculation of the resonance escape probability for heterogeneous reactor lattices.

It follows from this result that the resonance region over which it is necessary to account for absorption cross section in the region where the absorption rate in a given region is equal to the integral of the observed neutron absorption rate in a flux equal to that existing in the absence of the resonances. If, for example,  $\phi_0$  is the (constant) asymptotic flux per unit lethargy in the resonance region in the presence of the resonances, the total number of neutrons absorbed in this region per  $\text{cm}^3/\text{sec}$  in the presence of the resonances

or in terms of lethargy

include absorption in *all* resonances. For this reason, it is usual to write  $p$  in the form of Eq. (7-63), namely,

$$p = \exp \left[ - \frac{N_A I}{\xi \Sigma_p} \right], \quad (7-70)$$

where  $I$  is now regarded as a measured parameter.

The experimental and theoretical values of  $I$  for  $\text{U}^{238}$  and  $\text{Th}^{232}$ , two of the most important resonance absorbers, can be represented by an equation of the type

$$I = a \left( \frac{\Sigma_p \times 10^{24}}{N_A} \right)^c \quad (7-71)$$

where  $I$  is in barns and the parameters  $a$  and  $c$  are given in Table 7-2. It will be observed from Eq. (7-71) that  $I$  increases as the concentration of absorber in the system decreases. This is clearly to be anticipated on the basis of Eq. (7-62). However, substituting Eq. (7-71) into Eq. (7-70) gives

$$p = \exp \left[ - \frac{a}{\xi} \left( \frac{N_A}{\Sigma_p \times 10^{24}} \right)^{1-c} \right]. \quad (7-72)$$

which shows that  $p$  actually increases as the concentration of the absorber decreases, as would be expected physically.

### 7-8 Space-Dependent Moderation with Absorption

Up to this point the discussion of neutron moderation has been confined to infinite systems containing uniformly distributed sources. A little reflection will show, however, that these results are actually more general than they might appear at first. In particular, the formulas for the resonance escape probability derived in the preceding sections remain valid for *any* distribution of sources, provided the medium is still uniform and infinite. This is simply due to the fact that a neutron slowing down in the medium has no way of knowing whether there are other neutrons in the system or not; nor is it relevant to its own absorption probability. The formulas for  $p$  do not hold, of course, if the medium is finite in size or if the resonance absorbers are nonuniformly distributed in the system. The value of  $p$  then depends on the location of the source. A neutron emanating from a source near the surface of a reactor, for instance, is more likely to escape from the system before being absorbed than a similar neutron emitted in the interior.

It is often necessary to know the spatial distribution of the slowing-down density in systems containing resonance absorbers, in addition to the resonance escape probability. This can easily be found on the basis of the Fermi age model, by enlarging the derivation of the age equation given in Section 6-9 to include absorption. It will be recalled that this equation was derived by computing the number of neutrons arriving and interacting in the lethargy interval  $du$  in the volume element  $dV$  (cf. Eq. 6-68). With absorption present there is an additional loss of

neutrons in  $du$  and  $dV$  equal to  $\Sigma_a(u)\phi(\mathbf{r}, u) du dV$ , and the neutron balance equation (Eq. 6-68) is now

$$\operatorname{div} \mathbf{J}(\mathbf{r}, u) + \Sigma_a(u)\phi(\mathbf{r}, u) + \frac{\partial q_a(\mathbf{r}, u)}{\partial u} = 0, \quad (7-73)$$

where for convenience the slowing-down density with absorption has been denoted as  $q_a$ . Again if the validity of Fick's law is assumed and if  $\phi(\mathbf{r}, u)$  is expressed in terms of  $q_a(\mathbf{r}, u)$  by Eq. (6-71), then Eq. (7-73) becomes

$$\frac{D(u)}{\bar{\xi}\Sigma_s(u)} \nabla^2 q_a(\mathbf{r}, u) - \frac{\Sigma_a(u)}{\bar{\xi}\Sigma_s(u)} q_a(\mathbf{r}, u) = \frac{\partial q_a(\mathbf{r}, u)}{\partial u}. \quad (7-74)$$

Equation (7-74) can be put in a more convenient form by writing  $q_a(\mathbf{r}, u)$  as

$$q_a(\mathbf{r}, u) = q(\mathbf{r}, u) \exp \left[ - \int_0^u \frac{\Sigma_a(u)}{\bar{\xi}\Sigma_s(u)} du \right], \quad (7-75)$$

where, for the moment,  $q(\mathbf{r}, u)$  should be considered to be an unknown function. By direct substitution it is easily found that Eq. (7-75) satisfies Eq. (7-74) provided  $q(\mathbf{r}, u)$  satisfies the equation

$$\frac{D(u)}{\bar{\xi}\Sigma_s(u)} \nabla^2 q(\mathbf{r}, u) = \frac{\partial q(\mathbf{r}, u)}{\partial u}. \quad (7-76)$$

Aside from the change in variables from  $u$  to  $\tau$ , Eq. (7-76) is just the age equation as derived in Section 6-9. It follows therefore that the function  $q(\mathbf{r}, u)$  is the slowing-down density in the absence of absorption, which, of course, is why this notation was used in Eq. (7-75).

A comparison of Eqs. (7-75) and (7-66) (noting that  $du = -dE/E$ ) shows that the exponential multiplying  $q(\mathbf{r}, u)$  in Eq. (7-75) is equal to the resonance escape probability in the case of small absorption. Thus, the slowing-down densities with and without absorption are related by

$$q_a(\mathbf{r}, u) = q(\mathbf{r}, u)p(u). \quad (7-77)$$

This result shows that in the limit of weak absorption and provided that age theory is valid, slowing down and absorption can be treated as two separate and independent processes. That is, the spatial distribution of the neutrons can be computed as though there were no absorption, and the resonance escape probability can be computed as though the system were infinite.

Equation (7-77) is not strictly valid for most reactors, and moderation and absorption are normally interrelated processes. Nevertheless, in order to make analytical calculations possible, it is usual to assume that Eq. (7-77) holds in all cases. There is some justification for this assumption in the fact that resonance absorption is confined to such a narrow band of energies, that is, most resonance absorption occurs between approximately 10 eV and 100 eV. Above and below these energies the neutrons slow down very largely without absorption.

### 7-9 Fast Fission

Although almost all fissions in a thermal reactor are induced by neutrons of thermal energies, some fissions inevitably occur whenever fast neutrons strike fuel. This effect is of little consequence in thermal reactors containing highly enriched fuel, because the fuel concentration in reactors of this type is ordinarily so small that neutrons rarely collide with fuel nuclei while slowing down. In reactors fueled with natural or slightly enriched uranium, however, substantial amounts of  $U^{238}$  are usually present and the fissions induced by neutrons striking this isotope above the fission threshold may make a nonnegligible contribution to the criticality of the system. This is also true, of course, for reactors containing large amounts of any fissionable but nonfissile isotope.

Fast fissions are normally taken into account in thermal reactors by introducing a parameter known as the *fast-fission factor* and denoted by the symbol  $\epsilon$ . This quantity is defined as the ratio, for an infinite system, of the total number of fission neutrons produced in *all* fissions, fast and thermal, to the number produced by thermal fissions alone. In symbols,  $\epsilon$  is given by the expression

$$\epsilon = \frac{\int_0^{\infty} \phi(E) \Sigma_f(E) \nu(E) dE}{\int \phi(E) \Sigma_f(E) \nu(E) dE}, \quad (7-78)$$

where  $\Sigma_f(E)$  is the macroscopic fission cross section,  $\nu(E)$  is the average number of neutrons emitted in a fission induced by neutrons of energy  $E$ , and the integral in the denominator is carried out only over thermal energies.

The denominator in Eq. (7-78) can be evaluated in rather general terms using techniques discussed in the next chapter. The integral in the numerator, at least that portion of the integral above thermal energies, must be carried out numerically.

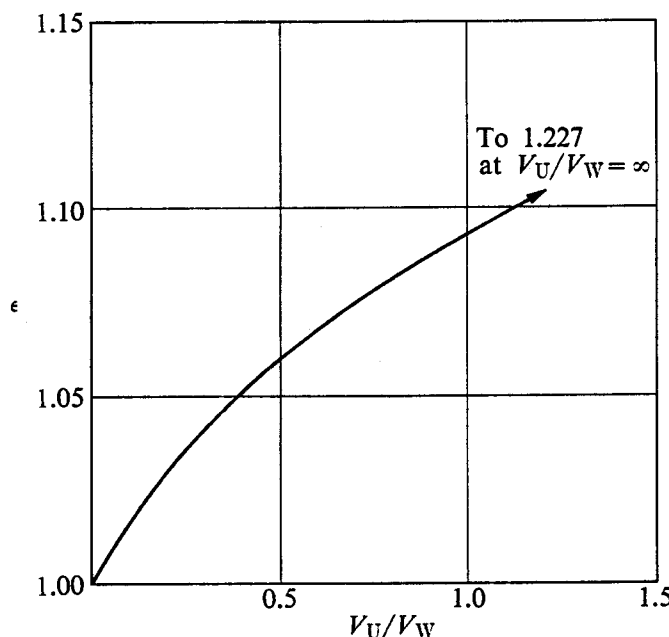


Fig. 7-4. The fast effect for uranium-water mixtures. (Based on data given by J. Chernick in BNL-622, August 1960.)

Figure 7-4 shows results of calculations of this type for mixtures of  $U^{238}$  and water. Although the calculations were carried out assuming that the system was homogeneous, it is usual to give  $\epsilon$  as a function of the uranium-water volume ratio  $V_U/V_W$  as shown in the figure. The ratio  $V_U/V_W$  therefore refers to the equivalent volumes of uranium and water based on the atom densities at which the calculations were performed. In other words, the system was assumed to be quasihomogeneous, as in Fig. 6-14. The curve in Fig. 7-4 can be represented approximately by the functions

$$\epsilon = \frac{1 + 0.987(V_U/V_W)}{1 + 0.805(V_U/V_W)} = \frac{1 + 0.690(N_{28}/N_W)}{1 + 0.563(N_{28}/N_W)}, \quad (7-79)$$

where  $N_{28}/N_W$  is the ratio of the atom density of  $U^{238}$  to the molecular density of the water. These formulas are useful in connection with criticality calculations of water-moderated reactors which will be considered in Chapter 9.

## References

- AMALDI, E., "The Production and Slowing Down of Neutrons," *Handbuch der Physik*. Berlin: Springer Verlag, Vol. 38, Part 2, 1959, pp. 1-659.
- DRESNER, L., *Resonance Absorption in Nuclear Reactors*. New York: Pergamon Press, 1960.
- GALANIN, A. D., *Thermal Reactor Theory*, 2nd ed. New York: Pergamon Press, 1960, Section 10.
- GLASSTONE, S., and M. C. EDLUND, *The Elements of Nuclear Reactor Theory*. Princeton, N.J.: Van Nostrand, 1952, Chapter 6.
- ISBIN, H. S., *Introductory Nuclear Reactor Theory*. New York: Reinhold, 1963, Chapter 3.
- MEGHREBLIAN, R. V., and D. K. HOLMES, *Reactor Analysis*. New York: McGraw-Hill, 1960, Chapter 4.
- NORDHEIM, L. W., "The Theory of Resonance Absorption," *Proc. Symp. Appl. Math.*, 11 (1961). Providence, R.I.: American Mathematical Society.
- NORDHEIM, L. W., "Resonance Absorption of Neutrons," Michigan Memorial Phoenix Project report of lectures delivered at Neutron Physics Conference, June 1961. (The notation used in this book in connection with resonance absorption was first introduced in this report.)
- Reactor Physics Constants*, U.S. Atomic Energy Commission Report, ANL-5800, 2nd ed, 1963, Section 3.6.4. A table of  $J(\zeta, \beta)$  is given on page 170.
- WEINBERG, A. M., and E. P. WIGNER, *The Physical Theory of Neutron Chain Reactors*. Chicago: University of Chicago Press, 1958, Chapter 10. The practical width was first defined by Wigner on page 685 of this reference.

## Problems

- 7-1. The radiation and neutron widths of the first three resonances in  $U^{238}$  are given in the table below. (a) Using the method developed in Section 7-1, compute the escape probabilities for the following mixtures of  $U^{238}$  and hydrogen.

- |   |   |
|---|---|
| (1) $N_U = N_H$ ; $T = 0^\circ\text{K}$   | (4) $N_U = 0.1 N_H$ ; $T = 0^\circ\text{K}$   |
| (2) $N_U = N_H$ ; $T = 20^\circ\text{C}$  | (5) $N_U = 0.1 N_H$ ; $T = 20^\circ\text{C}$  |
| (3) $N_U = N_H$ ; $T = 500^\circ\text{C}$ | (6) $N_U = 0.1 N_H$ ; $T = 500^\circ\text{C}$ |

(b) In each case, what is the probability that a neutron escapes capture in all three resonances?

$E_1(\text{eV})$	$\Gamma_\gamma(\text{mV})$	$\Gamma_n(\text{mV})$
6.67	26	1.52
10.2	25	0.0014
21.0	25	9.0

7-2. Neutrons slow down from 2 MeV in an infinite medium of hydrogen. What is the relative probability that they do not undergo a collision in the resonance region, say from 5 eV to 200 eV, that is, what is the probability that they jump over the resonance region entirely? Repeat the calculation for a graphite medium.

7-3. Show that

$$(a) \lim_{\zeta \rightarrow \infty} J(\zeta, \beta) = \frac{\pi}{2\sqrt{\beta(1 + \beta)}} \quad (b) \lim_{\beta \rightarrow \infty} J(\zeta, \beta) = \frac{\pi}{2\beta}$$

(c)  $\partial J / \partial \beta < 0$  (physically, this implies that resonance absorption increases with increasing concentration of absorbing nuclei). (d)  $\partial J / \partial \zeta < 0$  (physically, this implies that resonance absorption increases with increasing temperature).

7-4. Using the data in Problem 7-1, determine the practical width of the first resonance in  $\text{U}^{238}$  for a mixture of  $\text{U}^{238}$  and graphite in the following cases and compare with the energy loss per collision.

- |  |   |
|--|---|
| (a) $N_U = N_C; T = 0^\circ\text{K}$   | (d) $N_U = 0.01 N_C; T = 0^\circ\text{K}$   |
| (b) $N_U = N_C; T = 20^\circ\text{C}$  | (e) $N_U = 0.01 N_C; T = 20^\circ\text{C}$  |
| (c) $N_U = N_C; T = 500^\circ\text{C}$ | (f) $N_U = 0.01 N_C; T = 500^\circ\text{C}$ |

7-5. Neutrons slow down in an infinite medium consisting of a mixture of H and  $\text{U}^{238}$  with  $N_H = N_U$  at  $0^\circ\text{K}$ . (a) What is the probability that a neutron is absorbed in the resonance at  $E_1 = 6.68 \text{ eV}$  at energies outside the interval  $E_1 \pm \Gamma/2$ , where  $\Gamma$  is the natural width of the resonance? (b) What is the probability that a neutron is absorbed outside the interval  $E_1 \pm \Gamma_P/2$ , where  $\Gamma_P$  is the practical width?

7-6. Using the data in the table below, compute in the most appropriate way the escape probabilities for the 21.9 eV and 201 eV resonances in  $\text{Th}^{232}$  for the following mixtures of  $\text{Th}^{232}$  and  $\text{Be}^9$ .

- |  |   |
|--|---|
| (a) $N_{\text{Th}} = N_{\text{Be}}; T = 0^\circ\text{K}$   | (d) $N_{\text{Th}} = 0.01 N_{\text{Be}}; T = 0^\circ\text{K}$   |
| (b) $N_{\text{Th}} = N_{\text{Be}}; T = 20^\circ\text{C}$  | (e) $N_{\text{Th}} = 0.01 N_{\text{Be}}; T = 20^\circ\text{C}$  |
| (c) $N_{\text{Th}} = N_{\text{Be}}; T = 500^\circ\text{C}$ | (f) $N_{\text{Th}} = 0.01 N_{\text{Be}}; T = 500^\circ\text{C}$ |

$E_1(\text{eV})$	$\Gamma_\gamma(\text{mV})$	$\Gamma_n(\text{mV})$
21.8	25	2.0
129	22	3.5

7-7. A certain nucleus has a strong absorption resonance of width  $\Delta E$  at the energy  $E_r$ , where  $E_r$  is much less than the energy of the source neutrons and  $\Delta E \ll E_r$ . Assume

that all neutrons which strike the nucleus with energies within  $\Delta E$  are absorbed, and show that the escape probability for the resonance is

$$p = 1 - \frac{1}{\xi(1-\alpha)} \left[ \frac{\Delta E}{E_r} + \alpha \ln \left( 1 - \frac{\Delta E}{E_r} \right) \right] \approx 1 - \frac{\Delta E}{\xi E_r}.$$

7-8. Show that the resonance escape probability for a mixture of hydrogen and an infinitely heavy absorber (Eq. 7-9) can be derived from Eq. (7-31) by introducing the collision density  $F(E) = \Sigma_t(E)\phi(E)$  given in Eq. (7-5).

7-9. The first five resonances in  $U^{238}$  are at 6.67 eV, 10.2 eV, 21.0 eV, 36.8 eV, and 66.3 eV. For mixtures of  $U^{238}$  and graphite, are these resonances widely spaced in the sense of Section 7-4?

7-10. Estimate the probability that a 2-MeV neutron, emitted in an infinite body of water, will not be absorbed while slowing down to 1 eV.

7-11. Let  $r(u) = \Sigma_s(u)/\Sigma_t(u)$  be the probability that a neutron survives a collision at lethargy  $u$ . (a) If the neutron gains  $\xi$  in lethargy at each collision show that the resonance escape probability after  $n$  collisions is given by

$$p_n = \prod_{j=0}^{n-1} r(j\xi).$$

(b) Show that in the limit of continuous slowing down the escape probability from the interval  $du$  is approximately  $p(u+du)/p(u) = [r(u)]^{du/\xi}$ , and hence  $p(u)$  is

$$p(u) = \exp \left[ - \int_0^u \frac{\Sigma_a du}{\Sigma_t \xi} \right],$$

provided  $\Sigma_a/\Sigma_t \ll 1$ .

7-12. (a) Show that the NR approximation can be derived from the exact integral equation (Eq. 7-67) by replacing  $\phi(E)$  in the integrals by its asymptotic form in the absence of absorption. (b) Show also that the NRIM approximation follows from the same procedure, provided  $\alpha_A$  is placed equal to zero.

7-13. Generalize Eq. (7-67) to the case of neutrons slowing down in a mixture of several absorbing and moderating nuclei.

7-14. Neutrons slow down in an infinite medium of  $U^{238}$  and hydrogen with  $N_U = N_H$  at 20°C. What fraction of the neutrons which are captured in the resonances of  $U^{238}$  are captured in the first resonance at 6.67 eV?

7-15. Compute and plot the resonance escape probability for a homogeneous mixture of natural uranium and  $D_2O$  at room temperature as a function of the uranium concentration in gm/liter.

7-16. In the *spectral shift reactor* concept, the multiplication factor of the reactor (which is proportional to the resonance escape probability; cf. Section 9-1) is controlled over the lifetime of the reactor by varying the relative proportions of  $H_2O$  and  $D_2O$  in a  $H_2O-D_2O$  moderator. To illustrate this principle, consider an infinite homogeneous mixture of  $Th^{232}$  and a moderator of this type with  $N_{Th}/N_w = 1$ , where  $N_{Th}$  is the atom density (atoms/cm<sup>3</sup>) of the thorium and  $N_w$  is the molecular density (molecules/cm<sup>3</sup>) of both  $H_2O$  and  $D_2O$ . Compute and plot the resonance escape probability for this system as a function of the ratio  $N(H_2O)/N(D_2O)$ .

# 8

## Low-Energy Neutrons

It will be recalled from the introduction to Chapter 6 that it is convenient to divide the energy scale of neutrons in a thermal reactor into two regions defined by a cutoff energy  $E_m \approx 1$  eV. Above  $E_m$  the nuclei in the system can be assumed to be free, and the scattering of neutrons is a relatively simple affair. As a result, it is possible using straightforward analytical techniques to determine the energy-dependent flux,  $\phi(E)$ , for neutrons moving in a medium at these energies. These techniques formed the subject matter of the preceding two chapters.

It is considerably more difficult to determine  $\phi(E)$  at energies below  $E_m$ . Now the nuclei in the system are no longer free, and the scattering cross section is complicated by the various effects due to chemical binding which were discussed in Section 2-8. In particular, it will be recalled that the mass of a scattering nucleus is effectively increased over its value when the nucleus is free. Furthermore, in interacting with a molecule, a neutron may be scattered coherently from different nuclei or excite various vibrational, rotational, or translational modes; and, in interacting with a crystal, it may undergo Bragg scattering or excite vibrational modes (phonons) of the crystal.

In addition to the complicated nature of neutron scattering at low energies, the calculation of  $\phi(E)$  is also made difficult by the fact that, at energies of the order of the thermal energy of the nuclei, a neutron may *gain* energy ("up-scattering," as it is called) as well as *lose* energy ("down-scattering") in a collision with a nucleus. Indeed, the qualitative shape of the neutron spectrum, i.e.,  $\phi(E)$ , at energies up to about  $5kT$ , where  $k$  is Boltzmann's constant and  $T$  is the absolute temperature of the medium, is very largely determined by the presence of up-scattering. This low energy region, from  $E = 0$  to  $E \approx 5kT$ , is called the *thermal* or *quasi-Maxwellian* region. Up-scattering plays a less important role in the *transition* region from  $E \approx 5kT$  to  $E = E_m \approx 1$  eV. While some up-scattering is present at these energies, it no longer determines the qualitative shape of the neutron spectrum. Thus in the transition region,  $\phi(E)$  has much the same shape as in the moderating region, though modified somewhat by the effects of both chemical binding and up-scattering.

The presence of up-scattering in the thermal and transition regions can be seen in the scattering distribution function  $P(E \rightarrow E')$  (cf. Section 6-1). For example, it can be shown that for a monatomic hydrogen gas at the temperature  $T$ ,

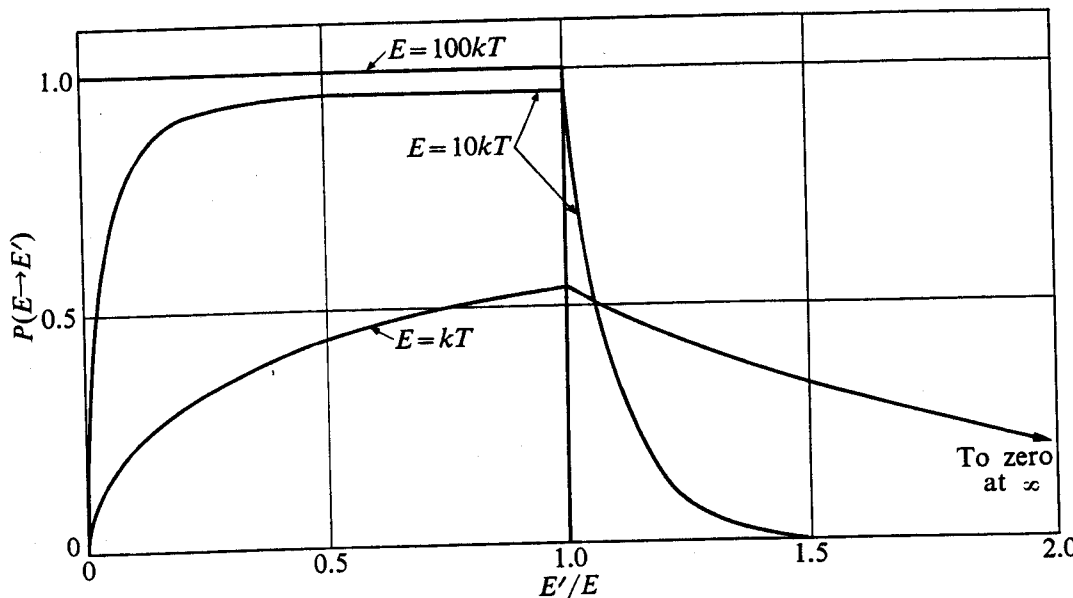


Fig. 8-1. Scattering distribution function  $P(E \rightarrow E')$  as a function of the ratio  $E'/E$  for a free monatomic hydrogen gas. The area under each curve is equal to unity.

$P(E \rightarrow E')$  is given by the expression

$$P(E \rightarrow E') = f(E) \begin{cases} \operatorname{erf} \sqrt{E'/kT}, & E' < E \\ \exp[(E - E')/kT] \operatorname{erf} \sqrt{E/kT}, & E' > E, \end{cases} \quad (8-1)$$

where  $f(E)$  is a normalization factor which is independent of  $E'$  (cf. Prob. 8-1) and  $\operatorname{erf }x$  is the error function (cf. Appendix II). The function  $P(E \rightarrow E')$  is shown in Fig. 8-1. It will be observed that for initial energies in the thermal region, i.e.,  $E \approx kT$ , there is a substantial likelihood that a neutron will be scattered to an energy  $E'$  greater than  $E$ . In the transition region,  $E \approx 10kT$ , it is evident from the figure that it is much less probable for a neutron to be up-scattered than down-scattered. Finally, for initial energies in the moderating region,  $E \sim 100kT$ , there is no up-scattering, and  $P(E \rightarrow E')$  is the familiar "rectangular" distribution function of constant magnitude. There are, of course, no chemical binding effects in the scattering of neutrons from a hypothetical gas of hydrogen atoms, and the scattering distribution functions for real materials are therefore considerably more complicated than the one shown in Fig. 8-1.

In the following sections, methods will be discussed for calculating  $\phi(E)$  at energies below  $E_m$ . The calculated spectra will then be applied in computations of various thermal reactor parameters.

### 8-1 Thermal Neutron Spectra

Consider an infinite homogeneous medium containing uniformly distributed sources emitting neutrons isotropically with an energy much greater than  $E_m$ . In this case, the energy-dependent flux  $\phi(E)$  is independent of position at all

energies. Above  $E_m$ , that is, in the moderating region,  $\phi(E)$  can be calculated by the methods given in the preceding chapters. In particular, if there are no strongly absorbing resonances in the energy region immediately above  $E_m$ ,  $\phi(E)$  in this region has the asymptotic behavior  $\phi(E) = \text{constant}/\xi E \Sigma_s(E)$ .

To calculate  $\phi(E)$  for energies below  $E_m$ , a neutron balance is set up in an energy interval  $dE$  at  $E$ . As indicated in Fig. 8-2, neutrons may arrive in  $dE$  as the result of down-scattering from energies above  $E_m$  or from both down-scattering and up-scattering from energies below  $E_m$ . In the steady state, the number of neutrons scattered into and interacting in  $dE$  must be equal.

It is convenient in calculations of low energy neutron spectra to treat the neutrons scattered into  $dE$  from collisions above  $E_m$  as source neutrons. Accordingly, the number of neutrons arriving in  $dE$  per  $\text{cm}^3/\text{sec}$  from the moderating region will be denoted by  $S(E) dE$ . The function  $S(E)$  can easily be computed if  $\phi(E)$  is known above  $E_m$  (see, for example, Prob. 8-2). However, the exact form of  $S(E)$  is not important for the present discussion.

Now let  $P(E' \rightarrow E) dE$  be the probability that a neutron scattered at the energy  $E'$  will appear with an energy between  $E$  and  $E + dE$ , where both  $E'$  and  $E$  lie below  $E_m$ . The number of neutrons scattered from  $dE'$  to  $dE$  per  $\text{cm}^3/\text{sec}$  is then

$$\Sigma_s(E') P(E' \rightarrow E) \phi(E') dE' dE,$$

and the total number reaching  $dE$  from collisions below  $E_m$  is

$$\int_{E'=0}^{E_m} \Sigma_s(E') P(E' \rightarrow E) \phi(E') dE' dE.$$

Adding to this the number of neutrons coming from collisions above  $E_m$  and equating to the number of interactions per  $\text{cm}^3/\text{sec}$  in  $dE$  gives

$$[\Sigma_s(E) + \Sigma_a(E)] \phi(E) = \int_0^{E_m} \Sigma_s(E') P(E' \rightarrow E) \phi(E') dE' + S(E), \quad (8-2)$$

where  $dE$  has been canceled from every term in the equation.

In calculations of neutron flux at low energies it is usual to replace the quantity  $\Sigma_s(E') P(E' \rightarrow E)$  in Eq. (8-2) by a single function, namely,

$$\Sigma_s(E') P(E' \rightarrow E) = \Sigma_s(E' \rightarrow E). \quad (8-3)$$

The function  $\Sigma_s(E' \rightarrow E)$  is called the *scattering kernel*. In view of Eq. (8-3),

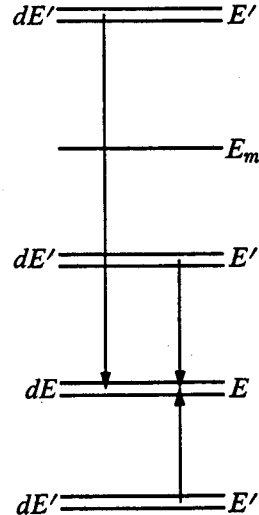


Fig. 8-2. Arrival of neutrons in  $dE$  from down-scattering above  $E_m$  and up- and down-scattering below  $E_m$ .

$\Sigma_s(E' \rightarrow E) dE$  is evidently the macroscopic cross section for a scattering interaction at  $E'$  which carries the neutron energy from  $E'$  to the interval  $dE$  at  $E$ . Since a scattered neutron must acquire an energy somewhere between  $E = 0$  and  $E = E_m$ , it follows that

$$\int_0^{E_m} \Sigma_s(E' \rightarrow E) dE = \Sigma_s(E'). \quad (8-4)$$

In terms of the scattering kernel, Eq. (8-2) can be written as

$$[\Sigma_s(E) + \Sigma_a(E)]\phi(E) = \int_0^{E_m} \Sigma_s(E' \rightarrow E)\phi(E') dE' + S(E). \quad (8-5)$$

Equation (8-5) is the fundamental equation underlying calculations of low-energy neutron spectra. In order to find  $\phi(E)$  it is necessary merely to insert the appropriate functions for  $\Sigma_s(E' \rightarrow E)$  and  $S(E)$  and solve the equation.

If Eq. (8-5) is integrated from  $E = 0$  to  $E = E_m$  there is obtained:

$$\begin{aligned} \int_0^{E_m} [\Sigma_s(E) + \Sigma_a(E)]\phi(E) dE &= \int_0^{E_m} \int_0^{E_m} \Sigma_s(E' \rightarrow E)\phi(E') dE' dE \\ &\quad + \int_0^{E_m} S(E) dE. \end{aligned} \quad (8-6)$$

In view of Eq. (8-4), however,

$$\int_0^{E_m} \int_0^{E_m} \Sigma_s(E' \rightarrow E)\phi(E') dE' dE = \int_0^{E_m} \Sigma_s(E')\phi(E') dE',$$

which is identical to the first term on the left-hand side of Eq. (8-6). It follows therefore that

$$\int_0^{E_m} \Sigma_a(E)\phi(E) dE = \int_0^{E_m} S(E) dE, \quad (8-7)$$

This result shows mathematically what is obvious physically, namely, that in the steady state the total number of neutrons scattered out of the moderating region per second must be equal to the number which are absorbed per second at energies below  $E_m$ .

**No sources, no absorption; the Maxwellian spectrum.** If there are no fast neutrons feeding the energy region below  $E_m$ , i.e., if  $S(E) = 0$ , and there is no absorption, Eq. (8-5) reduces to

$$\Sigma_s(E)\phi(E) = \int_0^{E_m} \Sigma_s(E' \rightarrow E)\phi(E') dE'. \quad (8-8)$$

Since the medium has been assumed to be infinite, the neutrons travel about in the medium indefinitely, much like the molecules in a gas. They continue to gain and lose energy, of course, as the result of repeated collisions with nuclei, but in the steady state the number of neutrons with energy in any interval  $dE$  must be inde-

pendent of time. In this case, it can be shown using statistical mechanics that the neutron flux is *Maxwellian*; that is, the flux  $\phi_M(E)$  satisfying Eq. (8-8) is given by the Maxwellian distribution

$$\phi_M(E) = \frac{2\pi n}{(\pi kT)^{3/2}} \left( \frac{2}{m} \right)^{1/2} E e^{-E/kT}, \quad (8-9)$$

where  $n$  is the density of neutrons,  $k$  is Boltzmann's constant,  $m$  is the neutron mass, and  $T$  is the temperature of the medium in degrees Kelvin. It should be noted particularly that  $\phi_M(E)$  depends only on the temperature of the medium and is independent of the nature of the scattering kernel.

The energy at which  $\phi_M(E)$  is a maximum is known as the *most probable energy* and will be denoted by  $E_T$ . Placing the derivative of Eq. (8-9) equal to zero it is easily found that

$$E_T = kT. \quad (8-10)$$

The speed of the neutrons having the energy  $E_T$  will be written as  $v_T$ , that is,

$$\frac{1}{2}mv_T^2 = kT. \quad (8-11)$$

When numerical values are substituted in Eqs. (8-10) and (8-11), the following useful formulas are obtained:

$$E_T = 8.617T \times 10^{-5} \text{ eV} \quad (8-12)$$

and

$$v_T = 1.284T^{1/2} \times 10^4 \text{ cm/sec}, \quad (8-13)$$

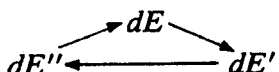
where  $T$  is in °K.

In the steady state and with no absorption, the number of neutrons scattered per second into and out of any energy interval  $dE$  clearly must be independent of time. This, of course, is the physical meaning of Eq. (8-8). In addition, however, it can be shown from statistical mechanics that when  $S(E) = \Sigma_a(E) = 0$  the number of neutrons scattered per second from  $dE$  to any other interval  $dE'$  is precisely equal to the number scattered back from  $dE'$  to  $dE$ . In terms of the scattering kernel defined above, this means that the relationship

$$\Sigma_s(E' \rightarrow E)\phi_M(E') = \Sigma_s(E \rightarrow E')\phi_M(E) \quad (8-14)$$

must hold for all  $E$  and  $E'$ . Equation (8-14) is known as the *condition of detailed balance*.\* The importance of this condition in calculations of low-energy neutron

\* It may be noted that the condition of detailed balance is a nontrivial law of nature, which is far from obvious physically. In particular, while Eq. (8-14) guarantees that the number of neutrons in  $dE$  is independent of time, it is not the only relationship of this kind which does so. The essential ingredient of the condition of detailed balance is that it rules out a balance at  $dE$  maintained by cyclic processes of the type



spectra stems from the fact that it places a restriction on the fundamental form of the scattering kernel. Since the kernel is necessarily the same whether or not there are neutron sources or absorption in the system, it follows that any kernel used to calculate  $\phi(E)$  must satisfy Eq. (8-14).

Incidentally, it may be noted that if Eq. (8-14) is substituted into Eq. (8-8), the latter equation is satisfied identically. This should come as no surprise. Thus while Eq. (8-14) represents a balance between each pair of intervals  $dE$  and  $dE'$ , Eq. (8-8) gives an overall balance between  $dE$  and *all*  $dE'$ . Since the neutrons satisfy a condition of *detailed* balance they surely must satisfy a condition of *overall* balance.

**Thermal spectra in general.** If there are sources present and the medium has a nonzero absorption cross section,  $\phi(E)$  depends in detail on the functions  $S(E)$  and  $\Sigma_a(E)$ , and on the nature of the scattering kernel. As already mentioned it is not usually difficult to determine  $S(E)$ . It is considerably more difficult, however, to find the kernel, due to the extremely complicated ways by which low-energy neutrons interact with matter. Calculations of the kernel lie well beyond the scope of this book and the reader should consult the references at the end of the chapter for further information on this subject. In any event, a number of kernels have been derived in recent years which adequately describe the low-energy scattering of neutrons in many of the materials important in nuclear engineering.

To determine the low-energy neutron spectrum in a given medium, the kernel appropriate to the medium is inserted, along with the source term,  $S(E)$ , into Eq. (8-5), and this equation is solved for  $\phi(E)$ . Unfortunately, in all cases the kernels are such complicated functions that it is not possible to obtain analytical

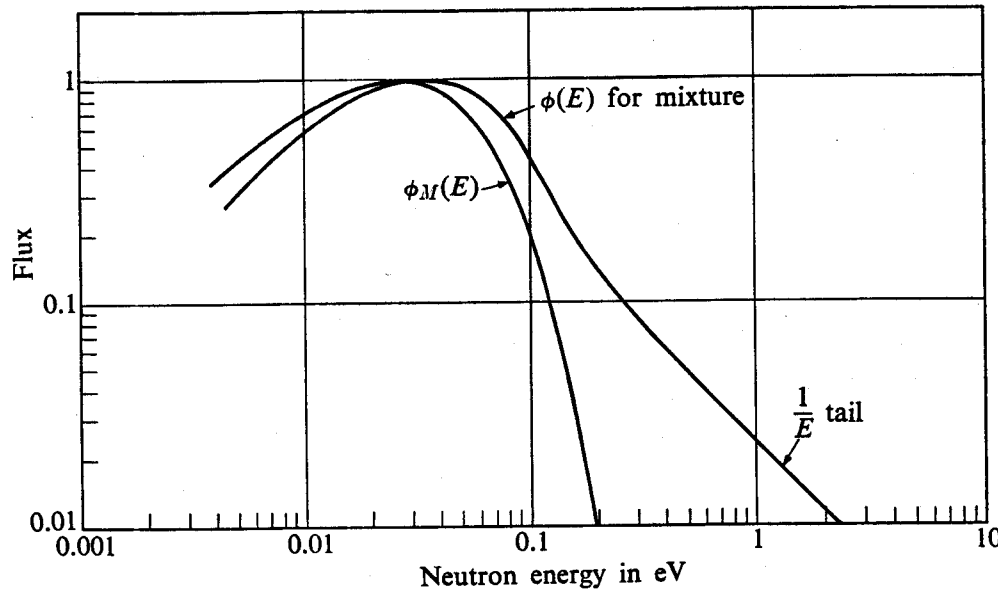


Fig. 8-3. Low-energy neutron flux for a mixture of  $H_2O$  and a  $1/v$  absorber (5.2 barns per hydrogen atom) at  $23^\circ C$  and the Maxwellian flux at the same temperature. (Based in part on General Atomics Report GA-5319.)

solutions for  $\phi(E)$ . Several techniques have been devised, however, for obtaining approximate numerical solutions to Eq. (8-5).

The results of calculations of this kind are illustrated in Fig. 8-3, where  $\phi(E)$  is shown for a mixture of water and a  $1/v$  absorber\* at 296° K (room temperature in San Diego, California). These calculations were performed using a kernel, developed by M. S. Nelkin, which takes into account the vibrations, hindered rotations, and translations of the water molecule. Also shown in the figure is the Maxwellian flux at the same temperature; both curves are normalized to maximum values of unity. It will be observed that the calculated flux consists of two more or less distinct parts. For energies up to about 0.15 eV,  $\phi(E)$  is similar in shape to the Maxwellian function. On the other hand, starting at about 1 eV,  $\phi(E)$  varies as  $1/E$ ; this, of course, is just the low-energy end of the flux in the moderating region. In the short transition region  $\phi(E)$  deviates somewhat from a  $1/E$  behavior, particularly near the end of the thermal region.

It should also be noted in Fig. 8-3 that the entire computed thermal spectrum is shifted to higher energies than the Maxwellian distribution. This is due to the fact that absorption at thermal energies tends to remove low-energy neutrons before they have had an opportunity to come to equilibrium with the system. Since neutrons slow down into the thermal region from higher energies, the result is an increase in the average energy of the thermal neutrons. The neutron distribution in this case is said to be *absorption hardened*. This effect is of minor significance in lightly fueled systems such as  $U^{235}$ -water research reactors, where the thermal absorption cross sections tend to be small compared with the thermal scattering cross sections. In the more heavily loaded reactors, however, which includes many power reactors, the absorption may be so great that the thermal energy distribution is substantially different from a Maxwellian distribution.

Although  $\phi(E)$  is not precisely Maxwellian when sources and absorption are present, it is often convenient to assume

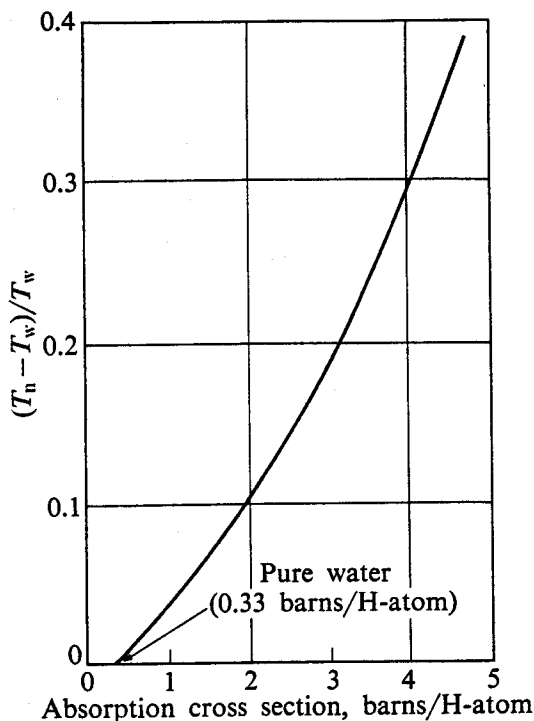


Fig. 8-4. The ratio  $(T_n - T_w)/T_w$  as a function of the total absorption cross section of a mixture of water and a  $1/v$  absorber. [Based on K. Burkart and W. Reichardt, *Proceedings of the Brookhaven Conference on Neutron Thermalization*, BNL-719 (C-32), Volume II, 1962, p. 318.]

\* A  $1/v$  absorber is a material whose low-energy absorption cross section varies as  $1/v$  (cf. Section 8-2).

that the thermal neutron spectrum is still Maxwellian in shape, though shifted by absorption hardening to higher energies. For example, a Maxwellian flux at a temperature of 440°K is found to give a fairly good fit to the thermal neutron spectrum shown in Fig. 8-3, and in this case  $T_n = 440^\circ\text{K}$  is said to be the *neutron temperature*. Clearly,  $T_n$  increases with the concentration of the absorber. This is indicated in Fig. 8-4 for a mixture of a  $1/v$  absorber and ordinary water. The figure shows measured values of the fraction  $(T_n - T_w)/T_w$ , where  $T_w$  is the water temperature, as a function of the total absorption cross section in barns per hydrogen atom. Similar curves have been obtained for other moderator-absorber mixtures and will be found in the references (see, in particular, ANL-5800). It should be emphasized, however, that the practice of representing the neutron flux at thermal energies by a Maxwellian distribution having a characteristic neutron temperature is, at best, only an approximation which should be used with caution. Except at small absorber concentrations, the thermal spectrum may depart too much from Maxwellian for the concept of neutron temperature to be meaningful.

**Finite media—diffusion cooling.** Up to this point, the discussion has been restricted to neutron spectra in infinite media generated by uniformly distributed isotropic sources. With finite media or nonuniform sources the problem of determining neutron spectra is complicated by various effects arising from the diffusion of the neutrons.

Consider, for example, a uniform, bare medium of arbitrary geometry. The system in question may be a reactor or an experimental assembly of the type to be discussed in Section 8-9 for measuring various diffusion parameters. It will now be shown that the low-energy spectrum in such a system differs from the spectrum in the corresponding infinite medium because of preferential leakage of neutrons from the high-energy end of the spectrum. This phenomenon, which is entirely analogous to evaporative cooling of a hot liquid, is known as *diffusion cooling*.

It will be shown in Section 8-9 and in Chapter 9 that the spatial distribution of the flux in a system of the type under discussion is given by the fundamental eigenfunction  $\varphi_1(\mathbf{r})$ . That is, the energy-dependent flux  $\phi(\mathbf{r}, E)$  can be written as

$$\phi(\mathbf{r}, E) = \phi(E)\varphi_1(\mathbf{r}), \quad (8-15)$$

where  $\phi(E)$  is the energy-dependent part of the flux and  $\varphi_1(\mathbf{r})$  satisfies

$$(\nabla^2 + B_1^2)\varphi_1(\mathbf{r}) = 0, \quad (8-16)$$

where  $B_1^2$  is the first eigenvalue (cf. Section 5-10). Similarly, the neutron density function  $n(\mathbf{r}, E)$  is given by

$$n(\mathbf{r}, E) = n(E)\varphi_1(\mathbf{r}), \quad (8-17)$$

and, of course,

$$\phi(\mathbf{r}, E) = n(\mathbf{r}, E)v(E), \quad (8-18)$$

where  $v(E)$  is the neutron speed.

The leakage of neutrons from the system in the energy element  $dE$  can be computed using diffusion theory; thus

$$\begin{aligned}\text{Number of neutrons in } dE \text{ leaking per sec} &= -D(E) \int_A \text{grad } \phi(\mathbf{r}, E) dE dA \\ &= -D(E) \int_V \nabla^2 \phi(\mathbf{r}, E) dE dV \\ &= D(E) B_1^2 \phi(E) dE \int_V \varphi_1(\mathbf{r}) dV,\end{aligned}$$

where use has been made of Eqs. (8-15) and (8-16). The total number of neutrons in the system in the interval  $dE$  is

$$\text{Total number of neutrons in } dE = \int_V n(\mathbf{r}, E) dE dV = n(E) dE \int_V \varphi_1(\mathbf{r}) dV.$$

The fraction of the neutrons in  $dE$  leaking per second is therefore

$$\frac{\text{Number of neutrons in } dE \text{ leaking per sec}}{\text{Total number of neutrons in } dE} = \frac{D(E) B_1^2 \phi(E)}{n(E)} = D(E) B_1^2 v(E). \quad (8-19)$$

It follows from Eq. (8-19) that the probability of a neutron leaking from the system increases with its speed. At thermal energies, however, there is a continual exchange of neutrons between different  $dE$ 's as a result of the repeated collisions of neutrons at these energies. Since the faster neutrons leak out more rapidly, this means that the energy distribution of the remaining neutrons is somewhat impoverished in fast neutrons, with the result that the remaining distribution is effectively cooled.

From a practical standpoint, the changes in the equilibrium neutron distribution due to diffusion cooling ordinarily need not be taken into account except in experiments involving very small systems from which there is considerable leakage. As noted earlier, reactors are designed so that there is little neutron leakage and it is not usually necessary, therefore, to include diffusion cooling in calculations of the low-energy neutron spectra for most reactors. Absorption hardening is a far more important phenomenon in reactors than diffusion cooling.

**The thermal flux.** In connection with calculations of thermal reactors it is expedient to introduce a quantity known as the *thermal flux*, denoted by  $\phi_T(\mathbf{r})$ . This is defined as the integral over thermal energies of the energy-dependent flux  $\phi(\mathbf{r}, E)$ , that is,

$$\phi_T(\mathbf{r}) = \int_0^{-5kT} \phi(\mathbf{r}, E) dE. \quad (8-20)$$

As discussed above,  $\phi(\mathbf{r}, E)$ , in the absence of diffusion cooling, can be represented approximately by

$$\phi(\mathbf{r}, E) = \frac{2\pi n(\mathbf{r})}{(\pi k T_n)^{3/2}} \left( \frac{2}{m} \right)^{1/2} E e^{-E/k T_n}, \quad (8-21)$$

where  $n(\mathbf{r})$  is the neutron density at  $\mathbf{r}$  and  $T_n$  is the neutron temperature. When Eq. (8-21) is inserted into Eq. (8-20) very little error is made if the integration is carried from zero to infinity, since the Maxwellian distribution dies off so rapidly beyond  $E \approx 5kT_n$ . Thus

$$\begin{aligned}\phi_T(\mathbf{r}) &= \int_0^\infty \phi(\mathbf{r}, E) dE = \frac{2\pi n(\mathbf{r})}{(\pi kT_n)^{3/2}} \left(\frac{2}{m}\right)^{1/2} \int_0^\infty E e^{-E/kT_n} \\ &= \frac{2}{\sqrt{\pi}} n(\mathbf{r}) \left(\frac{2kT_n}{m}\right)^{1/2}.\end{aligned}\quad (8-22)$$

In view of Eq. (8-11) this can also be written as

$$\phi_T(\mathbf{r}) = \frac{2}{\sqrt{\pi}} n(\mathbf{r}) v_T = 1.128 n(\mathbf{r}) v_T. \quad (8-23)$$

It should be noted from this result that since  $v_T$  depends upon the neutron temperature (cf. Eq. 8-13), it follows that  $\phi_T$  is also temperature dependent. If, for instance, the temperature is raised, the thermal flux increases, provided the neutron density is held constant.

## 8-2 Interaction Rates for Thermal Neutrons

In considering the interaction of thermal neutrons with nuclei in a thermal reactor it is necessary to take into account the fact that *both* the neutrons and nuclei are in thermal motion. The present section is therefore a generalization of the discussion of the Doppler effect given in Section 2-14, where only the nuclei were assumed to undergo thermal motion. In the following it is explicitly assumed that the neutrons interact with single, individual nuclei, so that the interactions can be described in terms of microscopic cross sections. It will be recalled from Section 2-8 that this is not possible, in general, for low-energy scattering since neutrons may be scattered simultaneously by a number of nuclei at these energies. The present discussion is limited, therefore, to absorption interactions such as radiative capture and fission.

Let  $n(\mathbf{v}) d\mathbf{v}$  be the number of neutrons/cm<sup>3</sup> at some point in the reactor moving with laboratory velocities between  $\mathbf{v}$  and  $\mathbf{v} + d\mathbf{v}$ , and similarly, let  $N(\mathbf{V}) d\mathbf{V}$  be the number of atoms/cm<sup>3</sup> moving with laboratory velocities between  $\mathbf{V}$  and  $\mathbf{V} + d\mathbf{V}$ . In a coordinate system in which these atoms are at rest, the neutrons approach the nuclei with the velocity  $\mathbf{v}_r = \mathbf{v} - \mathbf{V}$ , equal to the relative velocity of neutrons and nuclei. With respect to the nuclei, the neutrons comprise, in effect, a differential beam of intensity  $dI = n(\mathbf{v}) v_r d\mathbf{v}$ , where  $v_r = |\mathbf{v}_r|$ , and interact with the nuclei at the rate of

$$dF = n(\mathbf{v}) N(\mathbf{V}) \sigma(v_r) v_r d\mathbf{v} d\mathbf{V} \quad (8-24)$$

interactions per cm<sup>3</sup>/sec. The total interaction rate is then

$$F = \iint n(\mathbf{v}) N(\mathbf{V}) \sigma(v_r) v_r d\mathbf{v} d\mathbf{V}, \quad (8-25)$$

where the integration is carried over the (six) components of  $\mathbf{v}$  and  $\mathbf{V}$ . Equation (8-25) is a very general result which will now be applied to a number of different situations.

**Case (1):  $1/v$  absorption.** It will be recalled from Chapter 2 that the absorption cross sections of most nuclei at thermal energies vary as  $1/v_r$ . In this case,  $\sigma_a(v_r)$  can be written as

$$\sigma_a(v_r) = \sigma_a(v_{r0}) \frac{v_{r0}}{v_r}, \quad (8-26)$$

where  $v_{r0}$  is an arbitrary relative speed and  $\sigma_a(v_{r0})$  is the corresponding cross section. Introducing Eq. (8-26) into Eq. (8-25), the  $v_r$  cancels and the absorption rate becomes

$$F_a = \sigma_a(v_{r0}) v_{r0} \iint n(\mathbf{v}) N(\mathbf{V}) d\mathbf{v} d\mathbf{V} = N \sigma_a(v_{r0}) n v_{r0}, \quad (8-27)$$

where  $N$  and  $n$  are the atomic and neutron densities, respectively. This result shows that *the absorption rate for a  $1/v$  absorber is a constant, independent of the velocity distribution of either neutrons or nuclei.*

According to Eq. (8-27) the absorption rate depends only on a single arbitrary relative speed of neutron and nucleus. In computing  $F_a$  from Eq. (8-27) it is convenient to imagine that the nucleus is at rest in the laboratory system;  $v_{r0}$  is then an equally arbitrary *laboratory* speed of the neutron. In other words, the absorption rate for a  $1/v$  absorber can be calculated by assuming that all nuclei are at rest in the laboratory and that all neutrons have a single laboratory speed, despite the fact that both neutrons and nuclei have continuous velocity distributions (and *unspecified* velocity distributions, at that). Equation (8-27) can thus be written as

$$F_a = \Sigma_a(E_0) n v_0, \quad (8-28)$$

where  $v_0$  is an arbitrary laboratory speed of the neutrons and  $E_0$  is their corresponding energy.

It is the usual practice to tabulate thermal absorption cross sections at a laboratory energy of  $E_0 = 0.0253$  eV, which is equal to the most probable energy in a Maxwellian flux at  $20.46^\circ$  C. The corresponding speed is  $v_0 = 2200$  meters per second. It should be noted that  $E_0$  and  $v_0$  are simply the values of  $E_T$  and  $v_T$  evaluated at  $20.46^\circ$  C [cf. Eqs. (8-12) and (8-13)].

The quantity  $n v_0$  in Eq. (8-28) is called the 2200 *meters-per-second flux* and will be denoted by  $\phi_0$ , that is,

$$\phi_0 = n v_0. \quad (8-29)$$

It must be emphasized that this flux is *not* the same as the thermal flux,  $\phi_T$ , defined by Eq. (8-20). In particular, since according to Eq. (8-13),

$$\frac{v_T}{v_0} = \left( \frac{T}{T_0} \right)^{1/2}, \quad (8-30)$$

where  $T$  is the absolute temperature of the neutrons (the subscript  $n$  denoting neutron temperature will be dropped from here on) and  $T_0 = 273.15^\circ + 20.46^\circ = 293.61^\circ \text{ K}$ , it follows from Eqs. (8-23) and (8-29) that  $\phi_T$  and  $\phi_0$  are related by

$$\phi_T = \frac{2}{\sqrt{\pi}} \left( \frac{T}{T_0} \right)^{1/2} \phi_0. \quad (8-31)$$

In view of the fact that thermal neutrons have a continuous distribution of energies, the 2200 meters-per-second flux tends to be a somewhat artificial concept. Nevertheless, the fluxes of thermal reactors are often quoted in terms of  $\phi_0$  because this flux can easily be measured with a  $1/v$  detector. It is also much easier to make calculations of absorption rates using  $\phi_0$  rather than  $\phi_T$ , for regardless of the reactor temperature, the absorption rate for a  $1/v$  absorber is simply

$$F_a = \Sigma_a(E_0)\phi_0. \quad (8-32)$$

However, for calculations involving the transport of neutrons in a reactor, it is more appropriate to use the thermal flux, as will be shown later in this chapter.

The absorption rate for a  $1/v$  absorber can also be written in terms of the thermal flux. Thus in view of Eqs. (8-31) and (8-32),

$$F_a = \frac{\sqrt{\pi}}{2} \left( \frac{T_0}{T} \right)^{1/2} \Sigma_a(E_0)\phi_T. \quad (8-33)$$

This equation serves to define a useful quantity known as the *average thermal absorption cross section*, denoted by  $\bar{\Sigma}_a$ , which is defined as

$$\bar{\Sigma}_a = \frac{\sqrt{\pi}}{2} \left( \frac{T_0}{T} \right)^{1/2} \Sigma_a(E_0). \quad (8-34)$$

In terms of  $\bar{\Sigma}_a$  and  $\phi_T$ , the absorption rate can then be written

$$F_a = \bar{\Sigma}_a \phi_T. \quad (8-35)$$

**Case (2): non- $1/v$  absorption.** Some nuclei, namely those having an absorption resonance at very low energy, do not exhibit  $1/v$  absorption. Although only a comparatively few nuclei show such a non- $1/v$  behavior, the presence of these nuclei in a reactor may be a matter of some importance since a low-lying resonance usually leads to high values of  $\sigma_a$  in the thermal region. Non- $1/v$  absorption is found only in intermediate and heavy nuclei. In this case, the center-of-mass and laboratory coordinate systems are very nearly the same and  $v_r$  in Eq. (8-25) can be taken to be the laboratory speed of the neutrons. The absorption rate is then

$$\begin{aligned} F_a &= \iint n(\mathbf{v}) N(\mathbf{V}) \sigma_a(v) v \, d\mathbf{v} \, d\mathbf{V} \\ &= N \int n(\mathbf{v}) \sigma_a(v) v \, d\mathbf{v}. \end{aligned} \quad (8-36)$$

The dependent variable in the integral can be transformed from velocity to energy by noting that

$$n(v) dv = n(E) dE,$$

where  $E$  is the laboratory energy of the neutrons. Equation (8-36) then becomes

$$\begin{aligned} F_a &= N \int n(E) \sigma_a(E) v(E) dE \\ &= \int \Sigma_a(E) \phi(E) dE, \end{aligned} \quad (8-37)$$

where  $\phi(E) = n(E)v(E)$  is the energy-dependent flux (cf. Eq. 5-11).

The integral in Eq. (8-37) can be evaluated once the function  $\phi(E)$  is known. This can be found either by solving the neutron balance equation (Eq. 8-5) as discussed in the preceding section or from experiment. However, as already noted the neutron spectrum in systems with low absorption is well represented by a Maxwellian distribution function at a characteristic neutron temperature. Using a spectrum of this type, C. H. Westcott has numerically evaluated the integral in Eq. (8-37) for all of the important non- $1/v$  absorbers. The resulting value of  $F_a$  is a function of the neutron temperature and is given in the form\*

$$F_a = g_a(T) \Sigma_a(E_0) \phi_0, \quad (8-38)$$

where  $g_a(T)$ , the *non-1/v factor*, is a tabulated function and  $\Sigma_a(E_0)$  is the absorption cross section at 0.0253 eV. A short table of non- $1/v$  factors is given in Table 8-1.

In view of Eq. (8-31),  $F_a$  can also be written in terms of the thermal flux, that is,

$$F_a = \bar{\Sigma}_a \phi_T, \quad (8-39)$$

where  $\bar{\Sigma}_a$  is now given by

$$\bar{\Sigma}_a = \frac{\sqrt{\pi}}{2} g_a(T) \left( \frac{T_0}{T} \right)^{1/2} \Sigma_a(E_0). \quad (8-40)$$

Equations (8-38) and (8-40) are generalizations of Eqs. (8-32) and (8-34) since  $g_a(T) = 1$  for a  $1/v$ -absorber.

It should be noted that the above results apply to *any* absorption process which occurs at thermal energies in an intermediate or heavy nucleus. The number of thermal fissions per  $\text{cm}^3/\text{sec}$ , for example, is

$$F_f = \bar{\Sigma}_f \phi_T, \quad (8-41)$$

with

$$\bar{\Sigma}_f = \frac{\sqrt{\pi}}{2} g_f(T) \left( \frac{T_0}{T} \right)^{1/2} \Sigma_f(E_0), \quad (8-42)$$

where  $g_f(T)$ , the non- $1/v$  fission factor, must be included since fission cross sections tend to be slightly non- $1/v$ .

---

\* Equation (8-38) is a simplified version of Westcott's formulation of the non- $1/v$  absorption problem. See his report in the references for further details.

**Table 8-1**  
**Non- $1/v$  Factors\***

$T, ^\circ\text{C}$	Cd	In	Xe <sup>135</sup>	Sm <sup>149</sup>	U <sup>233</sup>	
	$g_a$	$g_a$	$g_a \dagger$	$g_a$	$g_a$	$g_f$
20	1.3203	1.0192	1.1581	1.6170	0.9983	1.0003
100	1.5990	1.0350	1.2103	1.8874	0.9972	1.0011
200	1.9631	1.0558	1.2360	2.0903	0.9973	1.0025
400	2.5589	1.1011	1.1864	2.1854	1.0010	1.0068
600	2.9031	1.1522	1.0914	2.0852	1.0072	1.0128
800	3.0455	1.2123	0.9887	1.9246	1.0146	1.0201
1000	3.0599	1.2915	0.8858	1.7568	1.0226	1.0284

$T, ^\circ\text{C}$	U <sup>235</sup>		U <sup>238</sup>	Pu <sup>239</sup>	
	$g_a$	$g_f$	$g_a$	$g_a$	$g_f$
20	0.9780	0.9759	1.0017	1.0723	1.0487
100	0.9610	0.9581	1.0031	1.1611	1.1150
200	0.9457	0.9411	1.0049	1.3388	1.2528
400	0.9294	0.9208	1.0085	1.8905	1.6904
600	0.9229	0.9108	1.0122	2.5321	2.2037
800	0.9182	0.9036	1.0159	3.1006	2.6595
1000	0.9118	0.8956	1.0198	3.5353	3.0079

\* Based on C. H. Westcott, "Effective Cross Section Values for Well-Moderated Thermal Reactor Spectra," AECL-1101, January 1962.

† Based on E. C. Smith, *et al.*, *Phys. Rev.* 115, 1693 (1959).

**Case (3): the general situation.** If  $\sigma_a(v_r)$  is not  $1/v$  or the target nuclei are not heavy as in the previous cases, it is necessary to evaluate the multiple integrals (there are six) in Eq. (8-25). The number of integrals can be reduced, however, provided the distribution functions of the neutrons and nuclei are both assumed to be purely Maxwellian with the *same* temperature.

From the kinetic theory of gases,  $n(\mathbf{v})$  and  $N(\mathbf{V})$  are then given by

$$n(\mathbf{v}) = n \left( \frac{m}{2\pi kT} \right)^{3/2} \exp \left( - \frac{mv^2}{2kT} \right) \quad (8-43)$$

and

$$N(\mathbf{V}) = N \left( \frac{M}{2\pi kT} \right)^{3/2} \exp \left( - \frac{MV^2}{2kT} \right), \quad (8-44)$$

where  $n$  and  $N$  are the neutron and atomic densities, and  $m$  and  $M$  are the neutron and atomic masses, respectively. Inserting these expressions into Eq. (8-25) gives

$$F_a = nN \left( \frac{mM}{4\pi^2 k^2 T^2} \right)^{3/2} \iint \exp \left( - \frac{mv^2 + MV^2}{2kT} \right) \sigma_a(v_r) v_r d\mathbf{v} d\mathbf{V}. \quad (8-45)$$

It is now convenient to change integration variables from  $v$  and  $V$  to  $v_r$  and  $c$ , where  $c$  is the velocity of the center of mass of the neutron and nucleus.\* The Jacobian of this transformation can easily be shown to be unity (cf. Prob. 8-11) so that  $dv dV = dv_r dc$ . Furthermore, the quantity  $\frac{1}{2}mv^2 + \frac{1}{2}MV^2$ , which appears in the exponential of Eq. (8-45) is the total kinetic energy of neutron and nucleus with respect to the laboratory, and this can be written as the sum of the kinetic energy of the particles with respect to the center of mass plus the energy of motion of the center of mass, that is,

$$\frac{1}{2}mv^2 + \frac{1}{2}MV^2 = \frac{1}{2}\mu v_r^2 + \frac{1}{2}(m+M)c^2. \quad (8-46)$$

With these results inserted into Eq. (8-45), the integrals separate so that

$$F_a = nN \left( \frac{mM}{4\pi^2 k^2 T^2} \right)^{3/2} \int \exp \left( -\frac{\mu v_r^2}{2kT} \right) \sigma_a(v_r) v_r dv_r \int \exp \left[ -\frac{(m+M)c^2}{2kT} \right] dc. \quad (8-47)$$

The second integration can easily be performed since the integrand is only a function of the magnitude of  $c$ . Thus shifting to spherical coordinates, the volume element becomes  $dc = 4\pi c^2 dc$ , and

$$\begin{aligned} & \int \exp \left[ -\frac{(m+M)c^2}{2kT} \right] dc \\ &= 4\pi \int_0^\infty \exp \left[ -\frac{(m+M)c^2}{2kT} \right] c^2 dc = \left( \frac{2\pi kT}{m+M} \right)^{3/2}. \end{aligned} \quad (8-48)$$

The same procedure can be followed for the integral over  $v_r$ , with the result

$$F_a = 4\pi n N \left( \frac{\mu}{2\pi kT} \right)^{3/2} \int_0^\infty \exp \left( -\frac{\mu v_r^2}{2kT} \right) \sigma_a(v_r) v_r^3 dv_r. \quad (8-49)$$

With a change in variables from  $v_r$  to  $E_c = \frac{1}{2}\mu v_r^2$ , the energy in the center-of-mass system, Eq. (8-49) becomes

$$\begin{aligned} F_a &= \frac{2\pi n N}{(\pi kT)^{3/2}} \left( \frac{2}{\mu} \right)^{1/2} \int_0^\infty e^{-E_c/kT} \sigma_a(E_c) dE_c \\ &= \int_0^\infty \Sigma_a(E_c) \phi_\mu(E_c) dE_c, \end{aligned} \quad (8-50)$$

where  $\Sigma_a(E_c) = N\sigma_a(E_c)$  and  $\phi_\mu(E_c)$  is given by

$$\phi_\mu(E_c) = \frac{2\pi n}{(\pi kT)^{3/2}} \left( \frac{2}{\mu} \right)^{1/2} E_c e^{-E_c/kT}. \quad (8-51)$$

---

\* The symbol  $c$  is used in the present section to denote the velocity of the center of mass, rather than the symbol  $v_0$  as in Chapter 2, to avoid confusion with the 2200 meters-per-second speed  $v_0$ .

Comparing Eq. (8-51) with Eq. (8-21) shows that  $\phi_\mu(E_c)$  is equal to the energy-dependent flux of particles of mass  $\mu$  having temperature  $T$ . Furthermore, since Eq. (8-50) is of the same form as Eq. (8-37) which was derived for stationary nuclei, it may be concluded that *the interaction rate between a Maxwellian distribution of neutrons and a Maxwellian distribution of nuclei, both distributions being at the same temperature, is equal to the interaction rate of a Maxwellian distribution of particles of mass  $\mu$  interacting at an energy  $E_c$  with stationary nuclei.* If the neutrons and nuclei are not Maxwellian at the same temperature the computation of the interaction rate is considerably more difficult and the reader should consult the references for further details. (See, in particular, Meghablian and Holmes, Chapter 4.)

### 8-3 Reactor Power

An important application of some of the concepts considered in the preceding section is the problem of computing the *thermal power* of a reactor. The term "thermal power" is used to connote the rate at which *heat* is produced in the reactor as the result of fissions in the fuel. Nuclear power installations are also rated in terms of their total output of electrical power. The electrical power is always smaller than the thermal power, of course, and depends upon the efficiency of the thermal to electrical conversion equipment (this usually is in the range of from 30 to 40%). Thermal power is usually written as megawatts (th); electrical power as megawatts (el).

For simplicity let it be assumed that the fissionable material is uniformly distributed in the fueled portion of the reactor. In this case, the macroscopic fission cross section is independent of position and the total fission rate in the reactor is

$$\int_V \int_{E=0}^{\infty} \Sigma_f(E) \phi(\mathbf{r}, E) dE dV \text{ fissions/sec,}$$

where  $V$  is the volume of the fueled region of the reactor. If the recoverable energy, in joules per fission is denoted by  $\gamma$  (when the recoverable energy is 200 MeV,  $\gamma = 3.20 \times 10^{-11}$  joules), the thermal power  $P$  is

$$P = \gamma \int_V \int_{E=0}^{\infty} \Sigma_f(E) \phi(\mathbf{r}, E) dE dV. \quad (8-52)$$

If the atom density of fissionable material is  $N_f$ , then  $\Sigma_f(E) = N_f \sigma_f(E)$ , where  $\sigma_f(E)$  is the microscopic fission cross section. In terms of  $M_f$ , the total mass of fissionable material in the reactor,  $N_f$  is given by

$$N_f = M_f N_0 / A V,$$

where  $N_0$  is Avogadro's number and  $A$  is the atomic mass number of the fissionable isotope. The thermal power can then be written as

$$P = \frac{\gamma M_f N_0}{A V} \int_V \int_{E=0}^{\infty} \sigma_f(E) \phi(\mathbf{r}, E) dE dV. \quad (8-53)$$

With the average value of  $\phi(\mathbf{r}, E)$  in the fueled portions of the reactor defined as

$$\bar{\phi}(E) = \frac{1}{V} \int_V \phi(\mathbf{r}, E) dV,$$

the power becomes

$$P = \frac{\gamma M_f N_0}{A} \int_0^\infty \sigma_f(E) \bar{\phi}(E) dE. \quad (8-54)$$

Equation (8-54) is a very general result which is valid for every type of reactor. For a thermal reactor, however, if all fissions are induced by thermal neutrons and it is possible to assume that  $\phi(E)$  is Maxwellian, the integral in Eq. (8-54) can be evaluated with the following result:

$$P = \left( \frac{\gamma M_f N_0}{A} \right) g_f(T) \sigma_f(E_0) \bar{\phi}_0, \quad (8-55)$$

or

$$P = \left( \frac{\gamma M_f N_0}{A} \right) \frac{\sqrt{\pi}}{2} g_f(T) \left( \frac{T_0}{T} \right)^{1/2} \sigma_f(E_0) \bar{\phi}_T. \quad (8-56)$$

Here  $\bar{\phi}_0$  and  $\bar{\phi}_T$  are the volume-averaged 2200 meters-per-second and thermal fluxes, respectively,  $g_f(T)$  is the non- $1/v$  fission factor,  $\sigma_f(E_0)$  is the thermal fission cross section,  $T$  is the neutron temperature in °K, and  $T_0 = 293.61$ ° K.

For U<sup>235</sup>, assuming a recoverable energy of 200 MeV per fission,  $P$  is given by

$$P = 4.73 M_f g_f(T) \bar{\phi}_0 \times 10^{-14} \text{ megawatts(th)} \quad (8-57)$$

$$= 7.19 M_f g_f(T) T^{-1/2} \bar{\phi}_T \times 10^{-13} \text{ megawatts(th)}, \quad (8-58)$$

where  $M_f$  is in kilograms. With other fuels and other values of the recoverable energy, the numerical factors in these equations are somewhat different.

#### 8-4 Average $\eta$ in a Thermal Flux

In Section 3-4 the parameter  $\eta(E)$  was defined as the average number of fission neutrons emitted when a neutron of energy  $E$  is absorbed by fuel. If the fuel consists of a single isotope,  $\eta(E)$  is given by

$$\eta(E) = \nu(E) \frac{\sigma_f(E)}{\sigma_a(E)}, \quad (8-59)$$

where  $\nu(E)$  is the average number of neutrons emitted per fission and  $\sigma_f$  and  $\sigma_a$  are the fission and absorption cross sections, respectively.

For calculations involving fission induced by thermal neutrons, it is convenient to introduce the quantity  $\eta_T$ , which is defined as the average number of fission neutrons emitted per thermal neutron absorbed in fuel. With a single isotope fuel  $\eta_T$  is therefore

$$\eta_T = \frac{\int \eta(E) \sigma_a(E) \phi(E) dE}{\int \sigma_a(E) \phi(E) dE} = \frac{\int \nu(E) \sigma_f(E) \phi(E) dE}{\int \sigma_a(E) \phi(E) dE}, \quad (8-60)$$

Table 8-2

Values of  $\eta_T$ , the Average Number of Fission Neutrons Emitted per Neutron Absorbed in a Thermal Flux, Assuming the Flux to be a Pure Maxwellian at the Temperature  $T^*$

$T, ^\circ\text{C}$	$\text{U}^{233}$	$\text{U}^{235}$	$\text{Pu}^{239}$
20	2.2837	2.0651	2.0347
100	2.2880	2.0632	1.9978
200	2.2908	2.0595	1.9468
400	2.2922	2.0504	1.8604
600	2.2917	2.0423	1.8107
800	2.2915	2.0366	1.7845
1000	2.2919	2.0328	1.7701

\* Based on C. H. Westcott, "Effective Cross Section Values for Well-Moderated Thermal Reactor Spectra," AECL-1101, January 1962.

where the integrals are carried out over thermal energies. If  $\phi(E)$  is assumed to be Maxwellian, and note is taken of the fact that  $v(E)$  is constant in the thermal region (cf. Section 3-4), Eq. (8-60) reduces to

$$\eta_T = v \frac{\bar{\sigma}_f}{\bar{\sigma}_a}, \quad (8-61)$$

where  $\bar{\sigma}_f$  and  $\bar{\sigma}_a$  are microscopic thermal average cross sections. From Eqs. (8-40) and (8-42),

$$\bar{\sigma}_a = \frac{\sqrt{\pi}}{2} g_a(T) \left( \frac{T_0}{T} \right)^{1/2} \sigma_a(E_0), \quad (8-62)$$

and

$$\bar{\sigma}_f = \frac{\sqrt{\pi}}{2} g_f(T) \left( \frac{T_0}{T} \right)^{1/2} \sigma_f(E_0), \quad (8-63)$$

in which  $g_a(T)$  and  $g_f(T)$  are the non- $1/v$  factors for absorption and fission, respectively. Inserting these expressions into Eq. (8-61) gives

$$\begin{aligned} \eta_T &= v \frac{g_f(T)\sigma_f(E_0)}{g_a(T)\sigma_a(E_0)} \\ &= \eta(E_0) \frac{g_f(T)}{g_a(T)}, \end{aligned} \quad (8-64)$$

where  $\eta(E_0)$  is the value of  $\eta$  at 0.0253 eV.

In view of Eq. (8-64) it is evident that if  $g_f(T)$  and  $g_a(T)$  had the same variation with temperature,  $\eta_T$  would be independent of temperature. In actual fact,  $g_f(T)$  and  $g_a(T)$  are slightly different for all fissile nuclei, and  $\eta_T$  is therefore a temperature-dependent quantity. This is shown in Table 8-2 where  $\eta_T$  is given as a function of temperature for the principal fissile isotopes.

When the fuel consists of a mixture of isotopes Eq. (8-64) must be modified somewhat. For instance, with natural uranium, it is easy to see that  $\eta_T$  becomes

$$\begin{aligned}\eta_T &= \nu^{25} \frac{\bar{\Sigma}_f}{\bar{\Sigma}_a} \\ &= \frac{\nu^{25} \Sigma_f^{25}(E_0) g_f^{25}(T)}{\Sigma_a^{25}(E_0) g_a^{25}(T) + \Sigma_a^{28}(E_0) g_a^{28}(T)},\end{aligned}\quad (8-65)$$

where the superscripts 25 and 28 refer to  $U^{235}$  and  $U^{238}$ , respectively. In terms of the value of  $\eta$  for natural uranium at 0.0253 eV, Eq. (8-65) can also be written as

$$\eta_T = \eta(E_0) \frac{[\Sigma_a^{25}(E_0) + \Sigma_a^{28}(E_0)] g_f^{25}(T)}{\Sigma_a^{25}(E_0) g_a^{25}(T) + \Sigma_a^{28}(E_0) g_a^{28}(T)}. \quad (8-66)$$

## 8-5 Diffusion of Thermal Neutrons

The diffusion of monoenergetic neutrons was considered in Chapter 5, and the diffusion of neutrons in the moderating region was discussed in Chapter 6. It is now appropriate to consider the diffusion of thermal neutrons.

The exact treatment of neutron diffusion at thermal energies is a very difficult problem which is well beyond the scope of this book. Nevertheless, it is possible to approximate the behavior of thermal neutrons by the following simple procedure. It will be recalled that as these neutrons move about they continually gain and lose energy in collisions with the nuclei. In the steady state, however, the number of neutrons in every energy interval is independent of time. If, therefore, only the average behavior of the neutrons is required, the fact that the energies of individual neutrons are continually changing may be ignored, and it can be assumed that all neutrons with energies in the interval between  $E$  and  $E + dE$  remain in this interval as they diffuse.

Considering time-independent diffusion first, it follows from these assumptions and from Eq. (5-48) that the neutrons between  $E$  and  $E + dE$  satisfy the equation

$$D(E) \nabla^2 \phi(\mathbf{r}, E) dE - \Sigma_a(E) \phi(\mathbf{r}, E) dE + s(\mathbf{r}, E) dE = 0, \quad (8-67)$$

where  $s(\mathbf{r}, E)$  is the energy spectrum of the sources in the system at the point  $\mathbf{r}$ . An energy-independent diffusion equation can now be obtained by integrating Eq. (8-67) over all thermal energies; that is,

$$\int D(E) \nabla^2 \phi(\mathbf{r}, E) dE - \int \Sigma_a(E) \phi(\mathbf{r}, E) dE + \int s(\mathbf{r}, E) dE = 0. \quad (8-68)$$

The average value of  $D$  in the thermal region is next defined as

$$\bar{D} = \frac{\int D(E) \nabla^2 \phi(\mathbf{r}, E) dE}{\int \nabla^2 \phi(\mathbf{r}, E) dE}. \quad (8-69)$$

It is now assumed that  $\phi(\mathbf{r}, E)$  can be written as a separable function of  $\mathbf{r}$  and  $E$ ,

that is, as the product of a function of  $\mathbf{r}$  multiplied by a function of  $E$ . In this case, the spatial variables cancel from Eq. (8-69) and  $\bar{D}$  becomes

$$\bar{D} = \frac{\int D(E)\phi(E) dE}{\int \phi(E) dE}. \quad (8-70)$$

Returning to Eq. (8-68) the first term can now be written as

$$\int D(E)\nabla^2\phi(\mathbf{r}, E) dE = \bar{D} \int \nabla^2\phi(\mathbf{r}, E) dE = \bar{D}\nabla^2\phi_T(\mathbf{r}),$$

where  $\phi_T(\mathbf{r})$  is the thermal flux at the point  $\mathbf{r}$ . The second term in Eq. (8-68) is the total neutron absorption rate, and from Eq. (8-39) this is

$$\int \Sigma_a(E)\phi(\mathbf{r}, E) dE = \bar{\Sigma}_a\phi_T(\mathbf{r}).$$

Here,  $\bar{\Sigma}_a$  is the thermal macroscopic absorption cross section at absolute temperature  $T$  as defined by Eq. (8-40). The integral over the source spectrum may be written as

$$\int s(\mathbf{r}, E) dE = s(\mathbf{r}),$$

where  $s(\mathbf{r})$  is the total number of neutrons emitted by the sources per  $\text{cm}^3/\text{sec}$  at thermal energies at  $\mathbf{r}$ .

With these results inserted into Eq. (8-68), the time-independent diffusion equation for thermal neutrons becomes

$$\bar{D}\nabla^2\phi_T(\mathbf{r}) - \bar{\Sigma}_a\phi_T(\mathbf{r}) + s(\mathbf{r}) = 0. \quad (8-71)$$

Upon dividing by  $\bar{\Sigma}_a$ , this equation can also be written as

$$L_T^2\nabla^2\phi_T(\mathbf{r}) - \phi_T(\mathbf{r}) + \frac{s(\mathbf{r})}{\bar{\Sigma}_a} = 0, \quad (8-72)$$

where

$$L_T^2 = \frac{\bar{D}}{\bar{\Sigma}_a} \quad (8-73)$$

is known as the *thermal diffusion area* and  $L_T$  is the *thermal diffusion length*. Since Eq. (8-72) is of the same form as the one-velocity diffusion equation, i.e., Eq. (5-48), the solutions obtained in Chapter 5 are also valid for the diffusion of thermal neutrons, provided  $L_T$  is substituted everywhere for  $L$ .

To evaluate  $\bar{D}$  from Eq. (8-70), it will be recalled from Section 5-6 that the diffusion coefficient is primarily a function of the scattering cross section, and for many moderators this is constant at thermal energies. There are, however, two important exceptions, namely  $\text{H}_2\text{O}$  and  $\text{D}_2\text{O}$ . The scattering cross sections of these moderators decrease with increasing energy according to the empirical relation

$$\Sigma_s(E) = \Sigma_s(E_0) \left( \frac{E_0}{E} \right)^m, \quad (8-74)$$

**Table 8-3**  
**Thermal Neutron Diffusion Parameters of Common Moderators at 20°C\***

Moderator	Density (gms/cm <sup>3</sup> )	$\bar{D}$ (cm)	$\Sigma_a$ (cm <sup>-1</sup> )	$L_T^2$ (cm <sup>2</sup> )	$L_T$ (cm)
H <sub>2</sub> O	1.00	0.16	0.0197	8.1	2.85
D <sub>2</sub> O†	1.10	0.87	$2.9 \times 10^{-5}$	$3.0 \times 10^4$	170
Be	1.85	0.50	$1.04 \times 10^{-3}$	480	21
BeO	2.96	0.47	$6.0 \times 10^{-4}$	790	28
Graphite‡	1.60	0.84	$2.4 \times 10^{-4}$	3500	59

\* Based on *Reactor Physics Constants*, U.S. Atomic Energy Commission Report ANL-5800, 2nd ed., 1963, Section 3.3.

† The diffusion properties of D<sub>2</sub>O are sensitive to the amount of H<sub>2</sub>O present.

‡ Graphite often contains impurities which affect its diffusion properties; the values given here are for highly-purified graphite.

where  $E_0 = 0.0253$  eV, and  $m = 0.470$  for H<sub>2</sub>O and  $m = 0.112$  for D<sub>2</sub>O. Since the diffusion coefficient varies inversely with scattering cross section it follows that\*

$$D(E) \approx D(E_0) \left( \frac{E}{E_0} \right)^m. \quad (8-75)$$

When  $D(E)$  from Eq. (8-75) is inserted into Eq. (8-70) and  $\phi(E)$  is assumed to be Maxwellian,  $\bar{D}$  becomes

$$\bar{D} = D(E_0) E_0^{-m} \frac{\int_0^\infty E^{m+1} e^{-E/kT} dE}{\int_0^\infty E e^{-E/kT} dE}. \quad (8-76)$$

In view of the formula

$$\int_0^\infty x^m e^{-ax} dx = \frac{\Gamma(m+1)}{a^{m+1}}, \quad (8-77)$$

where  $\Gamma(m+1)$  is the gamma function (this formula is a generalization of Eq. (5-118) for noninteger values of  $m$ ), Eq. (8-76) reduces to

$$\bar{D} = \Gamma(m+2) D(E_0) \left( \frac{kT}{E_0} \right)^m = \Gamma(m+2) D(E_0) \left( \frac{T}{T_0} \right)^m, \quad (8-78)$$

where  $T_0 = 293.61^\circ$  K. It may be noted that in the usual case  $m = 0$  and  $\bar{D} = D(E_0)$ , since  $\Gamma(2) = 1! = 1$ . The average thermal diffusion coefficient is thus ordinarily independent of temperature. From Eqs. (8-40) and (8-78)  $L_T^2$  is given by

$$L_T^2 = \frac{\bar{D}}{\Sigma_a} = \frac{2\Gamma(m+2)}{\sqrt{\pi g_a(T)}} \left( \frac{T}{T_0} \right)^{m+1/2} L_0^2, \quad (8-79)$$

\* In a more accurate calculation of  $\bar{D}$  it is necessary to take into account the variation of  $\cos \vartheta$  in the formula for  $D(E)$  (cf. Eq. 5-40).

Table 8-4

Thermal Diffusion Times,  $t_d$ , for Several Moderators as Computed from Eq. (8-82)

Moderator	$t_d$ , sec
H <sub>2</sub> O	$2.1 \times 10^{-4}$
D <sub>2</sub> O	0.14
Be	$3.9 \times 10^{-3}$
BeO	$6.7 \times 10^{-3}$
Graphite	0.017

where  $L_0^2 = D(E_0)/\Sigma_a(E_0)$  is the one-velocity diffusion area computed at 0.0253 eV, and  $g_a(T)$  is the non- $1/v$  factor. Measurements of  $\bar{D}$  and  $L_T$  are discussed in Section 8-9; measured values of these parameters are given in Table 8-3.

Before considering time-dependent diffusion of thermal neutrons it is convenient to introduce the concept of the *thermal diffusion time*. This parameter, which is denoted by  $t_d$ , is defined as the average time that a thermal neutron spends in an infinite system before it is captured. This may be found by noting that if  $\lambda_a(E)$  is the absorption mean free path at the energy  $E$ , then the mean lifetime of neutrons at this energy  $t(E)$  is

$$t(E) = \frac{\lambda_a(E)}{v(E)} = \frac{1}{\Sigma_a(E)v(E)}. \quad (8-80)$$

With  $1/v$  absorption,  $\Sigma_a(E) = \Sigma_a(E_0)v_0/v$ , and Eq. (8-80) gives

$$t(E) = \frac{1}{\Sigma_a(E_0)v_0}. \quad (8-81)$$

This result shows that for a  $1/v$  absorbing medium the mean lifetime of neutrons at the energy  $E$  is independent of energy, and it follows, therefore, that the *average* value of  $t(E)$  over the thermal distribution, that is  $t_d$ , is also given by Eq. (8-81); thus

$$t_d = \frac{1}{\Sigma_a(E_0)v_0} = \frac{\sqrt{\pi}}{2\Sigma_a v_T}, \quad (8-82)$$

where use has been made of Eqs. (8-30) and (8-34). If the medium does not exhibit  $1/v$  absorption,  $t_d$  will deviate somewhat from the value predicted by Eq. (8-82), but this is not important for most purposes. Values of  $t_d$  computed from Eq. (8-82) are given in Table 8-4 for several moderators.

The time-dependent thermal diffusion equation can now be derived by integrating the energy-dependent version of Eq. (5-44) over all thermal energies. The result is easily found to be

$$\bar{D}\nabla^2\phi_T(\mathbf{r}, t) - \bar{\Sigma}_a\phi_T(\mathbf{r}, t) + s(\mathbf{r}, t) = \frac{\partial n(\mathbf{r}, t)}{\partial t}, \quad (8-83)$$

where  $n(\mathbf{r}, t)$  is the density of thermal neutrons. From Eq. (8-23), however,

$$\phi_T(\mathbf{r}, t) = \frac{2}{\sqrt{\pi}} n(\mathbf{r}, t) v_T, \quad (8-84)$$

so that Eq. (8-83) can be written as

$$\bar{D} \nabla^2 \phi_T(\mathbf{r}, t) - \Sigma_a \phi_T(\mathbf{r}, t) + s(\mathbf{r}, t) = \frac{\sqrt{\pi}}{2v_T} \frac{\partial \phi_T(\mathbf{r}, t)}{\partial t}. \quad (8-85)$$

Finally, dividing by  $\Sigma_a$  and using Eqs. (8-73) and (8-82) gives

$$L_T^2 \nabla^2 \phi_T(\mathbf{r}, t) - \phi_T(\mathbf{r}, t) + \frac{s(\mathbf{r}, t)}{\Sigma_a} = t_d \frac{\partial \phi_T(\mathbf{r}, t)}{\partial t}. \quad (8-86)$$

This is the time-dependent diffusion equation for thermal neutrons.

## 8-6 Thermalization Time

In Section 6-17 a method was presented for estimating the time,  $t_m$ , called the *moderation time*, that it takes for a fission neutron to slow down out of the moderating region, i.e., to an energy of  $E = E_m$ . Neutrons continue to slow down, of course, at energies below  $E_m$  in thermal reactors, and the average time required for neutrons to slow down from  $E_m$  and come into thermal equilibrium with the system is called the *thermalization time*,  $t_{th}$ . The total *slowing down time*,  $t_s$ , from fission energies to thermal equilibrium is then the sum of the moderation and thermalization times, that is,

$$t_s = t_m + t_{th}. \quad (8-87)$$

The moderation time was computed in Section 6-17 by age theory. This method cannot be extended to energies below  $E_m$ , since in age theory it is assumed that the nuclei are free and the neutrons are only down-scattered. As noted in Section 8-1, chemical binding effectively increases the mass of the nuclei below  $E_m$  which, in turn, decreases the average energy loss per collision. In addition, a neutron may be up-scattered as well as down-scattered. It follows that the rate at which neutrons slow down decreases as soon as their energy falls below  $E_m$ .

To compute  $t_{th}$ , it is supposed that a pulse of neutrons of, for the moment, unspecified shape arrives at the transition region from the moderating region, as shown in Fig. 8-5. As the neutrons slow down, this pulse moves to lower energies until it eventually reaches the equilibrium shape and position indicated in the figure. The thermalization time can be computed by following the motion of this pulse. To do this, it is necessary to set up the time-dependent neutron balance equation describing the shape of the pulse at any time. Consider, therefore, the arrival and departure of neutrons in the energy interval  $dE$  at  $E$ . The rate of increase in the number of neutrons in  $dE$  is evidently equal to the number which arrive in  $dE$  per second minus the number scattered out of or absorbed in  $dE$  per second. Thus if  $n(E, t) dE$  is the density of neutrons in  $dE$  at the time  $t$ , it follows

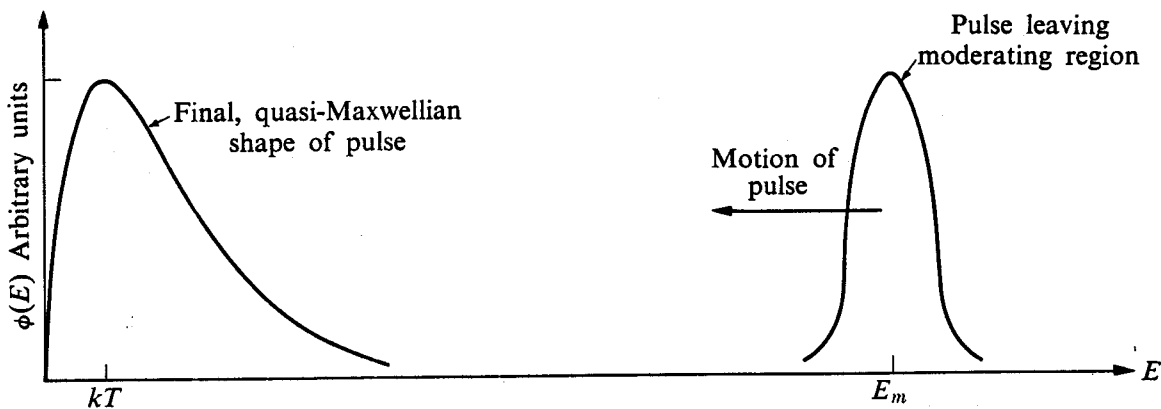


Fig. 8-5. The thermalization of a neutron pulse.

that  $n(E, t)$  must satisfy the equation

$$\frac{\partial n(E, t)}{\partial t} = \int_0^{E_m} \Sigma_s(E' \rightarrow E) \phi(E', t) dE' - [\Sigma_s(E) + \Sigma_a(E)] \phi(E, t). \quad (8-88)$$

It is not possible to obtain an exact analytical solution to Eq. (8-88). An estimate of the time behavior of  $n(E, t)$  can be found, however, by assuming that  $n(E, t)$  and  $\phi(E, t)$  are always Maxwellian but at a temperature which is a function of time. In this case, it can be shown that the temperature at time  $t$ ,  $T(t)$ , varies as

$$T(t) = T + (T_1 - T)e^{-\lambda t}, \quad (8-89)$$

where  $T$  is the ultimate temperature of the neutron distribution,  $T_1$  is the temperature of the pulse as it enters the transition region, and  $\lambda$  is a parameter given by

$$\lambda = \frac{2v_T M_2}{3\sqrt{\pi}}. \quad (8-90)$$

Here,  $v_T$  is the speed corresponding to the energy  $kT$  (cf. Eq. 8-11), and  $M_2$  is the *second moment of the scattering kernel*, defined as

$$M_2 = \frac{1}{(kT)^4} \int_0^{E_m} \int_0^{E_m} \Sigma_s(E' \rightarrow E) (E - E')^2 E' e^{-E'/kT} dE dE'. \quad (8-91)$$

From Eq. (8-89) it is seen that the temperature of the neutron pulse approaches the equilibrium temperature exponentially. Thus, as would be expected physically, it takes an infinite amount of time for the neutrons to come into equilibrium with the medium. However, the time constant  $\lambda^{-1}$  in Eq. (8-89) is some measure of the time required for a pulse to reach equilibrium, and it is therefore usual to write

$$t_{th} = \frac{1}{\lambda} = \frac{3\sqrt{\pi}}{2v_T M_2}. \quad (8-92)$$

**Table 8-5**  
**Moderation, Thermalization, and Diffusion Times in Microseconds**  
**of Moderators at Room Temperature**

Moderator	$t_m$	$t_{th}^*$	$t_d$
H <sub>2</sub> O	1.0	~5	210
D <sub>2</sub> O	8.1	~66	$1.4 \times 10^5$
Be	9.3	~45	$3.9 \times 10^3$
BeO	12	~72	$6.7 \times 10^3$
Graphite	23	~200	$1.7 \times 10^4$

\* Based on data given in ANL-5800 and by L. S. Kothari and V. P. Duggal, *Advances in Nuclear Science and Technology*, Vol. 2., New York: Academic Press, 1964.

It may be noted here that while  $t_m$  is a specific average time,  $t_{th}$ , as defined by Eq. (8-92), is actually a relaxation time. The adding of  $t_m$  and  $t_{th}$  to obtain the total slowing down time (cf. Eq. 8-87) is thus a little like adding apples and oranges. The important point, however, is that they are both fruit.

Values of  $t_{th}$ , the moderation time  $t_m$ , and the diffusion time  $t_d$ , are given in Table 8-5 for several moderators. It will be observed that in all cases  $t_{th}$  is much larger than  $t_m$ . Thus neutrons spend considerably longer reaching their equilibrium distribution in the thermal region than they do in moderating from fission energies. *The total slowing down time is therefore approximately equal to the thermalization time.*

It is also evident from Table 8-5 that  $t_d$  is much larger than  $t_{th}$ . This means that neutrons moderate and thermalize in a time which is short compared to the time that they subsequently spend diffusing as thermal neutrons. It will be shown in Section 8-8 that this circumstance considerably simplifies calculations of neutron slowing down and diffusion.

### 8-7 Age from Indium Resonance to Thermal

As pointed out in Section 6-14, the age of fission neutrons to thermal energies,  $\tau_T$ , cannot be measured directly because it is not possible to distinguish neutrons which have "just come into equilibrium" from those which have been diffusing about for some time. It is necessary therefore to measure  $\tau$  to some energy above the thermal region, usually to the 1.45 eV resonance of In<sup>115</sup>, and then calculate  $\tau$  from this energy to thermal.

According to the Fermi formula (cf. Eq. 6-76),  $\tau(E_{In} \rightarrow E_{th})$  is defined as

$$\tau(E_{In} \rightarrow E_{th}) = \int_{E_{th}}^{E_{In}} \frac{D}{\xi \Sigma_s} \frac{dE}{E}.$$

It is convenient now to change the variable of integration from energy to time, and

Table 8-6

Ages (in cm<sup>2</sup>) of Fission Neutrons to Indium Resonance,  $\tau_{In}$ ; Estimated Age From Indium Resonance to Thermal Energies,  $\tau(E_{In} \rightarrow E_{th})$ ; and the Total Age of Fission Neutrons to Thermal Energies,  $\tau_T^*$

Moderator	$\tau_{In}$	$\tau(E_{In} \rightarrow E_{th})$	$\tau_T$
H <sub>2</sub> O	~26	~1	~27
D <sub>2</sub> O	111	~20	~131
Be	85	~17	~102
BeO	80	~20	~100
Graphite	311	~57	~368

\* Based, in part, on data given in L. S. Kothari and V. P. Duggal, "Scattering of Thermal Neutrons from Solids and Their Thermalization Near Equilibrium," *Advances in Nuclear Science and Technology*, Vol. 2. New York: Academic Press, 1964.

follow, as in the preceding section, the thermalization of a pulse of neutrons from the time it enters the transition region to the time it comes to equilibrium with the system. From Eq. (6-75),

$$du = -\frac{dE}{E} = \xi \Sigma_s dx = \xi \Sigma_s v dt,$$

where  $v$  is the speed corresponding to the energy  $E$ . With  $t = 0$  being the time when the pulse is centered at 1.45 eV, it follows that

$$\tau(E_{In} \rightarrow E_{th}) = \int_0^\infty D(t)v(t) dt. \quad (8-93)$$

It will be observed that by changing the integration variable from energy to time, the rather artificial lower limit  $E_{th}$  on the integral has been eliminated. The parameters  $D(t)$  and  $v(t)$  in Eq. (8-93) are the average values of  $D$  and  $v$  in the flux  $\phi(E, t)$ ; for instance,

$$D(t) = \frac{\int_0^\infty D(E)\phi(E, t) dE}{\int_0^\infty \phi(E, t) dE}.$$

Both  $D(t)$  and  $v(t)$  can be computed using the method discussed in the preceding section. Thus as a first approximation  $\phi(E, t)$  can be assumed to be Maxwellian with a time-dependent temperature. Then both  $D(t)$  and  $v(t)$  are functions of  $T(t)$  which is given in Eq. (8-89). The final integration of Eq. (8-93) must be carried out numerically.

Values of  $\tau_{In}$  (the age of fission neutrons to indium resonance)  $\tau(E_{In} \rightarrow E_{th})$ , and  $\tau_T$  are given in Table 8-6 for the important moderators. It should be par-

ticularly noted in this table that in every case the age from fission energies to 1.45 eV is much larger than the age from 1.45 eV to thermal. Thus despite the fact that fission neutrons spend comparatively little time in moderating to 1.45 eV, the bulk of their migration occurs during this time. During the much longer thermalization time they move very little further from the source point. This is a very important result, for it means that it is possible to use age theory to compute the thermal slowing down distribution  $q_T(\mathbf{r})$  despite the fact that age theory is not valid at energies below the cutoff of the moderating region.

### 8-8 Slowing Down and Diffusion

According to the results of Section 8-6, fission neutrons quickly slow down to thermal energies and then spend a comparatively long time diffusing as thermal neutrons before being absorbed. It is possible, therefore, to describe the slowing down of neutrons and their subsequent diffusion as two distinct processes. Furthermore, since the thermal slowing-down density  $q_T(\mathbf{r})$  is equal to the number of neutrons becoming thermal per  $\text{cm}^3/\text{sec}$ ,  $q_T(\mathbf{r})$  is equivalent to a distributed source of thermal neutrons. Thus when  $q_T(\mathbf{r})$  is known, the thermal flux can be computed by the methods discussed in Chapter 5 for solving the diffusion equation.

For instance, if the diffusion kernel  $G_D(\mathbf{r}, \mathbf{r}')$  is known for a particular system, the flux can be obtained by evaluating the integral (cf. Eq. 5-79)

$$\phi_T(\mathbf{r}) = \int_V q_T(\mathbf{r}') G_D(\mathbf{r}, \mathbf{r}') dV', \quad (8-94)$$

where  $V$  is the volume of the system. In view of Eq. (6-136),  $q_T(\mathbf{r}')$  can also be expressed in terms of a slowing down kernel  $G_S(\mathbf{r}', \mathbf{r}'')$ , and Eq. (8-94) then takes the form

$$\phi_T(\mathbf{r}) = \iint s(\mathbf{r}'') G_S(\mathbf{r}', \mathbf{r}'') G_D(\mathbf{r}, \mathbf{r}') dV' dV''. \quad (8-95)$$

As an example of the use of Eq. (8-94), consider the slowing down and diffusion of neutrons emitted from an infinite planar source in an infinite medium. If the source emits  $S$  fast neutrons per  $\text{cm}^2/\text{sec}$  and if age theory is valid, the thermal slowing down density at  $x'$  is (cf. Eq. 6-96)

$$q_T(x') = \frac{S}{\sqrt{4\pi\tau_T}} e^{-x'^2/4\tau_T}. \quad (8-96)$$

The diffusion kernel in planar geometry is given by Eq. (5-82):

$$G_D(x, x') = \frac{L_T}{2D} e^{-|x-x'|/L_T}, \quad (8-97)$$

and from Eq. (8-94) the thermal flux is

$$\phi_T(x) = \frac{SL_T}{2D\sqrt{4\pi\tau_T}} \int_{-\infty}^{\infty} e^{-x'^2/4\tau_T} e^{-|x-x'|/L_T} dx'. \quad (8-98)$$

To evaluate the integral in Eq. (8-98) it is necessary to break the range of integration into two parts, namely,  $x' < x$  and  $x' > x$ . Then  $\phi_T(x)$  becomes

$$\begin{aligned}\phi_T(x) = \frac{SL_T}{2D\sqrt{4\pi\tau_T}} & \left[ \int_{-\infty}^x \exp\left(-\frac{x'^2}{4\tau_T} + \frac{x'}{L_T} - \frac{x}{L_T}\right) dx' \right. \\ & \left. + \int_x^\infty \exp\left(-\frac{x'^2}{4\tau_T} - \frac{x'}{L_T} + \frac{x}{L_T}\right) dx' \right]. \quad (8-99)\end{aligned}$$

These integrals can be expressed in terms of the error function which is defined by the integral (see Appendix II)

$$\operatorname{erf} x = \frac{2}{\sqrt{\pi}} \int_0^x e^{-t^2} dt. \quad (8-100)$$

By completing the square of the argument in the exponential, the first integral in Eq. (8-99) can be written as

$$\begin{aligned}\int_{-\infty}^x \exp\left(-\frac{x'^2}{4\tau_T} + \frac{x'}{L_T} - \frac{x}{L_T}\right) dx' \\ = \exp\left(\frac{\tau_T}{L_T^2} - \frac{x}{L_T}\right) \int_{-\infty}^x \exp\left(-\left(\frac{x'}{2\sqrt{\tau_T}} - \frac{\sqrt{\tau_T}}{L_T}\right)^2\right) dx'. \quad (8-101)\end{aligned}$$

Now by introducing the new variable

$$t = \frac{x'}{2\sqrt{\tau_T}} - \frac{\sqrt{\tau_T}}{L_T}, \quad (8-102)$$

Eq. (8-101) becomes

$$\begin{aligned}\int_{-\infty}^x \exp\left(-\frac{x'^2}{4\tau_T} + \frac{x'}{L_T} - \frac{x}{L_T}\right) dx' \\ = 2\sqrt{\tau_T} \exp\left(\frac{\tau_T}{L_T^2} - \frac{x}{L_T}\right) \int_{-\infty}^{x/2\sqrt{\tau_T} - \sqrt{\tau_T}/L_T} e^{-t^2} dt \\ = \sqrt{\pi\tau_T} \exp\left(\frac{\tau_T}{L_T^2} - \frac{x}{L_T}\right) \left[ \frac{2}{\sqrt{\pi}} \int_{-\infty}^0 e^{-t^2} dt + \frac{2}{\sqrt{\pi}} \int_0^{x/2\sqrt{\tau_T} - \sqrt{\tau_T}/L_T} e^{-t^2} dt \right] \\ = \sqrt{\pi\tau_T} \exp\left(\frac{\tau_T}{L_T^2} - \frac{x}{L_T}\right) \left[ 1 + \operatorname{erf}\left(\frac{x}{2\sqrt{\tau_T}} - \frac{\sqrt{\tau_T}}{L_T}\right) \right]. \quad (8-103)\end{aligned}$$

The second integral in Eq. (8-99) can be handled in the same way, and the final expression for the flux is

$$\begin{aligned}\phi_T(x) = \frac{SL_T e^{\tau_T/L_T^2}}{4D} & \left\{ e^{-x/L_T} \left[ 1 + \operatorname{erf}\left(\frac{x}{2\sqrt{\tau_T}} - \frac{\sqrt{\tau_T}}{L_T}\right) \right] \right. \\ & \left. + e^{x/L_T} \left[ 1 - \operatorname{erf}\left(\frac{x}{2\sqrt{\tau_T}} + \frac{\sqrt{\tau_T}}{L_T}\right) \right] \right\}. \quad (8-104)\end{aligned}$$

Although this result appears to be rather complicated,  $\phi_T$  can easily be computed using tables of the error function.

Other useful formulas for finding the thermal flux from a known slowing-down density can be obtained from the general solution to the diffusion equation given by Eqs. (5-88) and (5-89). For example, if the slowing-down density at the distance  $r$  from a point source in an infinite medium is  $q_T(r)$ , the diffusion equation is

$$\frac{1}{r^2} \frac{d}{dr} r^2 \frac{d\phi_T(r)}{dr} - \frac{1}{L_T^2} \phi_T(r) = - \frac{q_T(r)}{D}. \quad (8-105)$$

According to Eq. (5-88),  $\phi_T(r)$  can be found in terms of the homogeneous solutions to Eq. (8-105). To satisfy the requirement that  $\phi_T$  be finite at  $r = 0$  and go to zero as  $r \rightarrow \infty$ , it is appropriate to choose as homogeneous solutions the following functions:

$$\phi_{h1}(r) = \frac{e^{-r/L_T}}{r} \quad (8-106)$$

and

$$\phi_{h2}(r) = \frac{\sinh(r/L_T)}{r}. \quad (8-107)$$

These functions satisfy the homogeneous form of Eq. (8-105), and it will be noted that  $\phi_{h1}$  is singular at  $r = 0$  but goes to zero as  $r \rightarrow \infty$ , while  $\phi_{h2}$  has the reverse behavior. The Wronskian of these functions (cf. Eq. 5-90) is easily found to be  $1/r^2 L_T$ , and  $\phi_T(r)$  is then

$$\phi_T(r) = \frac{L_T}{D} \left[ \frac{\sinh(r/L_T)}{r} \int_r^\infty q_T(r') e^{-r'/L_T} r' dr' + \frac{e^{-r/L_T}}{r} \int_0^r q_T(r') \sinh(r'/L_T) r' dr' \right]. \quad (8-108)$$

In this expression the limits on the integrals have been adjusted so that  $\phi_T(r)$  remains finite at  $r = 0$  and vanishes as  $r \rightarrow \infty$ . These integrals can be computed numerically, and, provided the slowing-down density is accurately known (from either theory or experiment), the thermal flux determined in this way is reasonably precise. The only assumption implicit in Eq. (8-108) is the validity of diffusion theory for the thermal neutrons.

### 8-9 Measurements of the Thermal Diffusion Parameters

The formulas derived in this chapter and Chapter 5 for the thermal diffusion coefficient and the thermal diffusion length can be used to obtain good estimates of these parameters. However, the assumptions on which these formulas are based are not always valid, and, furthermore, the necessary cross-section data is frequently unreliable. For these reasons, it is usually advisable to determine  $D$  and  $L_T$  from experiment. (Measured values of  $D$  and  $L_T^2$  are given in Table 8-3.)

Two methods for measuring these parameters are widely used. The older of these involves the measurement of the spatial distribution of the steady-state thermal flux in an assembly of material called a *sigma pile*. In the second, and newer method, a sharp burst or *pulse* of neutrons is introduced into an assembly of material and the flux is measured as a function of time. As will be shown presently, it is possible to determine only the diffusion length in the steady-state experiments. Considerably more information about thermal diffusion parameters can be obtained from pulsed-neutron experiments.

**Sigma pile experiments.** In steady-state experiments it is necessary to provide some sort of steady neutron source; and small decay sources, e.g., Ra-Be sources, have been used for this purpose. From a practical standpoint, however, it is desirable to use as strong a source as possible. Reactors are therefore almost always used to provide source neutrons whenever accurate measurements are to be performed.

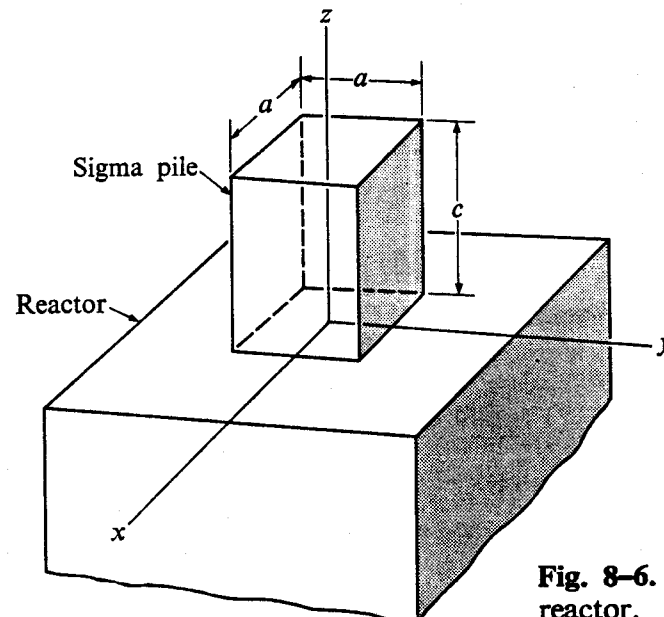


Fig. 8-6. Sigma pile atop a reactor.

Consider a large block of material (or tank if it is a liquid) placed atop the thermal column of a reactor as shown in Fig. 8-6. For simplicity, it will be assumed that the pile has a square cross section, each side of extrapolated length  $a$ , and an extrapolated height  $c$ . It will also be assumed that the thermal flux at the base of the pile,  $\phi_T(x, y, 0)$ , is known and is symmetric about the center of the pile. This will be the case if the thermal column is located at the center of the reactor. With  $\phi_T(x, y, 0)$  a symmetric function it necessarily follows that the flux throughout the pile must be an even function of both  $x$  and  $y$ .

Since the flux in the pile depends on all three rectangular coordinates, the diffusion equation is

$$\frac{\partial^2 \phi_T}{\partial x^2} + \frac{\partial^2 \phi_T}{\partial y^2} + \frac{\partial^2 \phi_T}{\partial z^2} - \frac{1}{L_T^2} \phi_T = 0. \quad (8-109)$$

This equation can be solved in terms of eigenfunctions (cf. Section 5-10). Now, however, since  $\phi_T$  is a function of three spatial variables it is convenient to use a *double eigenfunction series*.\* Thus a solution is assumed of the form

$$\phi_T(x, y, z) = \sum_{m,n \text{ odd}} f_{mn}(z) \cos \frac{m\pi x}{a} \cos \frac{n\pi y}{a}, \quad (8-110)$$

where the function  $f_{mn}(z)$  must be determined. It will be noted that Eq. (8-110) vanishes at the extrapolated sides of the pile and is an even function of  $x$  and  $y$  as required.

Substituting Eq. (8-110) into Eq. (8-109) yields

$$\begin{aligned} \sum_{m,n \text{ odd}} \left[ -\left(\frac{m\pi}{a}\right)^2 f_{mn} - \left(\frac{n\pi}{a}\right)^2 f_{mn} + \frac{d^2 f_{mn}}{dz^2} - \frac{1}{L_T^2} f_{mn} \right] \\ \times \cos \frac{m\pi x}{a} \cos \frac{n\pi y}{a} = 0. \end{aligned} \quad (8-111)$$

In view of the orthogonality of the eigenfunctions, each term in the series in Eq. (8-111) must be equal to zero. Thus the following differential equation for  $f_{mn}$  is obtained:

$$\frac{d^2 f_{mn}}{dz^2} - \gamma_{mn}^2 f_{mn} = 0, \quad (8-112)$$

where

$$\gamma_{mn}^2 = \frac{1}{L_T^2} + \left(\frac{m\pi}{a}\right)^2 + \left(\frac{n\pi}{a}\right)^2. \quad (8-113)$$

The solution to Eq. (8-112) which is zero when  $z = c$ , i.e., at the extrapolated top of the pile, is

$$f_{mn} = A_{mn} \sinh \gamma_{mn}(c - z), \quad (8-114)$$

where the  $A_{mn}$  are constants which remain to be determined.

From Eq. (8-110),  $\phi_T(x, y, z)$  may now be written as

$$\phi_T(x, y, z) = \sum_{m,n \text{ odd}} A_{mn} \sinh \gamma_{mn}(c - z) \cos \frac{m\pi x}{a} \cos \frac{n\pi y}{a}. \quad (8-115)$$

The constants  $A_{mn}$  can be found from the boundary condition at the base of the pile, where  $\phi_T(x, y, 0)$  is presumed to be known. From Eq. (8-115),

$$\phi_T(x, y, 0) = \sum_{m,n \text{ odd}} A_{mn} \sinh \gamma_{mn} c \cos \frac{m\pi x}{a} \cos \frac{n\pi y}{a}. \quad (8-116)$$

Next, multiplying both sides of this equation by  $\cos(m'\pi x/a) \cos(n'\pi y/a)$  and integrating over the base of the pile, it is easy to see that in view of the ortho-

---

\* A triple eigenfunction series in all variables,  $x$ ,  $y$ , and  $z$ , can also be used but the subsequent analysis is somewhat more complicated (cf. Prob. 8-23).

nality of the eigenfunctions  $A_{mn}$  is given by

$$A_{mn} = \frac{4}{a^2 \sinh \gamma_{mn} c} \int_{-a/2}^{a/2} \int_{-a/2}^{a/2} \phi_T(x, y, 0) \cos \frac{m\pi x}{a} \cos \frac{n\pi y}{a} dx dy. \quad (8-117)$$

Thus when the explicit form of the function  $\phi_T(x, y, 0)$  is known, the  $A_{mn}$  can be computed, and the thermal flux can be determined throughout the pile.

Actually, it is not necessary to know the absolute value of  $\phi_T$  in order to carry out measurements of the diffusion length. In these experiments the flux is measured along the center ( $z$ -axis) of the pile, so that placing  $x = y = 0$  in Eq. (8-115) gives

$$\phi_T(0, 0, z) = \sum_{m, n \text{ odd}} A_{mn} \sinh \gamma_{mn}(c - z). \quad (8-118)$$

All sigma piles are purposely constructed so that the height  $c$  is much larger than  $L_T$ , and as a consequence, there is a region in the pile, not too close to the top, where the quantity  $\gamma_{mn}(c - z)$  is much greater than unity. In particular, if  $\gamma_{11}(c - z) > 1$ , then this will be true for all values of  $m$  and  $n$  since according to Eq. (8-113) the  $\gamma_{mn}$  increase monotonically with  $m$  and  $n$ . Therefore, with Eq. (8-118) written in exponentials,

$$\phi_T(0, 0, z) = \frac{1}{2} \sum_{m, n \text{ odd}} A_{mn} [e^{\gamma_{mn}(c-z)} - e^{-\gamma_{mn}(c-z)}], \quad (8-119)$$

it is evident that except near the top of the pile the second term in this equation can be neglected. Then, upon defining the new constant  $C_{mn} = \frac{1}{2} A_{mn} e^{\gamma_{mn} c}$ , Eq. (8-119) becomes

$$\phi_T(0, 0, z) \approx \sum_{m, n \text{ odd}} C_{mn} e^{-\gamma_{mn} z}. \quad (8-120)$$

In view of the fact that  $\gamma_{11} < \gamma_{13}, \gamma_{31} < \gamma_{15}$ , etc., the first term in Eq. (8-120) is greater than the second term, which in turn is greater than (or possibly equal to) the third, and so on. Furthermore, in most experiments it turns out that  $C_{11} < C_{13} \approx C_{31} < C_{15}, \dots$  etc., so that over a certain distance along the center of the pile  $\phi_T$  is given by

$$\phi_T = C_{11} e^{-\gamma_{11} z} + C_{13} e^{-\gamma_{13} z} + \dots, \quad (8-121)$$

where the second term is much smaller than the first.

The diffusion length is determined with the aid of Eq. (8-121) in the following way. The thermal flux is measured as a function of  $z$  along the center of the pile. According to Eq. (8-121) the measured value of  $\phi_T$  varies approximately as  $\exp(-\gamma_{11} z)$ , and a plot of  $\ln \phi_T$  versus  $z$  therefore yields a rough estimate of  $\gamma_{11}$ . With this value of  $\gamma_{11}$ , an approximate value of  $L_T$  can now be computed from Eq. (8-113), and estimates can then be made of  $\gamma_{13}, \gamma_{31}, \gamma_{15}$ , etc. Then knowing even approximate values of the constants  $C_{11}, C_{13}$ , etc., the contribution of the higher terms in Eq. (8-121) can be estimated. These computations are repeated until a value of  $L_T$  is obtained that consistently reproduces the data. (A least-squares analysis of the data can also be used to obtain  $L_T$ .)

**Pulsed-neutron experiments.** In these experiments an assembly of the material under investigation is exposed to a short burst of neutrons. These neutrons are obtained when a burst of charged particles from an accelerator strikes a suitable target. For example, if the accelerator produces deuterons, a tritium target will give neutrons from the  $H^3(d, n)He^4$  reaction. The energy of the charged particles need not be high; the maximum value of the cross section for the  $H^3(d, n)He^4$  reaction, for instance, occurs at only about 100 keV. With modern techniques for pulsing accelerators, pulses of neutrons of the order of  $10-\mu$  sec duration can easily be obtained. Shorter burst widths are not required for the experiments under discussion.

In some experiments the neutrons are produced external to the assembly and enter the assembly through its surface. In many ways, however, it is preferable to produce the neutrons in the interior of the system. This is accomplished by locating the target at a convenient point (usually at the center) in the assembly and passing the charged particle beam through a small tube. For the purposes of the present discussion this latter technique will be assumed.

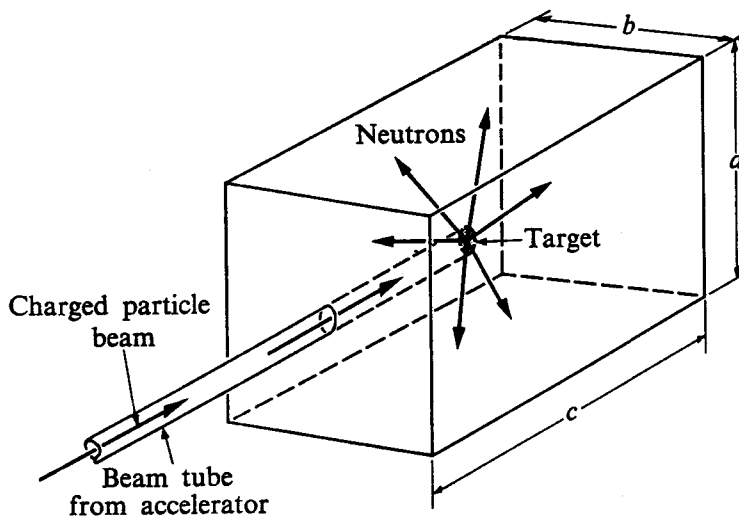


Fig. 8-7. Schematic drawing of the experimental arrangement for producing a pulse of neutrons in the center of a block of material.

Consider then a block of material of extrapolated dimensions  $a$ ,  $b$ ,  $c$ , at the center of which a burst of neutrons is introduced as indicated in Fig. 8-7. These neutrons are initially very energetic, having energies of several MeV, but they promptly slow down to thermal energies and then diffuse as thermal neutrons in the manner discussed in the preceding section. Furthermore, as shown in Section 8-6, the time required for the fast neutrons to slow down to thermal energies is considerably shorter than their thermal diffusion time, and it is possible to assume, therefore, that the burst of fast neutrons emanating from the target actually provides a burst of *thermal* neutrons distributed in some way within the assembly. In other words, the source of neutrons in the system can be taken to be

of the form

$$s(\mathbf{r}, t) = s(\mathbf{r}) \delta(t), \quad (8-122)$$

where  $s(\mathbf{r})$  is the spatial distribution of the thermalized neutrons and  $\delta(t)$  is the Dirac delta function. To simplify the present discussion it will also be assumed that  $s(\mathbf{r})$  is a symmetric function of position so that it can be expanded in terms of simple cosine eigenfunctions.

With the introduction of a burst of neutrons into an otherwise quiescent assembly, the thermal neutron flux quickly builds up from zero, and then somewhat more slowly returns to zero as the neutrons are absorbed or leak from the system. The flux is determined by the time-dependent diffusion equation (Eq. 8-86)

$$L_T^2 \nabla^2 \phi_T(\mathbf{r}, t) - \phi_T(\mathbf{r}, t) = t_d \frac{\partial \phi_T(\mathbf{r}, t)}{\partial t} - \frac{s(\mathbf{r}) \delta(t)}{\bar{\Sigma}_a}. \quad (8-123)$$

This equation can be solved using the eigenfunctions of the assembly. Thus let

$$\phi_T(\mathbf{r}, t) = \sum_{l,m,n \text{ odd}} T_{lmn}(t) \cos \frac{l\pi x}{a} \cos \frac{m\pi y}{b} \cos \frac{n\pi z}{c}, \quad (8-124)$$

where the functions  $T_{lmn}(t)$  must be determined. Similarly let

$$s(\mathbf{r}) = \sum_{l,m,n \text{ odd}} S_{lmn} \cos \frac{l\pi x}{a} \cos \frac{m\pi y}{b} \cos \frac{n\pi z}{c}. \quad (8-125)$$

Since the source function  $s(\mathbf{r})$  is presumably known, the constants  $S_{lmn}$  may be assumed to be known also.

Substituting Eqs. (8-124) and (8-125) into Eq. (8-123) and noting the orthogonality of the eigenfunctions yields the following equation for the functions  $T_{lmn}$ :

$$-(1 + B_{lmn}^2 L_T^2) T_{lmn}(t) = t_d \frac{dT_{lmn}(t)}{dt} - \frac{S_{lmn}}{\bar{\Sigma}_a} \delta(t), \quad (8-126)$$

where

$$B_{lmn}^2 = \left( \frac{l\pi}{a} \right)^2 + \left( \frac{m\pi}{b} \right)^2 + \left( \frac{n\pi}{c} \right)^2, \quad (8-127)$$

and  $l$ ,  $m$ , and  $n$  are odd integers. Writing this equation in standard form

$$dT_{lmn}(t) + \frac{1 + B_{lmn}^2 L_T^2}{t_d} T_{lmn}(t) dt = \frac{S_{lmn}}{t_d \bar{\Sigma}_a} \delta(t) dt, \quad (8-128)$$

it will be evident that the integrating factor is

$$\exp \left[ \frac{1 + B_{lmn}^2 L_T^2}{t_d} t \right].$$

The integration of Eq. (8-128) is carried out starting from a short time prior to the onset of the neutron burst, indicated by  $t = 0^-$ , when there is no flux in the

system. This gives

$$\begin{aligned} T_{lmn}(t) &= \frac{S_{lmn}}{t_d \sum_a} \exp \left[ -\frac{1 + B_{lmn}^2 L_T^2}{t_d} t \right] \int_{0^-} \delta(t) \exp \left[ \frac{1 + B_{lmn}^2 L_T^2}{t_d} t \right] dt \\ &= \frac{S_{lmn}}{t_d \sum_a} \exp \left[ -\frac{1 + B_{lmn}^2 L_T^2}{t_d} t \right]. \end{aligned} \quad (8-129)$$

The flux is then

$$\phi_T(\mathbf{r}, t) = \frac{1}{t_d \sum_a} \sum_{l,m,n \text{ odd}} S_{lmn} \exp \left[ -\frac{1 + B_{lmn}^2 L_T^2}{t_d} t \right] \cos \frac{l\pi x}{a} \cos \frac{m\pi y}{b} \cos \frac{n\pi z}{c}. \quad (8-130)$$

At this point it is observed that in view of Eq. (8-127) the parameters  $B_{lmn}^2$  form a monotonically increasing series, i.e.,  $B_{111}^2 < B_{311}^2 \approx B_{131}^2 \approx B_{113}^2 < B_{511}^2$ , etc. It follows that the second and all higher terms in Eq. (8-130) die out in time more rapidly than the first term. Eventually, therefore, the flux at every point in the assembly decreases as a single exponential:

$$\phi_T(t) = \text{const } e^{-\lambda t}, \quad (8-131)$$

where the decay constant is given by

$$\lambda = \frac{1 + B^2 L_T^2}{t_d}, \quad (8-132)$$

and  $B^2$  has been written for  $B_{111}^2$ .

Equation (8-132) forms the basis of pulsed-neutron experiments, which are carried out in the following steps. First, the flux is measured as a function of time after a burst of neutrons is produced in the assembly. According to Eq. (8-131) the flux ultimately decays exponentially, and from these data the value of  $\lambda$  can be determined for the assembly. These measurements are repeated for assemblies of varying sizes, and the resulting values of  $\lambda$  are plotted as a function of  $B^2$  as shown in Fig. 8-8. On the basis of the above derivation the result should be a

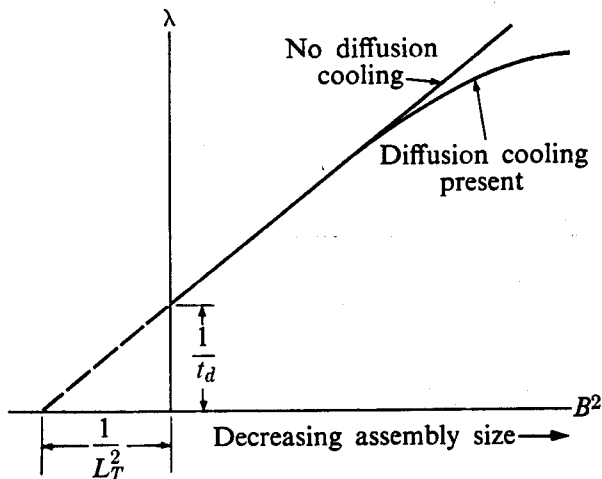


Fig. 8-8. The decay constant versus  $B^2$  in pulsed neutron experiments.

straight line which intercepts the negative  $B^2$ -axis at  $L_T^{-2}$ . Furthermore, the value of  $\lambda$  at  $B^2 = 0$  is simply  $t_d^{-1}$ , which is equal to  $\Sigma_a(E_0)v_0$  or  $2\bar{\Sigma}_a v_T / \sqrt{\pi}$  for a  $1/v$  absorber, so that  $\Sigma_a(E_0)$  or  $\bar{\Sigma}_a$  are also determined. This value of  $\bar{\Sigma}_a$  together with the measured value of  $L_T^2$  provides the value of  $D$  from Eq. (8-73). It will be evident that pulsed measurements yield substantially more information than the older steady-state method discussed earlier, and it is not surprising to find that sigma pile measurements are rapidly being replaced by pulsed-neutron techniques.

In conclusion, it should be mentioned that when experiments of this type are carried out it is found that a plot of  $\lambda$  versus  $B^2$  deviates from a straight line, as indicated in Fig. 8-8, at large values of  $B^2$ , that is, for small assemblies. This effect has been shown to be due primarily to diffusion cooling which was not included in the preceding derivation. Thus when diffusion cooling is taken into account, Eq. (8-132) becomes

$$\lambda = \frac{1}{t_d} + \frac{L_T^2}{t_d} B^2 - CB^4, \quad (8-133)$$

where the parameter  $C$  is known as the *diffusion cooling coefficient*. Methods have been devised for computing  $C$ , and these are discussed in the references.

## References

### General

GALANIN, A. D., *Thermal Reactor Theory*, 2nd ed. New York: Pergamon Press, 1960, Section 35.

*Reactor Physics Constants*. U.S. Atomic Energy Commission Report, ANL-5800, 2nd ed., 1963, Section 3.

WEINBERG, A. M., and E. P. WIGNER, *The Physical Theory of Neutron Chain Reactors*. Chicago: University of Chicago Press, 1958, Chapter 11.

### Neutron thermalization (theory and measurements)

BECKURTS, K. H. "Reactor Physics Research with Pulsed Neutron Sources," *Nucl. Instrum. Methods* **11**, 144 (1961).

BECKURTS, K. H., and K. WIRTZ, *Neutron Physics*. Berlin: Springer Verlag, 1958 (translated edition, 1964).

CORNGOLD, N., "Lectures on Neutron Thermalization," Ann Arbor: University of Michigan Report, MMPP-NPC-1962-1.

VON DARDEL, G. F., "The Interactions of Neutrons with Matter Studied with a Pulsed Neutron Source," *Trans. Roy. Inst. Technol. Stockholm* **75** (1954).

VON DARDEL, G. F., and N. G. SJOSTRAND, "Diffusion Measurements with Pulsed Neutron Sources," *Progr. Nucl. Energy Ser. I*, Vol. 2, p. 183 (1958).

HONECK, H. C., "A Review of the Methods for Computing Thermal Neutron Spectra," BNL-821 (T-319), June 1963. This report contains an extensive bibliography on methods for computing spectra.

KOTHARI, L. S., and V. P. DUGGAL, "Scattering of Thermal Neutrons from Solids and Their Thermalization Near Equilibrium," *Advances in Nuclear Science and Technology*, Vol. 2. New York: Academic Press, 1964.

NELKIN, M. S., "Neutron Thermalization," *Proceedings of Symposia in Applied Mathematics*, Volume XI. Providence, R.I.: American Mathematical Society, 1961.

YOUNG, J. C., and D. HUFFMAN, "Theoretical and Experimental Neutron Spectra," General Atomics Report GA-5319, May 22, 1964. This report contains an extensive compilation of measured and computed neutron spectra.

Proceedings of Brookhaven Conference on Neutron Thermalization, BNL-719 (1962).

#### Average thermal cross sections

MEGHREBLIAN, R. V., and D. K. HOLMES, *Reactor Analysis*. New York: McGraw-Hill, 1960, Section 4.7.

WESTCOTT, C. H. "Effective Cross-Section Values for Well-Moderated Thermal Reactor Spectra," AECL-1101, 3rd ed., January 1962.

#### Problems

8-1. The scattering kernel for neutrons in a gas of free hydrogen atoms at temperature  $T$  is given by

$$\Sigma_s(E \rightarrow E') = \frac{\Sigma_0}{E} \begin{cases} \operatorname{erf} \sqrt{E'/kT}, & E' < E, \\ \exp[(E - E')/kT] \operatorname{erf} \sqrt{E/kT}, & E' > E, \end{cases}$$

where  $\Sigma_0$  is a constant (the free cross section of hydrogen). (a) Show that this kernel satisfies the condition of detailed balance. (b) Compute the scattering cross section  $\Sigma_s(E)$  for neutrons in this hypothetical hydrogen gas. (c) Find the scattering distribution function  $P(E \rightarrow E')$ . (d) Show that for  $E \gg kT$ ,  $P(E \rightarrow E')$  reduces to its usual value for hydrogen, namely,  $P(E \rightarrow E') = 1/E$ . (e) What is the probability that a neutron of energy  $E = kT$  will be up-scattered?

8-2. Consider an infinite moderating medium throughout which  $S$  neutrons/cm<sup>3</sup>-sec are emitted at an energy much greater than  $E_m$ . Show that the source term  $S(E)$  in Eq. (8-2) is given by

$$S(E) = \frac{S}{E_m}$$

if the medium is hydrogen, and

$$S(E) = \begin{cases} \frac{S}{\xi(1 - \alpha)} \left( \frac{1}{E_m} - \frac{\alpha}{E} \right), & \alpha E_m < E < E_m, \\ 0, & E < \alpha E_m, \end{cases}$$

if the medium has  $A > 1$ .

8-3. What is the average energy of neutrons in a Maxwellian flux; that is, the average value of  $E$  over the flux distribution  $\phi_M(E)$ ?

8-4. The Maxwellian neutron density distribution function is given by

$$n_M(E) = \frac{2\pi n}{(\pi kT)^{3/2}} E^{1/2} e^{-E/kT}.$$

(a) Show that the most probable energy in this distribution is given by

$$E_{\text{most probable}} = \frac{1}{2}kT.$$

(b) Show that the average energy in this distribution is

$$\bar{E} = \frac{3}{2}kT.$$

8-5. Show that  $v_T$  (cf. Eq. 8-11) is the most probable speed in a Maxwellian density distribution (*not* flux). [Hint: First obtain the function  $n_M(v)$ , where  $n_M(v) dv = n_M(E) dE$ .]

8-6. The Bragg cutoff in graphite is at approximately 0.0018 eV. At what temperature is this the most probable energy of the neutrons in a Maxwellian flux?

8-7. It is common practice in giving low energy neutron spectra to plot  $E\phi(E)$  rather than  $\phi(E)$ . Show that the peak of the curve is at  $E_{\max} \approx 2kT$ .

8-8. Suppose that  $1/v$  absorbers are suddenly inserted uniformly into an infinite medium containing a well-established Maxwellian distribution of neutrons. (a) Show that the total density of neutrons in the medium steadily decreases in time, but that the neutron energy distribution, and hence the neutron temperature, does not change. (b) Discuss qualitatively the change in the energy distribution if the cross section of the absorbers varies as  $v^{-x}$ , where  $x \neq 1$ .

8-9. If the thermal neutrons in a reactor are assumed to be a perfect gas, compute the partial pressure of this gas for a 2200 m/sec flux of  $10^{13}$  neutrons/cm<sup>2</sup>-sec. ( $T = 100^\circ\text{C}$ .)

8-10. A water-moderated thermal reactor operating at 500°F has a computed average thermal flux of  $2 \times 10^{14}$  neutrons/cm<sup>2</sup>-sec. (a) Compute the rate at which neutrons are absorbed in the water. (Take the water to be of normal density.) (b) What concentration of the fission product Xe<sup>135</sup> gives the same absorption rate as in part (a)?

8-11. Show that the Jacobian of the transformation from the integration variables  $\mathbf{v}$  and  $\mathbf{V}$  to  $\mathbf{v}_r$  and  $\mathbf{c}$  in Eq. (8-45) is equal to unity.

8-12. A thermal reactor contains 350 gallons of ordinary water at room temperature and unit density. If the reactor operates at an average thermal flux of  $5 \times 10^{13}$  neutrons/cm<sup>2</sup>-sec, compute the concentrations of HDO and D<sub>2</sub>O in the reactor after 2 years of operation.

8-13. A U<sup>235</sup>-fueled thermal reactor operates at 100°C and produces 100 MW of thermal power. (a) If the fuel inventory at a particular time is 20 kg of U<sup>235</sup>, find the average 2200 meter/sec flux in the reactor. (b) Find the average thermal flux in the reactor. (c) At what rate is the fuel consumed?

8-14. A bare cubical reactor, of side  $a = 600$  cm, is fueled with U<sup>235</sup>. When it is operating at a thermal power of 10 MW at an average temperature of 150°C, the 2200 meter/sec flux is observed to be given approximately by the following formula:

$$\phi_0(x, y, z) = 10^{12} \cos\left(\frac{\pi x}{a}\right) \cos\left(\frac{\pi y}{a}\right) \cos\left(\frac{\pi z}{a}\right),$$

where  $x, y, z$  are measured from the center of the reactor. (a) How much U<sup>235</sup> is in the reactor? (b) How many moles of thermal neutrons are there in the entire reactor?

8-15. Compute the value of  $\eta_T$  for 2.5% enriched uranium as a function of temperature from  $T = 20^\circ\text{C}$  to  $500^\circ\text{C}$  and estimate the quantity  $(1/\eta_T)(d\eta_T/dT)$  (which is called the *temperature coefficient* of  $\eta_T$ ) for this fuel in this temperature range.

8-16. Find the limiting value of Eq. (8-104) as  $\tau_T \rightarrow 0$  and interpret the result.

8-17. Sources emitting  $S$  fast neutrons/cm<sup>3</sup>-sec are uniformly distributed throughout an infinite medium. Calculate the thermal flux if (a) there are no resonance absorbers present; (b) resonance absorbers are uniformly distributed throughout the medium.

8-18. Sources of monoenergetic fast neutrons are distributed in an infinite slab of moderator according to the function

$$s(x) = S \cos\left(\frac{\pi x}{a}\right),$$

where  $S$  is a constant and  $a$  is the thickness of the slab. (a) Assuming the validity of age theory and ignoring resonance capture, find the thermal slowing down density everywhere in the slab. (b) What fraction of the neutrons escape from the slab while slowing down? (c) Find the thermal flux in the slab. (d) What is the probability that a neutron leaks from the slab while diffusing at thermal energies?

8-19. A monodirectional beam of fast neutrons of energy  $E$  and intensity  $I_0$  is incident normally upon a semi-infinite body of water, i.e., the region  $0 \leq x < \infty$ . (a) Using the model of neutron slowing down in hydrogen discussed in Section 6-13, show that the thermal flux in the water is given *approximately* by

$$\phi_T(x) = \frac{I_0 \Sigma_s(E)/\bar{\Sigma}_a}{1 - \Sigma_s^2(E)L_T^2} \left[ e^{-\Sigma_s(E)x} - e^{-x/L_T} \right].$$

(b) Under what circumstances will  $\phi_T(x)$  have a maximum in the water? (c) If, by chance,  $\Sigma_s(E) = L_T^{-1}$ , what is  $\phi_T(x)$ ? Does  $\phi_T(x)$  have a maximum in this case?

8-20. An isotropic point source emitting  $S$  fast neutrons/sec is placed at the center of a bare cube of moderator of side  $a$ . Using age theory, show that the thermal flux in the moderator is given by

$$\phi_T(x, y, z) = \frac{8S}{V\bar{\Sigma}_a} \sum_{l, m, n \text{ odd}} \frac{e^{-B_{lmn}^2 \tau_T}}{1 + B_{lmn}^2 L_T^2} \cos\left(\frac{l\pi x}{a}\right) \cos\left(\frac{m\pi y}{a}\right) \cos\left(\frac{n\pi z}{a}\right),$$

where  $V = a^3$  is the volume of the cube.

8-21. An isotropic point source emits  $S$  fast neutrons/sec in an infinite moderator. (a) Using age theory, show that the thermal flux at the distance  $r$  from the source is given by

$$\phi_T(r) = \frac{Se^{\tau_T/L_T^2}}{8\pi \bar{D}r} \left[ e^{r/L_T} \operatorname{erf}\left(\frac{r}{2\sqrt{\tau_T}} + \frac{\sqrt{\tau_T}}{L_T}\right) + e^{-r/L_T} \operatorname{erf}\left(\frac{r}{2\sqrt{\tau_T}} - \frac{\sqrt{\tau_T}}{L_T}\right) - 2 \sinh \frac{r}{L_T} \right]$$

(b) Show that in the limit as  $\tau_T \rightarrow 0$ , this expression reduces to Eq. (5-64). (c) Compute and plot the thermal flux in an infinite graphite medium containing a radium-beryllium source emitting  $10^7$  neutrons/sec. (The value of  $\tau_T$  is approximately  $440 \text{ cm}^2$ .) [Hint: Use either Eq. (8-108) or the diffusion kernel for spherically symmetric source distributions derived in Problem 5-28.]

8-22. An isotropic point source emitting  $S$  fast neutrons/sec is located at the center of a bare cylindrical tank of moderator of radius  $R$  and height  $H$ . Using age theory, show

that the thermal flux in the tank is

$$\phi_T(r, z) = \frac{2S}{V\bar{\Sigma}_a} \sum_{\substack{m=1, 2, 3, \dots, n \\ \text{odd}}} \frac{e^{-B_{mn}^2 r T}}{(1 + B_{mn}^2 L_T^2) J_1^2(x_m)} J_0\left(\frac{x_m r}{R}\right) \cos\left(\frac{n\pi z}{H}\right),$$

where  $x_m$  is the  $m$ th zero of  $J_0(x)$  and

$$B_{mn}^2 = \left(\frac{x_m}{R}\right)^2 + \left(\frac{n\pi}{H}\right)^2.$$

[Hint: See Problem 6-23.]

8-23. Calculate the thermal flux in the rectangular parallelepiped sigma pile considered in Section 8-9, by expanding  $\phi_T(x, y, z)$  in the triple eigenfunction series

$$\phi_T(x, y, z) = \sum_{\substack{l, m, n \\ \text{odd}}} A_{lmn} \cos\left(\frac{l\pi x}{a}\right) \cos\left(\frac{m\pi y}{a}\right) \cos\left(\frac{n\pi z}{a}\right),$$

and show that the flux along the center of the pile reduces to Eq. (8-120) except near the top of the pile.

8-24. A cylindrical tank of moderator (sigma pile) of radius  $R$  and height  $H$  is placed atop a symmetrical source distribution of thermal neutrons which gives a flux  $\phi_{T0}(r)$  at the base of the tank. (a) With the origin of cylindrical coordinates at the center of the base of the tank, show that the thermal flux throughout the pile is given by

$$\phi_T(r, z) = \sum_{n=1} A_n J_0\left(\frac{x_n r}{R}\right) \sinh \gamma_n(H - z),$$

where  $x_n$  is the  $n$ th zero of  $J_0(x)$ ,

$$\gamma_n^2 = \left(\frac{x_n}{R}\right)^2 + \frac{1}{L_T^2},$$

and

$$A_n = \frac{2}{R^2 J_1^2(x_n) \sinh \gamma_n H} \int_0^R \phi_{T0}(r) J_0\left(\frac{x_n r}{R}\right) r dr.$$

(b) Show that except near the top of the tank the flux along the axis varies approximately as

$$\phi_T(0, z) \sim \sum_{n=1} C_n e^{-\gamma_n z}.$$

# 9

## Fermi Theory of the Bare Thermal Reactor

The production, diffusion, and slowing down of neutrons having been discussed in the preceding chapters, it is now possible to consider quantitatively the conditions which give rise to a critical reactor system. In the present chapter the discussion will be confined to bare thermal reactors; the criticality of reflected and nonthermal reactors is considered in Chapter 10.

### 9-1 Criticality of an Infinite Homogeneous Reactor

It is instructive to begin by considering the criticality of an infinite reactor consisting of a homogeneous mixture of fuel and moderator. It will be assumed that the ratio of the numbers of moderator atoms to fuel atoms is so large that the bulk of the fission neutrons slow down to thermal energies before they induce further fissions. In other words, the system is presumed to be thermal.

Because the system is infinite and uniform, the thermal flux and the slowing-down density are independent of position. Then according to the results of Section 8-2, the number of thermal neutrons absorbed per  $\text{cm}^3/\text{sec}$  at any point in the system is equal to  $\bar{\Sigma}_a \phi_T$ , where  $\bar{\Sigma}_a$  is the thermal macroscopic absorption cross section of the fuel-moderator mixture and  $\phi_T$  is the thermal flux. If the thermal absorption cross sections of the fuel and moderator are  $\bar{\Sigma}_{aF}$  and  $\bar{\Sigma}_{aM}$ , respectively,  $\bar{\Sigma}_a$  is evidently

$$\bar{\Sigma}_a = \bar{\Sigma}_{aF} + \bar{\Sigma}_{aM}. \quad (9-1)$$

The fraction of the thermal neutrons which are absorbed in fuel is known as the *thermal utilization* and is denoted by the symbol  $f$ . Since  $\bar{\Sigma}_{aF}\phi_T$  neutrons are absorbed per  $\text{cm}^3/\text{sec}$  in fuel and  $\bar{\Sigma}_a\phi_T$  in the fuel-moderator mixture, it follows that  $f$  is given by

$$f = \frac{\bar{\Sigma}_{aF}\phi_T}{\bar{\Sigma}_a\phi_T} = \frac{\bar{\Sigma}_{aF}}{\bar{\Sigma}_a} = \frac{\bar{\Sigma}_{aF}}{\bar{\Sigma}_{aF} + \bar{\Sigma}_{aM}}. \quad (9-2)$$

The parameter  $f$  is also equal to the relative probability that a thermal neutron will ultimately be absorbed in fuel in an infinite reactor.

In view of Eq. (9-2) the number of neutrons absorbed per  $\text{cm}^3/\text{sec}$  in fuel can be written as  $f\bar{\Sigma}_a\phi_T$ . The number of fission neutrons emitted per  $\text{cm}^3/\text{sec}$  as the

result of thermal fissions is therefore  $\eta_T f \bar{\Sigma}_a \phi_T$ , where  $\eta_T$  is the average number of fission neutrons emitted per thermal neutron absorbed by fuel (cf. Section 8-4). If, in addition to fissile isotopes, there are also nuclei such as  $U^{238}$  in the reactor which undergo fast fission, the total number of fission neutrons emitted per  $cm^3/sec$  becomes  $\eta_T f \epsilon \bar{\Sigma}_a \phi_T$ , where  $\epsilon$  is the fast-fission factor (cf. Section 7-9).

These fast neutrons slow down in elastic and inelastic collisions with the nuclei in the system, and as explained in Chapter 7 some of these neutrons may be captured in absorption resonances if intermediate or heavy nuclei are present in the reactor. In this case, although  $\eta_T f \epsilon \bar{\Sigma}_a \phi_T$  fast neutrons are produced per  $cm^3/sec$ , only  $\eta_T f p \epsilon \bar{\Sigma}_a \phi_T$  (where  $p$  is the resonance escape probability) neutrons actually succeed in slowing down to thermal energies.

The absorption of  $\bar{\Sigma}_a \phi_T$  neutrons in one generation thus eventually leads to the absorption of  $\eta_T f p \epsilon \bar{\Sigma}_a \phi_T$  neutrons in the next generation. As discussed in Chapter 4, the ratio of the number of fissions in one generation to the number in the generation immediately preceding is called the *multiplication factor*. Therefore, since the number of fissions is obviously proportional to the number of neutrons absorbed, it follows that for the system under discussion the multiplication factor is given by

$$k_\infty = \eta_T f p \epsilon. \quad (9-3)$$

The subscript on  $k_\infty$  signifies that this is the multiplication factor for an infinite system only.

Consider now the time behavior of an infinite reactor. To begin with, it will be obvious that in the absence of extraneous neutron sources (including spontaneous fissions) the flux in the reactor will remain zero after the system has been assembled since it requires at least one neutron to initiate a chain reaction. Suppose, however, that at time  $t = 0$  a uniform source emitting  $S$  fast neutrons per  $cm^3/sec$  is introduced throughout the system. The resulting buildup of a neutron flux can be found from the time-dependent diffusion equation (Eq. 8-86), in which the spatial derivatives do not appear, since  $\phi_T$  is independent of position. Thus  $\phi_T$  is given by the equation

$$-\phi_T + \frac{s}{\bar{\Sigma}_a} = t_d \frac{d\phi_T}{dt}, \quad (9-4)$$

where  $s$  is the source density of *thermal* neutrons, and  $t_d$  is the thermal diffusion time.

There are two parts to the thermal source term  $s$ , one coming from the extraneous neutron source and one from the fission neutrons. Since  $S$  source neutrons are produced per  $cm^3/sec$  and no neutrons can leak from an infinite system,  $pS$  of these neutrons eventually slow down per  $cm^3/sec$  throughout the reactor.\* At the same time, as discussed earlier, the fission neutrons thermalize at a rate of  $\eta_T f p \epsilon \bar{\Sigma}_a \phi_T$  neutrons per  $cm^3/sec$ , which, in view of Eq. (9-3), can

---

\* It is assumed here for simplicity that the source neutrons do not produce fast fissions.

also be written as  $k_\infty \bar{\Sigma}_a \phi_T$ . Hence,

$$s = pS + k_\infty \bar{\Sigma}_a \phi_T, \quad (9-5)$$

and Eq. (9-4) becomes

$$\frac{pS}{\bar{\Sigma}_a} + (k_\infty - 1)\phi_T = t_d \frac{d\phi_T}{dt}. \quad (9-6)$$

The solution to Eq. (9-6) which satisfies the initial condition  $\phi_T(0) = 0$  can readily be shown to be

$$\phi_T = \frac{pS/\bar{\Sigma}_a}{k_\infty - 1} \left[ \exp(k_\infty - 1) \frac{t}{t_d} - 1 \right]. \quad (9-7)$$

According to Eq. (9-7),  $\phi_T$  increases without limit if  $k_\infty > 1$ . However, it should be noted that  $\phi_T$  also goes to infinity when  $k_\infty = 1$ , although not exponentially. Placing  $k_\infty = 1$  in Eq. (9-6) gives  $d\phi_T/dt = pS/\bar{\Sigma}_a t_d$ , so that

$$\phi_T = \frac{pSt}{\bar{\Sigma}_a t_d}. \quad (9-8)$$

Thus if  $k_\infty = 1$ , the flux increases *linearly* with time. This result may be understood physically by noting that according to Eq. (8-23),  $\phi_T = 2nv_T/\sqrt{\pi}$ , where  $n$  is the thermal neutron density, and from Eq. (8-82),  $t_d = \sqrt{\pi}/2\bar{\Sigma}_a v_T$ . Substituting these expressions into Eq. (9-8) gives

$$n = pSt. \quad (9-9)$$

Equation (9-9) shows that if  $k_\infty = 1$ , the density of thermal neutrons in the system increases at the constant rate of  $pS$  neutrons per  $\text{cm}^3/\text{sec}$ . This behavior is due to the fact that with  $k_\infty = 1$ , a neutron introduced into the reactor is effectively never lost, since it is replaced by another neutron in each succeeding generation of the chain reaction. However, source neutrons enter the system at the rate of  $S$  per  $\text{cm}^3/\text{sec}$ , and  $pS$  of these eventually become thermal. The number of thermal neutrons in the reactor therefore increases at the rate of  $pS$  neutrons per  $\text{cm}^3/\text{sec}$  when  $k_\infty = 1$ , simply because of the continued accumulation of the thermalized source neutrons.

Finally, when  $k_\infty < 1$  in Eq. (9-7),  $\phi_T$  goes to a steady value of

$$\phi_T \rightarrow \frac{pS/\bar{\Sigma}_a}{1 - k_\infty}. \quad (9-10)$$

To understand the physical significance of Eq. (9-10), it is convenient to multiply both sides of the equation by  $\bar{\Sigma}_a$ ; this gives

$$\bar{\Sigma}_a \phi_T = \frac{pS}{1 - k_\infty}. \quad (9-11)$$

The left-hand side of this equation is equal to the number of thermal neutrons absorbed per  $\text{cm}^3/\text{sec}$  at any point in the reactor. The meaning of the right-hand side can be seen by noting that in view of the definition of  $k_\infty$ , the absorption of

$pS$  thermalized source neutrons gives rise to  $pSk_\infty$  new thermal neutrons. When these are absorbed,  $pSk_\infty^2$  new thermal neutrons are produced, and so on. Since the original source neutrons are assumed to be emitted continuously, the emission of  $S$  fast neutrons per  $\text{cm}^3/\text{sec}$  therefore leads to the production of

$$pS + pSk_\infty + pSk_\infty^2 + \dots = \frac{pS}{1 - k_\infty} \quad (9-12)$$

thermal neutrons per  $\text{cm}^3/\text{sec}$  throughout the system. In the steady state, however, the rates at which thermal neutrons are produced and absorbed must be equal, and this is the condition expressed by Eq. (9-11).

It should be clear from this discussion that regardless of the value of  $k_\infty$ , the introduction of a source into a quiescent assembly of fuel and moderator has the effect of producing a flux in the system. Suppose now that after having established a flux, the source is removed, say at the time  $t = t_0$ . Returning to Eq. (9-6), the solution with  $S = 0$  is

$$\phi_T = \phi_{T0} \exp \left[ (k_\infty - 1) \left( \frac{t - t_0}{t_d} \right) \right], \quad (9-13)$$

where  $\phi_{T0}$  is the thermal flux at  $t = t_0$ . From Eq. (9-13) it is seen that  $\phi_T$  still increases in time without limit when  $k_\infty > 1$ , and for this reason the reactor is said to be *supercritical* (cf. Section 4-1). On the other hand, if  $k_\infty < 1$ ,  $\phi_T$  decreases to zero and the reactor is *subcritical*. However, if  $k_\infty = 1$ , the flux remains at the constant value  $\phi_{T0}$  and the reactor is evidently *critical*.

To summarize these results:

- (i) If  $k_\infty > 1$ , an infinite reactor is supercritical, and the flux in the system increases without limit once the chain reaction is initiated, whether or not there is an extraneous neutron source in the system.
- (ii) If  $k_\infty < 1$ , the reactor is subcritical, and a flux cannot be maintained without an extraneous source of neutrons.
- (iii) If  $k_\infty = 1$ , the reactor is critical, and a steady flux will be maintained with no sources present, provided there is a flux in the system initially; if a source is present, the flux increases linearly in time.

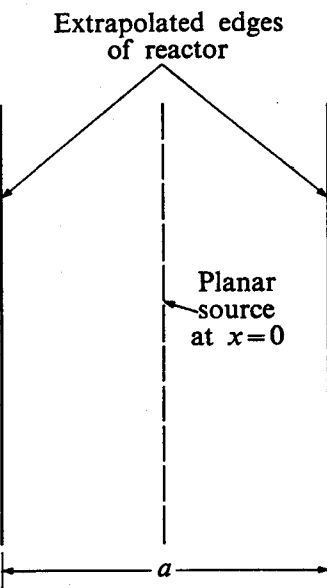
These conclusions apply, of course, only to the infinite reactor. However, it will be shown in the next section that they are also valid in somewhat modified form for the finite reactor.

## 9-2 The One-Region Finite Thermal Reactor

The results of the preceding section will now be generalized to thermal reactors of finite size. In the present discussion it will be assumed that the neutron moderation can be described by age theory, and since, as mentioned in Section 6-10, age theory cannot conveniently be used for systems consisting of more than one region, the remainder of the chapter will be limited to *bare* reactors. Reflected reactors are treated in Chapter 10.

Consider first an infinite bare slab reactor of extrapolated thickness  $a$ , composed of a homogeneous mixture of fuel and moderator. As discussed in the preceding section, the flux in the assembly will remain zero in the absence of spontaneous fissions or extraneous neutron sources. At time  $t = 0$  it will be assumed, therefore, that an infinite planar source emitting  $S$  fast neutrons per  $\text{cm}^2/\text{sec}$  is placed in the center of the reactor, as shown in Fig. 9-1.

Fig. 9-1. Bare slab reactor of extrapolated thickness  $a$  with planar source at center.



The subsequent behavior of the thermal flux is determined by the time-dependent diffusion equation in which the source density is replaced by the thermal slowing-down density as in Section 8-8; viz.,

$$L_T^2 \frac{\partial^2 \phi_T(x, t)}{\partial x^2} - \phi_T(x, t) + \frac{p}{\Sigma_a} q(x, \tau_T, t) = t_d \frac{\partial \phi_T(x, t)}{\partial t}, \quad (9-14)$$

which is equivalent to Eq. (9-4) for the infinite system. In Eq. (9-14),  $q(x, \tau_T, t)$  is the thermal slowing-down density *in the absence of resonance absorption*, and in view of the discussion in Section 7-8, the number of neutrons which actually become thermal per  $\text{cm}^3/\text{sec}$  at  $x$  is  $pq(x, \tau_T, t)$ . The flux must satisfy the boundary condition  $\phi_T(\pm a/2, t) = 0$ . Furthermore, from the symmetry of the problem it is evident that  $\phi_T$  must be an even function of  $x$ .

According to age theory,  $q(x, \tau, t)$  satisfies the equation

$$\frac{\partial^2 q(x, \tau, t)}{\partial x^2} = \frac{\partial q(x, \tau, t)}{\partial \tau}. \quad (9-15)$$

The function  $q(x, \tau, t)$  must satisfy the boundary condition  $q(\pm a/2, \tau, t) = 0$ , independent of the value of  $\tau$  (cf. Section 6-10), and it must also be an even function of  $x$ .

As in the preceding section, there are two sources of fast neutrons in the reactor, the planar source and the fission neutrons, and for simplicity it will be assumed that all of these neutrons are emitted at a single energy. The source condition at  $\tau = 0$  is then (cf. Eq. 6-77)

$$q(x, 0, t) = S \delta(x) + \eta_T f \epsilon \Sigma_a \phi_T(x, t). \quad (9-16)$$

The second term on the right-hand side gives the total number of fission neutrons produced per  $\text{cm}^3/\text{sec}$  at the point  $x$ . In view of the definition of  $k_\infty$ , Eq. (9-16)

can also be written as

$$q(x, 0, t) = S \delta(x) + \frac{k_\infty}{p} \bar{\Sigma}_a \phi_T(x, t). \quad (9-17)$$

Equations (9-14) and (9-15) can be solved in terms of the slab eigenfunctions discussed in Section 5-10. Thus solutions are assumed of the form

$$\phi_T(x, t) = \sum_{n \text{ odd}} A_n(t) \cos B_n x \quad (9-18)$$

and

$$q(x, \tau, t) = \sum_{n \text{ odd}} C_n(\tau, t) \cos B_n x, \quad (9-19)$$

where the functions  $A_n(t)$  and  $C_n(\tau, t)$  must be determined, and where

$$B_n = \frac{n\pi}{a}, \quad n = 1, 3, 5, \dots \quad (9-20)$$

Substituting Eq. (9-19) into the age equation [Eq. (9-15)] gives

$$-\sum_{n \text{ odd}} B_n^2 C_n(\tau, t) \cos B_n x = \sum_{n \text{ odd}} \frac{\partial C_n(\tau, t)}{\partial \tau} \cos B_n x. \quad (9-21)$$

In view of the orthogonality of the  $\cos B_n x$  functions, the corresponding terms on each side of this equation are equal, and the following differential equation for  $C_n(\tau, t)$  is obtained:

$$\frac{\partial C_n(\tau, t)}{\partial \tau} = -B_n^2 C_n(\tau, t). \quad (9-22)$$

The solution to this equation is

$$C_n(\tau, t) = T_n(t) e^{-B_n^2 \tau}, \quad (9-23)$$

where  $T_n(t)$  is a function of  $t$  to be determined later. If Eq. (9-23) is inserted into Eq. (9-19), the slowing-down density becomes

$$q(x, \tau, t) = \sum_{n \text{ odd}} T_n(t) e^{-B_n^2 \tau} \cos B_n x. \quad (9-24)$$

Next, substituting Eqs. (9-18) and (9-24) into Eq. (9-17), and noting that  $\delta(x) = (2/a) \sum_{n \text{ odd}} \cos B_n x$ , yields

$$\sum_{n \text{ odd}} T_n(t) \cos B_n x = \frac{2S}{a} \sum_{n \text{ odd}} \cos B_n x + \frac{k_\infty \bar{\Sigma}_a}{p} \sum_{n \text{ odd}} A_n(t) \cos B_n x, \quad (9-25)$$

so that

$$T_n(t) = \frac{2S}{a} + \frac{k_\infty \bar{\Sigma}_a}{p} A_n(t). \quad (9-26)$$

From Eq. (9-24),  $q(x, \tau, t)$  can then be written as

$$q(x, \tau, t) = \frac{2S}{a} \sum_{n \text{ odd}} e^{-B_n^2 \tau} \cos B_n x + \frac{k_\infty \bar{\Sigma}_a}{p} \sum_{n \text{ odd}} A_n(t) e^{-B_n^2 \tau} \cos B_n x. \quad (9-27)$$

Returning to Eq. (9-14) and inserting Eqs. (9-18) and (9-27) with  $\tau = \tau_T$ , the following equation is obtained:

$$\begin{aligned} -L_T^2 \sum_{n \text{ odd}} B_n^2 A_n(t) \cos B_n x - \sum_{n \text{ odd}} A_n(t) \cos B_n x + \frac{2pS}{a\bar{\Sigma}_a} \sum_{n \text{ odd}} e^{-B_n^2 \tau_T} \cos B_n x \\ + k_\infty \sum_{n \text{ odd}} A_n(t) e^{-B_n^2 \tau_T} \cos B_n x = t_d \sum_{n \text{ odd}} \frac{dA_n(t)}{dt} \cos B_n x. \end{aligned} \quad (9-28)$$

This equation can be put in a more convenient form by introducing the quantities

$$k_n = \frac{k_\infty e^{-B_n^2 \tau_T}}{1 + B_n^2 L_T^2} \quad (9-29)$$

and

$$t_n = \frac{t_d}{1 + B_n^2 L_T^2}. \quad (9-30)$$

By using these parameters and again noting that because of the orthogonality of the eigenfunctions the  $n$ th terms on each side of the equation are equal, Eq. (9-28) reduces to

$$t_n \frac{dA_n}{dt} = (k_n - 1)A_n + \frac{2pS k_n}{a\bar{\Sigma}_a k_\infty}. \quad (9-31)$$

The solution to Eq. (9-31), subject to the initial condition  $\phi_T(0) = 0$ , can easily be shown to be

$$A_n = \frac{2pS k_n}{a\bar{\Sigma}_a k_\infty (k_n - 1)} \left[ \exp(k_n - 1) \frac{t}{t_n} - 1 \right], \quad (9-32)$$

and from Eq. (9-18) the flux is therefore

$$\phi_T(x, t) = \frac{2pS}{a\bar{\Sigma}_a k_\infty} \sum_{n \text{ odd}} \left( \frac{k_n}{k_n - 1} \right) \left[ \exp(k_n - 1) \frac{t}{t_n} - 1 \right] \cos B_n x. \quad (9-33)$$

It can be seen from Eq. (9-33) that the time behavior of the flux following the insertion of the source depends upon the magnitudes of the parameters  $k_n$ . According to Eq. (9-20), the eigenvalues  $B_n$  increase monotonically with  $n$ , and from Eq. (9-29),  $k_n$  therefore forms a monotonically decreasing set, that is,

$$k_1 > k_3 > k_5 \dots \quad (9-34)$$

If, for instance,  $k_1$  is less than unity, all other  $k$ 's are also less than unity, and even

smaller. On the other hand, if  $k_1$  is greater than unity, a few additional  $k$ 's may also be greater than unity, but all the other  $k$ 's will be less than unity. Ordinarily, only  $k_1$  is ever greater than unity;  $k_3$  and all other  $k$ 's are then less than unity.

Suppose now that  $k_1 > 1$ , and  $k_3, k_5, \dots, < 1$ . From Eq. (9-33) the term with  $n = 1$ , that is, the fundamental, is seen to increase exponentially without limit with increasing time. The exponentials for all other terms are negative, however, since  $k_n - 1 < 0$ , and the harmonics with  $n = 3, 5, \dots$  all die out in time. The shape of the flux thus approaches the fundamental which increases exponentially with time. This reactor, of course, is supercritical.

Consider next the situation when  $k_1 < 1$ . In this case *all* of the time exponentials in Eq. (9-33) have negative exponents and the flux approaches the steady-state value

$$\phi_T \rightarrow \frac{2pS}{a\bar{\Sigma}_a k_\infty} \sum_{n \text{ odd}} \left( \frac{k_n}{1 - k_n} \right) \cos B_n x. \quad (9-35)$$

This is the flux in a subcritical reactor with an extraneous source and is a generalization of Eq. (9-10) for the finite reactor.

If  $k_1 = 1$ , all other  $k$ 's are less than unity, and all time exponentials in Eq. (9-33) except the first go to zero in time. The first term, however, behaves as

$$\frac{\exp(k_1 - 1)(t/t_1) - 1}{k_1 - 1},$$

which reduces to  $t/t_1$  in the limit as  $k_1 \rightarrow 1$ . The thermal flux is then given by

$$\phi_T = \frac{2pSk_1 t}{a\bar{\Sigma}_a k_\infty t_1} \cos B_1 x + \frac{2pS}{a\bar{\Sigma}_a k_\infty} \sum_{n>1 \text{ odd}} \left( \frac{k_n}{1 - k_n} \right) \cos B_n x. \quad (9-36)$$

The flux thus increases linearly with time in the fundamental mode. This result is simply a more complicated version of Eq. (9-8).

It follows from the above results that regardless of the value of the  $k$ 's, a flux is produced when a source is placed in the system. Suppose now that at  $t = t_0$  the source is removed from the reactor after the flux  $\phi_{T0}(x)$  has been established. With  $S = 0$  in Eq. (9-31),  $A_n$  is given by

$$A_n = A_{n0} \exp \left[ (k_n - 1) \left( \frac{t - t_0}{t_n} \right) \right], \quad (9-37)$$

and the flux becomes

$$\phi_T = \sum_{n \text{ odd}} A_{n0} \exp \left[ (k_n - 1) \left( \frac{t - t_0}{t_n} \right) \right] \cos B_n x. \quad (9-38)$$

The constants  $A_{n0}$  in this expression are the expansion coefficients of  $\phi_{T0}(x)$ , but their precise values are irrelevant in the present discussion.

Consider again the behavior of  $\phi_T$  for different values of  $k_n$ . If  $k_1 > 1$  but  $k_3, k_5, \dots, < 1$ , then the  $n = 1$  term in Eq. (9-38) increases exponentially while all

other terms go to zero. Thus the flux, in time, takes on the shape of the fundamental which increases in magnitude without limit. This reactor is supercritical.

If  $k_1 < 1$ , all other  $k$ 's are also less than unity, and all terms in Eq. (9-38) decrease to zero. The reactor in this case is evidently subcritical. However, it should be noted that since the  $k$ 's form a monotonically decreasing set, the exponential corresponding to  $k_3$  dies out faster than the exponential corresponding to  $k_1$ ; the exponential for  $k_5$  dies out faster than that for  $k_3$ ; and so on. Although all exponentials eventually go to zero, the *last* exponential to do so is therefore the one corresponding to the fundamental. Thus, even in a subcritical reactor the flux ultimately takes on the shape of the fundamental before it vanishes.

Finally, if  $k_1 = 1$ , the first term in Eq. (9-38) remains constant. All the other terms in the series go to zero, and the flux eventually reduces to the fundamental:

$$\phi_T \rightarrow A \cos B_1 x, \quad (9-39)$$

where  $A = A_{10}$ . The reactor is now critical since a time-independent flux is maintained in the system by the fission chain reaction alone, unsupported by the presence of an extraneous neutron source.

These conclusions are particularly important. To summarize:

(i) If  $k_1 > 1$ , the reactor is supercritical, and the flux approaches the fundamental which increases without limit once the chain reaction is initiated, whether or not there is an extraneous source in the system.

(ii) If  $k_1 < 1$  and a source is present, the flux approaches a steady-state distribution which is the sum of harmonics. If no source is present, the flux goes to zero, ultimately in the fundamental mode; the reactor in this case is subcritical.

(iii) If  $k_1 = 1$ , the reactor is critical, and the flux approaches the fundamental and maintains this steady-state distribution in the absence of sources, provided there is a flux in the system initially; if there are sources present, the flux ultimately increases linearly in the fundamental mode.\*

Although these conclusions have been derived for a slab reactor, they can be shown to be valid for any bare reactor. Incidentally, since the behavior of the reactor is determined only by the value of  $k_1$ , it is evident that  $k_1$  is actually the multiplication factor for the finite reactor. That this is indeed the case is shown in Section 9-4.

It should be especially noted from the preceding discussion that the larger its index  $n$  is, the more rapidly a harmonic dies out in time. In particular, all of the higher harmonics die out faster than the fundamental. This important result is

---

\* It is interesting to note that in view of these conclusions virtually all so-called critical reactors are actually subcritical due to the fact that there are extraneous sources of neutrons in most reactors. These neutrons either appear as the result of spontaneous fission or are emitted from startup sources which are left in the reactor after it reaches power. If such a reactor were truly critical, its flux and power would slowly increase with time. As a practical matter, however, these reactors are so close to critical they can be treated as exactly critical.

due to the following circumstances. It can easily be shown using the methods to be discussed in Section 9-4 that the leakage of neutrons from the surface of the reactor in the  $n$ th harmonic is proportional to  $B_n^2$ . Since the parameters  $B_n^2$  form a monotonically increasing set, it follows that the leakage of neutrons in these various modes increases with increasing  $n$ . Thus the higher harmonics die out faster than the fundamental simply because the neutrons which populate them escape more rapidly from the reactor.

For reasons that will be apparent shortly, the square of the first eigenvalue, that is,  $B_1^2$ , is known as the *buckling* of the system and the numerical subscript is omitted. The flux in the critical reactor then satisfies the equation

$$\frac{d^2\phi_T}{dx^2} + B^2\phi_T = 0. \quad (9-40)$$

This is often called the *reactor equation*—in this case, for the slab reactor.

The origin of the term “buckling” can be seen by solving Eq. (9-40) for  $B^2$ ; thus

$$B^2 = -\frac{1}{\phi_T} \frac{d^2\phi_T}{dx^2}. \quad (9-41)$$

The right-hand side of this equation is proportional to the *curvature* of  $\phi_T$ , so  $B^2$  is therefore a measure of the curvature of the flux, or, in other words, the extent to which the flux “buckles.” In an infinite, uniform reactor, for example, the flux is independent of position, Eq. (9-41) gives  $B^2 = 0$ , and the flux does not “buckle.” With a finite slab reactor on the other hand, since  $B^2 = \pi^2/a^2$ , the buckling of the flux increases with decreasing size of the system.

It may be noted that because Eq. (9-40) is homogeneous, any solution to the equation multiplied by a constant is also a solution. It follows that the reactor equation specifies the *shape* but not the *magnitude* of the flux. This is to be expected physically, for as shown in Section 8-3 the magnitude of the flux is determined by the operating power of the reactor and no mention was made of the reactor power in the arguments which led to Eq. (9-40). The shape of the flux in a critical reactor is the same whether the reactor is operating at one watt or one megawatt. This fact has a number of important practical consequences. In particular, it means that it is possible to determine experimentally the flux distribution in a reactor intended for operation at high power, by performing measurements in an assembly which duplicates the actual reactor but which operates at very low power. These measurements are discussed more fully in Section 10-7.

In a uniform slab reactor according to Eq. (9-39), the flux is

$$\phi_T = A \cos \frac{\pi x}{a}, \quad (9-42)$$

and the reactor power  $P$  per unit area of the slab is given by

$$P = \gamma \Sigma_f \int_{-a/2}^{a/2} \phi_T(x) dx. \quad (9-43)$$

Here  $\gamma$  is the recoverable energy per fission and  $\bar{\Sigma}_f$  is the thermal average macroscopic fission cross section. Inserting Eq. (9-42) into Eq. (9-43) and solving for  $A$  gives

$$A = \frac{\pi P}{2a\gamma\bar{\Sigma}_f},$$

so that

$$\phi_T = \frac{\pi P}{2a\gamma\bar{\Sigma}_f} \cos \frac{\pi x}{a}. \quad (9-44)$$

Equation (9-44) shows that the flux at any point is proportional to the reactor power, a conclusion that is entirely reasonable physically.

Returning to Eq. (9-27) it will be noted that if the reactor is critical, and no extraneous sources are present ( $S = 0$ ), all functions  $A_n(t)$  except the first vanish with time and the slowing-down density reduces to

$$q(x, \tau_T) \rightarrow \frac{k_\infty \bar{\Sigma}_a}{p} A e^{-B^2 \tau_T} \cos Bx. \quad (9-45)$$

In view of Eq. (9-39), it follows that

$$q(x, \tau_T) = \frac{k_\infty \bar{\Sigma}_a}{p} e^{-B^2 \tau_T} \phi_T(x). \quad (9-46)$$

According to Eq. (9-46) the flux and slowing-down density are proportional everywhere in the reactor. Although this result has been obtained for a slab reactor using age theory, it is a general theorem valid for *any one region reactor* and is independent of the way in which neutrons slow down, that is, whether age theory is valid or not. It does not hold, however, for multiregion reactors, as will be seen in Chapter 10.

### 9-3 Criticality for Other Reactor Geometries

It is not difficult to generalize the results of the preceding section to any one-region thermal reactor. The more general diffusion and age equations are then, respectively,

$$L_T^2 \nabla^2 \phi_T(\mathbf{r}, t) - \phi_T(\mathbf{r}, t) + \frac{p}{\bar{\Sigma}_a} q(\mathbf{r}, \tau_T, t) = t_d \frac{\partial \phi_T(\mathbf{r}, t)}{\partial t} \quad (9-47)$$

and

$$\nabla^2 q(\mathbf{r}, \tau, t) = \frac{\partial q(\mathbf{r}, \tau, t)}{\partial \tau}. \quad (9-48)$$

These equations can be solved by a procedure analogous to that used earlier. Expansions are assumed for the flux and slowing-down densities of the form

$$\phi_T(\mathbf{r}, t) = \sum A_n(t) \varphi_n(\mathbf{r}) \quad (9-49)$$

and

$$q(\mathbf{r}, \tau, t) = \sum C_n(\tau, t) \varphi_n(\mathbf{r}), \quad (9-50)$$

where  $\varphi_n(\mathbf{r})$  are eigenfunctions appropriate to the geometry of the reactor and satisfy the equation

$$\nabla^2 \varphi_n(\mathbf{r}) + B_n^2 \varphi_n(\mathbf{r}) = 0. \quad (9-51)$$

By proceeding as before, expressions for  $\phi_T(\mathbf{r}, t)$  and  $q(\mathbf{r}, \tau, t)$  can be obtained which are identical with those for the slab reactor except that the slab eigenfunctions are everywhere replaced by  $\varphi_n(\mathbf{r})$ . In this way all of the conclusions regarding the gross time behavior of the slab reactor discussed in Section 9-2 can be shown to apply to the more general system. In particular, any one-region thermal reactor will be critical provided  $k_1 = 1$ , where  $k_1$  is defined by Eq. (9-29). With no extraneous sources present, the thermal flux ultimately takes on the shape of the fundamental eigenfunction which, according to Eq. (9-51), is determined by the equation

$$\nabla^2 \phi_T(\mathbf{r}) + B^2 \phi_T(\mathbf{r}) = 0. \quad (9-52)$$

This is the reactor equation for the more general reactor. The first eigenvalue of the equation,  $B^2$ , is again called the *buckling*.

Finally, the magnitude of the flux is determined by the reactor power. As in Eq. (9-43),

$$P = \gamma \bar{\Sigma}_f \int_V \phi_T(\mathbf{r}) dV, \quad (9-53)$$

where the integral is now over the reactor volume. When the fundamental eigenfunction is known, Eq. (9-53) can be used to find the magnitude of  $\phi_T$ .

These results will now be applied to several important reactor geometries.

**Rectangular parallelepiped.** This reactor has extrapolated dimensions  $a$ ,  $b$ , and  $c$ , as shown in Fig. 9-2. The reactor equation is

$$\frac{\partial^2 \phi_T}{\partial x^2} + \frac{\partial^2 \phi_T}{\partial y^2} + \frac{\partial^2 \phi_T}{\partial z^2} + B^2 \phi_T = 0, \quad (9-54)$$

and since the flux must vanish at every point on the extrapolated surface, the boundary conditions are

$$\phi_T\left(\pm \frac{a}{2}, y, z\right) = \phi_T\left(x, \pm \frac{b}{2}, z\right) = \phi_T\left(x, y, \pm \frac{c}{2}\right) = 0.$$

Equation (9-54) can be solved by the method of separation of variables.\* Thus a solution is assumed of the form

$$\phi_T(x, y, z) = X(x) Y(y) Z(z), \quad (9-55)$$

where the three functions  $X$ ,  $Y$ , and  $Z$  must be determined. Substituting this

---

\* The solution to Eq. (9-54) can also be obtained by expanding  $\phi_T$  directly in a triple eigenfunction series. However, since the method of separation of variables is needed later in this chapter, it is instructive to illustrate this procedure at this point.

expression into Eq. (9-54) and dividing by  $\phi_T$  gives

$$\frac{1}{X} \frac{d^2 X}{dx^2} + \frac{1}{Y} \frac{d^2 Y}{dy^2} + \frac{1}{Z} \frac{d^2 Z}{dz^2} + B^2 = 0. \quad (9-56)$$

The first three terms in this equation are functions of only  $x$ ,  $y$ , and  $z$ , respectively, and their sum is equal to a constant. This is possible only if each term is itself a constant, that is, if

$$\frac{1}{X} \frac{d^2 X}{dx^2} = -\alpha^2, \quad (9-57)$$

$$\frac{1}{Y} \frac{d^2 Y}{dy^2} = -\beta^2, \quad (9-58)$$

$$\frac{1}{Z} \frac{d^2 Z}{dz^2} = -\gamma^2, \quad (9-59)$$

where from Eq. (9-56)

$$\alpha^2 + \beta^2 + \gamma^2 = B^2. \quad (9-60)$$

The solution to Eq. (9-57) is  $X(x) = A \cos \alpha x + C \sin \alpha x$ , but in view of the symmetry of the problem,  $C$  must be taken to be zero, since  $\sin \alpha x$  is an odd function. To satisfy the boundary conditions at  $x = \pm a/2$ ,  $\alpha$  must take on the familiar values

$$\alpha = \frac{l\pi}{a}, \quad l = 1, 3, 5, \dots \quad (9-61)$$

There is, therefore, an infinite set of functions satisfying Eq. (9-57) of the form

$$X_l(x) = A_l \cos \frac{l\pi x}{a}, \quad l = 1, 3, 5, \dots, \quad (9-62)$$

where  $A_l$  are arbitrary constants.

In a similar way, the separation constants in Eqs. (9-58) and (9-59) are given by

$$\beta_m = \frac{m\pi}{b} \quad \text{and} \quad \gamma_n = \frac{n\pi}{c}, \quad m, n = 1, 3, 5, \dots,$$

and the admissible functions  $Y(y)$  and  $Z(z)$  are

$$Y_m(y) = A'_m \cos \frac{m\pi y}{b}, \quad Z_n(z) = A''_n \cos \frac{n\pi z}{c},$$

where  $A'_m$  and  $A''_n$  are constants. In view of Eq. (9-55), a solution for  $\phi_T$  is

$$\phi_{Tlmn} = A_{lmn} \cos \frac{l\pi x}{a} \cos \frac{m\pi y}{b} \cos \frac{n\pi z}{c}, \quad (9-63)$$

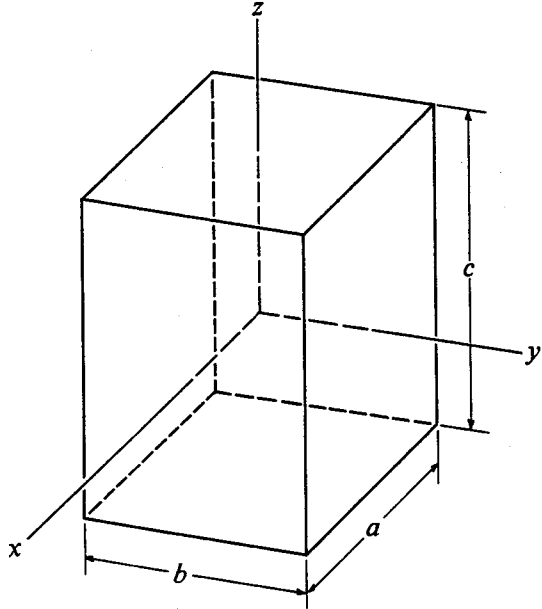


Fig. 9-2. Rectangular parallelepiped reactor of extrapolated dimensions  $a$ ,  $b$ , and  $c$ .

where  $A_{lmn}$  is a new constant:  $A_{lmn} = A_l A'_m A''_n$ . The function in Eq. (9-63) with the lowest indices, that is,  $l = m = n = 1$ , is evidently the fundamental, and the other functions are higher harmonics. With the critical reactor, as shown in Section 9-2, these harmonics die out in time and the steady-state flux reduces to

$$\phi_T = A \cos \frac{\pi x}{a} \cos \frac{\pi y}{b} \cos \frac{\pi z}{c}. \quad (9-64)$$

From Eq. (9-60) the buckling of the system is then

$$B^2 = \left(\frac{\pi}{a}\right)^2 + \left(\frac{\pi}{b}\right)^2 + \left(\frac{\pi}{c}\right)^2. \quad (9-65)$$

Finally, from Eq. (9-53) the constant  $A$  in Eq. (9-64) is easily found to be

$$A = \frac{\pi^3 P}{8V\gamma\Sigma_f}, \quad (9-66)$$

where  $V = abc$  is the reactor volume.

**Sphere.** Consider next a bare spherical reactor of extrapolated radius  $R$ . In this system the flux is a function only of  $r$  and the reactor equation is

$$\frac{1}{r^2} \frac{d}{dr} r^2 \frac{d\phi_T}{dr} + B^2 \phi_T = 0. \quad (9-67)$$

By substitution of  $\phi_T = w/r$ , as in Section 5-9, the general solution to this equation is seen to be

$$\phi_T = A \frac{\sin Br}{r} + C \frac{\cos Br}{r}. \quad (9-68)$$

The second term becomes infinite as  $r$  goes to zero and  $C$  must be taken to be zero. Therefore  $\phi_T$  is given by

$$\phi_T = A \frac{\sin Br}{r}. \quad (9-69)$$

The boundary condition  $\phi_T(R) = 0$  can be satisfied by requiring that  $BR = n\pi$ , where  $n$  is any integer. With  $n = 1$ , the buckling is

$$B^2 = \left(\frac{\pi}{R}\right)^2, \quad (9-70)$$

and the flux in a critical spherical reactor is then

$$\phi_T = A \frac{\sin(\pi r/R)}{r}. \quad (9-71)$$

Also, from Eq. (9-53), the constant  $A$  is

$$A = \frac{P}{4R^2\gamma\Sigma_f}. \quad (9-72)$$

**Infinite cylinder.** For an infinitely long, bare cylinder of extrapolated radius  $R$ , the flux is again a function only of  $r$ , and using the form of the Laplacian given in Eq. (5-46), the reactor equation is

$$\frac{1}{r} \frac{d}{dr} r \frac{d\phi_T}{dr} + B^2 \phi_T = 0. \quad (9-73)$$

In addition,  $\phi_T$  must satisfy the boundary condition  $\phi_T(R) = 0$ . Equation (9-73) is the ordinary Bessel equation (cf. Appendix II) whose general solution is

$$\phi_T = AJ_0(Br) + CY_0(Br).$$

The function  $Y_0(Br)$  is singular if  $r = 0$ , however, and so  $C = 0$ . Thus,  $\phi_T$  is given by

$$\phi_T = AJ_0(Br). \quad (9-74)$$

As discussed in Appendix II, the function  $J_0(x)$  has an infinite number of zeros at  $x = x_1, x_2, x_3, \dots$ , that is,  $J_0(x_1) = J_0(x_2) = J_0(x_3) = \dots = 0$ . The boundary condition at  $r = R$  will therefore be satisfied provided that  $B$  takes on the values of  $B_nR = x_n$ , where  $x_n$  is any of the zeros. Thus the reactor equation has the following solutions:

$$\phi_{Tn} = A_n J_0 \left( \frac{x_n r}{R} \right). \quad (9-75)$$

The smallest value of  $x_n$  is  $x_1 = 2.405$ . Therefore, the buckling for the infinite cylinder is

$$B^2 = \left( \frac{2.405}{R} \right)^2, \quad (9-76)$$

and the flux in the critical reactor is

$$\phi_T = AJ_0 \left( \frac{2.405r}{R} \right). \quad (9-77)$$

The constant  $A$  is again found from Eq. (9-53). Using the formula for the integral of Bessel functions given in Appendix II [cf. Eq. (II-52)], it is found that

$$A = \frac{2.405P}{2\pi R^2 \gamma \bar{\Sigma}_f J_1(2.405)} = \frac{0.738P}{R^2 \gamma \bar{\Sigma}_f}. \quad (9-78)$$

Here,  $P$  is the power per unit length of the reactor.

**Finite cylinder.** Finally, consider a bare cylinder of extrapolated radius  $R$  and extrapolated height  $H$ , as shown in Fig. 9-3. The flux in this reactor depends upon both  $r$  and  $z$ , and the reactor equation is now [cf. Eq. (5-46)]

$$\frac{1}{r} \frac{\partial}{\partial r} r \frac{\partial \phi_T}{\partial r} + \frac{\partial^2 \phi_T}{\partial z^2} + B^2 \phi_T = 0. \quad (9-79)$$

With the origin of the coordinate system located at the center of the cylinder, as shown in the figure, the boundary conditions are

$$\phi_T(R, z) = \phi_T\left(r, \pm \frac{H}{2}\right) = 0.$$

Using the separation of variables again, let

$$\phi_T = X(r)Z(z). \quad (9-80)$$

Substituting this expression into Eq. (9-79) and dividing by  $\phi_T$ , as in the earlier example, yields

$$\frac{1}{Xr} \frac{d}{dr} r \frac{dX}{dr} + \frac{1}{Z} \frac{d^2Z}{dz^2} + B^2 = 0. \quad (9-81)$$

The first and second terms depend only on  $r$  and  $z$ , respectively, and these can be placed equal to constants; that is,

$$\frac{1}{Z} \frac{d^2Z}{dz^2} = -\alpha^2 \quad (9-82)$$

and

$$\frac{1}{Xr} \frac{d}{dr} r \frac{dX}{dr} = -\beta^2, \quad (9-83)$$

where

$$B^2 = \alpha^2 + \beta^2. \quad (9-84)$$

In view of the boundary conditions at  $z = \pm H/2$ , the separation constant in Eq. (9-82) must be

$$\alpha_m = \frac{m\pi}{H}, \quad m = 1, 3, 5, \dots, \quad (9-85)$$

and  $Z(z)$  has the solutions

$$Z_m(z) = A_m \cos\left(\frac{m\pi z}{H}\right). \quad (9-86)$$

Also, as in the previous case,  $\beta_n$  is

$$\beta_n = \frac{x_n}{R}, \quad (9-87)$$

where  $x_n$  is the  $n$ th zero of  $J_0(x)$ , and  $X(r)$  is

$$X(r) = A_n J_0\left(\frac{x_n r}{R}\right). \quad (9-88)$$

By using the lowest values of  $m$  and  $n$ , the buckling is

$$B^2 = \left(\frac{2.405}{R}\right)^2 + \left(\frac{\pi}{H}\right)^2, \quad (9-89)$$

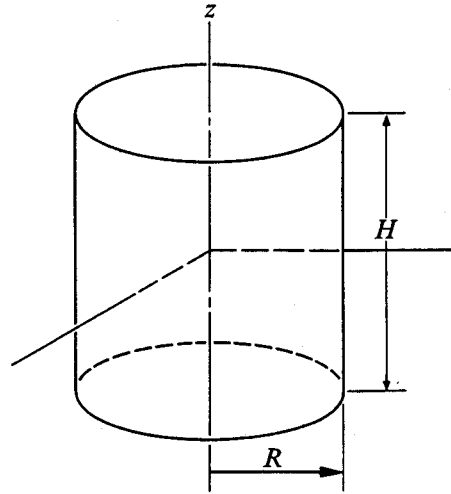
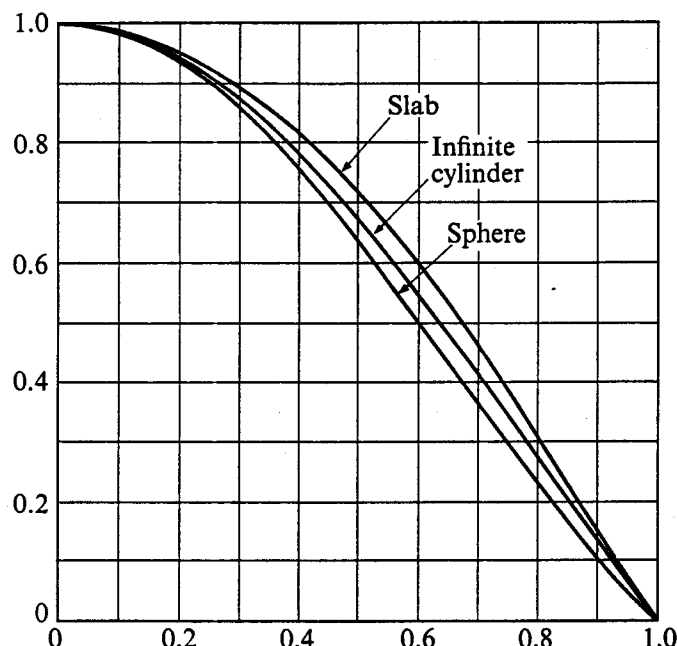


Fig. 9-3. Bare cylindrical reactor of extrapolated radius  $R$  and extrapolated height  $H$ .

**Table 9-1**  
**Bucklings and Fluxes of Critical Bare Reactors (All Dimensions Are Extrapolated)\***

Geometry	Dimensions	Buckling	Flux
Infinite slab	Thickness $a$	$\left(\frac{\pi}{a}\right)^2$	$\cos\left(\frac{\pi x}{a}\right)$
Rectangular parallelepiped	$a \times b \times c$	$\left(\frac{\pi}{a}\right)^2 + \left(\frac{\pi}{b}\right)^2 + \left(\frac{\pi}{c}\right)^2$	$\cos\left(\frac{\pi x}{a}\right) \cos\left(\frac{\pi y}{b}\right) \cos\left(\frac{\pi z}{c}\right)$
Infinite cylinder	Radius $R$	$\left(\frac{2.405}{R}\right)^2$	$J_0\left(\frac{2.405r}{R}\right)$
Finite cylinder	Radius $R$ Height $H$	$\left(\frac{2.405}{R}\right)^2 + \left(\frac{\pi}{H}\right)^2$	$J_0\left(\frac{2.405r}{R}\right) \cos\left(\frac{\pi z}{H}\right)$
Sphere	Radius $R$	$\left(\frac{\pi}{R}\right)^2$	$\frac{1}{r} \sin\left(\frac{\pi r}{R}\right)$

\* See text for details of the coordinate systems used.



**Fig. 9-4.** Neutron fluxes for the infinite slab, infinite cylinder, and sphere as a function of the fractional distance from their center to the surface. The fluxes are normalized to unity at the center.

and the flux in the critical system is

$$\phi_T(r, z) = AJ_0\left(\frac{2.405r}{R}\right)\cos\left(\frac{\pi z}{H}\right). \quad (9-90)$$

Finally, the constant  $A$  is found to be

$$A = \frac{2.405\pi P}{4V\gamma\bar{\Sigma}_f J_1(2.405)} = \frac{3.63P}{V\gamma\bar{\Sigma}_f}, \quad (9-91)$$

where  $V = \pi R^2 H$  is the volume of the reactor.

The bucklings and fluxes of the various reactors considered in this section are summarized in Table 9-1. The fluxes are also shown in Fig. 9-4 for the infinite slab, infinite cylindrical, and spherical reactors. These fluxes are normalized to unity at the center of each reactor and are plotted as a function of the fraction of the distance from the center to the surface of the reactor. It will be observed that all of these functions have approximately the same shape. However, it should be noted that the slope of the flux at the reactor surface is somewhat greater for the slab than for the cylinder, while it is greater for the cylinder than for the sphere. Since the neutron leakage is proportional to the (negative) slope, it follows that, other things being equal, the leakage of neutrons per unit area of the reactor surface is greater for the slab than for the cylinder, and greater for the cylinder than for the sphere.

#### 9-4 The Critical Equation

According to the results of Section 9-2, it is necessary that  $k_1 = 1$  in order for a bare reactor to be critical. From Eq. (9-29) this means that the following equation must be satisfied:

$$k_1 = \frac{k_\infty e^{-B^2\tau_T}}{1 + B^2 L_T^2} = 1. \quad (9-92)$$

This expression is known as the *critical equation*, and is valid for any bare, homogeneous, thermal reactor provided that the slowing down of the neutrons is adequately described by Fermi age theory. Equation (9-92) is a generalization of the criticality condition which was obtained in Section 9-1 for the infinite reactor, namely,  $k_\infty = 1$ . The additional factors multiplying  $k_\infty$  in Eq. (9-92) are due to the leakage of neutrons from the surface of the reactor, as will now be shown.

The total number of thermal neutrons which escape from the surface of the reactor per second is  $\int_A \mathbf{J} \cdot \mathbf{n} dA$ , where  $\mathbf{J}$  is the thermal neutron current,  $\mathbf{n}$  is a unit vector normal to the surface at  $dA$ , and the integral is over the entire surface  $A$  of the reactor. From Fick's law and the divergence theorem,

$$\int_A \mathbf{J} \cdot \mathbf{n} dA = \int_V \operatorname{div} \mathbf{J} dV = -D \int_V \nabla^2 \phi_T dV,$$

where  $V$  is the reactor volume. In view of the reactor equation (Eq. 9-52), the

total number of thermal neutrons leaking from the reactor is therefore\*

$$-\bar{D} \int_V \nabla^2 \phi_T dV = \bar{D} B^2 \int_V \phi_T dV.$$

The total number of thermal neutrons absorbed per second in the reactor is equal to  $\int_V \bar{\Sigma}_a \phi_T dV$ , and since the reactor properties have been assumed to be uniform, this can also be written as  $\bar{\Sigma}_a \int_V \phi_T dV$ .

Now it will be obvious that thermal neutrons in a reactor eventually either leak from the system or are absorbed somewhere in it; there is no other possibility.<sup>†</sup> The probability  $P_T$  that a thermal neutron is *absorbed*, or, in other words, that it does not leak from the system, is simply the number which is absorbed per second divided by the number which is absorbed plus the number which leaks per second, namely,

$$P_T = \frac{\bar{\Sigma}_a \int_V \phi_T dV}{\bar{\Sigma}_a \int_V \phi_T dV + \bar{D} B^2 \int_V \phi_T dV}.$$

The integrals are all identical and may be cancelled. Then, dividing by  $\bar{\Sigma}_a$ , this expression reduces to

$$P_T = \frac{1}{1 + B^2 L_T^2}, \quad (9-93)$$

which is one of the factors in Eq. (9-92). The quantity  $P_T$  is called the *thermal nonleakage probability*. For an infinite uniform reactor,  $B = 0$  and  $P_T = 1$ , as would be expected since in such a system there can be no leakage of thermal neutrons.

Consider next the escape of neutrons as they slow down from fission energies. The total number of fast neutrons produced in the reactor per second is  $(k_\infty \bar{\Sigma}_a / p) \int_V \phi_T dV$ . Of these, the number which thermalize per second in the system in the absence of resonance capture is  $\int_V q_T dV$ , where  $q_T$  is the thermal slowing-down density. However, in view of Eq. (9-46),  $q_T$  and  $\phi_T$  are proportional, and so

$$\int_V q_T dV = \frac{k_\infty \bar{\Sigma}_a e^{-B^2 \tau_T}}{p} \int_V \phi_T dV.$$

The relative probability  $P_F$  that a fast neutron *does not escape* while slowing down

\* It may be noted that this expression gives the leakage from the fundamental mode only. The leakage associated with the  $n$ th harmonic in a noncritical reactor can be found by replacing  $\phi_T$  by the  $n$ th eigenfunction and then proceeding as before. The leakage from the  $n$ th harmonic is then evidently proportional to  $B_n^2$ .

<sup>†</sup> Neutrons can undergo radioactive decay, of course, but this is a negligible effect in view of the lifetimes involved.

is equal to the ratio of the number which slow down to the original number produced; thus

$$P_F = \frac{\int_V q_T dV}{(k_\infty/p) \bar{\Sigma}_a \int_V \phi_T dV} = e^{-B^2 \tau_T}, \quad (9-94)$$

which is the second factor in Eq. (9-92). Again, if the reactor is infinite,  $B = 0$  and  $P_F = 1$ , as required.

With these results, the critical equation can be written as

$$k_\infty P_T P_F = 1. \quad (9-95)$$

For an infinite system  $P_T = P_F = 1$ , and Eq. (9-95) properly reduces to the critical condition for the infinite reactor, that is,  $k_\infty = 1$ . The physical meaning of the critical equation can now be seen from Eq. (9-95). In any critical reactor whether it is finite or infinite, the ratio of the number of fissions in succeeding generations of the chain reaction must be equal to unity. In the infinite system this ratio is just  $k_\infty$ . For the finite system, however, only those neutrons that are retained within the reactor are able to contribute to the continuation of the chain reaction, and this effectively reduces the multiplication factor of a finite reactor from  $k_\infty$  to  $k_\infty P_T P_F$ . Thus as mentioned earlier,  $k_1$  is the multiplication factor for the finite system, and in the future  $k_1$  will be denoted simply as  $k$ . The critical equation is then

$$k = k_\infty P_T P_F = 1. \quad (9-96)$$

## 9-5 Large Reactors

With a great many reactors, particularly large reactors, the slowing-down length  $\sqrt{\tau_T}$  is much smaller than the dimensions of the reactor. In this case, since  $B^2$  depends inversely on the reactor size, the quantity  $B^2 \tau_T$  is much less than unity and  $\exp(B^2 \tau_T) \approx 1 + B^2 \tau_T$ . The critical equation can therefore be written as

$$\begin{aligned} 1 &= \frac{k_\infty e^{-B^2 \tau_T}}{1 + B^2 L_T^2} \approx \frac{k_\infty}{(1 + B^2 L_T^2)(1 + B^2 \tau_T)} \\ &\approx \frac{k_\infty}{1 + B^2(L_T^2 + \tau_T)}. \end{aligned} \quad (9-97)$$

The quantity  $L_T^2 + \tau_T$  in Eq. (9-97) is known as the *thermal migration area*, and is denoted by  $M_T^2$ , that is,

$$M_T^2 = L_T^2 + \tau_T. \quad (9-98)$$

With this definition, Eq. (9-97) becomes

$$\frac{k_\infty}{1 + B^2 M_T^2} = 1. \quad (9-99)$$

As will be seen in the next section, this critical equation is much easier to use than Eq. (9-92) in certain problems of reactor criticality, since Eq. (9-99) is not transcendental in  $B^2$ . For reasons that will be discussed in Chapter 10, Eq. (9-99) is sometimes referred to as the critical equation of *modified one-group theory*.

The migration area has the following interesting interpretation. It will be recalled that  $\tau_T$  is equal to one-sixth the average square of the crow-flight distance from the point where a fast neutron first appears to the point where it slows down to thermal energies. Similarly,  $L_T^2$  is one-sixth the average square of the crow-flight distance from the point where a neutron becomes thermal to the point where it is finally absorbed. It follows, therefore, that  $M_T^2$  is equal to one-sixth the average crow-flight distance from the point where a fast neutron is born to the point where it is absorbed as a thermal neutron.

## 9-6 Practical Applications of the Critical Equation

Problems of reactor criticality that are met in practice are usually of two types. Either the dimensions of the reactor are specified and the designer must include enough fuel to assure criticality (and also provide for fuel burnup) or the reactor composition is given and the designer must determine the dimensions of the system which are required for criticality. Both of these problems will be considered in the present section. Since the theory developed in this chapter pertains only to one-region homogeneous reactors, the discussion will be limited to systems of this type.

In Cases I and II below, it will be assumed that the reactor contains no resonance absorbers and no nuclei such as  $U^{238}$  which undergo fast fission only. For these cases  $p = \epsilon = 1$ . Reactors with resonance absorption and fast fission are considered in Case III.

**Case I—determining the critical composition when size is given.** In order to make use of the critical equation (Eq. 9-92), it is first necessary to compute the parameters  $B^2$ ,  $k_\infty$ ,  $\tau_T$ , and  $L_T^2$ . To begin with, if the size and shape of a bare reactor have been specified,  $B^2$  can be computed immediately from the appropriate formula derived in Section 9-3. For example, if the reactor is a sphere with a diameter of 100 cm, then  $B^2 = (\pi/50)^2 = 39.5 \times 10^{-4} \text{ cm}^{-2}$ . The parameters  $k_\infty$ ,  $\tau_T$ , and  $L_T^2$  that satisfy the critical equation with this value of  $B^2$  must now be found.

The infinite multiplication factor with  $p = \epsilon = 1$  is simply  $k_\infty = \eta_T f$ . The constant  $\eta_T$  is determined by the nature of the fuel, and the thermal utilization  $f$  is given by (cf. Eq. 9-2)

$$f = \frac{\bar{\Sigma}_{aF}}{\bar{\Sigma}_{aF} + \bar{\Sigma}_{aM}}, \quad (9-100)$$

where  $\bar{\Sigma}_{aF}$  and  $\bar{\Sigma}_{aM}$  are the macroscopic thermal absorption cross sections of fuel and moderator, respectively. Since the critical composition is not known at this

point, the absolute values of  $\bar{\Sigma}_{aF}$  and  $\bar{\Sigma}_{aM}$  cannot be computed and it is convenient to introduce the quantity

$$Z = \frac{\bar{\Sigma}_{aF}}{\bar{\Sigma}_{aM}}. \quad (9-101)$$

Equation (9-100) then becomes

$$f = \frac{Z}{Z + 1}. \quad (9-102)$$

Calculations of homogeneous reactors not containing structural material or resonance absorbers are greatly simplified by the fact that the age of the fission neutrons can be taken to be the age for the moderator alone. This is because the concentration of fuel in such systems is always too small to affect significantly the slowing down of the neutrons. Thus in homogeneous aqueous reactors, for example,  $\tau_T$  is simply the average age of fission neutrons in water.

Finally,  $L_T^2$  is given by Eq. (8-73), where the absorption of neutrons in both fuel and moderator must be included, i.e.,

$$L_T^2 = \frac{\bar{D}}{\bar{\Sigma}_{aF} + \bar{\Sigma}_{aM}}. \quad (9-103)$$

Since very little fuel is necessary to make this type of reactor critical,  $\bar{D}$  can be taken to be the diffusion coefficient of the moderator. Thus dividing numerator and denominator of Eq. (9-103) by  $\bar{\Sigma}_{aM}$  gives

$$L_T^2 = \frac{L_{TM}^2}{1 + Z} = (1 - f)L_{TM}^2, \quad (9-104)$$

where  $L_{TM}^2$  is the thermal diffusion area of the moderator.

With these results, the critical equation becomes

$$\frac{k_\infty e^{-B^2\tau_T}}{1 + B^2 L_T^2} = \frac{\eta_T Z e^{-B^2\tau_T}}{1 + Z + B^2 L_{TM}^2} = 1. \quad (9-105)$$

Solving this equation for  $Z$ , it follows that

$$Z = \frac{1 + B^2 L_{TM}^2}{\eta_T e^{-B^2\tau_T} - 1}. \quad (9-106)$$

All of the parameters on the right-hand side of this equation are known and  $Z$  can be computed directly. Once  $Z$  has been obtained, the critical composition is known through Eq. (9-101). Finally, in view of the definition of  $Z$ , the critical mass of fuel,  $m_F$ , is

$$m_F = Z m_M \frac{M_F \bar{\sigma}_{aM}}{M_M \bar{\sigma}_{aF}}, \quad (9-107)$$

where  $m_M$  is the total mass of the moderator in the reactor,  $M_F$  and  $M_M$  are the molecular weights of fuel and moderator, respectively, and  $\bar{\sigma}_{aF}$  and  $\bar{\sigma}_{aM}$  are their

average thermal absorption cross sections. The assumption can usually be made in using Eq. (9-107) that the volume of fuel in the system is essentially zero;  $m_M$  is then just the normal density of the moderator multiplied by the reactor volume.

To illustrate this procedure, consider the problem of finding the critical mass of a spherical reactor of extrapolated radius 50 cm, consisting of an aqueous solution of highly enriched uranyl sulfate ( $\text{U}^{235}\text{O}_2\text{SO}_4$ ). The thermal absorption cross section of oxygen is essentially zero. For sulfur,  $\sigma_a = 0.5$  barns, while  $\sigma_a = 678$  barns for  $\text{U}^{235}$ . Thus since there is only one atom of sulfur per atom of uranium in the solution, the presence of the sulfur has negligible effect on the system and can be ignored. As already noted, the buckling is  $B^2 = 39.5 \times 10^{-4} \text{ cm}^{-2}$ , and from Tables 8-2, 8-3, and 8-6,  $\eta_T = 2.07$ ,  $\tau_T \approx 27 \text{ cm}^2$  and  $L_{TM}^2 = 8.1 \text{ cm}^2$ . From Eq. (9-106),  $Z = 1.21$ , and the ratio of the number of molecules of  $\text{UO}_2\text{SO}_4$  to molecules of water is therefore  $Z\sigma_{aw}/\sigma_{a25} = 1/850$ , where  $\sigma_{aw}$  and  $\sigma_{a25}$  are the microscopic absorption cross sections of water and  $\text{U}^{235}$ , respectively. Since there are about  $5.2 \times 10^5 \text{ gm}$  of water in the reactor, the critical mass of  $\text{U}^{235}$  is found from Eq. (9-107) to be 8.0 kg.

It is interesting to establish the fate of the fission neutrons in this system. The fast nonleakage probability is  $P_F = \exp(-B^2\tau_T) = 0.896$ , so that about 10% of the neutrons escape from the system while slowing down. The diffusion area in the critical reactor is  $L_T^2 = L_{TM}^2/(1 + Z) = 3.69 \text{ cm}^2$ , and the thermal nonleakage probability is therefore  $P_T = 1/(1 + B^2L_T^2) = 0.985$ . Thus only about 1.5% of the neutrons which reach thermal energies subsequently escape from the reactor. The thermal utilization is  $f = Z/(1 + Z) = 0.545$ , which means that 54.5% of the thermal neutrons that are captured in the reactor are absorbed by  $\text{U}^{235}$ . Finally,  $k_\infty = 2.07 \times 0.545 = 1.13$ , and  $k = k_\infty P_T P_F = 1.13 \times 0.896 \times 0.985 = 1.00$ , as required for criticality.

**Case II—determining critical size from given composition.** When the composition of a reactor is specified, it is a simple matter to obtain the nuclear parameters  $k_\infty$ ,  $\tau_T$ , and  $L_T^2$ , and the problem reduces to one of finding  $B^2$ . The critical equation, however, is transcendental in  $B^2$  and must be solved by numerical methods. The solution can be simplified by writing  $B^2\tau_T = x$ ; then Eq. (9-92) becomes

$$k_\infty e^{-x} = 1 + \left( \frac{L_T^2}{\tau_T} \right) x. \quad (9-108)$$

The quantity  $L_T^2/\tau_T$  is a dimensionless number and  $x$  can be found without difficulty. Once  $B^2$  is known, the dimensions of the reactor can be computed provided that the shape is given. If the reactor is a sphere, for instance, the radius is determined directly from the buckling.

With a large reactor, it is usually easier to use Eq. (9-99) than Eq. (9-92). The buckling is then given simply by

$$B^2 = \frac{k_\infty - 1}{M_T^2}. \quad (9-109)$$

Equation (9-109) often gives a good estimate of  $B^2$  to begin an iterative solution of Eq. (9-108).

As an illustration of this method, consider the reverse of the example in Case I. Let the concentration of  $\text{UO}_2\text{SO}_4$  be 24 gm/liter (which corresponds to a water-fuel molecular ratio of 850). It is then easy to obtain  $k_\infty = 1.13$  and  $L_T^2/\tau_T = 0.138$ , and from Eq. (9-108),  $x = 0.105$ . If the reactor is known to be spherical, the extrapolated radius is then  $R = \pi/B = \pi\sqrt{\tau_T/x} = 50$  cm.

**Case III—reactors with resonance absorption and/or fast fission.** In Cases I and II, resonance absorption and fast fission were not considered. The infinite multiplication factor then was  $k_\infty = \eta_T f$ , and since  $f$  obviously increases monotonically with increasing fuel concentration,  $k_\infty$  does also. In this case, there is only one fuel concentration which will give the value of  $k_\infty$  necessary to achieve criticality in a reactor of a given size. The inclusion of  $\epsilon$  in the calculation of  $k_\infty$  does not alter this general conclusion, since the fast-fission factor also increases monotonically with fuel concentration (cf. Fig. 7-4). However, when resonance absorbers are present, the situation is somewhat more involved. It will be recalled from Section 7-7 that the resonance escape probability *decreases* with

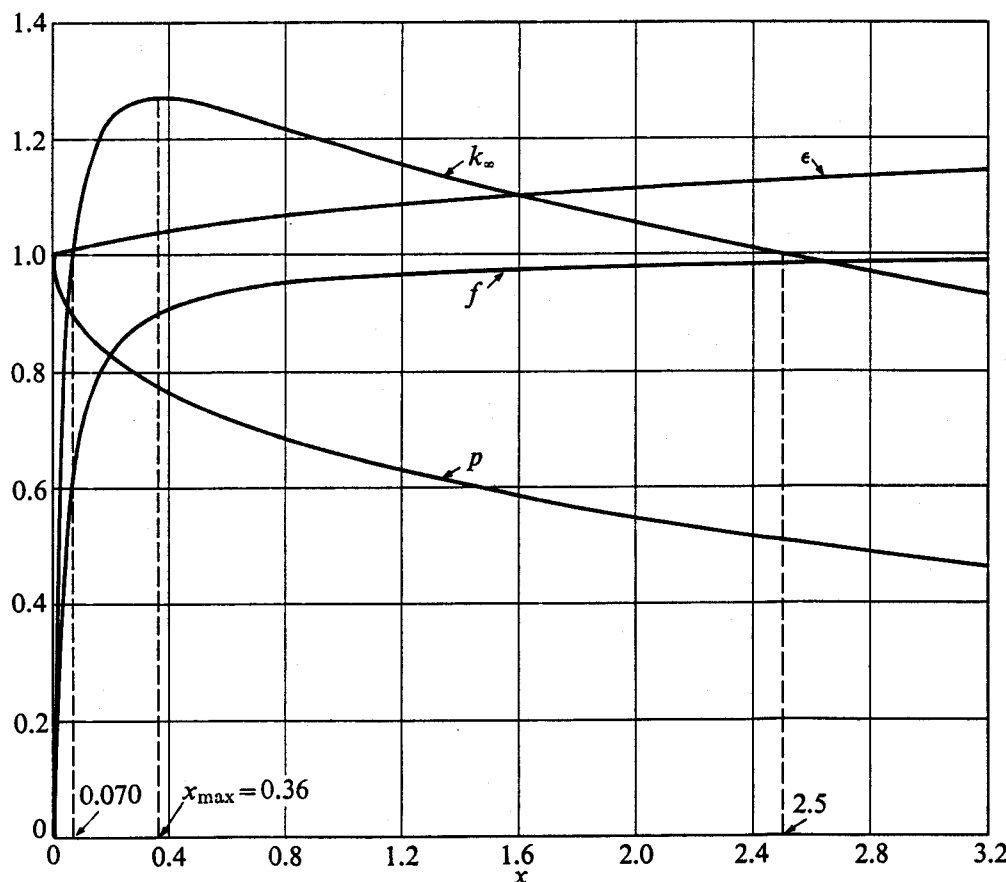


Fig. 9-5. The factors  $k_\infty$ ,  $\epsilon$ ,  $f$ , and  $p$  for a homogeneous mixture of 2%-enriched uranium and water as a function of  $x = (\text{atom density of uranium}) \div (\text{molecular density of water})$ .

increasing fuel concentration. Thus as  $f$  and  $\epsilon$  increase,  $p$  decreases, with the result that  $k_\infty$  passes through a maximum. As a consequence, there may be *two* different fuel concentrations which will give a critical system.

This situation is illustrated in Fig. 9-5 where  $k_\infty$  is shown for a homogeneous mixture of 2% enriched uranium and  $H_2O$ . As indicated in the figure,  $k_\infty = 1$  for  $x = N_{28}/N_w = 0.070$  and 2.5, and infinite reactors would be critical at these fuel concentrations. Finite reactors would require somewhat larger values of  $k_\infty$  due to neutron leakage. Indeed, if the leakage of neutrons is too great it may not be possible to achieve criticality at all, since according to Fig. 9-5,  $k_\infty$  is never larger than about 1.27.

The critical composition or compositions of a *finite* reactor of specified buckling can be found by plotting  $k$  versus composition, much as was done in Fig. 9-5 for the infinite reactor. The resulting curve differs slightly from Fig. 9-5 owing to the variation of the thermal nonleakage probability with fuel concentration. On the other hand, if the composition is given, all factors in the critical equation except  $B^2$  are determined, and in this situation,  $B^2$  and the critical dimensions can be found as in Case II above.

As a general rule reactors are designed with the fuel concentration which gives the largest value of  $k_\infty$ , or close to it. The computation of this optimum fuel concentration can be speeded somewhat by placing the derivative of  $k_\infty$  equal to zero. Consider, for example, the 2%-uranium- $H_2O$  system discussed above. The value of  $\eta_T$  at this enrichment as calculated from Eq. (8-65) is 1.744 and is, of course, independent of the concentration of the fuel. Then using Eq. (9-2) for  $f$ , Eq. (7-70) for  $p$ , and Eq. (7-79) for  $\epsilon$ ,  $k_\infty$  may be written as

$$\begin{aligned} k_\infty &= \eta_T f p \epsilon \\ &= \eta_T \frac{N_{25}\bar{\sigma}_{a25} + N_{28}\bar{\sigma}_{a28}}{N_{25}\bar{\sigma}_{a25} + N_{28}\bar{\sigma}_{a28} + N_w\bar{\sigma}_{aw}} \exp\left(-\frac{N_{28}I}{\xi N_w \sigma_{sw}}\right) \\ &\quad \times \frac{1 + 0.690(N_{28}/N_w)}{1 + 0.563(N_{28}/N_w)}, \end{aligned} \quad (9-110)$$

where according to Eq. (7-71) and Table 7-2,

$$I = 2.73 \left( \frac{N_w \sigma_{sw}}{N_{28}} \right)^{0.486}.$$

Introducing the parameters  $\beta$ ,  $\gamma$ , and  $x$  defined by

$$\beta = \frac{N_{25}\bar{\sigma}_{a25}}{N_{28}\bar{\sigma}_{a28}}, \quad \gamma = \frac{\bar{\sigma}_{a28}}{\bar{\sigma}_{aw}}, \quad x = \frac{N_{28}}{N_w},$$

and using  $\xi = 0.920$  and  $\sigma_{sw} \approx 44.8$  b, Eq. (9-110) reduces to

$$k_\infty = \eta_T \frac{x\gamma(\beta + 1)}{x\gamma(\beta + 1) + 1} \exp(-0.422x^{0.514}) \frac{1 + 0.690x}{1 + 0.563x}. \quad (9-111)$$

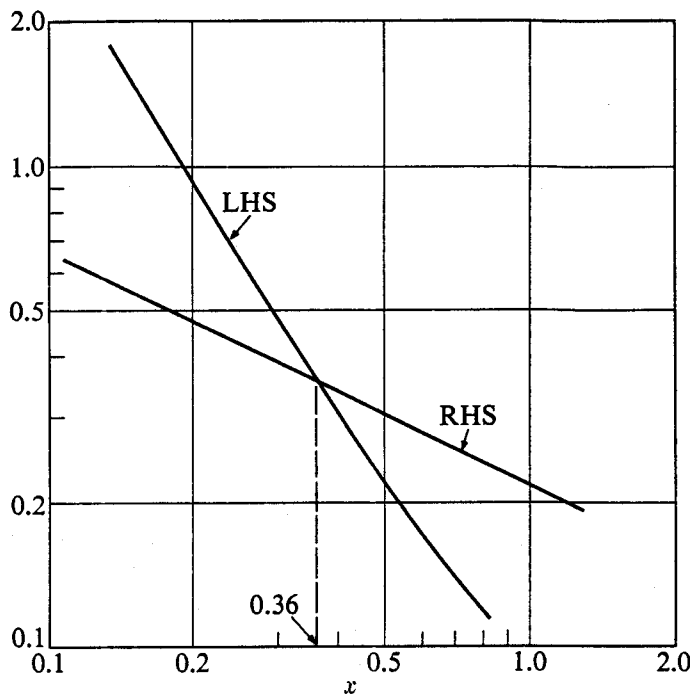


**Fig. 9-6.** The right-hand side (RHS) and left-hand side (LHS) of Eq. (9-113).

Taking logarithms preliminary to differentiating gives

$$\begin{aligned} \ln k_\infty = & \ln \eta_T + \ln x + \ln \gamma(\beta + 1) - \ln [x\gamma(\beta + 1) + 1] - 0.422x^{0.514} \\ & + \ln (1 + 0.690x) - \ln (1 + 0.563x). \end{aligned} \quad (9-112)$$

Placing the derivative of Eq. (9-112) equal to zero yields the following transcendental equation for the fuel concentration at which  $k_\infty$  is a maximum:

$$\frac{1}{x} - \frac{\gamma(\beta + 1)}{x\gamma(\beta + 1) + 1} + \frac{0.690}{1 + 0.690x} - \frac{0.563}{1 + 0.563x} = 0.217x^{-0.486}. \quad (9-113)$$

The value of  $x$  satisfying Eq. (9-113) may easily be found by plotting the two sides of the equation versus  $x$ , as shown in Fig. 9-6. For this purpose it is convenient to use a log-log plot, since the right-hand side of the equation is then a straight line. The left-hand side is a smoothly varying function which is easily computed. As indicated in the figure, the intersection of the curves occurs at  $x = 0.36$ . This is the fuel concentration which gives the largest value of  $k_\infty$ , as may be verified from Fig. 9-5.

### 9-7 Dependence of Critical Mass on Size and Composition

It is of interest to consider how the critical mass of a bare thermal reactor depends upon its size and composition. Figure 9-7 shows the critical composition and critical mass of a bare spherical reactor fueled with  $\text{U}^{235}$  and moderated by beryllium, as a function of the radius. These curves were computed using

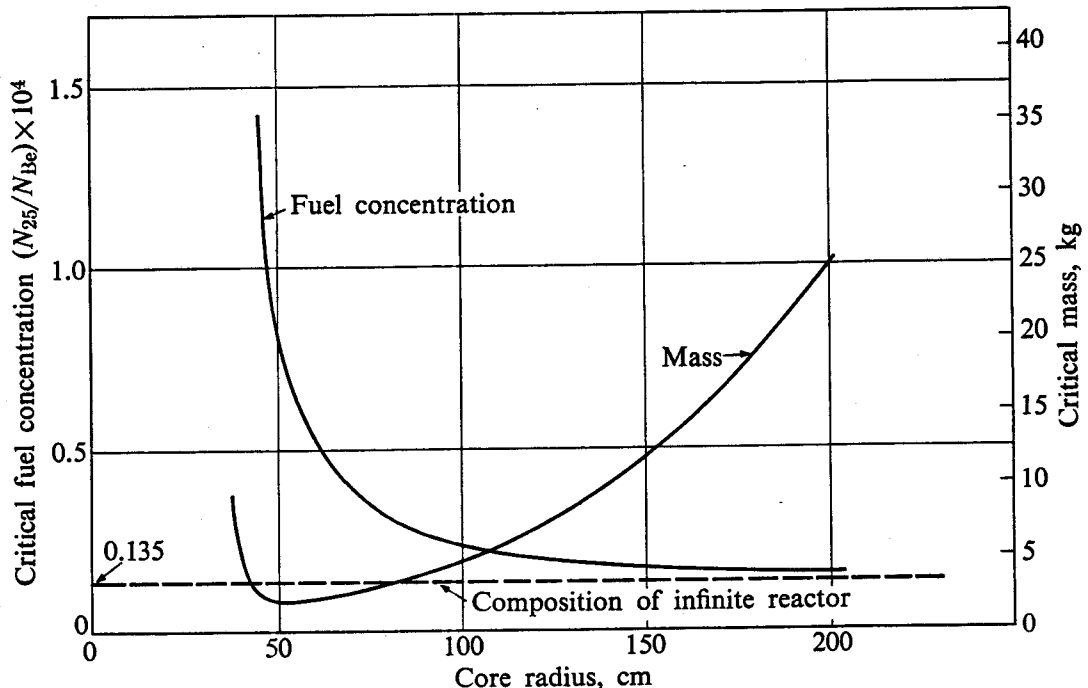


Fig. 9-7. Critical fuel concentration and critical mass of a bare spherical reactor fueled with  $\text{U}^{235}$  and moderated by beryllium as a function of its radius.

Eq. (9-92).\* It will be observed that at fuel-to-moderator ratios less than  $N_{25}/N_{Be} = 1.35 \times 10^{-5}$ , it is not possible to construct a critical system. This is the minimum fuel density for criticality and corresponds to the infinite reactor. With finite reactors, the critical fuel concentration increases with decreasing radius, due to the increasing leakage of neutrons. If the radius becomes too small, however, the necessary fuel density becomes so large that the system ceases to be a thermal reactor and the critical equation derived in this chapter is no longer valid. This is the reason why the curves do not extend to very small radii.

Although the critical composition decreases monotonically with increasing reactor radius, the critical mass at first decreases and then increases, passing through a minimum at about  $r = 50$  cm. The existence of this *minimum critical mass* is due to the following circumstances. With a small reactor there is a considerable leakage of neutrons from the system and the critical composition and mass are both high. As the radius increases, the leakage decreases and as a result the critical fuel-to-moderator ratio also decreases. However, it is easily shown that at small radii the fuel-to-moderator ratio decreases more rapidly than the volume increases, and the net effect is that the critical mass decreases. Beyond a certain point, this decreasing leakage of neutrons ceases to be as important as the increasing

\* Neutron production via the  $\text{Be}^9(n, 2n)$  reaction was not included in these calculations. These reactions can be taken into account by introducing a factor  $\epsilon$  similar in all respects to the fast-fission factor defined in Section 7-9. For pure beryllium this factor has a value of approximately 1.078 (cf. ANL-5800, Second Edition, p. 153).

volume of the reactor; the situation is reversed, and the critical mass now increases. As the reactor becomes very large the critical composition approaches that of the infinite system (only the fission neutrons near the surface can know that the system is finite rather than infinite) and the volume, and therefore critical mass, increases as  $r^3$ .

Although these conclusions pertain specifically to bare reactors and the computations are based on age theory, curves similar to those of Fig. 9-7 are found for all reactors, reflected and bare, and independent of the manner in which the neutrons slow down.

### 9-8 Optimum Reactor Shapes

It was shown in Section 9-3 that a reactor of specified composition will be critical if its dimensions give the required value of  $B^2$ . However, while  $B^2$  is uniquely determined by the dimensions of a reactor, the reverse is not necessarily true. That is, a given value of  $B^2$  does not always determine the dimensions of the reactor. Of course, with a spherical reactor, since  $B^2 = \pi^2/R^2$ ,  $B^2$  does determine  $R$ , but with a cylindrical reactor

$$B^2 = \left(\frac{2.405}{R}\right)^2 + \left(\frac{\pi}{H}\right)^2, \quad (9-89)$$

and any combination of values of  $R$  and  $H$  that gives the required value of  $B^2$  will result in a critical system. Since different values of  $R$  and  $H$  give different reactor volumes, it is reasonable to ask which choice of  $R$  and  $H$  leads to the reactor of least volume.

This, incidentally, is an important question in the design of many reactors. With a specified composition the amount of each material required in a reactor is roughly proportional to its volume. All other things being equal, therefore, the costs of materials tend to be minimized when the volume of the reactor is as small as possible.

To find the minimum critical volume of a cylindrical reactor, Eq. (9-89) is first solved for  $R^2$ :

$$R^2 = \frac{(2.405)^2}{B^2 - \pi^2/H^2}.$$

Substituting this into the formula for the volume of the cylinder yields

$$V = \pi R^2 H = \frac{\pi(2.405)^2 H}{B^2 - \pi^2/H^2}.$$

Differentiating with respect to  $H$  and placing the result equal to zero gives  $H = \pi\sqrt{3}/B$  and  $R = (2.405/B)\sqrt{3/2}$  for the optimum dimensions. The minimum volume is then

$$V_{\min} = \frac{3\sqrt{3}}{2} \frac{\pi^2(2.405)^2}{B^3} = \frac{148}{B^3}. \quad (9-114)$$

The ratio of the height to the radius of the reactor of minimum volume is

$$\frac{R}{H} = \frac{2.405}{\pi\sqrt{2}} = 0.55.$$

Thus the minimum volume of a cylindrical reactor is obtained when its diameter is approximately equal to its height. Although this conclusion is strictly valid only for a bare cylinder, the minimum volume reactor is usually assumed to have these dimensions, even when the reactor has a reflector, and the majority of cylindrical reactors are constructed in this shape. Cylinders of this type, with square cross sections in the axial plane, are known as *square cylinders*.

**Table 9-2**  
Reactors with Minimum Critical Volume

Geometry	Optimum dimensions	Minimum volume
Parallelepiped	$a = b = c$	$\frac{161}{B^3}$
Cylinder	$R = 0.55H$	$\frac{148}{B^3}$
Sphere	$R$	$\frac{130}{B^3}$

The optimum dimensions of a parallelepiped will not be derived here. However, it is easy to show (cf. Prob. 9-18) that the optimum shape is that of a cube, as might be expected. In this case the volume is given by

$$V_{\min} = \frac{3\sqrt{3}\pi^3}{B^3} = \frac{161}{B^3}. \quad (9-115)$$

The minimum volumes of the parallelepiped and cylinder reactors are given in Table 9-2 along with the volume of the spherical reactor of the same buckling. It will be observed that the sphere has the least volume of the three reactors. This is not surprising in view of the well-known fact that the sphere has the smallest surface-to-volume ratio of any solid. Thus the leakage of neutrons from the surface per volume of fissionable material is least for the sphere, and it follows that this reactor has the smallest critical volume.

### 9-9 Quasi-Homogeneous Reactors

Up to this point it has been assumed that reactors are homogeneous mixtures of fuel and moderator, whereas actually very few reactors are of this type. In most reactors the fuel is dispersed in some sort of structural material to form solid *fuel elements* which are arranged in a (usually) uniform lattice.

It is important to distinguish between two classes of reactors of this type. If the mean free path of neutrons at *any* energy is comparable to, or less than, the thickness of a fuel element, the reactor is said to be *heterogeneous*. The analysis of this kind of reactor is rather complicated (to put it mildly) and will be deferred until Chapter 11.

On the other hand, if the neutron mean free path at *all* energies is large compared with the thickness of the fuel element, the reactor is called *quasi-homogeneous*. Although a reactor of this kind is structurally heterogeneous, it is clearly homogeneous so far as the neutrons are concerned. Criticality calculations for a quasi-homogeneous reactor can therefore be made using the methods described in Section 9-6 for the equivalent homogeneous reactor. However, in these calculations it is usually necessary to find the number of fuel elements or the concentration of fuel in the elements required for criticality, rather than simply the fuel concentration in the moderator, as was the case with homogeneous reactors.

For this purpose it is convenient to introduce the following two quantities:

$$\gamma = \frac{V_S}{V_M}, \quad (9-116)$$

where  $V_S$  and  $V_M$  are the total volumes of the fuel elements and moderator in the reactor, respectively, and

$$s = \frac{\bar{\Sigma}_{aF}}{\bar{\Sigma}_{aS}}, \quad (9-117)$$

where  $\bar{\Sigma}_{aF}$  and  $\bar{\Sigma}_{aS}$  are the thermal absorption cross sections of the fuel and structure, respectively, within a single fuel element. The parameters  $\gamma$  and  $s$  are called, respectively, the *metal-to-moderator ratio* and the *fuel-to-structure ratio*.

As a simple example of a calculation involving a quasi-homogeneous reactor, consider a system in which there is no resonance absorption and no fast fission. The multiplication factor for the equivalent homogeneous reactor is then

$$k_\infty = \eta_T f = \frac{\eta_T \langle \bar{\Sigma}_{aF} \rangle}{\langle \bar{\Sigma}_{aF} \rangle + \langle \bar{\Sigma}_{aM} \rangle + \langle \bar{\Sigma}_{aS} \rangle}, \quad (9-118)$$

in which  $\eta_T$  refers to the fissile isotope and  $\langle \bar{\Sigma}_{aF} \rangle$ ,  $\langle \bar{\Sigma}_{aM} \rangle$ , and  $\langle \bar{\Sigma}_{aS} \rangle$  are the thermal macroscopic cross sections of fuel, moderator, and structure *averaged over the reactor volume*. Specifically, if there is a total of  $n_F$  atoms of fuel in the reactor volume  $V$ , then

$$\langle \bar{\Sigma}_{aF} \rangle = \left( \frac{n_F}{V} \right) \bar{\sigma}_{aF}, \quad (9-119)$$

where  $\bar{\sigma}_{aF}$  is the thermal averaged microscopic cross section of the fuel. In terms of the parameters  $\gamma$  and  $s$ , Eq. (9-118) can be written as

$$k_\infty = \frac{\eta_T s \gamma}{\gamma(s + 1) + (\bar{\Sigma}_{aM}/\bar{\Sigma}_{aS})}, \quad (9-120)$$

where  $\bar{\Sigma}_{aM}/\bar{\Sigma}_{aS}$  is the ratio of the macroscopic absorption cross sections of moderator and structural material computed at their normal densities.

Other reactor parameters can be computed for a quasi-homogeneous reactor in a similar manner. Thus the macroscopic absorption cross section averaged over the entire reactor  $\langle \bar{\Sigma}_a \rangle$  is easily seen to be given by the formula

$$\langle \bar{\Sigma}_a \rangle = \frac{\bar{\Sigma}_{aM}}{1 + \gamma} \left[ 1 + \gamma(s + 1) \frac{\bar{\Sigma}_{aS}}{\bar{\Sigma}_{aM}} \right], \quad (9-121)$$

and the average diffusion coefficient for the system is

$$\frac{1}{\langle D \rangle} = \frac{1}{\gamma + 1} \left[ \frac{1}{D_M} + \frac{\gamma}{D_S} \right], \quad (9-122)$$

where  $D_M$  and  $D_S$  are the diffusion coefficients of moderator and structure, respectively, computed at the normal densities of these materials. There is usually enough structural material in a quasi-homogeneous reactor to affect the neutron age substantially. The value of  $\tau_T$  must therefore be found as a function of  $\gamma$  from numerical computations, as shown in Fig. 6-14, or from experimental data.

The volume-averaged parameters given in Eqs. (9-120) through (9-122) are to be used in precisely the same way as the parameters for a homogeneous reactor, and once these are known as functions of  $\gamma$  and  $s$ , the conditions required for criticality can readily be determined. If the composition is given, for instance, these parameters are calculated using the above formulas and the critical size is found by the procedure given in Case II of Section 9-6. On the other hand, if the size of the system is given,  $k$  must be plotted as a function of  $\gamma$  or  $s$ , whichever is the variable parameter and the value (or values) of  $\gamma$  or  $s$  for which  $k = 1$  can be read from the graph.

## References

- GALANIN, A. D., *Thermal Reactor Theory*, 2nd ed. New York: Pergamon Press, 1960, Chapters 2, 3, and 5.
- GLASSTONE, S., and M. C. EDLUND, *The Elements of Nuclear Reactor Theory*. Princeton, N.J.: Van Nostrand, 1952, Chapter 7.
- ISBIN, H. S., *Introductory Nuclear Reactor Theory*. New York: Reinhold, 1963, Chapter 6.
- LITTLER, D. J., and J. F. RAFFLE, *An Introduction to Reactor Physics*, 2nd ed. New York: McGraw-Hill, 1957, Chapter 8.
- MEEM, J. L., *Two Group Reactor Theory*. New York: Gordon and Breach, 1964, Chapter 3.
- MEGHREBLIAN, R. V., and D. K. HOLMES, *Reactor Analysis*. New York: McGraw-Hill, 1960, Chapters 5 and 6.
- MURRAY, R. L., *Nuclear Reactor Physics*. Englewood Cliffs, N.J.: Prentice-Hall, 1957, Chapter 3.
- WEINBERG, A. M., and E. P. WIGNER. *The Physical Theory of Neutron Chain Reactors*. Chicago: University of Chicago Press, 1958, Chapters 12, 13, and 14.

## Problems

[Note: Except where otherwise stated, take the temperature in all problems to be room temperature.]

9-1. Show that the ratio of the slowing down time to the diffusion time in an infinite thermal reactor is given approximately by

$$\frac{t_s}{t_d} = \frac{1}{1-f} \left( \frac{t_s}{t_d} \right)_M,$$

where  $(t_s/t_d)_M$  is this ratio for moderator alone, and  $f$  is the thermal utilization.

9-2. Compute and compare the maximum to average thermal fluxes for the three principal bare reactor geometries:

- (a) sphere      (b) cube      (c) finite cylinder

9-3. (a) Show that a solution to the equation

$$\frac{1}{x^2} \frac{d}{dx} x^2 \frac{dy}{dx} + \left( \alpha^2 - \frac{2}{x^2} \right) y = 0$$

which is not singular at  $x = 0$  is

$$y = \frac{\sin \alpha x}{(\alpha x)^2} - \frac{\cos \alpha x}{\alpha x}.$$

(b) Using this result, find an expression for the buckling of a bare, homogeneous reactor having the shape of a hemisphere. [Hint: Use separation of variables in spherical coordinates, and try  $\cos \vartheta$  as a solution to the  $\vartheta$  equation.]

9-4. Consider the split, finite-cylindrical reactor shown in Fig. 9-8. (a) With the origin of coordinates at the center of the flat face of the reactor, show that the thermal flux is given by

$$\phi_T(r, \vartheta, z) = AJ_1 \left( \frac{x_1 r}{R} \right) \sin \vartheta \cos \left( \frac{\pi z}{H} \right),$$

where  $x_1 = 3.84$  is the first zero of  $J_1(x)$ , that is,  $J_1(x_1) = 0$ . (b) Show that the buckling is

$$B^2 = \left( \frac{x_1}{R} \right)^2 + \left( \frac{\pi}{H} \right)^2.$$

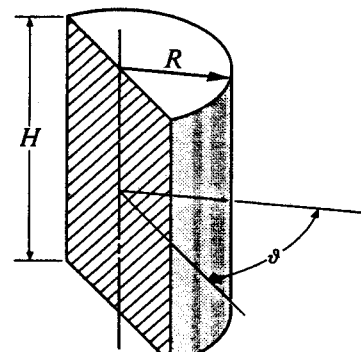


Figure 9-8

(c) Determine the constant  $A$  in terms of the reactor power. (d) What fraction of the thermal neutrons leaking from the reactor pass through the flat face?

9-5. A nonuniform distribution of thermal neutron sources  $s(r)$  is placed in an otherwise uniform bare subcritical thermal reactor. If  $s(r)$  is the first eigenfunction of the equation

$$\nabla^2 s(r) + B^2 s(r) = 0,$$

show that the equilibrium thermal flux consists only of the fundamental of the reactor equation.

9-6. Recalling that  $\operatorname{div} \mathbf{J} dV$  is equal to the net leakage of neutrons from  $dV/\text{sec}$  (cf. Section 5-3): (a) show that there is a net leakage of thermal neutrons from *every* volume element in a uniform, critical, bare, thermal reactor which is equal to  $B^2\phi_T(r) dV$  neutrons/sec, where  $dV$  is located at  $r$ ; (b) show that the probability that a neutron does not leak from a volume element is independent of the location or size of the element and is given by  $1/(1 + B^2L_T^2)$ ; (c) interpret this last result in terms of leakage from the reactor as a whole.

9-7. Compute the minimum critical concentrations at room temperature of  $\text{U}^{233}$ ,  $\text{U}^{235}$ , and  $\text{Pu}^{239}$  in the following moderators.

- (a)  $\text{H}_2\text{O}$       (b)  $\text{D}_2\text{O}$       (c) Be      (d) Graphite

9-8. A bare spherical reactor 100 cm in diameter is to be constructed of a homogeneous mixture of  $\text{D}_2\text{O}$  and  $\text{U}^{235}$ . The reactor is to be operated at a power of 10 MW(th) at 100°C. (a) Find the critical mass of the reactor. (b) Find the thermal flux throughout the reactor. (c) Find the slowing down density throughout the reactor in the proper units. (d) Find the probability that a neutron leaks from the system while slowing down and at thermal energies. (e) At what rate is the  $\text{U}^{235}$  consumed? (f) How many thermal neutrons are there in the entire reactor? (g) If the radius of the reactor were reduced would the critical mass of the system increase or decrease?

9-9. A bare reactor in the form of a square cylinder  $2\frac{1}{2}$  ft high contains a uniform mixture of  $\text{U}^{235}$  and Be and operates a power of 20 MW(th) at an average temperature of 500°C. (a) Find the critical mass (ignore the  $\text{Be}^9(n, 2n)$  reaction). (b) What fraction of the fission neutrons leak out while slowing down? (c) What is the probability that a neutron leaks from the system at thermal energies? (d) What is the maximum value of the thermal flux in the system? (e) Determine the effect of the  $\text{Be}(n, 2n)$  reaction on the critical mass of this reactor by using an equivalent fast fission factor  $\epsilon = 1.078$ . (f) Compute the average diffusion time in the reactor and compare this with the slowing down time.

9-10. At a fuel-processing plant, aqueous solutions of fully-enriched uranyl sulfate are to be carried through and/or stored in cylindrical pipes. If the maximum concentration of the uranyl sulfate is expected to be 100 gm/liter, what is the maximum size of pipe which can safely be used if an accidental criticality incident is to be averted?

9-11. It is costly to remove the power generated in a large research reactor. One measure of the merit of a research reactor used to produce thermal neutrons is, therefore, the ratio of the average thermal flux to the power. If a proposed (homogeneous) reactor is to be fueled with  $\text{U}^{235}$ , which of the four common moderators,  $\text{H}_2\text{O}$ ,  $\text{D}_2\text{O}$ , Be, or graphite, should be used to maximize this ratio? Assume, for simplicity, that the reactor is bare.

9-12. A large graphite reactor is constructed in the form of a bare cube and is fueled with lumps of natural uranium. The reactor has the following parameters:  $k_\infty = 1.0735$ ,  $f = 0.8964$ ,  $p = 0.8843$ ,  $\tau_T \approx 396 \text{ cm}^2$ , and  $L_T^2 \approx 325 \text{ cm}^2$ . When operating at a power of 25 MW(th) the maximum thermal flux is  $5 \times 10^{12} \text{ neutrons/cm}^2\text{-sec}$ . (a) Determine the critical size of the reactor. (b) How much  $\text{U}^{235}$  is present in the reactor? (c) If the natural uranium were replaced by pure  $\text{U}^{235}$ , what would be the new critical mass of the reactor? (d) What is the maximum value of the thermal flux in part (c) when the reactor operates at 25 MW(th)?

9-13. (a) Show that for a natural uranium-fueled reactor the conversion ratio  $C$ , i.e., the number of atoms of  $\text{U}^{238}$  converted to  $\text{Pu}^{239}$  per atom of  $\text{U}^{235}$  consumed (cf.

Section 4-3), is given by

$$C = \frac{\bar{\Sigma}_{a28}}{\bar{\Sigma}_{a25}} + \epsilon \eta_{T25}(1 - p)P_F,$$

where  $P_F$  is the fast nonleakage probability and the other symbols have their usual meanings. (b) Compute  $C$  for the reactor described in Problem 9-12. (c) Compute the rate of production of  $\text{Pu}^{239}$  when that reactor is operated at a power of 25 MW(th). (d) What fraction of the  $\text{Pu}^{239}$  production is due to thermal neutron absorption?

9-14. Determine the maximum value of  $k_\infty$  for a homogeneous mixture of natural uranium and

- (a)  $\text{H}_2\text{O}$       (b)  $\text{D}_2\text{O}$       (c) Be      (d) Graphite

[Note: Except for  $\text{H}_2\text{O}$ , take  $\epsilon = 1$ .]

9-15. Calculate the minimum enrichment of uranium necessary to achieve criticality with a homogeneous mixture of uranium and

- (a)  $\text{H}_2\text{O}$       (b) Be      (c)  $\text{BeO}$       (d) Graphite

[Note: Except for  $\text{H}_2\text{O}$ , take  $\epsilon = 1$ .]

9-16. Determine the minimum concentration of  $\text{D}_2\text{O}$  in  $\text{H}_2\text{O}$  necessary to obtain criticality with natural uranium, if the fuel is uniformly dispersed in the system. [Hint: Use the results of Problem 7-16.]

9-17. Compute and plot the critical mass and the fast and slow nonleakage probabilities for a spherical assembly of  $\text{U}^{235}$  and moderator as a function of the radius of the assembly for the following moderators.

- (a)  $\text{H}_2\text{O}$       (b)  $\text{D}_2\text{O}$       (c) Be      (d) Graphite

Determine the minimum critical mass in each case.

9-18. (a) Show that the critical mass of a uniform, bare, rectangular parallelepiped reactor of specified composition is a minimum when the reactor is a cube. (b) What is the reactor volume in this case? [Hint: Lagrange multipliers are useful in this problem (see any book on advanced calculus).]

9-19. Give a quantitative, physical explanation for the fact that the optimum finite bare cylindrical reactor is not precisely square.

9-20. The fuel elements of a certain reactor consist of thin fuel "sandwiches" as shown in Fig. 9-9. The "meat" is a uranium-aluminum alloy, 15% uranium by weight, with a density of approximately  $3.1 \text{ gm/cm}^3$ . The uranium is enriched to 90 atom % in  $\text{U}^{235}$ . These fuel elements are arranged in a regular array in a bare, square-cylindrical

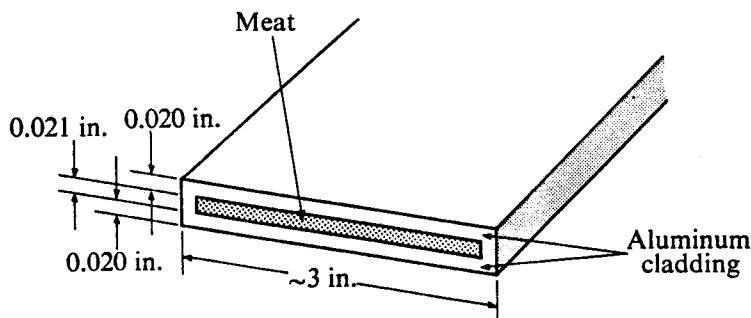


Figure 9-9

tank containing  $H_2O$  moderator-coolant of unit density. The ratio of the total fuel element volume to  $H_2O$  volume is 0.73. (a) Compute the thickness of the meat in thermal neutron mean free paths. (b) Compute  $k_\infty$ ,  $L_T^2$ , the critical dimensions, and the critical mass of the reactor. (Determine  $\tau_T$  from Fig. 6-14.) [Note: The fuel elements and reactor in question are similar to those of the Materials Testing Reactor (MTR) at Arco, Idaho.]

9-21. An isotropic point source emitting  $S$  fast neutrons/sec is placed at the center of a bare cylindrical subcritical assembly of radius  $R$  and height  $H$ . (a) Using age theory, show that the thermal flux at any point in the assembly is given by

$$\phi_T(r, z) = \frac{2pS}{V\bar{\Sigma}_a k_\infty} \sum_{\substack{m=1, 2, 3, \dots \\ n \text{ odd}}} \frac{k_{mn}}{(1 - k_{mn})J_1^2(x_m)} J_0\left(\frac{x_m r}{R}\right) \cos\left(\frac{n\pi z}{H}\right),$$

where  $V$  is the volume of the cylinder,  $x_m$  is the  $m$ th zero of  $J_0(x)$ ,

$$k_{mn} = \frac{k_\infty e^{-B_{mn}^2 \tau_T}}{1 + B_{mn}^2 L_T^2}, \quad \text{and} \quad B_{mn}^2 = \left(\frac{x_m}{R}\right)^2 + \left(\frac{n\pi}{H}\right)^2.$$

(b) Compute the maximum flux in the assembly if  $H = 2R = 5$  ft,  $S = 10^7$  neutrons/sec,  $k_\infty = 0.980$ ,  $p = 0.83$ ,  $\tau_T = 31.2 \text{ cm}^2$ ,  $L_T^2 = 2.8 \text{ cm}^2$ , and  $\bar{\Sigma}_a = 0.16 \text{ cm}^{-1}$ . [Hint: Use the results of Problem 6-23.]

9-22. If the source in Problem 9-21 were moved along the axis to the point  $(0, z_0)$ , show that the flux becomes

$$\begin{aligned} \phi_T(r, z) = & \frac{2pS}{V\bar{\Sigma}_a k_\infty} \sum_{m, n} \frac{k_{mn}}{1 - k_{mn}} \frac{J_0(x_m r/R)}{J_1^2(x_m)} \left[ \cos \frac{(2n - 1)\pi z}{H} \cos \frac{(2n - 1)\pi z_0}{H} \right. \\ & \left. + \sin \frac{2n\pi z}{H} \sin \frac{2n\pi z_0}{H} \right]. \end{aligned}$$

9-23. If the slowing down distance is small compared with the dimensions of the assembly in Problem 9-21,  $k_{mn}$  can be written as

$$k_{mn} = \frac{k_\infty}{1 + B_{mn}^2 M^2},$$

where  $M^2$  is the migration area. In this case, show that there is a region along the axis of the assembly, not near the center or the top of the tank, where the thermal flux varies as

$$\phi_T \sim e^{-\lambda z}.$$

Here  $\lambda$  is given by

$$\lambda^2 = \left(\frac{2.405}{R}\right)^2 - B_M^2,$$

where

$$B_M^2 = \frac{k_\infty - 1}{M^2}$$

is called the *materials buckling*. (A comparison of the formula for  $B_M^2$  and Eq. (9-109) shows that an assembly with parameters  $k_\infty$  and  $M^2$  will be critical provided  $B_M^2 = B^2$ ,

where  $B^2$ , the buckling, is the first eigenfunction of the reaction equation. In view of the above results, measurements of the thermal flux along the axis of the assembly give  $B_M^2$  directly, and this, in turn, can be used to determine the dimensions of the critical system, if a system of this composition can indeed be made critical. Such measurements are known as *exponential experiments.*) Hint: Note that the sum

$$\sum_{n \text{ odd}} C_n \cos\left(\frac{n\pi z}{H}\right)$$

appearing in Problem 9-21 can be approximated in the limit of large  $H$ , by treating  $n\pi/H = \xi$  as a continuous variable. Then

$$\sum_{n \text{ odd}} C_n \cos\left(\frac{n\pi z}{H}\right) \sim \int_0^\infty C(\xi) \cos \xi z \, d\xi.$$

# 10

## Multiregion Reactors—the Group Diffusion Method

The discussion of reactor criticality in the preceding chapter was limited to one-region bare reactors, and the neutron moderation was treated by Fermi age theory. Most reactors, however, are not bare; almost all have reflectors to reduce neutron leakage, and many have additional regions of fertile material. Since age theory cannot be used to describe the slowing down of neutrons in such multi-region systems, due to certain mathematical difficulties, it is necessary to turn to other methods of computation.

One of the most powerful ways of treating multiregion reactors is by the *group diffusion method*. In this method the energies of all the neutrons are divided into a number of energy groups. The neutrons within each group are then lumped together and their diffusion, scattering, absorption, and other interactions are described in terms of suitably averaged diffusion coefficients and cross sections, which are collectively known as *group constants*. An example of this procedure was encountered in Chapter 8 in connection with the diffusion of thermal neutrons. There it was shown how average diffusion coefficients, absorption cross sections, etc., can be computed for the thermal neutrons, and the diffusion equation for these neutrons was derived and applied to specific problems in Chapter 9.

The time behavior of multiregion reactors will not be considered in the present chapter, since the results derived in Chapter 9 for the bare reactor can be shown to apply with little modification in the multiregion case. Thus when the flux is found as a function of space and time for a multiregion reactor, a series of eigenfunctions is obtained similar to Eq. (9-38), each term of which is multiplied by an exponential function of time. In the absence of an extraneous neutron source, the flux will remain constant, that is, the reactor will be critical, only if the amplitude of the fundamental eigenfunction is independent of time. When this is the case, the higher harmonics in the series rapidly die out in time. The behavior of the multi-region reactor is therefore completely analogous to that of the bare reactor. With these results in mind, the present chapter is confined to the consideration of critical reactors only.

### 10-1 One Group of Neutrons

The simplest group diffusion problem involves only one group of neutrons, and for the purpose of illustration it will be assumed that these neutrons are all thermal neutrons. Thus the fact that fission neutrons actually appear in a reactor at high energies will be ignored and it will be assumed that they are emitted at thermal energies.

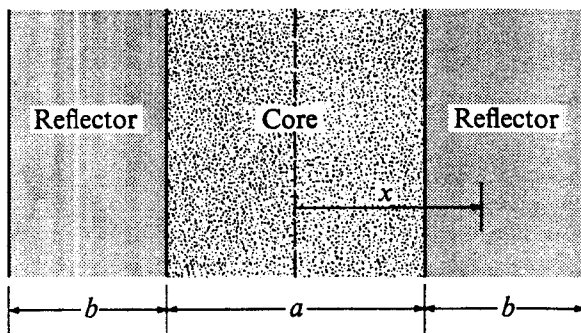


Fig. 10-1. The reflected slab reactor.

Consider now an infinite slab reactor of thickness  $a$  surrounded on both sides by a reflector of extrapolated thickness  $b$ , as shown in Fig. 10-1. The central region contains a homogeneous mixture of fuel and moderator, while the reflector consists of moderator alone. The center region corresponds to the core of a real reactor and its properties will be denoted by the subscript  $c$ . The reflector will be indicated by the subscript  $r$ .

Since it has been assumed that the reactor is critical and operating in a steady state, the flux is independent of time, and the diffusion equation for the neutrons in the core is

$$\bar{D}_c \frac{d^2\phi_{Tc}}{dx^2} - \bar{\Sigma}_{ac}\phi_{Tc} + \eta_T \bar{\Sigma}_{aFc}\phi_{Tc} = 0. \quad (10-1)$$

Here  $\phi_{Tc}$  is the thermal flux,  $\bar{\Sigma}_{ac}$  is the thermal absorption cross section of the fuel-moderator mixture,  $\bar{\Sigma}_{aFc}$  is the thermal absorption cross section of the fuel alone, and  $\bar{D}_c$  is the thermal diffusion coefficient, all for the core (cf. Section 8-5). The term  $\eta_T \bar{\Sigma}_{aFc}\phi_{Tc}$  in Eq. (10-1) is the number of fission neutrons produced per  $\text{cm}^3/\text{sec}$  in the core. Resonance absorption and fast fission can be ignored, since by hypothesis all neutrons in the system are thermal. It follows from the discussion in Section 9-1 that  $\eta_T \bar{\Sigma}_{aFc} = \eta_T f \bar{\Sigma}_{ac} = k_\infty \bar{\Sigma}_{ac}$ , and Eq. (10-1) becomes

$$\bar{D}_c \frac{d^2\phi_{Tc}}{dx^2} + (k_\infty - 1)\bar{\Sigma}_{ac}\phi_{Tc} = 0. \quad (10-2)$$

This equation can be put in the more convenient form

$$\frac{d^2\phi_{Tc}}{dx^2} + B_c^2 \phi_{Tc} = 0, \quad (10-3)$$

where  $B_c^2$  is defined by

$$B_c^2 = \frac{k_\infty - 1}{L_{Tc}^2}, \quad (10-4)$$

and  $L_{Tc}$  is the thermal diffusion length in the core.

The parameter  $B_c^2$  defined by Eq. (10-4) is called the buckling of the core, and is analogous to the buckling of a bare reactor discussed in Section 9-2. Again,  $B_c^2$  is a measure of the curvature or “buckling” of the flux, but in this case, only in the core of the reactor.

With a little rearrangement, Eq. (10-4) can be written as

$$\frac{k_\infty}{1 + B_c^2 L_{Tc}^2} = 1. \quad (10-5)$$

This equation is the critical equation for the system according to the one-group model. It is analogous to the critical equation for the bare reactor (cf. Eq. 9-92), and in fact can be obtained from Eq. (9-92) by placing  $\tau_T = 0$ . The critical value of the buckling must again be found by solving the diffusion equation as in Chapter 9.

The diffusion equation for the reflector is somewhat simpler than for the core, since the reflector is not a multiplying medium. The equation is

$$\frac{d^2 \phi_{Tr}}{dx^2} - \frac{1}{L_{Tr}^2} \phi_{Tr} = 0, \quad (10-6)$$

where  $\phi_{Tr}$  and  $L_{Tr}$  are, respectively, the thermal flux and thermal diffusion length in the reflector.

In order to determine the critical buckling and the flux in the reactor, it is necessary to solve Eqs. (10-3) and (10-6) subject to the usual boundary conditions. Equation (10-3) has the general solution

$$\phi_{Tc} = A \cos B_c x + C \sin B_c x,$$

but in view of the symmetry of the system, it is evident that  $\phi_{Tc}$  must be an even function, so that  $C = 0$ . The flux in the core is therefore

$$\phi_{Tc} = A \cos B_c x. \quad (10-7)$$

Consider next the reflector equation. The solution to Eq. (10-6) for positive values of  $x$ , which is zero at the extrapolated edge of the reflector, i.e., at  $x = a/2 + b$ , is

$$\phi_{Tr} = A' \sinh \left( \frac{(a/2) + b - x}{L_{Tr}} \right).$$

Because of the symmetry of the system, the solution which is valid for both positive

and negative values of  $x$  can be obtained by replacing  $x$  by the absolute value of  $x$ ; that is,

$$\phi_{Tr} = A' \sinh \left( \frac{(a/2) + b - |x|}{L_{Tr}} \right). \quad (10-8)$$

Since the flux must be continuous at the core-reflector interface, i.e., at  $|x| = a/2$ , it follows that

$$A \cos \frac{B_c a}{2} = A' \sinh \frac{b}{L_{Tr}}. \quad (10-9)$$

Similarly, the continuity of current at  $|x| = a/2$  gives

$$\bar{D}_c B_c A \sin \frac{B_c a}{2} = \frac{\bar{D}_r}{L_{Tr}} A' \cosh \frac{b}{L_{Tr}}. \quad (10-10)$$

When Eq. (10-10) is divided by Eq. (10-9), the constants  $A$  and  $A'$  cancel and the following equation is obtained:

$$\bar{D}_c B_c \tan \frac{B_c a}{2} = \frac{\bar{D}_r}{L_{Tr}} \coth \frac{b}{L_{Tr}}. \quad (10-11)$$

Equation (10-11) gives a relation between the buckling and the slab thickness which must be satisfied if the reactor is to be critical. Suppose, for example, that the properties and thickness of the reflector are specified. If the properties of the core are also given,  $B_c^2$  is known from Eq. (10-4), and the critical core thickness can be found by solving Eq. (10-11) directly for  $a$ . On the other hand, if  $a$  is given,  $B_c^2$  must be found by solving Eq. (10-11) numerically or graphically. Before plotting this equation, it is convenient to multiply both sides by  $a/2$  and divide by  $\bar{D}_c$ ; this gives

$$\frac{B_c a}{2} \tan \frac{B_c a}{2} = \frac{\bar{D}_r a}{2 \bar{D}_c L_{Tr}} \coth \frac{b}{L_{Tr}}. \quad (10-12)$$

The two sides of Eq. (10-12) are shown in Fig. 10-2 as functions of  $B_c a/2$ . The right-hand side (RHS) of the equation is independent of  $B_c$ , and since  $a$  is given, the RHS appears as a horizontal line. The left-hand side (LHS) varies with  $B_c a/2$  as shown. Negative values of  $B_c a/2$  are not of interest, for  $a$  is always positive, and  $B_c$  cannot be negative (cf. Eq. 10-4).

It will be observed from Fig. 10-2 that there are an infinite number of solutions to Eq. (10-12), one occurring at each intersection of the curves. Each of these intersections corresponds to one of the eigenvalues of the problem. However, all eigenvalues above the first are associated with harmonics of the flux which die out in a critical reactor, and it is only the first intersection of the curves that has a bearing on the criticality of the system.

It should also be noted in Fig. 10-2 that the first eigenvalue is found at a value of  $B_c a/2$  somewhat less than  $\pi/2$ . Had the reactor been bare, it will be recalled from Chapter 9 that the critical eigenvalue would occur when  $B_c a/2$  is exactly

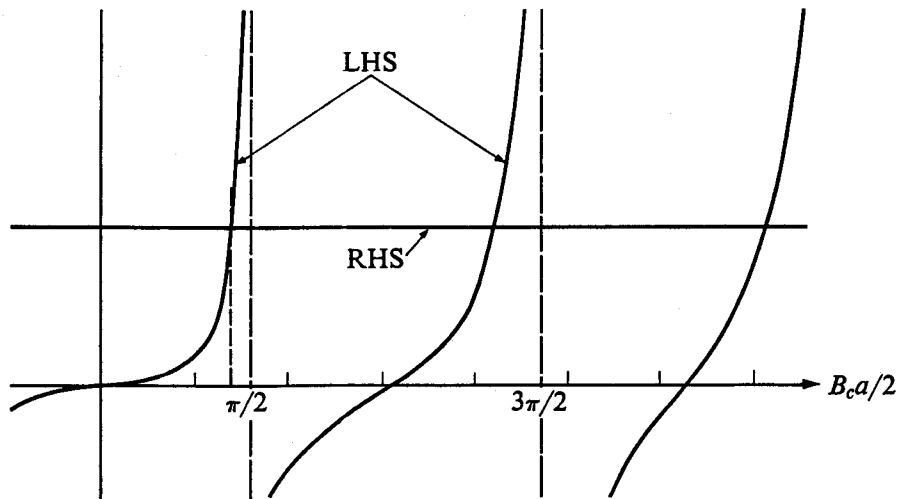


**Fig. 10-2.** The left-hand side (LHS) and right-hand side (RHS) of the one-group critical equation for the reflected slab reactor.

equal to  $\pi/2$ . Physically, this means that with a given core composition, i.e., a given value of  $B_c$ , the reflected reactor becomes critical with a smaller core than does the corresponding bare reactor. This, of course, is the reason why reactors have reflectors in the first place. In the limit as the thickness of the reflector goes to zero, that is, as the reactor approaches the bare system, the right-hand side of Eq. (10-12) becomes infinite. The horizontal line in Fig. 10-2 therefore rises and the first intersection is then at  $B_c a/2 = \pi/2$ . On the other hand, as the thickness of the reflector increases, the right-hand side of Eq. (10-12) decreases, the horizontal line in Fig. 10-2 moves downward and the first eigenvalue occurs at smaller and smaller values of  $B_c a/2$ . In the limit as the reflector becomes infinitely thick, that is,  $b \gg L_{Tr}$ , the right-hand side of Eq. (10-12) goes to the constant  $D_r a/2 D_c L_{Tr}$ . This limiting case gives the smallest core that will go critical with the specified composition and the given reflector material.

It will be recalled that in deriving Eq. (10-12) the constants  $A$  and  $A'$  cancel, and it is therefore not possible to determine the absolute value of the flux. This could hardly have been expected since, as discussed in Chapter 9, the magnitude of the flux depends upon the operating power of the reactor. It is possible to find  $A'$  in terms of  $A$ , however, so that the shape of the flux is known throughout the entire reactor. Thus from Eq. (10-9),

$$A' = A \frac{\cos(B_c a/2)}{\sinh(b/L_{Tr})},$$

and the flux is then

$$\phi_T(x) = A \begin{cases} \cos B_c x, & |x| \leq a/2, \\ \frac{\cos(B_c a/2) \sinh[(a/2 + b - |x|)/L_{Tr}]}{\sinh(b/L_{Tr})}, & |x| \geq a/2. \end{cases} \quad (10-13)$$

The constant  $A$  can be found in terms of the reactor power as in Section 9-2 by integrating  $\phi_T(x)$  over the power-producing region of the reactor, in this case,

the core. Thus, if  $P$  is the power per unit area of the reactor,  $\gamma$  is the recoverable energy per fission, and  $\bar{\Sigma}_{fc}$  is the average thermal fission cross section in the core, then

$$\begin{aligned} P &= \gamma \bar{\Sigma}_{fc} \int_{-a/2}^{a/2} \phi_{Tc}(x) dx = \gamma \bar{\Sigma}_{fc} A \int_{-a/2}^{a/2} \cos B_c x dx \\ &= \frac{2\gamma \bar{\Sigma}_{fc} A \sin(B_c a/2)}{B_c}. \end{aligned} \quad (10-14)$$

Therefore,  $A$  is given by

$$A = \frac{PB_c}{2\gamma \bar{\Sigma}_{fc} \sin(B_c a/2)}. \quad (10-15)$$

It may be mentioned at this point that the one-group critical equation (Eq. 10-5) becomes identical with the critical equation for large bare reactors given in Section 9-5 if  $L_{Tc}^2$  in Eq. (10-5) is replaced by the migration area  $M^2$ . The one-group model can thus be used for computations of large reactors by simply substituting  $M^2$  for  $L^2$ . It is for this reason that Eq. (9-99) was called the critical equation of "modified one-group theory."

The one-group model can also be used to make rough estimates of the critical size or composition of fast reactors. It will be recalled that in such systems the neutrons slow down to energies of the order of only 100 keV before inducing fissions. At these energies the fission and other cross sections vary smoothly with energy and it is possible to obtain useful estimates of the critical mass or dimensions by using only one group of neutrons. The necessary group constants can be computed as averages over the energy-dependent flux in exactly the same way as they were in the thermal case. However, instead of assuming that  $\phi(E)$  is similar to a Maxwellian as in Section 8-5, another, more appropriate function must be used for  $\phi(E)$ .

## 10-2 Two-Group Method

The one-group method is obviously limited by the fact that all neutrons are lumped together into only one group. A more accurate procedure, particularly for thermal reactors, is to split the neutrons into two groups. In this case the thermal neutrons are included in one group called the *thermal* or *slow group*, and all other neutrons are included in the *fast group*. The energy separating the two groups is thus of the order of  $5kT$ , as discussed in Chapter 8.

**Two-group constants.** The constants describing the thermal neutrons have already been derived in Chapter 8 and need no further elaboration. It is convenient at this point, however, to introduce a new notation. The thermal flux, which heretofore has been denoted by  $\phi_T$ , will now be written as  $\phi_2$ , where the subscript refers to the "second" or thermal neutron group.\* From Eq. (8-20)

---

\* It is the usual practice to denote by *ascending* numbers neutron groups of *decreasing* energy.

$\phi_2(\mathbf{r})$  is given by

$$\phi_2(\mathbf{r}) = \phi_T(\mathbf{r}) = \int_0^{-5kT} \phi(\mathbf{r}, E) dE. \quad (10-16)$$

In the present discussion the average thermal diffusion coefficient which was derived in Section 8-5 will be denoted by  $D_2$ , that is,

$$D_2 = \bar{D} = \Gamma(m + 2) D(E_0) \left( \frac{T}{T_0} \right)^m, \quad (10-17)$$

where  $m$  is the parameter related to the energy dependence of the scattering cross section at thermal energies (cf. Eq. 8-74),  $D(E_0)$  is the diffusion coefficient at 0.0253 eV,  $T_0 = 293.61^\circ$  K, and  $T$  is the neutron temperature. Similarly, the average thermal macroscopic absorption cross section will be denoted by  $\Sigma_2$  (cf. Eq. 8-40):

$$\Sigma_2 = \bar{\Sigma}_a = \frac{\sqrt{\pi}}{2} g_a(T) \Sigma_a(E_0) \left( \frac{T_0}{T} \right)^{1/2}, \quad (10-18)$$

where  $g_a(T)$  is the non- $1/v$  factor, and the other symbols have the same meaning as above.

The fast flux  $\phi_1(\mathbf{r})$  is defined by the integral

$$\phi_1(\mathbf{r}) = \int_{-5kT}^{\infty} \phi(\mathbf{r}, E) dE, \quad (10-19)$$

and the fast-diffusion coefficient  $D_1$  is defined as

$$D_1 = \frac{\int_{-5kT}^{\infty} D(E) \nabla^2 \phi(\mathbf{r}, E) dE}{\int_{-5kT}^{\infty} \nabla^2 \phi(\mathbf{r}, E) dE}. \quad (10-20)$$

According to Eq. (10-20),  $D_1$  will, in general, be a function of  $\mathbf{r}$  unless  $\phi(\mathbf{r}, E)$  can be written as a separable function of  $\mathbf{r}$  and  $E$ , namely, as the product of a function of  $\mathbf{r}$  times a function of  $E$ , that is,  $\phi(\mathbf{r}, E) = f(\mathbf{r})\phi(E)$ . This is never strictly true, but it must be assumed in order to carry out a two-group calculation. This being the case, Eq. (10-20) becomes

$$D_1 = \frac{\int_{-5kT}^{\infty} D(E) \phi(E) dE}{\int_{-5kT}^{\infty} \phi(E) dE}, \quad (10-21)$$

where  $\phi(E)$  is the energy-dependent flux.

The function  $\phi(E)$  to be used in Eq. (10-21) is rarely known exactly at the start of a two-group calculation, and it is a common practice to use the expression for  $\phi(E)$  which was derived in Chapter 6 for an infinite system. In Section 6-5 it was

**Table 10-1**  
**Fast-Group Constants for Various Moderators**

Moderator	$D_1$ , cm	$\Sigma_1$ , $\text{cm}^{-1}$	$\tau_T$ , $\text{cm}^2$
H <sub>2</sub> O	1.13	0.0419	~27
D <sub>2</sub> O	1.29	0.00985	131
Be	0.562	0.00551	102
C	1.016	0.00276	368

shown that in the asymptotic region

$$\phi(E) = \frac{\text{constant}}{\bar{\xi}(E)\Sigma_s(E)E}. \quad (10-22)$$

Since  $\Sigma_s(E)$  and  $\bar{\xi}(E)$  are often constant over much of the slowing-down region, it is frequently possible to write  $\phi(E) = \text{constant}/E$  in Eq. (10-21), and then

$$D_1 = \frac{\int_{-5kT}^{nkT} D(E) dE/E}{\int_{-5kT}^{nkT} dE/E}, \quad (10-23)$$

$n$  a large number. Values of  $D_1$  for several moderators are given in Table 10-1.

In the absence of resonance capture, neutrons are not ordinarily absorbed in the fast group, since the absorption cross section is so low at high energies. However, they can be lost from the fast group when, as the result of elastic and inelastic collisions, their energy falls into the thermal region. This disappearance of neutrons from the fast group is described in terms of a fictitious absorption cross section denoted by  $\Sigma_1$ . This is defined such that  $\Sigma_1\phi_1(\mathbf{r})$  is equal to the number of neutrons which slow down out of the fast group per  $\text{cm}^3/\text{sec}$  at the point  $\mathbf{r}$ .

To see the physical significance of  $\Sigma_1$ , consider the diffusion of fast neutrons emitted from a point source in an infinite, homogeneous moderator. These neutrons are described by a diffusion equation in which the rate of "absorption" at any point is given by  $\Sigma_1\phi_1$ . Except at the source itself, therefore, the fast flux is determined by

$$D_1\nabla^2\phi_1 - \Sigma_1\phi_1 = 0. \quad (10-24)$$

Equation (10-24) is identical in form with the equation describing the diffusion of monoenergetic neutrons emitted from a point source, which was discussed in detail in Chapter 5. It will be recalled from that discussion that the quantity  $L^2 = D/\Sigma_a$  is equal to one-sixth the average of the square of the crow-flight distance from the point where a neutron is emitted to the point where it is finally absorbed. By analogy, the quantity  $D_1/\Sigma_1$  in Eq. (10-24) must be equal to one-sixth the average of the square of the crow-flight distance from the source to the point where a neutron finally leaves the fast group, that is, to the point where the neutrons slow down into the thermal group. This, however, is precisely the definition of the

neutron age, so it must be concluded that

$$\frac{D_1}{\Sigma_1} = \tau_T, \quad (10-25)$$

where  $\tau_T$  is the age to thermal of the fast neutrons.

The numerical value of the cross section  $\Sigma_1$  for a two-group calculation is usually computed from Eq. (10-25). It will be recalled from Chapter 6 that  $\tau_T$  can be determined either by experiment or by numerical methods, and the value of  $\tau_T$  is therefore usually known. At the same time,  $D_1$  can easily be computed from Eq. (10-23), since  $D(E)$  is not usually a rapidly varying function of energy. The value of  $\Sigma_1$  is then simply

$$\Sigma_1 = \frac{D_1}{\tau_T}. \quad (10-26)$$

Values of  $\tau_T$  and  $\Sigma_1$  are also given in Table 10-1

According to the above discussion,  $\Sigma_1\phi_1$  neutrons slow down into the thermal group per  $\text{cm}^3/\text{sec}$  in the absence of resonance absorption. Thus in this case  $\Sigma_1\phi_1$  is equal to the thermal slowing-down density. When resonance absorbers are present, it follows from Section 7-8 that the slowing-down density is given by

$$q_T = p\Sigma_1\phi_1, \quad (10-27)$$

where  $p$  is the resonance escape probability.

**Two-group equations.** Consider a two-region thermal reactor consisting of a homogeneous multiplying core surrounded by a nonmultiplying reflector. For the moment the discussion will be limited to reactors in which the flux is a function of only one spatial variable. These reactors include the infinite slab, the infinite cylinder, and the sphere, all of which have reflectors whose thickness is either finite or infinite.

In a thermal reactor, neutrons appear in the fast group as the result of fissions induced by thermal neutrons. Thus, at the point  $r$ ,  $\eta_T\epsilon\Sigma_{2Fc}\phi_2(r)$  fast neutrons are produced per  $\text{cm}^3/\text{sec}$ , where  $\Sigma_{2Fc}$  is the average thermal absorption cross section of the fuel in the core. At the same time, neutrons are lost from the fast group by slowing down as explained above. In the steady state, the diffusion equation for the fast neutrons in the core is therefore

$$D_{1c}\nabla^2\phi_{1c} - \Sigma_{1c}\phi_{1c} + \eta_T\epsilon\Sigma_{2Fc}\phi_{2c} = 0. \quad (10-28)$$

From the definition of the infinite multiplication factor (cf. Section 9-1),  $\eta_T\epsilon\Sigma_{2Fc} = (k_\infty/p_c)\Sigma_{2c}$ , where  $\Sigma_{2c}$  is the slow-group absorption cross section of the fuel-moderator mixture, and  $p_c$  is the resonance escape probability. Equation (10-28) can then be written as

$$D_{1c}\nabla^2\phi_{1c} - \Sigma_{1c}\phi_{1c} + \frac{k_\infty}{p_c}\Sigma_{2c}\phi_{2c} = 0. \quad (10-29)$$

Consider now the slow group. Neutrons enter this group as the result of slowing down out of the fast group, and the thermal slowing-down density therefore appears as the source term in the thermal diffusion equation. Thus in view of Eq. (10-27) the slow flux in the core is described by the equation

$$D_{2c}\nabla^2\phi_{2c} - \Sigma_{2c}\phi_{2c} + p_c\Sigma_{1c}\phi_{1c} = 0. \quad (10-30)$$

By hypothesis, there is no fuel in the reflector, and consequently no source term appears in the diffusion equation for the fast neutrons in this region. This is then simply

$$D_{1r}\nabla^2\phi_{1r} - \Sigma_{1r}\phi_{1r} = 0. \quad (10-31)$$

It will be evident that all of the fast neutrons present in the reflector originate in leakage from the core. Many fast neutrons slow down in the reflector, however, and these give rise to a source term in the equation for the slow flux; namely,

$$D_{2r}\nabla^2\phi_{2r} - \Sigma_{2r}\phi_{2r} + \Sigma_{1r}\phi_{1r} = 0, \quad (10-32)$$

where it has been assumed that there are no resonance absorbers in the reflector.

**Solving the two-group equations.** To find the fast and slow fluxes and the condition for criticality of the reactor, it is necessary to solve the two-group equations for the core and the reflector. Beginning with the core, it will be noted that Eqs. (10-29) and (10-30) are *coupled* second-order differential equations, that is,  $\phi_2$  appears in the equation for  $\phi_1$  and, conversely,  $\phi_1$  appears in the equation for  $\phi_2$ . These equations can be *decoupled* by first solving Eq. (10-29) for  $\phi_{2c}$ :

$$\phi_{2c} = \frac{p_c}{k_\infty\Sigma_{2c}} (-D_{1c}\nabla^2\phi_{1c} + \Sigma_{1c}\phi_{1c}).$$

By substitution of this expression into Eq. (10-30), a fourth-order equation is obtained for  $\phi_{1c}$  alone, namely,

$$\tau_c L_c^2 \nabla^2 \nabla^2 \phi_{1c} - (\tau_c + L_c^2) \nabla^2 \phi_{1c} - (k_\infty - 1) \phi_{1c} = 0, \quad (10-33)$$

where

$$\tau_c = D_{1c}/\Sigma_{1c} \quad \text{and} \quad L_c^2 = D_{2c}/\Sigma_{2c}.$$

A fourth-order differential equation with constant coefficients such as Eq. (10-33) can be solved by factoring the equation. Thus Eq. (10-33) is written as

$$(\nabla^2 + \mu^2)(\nabla^2 - \lambda^2)\phi_{1c} = 0, \quad (10-34)$$

where  $\mu^2$  and  $\lambda^2$  are constants to be determined.\* The reason for the choice of signs in Eq. (10-34) will be clear presently. Upon expanding Eq. (10-34) and

---

\* Equation (10-34) cannot be factored further since  $\nabla^2$  is not the square of an operator; it is not  $(\text{grad})^2$  but rather  $\text{div grad}$ .

comparing the result with Eq. (10-33), it is found that  $\mu^2$  and  $\lambda^2$  must satisfy the relations

$$\mu^2 \lambda^2 = \frac{k_\infty - 1}{\tau_c L_c^2} \quad (10-35)$$

and

$$\lambda^2 - \mu^2 = \frac{1}{\tau_c} + \frac{1}{L_c^2}. \quad (10-36)$$

Next, solving Eq. (10-36) for  $\lambda^2$  and inserting this into Eq. (10-35) yields a quadratic equation for  $\mu^2$ . In a similar way, Eq. (10-36) can be solved for  $\mu^2$ , and substituting this into Eq. (10-35) yields a quadratic equation for  $\lambda^2$ . This pair of quadratic equations has only *two* different solutions, namely,

$$\mu^2 = \frac{1}{2\tau_c L_c^2} \left[ -(\tau_c + L_c^2) + \sqrt{(\tau_c + L_c^2)^2 + 4(k_\infty - 1)\tau_c L_c^2} \right] \quad (10-37)$$

and

$$\lambda^2 = \frac{1}{2\tau_c L_c^2} \left[ (\tau_c + L_c^2) + \sqrt{(\tau_c + L_c^2)^2 + 4(k_\infty - 1)\tau_c L_c^2} \right]. \quad (10-38)$$

Since  $k_\infty$  must be greater than unity for a critical reactor, both  $\mu^2$  and  $\lambda^2$  are positive and  $\mu$  and  $\lambda$  are therefore real. It was the desire to have the constants  $\mu$  and  $\lambda$  real that dictated the choice of signs in Eq. (10-34). It may be mentioned at this point that the computation of  $\mu$  from Eq. (10-37) is sometimes complicated by the fact that  $\mu^2$  is equal to the difference of two very nearly equal numbers. In this case it is expedient to first compute  $\lambda^2$  from Eq. (10-38) and then compute  $\mu^2$  from Eq. (10-35).

Equation (10-34) is equivalent to the two equations

$$(\nabla^2 + \mu^2)X = 0 \quad (10-39)$$

and

$$(\nabla^2 - \lambda^2)Y = 0, \quad (10-40)$$

and the general solution for  $\phi_{1c}$  is then the sum of the solutions for  $X$  and  $Y$ . Since Eqs. (10-39) and (10-40) are both second order, the solutions  $X$  and  $Y$  each consist of two independent functions. However, because of symmetry or other requirements, only one solution from each of the equations can ordinarily be used, and the general solution for  $\phi_{1c}$  is simply

$$\phi_{1c} = AX + CY, \quad (10-41)$$

where only the two constants  $A$  and  $C$  must be determined. For example, consider the uniform infinite slab reactor of thickness  $a$  surrounded by a reflector of thickness  $b$  which was treated by one-group theory in Section 10-1. Equation (10-39) then becomes

$$\left( \frac{d^2}{dx^2} + \mu^2 \right) X = 0,$$

**Table 10-2**  
**Two-Group Core Functions for Various Geometries**

Geometry	X	Y
Infinite slab	$\cos \mu x$	$\cosh \lambda x$
Infinite cylinder	$J_0(\mu r)$	$I_0(\lambda r)$
Sphere	$\frac{\sin \mu r}{r}$	$\frac{\sinh \lambda r}{r}$

which has as solutions  $\cos \mu x$  and  $\sin \mu x$ . In view of the symmetry of the reactor, the sine function clearly cannot be used. Similarly, Eq. (10-40) has the solutions  $\cosh \lambda x$  and  $\sinh \lambda x$ . Here the sinh function is odd and cannot be used. The fast flux in the core is therefore given by the expression

$$\phi_{1c} = A \cos \mu x + C \cosh \lambda x. \quad (10-42)$$

In the case of the infinite cylindrical reactor, Eq. (10-39) and Eq. (10-40) are, respectively,

$$\frac{1}{r} \frac{d}{dr} r \frac{dX}{dr} + \mu^2 X = 0 \quad (10-43)$$

and

$$\frac{1}{r} \frac{d}{dr} r \frac{dY}{dr} - \lambda^2 Y = 0. \quad (10-44)$$

The two solutions to Eq. (10-43) are  $J_0(\mu r)$  and  $J_1(\mu r)$ , while the solutions to Eq. (10-44) are  $I_0(\lambda r)$  and  $I_1(\lambda r)$ . However, both the functions  $J_0(\mu r)$  and  $J_1(\mu r)$  are singular at  $r = 0$  and cannot be used. For this problem the fast flux in the core is therefore

$$\phi_{1c} = AJ_0(\mu r) + CI_0(\lambda r).$$

Appropriate solutions to Eqs. (10-39) and (10-40) are summarized in Table 10-2 for the three most widely encountered reactor geometries.

With the fast flux in the core having been determined, the slow flux can now be found by assuming a solution of the form

$$\phi_{2c} = A'X + C'Y. \quad (10-45)$$

When this solution and Eq. (10-41) are substituted into Eq. (10-30), the following expression is obtained:

$$-(D_{2c}\mu^2 + \Sigma_{2c})A'X + p_c\Sigma_{1c}AX + (D_{2c}\lambda^2 - \Sigma_{2c})C'Y + p_c\Sigma_{1c}CY = 0, \quad (10-46)$$

where it has been noted that  $X$  and  $Y$  satisfy Eq. (10-39) and Eq. (10-40), respectively. Since  $X$  and  $Y$  are independent functions, Eq. (10-46) will not be satisfied unless the constants multiplying  $X$  and  $Y$  are identically zero. This leads

to the following relations between  $A$  and  $A'$  and  $C$  and  $C'$ :

$$\frac{A'}{A} = \frac{p_c \Sigma_{1c}/\Sigma_{2c}}{1 + \mu^2 L_c^2}, \quad \frac{C'}{C} = \frac{p_c \Sigma_{1c}/\Sigma_{2c}}{1 - \lambda^2 L_c^2}. \quad (10-47)$$

The slow flux can now be written as

$$\phi_{2c} = AS_1X + CS_2Y, \quad (10-48)$$

where  $S_1$  and  $S_2$  are constants defined by

$$S_1 = \frac{p_c \Sigma_{1c}/\Sigma_{2c}}{1 + \mu^2 L_c^2}, \quad S_2 = \frac{p_c \Sigma_{1c}/\Sigma_{2c}}{1 - \lambda^2 L_c^2}. \quad (10-49)$$

The quantities  $S_1$  and  $S_2$  are frequently called the *coupling coefficients* for the fast and slow fluxes.\*

Turning now to the reflector equations, Eqs. (10-31) and (10-32) may be written respectively as

$$\nabla^2 \phi_{1r} - \kappa_{1r}^2 \phi_{1r} = 0 \quad (10-50)$$

and

$$\nabla^2 \phi_{2r} - \kappa_{2r}^2 \phi_{2r} + \frac{\Sigma_{1r}}{D_{2r}} \phi_{1r} = 0, \quad (10-51)$$

where

$$\kappa_{1r}^2 = \frac{1}{\tau_r}, \quad \kappa_{2r}^2 = \frac{1}{L_r^2}. \quad (10-52)$$

The solution to Eq. (10-50) which properly vanishes at the extrapolated surface of the reflector can always be expressed in terms of only one function and one unknown constant. For example, it may readily be verified that for a slab reactor of core width  $a$  and reflector thickness  $b$ ,  $\phi_{1r}$  is

$$\phi_{1r} = F \sinh \kappa_{1r} \left( \frac{a}{2} + b - |x| \right), \quad (10-53)$$

where  $F$  is a constant. This function satisfies Eq. (10-50) and is zero at

$$|x| = \frac{a}{2} + b.$$

In general, the solution to Eq. (10-50) will be indicated by

$$\phi_{1r} = F Z_1. \quad (10-54)$$

---

\* Many workers prefer to have the coupling coefficients appear in the fast flux rather than the slow flux, and so write

$$\phi_{1c} = AS'_1X + CS'_2Y, \quad \phi_{2c} = AX + CY.$$

The coefficients  $S'_1$  and  $S'_2$  are then the reciprocals of those given in Eqs. (10-49).

**Table 10-3**  
**Two-Group Reflector Functions for Various Geometries**

Geometry	$Z$ (reflector thickness $b$ )	$Z$ (reflector thickness infinite)
Infinite slab	$\sinh \kappa \left( \frac{a}{2} + b -  x  \right)$	$e^{-\kappa x }$
Infinite cylinder	$I_0(\kappa r)K_0[\kappa(R + b)] - I_0[\kappa(R + b)]K_0(\kappa r)$	$K_0(\kappa r)$
Sphere	$\frac{\sinh \kappa(R + b - r)}{r}$	$\frac{e^{-\kappa r}}{r}$

Finally, the slow flux in the reflector can be found by assuming a solution to Eq. (10-51) of the form

$$\phi_{2r} = S_3 \phi_{1r} + GZ_2. \quad (10-55)$$

Here,  $S_3$  is another coupling constant,  $G$  is a constant, and  $Z_2$  is a solution to the equation

$$\nabla^2 Z_2 - \kappa_{2r}^2 Z_2 = 0, \quad (10-56)$$

which also is zero at the extrapolated surface of the reflector. By substituting Eq. (10-55) into Eq. (10-51) it is easy to show that the differential equation is indeed satisfied, provided that  $S_3$  has the value

$$S_3 = \frac{\Sigma_{1r}/D_{2r}}{\kappa_{2r}^2 - \kappa_{1r}^2} = \frac{D_{1r}/\Sigma_{2r}}{\tau_r - L_r^2}. \quad (10-57)$$

For the reflected slab reactor the slow flux in the reflector is therefore

$$\phi_{2r} = FS_3 \sinh \kappa_{1r} \left( \frac{a}{2} + b - |x| \right) + G \sinh \kappa_{2r} \left( \frac{a}{2} + b - |x| \right). \quad (10-58)$$

Table 10-3 lists the  $Z$ -functions for other geometries.

**The critical determinant.** Both the slow and fast fluxes and the slow and fast currents must be continuous at the core-reflector interface. Specifically, the following conditions must be satisfied:

$$\phi_{1c} = \phi_{1r}, \quad (10-59)$$

$$D_{1c}\phi'_{1c} = D_{1r}\phi'_{1r}, \quad (10-60)$$

$$\phi_{2c} = \phi_{2r}, \quad (10-61)$$

$$D_{2c}\phi'_{2c} = D_{2r}\phi'_{2r}. \quad (10-62)$$

In these equations all of the functions and their derivatives (indicated by primes) are evaluated at the core-reflector interface.

Inserting the solutions for the fluxes, namely, Eqs. (10-41), (10-48), (10-54), and (10-55), into Eqs. (10-59) through (10-62) gives the following set of equations:

$$AX + CY = FZ_1, \quad (10-63)$$

$$AD_{1c}X' + CD_{1c}Y' = FD_{1r}Z'_1, \quad (10-64)$$

$$AS_1X + CS_2Y = FS_3Z_1 + GZ_2, \quad (10-65)$$

$$AD_{2c}S_1X' + CD_{2c}S_2Y' = FD_{2r}S_3Z'_1 + GD_{2r}Z'_2. \quad (10-66)$$

All of the quantities in these equations are known in terms of reactor parameters except the constants  $A$ ,  $C$ ,  $F$ , and  $G$ . Therefore Eqs. (10-63) through (10-66) can be viewed as a set of four linear algebraic equations with these constants as unknowns. Written in a more standard way, these equations are

$$AX + CY - FZ_1 = 0, \quad (10-67)$$

$$AD_{1c}X' + CD_{1c}Y' - FD_{1r}Z'_1 = 0, \quad (10-68)$$

$$AS_1X + CS_2Y - FS_3Z_1 - GZ_2 = 0, \quad (10-69)$$

$$AD_{2c}S_1X' + CD_{2c}S_2Y' - FD_{2r}S_3Z'_1 - GD_{2r}Z'_2 = 0. \quad (10-70)$$

In this form it is recognized that all the equations are *homogeneous*; that is, the right-hand side of each is zero. However, in view of *Cramer's rule* regarding linear, homogeneous algebraic equations,\* Eqs. (10-67) through (10-70) can have no other solutions than  $A = C = F = G = 0$ , unless the determinant of the coefficients multiplying these unknowns is zero. Thus in order that the flux in the reactor be nonzero, it is necessary that

$$\begin{vmatrix} X & Y & -Z_1 & 0 \\ D_{1c}X' & D_{1c}Y' & -D_{1r}Z'_1 & 0 \\ S_1X & S_2Y & -S_3Z_1 & -Z_2 \\ D_{2c}S_1X' & D_{2c}S_2Y' & -D_{2r}S_3Z'_1 & -D_{2r}Z'_2 \end{vmatrix} = 0. \quad (10-71)$$

Equation (10-71) provides a relation, admittedly a somewhat complicated one, which must be satisfied if the reactor is to be critical. For this reason the left-hand side of the equation is known as the two-group *critical determinant*. Criticality can be obtained by adjusting either the physical properties or the size of the reactor in such a way that the critical determinant is precisely zero.

**Calculations of criticality.** Computations using the critical determinant can be simplified somewhat by dividing the first column by  $X$ , and the second by  $Y$ , and so on, and multiplying the third and fourth columns by  $-1$ . Equation

\* See any text on advanced calculus.

**Table 10-4**  
**Functions for Critical Determinant**

Geometry	$X'/X$	$Y'/Y$
Infinite slab of thickness $a$	$-\mu \tan \frac{\mu a}{2}$	$\lambda \tanh \frac{\lambda a}{2}$
Infinite cylinder of radius $R$	$-\mu \frac{J_1(\mu R)}{J_0(\mu R)}$	$\lambda \frac{I_1(\lambda R)}{I_0(\lambda R)}$
Sphere of radius $R$	$-\mu \left( \frac{1}{\mu R} - \cot \mu R \right)$	$\lambda \left( \coth \lambda R - \frac{1}{\lambda R} \right)$

Geometry	$Z'/Z$ (reflector thickness $b$ )	$Z'/Z$ (infinite reflector)
Infinite slab of thickness $a$	$-\kappa \coth \kappa b$	$-\kappa$
Infinite cylinder of radius $R$	$\kappa \frac{I_1(\kappa R)K_0[\kappa(R+b)] + I_0[\kappa(R+b)]K_1(\kappa R)}{I_0(\kappa R)K_0[\kappa(R+b)] - I_0[\kappa(R+b)]K_0(\kappa R)}$	$-\kappa \frac{K_1(\kappa R)}{K_0(\kappa R)}$
Sphere of radius $R$	$-\kappa \left( \frac{1}{\kappa R} + \coth \kappa b \right)$	$-\kappa \left( \frac{1}{\kappa R} + 1 \right)$

(10-71) then becomes

$$\begin{vmatrix} 1 & 1 & 1 & 0 \\ D_{1c} \frac{X'}{X} & D_{1c} \frac{Y'}{Y} & D_{1r} \frac{Z'_1}{Z_1} & 0 \\ S_1 & S_2 & S_3 & 1 \\ D_{2c} S_1 \frac{X'}{X} & D_{2c} S_2 \frac{Y'}{Y} & D_{2r} S_3 \frac{Z'_1}{Z_1} & D_{2r} \frac{Z'_2}{Z_2} \end{vmatrix} = 0. \quad (10-72)$$

The determinant can now be expanded by minors and with a little algebra the following equation is obtained:

$$\begin{aligned} \frac{X'}{X} = & \left[ D_{1c} D_{2r} (S_3 - S_1) \frac{Y'}{Y} \frac{Z'_2}{Z_2} + (D_{1r} D_{2c} S_2 - D_{1c} D_{2r} S_3) \frac{Y'}{Y} \frac{Z'_1}{Z_1} \right. \\ & + D_{1r} D_{2r} (S_1 - S_2) \frac{Z'_1}{Z_1} \frac{Z'_2}{Z_2} \Big] \div \left[ D_{1c} D_{2c} (S_2 - S_1) \frac{Y'}{Y} \right. \\ & \left. + (D_{1r} D_{2c} S_1 - D_{1c} D_{2r} S_3) \frac{Z'_1}{Z_1} + D_{1c} D_{2r} (S_3 - S_2) \frac{Z'_2}{Z_2} \right]. \quad (10-73) \end{aligned}$$

For additional ease in computation it is usually a good idea to multiply both

sides of Eq. (10-73) by the core radius for a cylindrical or spherical reactor, or by the half-thickness for a slab reactor. Both sides of the equation are then dimensionless (see the example later in this chapter).

The reason for writing Eq. (10-73) in the form above is that, in the usual case, the left-hand side of the equation is a rather rapidly varying and discontinuous function of the core composition and size, while the right-hand side is a more slowly varying function of these parameters. The composition or size required for criticality can then easily be obtained by plotting the two sides of the equation and finding the intersection of these curves. This procedure will be illustrated in an example later in this section. The functions

$$X'/X, \quad Y'/Y, \quad \text{and} \quad Z'/Z$$

are listed in Table 10-4.

**Determining the fluxes.** To find the fast and slow fluxes it is necessary to determine the constants  $A$ ,  $C$ ,  $F$ , and  $G$ . It is not possible, however, to find the absolute values of all of these constants, since it can be shown that if the determinant of the coefficients in Eqs. (10-67) through (10-70) is zero, as it must be for criticality, then these four equations are no longer independent. Therefore it is possible to determine only three of the constants in terms of  $A$ , for instance, but  $A$  itself will remain unknown. Thus the absolute value of the flux cannot be found from these equations. This is the same situation which was met previously in connection with the bare reactor in Chapter 9, and the one-group model of reflected reactors in Section 10-1. While it is possible to specify the *shape* of the flux in a critical reactor, its magnitude depends upon the operating power of the system and is not determined by the group equations.

To compute  $C$ ,  $F$ , and  $G$  in terms of  $A$ , Eqs. (10-67) through (10-69) are written as inhomogeneous equations, viz.,

$$CY - FZ_1 = -AX, \quad (10-74)$$

$$CD_{1c}Y' - FD_{1r}Z'_1 = -AD_{1c}X', \quad (10-75)$$

$$CS_2Y - FS_3Z_1 - GZ_2 = -AS_1X. \quad (10-76)$$

Then using Cramer's rule, it is found that

$$C = \frac{AX}{\beta Y} \left( D_{1c} \frac{X'}{X} - D_{1r} \frac{Z'_1}{Z_1} \right), \quad (10-77)$$

$$F = \frac{AX}{\beta Z_1} \left( D_{1c} \frac{X'}{X} - D_{1r} \frac{Y'}{Y} \right), \quad (10-78)$$

$$G = \frac{AX}{\beta Z_2} \left[ D_{1c}(S_2 - S_3) \frac{X'}{X} + D_{1c}(S_3 - S_1) \frac{Y'}{Y} + D_{1r}(S_1 - S_2) \frac{Z'_1}{Z_1} \right], \quad (10-79)$$

where  $\beta$  is a constant defined as

$$\beta = D_{1r} \frac{Z'_1}{Z_1} - D_{1c} \frac{Y'}{Y}. \quad (10-80)$$

All of the functions appearing in these equations are evaluated, of course, at the core-reflector interface.

To find the constant  $A$  it is necessary to compute the reactor power. Since only thermal fissions have been assumed to occur in the system and since there are no fissions in the reflector, the power is determined only by the function  $\phi_{2c}$ . Thus as in Eq. (10-14),

$$P = \gamma \Sigma_{2fc} \int \phi_{2c}(r) dV, \quad (10-81)$$

where  $\Sigma_{2fc}$  is the thermal fission cross section and the integration is carried out over the reactor core. With the infinite slab reactor, for instance,

$$\phi_{2c} = A \left[ \cos \mu x + \left( \frac{C}{A} \right) \cosh \lambda x \right], \quad (10-82)$$

where  $(C/A)$  is given by the Eq. (10-77), and so Eq. (10-81) gives

$$A = \frac{P}{2\gamma \Sigma_{2fc} \left[ \frac{1}{\mu} \sin \frac{\mu a}{2} + \frac{1}{\lambda} \left( \frac{C}{A} \right) \sinh \frac{\lambda a}{2} \right]}. \quad (10-83)$$

**Example.** As an illustration of the application of two-group theory, consider the problem of determining the critical radius of a spherical reactor at room temperature which is fueled with  $U^{235}$  and moderated by ordinary water. The reactor will be assumed to have an infinite water reflector. (An infinite reflector is one whose thickness is much larger than both the slowing-down and diffusion lengths in the reflector. Virtually all reactors have reflectors of this type.) The ratio of atoms of  $U^{235}$  to molecules of water in the core will be taken to be

$$\frac{N_{25}}{N_w} = \frac{1}{500}.$$

This is a somewhat higher fuel density than the 1/1120 ratio required for the criticality of an infinite system of this type. The critical core radius, critical mass, and expressions for the fast and slow fluxes must be found.

Since the density of fuel in the core is so small, the  $U^{235}$  can be viewed as merely an impurity in the water. The age of neutrons in the core is therefore the age in pure water, that is, about  $27 \text{ cm}^2$ . Furthermore, there is no fast fission and no resonance absorption. The constants and functions required for the computation are then as follows. (All numbers except  $k_\infty$  have been rounded off to three significant digits. However, during the course of a two-group calculation, it is wise to retain several additional digits and round off the numbers only at the end of the computation.)

*Core*

$$\text{Molecular density H}_2\text{O } (\times 10^{-24}): \quad N_{\text{W}} = \frac{1 \times 0.6023}{18.02} = 0.0335$$

$$\text{Atom density U}^{235} (\times 10^{-24}): \quad N_{25} = \frac{1}{500} \times 0.0335 = 6.70 \times 10^{-5}$$

$$\sigma_{a\text{W}} = 2\sigma_{a\text{H}} = 2 \times 0.332 = 0.664 \text{ barns} \quad \tau_c = 27 \text{ cm}^2$$

$$\sigma_{a25} = 678 \text{ barns} \quad \Sigma_{1c} = 0.0419 \text{ cm}^{-1}$$

$$D_{1c} = 1.13 \text{ cm} \quad D_{2c} = 0.16 \text{ cm}$$

$$\Sigma_{2c} = 0.886(N_{25}\sigma_{a25} + N_{\text{W}}\sigma_{a\text{W}}) = 0.060 \text{ cm}^{-1}$$

$$L_c^2 = D_{2\text{W}}/\Sigma_{2c} = 2.67 \text{ cm}^2 \quad \mu = 0.113$$

$$\eta_T = 2.07 \quad \lambda = 0.651$$

$$f = N_{25}\sigma_{a25}/(N_{25}\sigma_{a25} + N_{\text{W}}\sigma_{a\text{W}}) = 0.671 \quad S_1 = 0.676$$

$$k_\infty = \eta_T f = 1.390 \quad S_2 = -5.26$$

$$X = \frac{\sin \mu r}{r}$$

$$\frac{X'}{X} \text{ (evaluated at core radius)} = \mu \left( \cot \mu R - \frac{1}{\mu R} \right)$$

$$Y = \frac{\sinh \lambda r}{r}$$

$$\frac{Y'}{Y} \text{ (evaluated at core radius)} = \lambda \left( \coth \lambda R - \frac{1}{\lambda R} \right)$$

*Reflector*

$$D_{1r} = 1.13 \text{ cm} \quad L_r^2 = D_{2r}/\Sigma_{2r} = 8.12 \text{ cm}^2$$

$$\tau_r = 27 \text{ cm}^2 \quad \kappa_{1r} = 1/\sqrt{\tau_r} = 0.192 \text{ cm}^{-1}$$

$$\Sigma_{1r} = 0.0419 \text{ cm}^{-1} \quad \kappa_{2r} = 1/L_r = 0.351 \text{ cm}^{-1}$$

$$D_{2r} = 0.16 \text{ cm} \quad S_3 = 3.04$$

$$\Sigma_{2r} = 0.886N_{\text{W}}\sigma_{a\text{W}} = 0.0197 \text{ cm}^{-1}$$

$$Z = \frac{e^{-\kappa r}}{r}$$

$$\frac{Z'}{Z} \text{ (evaluated at core radius)} = \kappa \left( 1 + \frac{1}{\kappa R} \right)$$

Before using the critical equation, Eq. (10-73), it is convenient to multiply both sides by  $R$ . The two sides of the equation are now (the  $D$ 's cancel in RHS):

$$\text{LHS} = -\mu R \left( \cot \mu R - \frac{1}{\mu R} \right),$$

$$\text{RHS} = R \times \frac{2.37 \frac{Y'}{Y} \frac{Z'_2}{Z_2} - 8.30 \frac{Y'}{Y} \frac{Z'_1}{Z_1} + 5.93 \frac{Z'_1}{Z_1} \frac{Z'_2}{Z_2}}{5.93 \frac{Y'}{Y} + 2.37 \frac{Z'_1}{Z_1} - 8.30 \frac{Z'_2}{Z_2}}$$

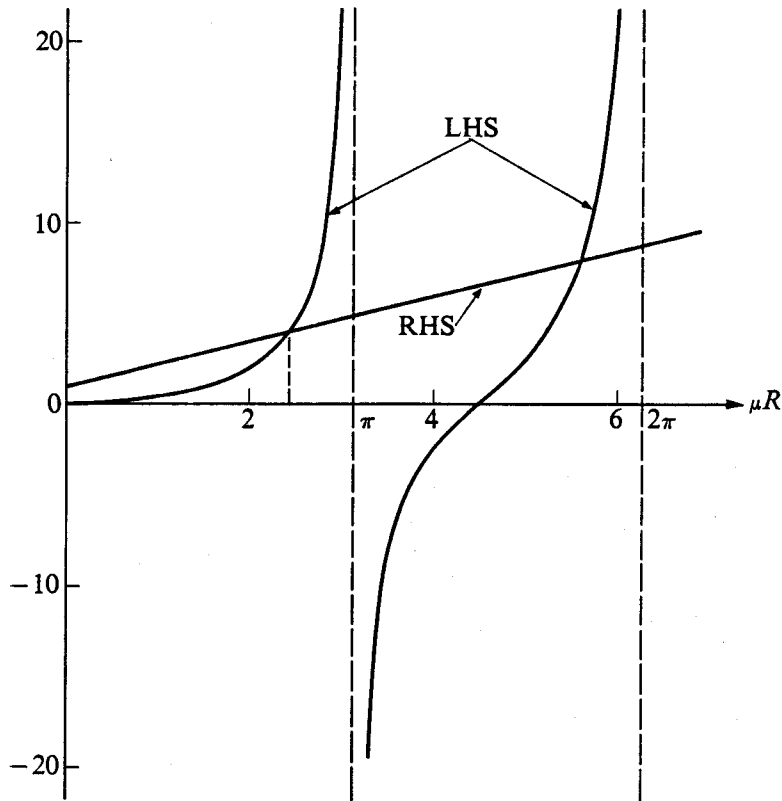


**Fig. 10-3.** The left-hand side (LHS) and right-hand side (RHS) of the two-group critical equation.

The functions LHS and RHS are plotted in Fig. 10-3 as a function of  $\mu R$ . It will be observed that RHS is a much smoother function than LHS, and is, in fact, linear in  $\mu R$  over the range of values of  $\mu R$  shown in the figure. Unfortunately, this linearity is not a general property of the right-hand side of the critical equation.

The first positive intersection of the curves in Fig. 10-3 occurs at  $\mu R = 2.47$ , which gives a critical radius  $R = 2.47/\mu = 21.9$  cm. The other intersections at larger values of  $\mu R$  correspond to harmonics that are not present if the reactor is critical and operating in the steady state. The similarity between Figs. 10-3 and 10-2 should be noted.

The critical mass  $m_{25}$  of  $\text{U}^{235}$  is

$$m_{25} = m_w \left( \frac{M_{25}}{M_w} \right) \left( \frac{N_{25}}{N_w} \right),$$

where  $m_w$  is the mass of water in the core,  $M_{25}$  and  $M_w$  are the molecular weights of  $\text{U}^{235}$  and water, respectively, and

$$\frac{N_{25}}{N_w} = \frac{1}{500}.$$

With  $R = 21.9$  cm,

$$m_w = \frac{4}{3}\pi R^3 = 41.6 \text{ kg} \quad \text{and} \quad m_{25} = 1.15 \text{ kg.}$$

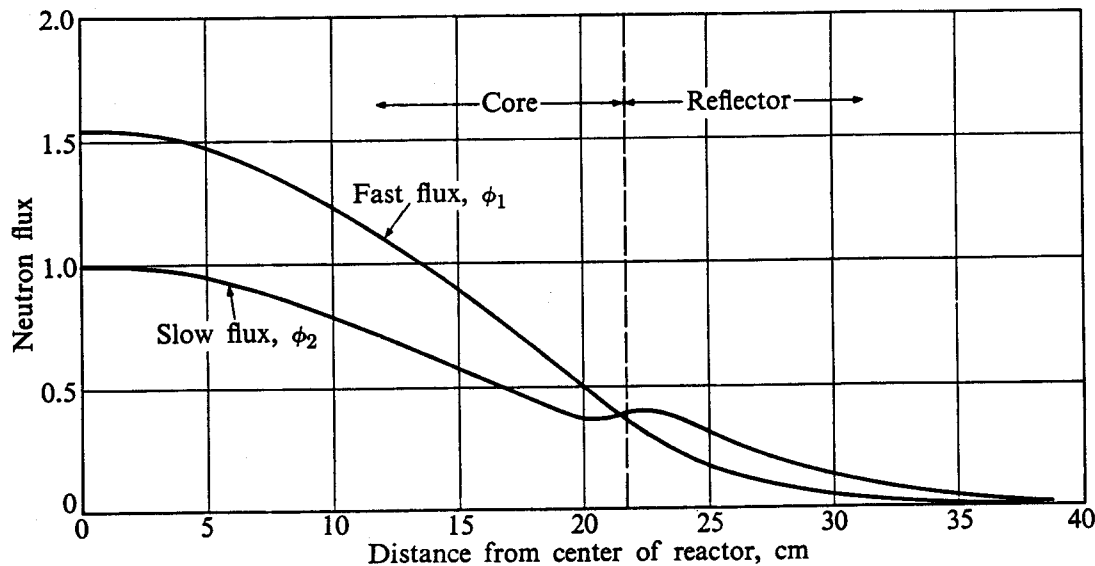


**Fig. 10-4.** The two-group fluxes for a water-moderated, water-reflected,  $\text{U}^{235}$ -fueled spherical reactor.

The constants in the expressions for the core and reflector fluxes Eqs. (10-41), (10-48), (10-54), and (10-55) are found from Eqs. (10-77) through (10-80). These fluxes are

$$\phi_{1c} = A \left( \frac{\sin 0.113r}{r} - 4.67 \times 10^{-8} \frac{\sinh 0.651r}{r} \right),$$

$$\phi_{2c} = 0.676A \left( \frac{\sin 0.113r}{r} + 3.64 \times 10^{-7} \frac{\sinh 0.651r}{r} \right),$$

$$\phi_{1r} = 39.6A \frac{e^{-0.192r}}{r},$$

$$\phi_{2r} = 120A \left[ \frac{e^{-0.192r}}{r} - 21.0 \frac{e^{-0.351r}}{r} \right].$$

These fluxes, normalized to  $\phi_{2c} = 1$  at the origin, are plotted in Fig. 10-4. As shown in the figure, the fast flux is larger than the thermal flux over the bulk of the core. This is due to the fact that the core material of this reactor is more effective in absorbing thermal neutrons than in moderating neutrons out of the fast group. To show this analytically, it is first noted that over most of the core the second terms in the expressions for the core fluxes are small compared with the first terms, so that the fluxes can be written approximately as  $\phi_{1c} \approx AX$  and  $\phi_{2c} \approx AS_1X$ . The ratio of fast flux to slow flux is therefore

$$\frac{\phi_{1c}}{\phi_{2c}} \approx \frac{1}{S_1} = \frac{1 + \mu^2 L_c^2}{p_c \Sigma_{1c}/\Sigma_{2c}} \approx \frac{\Sigma_{2c}}{\Sigma_{1c}}.$$

Inserting numerical values gives

$$\frac{\phi_{1c}}{\phi_{2c}} \approx \frac{0.06}{0.04} = 1.5,$$

which is about the ratio of the fluxes indicated in the figure.

It will also be observed in Fig. 10-4 that there is a small peak in the thermal flux in the reflector. This is one of the most striking results of two-group theory; no such phenomenon is predicted from one-group theory. The peaking of the thermal flux arises from the slowing down in the reflector of fast neutrons which escape from the core. Since the absorption cross section of the reflector is small, the thermalized neutrons accumulate in this region until they eventually diffuse back into the core, escape from the outer surface of the reflector, or are captured. Incidentally, the flux peak in the reflector is much more pronounced in many reactors than that indicated in Fig. 10-4.

**Partially reflected reactors.** The preceding calculations have been limited to reactors in which the flux is a function of only one spatial variable. The two-group method can be extended in a straightforward way to a few more complicated systems. These include the parallelepiped reactor reflected on two opposite faces, and the finite cylindrical reactor which is either reflected on the ends and bare on the side or reflected on the side and bare on the ends. Reactors of this type are called *partially reflected* and are shown in Fig. 10-5. Unfortunately, the mathematical problems associated with the *fully reflected* parallelepiped or finite cylinder (the two most commonly constructed reactors) are very difficult, and these reactors must be treated by special methods discussed in Section 10-6.

To illustrate the manner in which criticality calculations are carried out for partially reflected systems, consider a finite cylindrical reactor having an infinitely thick reflector on the side but bare on top and bottom (this reactor is like the one shown in Fig. 10-5(c), except that the reflector is infinite). The radius of the core is  $R$  and the extrapolated height is  $H$ . The center of coordinates will be taken to be at the center of the reactor. The two-group equations in the core are then the same as they were earlier [cf. Eqs. (10-29) and (10-30)], and the procedure for

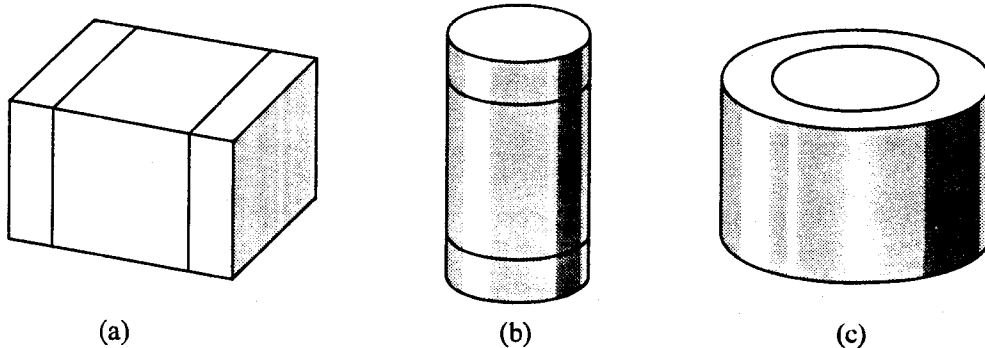


Fig. 10-5. Partially reflected reactors. The reflectors in each case may be infinite.

decoupling the equations is also unchanged. The fast and slow fluxes in the core can therefore be written as

$$\phi_{1c} = AX + CY, \quad (10-84)$$

$$\phi_{2c} = AS_1X + CS_2Y, \quad (10-85)$$

where  $S_1$  and  $S_2$  are given in Eqs. (10-49). The functions  $X$  and  $Y$  are still determined by Eqs. (10-39) and (10-40), but now both  $X$  and  $Y$  are functions of the two variables  $r$  and  $z$ . By inserting the Laplacian in cylindrical coordinates, Eqs. (10-39) and (10-40) become

$$\frac{1}{r} \frac{\partial}{\partial r} r \frac{\partial X}{\partial r} + \frac{\partial^2 X}{\partial z^2} + \mu^2 X = 0 \quad (10-86)$$

and

$$\frac{1}{r} \frac{\partial}{\partial r} r \frac{\partial Y}{\partial r} + \frac{\partial^2 Y}{\partial z^2} - \lambda^2 Y = 0. \quad (10-87)$$

The parameters  $\mu$  and  $\lambda$  are again found from Eqs. (10-37) and (10-38).

Equations (10-86) and (10-87) can be solved by the method of separation of variables which was introduced in Chapter 9. Thus letting  $X(r, z) = f(r)g(z)$  and substituting into Eq. (10-86) yields

$$\frac{d^2 g}{dz^2} + \alpha_1^2 g = 0 \quad (10-88)$$

and

$$\frac{1}{r} \frac{d}{dr} r \frac{df}{dr} + \alpha_2^2 f = 0, \quad (10-89)$$

where  $\alpha_1$  and  $\alpha_2$  are the separation constants and are related by

$$\alpha_1^2 + \alpha_2^2 = \mu^2. \quad (10-90)$$

The solution to Eq. (10-88) which is symmetric about the midplane of the cylinder is

$$g = \cos \alpha_1 z, \quad (10-91)$$

and, since both  $\phi_{1c}$  and  $\phi_{2c}$  must vanish on the extrapolated bare ends of the reactor, it is evident that

$$\alpha_1 = \frac{\pi}{H}. \quad (10-92)$$

The nonsingular solution to Eq. (10-89) is

$$f = J_0(\alpha_2 r), \quad (10-93)$$

and therefore

$$X = J_0(\alpha_2 r) \cos \left( \frac{\pi z}{H} \right). \quad (10-94)$$

By a similar argument, it is easy to show that the second flux function  $Y$  is given by

$$Y = I_0(\alpha_3 r) \cos\left(\frac{\pi z}{H}\right), \quad (10-95)$$

where

$$\alpha_3^2 = \lambda^2 + \left(\frac{\pi}{H}\right)^2. \quad (10-96)$$

Consider next the fluxes in the reflector; Eqs. (10-31) and (10-32) still hold and the solutions are again of the form given in Eqs. (10-54) and (10-55), that is

$$\phi_{1r} = FZ_1 \quad (10-97)$$

and

$$\phi_{2r} = S_3\phi_{1r} + GZ_2, \quad (10-98)$$

where  $S_3$  is given by Eq. (10-57), and  $F$  and  $G$  are constants. By following essentially the same procedure as with the core, the functions  $Z_1$  and  $Z_2$  are found to be

$$Z_1 = K_0(\beta_1 r) \cos\left(\frac{\pi z}{H}\right) \quad (10-99)$$

and

$$Z_2 = K_0(\beta_2 r) \cos\left(\frac{\pi z}{H}\right), \quad (10-100)$$

where  $\beta_1$  and  $\beta_2$  are defined by

$$\beta_1^2 = \kappa_{1r}^2 + \left(\frac{\pi}{H}\right)^2, \quad (10-101)$$

$$\beta_2^2 = \kappa_{2r}^2 + \left(\frac{\pi}{H}\right)^2. \quad (10-102)$$

The parameters  $\kappa_{1r}$  and  $\kappa_{2r}$  are given in Eqs. (10-52).

The boundary conditions at the core-reflector interface, namely, the continuity of fast and slow fluxes and currents, lead again to a set of four homogeneous algebraic equations of the same form as Eqs. (10-67) through (10-70), in which all functions of  $r$  are evaluated at  $r = R$ . However, the function  $\cos(\pi z/H)$  appears in every term and therefore cancels from all the equations. Thus a critical equation is obtained which is identical with Eq. (10-72) and its equivalent Eq. (10-73), except that  $\mu$ ,  $\lambda$ ,  $\kappa_1$ , and  $\kappa_2$  are replaced by  $\alpha_2$ ,  $\alpha_3$ ,  $\beta_1$ , and  $\beta_2$ , respectively. From this equation, the critical composition or size of the reactor and the fluxes can be found as in the example given earlier.

This procedure for handling the partially reflected cylinder can be extended without difficulty to other partially reflected reactors. These are discussed in the problems at the end of the chapter.

**Applications of two-group method.** It must be emphasized that the two-group method is not an exact technique for making reactor criticality calculations. Nevertheless, it does provide a relatively simple way of obtaining

reasonable estimates of critical mass or size, flux distributions, and so on. Two-group calculations are generally far more realistic than one-group calculations, particularly for thermal reactors. By contrast, the same degree of improvement is not obtained by going to two groups in the case of fast reactors, and first-order calculations of these systems can as well be made with one group as with two groups. Although two-group computations tend to be time consuming when done by hand, they can be carried out very rapidly on a computer. For this reason, the two-group method has been widely used for parametric studies of the gross characteristics of reactor systems.

It should be noted that the formulas developed in this section apply only to uniform reactors. As will be shown in the next section, however, even a reactor that is constructed in a uniform way becomes nonuniform soon after it is put into operation. It must be concluded, therefore, that the analytical formulation of two-group theory given in the present section is limited to newly assembled reactors, that is, to *clean* reactors.

It may also be mentioned at this point that reactors are never fueled with the minimum amount of fissile material required for criticality. This is for the obvious reason that once an atom of fuel has been consumed, such a system would no longer have the required critical mass, and it would fall subcritical. It is necessary, therefore, at the time a reactor is constructed to include more than the minimum fuel necessary for it to become critical. This excess fuel is compensated for by inserting nonfissionable neutron absorbers (control rods) into the reactor. As the fuel is consumed, the system is kept critical by removing the rods. These matters will be considered in detail in Chapters 13 and 14.

### 10-3 Two-Group Calculations of Nonuniform Reactors

It was possible to obtain analytical solutions to the two-group equations in the preceding section because all the nuclear parameters were assumed to be independent of position in the core and reflector. If, on the contrary, the parameters are not constants, then these solutions are no longer valid. Since reactors having nonuniform properties are frequently met in practice, it is necessary to consider how the criticality and the fluxes of such systems can be determined.

Reactors may be nonuniform for a number of reasons. For instance, they are sometimes deliberately constructed with nonuniform properties in an effort to obtain a more uniform power distribution within the core. Thus it can be shown that a uniform power density, or *flat power* as it is usually called, can be obtained by distributing the fuel, moderator, or absorbing poisons in an appropriate manner throughout the core. Reactors of this type operate more efficiently than ordinary uniform reactors, are more easily cooled, and usually have a longer useful life.

Even if a reactor is initially constructed with a uniform core, however, it will eventually become nonuniform as the result of nonuniform consumption of the fuel and the accompanying nonuniform accumulation of fission products (and

perhaps also the nonuniform conversion of fertile material). This, in turn, is due to the fact that at any point in the reactor the fuel is consumed at a rate of  $\Sigma_{2F}\phi_2$  atoms per  $\text{cm}^3/\text{sec}$ , where  $\Sigma_{2F}$  is the macroscopic absorption cross section of the fuel. Since  $\phi_2$  is higher near the center of the reactor, the fuel is consumed more rapidly in that region.

Although two-group calculations of nonuniform reactors cannot ordinarily be performed analytically, they can easily be carried out numerically. The following iterative scheme is widely used in practice. For simplicity, the discussion will be confined to the infinite slab reactor having a nonuniform core but with a uniform reflector; the method can easily be generalized to reactors of other geometries. Resonance capture and fast fission will also be ignored. Because the diffusion coefficients may be functions of position in a nonuniform reactor the two-group equations must be written in the form given in Eq. (5-43), that is,

$$\frac{d}{dx} \left( D_{1c} \frac{d\phi_{1c}}{dx} \right) - \Sigma_{1c}\phi_{1c} + \eta_T \Sigma_{2F} c \phi_{2c} = 0 \quad (10-103)$$

and

$$\frac{d}{dx} \left( D_{2c} \frac{d\phi_{2c}}{dx} \right) - \Sigma_{2c}\phi_{2c} + \Sigma_{1c}\phi_{1c} = 0. \quad (10-104)$$

In these equations, any or all of the nuclear parameters may be functions of position in the core. Since the reflector is uniform, the usual equations hold, namely,

$$D_{1r} \frac{d^2\phi_{1r}}{dx^2} - \Sigma_{1r}\phi_{1r} = 0 \quad (10-105)$$

and

$$D_{2r} \frac{d^2\phi_{2r}}{dx^2} - \Sigma_{2r}\phi_{2r} + \Sigma_{1r}\phi_{1r} = 0. \quad (10-106)$$

To begin the computations, it is necessary to specify both the size and composition of the reactor. Since these are never known at the start of the problem, educated guesses must be made wherever appropriate. For example, if the composition of the system is given, a guess must be made of its critical size. Contrariwise, if the size of the reactor is known, a guess must be made of the reactor's composition. Naturally, these guesses will not correspond to an exactly critical system, and the assumed reactor is therefore either subcritical or supercritical.

Next, arbitrary values are assigned to *one* of the fluxes throughout the entire reactor. For instance,  $\phi_2$  can be taken to be a constant in the core and zero in the reflector. This assumed function, which will be denoted by  $\phi_2^{(0)}$ , is now introduced into Eq. (10-103), which can be written as

$$\frac{d}{dx} \left( D_{1c} \frac{d\phi_{1c}}{dx} \right) - \Sigma_{1c}\phi_{1c} = -\eta_T \Sigma_{2F} c \phi_2^{(0)}. \quad (10-107)$$

This is a relatively simple inhomogeneous equation for  $\phi_{1c}$ , but since  $D_{1c}$ ,  $\Sigma_{1c}$ , and  $\Sigma_{2c}$  may be functions of position, it must be solved by numerical integration,

preferably on an electronic computer. At the core-reflector interface the solution is continued into the reflector by numerically integrating Eq. (10-105). This can be done in such a way that both the fast flux and fast current are continuous at that boundary. The result of these computations is a first estimate of the fast flux which will be denoted by  $\phi_1^{(1)}$ .

In the next step, the function  $\phi_1^{(1)}$  is inserted into Eqs. (10-104) and (10-106), and these equations are solved numerically, yielding an estimate of the thermal flux  $\phi_2^{(1)}$ . This, in turn, is inserted into Eqs. (10-103) and (10-105), giving another estimate of the fast flux  $\phi_1^{(2)}$ , and so on.

As these computations are repeated, an interesting and important phenomenon is observed. It is found, usually after only a few iterations, that although the *magnitudes* of the various fluxes change with each iteration, the *ratio* of either the fast or slow fluxes in successive iterations, for example,  $\phi_2^{(n+1)}/\phi_2^{(n)}$ , rapidly approaches a *constant, independent of position*. In other words, the spatial dependence of successive flux iterates becomes identical.

The origin of this behavior lies in the fact that each iteration in the calculation is actually equivalent to one cycle of the chain reaction. Thus the flux  $\phi_2^{(0)}$ , assumed at the beginning of the calculation, corresponds to a possible set of initial conditions in the reactor, that is, to the introduction of a specified distribution of thermal neutrons into the reactor at time  $t = 0$ . These thermal neutrons give rise to a fast flux via Eq. (10-103), and so on. Eventually, however, as shown in Chapter 9, the flux in the reactor approaches the fundamental eigenfunction, regardless of the initial state of the system, owing to the fact that the higher harmonics die out. The remaining fundamental then increases or decreases with time or remains constant, depending upon whether the system is supercritical, subcritical, or critical. Hence, the point in the calculation where the ratio  $C_n = \phi_2^{(n+1)}/\phi_2^{(n)}$  becomes independent of position corresponds to a time when the harmonics of the flux have died out in the reactor. Furthermore, the quantity  $C_n$  is clearly a measure of the criticality of the system. If  $C_n$  is greater than unity, for instance, the system is evidently supercritical; if  $C_n$  is less than unity, the system is subcritical.

For the sake of the discussion, suppose that after several iterations  $C_n$  turns out to be greater than unity. Physically this means that the size and composition of the reactor assumed at the beginning of the calculation have led to a supercritical system. If the size of the core is specified in the problem, it is necessary to reduce the fuel concentration. On the other hand, if the composition is specified initially, then the assumed core radius is too large and must be reduced. In either case, the calculations are repeated with new parameters and a new value of  $C_n$  is obtained. This procedure is continued and the resulting values of  $C_n$  are plotted as a function of the reactor size or composition. The critical size or composition then corresponds to the point where  $C_n = 1$ .\*

---

\* The time-consuming process of plotting  $C_n$  can be avoided by having the computer itself adjust the reactor size or composition after each iteration. The output of the calculation is then only the required conditions for criticality and a tabulation of the fluxes.

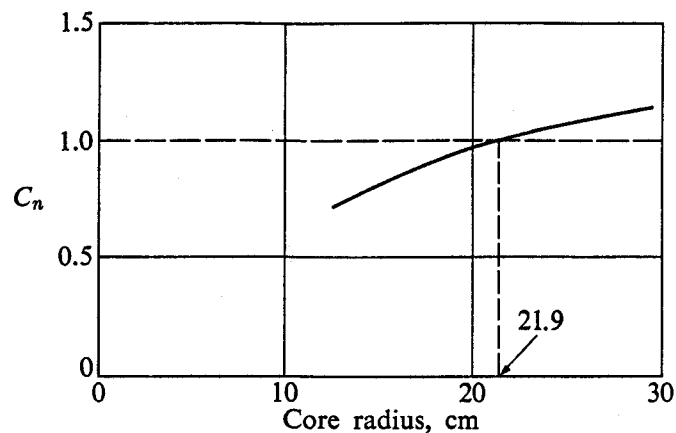


**Fig. 10-6.** The factor  $C_n$  in an iterative two-group computation of the reactor described in the example in Section 10-2. (Courtesy R. Poggi, Nuclear Technology Corporation.)

As a practical matter it is not necessary in computations of this kind to examine the spatial dependence of  $C_n$ , since this parameter ultimately converges to the multiplication factor of the system at any point in the reactor. Frequently, in order to improve the convergence of the calculations the quantity

$$C_n = \frac{\int \phi_i^{(n+1)}(\mathbf{r}) dV}{\int \phi_i^{(n)}(\mathbf{r}) dV}$$

is computed rather than the ratio of flux iterates at a single point.

The iterative technique can obviously be used for calculations of uniform as well as of nonuniform reactors. Figures 10-6 and 10-7 show the results of calculations of this type for the (uniform)  $U^{235}$ -water reactor which was discussed in the example in Section 10-2. In Fig. 10-6 computed values of  $C_n$  are plotted

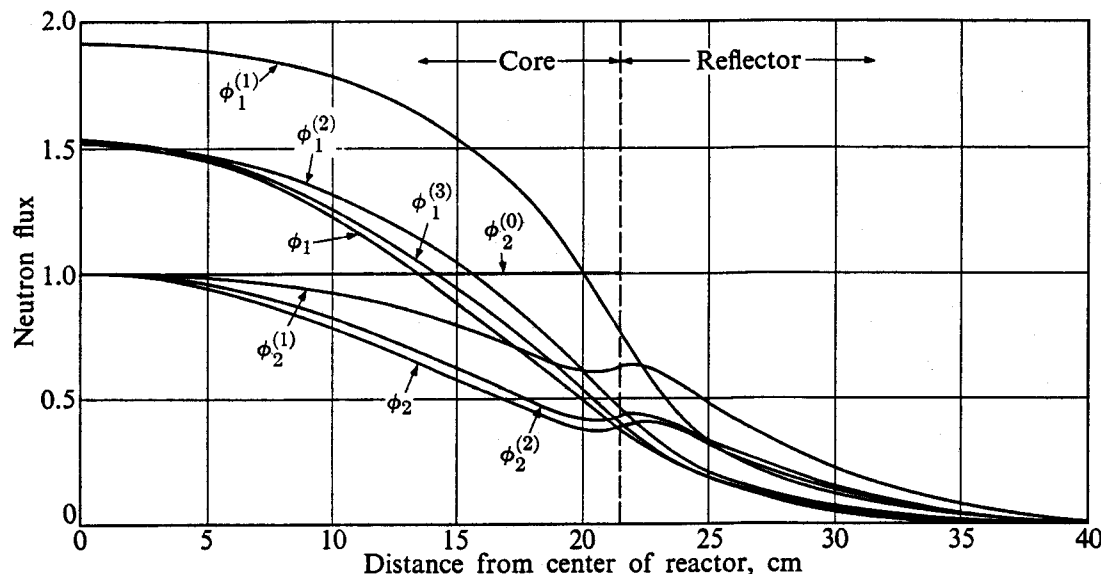


**Fig. 10-7.** Successive flux iterates and final fluxes from an iterative two-group computation of the reactor described in the example in Section 10-2. (Courtesy R. Poggi; Nuclear Technology Corporation.)

versus the core radius, and it is evident that the reactor is supercritical for  $R > 21.9$  cm and subcritical for  $R < 21.9$  cm. In other words, the critical radius is 21.9 cm. The sequence of flux iterates (normalized to unit slow flux at  $r = 0$ ) is shown in Fig. 10-7 for the critical reactor. As indicated in the figure, the initial slow flux was taken to be unity in the core and zero in the reflector. It should be particularly noted how quickly the flux approaches the fundamental.

## 10-4 The Multigroup Method

Calculations of reactor criticality can be greatly improved by the obvious device of increasing the number of neutron groups. In this way, the slowing down of fast neutrons in thermal reactors can be treated in a far more realistic fashion than in two-group theory. With fast and intermediate reactors, on the other hand, since it is the faster neutrons that cause the bulk of the fissions, a more detailed understanding of the behavior of these neutrons is of central importance in predicting criticality and other reactor properties. Multigroup calculations are therefore essential for the proper design of these reactors.

**Multigroup constants.** As the first step in a multigroup calculation, the entire range of neutron lethargy\* in the reactor is divided into  $N$  groups, which may or may not be of equal size (cf. Fig. 10-8). The flux  $\phi_g(\mathbf{r})$  of neutrons in the  $g$ th group is then defined by the integral

$$\phi_g(\mathbf{r}) = \int_{u_{g-1}}^{u_g} \phi(\mathbf{r}, u) du, \quad (10-108)$$

where  $u_g$  and  $u_{g-1}$  are the upper and lower lethargies of the group, respectively, and  $\phi(\mathbf{r}, u)$  is the lethargy-dependent flux at the point  $\mathbf{r}$ .

The diffusion of neutrons within each group is described by an average diffusion coefficient defined as

$$D_g = \frac{\int_{u_{g-1}}^{u_g} D(u) \nabla^2 \phi(\mathbf{r}, u) du}{\int_{u_{g-1}}^{u_g} \nabla^2 \phi(\mathbf{r}, u) du}. \quad (10-109)$$

If it is assumed again, as in Section 10-2, that the flux can be written as a separable function of space and lethargy, Eq. (10-109) becomes

$$D_g = \frac{1}{\phi_g} \int_{u_{g-1}}^{u_g} D(u) \phi(u) du, \quad (10-110)$$

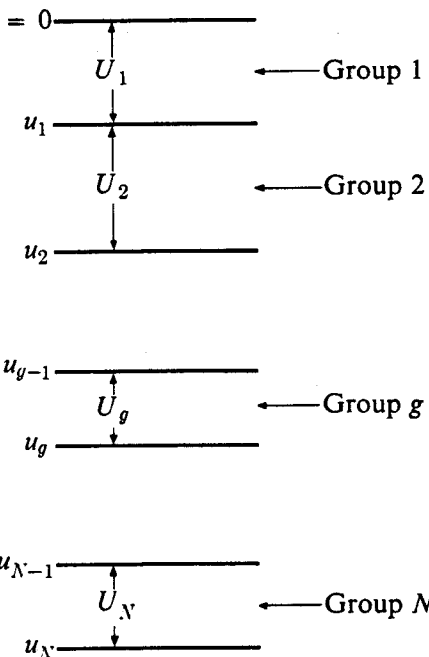


Fig. 10-8. The lethargy groups for a multigroup calculation.

\* In multigroup calculations it is somewhat more convenient to use the lethargy variable rather than energy.

where  $\phi(u)$  is the lethargy-dependent part of  $\phi(r, u)$  and  $\phi_g$  is the constant

$$\phi_g = \int_{u_{g-1}}^{u_g} \phi(u) du. \quad (10-111)$$

To evaluate the integral in Eq. (10-110) it is necessary to assume an appropriate form for  $\phi(u)$ . For thermal reactors this is often chosen to be  $\phi(u) = \text{constant}/\xi(u)\Sigma_s(u)$ , which is the lethargy-dependent flux in an infinite medium containing uniformly distributed sources (cf. Eq. 6-42). In many cases  $\xi(u)$  and  $\Sigma_s(u)$  are essentially constant within each group and it is then possible to take

$$\phi(u) = \text{constant}. \quad (10-112)$$

For simplicity this form for  $\phi(u)$  will be assumed in the present discussion. If the constant in Eq. (10-112) is denoted by  $A$ , then from Eq. (10-111),  $\phi_g = AU_g$ , where  $U_g$  is the width in lethargy of the  $g$ th group. From Eq. (10-110),  $D_g$  is therefore

$$D_g = \frac{1}{U_g} \int_{u_{g-1}}^{u_g} D(u) du. \quad (10-113)$$

If  $D(u)$  is approximately constant over the lethargy interval  $U_g$ , then  $D_g$  is simply the value of  $D$  at any lethargy within the group.

As in two-group theory, neutrons may disappear from a group either in an absorption interaction or as the result of elastic or inelastic scattering which increases their lethargy to that of another group. The true absorption within the  $g$ th group is described by the group absorption cross section  $\Sigma_{ag}$ :

$$\Sigma_{ag} = \frac{1}{\phi_g} \int_{u_{g-1}}^{u_g} \Sigma_a(u)\phi(u) du. \quad (10-114)$$

If it is assumed again that  $\phi(u)$  is constant, Eq. (10-114) becomes

$$\Sigma_{ag} = \frac{1}{U_g} \int_{u_{g-1}}^{u_g} \Sigma_a(u) du. \quad (10-115)$$

Similarly, the average elastic scattering cross section for the  $g$ th group is defined as

$$\Sigma_{sg} = \frac{1}{\phi_g} \int_{u_{g-1}}^{u_g} \Sigma_s(u)\phi(u) du, \quad (10-116)$$

which becomes

$$\Sigma_{sg} = \frac{1}{U_g} \int_{u_{g-1}}^{u_g} \Sigma_s(u) du. \quad (10-117)$$

Frequently,  $\Sigma_s$  is constant in the group and  $\Sigma_{sg}$  is then the actual macroscopic scattering cross section at any lethargy within the group.

The transfer of neutrons by scattering from one group to another is described by the *group transfer cross sections*, which are denoted by  $\Sigma(g \rightarrow h)$ . These are

defined so that  $\Sigma(g \rightarrow h)\phi_g(\mathbf{r})$  is equal to the number of neutrons which are transferred from the  $g$ th to the  $h$ th group per  $\text{cm}^3/\text{sec}$  at the point  $\mathbf{r}$ . Transfer cross sections can be written as the sum of two parts: the *elastic* transfer cross section  $\Sigma_s(g \rightarrow h)$  and the *inelastic* transfer cross section  $\Sigma_i(g \rightarrow h)$ .

Consider first the evaluation of  $\Sigma_s(g \rightarrow h)$ . The value of these constants depends on both the nuclear properties of the materials in the reactor and the number of groups used in the calculation. In particular, if the maximum increase in lethargy of a neutron undergoing an elastic collision is *less* than the width of every group, neutrons from one group can be elastically scattered only into the adjacent group; i.e., they cannot skip groups. In this case,  $\Sigma_s(g \rightarrow h)$  is zero unless  $h = g + 1$ , and the groups are said to be *directly coupled*, at least as far as elastic scattering is concerned. As shown in Chapter 6, the minimum energy of a neutron after an elastic collision is  $\alpha$  times its initial energy, and this is equivalent to an increase in lethargy of  $\ln(1/\alpha)$ . The condition for direct coupling by elastic scattering is therefore

$$\ln\left(\frac{1}{\alpha}\right) < U_g, \quad (10-118)$$

for all groups.

The constants  $\Sigma_s(g \rightarrow g + 1)$  can be computed for the directly coupled situation in the following way. From Eq. (10-116) the total number of scattering collisions per  $\text{cm}^3/\text{sec}$  in the  $g$ th group is  $\Sigma_{sg}\phi_g$ . If  $\bar{\xi}_g$  is the average lethargy increase in an elastic collision in the  $g$ th group (it must be remembered that, in general,  $\bar{\xi}$  is a function of energy; hence the subscript on  $\bar{\xi}_g$ , cf. Section 6-7), it follows that neutrons require  $U_g/\bar{\xi}_g$  collisions on the average in order to traverse that group. If there are  $\Sigma_{sg}\phi_g$  collisions per  $\text{cm}^3/\text{sec}$  in the  $g$ th group, there must be  $\Sigma_{sg}\phi_g \div U_g/\bar{\xi}_g = \bar{\xi}_g\Sigma_{sg}\phi_g/U_g$  neutrons scattered out of the  $g$ th group per  $\text{cm}^3/\text{sec}$ . Since these neutrons necessarily must enter the  $(g + 1)$ th group in the directly coupled case,  $\Sigma_s(g \rightarrow g + 1)$  is given by

$$\Sigma_s(g \rightarrow g + 1) = \frac{\bar{\xi}_g\Sigma_{sg}}{U_g}. \quad (10-119)$$

The calculation of the transfer cross sections in the nondirectly coupled case is straightforward in principle, but the results are more complicated than in the directly coupled situation. The simplest example of a calculation of this kind is that for a hydrogen moderator. A single collision with this nucleus can reduce the energy of a neutron to zero, so that neutrons can be scattered from any group to *all* groups at lower energy. Only the cross section  $\Sigma_s(g \rightarrow g + 1)$  will be derived here; the other cross sections for hydrogen are discussed in the problems.

Consider now the lethargy interval  $du'$  in the  $(g + 1)$ th group. Since neutrons can be scattered into  $du'$  as the result of collisions at *any* lethargy in the  $g$ th group, the number arriving per  $\text{cm}^3/\text{sec}$  in  $du'$  from this group is

$$\text{number scattered into } du' = du' \int_{u_{g-1}}^{u_g} \Sigma_s(u)\phi(u)P(u \rightarrow u') du,$$

where  $P(u \rightarrow u')$  is the probability distribution function for elastically scattered neutrons. The total number of neutrons transferred from the  $g$ th group to the  $(g + 1)$ th group is therefore

$$\text{number transferred} = \int_{u'=u_g}^{u_{g+1}} \int_{u=u_{g-1}}^{u_g} \Sigma_s(u) \phi(u) P(u \rightarrow u') du du'.$$

In view of the definition of  $\Sigma_s(g \rightarrow g + 1)$ , this number is equal to  $\Sigma_s(g \rightarrow g + 1)\phi_g$ , and it follows that

$$\Sigma_s(g \rightarrow g + 1) = \frac{1}{\phi_g} \int_{u'=u_g}^{u_{g+1}} \int_{u=u_{g-1}}^{u_g} \Sigma_s(u) \phi(u) P(u \rightarrow u') du du'. \quad (10-120)$$

If  $\phi(u)$  is again taken to be a constant and if, in addition,  $\Sigma_s(u)$  is reasonably constant in the lethargy interval defined by the  $g$ th group, then Eq. (10-120) can be written as

$$\Sigma_s(g \rightarrow g + 1) = \frac{\Sigma_s}{U_g} \int_{u'=u_g}^{u_{g+1}} \int_{u=u_{g-1}}^{u_g} P(u \rightarrow u') du du'. \quad (10-121)$$

For hydrogen (cf. Prob. 6-4)

$$P(u \rightarrow u') = e^{u-u'}, \quad (10-122)$$

and there is finally obtained

$$\begin{aligned} \Sigma_s(g \rightarrow g + 1) &= \frac{\Sigma_s}{U_g} (e^{u_g} - e^{u_{g-1}})(e^{-u_g} - e^{-u_{g+1}}) \\ &= \frac{\Sigma_s}{U_g} (1 - e^{-U_g})(1 - e^{-U_{g+1}}). \end{aligned} \quad (10-123)$$

The group transfer cross sections for inelastic scattering can be computed in much the same manner as for elastic scattering except, of course, that the inelastic probability distribution function (cf. Eq. 6-123) must be used in the above integrals. Since neutrons can lose such a large fraction of their energy in an inelastic interaction, the inelastic transfer cross sections frequently involve the coupling of several groups.

It is also necessary to define an average fission cross section for each group, and for the  $g$ th group this is

$$\begin{aligned} \Sigma_{fg} &= \frac{1}{\phi_g} \int_{u_{g-1}}^{u_g} \Sigma_f(u) \phi(u) du \\ &= \frac{1}{U_g} \int_{u_{g-1}}^{u_g} \Sigma_f(u) du, \end{aligned} \quad (10-124)$$

where  $\phi(u)$  is taken to be constant. It will be recalled from Chapter 3 that the prompt fission neutrons are emitted with a continuous energy spectrum (cf. Eq. 3-14). It is convenient to introduce the quantity  $x_g$  equal to the *fraction* of

these neutrons appearing in the  $g$ th group. Specifically, this is given by

$$\chi_g = \int_{u_{g-1}}^{u_g} \chi(u) du, \quad (10-125)$$

where  $\chi(u)$  is the fission spectrum *normalized to one emitted neutron*. Finally, it is necessary to take into account the fact that the average number of neutrons emitted per fission depends upon the energy of the incident neutron. For fissions induced by neutrons of the  $g$ th group, the average value of  $\nu$ , denoted by  $\nu_g$ , is

$$\begin{aligned} \nu_g &= \frac{1}{\phi_g} \int_{u_{g-1}}^{u_g} \nu(u) \phi(u) du \\ &= \frac{1}{U_g} \int_{u_{g-1}}^{u_g} \nu(u) du. \end{aligned} \quad (10-126)$$

**Multigroup equations.** With the various constants derived above, it is now possible to write diffusion equations describing the behavior of the neutrons within each group. In a region containing fuel, the equation for the first group, corresponding to the most energetic neutrons, is

$$D_1 \nabla^2 \phi_1(\mathbf{r}) - \Sigma_{a1} \phi_1(\mathbf{r}) - \left[ \sum_{h=2}^N \Sigma(1 \rightarrow h) \right] \phi_1(\mathbf{r}) + \chi_1 \sum_{h=1}^N \nu_h \Sigma_{fh} \phi_h(\mathbf{r}) = 0. \quad (10-127)$$

The second term gives the loss of neutrons due to absorption and the third term gives the loss of neutrons as the result of scattering from the first group to all other groups. The last term is equal to the total number of fission neutrons appearing in the first group as the result of fissions occurring in all other groups.

The diffusion equation for the  $g$ th group is evidently

$$\begin{aligned} D_g \nabla^2 \phi_g(\mathbf{r}) - \Sigma_{ag} \phi_g(\mathbf{r}) - \left[ \sum_{h>g}^N \Sigma(g \rightarrow h) \right] \phi_g(\mathbf{r}) + \sum_{h=1}^{g-1} \Sigma(h \rightarrow g) \phi_h(\mathbf{r}) \\ + \chi_g \sum_{h=1}^N \nu_h \Sigma_{fh} \phi_h(\mathbf{r}) = 0. \end{aligned} \quad (10-128)$$

Here again the second term represents the true absorption in the  $g$ th group; the third term gives the number of neutrons scattered from the  $g$ th group to all higher-numbered (lower-energy) groups; the fourth term is equal to the number of neutrons scattered into the  $g$ th group from all lower-numbered (higher-energy) groups; and the last term gives the number of fission neutrons produced in the  $g$ th group from fissions in all other groups. The group equations for regions that do not contain fuel are identical to Eq. (10-128) except that the last term does not appear.

**Bare reactor calculations.** Equation (10-128) represents a set of  $N$ -coupled partial differential equations; there is one such set for each region of the reactor. The numerical solution of these equations for a multiregion reactor must be carried out on an electronic computer. This problem will be considered later in this section. However, in one important case, namely the uniform bare reactor, the multigroup equations can be solved by hand in an hour or so using a desk calculator.

To proceed with the calculations it is necessary to assume that the extrapolation distance at the surface of the reactor is independent of energy and hence is the same for all groups. The reader will recall that this assumption was also necessary in Chapter 9 in order to treat the bare reactor by Fermi age theory. If this assumption is valid, it is easily shown that all group fluxes have the same spatial dependence. It is then possible to write

$$\phi_g(\mathbf{r}) = \phi_g F(\mathbf{r}), \quad (10-129)$$

where  $\phi_g$  is the magnitude of the  $g$ th flux, and  $F(\mathbf{r})$  satisfies the equation

$$\nabla^2 F(\mathbf{r}) + B^2 F(\mathbf{r}) = 0, \quad (10-130)$$

in which  $B^2$  is the buckling of each flux. Upon substituting Eq. (10-129) into Eq. (10-128) and noting Eq. (10-130), there is obtained

$$-\left[D_g B^2 + \Sigma_{ag} + \sum_{h>g}^N \Sigma(g \rightarrow h)\right] \phi_g + \sum_{h=1}^{g-1} \Sigma(h \rightarrow g) \phi_h + \chi_g \sum_{h=1}^N \nu_h \Sigma_{fh} \phi_h = 0. \quad (10-131)$$

This is a set of  $N$  linear homogeneous equations in the  $N$  unknowns  $\phi_1, \phi_2, \dots, \phi_N$ . By Cramer's rule such a homogeneous set can have no solution other than  $\phi_1 = \phi_2 = \dots = \phi_N = 0$  unless the determinant of the coefficients is zero. The critical size or composition of the reactor can therefore be determined by adjusting either the size or composition to give a zero value of the determinant, as was done in the two-group problem.

As a practical matter, it is not easy to handle a determinant of large order, and if more than three or four groups are involved, it is convenient to use the following iterative technique. To be specific, suppose that the reactor under study is a sphere of known properties and that it is required to find its critical radius  $R$ . As a first step, a guess is made of the value of  $R$  based either on experience or on other computations, for instance, a one-group calculation. In view of Eq. (10-130) and the discussion in Section 9-3, the fluxes have the shape  $F(r) = (\sin Br)/r$ . It follows that  $B^2 = (\pi/R)^2$ , and the assumed value of  $R$  gives a first estimate for  $B^2$ .

Next, a value is assigned to the quantity  $\sum_{h=1}^N \nu_h \Sigma_{fh} \phi_h$  in Eq. (10-131). It is usual to take this to be unity. The first group equation now contains only the

unknown flux  $\phi_1$  and can be solved directly giving

$$\phi_1 = \frac{\chi_1}{D_1 B^2 + \Sigma_{a1} + \sum_{h=2}^N \Sigma(1 \rightarrow h)}. \quad (10-132)$$

The second group equation, which involves only  $\phi_1$  and  $\phi_2$ , is next solved for  $\phi_2$  using the computed value of  $\phi_1$ ; this gives

$$\phi_2 = \frac{\chi_2 + \Sigma(1 \rightarrow 2)\phi_1}{D_2 B^2 + \Sigma_{a2} + \sum_{h=3}^N \Sigma(2 \rightarrow h)}. \quad (10-133)$$

In the same manner, all the  $N$  fluxes can be determined.

Once the fluxes have been found, they are used to compute the quantity  $\sum \nu_h \Sigma_{fh} \phi_h$ , which was initially assumed to be unity. If its computed value is indeed unity, the problem has been solved, and the original guess for the critical radius is correct. If, however,  $\sum \nu_h \Sigma_{fh} \phi_h$  is not unity, another value must be tried for  $B^2$  and the computations repeated. This process is continued until a consistent set of fluxes is obtained. The convergence of the technique can be improved by plotting the computed values of  $\sum \nu_h \Sigma_{fh} \phi_h$  versus  $B^2$ . In the usual case, however, only two or three iterations are necessary.

**Multiregion reactors.** If the reactor consists of more than one region, Eq. (10-128) and its counterparts for other regions must be solved numerically. These computations usually consist of an enlarged version of the iterative scheme discussed in Section 10-3 in connection with solving the two-group equations. As a first step, the dimensions of the reactor are assumed if the composition is given, or, conversely, the critical composition is assumed when the dimensions are given. As in the earlier discussion, this initial specification of the reactor will not correspond to a critical system.

Arbitrary values of the fluxes, denoted by  $\phi_g^{(0)}(\mathbf{r})$ , are next selected and inserted into the fission term of Eq. (10-128) for the *first* group. As noted in the preceding discussion, this equation contains no transfer coupling terms from other groups and can be written in the form\*

$$D_1 \nabla^2 \phi_1 - \Sigma_{a1} \phi_1 - \left[ \sum_{h=2}^N \Sigma(1 \rightarrow h) \right] \phi_1 = -\chi_1 \sum_{h=1}^N \nu_h \Sigma_{fh} \phi_h^{(0)}. \quad (10-134)$$

Equation (10-134) is an inhomogeneous equation which can easily be solved on a computer using standard numerical techniques. Furthermore, this solution can be continued across boundaries in the reactor in such a way that continuity of flux and current is assured. This calculation yields a first estimate of  $\phi_1$ , denoted by  $\phi_1^{(1)}$ .

Attention is next turned to the equation for the second group which contains transfer terms from only the first group. The assumed fluxes  $\phi_g^{(0)}$  are again used in

---

\* From here on, the spatial dependence of the fluxes will be omitted. It is to be understood that  $\phi_1 \equiv \phi_1(\mathbf{r})$ , etc.

this equation except that  $\phi_1^{(1)}$  may be introduced for the first-group flux. The solution to this equation gives an estimate  $\phi_2^{(1)}$  for  $\phi_2$ . This procedure is continued until estimates have been found for all the fluxes. These are now used instead of the original  $\phi_g^{(0)}$  in the fission term of the first-group equation and the calculations are repeated. This leads to new estimates of the fluxes  $\phi_g^{(2)}$ , and so on.

Again, as in the two-group calculations discussed earlier, it is found that the ratio of successive iterates of any of the group fluxes soon approaches a constant. In other words, with increasing values of  $n$ , the ratio  $\phi_g^{(n+1)}/\phi_g^{(n)}$  takes on a constant value, independent of position and independent of  $g$ . Denoting this constant by  $C$ , and using the same argument given in Section 10-3, it follows that if  $C > 1$ , the dimensions or composition assumed at the start of the computation lead to a supercritical reactor, whereas if  $C < 1$ , the assumed system is subcritical. Either the size or composition is now altered and the entire computation is repeated, giving a new value of  $C$ . This process is continued until a size or composition is obtained for which  $C = 1$ .

**Multigroup calculations in practice.** The accuracy of multigroup calculations naturally increases as the number of groups is increased, and computations involving as many as 50 groups have been carried out routinely. However, such elaborate computations tend to be costly in computer time. In the initial stages of the design of a reactor, therefore, the computations are usually carried out with only a few groups. These are sufficient for providing information regarding the general properties of the system. More elegant multigroup calculations are performed in the later stages in the design where greater detail is required.

Multigroup calculations involving many groups are also frequently performed for the sole purpose of providing values of the group constants for a few-group calculation. A 50-group computation, for example, gives a good estimate of the lethargy-dependent flux in a reactor, and few-group constants can be computed by averaging the relevant cross sections over this computed neutron spectrum. This makes it possible to carry out reasonably accurate parametric studies of a reactor using only a few groups at a considerable saving in computation time. In this connection, it may be mentioned that multigroup techniques can also be applied to thermal neutrons to provide thermal group constants. Thus the thermal neutrons are divided into a number of groups, group constants are defined, and multigroup equations are obtained of the same form as Eq. (10-128). However, in these calculations, the group transfer cross sections must be computed using an appropriate scattering kernel of the type discussed in Section 8-1.

Finally, it should be mentioned that although the multigroup equations derived in this section are based on diffusion theory, it is possible also to write multigroup equations in terms of transport theory. Needless to say, the resulting equations are more complicated than the ones discussed above, and they require considerably longer computation times. Nevertheless, the demand for increased precision in the design of reactors has led to the development of a number of transport-multigroup computer programs in recent years.

## 10-5 Reflector Savings

The concept of *reflector savings* is an important aid in many reactor calculations. This is defined as the *decrease* in the critical core dimensions of a reactor when the core is surrounded by a reflector. If, for instance, the critical radius of a bare spherical reactor is  $R_0$  without a reflector and  $R$  with a reflector, the reflector savings is defined as

$$\delta = R_0 - R. \quad (10-135)$$

The reflector savings can be determined by calculating the critical sizes of bare and reflected reactors of the same composition and then subtracting. Conversely, when  $\delta$  is known, the critical dimensions of a reflected reactor of specified composition can be found by solving the bare reactor problem. The actual size of the reflected system is then the bare dimensions minus  $\delta$ . The usefulness of the reflector savings lies in the fact that, as shown below,  $\delta$  is not a sensitive function of the properties of the reactor core. Values of  $\delta$  computed for one core composition can therefore be used for reactors with other, but similar, compositions.

Obviously, the most accurate value of  $\delta$  is obtained when the calculations of the critical dimensions of the bare and reflected reactors are as accurate as possible. For this reason, reflector savings are often computed by the multigroup method. A qualitative understanding of reflector savings can be obtained, however, from simple one-group theory. Consider, for example, the slab thermal reactor discussed in Section 10-1. The critical thickness  $a$  of the reflected core is determined by the critical equation

$$\bar{D}_c B_c \tan \frac{B_c a}{2} = \frac{\bar{D}_r}{L_{Tr}} \coth \frac{b}{L_{Tr}}, \quad (10-136)$$

where  $b$  is the extrapolated thickness of the reflector. The critical thickness of the *bare* slab, on the other hand, is simply  $a_0 = \pi/B_c$ .

The reflector savings for the slab reactor is defined as

$$\delta = \frac{1}{2}(a_0 - a). \quad (10-137)$$

The factor  $\frac{1}{2}$  appears in Eq. (10-137) due to the fact that there are two core-reflector interfaces. Solving Eq. (10-137) for  $a$  and substituting this into Eq. (10-136) results in

$$\bar{D}_c B_c \tan B_c \left( \frac{a_0}{2} - \delta \right) = \frac{\bar{D}_r}{L_{Tr}} \coth \frac{b}{L_{Tr}}. \quad (10-138)$$

Since  $B_c a_0/2 = \pi/2$ , Eq. (10-138) becomes

$$\bar{D}_c B_c \cot B_c \delta = \frac{\bar{D}_r}{L_{Tr}} \coth \frac{b}{L_{Tr}}. \quad (10-139)$$

Finally, inverting Eq. (10-139) gives the following formula for  $\delta$ :

$$\delta = \frac{1}{B_c} \tan^{-1} \left( \frac{\bar{D}_c B_c L_{Tr}}{\bar{D}_r} \tanh \frac{b}{L_{Tr}} \right). \quad (10-140)$$

Except for small reactors,  $B_c$  is much less than unity, and in Eq. (10-139),  $\cot B_c \delta \approx 1/B_c \delta$ . The reflector savings is then *independent of the buckling in the core* and is given by

$$\delta \approx \frac{\bar{D}_c}{\bar{D}_r} L_{Tr} \tanh \frac{b}{L_{Tr}}. \quad (10-141)$$

There are two limiting situations that can now be considered. First, if the reflector is very thin, that is,  $b \ll L_{Tr}$  (a most uncommon situation), then  $\tanh(b/L_{Tr}) \approx b/L_{Tr}$  and Eq. (10-141) becomes

$$\delta \approx \frac{\bar{D}_c}{\bar{D}_r} b. \quad (10-142)$$

The reflector savings in this case is seen to be proportional to the thickness of the reflector. On the other hand, with a thick reflector,  $b \gg L_{Tr}$ , so that  $\tanh(b/L_{Tr}) \approx 1$  and Eq. (10-141) reduces to the useful formula

$$\delta \approx \frac{\bar{D}_c}{\bar{D}_r} L_{Tr}. \quad (10-143)$$

As a practical matter, the function  $\tanh(b/L_{Tr})$  rises to its maximum value of unity very quickly with  $b/L_{Tr}$  (e.g.,  $\tanh 1.5 = 0.90$ ), and Eq. (10-143) is therefore valid provided the reflector is only one or two diffusion lengths in thickness. The reflector is then effectively infinite and there is little advantage in using a reflector which is any thicker. Since the diffusion length varies inversely with the absorption cross section, it also follows from Eq. (10-143) that the reflector savings increases with decreasing absorption cross section of the reflector. The critical dimensions of the core thus tend to be smaller when the material used for the reflector has a low absorption cross section. However, the thickness of material required for the reflector to be considered "infinite" is necessarily larger.

Similar one-group calculations of  $\delta$  can be carried out for reactors with other geometries. In all cases, the formulas for  $\delta$  reduce to Eqs. (10-141) through (10-143) provided the reactor cores are not too small. It may also be mentioned that the conclusions reached in this section which are based on one-group theory have somewhat wider applicability than might be expected. Thus more elegant multigroup calculations have been found to give *approximately* the same values of reflected savings, at least for thermal reactors.

## 10-6 Totally Reflected Reactors

Virtually all reactors are built with reflectors on all sides. Unfortunately, as mentioned in Section 10-2, the group diffusion equations cannot be solved analytically for two of the most important reactors of this type, namely, the totally reflected parallelepiped and finite cylinder. Fundamentally, this is due to the fact that separable solutions to the diffusion equation cannot be found which satisfy the boundary conditions at the core-reflector interfaces. This is true regardless

of the number of groups in the calculation. Satisfactory estimates of the critical composition or dimensions of these reactors can be obtained, however, from the following iterative scheme.

Consider, for example, the problem of finding, by one-group theory, the critical composition of a thermal reactor whose core is a cylinder of height  $H$  and radius  $R$ , which is surrounded on all sides by a reflector of thickness  $b$ . The critical equation in one-group theory is (cf. Eq. 10-5)

$$\frac{k_{\infty}}{1 + B_c^2 L_{Tc}^2} = 1,$$

where  $B_c$  is the buckling of the flux in the core. Since the dimensions of the reactor are given, the first problem is to find the value of  $B_c$  for the reactor. When this has been found, the critical composition of the system can be determined from the critical equation as was done in Section 9-6 (Case I).

To start the calculation, a guess is made of the axial reflector savings  $\delta_z$  arising from the reflectors on the ends of the reactor. The formula

$$\delta_z \approx \frac{\bar{D}_c}{\bar{D}_r} L_{Tr}$$

(cf. Eq. 10-143) is usually adequate for such a first guess. The actual reactor is

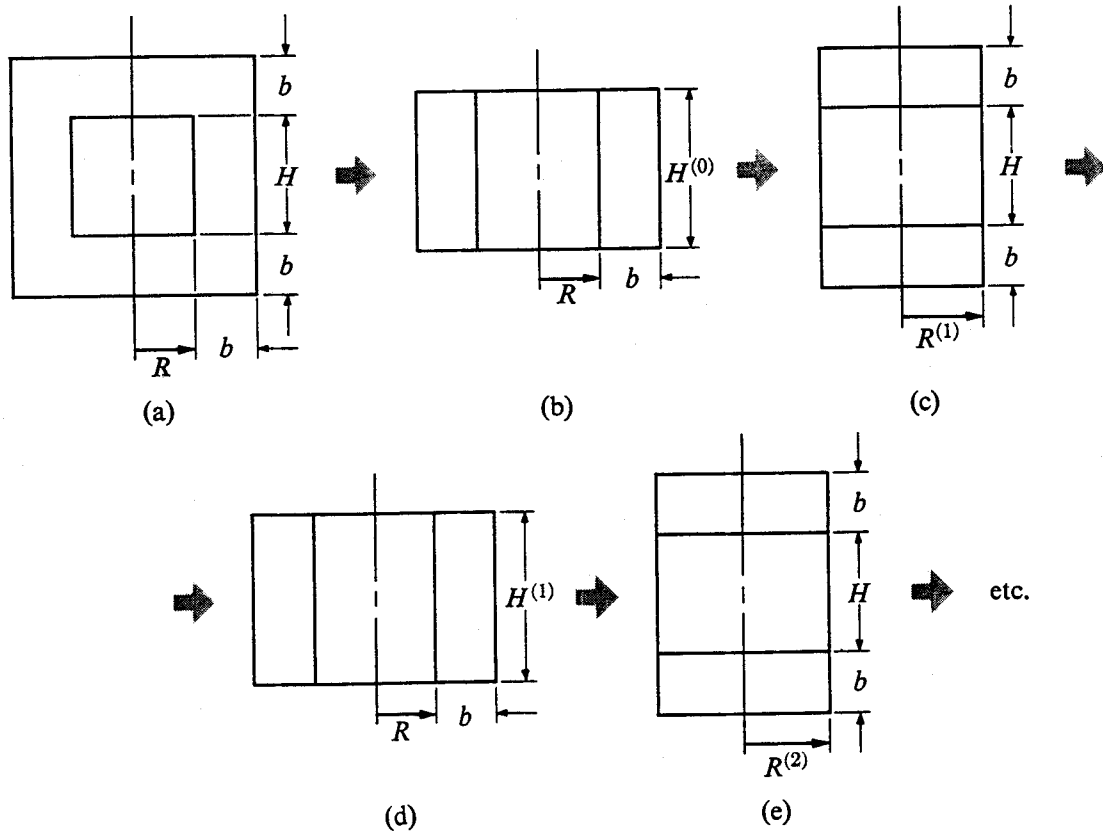


Fig. 10-9. Computation scheme for fully reflected cylindrical reactor.

now replaced by another reactor of the same radius but one which is bare on the ends and has a height  $H^{(0)} = H + 2\delta_z$ . This procedure is shown schematically in Fig. 10-9 (a and b).

The buckling of the new, partially reflected reactor can now be determined analytically by the procedure discussed in Section 10-2. Thus the diffusion equations for the core and reflector are, respectively,

$$\frac{1}{r} \frac{\partial}{\partial r} r \frac{\partial \phi_{Tc}}{\partial r} + \frac{\partial^2 \phi_{Tc}}{\partial z^2} + B_c^2 \phi_{Tc} = 0 \quad (10-144)$$

and

$$\frac{1}{r} \frac{\partial}{\partial r} r \frac{\partial \phi_{Tr}}{\partial r} + \frac{\partial^2 \phi_{Tr}}{\partial z^2} - \frac{1}{L_{Tr}^2} \phi_{Tr} = 0. \quad (10-145)$$

Using the method of separation of variables in the usual way, it is easy to show that the thermal fluxes in the core and reflector are

$$\phi_{Tc}(r, z) = AJ_0(\alpha r) \cos\left(\frac{\pi z}{H^{(0)}}\right), \quad (10-146)$$

$$\phi_{Tr}(r, z) = C\{I_0(\beta r)K_0[\beta(R + b)] - I_0[\beta(R + b)]K_0(\beta r)\} \cos\left(\frac{\pi z}{H^{(0)}}\right). \quad (10-147)$$

where

$$\alpha^2 = B_c^2 - \left(\frac{\pi}{H^{(0)}}\right)^2, \quad (10-148)$$

$$\beta^2 = \frac{1}{L_{Tr}^2} + \left(\frac{\pi}{H^{(0)}}\right)^2. \quad (10-149)$$

The equation giving the buckling for this reactor is obtained from the usual boundary conditions at the core-reflector interface at  $r = R$ . These conditions give the equation

$$-\bar{D}_c \alpha \frac{J_1(\alpha R)}{J_0(\alpha R)} = \bar{D}_r \beta \frac{I_1(\beta R)K_0[\beta(R + b)] + I_0[\beta(R + b)]K_1(\beta R)}{I_0(\beta R)K_0[\beta(R + b)] - I_0[\beta(R + b)]K_0(\beta R)}. \quad (10-150)$$

In Eq. (10-150) all parameters are known except  $\alpha$ , and this is found by solving the equation numerically. With  $\alpha$  known, an estimate of  $B_c$ , denoted as  $B_c^{(1)}$ , is obtained from Eq. (10-148). The radius of the equivalent *totally bare* cylindrical reactor is next determined by noting that for such a reactor, the buckling, height, and radius are related by (cf. Section 9-3)

$$B_c^2 = \left(\frac{2.405}{R}\right)^2 + \left(\frac{\pi}{H}\right)^2, \quad (10-151)$$

where in the present case  $B_c^{(1)}$  is used for  $B_c$  and  $H^{(0)}$  is used for  $H$ . This estimate of the radius of the bare reactor will be called  $R^{(1)}$ .

The original reactor is now replaced by another reactor that is bare on the sides, having the radius  $R^{(1)}$ , but which is reflected on the ends, as shown in Fig. 10-9(c). The buckling of this system can also be found analytically. The core and reflector equations are again given by Eqs. (10-144) and (10-145) and the fluxes are found to be

$$\phi_{Tc}(r, z) = A' J_0 \left( \frac{2.405r}{R^{(1)}} \right) \cos \gamma z, \quad (10-152)$$

$$\phi_{Tr}(r, z) = C' J_0 \left( \frac{2.405r}{R^{(1)}} \right) \sinh \xi \left( \frac{H}{2} + b - |z| \right), \quad (10-153)$$

where

$$\gamma^2 = B_c^2 - \left( \frac{2.405}{R^{(1)}} \right)^2, \quad (10-154)$$

$$\xi^2 = \frac{1}{L_{Tr}^2} + \left( \frac{2.405}{R^{(1)}} \right)^2. \quad (10-155)$$

Satisfying boundary conditions at the interface at  $z = H/2$  gives the equation

$$\overline{D}_c \gamma \tan \left( \frac{\gamma H}{2} \right) = \overline{D}_r \xi \coth \xi b. \quad (10-156)$$

Equation (10-156) is next solved for  $\gamma$ , and this value, together with Eq. (10-154), gives a new estimate  $B_c^{(2)}$  for the buckling. Then from Eq. (10-151), a new value of the equivalent bare height  $H^{(1)}$  of the system is obtained, and the calculations are repeated, starting with  $H^{(1)}$  instead of  $H^{(0)}$ . These computations are continued until the value of the buckling no longer changes on successive iterations. Once  $B_c$  is known, the critical composition of the core can be found by solving the critical equation as discussed earlier.\*

Iterative calculations of this type can be carried out with any number of groups. They tend to be rather time consuming, however, particularly when they involve more than a few groups. For this reason, multigroup calculations are often performed for the equivalent spherical reactor, that is, the spherical reactor having the same core volume. Most reactor cores are cylindrical, and most of these are square cylinders, i.e.,  $H = 2R$ , and the critical compositions of the equivalent spherical reactor and the actual reactor are very nearly the same. Incidentally, before lengthy iterative calculations of a totally reflected cylinder or parallelepiped are begun, it is wise to make calculations of the equivalent spherical reactor first. It is then possible to proceed with a good idea of what the result of the calculations should be.

---

\* It may be mentioned that it has not been established whether this iterative technique converges to the correct answer or not.

## 10-7 Experimental Determination of Critical Reactor Parameters

The computational methods described in this chapter are capable of providing good estimates of the critical composition or dimensions of a reactor, as well as the neutron flux. Nevertheless, before a reactor is constructed it is the usual practice to measure these and other reactor characteristics experimentally, unless the reactor under consideration is only slightly different from an existing reactor whose characteristics are well known. While the details of such measurements lie outside of the scope of this book, two of the more important experimental techniques will now be considered briefly.

**Critical experiments.** It has been pointed out repeatedly in this and the previous chapter that the critical mass and the shape of the fluxes are independent of the operating power of a reactor.\* For this reason it is possible to determine these important reactor characteristics in an assembly which duplicates the essential properties of the actual reactor (including structural material, coolant channels, control rods, etc.), but which operates at essentially zero power. A device of this kind is known as a *critical assembly*, and measurements made with such an assembly are called *critical experiments*. Since this assembly is not operated at significant power levels, elaborate heavy cooling equipment and large amounts of shielding around the reactor are not required. These are costly items in the construction of a power reactor; thus a critical assembly is a far less expensive device.

As an example of the use of a critical assembly, let it be supposed that the reactor being designed is to be moderated and reflected by normal-density water and fueled with rods of enriched uranium. In this case, the assembly is constructed in a tank large enough to accommodate both the core and the reflector. To hold the fuel rods in position, two or more grid plates, properly drilled with holes and aligned to provide the desired array of rods, are inserted into the tank. A small neutron source, one or more control rods, and a number of neutron detectors are also placed in the tank.

Up to this point, there is neither fuel nor water in the tank. A number of fuel rods are now inserted in the grid, water is admitted to the tank, and the control rods are slowly withdrawn. Since the system is presumably subcritical, the flux eventually becomes of the form (cf. Eq. 9-35)

$$\phi_T(\mathbf{r}) = \text{constant} \times \sum \frac{k_n}{1 - k_n} \phi_n(\mathbf{r}), \quad (10-157)$$

---

\* This is strictly true, of course, provided the properties of the reactor do not change substantially with power, due to accompanying changes in the temperature of the system. If the properties of the reactor are much different at the design power than at room temperature, the measurements discussed in this section should be performed at the appropriate elevated temperature, if possible. If this is not possible the data must be extrapolated to the operating temperature.

after the transients have died out. Although this formula was derived in Chapter 9 for a bare reactor and is based on age theory, an equation of the same type can be shown to be valid for more general systems. It will be recalled that the parameter  $k_1 = k$  is the multiplication factor of the assembly. From Eq. (10-157) it follows, therefore, that as the assembly approaches the critical state, that is, as  $k \rightarrow 1$ , the first term in the equation dominates the series, and the flux increases without limit.

With the first group of fuel rods in place, the flux is measured at one or more points in the system. The control rods are then reinserted, whereupon the flux falls rapidly to zero. More fuel rods are now inserted, the control rods are again withdrawn, and the flux is remeasured. In view of Eq. (10-157), the flux is now somewhat higher than in the first measurement, since the addition of fuel increases the multiplication factor of the system. This procedure is continued and at each step the reciprocal of the measured flux is plotted as a function of the number of fuel rods in the tank, as shown in Fig. 10-10. The number of rods which make the system critical is then found by extrapolating the curve, as indicated in the figure.

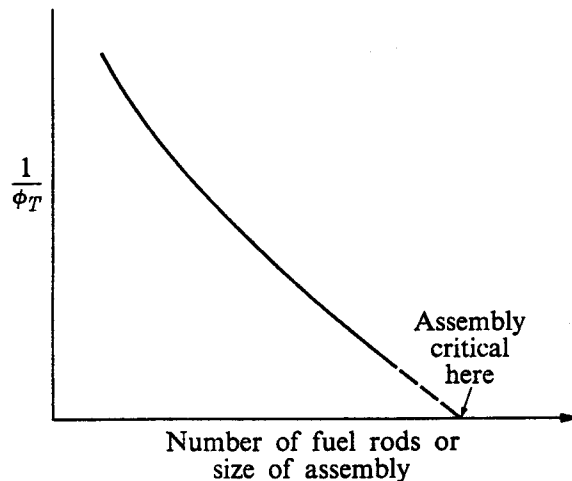


Fig. 10-10. The determination of critical size in a critical experiment.

Once the critical or near-critical state has been reached, the flux in the assembly will have the same shape as in the critical reactor and is measured throughout the system. Besides being used to determine the conditions for criticality and the flux distribution, critical experiments can also be used to measure a number of other important reactor properties such as control-rod effectiveness, conversion coefficients, and so on.

**Pulsed-neutron measurements.** In Section 9-2 it was shown that a flux is produced if a source is placed in a quiescent subcritical reactor, and when the source is removed, the flux decreases to zero, ultimately, in the fundamental mode. It is easy to show that the same situation can be obtained when a burst of neutrons is introduced into such an assembly. Thus from Eq. (9-38) the flux rises

and then ultimately decays as

$$\phi_T(\mathbf{r}, t) \rightarrow e^{-\lambda t} \phi_1(\mathbf{r}). \quad (10-158)$$

Here  $\phi_1$  is the fundamental eigenfunction of the reactor, and the decay constant  $\lambda$  is given by

$$\lambda = \frac{1 - k}{t_1}, \quad (10-159)$$

where  $k$  is the multiplication factor

$$k = \frac{k_\infty e^{-B^2 \tau_T}}{1 + B^2 L_T^2},$$

and

$$t_1 = \frac{t_d}{1 + B^2 L_T^2},$$

in which  $t_d$  is the mean diffusion time (cf. Eq. 8-82). By inserting the above formulas into Eq. (10-159),  $\lambda$  can be written as

$$\lambda = \frac{1 + B^2 L_T^2 - k_\infty e^{-B^2 \tau_T}}{t_d}. \quad (10-160)$$

Equation (10-160) is a generalization of Eq. (8-132) which was derived for non-fueled assemblies. In particular, it will be noted that when  $k_\infty = 0$ , the decay constants in the two cases become identical.

The above theoretical results form the basis of measurements of reactor properties using pulsed-neutron techniques similar to those discussed in Section 8-9. Thus a pulse of neutrons is introduced into a subcritical assembly having the same composition as the reactor under consideration, and the thermal flux is measured as a function of time at one or more points. These measurements give one value of  $\lambda$ . The size of the assembly is now increased, the experiments are repeated, and a new value of  $\lambda$  is obtained. In this way,  $\lambda$  is determined as a function of the size of the assembly and it is then plotted as a function of  $B^2$ . The resulting curve is illustrated in Fig. 10-11.

For large values of  $B^2$ , that is, when the assembly is small, the term  $k_\infty \exp(-B^2 \tau_T)$  in Eq. (10-160) vanishes, and  $\lambda$  is linear in  $B^2$  as shown in the figure. This is the same behavior which was encountered in Section 8-9 for nonfueled assemblies. The intercepts of the extrapolated, linear portion of the curve with the  $\lambda$ - and  $B^2$ -axes therefore determine  $t_d$  and  $L_T^2$ . In the present case, of course, these parameters refer to the fuel-moderator mixture (and whatever else is in the assembly) and not to the moderator alone.

As the assembly is made larger,  $B^2$  decreases, the term  $k_\infty \exp(-B^2 \tau_T)$  ceases to be negligible, and  $\lambda$  departs from its original linear behavior. Since according to Eq. (10-159),  $\lambda = 0$  when  $k = 1$ , it follows that the assembly is critical when it is sufficiently large that  $\lambda = 0$ . Thus by plotting  $\lambda$  versus  $B^2$  and extrapolating the curve to zero, it is possible to determine the critical size of the reactor using

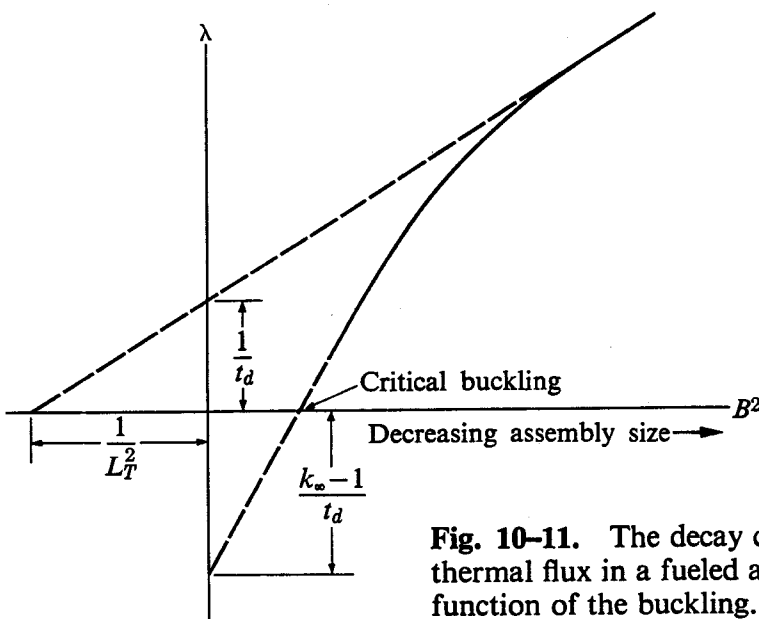


Fig. 10-11. The decay constant of the thermal flux in a fueled assembly as the function of the buckling.

this technique. Furthermore, with many assemblies the factor  $\exp(-B^2\tau_T)$  in Eq. (10-60) approaches a value near unity as the assembly approaches its critical size, owing to the fact that there is little leakage of fast neutrons from the critical system. In this case,  $\lambda$  varies as

$$\lambda \approx \frac{1 - k_\infty + B^2 L_T^2}{t_d}, \quad (10-161)$$

which is again linear in  $B^2$ . This explains the linear portion of the curve in Fig. 10-11 at small values of  $B^2$ . The intersection of this line with the  $\lambda$ -axis occurs at  $\lambda = -(k_\infty - 1)/t_d$ , so that by extrapolating this line as shown in the figure it is possible to determine  $(k_\infty - 1)/t_d$ . Since  $t_d$  is already known from measurements with the smaller assemblies, this means that the value of  $k_\infty$  is also determined.

Again, as in the case of measurements of nonmultiplying media discussed in Chapter 8, it is clear that more data about the system can be obtained by the pulsed-neutron technique than in static experiments on the same assembly. In particular, besides the critical dimensions of the reactor and the shape of the flux, it is also possible to determine the infinite multiplication factor, the thermal diffusion area, and the thermal diffusion time.

## References

- BONDARENKO, I. I., Editor, *Group Constants for Nuclear Reactor Calculations*. New York: Consultants Bureau, 1964.
- ETHERINGTON, H., Editor, *Nuclear Engineering Handbook*. New York: McGraw-Hill, 1958, Section 6-2.
- GALANIN, A. D., *Thermal Reactor Theory*, 2nd ed. New York: Pergamon Press, 1960, Chapters 2, 3, and 5.

GARABEDIAN, H. L., *Analytic Criticality Studies Associated with Neutron Diffusion Theory*. Vienna: IAEA Review Series No. 26, 1962.

GLASSTONE, S., and M. C. EDLUND, *The Elements of Nuclear Reactor Theory*. Princeton, N.J.: Van Nostrand, 1952, Chapter 8.

ISBIN, H. S., *Introductory Nuclear Reactor Theory*. New York: Reinhold, 1963, Chapter 7.

MEEM, J. L., *Two-Group Reactor Theory*. New York: Gordon and Breach, 1964, Chapter 7.

MEGHREBLIAN, R. V., and D. K. HOLMES, *Reactor Analysis*. New York: McGraw-Hill, 1960, Chapter 8.

MURRAY, R. L., *Nuclear Reactor Physics*. Englewood Cliffs, N.J.: Prentice-Hall, 1957, Chapter 5.

*Reactor Physics Constants*, U.S. Atomic Energy Commission Report ANL-5800, 2nd ed., 1963. The references at the end of Sections 3, 4, 6, and 7 of this report provide an extensive bibliography on criticality and other reactor measurements. See also Section 10 for a description of various computer codes.

SANGREN, W., *Digital Computers and Nuclear Reactor Calculations*. New York: Wiley, 1960.

WEINBERG, A. M., and E. P. WIGNER, *The Physical Theory of Neutron Chain Reactors*. Chicago: University of Chicago Press, 1958, Chapter 15.

YIFTAH, S., D. OKRENT, P. A. MOLDAUER, *Fast Reactor Cross Sections*, New York: Macmillan, 1960.

## Problems

10-1. (a) Using one-group theory, compute the critical composition of an infinite slab reactor of core thickness 50 cm, which is fueled with a homogeneous mixture of  $U^{235}$  and  $H_2O$  and has an infinite  $H_2O$  reflector. (b) If the reactor operates at an average power density of 25 watts/cm<sup>3</sup> and at an average temperature of 60°C, determine the thermal flux as a function of position in the reactor.

10-2. Using the one-group model, find the critical condition for the following thermal reactors. In each case, also find an expression for the flux throughout the reactor in terms of the reactor power.

- (a) Infinite cylinder, reflector thickness  $b$ .
- (b) Infinite cylinder, infinitely thick reflector.
- (c) Sphere, reflector thickness  $b$ .
- (d) Sphere, infinitely thick reflector.

10-3. Consider a spherical thermal reactor with an infinite reflector. The core is a homogeneous mixture of  $U^{235}$  and beryllium, and the reflector is also beryllium. Using one-group theory, compute and plot the critical  $U^{235}$  concentration ( $N_{25}/N_{Be}$ ) and the critical mass as a function of the core radius. What is the minimum critical mass? Compare with Fig. 9-7.

10-4. Using one-group theory, derive the critical equation for an infinite slab reactor consisting of three regions:

$$\begin{array}{lll} \text{Region 1 (core)} & |x| < a, & k_\infty > 1, \\ \text{Region 2 (blanket)} & a < |x| < b, & 0 < k_\infty < 1, \\ \text{Region 3 (reflector)} & b < |x|, & k_\infty = 0. \end{array}$$

10-5. The core of a spherical thermal reactor is 75 cm in radius and contains a uniform mixture of uranium, enriched to 2.5% U<sup>235</sup>, and 0.745 density H<sub>2</sub>O. The reactor has an infinite H<sub>2</sub>O reflector. Operating at a power of 100 MW(th) the average temperature of the core material is 550°C. (a) Using modified one-group theory, determine the critical fuel concentration and the critical mass. (b) Determine the thermal flux in the core. (c) At what rate is Pu<sup>239</sup> produced in the reactor?

10-6. Using microscopic cross section data and experimental values of  $\tau_T$ , compute the fast-group constants  $D_1$  and  $\Sigma_1$  for the following moderators.

- (a) H<sub>2</sub>O      (b) D<sub>2</sub>O      (c) Be      (d) Graphite

10-7. An isotropic point source emits  $S$  fast neutrons/sec in an infinite moderator.

(a) Show that according to two-group theory the thermal flux ( $\phi_2$ ) is given by

$$\phi_2(r) = \frac{SL_T^2}{4\pi r D_2(L_T^2 - \tau_T)} (e^{-r/L_T} - e^{-r/\sqrt{\tau_T}}).$$

(b) Show that in the limit as  $\tau_T \rightarrow 0$ , this formula reduces to Eq. (5-64). (c) What is  $\phi_2(0)$ ? (d) Compute and plot  $\phi_2(r)$  for the case given in Problem 8-21(c) and compare with the results of that problem.

10-8. Verify that there are only two independent solutions to Eqs. (10-35) and (10-36).

10-9. An infinite planar source emitting  $S$  fast neutrons/cm<sup>2</sup>-sec is placed at the center of a bare slab subcritical assembly of thickness  $a$ . (a) Show that the two-group fluxes in the assembly are given by

$$\phi_1 = \frac{2pS}{a\Sigma_2 k_\infty} \sum_{n \text{ odd}} \frac{k_n}{(1 - k_n) S_{1n}} \cos B_n x,$$

$$\phi_2 = \frac{2pS}{a\Sigma_2 k_\infty} \sum_{n \text{ odd}} \frac{k_n}{1 - k_n} \cos B_n x,$$

where  $B_n = n\pi/a$ ,

$$k_n = \frac{k_\infty}{(1 + B_n^2 L_T^2)(1 + B_n^2 \tau_T)},$$

and  $S_{1n}$  is the coupling coefficient for the  $n$ th mode (cf. Eq. 10-49):

$$S_{1n} = \frac{p\Sigma_1/\Sigma_2}{1 + B_n^2 L_T^2}.$$

(b) Compare  $\phi_2$  computed in part (a) with the expression for  $\phi_T$  given by Eq. (9-35) and interpret the similarity physically. [Note: Unfortunately, for reasons discussed in Chapter 15, the important problem of the reflected subcritical reactor cannot be handled by ordinary methods (cf. Prob. 15-22).]

10-10. Using the results of Problems 10-9 and 9-21, write down directly the two-group expression for the thermal flux in a bare cylindrical subcritical reactor containing a point source of fast neutrons at its center.

10-11. Verify the formulas for the two-group critical determinant (Eq. 10-73) and for the flux constants [Eqs. (10-77) through (10-80)].

- 10-12. Consider a critical bare spherical thermal reactor of radius  $R$  consisting of a homogeneous mixture of fuel and moderator. (a) Using two-group theory, derive expressions for the fast and slow fluxes. (b) Show that the slowing-down density is proportional to the thermal flux everywhere in the reactor. [This is another instance of the result given in Eq. (9-46).] (c) Derive formulas for the fast and slow nonleakage probabilities. (d) Show that the critical equation for the reactor is

$$\frac{k_{\infty}}{(1 + B^2 L_T^2)(1 + B^2 \tau_T)} = 1,$$

where  $B^2 = (\pi/R)^2$ .

- 10-13. Consider an infinite slab reactor of core thickness  $a$ , surrounded on both sides by infinite reflectors. The diffusion coefficients of core and reflector are identical. (a) Show that if  $\lambda \gg \mu$ , as is usually the case, the right-hand side of Eq. (10-73) is linear in  $\mu a$ . (b) Find the slope of this line and the value of RHS when  $\mu a = 0$ . (c) Repeat the calculation for a spherical reactor of core radius  $R$ , also having an infinite reflector.

- 10-14. Show that according to two-group theory, the fluxes in a bare cylindrical reactor of radius  $R$  and height  $H$  are given by

$$\begin{aligned}\phi_1 &= AJ_0\left(\frac{2.405r}{R}\right) \cos\left(\frac{\pi z}{H}\right), \\ \phi_2 &= AS_1J_0\left(\frac{2.405r}{R}\right) \cos\left(\frac{\pi z}{H}\right),\end{aligned}$$

where  $S_1$  is the first coupling coefficient.

- 10-15. A spherical reactor consists of a central core of radius  $a$ , containing a homogeneous mixture of a fissile isotope and moderator with an infinite multiplication constant  $k_{\infty c} > 1$ , surrounded by a blanket of radius  $b$ , containing a mixture of natural uranium and moderator with an infinite multiplication constant  $k_{\infty b} < 1$ . Calculate the elements of the two-group critical determinant and expressions for the fluxes throughout the reactor.

- 10-16. (a) Using two-group theory, find the critical core radius and critical mass of a spherical reactor fueled with  $U^{235}$  and moderated and reflected with ordinary water if the fuel to moderator ratio is  $N_{25}/N_w = 1/300$ . (b) Compute and plot the fast and thermal fluxes throughout the reactor. Take the reflector to be infinite.

- 10-17. The core of an infinite thermal slab reactor 100 cm thick consists of a homogeneous mixture of  $U^{233}$  and  $D_2O$ . The reflector is graphite and it may be taken to be infinite in thickness. (a) Using two-group theory, find the critical concentration of the fuel in gm/liter. (b) Find expressions for the fast and slow fluxes normalized to unit power/cm<sup>2</sup> of the core.

- 10-18. Which of the four common moderators,  $H_2O$ ,  $D_2O$ , Be, or graphite, should be used if it is desired to obtain the highest fast flux per unit power output of a thermal reactor? The reactor is to be fueled with a homogeneous mixture of this moderator and a fissile isotope. For simplicity, assume that the reactor is bare.

- 10-19. The core of a spherical reactor contains  $U^{235}$ -zirconium fuel elements with an atom ratio  $N_{Zr}/N_{25} = 200$ . Water of 0.80 density is both coolant and moderator in the core, and the metal-water volume ratio is 0.5. The reflector is unit density water and

may be considered infinite. The reactor operates at a power of 90 MW(th) at an average temperature of 550°C. (a) Using two-group theory, find the critical radius of the core and the critical mass. (b) Compute and plot the fluxes in the system. (c) What is the maximum to average thermal flux?

10–20. Using two-group theory, compute and plot as a function of the core radius the critical U<sup>235</sup> concentration and critical mass of the reactor described in Problem 10–3. Compare with Fig. 9–7. What is the minimum critical mass?

10–21. (a) Using two-group theory, determine the critical dimensions and critical mass of the reactor described in Problem 9–20, if the core tank is surrounded by an infinite beryllium reflector. For simplicity, make this calculation for the equivalent spherical reactor. (b) If the reactor operates at a power of 40 MW(th), compute the maximum and average thermal flux in the core.

10–22. Consider a reactor having a cubical core of side  $a$  which is reflected on two opposite sides by infinite reflectors. With the center of coordinates at the center of the reactor, show that the two-group fluxes are given by the following expressions:

$$\begin{aligned}\phi_{1c} &= (A \cos \alpha_1 x + C \cosh \alpha_2 x) \cos\left(\frac{\pi y}{a}\right) \cos\left(\frac{\pi z}{a}\right), \\ \phi_{2c} &= (AS_1 \cos \alpha_1 x + CS_2 \cosh \alpha_2 x) \cos\left(\frac{\pi y}{a}\right) \cos\left(\frac{\pi z}{a}\right), \\ \phi_{1r} &= Fe^{-\beta_1 |x|} \cos\left(\frac{\pi y}{a}\right) \cos\left(\frac{\pi z}{a}\right), \\ \phi_{2r} &= (FS_3 e^{-\beta_1 |x|} + Ge^{-\beta_2 |x|}) \cos\left(\frac{\pi y}{a}\right) \cos\left(\frac{\pi z}{a}\right),\end{aligned}$$

where

$$\begin{aligned}\alpha_1^2 &= \mu^2 - 2\left(\frac{\pi}{a}\right)^2, \\ \alpha_2^2 &= \lambda^2 + 2\left(\frac{\pi}{a}\right)^2, \\ \beta_i^2 &= \kappa_i^2 + 2\left(\frac{\pi}{a}\right)^2, \quad i = 1, 2.\end{aligned}$$

10–23. It is sometimes advantageous to have the thermal flux in a thermal reactor flat, i.e., constant in the fueled regions of the reactor. One way in which this can be done is by nonuniformly loading the fuel in an otherwise uniform reactor core. (a) Using the two-group model, show that the fuel distribution for flat thermal flux in a slab reactor of thickness  $a$  with an infinite reflector is given by

$$\Sigma_{2F}(x) = \frac{D_{2r}\kappa_{2r}(\kappa_{1r} + \kappa_{2r}) \cos \gamma x}{\gamma \tau_c \kappa_{1r} \sin(\gamma a/2)} + \frac{\Sigma_{2Mc}}{\eta_T - 1},$$

where  $\Sigma_{2F}$  and  $\Sigma_{2Mc}$  are the macroscopic absorption cross sections of the fuel and moderator (in the core) respectively,

$$\gamma^2 = \frac{\eta_T - 1}{\tau_c},$$

and the other symbols have their usual meanings. (b) Show that the critical thickness of the core is

$$a = \frac{2}{\gamma} \cot^{-1} \left[ \frac{D_{1r}\gamma}{D_{1r}\kappa_{1r}} - \frac{\eta_T \tau_c \Sigma_{2M} c \kappa_{1r} \gamma}{(\eta_T - 1) D_{2r} \kappa_{2r} (\kappa_{1r} + \kappa_{2r})} \right].$$

(c) Using the formulas as derived in (a) and (b) plot the fuel distribution, the fast and slow fluxes, and the power density for a slab reactor having a graphite core and graphite reflector and fueled with  $\text{U}^{235}$ . (d) Compare the critical mass in (c) with that of a uniform slab reactor of the same thickness. [It can be shown that the reactor with flat thermal flux *always* has a smaller critical mass than the uniform reactor. This is known as *Goertzel's theorem*; G. Goertzel, *J. Nuclear Energy* 2, 193 (1956).]

10-24. Choose appropriately-sized groups and estimate the three-group elastic transfer cross sections for the following moderators. (These group constants are to be used for computations of a *thermal* reactor.)

(a) Graphite      (b) Be      (c) BeO      (d)  $\text{D}_2\text{O}$

10-25. Show that if all groups are of the same width,  $U$ , in lethargy, the group transfer cross sections for hydrogen are given by

$$\Sigma_s(g \rightarrow h) = \frac{4\Sigma_{sg} e^{(g-h)}}{U} \sinh^2 \frac{U}{2}.$$

10-26. Consider a nondirectly coupled multigroup calculation in which all groups are of the same lethargy width,  $U$ , and in which neutrons can skip one (and only one) group. (a) Show that if the scattering is isotropic in the center-of-mass system the elastic transfer cross sections are given by

$$\begin{aligned} \Sigma_s(g \rightarrow g+1) &= \frac{\Sigma_{sg}}{U} \left[ \frac{2}{1-\alpha} (1 - \alpha U - e^{-U}) - \xi \right], \\ \Sigma_s(g \rightarrow g+2) &= \frac{\Sigma_{sg}}{U} \left[ \frac{1}{1-\alpha} (e^U + \alpha U - 1) + \xi \right], \\ \Sigma_s(g \rightarrow g+h) &= 0, \quad h > 2. \end{aligned}$$

(b) Compute  $\Sigma_s(g \rightarrow g)$ , the cross section for a neutron interacting in and remaining within the  $g$ th group. (c) Compute and interpret the sum  $\Sigma_s(g \rightarrow g) + \Sigma_s(g \rightarrow g+1) + \Sigma_s(g \rightarrow g+2)$ .

10-27. (a) Using the group constants given in Table 10-5,\* compute the critical radius and critical mass of a bare sphere of  $\text{Pu}^{239}$ . (b) Make a histogram plot of the energy-dependent flux in the reactor. (c) Would you classify this as a fast, intermediate, or thermal reactor? [Hint: By an appropriate change of variables in the multigroup equations, it will be seen that it is not necessary to convert to macroscopic cross sections until the end of the computation.]

10-28. A hypothetical fast reactor consists of a bare square-cylindrical tank, containing liquid sodium coolant and a uniform array of uranium fuel elements. The uranium is enriched to 25.6% in  $\text{U}^{235}$ , and the uranium-sodium volume ratio is 0.6. At the design

---

\* See next page.

**Table 10-5**  
**Multigroup Constants for Pu<sup>239</sup> (Microscopic Cross Sections in Barns)\***

g	Energy Range, MeV	$\nu$	$\chi$	$\sigma_{tr}$	$\sigma_f$	$\sigma_\gamma$	$\sigma(g \rightarrow h)$				
							$h = 2$	3	4	5	6
1	3.0– $\infty$	3.48	0.204	4.25	1.90	0.03	0.20	0.27	0.45	0.31	0.04
2	1.4–3.0	3.09	0.344	4.50	1.95	0.05	—	0.18	0.50	0.35	0.05
3	0.9–1.4	2.99	0.168	4.80	1.83	0.07	—	—	0.45	0.30	0.06
4	0.4–0.9	2.93	0.180	5.70	1.70	0.11	—	—	—	0.29	0.05
5	0.1–0.4	2.88	0.090	8.40	1.67	0.17	—	—	—	—	0.05
6	0.0–0.1	2.86	0.014	12.0	2.05	0.50	—	—	—	—	—

\* From ANL-5800, First Edition, p. 420.

**Table 10-6**  
**Three-Group Constants (Microscopic Cross Sections in Barns)\***

g	Energy Range, MeV	$\chi$	$U^{235}$					
			$\nu$	$\sigma_f$	$\sigma_\gamma$	$\sigma_{tr}$	$\sigma(g \rightarrow g + 1)$	$\sigma(g \rightarrow g + 2)$
1	1.35– $\infty$	0.575	2.7	1.29	0.08	4.5	1.00	0.50
2	0.4–1.35	0.326	2.53	1.27	0.13	5.7	0.50	—
3	0–0.4	0.099	2.47	1.77	0.49	10.0	—	—

$U^{238}$						
$g$	$\nu$	$\sigma_f$	$\sigma_\gamma$	$\sigma_{tr}$	$\sigma(g \rightarrow g + 1)$	$\sigma(g \rightarrow g + 2)$
1	2.6	0.524	0.036	4.6	1.41	0.64
2	2.47	0.01	0.13	5.8	0.25	—
3	—	—	0.26	9.6	—	—

$Na$				
$g$	$\sigma_\gamma$	$\sigma_{tr}$	$\sigma(g \rightarrow g + 1)$	$\sigma(g \rightarrow g + 2)$
1	0.0005	2.0	0.24	0.06
2	0.001	3.2	0.18	—
3	0.001	3.7	—	—

\* From ANL-5800, Second Edition, p. 581.

power level of 300 MW(th) the average temperature of the sodium is 750°F and its density is 53 lb/ft<sup>3</sup> (0.85 gm/cm<sup>3</sup>). (a) Using the data in Table 10-6, compute the critical size and critical mass ( $U^{235}$ ) of the reactor. (b) Compute the three-group fluxes in the reactor. (c) What fraction of the power is due to fissions in  $U^{238}$ ? (Assume that the recoverable energies/fission of  $U^{235}$  and  $U^{238}$  are both 200 MeV.) (d) At what rates are  $U^{235}$  and  $U^{238}$  consumed? (e) What is the conversion ratio at startup of the reactor? (f) At what rate is  $Pu^{239}$  produced in the entire reactor at startup? (g) Compute the saturation activity of the sodium [ $T_{1/2}(Na^{24}) = 15$  hr] in curies/cm<sup>3</sup>. [Note: This reactor is similar to the core of the Fermi Fast Breeder Reactor (cf. Section 4-4).]

10-29. The core of a spherical thermal reactor is 40 cm in radius and contains a uniform mixture of  $U^{233}$  and  $H_2O$ . Surrounding the core is an infinite  $H_2O$  reflector. The system operates at a power of 25 MW(th) at 150°C. The reflector savings for the reactor is known to be 3.0 cm. (a) Using two-group theory, find the critical mass of  $U^{235}$ . (b) Estimate the maximum fast and thermal fluxes.

10-30. Using one-group theory find an expression for the reflector savings of a reflected spherical reactor, and show that in the limit of infinite reflector thickness,  $\delta$  goes to the planar value, provided the radius of the core is sufficiently large.

10-31. Show that if the reflector savings is small compared with the dimensions of the reactor core,  $\delta$  is given approximately by the general formula

$$\delta \approx -\frac{\bar{D}_c L_r}{\bar{D}_r} \frac{\phi_r(a/L_r)}{\phi'_r(a/L_r)},$$

where  $\phi_r$  is the flux in the reflector,  $a$  is the reactor radius, or half-thickness in the case of the slab reactor, and the other symbols have their usual meanings.

10-32. Using one-group theory, find the critical mass of a square cylindrical reactor 100 cm high containing a uniform mixture of beryllium and  $U^{235}$  which is surrounded on all sides by an infinite beryllium reflector. Compare your answer with the critical mass of a reflected spherical reactor of the same core volume.

10-33. Discuss the application of the pulsed-neutron technique to measurements of the properties of a subcritical assembly having  $k_\infty < 1$ . In particular, what does the curve of  $\lambda$  versus  $B^2$  look like in this case?

# 11

## Heterogeneous Reactors

A reactor is said to be *heterogeneous* if the neutron mean free path at some energy is comparable to or less than the thickness of a fuel element. In this case, the flux distribution in the fuel may be substantially different from what it is in the moderator. This introduces complications into the analysis of a heterogeneous reactor which are not found in the analysis of homogeneous systems. A number of special methods have been developed for calculations of heterogeneous reactors, and some of the more elementary of these are considered in the present chapter. Ordinarily, only thermal reactors are heterogeneous and the discussion will be confined to these systems.

A large variety of fuel elements have been used in heterogeneous reactors. These often consist of plates or rods of natural uranium or uranium enriched in  $U^{235}$ , which are wrapped in some sort of cladding material. On the other hand, they may be an alloy of uranium and some structural material. Sometimes, hollow tubes filled with pellets of uranium oxide ( $UO_2$ ) are used. In any event, fuel elements generally consist of a mixture of fissile and nonfissile isotopes. Except for "clean" fuel elements, that is, fuel elements that have not been exposed to a neutron flux, various fission product poisons and newly produced isotopes such as  $U^{236}$  or  $Pu^{239}$  are also present. In discussing heterogeneous reactors, it will be convenient to refer to the entire fuel element as "fuel." Thus for the fuel elements described above, the "fuel" includes both the fissile and nonfissile isotopes of uranium, the oxygen in the  $UO_2$ , the structural materials, fission products, cladding,\* etc.

In many ways the analysis of a heterogeneous reactor is much like that of a homogeneous reactor. It is possible, for example, to define a multiplication factor for an infinite heterogeneous assembly as the number of fissions in one generation per fission in the preceding generation. Also, as in the homogeneous case, it is assumed that thermal neutron absorption, resonance absorption, and fast fission are processes which occur in more or less separate energy regions, so that it is possible to write  $k_\infty = \eta_T f_p \epsilon$ , where each of the four factors has essentially the same meaning as for a homogeneous reactor. However, these factors cannot be

---

\* In many treatments the cladding is handled separately (cf. Prob. 11-7).

computed from the formulas developed earlier for a homogeneous reactor, and much of the present chapter will be devoted to the derivation of new formulas appropriate for heterogeneous systems.

Once an expression for  $k_\infty$  is known, the critical size or composition of a heterogeneous reactor can be determined using one of the methods given in the preceding two chapters. For instance, if age theory is valid and the reactor is bare (or if the reflector savings is included to obtain the equivalent bare reactor), the critical equation is

$$\frac{k_\infty e^{-B^2\tau_T}}{1 + B^2L_T^2} = 1,$$

where appropriate values of  $\tau_T$  and  $L_T^2$  for a heterogeneous system must be used. On the other hand, if the reactor is reflected or consists of a number of regions of different composition, the requirements for criticality can be found from two-group or multigroup calculations.

### 11-1 Eta

By definition,  $\eta_T$  is equal to the average number of fission neutrons emitted per thermal neutron absorbed in fuel. Thus if the fuel consists of a mixture of fissile and nonfissile isotopes,  $\eta_T$  is given by

$$\eta_T = \frac{\sum \nu_n \bar{\Sigma}_{fn}}{\bar{\Sigma}_a}, \quad (11-1)$$

where  $\nu_n$  is the number of neutrons emitted per thermal fission in the  $n$ th isotope,  $\bar{\Sigma}_{fn}$  is the average thermal macroscopic fission cross section for this isotope, and  $\bar{\Sigma}_a$  is the average thermal absorption cross section for the fuel mixture. As explained in Chapter 8, the value of a thermal cross section depends upon the thermal neutron spectrum, and this spectrum must be known within the fuel in order to be able to calculate  $\eta_T$ . It is somewhat more difficult to obtain the spectrum in this case, however, than for the homogeneous systems discussed in Chapter 8. This is true because the neutrons in a heterogeneous reactor thermalize primarily in the moderator and then pass into the fuel. As a result, the neutron spectrum varies with position within the fuel, and can only be determined by elaborate space-dependent thermalization calculations. These calculations are beyond the scope of this book, and it will be assumed in this chapter that the thermal neutron spectrum in the fuel is Maxwellian and independent of position. The cross sections in Eq. (11-1) are then given by Eqs. (8-40) and (8-42).

### 11-2 Thermal Utilization

The thermal utilization is defined as the fraction of the thermal neutrons which are absorbed by the fuel in an infinite lattice of fuel lumps and moderator. The product  $\eta_T f$ , where  $\eta_T$  is defined in the preceding section, is then equal to the average number

of fission neutrons produced in thermal fission per thermal neutron absorbed in the infinite reactor. It follows from its definition that  $f$  is given by

$$f = \frac{\int \Sigma_{aF}(r)\phi(r) dV}{\int [\Sigma_{aF}(r) + \Sigma_{aM}(r)]\phi(r) dV}, \quad (11-2)$$

where  $\phi(r)$  is the thermal\* flux,  $\Sigma_{aF}(r)$  and  $\Sigma_{aM}(r)$  are the thermal\* macroscopic absorption cross sections of the fuel and moderator, respectively, and the integrations are carried out over the entire (infinite) reactor volume. Since in a heterogeneous reactor the fuel and moderator are separate, homogeneous regions, the quantities  $\Sigma_{aF}$  and  $\Sigma_{aM}$  are constants in their respective regions and Eq. (11-2) becomes

$$f = \frac{\Sigma_{aF} \int_{V_F} \phi(r) dV}{\Sigma_{aF} \int_{V_F} \phi(r) dV + \Sigma_{aM} \int_{V_M} \phi(r) dV}, \quad (11-3)$$

where  $V_F$  and  $V_M$  are the volumes of the fuel and moderator, respectively.

Equation (11-3) can be written more conveniently in terms of the average flux in the fuel,  $\bar{\phi}_F$ , and the average flux in the moderator,  $\bar{\phi}_M$ . These are defined as

$$\bar{\phi}_F = \frac{1}{V_F} \int_{V_F} \phi(r) dV \quad (11-4)$$

and

$$\bar{\phi}_M = \frac{1}{V_M} \int_{V_M} \phi(r) dV. \quad (11-5)$$

Inserting these quantities into Eq. (11-3) gives

$$f = \frac{\Sigma_{aF} V_F \bar{\phi}_F}{\Sigma_{aF} V_F \bar{\phi}_F + \Sigma_{aM} V_M \bar{\phi}_M} \quad (11-6)$$

or

$$f = \frac{\Sigma_{aF} V_F}{\Sigma_{aF} V_F + \Sigma_{aM} V_M (\bar{\phi}_M / \bar{\phi}_F)}. \quad (11-7)$$

If the average values of the flux in the fuel and moderator were identical, the ratio  $\bar{\phi}_M/\bar{\phi}_F$  would be equal to unity and Eq. (11-7) would reduce to the thermal utilization of the equivalent homogeneous system.† Thermal neutrons are absorbed more strongly by the fuel than by the moderator, however, and the thermal flux is therefore depressed within the fuel as indicated in Fig. 11-1. As a result,  $\bar{\phi}_F$

\* Throughout this section, the subscripts and bar averages denoting thermal values will be omitted.

† Note that  $\Sigma_{aF} V_F$  and  $\Sigma_{aM} V_M$  are the total absorption cross sections of fuel and moderator, respectively. The thermal utilization for the equivalent homogeneous mixture is therefore  $\Sigma_{aF} V_F / (\Sigma_{aF} V_F + \Sigma_{aM} V_M)$ .

is always somewhat less than  $\bar{\phi}_M$ , the quantity  $\bar{\phi}_M/\bar{\phi}_F$  is greater than unity, and from Eq. (11-7) it follows that *the thermal utilization of a heterogeneous system is less than that of a homogeneous mixture of the same materials.* For this reason, the ratio

$$\frac{\bar{\phi}_M}{\bar{\phi}_F} = \xi \quad (11-8)$$

is known as the *thermal disadvantage factor*.

This result can be viewed in another way. Since in a heterogeneous lattice the neutrons thermalize in the moderator and then pass into the fuel, the depression of the flux in the fuel is clearly caused by the absorption of some of the incoming neutrons by the nuclei near the surface of the lump. The nuclei in the interior regions of the lump are thus to some extent shielded by nuclei lying nearer to the surface. This phenomenon, which also has an important bearing on the resonance escape probability of a heterogeneous reactor, is called *self-shielding*.

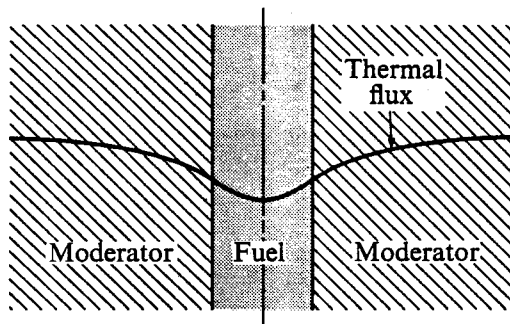


Fig. 11-1. Thermal neutron flux in and near a fuel rod.

It will be evident from the above formulas that  $f$  can be calculated once the thermal flux is known throughout the fuel and the moderator. Unfortunately, the flux cannot be found exactly except by elaborate numerical computations. Several approximate analytical methods have been derived which provide some good estimates of  $f$ , and two of the more widely used of these methods will be considered.

**Method of diffusion theory.** This is the oldest and probably one of the least reliable methods for computing the thermal utilization. The method is based on the assumption that diffusion theory is valid in the fuel as well as in the moderator. Several additional assumptions must be made in order to calculate  $f$  analytically, but these ordinarily introduce less error into the calculation than the use of diffusion theory in the fuel.

The first of these additional assumptions is that the thermal slowing-down density,  $q$ , is zero within the fuel. This is reasonable, physically, for although heavy fuel nuclei can moderate neutrons at high energy by inelastic scattering, these nuclei are not effective in slowing down neutrons near thermal energies.

It is also assumed that the thermal slowing-down density in the moderator is a constant, independent of position. The justification for this assumption lies in the

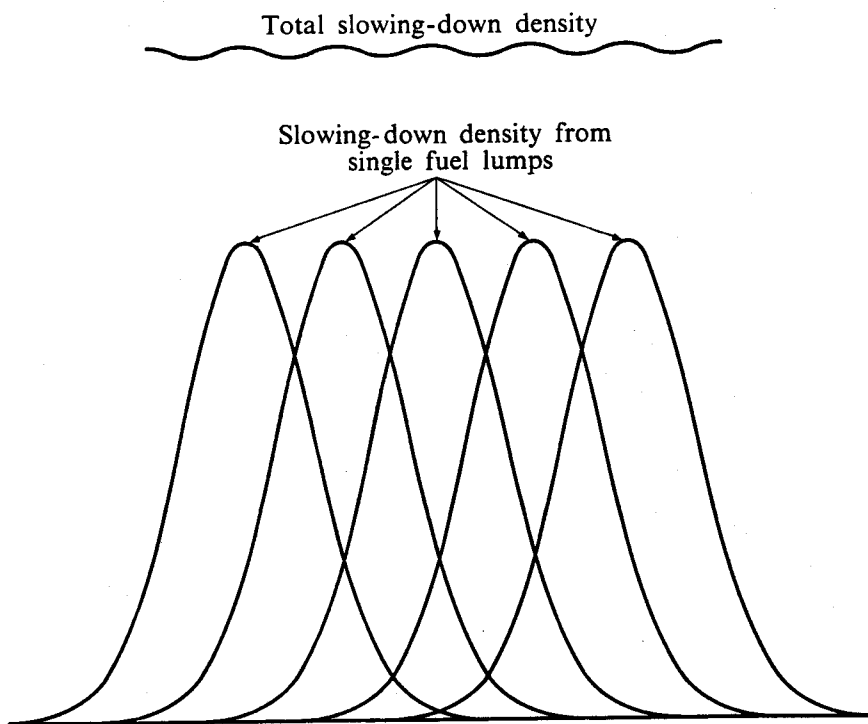


**Fig. 11-2.** The slowing-down density from individual fuel lumps and the total slowing-down density in a heterogeneous lattice.

fact that each fuel lump is the source of fast neutrons which slow down in the surrounding moderator. If age theory is valid, for instance, the thermal slowing-down distribution surrounding each lump is a Gaussian. Then if the distance between the centers of nearest lumps, which is called the *lattice spacing*, or *lattice pitch*, is small compared with the slowing-down distance  $\sqrt{\tau_T}$  these Gaussians overlap, as shown in Fig. 11-2, to produce a fairly constant value of  $q$ . (This assertion is discussed in Prob. 11-4.)

Next, it is convenient to divide the fuel-moderator lattice into *unit cells*, each containing one fuel lump at its center. Figure 11-3 shows two of the most commonly used lattices and the unit cells are indicated. Since all cells are identical in

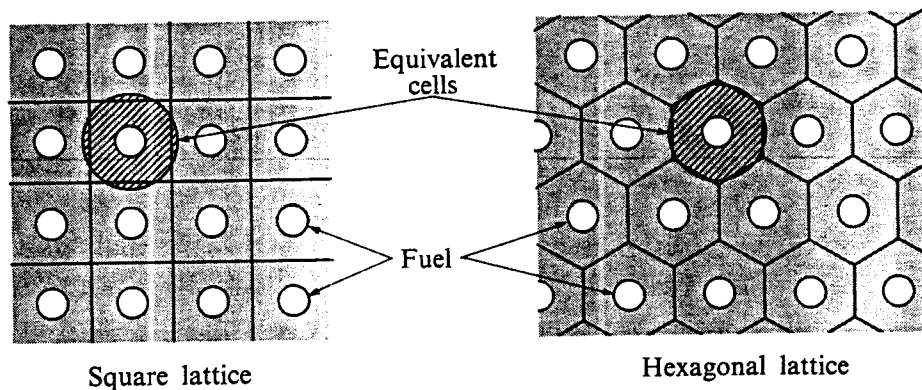


**Fig. 11-3.** Two typical heterogeneous lattices and equivalent cells for each.

an infinite uniform lattice, there can be no net flow of neutrons from one cell to another. It follows that *the current density is zero along the boundary of each cell.*

In order to calculate the flux within the cell it is necessary to replace the actual lattice cell by a cell having a somewhat more simple geometry. For instance, if the fuel lumps are in the form of cylinders, the actual cell is replaced by a cylindrical cell of the *same volume* as indicated in Fig. 11-3. Because there is no flow of thermal neutrons from one cell to another, the thermal neutron current may be taken to be zero on the surface of the equivalent cell. This procedure, of using an equivalent cell with a zero-current boundary condition, is known as the *Wigner-Seitz method*.

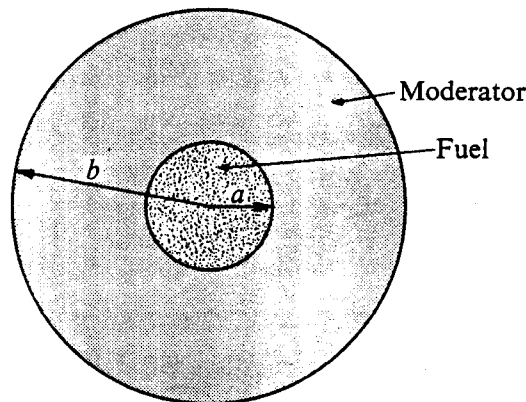


Fig. 11-4. Cylindrical equivalent cell.

With these assumptions the thermal flux throughout the equivalent cell can easily be computed by diffusion theory. Consider, for example, a cylindrical fuel rod of radius  $a$  in a cylindrical cell of radius  $b$  as shown in Fig. 11-4. The diffusion equations for the fluxes in the fuel and moderator are, respectively,

$$D_F \nabla^2 \phi_F - \Sigma_{aF} \phi_F = 0, \quad 0 < r < a, \quad (11-9)$$

and

$$D_M \nabla^2 \phi_M - \Sigma_{aM} \phi_M + q = 0, \quad a < r < b, \quad (11-10)$$

where  $D_F$  and  $D_M$  are the thermal diffusion coefficients for the fuel and moderator,  $\Sigma_{aF}$  and  $\Sigma_{aM}$  are the thermal absorption cross sections for the two regions, and  $q$  is the (constant) thermal slowing-down density in the moderator.

Dividing Eq. (11-9) by  $D_F$  and Eq. (11-10) by  $D_M$  yields

$$\nabla^2 \phi_F - \kappa_F^2 \phi_F = 0, \quad 0 < r < a \quad (11-11)$$

and

$$\nabla^2 \phi_M - \kappa_M^2 \phi_M + \frac{q}{D_M} = 0, \quad a < r < b, \quad (11-12)$$

where  $\kappa_F$  and  $\kappa_M$  are the reciprocals of the thermal diffusion lengths of fuel and moderator, respectively.

Because of the symmetry of the problem the fluxes are only a function of  $r$ , so that when the Laplacian is written in cylindrical coordinates Eqs. (11-11) and

(11-12) reduce to

$$\frac{d^2\phi_F}{dr^2} + \frac{1}{r} \frac{d\phi_F}{dr} - \kappa_F^2 \phi_F = 0, \quad 0 < r < a, \quad (11-13)$$

and

$$\frac{d^2\phi_M}{dr^2} + \frac{1}{r} \frac{d\phi_M}{dr} - \kappa_M^2 \phi_M + \frac{q}{D_M} = 0, \quad a < r < b. \quad (11-14)$$

Equation (11-13) will be recognized as the modified Bessel equation of zero order (cf. Appendix II), whose two independent solutions are  $I_0(\kappa_F r)$  and  $K_0(\kappa_F r)$ . However, the function  $K_0(\kappa_F r)$  is singular at  $r = 0$ , and since  $\phi_F$  must remain finite as  $r$  approaches zero, the solution to Eq. (11-13) is taken to be

$$\phi_F(r) = A I_0(\kappa_F r), \quad 0 < r < a, \quad (11-15)$$

where  $A$  is a constant to be determined.

Since Eq. (11-14) is inhomogeneous,  $\phi_M$  is the sum of the solutions to the homogeneous equation plus a particular solution. The homogeneous equation has the solution

$$A' I_0(\kappa_M r) + C' K_0(\kappa_M r),$$

and it is easy to see by direct substitution that the quantity  $q/\Sigma_{aM}$  is a particular solution. Hence  $\phi_M$  can be written as

$$\phi_M(r) = A' I_0(\kappa_M r) + C' K_0(\kappa_M r) + q/\Sigma_{aM}, \quad a < r < b. \quad (11-16)$$

The values of the constants  $A$ ,  $A'$ , and  $C'$  can be found in the usual way from the boundary conditions. It is convenient first to satisfy the boundary condition at the edge of the cell, that is, at  $r = b$ . Since the current there is zero, Eq. (11-16) gives

$$\phi'_M(b) = 0 = \kappa_M [A' I'_0(\kappa_M b) + C' K'_0(\kappa_M b)]. \quad (11-17)$$

With the identities (cf. Appendix II)

$$I'_0(x) = I_1(x), \quad K'_0(x) = -K_1(x), \quad (11-18)$$

Eq. (11-17) gives

$$C' = \frac{A' I_1(\kappa_M b)}{K_1(\kappa_M b)}.$$

By inserting this result into Eq. (11-16),  $\phi_M(r)$  becomes

$$\phi_M(r) = C [I_0(\kappa_M r) K_1(\kappa_M b) + K_0(\kappa_M r) I_1(\kappa_M b)] + q/\Sigma_{aM}, \quad (11-19)$$

where the new constant

$$C = \frac{A'}{K_1(\kappa_M b)}$$

has been introduced.

The two constants,  $A$  and  $C$ , remain undetermined and these can be found from the requirement that the flux and current be continuous at the fuel-moderator interface. Continuity of flux gives

$$AI_0(\kappa_F a) = C[I_0(\kappa_M a)K_1(\kappa_M b) + K_0(\kappa_M a)I_1(\kappa_M b)] + q/\Sigma_{aM}, \quad (11-20)$$

while continuity of current gives

$$AD_F \kappa_F I'_0(\kappa_F a) = CD_M \kappa_M [I'_0(\kappa_M a)K_1(\kappa_M b) + K'_0(\kappa_M a)I_1(\kappa_M b)], \quad (11-21)$$

which, by using again the identities in Eq. (11-18), may be written as

$$AD_F \kappa_F I_1(\kappa_F a) = CD_M \kappa_M [I_1(\kappa_M a)K_1(\kappa_M b) - K_1(\kappa_M a)I_1(\kappa_M b)]. \quad (11-22)$$

Equations (11-20) and (11-22) are a pair of linear algebraic equations which uniquely determine  $A$  and  $C$ . As it turns out, only one constant is needed to determine  $f$  and it is more convenient to compute  $A$  (or rather  $1/A$ ) than  $C$ . This is readily found to be

$$\frac{1}{A} = \frac{\Sigma_{aM}}{q} \left\{ I_0(\kappa_F a) - \frac{D_F \kappa_F I_1(\kappa_F a)[I_0(\kappa_M a)K_1(\kappa_M b) + K_0(\kappa_M a)I_1(\kappa_M b)]}{D_M \kappa_M [I_1(\kappa_M a)K_1(\kappa_M b) - K_1(\kappa_M a)I_1(\kappa_M b)]} \right\}. \quad (11-23)$$

The thermal utilization can now be calculated by noting that because there is no net flow of neutrons across the outer boundary of the cell, the number of neutrons slowing down within the cell per unit time must be equal to the number which are absorbed per unit time by the fuel and moderator in the cell. It follows that the thermal utilization is the ratio of the number of neutrons absorbed in the fuel to the number slowing down within the cell. The latter number can easily be computed since the slowing-down density has been assumed to be constant in the moderator and zero in the fuel. Thus, per unit length of the cell and per unit time,

$$\text{Number of neutrons slowing down in cell} = \pi(b^2 - a^2)q. \quad (11-24)$$

The number of neutrons absorbed per unit length of the fuel per unit time is given by the integral

$$\text{Number of neutrons absorbed in fuel} = 2\pi \Sigma_{aF} \int_0^a \phi_F(r)r dr. \quad (11-25)$$

By introducing Eq. (11-15), this becomes

$$\begin{aligned} \text{Number of neutrons absorbed in fuel} &= 2\pi \Sigma_{aF} A \int_0^a I_0(\kappa_F r)r dr \\ &= \frac{2\pi \Sigma_{aF} A a}{\kappa_F} I_1(\kappa_F a), \end{aligned} \quad (11-26)$$

where use has been made of the identity

$$\int_0^x I_0(x)x dx = xI_1(x).$$

**Table 11-1**  
**Lattice Functions for Planar and Spherical Geometry**

Geometry	<i>F</i>	<i>E</i>
Planar*	$\kappa_F a \coth \kappa_F a$	$\kappa_M(b - a) \coth \kappa_M(b - a)$
Spherical†	$\frac{\kappa_F^2 a^2}{3} \frac{\tanh \kappa_F a}{\kappa_F a - \tanh \kappa_F a}$	$\frac{\kappa_M^3 (b^3 - a^3)}{3 \kappa_M a} \left[ \frac{1 - \kappa_M b \coth \kappa_M(b - a)}{1 - \kappa_M^2 ab - \kappa_M(b - a) \coth \kappa_M(b - a)} \right]$

\* Slab fuel half-thickness  $a$ ; slab cell half-thickness  $b$ .

† Spherical fuel radius  $a$ ; spherical cell radius  $b$ .

**Table 11-2**  
**Thermal Diffusion Lengths of Fuels\***

Fuel	Reference density (gm/cm <sup>3</sup> )	$L_F$ (cm)	$\kappa_F$ (cm <sup>-1</sup> )
Natural uranium	18.9	1.55	0.645
$U_3O_8$	6.0	3.7	0.27
Thorium	11.2	2.7	0.37
$ThO_2$	6.0	4.1	0.24

\* Based on experiments performed in 1944 by R. S. Mulliken, *et al.*, CL-697 (the "Chicago Handbook"). These measurements apparently have not been repeated since that time.

If Eq. (11-26) is divided by Eq. (11-24), the thermal utilization is found to be

$$f = \frac{2 \Sigma_{aF} A a I_1(\kappa_F a)}{\kappa_F(b^2 - a^2) q}. \quad (11-27)$$

The ratio  $A/q$  is given by Eq. (11-23) so that  $f$ , or rather  $1/f$ , becomes

$$\frac{1}{f} = \frac{\Sigma_{aM} \kappa_F (b^2 - a^2)}{2 \Sigma_{aF} a} \left\{ \frac{I_0(\kappa_F a)}{I_1(\kappa_F a)} + \frac{D_F \kappa_F [I_0(\kappa_M a) K_1(\kappa_M b) + K_0(\kappa_M a) I_1(\kappa_M b)]}{D_M \kappa_M [I_1(\kappa_M b) K_1(\kappa_M a) - K_1(\kappa_M b) I_1(\kappa_M a)]} \right\}. \quad (11-28)$$

By introducing the *lattice functions* defined by

$$F(\kappa_F a) = \frac{\kappa_F a I_0(\kappa_F a)}{2 I_1(\kappa_F a)}, \quad (11-29)$$

$$E(\kappa_M a, \kappa_M b) = \frac{\kappa_M(b^2 - a^2)}{2a} \left[ \frac{I_0(\kappa_M a) K_1(\kappa_M b) + K_0(\kappa_M a) I_1(\kappa_M b)}{I_1(\kappa_M b) K_1(\kappa_M a) - K_1(\kappa_M b) I_1(\kappa_M a)} \right], \quad (11-30)$$

and noting that the ratio of the volumes of moderator and fuel is

$$\frac{V_M}{V_F} = \frac{\pi(b^2 - a^2)}{\pi a^2}, \quad (11-31)$$

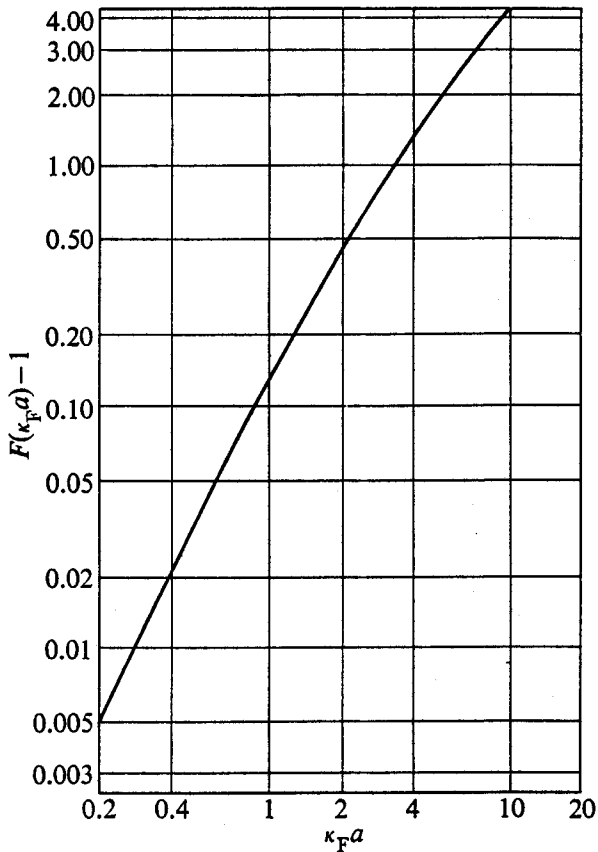


Fig. 11-5. The lattice function  $F(\kappa_F a) - 1$  for cylindrical rods. [From *The Reactor Handbook*, Vol. 1, p. 517, U. S. Atomic Energy Commission Report AECD-3645 (1955).]

Eq. (11-28) can be put in the following standard form:

$$\frac{1}{f} = \frac{\Sigma_{aM} V_M}{\Sigma_{aF} V_F} F(\kappa_F a) + E(\kappa_M a, \kappa_M b). \quad (11-32)$$

Although the above derivation was carried out for cylindrical fuel rods, an expression of the same form as Eq. (11-32) is found to hold for other geometries. The lattice functions are different, of course, and these are given in Table 11-1 for two other lattice geometries. It should be noted that in every case the  $F$  function depends only upon the diffusion length and the radius of the fuel, while  $E$  depends upon the diffusion length and the inner and outer radii of the moderator. Values of moderator diffusion lengths have been given in Table 8-3; those for the common fuels and breeding materials are given in Table 11-2. The  $F$  and  $E$  functions for cylindrical geometry are also shown in Figs. 11-5 and 11-6.

It is interesting to examine the physical significance of the lattice functions. The  $F$  function can readily be shown to be equal to the ratio of the flux at the surface of the fuel to the average value of the flux within the fuel. With cylindrical fuel rods, for example, the average flux  $\bar{\phi}_F$  is

$$\bar{\phi}_F = \frac{2\pi}{V_F} \int_0^a \phi_F(r) r dr = \frac{2\pi A}{V_F} \int_0^a I_0(\kappa_F r) r dr = \frac{2A}{\kappa_F a} I_1(\kappa_F a).$$

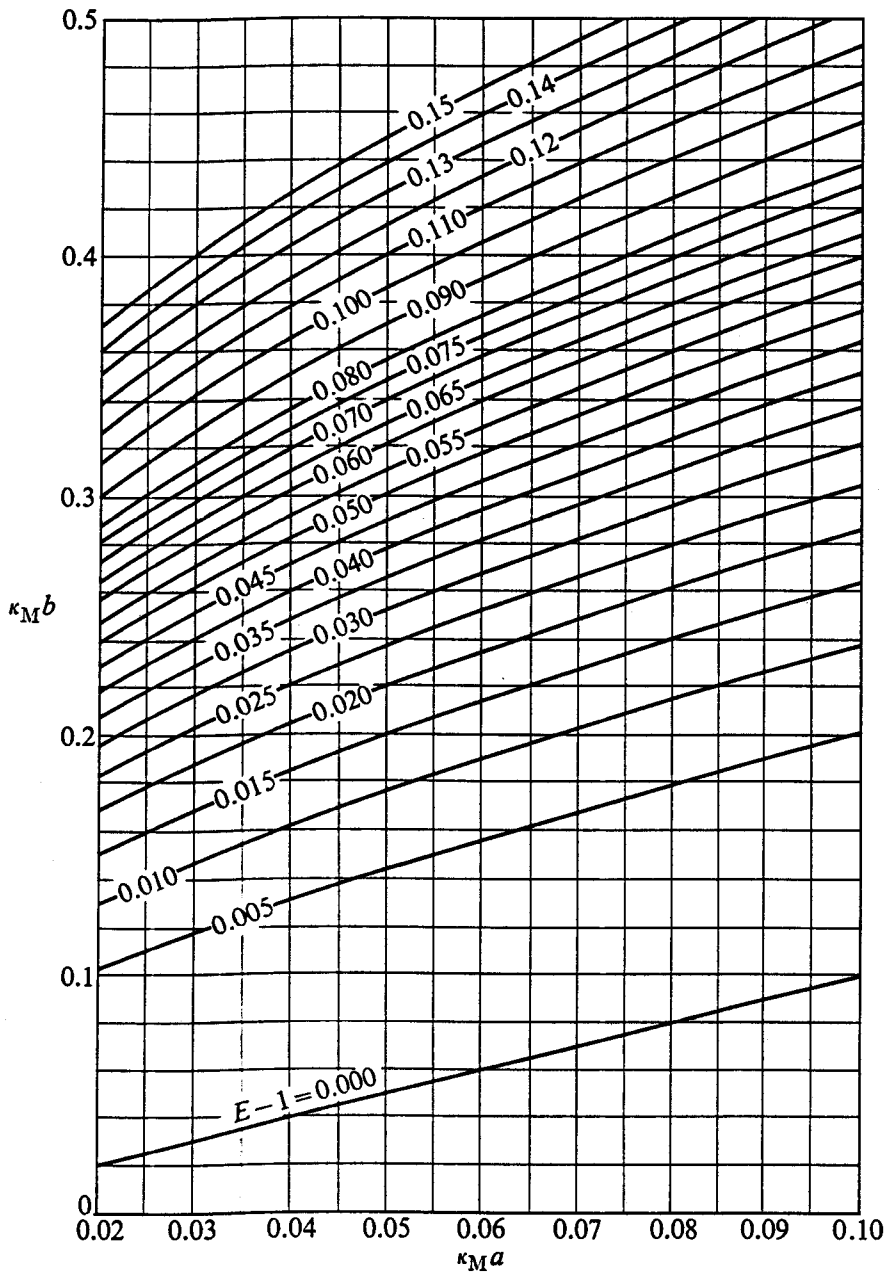


**Fig. 11-6.** Contours of the lattice function  $E(\kappa_M a, \kappa_M b) - 1$  for cylindrical rods. [From *The Reactor Handbook*, Vol. 1, p. 518, U. S. Atomic Energy Commission Report AECD-3645 (1955).]

The ratio in question is therefore

$$\frac{\phi_F(a)}{\bar{\phi}_F} = \frac{\kappa_F a I_0(\kappa_F a)}{2I_1(\kappa_F a)} = F(\kappa_F a).$$

Since  $\bar{\phi}_F < \phi_F(a)$ , it follows that  $F$  is always greater than unity.

The interpretation of the  $E$  function is somewhat more complicated. It will be recalled that the total number of neutrons which are absorbed per second by the

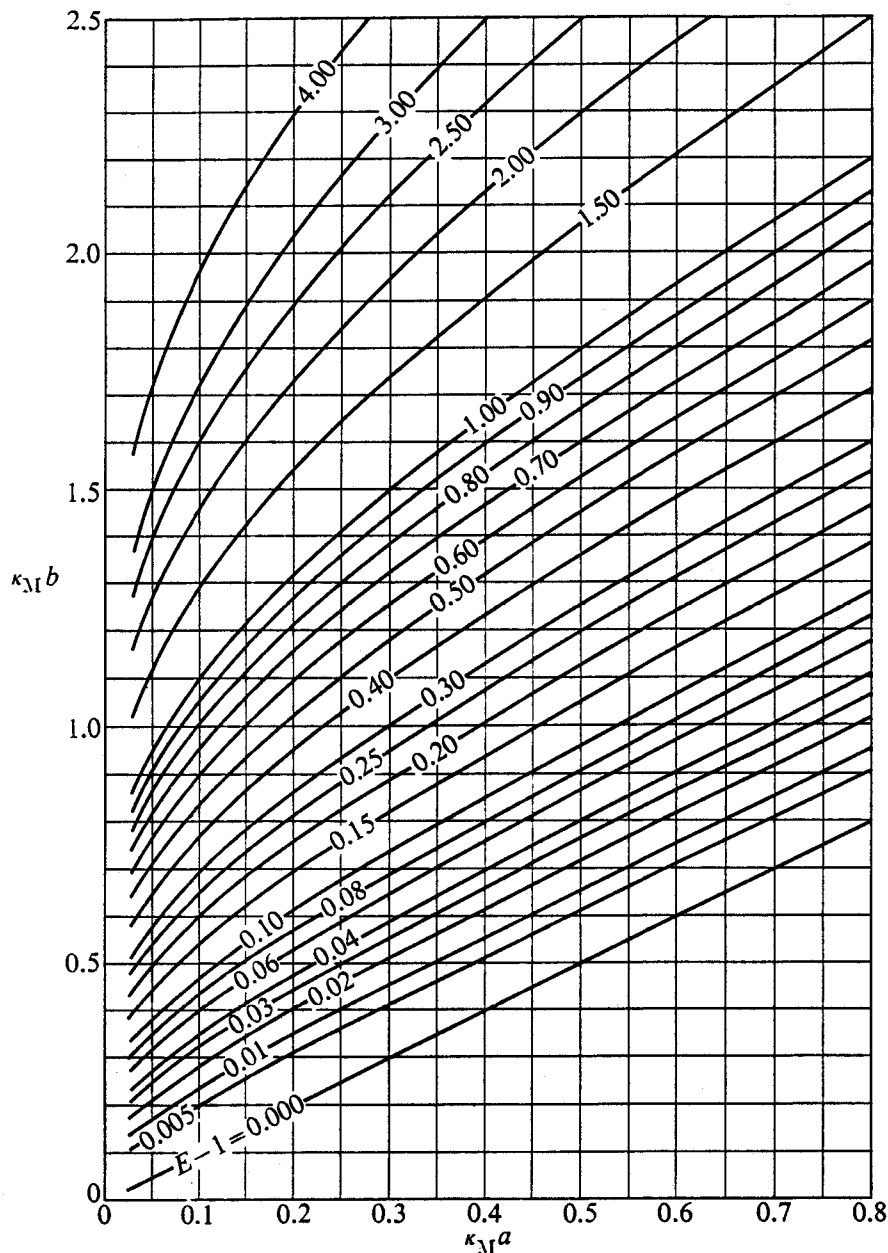


Figure 11-6 (Continued)

fuel and moderator is equal to  $qV_M$  (cf. Eq. 11-24). Then since there is no net flow of neutrons across the cell boundary the number of neutrons absorbed by the moderator is  $qV_M$  minus the number which flow into the fuel. Using Fick's law, the latter number is  $2\pi a D_M \phi'_M(a)$ ,\* so that  $qV_M - 2\pi a D_M \phi'_M(a)$  neutrons are absorbed per second in the moderator. If the flux throughout the moderator were equal to its value at the surface of the fuel, the absorption in the moderator would

\* There is no minus sign on this expression since this is the number of neutrons flowing in the *negative r* direction.

be  $V_M \Sigma_{aM} \phi_M(a)$ . The number of neutrons actually absorbed in excess of the number which would be absorbed if the flux were equal to  $\phi_M(a)$  is therefore

$$\text{Excess absorption in moderator} = [qV_M - 2\pi a D_M \phi'_M(a)] - V_M \Sigma_{aM} \phi_M(a).$$

Dividing by the number of neutrons absorbed in the fuel gives

$$\frac{\text{Excess absorption in moderator}}{\text{Absorption in fuel}} = -1 + \frac{V_M[q - \Sigma_{aM} \phi_M(a)]}{2\pi a D_M \phi'_M(a)}.$$

When Eq. (11-19) is substituted into the second term of this expression, this term reduces to the  $E$  function so that

$$\frac{\text{Excess absorption in moderator}}{\text{Absorption in fuel}} = E - 1.$$

This is the interpretation of the  $E$  function: Per neutron absorbed by the fuel,  $E - 1$  is equal to the number of neutrons absorbed in the moderator in excess of the number which would be absorbed if the flux were constant and equal to its value at the fuel surface. As a rule, the flux does not vary rapidly with position in the moderator. Consequently,  $E - 1$  is generally small, and  $E$  is only slightly greater than unity. By contrast, the flux may dip substantially within the fuel and  $F$  may be much greater than unity. In the usual case, therefore, it is the  $F$  function and not the  $E$  function which is responsible for the decrease in the thermal utilization of a heterogeneous system.

Because of the usual limitations of diffusion calculations, the value of  $f$  computed from the above formulas can be substantially in error. In particular, exact numerical calculations show, and experimental measurements confirm, that diffusion theory underestimates the depression of the flux in the fuel. Thus the values of  $F$  computed from diffusion theory formulas tend to be too small, which leads to an overestimate of  $f$ . Nevertheless, the diffusion theory method has been widely used, particularly in calculations of  $f$  for natural uranium-graphite reactors.

**The method of Amouyal, Benoist, and Horowitz.** The thermal utilization can be calculated with good accuracy using a technique developed by Amouyal, Benoist, and Horowitz (see the references at the end of the chapter), hereinafter denoted as ABH. Many of the same simplifying assumptions are used in this method as in the diffusion method. Thus the calculations are carried out only for the equivalent cell, and the current is taken to be zero at the outer surface of this cell. Furthermore, the thermal slowing-down density is taken to be constant in the moderator and zero in the fuel. For reasons that will be clear in a moment, it is also necessary to assume that all the thermal neutrons in the cell have the same energy. However, diffusion theory is not assumed to be valid, at least not in the fuel.

To begin the calculation, let  $G(\mathbf{r}, \mathbf{r}')$  be the one velocity flux at  $\mathbf{r}$  due to a unit source at  $\mathbf{r}'$ ; that is,  $G(\mathbf{r}, \mathbf{r}')$  is the exact kernel or Green's function describing the

transport of neutrons within the cell. Now let  $\mathbf{r}$  and  $\mathbf{r}'$  be points which lie in the fuel and moderator, respectively. With the (constant) slowing-down density  $q$  treated as a source term in the usual way, the flux  $\phi(\mathbf{r})$  at the point  $\mathbf{r}$  in the fuel due to the neutrons which thermalize throughout the moderator in the cell is

$$\phi(\mathbf{r}) = q \int_{V_M} G(\mathbf{r}, \mathbf{r}') dV'.$$

The total number of neutrons absorbed per second in the fuel is

$$\Sigma_{aF} \int_{V_F} \phi(\mathbf{r}) dV = \Sigma_{aF} q \int_{V_F} dV \int_{V_M} G(\mathbf{r}, \mathbf{r}') dV',$$

and the thermal utilization is this number divided by  $qV_M$ , the total number of neutrons slowing down per second in the cell:

$$f = \frac{\Sigma_{aF}}{V_M} \int_{V_F} dV \int_{V_M} G(\mathbf{r}, \mathbf{r}') dV'. \quad (11-33)$$

Equation (11-33), which is exact, is now transformed using the *reciprocity theorem* (cf. Section 5-12). It will be recalled that according to this theorem, the one-velocity flux at  $\mathbf{r}$  due to a unit source at  $\mathbf{r}'$  is identical with the one-velocity flux produced at  $\mathbf{r}'$  when the source is moved to  $\mathbf{r}$ . In symbols, the reciprocity theorem is

$$G(\mathbf{r}, \mathbf{r}') = G(\mathbf{r}', \mathbf{r}). \quad (11-34)$$

It must be emphasized that this theorem is exact and does not depend upon the validity of diffusion theory.

Inserting Eq. (11-34) into Eq. (11-33) and changing the order of integration yields

$$f = \frac{\Sigma_{aF}}{V_M} \int_{V_M} dV' \int_{V_F} G(\mathbf{r}', \mathbf{r}) dV. \quad (11-35)$$

Since the second variable in  $G(\mathbf{r}', \mathbf{r})$  represents the source point, it will be observed that  $f$  is now written in terms of an integral over sources *within the fuel*. Thus the original problem in which the neutrons flow from the moderator into the fuel has been replaced by a more convenient problem in which the neutrons originate in the fuel and are absorbed in the moderator.

The integral

$$\int_{V_F} G(\mathbf{r}', \mathbf{r}) dV$$

in Eq. (11-35) is by definition equal to the flux at  $\mathbf{r}'$  in the moderator produced by *uniformly distributed* unit sources in the fuel, and the expression

$$P = \frac{\Sigma_{aM}}{V_F} \int_{V_M} dV' \int_{V_F} G(\mathbf{r}', \mathbf{r}) dV \quad (11-36)$$

is the probability that a neutron produced by such sources will ultimately be absorbed in the moderator. Since a neutron must escape from the fuel before it can be captured in the moderator, it is reasonable to assume that  $P$  is proportional to the probability,  $P_F$ , that a neutron, uniformly produced within the fuel, will escape from the fuel without being absorbed. Hence  $P$  is written as

$$P = P_F P' \quad (11-37)$$

where  $P'$  is the probability that, once having escaped from the fuel, a neutron will ultimately be absorbed in the moderator and not return to and be absorbed in the fuel.

Combining the last three equations gives

$$f = \frac{\Sigma_{aF} V_F}{\Sigma_{aM} V_M} P_F P' \quad (11-38)$$

which with a little manipulation can be put in the form

$$\frac{1}{f} - 1 = \frac{\Sigma_{aM} V_M}{\Sigma_{aF} V_F} \frac{1}{P_F} + \frac{1 - f - P'}{f}. \quad (11-39)$$

This expression is to be compared with the standard form of the thermal utilization given in Eq. (11-32), which may be written as

$$\frac{1}{f} - 1 = \frac{\Sigma_{aM} V_M}{\Sigma_{aF} V_F} F + E - 1, \quad (11-40)$$

where  $F$  and  $E$  are the lattice functions. It will be recalled from the preceding discussion that in most cases  $E$  is approximately unity so that  $E - 1 \approx 0$ , and the  $E$  function has little influence on the value of  $f$ . On the other hand,  $f$  is sensitive to the value of the  $F$  function. The same situation holds in the present case; thus  $f$  is not sensitive to the value of  $P'$  but is sensitive to  $P_F$ . As a consequence,  $P'$  need not be calculated so accurately as  $P_F$ .

For the evaluation of  $P'$  it is assumed that the fuel is a strong absorber which does not scatter neutrons, and whose absorption mean free path is small compared to its physical dimensions. In this case every neutron which passes from the moderator into the fuel is absorbed there, and the fuel is said to be *black* to neutrons. Now let  $P_M$  be the probability that a neutron born uniformly and isotropically in the moderator crosses the surface between the fuel and moderator. If all neutrons entering the fuel were actually absorbed there, the fraction of the neutrons born in the moderator which are absorbed in the fuel would be equal to  $P_M$ . Since this is also the definition of the thermal utilization, it follows that in this situation  $P_M = f$ , and from Eq. (11-38),

$$P_M = \frac{\Sigma_{aF} V_F}{\Sigma_{aM} V_M} P_F P'. \quad (11-41)$$

For a strongly absorbing body and, in particular, one whose dimensions are large compared with an absorption mean free path, it can be shown that the escape probability  $P_F$  is given by\*

$$P_{F \text{ (black fuel lump)}} = \frac{S_F}{4V_F \Sigma_{aF}}, \quad (11-42)$$

where  $S_F$  is the surface area of the fuel. Substituting Eq. (11-42) into Eq. (11-41) and solving for  $P'$  gives

$$P' = \frac{4\Sigma_{aM} V_M P_M}{S_F}. \quad (11-43)$$

Equation (11-39) can now be written as

$$\frac{1}{f} - 1 = \frac{\Sigma_{aM} V_M}{\Sigma_{aF} V_F} \frac{1}{P_F} + \frac{1 - P_M}{P_M} - \frac{4\Sigma_{aM} V_M}{S_F}. \quad (11-44)$$

Equation (11-44) is the starting point for a calculation of the thermal utilization by the ABH method. It must be emphasized, however, that the last two terms in this equation are not exact since they were computed on the assumption that the fuel lump absorbs all neutrons incident upon it. As pointed out above, this is reasonable only because these terms do not contribute significantly to the value of  $f$ . In order to use Eq. (11-44), the quantities  $P_F$  and  $P_M$  must be computed.

**Calculation of  $P_F$ .** The calculation of  $P_F$ , the probability that neutrons produced uniformly within the fuel lump ultimately escape from the lump, is complicated by the fact that a neutron may be scattered several times within the fuel before escaping. In order to calculate  $P_F$ , it is necessary, therefore, to determine first the probabilities  $P_{F0}, P_{F1}, P_{F2}, \dots, P_{Fn}$ , that a neutron will escape without a collision, after one collision, after two collisions, etc.

To compute  $P_{F0}$ , let  $dV$  and  $dA$  be volume and surface elements of the fuel lump located at  $\mathbf{r}$  and  $\mathbf{r}'$ , respectively, and let  $d\Omega$  be the solid angle subtended by  $dA$  at  $dV$  (cf. Fig. 11-7). If the uniform source density in the fuel is denoted by  $s$ , the number of neutrons produced per second in  $dV$  moving into  $d\Omega$  is

$$\frac{s}{4\pi} dV d\Omega.$$

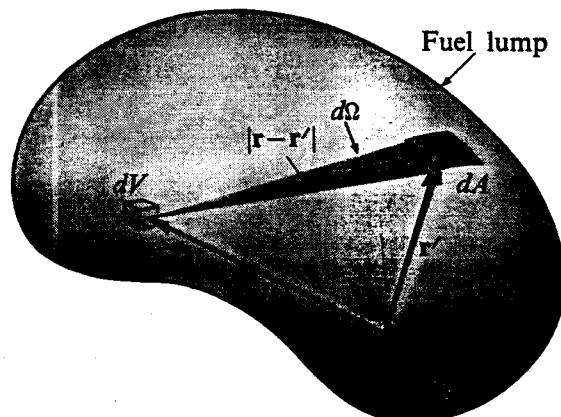


Fig. 11-7. Diagram for computing the escape probability from a lump of fuel.

\* The proof of Eq. (11-42) is somewhat lengthy. See Weinberg and Wigner, *The Physical Theory of Neutron Chain Reactors*. Chicago: University of Chicago Press, 1958, pp. 707-716; or Case, de Hoffmann, and Placzek, "Introduction to the Theory of Neutron Diffusion," U.S. Government Printing Office, Washington, D.C., 1953, Section 10.

For a strongly absorbing body and, in particular, one whose dimensions are large compared with an absorption mean free path, it can be shown that the escape probability  $P_F$  is given by\*

$$P_{F \text{ (black fuel lump)}} = \frac{S_F}{4V_F \Sigma_{aF}}, \quad (11-42)$$

where  $S_F$  is the surface area of the fuel. Substituting Eq. (11-42) into Eq. (11-41) and solving for  $P'$  gives

$$P' = \frac{4\Sigma_{aM} V_M P_M}{S_F}. \quad (11-43)$$

Equation (11-39) can now be written as

$$\frac{1}{f} - 1 = \frac{\Sigma_{aM} V_M}{\Sigma_{aF} V_F} \frac{1}{P_F} + \frac{1 - P_M}{P_M} - \frac{4\Sigma_{aM} V_M}{S_F}. \quad (11-44)$$

Equation (11-44) is the starting point for a calculation of the thermal utilization by the ABH method. It must be emphasized, however, that the last two terms in this equation are not exact since they were computed on the assumption that the fuel lump absorbs all neutrons incident upon it. As pointed out above, this is reasonable only because these terms do not contribute significantly to the value of  $f$ . In order to use Eq. (11-44), the quantities  $P_F$  and  $P_M$  must be computed.

**Calculation of  $P_F$ .** The calculation of  $P_F$ , the probability that neutrons produced uniformly within the fuel lump ultimately escape from the lump, is complicated by the fact that a neutron may be scattered several times within the fuel before escaping. In order to calculate  $P_F$ , it is necessary, therefore, to determine first the probabilities  $P_{F0}, P_{F1}$ ,  $P_{F2}, \dots, P_{Fn}$ , that a neutron will escape without a collision, after one collision, after two collisions, etc.

To compute  $P_{F0}$ , let  $dV$  and  $dA$  be volume and surface elements of the fuel lump located at  $\mathbf{r}$  and  $\mathbf{r}'$ , respectively, and let  $d\Omega$  be the solid angle subtended by  $dA$  at  $dV$  (cf. Fig. 11-7). If the uniform source density in the fuel is denoted by  $s$ , the number of neutrons produced per second in  $dV$  moving into  $d\Omega$  is

$$\frac{s}{4\pi} dV d\Omega.$$

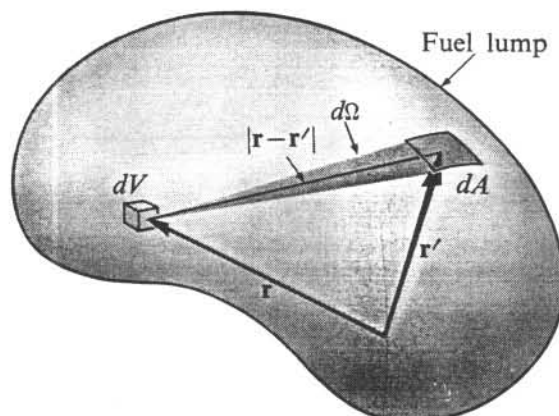


Fig. 11-7. Diagram for computing the escape probability from a lump of fuel.

\* The proof of Eq. (11-42) is somewhat lengthy. See Weinberg and Wigner, *The Physical Theory of Neutron Chain Reactors*. Chicago: University of Chicago Press, 1958, pp. 707–716; or Case, de Hoffmann, and Placzek, “Introduction to the Theory of Neutron Diffusion,” U.S. Government Printing Office, Washington, D.C., 1953, Section 10.

**Calculation of  $P_M$ .** The quantity  $P_M$ , the probability that a neutron born uniformly and isotropically in the moderator moves into the fuel lump which is assumed to be black to neutrons, could easily be computed if diffusion theory were valid. It would merely be necessary to compute, using Fick's law, the number of neutrons flowing into the fuel per neutron slowing down in the moderator. Diffusion theory is not valid, of course, particularly near the fuel since this has been assumed to be such a strong neutron absorber. This difficulty can be circumvented by using a boundary condition at the fuel surface, which, together with diffusion theory, gives the correct, or nearly correct, flux in the interior of the moderator. This is entirely analogous to the procedure for handling diffusion problems at a free surface which led to the concept of the extrapolation distance in Section 5-8.

In the present case, the boundary condition is written as

$$\frac{1}{\phi} \left. \frac{d\phi}{dr} \right|_{r=a} = \frac{1}{d}, \quad (11-48)$$

where  $a$  is the physical radius of the rod. The quantity  $d$ , which has dimensions of length, must be found from elaborate transport theory calculations. For purely absorbing cylindrical rods,  $d$  is only a function of the radius of the rod and the transport mean free path of the neutrons in the surrounding moderator, and is shown in Fig. 11-10. It is interesting to note that in the limit as the radius of the rod becomes large compared with  $\lambda_{tr}$ , the rod effectively becomes a slab, and  $d$  approaches the value  $0.71\lambda_{tr}$ . It will be recalled that this is the value of  $\phi'/\phi$  at a planar free surface, which is evidently black to neutrons (of all energy) since no neutrons return through such a surface. In this case, it follows that  $d$  can be interpreted as an extrapolation length and the boundary condition, Eq. (11-48), is equivalent to assuming that  $\phi$  vanishes at  $r = a - d$ . This, of course, makes little sense when  $d$  is comparable in size to  $a$ . As also indicated in Fig. 11-10,  $d$  approaches the value  $\frac{4}{3}\lambda_{tr}$  as  $a$  approaches zero. This result is discussed in Prob. 11-11.

The solution to the diffusion equation satisfying Eq. (11-48) at  $r = a$  and the Wigner-Seitz condition at  $r = b$  can be found in a straightforward way. With the flux in the moderator known,  $P_M$  is determined by the formula

$$P_M = \frac{2\pi a D_M \phi'_M(a)}{q V_M}.$$

The final expression for  $P_M$ , or better, for  $1/P_M$  is

$$\frac{1}{P_M} = \frac{V_M ad}{2V_F L_M^2} + E(\kappa_M a, \kappa_M b), \quad (11-49)$$

where  $E(\kappa_M a, \kappa_M b)$  is the lattice function defined in the preceding section (cf. Eq. 11-30).

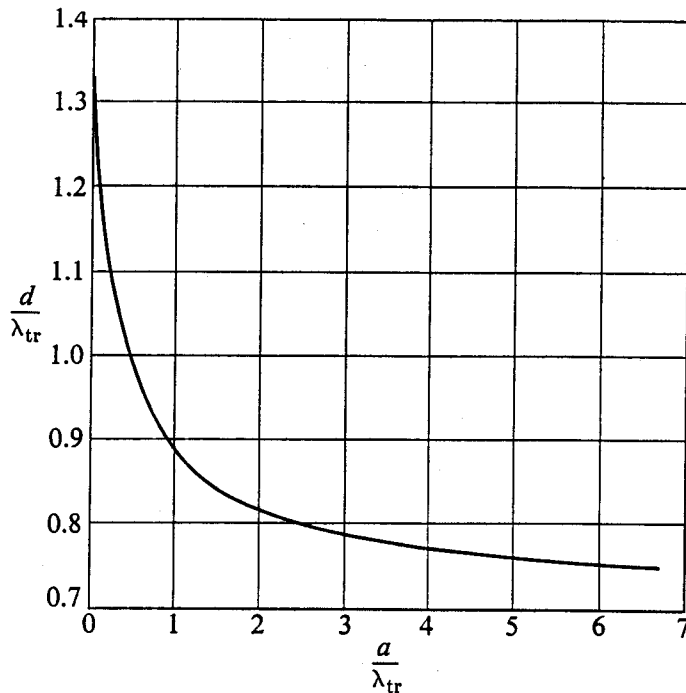


**Fig. 11-10.** The parameter  $d$  (in units of  $\lambda_{tr}$ , the transport mean free path of the surrounding medium) as a function of the radius (also in units of  $\lambda_{tr}$ ) of a purely absorbing cylinder. [Based on B. Davison, *Proceedings of the Physical Society*, London, A64, 881 (1951); and D. F. Zaretsky, *Proceedings of the International Conference at Geneva* 5, 529 (1955).]

When Eqs. (11-46) and (11-49) are substituted into Eq. (11-44), the following formula for the thermal utilization in cylindrical geometry is obtained:

$$\begin{aligned} \frac{1}{f} = & \frac{\Sigma_{aM} V_M}{\Sigma_{aF} V_F} \left\{ 1 + \frac{\Sigma_{aF} A}{\Sigma_{tF}} \left[ 1 + \alpha \left( \frac{\Sigma_{sF}}{\Sigma_{tF}} \right) + \beta \left( \frac{\Sigma_{sF}}{\Sigma_{tF}} \right)^2 \right] \right\} \\ & + \left( \frac{ad}{2L_M^2} - a\Sigma_{aM} \right) \frac{V_M}{V_F} + E(\kappa_M a, \kappa_M b). \end{aligned} \quad (11-50)$$

Calculations of  $f$  based on Eq. (11-50) have been found to give remarkably accurate results and this method is widely used for computations of thermal utilization.

**Numerical methods.** The thermal utilization can also be computed by solving the transport equation in the unit cell. These calculations cannot be carried out analytically, but they can be performed numerically with an electronic computer. It is also possible using numerical methods to determine the thermal neutron spectrum as a function of position in the cell. The dependence of the spectrum with position was specifically omitted in the analytical methods discussed above, since those methods were inherently one-velocity calculations. Ordinarily, however, the value of  $f$  is not particularly sensitive to the thermal spectrum.

### 11-3 Resonance Escape Probability

It was shown in the preceding section that the thermal utilization of a heterogeneous lattice is somewhat smaller than that of the equivalent homogeneous system, since the fuel nuclei near the surface of a fuel lump tend to shield the nuclei in the interior of the lump from the neutron flux of the surrounding moderator. Essentially the same phenomenon occurs for *resonance neutrons*, that is, neutrons having energies within the resonance region of the fuel. These neutrons are strongly absorbed by the nuclei near the surface of a fuel lump with the result that the nuclei in the interior of the fuel see a substantially smaller flux than they would otherwise see in a homogeneous system. The relative probability that a neutron will be captured in the resonances of the fuel is therefore *less* when the fuel is lumped than in the corresponding homogeneous system. This, in turn, means that the *resonance escape probability is greater for a heterogeneous lattice than for the equivalent homogeneous system.*

Lumping of the fuel also increases the resonance escape probability for another, purely geometrical, reason. With the fuel in the form of discrete lumps, some neutrons may slow down in the moderator to energies below the resonance region without ever encountering the fuel at resonance energies. However, the increase in  $p$  due to this effect is generally small compared with that caused by the drop in the flux of resonance neutrons in the fuel. In natural uranium-graphite reactors this effect has been found to increase  $p$  by only a few percent; with the more tightly packed lattices found in modern power reactors the effect is entirely negligible.

In recent years, it has become possible to compute  $p$  for a heterogeneous lattice with reasonably good accuracy. One of several computational procedures which have been developed will now be considered.

**The integral equation.** An exact equation was derived in Section 7-6 for determining the energy-dependent flux in a *homogeneous* mixture of moderator and resonance absorbers containing uniformly distributed sources of fast neutrons. By setting up a neutron balance in the energy interval  $dE$  at  $E$  it was easy to show that  $\phi(E)$  satisfied the following integral equation:

$$\begin{aligned} \Sigma_t(E)\phi(E) = & \frac{1}{1 - \alpha_A} \int_E^{E/\alpha_A} \Sigma_{sA}(E')\phi(E') \frac{dE'}{E'} \\ & + \frac{1}{1 - \alpha_M} \int_E^{E/\alpha_M} \Sigma_{sM}(E')\phi(E') \frac{dE'}{E'}, \end{aligned} \quad (11-51)$$

where the subscripts M and A refer to the moderator and absorber,\* respectively, and the other symbols have their usual meanings. Using standard numerical techniques,  $\phi(E)$  can be evaluated from Eq. (11-51) with the aid of an electronic computer. The resonance integral is then given by Eq. (7-69).

---

\* In Eq. (11-51) and the following discussion, it is assumed for simplicity that the absorber ( $\equiv$ fuel) and moderator are both single-nuclide materials.

The situation is obviously much more complicated in a heterogeneous lattice, for the flux is now a function of space as well as energy. To simplify the analysis, it will be assumed for the moment that neutrons at resonance energies cannot pass from one lump to another without having their energy drop to below the resonance region as the result of collisions in the intervening moderator. In this case, it is possible to treat each lattice cell separately and the lumps are said to be *isolated*. If, on the contrary, a resonance neutron can pass from one lump to another within the resonance region, the lumps are said to *interact*. Interacting fuel lumps are discussed later in this section.

It will be assumed that one fast neutron is emitted isotropically per  $\text{cm}^3/\text{sec}$  throughout the equivalent cell. As usual, the calculation of  $p$  then reduces to the problem of finding how many of these source neutrons escape capture in slowing down in the cell. For this purpose, it is necessary to set up neutron balance equations in both the fuel and moderator.

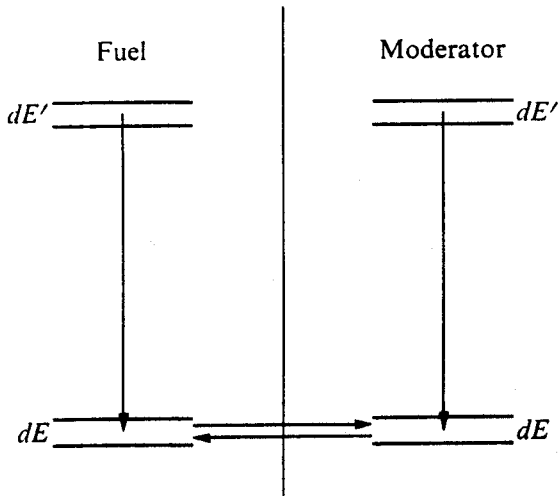


Fig. 11-11. Diagram for deriving the fuel-moderator balance equations.

Consider first the arrival and departure of neutrons in the energy interval  $dE$  in the fuel. As indicated schematically in Fig. 11-11, neutrons arrive in  $dE$  both as the result of scattering collisions at higher energies in the fuel and by traveling from the moderator into the fuel, having already acquired an energy within  $dE$  in the moderator.

Let  $\phi_F(E)$  be the average flux in the fuel. The total number of neutrons arriving in  $dE$  per sec from collisions in the fuel is then

$$\frac{V_F dE}{1 - \alpha_F} \int_E^{E/\alpha_F} \Sigma_{sF}(E') \phi_F(E') \frac{dE'}{E'}.$$

All of these neutrons do not necessarily interact within  $dE$  in the fuel; some neutrons may leave the fuel and have their next interaction in the moderator instead. If, as in the preceding section,  $P_{F0}(E)$  is the probability that a neutron of energy  $E$  escapes from the fuel without a collision, then  $1 - P_{F0}(E)$  is equal

to the probability that this neutron has its next interaction within the fuel. It follows therefore that

$$\frac{V_F [1 - P_{F0}(E)] dE}{1 - \alpha_F} \int_E^{E/\alpha_F} \Sigma_{sF}(E') \phi_F(E') \frac{dE'}{E'}$$

neutrons are scattered into and interact in  $dE$  in the fuel per sec.

Consider next the neutrons arriving in  $dE$  from the moderator. The number of these is equal to the number scattered into  $dE$  in the moderator multiplied by the probability  $P_{M0}(E)$  that a neutron of energy  $E$  in the moderator has its next collision in the fuel, namely,

$$\frac{V_M P_{M0}(E) dE}{1 - \alpha_M} \int_E^{E/\alpha_M} \Sigma_{sM}(E') \phi_M(E') \frac{dE'}{E'},$$

where  $\phi_M(E)$  is the average flux in the moderator. Adding the above terms gives the following neutron balance equation for the fuel:

$$V_F \Sigma_{tF}(E) \phi_F(E) = \frac{V_F [1 - P_{F0}(E)]}{1 - \alpha_F} \int_E^{E/\alpha_F} \Sigma_{sF}(E') \phi_F(E') \frac{dE'}{E'} + \frac{V_M P_{M0}(E)}{1 - \alpha_M} \int_E^{E/\alpha_M} \Sigma_{sM}(E') \phi_M(E') \frac{dE'}{E'}. \quad (11-52)$$

By precisely the same argument it is possible to derive the balance equation for the moderator. Thus since there is almost no absorption of neutrons in the moderator at resonance energies so that  $\Sigma_{tM} \approx \Sigma_{sM}$ , this equation is easily found to be

$$V_M \Sigma_{sM}(E) \phi_M(E) = \frac{V_F P_{F0}(E)}{1 - \alpha_F} \int_E^{E/\alpha_F} \Sigma_{sF}(E') \phi_F(E') \frac{dE'}{E'} + \frac{V_M [1 - P_{M0}(E)]}{1 - \alpha_M} \int_E^{E/\alpha_M} \Sigma_{sM}(E') \phi_M(E') \frac{dE'}{E'} \quad (11-53)$$

In order to compute the fluxes using the above balance equations it is necessary, of course, to specify the probabilities  $P_{F0}$  and  $P_{M0}$ . For this purpose, it is usual to assume that the flux is independent of position, i.e. "flat," in both the fuel and moderator. This is clearly not a good assumption; the flux, particularly at resonance energies, drops sharply within the interior of the fuel and it may be far from flat in the moderator. Nevertheless, because of a cancellation of errors discussed below, the results of calculations based on this assumption have been found to give good values of  $p$ .

With the fuel and moderator fluxes assumed to be flat it can be shown (cf. Prob. 11-17) using the reciprocity theorem (Eq. 11-34) that  $P_{F0}$  and  $P_{M0}$  are related by the equation

$$P_{F0} \Sigma_{tF} V_F = P_{M0} \Sigma_{sM} V_M. \quad (11-54)$$

As will be seen momentarily, Eq. (11-54) considerably simplifies calculations using the balance equations.

At this point it is convenient to note that the asymptotic solutions of Eqs. (11-52) and (11-53), i.e. the asymptotic fluxes in the absence of absorption, are the same in the fuel and moderator. Denoting these solutions by  $\phi_F^\infty$  and  $\phi_M^\infty$ , it can be shown by direct substitution and the use of Eq. (11-54) that

$$\phi_F^\infty = \phi_M^\infty = \frac{1}{\xi \bar{\Sigma}_p E}. \quad (11-55)$$

Here  $\bar{\Sigma}_p$  is given by

$$\bar{\Sigma}_p = \frac{1}{V} (\xi_F \Sigma_{pF} V_F + \xi_M \Sigma_{sM} V_M), \quad (11-56)$$

where  $\Sigma_{pF}$  is the potential scattering of the fuel (in the asymptotic region  $\Sigma_{sF} = \Sigma_{pF}$ ) and  $V = V_F + V_M$  is the total volume of the equivalent cell. It will be observed that Eq. (11-55) properly reduces to the homogeneous flux (Eq. 6-59) when  $V_F = V_M = V$ .

It is possible to decouple the heterogeneous balance equations by observing that the energy loss per collision with the moderator is always large compared with the practical width of the resonances in the fuel. In this case, it is reasonable to replace  $\phi_M$  in the second integral of Eq. (11-52) by  $\phi_M^\infty$ . This, in short, is the narrow resonance approximation for the moderator. Then since  $\Sigma_{sM}$  is a constant at resonance energies, this term becomes

$$\begin{aligned} \frac{V_M P_{M0}(E)}{1 - \alpha_M} \int_E^{E/\alpha_M} \Sigma_{sM}(E') \phi_M(E') \frac{dE'}{E'} &= \frac{V_M P_{M0}(E) \Sigma_{sM}}{\xi \bar{\Sigma}_p E} \\ &= \frac{V_F P_{F0}(E) \Sigma_{tF}(E)}{\xi \bar{\Sigma}_p E}, \end{aligned}$$

where use has been made of Eq. (11-54). Equation (11-52) now reduces to

$$\Sigma_{tF}(E) \phi_F(E) = \frac{1 - P_{F0}(E)}{1 - \alpha_F} \int_E^{E/\alpha_F} \Sigma_{sF}(E') \phi_F(E') \frac{dE'}{E'} + \frac{P_{F0}(E) \Sigma_{tF}(E)}{\xi \bar{\Sigma}_p E}. \quad (11-57)$$

This result shows that, based on the flat flux assumption, the flux in the fuel is determined by a single integral equation. It should furthermore be observed that  $P_{F0}$  appears in Eq. (11-57) with both signs. Hence any error in  $P_{F0}$  tends to be canceled in the computation of  $\phi_F$ . This presumably accounts for the good results obtained using the flat flux assumption.

When the appropriate values of  $P_{F0}(E)$  are substituted into Eq. (11-57) this equation can be solved for  $\phi_F(E)$  using standard numerical methods. The resonance escape probability at a single resonance can then be computed directly. The total

number of neutrons absorbed per second in the whole lump for a resonance at the energy  $E_i$  is

$$V_F \int_{E_i} \Sigma_{aF} \phi_F dE,$$

where the integration extends over energies near  $E_i$ . Since there are  $V$  fast neutrons produced in the cell per second, it follows that the escape probability for this resonance is

$$p_i = 1 - \frac{V_F}{V} \int_{E_i} \Sigma_{aF} \phi_F dE.$$

As in the homogeneous case (cf. Section 7-4), the resonance escape probability for a sequence of isolated resonances is

$$p = \prod_i p_i \approx \exp \left[ - \frac{V_F}{V} \int \Sigma_{aF} \phi_F dE \right],$$

which is usually written as

$$p = \exp \left[ - \frac{N_F V_F I}{\xi_F \Sigma_{pF} V_F + \xi_M \Sigma_{sM} V_M} \right], \quad (11-58)$$

where  $I$  is the resonance integral

$$I = \bar{\xi} \sum_p \int \sigma_{aF} \phi_F dE. \quad (11-59)$$

The numerical integration of Eqs. (11-57) and (11-59) forms the basis for the now standard technique for computing resonance escape in heterogeneous lattices consisting of isolated fuel lumps.

**The NR and NRIM approximations.** If the energy loss in an elastic collision with the fuel is large compared with the practical width of a resonance (the NR approximation; cf. Section 7-2), neutrons generally have no more than one collision within a resonance. It is then possible to replace  $\phi_F$  in the integral in Eq. (11-57) by its asymptotic form (Eq. 11-55) and perform the integration. In doing so, the scattering cross section of the fuel in the integral must be replaced by its (constant) potential scattering cross section  $\Sigma_{pF}$ . This takes into account the fact that in the NR approximation neutrons are scattered downward into the resonance from energies above the resonance, i.e., where  $\Sigma_{sF} = \Sigma_{pF}$ . This gives the following expression for the flux in the vicinity of the resonance:

$$\phi_F(E) = \frac{1}{\Sigma_{tF} \bar{\xi} \sum_p E} [(1 - P_{F0}) \Sigma_{pF} + P_{F0} \Sigma_{tF}]. \quad (11-60)$$

Inserting Eq. (11-60) into Eq. (11-59) gives

$$I(\text{NR}) = \int [\sigma_{pF} + P_{F0}(\sigma_{tF} - \sigma_{pF})] \frac{\sigma_{aF}}{\sigma_{tF}} \frac{dE}{E}. \quad (11-61)$$

When the energy loss per collision in the fuel is small compared with  $\Gamma_F$ , it will be recalled from Section 7-2 that, as a first approximation, it is reasonable to ignore energy losses in the fuel altogether. This is the basis of the NRIM approximation. The situation is more complicated for the heterogeneous system, however, because a neutron may now undergo repeated scattering in the fuel within a single resonance before escaping. For simplicity, it is usually assumed that the collision density is independent of position (flat) for all collisions. The *total* escape probability  $P_F$  can then be computed by considering a succession of collisions of the neutrons in the fuel. Thus if  $N$  neutrons are uniformly produced in the lump, then

$$\begin{aligned} NP_{F0} &\text{ neutrons escape without collision;} \\ N(1 - P_{F0}) &\text{ neutrons have a first collision in fuel;} \\ N(1 - P_{F0}) \frac{\sigma_{sF}}{\sigma_{tF}} &\text{ neutrons survive their first collision;} \\ N(1 - P_{F0}) \frac{\sigma_{sF}}{\sigma_{tF}} P_{F0} &\text{ neutrons escape after first collision;} \\ N(1 - P_{F0})^2 \frac{\sigma_{sF}}{\sigma_{tF}} &\text{ neutrons have a second collision;} \\ &\text{etc.} \end{aligned}$$

The total number of neutrons escaping is

$$NP_{F0} + N(1 - P_{F0}) \frac{\sigma_{sF}}{\sigma_{tF}} P_{F0} + N(1 - P_{F0})^2 \left( \frac{\sigma_{sF}}{\sigma_{tF}} \right)^2 P_{F0} + \dots,$$

so that the total escape probability is

$$P_F = \frac{P_{F0}}{1 - (1 - P_{F0})(\sigma_{sF}/\sigma_{tF})}. \quad (11-62)$$

In order to calculate the resonance integral in the NRIM approximation, it is merely necessary to replace  $P_{F0}$  in Eq. (11-61) by  $P_F$  from Eq. (11-62). At the same time,  $\sigma_{pF}$  must be set equal to zero since in the derivation of Eq. (11-60)  $\sigma_{pF}$  contributes to the scattering of neutrons into the resonance from higher energies, something that is specifically omitted in the NRIM approximation. The final expression for  $I$  is then

$$I(\text{NRIM}) = \int \frac{P_{F0}\sigma_{aF}}{1 - (1 - P_{F0})(\sigma_{sF}/\sigma_{tF})} \frac{dE}{E}. \quad (11-63)$$

**Wigner's approximation—equivalence theorems.** In order to evaluate the integrals in Eqs. (11-61) and (11-63), the escape probability  $P_{F0}$  must be specified. Unfortunately,  $P_{F0}$  is a very complicated function for all geometries so that the integrals in Eqs. (11-61) and (11-63) cannot be performed analytically. It is possible, however, to obtain good estimates for  $I$  by approximating  $P_{F0}$  by a simple function.

It can be shown that  $P_{F0}$  is only a function of the product  $\bar{r}\Sigma_{tF}$  where  $\bar{r}$  is the average length of a chord within the fuel lump and  $\Sigma_{tF}$  is the total cross section of

the fuel. By a somewhat involved geometrical calculation, it is also possible to show that  $\bar{r}$  is given by

$$\bar{r} = \frac{4V_F}{S_F}, \quad (11-64)$$

where  $V_F$  and  $S_F$  are the volume and surface area of the lump, respectively. It is now convenient to write  $P_{F0}$  in the form

$$P_{F0} = \frac{G(\bar{r}\Sigma_{tF})}{\bar{r}\Sigma_{tF}} = \frac{S_F G(\bar{r}\Sigma_{tF})}{4V_F \Sigma_{tF}}. \quad (11-65)$$

Here  $G(\bar{r}\Sigma_{tF})$  is called the *penetrability* of the lump and is equal to the probability that neutrons randomly incident on the surface of the lump are absorbed in the lump. For example, if the lump is large compared with an absorption mean free path, that is, if the lump is *black*, all of the incident neutrons are absorbed and  $G$  is unity. In this case, Eq. (11-65) reduces to

$$P_{F0} = \frac{1}{\bar{r}\Sigma_{tF}} = \frac{S_F}{4V_F \Sigma_{tF}}. \quad (11-66)$$

This result was used in the preceding section (cf. Eq. 11-42), where it was assumed that  $\Sigma_{aF} \approx \Sigma_{tF}$ . (In that situation  $\Sigma_{sF} \approx 0$  and  $P_{F0} \approx P_F$ .) On the other hand, as the size of the lump goes to zero, all neutrons escape from the lump so that  $P_{F0}$  must go to unity. This behavior, which is also shown in Fig. 11-8 for cylindrical lumps, suggests that  $P_{F0}$  may be represented by the expression

$$P_{F0} = \frac{1}{1 + \bar{r}\Sigma_{tF}}. \quad (11-67)$$

It will be noted that for  $\bar{r}\Sigma_{tF} \gg 1$  Eq. (11-67) reduces to Eq. (11-66), while for  $\bar{r}\Sigma_{tF} \ll 1$ , it approaches unity. Equation (11-67) is known as *Wigner's rational approximation* for  $P_{F0}$ .\*

In using Eq. (11-67) it is convenient to define a fictitious macroscopic cross section  $\Sigma_e$  by

$$\Sigma_e = \frac{1}{\bar{r}} \quad (11-68)$$

and a corresponding microscopic cross section  $\sigma_e$

$$\sigma_e = \frac{\Sigma_e}{N_F} = \frac{1}{N_F \bar{r}}, \quad (11-69)$$

\* A somewhat better representation for  $P_{F0}$  for small  $\bar{r}\Sigma_{tF}$  is

$$P_{F0} = \frac{1}{1 + \bar{r}\Sigma_{tF}/3},$$

(cf. Rothenstein in the References).

where, as usual,  $N_F$  is the atom density of the fuel. It should be noted that these fictitious cross sections are functions of the geometry of the lump but do not depend on neutron energy. Equation (11-67) can then be written as

$$P_{F0} = \frac{\Sigma_e}{\Sigma_e + \Sigma_{tF}} = \frac{\sigma_e}{\sigma_e + \sigma_{tF}}. \quad (11-70)$$

Introducing Eq. (11-70) into Eq. (11-61) gives

$$I(\text{NR}) = \int \frac{(\sigma_{pF} + \sigma_e)\sigma_{aF}}{\sigma_{tF} + \sigma_e} \frac{dE}{E}. \quad (11-71)$$

Writing  $\sigma_{tF} = \sigma_{aF} + \sigma'_{sF} + \sigma_{pF}$ , where  $\sigma'_{sF}$  is the anomalous scattering cross section of the fuel (cf. Section 2-8), and dividing numerator and denominator by  $\sigma_{pF} + \sigma_e$ , Eq. (11-71) becomes

$$I(\text{NR}) = \int \frac{\sigma_{aF}}{1 + (\sigma_{aF} + \sigma'_{sF})/(\sigma_{pF} + \sigma_e)} \frac{dE}{E}. \quad (11-72)$$

In a similar fashion, when Eq. (11-70) is substituted into Eq. (11-63), the corresponding expression in the NRIM approximation is

$$I(\text{NRIM}) = \int \frac{\sigma_e \sigma_{aF}}{\sigma_{aF} + \sigma_e} \frac{dE}{E}. \quad (11-73)$$

When the appropriate Doppler-broadened cross sections are inserted into Eqs. (11-72) or (11-73), formulas for the escape probabilities for single resonances can be obtained (see below).

It should be observed from Eqs. (11-72) and (11-73) that all factors in the integrals depend upon the properties of the fuel and are independent of the moderator. Furthermore, the geometry of the fuel lump only appears in the factor  $\sigma_e$ . It follows that *heterogeneous lattices with the same values of  $\sigma_e$  have the same resonance integrals regardless of the surrounding moderator*. This statement is known as the *first equivalence theorem* of resonance escape.

It is of some interest to compare Eqs. (11-72) and (11-73) with the corresponding resonance integrals of homogeneous reactors. According to Eq. (7-62), and in the notation of the present chapter where the resonance absorber has explicitly been taken to be fuel, the integrals are

$$I_{\text{homo}}(\text{NR}) = \int \frac{\sigma_{aF}}{1 + (\sigma_{aF} + \sigma'_{sF})/\sigma_p}, \quad (11-74)$$

and

$$I_{\text{homo}}(\text{NRIM}) = \int \frac{\sigma_p \sigma_{aF}}{\sigma_{aF} + \sigma_p} \frac{dE}{E}. \quad (11-75)$$

In Eq. (11-74),

$$\sigma_p = \frac{\Sigma_{sM}}{N_F} + \sigma_{pF} \quad (11-76)$$

is the potential scattering cross section per fuel atom of the fuel-moderator mixture, while in Eq. (11-75),

$$\sigma_p = \frac{\Sigma_{sM}}{N_F}, \quad (11-77)$$

the potential scattering cross section of the fuel having been placed equal to zero in the NRIM approximation. Comparing Eqs. (11-74) and (11-75) with Eqs. (11-72) and (11-73) shows that *a heterogeneous reactor with a given value of  $\sigma_{pF} + \sigma_e$  and a homogeneous reactor with a given value of  $\sigma_p$  will have the same resonance integrals provided*

$$\sigma_{pF} + \sigma_e = \sigma_p.$$

This is the *second equivalence theorem* of resonance escape.

These equivalence theorems are based, of course, on the rational approximation and are therefore not precise. However, despite the fact that they were derived above within the framework of the NR and NRIM approximations their validity does not depend upon the validity of these approximations. Thus it is also possible to establish the equivalence relations by comparing directly the integral equations for homogeneous and heterogeneous systems.

One trivial consequence of the equivalence theorems is that the formulas for the resonance integrals given in Chapter 7 in the NR and NRIM calculations of homogeneous mixtures can be carried over to the heterogeneous case by merely replacing  $\sigma_p$  by  $\sigma_{pF} + \sigma_e$  (cf. Prob. 11-19). It is not necessary to evaluate the integrals in Eqs. (11-72) and (11-73) anew. A far more important use of the equivalence theorems is in the comparison of calculations and measurements of heterogeneous resonance integrals with those of the corresponding homogeneous reactors.

In the foregoing, it was assumed that the fuel consists of a single isotope. If the fuel also contains a lightweight scatterer such as oxygen (as in  $\text{UO}_2$ ) it is not difficult to show that Eqs. (11-72) and (11-73) become

$$I(\text{NR}) = \int \frac{\sigma_{aF}}{1 + (\sigma_{aF} + \sigma'_{sF})/(\sigma_{pF} + \sigma_e + \sigma_m)} \frac{dE}{E} \quad (11-78)$$

and

$$I(\text{NRIM}) = \int \frac{(\sigma_e + \sigma_m)\sigma_{aF}}{\sigma_{aF} + \sigma_e + \sigma_m} \frac{dE}{E}, \quad (11-79)$$

where  $\sigma_m$  is the additional scattering cross section per fuel atom. The more general equivalence relations in this case are then as follows:

(1) heterogeneous lattices with the same value of  $\sigma_e + \sigma_m$  have the same resonance integral;

(2) heterogeneous and homogeneous reactors have the same resonance integrals provided

$$\sigma_{pF} + \sigma_e + \sigma_m = \sigma_p.$$

It must be emphasized that these relations were derived for and are therefore only applicable to fuel lattices consisting of isolated rods. They do not apply to closely packed lattices which are discussed below.

**Experimental data.** The resonance integral can be determined experimentally using the activation method described in Section 7-7, and considerable data has been accumulated for lattices consisting of isolated and interacting fuel lumps. It has been found that for isolated lumps this data can be represented by an equation of the form:

$$I = a + b \sqrt{\frac{S_F}{M_F}}, \quad (11-80)$$

where  $a$  and  $b$  are constants which depend on the nature of the fuel, and  $S_F$  and  $M_F$  are, respectively, the surface area and mass of the fuel. With cylindrical rods,  $S_F$  and  $M_F$  are the surface area and mass per unit length of the rod. Unfortunately, there does not appear to be simple, physical justification of the form of Eq. (11-80) and, indeed, it can be shown (cf. Nordheim) that the resonance integral cannot be represented precisely by an equation of this type. However, Eq. (11-80) reproduces the data satisfactorily within the accuracy of the experiments. Values of  $a$  and  $b$  are given in Table 11-3 for isolated lumps of several commonly used fuels. Data for more closely packed lattices can be found in the compilations such as ANL-5800. With  $I$  known,  $p$  can be computed directly from Eq. (11-58).

Table 11-3  
Measured Resonance Integral Constants\*

Fuel	$a$	$b$
$U^{238}$ (metal)	2.8	27.1
$U^{238}O_2$	3.0	28.0
$Th^{232}$ (metal)	3.9	14.8
$Th^{232}O_2$	3.4	17.3

\* W. G. Pettus and M. N. Baldwin, "Resonance Absorption in  $U^{238}$  Metal and Oxide Rods," Babcock and Wilcox Company Report BAW-1244, 1962; "Resonance Absorption in Thorium Metal and Oxide Rods," BAW-1286, 1963.

**Closely packed lattices.** Up to this point it has been assumed that the fuel lumps are so widely spaced that they do not interact with one another; that is, neutrons with energies in the resonance region do not pass from one lump to another. This assumption entered directly into the derivation of the neutron bal-

ance equation (Eq. 11-57) in that the escape probability from a single fuel lump  $P_{F0}$  was taken to be equal to the probability that a neutron in the lump has its next collision in the moderator. Clearly, if the fuel lumps interact, the next collision may take place in another lump. However, by redefining  $P_{F0}$  to be the probability that a neutron does in fact have its next collision in the moderator, i.e., excluding collisions in other lumps, the preceding calculations can be applied to closely packed lattices as well.

It is obviously much more difficult to compute this probability, denoted hereafter by  $P_{F0}^*$ , for an interacting lattice than for an isolated lump, and, in fact, this function cannot be determined exactly except by numerical methods. It can be shown, however, by an analysis which is too involved to be reproduced here, that  $P_{F0}^*$  is given approximately by the formula

$$P_{F0}^* = P_{F0} \frac{1 - C}{1 - (1 - \bar{r}\sum_{iF} P_{F0})C}, \quad (11-81)$$

where  $\bar{r}$  is the average chord length in one fuel lump (cf. Eq. 11-64) and  $C$  is called the *Dancoff-Ginsberg correction factor* for the lattice.

To determine  $C$  for a given lattice it is necessary to obtain the sum

$$C = \sum C_i \quad (11-82)$$

where  $C_i$  is the *lump-to-lump Dancoff-Ginsberg factor* and the sum is carried out over all lumps in the lattice. The parameters  $C_i$  are functions of two variables:  $a\Sigma_{iM}$  and  $d_i/a$ , where  $d_i$  is the distance to the  $i$ th lump and  $a$  is the radius of the lump (all lumps assumed to be identical). Extensive tables of  $C_i$  have been prepared and are given, for example, in the report ANL-5800. As would be expected physically, the value of  $C_i$  decreases sharply with increasing  $d_i/a$ , and it is usually necessary to include only a few terms in Eq. (11-82). In principle, it is no more difficult to use  $P_{F0}^*$  than  $P_{F0}$  in the calculations of  $I$  for a lattice than for an isolated lump.

It can also be shown that to a good approximation the effect of the interaction between fuel lumps in a closely packed lattice is equivalent to a reduction in the surface area of a single fuel lump by a factor of  $1 - C$ . Thus the resonance integral for such a lattice can be calculated from Eq. (11-80), using the constants in Table 11-3, by merely replacing  $S_F$  by  $(1 - C)S_F$ . The resonance escape probability for the lattice is then calculated from Eq. (11-58), as if the lattice were a single cell.

With the surface area of the fuel lump effectively diminished, it follows from Eq. (11-80) that the resonance integral is smaller for an interacting lattice than for a lattice of isolated lumps. Physically, this is because in the interacting case some of the neutrons that would ordinarily pass directly from the moderator into a lump are intercepted by neighboring lumps. In other words, each lump tends to be *shadowed* by its neighbors. It is this shadowing effect which is taken into account by the Dancoff-Ginsberg factor.

**Other methods for computing  $p$ .** The values of the resonance integral obtained by solving the integral equation (Eq. 11-57) using  $P_{F0}$  for isolated lumps and  $P_{F0}^*$  for interacting lumps are in good agreement with experiment. Nevertheless, the method is not exact due to the underlying assumption of flat flux in the fuel and moderator and the approximate nature of the Dancoff-Ginsberg correction factor. Furthermore, it is very difficult to extend the procedure to nonuniform lattices, that is, to lattices with varying distances between fuel lumps. In principle, the resonance integral can be computed exactly for all lattices by the Monte Carlo method (cf. Sections 5-10, 6-16, 7-6). The accuracy of these calculations is limited only by the accuracy of the input cross-section data and the duration of the computation. Monte Carlo calculations, however, usually require long computation times and such calculations are normally reserved either for the verification of other computational procedures or for situations where no other method can be applied. Monte Carlo is rarely used in production-line computations of resonance escape.

#### 11-4 The Fast Effect

Fast fission, that is, fission induced in fissionable but nonfissile material in an otherwise thermal reactor, was considered briefly in Section 7-9 for homogeneous systems. It will be recalled that this effect must be taken into account whenever there are substantial amounts of a fissionable isotope such as  $U^{238}$  or  $Th^{232}$  in a thermal reactor. As this is usually the case in a heterogeneous reactor, it is almost always necessary to include fast fission in calculations of this type of reactor.

Although only a few percent of all fissions taking place in a thermal reactor are fast fissions, these can have a significant bearing on the operation of the system. For example, in a natural uranium-graphite reactor, fast fission may account for upwards of one half of the value of  $k_\infty$  in excess of unity. This excess value of  $k_\infty$  is necessary not only to assure criticality, but also to compensate for the burnup of the fuel and to provide adequate control of the reactor at all times.

Fast fissions may also have a pronounced effect on the performance of a thermal breeder. It was pointed out in Chapter 4 that the breeding capability of a reactor is determined by the number of fast neutrons emitted per neutron absorbed in fuel, that is, by the value of  $\eta$ . Because of the fast effect the total number of neutrons produced per neutron absorbed in fuel is effectively increased from  $\eta$  to  $\eta\epsilon$ , where  $\epsilon$  is the fast fission factor. It is advisable, therefore, to design a thermal breeder to have as large a value of  $\epsilon$  as possible in order to maximize the breeding gain. Indeed, for fuels ( $U^{233}$ , in particular) with thermal values of  $\eta$  near 2, the value of  $\epsilon$  may mean the difference between success or failure in breeding.

**The definition of  $\epsilon$ .** The fast fission factor for a heterogeneous reactor must be defined with some care. It will be recalled that when the four-factor formula was derived in Chapter 9 it was implicitly assumed that fast fission and resonance absorption are processes which occur independently in different energy

regions. This is not entirely true; resonance absorption does occur to a small extent above the fission threshold  $E_f$ .

At the same time it may be noted that in the computation of the resonance escape probability given in the preceding section, it was assumed that the bulk of the slowing down of the fission neutrons occurs in the moderator. It is therefore only those neutrons which succeed in escaping from the fuel and subsequently slow down in the moderator which feed, so to speak, the resonance absorption calculation. However, nowhere in the calculations of  $p$  was the absorption of neutrons leaving the fuel *for the first time* included.

It will be evident that in defining the fast fission factor for a heterogeneous lattice it is important that the definition be consistent with the computations of  $p$ . Moreover, if possible, the omissions in the calculation of  $p$  should be corrected in the calculations of  $\epsilon$ . For this purpose, let  $E_l$  be an energy (say, in the low kilovolt region) below which prompt fission neutrons are not emitted, and below which it is unlikely that a neutron will appear as the result of inelastic scattering in the fuel. The neutrons present in the fuel below  $E_l$  then must have traveled into the fuel from the moderator. An appropriate definition of  $\epsilon$  is

$$\epsilon = \frac{\text{Number of neutrons slowing down below } E_l \text{ in the moderator}}{\text{Neutron produced in thermal fission}}. \quad (11-83)$$

This definition takes into account both the fast fission occurring above  $E_f$  and all resonance absorption occurring above  $E_l$ . The calculations of  $p$  discussed in the preceding section should not, of course, be carried out above  $E_l$ .

**The method of Spinrad, Fleishman, and Soodak.** The approximate value of  $\epsilon$  can be found by the following method which is due to Spinrad, Fleishman, and Soodak (SFS). For the moment, it will be assumed that the fuel lumps are so widely separated that collisions in the intervening moderator reduce the energies of neutrons emerging from a lump to below the fission threshold before they enter another lump. In this case, as in the preceding section, the lumps are said to be *isolated*. Closely packed lattices of *interacting* lumps will be considered later.

In the SFS method, it is assumed that once a neutron leaves the fuel it slows down in the moderator without returning to the fuel (at least not above the fission threshold).\* Based on this assumption a definition of  $\epsilon$  equivalent to the one given in Eq. (11-83) is

$$\epsilon = \frac{\text{Number of neutrons having first collisions in moderator}}{\text{Neutron produced in thermal fission}}; \quad (11-84)$$

Eq. (11-84) is known as Spinrad's definition of the fast fission factor.

---

\* A method which takes into account the return of neutrons from the moderator above the fission threshold has been given by H. Märkl and A. G. Fowler (see References).

To calculate  $\epsilon$ , all neutrons within the fuel lump are divided into three groups:

*Group 1.* This group contains all fission neutrons with energies above  $E_f$ . Neutrons are lost from this group by absorption, leakage from the lump, or scattering to below  $E_f$ .

*Group 2.* These are fission neutrons with energies below  $E_f$ . They are lost by absorption and leakage; it is assumed that neutrons are not scattered out of this group.

*Group 3.* This group contains the neutrons with energies below  $E_f$  which have been scattered out of Group 1. Neutrons are lost from this group by absorption or leakage. As in the case of Group 2, it is assumed that neutrons are not scattered out of this group.

It should be noted that the energy spectra of these three groups of neutrons are all different. The spectra of Group 1 and Group 2 neutrons are represented by portions of the prompt fission neutron spectrum above and below  $E_f$ , respectively, while the spectrum of Group 3 neutrons is given approximately by the inelastic neutron distribution function (cf. Eq. 2-89). The cross sections for each of these groups averaged over the appropriate spectra are defined as follows:

$\sigma_{1f}$  fission cross section, Group 1;

$\sigma_{1\gamma}$  capture cross section, Group 1;

$\sigma_{11}$  scattering cross section, Group 1, the scattered neutron remaining in Group 1;

$\sigma_{13}$  scattering cross section, Group 1, the scattered neutron falling into Group 3  
( $\sigma_{13}$  is a group transfer cross section as in Section 10-4);

$\sigma_{1t} = \sigma_{1f} + \sigma_{1\gamma} + \sigma_{11} + \sigma_{13}$  total cross section, Group 1;

$\sigma_{2\gamma}$  capture cross section, Group 2;

$\sigma_{22}$  scattering cross section, Group 2, the scattered neutron remaining in Group 2;

$\sigma_{2t} = \sigma_{2\gamma} + \sigma_{22}$  total cross section, Group 2;

$\sigma_{3\gamma}$  capture cross section, Group 3;

$\sigma_{33}$  scattering cross section, Group 3, the neutron remaining in Group 3;

$\sigma_{3t} = \sigma_{3\gamma} + \sigma_{33}$  total cross section, Group 3.

The fraction of the fission neutrons which are produced above and below the fission threshold will be denoted by  $x_1$  and  $x_2$ , respectively; that is

$$x_1 = \int_{E_f}^{\infty} x(E) dE \quad \text{and} \quad x_2 = \int_0^{E_f} x(E) dE,$$

where  $x(E)$  is the fission spectrum (cf. Eq. 3-14). It is customary in calculations of  $\epsilon$  to take  $E_f$  to be the energy at which the fission cross section rises to one-half of its plateau value (cf. Fig. 3-4). For both  $U^{238}$  and  $Th^{232}$ ,  $E_f$  is approximately 1.4 MeV; and in this case,  $x_1 = 0.561$  and  $x_2 = 1 - x_1 = 0.439$ . The average

number of neutrons emitted per fission induced by Group 1 neutrons will be written as  $\nu_1$ . Neutrons in Groups 2 and 3 are not capable of causing fast fission.

In addition to the above constants it is also necessary to know the average probability that a neutron in each of these groups will escape from or undergo a collision within the fuel. For simplicity, it is usually assumed that all fission neutrons are produced uniformly in the fuel and that all collision densities are independent of position in the fuel. The probability that a neutron escapes from the fuel without a collision is then given by the function  $P_{F0}$  which has been used repeatedly in the preceding sections. It will be remembered that  $P_{F0}$  is a function of the product  $\bar{r}\Sigma_{tF}$ , where  $\bar{r}$  is the average chord length of the lump. Since  $P_{F0}$  depends on the fuel cross section  $\Sigma_{tF}$ , its value is different for the three groups defined above. To simplify the notation, these probabilities will be denoted by  $P_1$ ,  $P_2$ , and  $P_3$ , where the subscript refers to the group number.

To calculate  $\epsilon$  based on the definition given in Eq. (11-84) it is merely necessary to determine the number of neutrons leaving the fuel for the first time from all groups, per neutron produced in thermal fission. To begin with, consider the neutrons in the first group. Per neutron emitted in thermal fission,  $x_1$  neutrons appear in this group. Of these,  $x_1P_1$  escape without collision while  $x_1(1 - P_1)$  have a first collision in the fuel. Such a collision produces, on the average,  $x_1\nu_1\sigma_{1f}/\sigma_{1t}$  fission neutrons in the first group while  $\sigma_{11}/\sigma_{1t}$  neutrons remain in the group after scattering. The total number of neutrons available in Group 1 after the first collision is thus

$$\frac{x_1(1 - P_1)(x_1\nu_1\sigma_{1f} + \sigma_{11})}{\sigma_{1t}} = x_1(1 - P_1)\beta_1,$$

where  $\beta_1 = (x_1\nu_1\sigma_{1f} + \sigma_{11})/\sigma_{1t}$ . Of this number,  $x_1P_1(1 - P_1)\beta_1$  neutrons escape without further collision while  $x_1(1 - P_1)^2\beta_1$  interact a second time. These produce  $x_1(1 - P_1)^2\beta_1^2$  neutrons, on the average, of which  $x_1P_1(1 - P_1)^2\beta_1^2$  escape, and so on.

The total number of neutrons escaping from the fuel in Group 1 after all collisions, per neutron produced in thermal fission, is therefore

$$x_1P_1 + x_1P_1(1 - P_1)\beta_1 + x_1P_1(1 - P_1)^2\beta_1^2 + \dots = \frac{x_1P_1}{1 - (1 - P_1)\beta_1}. \quad (11-85)$$

The total number of collisions in this group per thermal fission neutron is

$$x_1(1 - P_1) + x_1(1 - P_1)^2\beta_1 + x_1(1 - P_1)^3\beta_1^2 + \dots = \frac{x_1(1 - P_1)}{1 - (1 - P_1)\beta_1}.$$

The neutrons in Group 2 are produced in fission, that is, in the original thermal fission and in subsequent fissions induced by neutrons in Group 1. In particular,

$\chi_2$  neutrons are emitted per thermal fission neutron, and  $\chi_2\nu_1$  neutrons are emitted per fission in Group 1. Since there are a total of

$$\frac{\chi_1(1 - P_1)}{1 - (1 - P_1)\beta_1}$$

collisions in Group 1, and evidently

$$\frac{\chi_1(1 - P_1)\sigma_{1f}/\sigma_{1t}}{1 - (1 - P_1)\beta_1}$$

of these are fissions, it follows that the total number of neutrons entering Group 2, per neutron emitted in thermal fission, is

$$\chi_2 + \frac{\chi_2\nu_1\chi_1(1 - P_1)\sigma_{1f}/\sigma_{1t}}{1 - (1 - P_1)\beta_1}.$$

Consider now the fate of a neutron entering the second group. By definition  $P_2$  leave the fuel without collision and  $(1 - P_2)$  collide. After a collision

$$\frac{(1 - P_2)\sigma_{22}}{\sigma_{2t}} = (1 - P_2)\beta_2$$

neutrons remain in the group, where  $\beta_2 = \sigma_{22}/\sigma_{2t}$ . Of these,  $P_2(1 - P_2)\beta_2$  escape without further collision,  $(1 - P_2)^2\beta_2$  collide a second time, producing  $(1 - P_2)^2\beta_2^2$  neutrons, and so on. The total number escaping into the moderator per neutron entering the group is thus

$$P_2 + P_2(1 - P_2)\beta_2 + P_2(1 - P_2)^2\beta_2^2 + \dots = \frac{P_2}{1 - (1 - P_2)\beta_2}.$$

The number of neutrons leaving the lump in the second group per neutron produced in thermal fission is then

$$\left[ \chi_2 + \frac{\chi_2\nu_1\chi_1(1 - P_1)\sigma_{1f}/\sigma_{1t}}{1 - (1 - P_1)\beta_1} \right] \left[ \frac{P_2}{1 - (1 - P_2)\beta_2} \right]. \quad (11-86)$$

In a similar manner it is easy to show that

$$\frac{\chi_1(1 - P_1)\sigma_{13}/\sigma_{1t}}{1 - (1 - P_1)\beta_1}$$

neutrons are scattered into Group 3 from Group 1 per thermal fission neutron and that the fraction  $P_3/[1 - (1 - P_3)\beta_3]$  of these escape from the fuel, where  $\beta_3 = \sigma_{33}/\sigma_{3t}$ . The total leaving the fuel from Group 3 per fission neutron is therefore

$$\left[ \frac{\chi_1(1 - P_1)\sigma_{13}/\sigma_{1t}}{1 - (1 - P_1)\beta_1} \right] \left[ \frac{P_3}{1 - (1 - P_3)\beta_3} \right]. \quad (11-87)$$

**Table 11-4**  
**Three-Group Cross Sections (in Barns) for Computing  $\epsilon^*$**

Material	$\sigma_{1t}$	$\sigma_{1f}$	$\nu_1 \sigma_{1f}$	$\sigma_{11}$	$\sigma_{13}$	$\sigma_{1\gamma}$
$U^{238}$	4.52	0.549	1.56	1.89†	2.07†	0.054
$U^{238}O_2$	7.77	0.549	1.56	5.10†	2.07†	0.099
Material	$\sigma_{2t}$	$\sigma_{22}$	$\sigma_{2\gamma}$	$\sigma_{3t}$	$\sigma_{33}$	$\sigma_{3\gamma}$
$U^{238}$	6.05	5.91	0.138	5.66	5.53	0.135
$U^{238}O_2$	14.54	14.40	0.138	14.15	14.01	0.135

\* From M. R. Fleishman and H. Soodak, *Nuclear Sci. and Eng.* 7, 217 (1960).

† An additional 0.02 barn has been added to these cross sections to account for extra neutrons from the  $(n, 2n)$  reaction in  $U^{238}$ .

The total number of neutrons leaving the fuel in all groups per thermal fission neutron, that is,  $\epsilon$ , is given by the sum of Eqs. (11-85), (11-86), and (11-87):

$$\begin{aligned} \epsilon = & \frac{\chi_1 P_1}{1 - (1 - P_1)\beta_1} + \left[ \chi_2 + \frac{\chi_2 \nu_1 \chi_1 (1 - P_1) \sigma_{1f} / \sigma_{1t}}{1 - (1 - P_1)\beta_1} \right] \left[ \frac{P_2}{1 - (1 - P_2)\beta_2} \right] \\ & + \left[ \frac{\chi_1 (1 - P_1) \sigma_{13} / \sigma_{1t}}{1 - (1 - P_1)\beta_1} \right] \left[ \frac{P_3}{1 - (1 - P_3)\beta_3} \right], \quad (11-88) \end{aligned}$$

where, to recapitulate,

$$\beta_1 = \frac{\chi_1 \nu_1 \sigma_{1f} + \sigma_{11}}{\sigma_{1t}}, \quad (11-89)$$

$$\beta_2 = \frac{\sigma_{22}}{\sigma_{2t}}, \quad (11-90)$$

$$\beta_3 = \frac{\sigma_{33}}{\sigma_{3t}}. \quad (11-91)$$

Values of the cross sections and other constants needed for use in these equations are given in Table 11-4 for  $U^{238}$  and  $U^{238}O_2$ . It may be noted from the table that Group 2 and Group 3 cross sections are very nearly equal. Thus relatively little error is made by combining these two groups, and this is often done in practice.

It may be mentioned at this point that  $\epsilon$  is somewhat larger for a heterogeneous reactor than for the equivalent homogeneous reactor. This is true because there is a greater chance in the homogeneous case that a fission neutron will be scattered to below the fission threshold in a collision with the moderator before it has had an opportunity to interact with a fuel nucleus. When the fuel is lumped, however, a virgin fission neutron must pass through a region of fuel atoms before ever encountering the moderator, and this tends to increase the probability of a fast fission.

**Closely packed lattices.** Up to this point the discussion has been limited to isolated fuel lumps. If there is interaction between lumps,  $\epsilon$  can be calculated from Eq. (11-88) by replacing  $P_1$ ,  $P_2$ , and  $P_3$  by escape probabilities appropriately modified by the Dancoff-Ginsberg factors as in Eq. (11-81). It must be remembered, however, that this factor does not account precisely for the interaction between lumps, and the resulting values of  $\epsilon$  are therefore not exact. (In addition, of course, the SFS method is not exact to begin with.) For tightly packed lattices  $\epsilon$  can also be estimated by assuming that the system is homogeneous (cf. Fig. 7-4).

**Monte Carlo.** It is possible to compute  $\epsilon$  to any desired accuracy using the Monte Carlo method. Owing to the fact that the pertinent cross sections are smoothly varying functions at the energies of interest and because relatively few collisions are necessary to reduce the energy of a neutron to below the fission threshold, Monte Carlo calculations of  $\epsilon$  are less time consuming than many calculations using this method. Considerably less time is required to compute  $\epsilon$  than  $p$ , for example, for the same lattice and to the same degree of accuracy. For this reason, Monte Carlo is particularly suited for calculations of the fast effect.

### 11-5 The Value of $k_{\infty}$

In the preceding sections it was shown that the thermal utilization is smaller for a heterogeneous lattice than for a homogeneous mixture of the same materials, while the resonance escape probability and the fast fission factor are both larger. If the decrease in  $f$  is more than offset by the increase in  $p$  and  $\epsilon$ , the value of  $k_{\infty}$  will clearly be larger for the heterogeneous lattice than for the equivalent homogeneous system. This is the case for natural and for slightly enriched uranium. Thus up to an enrichment of approximately 5 percent  $U^{235}$ ,  $k_{\infty}$  is increased by lumping the fuel, while at higher enrichments it is decreased.

The effect of fuel lumping on the value of  $k_{\infty}$  was of considerable importance in the development of early reactors. At that time the only available fuel was natural uranium and the only abundant moderating materials were ordinary water and graphite. Unfortunately, numerous studies of the natural uranium-water system showed that even with lumping of the fuel  $k_{\infty}$  cannot be made large enough to provide a critical system. However, by lumping the fuel it was found possible to raise the value of  $k_{\infty}$  for the natural uranium-graphite system from a maximum value of about 0.85 for a homogeneous mixture, to sufficiently greater than unity to permit the operation of a critical reactor. Until enriched uranium and other moderators (in particular,  $D_2O$ ) became available, virtually all reactors were therefore of the natural uranium-graphite type.

It will be recalled from Section 9-6 (Case III) that  $k_{\infty}$  rises to a maximum value and then decreases as the concentration of fuel is raised in a homogeneous mixture of fuel (containing resonance absorbers) and moderator. Essentially the same phenomenon occurs in a heterogeneous system. For example, Fig. 11-12 shows values of  $f$ ,  $p$ ,  $\epsilon$  and  $k_{\infty}$  which were computed in connection with the design of the

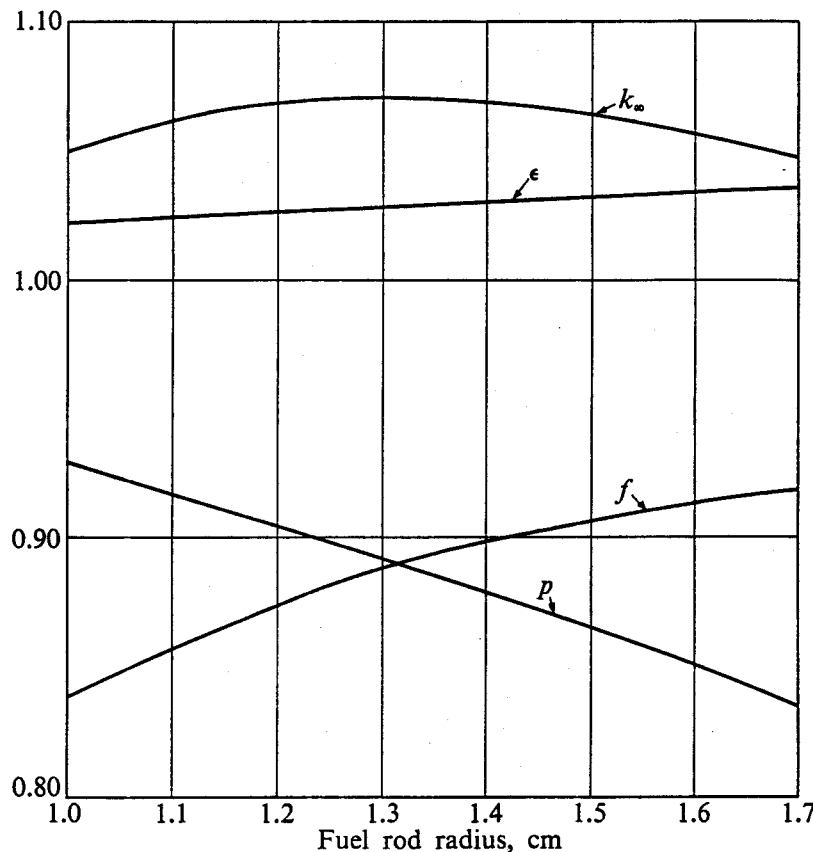


Fig. 11-12. Reactor parameters for the Brookhaven Research Reactor. [Based on I. Kaplan and J. Chernick, "The Brookhaven Nuclear Reactor: Theory and Nuclear Design Calculations," BNL-152 (January 1952).]

first lattice of the Brookhaven Research Reactor (a natural uranium-graphite reactor). In these calculations the lattice spacing was fixed so that an increasing fuel-rod size is equivalent to an increasing fuel concentration. Curves similar to those shown in Fig. 11-12 are found for all heterogeneous reactors.

It will be observed that the dependence of  $f$ ,  $p$ , and  $\epsilon$  in the case of this heterogeneous reactor is similar in all respects to the behavior of these parameters in the homogeneous case as shown in Fig. 9-5. Thus with increasing rod size,  $f$  and  $\epsilon$  increase monotonically while  $p$  decreases monotonically, with the result that  $k_{\infty}$  exhibits a broad maximum. There is hence an optimum rod size (concentration) for which  $k_{\infty}$  is the largest, and other things being equal, this is the rod which would normally be adopted for use in the reactor.

### 11-6 Other Reactor Parameters\*

In order to carry out criticality calculations for a heterogeneous reactor it is necessary to have values of  $\tau_T$ ,  $L_T^2$ , and  $D$  in addition to  $k_{\infty}$ . The more elementary methods for computing these parameters will now be considered.

\* In this section, bars denoting thermal averages are deleted.

**Calculation of  $\tau_T$ .** If the mean free path of fission neutrons for inelastic scattering is large compared with the size of the fuel lumps, the fission neutrons emerge from the lumps with an essentially virgin prompt neutron spectrum. If, in addition, the lumps are isolated in the sense of the preceding sections, these fission neutrons slow down in the surrounding moderator and  $\tau_T$  is simply the age of fission neutrons in the moderator.

When the inelastic mean free path is *not* large compared with the size of the lump, some fission neutrons may undergo inelastic scattering in the fuel. The energy distribution of the neutrons emerging from the fuel may then be substantially different from the prompt fission neutron spectrum. In this case, the age of the fission neutrons can be estimated by writing

$$\tau_T = \tau_{TM} P_{F0} + \tau'_{TM}(1 - P_{F0}) \quad (11-92)$$

or

$$\tau_T = \tau'_{TM} + (\tau_{TM} - \tau'_{TM})P_{F0}, \quad (11-93)$$

where  $\tau_{TM}$  is the age of fission neutrons in the moderator,  $\tau'_{TM}$  is the age of neutrons with a fission spectrum *degraded by one inelastic collision in the fuel*, and  $P_{F0}$  is the probability that a fission neutron will escape from the fuel without being inelastically scattered. The value of  $P_{F0}$  can be obtained from Fig. 11-8 by replacing  $\Sigma_{tF}$  with  $\Sigma_{if}$ , the macroscopic inelastic scattering cross section of the fuel.

The following formulas which are based on Eq. (11-93) have been widely used for computing  $\tau_T$ ; for natural uranium-graphite lattices:

$$\tau_T = 231 + 133P_{F0} \text{ cm}^2; \quad (11-94)$$

and for natural uranium-D<sub>2</sub>O lattices:

$$\tau_T = 97 + 23P_{F0} \text{ cm}^2. \quad (11-95)$$

The above equations neglect the volume of the lattice occupied by the fuel, and, indeed, this is usually small in an isolated lattice. The effect of the presence of the fuel can easily be included, however, by assuming that any neutron returning to the lump from the moderator has an energy below the inelastic threshold. Since elastic scattering by a heavy nucleus has little effect upon the energy of a neutron, it is reasonable to treat the fuel as a void region. Then by homogenizing the voids with the moderator, the final formula for  $\tau_T$  in an isolated lattice becomes

$$\tau_T = (1 + \gamma)^2 [\tau'_{TM} + (\tau_{TM} - \tau'_{TM})P_{F0}], \quad (11-96)$$

where

$$\gamma = V_F/V_M$$

is the fuel-to-moderator-volume ratio.

With tightly packed, interacting lattices it is usual to treat the system as if it were homogeneous. The age must be computed using one of the numerical methods described in Section 6-16 which gave rise to Fig. 6-14.

**Calculation of  $\Sigma_a$ ,  $D$ , and  $L_T^2$ .** The average value of the macroscopic absorption cross section for a heterogeneous lattice is defined as

$$\Sigma_a = \frac{\int \Sigma_a(\mathbf{r})\phi(\mathbf{r}) dV}{\int \phi(\mathbf{r}) dV}. \quad (11-97)$$

Since  $\Sigma_a(\mathbf{r})$  is a constant in the fuel and moderator, Eq. (11-97) can be written as

$$\Sigma_a = \frac{\Sigma_{aF}\bar{\phi}_F V_F + \Sigma_{aM}\bar{\phi}_M V_M}{\bar{\phi}_F V_F + \bar{\phi}_M V_M}, \quad (11-98)$$

where  $\bar{\phi}_F$  and  $\bar{\phi}_M$  are the average fluxes in the fuel and moderator, respectively.

An equation of the same form as Eq. (11-98) holds for the average transport cross section, namely,

$$\Sigma_{tr} = \frac{\Sigma_{trF}\bar{\phi}_F V_F + \Sigma_{trM}\bar{\phi}_M V_M}{\bar{\phi}_F V_F + \bar{\phi}_M V_M}. \quad (11-99)$$

The average diffusion coefficient of the lattice,  $D$ , is inversely proportional to  $\Sigma_{tr}$ , and it follows from Eq. (11-99) that

$$\frac{\bar{\phi}_F V_F + \bar{\phi}_M V_M}{D} = \frac{\bar{\phi}_F V_F}{D_F} + \frac{\bar{\phi}_M V_M}{D_M}, \quad (11-100)$$

where  $D_F$  and  $D_M$  are the diffusion coefficients of the fuel and moderator.

Solving Eq. (11-100) for  $D$  and dividing by  $\Sigma_a$  from Eq. (11-98) gives the average thermal diffusion area of the lattice:

$$L_T^2 = \frac{(\bar{\phi}_F V_F + \bar{\phi}_M V_M)^2}{[(\bar{\phi}_F V_F/D_F) + (\bar{\phi}_M V_M/D_M)](\Sigma_{aF}\bar{\phi}_F V_F + \Sigma_{aM}\bar{\phi}_M V_M)}. \quad (11-101)$$

This expression can be simplified by extracting the parameters  $D_M$  and  $\Sigma_{aM}$  from the denominator and by using the definitions of  $f$  given in Eq. (11-6) and the thermal disadvantage factor  $\xi$  given in Eq. (11-8). The resulting formula for  $L_T^2$  is

$$L_T^2 = (1 - f)L_{TM}^2 \frac{[1 + V_F/V_M\xi]^2}{1 + D_M V_F/D_F V_M \xi}, \quad (11-102)$$

where  $L_{TM}^2$  is the thermal diffusion area of the moderator. If the fuel volume is small compared to the moderator volume, and since  $\xi$  is always greater than unity, Eq. (11-102) reduces to

$$L_T^2 \approx (1 - f)L_{TM}^2, \quad (11-103)$$

which is also the formula for  $L_T^2$  for a homogeneous system (cf. Eq. 9-104).

Although Eqs. (11-98), (11-100), and (11-102) or (11-103) are often used in practice, they are not to be considered exact. For one thing, variations in the thermal neutron spectrum with position in the lattice were entirely ignored in the preceding derivations. More rigorous methods have been developed for computing the diffusion parameters, but these are beyond the scope of this book.

## References

### General

- CASE, K. M., F. DE HOFFMANN, and G. PLACZEK, "Introduction to the Theory of Neutron Diffusion," U.S. Government Printing Office, Washington, D.C., 1953. This report contains tables and curves of the collision probability  $P_C$ , where  $P_C = 1 - P_{F0}$ .
- CHERNICK, J., "Calculation Methods for Heterogeneous Systems," BNL-622, August 1960.
- GALANIN, A. D., *Thermal Reactor Theory*. New York: Pergamon Press, 1960, Chapters 4 and 10.
- GLASSSTONE, S., and M. C. EDLUND, *The Elements of Nuclear Reactor Theory*. Princeton, N.J.: Van Nostrand, 1952, Chapter 9.
- ISBIN, H. S., *Introductory Nuclear Reactor Theory*. New York: Reinhold, 1963, Chapter 15.
- MEEM, J. L., *Two Group Reactor Theory*. New York: Gordon and Breach, 1964, Chapter 9.
- MEGHREBLIAN, R. V., and D. K. HOLMES, *Reactor Analysis*. New York: McGraw-Hill, 1960, Chapter 10.
- MURRAY, R. L., *Nuclear Reactor Physics*. Englewood Cliffs, N.J.: Prentice-Hall, 1957, Chapter 4.
- Reactor Physics Constants*, United States Atomic Energy Commission Report, ANL-5800, 2nd ed., 1963, Section 4.
- WEINBERG, A. M., and E. P. WIGNER, *The Physical Theory of Neutron Chain Reactors*. Chicago: University of Chicago Press, 1958, Chapters 18 through 21.

### Thermal Utilization

- AMOUYAL, A., P. BENOIST, and J. HOROWITZ, "Nouvelle Methode de Determination du Facteur D'Utilisation Thermique D'Une Cellule," *J. Nuclear Energy* 6, 79-98 (1957).

Additional references, particularly to the diffusion method for computing  $f$ , will be found in the general references above.

### Resonance Escape

- DRESNER, L., *Resonance Absorption in Nuclear Reactors*. New York: Pergamon Press, 1960.
- NORDHEIM, L. W., "A New Calculation of Resonance Integrals," *Nuclear Sci. and Eng.* 12, 457 (1962).
- NORDHEIM, L. W., "The Theory of Resonance Absorption," *Proc. Symp. Appl. Math.* 11 (1961). Providence, R.I.: American Mathematical Society.
- ROTHENSTEIN, W., "Collision Probabilities and Resonance Integrals for Lattices," *Nuclear Sci. and Eng.* 7, 162 (1960).

### Fast Effect

- FLEISHMAN, M. R., and H. SOODAK, "Methods and Cross Sections for Calculating the Fast Effect," *Nuclear Sci. and Eng.* 7, 217 (1960).
- MÄRKL, H., and A. G. FOWLER, "A Generalized Method for Calculating the Fast Fission Effect in Coaxial Cylindrical Lattice Cells," *Nukleonik* 6, 39 (1964).
- SPINRAD, B. I., "Fast Effect in Lattice Reactors," *Nuclear Sci. and Eng.* 1, 455 (1956).

## Problems

11-1. Derive the following handy formulas for the radius  $b$  of the equivalent unit cell in terms of the lattice pitch  $s$ :

- (a)  $b = 0.564s$ , square lattice,
- (b)  $b = 0.525s$ , hexagonal lattice.

11-2. Show that the thermal disadvantage factor for a heterogeneous reactor is given by the formula

$$\xi = F + \frac{\Sigma_{aF} V_F}{\Sigma_{aM} V_M} (E - 1),$$

where  $F$  and  $E$  are the lattice functions.

11-3. Derive the lattice functions  $F$  and  $E$  given in Table 11-1 for (a) planar geometry, (b) spherical geometry.

11-4. (a) By treating fuel rods as line sources of fast neutrons, show that the slowing-down density at any point in an infinite square lattice of cylindrical rods is given by

$$q(x, y) = \frac{Q}{4\pi\tau} \sum_{m, n=-\infty}^{\infty} \exp[-[(x - ms)^2 + (y - ns)^2]/4\tau],$$

where  $Q$  is a constant,  $s$  is the lattice spacing (pitch), and  $x$  and  $y$  are measured from the axis of one rod. [Hint: See Problem 6-20.] (b) Using the identity (this is an instance of the *Poisson sum formula*)

$$\sum_{m=-\infty}^{\infty} e^{-(x-ms)^2/4\tau} = \frac{\sqrt{4\pi\tau}}{s} \sum_{m=-\infty}^{\infty} e^{-4\pi^2 m^2 \tau/s^2} \cos\left(\frac{2\pi mx}{s}\right),$$

show that  $q(x, y)$  reduces to

$$q(x, y) = \frac{Q}{s^2} \sum_{m, n=-\infty}^{\infty} \exp[-4\pi^2(m^2 + n^2)\tau/s^2] \cos\left(\frac{2\pi mx}{s}\right) \cos\left(\frac{2\pi ny}{s}\right).$$

(c) Using the result of part (b), show that the ratio of the slowing-down density at the edge of a cell to that at the center of a cell is of the order of  $1 - 8 \exp(-4\pi^2\tau/s^2)$ , and hence show that a criterion for the validity of the assumption that  $q$  is constant over the cell is

$$e^{4\pi^2\tau/s^2} \gg 8.$$

(d) Investigate the validity of the constant  $q$  assumption for the lattices described in Problems 11-9 and 11-10.

11-5. Show that the lattice functions in cylindrical geometry are given by the following expansions:

$$(a) F(x) = 1 + \frac{1}{2}\left(\frac{x}{2}\right)^2 - \frac{1}{12}\left(\frac{x}{2}\right)^4 + \dots$$

$$(b) E(x, y) = 1 + \frac{y^2}{2} \left[ \frac{y^2}{y^2 - x^2} \ln\left(\frac{y}{x}\right) - \frac{3}{4} + \frac{x^2}{4y^2} + \dots \right].$$

11-6. Using (1) diffusion theory and (2) the ABH method, calculate and plot the thermal utilization of a square lattice of natural uranium rods and graphite moderator as a function of the rod radius for (a) constant fuel-to-moderator-volume ratio of  $V_F/V_M = 1/50$ , (b) constant rod spacing of 10 inches. [Note: In part (a), fixing the ratio of  $V_F/V_M$  fixes the fuel concentration; increasing the rod radius then corresponds to increasing the heterogeneity of the system. In part (b), increasing the rod radius is equivalent to increasing both the fuel concentration and the heterogeneity.]

11-7. Fuel lumps are wrapped in cladding of volume  $V_S$  and macroscopic absorption cross section  $\Sigma_{as}$ . (a) Show that in diffusion theory the thermal utilization can be written approximately as

$$\frac{1}{f} = \frac{\Sigma_{aM} V_M}{\Sigma_{aF} V_F} F(\kappa_F a) + \frac{\Sigma_{as} V_S}{\Sigma_{aF} V_F} F(\kappa_F a) E(\kappa_M a, \kappa_M b) + E(\kappa_M a, \kappa_M b),$$

or, since ordinarily  $E(\kappa_M a, \kappa_M b) \approx 1$ ,

$$\frac{1}{f} = \frac{\Sigma_{aM} V_M + \Sigma_{as} V_S}{\Sigma_{aF} V_F} F(\kappa_F a) + E(\kappa_M a, \kappa_M b).$$

*Note:* The corresponding formula in the ABH method is

$$\frac{1}{f} = \frac{\Sigma_{aM} V_M + \Sigma_{as} V_S}{\Sigma_{aF} V_F} \frac{1}{P_F} + \frac{1}{P_M} - \frac{4\Sigma_{aM} V_M}{S_F}.$$

(b) Show that the *moderator* thermal utilization,  $f_M$ , that is, the probability that a thermal neutron is absorbed in the moderator, is given in diffusion theory by

$$f_M = 1 - f \left[ 1 + \frac{\Sigma_{as} V_S}{\Sigma_{aF} V_F} F(\kappa_F a) \right].$$

[Hint: In part (a) use the thin interface boundary conditions (cf. Section 5-8).]

11-8. In gas-cooled reactors the fuel elements are usually surrounded by comparatively vacuous coolant channels or gaps. By assuming that the thermal flux is constant across the channel, show that according to diffusion theory,  $f$  is given by

$$\frac{1}{f} = \frac{\Sigma_{aM} V_M}{\Sigma_{aF} V_F} F(\kappa_F a) + E(\kappa_M c, \kappa_M b),$$

where  $a$  is the radius of the fuel (equal to the inner radius of the gap);  $c$  is the outer radius of the gap (equal to the inner radius of the moderator); and  $b$  is the outer radius of the moderator. Note: More accurate formulas for  $f$  with coolant gaps are tabulated in ANL-5800, Second Edition, Section 4. The corresponding formula for  $f$  in the ABH method is

$$\begin{aligned} \frac{1}{f} &= \frac{\Sigma_{aM} V_M}{\Sigma_{aF} V_F} \left\{ 1 + \frac{\Sigma_{aF} A}{\Sigma_{tF}} \left[ 1 + \alpha \left( \frac{\Sigma_{sF}}{\Sigma_{tF}} \right) + \beta \left( \frac{\Sigma_{sF}}{\Sigma_{tF}} \right)^2 \right] + a \Sigma_{aF} \left( 1 - \frac{a}{c} \right) \right\} \\ &\quad + \frac{b^2 - c^2}{c^2} \left( \frac{cd}{2L_M^2} - c \Sigma_{aM} \right) + E(\kappa_M c, \kappa_M b). \end{aligned}$$

11-9. A large, air-cooled research reactor (the reactor in question is the first version of the Brookhaven Research Reactor) consists of a 25-ft cube of graphite penetrated by a

square array of 1369 air channels. The channels have a circular cross-sectional area of  $36 \text{ cm}^2$  and are spaced on 8-in. centers. Each air channel holds one fuel assembly, which consists of a finned aluminum cartridge containing several natural uranium slugs 1.1 in. in diameter. The six longitudinal fins extend along the full length of the cartridge to increase the transfer of heat to the air and to support the fuel in the center of each channel. The aluminum-uranium volume ratio is 0.2. (a) Using the formulas derived in Problems 11-7 and 11-8, estimate the thermal utilization of the lattice by the diffusion theory and ABH methods. (b) What fraction of the thermal neutrons are absorbed by the moderator? by aluminum? (c) What is the thermal utilization of the equivalent homogeneous lattice? [Note: In part (a) assume that all of the aluminum is located in a jacket surrounding the fuel. (The value  $f = 0.8984$  was computed by diffusion theory when this reactor was designed.)]

11-10. (a) Using the ABH method compute the thermal utilization of a hexagonal lattice of 0.384-in. radius  $\text{UO}_2$  rods ( $\rho = 7.53 \text{ gm/cm}^3$ ) and water, if the uranium is enriched to 1.3%  $\text{U}^{235}$  and the fuel-to-water-volume ratio is 0.25. (b) What is the thermal disadvantage factor for this lattice?

11-11. A small black cylinder of radius  $a$  is inserted in an infinite moderator which contains neutrons. Clearly, in the limit as  $a \rightarrow 0$  the cylinder cannot perturb the flux. (a) Assuming that the flux is isotropic, show that in this limit,  $d$  is given by

$$d = 4D = \frac{4}{3}\lambda_{\text{tr}},$$

where  $D$  and  $\lambda_{\text{tr}}$  refer to the moderator. (b) What is  $d$  in this limit for a sphere? [Hint: For part (a) use the result of Problem 5-6 to compute the current into the cylinder at its surface, and equate this to the current computed by Fick's law. Proceed similarly in part (b).]

11-12. The functions  $E_n(x)$ , which are defined in Appendix II, appear in many calculations of neutron escape probabilities (cf. Problems 11-13 and 11-14). Derive the following useful relations:

$$(a) \quad E_n(x) = \int_x^\infty E_{n-1}(u) du,$$

$$(b) \quad E_n(0) = \frac{1}{n-1}, \quad n > 1,$$

$$(c) \quad E_n(x) = \frac{1}{n-1} [e^{-x} - xE_{n-1}(x)], \quad n > 1,$$

$$(d) \quad E_n(x) = \frac{e^{-x}}{x} \left[ 1 - \frac{n}{x} + \frac{n(n+1)}{x^2} - \frac{n(n+1)(n+2)}{x^3} + \dots \right],$$

$$x \gg 1, n > 1.$$

11-13. A semi-infinite, uniform medium ( $0 \leq x < \infty$ ) contains monoenergetic, isotropic sources emitting  $S$  neutrons/ $\text{cm}^3\text{-sec}$ . Consider the neutrons emitted from a differential slab of thickness  $dx$ , located at a distance  $x$  from the surface of the medium. (a) Show that the current of neutrons from this slab which are emitted from the surface at  $x = 0$ , but which have not undergone a collision, is given by

$$dJ = \frac{Sx dx}{2} \int_x^\infty \frac{e^{-\Sigma_t u} du}{u^2} = \frac{S dx}{2} E_2(\Sigma_t x).$$

(b) Show that the probability  $P(x)$  that a neutron emitted at the distance  $x$  from the surface escapes without a collision is

$$P(x) = \frac{1}{2}E_2(\Sigma_t x).$$

(c) Show that the total current of neutrons leaving the medium without a collision is

$$J = \frac{S}{4\Sigma_t}.$$

11-14. Neutrons are emitted uniformly by isotropic sources throughout an infinite slab of thickness  $a$ . (a) Using the result of Problem 11-13, part (b), show that the probability that a neutron, emitted at the distance  $x$  from one surface of the slab, escapes from either surface without a collision is given by

$$P(x) = \frac{1}{2}\{E_2(\Sigma_t x) + E_2[\Sigma_t(a - x)]\}.$$

(b) Show that the *average* probability that a neutron escapes without a collision is

$$P_0 = \frac{1}{2\Sigma_t a} [1 - 2E_3(\Sigma_t a)].$$

(c) Plot  $P_0$  as a function of  $\Sigma_t a$ . (See Appendix II for a list of tabulations of  $E_n(x)$ .)

11-15. If the error in the resonance integral is estimated to be 10%, how much of an error does this introduce in calculations of  $p$ , when  $p$  is approximately 0.85?

11-16. (a) Compute the resonance escape probability for the reactor described in Problem 11-9. (b) What is the resonance escape probability for the equivalent homogeneous system? [Note: Ignore the presence of the aluminum. (The value  $p = 0.8783$  was obtained in the original design calculations of this reactor.)]

11-17. Using the reciprocity theorem show that

$$P_{F0}\Sigma_{tF}V_F = P_{M0}\Sigma_{tM}V_M.$$

[Hint: The probabilities  $P_{F0}$  and  $P_{M0}$  can be written as double integrals (cf. Eq. 11-36) of the Green's function for the *uncollided flux*. By its nature this Green's function must satisfy the reciprocity theorem. Do not use a diffusion kernel for this problem; the relevant neutrons do not diffuse.]

Table 11-5

$E_1(\text{eV})$	$\Gamma_\gamma(\text{mV})$	$\Gamma_n(\text{mV})$
6.67	26	1.52
398	40	7

11-18. Determine the practical widths of the  $\text{U}^{238}$  resonances whose properties are given in Table 11-5 for a lump of natural uranium at the following temperatures. In each case, compare  $\Gamma_P$  with the average energy loss per collision:

(a)  $T = 0^\circ\text{K}$

(b)  $T = 20^\circ\text{C}$

(c)  $T = 500^\circ\text{C}$

11-19. Consider a hexagonal lattice of 1-in. diameter natural uranium rods and ordinary water, with a metal-to-water-volume ratio of 1/3. Using the data in Problem 11-18, estimate the probabilities that a fission neutron will be captured in the 6.67 eV or the 398 eV resonance of  $\text{U}^{238}$  at the following temperatures:

$$(a) T = 0^\circ\text{K} \quad (b) T = 20^\circ\text{C} \quad (c) T = 500^\circ\text{C}$$

Compare with the same probabilities for the equivalent homogeneous system. [Note: The rods may be assumed to be isolated.]

11-20. Compute and plot as a function of rod-radius the resonance escape probability and the fast fission factor of the lattice described in Problem 11-6 (b).

11-21. Compute the fast fission factor for the reactor described in Problem 11-9. [Note: Using a method which predates the SFS method, the value  $\epsilon = 1.0299$  was obtained in the original design calculations of this reactor.]

11-22. Consider a natural uranium fuel rod, 1.1 in. in diameter. Using the SFS method, compute the fraction of fission neutrons that (a) leave the fuel without a collision; (b) are scattered within the fuel from above to below the fission threshold; (c) are captured in the fuel above and below the fission threshold.

11-23. (a) Using the results of Problems 11-6 and 11-20, determine the maximum value of  $k_\infty$  for the 10-in. lattice. (b) What is the value of  $k_\infty$  for the homogeneous system corresponding to  $(k_\infty)_{\max}$ ? [Note: In part (b) use  $\epsilon = 1$ .]

11-24. (a) Using the results of Problems 11-9, 11-16, and 11-21, compute  $k_\infty$  for the reactor described in Problem 11-9. (b) What is  $k_\infty$  for the equivalent homogeneous reactor?

11-25. A certain lattice consists of uranium metal rods 0.25 in. in diameter, enriched to 1.15%  $\text{U}^{235}$ , in ordinary water. The metal-to-water-volume ratio is 0.5. Compute (a)  $k_\infty$ ; (b) the ratio of the number of fissions in  $\text{U}^{238}$  to the number of fissions in  $\text{U}^{235}$ ; (c) the conversion ratio for this lattice at startup. [Note: The Dancoff-Ginsberg factor is 0.280; in part (c), see Problem 9-13.]

11-26. A subcritical assembly consists of a hexagonal lattice of aluminum clad, natural uranium rods in ordinary water. The rods are 1.20 in. in diameter including the cladding which is 0.040 in. thick. The lattice pitch is 1.80 in. (a) Compute  $k_\infty$  for this assembly. (Compute  $f$  by the ABH method; cf. Problem 11-7.) (b) Determine the optimum pitch, i.e., the one giving maximum  $k_\infty$ , for this lattice.

11-27. Estimate  $\tau_T$ ,  $\bar{D}$ ,  $\bar{\Sigma}_a$ , and  $L_T^2$  for the lattice described in (a) Problem 11-9; (b) Problem 11-25.

# 12

## Reactor Kinetics

For the most part, the preceding chapters have been concerned with the properties of critical reactors operating in the steady state. There was some discussion of the time behavior of noncritical reactors in Chapter 9, but this was primarily for the purpose of deriving the conditions for criticality, and many important aspects of the transient behavior of reactors were omitted. In the present chapter this transient behavior will be considered in more detail. This subject is usually called *reactor kinetics* or *reactor dynamics*.

A reactor will become supercritical or subcritical if its properties are changed in such a way that its multiplication factor becomes different from unity. These changes may occur in a number of ways, some of the more important of which are the following:

(a) *Control-rod motion.* Most reactors are controlled by moving rods of neutron-absorbing material which are inserted in their interiors. The movement of these *control rods* changes the absorption properties of the reactor, and this changes its multiplication factor. Control-rod motion, particularly during startup and shutdown, is the most frequently encountered reason for a reactor becoming noncritical.

(b) *Fuel burnup.* According to Section 3-6, fissionable material is consumed in an operating reactor at a rate proportional to the power of the system. Thus the amount of fuel in a reactor decreases in time, and this naturally has an effect on the multiplication factor.

(c) *Isotope production.* As discussed in Chapter 3, a large number of isotopes are produced in fission. Unfortunately, certain of these isotopes, known as *poisons*, are strong neutron absorbers and may substantially increase the absorption cross section of a reactor. In addition, if fertile materials such as  $\text{Th}^{232}$  or  $\text{U}^{238}$  are present, fissile nuclei will be produced (and, in part, consumed) in time and the appearance of these new isotopes will also affect the multiplication factor of the system.

(d) *Temperature changes.* Many reactor parameters depend upon temperature, and the multiplication factor of a reactor is therefore also temperature dependent. Reactor temperature, however, is usually a function of the operating power of the reactor, and changes in power level may lead to changes in the criticality of the system.

(e) *Environmental changes.* Some reactors are coupled to and are therefore affected by changes in their environment. The average absorption cross section of an air-cooled reactor, for example, depends upon the total amount of air present in the system. This, in turn, is a function of barometric pressure and air temperature, and the criticality of a reactor of this kind depends to some extent upon meteorological conditions.

(f) *Accidents.* Unforeseen events may suddenly change the properties and criticality of a reactor. For instance, if a coolant channel becomes clogged, some of the fuel rods, denied proper cooling, may increase in temperature to a point where they melt. The ensuing disassembly of portions of the fueled regions of the reactor obviously has a serious effect on the criticality of the system.

For these and other reasons a reactor may become supercritical or subcritical. In the present chapter, however, it will merely be assumed that a change in the multiplication factor occurs because of unspecified causes, and the central problem will be to determine the subsequent behavior of the noncritical reactor. Factors contributing to the change in the multiplication factor will be discussed in detail in Chapters 13 and 14.

### 12-1 Infinite Reactor with No Delayed Neutrons

Although the conclusions reached in Chapter 9 regarding the conditions for reactor criticality are strictly correct, that discussion of the time behavior of a non-critical reactor omitted one important factor affecting the dynamics of a reactor, namely, the *delayed neutrons*. It will be recalled from Chapter 3 that these neutrons appear long after the prompt neutrons, in six more or less well-defined distinct groups, each with its own characteristic energy and half-life (cf. Section 3-4). The fraction of the fission neutrons which are delayed is very small, (in the case of  $U^{235}$  only one neutron in about 150 is delayed) and for this reason it might be thought that they could be ignored. Quite the reverse is true, however, and were it not for these few delayed neutrons the control of nuclear reactors would be considerably more difficult than it actually is.

In order to understand the importance of delayed neutrons in reactor dynamics it is instructive to consider first the response of an infinite homogeneous reactor to a change in its multiplication factor in the *absence* of the delayed neutrons, that is, with only the prompt neutrons included. It will be assumed that up to the time  $t = 0$  the reactor is critical so that  $k_{\infty} = 1$ . Then at  $t = 0$ ,  $k_{\infty}$  is changed and the system becomes either supercritical or subcritical. An instantaneous change of this type, from one constant value of  $k_{\infty}$  to another, is called a *step change* in  $k_{\infty}$ .

Let  $l_p$  be the *prompt neutron lifetime*, that is, the average time from the emission of a prompt neutron in fission to the absorption of the neutron somewhere in the reactor. For example, in an infinite *thermal* reactor,  $l_p$  is the sum of the slowing-down time  $t_s$  and the diffusion time  $t_d$  (cf. Section 8-6) so that  $l_p = t_s + t_d$ . Since  $t_s \ll t_d$ , it follows that in this case  $l_p \approx t_d$ . On the other hand,  $l_p$  is much

less than  $t_s$  in intermediate and fast reactors due to the fact that the neutrons do not thermalize in these systems. Since the absorption of a prompt fission neutron initiates a new generation of fission neutrons, it will be clear that (in the absence of delayed neutrons)  $l_p$  is equal to the average time between successive generations of neutrons in a chain reaction, which is also known as the *mean generation time*.

In view of the definition of the multiplication factor (cf. Section 4-1), the absorption of one neutron in an infinite reactor leads, on the average, to the absorption of  $k_\infty$  neutrons in the next generation, that is,  $l_p$  sec later. It follows, therefore, that if  $N_F(t)$  is the number of fissions (which is proportional to the number of absorptions) occurring per  $\text{cm}^3/\text{sec}$  at the time  $t$  at any point in the system, the fission rate  $l_p$  sec later will be

$$N_F(t + l_p) = k_\infty N_F(t). \quad (12-1)$$

However, since

$$N_F(t + l_p) \approx N_F(t) + l_p \frac{dN_F(t)}{dt},$$

it follows that  $N_F(t)$  is determined by the equation

$$\frac{dN_F(t)}{dt} \approx \frac{(k_\infty - 1)}{l_p} N_F(t). \quad (12-2)$$

Integrating this equation gives

$$N_F(t) = N_F(0) e^{(k_\infty - 1)/l_p t}, \quad (12-3)$$

where  $N_F(0)$  is the fission rate at  $t = 0$ .

According to Eq. (12-3), the fission rate varies exponentially with time, and it is convenient to write

$$N_F(t) = N_F(0) e^{t/T}, \quad (12-4)$$

where  $T$  is called the *period* of the reactor. It will be evident that in the time  $T$  the fission rate either increases or decreases by the factor  $e$ , depending upon whether  $k_\infty - 1$  is positive or negative, and for this reason  $T$  is sometimes called the "e-folding time." In the present derivation, in which the delayed neutrons have been omitted, Eq. (12-3) gives

$$T = \frac{l_p}{k_\infty - 1}. \quad (12-5)$$

As an illustration of these results, consider an infinite thermal reactor consisting of a homogeneous mixture of  $\text{H}_2\text{O}$  and  $\text{U}^{235}$  in which  $k_\infty$  is increased by only 0.1 percent, that is, from  $(k_\infty)_0 = 1.000$  to  $k_\infty = 1.001$ . In this case, the prompt neutron lifetime  $l_p$  is equal to the mean diffusion time  $t_d$  of neutrons in the water-fuel mixture. According to Eq. (8-82)  $t_d$  is given by

$$t_d = \frac{\sqrt{\pi}}{2\bar{\Sigma}_{aF}v_T} = \frac{\sqrt{\pi}}{2(\bar{\Sigma}_{aF} + \bar{\Sigma}_{aM})v_T}, \quad (12-6)$$

where  $\bar{\Sigma}_{aF}$  and  $\bar{\Sigma}_{aM}$  are the average thermal macroscopic absorption cross sections of fuel and moderator, respectively. Equation (12-6) may also be written as

$$t_d = \frac{\sqrt{\pi}}{2\bar{\Sigma}_{aM}v_T} \frac{1}{1 + \bar{\Sigma}_{aF}/\bar{\Sigma}_{aM}} = t_{dM} \frac{1}{1 + \bar{\Sigma}_{aF}/\bar{\Sigma}_{aM}}, \quad (12-7)$$

where  $t_{dM}$  is the mean diffusion time for the moderator alone. Finally, from the definition of the thermal utilization given in Eq. (9-2),  $\bar{\Sigma}_{aF}/\bar{\Sigma}_{aM} = f/(1 - f)$ , and Eq. (12-7) reduces to

$$t_d = t_{dM}(1 - f). \quad (12-8)$$

Since the system was initially critical,  $(k_\infty)_0 = 1 = \eta_T f$ , and with  $\eta_T = 2.07$  for  $U^{235}$ ,  $f \approx 1/2$ . From Table 8-4 the mean diffusion time of thermal neutrons in pure water is  $2.1 \times 10^{-4}$  sec, so that from Eq. (12-8),  $t_d \approx 10^{-4}$  sec. Then from Eq. (12-5) it follows that

$$T = 10^{-4}/(1.001 - 1) = 0.1 \text{ sec.}$$

This is a very short period; in one second the reactor would pass through 10 periods and the fission rate (and power) would increase by a factor of  $e^{10} = 2.2 \times 10^4$ . Had the reactor originally been operating at 1 megawatt, the power would increase to 22,000 megawatts in only one second, if the system did not destroy itself first. A reactor with such a short period would be very difficult to control, to say the least. Although this result was derived for an infinite reactor, it will be shown later in this section that the mean-life of a neutron in a finite reactor is less than in an infinite system. The period of the corresponding finite reactor is therefore even shorter than computed above.

The situation is even worse with an intermediate or fast reactor due to the fact that the mean generation time in the absence of delayed neutrons is much shorter than for thermal reactors. For the Fermi Reactor (cf. Section 4-4), for example, the prompt neutron lifetime is only  $10^{-7}$  sec, and a 0.1 percent change in  $k_\infty$  would give a period of only  $10^{-4}$  sec.

Fortunately, due to the presence of the delayed neutrons, actual reactor periods are considerably longer than those computed in this section, and as a consequence reactors can be controlled rather easily.

## 12-2 Mean Generation Time with Delayed Neutrons

The underlying reason for the short periods of the reactors in the preceding section was the small value of the generation time, which in the absence of delayed neutrons is equal to the prompt neutron lifetime. When the delayed neutrons are included, the generation time is increased considerably and is equal to the sum of the prompt and delayed neutron lifetimes weighted by their relative yields. Let  $\beta_i$  be the fraction of the fission neutrons\* which appear in the  $i$ th group. The total

\* It must be emphasized that "fission neutrons" include both the prompt and delayed neutrons.

fraction of neutrons which are delayed is then

$$\beta = \sum_{i=1}^6 \beta_i, \quad (12-9)$$

so that the fraction  $1 - \beta$  of the fission neutrons is emitted as prompt neutrons. If  $l_p$  is again the prompt neutron lifetime, and  $l_i$  is the mean lifetime of a delayed neutron in the  $i$ th group *measured from the instant of fission to the time when the neutron is ultimately absorbed*, the mean-life of all fission neutrons, prompt and delayed, is

$$l = (1 - \beta)l_p + \sum_{i=1}^6 \beta_i l_i. \quad (12-10)$$

It may be noted at this point that the delayed neutrons slow down and are captured in a time which is short compared with the mean lifetime of their precursors. That is,  $t_s + t_d \ll \bar{t}_i$ , where  $\bar{t}_i$  is the mean-life of the precursors of the  $i$ th delayed group. Therefore, since one delayed neutron is emitted with the decay of each precursor, it follows that  $\bar{t}_i$  is also equal to the mean-life of a neutron in the  $i$ th group, that is,  $\bar{t}_i = l_i$ , and Eq. (12-10) reduces to

$$l = (1 - \beta)l_p + \sum_{i=1}^6 \beta_i \bar{t}_i. \quad (12-11)$$

Finally, since, according to Table 3-7,  $\beta \ll 1$  for all fissile nuclei, Eq. (12-11) can be written as

$$l \approx l_p + \sum_{i=1}^6 \beta_i \bar{t}_i. \quad (12-12)$$

Return now to the example of the  $U^{235}$ -fueled, water-moderated thermal reactor discussed earlier. Using the values given in Table 3-7 for  $U^{235}$ , the term  $\sum \beta_i \bar{t}_i$  in Eq. (12-12) is found to be 0.085 sec  $\approx$  0.1 sec. Again,  $l_p \approx 10^{-4}$  and from Eq. (12-12)  $l$  is about 0.1 sec, rather than  $10^{-4}$  sec as in Section 12-1, where the delayed neutrons were omitted. A 0.1 percent change in  $k_\infty$  according to Eq. (12-5) now leads to a period of  $T = 0.1/0.001 = 100$  sec. With this period it would take 100 sec for the reactor power to increase by a factor of  $e$  and the system could easily be controlled by the motion of control rods. It should be evident from this example, that the mean generation time and reactor period are determined very largely by the delayed rather than by the prompt neutrons. This is especially true for intermediate and fast reactors because of the very small prompt neutron lifetimes in these systems.

### 12-3 Infinite Reactor with Delayed Neutrons

Unfortunately, the precise effect of the delayed neutrons on the response of a reactor to a change in its multiplication factor cannot be found by simply replacing the mean generation time in the absence of delayed neutrons by the more

appropriate expression given in Eq. (12-12). Instead, it is necessary to consider in detail the production and subsequent decay of each of the delayed neutron precursors in the reactor. The analysis is rather complicated for a general reactor and it is expedient to begin by considering the infinite homogeneous thermal reactor. The thermal flux and concentrations of precursors are then independent of position and the results of the analysis will be independent of assumptions such as the validity of diffusion theory, the model of neutron slowing down, and so on. It will be shown in the next section that finite reactors behave in essentially the same way as the infinite thermal system.

**The reactivity equation.** Since the flux is independent of position in an infinite reactor, the equation of continuity for the thermal neutrons is (cf. Eq. 9-4)

$$-\phi_T(t) + \frac{q_T(t)}{\bar{\Sigma}_a} = t_d \frac{d\phi_T(t)}{dt}, \quad (12-13)$$

where  $q_T(t)$ , the thermal slowing-down density at the time  $t$ , has been used for the thermal source term. The function  $q_T(t)$  has two parts; one from the slowing down of the prompt neutrons and one from the slowing down of the delayed neutrons. Considering the prompt neutrons first, it will be noted that there are  $\bar{\Sigma}_f\phi_T(t)$  fissions per  $\text{cm}^3/\text{sec}$  throughout the reactor, where  $\bar{\Sigma}_f$  is the average thermal fission cross section. As a result, a total of  $\nu\epsilon\bar{\Sigma}_f\phi_T(t)$  fission neutrons are produced per  $\text{cm}^3/\text{sec}$ , of which the fraction  $(1 - \beta)$  are prompt and  $\beta$  are delayed.\* From Section 9-1,

$$\nu\epsilon\bar{\Sigma}_f\phi_T(t) = \frac{k_\infty}{p} \bar{\Sigma}_a\phi_T(t),$$

where  $\bar{\Sigma}_a$  is the absorption cross section of the fuel and moderator mixture. Thus assuming that the prompt neutrons slow down essentially instantaneously and taking into account resonance absorption, it follows that

$$p \times (1 - \beta) \frac{k_\infty}{p} \bar{\Sigma}_a\phi_T(t) = (1 - \beta)k_\infty\bar{\Sigma}_a\phi_T(t)$$

prompt neutrons thermalize per  $\text{cm}^3/\text{sec}$  throughout the reactor.

Consider next the delayed neutrons. If  $C_i(t)$  is the concentration at time  $t$  in atoms/ $\text{cm}^3$  of the precursors of the  $i$ th delayed group, and  $\lambda_i$  is their decay constant, then  $\lambda_i C_i(t)$  of these atoms decay per  $\text{cm}^3/\text{sec}$  (cf. Section 1-7). One delayed neutron is emitted with the decay of each precursor and assuming again that these neutrons thermalize instantaneously, the contribution to  $q_T(t)$  from all groups of delayed neutrons is  $p \sum_i \lambda_i C_i(t)$ , where the summation includes all

\* It was noted in Chapter 3 that the delayed fraction varies with the energy of the neutrons inducing fission. Strictly speaking, therefore, the values of  $\beta$  to be used for fast and thermal fissions should be different. This distinction is ignored in the present derivation.

groups. The total slowing-down density from both prompt and delayed neutrons is therefore

$$q_T(t) = (1 - \beta)k_\infty \bar{\Sigma}_a \phi_T(t) + p \sum_i \lambda_i C_i(t). \quad (12-14)$$

Inserting this result into Eq. (12-13) gives

$$[(1 - \beta)k_\infty - 1]\phi_T(t) + \frac{p}{\bar{\Sigma}_a} \sum_i \lambda_i C_i(t) = t_d \frac{d\phi_T(t)}{dt}. \quad (12-15)$$

From the above discussion,  $\beta(k_\infty/p)\bar{\Sigma}_a \phi_T(t)$  delayed neutrons are eventually emitted as the result of fissions occurring at time  $t$ , and of these  $\beta_i(k_\infty/p)\bar{\Sigma}_a \phi_T(t)$  are of the  $i$ th type. However, since only one delayed neutron is emitted per precursor it is evident that  $\beta_i(k_\infty/p)\bar{\Sigma}_a \phi_T(t)$  also must be the rate at which the  $i$ th precursor is formed per  $\text{cm}^3/\text{sec}$  at time  $t$  in the reactor. The precursors decay at the rate  $\lambda_i C_i(t)$  and their concentration at any time is determined by the equation

$$\frac{dC_i(t)}{dt} = \beta_i \frac{k_\infty}{p} \bar{\Sigma}_a \phi_T(t) - \lambda_i C_i(t). \quad (12-16)$$

Equations (12-15) and (12-16) are a set of seven coupled, linear, first-order differential equations with constant coefficients, which must be solved for  $\phi_T(t)$ . This can be done by assuming solutions of the form

$$\phi_T(t) = A e^{\omega t} \quad (12-17)$$

and

$$C_i(t) = C_i e^{\omega t}, \quad (12-18)$$

where  $A$ ,  $C_i$ , and  $\omega$  are constants to be determined. Because Eqs. (12-15) and (12-16) are linear,\* the sum of all possible solutions of this form will provide the general solution to the problem.

Inserting Eqs. (12-17) and (12-18) into Eq. (12-16) and solving for  $C_i$  gives

$$C_i = \frac{\beta_i k_\infty \bar{\Sigma}_a A}{p(\omega + \lambda_i)}. \quad (12-19)$$

When this result is substituted into Eq. (12-15), the constant  $A$  cancels from the equation and the following is obtained:

$$(1 - \beta)k_\infty - 1 + k_\infty \sum_i \frac{\lambda_i \beta_i}{\omega + \lambda_i} = \omega t_d. \quad (12-20)$$

Finally, if the constant  $\beta$  is replaced by  $\sum_i \beta_i$  and the equation is rearranged, it

---

\* The linearity of Eqs. (12-15) and (12-16) depends, of course, on  $k_\infty$ , which in the present discussion is a constant. In more realistic problems,  $k_\infty$  is a function of time and flux, and the equations cannot ordinarily be solved analytically (cf. Section 12-11).

can be put in the following form which is convenient for computations:

$$\frac{k_{\infty} - 1}{k_{\infty}} = \frac{\omega t_d}{1 + \omega t_d} + \frac{\omega}{1 + \omega t_d} \sum_i \frac{\beta_i}{\omega + \lambda_i}. \quad (12-21)$$

The quantity on the left-hand side of this equation is known as the *reactivity* of the infinite reactor and is given the symbol  $\rho$ ; thus

$$\rho = \frac{k_{\infty} - 1}{k_{\infty}}. \quad (12-22)$$

If  $k_{\infty}$  is greater than unity the reactor is evidently supercritical and  $\rho$  is positive, and in this case the reactor is said to have "positive reactivity." On the other hand, if  $k_{\infty}$  is less than unity, then the reactor is subcritical,  $\rho$  is negative, and the reactor possesses "negative reactivity." It should be noted that according to Eq. (12-22) the maximum value of  $\rho$  is unity, while  $\rho$  may have *any* negative value.

Incidentally, if the reactor is critical before the change in  $k_{\infty}$ , Eq. (12-22) may also be written as

$$\rho = \frac{k_{\infty} - (k_{\infty})_0}{k_{\infty}} \quad (12-23)$$

where  $(k_{\infty})_0 = 1$  is the multiplication factor of the initially critical system. The numerator in Eq. (12-23) is then simply the change in  $k_{\infty}$ , and hence for the infinite reactor the reactivity may be represented by

$$\rho = \frac{\Delta k_{\infty}}{k_{\infty}}. \quad (12-24)$$

Written in this form it is clear that  $\rho$  represents the *fractional change* in  $k_{\infty}$  and it is common therefore to specify reactivity in percent.

Equation (12-21) now becomes

$$\rho = \frac{\Delta k_{\infty}}{k_{\infty}} = \frac{\omega t_d}{1 + \omega t_d} + \frac{\omega}{1 + \omega t_d} \sum_i \frac{\beta_i}{\omega + \lambda_i}. \quad (12-25)$$

This equation is known as the *reactivity equation* and occasionally as the *inhour equation*. The origin of the latter term will be clarified in Section 12-6.

When the fractions in Eq. (12-25) are cleared, a seventh degree polynomial in  $\omega$  is obtained which has seven roots. Thus there are seven values of  $\omega$  for which the assumed functions in Eqs. (12-17) and (12-18) are solutions to the differential equations (12-15) and (12-16). The nature of the roots of Eq. (12-25) may be seen by plotting the right-hand side (RHS) of Eq. (12-25) as a function of  $\omega$  as shown in Fig. 12-1. It will be observed that the RHS = 0 for  $\omega = 0$  and increases monotonically to unity with increasingly positive values of  $\omega$ . When  $\omega$  is negative, however, the RHS is singular for the six values of  $\omega = -\lambda_i$  and at  $\omega = -1/t_d$ . Also, in the limit as  $\omega \rightarrow -\infty$ , RHS  $\rightarrow 1$ .

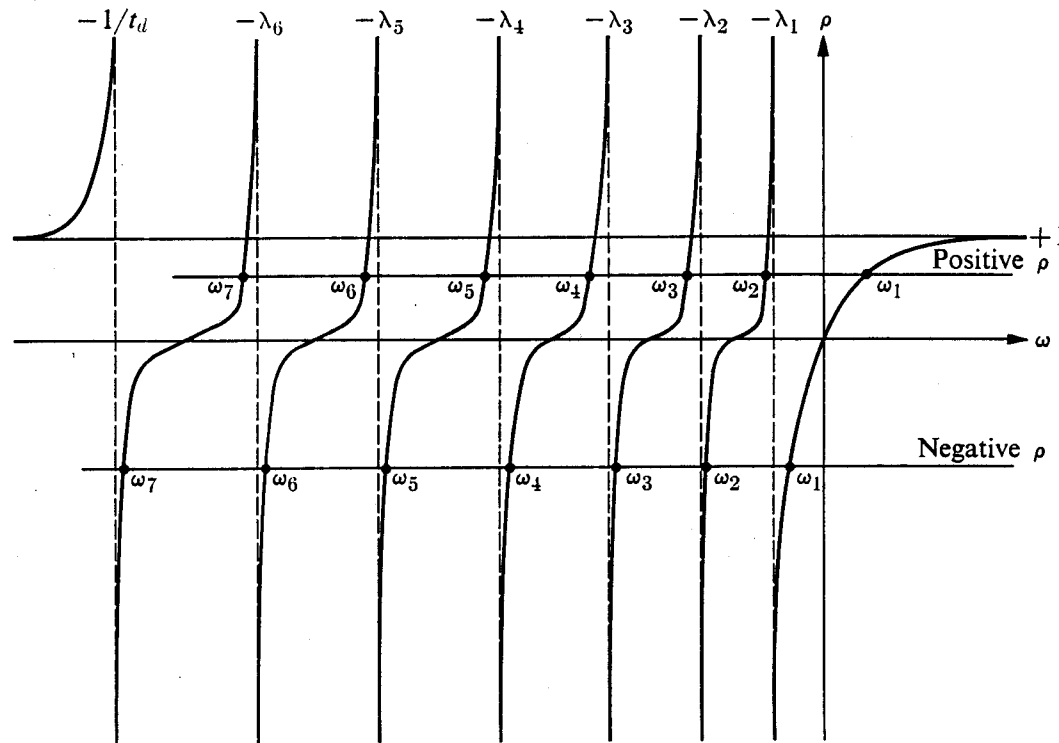


**Fig. 12-1.** Schematic drawing of the two sides of the reactivity equation showing the seven roots for positive and negative reactivity. The figure is not drawn to scale.

The roots of Eq. (12-25) are given by the intersections of the horizontal line representing the left-hand side of Eq. (12-25) with the right-hand side. As shown in the figure there are seven roots,  $\omega_1, \omega_2, \dots, \omega_7$ , for both positive and negative values of  $\rho$  (it must be remembered that  $\rho$  is confined to the range  $-\infty < \rho < 1$ ). The flux may then be written as the sum

$$\phi_T(t) = \phi_{T0}(A_1 e^{\omega_1 t} + A_2 e^{\omega_2 t} + \dots + A_7 e^{\omega_7 t}) = \phi_{T0} \sum_{j=1}^7 A_j e^{\omega_j t}, \quad (12-26)$$

where  $\phi_{T0}$  is the value of the flux at  $t = 0$ . Similarly, the concentration of the precursors of the  $i$ th type is

$$C_i(t) = C_{i0} \sum_{j=1}^7 B_{ij} e^{\omega_j t}, \quad (12-27)$$

where  $C_{i0}$  is the concentration at  $t = 0$ . The constants  $A_j$  and  $B_{ij}$ , of which there are a total of 49, must next be found.

**Determining the constants.** All but six of the constants in Eqs. (12-26) and (12-27) can be eliminated by inserting these equations into Eq. (12-16). This gives

$$C_{i0} \sum_{j=1}^7 B_{ij} \omega_j e^{\omega_j t} = \frac{\beta_i k_\infty \bar{\Sigma}_a \phi_{T0}}{p} \sum_{j=1}^7 A_j e^{\omega_j t} - \lambda_i C_{i0} \sum_{j=1}^7 B_{ij} e^{\omega_j t}. \quad (12-28)$$

Since this equation must hold for all values of  $t$ , the coefficients of corresponding exponentials (i.e., those having the same  $\omega_j$ ) are equal, so that

$$C_{i0}B_{ij} = \frac{\beta_i k_\infty \bar{\Sigma}_a \phi_{T0} A_j}{p(\omega_j + \lambda_i)}. \quad (12-29)$$

Equation (12-27) then reduces to

$$C_i(t) = \frac{\beta_i k_\infty \bar{\Sigma}_a \phi_{T0}}{p} \sum_{j=1}^7 \frac{A_j e^{\omega_j t}}{\omega_j + \lambda_i}. \quad (12-30)$$

Only the seven constants  $A_j$  now remain, and these can be determined from the initial conditions in the reactor. For instance, suppose the reactor was critical and operating in the steady state prior to the change in  $k_\infty$ . Then  $(k_\infty)_0 = 1$ , and the resonance escape probability is  $p_0$ . Since  $(dC_i/dt)_0 = 0$  at  $t = 0$ , it follows from Eq. (12-16) that

$$C_{i0} = \frac{\beta_i (k_\infty)_0 \bar{\Sigma}_a \phi_{T0}}{p_0 \lambda_i}. \quad (12-31)$$

From Eq. (12-30), however,

$$C_i(0) = C_{i0} = \frac{\beta_i k_\infty \bar{\Sigma}_a \phi_{T0}}{p} \sum_{j=1}^7 \frac{A_j}{\omega_j + \lambda_i}, \quad (12-32)$$

and comparing the last two equations it is evident that

$$\frac{p_0 k_\infty}{p (k_\infty)_0} \sum_{j=1}^7 \frac{A_j}{\omega_j + \lambda_i} = \frac{1}{\lambda_i}. \quad (12-33)$$

Finally, since  $\phi_T(0) = \phi_{T0}$ , Eq. (12-26) yields the condition

$$\sum_{j=1}^7 A_j = 1. \quad (12-34)$$

Equation (12-33) represents a set of six linear equations, one for each value of  $i$ , that is, one for each delayed group. These equations together with Eq. (12-34) uniquely specify the values of the seven constants  $A_j$  and the analytical solution is complete. Fortunately, as will be shown in the next section, it is not ordinarily necessary (nor is it appropriate) to compute the exact values of the  $A_j$  from Eqs. (12-33) and (12-34) in order to predict the response of a reactor to a change in its multiplication factor.

**Behavior of the flux.** As an example of the response of an initially critical reactor to a step change in  $k_\infty$ , consider the infinite  $U^{235}$ -water reactor which was discussed in Section 12-1, and again let

$$\Delta k_\infty = 0.001 \quad \text{and} \quad t_d = 10^{-4} \text{ sec.}$$

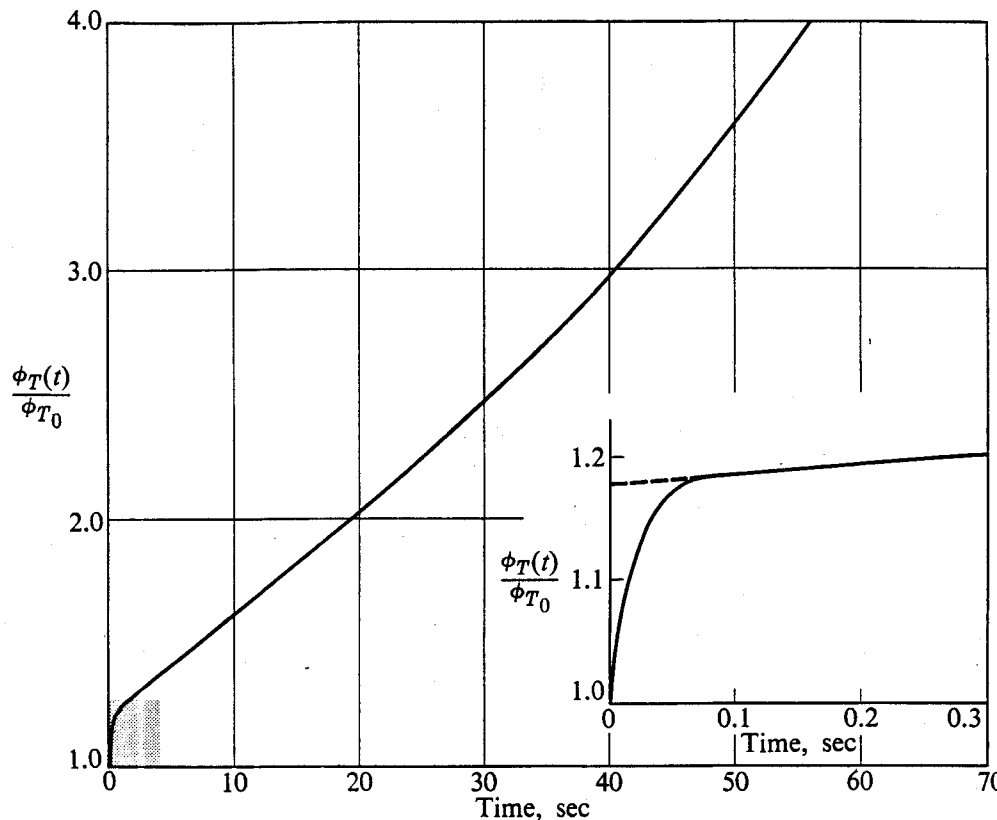


**Fig. 12-2.** Time behavior of thermal flux in infinite  $U^{235}$ -fueled,  $H_2O$ -moderated thermal reactor following step reactivity insertion of 0.001.

When the  $\omega_j$  and  $A_j$  are computed from Eqs. (12-25), (12-33), and (12-34),  $\phi_T(t)$  is found to be given by

$$\begin{aligned}\phi_T(t) = \phi_{T_0} & [1.446e^{0.0182t} - 0.0359e^{-0.0136t} - 0.140e^{-0.0598t} \\ & - 0.0637e^{-0.183t} - 0.0205e^{-1.005t} - 0.00767e^{-2.875t} \\ & - 0.179e^{-55.6t}].\end{aligned}\quad (12-35)$$

Figure 12-2 shows  $\phi_T(t)/\phi_{T_0}$  as a function of time after the change in  $k_\infty$ . It will be noted that the flux rises very suddenly at first, and then more slowly. Mathematically, the sudden rise is caused by the rapid decay of the exponential functions in Eq. (12-35) that have large arguments. Physically, this behavior is due to the fact that as soon as  $k_\infty$  is increased above unity the fission rate increases, more prompt neutrons are immediately generated, and the chain reaction begins to diverge on the prompt neutrons alone. However, this cannot continue indefinitely since the system is actually *subcritical* as far as the prompt neutrons are concerned. This is because only  $(1 - \beta)k_\infty$  new prompt neutrons are produced per cycle of the chain reaction, and in this case  $(1 - \beta)k_\infty = (1 - 0.0065) \times 1.001 = 0.994$ . The initial change in  $\phi_T(t)$  is thus similar to the sudden rise in flux which occurs when a neutron source is placed in a subcritical reactor. Following its initial rise caused by the prompt neutrons, the flux increases more slowly as the delayed

neutrons are emitted, and the subsequent behavior of the reactor is determined entirely by the delayed neutrons. This response of a reactor will be reconsidered in Section 12-7.

### 12-4 Response of a Bare Reactor to a Step-Change in Reactivity

It will now be shown that the results derived in the preceding section for the infinite reactor also hold with little modification for a finite reactor. For the most part the present discussion is limited to bare thermal reactors. The dynamics of reflected reactors is a somewhat more complicated subject, which requires mathematical techniques to be developed in Chapter 15. The slowing down of neutrons will be treated by age theory, and for the moment it will be assumed that the fission and delayed neutrons are emitted with the same energy. As a consequence, the ages of all neutrons to thermal energies can be taken to be equal.

For simplicity, the slab reactor will be considered first. It may be noted at the outset that the problem of finding the time behavior of such a reactor differs from that of the infinite reactor only in that the flux, the slowing-down density and the precursor concentrations, are all functions of space as well as time. As will be shown presently, this spatial variable can be eliminated by expanding these functions in appropriate eigenfunction series. The resulting equations are then identical in form with those for the infinite system.

**The bare slab reactor.** Consider a uniform slab thermal reactor of extrapolated thickness  $a$ . Up to the time  $t = 0$  it will be assumed that the reactor is critical and operating in a steady state, so that according to the discussion in Chapter 9 the multiplication factor  $k$  is equal to unity. The properties of the reactor are then changed *uniformly* throughout the entire slab so that for  $t > 0$ ,  $k$  is different from unity. It is desired to find the subsequent time behavior of the system, that is, for  $t > 0$ .

The thermal flux is a function of  $x$  and  $t$  and the diffusion equation is (cf. Eq. 9-14)

$$L_T^2 \frac{\partial^2 \phi_T(x, t)}{\partial x^2} - \phi_T(x, t) + \frac{p}{\bar{\Sigma}_a} q(x, \tau_T, t) = t_d \frac{\partial \phi_T(x, t)}{\partial t}, \quad (12-36)$$

where  $q(x, \tau_T, t)$  is the thermal slowing-down density in the absence of resonance capture as in Section 9-2. This function satisfies the age equation

$$\frac{\partial^2 q(x, \tau, t)}{\partial x^2} = \frac{\partial q(x, \tau, t)}{\partial \tau}. \quad (12-37)$$

Since the prompt and delayed neutrons have been assumed to be emitted with the same energy, the source condition for the slowing-down density at  $\tau = 0$  is

$$q(x, 0, t) = \sum_i \lambda_i C_i(x, t) + (1 - \beta) \frac{k_\infty}{p} \bar{\Sigma}_a \phi_T(x, t), \quad (12-38)$$

where  $C_i(x, t)$  is the concentration of precursors of the  $i$ th delayed group at  $x$  at the time  $t$ . Finally,  $C_i(x, t)$  satisfies an equation similar to Eq. (12-16), namely,

$$\frac{\partial C_i(x, t)}{\partial t} = \beta_i \frac{k_\infty}{p} \bar{\Sigma}_a \phi_T(x, t) - \lambda_i C_i(x, t). \quad (12-39)$$

All of these equations must be solved subject to the boundary conditions

$$q\left(\pm \frac{a}{2}, \tau, t\right) = 0 \quad \text{and} \quad \phi_T\left(\pm \frac{a}{2}, t\right) = 0,$$

for all values of  $t$  and  $\tau$ . This can be done in a straightforward way by expanding each of the functions  $\phi_T(x, t)$ ,  $C_i(x, t)$ , and  $q(x, \tau, t)$  in series of slab eigenfunctions  $\cos B_n x$ , where  $B_n = n\pi/a$ ,  $n = 1, 3, 5, \dots$ , which have been used repeatedly in earlier chapters. By proceeding in this way, the space dependence of these functions can be eliminated from each of the equations due to the orthogonality of the eigenfunctions. As noted above, the remaining time-dependent equations will then be found to be of the same form as those for the infinite reactor. Thus let

$$\phi_T(x, t) = \sum_{n \text{ odd}} \phi_n(t) \cos B_n x, \quad (12-40)$$

$$C_i(x, t) = \sum_{n \text{ odd}} C_{in}(t) \cos B_n x, \quad (12-41)$$

and

$$q(x, \tau, t) = \sum_{n \text{ odd}} q_n(\tau, t) \cos B_n x, \quad (12-42)$$

where the functions  $\phi_n(t)$ ,  $C_{in}(t)$ , and  $q_n(\tau, t)$  must be determined.

Substituting Eq. (12-42) into Eq. (12-37) gives

$$-\sum_{n \text{ odd}} B_n^2 q_n(\tau, t) \cos B_n x = \sum_{n \text{ odd}} \frac{\partial q_n(\tau, t)}{\partial \tau} \cos B_n x. \quad (12-43)$$

Because the orthogonality of the  $\cos B_n x$  functions (cf. Section 5-10) the  $n$ th terms on each side of Eq. (12-43) are equal, so that

$$\frac{\partial q_n(\tau, t)}{\partial \tau} = -B_n^2 q_n(\tau, t). \quad (12-44)$$

This equation has the solution

$$q_n(\tau, t) = T_n(t) e^{-B_n^2 \tau}, \quad (12-45)$$

where  $T_n(t)$  is an unknown function of  $t$ , and consequently Eq. (12-42) becomes

$$q(x, \tau, t) = \sum_{n \text{ odd}} T_n(t) e^{-B_n^2 \tau} \cos B_n x. \quad (12-46)$$

Inserting this result and Eqs. (12-40) and (12-41) into Eq. (12-38) gives

$$\begin{aligned} \sum_{n \text{ odd}} T_n(t) \cos B_n x &= \sum_{\substack{n \text{ odd} \\ i}} \lambda_i C_{in}(t) \cos B_n x \\ &\quad + (1 - \beta) \frac{k_\infty}{p} \bar{\Sigma}_a \sum_{n \text{ odd}} \phi_n(t) \cos B_n x. \end{aligned} \quad (12-47)$$

Again, in view of the orthogonality of the  $\cos B_n x$ , the  $n$ th terms in the equation are equal and so

$$T_n(t) = \sum_i \lambda_i C_{in}(t) + (1 - \beta) \frac{k_\infty}{p} \bar{\Sigma}_a \phi_n(t). \quad (12-48)$$

Next, if Eqs. (12-40) and (12-41) are substituted into Eq. (12-39) the result is

$$\sum_{n \text{ odd}} \frac{dC_{in}(t)}{dt} \cos B_n x = \beta_i \frac{k_\infty}{p} \bar{\Sigma}_a \sum_{n \text{ odd}} \phi_n(t) \cos B_n x - \lambda_i \sum_{n \text{ odd}} C_{in}(t) \cos B_n x, \quad (12-49)$$

and the orthogonality condition leads to

$$\frac{dC_{in}(t)}{dt} = \beta_i \frac{k_\infty}{p} \bar{\Sigma}_a \phi_n(t) - \lambda_i C_{in}(t). \quad (12-50)$$

In a similar way, when Eqs. (12-40) and (12-46) are substituted into Eq. (12-36), the resulting equation reduces to

$$-(1 + B_n^2 L_T^2) \phi_n(t) + \frac{p}{\bar{\Sigma}_a} T_n(t) e^{-B_n^2 \tau_T} = t_d \frac{d\phi_n(t)}{dt}. \quad (12-51)$$

Inserting Eq. (12-48) gives

$$\begin{aligned} -(1 + B_n^2 L_T^2) \phi_n(t) + \frac{p}{\bar{\Sigma}_a} e^{-B_n^2 \tau_T} \sum_i \lambda_i C_{in}(t) \\ + (1 - \beta) k_\infty e^{-B_n^2 \tau_T} \phi_n(t) = t_d \frac{d\phi_n(t)}{dt}. \end{aligned} \quad (12-52)$$

This equation can be simplified by introducing the quantities  $k_n$  and  $t_n$  defined in Section 9-2, namely,

$$k_n = \frac{k_\infty e^{-B_n^2 \tau_T}}{1 + B_n^2 L_T^2} \quad (12-53)$$

and

$$t_n = \frac{t_d}{1 + B_n^2 L_T^2}. \quad (12-54)$$

Equation (12-52) then becomes

$$t_n \frac{d\phi_n(t)}{dt} = [(1 - \beta) k_n - 1] \phi_n(t) + \frac{p k_n}{\bar{\Sigma}_a k_\infty} \sum_i \lambda_i C_{in}(t). \quad (12-55)$$

It may be noted at this point that Eqs. (12-50) and (12-55) are identical in form to Eqs. (12-15) and (12-16) for the infinite thermal reactor. As earlier, therefore, solutions may be found of the type

$$\phi_n(t) = A_n e^{\omega t} \quad (12-56)$$

and

$$C_{in}(t) = C_{in} e^{\omega t}. \quad (12-57)$$

Inserting these functions into Eq. (12-50) gives

$$C_{in} = \frac{\beta_i k_\infty \bar{\Sigma}_a A_n}{p(\omega + \lambda_i)}. \quad (12-58)$$

When this result and Eqs. (12-56) and (12-57) are introduced into Eq. (12-55), the constant  $A_n$  cancels from the equation, leaving

$$(1 - \beta)k_n - 1 + k_n \sum_i \frac{\lambda_i \beta_i}{\omega + \lambda_i} = \omega t_n, \quad (12-59)$$

which may be put in the more useful form

$$\frac{k_n - 1}{k_n} = \frac{\omega t_n}{1 + \omega t_n} + \frac{\omega}{1 + \omega t_n} \sum_i \frac{\beta_i}{\omega + \lambda_i}. \quad (12-60)$$

Equation (12-60) is the analog for the finite bare reactor of the reactivity equation for the infinite reactor (cf. Eq. 12-21). Thus any (uniform) change in the criticality of the system leads to various values of the  $k_n$  and  $t_n$ , and these values determine the seven roots in Eq. (12-60). Now, however, there are seven roots for *each value of n*. When all of these roots, denoted by  $\omega_{jn}$ , have been computed, the thermal flux in the slab reactor can be written as

$$\phi_T(x, t) = \sum_{j, n} A_{jn} e^{\omega_{jn} t} \cos B_n x. \quad (12-61)$$

Since prior to the change in  $k$  the reactor was assumed to be critical and operating in the steady state, the flux necessarily consisted of the fundamental mode only, so that

$$\phi_T(x, 0) = A \cos B_1 x. \quad (12-62)$$

Equating this to Eq. (12-61) at  $t = 0$  gives

$$A \cos B_1 x = \sum_{j, n} A_{jn} \cos B_n x. \quad (12-63)$$

Because of the orthogonality of the functions  $\cos B_n x$ , all of the constants  $A_{jn}$  must be zero for  $n \neq 1$ . This can be seen by multiplying both sides of Eq. (12-63) by  $\cos B_n x$  and integrating from  $x = -a/2$  to  $x = +a/2$ . Thus Eq. (12-61) reduces to

$$\phi_T(x, t) = \left[ \sum_j A_j e^{\omega_j t} \right] \cos B_1 x, \quad (12-64)$$

where, as usual, the subscript has been dropped for the fundamental mode. From Eq. (12-64) it must be concluded that *if the reactor is initially critical and operating in the fundamental mode and becomes supercritical or subcritical as the result of a uniform change in the system, the reactor will remain in the fundamental mode.* Furthermore, the magnitude of the flux increases or decreases as the sum of seven exponentials as does the flux in the infinite reactor. As will be shown presently, this theorem does not hold if the changes in the reactor are made in a nonuniform way.

It follows from this result that if the reactor is changed uniformly, Eq. (12-60) must be solved only for the case  $n = 1$ . Writing  $k$  for  $k_1$ , as usual, this equation is

$$\frac{k - 1}{k} = \frac{\omega t_1}{1 + \omega t_1} + \frac{\omega}{1 + \omega t_1} \sum_i \frac{\beta_i}{\omega + \lambda_i}. \quad (12-65)$$

The quantity on the left-hand side of this equation is known as the *reactivity* of the reactor, and as with the infinite reactor discussed in the last section, it is denoted by the symbol  $\rho$ , that is,

$$\rho = \frac{k - 1}{k} = \frac{\Delta k}{k}. \quad (12-66)$$

Equation (12-65) now reduces to

$$\rho = \frac{\omega t_1}{1 + \omega t_1} + \frac{\omega}{1 + \omega t_1} \sum_i \frac{\beta_i}{\omega + \lambda_i}. \quad (12-67)$$

This is the reactivity equation for the finite reactor.

It will be observed that Eq. (12-67) is identical with Eq. (12-25) except that  $t_d$ , the mean diffusion time, which is equal to the prompt neutron lifetime for the infinite reactor, is replaced by the parameter  $t_1$ . It may be inferred, therefore, that  $t_1$ , which is given by

$$t_1 = \frac{t_d}{1 + B^2 L_T^2}, \quad (12-68)$$

is the *effective prompt neutron lifetime in a finite reactor*. The factor  $1/(1 + B^2 L^2)$  is just the thermal nonleakage probability (cf. Section 9-4), and it follows from Eq. (12-68) that  $t_1$  is the mean diffusion time for the infinite reactor weighted by the probability that the prompt neutrons do not leak from the finite system. This means, of course, that the prompt neutron lifetime is smaller for a finite reactor than for the corresponding infinite reactor.

**Other reactor geometries.** The results derived above for the bare slab reactor can easily be shown to hold for all uniform bare reactors. To show this, it is merely necessary to replace the slab eigenfunctions  $\cos B_n x$  by the eigenfunctions  $\varphi_n(\mathbf{r})$  appropriate to the reactor. These are solutions to the equation

$$\nabla^2 \varphi_n(\mathbf{r}) + B_n^2 \varphi_n(\mathbf{r}) = 0, \quad (12-69)$$

which also satisfy the boundary condition  $\varphi_n(\mathbf{r}) = 0$  on the reactor surface. The flux following a uniform change in the multiplication properties of the system is then found to be given by a series similar to Eq. (12-61), namely,

$$\phi_T(\mathbf{r}, t) = \sum_{j, n} A_{jn} e^{\omega_{jn} t} \varphi_n(\mathbf{r}). \quad (12-70)$$

Furthermore, by the same argument which led to Eq. (12-64), if the system is initially critical and operating in the steady state, Eq. (12-70) reduces to

$$\phi_T(\mathbf{r}, t) = \left[ \sum_j A_j e^{\omega_j t} \right] \varphi_1(\mathbf{r}), \quad (12-71)$$

where the  $\omega_j$  are roots of Eq. (12-65). The constants  $A_j$  can be found using the same techniques discussed earlier for the infinite reactor.

**Nonuniform reactivity changes.** In the preceding discussion it was assumed that the properties of the reactor were suddenly changed uniformly throughout the entire system. As a practical matter, however, it is almost impossible to change a reactor in this way. Changes in a reactor are usually made non-uniformly, that is, the properties are altered differently at different points in the reactor. For example, when a control rod is moved, the physical properties of the reactor are only altered at the location of the rod; the properties of the remainder of the reactor are not affected.

To understand how a reactor responds to such a nonuniform change in its properties, it is important to recognize that the eigenfunctions of the reactor *after* a nonuniform change are not the same as the eigenfunctions of the original reactor. This is because mathematically the reactor after the change is a fundamentally different system, and either the differential equations determining the flux, or the boundary conditions, or both, are different from those for the original system. Furthermore, although the eigenfunctions of the new system are orthogonal to one another, they are *not* orthogonal to the eigenfunctions of the original reactor. For example, the first three eigenfunctions are shown schematically in Fig. 12-3 for a slab reactor before and after the introduction of a central control rod. It will be observed that the two sets of functions are quite different and there is no reason to expect the two sets to be orthogonal.

Let the eigenfunctions of the reactor for  $t > 0$  be denoted by  $\varphi_n^*(\mathbf{r})$  to distinguish them from the eigenfunctions  $\varphi_n(\mathbf{r})$  for  $t < 0$ . After the change in the system the flux according to Eq. (12-70) is given by

$$\phi(\mathbf{r}, t) = \sum_{j, n} A_{jn} e^{\omega_{jn} t} \varphi_n^*(\mathbf{r}). \quad (12-72)$$

Now if, prior to the change, the reactor was critical and in the steady state,  $\phi(\mathbf{r}, 0) = A \varphi_1(\mathbf{r})$ , and by placing  $t = 0$  in Eq. (12-72), it follows that

$$A \varphi_1(\mathbf{r}) = \sum_{j, n} A_{jn} \varphi_n^*(\mathbf{r}).$$

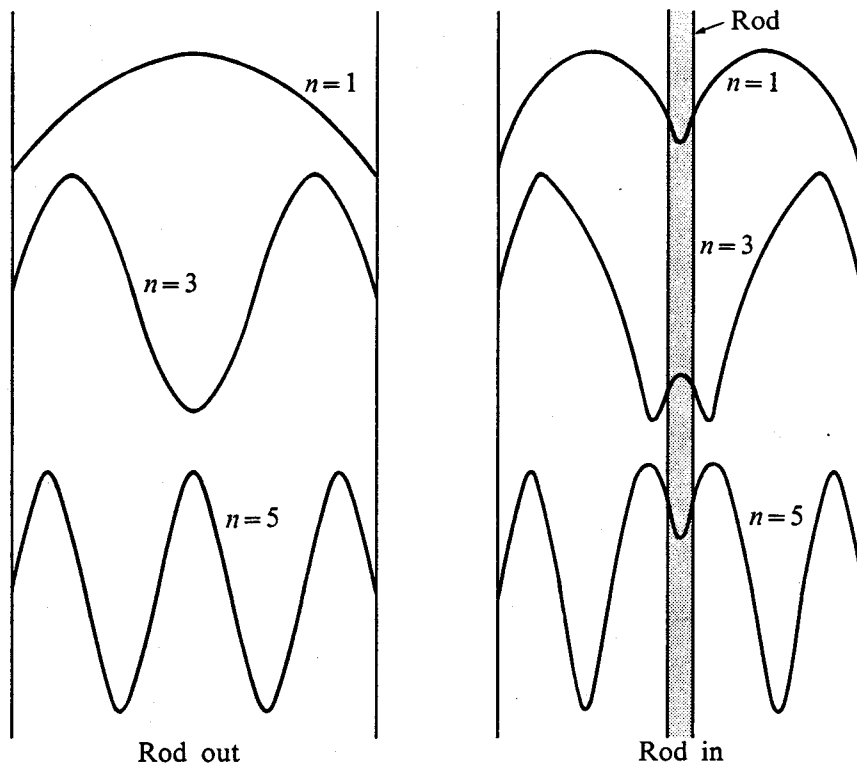


**Fig. 12-3.** First three eigenfunctions of slab reactor with and without central control rod. Only odd-numbered eigenfunctions appear because of the symmetry of the system.

This expression is similar to Eq. (12-63), but now since  $\varphi_1(\mathbf{r})$  is not orthogonal to the functions  $\varphi_n^*(\mathbf{r})$ , it is no longer true that the  $A_{jn}$  are zero for  $n > 1$ . On the contrary, all the  $A_{jn}$  are nonzero and it must be concluded that after a nonuniform change in a reactor the fundamental and higher harmonics† (of the new system) are present.

The higher harmonics do not persist, however, as may be seen from the following argument.‡ To begin with, let

$$\rho_n = \frac{k_n - 1}{k_n}. \quad (12-73)$$

This quantity, roughly speaking, is the reactivity associated with the  $n$ th harmonic. Since the eigenvalues form a monotonically increasing set, that is,

$$B_1 < B_2 < B_3, \dots,$$

it is evident from Eq. (12-53) that the  $k_n$  form a monotonically decreasing set,

† Recall that the fundamental is called the "first harmonic" (cf. Section 5-10).

‡ This argument is somewhat oversimplified, since the quantities  $k_n$  cannot be defined for a nonuniform reactor as easily as in Eq. (12-53), because the parameters  $\tau_T$ ,  $L_T^2$ , etc., may be space dependent. However, it is sufficient to think of the  $k_n$  as suitable averages over the reactor volume.

that is,  $k_1 > k_2 > k_3$ , etc. In actual fact,  $k_2$  is usually *substantially* less than  $k_1$ ,  $k_3$  is *substantially* less than  $k_2$ , and so on.

Suppose now that the multiplication factor  $k \equiv k_1$  is increased above unity, that is, the reactor becomes supercritical. For reasons which will be discussed in Section 12-8,  $k$  is rarely increased beyond about  $1 + \beta$ ; and since  $\beta \ll 1$  for all fuels, this means that  $k$  is never more than slightly greater than unity for positive reactivity changes. Therefore, since  $k_2 < k_1$ , it follows that  $k_2$  must be less than unity, and from Eq. (12-73)  $\rho_2$  must be negative. Similarly,  $\rho_3 < \rho_2 < 0$ , etc., so that *the reactivities associated with all harmonics above the fundamental are negative*. Now as shown in Fig. 12-1, all of the roots of the reactivity equation are negative when the reactivity is negative. Thus if  $\rho_n$  is negative for  $n > 1$ , the roots of Eq. (12-60) are also negative for  $n > 1$ , and it must be concluded that the harmonics in Eq. (12-72) die out in time even though the reactivity associated with the fundamental  $\rho_1 \equiv \rho$  is positive. On the other hand, had  $k$  originally been decreased below unity,  $\rho$  would be negative but the quantities  $\rho_2, \rho_3$ , etc., would be even *more* negative and the harmonics of the flux would die out much faster than the fundamental. In either case, the flux eventually assumes the shape of the fundamental eigenfunction of the changed reactor which then increases or decreases in time according to Eq. (12-71). To summarize, *if a reactor is originally critical and operating in the fundamental mode, the flux will remain in the fundamental after a change in the multiplication factor, provided the change is made uniformly. If the reactor is changed in a nonuniform manner the flux ultimately assumes the shape of the fundamental mode appropriate to the altered system after the harmonics of the flux have died out.*

**Other types of reactors.** While the above conclusions were derived for the thermal reactor, they can be shown to hold also for intermediate and fast reactors. Thus for any reactor the response to a step change in reactivity is determined by the general reactivity equation:

$$\rho = \frac{\omega l_p}{1 + \omega l_p} + \frac{\omega}{1 + \omega l_p} \sum_i \frac{\beta_i}{\omega + \lambda_i}, \quad (12-74)$$

where  $l_p$  is the prompt neutron lifetime. As noted earlier,  $l_p$  is much less for non-thermal reactors than for thermal reactors, and, as a consequence, the time behavior of these reactors is insensitive to the values of  $l_p$ . It is usually possible, in fact, to place  $l_p = 0$  in the reactivity equation for most nonthermal reactors.

It may also be mentioned here that the conclusions reached in this section, which were based on calculations of a bare reactor, also apply to reflected reactors provided an appropriate value is used for the prompt neutron lifetime in the reactivity equation. Unfortunately, the proof of this statement and a derivation of the formula for  $l_p$  require mathematical techniques to be developed in Chapter 15. On physical grounds, however, it may be said that since the reflector tends to

return neutrons to the core which would otherwise escape from the system, the effect of the reflector is to *increase* the prompt neutron lifetime over its value for the bare reactor. It follows that  $l_p$  for a reflected reactor generally lies between its value for the bare core and for the infinite reactor.

### 12-5 The Value of $\beta$

In the preceding sections it was assumed that both the prompt and delayed neutrons are emitted with the same energy, whereas in actual fact the delayed neutrons are considerably less energetic than the prompt neutrons. This has the following interesting effect on the kinetics of a finite reactor.

It should first be noted that if, as in most reactors, the fuel is a motionless solid, the prompt neutrons and their associated delayed neutrons are emitted in the reactor with the same spatial distribution.<sup>†</sup> The average fast leakage probability is therefore greater for the more energetic prompt neutrons since they spend a longer time slowing down than do the delayed neutrons. As a consequence, the fraction of the neutrons slowing down within a reactor which are delayed is somewhat increased over the fraction emitted per fission.

This can be taken into account by simply redefining the delayed neutron fractions. In particular, of the  $\beta_i$  neutrons emitted in the  $i$ th group per fission neutron,  $p\beta_i \exp(-B^2\tau_i)$  actually slow down in the reactor, where  $\tau_i$  is the age of the neutrons in this group. In the equations derived in the preceding sections, however, it was assumed that  $\tau_i = \tau_T$ , where  $\tau_T$  is the age of prompt fission neutrons. These equations can be corrected by using the effective fraction  $\beta_i^*$  defined as

$$\beta_i^* = \beta_i e^{B^2(\tau_T - \tau_i)}, \quad (12-75)$$

everywhere instead of  $\beta_i$ . Then the original, erroneous assumption that the age of all delayed neutrons is  $\tau_T$  gives the correct number of delayed neutrons slowing down in the system, namely,

$$p\beta_i^* \exp(-B^2\tau_T) = p\beta_i \exp(-B^2\tau_i).$$

With small water-moderated reactors  $\beta_i^*$  may be as much as 25% greater than  $\beta_i$ .

If the fuel consists of a mixture of isotopes, the value of  $\beta_i$  is the average of the delayed fractions for the isotopes, weighted by the number of fission neutrons emitted by each isotope. Suppose, for example, that the fuel for a thermal reactor is a mixture of the isotopes  $U^{235}$  and  $U^{238}$ . It will be recalled from the definition of the fast fission factor, that there are a total of  $\epsilon$  fast neutrons produced per neutron emitted in thermal fission. Per fission neutron there are therefore  $\epsilon^{-1}$  neutrons emitted from thermal fission in  $U^{235}$  and  $1 - \epsilon^{-1}$  neutrons emitted

<sup>†</sup> With fluid-fueled reactors the delayed neutron precursors may move a considerable distance before emitting their neutrons. This possibility leads to complications in the kinetics of circulating fuel reactors (cf. Meghrebian and Holmes, *op. cit.*, pp. 590 *et seq.*).

from fast fission in  $U^{238}$ . The effective value of  $\beta_i$  is then

$$\beta_i^* = \left[ \frac{\beta_i^{25}}{\epsilon} + \frac{\beta_i^{28}(\epsilon - 1)\nu^{28}}{\epsilon\nu^{25}} \right] e^{B^2(\tau_T - \tau_i)}. \quad (12-76)$$

The ratio of  $\nu^{28}$  to  $\nu^{25}$  in the second term is necessary because the kinetics and reactivity equations derived earlier are based on thermal fission, which in this example is fission in  $U^{235}$ .

## 12-6 The Stable Period

It was shown in Section 12-3 and Fig. 12-2 that the flux rises (or drops) very sharply following a step insertion of reactivity and thereafter assumes a more gradual rise (or drop). While the exact details of the behavior of the system immediately after a reactivity change are quite complicated, particularly when harmonics of the flux are present, the later behavior of the system can be handled rather easily.

Returning to Fig. 12-1, it will be observed that when  $\rho$  is positive there is one positive root of the reactivity equation. In this case, all of the exponentials except the first in Eq. (12-26) (or Eq. 12-71) decrease in time, and the behavior of the reactor is eventually dominated by the first term. On the other hand, when  $\rho$  is negative all roots to the reactivity equation are negative and all the exponentials die out in time. Now, however, the first exponential decreases more slowly than the others, and again the flux is dominated by the first term of Eq. (12-26).

In either case, therefore, whether  $\rho$  is positive or negative the flux eventually behaves as

$$\phi_T(t) \sim e^{\omega_1 t}, \quad (12-77)$$

where  $\omega_1$  is positive or negative, respectively, in the two cases. Equation (12-77) may also be written as

$$\phi_T(t) \sim e^{t/T}, \quad (12-78)$$

where

$$T = \frac{1}{\omega_1} \quad (12-79)$$

is known as the *stable period* of the reactor or simply as the reactor *period*. With the  $U^{235}$ -fueled, water-moderated reactor discussed in Section 12-3, for example, a step in reactivity of  $\rho = +0.001$  gave the value  $\omega_1 = 0.0182$  (cf. Eq. 12-35), and the stable period is therefore 55 sec.

Since the roots of the reactivity equation are functions of  $\rho$ , the delayed neutron fractions  $\beta_i$  and the prompt neutron lifetime  $t_p$  (which is equal to  $t_d$  for an infinite thermal reactor and  $t_1$  for a finite thermal reactor), it is possible to plot  $T = 1/\omega_1$  as a function of  $\rho$  for various values of prompt neutron lifetime and for each fissionable isotope. This is illustrated in Fig. 12-4, where the period is shown for positive and negative reactivities for a  $U^{235}$ -fueled reactor. These curves were computed using values of  $\beta_i$  and  $\lambda_i$  given in Table 3-7 for  $U^{235}$ .

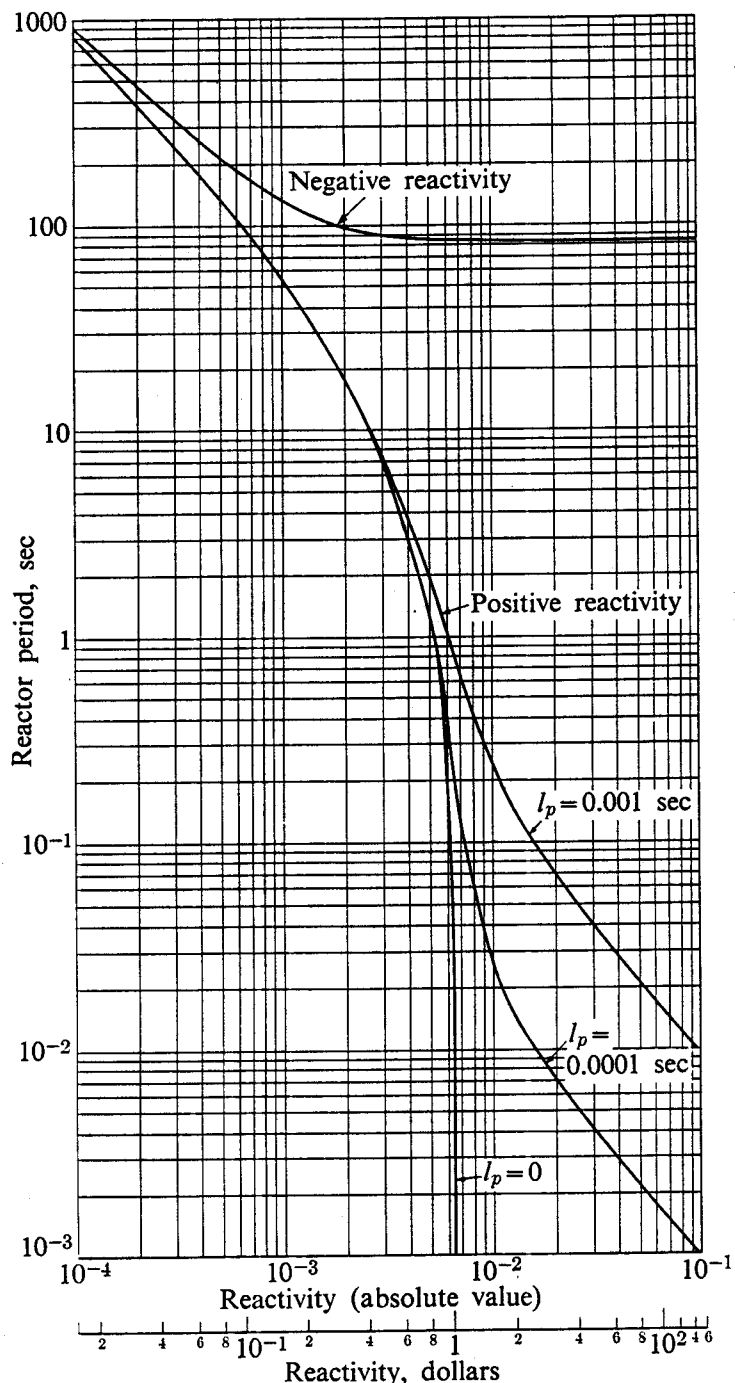


Fig. 12-4. Reactor period as a function of positive and negative reactivity for a  $\text{U}^{235}$ -fueled reactor.

Several things should be noted in Fig. 12-4. First, it will be observed that the period decreases monotonically with increasingly *positive* reactivity, but with *negative* reactivity the shortest period is only about 80 sec. The reason for this may be seen directly from the plot of the reactivity equation given in Fig. 12-1. Thus as  $\rho$  increases between 0 and +1, the first root clearly occurs at monotonically increasing values of  $\omega$ , which gives a monotonically decreasing period. By con-

trast, as  $\rho$  becomes increasingly negative the first root approaches  $\omega = -\lambda_1$ , giving the period  $T = 1/\lambda_1 \approx 80$  sec. The effect of this 80-sec period on reactor shutdown will be discussed in Section 12-10.

It should also be observed from Fig. 12-4 that the period is independent of the prompt neutron lifetime for periods longer than about 10 sec. Thus as would be expected physically, the longer periods are determined almost entirely by the delayed neutrons. Since the periods for negative  $\rho$  are never shorter than 80 sec, it follows that the prompt neutron lifetime has essentially no effect on the response of a reactor to insertions of negative reactivities.

With reactivities sufficient to give shorter periods, however, it is seen that the period is sensitive to  $l_p$ . This is especially true for  $\rho$  above  $\rho = \beta = 0.0065$ . As will be shown in Section 12-8 at reactivities greater than  $\rho = \beta$ , the reactor is critical on prompt neutrons alone and the delayed neutrons play little or no role in determining the reactor period. In particular, it will be seen from Fig. 12-4 that the period is zero for  $l_p = 0$  above  $\rho = \beta$ .

The stable period has been used to define a unit of reactivity known as the *inhour*. This is defined as the amount of positive reactivity required to produce a stable period of one hour. It will be evident from Fig. 12-4 that the inhour is a very small unit of reactivity. Thus a reactivity of merely  $+10^{-4}$  gives a period of only about 800 sec, which is much shorter than one hour. For this reason the inhour unit is limited in its usage to reactors in which only small reactivity changes are possible, namely, reactors with little built-in excess reactivity. Most modern reactors are capable of substantial reactivity changes, however, and with these reactors, reactivity is given absolute units, in percent, or in terms of the *dollar* unit which will be discussed in Section 12-8. Although the inhour unit is seldom used today, the reactivity equation is still often referred to as the inhour equation.

## 12-7 The Prompt Jump

It is usually impossible and also unnecessary to determine the precise behavior of a reactor immediately after a change in reactivity. If the reactivity is introduced uniformly and the system is originally in a steady state,  $\phi(t)$  can, of course, be found as the sum of seven exponentials. However, as mentioned in Section 12-4, spatially uniform changes in reactivity almost never occur in practice, and non-uniform changes in reactivity introduce harmonics into the flux. As a result, the numerical analysis of the early behavior of a reactor becomes hopelessly complicated.

Nevertheless, it is important for practical reasons to know to what level the flux will rise (or drop) when the reactivity is changed. This can be estimated in a straightforward way by assuming that the concentrations of the precursors remain constant immediately following the reactivity change. Also, since the harmonics quickly die out, it is only necessary to consider the behavior of the fundamental. Thus letting  $n = 1$  in Eq. (12-55) and writing  $\phi_T(t)$  and  $C_i(t)$  for the time depend-

ent parts of the flux and precursor concentrations, respectively, Eq. (12-55) becomes

$$t_1 \frac{d\phi_T(t)}{dt} = [(1 - \beta)k - 1]\phi_T(t) + \frac{pk}{\bar{\Sigma}_a k_\infty} \sum_i \lambda_i C_i(t). \quad (12-80)$$

By hypothesis, the second term on the right-hand side due to the delayed neutrons may now be taken to be constant.

If the reactor is initially in the steady state,

$$\frac{d\phi_T(t)}{dt} = 0$$

at  $t = 0$ ,  $k = 1$ , and Eq. (12-80) gives

$$\beta\phi_T(0) = \frac{pk}{\bar{\Sigma}_a k_\infty} \sum_i \lambda_i C_i(0),$$

where the ratio  $pk/\bar{\Sigma}_a k_\infty$  is evaluated at  $t = 0$ . Assuming that this ratio does not change significantly after the change in reactivity, Eq. (12-80) can be written as

$$t_1 \frac{d\phi_T(t)}{dt} = [(1 - \beta)k - 1]\phi_T(t) + \beta\phi_T(0). \quad (12-81)$$

The solution to this equation is easily found to be

$$\begin{aligned} \phi_T(t) &= \phi_T(0) \exp \frac{[(1 - \beta)k - 1]t}{t_1} \\ &+ \frac{\beta\phi_T(0)}{1 - (1 - \beta)k} \left\{ 1 - \exp \frac{[(1 - \beta)k - 1]t}{t_1} \right\}. \end{aligned} \quad (12-82)$$

If  $(1 - \beta)k < 1$ , both exponentials in Eq. (12-82) decrease in time with a period given by  $t_1/[1 - (1 - \beta)k] \approx t_1/(1 - k)$ . As shown in Section 12-1, this is the period of a reactor in the absence of delayed neutrons. The exponentials in Eq. (12-82) thus rapidly die out and the flux quickly assumes the value

$$\phi_T(t) \rightarrow \frac{\beta\phi_T(0)}{1 - (1 - \beta)k}. \quad (12-83)$$

In terms of reactivity, since  $k = 1/(1 - \rho)$  (cf. Eq. 12-66), Eq. (12-83) becomes

$$\phi_T(t) \rightarrow \frac{\beta(1 - \rho)}{\beta - \rho} \phi_T(0). \quad (12-84)$$

The flux thus jumps by the factor  $\beta(1 - \rho)/(\beta - \rho)$  very soon after the reactivity  $\rho$  is introduced into the system. It should be noted that this result holds whether  $\rho$  is positive or negative; the only requirement is that  $(1 - \beta)k < 1$ . Taken together, the prompt jump and the stable period discussed in the preceding section provide all the information usually required concerning the response of a reactor to a step change in reactivity.

### 12-8 The Prompt Critical Condition

It will be recalled that the multiplication factor of a reactor is directly proportional to the number of neutrons emitted per fission ( $\nu$ ). Since only the fraction  $1 - \beta$  of these are emitted as prompt neutrons, it follows that so far as the prompt neutrons are concerned, the multiplication factor of a reactor is equal to  $(1 - \beta)k$ . When this factor is less than unity for a supercritical reactor, the reactor is said to be *prompt subcritical*. In this case, the flux rises suddenly and then assumes a stable period, as discussed in the preceding sections. On the other hand, if  $(1 - \beta)k$  is greater than unity the chain reaction can continue to diverge on prompt neutrons alone. The delayed neutrons now play no role in governing the reactor period and the flux increases with the very short period determined by the prompt neutrons. The reactor is then said to be *prompt critical*, which is normally a dangerous situation.

Evidently the minimum condition for prompt criticality is

$$(1 - \beta)k = 1. \quad (12-85)$$

From Eq. (12-66),  $k = 1/(1 - \rho)$  and inserting this into Eq. (12-85) gives  $1 - \beta = 1 - \rho$  or

$$\beta = \rho. \quad (12-86)$$

Thus the reactivity required to bring a reactor to prompt critical is equal to the total delayed fraction  $\beta$ . Since  $\beta$  is much less than unity it is clear why positive reactivity changes are always such small numbers. Thus any reactivity insertion even approaching values of  $\beta$  necessarily represents an enormous change in the system when measured in terms of the response of the reactor.

The reactivity necessary for a reactor to become prompt critical, namely,  $\rho = \beta$ , is called, at least in the United States, a *dollar* of reactivity; one-one hundredth of this reactivity is known as one *cent*. It must be noted that the dollar is not an absolute unit of reactivity but depends upon both the fuel and the neutron leakage from the reactor (cf. Section 12-5). For U<sup>235</sup>-fueled reactors a dollar is usually worth about 0.0065 or 0.65% in reactivity, while it is worth substantially less for U<sup>233</sup>- or Pu<sup>239</sup>-fueled reactors (cf. Table 3-7). It follows that there are somewhat more stringent requirements on the amounts of reactivity that can be safely added to these reactors than for U<sup>235</sup>-fueled reactors.

### 12-9 Small Reactivities

When  $\rho$  is very small, the *first* root of the reactivity equation is also small, as can readily be seen from Fig. 12-1. In this case,  $\omega \ll \lambda_i$ , and it is possible to ignore the terms containing  $\omega$  in the denominator of the reactivity equation, Eq. (12-74). This equation then takes the form

$$\rho \approx \omega_1 \left( l_p + \sum_i \frac{\beta_i}{\lambda_i} \right) = \omega_1 \left( l_p + \sum_i \beta_i \bar{t}_i \right), \quad (12-87)$$

where  $\bar{t}_i$  is the mean-life of the  $i$ th precursor. The stable period is therefore

$$T = \frac{1}{\omega_1} = \frac{1}{\rho} \left( l_p + \sum_i \beta_i \bar{t}_i \right). \quad (12-88)$$

The numerator of this equation will be recognized from the discussion in Section 12-2 as the mean lifetime of fission neutrons when the delayed neutrons are included. Also, frequently,  $l_p \ll \sum_i \beta_i \bar{t}_i$  and Eq. (12-88) reduces to

$$T = \frac{1}{\rho} \sum_i \beta_i \bar{t}_i. \quad (12-89)$$

The range of validity of Eq. (12-89) may be estimated by writing the condition  $\omega \ll \lambda_i$  as  $1/\omega \gg 1/\lambda_i$ , which is equivalent to  $T \gg \bar{t}_i$ . The largest value of  $\bar{t}_i$  is about 80 sec, and it follows that Eq. (12-89) can be used provided  $T \gg 80$  sec. In practice, it is accurate enough for most purposes for reactivities up to about  $\rho = 0.0006$  or approximately 10 cents in a  $U^{235}$ -fueled reactor. For larger reactivities Eq. (12-89) substantially overestimates the reactor period.

## 12-10 Large Negative Reactivities; Scram and Shutdown

If several control rods are suddenly inserted into a reactor, that is, the reactor is *scrammed*, the reactivity of the system becomes large and negative. However, even if it were possible to insert an infinite negative reactivity, the flux would not fall to zero immediately. Thus placing  $\rho = -\infty$  in Eq. (12-84) for the prompt jump (in this instance, prompt drop), the result is

$$\phi_T(t) \rightarrow \beta \phi_T(0). \quad (12-90)$$

Equation (12-90) gives the theoretical minimum level to which the flux can drop soon after a scram.

In practice, it is seldom possible to insert rapidly more than about twenty dollars worth of negative reactivity (it is rarely possible to insert this much), which corresponds in a  $U^{235}$  reactor to a reduction in  $k$  to about 0.9. Using the values  $\rho = -20 \times 0.0065 = -0.13$  and  $\beta = 0.0065$  in Eq. (12-84) gives a prompt drop of

$$\phi_T(t) \rightarrow 0.054 \phi_T(0). \quad (12-91)$$

This is about ten times the value given by Eq. (12-90).

After the prompt drop in flux, the reactor goes on a stable period. As already noted in Section 12-6, if  $\rho = -\infty$ , the first root of the reactivity equation occurs at  $\omega_1 = -\lambda_1$ , the decay constant of the longest-lived precursor. The stable period is therefore  $T = -1/\lambda_1 = -80$  sec. This is the shortest stable (negative) reactor period possible, as is also shown in Fig. 12-4. The flux level cannot be reduced more rapidly and the shutdown of a reactor therefore requires a finite length of time. For example, suppose a reactor is considered to be shutdown when

its flux has been reduced by a factor of  $10^{10}$ . The minimum shutdown time,  $t_S$ , can then be found from the equation

$$e^{-t_S/T} = 10^{-10},$$

which gives  $t_S = 30$  min. This is the shutdown time following the (very short) prompt drop.

In some reactors the  $\gamma$ -rays from the decay of the accumulated fission products continue to produce neutrons by the  $(\gamma, n)$  reaction long after the shutdown procedure is begun, and the continued emission of these neutrons increases the time required for shutdown. This effect is particularly important in reactors containing large amounts of deuterium or beryllium or other materials having low photo-neutron thresholds.

### 12-11 Linear Change in Reactivity

Up to this point only step changes in reactivity have been considered. In the usual case, however, the multiplication factor of a reactor is changed gradually rather than instantaneously. This is necessarily the situation, for instance, when a control rod is inserted or removed from a reactor, due to its finite speed of motion. Also, in some reactor accidents reactivity is continually added to the system.

An approximate analysis of these problems can be carried out by assuming that the multiplication factor changes linearly with time. Then if the reactor is initially critical,  $k$  can be expressed as

$$k = 1 + at, \quad (12-92)$$

where  $a$  is a constant. Unfortunately, the exact response of a reactor to the function given in Eq. (12-92) presents a difficult mathematical problem, which is best handled on an electronic computer. However, a fair approximation to the reactor behavior can be obtained by assuming as in Section 12-7 that the precursor concentrations remain constant throughout the time when  $k$  is changing. In this case, the flux is again determined from Eq. (12-81), which now takes the form

$$t_1 \frac{d\phi_T(t)}{dt} = [-\beta + (1 - \beta)at]\phi_T(t) + \beta\phi_T(0). \quad (12-93)$$

Making the substitutions

$$\gamma = \frac{\beta}{\sqrt{2at_1(1 - \beta)}}, \quad y(t) = \gamma \left[ \frac{1 - \beta}{\beta} at - 1 \right], \quad (12-94)$$

Eq. (12-93) may be written as

$$d\phi_T(y) - 2y\phi_T(y)dy = 2\gamma\phi_T(0)dy. \quad (12-95)$$

The integrating factor for this equation is  $e^{-y^2}$ , so that

$$\phi_T[y(t)]e^{-y^2(t)} \Big|_{y(0)}^{y(t)} = 2\gamma\phi_T(0) \int_{y(0)}^{y(t)} e^{-y^2} dy. \quad (12-96)$$

The integral on the right-hand side can be expressed as the difference of two error functions, that is,

$$\int_{y(0)}^{y(t)} e^{-\nu^2} dy = \frac{\sqrt{\pi}}{2} \{ \text{erf}[y(t)] - \text{erf}[y(0)] \}. \quad (12-97)$$

The complete solution may then be written as

$$\phi_T(t) = \phi_T(0)e^{y^2(t)} \{ e^{-y^2(0)} + \gamma\sqrt{\pi} [\text{erf}[y(t)] - \text{erf}[y(0)]] \}. \quad (12-98)$$

This equation is often used to determine the response of a reactor to control rod motion and for the analysis of reactor accidents.

## References

- ASH, M., *Nuclear Reactor Kinetics*. New York: McGraw-Hill, 1965.
- GALANIN, A. D., *Thermal Reactor Theory*, 2nd ed. New York: Pergamon Press, 1960, Section 29.
- GLASSTONE, S., and M. C. EDLUND, *The Elements of Nuclear Reactor Theory*. Princeton, N.J.: Van Nostrand, 1952, Chapter 10.
- ISBIN, H. S., *Introductory Nuclear Reactor Theory*. New York: Reinhold, 1963, Chapter 9.
- KEEPIN, G. R., *Physics of Nuclear Kinetics*. Reading, Mass.: Addison-Wesley, 1965.
- MEEM, J. L., *Two Group Reactor Theory*. New York: Gordon and Breach, 1964, Chapter 5.
- MEGHREBLIAN, R. V., and D. K. HOLMES, *Reactor Analysis*. New York: McGraw-Hill 1960, Chapter 9.
- MURRAY, R. L., *Nuclear Reactor Physics*. Englewood Cliffs, N.J.: Prentice-Hall, 1957, Chapter 6.
- "Reactor Physics Constants," U.S. Atomic Energy Commission Report ANL-5800, 2nd ed., 1963, Section 5.
- SCHULTZ, M. A., *Control of Nuclear Reactors and Power Plants*, 2nd ed. New York: McGraw-Hill, 1961, Chapters 1, 2, 4, and 5.
- WEINBERG, A. M., and E. P. WIGNER, *The Physical Theory of Neutron Chain Reactors*. Chicago: University of Chicago Press, 1958, Chapter 17.

## Problems

12-1. Compute the prompt neutron lifetime for an infinite thermal reactor consisting of a homogeneous mixture of  $\text{U}^{235}$  and

- (a)  $\text{H}_2\text{O}$
- (b)  $\text{D}_2\text{O}$
- (c) Be
- (d) Graphite

12-2. Compute the mean life of fission neutrons in infinite, homogeneous, critical mixtures of  $\text{D}_2\text{O}$  and

- (a)  $\text{U}^{233}$
- (b)  $\text{U}^{235}$
- (c)  $\text{Pu}^{239}$

12-3. An infinite U<sup>235</sup>-fueled, H<sub>2</sub>O-moderated reactor operates at a constant power density of 100 watts(th)/cm<sup>3</sup>. Compute the concentrations in atoms/cm<sup>3</sup> of U<sup>235</sup> and each of the delayed neutron precursors.

12-4. A bare cylindrical tank 100 cm in diameter contains a homogeneous mixture of U<sup>235</sup> and ordinary water which is critical when the mixture fills the tank to a height of 100 cm. Compute the reactivity of the system when the tank is filled to 102 cm.

12-5. One day when a bare critical assembly, consisting of a 4-ft cube of thin plates of Be and U<sup>235</sup>, had just been brought to critical, the roof of the building collapsed on the assembly. (a) Take the roof to be equivalent to 2 in. of water, and estimate the reactivity introduced into the assembly in this accident. (b) What happens next?

12-6. Plot the right-hand side of the reactivity equation over the region  $-\lambda_1 < \omega < \infty$  for thermal reactors in the following cases.

- |  |   |
|--|---|
| (a) U <sup>233</sup> fuel, $l_p = 0$ sec       | (d) Pu <sup>239</sup> fuel, $l_p = 0$ sec       |
| (b) U <sup>233</sup> fuel, $l_p = 10^{-4}$ sec | (e) Pu <sup>239</sup> fuel, $l_p = 10^{-4}$ sec |
| (c) U <sup>233</sup> fuel, $l_p = 10^{-3}$ sec | (f) Pu <sup>239</sup> fuel, $l_p = 10^{-3}$ sec |

12-7. The approximate response of a reactor to a step insertion of reactivity can be obtained by assuming that there is only one delayed neutron group of yield  $\beta$  and mean life

$$\bar{t} = \sum_i \beta_i \bar{t}_i / \beta.$$

In this case, the reactivity equation is quadratic in  $\omega$ , and  $\phi(t)$  can be written as

$$\phi(t) = \phi_0 (A_1 e^{\omega_1 t} + A_2 e^{\omega_2 t}),$$

where  $t$  is the time measured from the reactivity change. (a) Calculate  $\omega_1$  and  $\omega_2$ . (b) Calculate  $A_1$  and  $A_2$ . (c) Show that for small reactivities

$$\begin{aligned} \omega_1 &\approx \frac{\lambda\rho}{\beta - \rho}, & \omega_2 &\approx -\frac{\beta - \rho}{l_p}, \\ A_1 &\approx \frac{\beta}{\beta - \rho}, & A_2 &\approx -\frac{\rho}{\beta - \rho}. \end{aligned}$$

(d) Compute and plot  $\phi(t)$  for a U<sup>235</sup>-fueled reactor with  $l_p = 10^{-4}$  sec and a step reactivity insertion of +0.1%. Compare with Fig. 12-2.

12-8. (a) Using one-group theory, show that the reactivity equation for a bare fast reactor is of the same form as for a thermal reactor. (b) Using delayed neutron data given in Table 3-8, determine the stable period of a U<sup>235</sup>-fueled fast reactor following a reactivity insertion of \$0.50. (Take  $l_p = 0$ .) [Hint: The *approximate* answer can be found by using Fig. 12-4. This determines the region of the new reactivity equation that must be plotted.]

12-9. A thermal reactor assembly consists of a homogeneous mixture of a fissile isotope and ordinary water in a bare 2.5 ft square cylinder. Compare the stable periods of the reactor for a step reactivity insertion of 0.1% if the fissile isotope is

- |                      |                      |                       |
|----------------------|----------------------|-----------------------|
| (a) U <sup>233</sup> | (b) U <sup>235</sup> | (c) Pu <sup>239</sup> |
|----------------------|----------------------|-----------------------|

[Note: In (a) and (c) use the results of Problem 12-6.]

12-10. In a bare, fast reactor, fueled with partially-enriched uranium, a substantial fraction of the fissions occur in the  $\text{U}^{238}$ . Show that in this case the reactivity equation is

$$\rho = \frac{\omega l_p}{1 + \omega l_p} + \frac{\omega \gamma^{25}}{1 + \omega l_p} \sum_{i=1}^6 \frac{\beta_i^{25}}{\omega + \lambda_i^{25}} + \frac{\omega \gamma^{28}}{1 + \omega l_p} \sum_{i=1}^6 \frac{\beta_i^{28}}{\omega + \lambda_i^{28}},$$

where  $\gamma^{25}$  and  $\gamma^{28}$  are the fractions of the fission neutrons emitted by  $\text{U}^{235}$  and  $\text{U}^{238}$ , respectively. [Hint: Set up the one-group flux equation and the equations for the concentrations of the 12 precursors; proceed as in the derivation of Eqs. (12-21) and (12-60).] Note: The above equation is valid for *any* (bare) reactor in which two nuclear species undergo fission.

12-11. A control rod worth \$0.90 is suddenly inserted into a large critical  $\text{U}^{235}$ -fueled thermal reactor. Plot the response of the system if  $l_p = 10^{-3}$  sec.

12-12. Show that the reactivity insertion in a thermal  $\text{U}^{235}$ -fueled reactor can never be greater than about \$80.

12-13. Show that the prompt jump formula for an infinite reactor (cf. Eq. 12-83) can be derived by summing successive generations of prompt neutrons, as was done in Section 9-1, assuming that the delayed neutrons represent a uniformly distributed source emitting  $S = \sum_i \lambda_i C_i(0)$  fast neutrons/cm<sup>3</sup>-sec.

12-14. Using Eq. (12-89), plot the stable period of a  $\text{U}^{235}$ -fueled reactor versus reactivity and compare with Fig. 12-4.

12-15. A control rod is inserted a short distance into a bare, critical reactor and as a result the reactor goes on a *long* (negative) stable period  $T$ . Show that the reactor would have gone on the same stable period had an absorbing nuclide of macroscopic cross section  $\bar{\Sigma}_{ap} = \ell\sqrt{\pi}/2t_d v_T T$  been distributed uniformly throughout the original critical reactor, where  $\ell$  is the mean generation time.

**Table 12-1**  
Delayed Photoneutron Data for  $\text{U}^{235}$  Fission Products in  $\text{D}_2\text{O}^*$

$i$	$\lambda_i(\text{sec}^{-1})$	$\beta_i \times 10^5$	$i$	$\lambda_i(\text{sec}^{-1})$	$\beta_i \times 10^5$
1	$6.26 \times 10^{-7}$	0.05	6	$1.50 \times 10^{-3}$	3.36
2	$3.63 \times 10^{-6}$	0.103	7	$4.81 \times 10^{-3}$	7.00
3	$4.37 \times 10^{-5}$	0.323	8	$1.69 \times 10^{-2}$	20.4
4	$1.17 \times 10^{-4}$	2.34	9	$2.77 \times 10^{-1}$	65.1
5	$4.28 \times 10^{-4}$	2.07	$\beta = \sum \beta_i = 100.75$		

\* From G. R. Keepin, *Physics of Nuclear Kinetics*, Addison-Wesley, Reading, Mass., 1965. The data in this table are for saturation fission product activity. For finite irradiation time  $t$ , the tabulated values of  $\beta_i$  each should be multiplied by the factor  $(1 - e^{-\lambda_i t})$ .

12-16. The production of neutrons from the  $(\gamma, n)$  reaction can have an important effect on the kinetic behavior of  $\text{D}_2\text{O}$ - and Be-moderated reactors. These neutrons can be traced to certain fission products which decay with the emission of energetic  $\gamma$ -rays.

It is possible, therefore, to treat photoneutrons as delayed neutrons having these fission products as precursors. Table 12-1 gives data for  $U^{235}$  fissions (saturation fission product activity) in  $D_2O$ . (a) Show that the reactivity equation for a  $D_2O$ -moderated reactor is

$$\rho = \frac{\omega l_p}{1 + \omega l_p} + \frac{\omega}{1 + \omega l_p} \sum_{i=1}^{15} \frac{\beta_i}{\omega + \lambda_i},$$

where  $i = 1, 2, \dots, 6$  refers to delayed fission neutrons and  $i = 7, 8, \dots, 15$  refers to delayed photoneutrons. (b) Compare the stable periods of an infinite,  $U^{235}$ -fueled,  $D_2O$ -moderated reactor, following a step reactivity insertion of \$0.10, with and without the delayed photoneutrons taken into consideration.

12-17. During the shutdown of a  $U^{235}$ -fueled reactor, with a prompt neutron lifetime of  $5 \times 10^{-4}$  sec, the power is observed to decrease by a factor of  $10^5$  in 20 min. A step insertion of how much reactivity was required to obtain this result?

12-18. A uniform, infinite, subcritical assembly of multiplication factor  $k_\infty$  contains uniformly distributed sources emitting  $S$  fast neutrons/cm<sup>3</sup>-sec. For  $t < 0$  the system is in the steady state, but at  $t = 0$  the sources are suddenly removed. (a) Show that the thermal flux quickly drops to the value

$$\phi_T(t) \rightarrow \frac{\beta k_\infty p S}{\Sigma_a(1 - k_\infty)[1 - (1 - \beta)k_\infty]} = \frac{\beta k_\infty \phi_T(0)}{1 - (1 - \beta)k_\infty},$$

where  $\phi_T(0)$  is the flux before the removal of the sources. (b) Compute the fractional change in the flux for a natural uranium-water assembly having  $k_\infty = 0.98$ . (c) Show that following the prompt drop the assembly goes on a stable period of approximately 80 sec. (d) Discuss quantitatively the prompt drop in flux in a *finite* subcritical assembly when a point source is suddenly removed. (e) Show how this drop in flux can be used to measure  $k_\infty$  of a subcritical assembly.

12-19. Reactivity is added to a  $U^{235}$ -fueled critical reactor ( $l_p = 10^{-3}$  sec) at the rate of approximately 6 cents/sec. (a) Using Eq. (12-98) compute and plot the fractional change in the power of the reactor up to 2 sec after the first insertion of reactivity. (b) How long would it take for the power to reach the same level if the total of 12 cents in reactivity were added in a single step?

# 13

## Changes in Reactivity

It was pointed out in the introduction to Chapter 12 that various properties of a reactor may change during the course of its operation. A number of these changes are considered in this chapter.

### 13-1 Changes in Temperature—Temperature Coefficients

Many of the parameters which determine the reactivity of a reactor, namely the thermal utilization, resonance escape probability, diffusion length, and so on, are functions of the temperature of the fuel, moderator, and coolant. Changes in the temperature of these reactor components therefore lead to changes in reactivity. Such temperature effects on reactivity must be understood if a reactor is to be properly controlled. For this purpose, various *temperature coefficients*, denoted by the symbol  $\alpha_T$ , are defined by the relation

$$\alpha_T = \frac{d\rho}{dT}, \quad (13-1)$$

where  $\rho$  is the reactivity of the system and  $T$  is the temperature of a specific component. Thus if  $T$  refers to the temperature of the fuel,  $\alpha_T$  is called the *fuel temperature coefficient*; if  $T$  is the moderator temperature,  $\alpha_T$  is called the *moderator temperature coefficient*; and so forth.

According to Eq. (12-66) the reactivity is given by  $\rho = 1 - k^{-1}$ , where  $k$  is the multiplication factor of the reactor, so that Eq. (13-1) is equivalent to

$$\alpha_T = \frac{1}{k^2} \frac{dk}{dT}. \quad (13-2)$$

In all cases of interest,  $k$  is close to unity and Eq. (13-2) may be written approximately as

$$\alpha_T \approx \frac{1}{k} \frac{dk}{dT}. \quad (13-3)$$

Equation (13-3) is a more convenient starting point for calculating temperature coefficients than either Eq. (13-1) or Eq. (13-2), and it will henceforth be taken to be the definition of  $\alpha_T$ .

Since  $k$  is always positive, it follows from Eq. (13-3) that  $dk/dT$  has the same algebraic sign as  $\alpha_T$ . Thus if  $\alpha_T$  is positive,  $dk/dT$  is also positive, and the multiplication factor of the reactor increases with increasing temperature. On the other hand, if  $\alpha_T$  is negative,  $dk/dT$  is negative, and the multiplication factor decreases with increasing temperature. The behavior of a reactor following a change in temperature depends upon the sign of  $\alpha_T$ . For example, if the temperature of a reactor component increases and its temperature coefficient is positive,  $k$  increases and, as a result, so also does the power. This, in turn, leads to a further increase in temperature, which again increases  $k$ , and so on. The power of the reactor continues to build up in this way until the reactor is brought under control by external intervention or the core melts, with all the unfortunate consequences this may entail. Had the temperature originally been reduced,  $k$  would have decreased, reducing the power, leading to a further drop in temperature, etc., and the reactor would have shut itself down. It is evident that reactors having positive temperature coefficients are inherently *unstable* with respect to changes in temperature.

Reactors with negative temperature coefficients behave quite differently. An increase in temperature now leads to a decrease in  $k$  which reduces the power level and tends to return the temperature to its original value. Similarly, a decrease in temperature results in an increase in  $k$  which increases the power and again returns the system to its initial temperature. Reactors having negative temperature coefficients are therefore *stable* with respect to temperature changes.

Such changes in temperature frequently accompany changes in the reactivity, and it follows that the response of a reactor to a reactivity change depends to some extent on the temperature coefficient as well as on the various neutron kinetics parameters that were discussed in Chapter 12. Consider, for instance, the behavior of a previously critical reactor following a step insertion of positive reactivity, say by the sudden removal of a control rod. As the reactor power increases the temperature does also, and if  $\alpha_T$  is positive this leads to a further increase in power, a further increase in temperature, and so on, with the result that, barring outside intervention, the power rises without limit as shown in Fig. 13-1. By contrast, if  $\alpha_T$  is negative, the reactivity decreases as the power and temperature increase. If  $\alpha_T$  is also small and the removal of heat from the reactor is sufficiently rapid, the power rises smoothly to a level, as indicated in the figure, where the temperature reduces the reactivity to zero. The reactor at this elevated power is now critical and remains at this power level indefinitely. Most power reactors behave in this way in response to a step insertion of reactivity. However, if  $\alpha_T$  is large and negative and/or the removal of heat is not sufficiently rapid, the rise in the temperature accompanying the initial rise in power may result in such a large drop in reactivity that the reactor falls subcritical before the heat generated in the system has been removed. The power in this case drops back to a level where the temperature and power are in the steady state, and the reactivity is zero. The result is the power "overshoot" illustrated in Fig. 13-1.

Although it is possible, in principle, to prevent large power excursions in a reactor having a positive temperature coefficient by the use of a fast and reliable

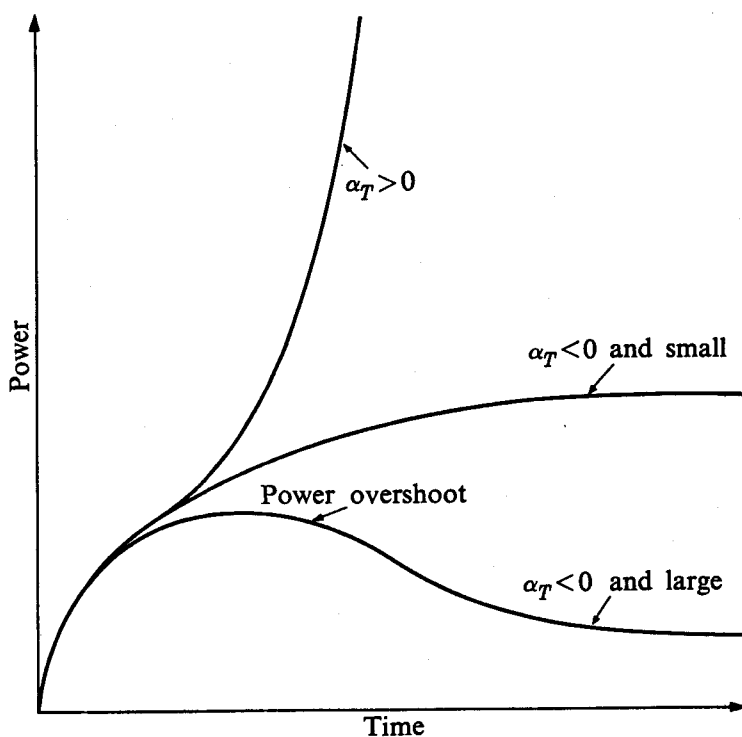


**Fig. 13-1.** Reactor power as a function of time after a step insertion of reactivity for three different temperature coefficients.

control system, it is generally considered advisable in the interest of safety to rely instead upon the inherent stability found in reactors having negative temperature coefficients. In this connection, it may be mentioned that in solid-fueled reactors (and this means most reactors) it is the temperature coefficient of the fuel which is usually of greatest importance in considerations of safety. This is because the fuel temperature responds almost immediately to changes in power, whereas the temperatures of the moderator or coolant must wait upon the transfer of heat from the fuel. For this reason, the fuel temperature coefficient is often called the *prompt temperature coefficient*. Virtually all reactors that have been built throughout the world have had negative prompt temperature coefficients, and in the United States the Atomic Energy Commission will not license a reactor that does not meet this requirement.

A reactor having a negative temperature coefficient will obviously have less reactivity at its operating temperature than it has in the shut-down condition at room temperature. This change in reactivity is known as the *temperature defect*. Since critical experiments are ordinarily carried out well below the intended operating temperature, the temperature coefficient must be known in order to assess the amount of excess reactivity needed to assure that the reactor will be critical when operating at full power.

In the following discussion it will be assumed for the most part that the temperature is independent of position at all times in the reactor. Thus when the temperature changes, it is assumed to change uniformly throughout the system. The

temperature coefficient to be derived in this case is called the *uniform temperature coefficient* or, sometimes, the *isothermal temperature coefficient*. Nonuniform temperature changes are best treated by perturbation methods which are considered in Chapter 15. For simplicity, the discussion will also be restricted to bare, thermal reactors.

Before proceeding, it must be noted that some reactor parameters are functions of the physical temperature of the medium,  $T$ , while others are functions of the neutron temperature,  $T_n$  (cf. Section 8-1). For example, in the expression for the macroscopic absorption cross section,  $\bar{\Sigma}_a = N\bar{\sigma}_a$ , the atom density,  $N$ , varies inversely with the temperature of the medium. Thus as  $T$  increases and the medium expands, the atom density decreases. The parameter  $\bar{\sigma}_a$  is a function of  $T_n$ , however, and only indirectly depends upon  $T$ . In order to be able to derive explicit relations for the various temperature coefficients, it will be assumed in this section that  $T_n$  is directly proportional to  $T$ , that is,

$$T_n = aT, \quad (13-4)$$

where  $a$  is a parameter which depends upon the properties of the medium, and both  $T$  and  $T_n$  are in degrees Kelvin.\*

**Temperature coefficients of a bare thermal reactor.** The multiplication factor of a bare thermal reactor is given by

$$k = k_\infty P_T P_F, \quad (13-5)$$

where

$$k_\infty = \eta_T f p \epsilon, \quad (13-6)$$

and  $P_T$  and  $P_F$  are the slow and fast nonleakage probabilities. As shown in Section 9-4,

$$P_T = \frac{1}{1 + B^2 L_T^2}, \quad (13-7)$$

and according to Fermi age theory,

$$P_F = e^{-B^2 r_T}. \quad (13-8)$$

To compute the uniform temperature coefficient, it is first convenient to take the logarithm of both sides of Eq. (13-5), namely,

$$\ln k = \ln k_\infty + \ln P_T + \ln P_F. \quad (13-9)$$

---

\* Throughout this section all *temperatures* are in degrees Kelvin. However, since one Kelvin degree is equal in size to one centigrade degree, temperature coefficients may be expressed equivalently in units of per °K or per °C. The latter unit will be used in this section.

Differentiating this equation term by term then gives

$$\alpha_T = \frac{1}{k} \frac{dk}{dT} = \frac{1}{k_\infty} \frac{dk_\infty}{dT} + \frac{1}{P_T} \frac{dP_T}{dT} + \frac{1}{P_F} \frac{dP_F}{dT}. \quad (13-10)$$

Each term in this equation is the temperature coefficient of the indicated parameter. That is,

$$\frac{1}{k_\infty} \frac{dk_\infty}{dT}$$

is the temperature coefficient of  $k_\infty$ , denoted by  $\alpha_T(k_\infty)$ ;

$$\frac{1}{P_T} \frac{dP_T}{dT}$$

is the temperature coefficient of  $P_T$ , denoted by  $\alpha_T(P_T)$ ; and so on. Thus from Eq. (13-10):

$$\alpha_T = \alpha_T(k_\infty) + \alpha_T(P_T) + \alpha_T(P_F). \quad (13-11)$$

Differentiating the logarithm of  $k_\infty$  gives

$$\frac{1}{k_\infty} \frac{dk_\infty}{dT} = \frac{1}{\eta_T} \frac{d\eta_T}{dT} + \frac{1}{f} \frac{df}{dT} + \frac{1}{p} \frac{dp}{dT} + \frac{1}{\epsilon} \frac{d\epsilon}{dT},$$

so that

$$\alpha_T(k_\infty) = \alpha_T(\eta_T) + \alpha_T(f) + \alpha_T(p) + \alpha_T(\epsilon). \quad (13-12)$$

Next, using Eq. (13-7) gives

$$\alpha_T(P_T) = \frac{1}{P_T} \frac{dP_T}{dT} = - \frac{B^2 L_T^2}{1 + B^2 L_T^2} \left[ \frac{1}{L_T^2} \frac{dL_T^2}{dT} + \frac{1}{B^2} \frac{dB^2}{dT} \right]$$

or

$$\alpha_T(P_T) = - \frac{B^2 L_T^2}{1 + B^2 L_T^2} [\alpha_T(L_T^2) + \alpha_T(B^2)]. \quad (13-13)$$

Similarly from Eq. (13-8),

$$\alpha_T(P_F) = \frac{1}{P_F} \frac{dP_F}{dT} = - B^2 \tau_T \left[ \frac{1}{\tau_T} \frac{d\tau_T}{dT} + \frac{1}{B^2} \frac{dB^2}{dT} \right]$$

or

$$\alpha_T(P_F) = - B^2 \tau_T [\alpha_T(\tau_T) + \alpha_T(B^2)]. \quad (13-14)$$

It is clear from Eqs. (13-11) through (13-14) that in order to calculate the temperature coefficient of the reactor, it is first necessary to determine the temperature coefficients of each of the parameters,  $\eta_T$ ,  $f$ ,  $p$ ,  $\epsilon$ ,  $L_T^2$ ,  $\tau_T$ , and  $B^2$ . These will now be considered in turn.

**Temperature coefficient of  $\eta_T$ .** If the fuel consists of a single fissile isotope,  $\eta_T$  is given by (cf. Eq. 8-61)

$$\eta_T = \nu \frac{\bar{\sigma}_f}{\bar{\sigma}_a}, \quad (13-15)$$

where  $\bar{\sigma}_f$  and  $\bar{\sigma}_a$  are the average thermal fission and absorption cross sections, respectively. Since  $\nu$  is essentially constant at thermal energies, the temperature coefficient of  $\eta_T$  is entirely due to variations with temperature of the ratio  $\bar{\sigma}_f/\bar{\sigma}_a$ . If both  $\bar{\sigma}_f$  and  $\bar{\sigma}_a$  are  $1/v$  or deviate from  $1/v$  in the same way, the temperature coefficient of  $\eta_T$  is clearly zero. Neither of these conditions is satisfied by the practical fissile fuels, as can be seen from Table 8-2, where values of  $\eta_T$  are given as a function of temperature. It will be observed that  $\eta_T$  decreases with increasing temperature for  $U^{235}$  and  $Pu^{239}$  and increases with temperature for  $U^{233}$ . Thus the temperature coefficient of  $\eta_T$  is negative for  $U^{235}$  and  $Pu^{239}$  and positive for  $U^{233}$ . At  $T_n = 373^\circ K$  ( $100^\circ C$ ),  $\alpha_T(\eta_T)$  is about  $-3 \times 10^{-5}/^\circ C$  for  $U^{235}$ ,  $-5 \times 10^{-4}/^\circ C$  for  $Pu^{239}$ , and  $+4 \times 10^{-5}/^\circ C$  for  $U^{233}$ .

If, as in solid-fueled reactors, the fuel elements consist of a mixture of fissile and nonfissile isotopes,  $\eta_T$  is given by (cf. Eq. 11-1)

$$\eta_T = \frac{\sum \nu_n \bar{\Sigma}_{fn}}{\bar{\Sigma}_a}, \quad (13-16)$$

where  $\nu_n$  and  $\bar{\Sigma}_{fn}$  refer to the  $n$ th fissile isotope and  $\bar{\Sigma}_a$  includes all nuclides in the fuel element. The temperature coefficient of  $\eta_T$  in this case is best found by computing  $\eta_T$  from Eq. (13-16) for several temperatures using non- $1/v$  factors from Table 8-1 and differencing the results. In the important case of natural uranium,  $\eta_T$  is found to be essentially constant up to about  $T_n = 575^\circ K$  ( $\sim 300^\circ C$ ) where it begins to decrease, giving a negative temperature coefficient above this temperature of about  $-10^{-4}/^\circ C$ .

The foregoing method for finding  $\alpha_T(\eta_T)$  is based, of course, on the Westcott formalism (cf. Section 8-2) for computing average thermal cross sections. In that formalism, it will be recalled, the thermal spectrum is assumed to be Maxwellian (a  $1/E$  tail is also added to the Maxwellian in the general case). If there is reason to believe that the spectrum of the thermal neutrons deviates substantially from a Maxwellian (plus a  $1/E$  tail), a detailed thermalization calculation should be carried out to determine the actual spectrum. Calculations of this type are especially necessary for heterogeneous reactors, as the thermal spectrum in solid fuel elements may be far from Maxwellian and may also vary with position within the fuel.

**Temperature coefficient of  $f$ .** The thermal utilization of a homogeneous reactor is given by the formula

$$f = \frac{\bar{\Sigma}_{aF}}{\bar{\Sigma}_{aF} + \bar{\Sigma}_{aM}}, \quad (13-17)$$

where  $\bar{\Sigma}_{aF}$  and  $\bar{\Sigma}_{aM}$  are the average thermal absorption cross sections of the fuel and moderator, respectively. Differentiating  $f$  with respect to the temperature of the fuel-moderator mixture gives

$$\frac{1}{f} \frac{df}{dT} = \frac{\bar{\Sigma}_{aM}}{\bar{\Sigma}_{aF} + \bar{\Sigma}_{aM}} \left[ \frac{1}{\bar{\Sigma}_{aF}} \frac{d\bar{\Sigma}_{aF}}{dT} - \frac{1}{\bar{\Sigma}_{aM}} \frac{d\bar{\Sigma}_{aM}}{dT} \right], \quad (13-18)$$

so that

$$\alpha_T(f) = (1 - f)[\alpha_T(\bar{\Sigma}_{aF}) - \alpha_T(\bar{\Sigma}_{aM})]. \quad (13-19)$$

The first term in Eq. (13-19) is

$$\begin{aligned} \alpha_T(\bar{\Sigma}_{aF}) &= \frac{1}{N_F \bar{\sigma}_{aF}} \frac{d(N_F \bar{\sigma}_{aF})}{dT} \\ &= \frac{1}{N_F} \frac{dN_F}{dT} + \frac{1}{\bar{\sigma}_{aF}} \frac{d\bar{\sigma}_{aF}}{dT} \\ &= \alpha_T(N_F) + \alpha_T(\bar{\sigma}_{aF}). \end{aligned} \quad (13-20)$$

The atom density of the fuel is directly proportional to the physical density of the mixture, and hence it is inversely proportional to its specific volume ( $\text{cm}^3/\text{gram}$ ). Thus

$$N_F \sim \frac{1}{v}, \quad (13-21)$$

where  $v$  is the specific volume of the mixture. Differentiating  $\ln N_F \sim -\ln v$  gives

$$\alpha_T(N_F) = -\frac{1}{v} \frac{dv}{dT} = -\beta, \quad (13-22)$$

where  $\beta$  is the coefficient of volume expansion of the mixture at constant pressure. Equation (13-22) reflects the obvious fact that as the temperature rises and the mixture expands, the atom density is reduced. Table 13-1 gives values of  $\beta$  for a number of solids at about  $20^\circ\text{C}$  ( $\beta$  depends on temperature), and Fig. 13-2 shows  $\beta$  for  $\text{H}_2\text{O}$  and  $\text{D}_2\text{O}$  as a function of temperature.

**Table 13-1**  
Coefficients of Volume Expansion near  $20^\circ\text{C}^*$

Material	$\beta \times 10^5/\text{ }^\circ\text{C}$	Material	$\beta \times 10^5/\text{ }^\circ\text{C}$
Aluminum	7.1	Thorium	3.3
Beryllium	3.5	Uranium	4.5
Graphite	0.6-1.5	$\text{UO}_2$	$\sim 1.5$
Stainless steel (type 347)	5.0	Zirconium	1.5

\* Based in part on *The Reactor Handbook*, Volume 3, Materials, U.S. Atomic Energy Commission Report No. AECD-3647, Appendix A.1 (1955).

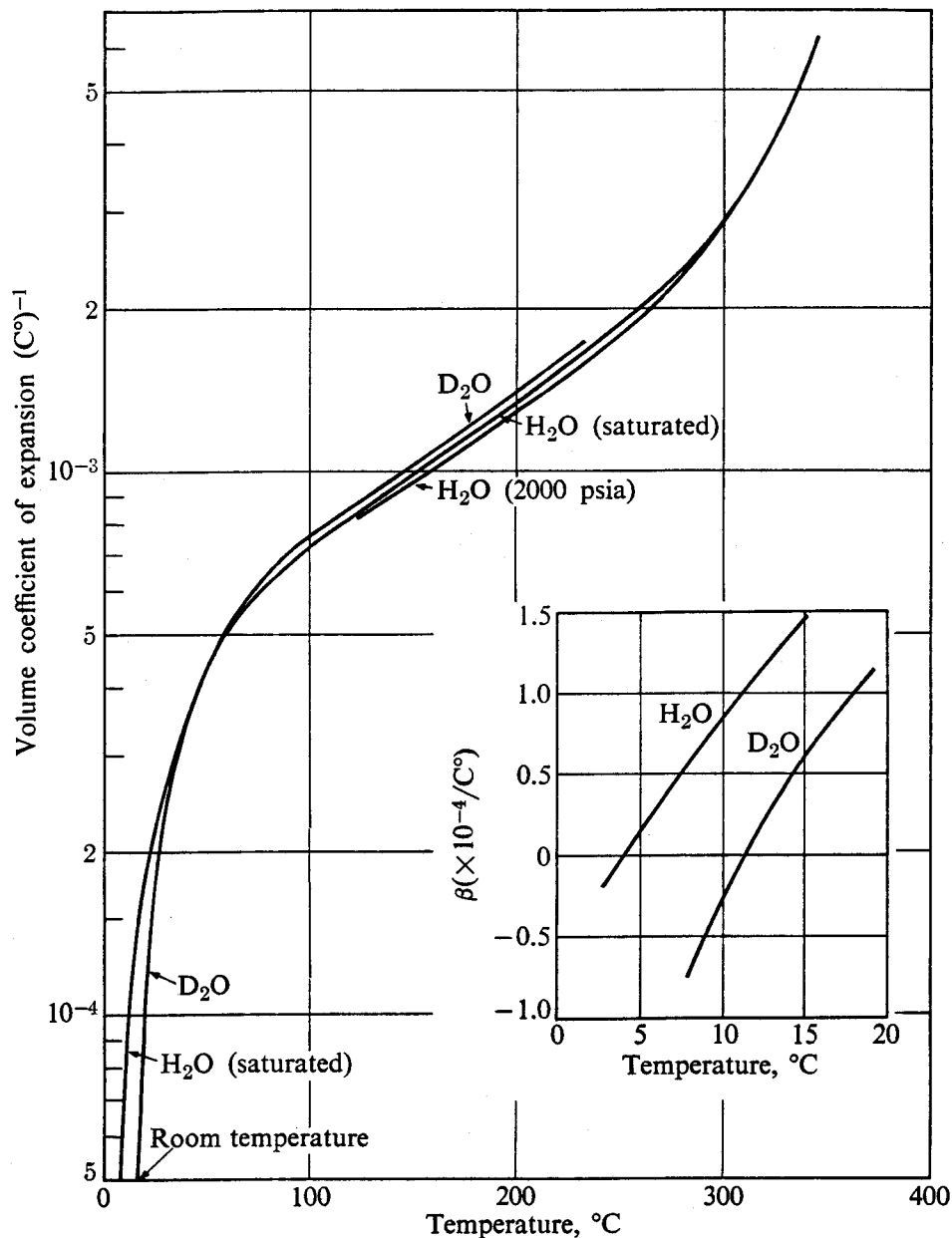


Fig. 13-2. Volume coefficients of expansion of water and heavy water. (From J. A. Larrimore, "Temperature Coefficients of Reactivity in Homogenized Thermal Nuclear Reactors," Ph.D. Thesis, M.I.T., September 1962).

In Section 8-2 it was shown that the average thermal absorption cross section depends upon the neutron temperature  $T_n$  as

$$\bar{\sigma}_a \sim \frac{g_a(T_n)}{\sqrt{T_n}}, \quad (13-23)$$

where  $g_a(T_n)$  is the non-1/ $v$  factor. The second term in Eq. (13-20) thus becomes

$$\alpha_T(\bar{\sigma}_{aF}) = a\alpha_{T_n}(g_{aF}) - 1/2T, \quad (13-24)$$

where  $\alpha_{T_n}(g_{aF})$  is the temperature coefficient of  $g_{aF}$  with respect to the neutron temperature, and use has been made of Eq. (13-4).

In view of Eqs. (13-22) and (13-24), the temperature coefficient of  $\bar{\Sigma}_{aF}$  is

$$\alpha_T(\bar{\Sigma}_{aF}) = -\beta + a\alpha_{T_n}(g_{aF}) - \frac{1}{2T}. \quad (13-25)$$

A similar expression holds for  $\alpha_T(\bar{\Sigma}_{aM})$ . Substituting these results into Eq. (13-19), the temperature coefficient of  $f$  reduces to

$$\alpha_T(f) = a(1 - f)[\alpha_{T_n}(g_{aF}) - \alpha_{T_n}(g_{aM})]. \quad (13-26)$$

Thus for a homogeneous reactor,  $\alpha_T(f)$  is only a function of the temperature coefficients of the non- $1/v$  factors of the fuel and moderator. In all cases, however, absorption cross sections of moderators are  $1/v^*$  and Eq. (13-26) becomes simply

$$\alpha_T(f) = a(1 - f)\alpha_{T_n}(g_{aF}). \quad (13-27)$$

The parameter  $a$  in Eq. (13-27) is of the order of unity, while the factor  $(1 - f)$  varies from about 0.1 to 0.3. Furthermore, the temperature coefficient of  $g_{aF}$  is generally quite small (with the exception of  $Pu^{239}$ ); representative values are given in Table 13-2 for several nuclei at  $775^\circ K$  ( $\sim 500^\circ C$ ). Hence except for  $Pu^{239}$ -fueled reactors, the temperature coefficient of  $f$  for a homogeneous system is of the order of  $10^{-6}/^\circ C$  and it can be neglected in comparison with other temperature coefficients.

If a reactor is quasihomogeneous, that is, if the fuel is contained in thin fuel elements,  $f$  is given by (cf. Section 9-9)

$$f = \frac{\bar{\Sigma}_{aF}V_F}{\bar{\Sigma}_{aF}V_F + \bar{\Sigma}_{aM}V_M + \bar{\Sigma}_{aS}V_S}, \quad (13-28)$$

where  $\bar{\Sigma}_{aF}$ ,  $\bar{\Sigma}_{aM}$ , and  $\bar{\Sigma}_{aS}$  are the average thermal absorption cross sections of the fuel, moderator, and structure, respectively, and  $V_F$ ,  $V_M$ , and  $V_S$  are the volumes of

**Table 13-2**  
Temperature Coefficient of Non- $1/v$  Absorption Factors at  $T_n = 775^\circ K$  ( $\sim 500^\circ C$ )

Isotope	$\alpha_{T_n}(g_{aF})/^\circ C$
$U^{233}$	$+3.1 \times 10^{-5}$
$U^{235}$	$-3.5 \times 10^{-5}$
$U^{238}$	$+1.8 \times 10^{-5}$
$Pu^{239}$	$+1.4 \times 10^{-3}$

\* The presence of fission product poisons in the moderator is ignored in this treatment.

these materials. Since the fuel is dispersed in the structure,  $V_F \approx V_S$ . Differentiating  $\ln f$  in the usual way gives

$$\alpha_T(f) = (1 - f)\alpha_T(\bar{\Sigma}_{aF}V_F) - f_M\alpha_T(\bar{\Sigma}_{aM}V_M) - f_S\alpha_T(\bar{\Sigma}_{aS}V_S), \quad (13-29)$$

where

$$f_M = \frac{\bar{\Sigma}_{aM}V_M}{\bar{\Sigma}_{aF}V_F + \bar{\Sigma}_{aM}V_M + \bar{\Sigma}_{aS}V_S} \quad (13-30)$$

and

$$f_S = \frac{\bar{\Sigma}_{aS}V_S}{\bar{\Sigma}_{aF}V_F + \bar{\Sigma}_{aM}V_M + \bar{\Sigma}_{aS}V_S}. \quad (13-31)$$

Equation (13-29) can also be written as

$$\begin{aligned} \alpha_T(f) &= (1 - f)\alpha_T(\bar{\sigma}_{aF}) - f_M\alpha_T(\bar{\sigma}_{aM}) - f_S\alpha_T(\bar{\sigma}_{aS}) \\ &\quad + (1 - f)\alpha_T(N_FV_F) - f_M\alpha_T(N_MV_M) - f_S\alpha_T(N_SV_S). \end{aligned} \quad (13-32)$$

In Eq. (13-32)  $N_FV_F$ ,  $N_MV_M$ , and  $N_SV_S$  are the total numbers of fuel, moderator, and structure atoms in the reactor. The fuel and structure are both solids, of course, so that  $N_FV_F$  and  $N_SV_S$  do not change as the temperature of the reactor is changed. If, in addition, the moderator is a solid,  $N_MV_M$  is also constant and the last three terms of Eq. (13-32) are zero. Furthermore, as already noted, the temperature coefficients of  $\bar{\sigma}_{aF}$  (with the exception of  $Pu^{239}$ ),  $\bar{\sigma}_{aM}$  and  $\bar{\sigma}_{aS}$  are negligible, and it follows that again  $\alpha_T(f) \approx 0$ .

The situation is somewhat more complicated when the moderator (or coolant) is a liquid. As may be seen by comparing Table 13-1 and Fig. 13-2, the coefficients of expansion of liquids are much larger than those of solids. Consequently, as the temperature of a reactor is raised, the moderator expands more rapidly than the solid parts of the system, and, assuming that the pressure does not change, some of the moderator is expelled from the reactor. The volume occupied by the moderator in the reactor may be taken to be constant, since this is determined by structural parts of the reactor, all of which are metallic. Then noting that  $N_FV_F$  and  $N_SV_S$  are constant, Eq. (13-32) reduces to

$$\begin{aligned} \alpha_T(f) &= -f_M\alpha_T(N_M) \\ &= f_M\beta_M, \end{aligned} \quad (13-33)$$

where  $\beta_M$  is the coefficient of expansion of the moderator.

It will be observed from Eq. (13-33) that  $\alpha_T(f)$  is *positive* for a liquid-moderated (cooled) reactor. Physically, this is due to the fact that with some of the moderator expelled from the reactor, the relative concentration of the fuel in the system is higher, and the probability that a thermal neutron is absorbed in fuel is also higher.

For a heterogeneous reactor the thermal utilization is given by (cf. Eq. 11-7)

$$f = \frac{\bar{\Sigma}_{aF}V_F}{\bar{\Sigma}_{aF}V_F + \bar{\Sigma}_{aM}V_M}, \quad (13-34)$$

where  $\xi$  is the disadvantage factor. By differentiating  $f$  and taking note of the above results for homogeneous and quasihomogeneous reactors, it is easy to show that

$$\alpha_T(f) = - (1 - f)\alpha_T(\xi) \quad (13-35)$$

for solid-moderated reactors, and

$$\alpha_T(f) = - (1 - f)[\alpha_T(\xi) - \beta_M] \quad (13-36)$$

for liquid-moderated reactors.

In the diffusion approximation,  $\xi$  is determined by the lattice functions  $F$  and  $E$ , and these functions, in turn, depend upon the thermal diffusion length of the fuel and moderator. In the method of Amouyal, Benoist, and Horowitz,  $\xi$  is related to the  $E$  function and to the escape probability of the fuel, the latter being a function of the thermal cross sections of the fuel. The temperature coefficient of  $\xi$  can be estimated by differentiating these various functions with respect to temperature. These computations are rather complicated, however, and will not be derived here; a special case is given in Prob. 13-3. In any event, it turns out that  $\alpha_T(\xi)$  is *always negative*, and from Eqs. (13-35) and (13-36) it follows that the temperature coefficient of  $f$  is positive. The reason for this may be seen most clearly in the diffusion approximation. It will be shown later in this section that the thermal diffusion length increases with temperature. As the diffusion length increases, the flux in the unit cell tends to flatten, that is, the depression of the flux across the cell becomes less pronounced, and this leads to a smaller value of  $\xi$ . Thus  $\xi$  decreases with increasing temperature, and  $\alpha_T(\xi)$  is negative.

It should be mentioned that the above procedure for computing  $\alpha_T(f)$  for a heterogeneous reactor may be substantially in error, due to the fact that it does not take into account the actual spectrum of the thermal neutrons throughout the unit cell and the way this spectrum changes with temperature. Accurate methods have been developed to handle this problem, but they lie beyond the scope of this book.

**Temperature coefficient of  $p$ .** The resonance escape probability in a homogeneous reactor depends on temperature by virtue of the Doppler effect. It was shown in Chapter 7 that because of this effect resonance absorption increases with increasing temperature. This, in turn, tends to give the resonance escape probability a negative temperature coefficient. With homogeneous and quasi-homogeneous reactors, however, the fuel concentration is usually so low that this effect is ordinarily negligible, and  $\alpha_T(p) \approx 0$ . It is only necessary therefore to consider heterogeneous reactors.

From Eq. (11-58) the resonance escape probability for a heterogeneous reactor is given by

$$p = \exp \left[ - \frac{N_F V_F I}{\xi_F \sum_p V_F + \xi_M \sum_M V_M} \right], \quad (13-37)$$

where  $I$  is the resonance integral. The *prompt temperature coefficient* of  $p$  can be calculated by assuming that the temperature of the moderator remains constant while the temperature of the fuel changes in response to a change in the power level of the reactor. In this case, the temperature dependence of the right-hand side of Eq. (13-37) is entirely due to the factor  $I$ . The product  $N_F V_F$ , in particular, is constant since this is the total number of fuel atoms in the fuel rods. Differentiating  $\ln p$  gives

$$\alpha_{\text{prompt}}(p) = - \frac{N_F V_F}{\xi_F \sum_p V_F + \xi_M \sum_s V_M} \frac{dI}{dT} = -\alpha_T(I) \ln\left(\frac{1}{p}\right). \quad (13-38)$$

Thus the prompt temperature coefficient is primarily a function of the temperature coefficient of the resonance integral.

The value of  $\alpha_T(I)$  can be found by measuring  $I$  at several temperatures or by calculating  $I$  as a function of temperature using one of the techniques described in Section 11-3. Both theory and experiment show that for  $\text{U}^{238}$  and  $\text{Th}^{232}$  and their oxides and in the temperature range from about  $300^\circ\text{K}$  to  $1500^\circ\text{K}$ ,  $I$  can be represented by the formula

$$I(T) = I(300^\circ) [1 + \beta_I (\sqrt{T} - \sqrt{300})], \quad (13-39)$$

where  $T$  is the temperature in degrees Kelvin. Except for very small fuel rods the parameter  $\beta_I$  has been found to be *approximately* linear in the surface to mass ratio of the fuel (cf. Section 11-3), that is,

$$\beta_I = c + d \left( \frac{S_F}{M_F} \right). \quad (13-40)$$

The constants  $c$  and  $d$  are given in Table 13-3. From Eq. (13-39) the temperature coefficient of  $I$  is

$$\alpha_T(I) = \frac{1}{I} \frac{dI}{dT} = \frac{I(300^\circ)}{I(T)} \frac{\beta_I}{2\sqrt{T}}, \quad (13-41)$$

which is always positive. Inserting Eq. (13-41) into Eq. (13-38) gives

$$\alpha_{\text{prompt}}(p) = - \frac{I(300^\circ)}{I(T)} \frac{\beta_I}{2\sqrt{T}} \ln\left(\frac{1}{p}\right). \quad (13-42)$$

By substituting  $dI/dT$  directly into the first line of Eq. (13-38) the following somewhat preferable formula is obtained for  $\alpha_{\text{prompt}}(p)$ :

$$\alpha_{\text{prompt}}(p) = - \frac{\beta_I}{2\sqrt{T}} \ln\left[\frac{1}{p(300^\circ)}\right], \quad (13-43)$$

where  $p(300^\circ)$  is the value of  $p$  at  $300^\circ\text{K}$ .

The ultimate behavior of the resonance escape probability, after the moderator has had an opportunity to heat up, depends upon whether the moderator is a

**Table 13-3**  
**The Constants  $c$  and  $d$  in the Formula for  $\beta_I$**

Fuel	$c \times 10^4$	$d \times 10^4$
$U^{238}$ (metal)*	48	64
$U^{238}O_2^*$	61	47
Th†	85	134
$ThO_2$ †	97	120

\* From W. G. Pettus and M. N. Baldwin, "Resonance Absorption in  $U^{238}$  Metal and Oxide Rods." Babcock and Wilcox Company Report No. BAW-1244, April 1962.

† Based on values of  $I$  computed by L. W. Nordheim, "A New Calculation of Resonance Integrals." *Nuclear Sci. and Eng.* 12, 457 (1962).

solid or a liquid. With a solid-moderated system the total number of fuel atoms and moderator atoms in the reactor is independent of temperature, so that the quantity

$$\frac{N_F V_F}{\xi_F \Sigma_{pF} V_F + \xi_M \Sigma_{sM} V_M}$$

in Eq. (13-37) is constant. In this case the "ultimate" (uniform) temperature coefficient of  $p$  is equal to its prompt temperature coefficient and is given by Eq. (13-42) or Eq. (13-43).

With a liquid-moderated reactor, an increase in temperature of both moderator and fuel leads to a net expulsion of some of the moderator from the reactor. The calculation of this effect is greatly simplified by noting that in most practical problems the first term in the denominator of Eq. (13-37) is negligible compared to the second term, that is,  $\xi_F \Sigma_{pF} V_F \ll \xi_M \Sigma_{sM} V_M$ , so that

$$p \approx \exp \left[ - \frac{N_F V_F I}{\xi_M \Sigma_{sM} V_M} \right]. \quad (13-44)$$

Since a liquid moderator is ordinarily held in a metal tank of some sort, it may reasonably be assumed that the ratio  $V_F/V_M$  remains constant during the change in temperature. The atom densities of fuel and moderator then change because of their differing coefficients of expansion. Using Eq. (13-44), the temperature coefficient of  $p$  can then be written as

$$\begin{aligned}
 \alpha_T(p) &= - \frac{V_F I}{\xi_M \sigma_{sM} V_M} \frac{d}{dT} \left( \frac{N_F}{N_M} \right) - \frac{N_F V_F}{\xi_M \Sigma_{sM} V_M} \frac{dI}{dT} \\
 &= - [\alpha_T(N_F) - \alpha_T(N_M) + \alpha_T(I)] \ln \left( \frac{1}{p} \right) \\
 &= - [-\beta_F + \beta_M + \alpha_T(I)] \ln \left( \frac{1}{p} \right),
 \end{aligned} \quad (13-45)$$

where  $\beta_F$  and  $\beta_M$  are the coefficients of expansion of the fuel and moderator. As already noted,  $\beta_F \ll \beta_M$ , so that Eq. (13-45) reduces to

$$\alpha_T(p) = - [\beta_M + \alpha_T(I)] \ln \left( \frac{1}{p} \right). \quad (13-46)$$

Equation (13-46) shows that the expansion and expulsion of moderator from the reactor contributes to the negative temperature coefficient of  $p$  for a liquid-moderated reactor. This is because the expulsion of moderator reduces the ratio of moderator atoms to fuel atoms, which is equivalent to increasing the concentration of fuel in the system. As discussed in Chapter 7,  $p$  decreases with increasing fuel concentration.

It is interesting to see how Eq. (13-46) applies to a water-moderated reactor. From Fig. 13-2,  $\beta_M \approx 2 \times 10^{-4}/^\circ\text{C}$  at room temperature, while at about  $250^\circ\text{C}$  (a reasonable operating temperature for a water reactor)  $\beta_M \approx 2 \times 10^{-3}/^\circ\text{C}$ . On the other hand, using Table 13-3 and Eq. (13-41),  $\alpha_T(I)$  is seen to be of the order of  $10^{-4}/^\circ\text{C}$  for all fuels and does not vary much with temperature. In view of Eq. (13-46), it may be concluded that while Doppler broadening makes a substantial contribution to  $\alpha_T(p)$  at room temperature, it has a small effect at operating temperatures. Doppler broadening is still responsible, of course, for the *prompt* temperature coefficient at all temperatures.

As shown above, the resonance absorption of neutrons increases with increasing temperature. In a thermal reactor this absorption occurs for the most part in nonfissile nuclei such as  $\text{U}^{238}$  or  $\text{Th}^{232}$ . There is also some additional absorption of neutrons in the resonances of whatever fissile nuclei are present in the system, and as a result there is an increase in the fission rate; but this effect is usually negligible in thermal reactors where the vast majority of fissions take place at thermal energies. With a fast reactor, however, virtually all of the fissions occur following the absorption of neutrons in resonances (most of them overlapping, so that the observed fission cross section appears smooth) of fissile nuclei, and an increase in the temperature of the fuel necessarily leads to a prompt increase in the fission rate, unless there are sufficient nonfissile absorbers present to offset this effect. In a system such as the Fermi Fast Reactor (cf. Section 4-4), for example, which is fueled with a mixture of  $\text{U}^{235}$  and  $\text{U}^{238}$ , it has been shown that the atom ratio  $N^{28}/N^{25}$  must be greater than about 3 in order to assure that the prompt temperature coefficient of the fuel is negative. Fortunately, this does not place a serious restriction on the design of this type of reactor, since at least this much  $\text{U}^{238}$  would normally be included in the system in order to enhance the breeding gain.

**Temperature coefficient of  $\epsilon$ .** The fast fission factor is independent of temperature in a homogeneous reactor, and  $\alpha_T(\epsilon) = 0$  for this type of system. With a heterogeneous reactor  $\epsilon$  may change slightly with temperature for two reasons. First, the thermal expansion of the fuel lumps leads to a decrease in the parameter  $\bar{\Sigma}_{tF}$  which determines the escape probabilities of the fast neutrons from

the fuel (cf. Section 11-4), and, as a consequence, these probabilities increase somewhat. At the same time, an increase in temperature tends to flatten the thermal flux in the fuel for the reasons given earlier in this section. The resulting change in the spatial distribution of the primary fissions can be shown to decrease the escape probability of the primary fission neutrons from the fuel. These are both minor effects, however, and the temperature coefficient of  $\epsilon$  is usually small compared with other reactor temperature coefficients.\* The value of  $\alpha_T(\epsilon)$  therefore will not be considered further here.

**Temperature coefficient of  $L_T^2$ .** By definition,  $L_T^2$  is given by (cf. Section 8-5)

$$L_T^2 = \frac{\bar{D}}{\Sigma_a}, \quad (13-47)$$

so that

$$\alpha_T(L_T^2) = \alpha_T(\bar{D}) - \alpha_T(\Sigma_a). \quad (13-48)$$

With a homogeneous reactor, according to Eq. (8-78),

$$\bar{D} = \Gamma(m + 2)D(E_0)\left(\frac{T_n}{T_{n0}}\right)^m, \quad (13-49)$$

where  $m$  is a constant,  $D(E_0)$  is the diffusion coefficient at 0.025 eV,  $T_n$  is the neutron temperature in degrees Kelvin and

$$T_{n0} = 293.61^\circ\text{K}.$$

Differentiating  $\ln \bar{D}$  and noting that  $D(E_0)$  varies inversely with atom density, the temperature coefficient of  $\bar{D}$  is easily found to be

$$\alpha_T(\bar{D}) = \beta + \frac{m}{T}, \quad (13-50)$$

where  $\beta$  is the coefficient of expansion of the fuel-moderator mixture and  $T$  is the temperature of the medium.

For a homogeneous reactor,  $\Sigma_a$  is

$$\bar{\Sigma}_a = \bar{\Sigma}_{aF} + \bar{\Sigma}_{aM}. \quad (13-51)$$

Assuming that only the fuel is non- $1/v$  and using Eq. (13-25),  $\alpha_T(\bar{\Sigma}_a)$  is

$$\alpha_T(\bar{\Sigma}_a) = -\beta + fa\alpha_{T_n}(g_{aF}) - \frac{1}{2T}. \quad (13-52)$$

Here,  $f$  is the thermal utilization and  $g_{aF}$  is the non- $1/v$  factor for the fuel. If the moderator is non- $1/v$  or contains non- $1/v$  absorbers, the term  $(1 - f) \times a\alpha_{T_n}(g_{aM})$  must be added to Eq. (13-52).

---

\* The temperature coefficient of  $\epsilon$  may not be negligible, however, in closely packed lattices of interacting rods.

Upon introducing Eqs. (13-50) and (13-52) into Eq. (13-48), the temperature coefficient of  $L_T^2$  for a homogeneous reactor becomes

$$\alpha_T(L_T^2) = 2\beta + \frac{m + 1/2}{T} - f\alpha_{T_n}(g_{aF}). \quad (13-53)$$

The last term in this equation is usually small compared to the other terms, and  $\alpha_T(L_T^2)$  is generally positive.

The calculation of  $\alpha_T(L_T^2)$  for a quasihomogeneous reactor is straightforward in principle, but complicated in detail. From the discussion in Section 9-9,  $\bar{D}$ , or rather  $1/\bar{D}$ , can be written as

$$\frac{1}{\bar{D}} = \frac{1}{\bar{D}_S} \frac{V_S}{V} + \frac{1}{\bar{D}_M} \frac{V_M}{V}, \quad (13-54)$$

where  $\bar{D}_S$  and  $\bar{D}_M$  are the diffusion coefficients for the structure (fuel-elements) and moderator, respectively;  $V_S$  and  $V_M$  are the volumes of these materials; and

$$V = V_S + V_M.$$

The temperature coefficient of  $\bar{D}$  is then

$$\alpha_T(\bar{D}) = \frac{\bar{D}V_S}{\bar{D}_S V} \alpha_T(\bar{D}_S) + \frac{\bar{D}V_M}{\bar{D}_M V} \alpha_T(\bar{D}_M). \quad (13-55)$$

Similarly,

$$\bar{\Sigma}_a = \bar{\Sigma}_{aF} \frac{V_S}{V} + \bar{\Sigma}_{aM} \frac{V_M}{V} + \bar{\Sigma}_{aS} \frac{V_S}{V} \quad (13-56)$$

and

$$\alpha_T(\bar{\Sigma}_a) = \frac{\bar{\Sigma}_{aF}}{\bar{\Sigma}_a} \frac{V_S}{V} \alpha_T(\bar{\Sigma}_{aF}) + \frac{\bar{\Sigma}_{aM}}{\bar{\Sigma}_a} \frac{V_M}{V} \alpha_T(\bar{\Sigma}_{aM}) + \frac{\bar{\Sigma}_{aS}}{\bar{\Sigma}_a} \frac{V_S}{V} \alpha_T(\bar{\Sigma}_{aS}). \quad (13-57)$$

In the derivation of Eq. (13-55) and (13-57) the ratios  $V_S/V$  and  $V_M/V$  were taken to be constant. Changes in  $\bar{D}$  or  $\bar{\Sigma}_a$  due to the expansion and expulsion of a liquid moderator are included in  $\alpha_T(\bar{D}_M)$  and  $\alpha_T(\bar{\Sigma}_{aM})$ . The temperature coefficient of  $L_T^2$  is now obtained by inserting Eqs. (13-55) and (13-57) into Eq. (13-48). Each temperature coefficient in the resulting expression can then be evaluated using the formulas for the homogeneous case.

With a heterogeneous reactor, and, for simplicity, one whose fuel volume is small compared with the moderator volume,  $L_T^2$  is (cf. Eq. 11-103)

$$L_T^2 = (1 - f)L_{TM}^2, \quad (13-58)$$

where  $L_{TM}$  is the diffusion length of the moderator. It follows from Eq. (13-58) that

$$\begin{aligned} \alpha_T(L_T^2) &= \alpha_T(1 - f) + \alpha_T(L_{TM}^2) \\ &= -\frac{f}{1-f} \alpha_T(f) + \alpha_T(L_{TM}^2). \end{aligned} \quad (13-59)$$

In the usual case, the first term in Eq. (13-59) is small compared to the second, and

$$\alpha_T(L_T^2) \approx \alpha_T(L_{TM}^2), \quad (13-60)$$

where  $\alpha_T(L_{TM}^2)$  (which is positive) is given by Eq. (13-53).

The significance of a positive temperature coefficient of  $L_T^2$  will be discussed later in this section.

**Temperature coefficient of  $\tau_T$ .** A change in temperature affects the age of fission neutrons in two ways. First, it changes the density of the medium, and second, it changes the energy range over which the neutrons slow down. The latter effect is usually negligible compared to the former, however, and only density effects ordinarily need to be considered. If the reactor consists of a homogeneous mixture of fuel and moderator, the age is inversely proportional to the square of the atom density of the moderator, that is,

$$\tau_T \sim \frac{1}{N_M^2}. \quad (13-61)$$

This conclusion can be seen directly from the Fermi age formula (cf. Eq. 6-73), but it is also true whether age theory is valid or not. From Eq. (13-61) it follows that

$$\alpha_T(\tau_T) = -2\alpha_T(N_M) = 2\beta, \quad (13-62)$$

where use has been made of Eq. (13-22).

With quasihomogeneous or heterogeneous reactors, it will be recalled that  $\tau_T$  must be found from elaborate calculations, some results of which were shown in Fig. 6-14 for mixtures of various metals and water. These results can be used directly to give  $\alpha_T(\tau_T)$  for such systems. Thus in the case of metal-water mixtures, a change in temperature has the effect of reducing the atom density of the water relative to that of the fuel, which is equivalent to increasing the metal-to-water-volume ratio, and, at the same time, reducing the atom density of the equivalent homogeneous mixture. In particular, a change in temperature of  $\Delta T$  gives a change in the metal-to-water ratio of approximately

$$\Delta \left( \frac{V_F}{V_M} \right) = (\beta_M - \beta_F) \Delta T. \quad (13-63)$$

The change in age corresponding to this change in  $V_F/V_M$  can be read from the appropriate curve in Fig. 6-14. This must be multiplied by the square of the increase in the atom density of the medium, namely,

$$\left[ 1 + \frac{V_F}{V_M} \Delta \left( \frac{V_F}{V_M} \right) \right]^2 \approx 1 + 2 \left( \frac{V_F}{V_M} \right) \beta_M \Delta T.$$

The resulting value of  $\Delta\tau_T$  can be used to calculate  $\alpha_T(\tau_T)$  from the formula

$$\alpha_T(\tau_T) \approx \frac{1}{\tau_T} \frac{\Delta\tau_T}{\Delta T}. \quad (13-64)$$

The appropriate  $\Delta T$  to be used in these computations can be found by trial and error. It will be obvious on intuitive grounds that  $\alpha_T(\tau_T)$  is always positive.

**Temperature coefficient of  $B^2$ .** If the reactor is fixed in size so that it cannot expand and contract with temperature changes, the temperature coefficient of the buckling is zero. In the following, it will be assumed that the size of the reactor is *not* constrained in any way.

The buckling of any bare reactor is proportional to the sum of one or more terms of the form

$$B^2 \sim \frac{1}{x^2}, \quad (13-65)$$

where  $x$  is one of the linear dimensions of the reactor. The temperature coefficient of  $B^2$  is thus given by

$$\alpha_T(B^2) = -2\alpha_T(x), \quad (13-66)$$

where  $\alpha_T(x)$  is the ordinary coefficient of *linear* expansion of the system. It can easily be verified that the coefficient of volume expansion  $\beta$  is related to  $\alpha_T(x)$  by the formula  $\beta = 3\alpha_T(x)$ , so that Eq. (13-66) can also be written as

$$\alpha_T(B^2) = -\frac{2}{3}\beta. \quad (13-67)$$

The parameter  $\beta$  is positive, and it follows from Eq. (13-67) that  $\alpha_T(B^2)$  is always negative. Thus  $B^2$  decreases with increasing temperature as would be expected physically, since the dimensions of the system increase with temperature. This means that the leakage of neutrons from the reactor *decreases* as the temperature rises, which, in turn, tends to give a reactor a positive temperature coefficient. However, reactors are either solid throughout or are contained in solid vessels of some sort, and as already noted  $\beta$  is very small for all solids. It is generally possible, therefore, to neglect the effect of changes in buckling on the overall temperature coefficient of a reactor.

**Temperature coefficients of  $P_T$  and  $P_F$ .** As shown in the preceding discussion, the temperature coefficients of  $L_T^2$  and  $\tau_T$  are positive while the temperature coefficient of  $B^2$  is negative. In view of Eqs. (13-13) and (13-14), this means that the temperature coefficients of both the slow and fast nonleakage probabilities are *negative* provided  $|\alpha_T(B^2)| < |\alpha_T(L_T^2)|$  and  $|\alpha_T(B^2)| < |\alpha_T(\tau_T)|$ . These inequalities usually hold, for as noted above  $\alpha_T(B^2)$  is small. The fact that positive temperature coefficients of  $L_T^2$  and  $\tau_T$  contribute to the overall stability of a reactor

should come as no surprise. Thus a glance at the formulas for  $P_T$  and  $P_F$  shows that both of these nonescape probabilities decrease as  $L_T^2$  and  $\tau_T$  increase, an observation that should be obvious on physical grounds.

**Temperature coefficients—summary.** The sign and relative magnitude of each of the various temperature coefficients discussed in this section are summarized in Table 13-4 for a nominal thermal heterogeneous reactor. All reactors, of course, do not have the temperature coefficients shown in the table; these values are merely representative. It will be evident from the table that the temperature coefficient of  $p$  is the most important factor contributing to the negative temperature coefficient of  $k_\infty$ . Also, the temperature coefficients of  $P_T$  and  $P_F$  are often small compared with the temperature coefficient of  $p$  and it follows that it is the resonance absorption which provides the overall negative temperature coefficient for the system. In addition, of course, resonance absorption gives a reactor of this type a prompt negative temperature coefficient. If a reactor contains no resonance absorbers the system must be designed with some care, for the temperature coefficient in this case is less negative and may even be positive.\*

Table 13-4  
Temperature Coefficients of a Nominal, Heterogeneous Thermal Reactor

Reactor parameter	Temperature coefficient	Reactor parameter	Temperature coefficient
$\eta_T$	+ or -; small, except for $\text{Pu}^{239}$	$L_T^2$	+
$f$	+; small	$\tau_T$	+
$p$	-; large	$B^2$	-; small
$\epsilon$	+ or -; small	$P_T$	-
$k_\infty$	-	$P_F$	-
		$k$	-

Finally, it must be emphasized that the calculations of temperature coefficients given in this section have been carried out only for the simplest type of systems, namely, bare thermal reactors. Temperature coefficients of other reactors, namely, intermediate or fast reactors and reflected or multiregion reactors, can be determined in either of two ways. One method is to compute the multiplication factor by a multigroup calculation (cf. Section 10-4) in which the group constants have been appropriately modified to account for a change in temperature of one or more components of the reactor. The computed change in the multiplication factor accompanying this temperature change gives the temperature coefficient

\* The presence of resonance absorption does not guarantee, however, that the temperature coefficient of a reactor will be negative.

directly. However, this procedure is not satisfactory for localized, nonuniform changes in temperature; these changes are better handled using perturbation theory which is discussed in Chapter 15.

### 13-2 Fission-Product Poisoning

Two fission fragments are produced in virtually every fission. Some of these nuclei and their progeny have substantial absorption cross sections, and their appearance in a reactor tends to reduce the multiplication factor. For this reason, these nuclei are known as *fission-product poisons*. Since absorption cross sections decrease rapidly with increasing neutron energy, such poisons are of greatest importance in thermal reactors, and the present section is limited to reactors of this type. It will also be necessary, for the moment, to restrict the discussion to the infinite homogeneous reactor.

To a good approximation, the only effect of fission-product poisons on the multiplication factor is on the thermal utilization. Thus the reactivity equivalent of poisons in a previously critical reactor can be written as

$$\rho = \frac{k'_\infty - k_\infty}{k'_\infty} = \frac{f' - f}{f'}, \quad (13-68)$$

where the primed parameters refer to the poisoned reactor. In the absence of poisons,  $f$  is given by

$$f = \frac{\bar{\Sigma}_{aF}}{\bar{\Sigma}_{aF} + \bar{\Sigma}_{aM}}, \quad (13-69)$$

where  $\bar{\Sigma}_{aF}$  and  $\bar{\Sigma}_{aM}$  are the macroscopic thermal absorption cross sections of the fuel and everything else except the fuel, respectively. With poisons present,  $f$  becomes

$$f' = \frac{\bar{\Sigma}_{aF}}{\bar{\Sigma}_{aF} + \bar{\Sigma}_{aM} + \bar{\Sigma}_{aP}}, \quad (13-70)$$

where  $\bar{\Sigma}_{aP}$  is the macroscopic cross section of the poison. From Eq. (13-68) the reactivity due to the poisons is then

$$\rho = \frac{f' - f}{f'} = - \frac{\bar{\Sigma}_{aP}}{\bar{\Sigma}_{aF} + \bar{\Sigma}_{aM}}. \quad (13-71)$$

Equation (13-71) can be put in a more convenient form by writing the multiplication factor of the unpoisoned reactor as

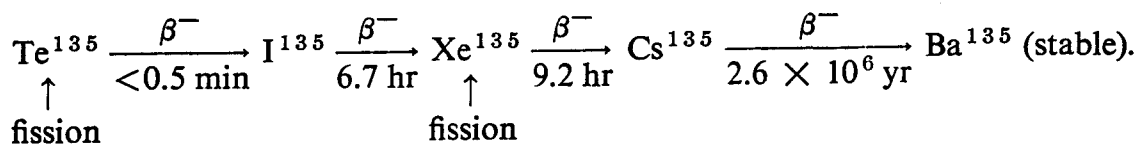
$$\begin{aligned} k_\infty &= 1 = \eta_T f p \epsilon = \frac{\eta_T p \epsilon \bar{\Sigma}_{aF}}{\bar{\Sigma}_{aF} + \bar{\Sigma}_{aM}} \\ &= \frac{\nu p \epsilon \bar{\Sigma}_f}{\bar{\Sigma}_{aF} + \bar{\Sigma}_{aM}}, \end{aligned} \quad (13-72)$$

where  $\bar{\Sigma}_f$  is the macroscopic fission cross section. Solving Eq. (13-72) for  $\bar{\Sigma}_{aF} + \bar{\Sigma}_{aM}$  and inserting this into Eq. (13-71) gives

$$\rho = - \frac{\bar{\Sigma}_{aP}/\bar{\Sigma}_f}{\nu p \epsilon}. \quad (13-73)$$

Equation (13-73) is in a form which is suitable for calculations of fission-product poisoning.

**Xenon-135.** The most important fission product poison is  $Xe^{135}$ , whose thermal (2200 m/sec) absorption cross section is  $2.7 \times 10^6$  barns and non- $1/v$  (the non- $1/v$  factor is given in Table 8-1). This isotope is formed as the result of the decay of  $I^{135}$ , and also is produced directly in the fission of  $U^{235}$ . The  $I^{135}$  is not formed in fission but appears as the result of the decay of  $Te^{135}$  (tellurium-135). These processes and their half-lives are summarized below:



In view of the fact that  $Te^{135}$  decays so rapidly to  $I^{135}$ , it is possible to assume that the  $I^{135}$  is produced directly in fission. The effective yields of  $I^{135}$  and  $Xe^{135}$  for the three fissile nuclei are given in Table 13-5; the decay constants of these isotopes are shown in Table 13-6.

Because the xenon is produced in part by the decay of the iodine, the xenon concentration at any time depends upon the iodine concentration. This, in turn, is determined by the rate equation

$$\frac{dI}{dt} = \gamma_I \bar{\Sigma}_f \phi_T - \lambda_I I, \quad (13-74)$$

where  $I$  is the number of  $I^{135}$  atoms/cm<sup>3</sup>,  $\gamma_I$  is the effective yield of this isotope, and  $\bar{\Sigma}_f$  is the average thermal fission cross section.

One atom of  $Xe^{135}$  is formed with the decay of each atom of  $I^{135}$  so that the total rate of formation of  $Xe^{135}$  is  $\lambda_I I + \gamma_X \bar{\Sigma}_f \phi_T$ , where  $\gamma_X$  is the fission yield of

Table 13-5  
Fission-Product Poison Yields (Atoms per Fission) from Thermal Fission\*

Isotope	$U^{233}$	$U^{235}$	$Pu^{239}$
$I^{135}$	0.051	0.061	0.055
$Xe^{135}$	—	0.003	—
$Pm^{149}$	0.0066	0.0113	0.019

\* From ANL-5800, 2nd ed., pp. 394 and 399.

**Table 13-6**  
**Decay Constants for Fission Product Poisoning Calculations**

Isotope	$\lambda$ (sec $^{-1}$ )	$\lambda$ (hr $^{-1}$ )
I <sup>135</sup>	$2.87 \times 10^{-5}$	0.1035
Xe <sup>135</sup>	$2.09 \times 10^{-5}$	0.0753
Pm <sup>149</sup>	$3.56 \times 10^{-6}$	0.0128

the xenon. The Xe<sup>135</sup> disappears both as the result of its natural radioactive decay and also because of neutron absorption. The xenon rate equation is therefore

$$\frac{dX}{dt} = \lambda_I I + \gamma_X \bar{\Sigma}_f \phi_T - \lambda_X X - \bar{\sigma}_{aX} \phi_T X, \quad (13-75)$$

where  $X$  is the Xe<sup>135</sup> concentration in atoms/cm<sup>3</sup> and  $\bar{\sigma}_{aX}$  is the average thermal absorption cross section of Xe<sup>135</sup> at the appropriate neutron temperature (cf. Eq. 8-40).

In an operating reactor the quantities  $\bar{\Sigma}_f$  and  $\phi_T$  may be functions of time, and the solutions to Eqs. (13-74) and (13-75) depend upon the nature of these functions. Tables have been prepared from which it is possible to determine the iodine and xenon concentrations under rather broad assumptions regarding the mode of operation of the reactor. These tables are noted in the references. Several special solutions to Eqs. (13-74) and (13-75) will now be considered.

**Equilibrium xenon.** Because the half lives of the I<sup>135</sup> and Xe<sup>135</sup> are so short and the absorption cross section of the xenon is so large, the concentrations of these isotopes, in all reactors except those operating at very low flux, quickly rise to their saturation or equilibrium values,  $I_\infty$  and  $X_\infty$ , provided the flux and macroscopic fission cross section do not change significantly in the interim. These concentrations can be found by placing the time derivatives in Eqs. (13-74) and (13-75) equal to zero. Thus from Eq. (13-74),

$$I_\infty = \frac{\gamma_I \bar{\Sigma}_f \phi_T}{\lambda_I}, \quad (13-76)$$

and from Eq. (13-75),

$$\begin{aligned} X_\infty &= \frac{\lambda_I I_\infty + \gamma_X \bar{\Sigma}_f \phi_T}{\lambda_X + \bar{\sigma}_{aX} \phi_T} \\ &= \frac{(\gamma_I + \gamma_X) \bar{\Sigma}_f \phi_T}{\lambda_X + \bar{\sigma}_{aX} \phi_T}. \end{aligned} \quad (13-77)$$

The macroscopic absorption cross section of the xenon is then

$$\bar{\Sigma}_{aX} = X_\infty \bar{\sigma}_{aX} = \frac{(\gamma_I + \gamma_X) \bar{\Sigma}_f \phi_T \bar{\sigma}_{aX}}{\lambda_X + \bar{\sigma}_{aX} \phi_T}. \quad (13-78)$$

The form of Eq. (13-78) can be improved by dividing the numerator and denominator of the right-hand side by  $\bar{\sigma}_{aX}$ . This gives

$$\bar{\Sigma}_{aX} = \frac{(\gamma_I + \gamma_X)\bar{\Sigma}_f\phi_T}{\phi_X + \phi_T}, \quad (13-79)$$

where  $\phi_X$  is a temperature-dependent parameter having the dimensions of flux:

$$\phi_X = \frac{\lambda_X}{\bar{\sigma}_{aX}} = 0.756 \times 10^{13} \text{ cm}^{-2} \text{ sec}^{-1} \quad (13-80)$$

at  $T = 20^\circ\text{C}$ . From Eq. (13-75) it can be seen that  $\phi_X$  is the thermal flux at which the disappearance rates of  $\text{Xe}^{135}$  by neutron absorption and natural decay are equal.

Upon inserting Eq. (13-79) into Eq. (13-73), the reactivity equivalent of equilibrium xenon is found to be

$$\rho = -\frac{\gamma_I + \gamma_X}{\nu p \epsilon} \frac{\phi_T}{\phi_X + \phi_T}. \quad (13-81)$$

There are now two situations to be considered. First, if  $\phi_T \ll \phi_X$ , Eq. (13-81) reduces to

$$\rho = -\frac{(\gamma_I + \gamma_X)\phi_T}{\nu p \epsilon \phi_X}, \quad (13-82)$$

and it is seen that in this low-flux case,  $-\rho$  increases linearly with  $\phi_T$ . On the other hand, if  $\phi_T \gg \phi_X$ ,  $-\rho$  takes on its maximum value

$$\rho = -\frac{\gamma_I + \gamma_X}{\nu p \epsilon}. \quad (13-83)$$

To get some idea of the magnitude of the equilibrium xenon poisoning effect, suppose that a reactor is fueled with  $\text{U}^{235}$  and contains no resonance absorbers or fissionable material other than  $\text{U}^{235}$ . In this case,  $p = \epsilon = 1$ , and Eq. (13-83) gives

$$\rho = -\frac{\gamma_I + \gamma_X}{\nu} = -\frac{0.064}{2.44} = -2.62\%,$$

or about four dollars and change. This is the maximum reactivity due to equilibrium xenon in a  $\text{U}^{235}$ -fueled reactor. If the reactor contains resonance absorbers, the maximum reactivity will be somewhat higher.

**Xenon after shutdown—reactor deadtime.** Although the fission production of  $\text{Xe}^{135}$  ceases when a reactor is shut down, this isotope continues to be produced as the result of the decay of the  $\text{I}^{135}$  present in the system. The xenon concentration therefore initially increases after shutdown, although it eventually disappears by its own decay.

If the iodine concentration at shutdown is  $I_0$ , its concentration at a time  $t$  later is given by

$$I(t) = I_0 e^{-\lambda_I t}. \quad (13-84)$$

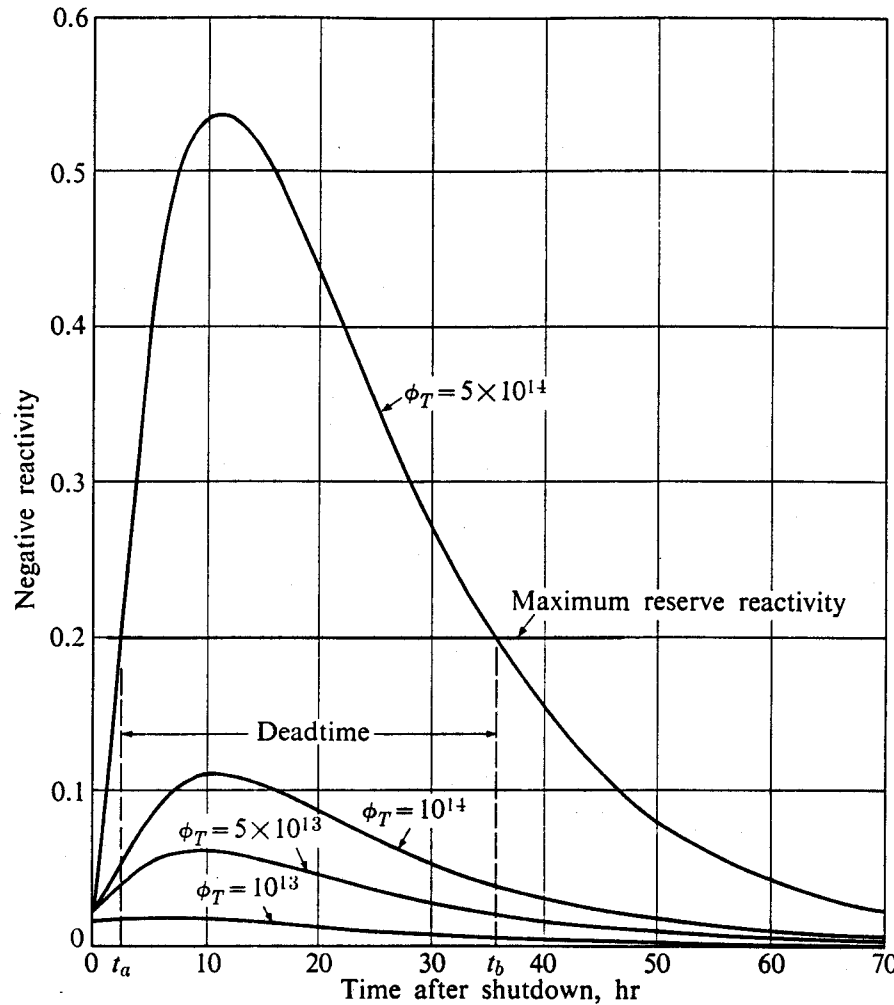


Fig. 13-3. Xenon-135 buildup after shutdown for several values of the operating flux before shutdown.

Inserting this function into Eq. (13-75) and noting that  $\phi_T = 0$  after shutdown, the resulting concentration of  $\text{Xe}^{135}$  is found to be

$$X(t) = X_0 e^{-\lambda_X t} + \frac{\lambda_I I_0}{\lambda_I - \lambda_X} (e^{-\lambda_X t} - e^{-\lambda_I t}). \quad (13-85)$$

Had the xenon and iodine reached equilibrium prior to shutdown,  $I_0$  and  $X_0$  are given by Eqs. (13-76) and (13-77), and the reactivity equivalent of the xenon becomes

$$\rho = -\frac{1}{\nu p \epsilon} \left[ \frac{(\gamma_I + \gamma_X)\phi_T}{\phi_X + \phi_T} e^{-\lambda_X t} + \frac{\gamma_I \phi_T}{\phi_I - \phi_X} (e^{-\lambda_X t} - e^{-\lambda_I t}) \right]. \quad (13-86)$$

Here,  $\phi_I$  is the temperature-dependent parameter

$$\phi_I = \frac{\lambda_I}{\sigma_{aX}} = 1.038 \times 10^{13} \text{ cm}^{-2} \text{ sec}^{-1} \quad (13-87)$$

at  $T = 20^\circ\text{C}$ , and  $\phi_T$  is evaluated, of course, prior to shutdown.

Figure 13-3 shows the (negative) reactivity due to xenon buildup after shutdown in a  $\text{U}^{235}$ -fueled reactor for four values of the flux prior to shutdown. As shown in the figure, the reactivity rises to a maximum, which occurs at about 10 hours after shutdown, and then decreases to zero. It should be particularly noted that the (negative) reactivity rise is greatest in reactors which have been operating at the highest flux before shutdown. This is true simply because the accumulated concentration of  $\text{I}^{135}$  at shutdown is greatest in these reactors.

The post-shutdown buildup of xenon is of little importance in low-flux reactors, but may be troublesome in reactors designed to operate at high flux. In particular, if at any time after the shutdown of a reactor the positive reactivity available by removing all control rods is less than the negative reactivity due to the xenon, the reactor cannot be restarted until the xenon has decayed. This situation is indicated in Fig. 13-3 where the horizontal line represents a hypothetical reserve reactivity. It will be clear from the figure that during the time interval from  $t_a$  to  $t_b$  the reactor which previously operated at a flux of  $5 \times 10^{14}$  cannot be restarted. This period is known as the *reactor deadtime*. The existence of a deadtime can be of major significance in the operation of any high-flux reactor, but it is of greatest importance

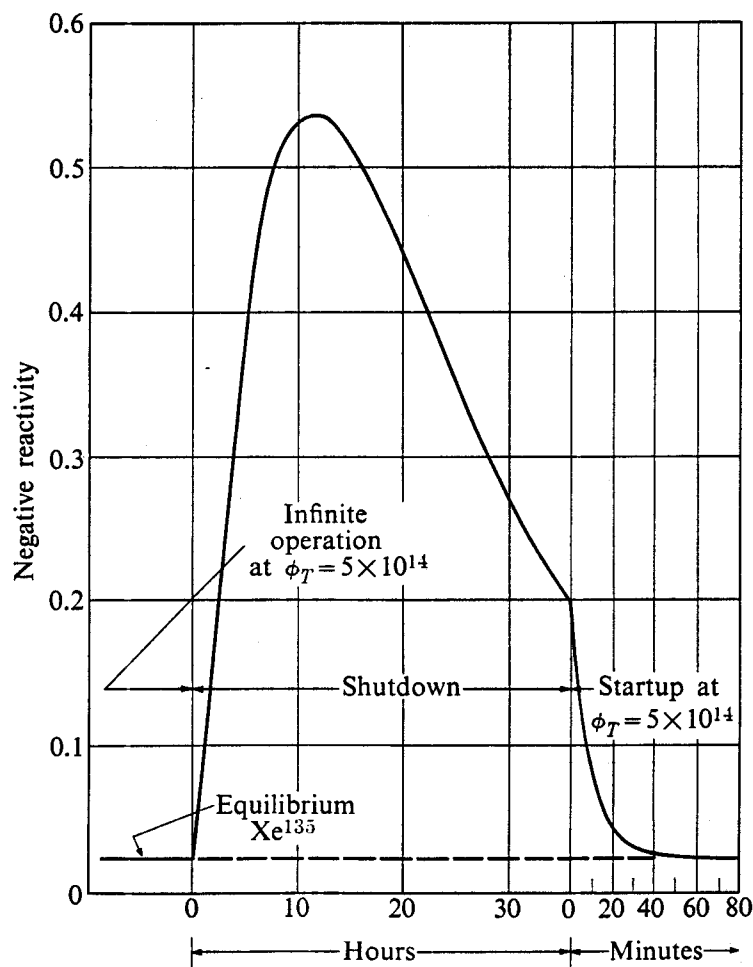


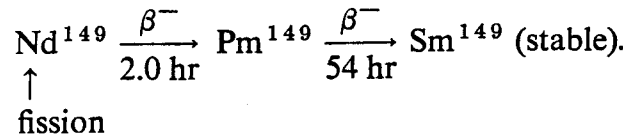
Fig. 13-4. Xenon-135 buildup after shutdown and burnout after startup.

in mobile systems which may be prone to accidental scrams. This is especially true near the end of reactor life when the available excess reactivity may be very small.

It must be emphasized that the absorption cross section of  $Xe^{135}$  is large only at thermal energies. Consequently the operational problems arising from xenon buildup are found only with thermal reactors; intermediate and fast reactors are immune from these problems. Indeed, as mentioned in Chapter 4, this fact was one of the principal motivations for the construction of the Submarine Intermediate Reactor (the SIR) which originally powered the American submarine Seawolf, and it remains one of the few attractive features of an intermediate reactor.

If a reactor is restarted while a large amount of xenon is present in the system, the subsequent burnout of this poison substantially *increases* the reactivity of the reactor. This is shown in Fig. 13-4 for a reactor that is returned to full-power just at the end of the deadtime. To compensate for this increasing reactivity, the control rods which were originally withdrawn to return the reactor to critical must be reinserted to some extent.

**Samarium-149.** The thermal (2200 m/sec) cross section of  $Sm^{149}$  is 40,800 barns and non- $1/v$  (cf. Table 8-1; the average thermal cross section at 20°C is 58,500 barns). Although this isotope is much less of a nuisance in a reactor than  $Xe^{135}$ , it must also be included separately in reactor calculations.  $Sm^{149}$  is not formed directly in fission but appears as the result of the decay of  $Nd^{149}$  (neodymium-149) as follows:



Because the  $Nd^{149}$  decays comparatively rapidly to  $Pm^{149}$  (promethium-149), the  $Pm^{149}$  may be assumed to be produced directly in fission with the yield  $\gamma_P$  (cf. Table 13-5). The concentration  $P$  of the promethium in atoms/cm<sup>3</sup> is then determined by the equation

$$\frac{dP}{dt} = \gamma_P \bar{\Sigma}_f \phi_T - \lambda_P P, \quad (13-88)$$

where  $\lambda_P$  is given in Table 13-6. Since the samarium is stable, it disappears only as the result of neutron capture. The relevant equation is then

$$\frac{dS}{dt} = \lambda_P P - \bar{\sigma}_{as} \phi_T S, \quad (13-89)$$

where  $S$  is the atom density of  $Sm^{149}$  and  $\bar{\sigma}_{as}$  is its average thermal absorption cross section (cf. Eq. 8-40).

**Equilibrium samarium.** Since the absorption cross section of  $Sm^{149}$  is much less than that of  $Xe^{135}$  and the half-life of  $Pm^{149}$  is longer than those of  $I^{135}$  and  $Xe^{135}$ , it follows that it takes somewhat longer for the promethium and

samarium concentrations to reach their equilibrium values than it does for xenon. Nevertheless, in all reactors except those operating at very low flux, these isotopes come into equilibrium in, at most, a few days' time (cf. Prob. 13-20).

Placing the time derivatives in Eqs. (13-88) and (13-89) equal to zero, these equilibrium concentrations are found to be

$$P_{\infty} = \frac{\gamma_P \bar{\Sigma}_f \phi_T}{\lambda_P}, \quad (13-90)$$

and

$$S_{\infty} = \frac{\gamma_P \bar{\Sigma}_f}{\bar{\sigma}_{aS}}. \quad (13-91)$$

The macroscopic absorption cross section of equilibrium  $\text{Sm}^{149}$  is then

$$\bar{\Sigma}_{aS} = \gamma_P \bar{\Sigma}_f, \quad (13-92)$$

and from Eq. (13-73) this is equivalent to the reactivity

$$\rho = - \frac{\gamma_P}{\nu p \epsilon}. \quad (13-93)$$

It should be particularly noted that this reactivity is independent of the flux or power of the reactor. By contrast, it will be recalled that the reactivity due to  $\text{Xe}^{135}$  increases with the flux at fluxes less than  $\phi_X$ . Using the value of  $\gamma_P$  given in Table 13-5 for  $\text{U}^{235}$ , Eq. (13-93) gives

$$\rho = - \frac{0.0113}{2.44} = -0.463\%,$$

or about 72 cents.

**Samarium after shutdown.** After shutdown,  $\text{Sm}^{149}$  builds up as the accumulated  $\text{Pm}^{149}$  decays. However, unlike  $\text{Xe}^{135}$  which undergoes beta decay,  $\text{Sm}^{149}$  is stable and remains in a reactor until the system is brought back to critical, whereupon it is removed by neutron absorption.

With the concentrations of promethium and samarium at shutdown denoted by  $P_0$  and  $S_0$ , respectively, the samarium concentration at the time  $t$  later is [cf. Eqs. (13-88) and (13-89)]

$$S(t) = S_0 + P_0(1 - e^{-\lambda_P t}). \quad (13-94)$$

As  $t \rightarrow \infty$ , the samarium concentration approaches  $S_0 + P_0$ , which it clearly must, since eventually all the promethium decays to samarium. If the promethium and samarium are at their equilibrium concentrations prior to shutdown,  $P_0$  and  $S_0$  are given by Eqs. (13-90) and (13-91). The post-shutdown reactivity due to  $\text{S}^{149}$  can then be written as

$$\rho = - \frac{\gamma_P}{\nu p \epsilon} \left[ 1 + \frac{\phi_T}{\phi_S} (1 - e^{-\lambda_P t}) \right], \quad (13-95)$$

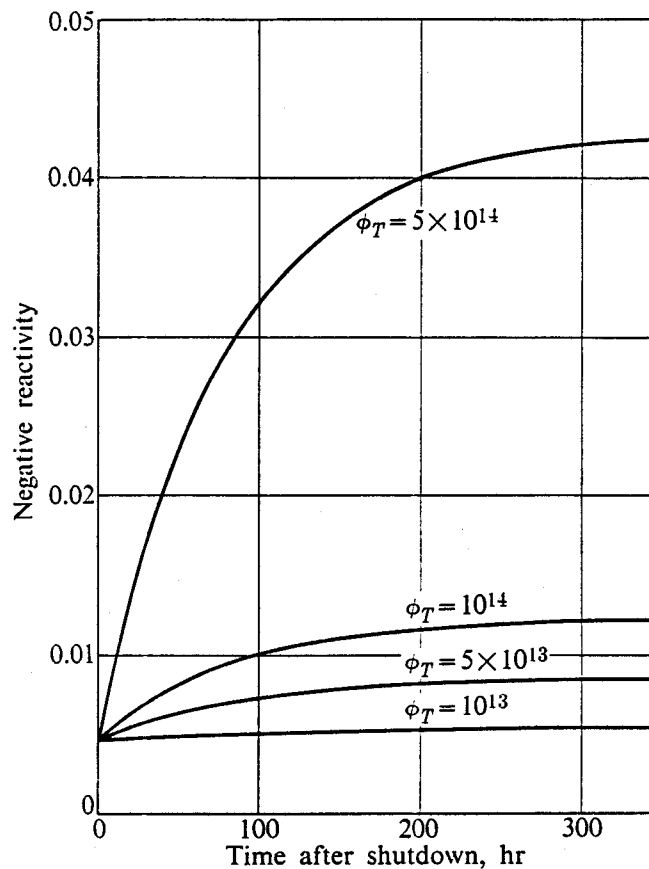


Fig. 13-5. Samarium-149 buildup after shutdown for various values of the operating flux.

where  $\phi_S$  is defined as

$$\phi_S = \frac{\lambda_P}{\bar{\sigma}_{aS}} = 6.095 \times 10^{13} \text{ cm}^{-2} \text{ sec}^{-1} \quad (13-96)$$

at 20°C.

Equation (13-95) is shown in Fig. 13-5 for a U<sup>235</sup>-fueled reactor operated at four different values of  $\phi_T$  before shutdown. It will be observed that although the equilibrium samarium is independent of the flux, the post-shutdown samarium increases with increasing flux. Thus, according to Eq. (13-95) the maximum value of  $-\rho$  is

$$\rho = -\frac{\gamma_P}{\nu p \epsilon} \left( 1 + \frac{\phi_T}{\phi_S} \right), \quad (13-97)$$

which increases linearly with  $\phi_T$ .

As in the case of post-shutdown xenon poisoning, the burnup of the accumulated Sm<sup>149</sup> tends to increase the reactivity of the system when a reactor is restarted after shutdown, as shown in Fig. 13-6. Since Sm<sup>149</sup> is stable, this effect occurs regardless of how long after shutdown the restartup occurs. By contrast, it will be recalled that Xe<sup>135</sup> decays after shutdown, and this effect is apparent for Xe<sup>135</sup> only when the reactor is brought to critical a day or so after shutdown.

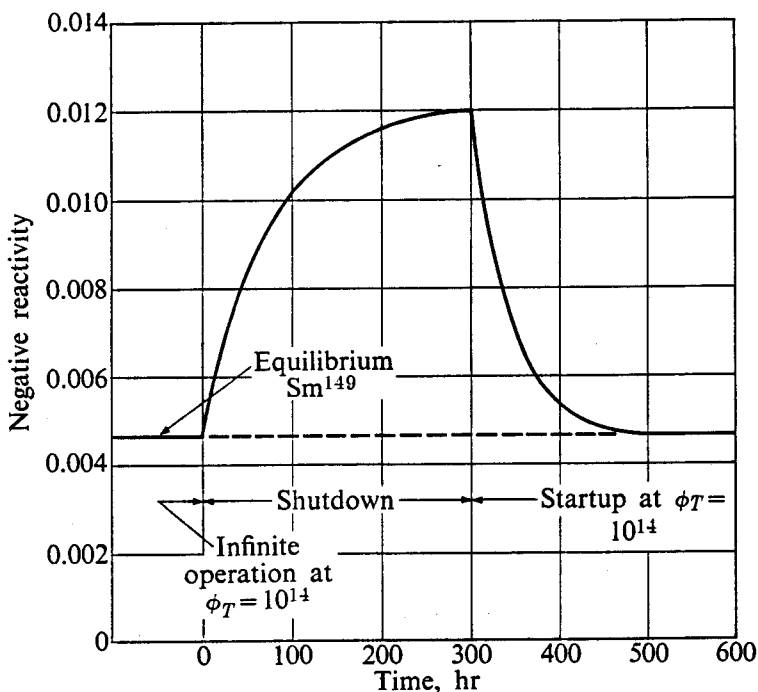


Fig. 13-6. Samarium-149 buildup after shutdown of a reactor operating at a flux  $\phi_T = 10^{14}$  and the subsequent burnout of the samarium after startup.

**Xenon and samarium at constant power.** In the derivations of the concentrations of equilibrium xenon and samarium given earlier, it was assumed that  $\bar{\Sigma}_f$  and  $\phi_T$  were constant, whereas in most reactors (at least in power reactors) these parameters are actually functions of time. Thus  $\bar{\Sigma}_f$  decreases due to the burnup of the fuel, and  $\phi_T$  must be increased if the reactor is to be operated at constant power. (These matters are discussed more fully in the next section.) However, for times of the order of the mean-lives for radioactive decay and/or disappearance by neutron absorption of  $\text{Xe}^{135}$ ,  $\text{Sm}^{149}$  and their precursors, the changes in  $\bar{\Sigma}_f$  and  $\phi_T$  are normally small. It is usually possible to assume, therefore, that the  $\text{Xe}^{135}$  and  $\text{Sm}^{149}$  are always at equilibrium. The macroscopic cross sections of these isotopes can then be found as functions of time by introducing the functions  $\bar{\Sigma}_f(t)$  and  $\phi_T(t)$  into Eqs. (13-79) and (13-92); thus

$$\bar{\Sigma}_{aX}(t) = \frac{(\gamma_I + \gamma_X)\bar{\Sigma}_f(t)\phi_T(t)}{\phi_X + \phi_T(t)} \quad (13-98)$$

and

$$\bar{\Sigma}_{aS}(t) = \gamma_P\bar{\Sigma}_f(t). \quad (13-99)$$

**Permanent poisons.** Many other fission products in addition to  $\text{Xe}^{135}$  and  $\text{Sm}^{149}$  are formed in a reactor, and like these isotopes some are stable and some are radioactive. However, no fission products with absorption cross sections comparable to those of  $\text{Xe}^{135}$  and  $\text{Sm}^{149}$  are produced with yields sufficiently

large to warrant individual treatment. The majority of these additional fission products have far smaller cross sections, and once they appear in a reactor there is little probability that they will be removed by neutron absorption during the lifetime of the reactor. For instance, if an isotope has a 100-barn thermal absorption cross section and the thermal flux is, say,  $10^{13} \text{ cm}^{-2} \text{ sec}^{-1}$ , the probability of absorption per sec per atom is  $100 \times 10^{-24} \times 10^{13} = 10^{-9} \text{ sec}^{-1}$ . This is equivalent to a mean lifetime for the atom of  $10^9 \text{ sec}$  or about 30 years. Thus unless such a fission product is radioactive its appearance may be considered to be a permanent change in the composition of the reactor.

Numerous studies of the accumulation of permanent fission-product poisons have shown that these poisons are produced at the rate of approximately 50 barns per fission in a reactor fueled with  $\text{U}^{235}$ . In reactors fueled with other fissile isotopes, this cross section is slightly different due to the fact that the fission product yield distributions are different for other fissile nuclei (cf. Fig. 3-7). Although this cross section is an average over a great many fission products, it is convenient to ascribe the absorption to one isotope. In other words, it is assumed that one atom with the thermal absorption cross section  $\bar{\sigma}_{pp} \approx 50$  barns is produced per fission. More complete studies have also provided the energy dependence of the permanent poison cross section for use in multigroup calculations (cf. ANL-5800 in references).

This 50 barns/fission does not include the cross sections of nuclei that may be formed by parasitic absorption in the fuel. For example,  $\text{U}^{236}$ , which is produced by thermal neutron absorption in  $\text{U}^{235}$ , has an absorption cross section of 7 barns. Since the capture-to-fission ratio of  $\text{U}^{235}$  is  $\alpha = \sigma_\gamma/\sigma_f = 0.17$ , about  $0.17 \times 7 = 1.2$  barns of permanent poisons are added per fission. This cross section per fission should be added to the permanent poison cross section.

**Nonuniform poisoning.** Up to this point it has been assumed that the various fission product poisons are produced uniformly throughout an infinite system. In a finite reactor, the poisons accumulate with a nonuniform distribution, since the flux and power are now functions of position. The reactivity due to the poisons in this case cannot be attributed simply to a change in the thermal utilization because this parameter is only defined for a uniform system; in other words, Eq. (13-73) does not apply to a finite reactor. However, the preceding formulas giving the poison concentrations remain valid at each point in the reactor. Thus the equilibrium xenon cross section at the point  $\mathbf{r}$  is (cf. Eq. 13-79)

$$\Sigma_{ax}(\mathbf{r}) = \frac{(\gamma_I + \gamma_X)\bar{\Sigma}_f(\mathbf{r})\phi_T(\mathbf{r})}{\phi_X + \phi_T(\mathbf{r})}; \quad (13-100)$$

the equilibrium samarium cross section is (cf. Eq. 13-92)

$$\Sigma_{as}(\mathbf{r}) = \gamma_P \bar{\Sigma}_f(\mathbf{r}); \quad (13-101)$$

and so on. The effect of these nonuniform poison distributions on the criticality

of the reactor can be found by using the iterative-numerical method introduced in Section 10-3. This method will be reconsidered later in this chapter. An approximate analytical procedure for computing the reactivity equivalent of these poisons is discussed in Chapter 15.

**Xenon oscillations.** In a finite thermal reactor the nonuniform production of  $\text{Xe}^{135}$  and its nonuniform consumption by neutron absorption may lead to an interesting instability in the system. Suppose that without changing the total power, the flux is increased in one region of the reactor and simultaneously decreased in another region. This may happen, for example, if control rods are inserted into one region and at the same time withdrawn from another. In the region of increased flux, the xenon now burns out more rapidly than it did prior to the change, and its concentration decreases. This decrease in xenon concentration leads to a higher reactivity in this region, which, in turn, leads to an increased flux. This again leads to increased local xenon burnup, increased local reactivity, increased flux, and so on.

Meanwhile, in the region of decreased flux, the xenon concentration increases due to its reduced burnup and to the continued decay of the existing iodine which was produced in the original, higher flux. This increased xenon concentration decreases the reactivity in this region, which reduces the flux, in turn, increasing the xenon concentration, and so on. The thermal flux, and hence the power density, thus decreases in this region while it increases in the other, the total power of the reactor remaining constant.

These local power excursions do not continue without limit, however. In the region of increased flux, the production of xenon from the decay of the iodine, which is now being formed more rapidly in this region, ultimately reduces the reactivity there and the flux and power eventually decrease. Likewise, in the region of reduced flux, the accumulated xenon eventually decays, increasing the local reactivity and reversing the flux and power transient in that region.

In this way, the flux and power of a reactor may oscillate between different regions until some action is taken to counteract them, say, by the motion of control rods. Calculations, too lengthy to be reproduced here, show that these oscillations have a period of from about 15 to 30 hours. It has also been shown that xenon oscillations may only occur in large reactors, and, of course, only in reactors having fluxes greater than about  $10^{13}$  neutrons per  $\text{cm}^2/\text{sec}$ , at which xenon burnup is as pronounced as xenon decay.

Because xenon oscillations occur at constant power they may go unnoticed unless the flux and/or power density distributions are monitored at several points in the reactor. This must be done in order to prevent such oscillations, since they represent something of a hazard to the safe operation of a reactor. Conceivably, they may lead to dangerously high local temperatures and even to fuel meltdown. In any event, these oscillations, if permitted to continue, burden the core materials with unnecessary temperature cycling which may result in premature materials failure.

### 13-3 Burnup and Conversion

Fuel is not consumed uniformly in an operating reactor, nor is fertile material converted uniformly, except in rare instances where the power density is uniform throughout the fueled portions of the reactor. As a consequence, the concentrations of the fissile isotopes, in general, are functions of both space and time. Equations determining these concentrations are derived in this section; their solutions will be discussed in the next section.

Suppose, for the moment, that the reactor is fueled with a single fissile isotope and that no fertile material is present. If  $N_F(r, t)$  is the atom density of this isotope at the point  $r$  and time  $t$ , its depletion is determined by the equation

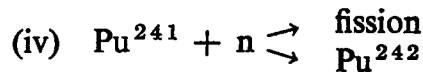
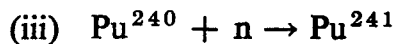
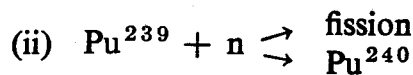
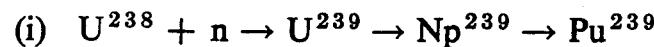
$$\frac{dN_F(r, t)}{dt} = -N_F(r, t)\bar{\sigma}_{aF}\phi_T(r, t), \quad (13-102)$$

where  $\bar{\sigma}_{aF}$  is the thermal absorption cross section. This equation has the formal solution

$$N_F(r, t) = N_F(r, 0) \cdot \exp \left[ -\bar{\sigma}_{aF} \int_0^t \phi_T(r, t) dt \right]. \quad (13-103)$$

If the flux is known as a function of time throughout the reactor,  $N_F(r, t)$  can be found by evaluating the integral in Eq. (13-103). However, the flux and fuel distributions are inter-related, that is, the flux distribution at any time depends upon the fuel distribution, and vice versa. For this reason,  $\phi_T(r, t)$  cannot be determined independently of  $N_F(r, t)$ ; these functions must be computed simultaneously and, except in special cases, this can only be done numerically.

If a reactor is fueled with a pure fissile isotope, the excess reactivity of the system continually decreases in time as this isotope is consumed and fission products accumulate. However, with fertile material present, the decreasing reactivity due to the burnup of the original fissile isotope is compensated to some extent by the production of new fissile isotopes. Consider, for example, a thermal reactor fueled with natural or partially-enriched uranium. In a reactor of this type, the reactivity tends to be maintained by the formation of isotopes of plutonium. The most important of these isotopes is  $Pu^{239}$ , but  $Pu^{241}$  may also have a substantial effect on the reactivity, particularly at high burnup. The pertinent reactions are the following:\*




---

\* The properties of the various isotopes are given in Appendix I.

Isotopes heavier than Pu<sup>241</sup> need not be considered because the absorption cross section of Pu<sup>242</sup> is small ( $\sim 30$  barns).

The Pu<sup>239</sup> is formed as the result of the absorption of thermal and resonance neutrons by U<sup>238</sup>, and it disappears as the result of thermal neutron absorption. The rate of formation of Pu<sup>239</sup> from resonance absorption can be expressed in terms of the resonance escape probability. Thus the number of neutrons absorbed in the resonances of U<sup>238</sup> is  $(1 - p)$  times the number of neutrons which slow down per second throughout the reactor. Since the reactor contains three fissile isotopes, namely, U<sup>235</sup>, Pu<sup>239</sup>, and Pu<sup>241</sup>, this number is

$$\epsilon P_F (\nu_{25} N_{25} \bar{\sigma}_{f25} + \nu_{49} N_{49} \bar{\sigma}_{f49} + \nu_{41} N_{41} \bar{\sigma}_{f41}) \phi_T,$$

where  $N_{25}$ ,  $N_{49}$ , and  $N_{41}$  are the concentrations (all functions of space and time) of the U<sup>235</sup>, Pu<sup>239</sup>, and Pu<sup>241</sup>, respectively,\*  $\epsilon$  is the fast fission factor, and  $P_F$  is the fast nonleakage probability. The concentration of Pu<sup>239</sup> is then determined by the rate equation

$$\frac{dN_{49}}{dt} = N_{28} \bar{\sigma}_{a28} \phi_T + (1 - p) \epsilon P_F (\nu_{25} N_{25} \bar{\sigma}_{f25} + \nu_{49} N_{49} \bar{\sigma}_{f49} + \nu_{41} N_{41} \bar{\sigma}_{f41}) \phi_T - N_{49} \bar{\sigma}_{a49} \phi_T. \quad (13-104)$$

The first and last terms in this equation are the rates of formation and disappearance of Pu<sup>239</sup> due to thermal neutron absorption.

The concentrations of Pu<sup>240</sup> and Pu<sup>241</sup> can be found from the rate equations

$$\frac{dN_{40}}{dt} = (N_{49} \bar{\sigma}_{\gamma49} - N_{40} \bar{\sigma}_{a40}) \phi_T \quad (13-105)$$

and

$$\frac{dN_{41}}{dt} = (N_{40} \bar{\sigma}_{a40} - N_{41} \bar{\sigma}_{a41}) \phi_T. \quad (13-106)$$

Resonance absorption in Pu<sup>240</sup> is neglected in these equations; it should be included in accurate computations involving high burnup.

### 13-4 Reactor Properties Over Life—Estimating Core Life

The prediction of the physical properties of a reactor throughout its life is one of the most important problems in reactor design. For one thing, unless these properties are known it is not possible to determine how much fuel should be loaded into the core in order to obtain the required power for a specified period. If there is too little fuel, the reactor will prematurely fall subcritical. On the other hand, it is clearly not economical to include enough fuel to keep the reactor oper-

---

\* Note that according to the code given in Section 3-2, U<sup>235</sup> = "25"; U<sup>238</sup> = "28"; Pu<sup>239</sup> = "49"; Pu<sup>241</sup> = "41"; etc.

ing longer than the properties of the reactor materials permit. The reactor behavior over life must also be understood in order to design a proper control system, and for many other reasons.

**The infinite thermal reactor.** The general problem of computing reactor properties over life is rather complicated, and it is instructive to begin with the infinite, homogeneous, thermal reactor. All reactor properties are then independent of position. For the moment, it will also be assumed that the system is fueled with a single fissile isotope such as U<sup>235</sup> and that no fertile material or resonance absorbers are present.

At startup, the reactor must be fueled with more fissile material than required for criticality in order to provide for the burnup of the fuel and for other reactivity changes. To compensate for this excess fuel, control rods are inserted into the reactor and then slowly withdrawn to keep the system critical as the fuel is consumed and poisons accumulate. In the present problem, it is convenient to simulate these control rods by a uniformly distributed control poison of macroscopic absorption cross section  $\bar{\Sigma}_C(t)$ . The magnitude of  $\bar{\Sigma}_C(t)$  must be continuously adjusted so that the reactor remains critical from startup to final shutdown. It is easily shown (cf. Prob. 13-29) that  $\bar{\Sigma}_C(t)$  also is proportional to the excess reactivity of the reactor compensated at any time by the control rods. In the absence of resonance absorption or fast fission, the multiplication factor is  $k_\infty = \eta_T f$ . It follows that  $\bar{\Sigma}_C(t)$  must be varied in such a way that at all times

$$k_\infty = \frac{\eta_T \bar{\Sigma}_{aF}(t)}{\bar{\Sigma}_{aF}(t) + \bar{\Sigma}_{aM} + \bar{\Sigma}_{aP}(t) + \bar{\Sigma}_C(t)} = 1, \quad (13-107)$$

where  $\bar{\Sigma}_{aF}(t)$ ,  $\bar{\Sigma}_{aM}$ , and  $\bar{\Sigma}_{aP}(t)$  are the macroscopic absorption cross sections of the fuel (fissile isotope), moderator, and fission product poisons, respectively.

To picture the way in which the control poison must be changed with time, Eq. (13-107) may be solved for  $\bar{\Sigma}_C(t)$ :

$$\bar{\Sigma}_C(t) = (\eta_T - 1)\bar{\Sigma}_{aF}(t) - \bar{\Sigma}_{aM} - \bar{\Sigma}_{aP}(t). \quad (13-108)$$

As time goes on,  $\bar{\Sigma}_{aF}(t)$  decreases while  $\bar{\Sigma}_{aP}(t)$  increases, with the result that  $\bar{\Sigma}_C(t)$  steadily drops to zero. The time  $t_l$ , when  $\bar{\Sigma}_C(t) = 0$ , corresponds to the time when all of the (simulated) control rods have been removed from the system. At this time there is no positive reactivity remaining in the system, and it can no longer be kept critical. Hence,  $t_l$  is the end of life of the reactor.

As a specific example of the use of Eq. (13-108), let it be supposed that the reactor is operated at constant power throughout its life. In order to calculate  $t_l$  for a given initial fuel loading, the quantities  $\bar{\Sigma}_{aF}(t)$  and  $\bar{\Sigma}_{aP}(t)$  must first be computed. Since the power density is proportional to the number of neutrons absorbed per second in the fuel, it follows that the quantity  $\bar{\Sigma}_{aF}(t)\phi_T(t)$  must be constant. In particular,

$$\bar{\Sigma}_{aF}(t)\phi_T(t) = \bar{\Sigma}_{aF}(0)\phi_T(0), \quad (13-109)$$

where  $\Sigma_{aF}(0)$  and  $\phi_T(0)$  are the cross section and flux evaluated at the startup of the system, that is, at  $t = 0$ . A fissile atom is consumed when it absorbs a neutron, and accordingly the concentration of fuel at time  $t$  is given by

$$\begin{aligned} N_F(t) &= N_F(0) - \Sigma_{aF}(0)\phi_T(0)t \\ &= N_F(0)[1 - \bar{\sigma}_{aF}\phi_T(0)t]. \end{aligned} \quad (13-110)$$

The quantity  $\bar{\sigma}_{aF}\phi_T(0)t$  in Eq. (13-110) is the fraction of the fissile atoms consumed up to the time  $t$ . For example, when  $\bar{\sigma}_{aF}\phi_T(0)t = 0.50$ , one half of the fuel has been consumed.\* Multiplying Eq. (13-110) by  $\bar{\sigma}_{aF}$  gives

$$\Sigma_{aF}(t) = \Sigma_{aF}(0)[1 - \bar{\sigma}_{aF}\phi_T(0)t]. \quad (13-111)$$

The flux can be found by substituting Eq. (13-111) into Eq. (13-109):

$$\Sigma_{aF}(t)\phi_T(t) = \Sigma_{aF}(0)[1 - \bar{\sigma}_{aF}\phi_T(0)t]\phi_T(t) = \Sigma_{aF}(0)\phi_T(0).$$

Solving for  $\phi_T(t)$ , the result is

$$\phi_T(t) = \frac{\phi_T(0)}{1 - \bar{\sigma}_{aF}\phi_T(0)t}. \quad (13-112)$$

Thus, as expected, for a reactor operating at constant power density, the flux must be increased in order to compensate for the decreasing fuel concentration.

Consider now the fission-product poisons. The equilibrium  $Xe^{135}$  cross section is (cf. Eq. 13-98)

$$\begin{aligned} \Sigma_{aX}(t) &= \frac{(\gamma_I + \gamma_X)\bar{\Sigma}_f(t)\phi_T(t)}{\phi_X + \phi_T(t)} \\ &= \frac{(\gamma_I + \gamma_X)\bar{\Sigma}_f(0)\phi_T(0)}{\phi_X + \phi_T(t)}. \end{aligned} \quad (13-113)$$

Similarly, the equilibrium  $Sm^{149}$  cross section is (cf. Eq. 13-99)

$$\bar{\Sigma}_{aS}(t) = \gamma_P\bar{\Sigma}_f(t). \quad (13-114)$$

In Eqs. (13-113) and (13-114),  $\bar{\Sigma}_f(t)$  is the macroscopic fission cross section and is equal to  $\Sigma_{aF}(t)/(1 + \alpha)$ , where  $\Sigma_{aF}(t)$  is given by Eq. (13-111) and  $\alpha$  is the capture-to-fission ratio. The permanent poisons accumulate at the rate of  $\bar{\sigma}_{pp}$  barns per fission so that at time  $t$  their macroscopic cross section is

$$\bar{\Sigma}_{pp} = \bar{\sigma}_{pp}\bar{\Sigma}_f(t)\phi_T(t)t = \bar{\sigma}_{pp}\bar{\Sigma}_f(0)\phi_T(0)t. \quad (13-115)$$

---

\* It must be remembered that a very substantial fraction of the *fissile* material in most reactors can be consumed before radiation damage leads to materials failure. (See the discussion at the end of Section 3-6.)

When Eqs. (13-111) through (13-115) are substituted into Eq. (13-108), the control poison required to keep the reactor critical at any time is found to be

$$\begin{aligned}\bar{\Sigma}_C(t) = & (\eta_T - 1)\bar{\Sigma}_{aF}(0)[1 - \bar{\sigma}_{aF}\phi_T(0)t] - \bar{\Sigma}_{aM} - \frac{(\gamma_I + \gamma_X)\bar{\Sigma}_f(0)\phi_T(0)}{\phi_X + \phi_T(t)} \\ & - \gamma_P\bar{\Sigma}_f(0)[1 - \bar{\sigma}_{aF}\phi_T(0)t] - \bar{\sigma}_{pp}\bar{\Sigma}_f(0)\phi_T(0)t.\end{aligned}\quad (13-116)$$

The lifetime of the reactor can be found by introducing the formula for  $\phi_T(t)$  from Eq. (13-112) into the third term of the right-hand side of Eq. (13-116) and then solving the equation  $\bar{\Sigma}_C(t_l) = 0$  for  $t_l$ . The resulting expression is quadratic in  $t_l$ . However, if either  $\phi_T(t) \ll \phi_X$  or  $\phi_T(t) \gg \phi_X$  for all  $t$ , Eq. (13-116) is linear in  $t_l$  and simple formulas for  $t_l$  can be obtained. Thus if  $\phi_T(t) \ll \phi_X$ ,  $t_l$  can be put in the form

$$t_l = \frac{\eta_T \rho_{ex}(1 + \alpha) - (\gamma_I + \gamma_X)\phi_T(0)/\phi_X - \gamma_P}{[(\eta_T - 1)(1 + \alpha)\bar{\sigma}_{aF} - \gamma_P\bar{\sigma}_{aF} + \bar{\sigma}_{pp}]\phi_T(0)}, \quad (13-117)$$

where  $\rho_{ex} = [k_\infty(0) - 1]/k_\infty(0)$  is the excess reactivity at startup and  $\alpha$  is the capture-to-fission ratio (cf. Section 3-4). On the other hand, when  $\phi_T(t) \gg \phi_X$ ,  $t_l$  is

$$t_l = \frac{\eta_T \rho_{ex}(1 + \alpha) - (\gamma_I + \gamma_X + \gamma_P)}{[(\eta_T - 1)(1 + \alpha)\bar{\sigma}_{aF} - (\gamma_I + \gamma_X + \gamma_P)\bar{\sigma}_{aF} + \bar{\sigma}_{pp}]\phi_T(0)}. \quad (13-118)$$

As seen from these formulas, the lifetime of the reactor is inversely proportional to the initial flux in the system. This, of course, would be expected on intuitive grounds.

In the preceding discussion, it was presumed that the reactor is kept in operation until all of the control rods have been removed, at which time the reactor falls subcritical. It may be mentioned that it is not always a sound practice to operate a reactor in this manner. In particular, many reactors are operated only as long as it is possible to over-ride the post-shutdown buildup of  $Xe^{135}$ . This is then taken to be the end of the life of the reactor (or, more accurately, of the reactor core). This criterion for end of life is often adopted for the reactors used to power ships. A reactor aboard a ship may be subject to accidental shutdowns, and unless it is able to over-ride the xenon buildup the ship will remain "dead in the water" during the deadtime of the reactor—an embarrassing state of affairs, to say the least. The above results are easily generalized to this case. Thus if the minimum allowable control poison is  $\bar{\Sigma}_{C\min}$ , the lifetime may be found by solving the relation

$$\bar{\Sigma}_C(t_l) = \bar{\Sigma}_{C\min}, \quad (13-119)$$

where  $\bar{\Sigma}_C(t_l)$  is given by Eq. (13-116) for the constant power reactor.

Up to this point it has been assumed that the reactor does not contain fertile material. If such material is present, the newly produced fissile isotopes tend to support the criticality of the system. The control requirements over time are then

somewhat different from those derived above. Suppose, for instance, that the (infinite) reactor is fueled with a mixture of  $U^{235}$  and  $U^{238}$  (natural or partially-enriched uranium), and is again operated at constant power density. There is now a contribution to the power from thermal fissions occurring in  $Pu^{239}$  and  $Pu^{241}$  as well as from fission in  $U^{235}$ .\* The power density  $P_d$ , in watts/cm<sup>3</sup>, is thus

$$\gamma(N_{25}\bar{\sigma}_{f25} + N_{49}\bar{\sigma}_{f49} + N_{41}\bar{\sigma}_{f41})\phi_T = P_d, \quad (13-120)$$

where  $\gamma$  is the recoverable energy per fission in joules (assumed the same for all isotopes).

Solving Eq. (13-120) for  $\phi_T$  and substituting this into Eqs. (13-102), (13-104), (13-105), and (13-106), the following equations are obtained for determining the  $U^{235}$ ,  $Pu^{239}$ , and  $Pu^{241}$  concentrations as a function of time:

$$\frac{\gamma}{P_d}(N_{25}\bar{\sigma}_{f25} + N_{49}\bar{\sigma}_{f49} + N_{41}\bar{\sigma}_{f41}) \frac{dN_{25}}{dt} = N_{25}\bar{\sigma}_{a25}, \quad (13-121)$$

$$\begin{aligned} \frac{\gamma}{P_d}(N_{25}\bar{\sigma}_{f25} + N_{49}\bar{\sigma}_{f49} + N_{41}\bar{\sigma}_{f41}) \frac{dN_{49}}{dt} &= N_{28}\bar{\sigma}_{a28} \\ &+ (1 - p)\epsilon(\nu_{25}N_{25}\bar{\sigma}_{f25} + \nu_{49}N_{49}\bar{\sigma}_{f49} + \nu_{41}N_{41}\bar{\sigma}_{f41}) - N_{49}\bar{\sigma}_{a49}, \end{aligned} \quad (13-122)$$

$$\frac{\gamma}{P_d}(N_{25}\bar{\sigma}_{f25} + N_{49}\bar{\sigma}_{f49} + N_{41}\bar{\sigma}_{f41}) \frac{dN_{40}}{dt} = N_{49}\bar{\sigma}_{\gamma49} - N_{40}\bar{\sigma}_{a40}, \quad (13-123)$$

$$\frac{\gamma}{P_d}(N_{25}\bar{\sigma}_{f25} + N_{49}\bar{\sigma}_{f49} + N_{41}\bar{\sigma}_{f41}) \frac{dN_{41}}{dt} = N_{40}\bar{\sigma}_{a40} - N_{41}\bar{\sigma}_{a41}. \quad (13-124)$$

This set of coupled, nonlinear equations can be solved using an electronic computer. With the  $U^{235}$ ,  $Pu^{239}$ , and  $Pu^{241}$  concentrations known, the flux is determined from Eq. (13-120). The control poison can be calculated by introducing all of these results into Eq. (13-108). The lifetime is then found, as in the previous example, by placing

$$\bar{\Sigma}_{aC}(t_l) = 0 \quad \text{or} \quad \bar{\Sigma}_{aC}(t_l) = \bar{\Sigma}_{C\min}.$$

Figure 13-7 shows the results of calculations of this type for a reactor fueled with 2.7% enriched uranium and operating at a power density of 70 watts/cm<sup>3</sup> with an initial flux of  $2 \times 10^{13} \text{ cm}^{-2} \text{ sec}^{-1}$ . The resonance escape probability and fast fission factor were taken to be 0.814 and 1.044, respectively. The thermal utilization at startup was 0.71, which corresponds to an initial excess reactivity of about 20%. (These parameters are similar to those of the Yankee Reactor at Rowe, Massachusetts.) As indicated in the figure, the control poison (or excess reactivity) does not decrease linearly† as it would if there were no buildup of  $Pu^{239}$  and  $Pu^{241}$ ; instead, there is a slight concavity to the curve. The sudden drop in reactivity near startup is due to the accumulation of equilibrium  $Xe^{135}$

\* The power produced by fast fission in  $U^{238}$  is ignored here.

† Note that Eq. (13-116) is almost linear in  $t$ .

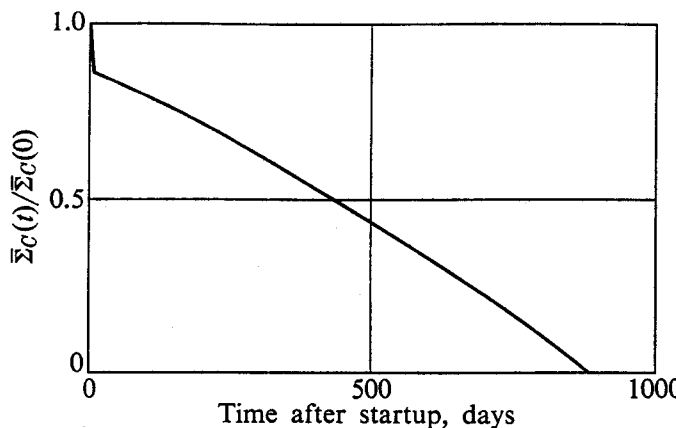


Fig. 13-7. Control poison as a function of time after startup of a thermal reactor fueled with 2.7% enriched uranium. (Courtesy of B. Pellaud, Consolidated Edison Company of New York.)

and  $\text{Sm}^{149}$  which occurs during the first few days of operation. With any reactor started from a clean-cold condition there is also a drop in reactivity (the temperature defect) due to the negative temperature coefficient of the system. This is not shown in Fig. 13-7, the reactor having been assumed to be at a fixed temperature.

The reactivity buildup due to  $\text{Pu}^{239}$  and  $\text{Pu}^{241}$  is more pronounced for a reactor fueled with natural uranium. This is shown in Fig. 13-8 for a reactor assumed to operate at a power density of 0.5 watt/cm<sup>3</sup> with an initial flux of  $10^{13} \text{ cm}^{-2} \text{ sec}^{-1}$ . For this reactor,  $p = 0.85$ ,  $\epsilon = 1.031$ , and the initial excess reactivity was 5.5%. It will be observed that after the initial drop in reactivity due to the buildup of equilibrium xenon and samarium, the curve rises and after about 700 days from startup  $\Sigma c(t)$  almost reaches its initial value. At this time the control rods which were removed to compensate for the poison buildup are back in their starting positions. In some reactors the rise in reactivity accompanying the buildup of plutonium isotopes may actually exceed the excess reactivity at startup.

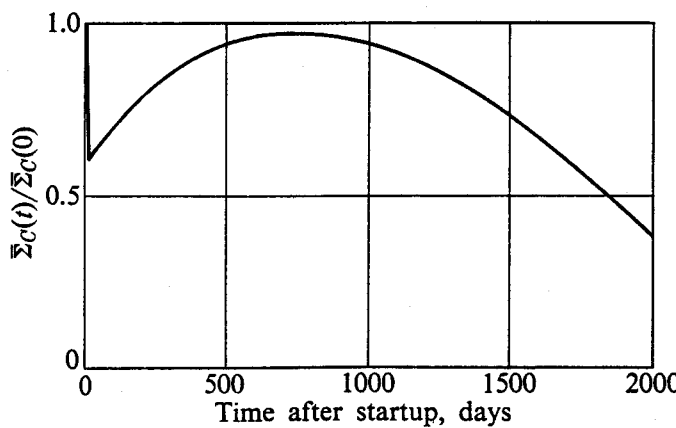


Fig. 13-8. Control poison as a function of time after startup of a thermal reactor fueled with natural uranium. (Courtesy of B. Pellaud, Consolidated Edison Company of New York.)

**The finite thermal reactor.** The procedure for estimating the properties of a finite reactor over its lifetime is essentially the same as it is for the infinite reactor, except that now these properties are functions of space as well as time. For simplicity, the present discussion is confined to a two-region thermal reactor, consisting of a core and reflector, which is fueled with a pure fissile isotope. The space-dependence of the flux will be found using two-group theory, and it will be assumed that the reactor operates at constant power. In the notation of two-group theory, this means that

$$P = \gamma\sigma_{2f} \int_V N_F(\mathbf{r}, t)\phi_2(\mathbf{r}, t) dV = \text{constant}, \quad (13-125)$$

where  $P$  is the total reactor power,  $\gamma$  is the recoverable energy per fission,  $\sigma_{2f}$  is the thermal fission cross section, and  $\phi_2(\mathbf{r}, t)$  is the thermal flux.

The control-rod distribution at any time will be simulated by a thermal control poison  $\Sigma_C(\mathbf{r}, t)$ , which is varied in such a way that the reactor remains critical throughout its lifetime. Within limits, the spatial distribution of the control rods is at the discretion of the operator of the reactor. That is, at any time the reactor can be kept critical with different arrangements of the control rods, and at the start of a lifetime calculation it must be decided how the control rods are to be moved over the life of the core. Such a plan of rod motions is known as a *control-rod program*. One of the objectives of calculations of reactor properties over life is to determine the rod program which is most suitable for the reactor under consideration. Lifetime calculations are usually carried out, therefore, for a variety of rod programs. For the purpose of illustration, a very simple rod program will be used. Thus it will be assumed that at all times the rods are distributed uniformly throughout the core. In this case,  $\Sigma_C(\mathbf{r}, t)$  is the function

$$\Sigma_C(r, t) = \begin{cases} \Sigma_C(t), & r < a, \\ 0, & r > a, \end{cases} \quad (13-126)$$

where  $a$  is the radius of the core. Only the magnitude of  $\Sigma_C(t)$  is then at the disposal of the reactor operator for maintaining the criticality of the system.

Because of the continually changing distributions of fuel and poisons, the thermal absorption and fission cross sections in the core are functions of space and time. However, these changing distributions have little or no effect upon the slowing-down properties of the core nor upon the diffusion coefficients, and these can usually be assumed to remain constant. For the core, therefore, the two group equations describing the critical reactor at time  $t$  are

$$D_1 \nabla^2 \phi_1(\mathbf{r}, t) - \Sigma_1 \phi_1(\mathbf{r}, t) + \eta_T \Sigma_{2F}(\mathbf{r}, t) \phi_2(\mathbf{r}, t) = 0 \quad (13-127)$$

and

$$D_2 \nabla^2 \phi_2(\mathbf{r}, t) - [\Sigma_{2F}(\mathbf{r}, t) + \Sigma_{2M} + \Sigma_{2P}(\mathbf{r}, t) + \Sigma_C(t)] \phi_2(\mathbf{r}, t) + \Sigma_1 \phi_1(\mathbf{r}, t) = 0. \quad (13-128)$$

In these equations,  $\Sigma_{2F}(\mathbf{r}, t)$ ,  $\Sigma_{2M}$ ,  $\Sigma_{2P}(\mathbf{r}, t)$ , and  $\Sigma_C(t)$  are the average thermal macroscopic absorption cross sections of the fuel, moderator (and structure), fission product poisons, and control poison, respectively. Since the properties of the reflector presumably do not change over the reactor lifetime, the reflector equations are given by Eqs. (10-50) and (10-51).

Using a computer, Eqs. (13-127) and (13-128) can readily be solved by replacing the continuous operation of the reactor with a stepwise operation. The reactor lifetime is first divided into a number of time intervals of length  $\Delta t$ . The parameters of the core are then assumed to remain constant during  $\Delta t$ , and these are used to calculate the core parameters for the next interval, using the equations derived earlier in this chapter. For instance, the fuel concentration at  $t + \Delta t$ , in terms of its concentration at time  $t$  according to Eq. (13-103), is given by

$$N_F(\mathbf{r}, t + \Delta t) = N_F(\mathbf{r}, t)e^{-\sigma_{2F}\phi_2(\mathbf{r}, t)\Delta t}, \quad (13-129)$$

so that

$$\Sigma_{2F}(\mathbf{r}, t + \Delta t) = \Sigma_{2F}(\mathbf{r}, t)e^{-\sigma_{2F}\phi_2(\mathbf{r}, t)\Delta t}. \quad (13-130)$$

The fission product poison cross section  $\Sigma_{2P}(\mathbf{r}, t)$  consists of three terms arising from the  $Xe^{135}$ , the  $Sm^{149}$ , and the permanent poisons. To find the concentration of the xenon at  $t + \Delta t$ , Eq. (13-74) is solved for the  $I^{135}$  concentration assuming that  $\bar{\Sigma}_f$  and  $\phi_T$  are constant, and the result is substituted into the solution of Eq. (13-75). The final expression for the  $Xe^{135}$  cross section is

$$\begin{aligned} \Sigma_{2X}(\mathbf{r}, t + \Delta t) &= \frac{(\gamma_I + \gamma_X)\Sigma_{2f}(\mathbf{r}, t)\phi_2(\mathbf{r}, t)}{\phi_X + \phi_2(\mathbf{r}, t)} \\ &+ \frac{\lambda_I N_I(\mathbf{r}, t) - \gamma_I \Sigma_{2f}(\mathbf{r}, t)\phi_2(\mathbf{r}, t)}{\phi_X - \phi_I + \phi_2(\mathbf{r}, t)} [e^{-\lambda_I \Delta t} - e^{-\lambda_X [1 + \phi_2(\mathbf{r}, t)/\phi_X] \Delta t}] \\ &+ \left[ \Sigma_{2X}(\mathbf{r}, t) - \frac{(\gamma_I + \gamma_X)\Sigma_{2f}(\mathbf{r}, t)\phi_2(\mathbf{r}, t)}{\phi_X + \phi_2(\mathbf{r}, t)} \right] e^{-\lambda_X [1 + \phi_2(\mathbf{r}, t)/\phi_X] \Delta t}. \end{aligned} \quad (13-131)$$

In this equation,  $N_I(\mathbf{r}, t)$  is the concentration of the iodine and the other symbols have the same meaning as in Section 13-2. The  $Sm^{149}$  cross section can be found in a similar manner from Eqs. (13-88) and (13-89); this is

$$\begin{aligned} \Sigma_{2S}(\mathbf{r}, t + \Delta t) &= \gamma_P \Sigma_{2f}(\mathbf{r}, t) + \left[ \frac{\lambda_P N_P(\mathbf{r}, t) - \gamma_P \Sigma_{2f}(\mathbf{r}, t)\phi_2(\mathbf{r}, t)}{\phi_2(\mathbf{r}, t) - \phi_S} \right] [e^{-\lambda_P \Delta t} - e^{-\lambda_P [\phi_2(\mathbf{r}, t)/\phi_S] \Delta t}] \\ &+ [\Sigma_{2S}(\mathbf{r}, t) - \gamma_P \Sigma_{2f}(\mathbf{r}, t)] e^{-\lambda_P [\phi_2(\mathbf{r}, t)/\phi_S] \Delta t}, \end{aligned} \quad (13-132)$$

where  $N_P(\mathbf{r}, t)$  is the  $Pm^{149}$  concentration. Finally, the macroscopic cross section of the permanent poisons is

$$\Sigma_{2pp}(\mathbf{r}, t + \Delta t) = \Sigma_{2pp}(\mathbf{r}, t) + \bar{\sigma}_{pp} \Sigma_{2f}(\mathbf{r}, t) \phi_2(\mathbf{r}, t) \Delta t, \quad (13-133)$$

where  $\bar{\sigma}_{pp} \approx 50$  barns.

Equations (13-127) and (13-128) are first solved at  $t = 0$ , that is, at the startup of the reactor using the iterative procedure given in Section 10-3. In this calculation the dimensions of the reactor as well as the initial fuel loading must be specified. The object of the calculation is simply to find the magnitude of the control poison which must be included in the reactor at startup to compensate for the excess fuel. In short, the parameter  $\Sigma_C(0)$  is treated as the eigenvalue of the problem. The computation proceeds as follows. A value of  $\Sigma_C(0)$  is guessed, and one of the fluxes, say  $\phi_2^{(0)}$  is assumed throughout the reactor. This flux is used in Eq. (13-127) to compute a first estimate,  $\phi_1^{(1)}$ , of the fast flux;  $\phi_1^{(1)}$  is then used in Eq. (13-128) to compute  $\phi_2^{(1)}$ ; and so on. For the reasons explained in Section 10-3, the ratio  $\phi^{(n+1)} / \phi^{(n)}$  for either flux soon approaches a constant  $C$ , which is the multiplication factor of the reactor. If  $C$  is less than unity the reactor is subcritical, which means that the original choice for  $\Sigma_C(0)$  was too large. On the other hand, if  $C$  is greater than unity the reactor is supercritical and  $\Sigma_C(0)$  was too small. In either case, the value of  $\Sigma_C(0)$  is changed, the computations are repeated and a new value of  $C$  is determined. This procedure is continued until a value of  $\Sigma_C(0)$  is obtained which corresponds to a critical system at startup.

In addition to the critical value of  $\Sigma_C$ , this calculation also gives the relative values of each flux throughout the reactor, that is, values of the fluxes multiplied by a constant. The magnitude of this constant is determined by the operating power of the reactor, and can be found by numerically performing the integration in Eq. (13-125).

With the fluxes known at startup, the values of the various parameters can be computed at  $t = \Delta t$  by using Eqs. (13-130) through (13-133). The criticality calculations are then repeated until a new value of the control poison  $\Sigma_C(\Delta t)$  is found. Using the fluxes computed for  $t = \Delta t$ , new parameters are computed for  $t = 2 \Delta t$ , and so on. In this way, the computations are carried from interval to interval until the value of  $\Sigma_C(t)$  falls below some specified minimum value. This corresponds, as with the infinite system discussed earlier, to the end of life of the reactor core.

These calculations can also be carried out by using the multigroup equations, and naturally the results are more accurate than those of two-group theory. However, multigroup criticality calculations require considerably more computer time, and since a criticality search must be performed for every time interval, repeated multigroup lifetime calculations can become quite costly. In practice, therefore, preliminary lifetime studies are usually carried out with two or at most only a few groups. Multigroup calculations are made after the design specifications have been more or less frozen. The results of lifetime calculations can also be greatly improved by simulating the control rod distribution more accurately. This can be done, as mentioned in Section 14-7, by the use of two or three dimensional multigroup computer codes with which it is possible to represent the actual shape of the rods and their distribution in the reactor.

The preceding discussion was restricted to homogeneous reactors. Lifetime calculations of heterogeneous reactors are considerably more difficult to carry

out due to the fact that in these reactors the consumption of fissile nuclei, the production of fission products, and the conversion of fertile material all occur non-uniformly in each fuel element as well as nonuniformly throughout the reactor. The analysis of the properties of the system over its lifetime can only be accomplished with elaborate numerical methods which are beyond the scope of this book.

It should be pointed out that even elegant lifetime calculations may be subject to considerable error. This is due to the inherent difficulties in properly describing the system, on the one hand, and also because in lifetime calculations there tends to be an accumulation of errors. Thus an error of any sort (a numerical error or an inaccuracy in the description of the system) in the calculation for any  $\Delta t$  has an effect on the calculations for all subsequent  $\Delta t$ . It is not unusual therefore for the results of reactor lifetime calculations to be in error by as much as several hundred percent.

## References

### General

GALANIN, A. D., *Thermal Reactor Theory*, 2nd ed. New York: Pergamon Press, 1960, Chapters 7 and 8.

GLASSTONE, S., and M. C. EDLUND, *The Elements of Nuclear Reactor Theory*. Princeton, N.J.: Van Nostrand, 1952, Chapter 11.

ISBIN, H. S., *Introductory Nuclear Reactor Theory*. New York: Reinhold, 1963, Chapter 16.

MEEM, J. L., *Two-Group Reactor Theory*. New York: Gordon and Breach, 1964, Chapter 5.

MEGHREBLIAN, R. V., and D. K. HOLMES, *Reactor Analysis*. New York: McGraw-Hill, 1960, Chapters 6 and 9.

MURRAY, R. L., *Nuclear Reactor Physics*. Englewood Cliffs, N.J.: Prentice-Hall, 1957, Chapters 7 and 8.

SCHULTZ, M. A., *Control of Nuclear Reactors and Power Plants*. 2nd ed., New York: McGraw-Hill, 1961, Chapters 2, 5, 8, 11 through 13.

WEINBERG, A. M., and E. P. WIGNER, *The Physical Theory of Neutron Chain Reactors*. Chicago: University of Chicago Press, 1958, Chapters 14 and 16.

### Temperature Coefficients

DRESNER, L., *Resonance Absorption in Nuclear Reactors*. New York: Pergamon Press, 1960, Chapter 7.

LARRIMORE, J. A., "Temperature Coefficients of Reactivity in Homogenized Thermal Nuclear Reactors," Department of Nuclear Engineering, M.I.T., Thesis (Ph.D), September 1962. This thesis contains an excellent review of calculations and measurements of temperature coefficients.

NORDHEIM, L. W., "A New Calculation of Resonance Integrals," *Nuclear Sci. and Eng.* 12, 457 (1962).

### Fission Product Poisoning

CLARK, H. K., and J. C. ENGLISH, "Xenon Tables," E. I. duPont de Nemours and Co. Savannah River Laboratory Report DP-200, May 1957.

ENGLISH, J. C., and T. C. GORRELL, "Samarium Tables," E. I. duPont de Nemours and Co., Savannah River Laboratory Report DP-557, February 1961.

RANDALL, D., and D. S. ST. JOHN, "Xenon Spatial Oscillations," Nucleonics 16, 82 (March 1958).

"Reactor Physics Constants," U.S. Atomic Energy Commission Report ANL-5800, 2nd ed., 1963, Section 5.2.

### Problems

13-1. Let  $x_i$  be any temperature-dependent reactor parameter. (a) If

$$x = \prod_i^n x_i,$$

show that

$$\alpha_T(x) = \sum_i^n \alpha_T(x_i).$$

(b) If

$$x = \sum_i^n x_i,$$

show that

$$\alpha_T(x) = \sum_i^n \left( \frac{x_i}{x} \right) \alpha_T(x_i).$$

13-2. Using Table 8-2, determine  $\alpha_T(\eta_T)$  from 20°C to 1000°C for

- (a)  $U^{233}$       (b)  $U^{235}$       (c)  $Pu^{239}$

13-3. (a) Using the expressions for the cylindrical lattice functions given in Problem 11-5, show that

$$\begin{aligned} \frac{dF}{dT} &\approx -\frac{1}{4T} \left[ \frac{(\kappa_F a)^2}{4} - \frac{(\kappa_F a)^4}{48} + \dots \right], \\ \frac{dE}{dT} &\approx -\frac{E - 1}{2T}. \end{aligned}$$

(b) Show that according to diffusion theory the temperature coefficient of  $f$  for a solid-moderated heterogeneous reactor is

$$\alpha_T(f) = \frac{f}{4T} \left\{ \frac{\Sigma_{aM} V_M}{\Sigma_{aF} V_F} \left[ \frac{(\kappa_F a)^2}{4} - \frac{(\kappa_F a)^4}{48} + \dots \right] + 2(E - 1) \right\}.$$

(c) Find an expression for  $\alpha_T(f)$  if each fuel rod is surrounded by a thin layer of cladding and there is an air gap between the fuel and moderator (cf. Problems 11-7 and 11-8).

- 13-4. Compute  $\alpha_{\text{prompt}}(p)$  and  $\alpha_T(k_\infty)$  for the lattice described in Problem 11-19.  
 13-5. One effect of a change in temperature on the age of fission neutrons is a change in the energy interval over which the neutrons slow down. (a) By writing  $\tau_T$  as

$$\tau_T = \int_{aT}^{E_0} \frac{D}{\xi \Sigma_s} \frac{dE}{E},$$

where  $a$  is some constant and  $T$  is the temperature, show that for a homogeneous system,

$$\alpha_T(\tau_T) = 2\beta - \frac{D}{\xi \Sigma_s \tau_T T}.$$

- (b) Does this calculation overestimate or underestimate this effect? Explain. (c) Compute  $\alpha_T(\tau_T)$  for graphite and  $H_2O$  at room temperature.

13-6. The core of a certain reactor consists of thin  $U^{235}$ -aluminum sandwiches (cf. Problem 9-20) in an  $H_2O$  moderator-coolant. The metal-to-water-volume ratio is 1.0, and the ratio of aluminum atoms to  $U^{235}$  atoms is 150. The reactor operates at a power of 75 MW(th) at an average temperature of 200°C. Compute the temperature coefficients of this reactor assuming that the core is bare.

13-7. For the reactor described in Prob. 11-9, compute (a) the prompt temperature coefficient, (b)  $\alpha_T(k_\infty)$ , (c)  $\alpha_T(k)$ . [Hint: In (b) compute  $\alpha_T(f)$  using diffusion theory and the result of Problem 13-3.]

13-8. The escape probability,  $P_{FO}$ , for a cylindrical rod of radius  $a$  is a function of  $\Sigma_t a$ , where  $\Sigma_t$  is the total cross section (cf. Fig. 11-8). (a) Show that the temperature coefficient of  $\Sigma_t a$  is given by

$$\alpha_T(\Sigma_t a) = -\frac{2}{3}\beta,$$

where  $\beta$  is the coefficient of volume expansion of the fuel. (b) Using the result of part (a), estimate the temperature coefficient of  $P_{FO}$  for fission neutrons in a natural uranium rod of radius 1.4 cm. (c) Estimate the temperature coefficient of  $\epsilon$  for a lattice of these rods assuming that the rods do not interact. [Note: The quantity  $\alpha_T(P_{FO})$  also is important in determining the temperature coefficient of  $f$  according to the ABH method.]

13-9. Suppose that at time  $t = 0$ , either intentionally or by accident, a large amount of reactivity (many dollars) is suddenly inserted into a reactor having a negative temperature coefficient. The response of the system can be estimated by (1) ignoring the delayed neutrons (the reactor is prompt critical, in any case), and (2) assuming that the heat generated in the transient remains within the reactor.

Let  $W(t)$  be the total energy released per  $\text{cm}^3$  in the reactor from the onset of the reactivity change to time  $t$ . The equations describing the incident are then

$$\frac{d\phi_T(t)}{dt} = \frac{k_\infty(t) - 1}{l_p} \phi_T(t),$$

$$k_\infty(t) = k_\infty(0) - \alpha_T k_\infty(0)[T(t) - T(0)],$$

$$C_p[T(t) - T(0)] = W(t),$$

$$W(t) = \gamma \Sigma_f \int_0^t \phi_T(t') dt',$$

where  $k_\infty(0)$  is the initial (changed) value of  $k_\infty$ ,  $T$  is the reactor temperature,  $C_p$  is the specific heat per  $\text{cm}^3$  of the reactor,  $\gamma$  is the recoverable energy per fission, and  $\alpha_T$  is the *magnitude* of the negative temperature coefficient. (a) Show that

$$\frac{d\phi_T}{dt} = \frac{k_\infty(0) - 1}{l_p \gamma \bar{\Sigma}_f} \frac{dW}{dt} - \frac{\alpha_T k_\infty(0)}{l_p C_p \gamma \bar{\Sigma}_f} W \frac{dW}{dt},$$

and hence

$$\phi_T(t) = \phi_T(0) + \frac{k_\infty(0) - 1}{l_p \gamma \bar{\Sigma}_f} W(t) - \frac{\alpha_T k_\infty(0)}{2 l_p C_p \gamma \bar{\Sigma}_f} W^2(t).$$

(b) Writing the result in part (a) as

$$\frac{dW(t)}{dt} = P_0 + \frac{1}{\theta_0} W(t) - \frac{\alpha_T}{2 C_p \theta_0 \rho} W^2(t),$$

where  $P_0 = \gamma \bar{\Sigma}_f \phi_T(0)$  is the initial power density of the reactor,  $\theta_0 = l_p/[k_\infty(0) - 1]$  is the initial reactor period, and  $\rho$  is the initial reactivity insertion, show that

$$W(t) = \frac{2P_0\theta_0(e^{t/\theta} - 1)}{[(\theta_0/\theta) - 1]e^{t/\theta} + [(\theta_0/\theta) + 1]},$$

where

$$\theta = \frac{\theta_0}{\sqrt{1 + 2\alpha_T P_0 \theta_0 / C_p \rho}}.$$

(c) Show that the total heat release is

$$W(\infty) = \frac{2P_0\theta_0}{(\theta_0/\theta) - 1},$$

and the total temperature rise in the transient is

$$\Delta T = \frac{2P_0\theta_0/C_p}{(\theta_0/\theta) - 1}.$$

(d) Show that the flux is given by

$$\phi_T(t) = \phi_T(0) \frac{4(\theta_0/\theta)^2 e^{t/\theta}}{\{( (\theta_0/\theta) - 1) e^{t/\theta} + [(\theta_0/\theta) + 1]\}^2}.$$

(e) Show that the flux rises to a maximum at the time

$$t_{\max} = \theta \ln \left[ \frac{(\theta_0/\theta) + 1}{(\theta_0/\theta) - 1} \right]$$

and that the maximum flux is

$$\phi_{T_{\max}} = \frac{\phi_T(0)}{1 - (\theta/\theta_0)^2}.$$

[Note: This analysis of a reactor transient is known as *Fuchs' model*.]

13-10. Using the formulas derived in the preceding problem, plot the response of a small research reactor, originally operating at a power of 0.1 watt, following the step insertion

of §3. Determine the maximum flux, the total energy release and the final temperature of the system. *Note:* The reactor has the following parameters:

$$\begin{aligned}\alpha_T &= -3.6 \times 10^{-4} / ^\circ C, \\ l_p &= 10^{-4} \text{ sec}, \\ \bar{\Sigma}_f &= 0.074 \text{ cm}^{-1}, \\ C_p &= 2 \text{ joules/cm}^3 \cdot ^\circ C = 0.48 \text{ calories/cm}^3 \cdot ^\circ C, \\ \text{Core volume} &= 1.23 \times 10^4 \text{ cm}^3.\end{aligned}$$

13-11. Compute and plot the ratio of the atom densities of equilibrium  $Xe^{135}$  and  $U^{235}$  as a function of thermal flux in a reactor operating at constant flux.

13-12. Consider a natural uranium-fueled subcritical assembly of the type used for instructional purposes. (a) If the average thermal flux is  $5 \times 10^4$  neutrons/cm<sup>2</sup>-sec, how long must the assembly be operated for the  $Xe^{135}$  concentration to reach 90% of its equilibrium value? (b) Repeat the calculation for  $Sm^{149}$ . (c) Roughly how much reactivity do these concentrations of isotopes represent?

13-13. In the xenon tables of Clark and English (cf. references), the  $I^{135}$  and  $Xe^{135}$  concentrations are written as

$$\begin{aligned}I &= A + BI_0, \\ X &= C + DI_0 + EX_0,\end{aligned}$$

where  $I_0$  and  $X_0$  are known concentrations at time  $t_0$ . The quantities  $A$ ,  $B$ ,  $C$ ,  $D$ , and  $E$  are tabulated as functions of the elapsed time from  $t_0$ , assuming that the flux and fuel cross sections remain constant. (a) Find expressions for  $A$ ,  $B$ , etc. (b) Show how the tables could be used to determine the  $Xe^{135}$  concentration at any time after a number of changes in flux.

13-14. Show that an hour or so after the startup of a clean reactor having a thermal flux  $\phi_T \gg \phi_X$ , the  $Xe^{135}$  concentration is given approximately by

$$X(t) = X_\infty(1 - e^{-\lambda_I t}).$$

Interpret this result physically.

13-15. (a) Show that for a reactor operating at constant flux before shutdown, the maximum  $Xe^{135}$  buildup occurs at the time  $t_{\max}$  after shutdown where

$$t_{\max} = \frac{1}{\lambda_I - \lambda_X} \ln \left[ \frac{\lambda_I / \lambda_X}{1 + (\gamma_I + \gamma_X)(\phi_I - \phi_X) / \gamma_I(\phi_X + \phi_T)} \right].$$

(b) Show that  $t_{\max}$  is not sensitive to the value of  $\phi_T$  in those cases where xenon poisoning is important, and that  $t_{\max} \approx 11.3$  hr. (c) Derive an expression for  $\rho_{\max}$ , the maximum reactivity of post-shutdown  $Xe^{135}$ , in terms of the reactivity of equilibrium  $Xe^{135}$ , and compute  $\rho_{\max}$  for a  $U^{235}$ -fueled reactor operating at a flux of  $\phi_T = 10^{14}$  neutrons/cm<sup>2</sup>-sec prior to shutdown.

13-16. Show that there is no post-shutdown buildup of  $Xe^{135}$  in a  $U^{235}$ -fueled reactor operating at constant flux  $\phi_T$  provided

$$\phi_T \leq \frac{\gamma_X}{\gamma_I} \phi_X = 3.7 \times 10^{11} \text{ neutrons/cm}^2 \cdot \text{sec.}$$

13-17. A U<sup>235</sup>-fueled reactor operates at a power of 100 MW(th) at an average thermal flux of  $2 \times 10^{14}$  neutrons/cm<sup>2</sup>-sec. Long after startup, when the reactor has 10% reserve reactivity, the reactor is scrammed. Compute (a) the time to the onset of the deadtime; (b) the duration of the deadtime.

13-18. The reactor in Problem 13-17 is returned to critical at a power of 100 MW(th) immediately after the end of the deadtime. Compute and plot the rise in reactivity as a function of time after startup.

13-19. What is the minimum level to which the power of the operating reactor in Problem 13-17 may suddenly be dropped if there is to be no deadtime?

13-20. Compute and plot as a function of flux the time after startup of a clean thermal reactor that the Sm<sup>149</sup> concentration reaches 90% of its saturation (equilibrium) value.

13-21. Compare the effects of equilibrium Xe<sup>135</sup> and Sm<sup>149</sup> in thermal reactors fueled with U<sup>233</sup>, U<sup>235</sup>, and Pu<sup>239</sup>.

13-22. (a) At what flux levels are the reactivities of equilibrium Xe<sup>135</sup> and Sm<sup>149</sup> equal in a U<sup>235</sup>-fueled reactor? (b) How long does it take for these isotopes to reach 90% of their equilibrium values in this flux?

13-23. Show that when a reactor is operated at constant power the concentration of Sm<sup>149</sup> is given approximately by the formula

$$S(t) = \frac{\gamma_p \bar{\Sigma}_f(t)}{\bar{\sigma}_{as}} \left\{ 1 - \left[ \frac{\phi_T(0)}{\phi_T(t)} \right]^m \right\},$$

where

$$m = \frac{\bar{\sigma}_{as}}{\bar{\sigma}_{af}}.$$

[Note: This is a somewhat more accurate expression than Eq. (13-99).]

13-24. Compute  $\alpha_T(f)$  for an infinite reactor consisting of a homogeneous mixture of U<sup>235</sup> and pressurized H<sub>2</sub>O, operating with negligible excess reactivity at a power density of 150 watts/cm<sup>3</sup> at 300°C. Include effects due to equilibrium xenon and samarium, but ignore permanent poisons.

13-25. An atom of U<sup>235</sup> is placed in a thermal flux of  $2 \times 10^{13}$  neutrons/cm<sup>2</sup>-sec. What is the probability that this atom will not disappear by neutron absorption in a period of one year?

13-26. The quantity

$$\theta(t) = \int_0^t \phi(t') dt'$$

is known as *flux-time*. Derive expressions in terms of this variable for the concentrations of U<sup>235</sup> and the isotopes of plutonium in a natural uranium-fueled thermal reactor.

13-27. A large thermal reactor fueled with natural uranium operates at constant flux over its life. Derive expressions for the concentrations of U<sup>235</sup>, Pu<sup>239</sup>, and Pu<sup>241</sup> as a function of time. [Note: Ignore the production of Pu<sup>239</sup> from resonance capture of Pu<sup>241</sup> fission neutrons.]

13-28. A thermal reactor is initially fueled with a mixture of U<sup>235</sup> and Th<sup>232</sup>. As time goes on, the converted isotope U<sup>233</sup> accumulates as the U<sup>235</sup> is consumed. (a) Show that the concentrations of U<sup>235</sup>, Pa<sup>233</sup>, and U<sup>233</sup> at any time are given by the equations

(resonance capture in the thorium neglected)

$$\begin{aligned}\frac{dN_{25}}{dt} &= - N_{25}\bar{\sigma}_{a25}\phi_T, \\ \frac{dN_{13}}{dt} &= N_{02}\bar{\sigma}_{a02}\phi_T - \lambda_{13}N_{13}, \\ \frac{dN_{23}}{dt} &= \lambda_{13}N_{13} - N_{23}\bar{\sigma}_{a23}\phi_T.\end{aligned}$$

- (b) Solve these equations assuming that  $\phi_T$  and the thorium concentration are constant.  
 (c) Determine graphically the cross-over time at which the fission rates of  $U^{235}$  and  $U^{233}$  are equal if the original concentration of the  $U^{235}$  is  $N_{25}(0)/N_{02} = 1/100$  and the reactor operates at a flux of  $2 \times 10^{13}$  neutrons/cm<sup>2</sup>-sec.

13-29. Show that the excess reactivity at the time  $t$  controlled by the poison  $\Sigma_C(t)$  is given by

$$\rho(t) = \frac{\Sigma_C(t)}{\eta_T \bar{\Sigma}_{aF}(t)},$$

where  $\bar{\Sigma}_{aF}(t)$  is the absorption cross section of the fuel.

13-30. If the excess reactivity of the reactor described in Problem 13-6 is 25% at startup, compute, by two-group theory, the bare, critical radius of this reactor.

13-31. Using the formulas derived in Problem 13-27, compute and plot the concentrations of  $U^{235}$ ,  $Pu^{239}$ , and  $Pu^{241}$  as a function of time in a natural uranium-graphite reactor operating at a constant flux of about  $2 \times 10^{12}$  neutrons/cm<sup>2</sup>-sec and an initial power density of 0.1 watts/cm<sup>3</sup>. Other reactor parameters at startup are  $f = 0.898$ ,  $p = 0.878$ ,  $\epsilon = 1.030$ .

13-32. The core of a large  $U^{235}$ -fueled,  $D_2O$ -moderated reactor must be capable of operating at a power density of 85 watts/cm<sup>3</sup> for one year. Neglecting temperature effects, estimate (a) the average thermal flux at startup and shutdown, (b) the excess reactivity at startup, (c) the  $U^{235}$  concentration in gm/cm<sup>3</sup> at startup and shutdown.

13-33. The excess reactivity (and hence the number of control rods), which must be included in a reactor in order to obtain a desired lifetime, can be reduced by the use of a *burnable poison*. This is an isotope having a large absorption cross section ( $B^{10}$  is often used for this purpose) which is converted to an isotope of low absorption cross section as the result of neutron absorption. The increase in reactivity due to the burnup of this poison compensates to some extent for the decrease in reactivity due to fuel burnup and the accumulation of fission-product poisons. (a) Show that regardless of the way in which the reactor is operated (e.g., constant flux or constant power) the following relation holds:

$$N_B(t) = N_B(0) \left[ \frac{N_F(t)}{N_F(0)} \right]^{\sigma_{aB}/\sigma_{aF}},$$

where  $N_B$  and  $\sigma_{aB}$  are the concentration and absorption cross section of the poison, respectively. (b) If the reactor operates at constant power, show that

$$N_B(t) = N_B(0)[1 - \sigma_{aF}\phi_T(0)t]^{\sigma_{aB}/\sigma_{aF}},$$

where  $\phi_T(0)$  is the flux at startup.

13-34. Derive an expression for the life of a fissile-fueled research reactor which operates at constant thermal flux. For simplicity, assume that the reactor is infinite.

13-35. A certain quasihomogeneous reactor has the following properties at startup:

Core dimensions	cube, 20 in. on a side
Fuel	8.55 kg U <sup>235</sup>
Burnable poison	21.1 gm B <sup>10</sup>
Moderator	H <sub>2</sub> O, normal density
Fuel elements	stainless steel
Metal-to-water-volume ratio	0.25
Average thermal flux	$2.7 \times 10^{13}$ neutrons/cm <sup>2</sup> -sec

(a) By considering the equivalent infinite system, compute and plot the excess reactivity of the reactor as a function of time after startup. (b) Estimate the reactor life if the minimum allowable excess reactivity is to be 3.0%. (c) Estimate the reactor life if there were no burnable poison but the reactor had the same initial excess reactivity. [Note: The reactor is to be operated at constant power over its lifetime.]

# 14

## Control Rods

As explained at the beginning of Chapter 12, it is necessary, in order to keep a reactor critical, to compensate for changes which occur in the system due to the burnup of the fuel, the production of isotopes, changes in temperature, and so on. In most reactors this is accomplished by *control rods*, which are also used to start up and shut down a reactor or change its power level.

In the early days of the nuclear industry, reactors were controlled with comparatively few rods. These were invariably cylindrical in shape and made of a strong thermal neutron absorber such as cadmium [ $\sigma_a(0.025 \text{ eV}) = 2450 \text{ b}$ ]. Their diameter was substantially greater than the absorption mean free path of thermal neutrons, and all thermal neutrons striking this kind of rod were therefore absorbed. Such strongly absorbing rods are said to be *black*.

Black rods are not used as frequently today for a number of reasons. For one thing, strongly absorbing rods badly distort the flux in their vicinity, and this gives rise to undesirable power and temperature distributions. Less strongly absorbing materials such as hafnium [ $\sigma_a(0.025 \text{ eV}) = 105 \text{ b}$ ] or steel containing small amounts of boron are therefore used for the rods in most modern reactors. These rods are also comparatively thin, so that while they are good neutron absorbers, all thermal neutrons striking them are not absorbed. Rods of this type are called *grey*.

The control rods used in many modern reactors are not cylindrical, but are fabricated in various shapes such as the cruciform or cross-like rod. Rods of this shape fit snuggly into an array of fuel assemblies and are widely used in reactors, particularly water-moderated reactors, that have tight fuel lattices. This type of rod has the additional advantage over the cylindrical rod in that it can be cooled more easily. This is particularly important in power reactors where a rod may become very hot unless properly cooled.

When a rod is removed from a solid-moderated reactor, the region originally occupied by the rod remains behind as a vacant space, while in a liquid-moderated reactor the region may fill with moderator. In either case, the replacing of a strongly absorbing rod by a void or a weak absorber tends to peak the flux in this region. To avoid this situation, it is common practice to attach a region of fuel or mildly absorbing structural material to the end of the rod. Such rod *followers*, as these extensions to a control rod are called, reduce the peaking of the flux, and if the followers are fueled they may substantially increase the reactivity equivalent

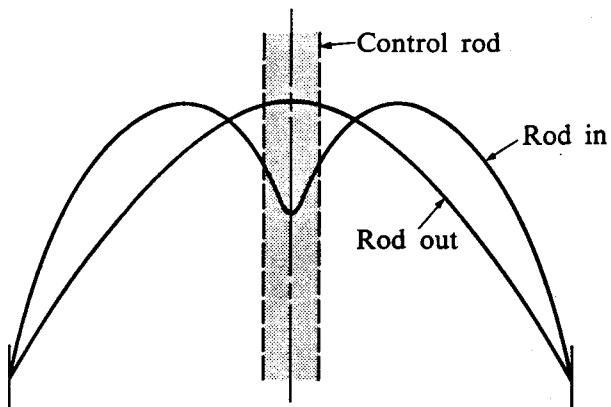


Fig. 14-1. Flux in a bare reactor with and without central control rod.

of the rod. Thus in this case, fuel is simultaneously introduced into the system as the rod is extracted.

The insertion of a control rod in a reactor changes its multiplication factor in two ways. First, of course, the rod simply absorbs neutrons. At the same time, however, the rod distorts the flux in such a way that the leakage of neutrons from the system is increased. This can be seen in Fig. 14-1, where the flux is shown in a bare cylindrical reactor before and after a single rod is inserted. It will be observed that the curvature or buckling of the flux is *greater* when the rod is present. The gradient of the flux at the surface of the reactor is therefore greater, and so also is the leakage current. With many reactors these two effects of a control rod, i.e., increased absorption and increased leakage, are about equally important in determining the effect of the rod upon the multiplication factor of the system (cf. Prob. 14-4).

The amount of reactivity which the control rods must be capable of providing depends upon the nature of the reactor, the desired core lifetime, and many other factors. Table 14-1 gives the required control for two reactors, the Pressurized Water Reactor (PWR),\* which is a 230 megawatt(th) thermal reactor, and the Fermi Reactor,† a 300 megawatt(th) fast reactor. It will be observed that the control requirements for the Fermi Reactor are considerably smaller than for the PWR.‡ There are several reasons for this. First, it can easily be shown that temperature changes have a much smaller effect on a fast reactor than on a thermal reactor. At the same time, xenon, samarium, and the other thermal poisons have no effect on a fast reactor since there are essentially no thermal neutrons in the system. Finally, the small reactivity compensation for burnup with the Fermi Re-

\* Duquesne Light Co., Shippingport, Pennsylvania.

† See Section 4-4.

‡ All thermal reactors do not have such large control requirements as the PWR. Thus, Yankee requires 20%, Dresden 16%, the Savannah 15%, and so on. Furthermore, the recent introduction of continuous refueling (also called *on-line refueling*) will considerably reduce the required control reactivity of all reactors.

**Table 14-1**  
**Control Requirements (in %) of Two Reactors**

	PWR	Fermi
Temperature compensation	3.0	0.15
Equilibrium xenon	3.0	0
Xenon override	3.0	0
Equilibrium samarium	1.0	0
Fuel burnup, permanent poisons, isotope production	10.0	0.32
Actual control system capability	25.0	6.69

actor is due to the fact that portions of this reactor are refueled about every two weeks.

While all reactors, thermal or fast, do not have the same control requirements as the PWR or the Fermi Reactor, Table 14-1 illustrates many of the factors which must be taken into consideration in designing the control system of every reactor. Once these control requirements have been established, the number, composition, and arrangement of the control rods which are needed to fulfill these requirements must next be determined. Methods for calculating the reactivity equivalents of a single rod and an array of rods are considered in this chapter. For the most part, the discussion is restricted to rods in thermal reactors; the (less difficult) problem of rods in fast reactors is considered briefly in Section 14-7.

### 14-1 Control-Rod Worth

As already mentioned, control rods are used in two fundamentally different ways. They are either inserted and withdrawn rather quickly during startup, shutdown, and changes in power, or they are moved slowly to compensate for fuel burnup and other long-term changes in the properties of the system. It is important to recognize that these two modes of operation are quite different physically. In particular, when the rods are moved quickly the reactor becomes supercritical or subcritical, whereas when they are moved slowly the reactor remains critical or nearly so. It is not surprising, therefore, that the quantitative measure of the effect of the rods on the reactor, that is, the *worth* of the rods, is defined differently in the two cases.

Consider an example of the first use of a control rod. It will be assumed that the reactor is initially critical and that no rods are present in the reactor. Then suddenly a rod is inserted fully into the system, and as a result the reactor immediately falls subcritical. The insertion of the rod clearly represents a nonuniform change in the reactor, since the rod does not extend over the entire reactor. The eigenfunctions of the reactor with the rod present are therefore different from the eigenfunctions with the rod removed. Consequently, as explained in Section 12-4,

the time-dependent flux following the insertion of the rod is a superposition of the eigenfunctions of the new reactor, that is, the reactor containing the rod, each multiplied by seven exponential time factors, one for each solution of the reactivity equation. The harmonics, however, die out more rapidly than the fundamental, and the flux ultimately assumes the shape of the fundamental, which dies out as  $\exp(-t/T)$ , where  $T$  is the stable period. The worth of a control rod used in this manner is defined as the *magnitude* of the reactivity insertion required to place the reactor on this stable period.

To derive an explicit formula for rod worth, it is convenient to treat the rod as a region *external* to the reactor. Thus with a cylindrical rod of radius  $a$  inserted along the axis of a cylindrical reactor of radius  $R$ , the "reactor" is taken to be the annular region between the surface of the rod and the outer surface of the reactor, that is, the region defined by  $a \leq r \leq R$ . In this way, the actual nonuniform reactor (reactor plus control rod) is replaced by a uniform, one region (annular) reactor, and all of the formulas derived in earlier chapters for uniform reactors can be applied in the control-rod problem. Furthermore, it is assumed that there is no hole for the rod in the original reactor, and that as the rod is inserted a cylinder of core material equal in size to the rod is forced out of the reactor. Similarly, when the rod is withdrawn the hole is assumed to fill with core material. This situation is realized in practice if the rod is equipped with a follower composed of core material.

Denoting the rod worth by the symbol  $\rho_w$ , it follows from the above definition and the formula for reactivity (cf. Eq. 12-66) that

$$\rho_w = |\rho| = \frac{1 - k}{k}, \quad (14-1)$$

where  $k$  is the multiplication factor of the reactor *after* the rod has been inserted. For the moment, it will be convenient to make calculations of  $\rho_w$  using modified one-group theory. Then from Section 9-5,  $k$  is given by\*

$$k = \frac{k_\infty}{1 + B^2 M^2}, \quad (14-2)$$

where  $B^2$  is the buckling of the reactor with the rod inserted. In view of the fact that the physical properties of the reactor material do not change as the result of the rod motion, the parameters  $k_\infty$  and  $M^2$  in Eq. (14-2) are constant. Only  $B^2$  changes because of the motion of the rod.

Since the reactor was assumed to be critical before the rod was inserted, the original multiplication factor,  $k_0$ , was unity, that is,

$$k_0 = \frac{k_\infty}{1 + B_0^2 M^2} = 1, \quad (14-3)$$

---

\* Because the formulas dealing with control rods are so complicated, subscripts denoting thermal values of reactor parameters are omitted in this chapter, except in Section 14-7.

where  $B_0^2$  is the initial buckling of the reactor. Substituting Eqs. (14-2) and (14-3) into (14-1) gives

$$\rho_w = \frac{k_0 - k}{k} = \frac{(B^2 - B_0^2)M^2}{1 + B_0^2 M^2}. \quad (14-4)$$

If the reactivity equivalent of a rod is small, as is often the case, then  $B \approx B_0$  and Eq. (14-4) can be simplified; thus

$$\begin{aligned} \rho_w &= \frac{(B - B_0)(B + B_0)M^2}{1 + B_0^2 M^2} \\ &\approx \frac{2M^2 B_0 \Delta B}{1 + B_0^2 M^2}. \end{aligned} \quad (14-5)$$

Returning now to the case in which the rod is withdrawn slowly to compensate for the reactivity changes, it should first be noted that the physical properties of the core material are somewhat different when the rod is finally withdrawn than when it was initially inserted. It is the usual practice, therefore, to define the worth of such a rod in terms of the changes in the properties of the system for which it can compensate. In particular, the rod worth is written as

$$\rho_w = \frac{k_\infty - (k_\infty)_0}{(k_\infty)_0} \quad (14-6)$$

or

$$\rho_w = \frac{k_\infty - (k_\infty)_0}{k_\infty}, \quad (14-7)$$

where  $k_\infty$  and  $(k_\infty)_0$  are the infinite multiplication factors of the core with the rod inserted and withdrawn, respectively. Equations (14-6) and (14-7) are essentially equivalent since in practice the difference between  $k_\infty$  and  $(k_\infty)_0$  is usually small. Denoting the initial and final migration areas by  $M^2$  and  $M_0^2$ , respectively,  $k_\infty$  and  $(k_\infty)_0$  are given by

$$k_\infty = 1 + B^2 M^2 \quad (14-8)$$

and

$$(k_\infty)_0 = 1 + B_0^2 M_0^2. \quad (14-9)$$

From Eq. (14-6) it follows that the rod worth is

$$\rho_w = \frac{B^2 M^2 - B_0^2 M_0^2}{1 + B_0^2 M_0^2}. \quad (14-10)$$

If the changes in the system compensated by one rod are small so that  $M^2 \approx M_0^2$ , it will be seen that Eq. (14-10) reduces to Eq. (14-4). Thus in this case the two definitions of rod worth are equivalent. Furthermore, if the rod worth is small, Eq. (14-10) reduces to Eq. (14-5). It is common practice, therefore, to use either Eq. (14-4) or Eq. (14-5) for one group calculations of rod worth regardless of the way in which the rod is used for control purposes.

With two-group theory it is somewhat easier to define rod worth by Eq. (14-6) than by Eq. (14-1), although an equivalent definition based on reactor period can be given. The two-group formula for  $k_\infty$  can be found by solving Eq. (10-37) for  $k_\infty$ . The result is

$$k_\infty = (1 + \mu^2\tau)(1 + \mu^2L^2), \quad (14-11)$$

where  $\mu^2$  [one of the two-group parameters defined by Eq. (10-37)],  $k_\infty$ ,  $\tau$ , and  $L^2$  refer to the reactor with the rod inserted. With the rod removed ( $k_\infty$ )<sub>0</sub> is

$$(k_\infty)_0 = (1 + \mu_0^2\tau_0)(1 + \mu_0^2L_0^2), \quad (14-12)$$

where all parameters refer to the reactor with the rod out. From Eq. (14-6) the rod worth is then

$$\rho_w = \frac{(1 + \mu^2\tau)(1 + \mu^2L^2) - (1 + \mu_0^2\tau_0)(1 + \mu_0^2L_0^2)}{(1 + \mu_0^2\tau_0)(1 + \mu_0^2L_0^2)}. \quad (14-13)$$

If the reactor is large compared to the slowing-down length ( $\sqrt{\tau}$ ) or the diffusion length, the terms in  $\mu^4$  or  $\mu_0^4$  in Eq. (14-13) can be ignored, and this equation reduces to

$$\rho_w = \frac{\mu^2M^2 - \mu_0^2M_0^2}{1 + \mu_0^2M_0^2}. \quad (14-14)$$

The similarity between Eqs. (14-14) and (14-10) will be immediately apparent. Furthermore, from the argument following Eq. (14-10), it is often true that  $M^2 \approx M_0^2$  and Eq. (14-14) becomes

$$\rho_w = \frac{(\mu^2 - \mu_0^2)M^2}{1 + \mu_0^2M^2}. \quad (14-15)$$

Finally, if the rod worth is small,  $\rho_w$  can be written as

$$\rho_w \approx \frac{2M^2\mu_0\Delta\mu}{1 + \mu_0^2M^2}. \quad (14-16)$$

This result, which will be recognized as the two-group version of Eq. (14-5), is the most commonly used expression for computations of rod worth in two-group theory.

In the following sections explicit expressions for  $\rho_w$  will be derived based on the above formulas. The discussion will be restricted to bare reactors; reflected reactors can be treated approximately by including the reflector savings in the dimensions of the bare system. A more accurate analysis of reflected reactors leads to computations which must be performed on an electronic computer. For the moment, the discussion will also be confined to the most commonly encountered systems, namely, cylindrical thermal reactors. As will be shown in Section 14-6,

the worth of a control rod of arbitrary shape can be computed in terms of the worth of an equivalent cylindrical rod. It is logical therefore to begin by considering cylindrical rods in some detail.

## 14-2 One Central Rod—Modified One-Group Theory

Although one-group theory (or modified one-group theory) ordinarily does not provide more than a rough estimate of control-rod worth, it illustrates the general approach to control-rod calculations. Consider, therefore, a bare homogeneous thermal reactor of extrapolated radius  $R$  and height  $H$  having at its center a single rod of radius  $a$ . (If the reactor is reflected the reactor dimensions include the reflector savings.) As in the preceding section, it will be assumed that as the rod is withdrawn the hole that would ordinarily remain behind fills with core material, and contrariwise, as the rod is inserted, a cylinder of the reactor core is forced out of the system. Unless the rod is equipped with a rod follower, this assumption overestimates the worth of the rod.\*

In view of Eq. (14-4) or Eq. (14-5) the rod worth is determined by the bucklings of the system, that is, the first eigenvalues of the reactor equation, with the rod inserted and withdrawn. In both cases the flux satisfies the reactor equation

$$\nabla^2\phi_T + B^2\phi_T = 0.$$

With the rod out the flux is given by (cf. Section 9-3)

$$\phi_{T0}(r, z) = AJ_0\left(\frac{2.405r}{R}\right) \cos\left(\frac{\pi z}{H}\right), \quad (14-17)$$

and the buckling  $B_0^2$  is

$$B_0^2 = \left(\frac{2.405}{R}\right)^2 + \left(\frac{\pi}{H}\right)^2. \quad (14-18)$$

The quantity  $(2.405/R)^2$ , which is often called the radial buckling, will be given the symbol  $\alpha_0^2$ , so that

$$B_0^2 = \alpha_0^2 + \left(\frac{\pi}{H}\right)^2. \quad (14-19)$$

The criticality problem with the rod inserted is complicated by the fact that the rod is a strong absorber of neutrons (although not necessarily black), and diffusion theory is not applicable in or near the rod. This difficulty can be circumvented by simply considering the rod to be a region external to the reactor as discussed in the preceding section. Diffusion theory can then be employed in regions up to the edge of the rod by using an appropriate boundary condition at the rod-reactor interface. This is precisely the same procedure as that used in Section 11-2 for

---

\* The error introduced by this assumption can be corrected using methods discussed in Chapter 15.

the calculation of the thermal utilization by the method of Amouyal, Benoist, and Horowitz.

Thus the boundary condition at the rod surface is written as

$$\frac{1}{\phi_T} \left. \frac{d\phi_T}{dr} \right|_{r=a} = \frac{1}{d}, \quad (14-20)$$

where  $a$  is the physical radius of the rod, and  $d$  is the linear extrapolation distance, which, in general, depends upon the radius of the rod and the scattering properties of the rod and core material. Figure 11-10 shows  $d$  for black rods. Values of  $d$  for grey rods will be found in the references at the end of the chapter (see, in particular, ANL-5800).\*

With the rod inserted in the reactor there is no reason to exclude solutions to the reactor equation which are singular at  $r = 0$ , since the region occupied by the rod is considered to be external to the reactor. With the rod present, the flux may then be assumed of the form

$$\phi_T(r) = A \left[ J_0(\alpha r) - \frac{J_0(\alpha R)}{Y_0(\alpha R)} Y_0(\alpha r) \right] \cos \left( \frac{\pi z}{H} \right), \quad (14-21)$$

where

$$B^2 = \alpha^2 + \left( \frac{\pi}{H} \right)^2. \quad (14-22)$$

As may readily be seen, this function satisfies the reactor equation and also vanishes for  $r = R$  and  $z = \pm H/2$ , that is, at the surface of the reactor. Next, applying the boundary condition at the rod-reactor interface, Eq. (14-20) gives

$$\frac{\alpha [J'_0(\alpha a) - J_0(\alpha R) Y'_0(\alpha a) / Y_0(\alpha R)]}{J_0(\alpha a) - J_0(\alpha R) Y_0(\alpha a) / Y_0(\alpha R)} = \frac{1}{d}. \quad (14-23)$$

Using the identities  $J'_0(\alpha a) = -J_1(\alpha a)$  and  $Y'_0(\alpha a) = -Y_1(\alpha a)$ , this becomes

$$-\frac{\alpha [J_1(\alpha a) - J_0(\alpha R) Y_1(\alpha a) / Y_0(\alpha R)]}{J_0(\alpha a) - J_0(\alpha R) Y_0(\alpha a) / Y_0(\alpha R)} = \frac{1}{d}. \quad (14-24)$$

---

\* Although the curve of  $d$  versus  $a$  shown in Figure 11-10 and values of  $d$  for grey rods given in the references have been used in control rod calculations for many years, it should be recognized that these values are by no means exact. In particular, they are based on *one-velocity* transport theory calculations for a rod placed in an *infinite, source-free, nonabsorbing* medium into which neutrons enter only from *infinity*. Clearly, these assumptions do not reproduce the conditions actually found in a reactor. Thus reactors are finite; thermal neutrons are not monoenergetic and appear as distributed (thermalized) sources throughout the system; and, finally, all reactor materials absorb neutrons. Unfortunately, exact values of  $d$  have not been obtained as yet due to certain computational difficulties. There is reason to believe, however, that the exact values are somewhat larger than those currently in use. [Cf. G. C. Pomraning, "On the Linear Extrapolation Distance," *Nuclear Science and Engineering* 16, 239 (1963).]

Equation (14-24) is the critical condition for the reactor with the rod inserted. The smallest positive value of  $\alpha$ , which satisfies this equation, that is, the first eigenvalue, must next be determined by numerical or graphical methods. Once this value of  $\alpha$  is known,  $B^2$  can be computed from Eq. (14-22), and  $\rho_w$  is then given by Eqs. (14-4) or (14-5). It must be emphasized that it is necessary to set up and solve the critical equation simply because this equation determines the buckling, i.e., first eigenvalue of the reactor with the rod present. As explained in Section 14-1, this reactor may not actually be critical.

If the rod and its worth are both small, an approximate solution to Eq. (14-24) can easily be found. Thus according to the formulae in Appendix II, if  $\alpha \ll 1$ , then

$$\begin{aligned} J_0(\alpha a) &\approx 1, \quad J_1(\alpha a) \approx 0, \\ Y_0(\alpha a) &\approx -\frac{2}{\pi} \left[ 0.116 + \ln \left( \frac{1}{\alpha_0 a} \right) \right] = -\frac{2}{\pi} \left[ 0.116 + \ln \left( \frac{R}{2.405 a} \right) \right], \\ Y_1(\alpha a) &\approx -\frac{2}{\pi \alpha a}. \end{aligned}$$

Furthermore, letting  $\alpha = \alpha_0 + \Delta\alpha$ , the Bessel functions evaluated at  $r = R$  can be expanded as

$$\begin{aligned} J_0(\alpha R) &= J_0(\alpha_0 R + R \Delta\alpha) \\ &\approx J_0(\alpha_0 R) + J'_0(\alpha_0 R) R \Delta\alpha \\ &= J_0(\alpha_0 R) - J_1(\alpha_0 R) R \Delta\alpha. \end{aligned} \tag{14-25}$$

However,

$$J_0(\alpha_0 R) = J_0(2.405) = 0$$

and

$$J_1(\alpha_0 R) = J_1(2.405) = 0.519,$$

so that  $J_0(\alpha R) \approx -0.519 R \Delta\alpha$ . Also,  $Y_0(\alpha R) \approx Y_0(\alpha_0 R) = 0.510$ .

When these results are substituted into Eq. (14-24) and the equation is solved for  $\Delta\alpha$ , the following expression is obtained:

$$\Delta\alpha = \frac{1.54}{R} \left[ 0.116 + \ln \left( \frac{R}{2.405 a} \right) + \frac{d}{a} \right]^{-1}. \tag{14-26}$$

From Eq. (14-22), however,

$$\alpha_0 \Delta\alpha \approx B_0 \Delta B, \tag{14-27}$$

so that from Eq. (14-26) and Eq. (14-5),

$$\rho_w = \frac{7.43 M^2}{(1 + B_0^2 M^2) R^2} \left[ 0.116 + \ln \left( \frac{R}{2.405 a} \right) + \frac{d}{a} \right]^{-1}, \tag{14-28}$$

where  $B_0^2$  is given by Eq. (14-19). This is the reactivity worth of a small central cylindrical control rod according to modified one-group theory.

### 14-3 Two-Group Theory of Control Rod

The preceding one-group calculation tends to overestimate control-rod worth. This is because in the one-group model it is implicitly assumed that the rod absorbs neutrons of all energies at the same rate, whereas in actual fact control rods absorb fast neutrons to a far lesser extent than thermal neutrons. This can be taken into account approximately by going to a two-group calculation. Multigroup calculations are necessary if even greater accuracy is desired.

With the rod absent, the two-group fluxes are given by (cf. Prob. 10-14)

$$\phi_1(r, z) = AJ_0\left(\frac{2.405r}{R}\right) \cos\left(\frac{\pi z}{H}\right) \quad (14-29)$$

and

$$\phi_2(r, z) = AS_1J_0\left(\frac{2.405r}{R}\right) \cos\left(\frac{\pi z}{H}\right), \quad (14-30)$$

where  $S_1$  is the coupling coefficient defined by Eq. (10-49). The parameter  $\mu_0^2$ , which is equal to the buckling for the bare reactor with the rod withdrawn, is

$$\mu_0^2 = \left(\frac{2.405}{R}\right)^2 + \left(\frac{\pi}{H}\right)^2. \quad (14-31)$$

When the rod is fully inserted the fast and thermal fluxes are given by

$$\phi_1(r, z) = AX(r, z) + CY(r, z) \quad (14-32)$$

and

$$\phi_2(r, z) = AS_1X(r, z) + CS_2Y(r, z). \quad (14-33)$$

Here  $S_1$  and  $S_2$  are the coupling constants (cf. Eq. 10-49) and the functions  $X(r, z)$  and  $Y(r, z)$  satisfy the equations

$$(\nabla^2 + \mu^2)X(r, z) = 0 \quad (14-34)$$

and

$$(\nabla^2 - \lambda^2)Y(r, z) = 0, \quad (14-35)$$

where  $\mu^2$  and  $\lambda^2$  are given by Eqs. (10-37) and (10-38).

The fluxes must satisfy a number of boundary conditions. In particular, both  $\phi_1$  and  $\phi_2$  must vanish at  $z = \pm H/2$  and at  $r = R$ . Furthermore, at  $r = a$  the thermal flux must satisfy the condition

$$\frac{1}{\phi_2} \frac{d\phi_2}{dr} \Big|_{r=a} = \frac{1}{d}, \quad (14-36)$$

as in the one-group problem. Finally, since the fast neutrons are not appreciably absorbed by the rod, there can be no net current of fast neutrons into the rod so that

$$\frac{d\phi_1}{dr} \Big|_{r=a} = 0. \quad (14-37)$$

By separation of variables, or better, by direct substitution, it is easy to see that the functions

$$X(r, z) = \left[ J_0(\alpha r) - \frac{J_0(\alpha R)}{Y_0(\alpha R)} Y_0(\alpha r) \right] \cos\left(\frac{\pi z}{H}\right) \quad (14-38)$$

and

$$Y(r, z) = \left[ K_0(\beta r) - \frac{K_0(\beta R)}{I_0(\beta R)} I_0(\beta r) \right] \cos\left(\frac{\pi z}{H}\right), \quad (14-39)$$

where

$$\alpha^2 + \left(\frac{\pi}{H}\right)^2 = \mu^2 \quad (14-40)$$

and

$$\beta^2 - \left(\frac{\pi}{H}\right)^2 = \lambda^2, \quad (14-41)$$

satisfy both Eqs. (14-34) and (14-35) and the boundary conditions at the surface of the reactor. For future reference, it may be noted here that  $\alpha^2$  and  $\beta^2$  are closely related parameters. Thus subtracting Eq. (14-40) from Eq. (14-41) gives

$$\beta^2 = \alpha^2 + \lambda^2 - \mu^2 + 2\left(\frac{\pi}{H}\right)^2. \quad (14-42)$$

However, from Eq. (10-36),

$$\lambda^2 - \mu^2 = \frac{1}{\tau} + \frac{1}{L^2},$$

and Eq. (14-42) reduces to

$$\beta^2 = \alpha^2 + \frac{1}{\tau} + \frac{1}{L^2} + 2\left(\frac{\pi}{H}\right)^2. \quad (14-43)$$

Substituting Eqs. (14-38) and (14-39) into Eq. (14-33) and then into Eq. (14-36) gives

$$\begin{aligned} \frac{1}{d} &= \frac{AS_1\alpha \left[ J'_0(\alpha a) - \frac{J_0(\alpha R)}{Y_0(\alpha R)} Y'_0(\alpha a) \right] + CS_2\beta \left[ K'_0(\beta a) - \frac{K_0(\beta R)}{I_0(\beta R)} I'_0(\beta a) \right]}{AS_1 \left[ J_0(\alpha a) - \frac{J_0(\alpha R)}{Y_0(\alpha R)} Y_0(\alpha a) \right] + CS_2 \left[ K_0(\beta a) - \frac{K_0(\beta R)}{I_0(\beta R)} I_0(\beta a) \right]} \\ &= - \frac{AS_1\alpha \left[ J_1(\alpha a) - \frac{J_0(\alpha R)}{Y_0(\alpha R)} Y_1(\alpha a) \right] + CS_2\beta \left[ K_1(\beta a) + \frac{K_0(\beta R)}{I_0(\beta R)} I_1(\beta a) \right]}{AS_1 \left[ J_0(\alpha a) - \frac{J_0(\alpha R)}{Y_0(\alpha R)} Y_0(\alpha a) \right] + CS_2 \left[ K_0(\beta a) - \frac{K_0(\beta R)}{I_0(\beta R)} I_0(\beta a) \right]}. \end{aligned} \quad (14-44)$$

The ratio  $C/A$  may now be found by inserting Eq. (14-32) into Eq. (14-37), viz.,

$$\frac{C}{A} = - \frac{\alpha}{\beta} \frac{J_1(\alpha a) - \frac{J_0(\alpha R)}{Y_0(\alpha R)} Y_1(\alpha a)}{K_1(\beta a) + \frac{K_0(\beta R)}{I_0(\beta R)} I_1(\beta a)}. \quad (14-45)$$

Introducing this expression into Eq. (14-44) gives finally

$$\begin{aligned} \frac{1}{d} = & -\alpha\beta(S_1 - S_2) \left[ J_1(\alpha a) - \frac{J_0(\alpha R)}{Y_0(\alpha R)} Y_1(\alpha a) \right] \left[ K_1(\beta a) + \frac{K_0(\beta R)}{I_0(\beta R)} I_1(\beta a) \right] \\ & \div \left\{ \beta S_1 \left[ J_0(\alpha a) - \frac{J_0(\alpha R)}{Y_0(\alpha R)} Y_0(\alpha a) \right] \left[ K_1(\beta a) + \frac{K_0(\beta R)}{I_0(\beta R)} I_1(\beta a) \right] \right. \\ & \left. - \alpha S_2 \left[ J_1(\alpha a) - \frac{J_0(\alpha R)}{Y_0(\alpha R)} Y_1(\alpha a) \right] \left[ K_0(\beta a) - \frac{K_0(\beta R)}{I_0(\beta R)} I_0(\beta a) \right] \right\}. \end{aligned} \quad (14-46)$$

Equation (14-46) is the critical equation for the reactor with the rod inserted. The right-hand side of this equation is a function of the two parameters,  $\alpha$  and  $\beta$ . However, according to Eq. (14-43)  $\beta$  is directly related to  $\alpha$ , so that Eq. (14-46) may be considered to be a function of  $\alpha$  only. The critical value of  $\alpha$  can therefore be found by either numerical or graphical methods. This value of  $\alpha$  determines  $\mu^2$  through Eq. (14-40). The rod worth is then obtained by inserting  $\mu^2$  and  $\mu_0^2$  into Eq. (14-13) or Eq. (14-14).

If the rod is small, that is, if  $a \ll R$ , and also if  $L \ll R$ ,  $H$  and  $\sqrt{\tau} \ll R$ ,  $H$  (which is true except in very small cores), Eq. (14-46) can be simplified as was done in the one group calculation. Thus when these conditions are satisfied it is possible to write

$$\begin{aligned} J_0(\alpha a) &\approx 1, \quad J_1(\alpha a) \approx 0, \\ Y_0(\alpha a) &\approx -\frac{2}{\pi} \left[ 0.116 + \ln \left( \frac{1}{\alpha a} \right) \right], \quad Y_1(\alpha a) \approx -\frac{2}{\pi \alpha a}, \\ K_0(\beta a) &\approx 0.116 + \ln \left( \frac{1}{\beta a} \right), \quad K_1(\beta a) \approx \frac{1}{\beta a}. \end{aligned}$$

Also, as in the preceding section,

$$J_0(\alpha R) \approx -0.519 R \Delta \alpha \quad \text{and} \quad Y_0(\alpha R) \approx 0.510.$$

Furthermore, when  $\beta a$  is small,

$$K_0(\beta a) - \frac{K_0(\beta R)}{I_0(\beta R)} I_0(\beta a) \approx K_0(\beta a) \quad (14-47)$$

and

$$K_1(\beta a) - \frac{K_0(\beta R)}{I_0(\beta R)} I_1(\beta a) \approx K_1(\beta a). \quad (14-48)$$

Inserting these approximations into Eq. (14-46) and solving for  $\Delta \alpha$  yields

$$\Delta \alpha = \frac{1.54}{R} \left[ 0.116 \left( 1 - \frac{S_2}{S_1} \right) - \frac{S_2}{S_1} \ln \left( \frac{1}{\beta a} \right) + \ln \left( \frac{1}{\alpha a} \right) + \frac{d}{a} \left( 1 - \frac{S_2}{S_1} \right) \right]^{-1}. \quad (14-49)$$

From Eq. (14-40),

$$\alpha \Delta \alpha \approx \alpha_0 \Delta \alpha = \mu_0 \Delta \mu. \quad (14-50)$$

Also, from Eq. (14-41), and noting that  $\mu^2 \ll \lambda^2$ ,

$$\beta^2 \approx \lambda^2 \approx \frac{1}{\tau} + \frac{1}{L^2}, \quad (14-51)$$

so that

$$\beta \approx \frac{M}{L\sqrt{\tau}}. \quad (14-52)$$

When these results are introduced into Eq. (14-16), the worth of a small central control rod is found to be

$$\begin{aligned} \rho_w = & \frac{7.43M^2}{(1 + \mu_0^2 M^2)R^2} \left[ 0.116 \left( 1 - \frac{S_2}{S_1} \right) - \frac{S_2}{S_1} \ln \left( \frac{L\sqrt{\tau}}{aM} \right) \right. \\ & \left. + \ln \left( \frac{R}{2.405a} \right) + \frac{d}{a} \left( 1 - \frac{S_2}{S_1} \right) \right]^{-1}. \end{aligned} \quad (14-53)$$

According to Eq. (10-49), the ratio  $S_2/S_1$  is given by

$$\frac{S_2}{S_1} = \frac{1 + \mu^2 L^2}{1 - \lambda^2 L^2}. \quad (14-54)$$

It can easily be shown from Eqs. (10-37) and (10-38) that for small values of  $\tau$ ,  $S_2/S_1$  is proportional to  $\tau$ . Thus in the limit as  $\tau \rightarrow 0$ , which corresponds to a one-group situation, Eq. (14-53) properly reduces to the one-group formula given by Eq. (14-28).

#### 14-4 The Eccentric Control Rod

The calculation of control-rod worth is somewhat more involved when the rod is not located along the axis of the reactor. For simplicity, the present discussion will therefore be confined to the modified one-group model.

It is convenient to set up two coordinate systems; one centered on the axis of the reactor, and the other centered on the axis of the rod (cf. Fig. 14-2). Any point in the reactor then has coordinates  $(r, \vartheta)$  with respect to the first coordinate system and  $(\xi, \psi)$  with respect to the other. It should be especially noted that  $\vartheta$  is measured from the line joining the axis of the reactor with the axis of the rod. In view of the symmetry of the problem, the flux must therefore be an even function of  $\vartheta$ .

As in the previous section, the rod is replaced by the boundary condition, Eq. (14-20), at the rod-reactor interface. The flux must then be found throughout the core excluding the region occupied by the rod. Since the solution need not be finite in this excluded region, it is possible to write the flux as the sum of a function,  $\phi_r$ , which is regular (nonsingular) over the entire core, plus another function,  $\phi_i$ , which is irregular (singular) within the rod. Thus

$$\phi_T = \phi_r + \phi_i. \quad (14-55)$$

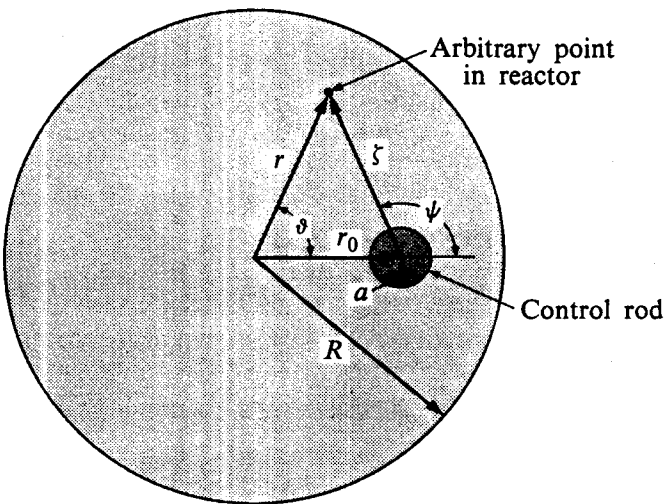


Fig. 14-2. An eccentric control rod in a bare cylindrical reactor.

It may readily be verified that the general solution to the reactor equation which is nonsingular throughout the reactor and which is even in  $\vartheta$  is of the form

$$\phi_r = \cos\left(\frac{\pi z}{H}\right) \sum_{m=0}^{\infty} A_m J_m(\alpha r) \cos m\vartheta, \quad (14-56)$$

where  $A_m$  are constants to be determined and, as usual,

$$B^2 = \alpha^2 + \left(\frac{\pi}{H}\right)^2. \quad (14-57)$$

The behavior of the flux in the vicinity of the rod is determined to a large extent by the function  $\phi_i$ , since this varies so rapidly near the rod. However, if the radius of the rod is small compared with the radius of the reactor, the flux will tend to be rather symmetric about the rod. In other words,  $\phi_i$  can be taken to be the singular solution to the reactor equation in the coordinate system  $(\xi, \psi)$  which is independent of  $\psi$ , namely,

$$\phi_i = A \cos\left(\frac{\pi z}{H}\right) Y_0(\alpha\xi). \quad (14-58)$$

The complete solution for the flux from Eq. (14-55) is then

$$\phi_T = \cos\left(\frac{\pi z}{H}\right) \left[ \sum_{m=0}^{\infty} A_m J_m(\alpha r) \cos m\vartheta + A Y_0(\alpha\xi) \right]. \quad (14-59)$$

From the addition theorem for Bessel functions\*

$$Y_0(\alpha\xi) = Y_0(\alpha r)J_0(\alpha r_0) + 2 \sum_{m=1}^{\infty} Y_m(\alpha r)J_m(\alpha r_0) \cos m\vartheta, \quad (14-60)$$

---

\* See any book on advanced calculus or function theory.

Eq. (14-59) becomes

$$\phi_T = \cos\left(\frac{\pi z}{H}\right) \left\{ A Y_0(\alpha r) J_0(\alpha r_0) + A_0 J_0(\alpha r) \right. \\ \left. + \sum_{m=1}^{\infty} [A_m J_m(\alpha r) + 2A Y_m(\alpha r) J_m(\alpha r_0)] \cos m\vartheta \right\}. \quad (14-61)$$

The flux must vanish at  $r = R$  for all values of  $\vartheta$ , and from Eq. (14-61) it follows that

$$A_0 = - \frac{A Y_0(\alpha R) J_0(\alpha r_0)}{J_0(\alpha R)} \quad (14-62)$$

and

$$A_m = - \frac{2A Y_m(\alpha R) J_m(\alpha r_0)}{J_m(\alpha R)}. \quad (14-63)$$

Introducing the quantity  $\delta_m$  defined by

$$\delta_m = \begin{cases} 1, & m = 0, \\ 2, & m > 0, \end{cases} \quad (14-64)$$

Eq. (14-59) can be written as

$$\phi_T = A \cos\left(\frac{\pi z}{H}\right) \left[ Y_0(\alpha \xi) - \sum_{m=0}^{\infty} \frac{\delta_m Y_m(\alpha R) J_m(\alpha r_0)}{J_m(\alpha R)} J_m(\alpha r) \cos m\vartheta \right]. \quad (14-65)$$

The boundary condition at the surface of the rod is

$$\frac{1}{\phi_T} \frac{d\phi_T}{d\xi} \Big|_{\xi=a} = \frac{1}{d}. \quad (14-66)$$

This condition can now be satisfied by noting that the regular part of  $\phi_T$ , which is given by the summation in Eq. (14-65), is relatively constant near the rod. In this region, therefore, since the rod is located at  $\vartheta = 0$ ,

$$\phi_T(\xi) \approx A \cos\left(\frac{\pi z}{H}\right) \left[ Y_0(\alpha \xi) - \sum_{m=0}^{\infty} \frac{\delta_m Y_m(\alpha R) J_m^2(\alpha r_0)}{J_m(\alpha R)} \right]. \quad (14-67)$$

Using this function in Eq. (14-66) gives

$$\frac{1}{d} = - \frac{\alpha Y_1(\alpha a)}{Y_0(\alpha a) - \sum_{m=0}^{\infty} \delta_m Y_m(\alpha R) J_m^2(\alpha r_0) / J_m(\alpha R)}. \quad (14-68)$$

Equation (14-68) is the one-group critical equation for the eccentric rod. The worth of the rod can now be found by first solving Eq. (14-68) for  $\alpha$  and then computing  $B^2$  from Eq. (14-57). The worth is then given by Eq. (14-4) or (14-5).

To simplify the computations, it may be noted that the higher terms in the series in the denominator of Eq. (14-68) make decreasing contributions to the sum, and as a rough approximation, the series may be truncated after the first

term. Also, if  $a \ll R$ , it is possible as in the preceding sections to write

$$Y_0(\alpha a) \approx -\frac{2}{\pi} [0.116 + \ln(1/\alpha a)],$$

$$Y_1(\alpha a) \approx -2/\pi \alpha a, \quad Y_0(\alpha R) \approx 0.510, \quad J_0(\alpha R) \approx -0.519R \Delta\alpha.$$

When these formulas are introduced into Eq. (14-68), the resulting equation can be solved for  $\Delta\alpha$ . An expression for  $\Delta B$  can then be obtained using Eq. (14-27). Finally, when  $\Delta B$  is substituted into Eq. (14-5), the rod worth is found to be

$$\rho_w = \frac{7.43M^2}{(1 + B_0^2 M^2)R^2} J_0^2\left(\frac{2.405r_0}{R}\right) \left[0.116 + \ln\left(\frac{R}{2.405a}\right) + \frac{d}{a}\right]^{-1}. \quad (14-69)$$

A comparison of Eq. (14-69) with Eq. (14-28) shows that according to one-group theory the effectiveness of an eccentric rod is equal to the effectiveness of a central rod multiplied by the factor  $J_0^2(2.405r_0/R)$ . This factor is just the square of the thermal flux at  $r_0$ , normalized to unity at  $r = 0$ . The physical reason for the reduction in the worth of the rod with increasing distance from the axis of the reactor is simply that the rod absorbs fewer neutrons in the lower flux. The reason why the worth involves the *square* of the flux will be discussed in Chapter 15.

### 14-5 Ring of Rods

Reactors are never constructed with only one control rod. They always contain a number of rods arranged in one or more rings, and frequently there is also a rod at the reactor center. Since the analysis is quite tedious for more complicated cases, the present section is limited to a single ring of  $N$  equally spaced rods and the one-group model will be used throughout.

Generalizing the case of the single eccentric rod, it is reasonable to assume a solution for the flux of the form

$$\phi_T = A \sum_{n=1}^N Y_0(\alpha \xi_n) + \sum_{m=0}^{\infty} A_m J_m(\alpha r) \cos m\vartheta, \quad (14-70)$$

where  $\xi_n$  is a radial variable measured from the center of the  $n$ th rod, and  $\vartheta$  is measured clockwise from an arbitrarily chosen first rod, as shown in Fig. 14-3. Each of the terms in the first summation corresponds to a single rod, and in view of the symmetry of the system all of these terms must be equal. It should also be noted that since the rods are equally spaced the flux is an even function of  $\vartheta$ ; hence the use of  $\cos m\vartheta$  in Eq. (14-70).

Expanding the  $Y_0(\alpha \xi_n)$  functions by the Bessel function addition theorem, Eq. (14-60) gives

$$Y_0(\alpha \xi_n) = Y_0(\alpha r) J_0(\alpha r_0) + 2 \sum_{m=1}^{\infty} Y_m(\alpha r) J_m(\alpha r_0) \cos m\vartheta_n. \quad (14-71)$$

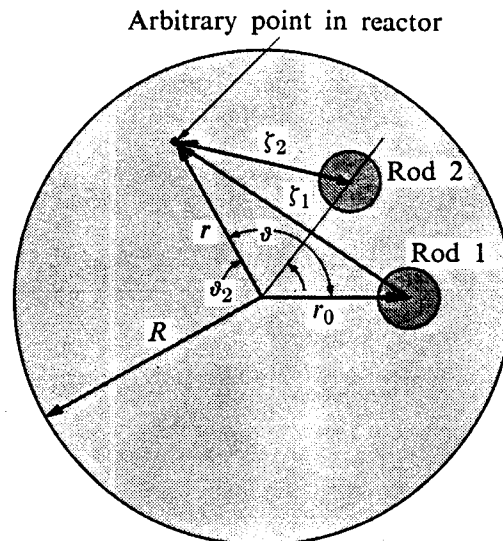


Fig. 14-3. Ring of control rods in a bare cylindrical reactor.

In this expression  $\vartheta_n$  is an angle measured clockwise from the  $n$ th rod, and  $\vartheta_1 \equiv \vartheta$  (cf. Fig. 14-3). The flux then becomes

$$\begin{aligned}\phi_T = A & \left[ NY_0(\alpha r)J_0(\alpha r_0) + 2 \sum_{m=1}^{\infty} \sum_{n=1}^N Y_m(\alpha r)J_m(\alpha r_0) \cos m\vartheta_n \right] \\ & + \sum_{m=0}^{\infty} A_m J_m(\alpha r) \cos m\vartheta.\end{aligned}\quad (14-72)$$

Consider now the second term in Eq. (14-72). From Fig. 14-3 it is seen that

$$\vartheta_n = \vartheta - \frac{2\pi(n-1)}{N}. \quad (14-73)$$

Writing  $\cos m\vartheta_n$  in exponential form, the sum on  $n$  in the second term becomes

$$\begin{aligned}\sum_{n=1}^N \cos m\vartheta_n &= \frac{1}{2} \sum_{n=1}^N \left\{ \exp \left[ im \left( \vartheta - \frac{2\pi(n-1)}{N} \right) \right] \right. \\ &\quad \left. + \exp \left[ -im \left( \vartheta - \frac{2\pi(n-1)}{N} \right) \right] \right\}.\end{aligned}\quad (14-74)$$

Each of these sums can be written in closed form using the familiar formula

$$\sum_{n=1}^N x^{n-1} = \frac{1-x^N}{1-x}, \quad (14-75)$$

where in the present instance  $x = \exp(-2\pi mi/N)$ . The first sum is then

$$\sum_{n=1}^N \exp \left[ im \left( \vartheta - \frac{2\pi(n-1)}{N} \right) \right] = e^{im\vartheta} \left[ \frac{1-e^{-2\pi mi}}{1-e^{-2\pi mi/N}} \right]. \quad (14-76)$$

The numerator of this expression is zero for every value of  $m$ , since  $\exp(-2\pi mi) = 1$ . On the other hand, the denominator is zero only when  $m/N$  is an integer. In this case, the fraction in Eq. (14-76) is indeterminate and has the value  $N$ . Thus

$$\sum_{n=1}^N \exp \left[ im \left( \vartheta - \frac{2\pi(n-1)}{N} \right) \right] = \begin{cases} Ne^{im\vartheta}, & m = N, 2N, 3N, \dots, \\ 0, & \text{otherwise.} \end{cases} \quad (14-77)$$

A similar result is obtained for the second sum in Eq. (14-74), and it follows that

$$\sum_{n=1}^N \cos m\vartheta_n = \begin{cases} N \cos m\vartheta, & m = N, 2N, 3N, \dots, \\ 0, & \text{otherwise.} \end{cases} \quad (14-78)$$

The flux is therefore

$$\begin{aligned} \phi_T = A & \left[ NY_0(\alpha r)J_0(\alpha r_0) + 2N \sum_{m/N \text{ integer}}^{\infty} Y_m(\alpha r)J_m(\alpha r_0) \cos m\vartheta \right] \\ & + \sum_{m=0}^{\infty} A_m J_m(\alpha r) \cos m\vartheta. \end{aligned} \quad (14-79)$$

The boundary condition  $\phi(R) = 0$  can now be satisfied for all values of  $\vartheta$ , and from Eq. (14-79) this gives

$$A_0 = - \frac{AN Y_0(\alpha R)J_0(\alpha r_0)}{J_0(\alpha R)}, \quad (14-80)$$

$$A_m = - \frac{2AN Y_m(\alpha R)J_m(\alpha r_0)}{J_m(\alpha R)}, \quad m = N, 2N, 3N, \dots, \quad (14-81)$$

$$A_m = 0, \quad m \neq 0, N, 2N, 3N, \dots \quad (14-82)$$

Thus returning to Eq. (14-70), the flux can be written as

$$\phi_T = A \left\{ \sum_{n=1}^N Y_0(\alpha \xi_n) - N \sum_{\substack{m=0 \\ m/N \text{ integer}}}^{\infty} \frac{\delta_m Y_m(\alpha R)J_m(\alpha r_0)}{J_m(\alpha R)} J_m(\alpha r) \cos m\vartheta \right\}, \quad (14-83)$$

where  $\delta_m$  is defined by Eq. (14-64).

It is now necessary to satisfy the boundary conditions at the surface of the rods. Because of the symmetry of the problem, however, it is only necessary to consider one rod. In the neighborhood of the rod number 1, the variables  $\xi_2, \xi_3, \dots, \xi_N$  are roughly constant, provided the rods are not too closely spaced. It is possible, therefore, to replace the variables  $\xi_n$  for  $n > 1$  by the constants  $b_{1n}$ , where  $b_{1n}$  is the distance from the center of the first rod to the center of the  $n$ th rod. From Fig. 14-4, it is easy to see that  $b_{1n}$  is given by

$$b_{1n} = 2r_0 \sin \frac{(n-1)\pi}{N}. \quad (14-84)$$

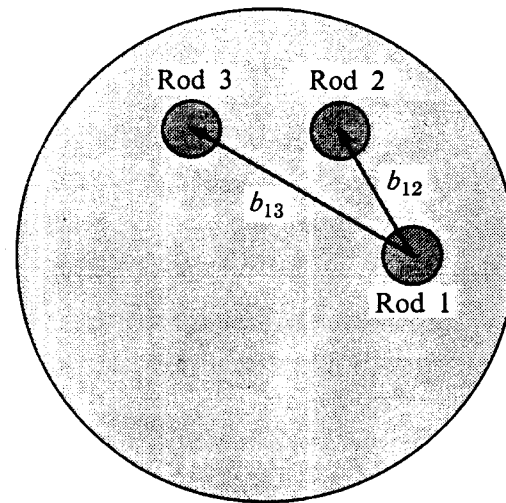


Fig. 14-4. The distance  $b_{1n}$  for a ring of control rods.

With rod 1 arbitrarily located at  $\vartheta = 0$ , Eq. (14-83) becomes

$$\phi_T(\xi_1) \approx A \left\{ Y_0(\alpha\xi_1) + \sum_{n=2}^N Y_0(\alpha b_{1n}) - N \sum_m \frac{\delta_m Y_m(\alpha R) J_m^2(\alpha r_0)}{J_m(\alpha R)} \right\}. \quad (14-85)$$

All quantities in Eq. (14-85) except  $\xi_1$  are constant near the first rod. Inserting Eq. (14-85) into the boundary condition, Eq. (14-66), the one-group critical equation for the reactor with a ring of rods is found to be

$$\frac{1}{d} = - \frac{\alpha Y_1(\alpha a)}{Y_0(\alpha a) + \sum_{n=2}^N Y_0(\alpha b_{1n}) - N \sum_m \delta_m Y_m(\alpha R) J_m^2(\alpha r_0) / J_m(\alpha R)}. \quad (14-86)$$

This equation must be solved by numerical or graphical methods for  $\alpha$ , and this value is used in the usual way to compute the worth of the ring of rods.

If  $a \ll R$ , Eq. (14-86) can be simplified as in the preceding sections [cf. discussion following Eq. (14-68)] with the following result:

$$\rho_w = \frac{7.43 M^2 N}{(1 + B_0^2 M^2) R^2} J_0^2 \left( \frac{2.405 r_0}{R} \right) \times \left[ 0.116 + \ln \left( \frac{R}{2.405 a} \right) + \frac{d}{a} - \frac{\pi}{2} \sum_{n=2}^N Y_0 \left( \frac{2.405 b_{1n}}{R} \right) \right]^{-1}. \quad (14-87)$$

Comparison of this expression with Eq. (14-69) shows that were it not for the term containing the summation, the worth of a ring of  $N$  rods would be simply  $N$  times the worth of a single rod located at the same distance from the reactor axis. This

would be the case if the rods acted independently. In actual fact, however, the presence of each rod changes the worth of all others by distorting the flux in their vicinity. The summation term in Eq. (14-87) accounts for the distortion of the flux at one rod due to the other rods.

To see the effect of the interaction of one rod upon another it is instructive to consider a ring consisting of only two rods. In this case, the summation in Eq. (14-87) reduces to only one term with  $b_{1n} = 2r_0$ . For two rods, therefore, according to one-group theory,

$$\rho_w = \frac{14.86M^2}{(1 + B_0^2 M^2)R^2} J_0^2\left(\frac{2.405r_0}{R}\right) \times \left[0.116 + \ln\left(\frac{R}{2.405a}\right) + \frac{d}{a} - \frac{\pi}{2} Y_0\left(\frac{4.81r_0}{R}\right)\right]^{-1}. \quad (14-88)$$

The function  $Y_0(x)$ , which is shown in Fig. II-2, is negative for  $x$  less than about 0.90 and positive for  $x$  greater than 0.90. Thus from Eq. (14-88), if  $4.81r_0/R < 0.90$ , that is,  $r_0 < 0.19R$ , the worth of the two rods is *less* than twice the worth of the two rods acting independently (cf. Eq. 14-69). This reduction in effectiveness per rod is due to the fact that the flux at each rod is reduced by the presence of the other, an effect known as *shadowing*.

On the other hand, if the rods are so placed that  $r_0 > 0.19R$ , then  $Y_0(4.81r_0/R)$  is positive and the worth of the two rods is *greater* than the sum of the worths of

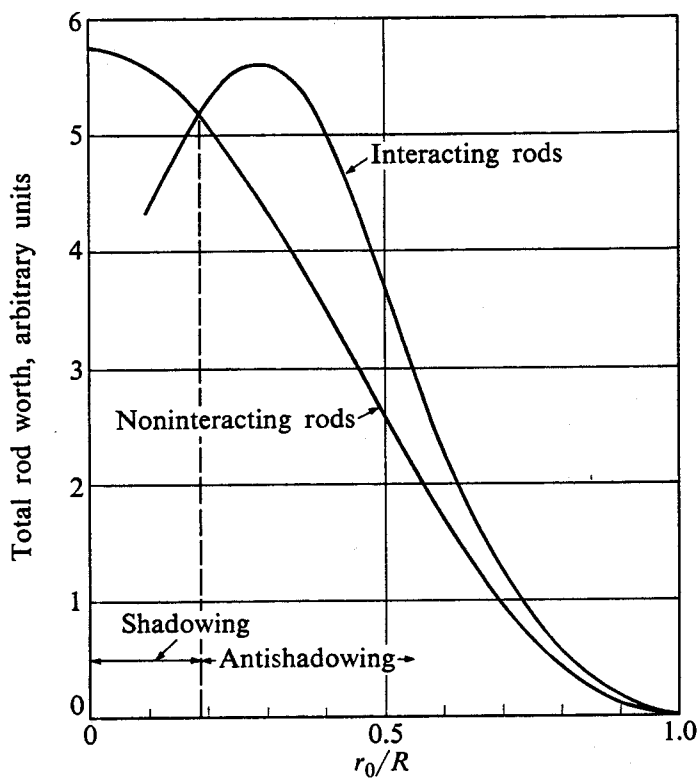


**Fig. 14-5.** The worth of two diametrically opposite control rods as a function of their distance from the axis of a cylindrical reactor, with and without interaction.

each rod acting alone. This effect, which is known as *antishadowing*, is caused by the increase in flux at each rod due to the other. This situation is illustrated in Fig. 14-5, where the worth (arbitrary units) of two rods is shown, with and without the interference term  $Y_0(4.81r_0/R)$ , as a function of their location in a reactor. The regions of shadowing and antishadowing are clearly evident.

### 14-6 Noncylindrical Rods

It was noted in the introduction to this chapter that for a number of reasons cylindrical rods are not used as frequently in reactors as they once were. Noncylindrical rods, particularly cruciform rods, have largely replaced cylindrical rods in many types of reactors. The worth of an isolated noncylindrical rod may be determined analytically by first finding the radius of the equivalent cylindrical rod. This radius is then used in the appropriate formulas derived in the preceding sections for the worth of the cylindrical rod. This procedure is not applicable to closely spaced or overlapping rods, which are often found in reactors having many cruciform rods. These must be treated by approximate analytical procedures or by numerical methods both of which are discussed in the next section.

The equivalent radius of a noncylindrical rod is found by solving the diffusion equation, subject to the usual boundary conditions at the rod surface. In view of the complicated geometry of the problem, the mathematical analysis is too involved to be reproduced here. Furthermore, it is not possible to obtain exact expressions for the equivalent radius except in special cases. However, if the effective radius is small compared with the diffusion length in the reactor core material, as is frequently the case, the effective radius  $a$  is given by the following formulas:

*Infinite flat ribbon.* If the ribbon has width  $w$  and essentially zero thickness, then

$$a = \frac{w}{4}. \quad (14-89)$$

*Cruciform rod.* If the span of the cross is  $w$ , then

$$a = \frac{w\sqrt{2}}{4} = 0.371w. \quad (14-90)$$

The formulas for the effective radius are considerably more complicated when  $a$  is not small compared to the reactor diffusion length, and the reader should consult the references at the end of the chapter for the effective radius in this case (see, especially, ANL-5800).

### 14-7 Many Rods

As mentioned earlier, many reactors, particularly power reactors, are designed with a large number of control rods, each rod having a relatively small worth. In this case, it is not usually practical to determine the worth of the entire array by using an analysis like that in Section 14-5 for a ring of rods, since the mathematics is too involved, and other methods must be used.

If the rods are arranged in a regular array, it is possible to compute their effectiveness by a procedure similar to that used to treat heterogeneous reactors. The reactor is first divided into cells, each containing one rod at its center. The *rod utilization*,  $f_R$ , is then defined as the number of thermal neutrons absorbed in the rod per neutron thermalizing in the cell. To compensate for the rods it is necessary to increase the thermal utilization of the system by the factor  $(1 - f_R)^{-1}$  to maintain criticality. Using Eq. (14-1) or Eq. (14-7), the worth of the array is therefore

$$\rho_w = \frac{k_\infty(1 - f_R)^{-1} - k_\infty}{k_\infty(1 - f_R)^{-1}} = f_R. \quad (14-91)$$

The computation of  $f_R$  is quite straightforward. The diffusion equation is solved in the cell using Wigner-Seitz boundary conditions at the outer boundary of the cell and Eq. (14-20) at the rod surface. The resulting expression for  $f_R$  is

$$\frac{1}{f_R} = \frac{(R_c^2 - a^2)d}{2aL_T^2} + E(\kappa a, \kappa R_c), \quad (14-92)$$

where  $R_c$  is the cell radius,  $a$  is the radius (or effective radius) of the rod,  $d$  is given by Eq. (14-20),  $\kappa = 1/L_T$  is the reciprocal thermal diffusion length in the core material, and  $E(\kappa a, \kappa R_c)$  is the lattice function (cf. Section 11-2)

$$E(\kappa a, \kappa R_c) = \frac{\kappa(R_c^2 - a^2)}{2a} \left[ \frac{I_0(\kappa a)K_1(\kappa R_c) + K_0(\kappa a)I_1(\kappa R_c)}{I_1(\kappa R_c)K_1(\kappa a) - K_1(\kappa R_c)I_1(\kappa a)} \right]. \quad (14-93)$$

In many cases this formula can be simplified (cf. Prob. 11-5).

The above technique is not applicable to reactors containing relatively large and closely spaced cruciform rods such as are often found in water reactors. In this case the following method due to A. F. Henry may be used. The reactor is again divided into cells, but now each cell is partly bounded by the blades of two rods as shown in Fig. 14-6. The rod utilization is then found by computing the ratio of the number of neutrons flowing into the blades per neutron thermalized in the cell.

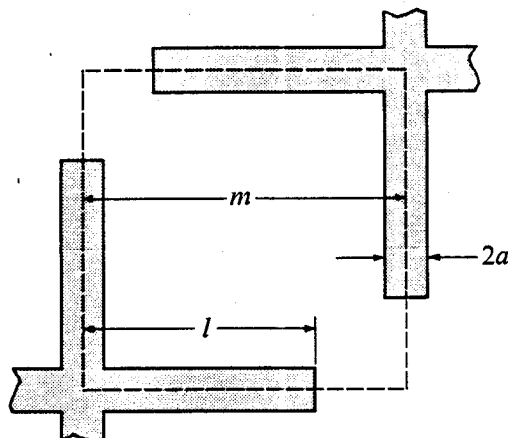


Fig. 14-6. Cell for calculation of worth of closely spaced cruciform rods.

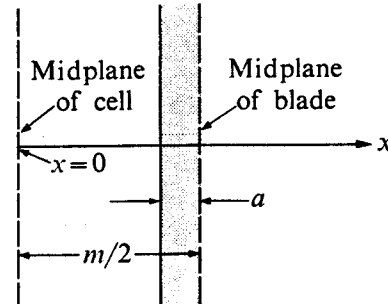


Fig. 14-7. Slab geometry for solution of diffusion equation.

In view of the complicated geometry of the problem it is not possible to obtain an exact analytical expression for  $f_R$ . An estimate of  $f_R$  can be made, however, by solving the diffusion equation in infinite slab geometry with the blade along one boundary as in Fig. 14-7. The diffusion equation is then

$$\bar{D} \frac{d^2\phi_T}{dx^2} - \bar{\Sigma}_a \phi_T = -q_T, \quad (14-94)$$

where  $\bar{D}$  and  $\bar{\Sigma}_a$  refer to the core material and  $q_T$  is the slowing-down density, assumed constant throughout the cell. The flux must be an even function and satisfy the boundary condition (note that  $\phi'_T$  is negative)

$$\frac{1}{\phi_T} \frac{d\phi_T}{dx} = - \frac{1}{d} \quad (14-95)$$

at the blade surface, that is, at  $x = (m/2) - a$ . If the rods are black,  $d = 0.71\lambda_{tr} = 3 \times 0.71\bar{D}$  (cf. Fig. 11-10). It is readily seen that  $\phi_T(x)$  is given by

$$\phi_T(x) = \frac{q_T}{\bar{\Sigma}_a} \left[ 1 - \frac{\cosh(x/L_T)}{(d/L_T) \sinh[(m-2a)/2L_T] + \cosh[(m-2a)/2L_T]} \right]. \quad (14-96)$$

The quantity  $f_R$  is now obtained by multiplying the current at the surface of the blade [computed from Eq. (14-96)] by the length of the blades which border the cell, and dividing by the total number of neutrons thermalized in the cell. The final result is

$$\rho_w = f_R = \frac{4(l-a)L_T}{(m-2a)^2} \frac{1}{(d/L_T) + \coth[(m-2a)/2L_T]}. \quad (14-97)$$

In view of the nature of the above derivation, Eq. (14-97) only provides a rough estimate of the worth of the assembly of rods. More exact values can be obtained, however, by solving the diffusion equation numerically in two dimensions using an electronic computer. It is then possible to take into account the actual shape of the rods and the fraction of each cell bordered by the rod blades. Computer programs have also been written for two dimensional multigroup calculations of this nature. Such calculations are particularly important if the control rods absorb neutrons at energies above thermal to any appreciable extent.

Another method which is often used to estimate the worth of a large array of rods is to replace the rods by an equivalent distribution of poisons. If the rods are spaced uniformly in a region of the reactor, for example, these rods are replaced by a uniform distribution of poisons in this region. If the rods are arranged in many concentric rings, they may be replaced by concentric annular regions of different absorption cross section. The worth of the array of rods is then found by comparing the multiplication factor of the poisoned and unpoisoned reactors computed from a one-group or a multigroup calculation. This procedure is particularly reasonable for fast reactors since in these reactors the mean free path of fast neutrons is always much larger than the dimensions of a control rod.

## References

### General

ETHERINGTON, H., Editor, *Nuclear Engineering Handbook*. New York: McGraw-Hill, 1958, Section 8-1.

GALANIN, A. D., *Thermal Reactor Theory*, 2nd ed. New York: Pergamon Press, 1960, Section 31.

GLASSTONE, S., and M. C. EDLUND, *The Elements of Nuclear Reactor Theory*. Princeton, N.J.: Van Nostrand, 1952, Chapter 11.

ISBIN, H. S., *Introductory Nuclear Reactor Theory*. New York: Reinhold, 1963, Section 16-7.

MEEM, J. L., *Two-Group Reactor Theory*. New York: Gordon and Breach, 1964, Chapter 8.

MEGHREBLIAN, R. V., and D. K. HOLMES, *Reactor Analysis*. New York: McGraw-Hill, 1960, Chapter 11.

MURRAY, R. L., *Nuclear Reactor Physics*. Englewood Cliffs, N.J.: Prentice-Hall, 1957, Chapter 8.

SCHULTZ, M. A., *Control of Nuclear Reactors and Power Plants*, 2nd ed. New York: McGraw-Hill, 1961, Chapter 8.

SOODAK, H., Editor, *Reactor Handbook*, 2nd ed., Vol. III, Part A. New York: Wiley, 1962, Section 4.6.

WEINBERG, A. M., and E. P. WIGNER, *The Physical Theory of Neutron Chain Reactors*. Chicago: University of Chicago Press, 1958, Chapter 22.

### Special

HENRY, A. F., U.S. Atomic Energy Commission Report TID-7532, Part 1 (1957), p. 3. Henry's method for treating cruciform rods is explained in this report.

"Reactor Physics Constants," U.S. Atomic Energy Commission Report ANL-5800, 2nd ed., 1963, Section 5.1. Values of  $d$  for grey and black rods and the equivalent radii of noncylindrical rods are reproduced from the original papers in Section 5.1 of this report.

SPINKS, N., "The Extrapolation Distance at the Surface of a Grey Cylindrical Control Rod," *Nuclear Science and Engineering* 22, 87 (1965). Tables relating the extrapolation distances of black and grey rods are given in this paper as a function of the "blackness" of the rods.

## Problems

14-1. An infinite sheet of absorber of thickness  $a$  is placed in an infinite medium containing uniformly distributed sources emitting  $S$  neutrons/cm<sup>3</sup>-sec. (a) Using one-group theory, derive an expression for the thermal flux in the medium. (b) Show that the number of neutrons absorbed/cm<sup>2</sup>-sec of the sheet is equal to  $2SL_T^2/(L_T + d) \approx 2SL_T$ , when  $d \ll L_T$ .

14-2. At startup, a hypothetical, U<sup>235</sup>-fueled, H<sub>2</sub>O-moderated and reflected reactor is critical with a single, heavily borated rod 1 in. in diameter fully inserted at its center. The reactor core is a square cylinder 76 cm in height and operates at a power of 100 MW(th). The reflector savings is approximately 3 cm. Using modified one-group theory

estimate (a) the excess reactivity at startup, (b) the thermal flux throughout the reactor core, (c) the rate at which heat is generated in the control rod.

14-3. A uniform sphere of moderator of extrapolated radius  $R$  is exposed to a burst of fast neutrons and the decay constant  $\lambda$  of the fundamental mode is measured. An absorbing sphere of radius  $a$  is then placed at the center of the sphere and the decay constant  $\lambda'$  is measured. (a) Using one-group theory, derive an expression determining the change  $\Delta\lambda = \lambda' - \lambda$ . (b) In the limit of small  $a$ , derive an explicit formula for  $\Delta\lambda$ , and show that  $\Delta\lambda$  varies inversely with the volume of the moderator sphere.

14-4. An infinite, bare cylindrical reactor is critical with a cylindrical control rod along its axis. (a) Using one-group theory, derive expressions for the probability that a thermal neutron (i) is absorbed by the rod, (ii) escapes from the surface of the reactor, (iii) is absorbed in the reactor core material. (b) Show that the increase in the number of neutrons leaking/sec from the surface due to the presence of the rod is comparable to the number of neutrons absorbed/sec in the rod.

14-5. A cylindrical rod 1 cm in radius is suddenly inserted along the axis of an initially critical thermal reactor. The reactor is a square cylinder 85 cm high (including reactor savings). It is fueled with  $U^{235}$  and moderated with  $H_2O$ . (a) Assuming that the rod is black to thermal neutrons, estimate the reactivity introduced by the rod using one-group theory. (b) Repeat part (a) using two-group theory. (c) Determine the stable period of the reactor following the insertion of the rod.

14-6. A small absorbing sphere of radius  $a$  is placed at the center of a spherical reactor of radius  $R$  (including reflector savings). (a) Derive an expression determining the worth of the sphere using one-group theory. (b) Repeat part (a) using two-group theory. (c) Find explicit expressions in both one- and two-group theory for the worth of the sphere in the limit of small  $a$ .

14-7. (a) Using two-group theory derive a critical equation determining the worth of a large sheet of black absorber which is used in case of emergency as a safety "rod" to divide in half a cubical reactor (length of side  $a$ ). (b) If the sheet is grey to thermal neutrons, show that according to two-group theory its worth is given approximately by

$$\rho_w = \frac{4M^2}{(1 + \mu_0^2\tau)(1 + \mu_0^2L^2)ad} \left\{ \frac{S_2}{S_1} \left[ \frac{L\sqrt{\tau}}{Md} \tanh \left( \frac{Ma}{2L\sqrt{\tau}} \right) + 1 \right] + 1 \right\}^{-1}.$$

(c) Compare the results of parts (a) and (b) with similar one-group calculations.

14-8. If the reactor in the preceding problem is 100 cm on a side, fueled with  $U^{235}$  and moderated with Be, compute the worth of the black sheet using two-group theory.

14-9. (a) Using two-group theory, derive an expression determining the worth of an eccentric cylindrical control rod in a bare cylindrical reactor. (b) Show that in two-group theory, as in one-group theory, the worth of a small eccentric rod is equal to the worth of a central rod multiplied by the square of the radial part of the thermal flux at its actual location.

14-10. (a) Using one-group theory, derive an expression determining the worth of a central rod surrounded by a ring of  $N$  equally spaced similar rods. (b) Derive an explicit formula for the total worth of the rods in the limit of small rod size. (c) In the special case of  $N = 2$ , discuss quantitatively the conditions under which the worth of the three rods is a maximum.

14-11. A bare critical assembly consists of a cubic array of beryllium blocks and evenly spaced, thin sheets of  $U^{235}$  metal. The assembly, which is 5 ft on a side, is critical with no control rods present. (a) Using two-group theory, determine the mass of  $U^{235}$  in the assembly. (b) Estimate the worth of a single black cruciform rod 0.25 in. thick of 3-in. span fully inserted at the center of the assembly.

14-12. The Yankee Reactor at Rowe, Massachusetts, contains a square array of cruciform control rods 27.6 cm between centers ( $m = 19.5$  cm in Fig. 14-6). The blades are 0.672 cm thick and have a span of 20.0 cm. The average thermal neutron diffusion length of the fuel-moderator mixture is 1.8 cm, and  $\bar{\Sigma}_a$  is  $0.114 \text{ cm}^{-1}$ . The rods are black to thermal neutrons. Estimate the total worth of the rods.

14-13. If the reactor described in Problems 13-6 and 13-30 is to be controlled by a uniform array of black cruciform control rods of 10 cm span and 0.5 cm thickness, approximately how many rods will be necessary?

14-14. If the width of a blade of a cruciform rod is comparable to the side of a control cell, i.e.,  $l \approx m$  (cf. Fig. 14-6), it is reasonable, as a first approximation, to assume that the cell is completely surrounded by control rods. (a) Using this model and one-group theory find an expression for the thermal flux in such a square cell. (b) Find an expression determining the worth of the rods. [Hint: In part (a), assume for simplicity that the flux vanishes an extrapolation length into the rod and use a double eigenfunction expansion. (Eigenfunctions satisfying the condition  $\phi'/\phi = -1/d$  at the rod surface can also be used.)]

14-15. By assuming that the cell in Problem 14-14 is cylindrical rather than square, derive an expression for the worth of the rods in one-group theory.

# 15

## Perturbation Theory

It is often necessary to compute the effect of small changes or *perturbations* on the behavior of a reactor. If the perturbation occurs uniformly throughout the entire reactor or a region thereof, the problem can be handled by the methods developed in the earlier chapters. For instance, the effect of a uniform change in the core of a reactor can be found by computing new group constants for this region and then performing a two-group or multigroup calculation as discussed in Chapter 10. However, this procedure is not satisfactory for small perturbations, for the effect of the perturbation may be lost in the computations as the result of round-off errors. Problems involving small uniform perturbations can also be handled by differentiation, as was done in Chapter 13 in the calculation of the uniform temperature coefficient, but as noted in that chapter, this technique is restricted to only the most simplified reactor models.

Uniform perturbations are met very rarely in practice, and most of the changes which occur in the course of the operation of a reactor are nonuniform. There are numerous examples of such nonuniform perturbations. Small pieces of foreign material or instrumentation are continually being inserted and withdrawn from research and test reactors; while in power reactors, although foreign materials are seldom intentionally inserted, other kinds of nonuniform perturbations occur, such as those due to nonuniform fuel burnup and nonuniform poison accumulation. Unpredicted or unintentional conditions may also develop, such as the onset of boiling in a liquid-moderated or cooled reactor or the sudden melt-down of a fuel element.

In principle, the effect of nonuniform perturbations on the performance of a reactor can be found by performing a multigroup calculation in which the perturbations are represented by appropriate space-dependent group constants. With small, localized perturbations, however, this procedure is not usually practical. By its very nature, a localized perturbation requires that a multigroup calculation be carried out in at least two but more probably in three dimensions; and, as mentioned in Section 10-4, such calculations are very costly. Fortunately, problems of this type can be handled by *perturbation theory*, provided the perturbation is not so large as to distort substantially the flux in the neighborhood of the perturbation. This technique is not limited to problems involving localized perturbations; the effect on a reactor of all (small) nonuniform changes as well as uniform changes can also be determined by perturbation theory.

### 15-1 Reactivity and Perturbations

Consider, for a moment, a uniform, bare, thermal reactor. Its multiplication factor is\*

$$k = \eta f p \epsilon P_L, \quad (15-1)$$

where  $P_L$  is the total nonleakage probability. Equation (15-1) can also be written as

$$k = \nu \left( \frac{\Sigma_f}{\Sigma_{aF}} f p \epsilon P_L \right), \quad (15-2)$$

in which  $\Sigma_f$  and  $\Sigma_{aF}$  are the macroscopic fission and absorption cross sections of the fuel, respectively. Denoting the factors in the parentheses by the symbol  $g$ , Eq. (15-2) becomes

$$k = \nu g. \quad (15-3)$$

If the reactor is critical it follows that

$$\nu g = 1. \quad (15-4)$$

Suppose now that a *uniform* change of some sort occurs throughout the reactor. As a result, one or more of the parameters included in the factor  $g$  will be altered and the reactor will become supercritical or subcritical, depending upon the nature of the perturbation. If the new value of  $g$  is  $g'$ , the new multiplication factor is

$$k' = \nu g' \neq 1, \quad (15-5)$$

and the reactivity of the perturbed system is (cf. Eq. 12-66)

$$\rho = \frac{k' - k}{k'} = \frac{g' - g}{g'}. \quad (15-6)$$

In view of the fact that the multiplication factor is proportional to  $\nu$ , the perturbed reactor obviously could be returned to critical if it were possible to change the value of  $\nu$  in such a way as to compensate for the changed value of  $g$ . Although this, of course, is impossible since  $\nu$  is a constant of nature, it is convenient nevertheless in perturbation problems to describe the effect of the perturbation in terms of the compensatory change in  $\nu$  required to maintain criticality. Denoting the required value of  $\nu$  by  $\nu'$ , this is defined so that

$$\nu' g' = 1. \quad (15-7)$$

From Eq. (15-6), the reactivity of the perturbed reactor can then be written as

$$\rho = - \frac{\nu' - \nu}{\nu} = - \frac{\Delta \nu}{\nu}. \quad (15-8)$$

\* Throughout this chapter the symbols denoting thermal averages and thermal flux will be omitted to simplify the notation.

Up to this point, the discussion has been restricted to the uniform, bare, thermal reactor and to uniform perturbations. The above results can be generalized, however, to other situations. In particular, it can be shown that for *any* reactor the requirement for criticality can be put in the form

$$\nu g = 1, \quad (15-9)$$

where  $g$  is some constant determined by the composition and dimensions of the system.\* It must be emphasized that Eq. (15-9) applies whether the reactor is uniform or not. Thus whenever a reactor is perturbed, the  $g$  factor is changed, but regardless of the nature of the perturbation, the system can be returned to critical by an appropriate change in  $\nu$ . The quantity  $\Delta\nu/\nu$  given in Eq. (15-8) can be used, therefore, to express the effect on a reactor of any kind of perturbation. Methods for computing  $\Delta\nu/\nu$  are considered in the following sections. Since these methods involve a number of mathematical techniques which may not be familiar to the reader, it is necessary to pause at this point for a little mathematics.

## 15-2 Some Mathematical Preliminaries

Throughout much of the present chapter it will be convenient to write differential equations in an abbreviated form by using operators of one type or another. Consider, for example, the one-group equation for a critical slab reactor. If the reactor is not uniform this equation is of the form

$$\frac{d}{dx} D(x) \frac{d\phi}{dx} + F(x)\phi = 0, \quad (15-10)$$

where  $D(x)$  is the diffusion coefficient and  $F(x)$  is a function which depends upon the multiplying and absorption properties of the system. Equation (15-10) can be written succinctly as

$$M\phi = 0, \quad (15-11)$$

where  $M$  is the operator

$$M = \frac{d}{dx} D(x) \frac{d}{dx} + F(x). \quad (15-12)$$

In connection with the calculations considered later in this chapter, it is necessary to introduce a new equation, which is related to Eq. (15-11), known as the *adjoint equation*:

$$M^+\psi = 0. \quad (15-13)$$

The operator  $M^+$  is known as the *adjoint* of  $M$  and is related to  $M$  in a manner to be described momentarily. The function  $\psi$  is called the *adjoint function* by mathe-

---

\* If the reactor fuel is a mixture of isotopes an appropriate average value of  $\nu$  is to be used in Eq. (15-9); with fast reactors, where  $\nu$  may be a function of energy, an appropriately normalized  $\nu$  must be used.

maticians; in nuclear engineering  $\psi$  is usually referred to as the *adjoint flux* or the *importance function*.\* In addition to satisfying Eq. (15-13),  $\psi$  is required to satisfy the same boundary conditions as  $\phi$ . Hence if the extrapolated thickness of the slab reactor is  $a$ ,  $\psi$  must vanish at  $x = \pm a/2$ . The physical significance of  $\psi$  will be discussed in detail later.

It should be noted that Eq. (15-13) and the boundary conditions determine the shape of the function  $\psi$  but do not specify its absolute magnitude. This is analogous to the situation with the flux. Thus it will be recalled that the magnitude of the flux is determined by the operating power of the reactor and cannot be found simply by solving the differential equation subject to the boundary conditions. As will be seen later, however, the magnitude of  $\psi$  is not required in practical calculations and it will therefore remain unspecified.

The adjoint operator  $M^+$  is defined as the operator which satisfies the following relation:

$$\int_{-a/2}^{a/2} u M v \, dx = \int_{-a/2}^{a/2} v M^+ u \, dx, \quad (15-14)$$

where  $u$  and  $v$  are *any* two functions which vanish at  $x = \pm a/2$ . To find an explicit expression for  $M^+$  it is merely necessary to insert  $M$  into the integral on the left-hand side of Eq. (15-14) and integrate by parts wherever required to transfer the various operations from  $v$  to  $u$ . In this way it is easy to see that

$$\begin{aligned} \int_{-a/2}^{a/2} u \left[ \frac{d}{dx} D \frac{d}{dx} + F \right] v \, dx &= (u D v' - u' D v) \Big|_{-a/2}^{a/2} \\ &\quad + \int_{-a/2}^{a/2} v \left[ \frac{d}{dx} D \frac{d}{dx} + F \right] u \, dx. \end{aligned} \quad (15-15)$$

Since both  $u$  and  $v$  are zero at the limits, the first term on the right vanishes and it follows that

$$\int_{-a/2}^{a/2} u M v \, dx = \int_{-a/2}^{a/2} v M u \, dx. \quad (15-16)$$

Comparing this result with Eq. (15-14), it is evident that

$$M^+ = M. \quad (15-17)$$

Thus the operator and its adjoint are identical and in this case the operator  $M$  is said to be *self-adjoint*. In view of the fact that Eqs. (15-11) and (15-13) are homogeneous and both  $\phi$  and  $\psi$  vanish at  $x = \pm a/2$ , it also follows that  $\phi$  and  $\psi$  are everywhere proportional.

These results, which up to this point have been limited to operators in one variable, can easily be extended to multivariable operators. For example, the

---

\* It may be of interest to mention that in quantum mechanics adjoint functions are called "bras" (cf. P.A.M. Dirac, *Principles of Quantum Mechanics*, 4th ed., London: Oxford University Press, 1958).

general one-group diffusion operator is

$$M = \operatorname{div} D \operatorname{grad} + F, \quad (15-18)$$

where  $D$  and  $F$  are functions of position within a reactor of volume  $V$ . The adjoint of  $M$  is now defined by the equation

$$\int_V u M v dV = \int_V v M^+ u dV, \quad (15-19)$$

where  $u$  and  $v$  vanish on the surface of  $V$ .

To find an explicit expression for  $M^+$ , it is first observed that the function  $F$  is obviously self-adjoint and it is necessary therefore to determine only the adjoint of the operator  $\operatorname{div} D \operatorname{grad}$ . In this connection the following vector identity is useful:

$$w \operatorname{div} \mathbf{W} = \operatorname{div} w \mathbf{W} - \mathbf{W} \cdot \operatorname{grad} w, \quad (15-20)$$

in which  $w$  and  $\mathbf{W}$  are scalar and vector functions, respectively. Then

$$\int_V u \operatorname{div} D \operatorname{grad} v dV = \int_V \operatorname{div} (uD \operatorname{grad} v) dV - \int_V D \operatorname{grad} v \cdot \operatorname{grad} u dV.$$

From the divergence theorem, however,

$$\int_V \operatorname{div} (uD \operatorname{grad} v) dV = \int_A u D \operatorname{grad} v \cdot \mathbf{n} dA = 0,$$

since  $u = 0$  on the surface of the reactor, so that

$$\int_V u \operatorname{div} D \operatorname{grad} v dV = - \int_V D \operatorname{grad} u \cdot \operatorname{grad} v dV. \quad (15-21)$$

Using the above identity again (this is the equivalent of integrating by parts twice, as done earlier), it is seen that

$$\begin{aligned} \int_V D \operatorname{grad} u \cdot \operatorname{grad} v dV &= \int_V \operatorname{div} (v D \operatorname{grad} u) dV - \int_V v \operatorname{div} D \operatorname{grad} u dV \\ &= - \int_V v \operatorname{div} D \operatorname{grad} u dV. \end{aligned}$$

Substituting this result into Eq. (15-21) gives

$$\int_V u \operatorname{div} D \operatorname{grad} v dV = \int_V v \operatorname{div} D \operatorname{grad} u dV, \quad (15-22)$$

which shows that the operator in Eq. (15-18) is self-adjoint.

The above results are more general than they may at first appear due to the fact that  $D$  and  $F$  are arbitrary functions of position. The preceding operators can be used, therefore, to describe any nonuniform, reflected, or multiregion reactor by an appropriate choice of the functional form of these parameters. For example, if the reactor consists of a uniform core and a uniform reflector with different

physical properties,  $D$  and  $F$  are taken to be step functions, i.e., functions having one value in the core and another value in the reflector. Hence it may be concluded that *all one-group diffusion operators are self-adjoint.*

Turning now to two-group theory, the flux equations are

$$\operatorname{div} D_1 \operatorname{grad} \phi_1 - \Sigma_1 \phi_1 + \nu \epsilon \Sigma_{2f} \phi_2 = 0, \quad (15-23)$$

$$\operatorname{div} D_2 \operatorname{grad} \phi_2 - \Sigma_2 \phi_2 + p \Sigma_1 \phi_1 = 0. \quad (15-24)$$

Here,  $\Sigma_{2f}$  is the macroscopic fission cross section for the slow group and the other parameters are the same as used in Chapter 10. All of these parameters (except  $\nu$ ) may be functions of position, so that, as in the preceding example, Eqs. (15-23) and (15-24) are applicable to multiregion as well as one-region reactors.

Equations (15-23) and (15-24) can be put in a more tractable form by considering  $\phi_1$  and  $\phi_2$  as the components of a two-component vector  $\phi$ . This vector is conveniently represented by a one-column matrix, namely,

$$\phi = \begin{pmatrix} \phi_1 \\ \phi_2 \end{pmatrix}. \quad (15-25)$$

Then by defining the *matrix operator*  $M$  as

$$M = \begin{pmatrix} \operatorname{div} D_1 \operatorname{grad} - \Sigma_1 & \nu \epsilon \Sigma_{2f} \\ p \Sigma_1 & \operatorname{div} D_2 \operatorname{grad} - \Sigma_2 \end{pmatrix} \quad (15-26)$$

and following the rules of matrix multiplication,\* Eqs. (15-23) and (15-24) can

\* If  $M$  is the  $2 \times 2$  matrix

$$M = \begin{pmatrix} m_{11} & m_{12} \\ m_{21} & m_{22} \end{pmatrix},$$

then

$$M\phi = \begin{pmatrix} m_{11} & m_{12} \\ m_{21} & m_{22} \end{pmatrix} \begin{pmatrix} \phi_1 \\ \phi_2 \end{pmatrix} = \begin{pmatrix} m_{11}\phi_1 + m_{12}\phi_2 \\ m_{21}\phi_1 + m_{22}\phi_2 \end{pmatrix}.$$

In general, if  $M$  is an  $N \times N$  matrix and operates on an  $N$ -component vector the result is

$$M\phi = \begin{pmatrix} \sum_n m_{1n}\phi_n \\ \sum_n m_{2n}\phi_n \\ \vdots \\ \sum_n m_{Nn}\phi_n \end{pmatrix}$$

where all the sums are carried out from  $n = 1$  to  $n = N$ .

be written as the single equation

$$\mathbf{M}\phi = 0. \quad (15-27)$$

The adjoint equation is

$$\mathbf{M}^+\psi = 0, \quad (15-28)$$

where  $\mathbf{M}^+$ , the adjoint operator, is another matrix and  $\psi$ , the adjoint function, is a two-component vector. The operator  $\mathbf{M}^+$  is defined by an expression similar to those used earlier, namely,

$$\int_V \mathbf{u} \mathbf{M} \mathbf{v} dV = \int_V \mathbf{v} \mathbf{M}^+ \mathbf{u} dV, \quad (15-29)$$

where  $\mathbf{u}$  and  $\mathbf{v}$  are any two-component vectors, all of whose components vanish at the surface of the reactor. Incidentally, in connection with Eq. (15-29) it should be noted that in evaluating a product of vectors the first vector must be written as a row matrix rather than a column matrix. For instance, the product  $\mathbf{u}\mathbf{v}$  is

$$(u_1 \ u_2) \begin{pmatrix} v_1 \\ v_2 \end{pmatrix} = u_1 v_1 + u_2 v_2, \quad (15-30)$$

which is a scalar. In Eq. (15-29) the quantity  $\mathbf{M}\mathbf{v}$  is a vector, and the product  $\mathbf{u}\mathbf{M}\mathbf{v}$  is therefore a scalar.

The elements of the operator  $\mathbf{M}^+$  can be found by expanding both sides of Eq. (15-29). Thus let

$$\mathbf{M}^+ = \begin{pmatrix} \mu_{11} & \mu_{12} \\ \mu_{21} & \mu_{22} \end{pmatrix} \quad (15-31)$$

where  $\mu_{11}$ ,  $\mu_{12}$ , etc., must be determined. Substituting  $\mathbf{M}$  and  $\mathbf{M}^+$  into Eq. (15-29) and carrying out the multiplication gives

$$\begin{aligned} \int_V u_1 m_{11} v_1 dV + \int_V u_1 m_{12} v_2 dV + \int_V u_2 m_{21} v_1 dV + \int_V u_2 m_{22} v_2 dV \\ = \int_V v_1 \mu_{11} u_1 dV + \int_V v_1 \mu_{12} u_2 dV + \int_V v_2 \mu_{21} u_1 dV + \int_V v_2 \mu_{22} u_2 dV, \end{aligned} \quad (15-32)$$

where  $m_{11}$ ,  $m_{12}$ , etc., are the elements of  $\mathbf{M}$  (cf. Eq. 15-26).

As seen in Eq. (15-26)  $m_{11}$  is a one-group operator and is therefore self-adjoint. Thus

$$\int_V u_1 m_{11} v_1 dV = \int_V v_1 m_{11} u_1 dV,$$

and the first term on each side of Eq. (15-32) will be identical if  $\mu_{11}$  is taken equal to  $m_{11}$ . By a similar argument

$$\mu_{22} = m_{22}.$$

The remaining elements of  $\mathbf{M}^+$  can easily be identified by noting that the operators  $m_{12}$  and  $m_{21}$  are merely functions and are also self-adjoint. Equation (15-32) is

then satisfied if  $\mu_{12} = m_{21}$  and  $\mu_{21} = m_{12}$ . Hence  $\mathbf{M}^+$  is given by

$$\mathbf{M}^+ = \begin{pmatrix} \operatorname{div} D_1 \operatorname{grad} - \Sigma_1 & p\Sigma_1 \\ \nu\Sigma_{2f} & \operatorname{div} D_2 \operatorname{grad} - \Sigma_2 \end{pmatrix}. \quad (15-33)$$

Comparing Eq. (15-33) with Eq. (15-26) shows that  $\mathbf{M}^+$  is *not* the same as  $\mathbf{M}$ , and it must be concluded that the operator  $\mathbf{M}$  is not self-adjoint. In particular,  $\mathbf{M}^+$  is the *transpose\** of the matrix  $\mathbf{M}$ . Since  $\mathbf{M}$  is not self-adjoint, it also follows that the adjoint function and the flux are not proportional as they were in the one-group problem; they may now be quite different functions.

These conclusions can be generalized in an obvious way to the multigroup equations. If there are  $N$  equations, the flux is written as an  $N$ -component vector, and the multigroup operator is an  $N \times N$  matrix. In this case, the adjoint operator can be shown to be transpose of the multigroup operator, as would be expected.

### 15-3 One-Group Perturbation Theory

Consider a critical reactor described by one-group theory. The flux is then given by the equation

$$\operatorname{div} D \operatorname{grad} \phi + (\nu\Sigma_f - \Sigma_a)\phi = 0, \quad (15-34)$$

where  $\Sigma_f$  and  $\Sigma_a$  are the macroscopic fission and absorption cross sections, respectively. The quantities  $D$ ,  $\Sigma_f$ , and  $\Sigma_a$  may all be functions of position. As explained in the preceding section this equation can also be written as

$$M\phi = 0, \quad (15-35)$$

where  $M$  is the operator

$$M = \operatorname{div} D \operatorname{grad} + \nu\Sigma_f - \Sigma_a. \quad (15-36)$$

Suppose now that for some reason  $\Sigma_f$  and/or  $\Sigma_a$  are changed so that  $\Sigma_f \rightarrow \Sigma'_f$  and  $\Sigma_a \rightarrow \Sigma'_a$ . For the moment, it will be assumed that  $D$  does not change. Since both  $\Sigma_f$  and  $\Sigma'_f$  may be functions of position, the difference between  $\Sigma_f$  and  $\Sigma'_f$ , in general, is also a function of position. This function is denoted by the symbol  $\delta\Sigma_f$ ,† so that  $\Sigma'_f$  can be written as

$$\Sigma'_f = \Sigma_f + \delta\Sigma_f \quad (15-37)$$

and similarly

$$\Sigma'_a = \Sigma_a + \delta\Sigma_a. \quad (15-38)$$

As a result of these perturbations, the reactor becomes either subcritical or supercritical. As explained in Section 15-1, however, the system could be returned

\* The transpose of a matrix whose elements are  $m_{ij}$  is defined as the matrix with elements  $\mu_{ij} = m_{ji}$ .

† The symbol  $\delta$  is borrowed from the calculus of variations. (See, for instance, F. B. Hildebrand, *Methods of Applied Mathematics*. New York: Prentice-Hall, 1952, Chapter 2.)

to critical were it possible to change the value of  $\nu$  to an appropriate new value  $\nu'$ . The flux  $\phi'$  in the perturbed critical reactor would then satisfy the equation:

$$\operatorname{div} D \operatorname{grad} \phi' + (\nu' \Sigma'_f - \Sigma'_a) \phi' = 0, \quad (15-39)$$

which can be put in the form

$$M' \phi' = 0, \quad (15-40)$$

where  $M'$  is the operator

$$M' = \operatorname{div} D \operatorname{grad} + \nu' \Sigma'_f - \Sigma'_a. \quad (15-41)$$

Inserting Eqs. (15-37) and (15-38) and writing  $\nu' = \nu + \Delta\nu$ ,  $M'$  becomes

$$\begin{aligned} M' &= \operatorname{div} D \operatorname{grad} + (\nu + \Delta\nu)(\Sigma_f + \delta\Sigma_f) - (\Sigma_a + \delta\Sigma_a) \\ &= M + \nu \delta\Sigma_f + \Delta\nu \Sigma_f + \Delta\nu \delta\Sigma_f - \delta\Sigma_a. \end{aligned} \quad (15-42)$$

Perturbation theory can only be used in connection with small changes in a reactor. For this reason, the term  $\Delta\nu \delta\Sigma_f$  in Eq. (15-42) can be ignored since it involves the product of two small quantities. Equation (15-42) then reduces to

$$M' = M + \nu \delta\Sigma_f + \Delta\nu \Sigma_f - \delta\Sigma_a. \quad (15-43)$$

This can also be written as

$$M' = M + P, \quad (15-44)$$

where

$$P = \nu \delta\Sigma_f + \Delta\nu \Sigma_f - \delta\Sigma_a \quad (15-45)$$

is called the *perturbation operator*. Equation (15-39) is then simply

$$(M + P)\phi' = 0. \quad (15-46)$$

The reactivity introduced by the perturbation can be found by the following procedure. Ignoring for the moment the fact that the operator  $M$  is self-adjoint, the equation adjoint to Eq. (15-35) is

$$M^+ \psi = 0. \quad (15-47)$$

Multiplying this equation by  $\phi'$  and Eq. (15-46) by  $\psi$ , subtracting, and integrating over the volume of the reactor yields

$$\int_V \psi(M + P)\phi' dV - \int_V \phi' M^+ \psi dV = 0, \quad (15-48)$$

or

$$\int_V (\psi M \phi' - \phi' M^+ \psi) dV + \int_V \psi P \phi' dV = 0. \quad (15-49)$$

In view of the definition of the adjoint operator given in the preceding section

(cf. Eq. 15-19), the first integral vanishes, so that

$$\int_V \psi P \phi' dV = 0, \quad (15-50)$$

Inserting the expression for  $P$  from Eq. (15-45) and solving for  $\Delta\nu/\nu$  gives the following result:

$$\rho = -\frac{\Delta\nu}{\nu} = \frac{\int_V \psi(\nu \delta\Sigma_f - \delta\Sigma_a)\phi' dV}{\nu \int_V \psi \Sigma_f \phi' dV}. \quad (15-51)$$

This equation cannot be used as it stands to compute  $\rho$  since the perturbed flux  $\phi'$  is not known. However, if the perturbation of the reactor is small,  $\phi'$  will not differ significantly from  $\phi$ . In this case,  $\phi'$  can be replaced by  $\phi$  and Eq. (15-51) becomes\*

$$\rho = \frac{\int_V \psi(\nu \delta\Sigma_f - \delta\Sigma_a)\phi dV}{\nu \int_V \psi \Sigma_f \phi dV}. \quad (15-52)$$

At this point it may be noted that the one-group operator is self-adjoint so that  $\psi$  is proportional to  $\phi$ . Equation (15-52) then reduces to

$$\rho = \frac{\int_V (\nu \delta\Sigma_f - \delta\Sigma_a)\phi^2 dV}{\nu \int_V \Sigma_f \phi^2 dV}. \quad (15-53)$$

Equation (15-53) shows that the effect of a perturbation in  $\Sigma_f$  or  $\Sigma_a$  is obtained by weighting the perturbation by the *square* of the flux. For example, suppose that a small absorber of volume  $V_p$  and absorption cross section  $\Sigma_{ap}$  is inserted in the reactor at the point  $\mathbf{r}_0$ . This perturbation can be represented approximately by the function

$$\delta\Sigma_a = \Sigma_{ap} V_p \delta(\mathbf{r} - \mathbf{r}_0), \quad (15-54)$$

where  $\delta(\mathbf{r} - \mathbf{r}_0)$  is the Dirac delta function.† There is no perturbation in  $\Sigma_f$ , so  $\delta\Sigma_f = 0$ . Inserting Eq. (15-54) into Eq. (15-53) gives

$$\begin{aligned} \rho &= -\frac{\int_V \delta\Sigma_a \phi^2 dV}{\nu \int_V \Sigma_f \phi^2 dV} \\ &= -\frac{\Sigma_{ap} V_p \phi^2(\mathbf{r}_0)}{\nu \int_V \Sigma_f \phi^2 dV}. \end{aligned} \quad (15-55)$$

Thus the effect on the reactivity of placing the absorber at  $\mathbf{r}_0$  is weighted by the square of the flux at that point. For this reason the quantity  $\phi^2(\mathbf{r})$  is called the

\* It can be shown that the replacement of  $\phi'$  by  $\phi$  represents the same order of approximation (namely first-order) as the omission of products such as  $\Delta\nu \delta\Sigma_f$  in Eq. (15-42). (See any book on quantum mechanics.)

† The use of the same symbol to denote both a perturbation and the Dirac  $\delta$ -function is an unfortunate but well-established tradition.

*statistical weighting function* or the *statistical weight* of the point  $\mathbf{r}$ . Incidentally, it should be observed that Eq. (15-55) has the correct sign. Obviously, inserting an absorber into a critical reactor causes its reactivity to become negative; i.e., the reactor falls subcritical.

Up to this point only changes in  $\Sigma_f$  and  $\Sigma_a$  have been considered. It will now be supposed that  $D$  is changed while  $\Sigma_f$  and  $\Sigma_a$  remain fixed. In this case,

$$D \rightarrow D' = D + \delta D,$$

and the operator for the perturbed system can again be written as

$$\mathcal{M}' = \mathcal{M} + P,$$

where now the perturbation operator is

$$P = \operatorname{div} \delta D \operatorname{grad} + \Delta\nu \Sigma_f. \quad (15-56)$$

Proceeding in the same manner as before gives

$$\int_V \psi P \phi' dV \approx \int_V \psi P \phi dV = 0.$$

Inserting Eq. (15-56) for  $P$ , and again noting that since the operators are self-adjoint  $\psi$  is proportional to  $\phi$ , the reactivity is found to be

$$\rho = -\frac{\Delta\nu}{\nu} = \frac{\int_V \phi \operatorname{div} \delta D \operatorname{grad} \phi dV}{\nu \int_V \Sigma_f \phi^2 dV}. \quad (15-57)$$

This expression can be written in a better form by using the identity given in Eq. (15-20). Thus

$$\int_V \phi \operatorname{div} \delta D \operatorname{grad} \phi dV = \int_V \operatorname{div} (\phi \delta D \operatorname{grad} \phi) dV - \int_V \delta D (\nabla \phi)^2 dV.$$

From the divergence theorem the first term on the right is

$$\int_V \operatorname{div} (\phi \delta D \operatorname{grad} \phi) dV = \int_A \phi \delta D \operatorname{grad} \phi \cdot \mathbf{n} dA = 0,$$

since  $\phi$  vanishes on the surface. Hence Eq. (15-57) becomes

$$\rho = -\frac{\int_V \delta D (\nabla \phi)^2 dV}{\nu \int_V \Sigma_f \phi^2 dV}. \quad (15-58)$$

It will be seen from Eq. (15-58) that changes in  $D$  are weighted by  $(\nabla \phi)^2$ , rather than by  $\phi^2$  as in the previous case. Also, it should be noted that an increase in  $D$ , i.e., a positive  $\delta D$ , again leads to a negative value of  $\rho$ . Physically, this is due to the fact that the neutron current increases with increasing  $D$ . A positive  $\delta D$  thus results in additional leakage of neutrons from the reactor, causing the originally critical reactor to fall subcritical.

If  $D$ ,  $\Sigma_a$ , and  $\Sigma_f$  are all changed simultaneously, the total reactivity is simply the sum of the reactivities given by Eqs. (15-53) and (15-58). In this case,  $\rho$  is

$$\rho = \frac{\int_V [(\nu \delta\Sigma_f - \delta\Sigma_a)\phi^2 - \delta D (\nabla\phi)^2] dV}{\nu \int_V \Sigma_f \phi^2 dV}. \quad (15-59)$$

It must be emphasized that the integrals in Eq. (15-59) are carried out over the entire reactor, though generally they may be zero over a portion of the system. For example, with a two-region reactor consisting of a core and reflector,  $\Sigma_f$  and  $\delta\Sigma_f$  are both zero in the reflector so that  $\rho$  can be written as

$$\rho = \frac{1}{\nu \int_{\text{core}} \Sigma_f \phi^2 dV} \left\{ \int_{\text{core}} [(\nu \delta\Sigma_f - \delta\Sigma_a)\phi^2 - \delta D (\nabla\phi)^2] dV \right. \\ \left. - \int_{\text{reflector}} [\delta\Sigma_a \phi^2 + \delta D (\nabla\phi)^2] dV \right\}. \quad (15-60)$$

The various one-group perturbation formulas developed in this section are necessarily limited by the inadequacies inherent in the one-group method. For example, it will be recalled that the peaking of the thermal flux in the reflector is not predicted by one-group theory. Thus the effect of placing an absorber in the reflector cannot be determined accurately with one-group perturbation theory. The one-group formulas also are not applicable to problems involving changes in the moderating properties of the system or the production of fast neutrons, because these things simply are not included in one-group theory. The above formulas are limited therefore to changes in the one-group absorption cross section and diffusion coefficient, and may be used only for perturbations occurring where one-group theory gives accurate values of the flux.

In applying Eq. (15-59) to various problems, it should be remembered that the absorption cross section  $\Sigma_a$  includes both capture and fission by the fuel. While a change in  $\Sigma_a$  does not necessarily imply a change in  $\Sigma_f$ , a change in  $\Sigma_f$  always gives rise to a change in  $\Sigma_a$ . In particular, since the absorption cross section of the fuel,  $\Sigma_{aF}$ , is related to the fission cross section,  $\Sigma_f$ , by (cf. Section 3-3)

$$\Sigma_{aF} = (1 + \alpha)\Sigma_f, \quad (15-61)$$

where  $\alpha$  is the capture-to-fission ratio, there is a change in  $\Sigma_a$  of

$$\delta\Sigma_a = \delta\Sigma_{aF} = (1 + \alpha) \delta\Sigma_f \quad (15-62)$$

associated with a change in  $\Sigma_f$  of  $\delta\Sigma_f$ .

#### 15-4 Two-Group Perturbation Theory

For the various reasons mentioned above, one-group perturbation theory has very limited applications. A much wider range of problems can be handled in two-group theory. Still greater accuracy can be attained with multigroup perturbation methods. The present section will be confined to thermal reactors.

**The two-group perturbation formulas.** Using the matrix and vector notation introduced in Section 15-2, the two group equations for an unperturbed, critical reactor may be written as

$$\mathbf{M}\phi = 0, \quad (15-63)$$

where  $\phi$  is the two-component vector flux given by Eq. (15-25) and  $\mathbf{M}$  is the matrix operator defined by Eq. (15-26).

Suppose now that all reactor parameters except  $p$ ,  $\epsilon$ ,\* and the diffusion coefficients  $D_1$  and  $D_2$  undergo small changes. In the notation of Eqs. (15-23) and (15-24),

$$\Sigma_1 \rightarrow \Sigma_1 + \delta\Sigma_1, \quad \Sigma_2 \rightarrow \Sigma_2 + \delta\Sigma_2, \quad \Sigma_{2f} \rightarrow \Sigma_{2f} + \delta\Sigma_{2f}.$$

As the result of these changes the reactor is no longer critical but, as discussed previously, the system can be returned to critical by a suitable change in  $\nu$ . The flux in the perturbed reactor is then determined by the equation

$$\mathbf{M}'\phi' = 0 \quad (15-64)$$

where  $\mathbf{M}'$  is the perturbed reactor operator.

Inserting the above parameter changes into the matrix operator given in Eq. (15-26) and neglecting products of small quantities in the usual way, it is easy to show that  $\mathbf{M}'$  can be written as

$$\mathbf{M}' = \mathbf{M} + \mathbf{P}, \quad (15-65)$$

where  $\mathbf{P}$  is the perturbation operator

$$\mathbf{P} = \begin{pmatrix} -\delta\Sigma_1 & \epsilon(\Delta\nu \Sigma_{2f} + \nu \delta\Sigma_{2f}) \\ p \delta\Sigma_1 & -\delta\Sigma_2 \end{pmatrix}. \quad (15-66)$$

To find the reactivity introduced into the system by this perturbation the procedure is essentially the same as it was in one-group theory, with the exception that the reactor operators are now matrices and the fluxes and adjoints are both two-component vectors. First, the adjoint equation

$$\mathbf{M}^+\psi = 0 \quad (15-67)$$

is multiplied by the perturbed flux  $\phi'$ ; the perturbed equation

$$(\mathbf{M} + \mathbf{P})\phi' = 0 \quad (15-68)$$

is multiplied by the adjoint function  $\psi$ ; and the two equations are then subtracted

---

\* The resonance escape probability and fast fission factor are not functions of position in the same sense as the other reactor parameters, and they are assumed in this section to remain constant. Perturbation problems involving resonance absorbers and fast fission are best handled by multigroup methods.

and integrated over the volume of the reactor. The result is

$$\int_V \psi(\mathbf{M} + \mathbf{P})\phi' dV - \int_V \phi'\mathbf{M}^+\psi dV = 0, \quad (15-69)$$

or

$$\int_V (\psi\mathbf{M}\phi' - \phi'\mathbf{M}^+\psi) dV + \int_V \psi\mathbf{P}\phi' dV = 0. \quad (15-70)$$

Again, in view of the definition of the adjoint operator, the first integral vanishes and Eq. (15-70) reduces to

$$\int_V \psi\mathbf{P}\phi' dV = 0. \quad (15-71)$$

Introducing Eq. (15-66) for  $\mathbf{P}$  and replacing  $\phi'$  by  $\phi$ , as usual, the final expression for the reactivity is found to be

$$\rho = -\frac{\Delta\nu}{\nu} = \frac{1}{Q} \left[ - \int_V \delta\Sigma_1 \psi_1 \phi_1 dV + \epsilon\nu \int_V \delta\Sigma_{2f} \psi_1 \phi_2 dV + p \int_V \delta\Sigma_1 \psi_2 \phi_1 dV - \int_V \delta\Sigma_2 \psi_2 \phi_2 dV \right], \quad (15-72)$$

where

$$Q = \epsilon\nu \int_V \Sigma_{2f} \psi_1 \phi_2 dV. \quad (15-73)$$

As in one-group perturbation theory if the diffusion coefficients are also perturbed, the calculation of  $\rho$  is somewhat more complicated. Nevertheless, by performing operations similar to those discussed in the preceding section it is not difficult to show that in this more general case the reactivity is given by

$$\rho = \frac{1}{Q} \left[ - \int_V \delta D_1 \nabla \psi_1 \cdot \nabla \phi_1 dV - \int_V \delta\Sigma_1 \psi_1 \phi_1 dV + \epsilon\nu \int_V \delta\Sigma_{2f} \psi_1 \phi_2 dV + p \int_V \delta\Sigma_1 \psi_2 \phi_1 dV - \int_V \delta D_2 \nabla \psi_2 \cdot \nabla \phi_2 dV - \int_V \delta\Sigma_2 \psi_2 \phi_2 dV \right], \quad (15-74)$$

where  $Q$  is given by Eq. (15-73).

It should be noted in applying Eqs. (15-72) and (15-74) that a change in  $\Sigma_{2f}$ , the macroscopic thermal fission cross section, necessarily implies a change in  $\Sigma_2$ , the total macroscopic thermal absorption cross section. Thus, as explained in Section 15-3, a variation  $\delta\Sigma_{2f}$  gives the variation  $\delta\Sigma_2$ :

$$\delta\Sigma_2 = (1 + \alpha) \delta\Sigma_{2f}, \quad (15-75)$$

where  $\alpha$  is the capture-to-fission ratio.

**Computing the adjoint function.** In order to use the above perturbation formulas, both the fluxes and adjoint functions must be computed for the unperturbed reactor. Methods for calculating the fluxes were discussed in detail in Chapter 10; the adjoint functions remain to be found.

Consider first a two-region reactor consisting of a uniform core with a uniform reflector. The two-group equations in the core are then (cf. Section 10-2)

$$D_{1c}\nabla^2\phi_{1c} - \Sigma_{1c}\phi_{1c} + \nu\epsilon\Sigma_{2fc}\phi_{2c} = 0, \quad (15-76)$$

$$D_{2c}\nabla^2\phi_{2c} - \Sigma_{2c}\phi_{2c} + p\Sigma_{1c}\phi_{1c} = 0, \quad (15-77)$$

and, in the reflector,

$$D_{1r}\nabla^2\phi_{1r} - \Sigma_{1r}\phi_{1r} = 0, \quad (15-78)$$

$$D_{2r}\nabla^2\phi_{2r} - \Sigma_{2r}\phi_{2r} + \Sigma_{1r}\phi_{1r} = 0. \quad (15-79)$$

From Chapter 10 it will be recalled that the solutions to the core equations can be written in the form

$$\phi_{1c} = AX + CY, \quad (15-80)$$

$$\phi_{2c} = AS_1X + CS_2Y, \quad (15-81)$$

where  $A$  and  $C$  are constants and  $X$  and  $Y$  are functions satisfying

$$(\nabla^2 + \mu^2)X = 0, \quad (15-82)$$

$$(\nabla^2 - \lambda^2)Y = 0. \quad (15-83)$$

The parameters  $\mu^2$  and  $\lambda^2$  are given by Eqs. (10-37) and (10-38), and the coupling coefficients  $S_1$  and  $S_2$  are

$$S_1 = \frac{p\Sigma_{1c}/\Sigma_{2c}}{1 + \mu^2 L_c^2}, \quad S_2 = \frac{p\Sigma_{1c}/\Sigma_{2c}}{1 - \lambda^2 L_c^2}. \quad (15-84)$$

The two-group fluxes in the reflector are

$$\phi_{1r} = FZ_1, \quad (15-85)$$

$$\phi_{2r} = FS_3Z_1 + GZ_2, \quad (15-86)$$

where  $F$  and  $G$  are constants and  $Z_1$  and  $Z_2$  satisfy

$$(\nabla^2 - \kappa_{1r}^2)Z_1 = 0, \quad (15-87)$$

$$(\nabla^2 - \kappa_{2r}^2)Z_2 = 0, \quad (15-88)$$

with

$$\kappa_{1r}^2 = \frac{1}{\tau_r}, \quad \kappa_{2r}^2 = \frac{1}{L_r^2}. \quad (15-89)$$

The coupling coefficient  $S_3$  is given by

$$S_3 = \frac{\Sigma_{1r}/D_{2r}}{\kappa_{2r}^2 - \kappa_{1r}^2}. \quad (15-90)$$

Three of the four constants  $A$ ,  $C$ ,  $F$ , and  $G$  are specified in terms of the fourth by the boundary conditions at the core-reflector interface [cf. Eqs. (10-77) through (10-80)]. The fourth constant is determined by the operating power of the reactor.

The two-group equations written in operator form are

$$\mathbf{M}\phi = 0,$$

where

$$\mathbf{M} = \begin{pmatrix} D_{1c}\nabla^2 - \Sigma_{1c} & \nu\epsilon\Sigma_{2fc} \\ p\Sigma_{1c} & D_{2c}\nabla^2 - \Sigma_{2c} \end{pmatrix} \quad (15-91)$$

in the core, and

$$\mathbf{M} = \begin{pmatrix} D_{1r}\nabla^2 - \Sigma_{1r} & 0 \\ \Sigma_{1r} & D_{2r}\nabla^2 - \Sigma_{2r} \end{pmatrix} \quad (15-92)$$

in the reflector.

The adjoint equations in operator form are

$$\mathbf{M}^+\psi = 0,$$

where  $\mathbf{M}^+$  is given by the transpose of  $\mathbf{M}$ , namely

$$\mathbf{M}^+ = \begin{pmatrix} D_{1c}\nabla^2 - \Sigma_{1c} & p\Sigma_{1c} \\ \nu\epsilon\Sigma_{2fc} & D_{2c}\nabla^2 - \Sigma_{2c} \end{pmatrix} \quad (15-93)$$

in the core, and

$$\mathbf{M}^+ = \begin{pmatrix} D_{1r}\nabla^2 - \Sigma_{1r} & \Sigma_{1r} \\ 0 & D_{2r}\nabla^2 - \Sigma_{2r} \end{pmatrix} \quad (15-94)$$

in the reflector. Written out in detail, the adjoint equations in the core are

$$D_{1c}\nabla^2\psi_{1c} - \Sigma_{1c}\psi_{1c} + p\Sigma_{1c}\psi_{2c} = 0, \quad (15-95)$$

$$D_{2c}\nabla^2\psi_{2c} - \Sigma_{2c}\psi_{2c} + \nu\epsilon\Sigma_{2fc}\psi_{1c} = 0; \quad (15-96)$$

in the reflector, they are

$$D_{1r}\nabla^2\psi_{1r} - \Sigma_{1r}\psi_{1r} + \Sigma_{1r}\psi_{2r} = 0, \quad (15-97)$$

$$D_{2r}\nabla^2\psi_{2r} - \Sigma_{2r}\psi_{2r} = 0. \quad (15-98)$$

In view of the fact that the adjoint equations are identical in form to the flux equations (both are coupled, linear, second-order differential equations with constant coefficients), the adjoint functions, like the flux, must consist of linear combinations of the functions  $X$ ,  $Y$ ,  $Z_1$ , and  $Z_2$ . It is desirable to write these solutions in the form

$$\psi_{1c} = A^+S_1^+X + C^+S_2^+Y, \quad (15-99)$$

$$\psi_{2c} = A^+X + C^+Y, \quad (15-100)$$

in the core, and

$$\psi_{1r} = F^+Z_1 + G^+S_3^+Z_2, \quad (15-101)$$

$$\psi_{2r} = G^+Z_2, \quad (15-102)$$

in the reflector. In these equations  $A^+$ ,  $C^+$ ,  $F^+$ , and  $G^+$  are constants and  $S_1^+$ ,  $S_2^+$ , and  $S_3^+$  are coupling coefficients which remain to be determined.

The procedure for finding  $S_1^+$ ,  $S_2^+$ , and  $S_3^+$  is the same as it was in Chapter 10 for the flux coupling coefficients. Thus, substituting Eqs. (15-99) and (15-100) into Eq. (15-95) and noting that  $X$  and  $Y$  are independent functions, it is found that

$$S_1^+ = \frac{p}{1 + \mu^2 \tau_c} \quad (15-103)$$

and

$$S_2^+ = \frac{p}{1 - \lambda^2 \tau_c}. \quad (15-104)$$

Similarly, substituting Eqs. (15-101) and (15-102) into Eq. (15-97) gives

$$S_3^+ = \frac{1}{1 - \kappa_{2r}^2/\kappa_{1r}^2} = \frac{L_r^2}{L_r^2 - \tau_r}. \quad (15-105)$$

It will be recalled from Section 15-2 that the adjoint function is required to satisfy the same boundary conditions as the flux. The requirement that  $\psi$  vanish at the extrapolated surface of the reflector is satisfied by the functions  $X$ ,  $Y$ ,  $Z_1$ , and  $Z_2$  as defined in Chapter 10. At the core-reflector interface the adjoint fluxes must also satisfy continuity conditions similar to those given in Eqs. (10-59) through (10-62), namely,

$$\psi_{1c} = \psi_{1r}, \quad (15-106)$$

$$D_{1c}\psi'_{1c} = D_{1r}\psi'_{1r}, \quad (15-107)$$

$$\psi_{2c} = \psi_{2r}, \quad (15-108)$$

$$D_{2c}\psi'_{2c} = D_{2r}\psi'_{2r}, \quad (15-109)$$

where all functions and their derivatives are evaluated at the interface. As in Section 10-2, when Eqs. (15-99) through (15-102) are inserted into Eqs. (15-106) through (15-109), a set of four homogeneous linear algebraic equations is obtained from which it is possible to determine three of the constants  $A^+$ ,  $C^+$ ,  $F^+$ , and  $G^+$  in terms of a fourth. Carrying out this procedure gives

$$C^+ = \frac{A^+ X}{\beta^+ Y} \left( D_{2c} \frac{X'}{X} - D_{2r} \frac{Z'_2}{Z_2} \right), \quad (15-110)$$

$$F^+ = \frac{A^+ X}{\beta^+ Z_1} \left[ D_{2c}(S_2^+ - S_3^+) \frac{X'}{X} + D_{2c}(S_3^+ - S_1^+) \frac{Y'}{Y} + D_{2r}(S_1^+ - S_2^+) \frac{Z'_2}{Z_2} \right], \quad (15-111)$$

$$G^+ = \frac{A^+ X}{\beta^+ Z_2} \left( D_{2c} \frac{X'}{X} - D_{2c} \frac{Y'}{Y} \right), \quad (15-112)$$

where  $\beta^+$  is defined by

$$\beta^+ = D_{2r} \frac{Z'_2}{Z_2} - D_{2c} \frac{Y'}{Y}. \quad (15-113)$$

The constant  $A^+$  is not determined and the absolute magnitudes of the adjoint fluxes are therefore left arbitrary. As mentioned earlier, however, these are not needed since the magnitudes of the adjoint fluxes (and, incidentally, also the

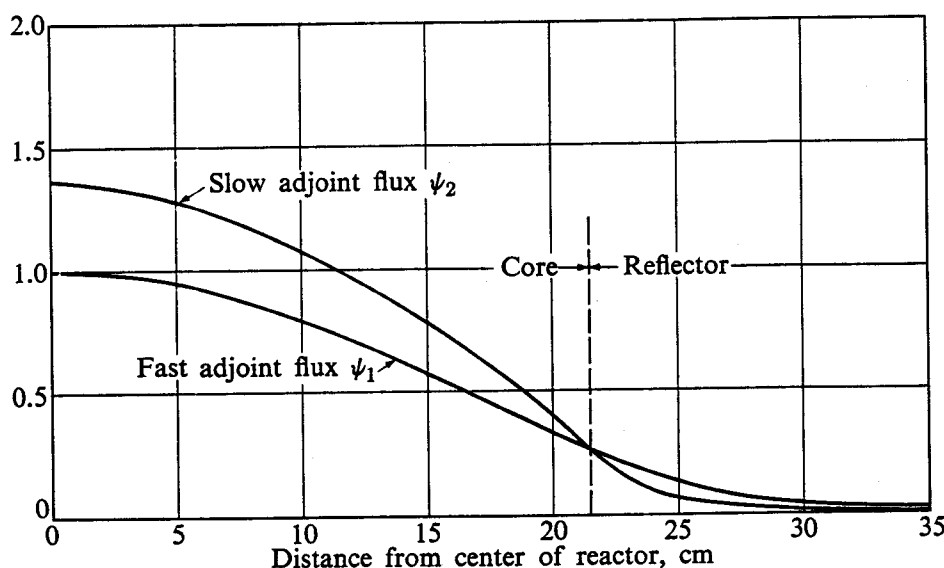


Fig. 15-1. The two-group adjoint fluxes for the reactor described in Section 10-2.

fluxes themselves) do not appear in perturbation formulas. [See, for example, Eqs. (15-72) or (15-74).]

As an illustration of the procedure for computing two-group adjoint fluxes, it is convenient to return to the example of the reflected spherical reactor discussed in Section 10-2. Then using Eqs. (15-110) through (15-113) the adjoint fluxes are found to be

$$\psi_{1c}(r) = 0.735A^+ \left[ \frac{\sin 0.113r}{r} + 2.36 \times 10^{-8} \frac{\sinh 0.651r}{r} \right],$$

$$\psi_{2c}(r) = A^+ \left[ \frac{\sin 0.113r}{r} - 2.58 \times 10^{-7} \frac{\sinh 0.651r}{r} \right],$$

$$\psi_{1r}(r) = 39.9A^+ \left[ \frac{e^{-0.192r}}{r} - 364 \frac{e^{-0.351r}}{r} \right],$$

$$\psi_{2r}(r) = 878A^+ \left[ \frac{e^{-0.351r}}{r} \right].$$

These functions, normalized to  $\psi_{1c} = 1$  at the origin, are plotted in Fig. 15-1. The physical reason for the shape of the functions shown in the figure will be discussed at the end of the next section.

If the core and reflector are not uniform regions as in this example, the adjoint fluxes can be found by solving the adjoint equations using the iterative numerical technique given in Section 10-3. This method is also convenient for computing the adjoint fluxes in a multigroup perturbation calculation.

Incidentally, it is interesting to note that if the reactor is bare, the constant  $C^+$  in Eqs. (15-99) and (15-100) must be taken to be zero in order to satisfy the boundary condition at the extrapolated surface of the reactor. The adjoint fluxes

then reduce to

$$\psi_1 = A^+ S_1^+ X \quad (15-114)$$

and

$$\psi_2 = A^+ X. \quad (15-115)$$

It will be recalled (cf. Prob. 10-14) that for a bare reactor the fluxes are of the same form, namely,

$$\phi_1 = AX$$

and

$$\phi_2 = AS_1X.$$

Thus the fluxes and their adjoints all have the same shape in a reactor of this type. This result is also true in the multigroup case.

### 15-5 Physical Interpretation of the Adjoint Flux

To understand the physical significance of the one-group adjoint flux, consider the reactivity introduced into an originally critical reactor by the insertion of a small absorber at the point  $\mathbf{r}_0$ . If the absorber (which is assumed not to scatter neutrons) has the volume  $V_p$  and macroscopic absorption cross section  $\Sigma_{ap}$ , the perturbation is given by the usual formula

$$\delta\Sigma_a = \Sigma_{ap} V_p \delta(\mathbf{r} - \mathbf{r}_0), \quad (15-116)$$

and according to Eq. (15-52) the reactivity is

$$\rho = - \frac{\Sigma_{ap} V_p \psi(\mathbf{r}_0) \phi(\mathbf{r}_0)}{\nu \int_V \psi \Sigma_f \phi dV}. \quad (15-117)$$

The denominator in Eq. (15-117) is a constant which depends upon the normalizations of the functions  $\psi$  and  $\phi$ , but is independent of the nature of the perturbation. Denoting this term by the symbol  $C^{-1}$  and solving Eq. (15-117) for  $\psi(\mathbf{r}_0)$ , the result is

$$\psi(\mathbf{r}_0) = - \frac{\rho}{C \Sigma_{ap} V_p \phi(\mathbf{r}_0)}. \quad (15-118)$$

The quantity  $\Sigma_{ap} V_p \phi(\mathbf{r}_0)$  is equal to the total number of neutrons absorbed per second in the absorber, and it follows from Eq. (15-118) that the *one group adjoint function*  $\psi(\mathbf{r}_0)$  is proportional to the (negative) change in reactivity of the reactor per neutron absorbed per second at  $\mathbf{r}_0$ . If, for example, the absorber is placed at a point where  $\psi(\mathbf{r}_0)$  is small, the reactivity will also be small. In other words,  $\psi(\mathbf{r}_0)$  measures the *importance* of the point  $\mathbf{r}_0$  with respect to the reactivity introduced by an absorber located at that point, and it is for this reason that  $\psi$  is also called the *importance function*.

Suppose now that a small piece of fissile material of volume  $V_p$  and of macroscopic fission and absorption cross sections  $\Sigma_{fp}$  and  $\Sigma_{ap}$ , respectively, is inserted

at  $\mathbf{r}_0$ . The perturbations in these cross sections may be written as

$$\delta\Sigma_f = \Sigma_{fp}V_p \delta(\mathbf{r} - \mathbf{r}_0) \quad (15-119)$$

and

$$\delta\Sigma_a = \Sigma_{ap}V_p \delta(\mathbf{r} - \mathbf{r}_0). \quad (15-120)$$

Then according to Eq. (15-52) the reactivity of the system becomes

$$\rho = \frac{(\nu\Sigma_{fp} - \Sigma_{ap})V_p\psi(\mathbf{r}_0)\phi(\mathbf{r}_0)}{\nu \int_V \psi \Sigma_f \phi dV}. \quad (15-121)$$

Again, denoting the denominator by  $C^{-1}$  and solving for  $\psi(\mathbf{r}_0)$  gives

$$\psi(\mathbf{r}_0) = \frac{\rho}{C(\nu\Sigma_{fp} - \Sigma_{ap})V_p\phi(\mathbf{r}_0)}. \quad (15-122)$$

The term  $(\nu\Sigma_{fp} - \Sigma_{ap})V_p\phi(\mathbf{r}_0)$  is equal to the *net* number of neutrons introduced per second in the reactor at the point  $\mathbf{r}_0$  by the fissile material. It follows from Eq. (15-122) that  $\psi(\mathbf{r}_0)$  is proportional to the (positive) reactivity per (net) neutron introduced per second by fissile material located at  $\mathbf{r}_0$ . In view of this result and the conclusions of the preceding paragraph, it is evident that the adjoint function represents the relative importance of *any* local change at the point  $\mathbf{r}_0$  which either introduces or removes neutrons from the system.

In a similar way the physical significance of the two-group adjoint fluxes can easily be established. As would be expected, the functions  $\psi_1(\mathbf{r}_0)$  and  $\psi_2(\mathbf{r}_0)$  are proportional, respectively, to the reactivities resulting from perturbations which introduce or remove neutrons from the fast or slow groups. For example, if a slow neutron absorber (which does not scatter neutrons) of volume  $V_p$  and thermal cross section  $\Sigma_{2p}$  is introduced at  $\mathbf{r}_0$ , the perturbation is

$$\delta\Sigma_2 = \Sigma_{2p}V_p \delta(\mathbf{r} - \mathbf{r}_0), \quad (15-123)$$

and from Eq. (15-74) the resulting reactivity is

$$\rho = -\frac{1}{Q} \Sigma_{2p}V_p\psi_2(\mathbf{r}_0)\phi_2(\mathbf{r}_0). \quad (15-124)$$

The quantity  $\Sigma_{2p}V_p\phi_2(\mathbf{r}_0)$  is the number of neutrons removed per second by the absorber while the value of  $Q$  is independent of the presence of the absorber. Thus, as predicted, the slow adjoint flux,  $\psi_2(\mathbf{r}_0)$ , is proportional to the reactivity per thermal neutron absorbed per second at  $\mathbf{r}_0$ .

If, on the other hand, a piece of fissile material of fission and absorption cross sections  $\Sigma_{2fp}$  and  $\Sigma_{2p}$  is placed at  $\mathbf{r}_0$ , the perturbations are

$$\delta\Sigma_{2f} = \Sigma_{2fp}V_p \delta(\mathbf{r} - \mathbf{r}_0), \quad \delta\Sigma_2 = \Sigma_{2p}V_p \delta(\mathbf{r} - \mathbf{r}_0) \quad (15-125)$$

and the reactivity is

$$\rho = \frac{1}{Q} [\epsilon\nu\Sigma_{2fp}V_p\psi_1(\mathbf{r}_0)\phi_2(\mathbf{r}_0) - \Sigma_{2p}V_p\psi_2(\mathbf{r}_0)\phi_2(\mathbf{r}_0)]. \quad (15-126)$$

The second term in the brackets is the loss in reactivity due to the absorption of slow neutrons by the sample, while the first term gives the increase in reactivity from the additional fissions. Since there are a total of  $\epsilon\nu\Sigma_{2fp}V_p\phi_2(r_0)$  neutrons produced per second from the sample it is evident that  $\psi_1(r_0)$  is proportional to the gain in reactivity per neutron produced per second in the fast group at  $r_0$ .

The above results may be summarized as follows. *The group adjoint function  $\psi_n(r)$  is proportional to the gain or loss in reactivity of a reactor due to the insertion or removal of one neutron per second in the group at the point  $r$ .* Another physical interpretation of this interesting function is given in the problems (cf. Prob. 15-12).

It is now possible to give a physical explanation for the shape of the adjoint fluxes shown in Fig. 15-1. As seen in the figure, the adjoint functions have somewhat a reverse behavior from the fluxes shown in Fig. 10-4. In particular, the fast adjoint is less than the slow adjoint in the core although the fast flux is greater than the slow flux in the same region. From the discussion in Section 10-2, it will be recalled that the reason why  $\phi_{2c}$  is less than  $\phi_{1c}$  is that the thermal absorption cross section in the core is greater than the slowing-down cross section. As a result, the thermal flux is depressed below the value of the fast flux. Viewed in a different way, the fact that  $\Sigma_{2c} > \Sigma_{1c}$  also means that neutrons introduced into the slow group are absorbed at a greater rate and therefore contribute more directly to the chain reaction than neutrons introduced into the fast group. This is equivalent to saying that neutrons added to the slow flux are *more important* than neutrons added to the fast group, and this is the reason why the fast and slow adjoints or importance functions have a behavior which is the reverse of that shown by the fluxes. In short, it takes more fast neutrons than slow neutrons (more precisely,  $\phi_{1c} > \phi_{2c}$ ) to keep the reactor described in Section 10-2 critical. Neutron for neutron (or "flux for flux") the slow neutrons have a greater effect on the reactor than the fast neutrons, and hence  $\psi_{1c} < \psi_{2c}$  as shown in Fig. 15-1. It must be emphasized, of course, that these conclusions only apply to the reactor in question. The physical principles are applicable, however, to all reactors.

## 15-6 Some Applications of Perturbation Theory

There are a great many reactor problems which can appropriately be treated by perturbation theory. A few of these will now be discussed for the purpose of illustrating the use of the perturbation formulas derived in the preceding sections.

**Partially inserted control rod.** Perturbation theory cannot be used to determine the worth of a control rod unless the rod is a weak absorber of neutrons. With strongly absorbing rods, the worth must be computed using the methods which were given in Chapter 14. It will be recalled that in Chapter 14 it was always assumed that the rods were fully inserted in the reactor. If the rods are partially inserted, the problem is too complicated to be handled by ordinary analytical methods. In this case, perturbation theory can be used to provide a satisfactory estimate of the worth of the partially inserted rod relative to its worth when fully inserted.

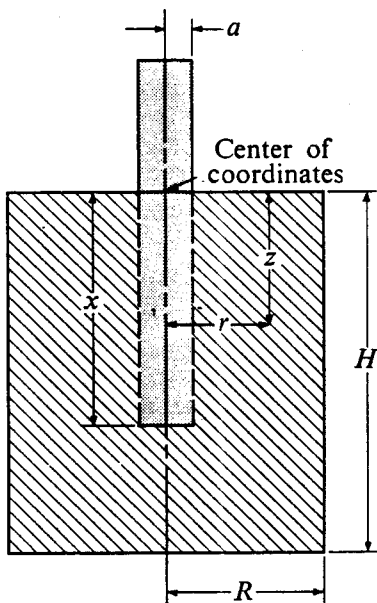


Fig. 15-2. Control rod partially inserted along the axis of a bare cylindrical reactor.

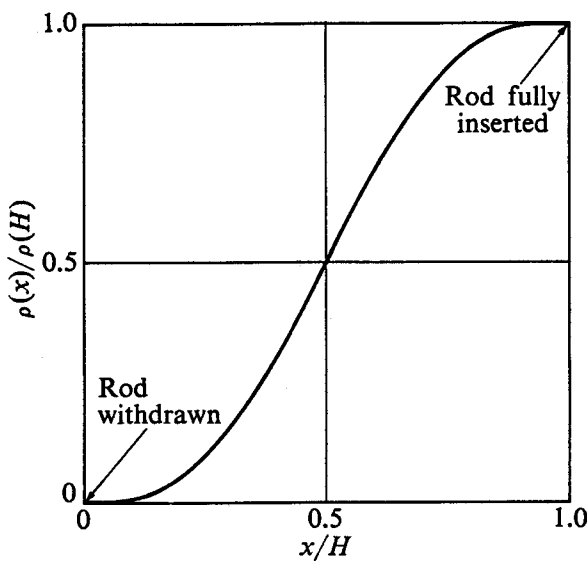


Fig. 15-3. The worth of a partially inserted control rod as a function of its distance of insertion.

The present discussion will be limited to a central rod of radius  $a$  located in a bare cylindrical reactor of extrapolated radius  $R$  and height  $H$ , as shown in Fig. 15-2. It will be assumed that the rod absorbs but does not scatter neutrons. For simplicity, one-group theory will be used; the two-group problem is given in the exercises at the end of the chapter (cf. Prob. 15-13). It is convenient to take the center of the coordinate system at the top of the cylinder (cf. Fig. 15-2). Then with the rod inserted the distance  $x$ , the perturbation is

$$\delta\Sigma_a = \begin{cases} \Sigma_{ap}, & 0 \leq z \leq x, \quad 0 \leq r \leq a, \\ 0, & \text{otherwise,} \end{cases} \quad (15-127)$$

where  $\Sigma_{ap}$  is the macroscopic absorption cross section of the rod. In this coordinate system the unperturbed flux is

$$\phi(r, z) = AJ_0\left(\frac{2.405r}{R}\right) \sin\left(\frac{\pi z}{H}\right). \quad (15-128)$$

Introducing Eqs. (15-127) and (15-128) into Eq. (15-53) and noting that the volume element is  $2\pi r dr dz$ , the reactivity due to the rod inserted the distance  $x$  is

$$\rho(x) = -\frac{2\pi A^2 \Sigma_{ap} \int_0^a J_0^2(2.405r/R)r dr \int_0^x \sin^2(\pi z/H) dz}{\nu \int_V \Sigma_f \phi^2 dV}. \quad (15-129)$$

When the rod is fully inserted the reactivity is

$$\rho(H) = -\frac{2\pi A^2 \Sigma_{ap} \int_0^a J_0^2(2.405r/R)r dr \int_0^H \sin^2(\pi z/H) dz}{\nu \int_V \Sigma_f \phi^2 dV}. \quad (15-130)$$

Dividing the last two equations gives

$$\rho(x) = \rho(H) \frac{\int_0^x \sin^2(\pi z/H) dz}{\int_0^H \sin^2(\pi z/H) dz} = \rho(H) \left[ \frac{x}{H} - \frac{1}{2\pi} \sin\left(\frac{2\pi x}{H}\right) \right]. \quad (15-131)$$

In using Eq. (15-131), the fully-inserted worth  $\rho(H)$  is to be computed by using the methods of Chapter 14 or is to be determined from experiment. Since only relative worths appear in Eq. (15-131), this formula then can be applied even to strongly absorbing rods. Incidentally, despite the fact that Eq. (15-131) was derived for a central rod, it also gives the worth of a partially inserted eccentric rod, provided the appropriate value is used for  $\rho(H)$ .

Equation (15-131) is plotted in Fig. 15-3. It will be observed that the greatest change in the reactivity per unit distance of insertion, i.e., the maximum derivative of  $\rho(x)$ , occurs when the rod is half-way inserted. This is due to the fact that when the end of the rod is in the center of the reactor it is moving in the region of greatest importance.

**Nonuniform fission-product poisoning.** It was shown in Chapter 13 that fission-product poisons generally do not accumulate uniformly in a reactor, and exact numerical methods were discussed in that chapter for handling problems involving nonuniform poison distributions. Certain problems of this type can also be treated by perturbation theory.

Consider, for example, the reactivity equivalent of equilibrium  $Xe^{135}$ . According to Eq. (13-100) the equilibrium xenon concentration at the point  $r$  in atoms/cm<sup>3</sup> is given by

$$X_\infty(r) = \frac{(\gamma_I + \gamma_X)\Sigma_f(r)\phi(r)/\sigma_{aX}}{\phi_X + \phi(r)}, \quad (15-132)$$

where the symbols\* are all defined in Section 13-2. To find the reactivity due to this distribution of poisons by perturbation theory, the entire poison distribution is treated as the perturbation, that is,

$$\delta\Sigma_a = X_\infty(r)\sigma_{aX}. \quad (15-133)$$

Scattering by the xenon can be neglected since its absorption cross section is so large compared with its scattering cross section. Using the one-group perturbation formula (Eq. 15-53) the reactivity is then

$$\rho = -\frac{(\gamma_I + \gamma_X)}{\nu \int_V \Sigma_f \phi^2 dV} \int_V \frac{\Sigma_f \phi^3}{\phi_X + \phi} dV. \quad (15-134)$$

Except in special cases, Eq. (15-134) must be evaluated numerically.

---

\* The symbols denoting thermal averages of the cross sections and the flux are omitted for simplicity.

**Danger coefficients.** The effect on a reactor of introducing a small amount of foreign material is often expressed in terms of the *danger coefficient*. This is defined as the change in the reactivity of the system per gram (or, frequently, per mole) of the material, and will be denoted as  $\rho_D$ . This coefficient, which is a function of the location of the material, can be computed by perturbation theory. Since a foreign material generally alters the moderating as well as the absorption properties of a reactor, it is usually necessary to calculate danger coefficients with two-group (or multigroup) perturbation theory.

For the moment it will be assumed that the foreign material is neither fissile nor fissionable. It will also be assumed that no displacement of reactor material occurs when the foreign matter is introduced in the system. This is the case, for instance, when a sample is placed in a vacant beam tube. Then, noting that 1 gram of material occupies  $d_0^{-1}$  cm<sup>3</sup>, where  $d_0$  is its normal density, the perturbations in the two-group parameters, when the material is inserted at the point  $r_0$ , are

$$\delta\Sigma_1 = \frac{1}{d_0} \Sigma_{1p} \delta(r - r_0), \quad \delta\Sigma_2 = \frac{1}{d_0} \Sigma_{2p} \delta(r - r_0), \quad (15-135)$$

$$\delta D_1 = \frac{1}{d_0} D_{1p} \delta(r - r_0), \quad \delta D_2 = \frac{1}{d_0} D_{2p} \delta(r - r_0), \quad (15-136)$$

where  $\Sigma_{1p}$ ,  $\Sigma_{2p}$ ,  $D_{1p}$ , and  $D_{2p}$  are the two-group parameters for the material at normal density. Inserting the above perturbations into Eq. (15-74) gives the following formula for the danger coefficient:

$$\rho_D = \frac{1}{Qd_0} \left[ -D_{1p} \nabla \psi_1(r_0) \cdot \nabla \phi_1(r_0) - \Sigma_{1p} \psi_1(r_0) \phi_1(r_0) + p \Sigma_{1p} \psi_2(r_0) \phi_1(r_0) - D_{2p} \nabla \psi_2(r_0) \cdot \nabla \phi_2(r_0) - \Sigma_{2p} \psi_2(r_0) \phi_2(r_0) \right], \quad (15-137)$$

where  $Q$  is given by Eq. (15-73).

If the reactor is liquid moderated, the introduction of foreign material may simultaneously displace reactor material. In this case the perturbations may be written as

$$\delta\Sigma_1 = \frac{1}{d_0} (\Sigma_{1p} - \Sigma_1) \delta(r - r_0), \quad \delta\Sigma_2 = \frac{1}{d_0} (\Sigma_{2p} - \Sigma_2) \delta(r - r_0), \quad (15-138)$$

$$\delta D_1 = \frac{1}{d_0} (D_{1p} - D_1) \delta(r - r_0), \quad \delta D_2 = \frac{1}{d_0} (D_{2p} - D_2) \delta(r - r_0), \quad (15-139)$$

where  $\Sigma_1$ ,  $\Sigma_2$ ,  $D_1$ , and  $D_2$  refer to the displaced reactor material. When these expressions are used in Eq. (15-74), a formula is obtained which is similar to, but much more complicated than, Eq. (15-137). If the inserted material is fissile, it is

necessary to add the perturbations

$$\delta\Sigma_{2f} = \frac{1}{d_0} \Sigma_{2fp} \delta(\mathbf{r} - \mathbf{r}_0), \quad \delta\Sigma_2 = \frac{1}{d_0} (1 + \alpha) \Sigma_{2fp} \delta(\mathbf{r} - \mathbf{r}_0) \quad (15-140)$$

or

$$\delta\Sigma_{2f} = \frac{1}{d_0} (\Sigma_{2fp} - \Sigma_{2f}) \delta(\mathbf{r} - \mathbf{r}_0), \quad \delta\Sigma_2 = \frac{1}{d_0} (1 + \alpha) (\Sigma_{2fp} - \Sigma_{2f}) \delta(\mathbf{r} - \mathbf{r}_0), \quad (15-141)$$

depending upon whether or not fuel material is displaced by the inserted material.

Danger coefficients can be measured by observing the stable period of an originally critical reactor following the insertion of a small quantity of material. The reactivity of the system is related to the period in the manner discussed in Chapter 12. Measurements of this type can also be used to determine absorption cross sections. For example, if the scattering cross section is small compared with the absorption cross section and the sample is located at a point where the gradient of the flux is small, the reactivity, according to Eq. (15-137), is proportional to  $\Sigma_{2p}/d_0$ . Therefore, by comparing the periods of a reactor when samples of known and unknown absorption cross sections are inserted at the same point, it is possible to measure an unknown cross section in terms of the known cross section. Unfortunately, in most instances where this method is most useful, the scattering cross section is not small compared with the absorption cross section, and appropriate corrections must be made.

## 15-7 Orthogonality and Adjointness

Throughout much of this book eigenfunction expansions have been utilized in solving a variety of problems. The reader may recall, however, that these expansions were used only in connection with *one-group* problems. The application of eigenfunctions in two-group or multigroup problems has been carefully avoided. The reason for this apparent inconsistency is related to the orthogonality properties of the eigenfunctions. Thus as will now be shown, two-group and multigroup eigenfunctions do not form orthogonal sets in the usual sense.

Before discussing the more general problem, it will be helpful first to review the orthogonality of the one-group eigenfunctions. Consider therefore a uniform, bare reactor which may or may not be critical. For simplicity the delayed neutrons will be ignored; in any event, they do not alter the results of the present argument. The one-group time-dependent equation is then

$$D\nabla^2\phi(\mathbf{r}, t) + (k_\infty - 1)\Sigma_a\phi(\mathbf{r}, t) = \frac{1}{v} \frac{\partial\phi(\mathbf{r}, t)}{\partial t}. \quad (15-142)$$

As in Chapter 9, if separable solutions of the form

$$\phi(\mathbf{r}, t) = \phi(\mathbf{r})T(t)$$

are sought, the function  $T(t)$  is given by  $T(t) = e^{\omega t}$ , where  $\omega$  is the separation constant. The space-dependent part of the flux then satisfies the equation

$$D\nabla^2\phi(\mathbf{r}) + (k_\infty - 1)\Sigma_a\phi(\mathbf{r}) = \frac{\omega}{v}\phi(\mathbf{r}) \quad (15-143)$$

or

$$D\nabla^2\phi(\mathbf{r}) + \left[(k_\infty - 1)\Sigma_a - \frac{\omega}{v}\right]\phi(\mathbf{r}) = 0. \quad (15-144)$$

Writing

$$B^2 = \frac{(k_\infty - 1)\Sigma_a - \omega/v}{D}, \quad (15-145)$$

Eq. (15-144) reduces to the reactor equation

$$\nabla^2\phi(\mathbf{r}) + B^2\phi(\mathbf{r}) = 0. \quad (15-146)$$

It has already been shown that Eq. (15-146) is an eigenvalue equation. That is, there are only certain values of  $B^2$ , denoted by  $B_n^2$ , for which there are nontrivial solutions to the equation which also satisfy the boundary conditions. Thus Eq. (15-146) must be written as

$$\nabla^2\phi_n(\mathbf{r}) + B_n^2\phi_n(\mathbf{r}) = 0. \quad (15-147)$$

Now since  $B^2$  and  $\omega$  are related through Eq. (15-145) it will be clear that  $\omega$  may have only certain values,  $\omega_n$ , and it follows that  $\omega_n$  may also be considered to be an eigenvalue of Eq. (15-144). This equation can therefore be written as

$$[D\nabla^2 + (k_\infty - 1)\Sigma_a]\phi_n(\mathbf{r}) = \frac{\omega_n}{v}\phi_n(\mathbf{r}) \quad (15-148)$$

or, equivalently, as

$$vM\phi_n(\mathbf{r}) = \omega_n\phi_n(\mathbf{r}), \quad (15-149)$$

where  $M$  is the one-group reactor operator:

$$M = D\nabla^2 + (k_\infty - 1)\Sigma_a. \quad (15-150)$$

Equation (15-149) presents the reactor equation in a form which is convenient for discussing the orthogonality of the eigenfunctions.

To demonstrate this orthogonality, the equation for the  $m$ th eigenfunction, namely

$$vM\phi_m(\mathbf{r}) = \omega_m\phi_m(\mathbf{r}), \quad (15-151)$$

is multiplied by  $\phi_n(\mathbf{r})$ , while Eq. (15-149) is multiplied by  $\phi_m(\mathbf{r})$ . The two equations are then subtracted and integrated over the volume of the reactor; the result is

$$v \int_V [\phi_m(\mathbf{r})M\phi_n(\mathbf{r}) - \phi_n(\mathbf{r})M\phi_m(\mathbf{r})] dV = (\omega_n - \omega_m) \int_V \phi_m(\mathbf{r})\phi_n(\mathbf{r}) dV. \quad (15-152)$$

It was shown in Section 15-2 that all one-group operators are self-adjoint, so that

$$\int_V \phi_m(\mathbf{r}) M \phi_n(\mathbf{r}) dV = \int_V \phi_n(\mathbf{r}) M \phi_m(\mathbf{r}) dV. \quad (15-153)$$

The left-hand side of Eq. (15-152) therefore vanishes and this equation reduces to

$$\int_V \phi_m(\mathbf{r}) \phi_n(\mathbf{r}) dV = 0, \quad (15-154)$$

when  $m \neq n$ . This shows that *the eigenfunctions of the one-group equation form an orthogonal set*. Although this result was derived for a uniform reactor, it can be shown to be valid for a nonuniform reactor by simply treating  $M$  as a space-dependent operator. It will be recalled that  $M$  is still self-adjoint in this more general situation.

The above procedure can easily be extended to two-group or multigroup problems. The two-group equations analogous to Eq. (15-142) are

$$D_1 \nabla^2 \phi_1 - \Sigma_1 \phi_1 + \epsilon v \Sigma_{2f} \phi_2 = \frac{1}{v_1} \frac{\partial \phi_1}{\partial t}, \quad (15-155)$$

$$D_2 \nabla^2 \phi_2 - \Sigma_2 \phi_2 + p \Sigma_1 \phi_1 = \frac{1}{v_2} \frac{\partial \phi_2}{\partial t}, \quad (15-156)$$

where  $v_1$  and  $v_2$  are the average speeds of the neutrons in the fast and slow groups, respectively. These equations may be written in operator form as

$$\mathbf{vM}\phi = \frac{\partial \phi}{\partial t}, \quad (15-157)$$

where  $\mathbf{M}$  is the two-group operator defined earlier,  $\phi$  is the two-component flux, and  $\mathbf{v}$  is the diagonal matrix

$$\mathbf{v} = \begin{pmatrix} v_1 & 0 \\ 0 & v_2 \end{pmatrix}. \quad (15-158)$$

If separable solutions to Eq. (15-157) are sought as in the one-group problem, the resulting eigenfunction equation is

$$\mathbf{vM}\phi_n = \omega_n \phi_n. \quad (15-159)$$

However, unlike the one-group eigenfunctions, the eigenfunctions determined by Eq. (15-159) do not form an orthogonal set. Thus multiplying Eq. (15-159) by  $\phi_m$  and the corresponding equation for the  $m$ th eigenfunction by  $\phi_n$ , subtracting, and integrating gives

$$\int_V [\phi_m \mathbf{vM}\phi_n - \phi_n \mathbf{vM}\phi_m] dV = (\omega_n - \omega_m) \int_V \phi_m \phi_n dV. \quad (15-160)$$

Since  $\mathbf{M}$  (or rather  $\mathbf{vM}$ ) is not self-adjoint, the left-hand side of this equation does not vanish as it did in the one-group case. It must be concluded, therefore, that *the eigenfunctions of the two-group operator do not form an orthogonal set*.

Consider now the eigenfunctions of the equation adjoint to Eq. (15-159). It can easily be shown (cf. Prob. 15-19) that the eigenvalues of this adjoint equation are precisely the same as the eigenvalues of the flux equation. The  $m$ th adjoint eigenfunction therefore satisfies the equation

$$\mathbf{M}^+ \mathbf{v} \psi_m = \omega_m \psi_m. \quad (15-161)$$

It should be noted that the  $\mathbf{v}$ -matrix must be written *following* the operator  $\mathbf{M}^+$  as can be verified by carrying out the matrix multiplication term by term. Multiplying this equation by  $\phi_n$  and Eq. (15-159) by  $\psi_m$ , subtracting, and integrating over the volume of the reactor gives

$$\int_V [\psi_m \mathbf{v} \mathbf{M} \phi_n - \phi_n \mathbf{M}^+ \mathbf{v} \psi_m] dV = (\omega_n - \omega_m) \int_V \psi_m \phi_n dV. \quad (15-162)$$

From the definition of the adjoint operator,

$$\int_V \psi_m \mathbf{v} \mathbf{M} \phi_n dV = \int_V \phi_n (\mathbf{v} \mathbf{M})^+ \psi_m dV. \quad (15-163)$$

It is easy to show that the adjoint of the product of two operators is the product of their adjoints in reverse order. Furthermore, since the matrix  $\mathbf{v}$  is diagonal,  $\mathbf{v}^+ = \mathbf{v}$ . Equation (15-163) then reduces to

$$\int_V \psi_m \mathbf{v} \mathbf{M} \phi_n dV = \int_V \phi_n \mathbf{M}^+ \mathbf{v} \psi_m dV. \quad (15-164)$$

The left-hand side of Eq. (15-162) therefore vanishes, and the result is obtained that

$$\int_V \psi_m \phi_n dV = 0, \quad (15-165)$$

when  $m \neq n$ . Thus the *two-group flux eigenfunctions are orthogonal to the two-group adjoint functions*. This conclusion can be generalized to the multigroup case. Thus regardless of the number of groups, corresponding flux and adjoint eigenfunctions are orthogonal. The flux and adjoint eigenfunctions in this case are said to form a *biorthogonal set*.

The biorthogonality of the eigenfunctions and their adjoints is of enormous importance in reactor theory. In particular, it means that it is possible to expand any reasonably well-behaved multi-component vector function in a series of eigenfunctions, and determine the expansion coefficients even though these functions are not orthogonal among themselves. Thus if the function  $f(\mathbf{r})$  is expanded as

$$f(\mathbf{r}) = \sum A_n \phi_n(\mathbf{r}), \quad (15-166)$$

the coefficients  $A_n$  can be found by multiplying both sides of the equation by  $\psi_m(\mathbf{r})$  and integrating over the reactor volume. The biorthogonality condition

then gives

$$A_n = \frac{\int_V \psi_n(\mathbf{r}) f(\mathbf{r}) dV}{\int_V \psi_n(\mathbf{r}) \phi_n(\mathbf{r}) dV}. \quad (15-167)$$

Using expansions such as Eq. (15-167), it is possible to treat a number of important reactor problems which were omitted in the earlier chapters of this book. These include the multigroup theory of subcritical reactors, the kinetics of reflected reactors, and so on. Some of these problems are discussed in the exercises at the end of the chapter.

## References

- GALANIN, A. D., *Thermal Reactor Theory*, 2nd ed. New York: Pergamon Press, 1960, Chapter 6.
- GLASSTONE, S., and M. C. EDLUND, *The Elements of Nuclear Reactor Theory*. Princeton, N.J.: Van Nostrand, 1952, Chapter 13.
- ISBIN, H. S., *Introductory Nuclear Reactor Theory*. New York: Reinhold, 1963, Chapter 12.
- MEGHREBLIAN, R. V., and D. K. HOLMES, *Reactor Analysis*. New York: McGraw-Hill, 1960, Chapter 13.
- MORSE, P. M., and H. FESHBACH, *Methods of Theoretical Physics*. New York: McGraw-Hill, 1953, Chapter 13.
- MURRAY, R. L., *Nuclear Reactor Physics*. Englewood Cliffs, N.J.: Prentice-Hall, 1957, Chapter 8.
- WEINBERG, A. M., and E. P. WIGNER, *The Physical Theory of Neutron Chain Reactors*. Chicago: University of Chicago Press, 1958, Chapter 16.

## Problems

- 15-1. (a) Show that the operator adjoint to

$$M = f_0(x) \frac{d^n}{dx^n} + f_1(x) \frac{d^{n-1}}{dx^{n-1}} + \cdots + f_{n-1}(x) \frac{d}{dx} + f_n(x)$$

is

$$M^+ = (-)^n \frac{d^n}{dx^n} f_0(x) + (-)^{n-1} \frac{d^{n-1}}{dx^{n-1}} f_1(x) + \cdots - \frac{d}{dx} f_{n-1}(x) + f_n(x).$$

- (b) In the special case of  $n = 2$ , derive a relationship between  $f_0(x)$  and  $f_1(x)$  which must be satisfied if the operator is to be self-adjoint.

- 15-2. Show explicitly that the one-group operator for a reflected slab reactor is self-adjoint.

- 15-3. A live, but slow-moving fish, approximately 0.2 liter in volume, is tossed into a critical swimming-pool reactor by a disgruntled nuclear engineering student. The reactor core may be treated as a sphere 60 cm in diameter containing a concentration of  $U^{235}$  sufficient to achieve criticality, and the pool may be taken to be infinite. The moderating

properties of the fish are the same as those of water, and its average macroscopic absorption cross section is  $\Sigma_a \approx 0.1 \text{ cm}^{-1}$ . (a) Using one-group theory, compute and plot the negative reactivity introduced by the fish as a function of its position in the pool. (b) Determine the stable period of the reactor as a function of the position of the fish. [Note: Where the facilities are available, this makes a splendid experiment.]

15-4. Using one-group perturbation theory, derive a formula for the effectiveness of a small cylindrical control rod of radius  $a$  located in a bare cylindrical reactor (a) at the axis, (b) off-axis. Compare your formulas with those derived in Chapter 14.

15-5. In computing the effectiveness of control rods in Chapter 14, it was assumed that when a control rod is removed from a reactor the space occupied by the rod is filled with core material, and conversely, when a rod is inserted a slug of core material is expelled from the reactor. In other words, it was assumed that each rod has a fueled follower. (a) Derive one-group and two-group formulas for the error introduced by this assumption if the rod does not have such a follower. (b) Evaluate this error for the control rod described in Problem 14-2.

15-6. In a pulsed-neutron experiment with a bare assembly of moderator, the thermal flux is measured with a small detector, located at the point  $r_0$ , having volume  $V_d$  and macroscopic absorption cross section  $\bar{\Sigma}_{ad}$ . Using one-group perturbation theory, show that the presence of the detector changes the observed decay constant by approximately

$$\Delta\lambda = \frac{v_T V_d \bar{\Sigma}_{ad} \phi_T^2(r_0)}{\int \phi_T^2 dV},$$

where  $v_T$  is the speed of neutrons having the energy  $kT$  (cf. Eq. 8-11).

15-7. Verify the formulas for  $C^+$ ,  $F^+$ , and  $G^+$  given in Eqs. (15-110) through (15-112).

15-8. Compute and plot the two-group fluxes and adjoint fluxes for the reactors described in (a) Problem 10-16, (b) Problem 10-17, (c) Problem 10-19.

15-9. Show that the adjoint of the multigroup operator is the transpose of the multigroup operator.

15-10. (a) Write down the reactor operator for a directly coupled multigroup calculation. (b) What is the adjoint operator?

15-11. A small void forms (for instance, by boiling) at the center of a critical, bare, spherical, thermal reactor containing no resonance absorbers. (a) Using two-group perturbation theory, show that if the reactor consists of a liquid fuel-moderator mixture of fixed density, the reactor falls subcritical. (b) Show that if the reactor is quasihomogeneous with a liquid moderator-coolant and the void forms in the liquid, the reactor becomes supercritical unless  $\pi^4 \tau_T L_T^2 / R^4 \geq 1$ , where  $R$  is the radius of the reactor. [Hint: Treat the void as a medium with negative atom density; in part (b),  $\delta\Sigma_{2f} = 0$ .]

15-12. At the time  $t = 0$  a neutron is introduced into a critical reactor at the point  $r_0$ . In one-group theory the flux at  $t = 0$  becomes  $\phi(r, 0) = A\varphi_1(r) + v\delta(r - r_0)$ , where  $A$  is a constant depending upon the initial power of the reactor,  $\varphi_1(r)$  is the fundamental eigenfunction, and  $v$  is the one-group speed. With the introduction of the neutron, the neutron balance is disturbed (although the reactor is still critical) and for  $t > 0$  the flux can be written as

$$\phi(r, t) = \sum C_n \varphi_n(r) e^{\omega_n t},$$

where  $\omega_n < 0$  for  $n > 1$ . Determine the constants  $C_n$  and show that the ultimate flux at any point in the reactor is larger than the initial flux ( $t < 0$ ) by an amount which is proportional to the importance of the point  $r_0$ .

15-13. Using two-group perturbation theory, derive an expression for the relative worth of a partially inserted control rod in a bare cylindrical reactor, and compare with Eq. (15-131). Explain your result physically.

15-14. In an effort to obtain a uniform flux and also to simplify the control system, the control rods in most power reactors are usually *ganged*, that is, connected to the control circuitry in such a way that several rods (a "gang") move together. (a) If all the rods in the reactor, whose lifetime control requirements are shown in Fig. 13-7, operate as one gang (a most unlikely situation), plot the relative distance of insertion of the rods as a function of time from startup to shutdown. (b) If the rods operate in two gangs of equal worth, plot their distance of insertion if the second group of rods is not moved until the first is entirely removed from the reactor.

15-15. A large, natural uranium-fueled, graphite-moderated research reactor is a bare cube 25 ft on a side. With the reactor operating at a power of 25 MW(th), the maximum thermal flux is  $5 \times 10^{12}$  neutrons/cm<sup>2</sup>-sec. Calculate the negative reactivity due to equilibrium Xe<sup>135</sup>.

15-16. (a) Using one-group perturbation theory, derive a formula for the reactivity due to equilibrium Sm<sup>149</sup>. (b) Apply this formula to the reactor described in the preceding problem.

15-17. Using the results of Problems 10-16 and 15-8, compute the danger coefficient at the center of the reactor described in Problem 10-16 for the following substances: (a) D<sub>2</sub>O (in a small container), (b) Be, (c) Fe, (d) U<sup>235</sup>.

15-18. For some reason, the temperature suddenly increases by the amount  $\Delta T$  throughout a cylindrical region of radius  $a$  along the center of a critical, bare, cylindrical reactor of radius  $R$ . The reactor is homogeneous and contains no resonance absorbers. By treating as perturbations the changes in the reactor parameters arising from the change in temperature, compute by one-group theory the reactivity introduced into the reactor by this local temperature rise.

15-19. Show that corresponding eigenvalues of the reactor operator and its adjoint are equal.

15-20. Show that the transpose of the product of two matrices is equal to the product of their transposes but in reverse order.

15-21. A point source emitting a continuous spectrum of neutrons is placed in a medium of arbitrary geometry. (a) Show that the multigroup diffusion kernel is determined by the equation

$$MG(r, r') = S \delta(r - r'),$$

where  $M$  is a multigroup operator and  $S$  is the source vector whose  $j$ th component is equal to the fraction of the source neutrons emitted in the  $j$ th group. (b) Write down  $M$  for a medium which does not contain fissionable material. (c) What is  $M^+$  for the medium in (b)? (d) Show that the reciprocity theorem is  $G^+(r, r') = G(r', r)$ , where  $G^+(r, r')$  satisfies the equation

$$M^+G^+(r, r') = S \delta(r - r').$$

15-22. Show that the two-group fluxes in a reflected subcritical reactor are given formally by the expression

$$\phi(\mathbf{r}) = \int S(\mathbf{r}') G(\mathbf{r}, \mathbf{r}') dV',$$

where  $S(\mathbf{r}')$  is the source vector (cf. Problem 15-21) and

$$G(\mathbf{r}, \mathbf{r}') = \sum_n \frac{\phi_n(\mathbf{r})\psi_n(\mathbf{r}')}{\omega_n \int \psi_n \phi_n dV}.$$

## **APPENDIX I**

# **Miscellaneous Constants and Data**

**Table I-1**  
**Physical Constants\***

Quantity	Symbol or definition	Value
Avogadro's number	$N_A$	$0.602252 \times 10^{24} (\text{gm}\cdot\text{mole})^{-1}$
Boltzmann's constant	$k$	$1.38054 \times 10^{-16} \text{ erg } (\text{°K})^{-1}$
		$8.617065 \times 10^{-5} \text{ eV } (\text{°K})^{-1}$
Classical electron radius	$r_e = e^2/m_e c^2$	$2.81777 \times 10^{-13} \text{ cm}$
Electron rest mass	$m_e$	$9.1091 \times 10^{-28} \text{ gm}$ $5.48597 \times 10^{-4} \text{ amu}$ $0.511006 \text{ MeV}$
Elementary charge	$e$	$1.60210 \times 10^{-19} \text{ coul}$
Fine structure constant	$e^2/\hbar c$	$7.29720 \times 10^{-3}$ $1/137.0388$
Neutron rest mass	$M_n$	$1.67482 \times 10^{-24} \text{ gm}$ $1.0086654 \text{ amu}$ $939.550 \text{ MeV}$
Planck's constant divided by $2\pi$	$\hbar$	$1.05450 \times 10^{-27} \text{ erg}\cdot\text{sec}$ $6.58199 \times 10^{-16} \text{ eV}\cdot\text{sec}$
Proton rest mass	$M_p$	$1.67252 \times 10^{-24} \text{ gm}$ $1.0072766 \text{ amu}$ $938.256 \text{ MeV}$
Speed of light	$c$	$2.997925 \times 10^{10} \text{ cm}\cdot\text{sec}^{-1}$

\* The values are those recommended by the Committee on Fundamental Constants of the National Academy of Sciences-National Research Council. See *Physics Today*, February 1964, p. 48.

## **APPENDIX I**

# **Miscellaneous Constants and Data**

**Table I-1**  
**Physical Constants\***

Quantity	Symbol or definition	Value
Avogadro's number	$N_A$	$0.602252 \times 10^{24} (\text{gm}\cdot\text{mole})^{-1}$
Boltzmann's constant	$k$	$1.38054 \times 10^{-16} \text{ erg } (\text{°K})^{-1}$
Classical electron radius	$r_e = e^2/m_e c^2$	$8.617065 \times 10^{-5} \text{ eV } (\text{°K})^{-1}$
Electron rest mass	$m_e$	$2.81777 \times 10^{-13} \text{ cm}$
Elementary charge	$e$	$9.1091 \times 10^{-28} \text{ gm}$
Fine structure constant	$e^2/\hbar c$	$5.48597 \times 10^{-4} \text{ amu}$
Neutron rest mass	$M_n$	$0.511006 \text{ MeV}$
Planck's constant divided by $2\pi$	$\hbar$	$1.60210 \times 10^{-19} \text{ coul}$
Proton rest mass	$M_p$	$7.29720 \times 10^{-3}$
Speed of light	$c$	$1/137.0388$
		$1.67482 \times 10^{-24} \text{ gm}$
		$1.0086654 \text{ amu}$
		$939.550 \text{ MeV}$
		$1.05450 \times 10^{-27} \text{ erg}\cdot\text{sec}$
		$6.58199 \times 10^{-16} \text{ eV}\cdot\text{sec}$
		$1.67252 \times 10^{-24} \text{ gm}$
		$1.0072766 \text{ amu}$
		$938.256 \text{ MeV}$
		$2.997925 \times 10^{10} \text{ cm}\cdot\text{sec}^{-1}$

\* The values are those recommended by the Committee on Fundamental Constants of the National Academy of Sciences-National Research Council. See *Physics Today*, February 1964, p. 48.

**Table I-2**  
**Units and Conversion Factors**

1 eV	$1.60210 \times 10^{-19}$ joule $1.60210 \times 10^{-12}$ erg
1 MeV	$10^6$ eV $1.60210 \times 10^{-13}$ joule
1 amu	$1.660438 \times 10^{-24}$ gm 931.478 MeV $1.49232 \times 10^{-3}$ erg
1 joule	$10^7$ erg
1 watt	1 joule/sec
1 day	86400 sec
1 mean year	365.25 days $3.156 \times 10^7$ sec
1 curie	$3.7000 \times 10^{10}$ disintegrations/sec
1°K	$8.617065 \times 10^{-5}$ eV
1 kg	2.205 lb
1 in.	2.540 cm
1 ft	30.48 cm
1 ft <sup>3</sup>	$2.832 \times 10^4$ cm <sup>3</sup>
1 hp	0.7457 kW
0°K	-273.15°C

**Table I-3**  
**Some Isotopes of Importance in Nuclear Engineering**

Atomic number	Isotope	Abundance, atom %	half-life	$\sigma_a,^*$ barns	$\sigma_f,^*$ barns
0	n		12 m		
1	H <sup>1</sup>	99.985		332 mb	
	H <sup>2</sup>	0.015		0.5 mb	
	H <sup>3</sup>		12.26 y		
3	Li <sup>6</sup>	7.42		945	
	Li <sup>7</sup>	92.58		37 mb	
5	B <sup>10</sup>	19.6		3837	
	B <sup>11</sup>	80.4		5 mb	
6	C <sup>12</sup>	98.89		3.4 mb	
	C <sup>13</sup>	1.11		0.9 mb	
	C <sup>14</sup>		5770 y		
7	N <sup>14</sup>	99.63		1.85	
	N <sup>15</sup>	0.37		24 $\mu$ b	
8	O <sup>16</sup>	99.759		0.178 mb	
	O <sup>17</sup>	0.037		0.235	
	O <sup>18</sup>	0.204		0.21 mb	
53	I <sup>135</sup>		6.7 h		
54	Xe <sup>135</sup>		9.2 h	2.7 $\times$ 10 <sup>6</sup> †	
61	Pm <sup>149</sup>		54.4 h		
62	Sm <sup>149</sup>	13.83		40,800†	
90	Th <sup>232</sup>	100	1.41 $\times$ 10 <sup>10</sup> y	7.4	
	Th <sup>233</sup>		22.1 m	1500	15
92	U <sup>233</sup>		1.62 $\times$ 10 <sup>5</sup> y	573.1†	524.5†
	U <sup>234</sup>	0.0057	2.48 $\times$ 10 <sup>5</sup> y	95	
	U <sup>235</sup>	0.72	7.13 $\times$ 10 <sup>8</sup> y	678.2†	577.1†
	U <sup>236</sup>		2.39 $\times$ 10 <sup>7</sup> y	6	
	U <sup>238</sup>	99.27	4.51 $\times$ 10 <sup>9</sup> y	2.73	
	U <sup>239</sup>		23.5 m	22	14
94	Pu <sup>239</sup>		24360 y	1014.5†	740.6†
	Pu <sup>240</sup>		6760 y	286	0.03
	Pu <sup>241</sup>		13 y	1375	950
	Pu <sup>242</sup>		3.79 $\times$ 10 <sup>5</sup> y	30	<0.2

\* Cross sections at 0.0253 eV or 2200 m/sec. (From BNL-325, 2nd ed. 1958 plus supplements 1 and 2, 1960, 1964, and 1965.)

† Non-1/v absorber; see Table 8-1, p. 255, for non-1/v factor.

**Table I-4**  
**Properties of the Elements and Certain Molecules**

Element or molecule	Symbol	Atomic number	Atomic or molecular weight*	Nominal density, gm/cm <sup>3</sup>	Atoms or molecules per cm <sup>3</sup> †	$\sigma_{a,\dagger}$ barns	$\Sigma_{a,\dagger}$ cm <sup>-1</sup>	$\Sigma_{s,\dagger}$ cm <sup>-1</sup>
Actinium	Ac	89	227	26.9815	2.699	0.06024	800	0.08434
Aluminum	Al	13	121.75	6.62	0.03275	5.5	0.1801	0.1408
Antimony	Sb	51	39.948	Gas	0.63	1.5		
Argon	Ar	18	74.9216	5.73	0.04606	4.5	6	0.2073
Arsenic	As	33	137.34	3.5	0.01535	1.2	8	0.01842
Barium	Ba	56	9.0122	1.85	0.1236	0.0095	7.0	0.0011174
Beryllium	Be	4	25.0116	2.96	0.07127	0.0095	6.8	0.0006771
Beryllium oxide	BeO		208.980	9.80	0.02824	0.034	9	0.0009602
Bismuth	Bi	83	10.811	2.3	0.1281	759	4	0.4846
Boron	B	5	79.909	3.12	0.02351	6.7	6	0.2542
Bromine	Br	35	112.40	8.65	0.04635	2450	7	0.5124
Cadmium	Cd	48	40.08	1.55	0.02329	0.43	3.0	0.1411
Calcium	Ca	20						0.3245
Carbon (graphite)**	C	6	12.01115	1.60	0.08023	0.0034	4.8	0.0002728
Cerium	Ce	58	140.12	6.78	0.02914	0.7	9	0.02040
Cesium	Cs	55	132.905	1.9	0.008610	30	20	0.2623
Chlorine	Cl	17	35.453	Gas		33	16	0.1722
Chromium	Cr	24	51.996	7.19	0.08328	3.1	3	0.2582
Cobalt	Co	27	58.9332	8.8	0.08993	37	7	0.2498
Columbium (see niobium)								0.6295
Copper	Cu	29	63.54	8.96	0.08493	3.8	7.2	0.6115
Deuterium	D	1	2.01410	Gas		0.0005		
Dysprosium	Dy	66	162.50	8.56	0.03172	940	100	3.172

Erbium	68	167.26	9.16	0.03203	160	15	5.125	0.4805
Europium	63	151.96	5.22	0.02069	4300	8	88.97	0.1655
Fluorine	F	9	18.9984	Gas	0.0098	3.9		
Gadolinium	Gd	64	157.25	7.95	0.03045	46,000	4	0.1218
Gallium	Ga	31	69.72	5.91	0.05105	3.0	0.1532	
Germanium	Ge	32	72.59	5.36	0.04447	2.4	3	0.1067
Gold	Au	79	196.967	19.32	0.05907	98.8	9.3	0.1334
Hafnium	Hf	72	178.49	13.36	0.04508	105	8	0.5494
Heavy water††	D <sub>2</sub> O		20.0276	1.105	0.03323	0.0010	13.6	0.3606
Helium	He	2	4.0026	Gas	≤ 0.050	0.8	3.323 × 10 <sup>-5</sup>	0.4519
Holmium	Ho	67	164.930	8.76	0.03199	65	2.079	
Hydrogen	H	1	1.00797	Gas	0.332			
Illinium (see promethium)	In	49	114.82	7.31	0.03834	194	2.2	7.438
Indium	I	53	126.9044	4.93	0.02340	6.4	3.6	0.1498
Iodine	Ir	77	192.2	22.5	0.07050	460	32.43	0.08242
Iridium	Fe	26	55.847	7.87	0.08487	2.53	11	0.2147
Iron	Kr	36	83.80	Gas	24	7.2		0.9336
Krypton	La	57	138.91	6.19	0.02684	8.9	15	0.2389
Lanthanum	Pb	82	207.21	11.34	0.03348	0.17	11	0.005692
Lead	Li	3	6.939	0.53	0.04600	71	1.4	0.4026
Lithium	Lu	71	174.91	9.74	0.03354	80	11	0.3683
Lutetium	Mg	12	24.312	1.74	0.04310	0.063	3.266	0.0644
Magnesium	Mn	25	54.9380	7.43	0.08145	13.3	4	0.002715
Manganese	Hg	80	200.59	13.55	0.04068	360	2.3	0.1724
Mercury	Mo	42	95.94	10.2	0.06403	2.6	20	1.083
Molybdenum	Nd	60	144.24	6.98	0.02914	50	7	0.1873
Neodymium	Ne	10	20.183	Gas	0.032	16	14.64	0.8136
Neon	Ni	28	58.71	8.90	0.09130	4.6	7	0.4482
Nickel	Nb	41	92.906	8.57	0.05555	1.1	1.457	0.4662
Niobium	N	7	14.0067	Gas	0.03296	1.85	10	1.597
Nitrogen								0.2778
								0.3626
								0.005603

(Cont.)

Table I-4 (*Continued*)

Element or molecule	Symbol	Atomic number	Atomic or molecular weight*	Nominal density, gm/cm <sup>3</sup>	Atoms or molecules per cm <sup>3</sup> †	$\sigma_a, \dagger$ barns	$\sigma_a, \dagger$ barns	$\Sigma_a, \dagger$ cm <sup>-1</sup>	$\Sigma_s, \dagger$ cm <sup>-1</sup>
Osmium	Os	76	190.2	22.5	0.07124	15	11	1.069	0.7836
Oxygen	O	8	15.9994	Gas	<0.0002	4.2	4.2		
Palladium	Pd	46	106.4	12.0	0.06792	8	3.6	0.5434	0.2445
Phosphorus (yellow)	P	15	30.9738	1.82	0.03539	0.19	5	0.006724	0.1770
Platinum	Pt	78	195.09	21.45	0.06622	10	10	0.6622	0.6622
Plutonium	Pu	94	239	19.6	0.04939	$\sigma_a = 1015$ $\sigma_f = 741$	9.6	49.88	0.4741
Polonium	Po	84	210	9.51	0.02727	2.1	1.5	0.02783	0.01988
Potassium	K	19	39.102	0.86	0.01325	12	4	0.1965	0.1159
Praseodymium	Pr	59	140.907	6.78	0.02898				
Promethium	Pm	61							
Protactinium	Pa	91	231			210			
Radium	Ra	88	226	5.0	0.01332	20		0.2664	
Rhenium	Re	75	186.2	20	0.06596	85	14	5.607	0.9234
Rhodium	Rh	45	102.905	12.41	0.07263	155	5	11.26	0.3632
Rubidium	Rb	37	85.47	1.53	0.01078	0.73	12	0.007869	0.1294
Ruthenium	Ru	44	101.07	12.2	0.07270	2.5	6	0.1818	0.4362
Samarium	Sm	62	150.35	6.93	0.02776	5800	5	161.0	0.1388
Scandium	Sc	21	44.956	2.5	0.03349	23	24	0.7703	0.8038
Selenium	Se	34	78.96	4.81	0.03669	12	11	0.4403	0.4036
Silicon	Si	14	28.086	2.33	0.04996	0.16	1.7	0.1164	0.08493
Silver	Ag	47	107.870	10.49	0.05857	63	6	3.690	0.3514
Sodium	Na	11	22.9898	0.97	0.02541	0.53	4	0.01347	0.1016
Strontium	Sr	38	87.62	2.6	0.01787	1.3	10	0.02323	0.1787
Sulfur (yellow)	S	16	32.064	2.07	0.03888	0.52	1.1	0.2022	0.04277

Tantalum	73	180.948	16.6	0.05525	21	5	1.160	0.2763
Technetium	Tc	43	99	0.02945	22	5	0.1384	0.1473
Tellurium	Te	52	127.60	6.24	4.7	1.452		
Terbium	Tb	65	158.924	8.33	0.03157	46	0.1152	0.4889
Thallium	Tl	81	204.37	11.85	0.03492	3.3	0.2249	0.3829
Thorium	Th	90	232.038	11.71	0.03039	7.4	4.143	0.2320
Thulium	Tm	69	168.934	9.35	0.03314	125	4	0.02333
Tin	Sn	50	118.69	7.298	0.03703	0.63	0.3459	0.1481
Titanium	Ti	22	47.90	4.51	0.05670	6.1	5	0.2268
Tungsten	W	74	183.85	19.2	0.06289	19	1.195	0.3145
Uranium	U	92	238.03	19.1	0.04833	$\sigma_a = 7.6$ $\sigma_f = 4.2$	0.3673	0.4011
Vanadium	V	23	50.942	6.1	0.07212	4.9	5	0.3534
Water	H <sub>2</sub> O		18.0153	1.0	0.03343	0.664	103	0.2030
Xenon	Xe	54	131.30	Gas	24	4.3		0.3606
Ytterbium	Yb	70	173.04	7.01	0.02440	37	12	3.443
Yttrium	Y	39	88.905	5.51	0.03733	1.3	0.9208	0.2928
Zinc	Zn	30	65.37	7.133	0.06572	1.10	3	0.1120
Zirconium	Zr	40	91.22	6.5	0.04291	0.18	0.07229	0.2366
						8	0.007724	0.3433

\* Based on C<sup>12</sup> = 12.00000 amu.

† Four-digit accuracy for computational purposes only; last digit(s) usually is not meaningful.

‡ Cross sections at 0.0253 eV or 2200 m/sec. The scattering cross sections, except for those of H<sub>2</sub>O and D<sub>2</sub>O, are measured values in a thermal neutron spectrum and are assumed to be 0.0253 eV values because  $\sigma_a$  is usually constant at thermal energies. The errors in  $\sigma_a$  tend to be large, and the tabulated values of  $\sigma_a$  should be used with caution. (From BNL-325, 2nd ed., 1958 plus supplements 1 and 2, 1960, 1964, and 1965.)

\*\* The value of  $\sigma_a$  given in the table is for pure graphite. Commercial reactor-grade graphite contains varying amounts of contaminants and  $\sigma_a$  is somewhat larger, say, about 0.0048 barns, so that  $\Sigma_a \approx 0.003851 \text{ cm}^{-1}$ .

†† The value of  $\sigma_a$  given in the table is for pure D<sub>2</sub>O. Commercially available heavy water contains small amounts of ordinary water and  $\sigma_a$  in this case is somewhat larger.

## **APPENDIX II**

# **Special Functions**

The properties of several transcendental functions which are important in reactor theory are summarized in this Appendix. References to these functions and available tabulations are given at the end of the Appendix.

### **II-1 The Delta Function-Singular Source Distributions**

The *delta function*, written  $\delta(x)$ , is defined to be zero for all values of  $x$  except  $x = 0$ . The integral of  $\delta(x)$  is finite, however, provided the range of integration includes the point at  $x = 0$ , and the value of this integral is taken to be unity. In summary,

$$\delta(x) = 0, \quad x \neq 0 \quad (\text{II-1})$$

$$\int_a^b \delta(x) dx = \begin{cases} 1, & \text{if } a < 0 < b, \\ 0, & \text{otherwise.} \end{cases} \quad (\text{II-2})$$

The defining relations do not include the possibility that either  $a$  or  $b$  may be zero, and it is necessary to extend the definition of  $\delta(x)$  as follows:

$$\int_0^a \delta(x) dx = - \int_a^0 \delta(x) dx = \frac{1}{2}. \quad (\text{II-3})$$

Integrals involving delta functions can easily be evaluated. Consider, for instance, the integral

$$\int_{-\infty}^{\infty} f(x) \delta(x) dx.$$

Since  $\delta(x)$  is zero everywhere except at  $x = 0$ , there is no contribution to the integral except at that point. However, unless  $f(x)$  is singular at  $x = 0$ , it will change very little in a small interval near  $x = 0$  and can be taken out of the integral; thus

$$\int_{-\infty}^{\infty} f(x) \delta(x) dx \approx f(0) \int_{-\epsilon}^{\epsilon} \delta(x) dx = f(0), \quad (\text{II-4})$$

where  $\epsilon$  is an arbitrary small number. If  $f(x)$  is singular at  $x = 0$ , the integral

does not exist. Although the limits on the above integral are from  $-\infty$  to  $+\infty$ , Eq. (II-4) is valid for any range of integration which includes the point  $x = 0$ . Thus,

$$\int_a^b f(x) \delta(x) dx = \begin{cases} f(0), & \text{if } a < 0 < b, \\ \frac{1}{2}f(0), & \text{if } a = 0, \\ 0, & \text{otherwise,} \end{cases} \quad (\text{II-5})$$

provided  $f(0)$  exists.

In terms of the above definitions it is easy to derive the following relations:

$$\delta(x - x') = 0, \quad x \neq x', \quad (\text{II-6})$$

$$\int_a^b f(x) \delta(x - x') dx = \begin{cases} f(x'), & \text{if } a < x' < b, \\ \frac{1}{2}f(x'), & \text{if } a = x', \\ 0, & \text{otherwise,} \end{cases} \quad (\text{II-7})$$

provided  $f(x')$  exists.

It is important to note that  $\delta(x)$  is an *even* function; that is,  $\delta(-x) = \delta(x)$ . This can be seen by letting  $f(x)$  in Eq. (II-4) be any odd function and noting that the integral of the product of an even function and an odd function is zero.

Singular source distribution functions can usually be written in terms of delta functions. However, the appropriate representation of such a source function depends upon both the nature of the source and the geometry of the system under consideration. For example, the neutron source density  $s(x)$  for a planar source lying in the  $YZ$  plane at  $x = 0$  and emitting  $S$  neutrons/cm<sup>2</sup> per sec can be represented by

$$s(x) = S \delta(x). \quad (\text{II-8})$$

For an isotropic point source located at the origin and emitting  $S$  neutrons/sec, the source density is given in rectangular coordinates by

$$s(x, y, z) = S \delta(x) \delta(y) \delta(z). \quad (\text{II-9})$$

It will be noted that the integral of  $s(x, y, z)$  over all space is equal to  $S$ . This result must be obtained regardless of the coordinate system used to represent the source. Thus in spherical coordinates, a point source at the origin is represented by

$$s(r) = \frac{S \delta(r)}{2\pi r^2}. \quad (\text{II-10})$$

The integral of this density function is

$$\int_{\text{all space}} s(r) dV = \int_0^\infty \frac{S \delta(r)}{2\pi r^2} 4\pi r^2 dr = 2S \int_0^\infty \delta(r) dr = S,$$

in view of Eq. (II-3).

The density function in cylindrical coordinates for an infinite line source at  $r = 0$  emitting  $S$  neutrons/cm per sec is

$$s(r) = \frac{S \delta(r)}{\pi r}. \quad (\text{II-11})$$

It is often necessary to have expansions of the various singular source functions in eigenfunctions of the infinite slab, infinite cylinder, and sphere. These are given by the following formulas:

Infinite slab, thickness  $a$  ( $-a/2 \leq x \leq a/2$ ), planar source at  $x'$ :

$$S \delta(x - x') = \frac{2S}{a} \left[ \sum_{n \text{ odd}} \cos\left(\frac{n\pi x}{a}\right) \cos\left(\frac{n\pi x'}{a}\right) + \sum_{n \text{ even}} \sin\left(\frac{n\pi x}{a}\right) \sin\left(\frac{n\pi x'}{a}\right) \right] \quad (\text{II-12})$$

Infinite cylinder, radius  $R$ , infinite line source at  $r = 0$ :

$$\frac{S \delta(r)}{\pi r} = \frac{S}{\pi R^2} \sum_{n=1}^{\infty} J_0(x_n r/R) / J_1^2(x_n), \quad (\text{II-13})$$

where  $J_0(x_n) = 0$ ;

Sphere, radius  $R$ , point source at  $r = 0$ :

$$\frac{S \delta(r)}{2\pi r^2} = \frac{S}{2rR^2} \sum_{n=1}^{\infty} n \sin\left(\frac{n\pi r}{R}\right). \quad (\text{II-14})$$

## II-2 The Exponential Integral Function

The function  $Ei(-x)$  defined by

$$-Ei(-x) = \int_x^{\infty} \frac{e^{-u}}{u} du, \quad x > 0, \quad (\text{II-15})$$

is known as the *exponential integral function*. This function appears in many problems of neutron diffusion. At  $x = 0$ ,  $-Ei(-x)$  is singular but then decreases to zero more rapidly than  $e^{-x}$  as shown in Fig. II-1.

## II-3 The Functions $E_n(x)$

The functions  $E_n(x)$  are generalizations of the exponential integral function. These are defined as follows:

$$E_n(x) = \int_1^{\infty} \frac{e^{-xu}}{u^n} du, \quad (\text{II-16})$$

which can also be written as

$$E_n(x) = x^{n-1} \int_x^{\infty} \frac{e^{-u}}{u^n} du. \quad (\text{II-17})$$

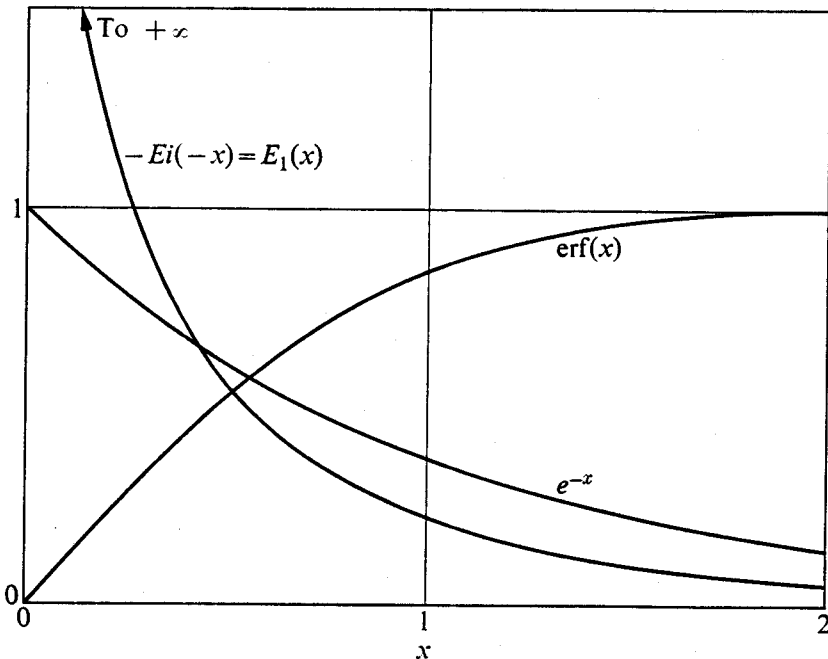


Fig. II-1. The exponential, exponential-integral, and error functions.

When  $n = 0$ , the integral can be carried out with the result

$$E_0(x) = \frac{e^{-x}}{x}. \quad (\text{II-18})$$

When  $n = 1$ ,

$$E_1(x) = \int_x^{\infty} \frac{e^{-u} du}{u} = -Ei(-x). \quad (\text{II-19})$$

Using integration by parts it is easy to show that

$$E_n(x) = \frac{1}{n-1} [e^{-x} - xE_{n-1}(x)], \quad n > 1. \quad (\text{II-20})$$

It follows from Eq. (II-20) that for  $n > 1$  the  $E_n(x)$  functions can be expressed in terms of  $E_1(x) = -Ei(-x)$ . However, since diffusion problems often involve functions with  $n = 3$  or  $n = 4$ , it is easier to use tabulated values of  $E_n(x)$  rather than expressions involving  $-Ei(-x)$ . For other properties of  $E_n(x)$  see Problem 11-12.

#### II-4 The Error Function

The *error function*, which is denoted by  $\text{erf}(x)$ , is defined by the integral

$$\text{erf}(x) = \frac{2}{\sqrt{\pi}} \int_0^x e^{-u^2} du. \quad (\text{II-21})$$

This function is the area under the Gaussian function  $2e^{-u^2}/\sqrt{\pi}$  from  $u = 0$

to  $u = x$ . It follows that  $\text{erf}(x)$  is a monotonically increasing function of  $x$  as shown in Fig. II-1. The total area under the Gaussian from  $u = 0$  to  $u = \infty$  is unity, so that  $\text{erf}(\infty) = 1$ .

The Maclaurin series for  $\text{erf}(x)$  is

$$\text{erf}(x) = \frac{2}{\sqrt{\pi}} \left( x - \frac{x^3}{3 \cdot 1!} + \frac{x^5}{5 \cdot 2!} - \frac{x^7}{7 \cdot 3!} + \dots \right), \quad (\text{II-22})$$

and for large  $x$ ,

$$\text{erf}(x) = 1 - \frac{e^{-x^2}}{x\sqrt{\pi}} \left[ 1 - \frac{1}{2x^2} + \frac{1 \cdot 3}{(2x^2)^2} - \frac{1 \cdot 3 \cdot 5}{(2x^2)^3} + \dots \right]. \quad (\text{II-23})$$

## II-5 Bessel Functions

The solutions of reactor problems in cylindrical coordinates frequently involve *Bessel functions*. Some useful properties of these functions are summarized here.

**Ordinary Bessel functions.** Bessel's equation is:

$$\frac{d^2\phi}{dx^2} + \frac{1}{x} \frac{d\phi}{dx} + \left( \alpha^2 - \frac{n^2}{x^2} \right) \phi = 0, \quad (\text{II-24})$$

where  $\alpha$  and  $n$  are constants. If  $n$  is *not* an integer or zero, the two independent solutions to this equation are denoted by

$$\phi(x) = \begin{cases} J_n(\alpha x), \\ J_{-n}(\alpha x). \end{cases} \quad (\text{II-25})$$

If  $n$  is an integer or zero, however, these two functions are not independent, and the two solutions are usually written as\*

$$\phi(x) = \begin{cases} J_n(\alpha x), \\ Y_n(\alpha x). \end{cases} \quad (\text{II-26})$$

The functions  $J_n(z)$  and  $Y_n(z)$  are known as *ordinary Bessel functions of the first and second kind*, respectively. In the following it will be assumed that  $n$  is an integer or zero and that  $z$  is real; this is the case in most reactor problems.

The function  $J_n(z)$  is finite for all values of  $z$ ;  $J_0(z)$  is shown in Fig. II-2. About the origin,  $J_n(z)$  has the following series expansion:

$$J_n(z) = \frac{1}{n!} \left( \frac{z}{2} \right)^n \left[ 1 - \frac{(z/2)^2}{1!(n+1)} + \frac{(z/2)^4}{2!(n+1)(n+2)} - \dots \right]. \quad (\text{II-27})$$

---

\* In German texts and in much of the recent literature of mathematical physics the function  $Y_n(z)$  is denoted by  $N_n(z)$ .

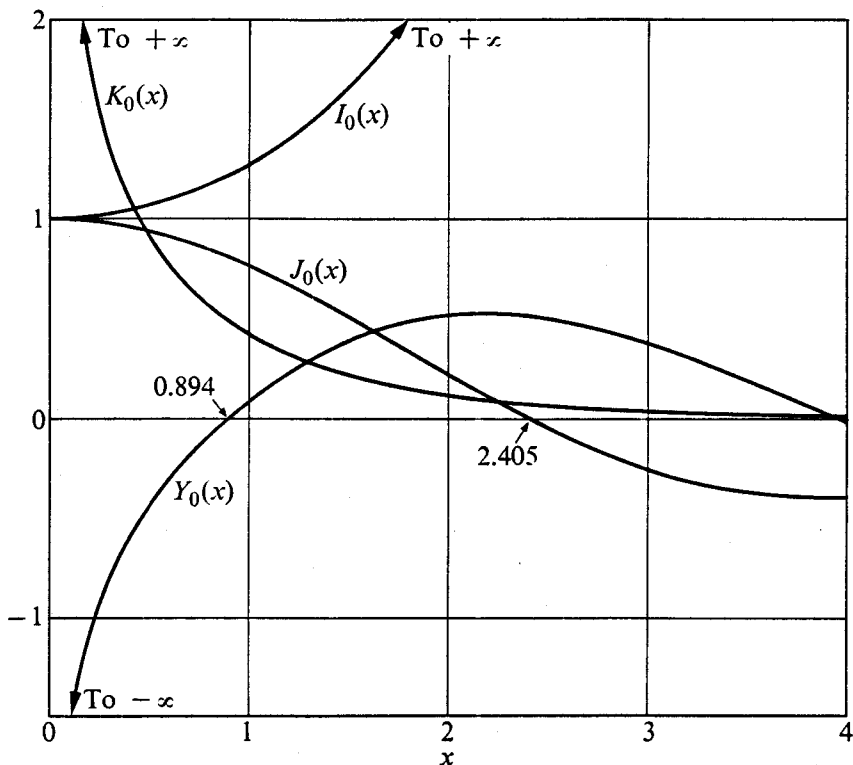


Fig. II-2. Ordinary and modified Bessel functions of zero order.

For large values of  $z$ ,  $J_n(z)$  has the asymptotic behavior:

$$J_n(z) \xrightarrow{z \rightarrow \infty} \sqrt{\frac{2}{\pi z}} \cos \left[ z - \frac{\pi}{2} (n + \frac{1}{2}) \right]. \quad (\text{II-28})$$

The function  $Y_n(z)$  is singular at  $z = 0$  and is given by the following series:

$$\begin{aligned} Y_n(z) &= \frac{2}{\pi} \left[ \ln \left( \frac{z}{2} \right) + \gamma - \frac{1}{2} \sum_{s=1}^n \left( \frac{1}{s} \right) \right] J_n(z) \\ &\quad - \frac{1}{\pi} \sum_{m=0}^{n-1} \frac{(n-m-1)!}{m!(z/2)^{n-2m}} \\ &\quad - \frac{1}{\pi} \sum_{m=1}^{\infty} (-1)^m \frac{(z/2)^{n+2m}}{m!(n+m)!} \sum_{s=1}^m \left( \frac{1}{s} + \frac{1}{s+n} \right), \end{aligned} \quad (\text{II-29})$$

where  $\gamma = 0.57722$  is Euler's constant. When  $n = 0$ , the summation in the first bracket and the sum from  $m = 0$  to  $m = n - 1$  in the second term do not appear. Equation (II-29) then reduces to

$$Y_0(z) = \frac{2}{\pi} [\ln z - 0.11593] J_0(z) - \frac{2}{\pi} \sum_{m=1}^{\infty} (-1)^m \frac{(z/2)^{2m}}{(m!)^2} \sum_{s=1}^m \left( \frac{1}{s} \right). \quad (\text{II-30})$$

For small values of  $z$ ,  $Y_n(z)$  behaves as

$$Y_n(z) \xrightarrow[z \rightarrow 0]{} \frac{2}{\pi} [\ln z - 0.11593], \quad n = 0, \quad (\text{II-31})$$

$$\xrightarrow[z \rightarrow 0]{} - \frac{(n-1)!}{\pi} \left(\frac{2}{z}\right)^n, \quad n = 1, 2, 3, \dots \quad (\text{II-32})$$

For large  $z$ ,  $Y_n(z)$  has the asymptotic form

$$Y_n(z) \xrightarrow[z \rightarrow \infty]{} \sqrt{\frac{2}{\pi z}} \sin \left[ z - \frac{\pi}{2} (n + \frac{1}{2}) \right]. \quad (\text{II-33})$$

It may also be noted that

$$\begin{aligned} J_{-n}(z) &= (-1)^n J_n(z), \\ Y_{-n}(z) &= (-1)^n Y_n(z). \end{aligned} \quad (\text{II-34})$$

**Modified Bessel functions.** If the quantity  $\alpha^2$  in Eq. (II-24) is negative, Bessel's equation takes the form

$$\frac{d^2\phi}{dx^2} + \frac{1}{x} \frac{d\phi}{dx} - \left( \alpha^2 + \frac{n^2}{x^2} \right) \phi = 0. \quad (\text{II-35})$$

When  $n$  is not an integer or zero, the two independent solutions are denoted by

$$\phi(x) = \begin{cases} I_n(\alpha x), \\ I_{-n}(\alpha x). \end{cases} \quad (\text{II-36})$$

Again, if  $n$  is zero or an integer, these functions are not independent and the two solutions are written as

$$\phi(x) = \begin{cases} I_n(\alpha x), \\ K_n(\alpha x). \end{cases} \quad (\text{II-37})$$

The functions  $I_n(z)$  and  $K_n(z)$  are called, respectively, *modified Bessel functions of the first and second kind*.\* They are related to the ordinary Bessel functions as follows:

$$I_n(z) = i^{-n} J_n(iz) \quad (\text{II-38})$$

and

$$K_n(z) = \frac{\pi}{2} i^{n+1} [J_n(iz) + i Y_n(iz)]. \quad (\text{II-39})$$

The series expansion of  $I_n(z)$  can be obtained from Eqs. (II-27) and (II-38); thus

$$I_n(z) = \frac{1}{n!} \left(\frac{z}{2}\right)^n \left[ 1 + \frac{(z/2)^2}{1!(n+1)} + \frac{(z/2)^4}{2!(n+1)(n+2)} + \dots \right]. \quad (\text{II-40})$$

---

\* Modified Bessel functions are sometimes called *hyperbolic Bessel functions*.

For large values of  $z$ ,  $I_n(z)$  behaves as

$$I_n(z) \xrightarrow{z \rightarrow \infty} \frac{1}{\sqrt{2\pi z}} e^z. \quad (\text{II-41})$$

Like  $Y_n(z)$ , the function  $K_n(z)$  is singular at  $z = 0$  (cf. Eq. II-29). The series representation about this point is

$$\begin{aligned} K_n(z) &= (-1)^{n+1} \left[ \ln \left( \frac{z}{2} \right) + \gamma - \frac{1}{2} \sum_{s=1}^n \left( \frac{1}{s} \right) \right] I_n(z) \\ &\quad + \frac{1}{2} \sum_{m=0}^{n-1} (-1)^m \frac{(n-m-1)!}{m!(z/2)^{n-2m}} \\ &\quad + (-1)^n \frac{1}{2} \sum_{m=0}^{\infty} \frac{(z/2)^{n+2m}}{m!(m+n)!} \sum_{s=1}^m \left( \frac{1}{s} + \frac{1}{s+n} \right). \end{aligned} \quad (\text{II-42})$$

The similarity between this expansion and that of  $Y_n(z)$  should be noted. For  $n = 0$ , Eq. (II-42) gives

$$K_0(z) = -[\ln z - 0.11593] I_0(z) + \sum_{m=0}^{\infty} \frac{(z/2)^{2m}}{(m!)^2} \sum_{s=1}^m \left( \frac{1}{s} \right). \quad (\text{II-43})$$

For small values of  $z$ ,  $K_n(z)$  behaves as

$$K_n(z) \xrightarrow{z \rightarrow 0} -[\ln z - 0.11593], \quad n = 0, \quad (\text{II-44})$$

$$K_n(z) \xrightarrow{z \rightarrow 0} \frac{1}{2}(n-1)! \left( \frac{2}{z} \right)^n, \quad n = 1, 2, 3, \dots \quad (\text{II-45})$$

For large  $z$ ,

$$K_n(z) \xrightarrow{z \rightarrow \infty} \sqrt{\frac{\pi}{2z}} e^{-z}. \quad (\text{II-46})$$

Relations similar to those given in Eq. (II-34) are

$$I_{-n}(z) = I_n(z), \quad K_{-n}(z) = K_n(z). \quad (\text{II-47})$$

**Some useful formulas.** The following formulas, which are written in terms of  $J_n(z)$ , are also valid for  $Y_n(z)$  and for any linear combination of  $J_n(z)$  and  $Y_n(z)$ :

$$\frac{2n}{z} J_n(z) = J_{n-1}(z) + J_{n+1}(z), \quad (\text{II-48})$$

$$2 \frac{dJ_n(z)}{dz} = J_{n-1}(z) - J_{n+1}(z), \quad \frac{dJ_0(z)}{dz} = -J_1(z), \quad (\text{II-49})$$

$$\int J_n^2(z) z dz = \frac{1}{2} z^2 [J_n^2(z) - J_{n-1}(z) J_{n+1}(z)], \quad (\text{II-50})$$

$$\int J_0^2(z) z dz = \frac{1}{2} z^2 [J_0^2(z) + J_1^2(z)], \quad (\text{II-51})$$

$$\int J_1(z) dz = -J_0(z), \quad \int J_0(z) z dz = z J_1(z). \quad (\text{II-52})$$

Important relations connecting  $J_n(z)$  and  $Y_n(z)$  are the following:

$$J_n(z) Y_{n-1}(z) - J_{n-1}(z) Y_n(z) = \frac{2}{\pi z}, \quad (\text{II-53})$$

$$J_n(z) \frac{dY_n(z)}{dz} - \frac{dJ_n(z)}{dz} Y_n(z) = \frac{2}{\pi z}, \quad (\text{II-54})$$

$$(\alpha^2 - \beta^2) \int J_0(\alpha z) J_0(\beta z) z dz = \alpha z J_1(\alpha z) J_0(\beta z) - \beta z J_0(\alpha z) J_1(\beta z), \quad (\text{II-55})$$

$$(\alpha^2 - \beta^2) \int J_n(\alpha z) J_n(\beta z) z dz = \beta z J_n(\alpha z) J_{n-1}(\beta z) - \alpha z J_{n-1}(\alpha z) J_n(\beta z). \quad (\text{II-56})$$

Equations (II-55) and (II-56) are also valid for integrals of products of ordinary Bessel functions of the first and second kind such as  $J_n(\alpha z) Y_n(\beta z)$ .

The formulas involving modified Bessel functions similar to those given above for  $J_n(z)$  and  $Y_n(z)$  are not the same for  $K_n(z)$  as they are for  $I_n(z)$ , and these must be written separately. For  $I_n(z)$ ,

$$\frac{2n}{z} I_n(z) = I_{n-1}(z) - I_{n+1}(z), \quad (\text{II-57})$$

$$2 \frac{dI_n(z)}{dz} = I_{n-1}(z) + I_{n+1}(z), \quad \frac{dI_0(z)}{dz} = I_1(z), \quad (\text{II-58})$$

$$\int I_n^2(z) z dz = \frac{1}{2} z^2 [I_n^2(z) - I_{n-1}(z) I_{n+1}(z)], \quad (\text{II-59})$$

$$\int I_0^2(z) z dz = \frac{1}{2} z^2 [I_0^2(z) - I_1^2(z)], \quad (\text{II-60})$$

$$\int I_1(z) dz = I_0(z); \quad \int I_0(z) z dz = z I_1(z). \quad (\text{II-61})$$

For  $K_n(z)$ ,

$$-\frac{2n}{z} K_n(z) = K_{n-1}(z) - K_{n+1}(z), \quad (\text{II-62})$$

$$-2 \frac{dK_n(z)}{dz} = K_{n-1}(z) + K_{n+1}(z); \quad \frac{dK_0(z)}{dz} = -K_1(z), \quad (\text{II-63})$$

$$\int K_n^2(z) z dz = \frac{1}{2} z^2 [K_n^2(z) - K_{n-1}(z) K_{n+1}(z)], \quad (\text{II-64})$$

$$\int K_0^2(z) z dz = \frac{1}{2} z^2 [K_0^2(z) - K_1^2(z)], \quad (\text{II-65})$$

$$\int K_1(z) dz = -K_0(z); \quad \int K_0(z) z dz = -z K_1(z). \quad (\text{II-66})$$

It is important to note that the relation  $Z'_0(z) = -Z_1(z)$  holds for every Bessel function *except*  $I_0(z)$ .

Relations analogous to Eqs. (II-53) and (II-54) are

$$I_n(z) K_{n-1}(z) + I_{n-1}(z) K_n(z) = \frac{1}{z}, \quad (\text{II-67})$$

$$\frac{dI_n(z)}{dz} K_n(z) - I_n(z) \frac{dK_n(z)}{dz} = \frac{1}{z}. \quad (\text{II-68})$$

**Orthogonality.** The Bessel function  $J_0(z)$  has an infinite number of zeros, i.e., values of  $z$  where the function is zero. If these values of  $z$  are denoted by  $x_n$  then it follows that  $J_0(x_n) = 0$ .

Consider now the functions  $J_0(x_m z/R)$  and  $J_0(x_n z/R)$ . Both of these functions vanish at  $z = R$  and are unity at  $z = 0$ . Using Eqs. (II-51) and (II-55), it can be shown that the integral

$$\int_0^R J_0\left(\frac{x_m z}{R}\right) J_0\left(\frac{x_n z}{R}\right) z \, dz = \begin{cases} 0, & m \neq n, \\ \frac{R^2}{2} J_1^2(x_n), & m = n. \end{cases} \quad (\text{II-69})$$

Equation (II-69) expresses the orthogonality of the Bessel functions. This orthogonality can be used to expand any well-behaved function in a series of Bessel functions in the region from  $z = 0$  to  $z = R$ . Thus let

$$f(z) = \sum_{n=1}^{\infty} C_n J_0\left(\frac{x_n z}{R}\right), \quad (\text{II-70})$$

where  $C_n$  are constants. Multiplying both sides of this equation by  $J_0(x_m z/R)$  and by the *weighting function*  $z$  and integrating from  $z = 0$  to  $z = R$  gives the following formula for  $C_n$ :

$$C_n = \frac{2}{R^2 J_1^2(x_n)} \int_0^R f(z) J_0\left(\frac{x_n z}{R}\right) z \, dz. \quad (\text{II-71})$$

## References

### Delta functions

DIRAC, P. A. M., *The Principles of Quantum Mechanics*, 4th ed., London: Oxford University Press, 1958. This book contains a lengthy discussion on the delta function by the originator of this function.

MORSE, P. M., and H. FESHBACH, *Methods of Theoretical Physics*. New York: McGraw-Hill, 1953. A great many practical applications of the delta function are given in this reference.

### The exponential integral function

There are many tabulations of  $-Ei(-x)$ . See, for example:

ETHERINGTON, H., Editor, *Nuclear Engineering Handbook*. New York: McGraw-Hill, 1958, pp. 1-119.

"Handbook of Mathematical Functions," NBS Applied Mathematics Series No. 55, Washington, D.C.: U. S. Government Printing Office, p. 227.

JAHNKE, E., F. EMDE, and F. LÖSCH, *Tables of Higher Functions*, 6th ed., New York: McGraw-Hill, 1960.

### The $E_n(x)$ functions

CASE, K. M., F. DE HOFFMANN, and G. PLACZEK, *Introduction to the Theory of Neutron Diffusion*. Washington, D. C.: U. S. Government Printing Office, 1953, p. 153. The properties of  $E_n(x)$  and tables of  $E_n(x)$  for  $n$  up to 4 are given in this document.

ETHERINGTON, H., *op. cit.*, pp. 1-120. Tables of  $E_0(x)$ ,  $E_1(x)$  and  $E_2(x)$  are given here.

GOLDSTEIN, H., *Fundamental Aspects of Reactor Shielding*, Reading, Mass.: Addison-Wesley, 1959, Appendix C.

"Handbook of Mathematical Functions," *op. cit.*, p. 227.

### The error function

This function has applications in many fields other than nuclear engineering, and it has been widely tabulated. See, for instance, the following:

ETHERINGTON, H., *op. cit.*, pp. 1-124. [The definition of  $\text{erf}(x)$  given on pp. 3-94 of this reference is different from Eq. (II-21). However, the tables in this reference are based on the more usual definition given by Eq. (II-21).]

"Handbook of Mathematical Functions," *op. cit.*, p. 295.

JAHNKE, E., *et al*, *op. cit.*, p. 17.

### Bessel functions

Virtually all books on advanced calculus and function theory include sections on Bessel functions. Convenient tabulations are included in the following:

ETHERINGTON, H., *op. cit.*, pp. 1-94. The ordinary and modified Bessel functions of zero and first order are tabulated here.

"Handbook of Mathematical Functions," *op. cit.*, pp. 355 *et seq.*

JAHNKE, E., *et al*, *op. cit.* The notation  $N_n = Y_n$  is used in this reference.

"Tables of Bessel Functions  $Y_0$ ,  $Y_1$ ,  $K_0$ ,  $K_1$ ,  $0 \leq X \leq 1$ ," Applied Mathematics Series, National Bureau of Standards, Washington, D. C.: U. S. Government Printing Office. These tables can be used when the argument of these functions is small. They are particularly valuable in many reactor calculations and, in fact, were computed during World War II specifically for the Manhattan Project.